EXPANSIVE AND COLLAPSING BEHAVIOUR OF VOLUME CHANGE SOILS

A Thesis presented to the

DEPARTMENT OF CIVIL ENGINEERING

UNIVERSITY OF CAPE TOWN

In partial* fulfilment of the requirements for the degree of Master of Science in Engineering

by

TIBERIO J.V. DE SOUSA VINAGRE

1990

* *This candidate has successfully completed five postgraduate courses (30 credit points) in partial fulfilment of the requirements for the M.Sc.Eng. degree, and therefore this thesis should be less than one half of the value of an M.Sc. thesis submitted in complete fulfilment of the requirements for the degree. For details of courses taken, see page 1 in Appendix I.*

The University of Cape Town has been given the right to reproduce this thesis in whole or in part. Copyright is held by the author.

The copyright of this thesis vests in the author. No quotation from it or information derived from it is to be published without full acknowledgement of the source. The thesis is to be used for private study or non-commercial research purposes only.

Published by the University of Cape Town (UCT) in terms of the non-exclusive license granted to UCT by the author.

University of Cape Town

ACKNOWLEDGEMENTS

I would like to express my gratitude to all those people who have contributed to this thesis, and in particular to:

Professor A.D.W. Sparks, my supervisor, who has been a source of advice and guidance, friendship and encouragement.

I thank the University of Cape Town, and specially the Department of Civil Engineering.

University of Cape T

This thesis is dedicated to:

Jacqueline, Jacques, Paulo and Tibério.

DECLARATION

The author hereby declares that, except where otherwise stated, the content of this thesis is his own work and has not been submitted for a degree at another University.

signature removed

Signed: Tiberio J.V. de Sousa Vinagre

University of Cape T

PREFACE

This thesis is designed to achieve three goals:

Goal One - to introduce the reader to soils exhibiting expansive and/or collapsing behaviour;
Goal Two - to provide an in depth understanding of aspects of this behaviour, obtained from an extensive study of these soil types; and,
Goal Three - to serve as a reference for future research work (a recommendation for further research proposed in Chapter Ten of this thesis).

The thesis is divided in two main parts.
In the first part representative soil types were selected on the basis of their properties and expected engineering behaviour. The soil structure and clay minerals were also studied in part one of this thesis.
The second part of the thesis deals with aspects of expansive and collapsing behaviour of soils. Chapter three provides the introduction to the subsequent chapters on expansive and collapsing behaviour of volume change soils.

The chapters in the first part of Volume I of this thesis.

Chapter one deals with the origin, physical properties and selection of the natural soils used throughout this thesis. The chapter is divided into three main sections :

I - describes the geology of the areas where the natural soils where obtained, namely the Cape Peninsula and Durban areas, as well as the origin and formation of expansive and collapsing soils;
II - provides the preliminary engineering properties for all the soil samples obtained in the field investigation; and,
III - selects the natural soil types to be used in the thesis, and introduces the artificial or made up soils.
The purpose of chapter one is therefore, to identify suitable soil types on the basis of their physical and engineering properties.

University of Cape T

The purpose of chapter two is threefold:

1) - To define the macro structure of the soil types, previously selected in chapter one, by visual appearance, particle size distribution, pH value, and the relationship between soil density and water content;
2) - To observe their micro structure by means of scanning electron microscopy; (see also Appendix) and,
3) - To identify the clay minerals which are present in each soil type, using X-ray diffraction techniques (see also Appendix).
The soil structure and clay minerals are of fundamental importance to characterize the behaviour of each soil type.

Artificially prepared soils were also used in order to result in a closer control of structure, measureable engineering properties, and the expected volume change behaviour.

The flow chart for each type of soil sample testing method used in Chapters One and Two is as follows:-

START:

Soil sample (after field investigation)
Obtained:-
Linear Shrinkage;
Liquid Limit;
Plasticity Index;
% Clay Size.

SELECTION OF SOIL TYPES

Selected soil types
Determined:-
Linear Shrinkage;
Liquid Limit;
Plastic Limit;
Plasticity Index;
Shrinkage Limit;
% Sand;
% Silt;
% Clay;
Specific Gravity.

University of Cape T

Macro study (natural or artificial soil)
Defined:
Visual appearance;
Particle size distribution;
pH value;
Soil density vs. water content relationships.

Micro study (natural or artificial soil)
Observations of micro structure: Scanning electron microscopy.
Identification of clay minerals: X-ray diffraction.

The chapters of the second part of volume I of the thesis.

An introduction to the rest of the thesis is given in Chapter 3.
The remaining chapters describe measured parameters.

Volume two.

For reading convenience, this dissertation has been divided into two separate volumes.

Observed data are provided in Appendices in a Separate Volume. Thus the reader may examine the chapters in this volume and refer to the appendices in volume two, at the same time.

University of Cape T

EXPANSIVE AND COLLAPSING BEHAVIOUR OF VOLUME CHANGE SOILS

VOLUME ONE - INDEX OF CONTENTS

SECTION		PAGE
TITLE PAGE		I
ACKNOWLEDGEMENTS		II
DECLARATION		III
PREFACE		IV
INDEX OF CONTENTS		VII
LIST OF FIGURES		XIX
LIST OF TABLES		LII
LIST OF PHOTOGRAPHIC PLATES		LV
NOMENCLATURE		LVII
BIBLIOGRAPHY		LXIV
CHAPTER ONE: THE SOIL TYPES		
1.1	Introduction and purpose.	1/1
1.2	Geology of the Cape Peninsula.	1/1
	Introduction to the area and its physiography.	1/1
	Geological formations.	1/3
1.3	Geology of the Durban area.	1/9
	Introduction to the area and its topography.	1/9
	Geological formations near Durban.	1/10
1.4	Expansive and collapsing Soils.	1/18
	Expansive Soils.	1/18
	Collapsing Soils.	1/21
	Residual soils.	1/25
	Distribution of expansive and collapsing soils.	1/25
1.5	Soil samples.	1/26
	Preliminary field investigations.	1/26
	Laboratory tests.	1/26
	Tabulation of results.	1/27
	Plasticity Index and Liquid Limit.	1/30
1.6	Selection of soil types.	1/31
	The criteria adopted.	1/31
	Introduction to Soil States - Consistency Limits.	1/32
	Initial selection of natural soil types.	1/32
	Definition of test procedures.	1/33
	Soil sampling and description of profiles.	1/34
	In Situ Tests.	1/42
	Natural water content of undisturbed samples.	1/45
	Selection of soil types.	1/45
1.7	Conclusions for Chapter One.	1/47
1.8	References for Chapter One.	1/49

University of Cape T

CHAPTER TWO:
SOIL STRUCTURE AND CLAY MINERALS

2.1 Introduction and objectives.	2/1
2.2 Macro studies.	2/1
2.2.1 Natural and artificial soil types.	2/2
Visual appearance of the Natural Soil Types.	2/2
Visual appearance of the Artificial Soil Types.	2/3
2.2.2 Particle size distribution.	2/4
Natural soils.	2/5
Artificial soils.	2/12
2.2.3 pH value of each soil type.	2/15
2.2.4 Soil density versus water content relationship.	2/16
2.3 Micro studies - I	2/28
Observations of soil structure by means of Scanning Electron Microscopy.	2/28
2.3.1 Introduction.	2/28
2.3.2 Basic theory, modes of operation and application.	2/28
2.3.3 Clay separation of samples for Scanning Electron Microscopy and X-Ray Diffraction.	2/39
2.3.4 Preparation of clay samples and SEM testing.	2/39
2.3.5 The photographic plates.	2/41
2.4 Micro studies - II	
Use of X-ray Diffraction data to identify the clay minerals.	2/45
2.4.1 Introduction.	2/45
2.4.2 Introduction to Mineralogy and the Clay Minerals.	2/45
2.4.3 Application of X-rays to the study of crystals.	2/98
2.4.4 X-ray Diffraction: Preparation and testing of samples.	2/104
2.4.5 X-Ray Diffraction - Analysis of test data.	2/110
2.5 Conclusions for chapter two.	2/114
2.5.1 Engineering properties.	2/114
2.5.2 Micro structure.	2/118
2.5.3 Clay minerals.	2/119
2.6 References for Chapter Two.	2/122

CHAPTER THREE:
INTRODUCTION TO EXPANSIVE AND COLLAPSING BEHAVIOUR

3.1 Introduction and definitions.	3/1
3.2 Outline of the main testing methods.	3/2
3.3 Summary of the chapters ahead.	3/3

University of Sheffield

CHAPTER FOUR:
FREE SHRINKAGE AND FREE SWELL PATHS

4.1	Introduction.	4/1
4.2	Definition.	4/1
4.3	The parameters which were investigated.	4/2
4.4	Reasons for using the type of plot shown in Figure 4.01.	4/4
4.5	Types of sample preparation.	4/7
4.6	Test method - includes visual sequence.	4/8
4.7	Summary of test results for each soil type.	4/10
4.7.1	Natural Soil Types.	4/10
4.7.2	Artificial Soil Types.	4/51
4.8	Conclusions for Chapter Four.	4/68
4.8.1	The Free Expansion Limit.	4/68
4.8.2	Free Swell Paths.	4/83
4.9	References for Chapter Four.	4/101

CHAPTER FIVE:
FITTING STRESS SCALES TO OBSERVED DATA

5.1	Introduction.	5/1
5.2	Definitions.	5/1
5.3	The parameters which are being investigated.	5/2
5.4	Stress scales and the type of plot shown in Figure 5.02.	5/4
5.5	Preparation of test samples.	5/7
5.6	The two main types of tests.	5/8
5.6.1	Consolidometer test.	5/8
5.6.2	Triaxial test.	5/9
5.7	Analysis of test results for each soil type.	5/12
5.7.1	Natural Soil Types - Remoulded Samples.	5/13
5.7.2	Natural Soil Types - Undisturbed Samples.	5/23
5.7.3	Artificial Soil Types.	5/27
5.8	Conclusions for Chapter Five: Fitting stress scales.	5/36
5.8.1	Natural Soil Types - Remoulded Samples.	5/36
5.8.2	Natural Soil Types - Undisturbed Samples.	5/46
5.9	References for Chapter Five.	5/58

University of Cape T

CHAPTER SIX:
ONE-DIMENSIONAL EXPANSION OR COLLAPSE

6.1 Introduction. 6/1
6.2 Concepts and definitions. 6/1
6.3 The parameters which are being investigated. 6/3
6.4 Reasons for using the types of plot shown in Figures 6.01-02. 6/5
6.5 Some specific objectives for this chapter. 6/7
6.6 Preparation of test samples. 6/8
6.7 Test method. 6/8
6.8 Summary of test results for each soil type. 6/10
6.8.1 Natural Soil Types. 6/10
6.8.2 Artificial Soil Types. 6/68
6.9 Analysis of test results. 6/86
6.9.1 Stress Scales: Void Ratio versus Water Ratio. 6/87
6.9.2 Void Ratio vs Effective Vertical Pressure vs Water Ratio. 6/112
6.10 Conclusions for Chapter Six. 6/146
6.10.1 Site 11, Rosebank - Expansion or Collapse of samples due to wetting. 6/147
6.10.2 Site 36, Rondebosch - Expansion or Collapse of samples due to wetting. 6/153
6.10.3 Site 30, Hout Bay - Expansion or Collapse of samples due to wetting. 6/155
6.10.4 Site A, Berea Road - Expansion or Collapse of samples due to wetting. 6/157
6.10.5 Site 7, Mowbray - Expansion or Collapse of samples due to wetting. 6/159
6.10.6 Sites 'B' Francois Road, 'C' Margaret Mayton Avenue and 'D' Rose Hill - Expansion or Collapse of samples due to wetting. 6/161
6.10.7 Site 48, Lady Grey - Expansion or Collapse of samples due to wetting. 6/162
6.10.8 Kaolin K.1 (13% Clay size), K.2 (20% clay), and K.3 (8.5% clay size) - Expansion or Collapse of samples due to wetting. 6/163
6.10.9 Bentonite B.1 (13.5% clay size), B.2 (7% clay) B.3 (11.5% clay), B.4 (15.5% clay), and Bentonite B.5 (35% clay) Expansion or Collapse of samples due to wetting. 6/164
6.11 References for Chapter Six. 6/166

University of Cape T

CHAPTER SEVEN:
SWELL PRESSURES

7.1	Introduction.	7/1
7.2	Definitions.	7/1
7.3	The parameters which are being investigated.	7/2
7.4	Swell pressures and the type of plot shown in Figure 7.02.	7/4
7.5	Preparation of test samples.	7/7
7.6	Test method.	7/7
7.7	Test results for each soil type.	7/9
7.8	Analysis of test results.	7/33
7.8.1	Void Ratio versus Effective Vertical Pressure.	7/34
7.8.2	Void Ratio vs Effective Vertical Pressure vs Water Ratio.	7/45
7.9	Conclusions for Chapter Seven.	7/56
7.10	References for Chapter Seven.	7/68

CHAPTER EIGHT:
AXISYMMETRIC STRESS BEHAVIOUR OF
EXPANSIVE AND COLAPSING SOILS

8.1	Introduction.	8/1
8.2	Concepts and definitions.	8/2
8.3	The parameters which are being investigated.	8/3
8.4	Reasons for using the types of plot shown in Figures 8.01, 8.02, and 8.03.	8/7
8.5	Some specific objectives.	8/8
8.6	Preparation of test samples.	8/9
8.7	Test method.	8/9
8.8	Measurement of horizontal strains, or stresses.	8/14
8.9	Analysis of test results.	8/20
8.10	Conclusions for Chapter Eight.	8/40
8.10.1	Stress Scales - Void Ratio versus Water Ratio.	8/41
8.10.2	Void Ratio versus Effective Vertical Pressure.	8/46
8.10.3	Void Ratio vs Effective Vertical Pressure vs Water Ratio.	8/49
8.10.4	Void Ratio vs Effective Horizontal Stress vs Water Ratio.	8/54
8.10.5	Void Ratio vs Effective Average Stress vs Water Ratio.	8/59
8.11	References for Chapter Eight.	8/67

University of Cape T

CHAPTER NINE:
ALL ROUND, THREE-DIMENSIONAL,
EXPANSION OR COLLAPSE

9.1	Introduction.	9/1
9.2	Concepts and definitions.	9/2
9.3	The parameters which are being investigated.	9/3
9.4	Reasons for using the types of plot shown in Figures 9.01 to 9.02.	9/6
9.5	Some specific objectives for this chapter.	9/6
9.6	Preparation of test samples.	9/7
9.7	Test method.	9/8
9.8	Test results for the soil types investigated.	9/10
9.9	Analysis of the test results.	9/16
9.10	Conclusions for Chapter Nine.	9/19
9.9.1	Void Ratio vs Effective All Round Pressure vs Water Ratio.	9/17
9.11	References for Chapter Nine.	9/22

CHAPTER TEN:
CONCLUDING SUMMARY AND FURTHER THOUGHTS

10.1	Introduction.	10/1
10.2	Concluding summary for part one of the thesis.	10/1
10.2.1	The Soil Types and their Macro Structure.	10/1
10.3	Concluding summary for part two of the theses.	10/11
10.3.1	Free Expansion Limit.	10/11
10.3.2	Relationship between Free Expansion Limit and the Consistency Limits.	10/12
10.3.3	Free Swell Paths.	10/16
10.3.4	Expansion or Collapse of samples due to wetting.	10/49
10.3.5	Swell Pressures, Consistency Limits and Stress Scales.	10/60
10.3.6	Vertical Pressures versus Horizontal Pressures, or Stresses.	10/62
10.3.7	Stress Paths of 'p' versus 'q'.	10/66
10.4	Stress Paths.	10/69
10.5	Compacted Soils vs Soils which dry from slurries.	10/70
10.6	Free Swell Curves.	10/71
10.7	Time versus Swell and/or Settlement behaviour.	10/72
10.8	Concluding remark.	10/72

University of Cape T

EXPANSIVE AND COLLAPSING BEHAVIOUR OF VOLUME CHANGE SOILS

VOLUME TWO

INDEX OF CONTENTS

SECTION	PAGE
TITLE PAGE	I
PREFACE	II
INDEX OF CONTENTS	III
FIGURES	IX
TABLES	XXVI
APPENDIX A: SOIL SAMPLING, INDICATOR AND CLASSIFICATION TEST PROCEDURES AND RESULTS	A/1
A.1 Introduction.	A/1
A.2 Soil sampling.	A/2
A.3 Preparation of soil samples for testing.	A/7
A.4 Indicator and classification test procedures.	A/11
A.4.1 Linear Shrinkage.	A/11
A.4.2 Liquid Limit.	A/13
A.4.3 Plastic Limit.	A/16
A.4.4 Plasticity Index.	A/18
A.4.5 Shrinkage Limit.	A/19
A.4.6 Particle size analysis.	A/23
A.4.7 Specific Gravity.	A/34
A.4.8 pH value of soil suspension.	A/37
A.5 Compaction tests.	A/39
A.6 References for Appendix A.	A/43
A.7 Test results.	A/45
A.7.1 Consistency Limits (Part 1): Liquid Limit; Linear Shrinkage; Plastic Limit; and Plasticity Index.	A/45
A.7.2 Consistency Limits (Part 2): Shrinkage Limit.	A/61
A.7.3 Particle Size Distribution.	A/95
A.7.4 Specific Gravity.	A/103
A.7.5 pH measurements.	A/104
A.7.6 Standard and Modified AASHTO compaction tests.	A/105
A.7.7 Test Data Sheets.	A/115

University of Cape T

APPENDIX B:
SCANNING ELECTRON MICROSCOPY AND X-RAY DIFFRACTION
- PREPARATION OF CLAY SAMPLES AND TEST DATA
B.1 Introduction. B/1
B.2 Clay separation of samples for Scanning Electron Microscopy and X-ray Diffraction. B/1
Initial preparation of samples for SEM & X-ray D. B/1
Clay separation of soil samples. B/2
Sediment laboratory procedure. B/2
B.3 Preparation of clay samples and SEM testing. B/5
Test procedure using the emissive mode. B/5
Final preparation and testing of samples at UCT. B/7
B.4 X-ray diffraction: Preparation and testing of samples. B/8
Preparation of clay samples for X-ray diffraction. B/8
X-ray diffraction test method. B/10
X-ray diffraction equipment. B/10
B.5 X-ray diffraction test traces. B/11
Traces (or plots) carried out for each soil type. B/11
X-ray diffraction data output. B/13
B.6 References for Appendix B. B/42

APPENDIX C:
FREE SHRINKAGE AND FREE SWELL
-TEST PROCEDURE AND RESULTS C/1
C.1 Introduction. C/1
C.2 Test Procedure. C/1
Preparation of test samples. C/1
- Remoulded test samples. C/1
- Compacted samples. C/2
- Undisturbed samples. C/2
Apparatus required. C/2
Procedure. C/3
Calculations and report. C/4
C.3 References for Appendix C. C/5
C.4 Test results. C/6
C.4.1 Natural Soils. C/6
C.4.2 Artificial Soils. C/50
C.4.3 Test Data Sheet. C/64

University of Cape T

APPENDIX D:
CONSOLIDOMETER AND TRIAXIAL
-TEST PROCEDURES AND RESULTS D/1

D.1 Consolidometer:
One-dimensional consolidation test procedure. D/1
Introduction. D/1
Apparatus required. D/1
Procedure. D/3
Calculations. D/6
Calibration test. D/8
Percentage of consolidation. D/9
D.2 Triaxial:
Isotropic consolidation test procedure. D/10
Introduction. D/10
Apparatus required. D/10
Getting organized. D/11
Operational procedure for setting up the de-airing system. D/12
Operational procedure (refer to Figure D.03). D/13
Calibration of equipment. D/13
Measurement of masses and dimensions, and positioning of the soil sample. D/13
Assembly of triaxial components - refer to Figure D.04. D/14
Testing. D/17
Test sheet and calculations. D/19
Calibration test. D/21
D.3 References for Appendix D. D/23
D.4 Test results. D/24
D.4.1 Natural Soils. D/24
D.4.2 Artificial Soils. D/34

University of Oulu

APPENDIX E:
CONSOLIDOMETER TESTS FOR EXPANSIVE AND COLLAPSING SOILS - TEST PROCEDURES AND RESULTS E/1
E.1 Introduction. E/1
E.2 Test procedure. E/1
Preparation of test samples. E/1
- Remoulded samples. E/1
- Compacted samples. E/2
- Undisturbed samples. E/2
Apparatus required. E/2
Procedure. E/2
Calculations and report. E/5
Calibration tests. E/7
E.3 References for Appendix E. E/11
E.4 Test results for natural soils.
(Remoulded and Undisturbed samples). E/12
E.4.1 Site 11 - Rosebank, Cape. E/12
E.4.2 Site 36 - Rondebosch, Cape. E/41
E.4.3 Site 30 - Hout Bay, Cape. E/60
E.4.4 Site A - Berea Road, Durban. E/72
E.4.5 Site 7 - Mowbray, Cape. E/83
E.4.6 Site B - Francois Road, Durban. E/93
E.4.7 Site C - Margaret Mayton Avenue, Durban. E/96
E.4.8 Site D - Rose Hill, Durban. E/99
E.4.9 Site 48 - Lady Grey District Farm Unity, Natal. E/102
E.5 Test results for artificial soils. E/105
E.5.1 Kaolin K.1 (13% clay size). E/105
E.5.2 Kaolin K.2 (20% clay size). E/108
E.5.3 Kaolin K.3 (8.5% clay size). E/111
E.5.4 Bentonite B.1 (3.5% clay size). E/114
E.5.5 Bentonite B.2 (7% clay size). E/118
E.5.6 Bentonite B.3 (11.5% clay size). E/122
E.5.7 Bentonite B.4 (15.5% clay size). E/125
E.5.8 Bentonite B.5 (35% clay size). E/129

University of Cape Town

APPENDIX F:
SWELL PRESSURE TESTS FOR EXPANSIVE SOILS
- TEST PROCEDURE AND RESULTS F/1
F.1 Introduction. F/1
F.2 Test procedure. F/1
Preparation of test samples. F/1
- Remoulded samples. F/1
- Compacted samples. F/1
- Undisturbed samples. F/2
Apparatus required. F/2
Procedure. F/2
Calculations and report. F/4
F.3 References for Appendix F. F/6
F.4 Test results for Natural Soil Types. F/7
F.4.1 Site 11 - Rosebank, Cape. F/7
F.4.2 Site 36 - Rondebosch, Cape. F/20
F.4.3 Site 30 - Hout Bay, Cape. F/30
F.4.4 Site A - Berea Road, Durban. F/36
F.4.5 Site 7 - Mowbray, Cape. F/38

APPENDIX G:
CONSOLIDOMETER TESTS WITH LATERAL PRESSURE MEASUREMENTS
- TEST PROCEDURES AND RESULTS G/1
G.1 Introduction. G/1
G.2 Test procedure. G/1
Preparation of test samples. G/1
- Remoulded samples. G/2
- Compacted samples. G/2
- Undisturbed samples. G/2
Apparatus required. G/2
G.2.1 The One-dimensional Consolidometer Test. G/4
Calibration of equipment. G/4
Calculations and report. G/7
Calibration tests. G/9
G.2.2 The One-dimensional Consolidation Test for Expansive and Collapsing Soils. G/11
Calibration of equipment. G/11
Calculations and report. G/14
Calibration test. G/15
G.2.3 The Swell Pressure Test for Expansive Soils. G/16
Calibration of equipment. G/16
Calculations and report. G/17
G.3 Measurement of Horizontal Strains, or Pressures. G/18
The stainless steel strain unit. G/18
The ring/meambrane unit. G/19
G.4 References for Appendix G. G/21
G.5 Test results for Natural Soil Types. G/22
G.5.1 Site 11 - Rosebank, Cape. G/22
G.5.2 Site 36 - Rondebosch, Cape. G/45
G.5.3 Site A - Berea Road, Durban. G/49
G.5.4 Site 7 - Mowbray, Cape. G/52
G.5.5 Site 48 - Lady Grey District Farm Unity, Natal. G/55

University of Cape T

APPENDIX H:
TRIAXIAL TESTS FOR EXPANSIVE AND COLLAPSING SOILS
- TEST PROCEDURES AND RESULTS H/1
H.1 Introduction. H/1
H.2 Test procedure. H/1
Preparation of test samples. H/1
- Compacted samples. H/1
- Undisturbed samples. H/1
Apparatus required. H/2
Procedure. H/2
Testing. H/3
Calculations and report. H/4
H.3 'KO' and stress/strain drained test. H/6
H.4 References for Appendix H. H/6
H.5 Test results for Natural Soil Types. H/7
H.5.1 Site 11 - Rosebank, Cape. H/7
H.5.2 Site A - Berea Road, Durban. H/11

APPENDIX I:
POSTGRADUATE COURSES COMPLETED AND
EXPERIMENTAL RESULTS USED FOR PUBLICATION I/1
I.1 Postgraduate courses completed. I/1
I.2 Experimental results used for publication. I/4

POSTCRIPT

The manuscript of this thesis was prepared in electronic form.
Text and graphics were processed and formatted using the following computer programs:

1. Microsoft Word (version 5.0) - word processing;
2. Microsoft Chart (ver. 3.0) - chart program;
3. Statgraphics (ver. 2.1) - statistical graphical system;
4. Perspective (ver. 1.2) - business & scientific graphics;
5. Pizazz Plus - screen capture and print facility;
6. Lotus 123 (ver. 2.01) - spreadsheet and graphics.

The operating system used was MS Dos 3.21.

The hardware consisted of the following: PC-XT IBM compatible, with 640 Kb Ram; Intel's 8088 processor, and 8087 numerical co-processor; 30 Mb hard disk.

University of Cape T

LIST OF FIGURES

CHAPTER ONE

Number Title

1.01: Aerial view of Cape Peninsula area.- includes location and soil samples obtained in field investigations.
1.02: The Derban area - includes the location of the Berea Red Sand formation.
1.03: Cross sections through the areas shown in Figure 1.02 - illustrates distrubution of the Red Sand.
1.04: Distribution of expansive clays and collapsing sands.
1.05: Plasticity chart - includes plotted values of Plasticity Index and Liquid Limit, for each site listed in Table 1.03.
1.06: Site 11, Rosebank - (i) Location, and (ii) Soil profile.
1.07: Site 36, Rondebosch - (i) Location, and (ii) Soil profile.
1.08: Site 30, Hout Bay - (i) Location, and (ii) Soil profile.
1.09: Site 7, Mowbray - (i) Location, and (ii) Soil profile.
1.10: Site 45, Bellville - (i) Location, and (ii) Soil profile.
1.11: Site 48, Lady Grey - (i) Location, and (ii) Soil profile.
1.12: Mowbray site - in situ test results for S.P.T.'s and Dutch Probes.
1.13: Plasticity characteristics of the soil types selected.

CHAPTER TWO

2.01: Particle size distribution - site 11, Rosebank.
2.02: Particle size distribution - site 36, Rondebosch.
2.03: Particle size distribution - site 30, Hout Bay.
2.04: Particle size distribution - site A, Berea Road (Durban).
2.05: Particle size distribution - site 7, Mowbray.
2.06: Particle size distribution - (i) site 45, Bellville, and (ii) site 48, Lady Grey.
2.07: Particle size distribution - (i) site B, Francois Road, (ii) site C, Margaret Mayton Avenue, and (iii) site D, Rose Hill (all sites in Durban).
2.08: Particle size distribution - Kaolin K.1 (13%), K.2 (20%), and K.3 (10%).
2.09: Particle size distribution - Bentonite B.1 (3.5%), B.2 (7%), B.3 (11.5%), B.4 (15.5%), and B.5 (35%).

University of Cape T

Number	Title
2.10:	Site 11, Rosebank - relationships of water ratio versus dry density, void ratio, porosity and degree of saturation.
2.11:	Site 36, Rondebosch - relationships of water ratio versus dry density, void ratio, porosity and degree of saturation.
2.12:	Site 30, Hout Bay - relationships of water ratio versus dry density, void ratio, porosity and degree of saturation.
2.13:	Site A, Berea Road - relationships of water ratio versus dry density, void ratio, porosity and degree of saturation.
2.14:	Site 7, Mowbray - relationships of water ratio versus dry density, void ratio, porosity and degree of saturation.
2.15:	Diagram illustrating details of a transmission electron optical system, light optical system, and Scanning Electron Microscope.
2.16:	Electron sensor - the detector system for the SEM.
2.17:	Major modes of imaging in the SEM.
2.18:	Structural arrangements of the SiO_4 tetrahehra units, as defined in Table 2.10 - (i) nesosilicates, (ii) sorosilicates, (iii) cyclosilicates, (iv) inosilicates, (v) phyllosilicates, and (vi) tectosilicates.
2.19:	Distribution of Soil Groups over Africa, Europe, South America, and parts of the other continents.
2.20:	The structure of ordinary ice.
2.21:	Adsorbed water density on Na-montmorillonite.
2.22:	Dielectric dispersion of adsorbed water as a function of water content.
2.23:	Nuclear magnetic resonance line width with water adsorbed on clay (after Pickett and Lemcoe).
2.24:	Spontaneous freezing temperature as a function of capillary diameter (from Hosler and Hosler).
2.25:	Change in strength of sand-clay mixtures with time and water content for different clays.
2.26:	Variation of lateral dimension of an unconstrained tetrahedral sheet as a function of Si, Al.
2.27:	Distorted oxygen network - (i) in trioctahedral xanthophyllite, and (ii) at the octahedral-tetrahedral junction in dioctahedral margarite (also included in Table 2.14).
2.28:	Montmorillonite structure - (1) oxygen, (2) hydroxyl, (3) aluminium, (4) magnesium, (5) sorbed cation, (6) silicon, (7) water molecule, (8) hydroxyl bond, (9) hydrogen bond, and (10) electrovalent bond.

University of Cape Town

Number Title

2.29: The relation between free swelling and b-dimension for Na-montmorillonites.
2.30: Relation between b-dimension and water content for six Na-saturated dioctahedral montmorillonites - reproducibility of b-dimension = ± 0.001 Å at low water content, ± 0.003 at high water content.
2.31: Relation between c-axis spacing and water content for Na-montmorillonite.
2.32: (a) Diagram of the arrangement of water molecules (open circles) in ice; (b) Ditrigonal symmetry of the surface of a dry montmorillonite; and (c) Regular hexagonal symmetry of the surface of idealized montmorillonite.
2.33: The relation between dF, the change in free energy, and n, the number of grams of water transferred from pure bulk water to 1g of air-dried Na- montmorillonite (from Ravina and Low).
2.34: The electromagnetic spectrum.
2.35: (A) Scattering of X-rays by a row of equally spaced, identical atoms; (B) Conditions for X-ray diffraction from a row of atoms.
2.36: (A) Diffraction cones from row of atoms; (B) Diffraction cones from three noncoplanar rows of scattering atoms, intersecting in a common line.
2.37: Reflection from a crystal structure.
2.38: Site 11, trace 1.A - 3^{o} 30^{o} 2θ Mg-saturated.
2.39: (i) Site 11, trace 1.B - 24^{o} $25\frac{1}{2}^{o}$ 2θ Mg-saturated ($\frac{1}{4}^{o}$ 2θ/min.); (ii) Site 11, trace 1.C - 3^{o} 13^{o} 2θ Mg-saturated, Ethylene glycolated (2^{o} 2θ/min.).
2.40: Site 11, trace 8.D - 3^{o} 30^{o} 2θ Mg-saturated (previously heated to 550°C for 1 hr, following which it was allowed to cool and then placed in a desiccator until testing).
2.41: (i) Site 11, trace 15.E - 3^{o} 30^{o} 2θ Mg-saturated, previously heated to 105°C overnight, allowed to cool and placed in a desiccator until testing; (ii) Site 11, trace 15.C - 3^{o} 13^{o} 2θ Mg-saturated, Ethylene glycolated.
2.42: Particle size grading envelope for all the natural soil types - sites 11, 36, 30, A, 7, 48, 45, B, C and D. (Comment: Dips in grading curves should not exist).
2.43: Particle size grading envelope for all artificial soil types - Kaolin K.1 (13%), K.2 (20%), and K.3 (10%), and Bentonite B.1 (3.5%), B.2 (7%), B.3 (11.5%), B.4 (15.5%), and B.5 (35%).
2.44: Adsorbed water density on Na-montmorillonite.
2.45: The relation between free swelling and b-dimension for Na-montmorillonites.

University of Cape Town

CHAPTER FOUR

Number Title

4.01a: Relationship between the void ratio (or total volume) and the water content - includes degrees of saturation.
4.01b: Relationship between void ratio and water content - includes drying/wetting and shrinkage limit.
4.01c: Relationship between void ratio and water content - includes the three types of expansion.
4.02: Void ratio versus water content plot - starting grid for the swelling paths.
4.03: Site 11, Rosebank [Remoulded, M1≥LL] - Free Shrinkage Paths.
4.04: Site 11, Rosebank [Remoulded, M1≥LL] - Free Swell Paths. (After shrinking to points on Figure 4.03).
4.05: Site 11, Rosebank [Remoulded, M1<LL] - Free Shrinkage Paths.
4.06: Site 11, Rosebank [Remoulded, M1<LL] - Free Swell Paths. (After shrinking to points on Figure 4.05).
4.07: Site 11, Rosebank [Remoulded, M2] - Free Shrinkage Paths.
4.08: Site 11, Rosebank [Remoulded, M2] - Free Swell Paths. (After shrinking to points on Figure 4.07).
4.09: Site 11, Rosebank [Compacted] - Free Shrinkage Paths.
4.10: Site 11, Rosebank [Compacted] - Free Swell Paths. (After shrinking to points on Figure 4.09).
4.11: Site 11, Rosebank [Undisturbed] - Free Shrinkage Paths.
4.12: Site 11, Rosebank [Undisturbed] - Free Swell Paths. (After shrinking to points on Figure 4.11).
4.13: Site 36, Rondebosch [Remoulded] - Free Shrinkage Paths.
4.14: Site 36, Rondebosch [Remoulded] - Free Swell Paths. (After shrinking to points on Figure 4.13).
4.15: Site 36, Rondebosch [Compacted] - Free Shrinkage Paths.
4.16: Site 36, Rondebosch [Compacted] - Free Swell Paths. (After shrinking to points on Figure 4.15).
4.17: Site 36, Rondebosch [Undisturbed] - Free Shrinkage Paths.
4.18: Site 36, Rondebosch [Undisturbed] - Free Swell Paths. (After shrinking to points on Figure 4.17).
4.19: Site 30, Hout Bay [Remoulded] - Free Shrinkage Paths.
4.20: Site 30, Hout Bay [Remoulded] - Free Swell Paths. (After shrinking to points on Figure 4.19).
4.21: Site 30, Hout Bay [Undisturbed] - Free Shrinkage Paths.

University of Cape Town

Number	Title
4.22:	Site 30, Hout Bay [Undisturbed] - Free Swell Paths. (After shrinking to points on Figure 4.21).
4.23:	Site A, Berea Road (Durban) [Remoulded] - Free Shrinkage Paths.
4.24:	Site A, Berea Road (Durban) [Remoulded] - Free Swell Paths. (After shrinking to points on Figure 4.23).
4.25:	Site A, Berea Road (Durban) [Compacted] - Free Shrinkage Paths.
4.26:	Site A, Berea Road (Durban) [Compacted] - Free Swell Paths. (After shrinking to points on Figure 4.25).
4.27:	Site A, Berea Road (Durban) [Undisturbed] - Free Shrinkage Paths.
4.28:	Site A, Berea Road (Durban) [undisturbed] - Free Swell Paths. (Starts from points on Figure 4.27).
4.29:	Site 7, Mowbray [Remoulded] - Free Shrinkage Paths.
4.30:	Site 7, Mowbray [Remoulded] - Free Swell Paths. (After shrinking to points on Figure 4.29).
4.31:	Site 7, Mowbray [Compacted and Undisturbed] - Free Shrinkage Paths. (After shrinking to points on Figure 4.31).
4.32:	Site 7, Mowbray [Compacted and Undisturbed] - Free Swell Paths. (After shrinking to points on Figure 4.31).
4.33:	Site B, Francois Road (Durban) [Remoulded - Free Shrinkage Paths.
4.34:	Site B, Francois Road (Durban) [Remoulded] - Free Swell Paths. (After shrinking to points on Figure 4.33).
4.35:	Site C, Margaret Mayton Avenue (Durban) [Remoulded] - Free Shrinkage Paths.
4.36:	Site C, Margaret Mayton Avenue (Durban) [Remoulded] - Free Swell Paths. (After shrinking to points on Figure 4.35).
4.37:	Site D, Rose Hill (Durban) [Remoulded] - Free Shrinkage Paths.
4.38:	Site D, Rose Hill (Durban) [Remoulded] - Free Swell Paths. (After shrinking to points on Figure 4.37).
4.39:	Kaolin K.1 (13%) - Free Shrinkage Paths.
4.40:	Kaolin K.1 (13%) - Free Swell Paths. (After shrinking to points on Figure 4.39).
4.41:	Kaolin K.2 (20%) - Free Shrinkage Paths.
4.42:	Kaolin K.2 (20%) - Free Swell Paths. (After shrinking to points on Figure 4.41).
4.43:	Kaolin K.3 (8.5%) - Free Shrinkage Paths.
4.44:	Kaolin K.3 (8.5%) - Free Swell Paths. (After shrinking to points on Figure 4.43).

University of Cape Town

Number	Title
4.45:	Bentonite B.1 (3.5%) - Free Shrinkage Paths.
4.46:	Bentonite B.1 (3.5%) - Free Swell Paths. (After shrinking to points on Figure 4.45).
4.47:	Bentonite B.2 (7%) - Free Shrinkage Paths.
4.48:	Bentonite B.2 (7%) - Free Swell Paths. (After shrinking to points on Figure 4.47).
4.49:	Bentonite B.3 (11.5%) - Free Shrinkage Paths.
4.50:	Bentonite B.3 (11.5%) - Free Swell Paths. (After shrinking to points on Figure 4.49).
4.51:	Bentonite B.4 (15.5%) - Free Shrinkage Paths.
4.52:	Bentonite B.4 (15.5%) - Free Swell Paths. (After shrinking to points on Figure 4.51).
4.53:	Bentonite B.5 (35%) - Free Shrinkage Paths.
4.54:	Bentonite B.5 (35%) - Free Swell Paths. (After shrinking to points on Figure 4.53).
4.55:	Site 11, Rosebank [Remoulded and Compacted Samples] - Initial Void Ratio 'e_i' versus final Water Ratio 'wr_f' (Free Expansion Limit).
4.56:	Site 11, Rosebank [Remoulded and Compacted Samples] - Initial Water Ratio 'wr_i' versus final Water Ratio 'wr_f' (Free Expansion Limit).
4.57:	Site 36, Rondebosch [Remoulded and Compacted Samples] - Initial Void Ratio 'e_i' versus final Water Ratio 'wr_f' (Free Expansion Limit).
4.58:	Site 36, Rondebosch [Remoulded and Compacted Samples] - Initial Water Ratio 'wr_i' versus final Water Ratio 'wr_f' (Free Expansion Limit).
4.59:	Site 30, Hout Bay [Remoulded Samples] - Initial Void Ratio 'e_i' versus final Water Ratio 'wr_f' (Free Expansion Limit).
4.60:	Site 30, Hout Bay [Remoulded Samples] - Initial Water Ratio 'wr_i' versus final Water Ratio 'wr_f' (Free Expansion Limit).
4.61:	Site A, Berea Road [Remoulded and Compacted Samples] - Initial Void Ratio 'e_i' versus final Water Ratio 'wr_f' (Free Expansion Limit).
4.62:	Site A, Berea Road [Remoulded and Compacted Samples] - Initial Water Ratio 'wr_i' versus final Water Ratio 'wr_f' (Free Expansion Limit).
4.63:	Site 7, Mowbray [Remoulded and Compacted Samples] - Initial Void Ratio 'e_i' versus final Water Ratio 'wr_f' (Free Expansion Limit).
4.64:	Site 7, Mowbray [Remoulded and Compacted Samples] - Initial Water Ratio 'wr_i' versus final Water Ratio 'wr_f' (Free Expansion Limit).
4.65:	Kaolin K.1 (13% clay size) - Initial Void Ratio 'e_i' versus final Water Ratio 'wr_f' (Free Expansion Limit).

Number	Title
4.66:	Kaolin K.1 (13% clay size) - Initial Water Ratio 'wr_i' versus final Water Ratio 'wr_f' (Free Expansion Limit).
4.67:	Kaolin K.2 (20% clay size) - Initial Void Ratio 'e_i' versus final Water Ratio 'wr_f' (Free Expansion Limit).
4.68:	Kaolin K.2 (20% clay size) - Initial Water Ratio 'wr_i' versus final Water Ratio 'wr_f' (Free Expansion Limit).
4.69:	Kaolin K.3 (10% clay size) - Initial Void Ratio 'e_i' versus final Water Ratio 'wr_f' (Free Expansion Limit).
4.70:	Kaolin K.3 (10% clay size) - Initial Water Ratio 'wr_i' versus final Water Ratio 'wr_f' (Free Expansion Limit).
4.71:	Bentonite B.1 (3.5% clay size) - Initial Void Ratio 'e_i' versus final Water Ratio 'wr_f' (Free Expansion Limit).
4.72:	Bentonite B.1 (3.5% clay size) - Initial Water Ratio 'wr_i' versus final Water Ratio 'wr_f' (Free Expansion Limit).
4.73:	Bentonite B.2 (7% clay size) - Initial Void Ratio 'e_i' versus final Water Ratio 'wr_f' (Free Expansion Limit).
4.74:	Bentonite B.2 (7% clay size) - Initial Water Ratio 'wr_i' versus final Water Ratio 'wr_f' (Free Expansion Limit).
4.75:	Bentonite B.3 (11.5% clay size) - Initial Void Ratio 'e_i' versus final Water Ratio 'wr_f' (Free Expansion Limit).
4.76:	Bentonite B.3 (11.5% clay size) - Initial Water Ratio 'wr_i' versus final Water Ratio 'wr_f' (Free Expansion Limit).
4.77:	Bentonite B.4 (15.5% clay size) - Initial Void Ratio 'e_i' versus final Water Ratio 'wr_f' (Free Expansion Limit).
4.78:	Bentonite B.4 (15.5% clay size) - Initial Water Ratio 'wr_i' versus final Water Ratio 'wr_f' (Free Expansion Limit).
4.79:	Bentonite B.5 (35% clay size) - Initial Void Ratio 'e_i' versus final Water Ratio 'wr_f' (Free Expansion Limit).
4.80:	Bentonite B.5 (35% clay size) - Initial Water Ratio 'wr_i' versus final Water Ratio 'wr_f' (Free Expansion Limit).
4.81:	Site 11, Rosebank [Remoulded and Compacted samples] - Plots of Void Ratio 'e' versus Water Ratio 'wr' for the Free Swell Paths over the full range of Degree of Saturation 'Sr'.

University of Cape Town

Number Title

4.82: Site 36, Rondebosch [Remoulded and Compacted samples] - Plots of Void Ratio 'e' versus Water Ratio 'wr' for the Free Swell Paths over the full range of Degree of Saturation 'Sr'.
4.83: Site 30, Hout Bay [Remoulded samples] - Plots of Void Ratio 'e' versus Water Ratio 'wr' for the Free Swell Paths over the full range of Degree of Saturation 'Sr'.
4.84: Site A, Berea Road [Remoulded and Compacted samples] - Plots of Void Ratio 'e' versus Water Ratio 'wr' for the Free Swell Paths over the full range of Degree of Saturation 'Sr'.
4.85: Site 7, Mowbray [Remoulded and Compacted samples] - Plots of Void Ratio 'e' versus Water Ratio 'wr' for the Free Swell Paths over the full range of Degree of Saturation 'Sr'.
4.86: Site 'B' Francois Road [Remoulded samples] - Plots of Void Ratio 'e' versus Water Ratio 'wr' for the Free Swell Paths over the full range of Degree of Saturation 'Sr'.
4.87: Site 'C', Margaret Mayton Avenue [Remoulded sample] - Plots of Void Ratio 'e' versus Water Ratio 'wr' for the Free Swell Paths over the full range of Degree of Saturation 'Sr'.
4.88: Site 'D' Rose Hill [Remoulded sample] - Plots of Void Ratio 'e' versus Water Ratio 'wr' for the Free Swell Paths over the full range of Degree of Saturation 'Sr'.
4.89: Kaolin K1 (13% clay size) - Plots of Void Ratio 'e' versus Water Ratio 'wr' for the Free Swell Paths over the full range of Degree of Saturation 'Sr'.
4.89: Kaolin K1 (13% clay size) - Plots of Void Ratio 'e' versus Water Ratio 'wr' for the Free Swell Paths over the full range of Degree of Saturation 'Sr'.
4.90: Kaolin K2 (20% clay size) - Plots of Void Ratio 'e' versus Water Ratio 'wr' for the Free Swell Paths over the full range of Degree of Saturation 'Sr'.
4.91: Kaolin K3 (10% clay size) - Plots of Void Ratio 'e' versus Water Ratio 'wr' for the Free Swell Paths over the full range of Degree of Saturation 'Sr'.
4.92: Bentonite B1 (3.5% clay size) - Plots of Void Ratio 'e' versus Water Ratio 'wr' for the Free Swell Paths over the full range of Degree of Saturation 'Sr'.
4.93: Bentonite B2 (7% clay size) - Plots of Void Ratio 'e' versus Water Ratio 'wr' for the Free Swell Paths over the full range of Degree of Saturation 'Sr'.
4.94: Bentonite B3 (11.5% clay size) - Plots of Void Ratio 'e' versus Water Ratio 'wr' for the Free Swell Paths over the full range of Degree of Saturation 'Sr'.

University of Cape Town

Number Title

4.95: Bentonite B4 (15.5% clay size) - Plots of Void Ratio 'e' versus Water Ratio 'wr' for the Free Swell Paths over the full range of Degree of Saturation 'Sr'.
4.96: Bentonite B5 (35% clay size) - Plots of Void Ratio 'e' versus Water Ratio 'wr' for the Free Swell Paths over the full range of Degree of Saturation 'Sr'.

CHAPTER FIVE

5.01: Relationship between the void ratio and the logarithm of the effective pressure (or stress).
5.02: Relationship between the void ratio and the water ratio (or water content). Based on Rosebank S.11. Pressure Values on the left of the line are 'average' pressures for one-dimensional consolidation, computed by assuming that the average pressure is equal to half the vertical applied pressure.
5.03: Site 11, Rosebank [Remoulded] - (Top) One-dimensional consolidation, results from two different samples and (Bottom) Isotropic consolidation in triaxial.
5.04: Site 36, Rondebosch [Remoulded] - (Top) One-dimensional consolidation, and (Bottom) Isotropic consolidation.
5.05: Site 30, Hout Bay [Remoulded] - (Top) One-dimensional consolidation, and (Bottom) Isotropic consolidation.
5.06: Site A, Berea Road (Durban) [Remoulded] - (Top) One-dimensional consolidation, and (Bottom) Isotropic consolidation.
5.07: Site 7, Mowbray [Remoulded] - (Top) One-dimensional consolidation, and (Bottom) Isotropic consolidation.
5.08: Site 45, Bellville [Remoulded] - One-dimensional consolidation.
5.09: Site B, Francois Road (Durban) [Remoulded] - One-dimensional consolidation.
5.10: Site C, Margaret Mayton Avenue (Durban) [Remoulded] - One-dimensional consolidation.
5.11: Site D, Rose Hill (Durban) [Remoulded] - One-dimensional consolidation.
5.12: Site 11, Rosebank [Undisturbed] - (Top) One-dimensional consolidation, and (Bottom) Isotropic consolidation.
5.13: Site 36, Rondebosch [Undisturbed] - One- dimensional consolidation.

University of the Witwatersrand

Number	Title
5.14:	Site 30, Hout Bay [Undisturbed] - One- dimensional consolidation.
5.15:	Kaolin K.1 (13% clay size) - One-dimensional consolidation.
5.16:	Kaolin K.2 (20% clay size) - (Top) One-dimensional consolidation; and (Bottom) Isotropic consolidation.
5.17:	Kaolin K.3 (8.5% clay size) - (Top) One-dimensional consolidation, and (Bottom) Isotropic consolidation.
5.18:	Bentonite B.1 (3.5% clay size) - One-dimensional consolidation.
5.19:	Bentonite B.2 (7% clay size) - (Top) One-dimensional consolidation; and (Bottom) Isotropic consolidation.
5.20:	Bentonite B.3 (11.5% clay size) - One-dimensional consolidation.
5.21:	Bentonite B.4 (15.5% clay size) - (Top) (i) One-dimensional consolidation, and (Bottom) Isotropic consolidation.
5.22:	Bentonite B.5 (35% clay size) - (Top) One- dimensional consolidation, and (Bottom) Isotropic consolidation.
5.23:	Site 11, Rosebank [Remoulded] - Stress Scales. [From Figure 5.03]. Pressure values on the left of the line are 'average' pressures for one-dimensional consolidation computed by assuming that the average pressure is equal to half the vertical applied pressure.
5.24:	Site 36, Rondebosch [Remoulded] - Stress scales, [From Figure 5.04].
5.25:	Site 30, Hout Bay [Remoulded] - Stress scales. [From Figure 5.05].
5.26:	Site A, Berea Road (Durban) [Remoulded] - Stress scales. [From Figure 5.06].
5.27:	Site 7, Mowbray [Remoulded] - Stress scales. [From Figure 5.07].
5.28:	Site 45, Bellville [Remoulded] - Stress scales. [From Figure 5.08].
5.29:	Francois Road (Durban) [Remoulded] - Stress scales. [From Figure 5.09].
5.30:	Site C, Margaret Mayton Avenue (Durban) [Remoulded] - Stress scales. [From Figure 5.10].
5.31:	Site D, Rose Hill (Durban) [Remoulded] - Stress scales. [From Figure 5.11]. Pressure values on the left of the line are 'average' pressures for one-dimensional consolidation computed by assuming that the average pressure is equal to half the vertical applied pressure.

University of Cape Town

Number Title

5.32: Site 11, Rosebank [Undisturbed] - Stress Scales. [From Figure 5.12]. Pressure values on the left of the line are 'average' pressures for one-dimensional consolidation computed by assuming that the average pressure is equal to half the vertical applied pressure.
5.33: Site 36, Rondebosch [Undisturbed] - Stress scales. [From Figure 5.13].
5.34: Site 30, Hout Bay [Undisturbed] - Stress scales. [From Figure 5.14].
5.35: Kaolin K.1 (13% clay size) - Stress scales. [From Figure 5.15]. Pressure values on the left of the line are 'average' pressures for one-dimensional consolidation computed by assuming that the average pressure is equal to half the vertical applied pressure.
5.36: Kaolin K.2 (20% clay size) - Stress scales. [From Figure 5.16].
5.37: Kaolin K.3 (8.5% clay size) - Stress scales. [From Figure 5.17].
5.38: Bentonite B.1 (3.5% clay size) - Stress scales. [From Figure 5.18].
5.39: Bentonite B.2 (7% clay size) - Stress scales. [From Figure 5.19].
5.40: Bentonite B.3 (11.5% clay size) - Stress scales. [From Figure 5.20].
5.41: Bentonite B.4 (15.5% clay size) - Stress scales. [From Figure 5.21].
5.42: Bentonite B.5 (35% clay size) - Stress scales. [From Figure 5.22].

CHAPTER SIX

6.01: Site 11, Rosebank -Relationship between the void ratio `e' and the water ratio `Ω', or `wr', for the full test path.
6.02: Relationship between the void ratio `e' and the effective vertical pressure (or stress) `peV', for the full test path.
6.03: Site 11, Rosebank - [1 Kpa during wetting] Relationship between the void ratio `e' and the water ratio `wr'. Read in conjunction with Figure 6.04.
6.04: Site 11, Rosebank - [1 Kpa during wetting] Relationship between the void ratio `e' and the effective vertical pressure (or stress) `peV'.

University of Cape Town

Number Title

6.05: Site 11, Rosebank - [settles overnight under 50 Kpa and carries this load during wetting] Relationship between the void ratio `e' and the water ratio `wr'. Read in conjunction with Figure 6.06.
6.06: Site 11, Rosebank - [50 Kpa during wetting] Relationship between the void ratio `e' and the effective vertical pressure (or stress) `peV'.
6.07: Site 11, Rosebank - [100 Kpa during wetting] Relationship between the void ratio `e' and the water ratio `wr'.
6.08: Site 11, Rosebank - [100 Kpa during wetting] Relationship between the void ratio `e' and the effective vertical pressure (or stress) `peV'.
6.09: Site 11, Rosebank - [400 Kpa during wetting] Relationship between the void ratio `e' and the water ratio `wr'.
6.10: Site 11, Rosebank - [400 Kpa during wetting] Relationship between the void ratio `e' and the effective vertical pressure (or stress) `peV'.
6.11: Site 11, Rosebank [Compacted] - [100 Kpa during wetting] Relationship between the void ratio `e' and the water ratio `wr'.
6.12: Site 11, Rosebank - [100 Kpa during wetting] Relationship between the void ratio `e' and the effective vertical pressure (or stress) `peV'.
6.13: Site 11, Rosebank [Undisturbed] - [100 Kpa during wetting] Relationship between the void ratio `e' and the water ratio `wr'.
6.14: Site 11, Rosebank [Undisturbed] - [100 Kpa during wetting] Relationship between the void ratio `e' and the effective vertical pressure (or stress) `peV'.
6.15: Site 36, Rondebosch - [1 Kpa during wetting] Relationship between the void ratio `e' and the water ratio `wr'. Read in conjunction with Figure 6.16.
6.16: Site 36, Rondebosch - [1 Kpa during wetting] Relationship between the void ratio `e' and the effective vertical pressure (or stress) `peV'.
6.17: Site 36, Rondebosch - [50 Kpa during wetting] Relationship between the void ratio `e' and the water ratio `wr'.
6.18: Site 36, Rondebosch - [50 Kpa during wetting] Relationship between the void ratio `e' and the effective vertical pressure (or stress) `peV'.
6.19: Site 36, Rondebosch - [100 Kpa during wetting] Relationship between the void ratio `e' and the water ratio `wr'.
6.20: Site 36, Rondebosch - [100 Kpa during wetting] Relationship between the void ratio `e' and the effective vertical pressure (or stress) `peV'.

University of Cape Town

Number Title

6.21: Site 36, Rondebosch - [400 Kpa during wetting] Relationship between the void ratio `e' and the water ratio `wr'.
6.22: Site 36, Rondebosch - [400 Kpa during wetting] Relationship between the void ratio `e' and the effective vertical pressure (or stress) `peV'.
6.23: Site 36, Rondebosch [Compacted] - [100 Kpa during wetting] Relationship between the void ratio `e' and the water ratio `wr'.
6.24: Site 36, Rondebosch [Compacted] - [100 Kpa during wetting] Relationship between the void ratio `e' and the effective vertical pressure (or stress) `peV'.
6.25: Site 36, Rondebosch [Undisturbed] - [100 Kpa during wetting] Relationship between the void ratio `e' and the water ratio `wr'.
6.26: Site 36, Rondebosch [Undisturbed] - [100 Kpa during wetting] Relationship between the void ratio `e' and the effective vertical pressure (or stress) `peV'.
6.27: Site 30, Hout Bay - [1 Kpa during wetting] Relationship between the void ratio `e' and the water ratio `wr'. Read in conjunction with Figure 6.28.
6.28: Site 30, Hout Bay - [1 Kpa during wetting] Relationship between the void ratio `e' and the effective vertical pressure (or stress) `peV'.
6.29: Site 30, Hout Bay - [50 Kpa during wetting] Relationship between the void ratio `e' and the water ratio `wr'.
6.30: Site 30, Hout Bay - [50 Kpa during wetting] Relationship between the void ratio `e' and the effective vertical pressure (or stress) `peV'.
6.31: Site 30, Hout Bay - [100 Kpa during wetting] Relationship between the void ratio `e' and the water ratio `wr'.
6.32: Site 30, Hout Bay - [100 Kpa during wetting] Relationship between the void ratio `e' and the effective vertical pressure (or stress) `peV'.
6.33: Site 30, Hout Bay [Undisturbed] - [100 Kpa during wetting] Relationship between the void ratio `e' and the water ratio `wr'.
6.34: Site 30, Hout Bay [Undisturbed] - [100 Kpa during wetting] Relationship between the void ratio `e' and the effective vertical pressure (or stress) `peV'.
6.35: Site A, Berea Road (Durban) - [100 Kpa during wetting] Relationship between the void ratio `e' and the water ratio `wr'. Read in conjunction with Figure 6.36.
6.36: Site A, Berea Road (Durban) - [100 Kpa during wetting] Relationship between the void ratio `e' and the effective vertical pressure (or stress) `peV'.

University of Cape Town

Number Title

6.37: Site A, Berea Road (Durban) [Compacted] - [100 Kpa during wetting] Relationship between the void ratio `e' and the water ratio `wr'.
6.38: Site A, Berea Road (Durban) [Compacted] - [100 Kpa during wetting] Relationship between the void ratio `e' and the effective vertical pressure (or stress) `peV'.
6.39: Site A, Berea Road (Durban) [Undisturbed Air dried] - [100 Kpa during wetting] Relationship between the void ratio `e' and the water ratio `wr'.
6.40: Site A, Berea Road (Durban) [Undisturbed Air dried] - [100 Kpa during wetting] Relationship between the void ratio `e' and the effective vertical pressure (or stress) `peV'.
6.41: Site 7, Mowbray - [100 Kpa during wetting] Relationship between the void ratio `e' and the water ratio `wr'. Read in conjunction with Figure 6.42.
6.42: Site 7, Mowbray - [100 Kpa during wetting] Relationship between the void ratio `e' and the effective vertical pressure (or stress) `peV'.
6.43: Site 7, Mowbray [Compacted] - [100 Kpa during wetting] Relationship between the void ratio `e' and the water ratio `wr'.
6.44: Site 7, Mowbray [Compacted] - [100 Kpa during wetting] Relationship between the void ratio `e' and the effective vertical pressure (or stress) `peV'.
6.45: Site 7 Mowbray [Undisturbed] - [100 Kpa during wetting] Relationship between the void ratio `e' and the water ratio `wr'.
6.46: Site 7, Mowbray [Undisturbed] - [100 Kpa during wetting] Relationship between the void ratio `e' and the effective vertical pressure (or stress) `peV'.
6.47: Site B, Francois Road (Durban) - [100 Kpa during wetting] Relationship between the void ratio `e' and the water ratio `wr'. Read in conjunction with Figure 6.48.
6.48: Site B, Francois Road (Durban) - [100 Kpa during wetting] Relationship between the void ratio `e' and the effective vertical pressure (or stress) `peV'.
6.49: Site C, Margaret Mayton Avenue (Durban) - [100 Kpa during wetting] Relationship between the void ratio `e' and the water ratio `wr'.
6.50: Site C, Margaret Mayton Avenue (Durban) - [100 Kpa during wetting] Relationship between the void ratio `e' and the effective vertical pressure (or stress) `peV'.
6.51: Site D, Rose Hill (Durban) - [100 Kpa during wetting] Relationship between the void ratio `e' and the water ratio `wr'.

University of Cape Town

Number Title

6.52: Site D, Rose Hill (Durban) - [100 Kpa during wetting] Relationship between the void ratio `e' and the effective vertical pressure (or stress) `peV'.
6.53: Site 48, Lady Grey (Natal) - [100 Kpa during wetting] Relationship between the void ratio `e' and the water ratio `wr'. Test by Ballantyne.
6.54: Site 48, Lady Grey (Natal) - [100 Kpa during wetting] Relationship between the void ratio `e' and the effective vertical pressure (or stress) `peV'. Test by Ballantyne.
6.55: Kaolin K.1 (13% clay size) - [100 Kpa during wetting] Relationship between the void ratio `e' and the water ratio `wr'. Read in conjunction with Figure 6.56.
6.56: Kaolin K.1 (13% clay size) - [100 Kpa during wetting] Relationship between the void ratio `e' and the effective vertical pressure (or stress) `peV'.
6.57: Kaolin K.2 (20% clay size) - [100 Kpa during wetting] Relationship between the void ratio `e' and the water ratio `wr'.
6.58: Kaolin K.2 (20% clay size) - [100 Kpa during wetting] Relationship between the void ratio `e' and the effective vertical pressure (or stress) `peV'.
6.59: Kaolin K.3 (8.5% clay size) - [100 Kpa during wetting] Relationship between the void ratio `e' and the water ratio `wr'.
6.60: Kaolin K.3 (8.5% clay size) - [100 Kpa during wetting] Relationship between the void ratio `e' and the effective vertical pressure (or stress) `peV'.
6.61: Bentonite B.1 (3.5% clay size) - [100 Kpa during wetting] Relationship between the void ratio `e' and the water ratio `wr'. Read in conjunction with Figure 6.62.
6.62: Bentonite B.1 (3.5% clay size) - [100 Kpa during wetting] Relationship between the void ratio `e' and the effective vertical pressure (or stress) `peV'.
6.63: Bentonite B.2 (7% clay size) - [100 Kpa during wetting] Relationship between the void ratio `e' and the water ratio `wr'.
6.64: Bentonite B.2 (7% clay size) - [100 Kpa during wetting] Relationship between the void ratio `e' and the effective vertical pressure (or stress) `peV'.
6.65: Bentonite B.3 (11.5% clay size) - [100 Kpa during wetting] Relationship between the void ratio `e' and the water ratio `wr'.
6.66: Bentonite B.3 (11.5% clay size) - [100 Kpa during wetting] Relationship between the void ratio `e' and the effective vertical pressure (or stress) `peV'.
6.67: Bentonite B.4 (15.5% clay size) - [100 Kpa during wetting] Relationship between the void ratio `e' and the water ratio `wr'.

University of Cape Town

Number Title

6.68: Bentonite B.4 (15.5% clay size) - [100 Kpa during wetting] Relationship between the void ratio `e' and the effective vertical pressure (or stress) `peV'.
6.69: Bentonite B.5 (35% clay size) - [100 Kpa during wetting] Relationship between the void ratio `e' and the water ratio `wr'.
6.70: Bentonite B.5 (35% clay size) - [100 Kpa during wetting] Relationship between the void ratio `e' and the effective vertical pressure (or stress) `peV'.
6.71: Site 11, Rosebank [Remoulded] - Void ratio `e' versus water ratio `wr'.
Volume change, due to wetting, shown while carrying 1 Kpa only. Scales are from other tests (Chapter 5).
6.72: Site 11, Rosebank [Remoulded] - Void ratio `e' versus water ratio `wr'.
Volume change, due to wetting, shown while carrying 50 Kpa only. Scales are from other tests (Chapter 5).
6.73: Site 11, Rosebank [Remoulded] - Void ratio `e' versus water ratio `wr'.
Volume change, due to wetting, shown while carrying 100 Kpa only. Scales are from other tests (Chapter 5).
6.74: Site 11, Rosebank [Remoulded] - Void ratio `e' versus water ratio `wr'.
Volume change, due to wetting, shown while carrying 400 Kpa only. Scales are from other tests (Chapter 5).
6.75: Site 11, Rosebank [Compacted] - Void ratio `e' versus water ratio `wr'.
Volume change, due to wetting, shown while carrying 100 Kpa only. Scales are from other tests (Chapter 5).
6.76: Site 11, Rosebank [Undisturbed] - Void ratio `e' versus water ratio `wr'.
Volume change, due to wetting, shown while carrying 1 Kpa only. Scales are from other tests (Chapter 5).
6.77: Site 36, Rondebosch [Remoulded] - Void ratio `e' versus water ratio `wr'.
Volume change, due to wetting, shown while carrying 1 Kpa; 50 Kpa; 100 Kpa; and, 400 Kpa. Scales are from other tests (Chapter 5).
6.78: Site 36, Rondebosch [Compacted and Undisturbed] - Void ratio `e' versus water ratio `wr'.
Volume change, due to wetting, shown while carrying 100 Kpa only. Scales are from other tests (Chapter 5).

University of Cape Town

Number Title

6.79: Site 30, Hout Bay [Remoulded] - Void ratio `e' versus water ratio `wr'.
Volume change, due to wetting, shown while carrying 1 Kpa, 50 Kpa, and 100 Kpa only. Scales are from other tests (Chapter 5).
6.80: Site 30, Hout Bay [Undisturbed] - Void ratio 'e' versus water ratio `wr'.
Volume change, due to wetting, shown while carrying 100 Kpa only. Scales are from other tests (Chapter 5).
6.81: Site A, Berea Road (Durban) [Remoulded] - Void ratio `e' versus water ratio `wr'.
Volume change, due to wetting, shown while carrying 100 Kpa only. Scales are from other tests (Chapter 5).
6.82: Site A, Berea Road (Durban) [Compacted and Undisturbed] - Void ratio `e' versus water ratio `wr'.
Volume change, due to wetting, shown while carrying 100 Kpa only. Scales are from other tests (Chapter 5).
6.83: Site 7, Mowbray [Remoulded] - Void ratio `e' versus water ratio `wr'.
Volume change, due to wetting, shown while carrying 100 Kpa only. Scales are from other tests (Chapter 5).
6.84: Site 7, Mowbray [Compacted and Undisturbed] - Void ratio `e' versus water ratio `wr'.
Volume change, due to wetting, shown while carrying 100 Kpa only. Scales are from other tests (Chapter 5).
6.85: Site B, Francois Road (Durban) [Remoulded] - Void ratio `e' versus water ratio `wr'.
Volume change, due to wetting, shown while carrying 100 Kpa only. Scales are from other tests (Chapter 5).
6.86: Site C, Margaret Mayton Avenue (Durban) -[Remoulded] Void ratio `e' versus water ratio `wr'.
Volume change, due to wetting, shown while carrying 100 Kpa only. Scales are from other tests (Chapter 5).
6.87: Site D, Rose Hill (Durban) [Remoulded] - Void ratio `e' versus water ratio `wr'.
Volume change, due to wetting, shown while carrying 100 Kpa only. Scales are from other tests (Chapter 5).
6.88: Kaolin K.1 (13% clay size) [Remoulded] - Void ratio `e' versus water ratio `wr'.
Volume change, due to wetting, shown while carrying 100 Kpa only. Scales are from other tests (Chapter 5).

University of Cape Town

Number Title

6.89: Kaolin K.2 (20% clay size) [Remoulded] - Void ratio `e' versus water ratio `wr'.
6.90: Kaolin K.3 (8.5% clay size) [Remoulded] - Void ratio `e' versus water ratio `wr'.
6.91: Bentonite B.1 (3.5% clay size) [Remoulded] - Void ratio `e' versus water ratio `wr'. Volume change, due to wetting, shown while carrying 100 Kpa only. Scales are from other tests (Chapter 5).
6.92: Bentonite B.2 (7% clay size) [Remoulded] - Void ratio `e' versus water ratio `wr'.
6.93: Bentonite B.3 (11.5% clay size) [Remoulded] - Kpa] Void ratio `e' versus water ratio `wr'.
6.94: Bentonite B.4 (15.5% clay size) [Remoulded] - Void ratio `e' versus water ratio `wr'.
6.95: Bentonite B.5 (35% clay size) [Remoulded] - Void ratio `e' versus water ratio `wr'.
6.96: Site 11, Rosebank [Remoulded, 1 Kpa] - Void ratio `e' vs effective vertical pressure `peV' vs water ratio `wr' for the full test path.
6.97: Site 11, Rosebank - [Remoulded, 50 Kpa] Void ratio `e' vs effective vertical pressure `peV' vs water ratio `wr'.
6.98: Site 11, Rosebank - [Remoulded, 100 Kpa] Void ratio `e' vs effective pressure `peV' vs water ratio `wr'.
6.99: Site 11, Rosebank [Remoulded, 400 Kpa] Void ratio `e' vs effective vertical pressure `peV' vs water ratio `wr'.
6.100: Site 11, Rosebank - [Compacted, 100 Kpa] Void ratio `e' vs effective vertical pressure `peV' vs water ratio `wr'.
6.101: Site 11, Rosebank - [Undisturbed, 100 Kpa] Void ratio `e' vs effective vertical pressure `peV' vs water ratio `wr'.
6.102: Site 36, Rondebosch - [Remoulded, 1 Kpa] Void ratio `e' vs effective vertical pressure `peV' vs water ratio `wr'.
6.103: Site 36, Rondebosch - [Remoulded, 50 Kpa] Void ratio `e' vs effective vertical pressure `peV' vs water ratio `wr'.
6.104: Site 36, Rondebosch - [Remoulded, 100 Kpa] Void ratio `e' vs effective vertical pressure `peV' vs water ratio `wr'.
6.105: Site 36, Rondebosch - [Remoulded, 400 Kpa] Void ratio `e' vs effective vertical pressure `peV' vs water ratio `wr'.
6.106: Site 36, Rondebosch - [Compacted, 100 Kpa] Void ratio `e' vs effective vertical pressure `peV' vs water ratio `wr'.

University of Cape Town

Number Title

6.107: Site 36, Rondebosch - [Undisturbed, 100 Kpa] Void ratio `e' vs effective vertical pressure `peV' vs water ratio `wr'.
6.108: Site 30, Hout Bay - [Remoulded, 1 Kpa] Void ratio `e' vs effective vertical pressure `peV' vs water ratio `wr'.
6.109: Site 30, Hout Bay - [Remoulded, 50 Kpa] Void ratio `e' vs effective vertical pressure `peV' vs water ratio `wr'.
6.110: Site 30, Hout Bay - [Remoulded, 100 Kpa] Void ratio `e' vs effective vertical pressure `peV' vs water ratio `wr'.
6.111: Site 30, Hout Bay - [Undisturbed, 100 Kpa] Void ratio `e' vs effective vertical pressure `peV' vs water ratio `wr'.
6.112: Site A, Berea Road (Durban) - [Remoulded, 100 Kpa] Void ratio `e' vs effective vertical pressure `peV' vs water ratio `wr'.
6.113: Site A, Berea Road (Durban) - [Compacted, 100 Kpa] Void ratio `e' vs effective vertical pressure `peV' vs water ratio `wr'.
6.114: Site A, Berea Road (Durban) - [Undisturbed, 100 Kpa] Void ratio `e' vs effective vertical pressure `peV' vs water ratio `wr'.
6.115: Site 7, Mowbray, - [Remoulded, 100 Kpa] Void ratio `e' vs effective vertical pressure `peV' vs water ratio `wr'.
6.116: Site 7, Mowbray - [Compacted, 100 Kpa] Void ratio `e' vs effective vertical pressure `peV' vs water ratio `wr'.
6.117: Site 7, Mowbray, - [Undisturbed, 100 Kpa] Void ratio `e' vs effective vertical pressure `peV' vs water ratio `wr'.
6.118: Site B, Francois Road (Durban) - [Remoulded, 100 Kpa] Void ratio `e' vs effective vertical pressure `peV' vs water ratio `wr'.
6.119: Site C, Margaret Mayton Avenue (Durban) - [Remoulded, 100 Kpa] Void ratio `e' vs effective vertical pressure `peV' vs water ratio `wr'.
6.120: Site D, Rose Hill (Durban) - [Remoulded, 100 Kpa] Void ratio `e' vs effective vertical pressure `peV' vs water ratio `wr'.
6.121: Site 48, Lady Grey (Natal) - [Undisturbed, 100 Kpa] Void ratio `e' vs effective vertical pressure `peV' vs water ratio `wr'.
6.122: Kaolin K.1 (13% clay size) - [100 Kpa] Void ratio `e' vs effective vertical pressure `peV' vs water ratio `wr'.
6.123: Kaolin K.2 (20% clay size) - [100 Kpa] Void ratio `e' vs effective vertical pressure `peV' vs water ratio `wr'.

University of Cape Town

Number Title

6.124: Kaolin K.3 (8.5% clay size) - [100 Kpa] Void ratio `e' vs effective vertical presure `peV' vs water ratio `wr'.
6.125: Bentonite B.1 (3.5% clay size) - [100 Kpa] Void ratio `e' vs effective vertical pressure `peV' vs water ratio `wr'.
6.126: Bentonite B.2 (7% clay size) - [100 Kpa] Void ratio `e' vs effective vertical pressure `peV' vs water ratio `wr'.
6.127: Bentonite B.3 (11.5% clay size) - [100 Kpa] Void ratio `e' vs effective vertical pressure `peV' vs water ratio `wr'.
6.128: Bentonite B.4 (15.5% clay size) - [100 Kpa] Void ratio `e' vs effective vertical pressure `peV' vs water ratio `wr'.
6.129: Bentonite B.5 (35% clay size) - [100 Kpa] Void ratio `e' vs effective vertical pressure `peV' vs water ratio `wr'.
6.130: Site 11, Rosebank [Remoulded 0.8 - 1 Kpa] - Relationship between Water Content 'w_i', before wetting and Percentage Volume Change, after wetting.
6.131: Site 11, Rosebank [Remoulded 49.0 - 54.6 Kpa] - Relationship between Water Content 'w_i', before wetting and Percentage Volume Change, after wetting.
6.132: Site 11, Rosebank [Remoulded 98.1 - 109.9 Kpa] - Relationship between Water Content 'w_i', before wetting and Percentage Volume Change, after wetting.
6.133: Site 11, Rosebank [Remoulded 392.3 - 433.7 Kpa] - Relationship between Water Content 'w_i', before wetting and Percentage Volume Change, after wetting.
6.134: Site 11, Rosebank [Compacted 107.3 - 108.4 Kpa] - Relationship between Water Content 'w_i', before wetting and Percentage Volume Change, after wetting.
6.135: Site 11, Rosebank [Undisturbed 98.1 - 107.3 Kpa] - Relationship between Water Content 'w_i', before wetting and Percentage Volume Change, after wetting.
6.136: Site 36, Rondebosch [Remoulded 0.8 - 430.3 Kpa] - Relationship between Water Content 'w_i', before wetting and Percentage Volume Change, after wetting.
6.137: Site 36, Rondebosch [Compacted 107.5 Kpa and undisturbed 98.1 Kpa] - Relationship between Water Content 'w_i', before wetting and Percentage Volume Change, after wetting.
6.138: Site 30, Hout Bay [Remoulded 1.0 - 107.3 Kpa] - Relationship between Water Content 'w_i', before wetting and Percentage Volume Change, after wetting.
6.139: Site 30, Hout Bay [Undisturbed, 107.6 Kpa] - Relationship between Water Content 'w_i', before wetting and Percentage Volume Change, after wetting.

University of Cape Town

Number Title

6.140: Site A, Berea Road [Remoulded 98.1 - 107.3 Kpa] - Relationship between Water Content 'w_i', before wetting and Percentage Volume Change, after wetting.
6.141: Site A, Berea Road [Compacted 107.3 Kpa and undisturbed 98.1 Kpa] - Relationship between Water Content 'w_i', before wetting and Percentage Volume Change, after wetting.
6.142: Site 7, Mowbray [Remoulded 98.1 - 107.3 Kpa] - Relationship between Water Content 'w_i', before wetting and Percentage Volume Change, after wetting.
6.143: Site 7, Mowbray [Compacted 107.3 Kpa, and undisturbed 107.3 Kpa] - Relationship between Water Content 'w_i', before wetting and Percentage Volume Change, after wetting.
6.144: Site 'B' Francois Road, site 'C' Margaret Mayton Avenue and site 'D' Rose Hill [Remoulded 98.1 - 107.3 Kpa] - Relationship between Water Content 'w_i', before wetting and Percentage Volume Change, after wetting.
6.145: Site 48, Lady Grey [Undisturbed, 98.1 Kpa] - Relationship between Water Content 'w_i', before wetting and Percentage Volume Change, after wetting.
6.146: Kaolin K.1 (13% clay size), K.2 (20% clay), and Kaolin K.3 (8.5% clay size([Artificial soil types Remoulded, 98.1 Kpa] - Relationship between Water Content 'w_i', before wetting and Percentage Volume Change, after wetting.
6.147: Bentonite B.1 (3.5% clay size), B.2 (7% clay), B.3 (11.5%) B.4 (15.5%) and Bentonite B.5 (35% clay size) [Artificial soil types Remoulded, 98.1 Kpa] - Relationship between Water Content 'w_i', before wetting and Percentage Volume Change, after wetting.

CHAPTER SEVEN

7.01: Relationship between the void ratio `e' and the water ratio `wr' or `Ω', (or alternatively use the water content). For description of curve see section 7.3.
7.02: Relationship between the void ratio `e' and water ratio `wr' or `Ω', for the controlled wetting stage - includes the maximum and final values of swell pressure.
7.03: Site 11, Rosebank [Remoulded samples] - Void ratio `e' versus water ratio `wr', for the controlled wetting path (includes swell pressures due to wetting while confined).

University of Cape Town

Number	Title
7.04:	Site 11, Rosebank [Remoulded samples] - Void ratio `e' versus water ratio `wr', for the full test path (includes free-shrinkage and unloading paths). Horizontal portions are for wetting of confined samples.
7.05:	Site 11, Rosebank [Compacted samples] - Void ratio `e' versus water ratio `wr', for the controlled wetting path (includes swell pressures while confined).
7.06:	Site 11, Rosebank [Compacted samples] - Void ratio `e' versus water ratio `wr', for the full test path (includes free-shrinkage and unloading paths).
7.07:	Site 11, Rosebank [Undisturbed samples] - Void ratio `e' versus water ratio `wr', for the controlled wetting path (includes swell pressures).
7.08:	Site 11, Rosebank [Undisturbed samples] - Void ratio `e' versus water ratio `wr', for the full test path (includes free shrinkage and unloading path).
7.09:	Site 36, Rondebosch [Remoulded samples] - Void ratio `e' versus water ratio `wr', for the controlled wetting path (includes swell pressures).
7.10:	Site 36, Rondebosch [Remoulded samples] - Void ratio `e' versus water ratio `wr', for the full test path (includes free-shrinkage and unloading paths).
7.11:	Site 36, Rondebosch [Compacted sample] - Void ratio `e' versus water ratio `wr', for the controlled wetting path (includes swell pressures).
7.12:	Site 36, Rondebosch [Compacted sample] - Void ratio `e' versus water ratio `wr', for the full test path (includes free-shrinkage and unloading paths).
7.13:	Site 36, Rondebosch [Undisturbed sample] - Void ratio `e' versus water ratio `wr', for the controlled wetting path (includes swell pressures).
7.14:	Site 36, Rondebosch [Undisturbed sample] - Void ratio `e' versus water ratio `wr', for the full test path (includes free-shrinkage and unloading paths).
7.15:	Site 30, Hout Bay [Remoulded samples] - Void ratio `e' versus water ratio `wr', for the controlled wetting path (includes swell pressures).
7.16:	Site 30, Hout Bay [Remoulded samples] - Void ratio `e' versus water ratio `wr', for the full test path (includes free-shrinkage and unloading paths).
7.17:	Site 30, Hout Bay [Undisturbed sample] - Void ratio `e' versus water ratio `wr', for the controlled wetting path (includes swell pressures).
7.18:	Site 30, Hout Bay [Undisturbed sample] - Void ratio `e' versus water ratio `wr', for the full test path (includes free-shrinkage and unloading paths).
7.19:	Site A, Berea Road (Durban) [Compacted sample] - Void ratio `e' versus water ratio `wr', for the controlled wetting path (includes swell pressures).

University of Cape Town

Number	Title
7.20:	Site A, Berea Road (Durban) [Compacted sample] - Void ratio `e' versus water ratio `wr', for the full test path (includes free-shrinkage and unloading paths).
7.21:	Site 7, Mowbray [Remoulded samples] - Void ratio `e' versus water ratio `wr', for the controlled wetting path (includes swell pressures).
7.22:	Site 7, Mowbray [Remoulded sample] - Void ratio `e' versus water ratio `wr', for the full test path (includes free-shrinkage and unloading paths).
7.23:	Site 7, Mowbray [Undisturbed sample] - Void ratio `e' versus water ratio `wr', for the controlled wetting path (includes swell pressures).
7.24:	Site 7, Mowbray [Undisturbed sample] - Void ratio `e' versus water ratio `wr', for the full test path (includes free-shrinkage and unloading paths.)
7.25:	Site 11, Rosebank [Remoulded samples] - Void ratio `e' versus effective vertical pressure `peV', for the full test path.
7.26:	Site 11, Rosebank [Compacted samples] - Void ratio `e' versus effective vertical pressure `peV', for the full test path.
7.27:	Site 11, Rosebank [Undisturbed samples] - Void ratio `e' versus effective vertical pressure `peV', for the full test path.
7.28:	Site 36, Rondebosch [Remoulded samples] - Void ratio `e' versus effective vertical pressure `peV', for the full test path.
7.29:	Site 36, Rondebosch [Compacted sample] - Void ratio `e' versus effective vertical pressure `peV', for the full test path.
7.30:	Site 36, Rondebosch [Undisturbed sample] - Void ratio `e' versus effective vertical pressure `peV', for the full test path.
7.31:	Site 30, Hout Bay [Remoulded samples] - Void ratio `e' versus effective vertical pressure `peV', for the full test path.
7.32:	Site 30, Hout Bay [Undisturbed sample] - Void ratio `e' versus effective vertical pressure `peV', for the full test path.
7.33:	Site A, Berea Road (Durban) [Compacted sample] - Void ratio `e' versus effective vertical pressure `peV', for the full test path.
7.34:	Site 7, Mowbray [Remoulded samples] - Void ratio `e' versus effective vertical pressure `peV', for the full test path.
7.35:	Site 7, Mowbray [Undisturbed sample] - Void ratio `e' versus effective vertical pressure `peV', for the full test path.

University of Cape Town

Number	Title
7.36:	Site 11, Rosebank [Remoulded samples] - Void ratio `e' vs effective vertical pressure `peV' vs water ratio `wr', for the full test path.
7.37:	Site 11, Rosebank [Compacted samples] - Void ratio `e' vs effective vertical pressure `peV' vs water ratio `wr', for the full test path.
7.38:	Site 11, Rosebank [Undisturbed samples] - Void ratio `e' vs effective vertical pressure `peV' vs water ratio `wr', for the full test path.
7.39:	Site 36, Rondebosch [Remoulded samples] - Void ratio `e' vs effective vertical pressure `peV' vs water ratio `wr', for the full test path.
7.40:	Site 36, Rondebosch [Compacted sample] - Void ratio `e' vs effective vertical pressure `peV' vs water ratio `wr', for the full test path.
7.41:	Site 36, Rondebosch [Undisturbed sample] - Void ratio `e' vs effective vertical pressure `peV' vs water ratio `wr', for the full test path.
7.42:	Site 30, Hout Bay [Remoulded samples] - Void ratio `e' vs effective vertical pressure `peV' vs water ratio `wr', for the full test path.
7.43:	Site 30, Hout Bay [Undisturbed sample] - Void ratio `e' vs effective vertical pressure `peV' vs water ratio `wr', for the full test path.
7.44:	Site A, Berea Road (Durban) [Compacted sample] - Void ratio `e' vs effective vertical pressure `peV' vs water ratio `wr', for the full test path.
7.45:	Site 7, Mowbray [Remoulded samples] - Void ratio `e' vs effective vertical pressure `peV' vs water ratio `wr' for the full test path.
7.46:	Site 7, Mowbray [Undisturbed sample] - Void ratio `e' vs effective vertical pressure `peV' vs water ratio `wr', for the full test path.
7.47:	Site 11, Rosebank [Remoulded samples] - Void ratio `e' vs water ratio `wr', over the full range of degree of saturation, for swelling against constraint (includes stress scales, "average stresses" `peAV' and consistency limits). These average stresses have been taken to be half of those shown on Figure 7.03. Stress Scales on inclined line were found by other tests.
7.48:	Site 11, Rosebank [Compacted samples] - Void ratio `e' vs water ratio `wr', over the full range of degree of saturation, for swelling against constraint (includes stress scales, "average stresses" `peAV' and consistency limits).
7.49:	Site 11, Rosebank [Undisturbed samples] - Void ratio `e' vs water ratio `wr', for swelling against constraint (includes stress scales and "average stresses" `peAV').

University of Cape Town

Number Title

7.50: Site 36, Rondebosch [Remoulded samples] - Void ratio `e' vs water ratio `wr', over the full range of degree of saturation, for swelling against constraint (includes stress scales, "average stresses" `peAV' and consistency limits).
7.51: Site 36, Rondebosch [Compacted sample] - Void ratio `e' vs water ratio `wr', over the full range of degree of saturation, for swelling against constraint (includes stress scales, "average stresses" `peAV' and consistency limits).
7.52: Site 36, Rondebosch [Undisturbed sample] - Void ratio `e' vs water ratio `wr', for swelling against constraint (includes stress scales and "average stresses" `peAV').
7.53: Site 30, Hout Bay [Remoulded samples] - Void ratio `e' vs water ratio `wr', over the full range of degree of saturation, for swelling against constraint (includes stress scales, "average stresses" `peAV' and consistency limits).
7.54: Site 30, Hout Bay - [Undisturbed sample] Void ratio `e' vs water ratio `wr', for swelling against constraint (includes stress scales and "average stresses" `peAV').
7.55: Site A, Berea Road (Durban) [Compacted sample] - Void ratio `e' vs water ratio `wr', over the full range of degree of saturation, for swelling against constraint (includes stress scales, "average stresses" `peAV' and consistency limits).
7.56: Site 7, Mowbray [Remoulded samples] - Void ratio `e' vs water ratio `wr', over the full range of degree of saturation, for swelling against constraint (includes stress scales, "average stresses" `peAV' and consistency limits).
7.57: Site 7, Mowbray [Undisturbed sample] - Void ratio `e' vs water ratio `wr', for swelling against constraint (includes stress scales and "average stresses" `peAV').

CHAPTER EIGHT

8.01: Relationship between the void ratio `e' and the water ratio 'wr', or `Ω', for the full test path. See Section 8.3 for description.
8.02: Relationship between the void ratio `e' and the effective vertical pressure (or stress) `peV'.
8.03: Relationship between the void ratio `e' and the effective horizontal pressure (or stress) `peH'. The latter is measured by using the horizontal confining ring fitted with electrical strain gauge.

University of Cape Town

Number	Title
8.04:	Site 11, Rosebank - [One-D Consolidation] Relationship between the void ratio `e' and the effective vertical pressure (or stress) `peV'.
8.05:	Site 11, Rosebank - [One-D Consolidation] Relationship between the void ratio `e' and the effective horizontal pressure (or stress) `peH'.
8.06:	Site 11, Rosebank - [Left overnight at 50 kpa and then wetted under this pressure] Relationship between the void ratio `e' and the water ratio `wr', for the full test path.
8.07:	Site 11, Rosebank - [50 kpa] Relationship between the void ratio `e' and the effective vertical pressure (or stress) `peV'.
8.08:	Site 11, Rosebank - [50 kpa] Relationship between the void ratio `e' and the effective horizontal pressure (or stress) `peH'.
8.09:	Site 11, Rosebank - [100 kpa] Relationship between the void ratio `e' and the water ratio `wr', for the full test path.
8.10:	Site 11, Rosebank - [100 kpa] Relationship between the void ratio `e' and the effective vertical pressure (or stress) `peV'.
8.11:	Site 11, Rosebank - [100 kpa] Relationship between the void ratio `e' and the effective horizontal pressure (or stress) `peH'.
8.12:	Site 11, Rosebank - [400 kpa] Relationship between the void ratio `e' and the water ratio `wr', for the full test path.
8.13:	Site 11, Rosebank - [400 kpa] Relationship between the void ratio `e' and the effective vertical pressure (or stress) `peV'.
8.14:	Site 11, Rosebank - [400 kpa] Relationship between the void ratio `e' and the effective horizontal pressure (or stress) `peH'.
8.15:	Site 11, Rosebank - [Swell Pressure] Relationship between the void ratio `e' and the water ratio `wr', for the full test path.
8.16:	Site 11, Rosebank - [Swell Pressure] Relationship between the void ratio `e' and the effective vertical pressure `peV'.
8.17:	Site 11, Rosebank - [Swell Pressure] Relationship between the void ratio `e' and the effective horizontal pressure `peH'.
8.18:	Site 36, Rondebosch - [100 kpa] Relationship between the void ratio `e' and the water ratio `wr', for the full test path.
8.19:	Site 36, Rondebosch - [100 kpa] Relationship between the void ratio `e' and the effective vertical pressure `peV'.

University of Cape Town

Number	Title
8.20:	Site 36, Rondebosch - [100 kpa] Relationship between the void ratio `e' and the effective horizontal pressure `peH'.
8.21:	Site A, Berea Road (Durban) - [100 kpa] Relationship between the void ratio `e' and the water ratio `wr'.
8.22:	Site A, Berea Road (Durban) - [100 kpa] Relationship between the void ratio `e' and the effective vertical pressure `peV'.
8.23:	Site A, Berea Road (Durban) - [100 kpa] Relationship between the void ratio `e' and the effective horizontal pressure `peH'.
8.24:	Site 7, Mowbray - [100 kpa] Relationship between the void ratio `e' and the water ratio `wr'.
8.25:	Site 7, Mowbray - [100 kpa] Relationship between the void ratio `e' and the effective vertical pressure `peV'.
8.26:	Site 7, Mowbray - [100 kpa] Relationship between the void ratio `e' and the effective horizontal pressure `peH'.
8.27:	Site 48, Lady Grey (Natal) - [100 kpa] Relationship between the void ratio `e' and the water ratio `wr'.
8.28:	Site 48, Lady Grey (Natal) - [100 kpa] Relationship between the void ratio `e' and the effective vertical pressure `peV'.
8.29:	Site 48, Lady Grey (Natal) - [100 kpa] Relationship between the void ratio `e' and the effective horizontal pressure `peH'.
8.30:	Site 11, Rosebank - [50 kpa; 100 kpa; 400 kpa; Swell Pressure] Void ratio `e' versus water ratio `wr'. The average pressures shown are the average of the vertical pressure and two equal horizontal pressures which are measured.
8.31:	Site 36, Rondebosch - [Settled overnight under 100 kpa and then wetted while carrying this pressure] Void ratio `e' versus water ratio `wr'.
8.32:	Site A, Berea Road (Durban) - [100 kpa] Void ratio `e' versus water ratio `wr'.
8.33:	Site 7, Mowbray - [100 kpa] Void ratio `e' versus water ratio `wr'.
8.34:	Site 48, Lady Grey (Natal) - [100 kpa] Void ratio `e' versus water ratio `wr'.
8.35:	Site 11, Rosebank - [One-dimensional; 50 kpa; 100 kpa; 400 kpa; Swell Pressure] Void ratio `e' versus effective vertical pressure `peV'.
8.36:	Site 36, Rondebosch - [100 kpa] Void ratio `e' versus effective vertical pressure `peV'.
8.37:	Site A, Berea Road (Durban) - [100 kpa] Void ratio `e' versus effective vertical pressure `peV'.
8.38:	Site 7, Mowbray - [100 kpa] Void ratio `e' versus effective vertical pressure `peV'.

University of Cape Town

Number	Title
8.39:	Site 48, Lady Grey (Natal) - [100 kpa] Void ratio `e' versus effective vertical pressure `peV'.
8.40:	Site 11, Rosebank - [50 kpa; 100 kpa; 400 kpa; Swell Pressure] Void ratio `e' versus effective vertical pressure `peV' versus water ratio `wr'.
8.41:	Site 36, Rondebosch - [100 kpa] Void ratio `e' versus effective vertical pressure `peV' versus water ratio `wr'.
8.42:	Site A, Berea Road (Durban) - [100 kpa] Void ratio `e' versus effective vertical pressure `peV' versus water ratio `wr'.
8.43:	Site 7, Mowbray - [100 kpa] Void ratio `e' versus effective vertical pressure `peV' versus water ratio `wr'.
8.44:	Site 48, Lady Grey (Natal) - [100 kpa] Void ratio `e' versus effective vertical pressure `peV' versus water ratio `wr'.
8.45:	Site 11, Rosebank - [50 kpa; 100kpa; 400 kpa; Swell Pressure] Void ratio `e' versus effective horizontal stress `peH' versus water ratio `wr'.
8.46:	Site 36, Rondebosch - [100 kpa] Void ratio `e' versus effective horizontal stress `peH' versus water ratio `wr'.
8.47:	Site A, Berea Road (Durban) - [100 kpa] Void ratio `e' versus effective horizontal stress `peH' versus water ratio `wr'.
8.48:	Site 7, Mowbray - [100 kpa] Void ratio `e' versus effective horizontal stress `peH' versus water ratio `wr'.
8.49:	Site 48, Lady Grey (Natal) - [100 kpa] Void ratio `e' versus effective horizontal stress `peH' versus water ratio `wr'.
8.50:	Site 11, Rosebank - [50 kpa; 100kpa; 400 kpa; Swell Pressure] Void ratio `e' versus effective average stress `peAV' versus water ratio `wr'.
8.51:	Site 36, Rondebosch - [100 kpa] Void ratio `e' versus effective average stress `peAV' versus water ratio `wr'.
8.52:	Site A, Berea Road (Durban) - [100 kpa] Void ratio `e' versus effective average stress `peAV' versus water ratio `wr'.
8.53:	Site 7, Mowbray - [100 kpa] Void ratio `e' versus effective average stress `peAV' versus water ratio `wr'.
8.54:	Site 48, Lady Grey (Natal) - [100 kpa] Void ratio `e' versus effective average stress `peAV' versus water ratio `wr'.

University of Cape Town

CHAPTER NINE

Number Title

9.01: Sample S.11-T3 [Undisturbed] Drained triaxial, isotropically consolidation overnight, wetted by increments, further consolidation, then unloading. Relationship between the void ratio `e' and the water ratio `wr' or `Ω', for the full test path.
9.02: Relationship between the void ratio `e', and the effective all round pressure (or stress) `peAR', for the full test path.
9.03: Site 11, Rosebank - [Undisturbed - 100 kpa] Relationship between the void ratio `e' and the water ratio `wr'.
9.04: Site 11, Rosebank - [Undisturbed - 100 kpa] Relationship between the void ratio `e' and the effective all round pressure `peAR'.
9.05: Site 11, Rosebank - [Compacted - 100 kpa] Relationship between the void ratio `e' and the water ratio `wr'.
9.06: Site 11, Rosebank - [Compacted - 100 kpa] Relationship between the void ratio `e' and the effective all round pressure `peAR'.
9.07: Site A, Berea Road (Durban) - [Undisturbed - 100 kpa] Relationship between the void ratio `e' and the water ratio `wr'.
9.08: Site A, Berea Road (Durban) - [Undisturbed - 100 kpa] Relationship between the void ratio `e' and the effective all round pressure `peAR'.
9.09: Site A, Berea Road (Durban) - [Compacted - 100 kpa] Relationship between the void ratio `e' and the water ratio `wr'.
9.10: Site A, Berea Road (Durban) - [Compacted - 100 kpa] Relationship between the void ratio `e' and the effective all round pressure `peAR'.
9.11: Site 11, Rosebank - [U & C - 100 kpa] Void ratio `e' versus effective all round pressure `peAR' versus water ratio 'wr'.
9.12: Site A, Berea Road (Durban) - [U & C - 100 kpa] Void ratio `e' versus effective all round pressure `peAR' versus water ratio 'wr'.
9.13: Site 11, Rosebank - [U & C - 100 kpa during wetting] Void ratio `e' versus water ratio 'wr', under an all round pressure `peAR' of 103.4 Kpa.
9.14: Site A, Berea Road (Durban) - [U & C - 100 kpa during wetting] Void ratio `e' versus water ratio 'wr', under an all round pressure `peAR' of 103.4 Kpa.

University of Cape Town

CHAPTER TEN

Number Title

10.01: Consistency Limits - Natural Soil Types.
10.02: Consistency Limits - Artificial Soil Types.
10.03: Particle Size Distribution [Percentages of sand, silt and clay] - Natural Soil Types.
10.04: Particle Size Distribution [Percentages of sand, silt and clay] - Artificial Soil Types.
10.05: Specific Gravity - Natural Soil Types.
10.06: Specific Gravity - Artificial Soil Types.
10.07: pH Values - Natural and artificial soil types.
10.08: Dry Density versus Water Ratio [Mod] includes values of void ratio, porosity and degree of saturation.
10.09: Dry Density versus Water Ratio [Std] includes values of void ratio, porosity and degree of saturation.
10.10: Relation between b-dimension and water content for six Na-saturated dioctahedral montmorillonites.
10.11: Free Expansion Limit - Natural Soil Types.
10.12: Free Expansion Limit - Artificial Soil Types.
10.13: Relationship between Free Expansion Limit and Liquid Limit.
10.14: Relationship between Free Expansion Limit and Plastic Limit.
10.15: Relationship between Free Expansion Limit and Plasticity Index.
10.16: Relationship between Free Expansion Limit and Linear Shrinkage.
10.17: Site 11, Rosebank - Constant 'C' as function of degree of saturation 'Sr', in the Free Swell Paths.
10.18: Site 11, Rosebank - Constant 'C' as function of degree of saturation 'Sr' and void ratio 'e', in the Free Swell Path.
10.19: Site 36, Rondebosch - 'C' as function of 'Sr', in the Free Swell Paths.
10.20: Site 36, Rondebosch - 'C' as function of 'Sr' and 'e', in the Free Swell Path.
10.21: Site 30, Hout Bay - 'C' as function of 'Sr', in the Free Swell Paths.
10.22: Site 30, Hout Bay - 'C' as function of 'Sr' and 'e', in the Free Swell Path.
10.23: Site A, Berea Road - 'C' as function of 'Sr', in the Free Swell Paths.
10.24: Site A, Berea Road - 'C' as function of 'Sr' and 'e', in the Free Swell Path.
10.25: Site 7, Mowbray - 'C' as function of 'Sr', in the Free Swell Paths.
10.26: Site 7, Mowbray - 'C' as function of 'Sr' and 'e', in the Free Swell Path.

University of Cape Town

Number	Title
10.27:	Site B, Francois Road - 'C' as function of 'Sr', in the Free Swell Paths.
10.28:	Site B, Francois Road - 'C' as function of 'Sr' and 'e', in the Free Swell Path.
10.29:	Site C, Margaret Mayton Avenue - 'C' as function of 'Sr', in the Free Swell Paths.
10.30:	Site C, Margaret Mayton Avenue - 'C' as function of 'Sr' and 'e', in the Free Swell Path.
10.31:	Site D, Rose Hill - 'C' as function of 'Sr', in the Free Swell Paths.
10.32:	Site D, Rose Hill - 'C' as function of 'Sr' and 'e', in the Free Swell Path.
10.33:	Kaolin K.1 (13% clay size) - 'C' as function of 'Sr', in the Free Swell Paths.
10.34:	Kaolin K.1 (13% clay size) - 'C' as function of 'Sr' and 'e', in the Free Swell Path.
10.35:	Kaolin K.2 (20% clay size) - 'C' as function of 'Sr', in the Free Swell Paths.
10.36:	Kaolin K.2 (20% clay size) - 'C' as function of 'Sr' and 'e', in the Free Swell Path.
10.37:	Kaolin K.3 (8.5% clay size) - 'C' as function of 'Sr', in the Free Swell Paths.
10.38:	Kaolin K.3 (8.5% clay size) - 'C' as function of 'Sr' and 'e', in the Free Swell Path.
10.39:	Bentonite B.1 (3.5% clay size) - 'C' as function of 'Sr', in the Free Swell Paths.
10.40:	Bentonite B.1 (3.5% clay size) - 'C' as function of 'Sr' and 'e', in the Free Swell Path.
10.41:	Bentonite B.2 (7% clay size) - 'C' as function of 'Sr', in the Free Swell Paths.
10.42:	Bentonite B.2 (7% clay size) - 'C' as function of 'Sr' and 'e', in the Free Swell Path.
10.43:	Bentonite B.3 (11.5% clay size) - 'C' as function of 'Sr', in the Free Swell Paths.
10.44:	Bentonite B.3 (11.5% clay size) - 'C' as function of 'Sr' and 'e', in the Free Swell Path.
10.45:	Bentonite B.4 (15.5% clay size) - 'C' as function of 'Sr', in the Free Swell Paths.
10.46:	Bentonite B.4 (15.5% clay size) - 'C' as function of 'Sr' and 'e', in the Free Swell Path.
10.47:	Bentonite B.5 (35% clay size) - 'C' as function of 'Sr', in the Free Swell Paths.
10.48:	Bentonite B.5 (35% clay size) - 'C' as function of 'Sr' and 'e', in the Free Swell Path.
10.49:	Site 11, Rosebank [Remoulded and Compacted samlpes] - Water Content 'w_i' and Void Ratio 'e_i', before wetting, and the Percentage Volume Change, after wetting.

University of Cape Town

LIST OF TABLES

CHAPTER ONE

Number Title

1.01: Geological units.
1.02: Geological units.
1.03: Summary of the test results for all the preliminary soil investigations.
1.04: Basic engineering properties of the natural soil types - the initial selection.
1.05: Results for the three test holes at Bellville.
1.06: Soil types - summary of the measured engineering properties for, as defined for Table 1.04.
1.07: Soil types grouped according to their plasticity characteristics.

CHAPTER TWO

2.01: Soil types - pH values, as defined above (refer to Appendix A).
2.02: Site 11, Rosebank - compaction tests.
2.03: Site 36, Rondebosch - compaction tests.
2.04: Site 30, Hout Bay - compaction tests.
2.05: Site A, Berea Road - compaction tests.
2.06: Site 7, Mowbray - compaction tests.
2.07: Correlation between the soil type, the specimen number and scale of each SEM photomicrograph.
2.08: Average amounts of the elements in crustal rocks - in weight percent for the common elements (as indicated by %) and in parts per million (no unit indicated) for the less abundant ones.
2.09: Average composition of crustal rocks.
2.10: Classification of Silicate Structures.
2.11: Average Mineral Composition of some Common Rocks.
2.12: Classification of the clay minerals - according to Grim.
2.13: Summary of the principal characteristics of the clay mineral groups.
2.14: Octahedral sheet thickness.
2.15: Tetrahedral sheet thicknesses.
2.16: Site 11, Rosebank - interplanar spacing 'd' for each main peak observed in the X-ray diffraction traces.
2.17: Site 36, Rondebosch - interplanar spacing 'd' for each main peak observed in the X-ray diffraction traces.
2.18: Site 30, Hout Bay - interplanar spacing 'd' for each main peak observed in the X-ray diffraction traces.
2.19: Site A, Berea Road (Durban) - interplanar spacing 'd' for each main peak observed in the X-ray diffraction traces.

University of Cape Town

Number Title

2.20: Site 7, Mowbray - interplanar spacing 'd' for each main peak observed in the X-ray diffraction traces.
2.21: Artificial soil Kaolin 'K' - interplanar spacing 'd' for each main peak observed in the X-ray diffraction traces.
2.22: Artificial soil Bentonite 'B' - interplanar spacing 'd' for each main peak observed in the X-ray diffraction traces.
2.23: Soil density versus water ratio for natural soil types - includes values of void ratio, porosity and degree of saturation.
2.25: Site 11, Rosebank - interplanar spacing `d' for each visible peak in the X-ray diffraction traces.
2.26: Site 36, Rondebosch - interplanar spacing `d' for each visible peak in the X-ray diffraction traces.
2.27: Site 30, Hout Bay - interplanar spacing `d' for each visible peak in the X-ray diffraction traces.
2.28: Site A, Berea Road (Durban) - interplanar spacing `d' for each visible peak in the X-ray diffraction traces.
2.29: Site 7, Mowbray - interplanar spacing `d' for each visible peak in the X-ray diffraction traces.
2.30: Artificial soil Kaolin `K' - interplanar spacing `d' for each visible peak in the X-ray diffraction traces.
2.31: Artificial soil Bentonite `BE' - interplanar spacing `d' for each visible peak in the X-ray diffraction traces.
2.32: Elemental analysis of samples - includes all natural soil types (sites 11, 36, 30, A, and 7) and artificial ones (kaolin `K' and bentonite `BE').
2.33: Mineralogical Analysis of samples - includes all natural soil types (sites 11, 36, 30, A, and 7) and artificial ones (kaolin `K' and bentonite `BE').

CHAPTER FOUR

4.01: Natural Soils - samples used for Free Shrinkage and Free Swell tests.
4.02: Artificial Soils - samples used for Free Shrinkage and Free Swell tests.
4.03: Natural & Artificial Soils [Remoulded, Compacted and Undisturbed] - Free Expansion Limit 'FEL' values.

University of Cape Town

CHAPTER FIVE

Number Title

5.01: Natural Soils - Remoulded samples used for one-dimensional (consolidometer) and isotropic (triaxial) tests.
5.02: Natural Soils - undisturbed samples used for one-dimensional (consolidometer) and isotropic (triaxial) tests.
5.03: Artificial soils - samples used for one-dimensional (consolidometer) and isotropic (triaxial) tests.

CHAPTER SIX

6.01: Natural Soils - samples used for one-dimensional consolidation tests (expansive and collapsing soils).
6.02: Artificial soils - remoulded samples used for the one-dimensional consolidation tests [100 Kpa effective pressure applied in all tests].

CHAPTER SEVEN

7.01: Samples of natural soils used for swell pressure tests.

CHAPTER EIGHT

8.01: Natural soil samples used for consolidometer tests with horizontal strain, or stress, measurements.

CHAPTER NINE

9.01: Natural soils - samples used for triaxial tests for expansive and collapsing soils.

University of Cape Town

LIST OF PHOTOGRAPHIC PLATES

CHAPTER TWO

Number	Title
2.01:	The Cambridge S180 scanning electron microscope.
2.02:	Site 11, Rosebank - SEM photomicrograph of clay sample.
2.03:	(LHS) Site 36, Rondebosch; and; (RHS) Site 30, Hout Bay - SEM photomicrographs of samples.
2.04:	(LHS) Site A, Berea Road (Durban); (RHS) Site 7, Mowbray - SEM photomicrographs of samples.
2.05:	(LHS) Kaolin Clay 'K'; and, (RHS) Bentonite Clay 'B' - SEM photomicrographs of clay samples.

CHAPTER FOUR

4.01:	(i) Unit filled with mercury; (ii) Zero reading obtained by pressing flat plate with 3 prongs, into mercury and removing the excess; (iii) Sample is placed on top of mercury, and (iv) pressed down under it; (v) Bits of mercury are brushed into glass beaker; (vi) Masses of sample (LHS) and beaker plus mercury (RHS) are recorded.

CHAPTER FIVE

5.01:	(i) Remoulded soil samples - 1. triaxial, 2. free shrinkage/swell, and 3. water content; (ii) Parts for triaxial test - 1. 1½ inches diameter tube, 2. dolly, 3. filter papers and porous plates, 4. filter drains, 5. loading cap, 6. rubber membrane, 7. twin walled tube, 8. and 9. rubber `O' rings; (iii) Ready to start test - inlet/outlet valves (left to right - cell pressure 'in'; air 'out', and water 'out' - respectively); (iv) Pressure supply board; (v) Volume and pore water pressure board; (vi) At end of test - sample with filter drains.

University of Cape Town

CHAPTER EIGHT

Number Title

8.01: [Fitting strain gauges]: 1. Emery paper; 2. Cotton wool and buds; 3. Acetone; 4. Strain gauges; 5. Tweezers, glass plate and scotch tape; 6. Cement; 7. Soldier, soldier iron and tin; 8. Electric wires, connectors and screwdriver; and, 9. Strain gauge cement.

8.02: [Stainless steel ring with strain gauges and expansion joint used]: 1. Stainless steel ring with strain gauges; 2. Epidermix 317 (activator and base); 3. Plycol type 347; and, 4. Outer ring.

8.03: [Calibration of the `Strain Unit']: Background (LHS) - The dead weight tester; Middle ground - The rubber hose unit plus strain unit; Foreground (RHS) - The strain gauge measuring device.

8.04: [Parts used in specially made container]: 1. Base plate; 2. Filter paper (Bottom piece); 3. The strain unit; 4. Filter paper (top piece); 5, 5A and 5B. Top plate - steel or perspex; 6. Top cover; 7. Plastic cover; 8. Rubber `O' ring.

8.05: [LHS - Equipment ready to be assembled for the Consolidometer Test]: 1. Strain unit; 2. Connecting board; 3. Strain gauge measuring device.

8.06: [RHS - Consolidometer test with horizontal strain measurement]: Equipment assembled and test in operation.

University of Cape Town

NOMENCLATURE

A = cross-sectional area of sedimentation cylinder, cm^2.
a = average x-sectional area after change δl in length.
a = parameter (or dimension) = cell edge in the x direction.
AASHTO = American Association of State Highway and Transportation Officials.
Activity = PI/ % Clay.
ADS = mass of air dried soil sample.
ao = initial cross sectional area.
AR = adjusted hydrometer reading = $[R + CR - G_{SL}]$.
ASTM = American Society for Testing and Materials.
atm = atmosphere standard (1 atm = 101325 Pa).
a_v = coefficient of compressibility.

B = bentonite.
b = parameter (or dimension) = cell edge in the y direction.
Bore = borehole.
bot. = bottom.

$$C = \text{constant} = \left| \frac{105}{W} \times \frac{G_S}{G_S - G_{SL}} \right|$$

C = compacted.
c = cohesion.
c = velocity of propagation (electromagnetic radiation).
$CaCO_3$ = Calcium carbonate.
cc_3 = cubic centimetres.
cm^3 = cubic centimetres.
Clay = particle size smaller than 0,002 mm.
clk. = chalk.
CM = hygroscopic moisture correction factor.
CO_2 = carbon dioxide.
coords = coordinates.
cm = centimetres.
CR = composite correction for hydrometer reading.
cre. = cream (colour).
CRT = cathode ray tube.
CSIR = Council for Scientific and Industrial Research.
CStd = Consolidometer Standard.
c_v = coefficient of consolidation.

University of Cape Town

D = diameter of soil particle in milimeters.
D = diameter of soil sample (inside the steel ring).
d = interplanar spacing.
d_{060} = interplanar spacing - determines 'b' dimension (or parameter).
d_{400} = interplanar spacing - determines 'a' dimension (or parameter).
D_D = dry density ie. specific weight, KN/m^3.
deg = degrees.
dF = change in free energy.
dim = dimensional.
dk. = dark (colour).
D_W = wet density ie. specific weight, KN/m^3.

E = east (direction).
e = void ratio.
e = energy.
eg = for example.
emb. = embankment.
etc = etcetera.

$f_{at'N'}$ = linear shrinkage correcting coefficient.
ft = foot, feet (measurement).
FS/FS = free shrinkage / free swell.

g = grams.
gre. = greenish (colour).
gry. = grey (colour).
G_S = specific gravity (ie. relative mass density) of soil particles.
$G_{S`Hg'}$ = specific gravity of mercury.
G_{SL} = specific gravity of suspending medium.

H = average thickness of compressible layer (for the load increment) or distance to a drainage surface.
h = Plank's constant.
H^+ = hydrogen-ion.
Hg = mass of mercury.
hi = corrected vertical deflection.
H-O-H = hydrogen-oxygen-hydrogen.
hr = hour(s).
Ht = height.
ht = original height of sample.
H_2O = water.
H_2O_2 = hydrogen peroxide.

ie = that is.
in_2 = inch(s).
in^2 = square inch.
I_p = plasticity index.

J/m^3 = joule per cubic meter.
jw = unit mass of water (g/cm^3).

University of Cape Town

K = kaolin.
K = constant depending on the temperature of suspension and the specific gravity G_S.

$$K = \frac{\text{relative density of water at Tx}}{\text{relative density of water at } 20^{o}C.}$$

k = coefficient of permeability.
kg = kilogram.
kg/m^3 = kilogram per cubic meter.
km = kilometer.
KN/m^2 = kilonewton per square meter.
KN/m^3 = kilonewton per cubic meter.
Kpa = kilopascal (10^3 x Pa).

L = the effective depth or distance from the surface of the suspension to the level at which density of the suspension is being measured.
L = effective depth cm.
L_1 = distance along the stem of the hydrometer from the top of the bulb to the mark for a hydrometer reading, cm.
L_2 = overall length of the hydrometer bulb, cm.
lb/ft^3 = pound per cubic foot.
lbs = pounds.
LHS = Left hand side.
LL = Liquid Limit.
Lo = initial length.
Log = logarithm of a number to the base e (2.718281828).
$Log_{10}p$ = logarithm of p to the base 10.
$Log(H^+)$ = logarithm of the hydrogen ion concentration of a solution.
lt = light (colour).

M = mass of moist compacted soil.
M = mass of moist/dry soil.
M = method.
m = metre.
MD_D = maximum dry density.
$M_D(g)$ = mass of oven dry soil.
M(g) = compacted soil.
mid = middle.
min = minute.
ml = millilitre.
mm = millimetre.
M-O bond (length of) = Monoclinic structure - Oxygen.
MW = molecular weight.
MW_D = maximum wet density.

University of Cape Town

N = coefficient of viscosity of the suspended medium water in poises varies with temperature.
N = normality of a solute (ie, number of moles of solute per 1000 g of solvent carbonate removed).
N/m^2 = newton per square metre.
n = porosity.
n = no. of grams of water transfered from pure bulk water to 1g of air-dried Na-montmorillonite.
N = exact number of blows recorded.
NBRI = National Building Research Institute.
nm = nanometre (1 nm = 1 x 10^{-9}m).
no = number.
NP = non plastic.
NW = north west.

octah = octahedral.
ODS = mass of oven dried soil used in the dry sieve analysis.
O-H = oxygen-hydrogen bond.
OH^- = hydroxide-ion.
OMC = optimum moisture content.
One-D = One-dimensional.
O-O = oxygen-oxygen.
O-O bond (length of) = oxygen-oxygen.
ora = orange (colour).
O ring = rubber ring, O shape.

P = poise (pascal second - Pa.s).
P = percentage of soil remaining in suspension at the level at which the hydrometer measures the density of suspension.
p = vertical stress plus horizontal stress divided by 2.
Pa = pascal (N/m^2).
Pa.s = pascal second.
P_{AVE} = average pressure.
pe = pressure (effective) = effective pressure.
peAR = effective all round pressure.
peAV = effective average stress.
peH = effective horizontal stress.
peV = effective vertical pressure.
pH = degree of effective acidity or alkalinity of a solution, pH = - Log(H^+).
pH = degree of acidity of the soil sample.
phi = value (-ve logarithm to the base 2 of the size in mm).
PI = Plasticity Index.
PL = Plastic Limit.
P_2O_5 = phospheros pentoxide.
podsol = grey colour and appearance of silicons soil horizon (Russian Purpose - pod, meaning under, and zola, ash).
ppm = parts per million.
P/Po = relative water vapour pressure.
pt = pressure (total) = total pressure.

University of Cape Town

q = difference between the vertical and horizontal stresses divided by 2.
q_u = estimated unconfined compression strength.

R = corrected hydrometer reading.
R = molar gas constant.
red = reddish.
Ref = reference.
RHS = Right hand side.

S = estimated shear strength (Kpa).
S = site.
Sand = particle size smaller than 2 mm.
SE = south east.
sec = seconds.
SEM = scanning electron microscopy.
SG = (not used) see G_S.
Silt = particle size smaller than 0,02 mm.
SP = slightly plastic.
SPT = Standard Penetration Test, number of blows per 300 mm.
Sr = ds = degree of saturation.
Std = standard (as in Standard AASHTO).
sq. m = square meter.

T = interval of time from the start of sedimentation to the recording of the reading.
T = temperature.
t = time (minutes) for a percentage of the consolidation process to take place.
Tarr = tarr (1 Tarr = 133,32237 Pa).
Temp = temperature.
Ti = observed temperature of water (^{o}C).
T-O bond (length of) = trigonal or triclinic structure-oxygen.
trn. = trench.
Tv = time factor (dimensionless quality).
Tx = soil water temperature.

U = value of degree of consolidation.
U = undisturbed.
UCT = University of Cape Town.

v = frequency.
V_B = volume of hydrometer bulb, cm^3.
Vi = initial volume.
Vo = original volume.
Vol = volume.
vs = versus.
V_S = volume of soil grains.
$V_S(cm^3)$ = volume of solids.
V_T = total volume of soil mass.
V_T = volume of compacted mould.
Vv = volume of voids.
Vw = volume of water in soil.

University of Cape Town

W = west.
W = calculated mass of oven dried soil used in hydrometer analysis.
w = water content.
w = water content of moist soil.
w = wavelength (electromagnetic waves).
Wa = mass of G_S bottle with water at desired temp 'Tx' (g).
Wb = mass of G_S bottle with soil-water at temp 'Tx' (g).
W_{ci} = initial water content.
W_{cf} = final water content.
w_D = density of water.
Wf = mass of G_S bottle (g).
w_{FE} = Free Expansion Limit.
w_L = liquid limit.
w_{Ls} = linear shrinkage.
Wo = mass of oven dry soil (g).
w_P = plastic limit.
w_S = shrinkage limit.
WS = wet sieving.
Wt = weight.
w_W = natural water content.

x = x-axis of plane.
x' = x coordinates.
X-ray D = X-ray diffraction.

y = y-axis of plane.
y' = y coordinates.
yel = yellow.

z = z-axis of plane.
z' = z coordinates.

^oC = degree centigrade.
3-D = three-dimensional.
% = percentage.
± = plus minus.
+ve = positive.
-ve = negative.
> = greater than.
≥ = greater than or equal to.
< = less than.
Ω = wr = water ratio.
π = pi (3.141592654).
δe = change in void ratio.
δl = change in length.
δp = change in effective pressure.
δv = change in volume.
∞ = infinity.
ϵ = axial strain (δl/Lo).
Å = ångstrom (1 Å = 0,1 nm = 0,000 000 000 1 m).
μm = micron (1 μm = 1 x 10^{-6}m).

University of Cape Town

£ = adsorbed water density.
θ = surface coverage.
v = partial molar volume of water in clay.
F-Fo = relative partial molar free energy of water.
≈ = approximately equal.

University of Cape Town

11. ERRERA, L.A. (1977): Stress Paths and Collapsing Soils - M.Sc. Thesis. Department of Civil Engineering, University of Cape Town.

12. KNIGHT, K. (1961): The Collapse of Structure of Sandy Sub-soils on Wetting - Ph.D. thesis. Department of Civil Engineering, University of the Witwatersrand.

13. HOLMES, A. (1970): Principles of Engineering Geology - 2nd edition. Thomas Nelson and Sons Ltd., Great Britain.

14. JENNINGS, J.E., BRINK, A.B.A., and WILLIAMS, A.A.B. (1973): Revised Guide to Soil Profiling for Civil Engineering Purposes in Southern Africa. Transactions of the S.A.I.C.E., Volume 15, Number 1, January 1973.

15. TERZAGHI, K., and PECK, R.B. (1967): Soil Mechanics in Engineering Practise - 2nd edition. J. WILEY and Sons Inc.

16. DE S. VINAGRE, T.J.V. (1976/77): Masters Thesis - Diaries One, Two, Three, Four, Five, and Six.

17. SPARKS, A.D.W. (1963): Discussion in Section A - Expansive and Collapsing Soils and Soil Moisture; and, Section C - Soil Types and Soil Mapping. Proceedings, 3rd Regional Conference for Africa on Soil Mechanics and Foundation Engineering, Salisbury.

18. ANNUAL BOOK OF A.S.T.M. STANDARDS, PART 19 (1976): Natural Building Stones; Soil and Rock; Peats, Mosses, and Humus. American Society for Testing and Materials.

19. BOWLES, J.E. (1970): Engineering Properties of Soils and their Measurement. McGraw-Hill Book Company.

20. BALLANTINE, P.A. (1978): Consolidometer tests to determine the stress path in a soil subject to vertical load - post B.Sc. thesis tests for Prof. Sparks. Department of Civil Engineering, University of Cape Town.

21. LIEBENBERG AND STANDER Consulting Engineers (1976): Report to the Architects J. Boyd & Associates in association with R. Nixon and A.C. Orsmond - "Subsoil Investigation carried out at the site of the proposed extension to the Trigonometrical Survey Office, Mowbray, Cape Town", dated January 1976.

22. DE S. VINAGRE, T.J.V. (1977): Soils Report for Site Investigation of New Church at La Rochelle, Bellville - for Mr. A. Ellmer (Architect). Department of Civil Engineering, University of Cape Town.

University of Cape Town

23. LAMBE, T.W. (1965): Soil Testing for Engineers. The Massachusets Institute of Technology. Published by J. Wiley & Sons, New York, USA.

24. THE AMERICAN ASSOCIATION OF STATE HIGHWAY AND TRANSPORTATION OFFICIALS `AASHTO' (1974): Standard Specifications for Transportation Materials and Methods of Sampling and Testing - Part II, Methods of Sampling and Testing. Eleventh Edition - Published by the American Association of State Highway and Transportation Officials, Washington DC.

25. BRITISH STANDARDS INSTITUTION (1975): BS 1377 - Methods of test for `Soils for civil engineering purposes'; BS 812 - Methods for `Sampling and testing of mineral aggregates, sands and fillers. Published by the British Standards Institute, London.

26. AKROYD, T.N.W. (1964): Laboratory testing in Soil Engineering. Published by Soil Mechanics Limited, London.

27. SOIL MECHANICS DIVISION, NATIONAL INSTITUTE FOR ROAD RESEARCH (1968): Manual of Laboratory Tests in Soil Mechanics. Council for Scientific and Industrial Research, South Africa.

28. SOUTH AFRICAN BUREAU OF STANDARDS (1976): Standard Methods - SABS Method 852. Council of the S.A. Bureau of Standards.

29. TECHNICAL METHODS FOR HIGHWAYS (1979): Standard Methods of Testing Road Construction Materials - TMH1. Published by the National Institute for Transport and Road Research of the Council for Scientific and Industrial Research, Pretoria.

30. GRINDLEY, E.N. (1969): The U.C.T. `Manual of Practical Physics'. Revised sixth edition, published by the University of Cape Town.

31. LANGE'S HANDBOOK OF CHEMISTRY - tenth revised edition, 1961.

32. ABBE, E. (1873): The Theory of Microscope Image Formation.

33. OATLEY, C.W. (1972): The Scanning Electron Microscope. Published by the Cambridge University Press, London.

34. MEAKING, J.D., and FALLON, L.M. (1973): Low magnification scanning electron microscopy. In Scanning Electron Microscopy/1973, O. Johari and I. Corvin, eds. IITRI 6, 145 - 150.

University of Cape Town

35. MEE, P.E. (1972): Microscopy and its contribution to computer technology. Microstructures, October/November 1972.

36. SCHARF, D. (1977): Magnifications - Photography with the Scanning Electron Microscope. Schocken Books, New York.

37. Electron Microscope Unit (1976/77) R.W. James Physics Building, University of Cape Town: Pamphlet for the electron microscopy services provided by the unit, issued in 1977, ABC press.

38. ROGERS, J. (1971): Sedimentology of Quarternary Deposits on the Agulhas Bank. Bulletin No. 1, S.A. Nat. Committee for Oceanographic Research.

39. VAN ANDEL, T.H., and FRANKLIN, K. (1968): Sediment laboratory procedure - Unpublished manual. Oceanographic Dept., Oregon State University.

40. KRUMBEIN, W.C. (1934): Size frequency distribution of sediments. J. Sediment Petrol., 4; 65-77.

41. HURLBUT, C.S., and KLEIN, C. (1977): Manual of Mineralogy - 19th Edition (after J.D. Dana). Published by J. Wiley & Sons Inc.

42. MANSON, B. (1966): Principles of Geochemistry - 3rd Edition. J. Wiley & Sons, New York.

43. PAULING, L. (1960): The Nature of the Chemical Bond - 3rd Edition. Cornell University Press, Ithaca, 644 pp.

44. COMPANION, A.L. (1964): Chemical Bonding. McGraw-Hill Book Company.

45. GRIM, R.E. (1968): Clay Mineralogy - 2nd Edition. McGraw-Hill Book Company.

46. LYONS, T.L., and BUCKMAN, H.O. (1943): The Nature and Properties of Soils. Macmillan, New York.

47. WINTERS, E. and SIMONSON, R.W. (1951): The Subsoil. Advan. Agron., 3:2-92.

48. JACKSON M.L. (1959): Frequency Distribution of Clay Minerals in Major Great Soil Groups as related to the Factors of Soil Formation. Proceedings of the 6th National Clay Conference, pp. 133-143, Pergamon Press, New York.

49. DEER, W.A., HOWIE, R.A., and ZUSSMAN, J. (1969): An Introduction to the Rock Forming Minerals - 5th Impression. Longman's, Green and Co. Ltd., London.

University of Cape Town

50. BROWN, G. (1955): Report of the Clay Minerals Group Sub-Committee on Nomenclature of Clay Minerals, Clay Minerals Bull. 2(13): 294-302.

51. EISENBERG, D. and KANZMANN, W. (1969): The structure and properties of Water. Oxford Univ. Press, New York.

52. Florentine Acadamy (about 1658): Saggi di Naturali Esperienze. English translations in Phil. Trans. 5, 2020 (1670); and, in Essayes of Natural Experiments, translated by R. Waler (1684); Johnson Reprint Corporation, New York, 1964.

53. BRIDGMAN, P.W. (1926): The effect of increased pressure in Lowering the viscosity of cold water. Proc. Acad. Arts Sci. 61, 57.

54. MARTIN, R.T. (1960): Adsorbed Water on Clay: A Review. Peoceedings of 9th National Conference on Clays and Clay Minerals - Clays and Clay Minerals, vol.9.

55. DE WIT, C.T., and ARENS, P.L. (1950): Moisture content and density of some clay minerals and some remarks on the hydration pattern of clay. Trans. 4th Int. Cong. Soil Sci., V.2, pp. 59-62.

56. MACKENZIE, R.C. (1958): Density of water sorbed on montmorillonite. Nature v.181, p. 334.

57. MOONEY, R.W., KEENAN, A.G. and WOOD, L.A. (1952): Adsorption of water vapour on montmorillonite. II: J. Amer. Chem. Soc., v.74, pp. 1371-1374.

58. NORRISH, K. (1954): The swelling of montmorillonite. Faraday Society Discussion no. 18, pp. 120-134.

59. ANDERSON, D.M. and LOW, P.F. (1958): The density of water adsorbed by Li-, Na-, and K-bentonite. Soil Sci. Soc. Amer. Proc., vol.22, pp. 99-103.

60. HILL, T.C. (1950): Statistical mechanics of adsorption, IX, Adsorption thermodynamics and solution thermodynamics. J. Chem. Phys. v.18, pp. 246-256.

61. QUIRK, J.P. (1955): Significance of surface areas calculated from water vapor sorption isotherms by use of the BET equation. Soil Sci., vol.80, pp. 423-430.

62. SIENKO, J.M. and PLANE, R.A. (1966): "Chemistry: Principles and Applications" - International Student Edition. McGraw-Hill Inc.

University of Cape Town

63. MUIR, J. (1954): Dielectric loss in water films adsorbed by some silicate clay minerals. Trans. Faraday Soc., v.50, pp. 249-254.

64. DEEG, E. and HUBER, O. (1955): Dielectric constant of clays in decimeter wavelength as a function of water content. Ber. dtch. keram. Ges., v.32, pp. 261-272.

65. PICKETT, A.G. and LEMCOE, M.M. (1959): An investigation of shear strength of the clay-water system by radio-frequency spectroscopy. J. Geophys. Res. v.64, pp. 1579-1586.

66. HOSLER, C.L. and HOSLER, C.R. (1955): An investigation of the freezing of water in capillaries. Trans. Amer. Geophys. Un., v.36, pp. 126-132.

67. GRIM, R.E. and CUTHBERT F.C. (1945): Some clay-water properties of certain clay minerals. J. Amer. Ceram. Soc. v.28 pp. 90-95.

68. BAILEY, S.W. (1966): The status of Clay Mineral Structures. Clay and Clay Minerals - Proceedings of xiv National Conference at Berkley, California.

69. VEITCH, L.G., and RADOSLOVICH, E.W. (1963): The cell dimensions and summetry of layer-lattice silicates. III, Octahedral ordering: Amer. Min. 48, 62-75.

70. LINDGVIST, B. (1962): Polymorphic phase changes during heating of dioctrahedral layer silicates. Geol. Foren. Forhandl. 84, 224-9.

71. TAKEUCHI, Y. (1965): Structures of brittle micas. Clays and Clay Minerals, Pro. 13th Conf., Pergamon Press, New York.

72. EIRISH, M.V. and TRET'YAKOVA, L.I. (1970): The role of sorptive layers in the formation and change of the crystal structure of montmorillonite. Clay Minerals, v.8, pp. 255-266.

73. DAVIDTZ, J.C. and LOW, P. F. (1970): Relation between crystal-lattice configuration and swelling of montmorillonites. Clays and Clay Minerals, vol.18, pp. 325-332.

74. OVERBECK, J.Th.G. (1966): Colloid stability in aqueous and nonaqueous media. Discussions Faraday Society no. 42, pp. 7-13.

University of Cape Town

75. RADOSLOVICH, E.W. (1962): The cell dimensions and symmetry of layer-lattice silicates - II. Regression relations: Am. Mineralogist 47, 617-636.

76. FOSTER, M.D. (1955): The relation between composition and swelling in clays. Clays and Clay Minerals, 3, 205-220.

77. LOW, P.F. and ANDERSON, D.M. (1958): Osmotic pressure equations for determining thermodynamic properties of soil water. Soil Sci. 86, 251-253.

78. RAVINA, I. and LOW, P.F. (1972): Relation between swelling, water properties and b-dimension in montmorillonite-water systems. Clays and Clay Minerals, vol.20, pp. 109-123.

79. NUFFIELD, E.W. (1966): X-Ray Diffraction Methods. John Wiley & Sons Inc., New York.

80. HALLIDAY, D. and RESNICK, R. (1970): Fundamentals of Physics. A Wiley International Edition.

81. FANG, J.H. and BLOSS, F.D. (1966): X-ray Diffraction Tables. Southern University Press.

82. CARVER, R.E. (1971): Procedures in Sedimentary Petrology. Wiley Interscience.

83. BROWN, G. (1972): The X-ray Identification and Crystal Structures of Clay Minerals. Mineralogical Society, London.

84. SPARKS, A.D.W. (1961): "Partly Saturated Soils - classification; compressibility of the fluid phase; stress equations" - M.Sc. (Eng) thesis. University of the Witwatersrand.

85. SPARKS, A.D.W. (1967): A theory of consolidation for partially saturated soils. The Civil Engineer in South Africa, S.A.I.C.E., accepted October 1960, published July 1967.

86. SPARKS, A.D.W. (1975): Discussions, Vol.II, Proceedings of the Sixth Regional Conference for Africa on Soil Mechanics and Foundation Engineering; Durban, South Africa, September 1975.

87. BRACKLEY, I.J.A. (1975): A model of unsaturated clay structure and its application to swell behaviour. Sixth Regional Conf. for Africa on Soil Mech. and Foundation Eng., Durban, South Africa.

88. BISHOP, A.W. and HENKEL, D.J. (1962): The Measurement of Soil properties in the triaxial test - Second Edition Edward Arnold (Publishers) Ltd., London.

University of Cape Town

89. SPARKS, A.D.W. (1963): Various Aspects of Soil Moisture. Regional Conf. for Africa of Int. Soc of Soil Mechanics & Foundation Engineering. Salisbury, Rhodesia (Zimbabwe).

90. SPARKS, A.D.W. (1959): A Semigraphical Method for determining the Initial Compression during Consolidation in a Partially Saturated Soil. 2nd African Regional Conf. on Soil Mechanics & Foundation Engineering.
Lourenco Marques, 1959.

91. SPARKS, A.D.W. Prof. (Supervisor) Discussions with the writer.

University of Cape Town

CHAPTER ONE *

THE SOIL TYPES

1.1 INTRODUCTION AND PURPOSE

This chapter deals with the origin, physical properties and selection of the natural soil types used throughout the thesis. The chapter is divided into three main sections:

(1) The first portion describes the geology of the areas where natural soils where obtained, namely Cape Peninsula and Durban, as well as the origin and formation of expansive and collapsing soils;
(2) The second portion provides basic engineering properties for all soil samples obtained in preliminary field investigations;
(3) The third portion describes the selection of natural soil types used in this thesis.

The purpose of this chapter is to identify suitable soil types on the basis of their physical properties and measured engineering properties - the main emphasis is upon their subsequent engineering behaviour upon wetting.

1.2 GEOLOGY OF THE CAPE PENINSULA

Introduction to the area and its physiography:-

The area is densely populated, except in the mountainous areas of the Peninsula and the hills around Tygerberg and Durbanville.
The Cape Peninsula has a Mediterranean climate with hot dry summers and cool, wet winters. Mean Annual Rainfall for the area is 550 mm. Average climatic conditions for the area are as follows (see "Captour", Ref. 3):

Season	*Day temperature, ^{o}C [maximum/minimum]*	*Rain [days]*	*Sun daily [hours]*	*Humidity [%]*
Summer	26/16	7	11	70
Autumn	23/11	9	8	76
Winter	17/07	14	6	81
Spring	21/10	11	9	74

At Table Mountain, the Cape Peninsula reaches a maximum altitude of 1086m. It is bordered on the east by the extensive Cape Flats on which the highest dunes are only 65m above Sea Level. Farther east the Tygerberg Ridge is 456 m high at Kanokop.

---

* - *Observations are in Appendix A.*

University of Cape Town

Upon weathering, the resistant sandstones of the Table Mountain Group have given rise to steep cliffs on the Peninsula as compared with the rolling hilly landscape characterizing granite and Malmesbury rock terrain. The Diep, Mosselbank, Elsieskraal, Liesbeek, Salt and Kuils Rivers constitute the major drainage systems, with a few smaller streams in the mountainous Peninsula. They all are influenced by wind blown sand.

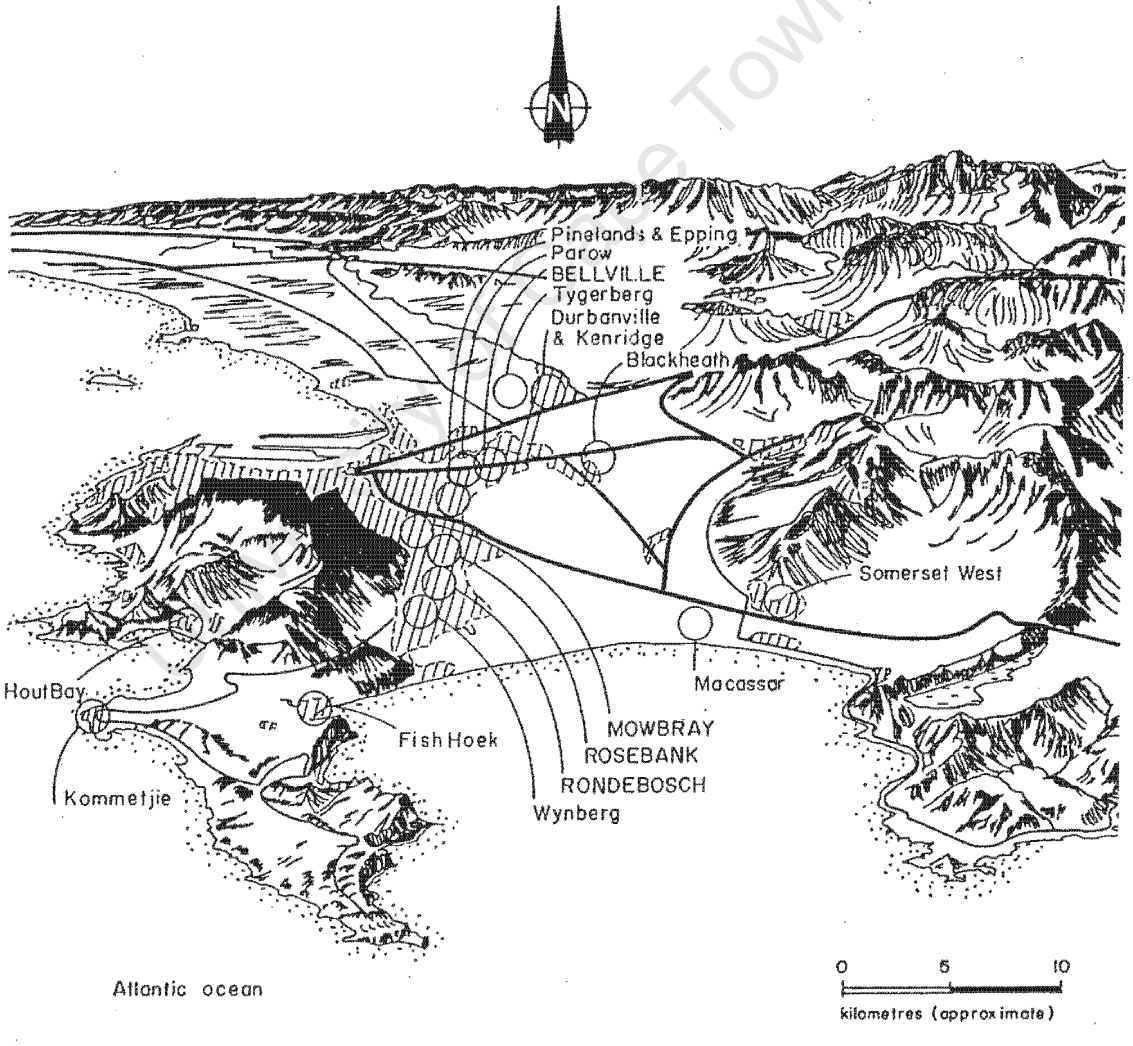

Figure 1.01: Aerial view of Cape Peninsula area - includes location of soil samples obtained in field investigations[1].

[1] - *refer to sections 1.5 and 1.6 of this chapter.*

The Cape Peninsula area is covered by Sheets 3318CD, 3318DC, 3418AB&AD, and 3418BA (scale of 1:50000) - published by the Geological Survey, Department of Mineral and Energy Affairs, 1984. The area extends from the sea northwards to latitude 33 (degrees) 45 (minutes) South, and eastwards to longitude 18 (deg) 45 (min) East.

Geological formations:-

The Geological units present in the area are summarized in Table 1.01.

Table 1.01: Geological units[1].

	Super-group	Group	Formation	Lithology
Tertiary and Quaternary				Alluvium; Scree grading into gritty sand; White sand with comminuted shell; Light grey to pale red soil; Loamy soil; Brack calcareous soil; Beach-terrace deposits; Ferricrete and silcrete; Surface limestone, calcareous sand, consolidated and partly layered.
Carboniferous to Jurassic				Dykes of dolerite, hornblende lamprophyre trachyte.
Ordovician	Cape	Table Mountain	Parkuis Peninsula Graafwater	Sandy tillite; Quartzitic sandstone; Finely bedded sandstone, siltstone and mudstone. Agglomerate and basalt.
Cape Granite Suite		Peninsula pluton Kuils River-Helderberg pluton		Coarse prophyritic, granite locally medium medium grained, with inclusions.
		Malmesbury	Tygerberg	Greywacke, phyllite, quartzitic sandstone with volcanic intercalations.

[1] - *by J.N. Theron, Ref. 4.*

University of Cape Town

Malmesbury Group: Oldest rocks in local sequence.

The Malmesbury group was deformed under influence of pressure from the east into a series of north-westerly directed narrow parallel synclines and anticlines. The general strike is consistent at about N, NW[1]. The Tygerberg formation of the Malmesbury group, consists predominantly of irregular alternations of grey to green phyllitic shale, siltstone, and massively bedded medium to fine grained quartzitic greywacke. The rocks of this formation are present over a large part of the area, mostly covered by surficial sediments, and frequently deeply weathered to a red brown or yellow clay. The occurrences in the Bellville - Durbanville area are characterized by considerably more extensive development of siltstone, greywacke and sandstone zones. Individual arenaceous layers vary in thickness from 0.25 m - 3.0 m. Many of these units can be followed as marker horizons over long distances, although drilling has demonstrated that the continuity of the more sandy units, is exceedingly variable. Well developed small scale bedding[2] and the accompanying alternation of fairly continuous light - coloured siltstone and mica rich sandstone and shale layers occur throughout. The presence of granite close to the present surface is manifested by hornfelsic nature of the outcrops in the area and the general presence of typical metamorphic spotting.

The continuity of many of the individual thin greywacke or siltstone layers, the rapid variations in lithology and the small scale sedimentary structures point to a rapid alternation of relatively weak streams with deposition of siltstone and the pelitic material during quiescence. Igneous rocks were emplaced towards the end of the Malmesbury orogenic cycle. Different phases of medium to coarse grained porphyric granite with subsidiary bodies and dykes of aplite, granodiorite, lamprophyre, trachyte and basic rocks are present.

Cape Granite Suite: The Cape Peninsula and Kuilsriver - Helderberg Plutons.

The Cape Peninsula pluton consists mainly of grey coarse grained biotite granite characterized by large feldspar phenocrysts. In addition to metamorphosed Malmesbury inclusions, in all stages of assimilation, widely spread, tourmaline rich clots are present in the granite. The grey coarse grained, porphyric biotite granite gives rise to massive round blocks characterized by prominently weathering, twinned orthoclase phenocrysts averaging 40 mm in length but which can attain measurements of 60 by 40 mm or even more. Otherwise the granite consists of quartz, muscovite, plagioclase and cordierite and contains accessory tourmaline, apatite, zircon, magnetite, pypite and sometimes also almandine garnet.

---

[1] - *north, north west.*
[2] - *of the order of 1 mm.*

University of Cape Town

These rocks occupy the whole Peninsula south and west of the granite contact with the Malmesbury rocks. The granite is intrusive into sediments of the Tygerberg formation of the Malmesbury group and is unconformally overlain by Table Mountain sandstone. The granite has two joint systems, each consisting of two sets which are approximately at right angles. The most prominent trend is W,NW - E,SE[1], which dips near to vertical.

The Kuils River - Helderberg pluton consists predominantly of leucocratic, fine to medium grained quartz feldspar granite. Tourmaline rich nodules and zones are widespread and coarse porphyritic biotite granite very like that of the Peninsula is also encountered.
A fine grained granite characterizes the wall of the pluton and is predominant in the Durbanville area. The granite at Kuilsriver is mainly a leucocratic, fine to medium grained, quartz feldspar tourmaline granite.
Analysis of several granitic samples show the following relationship; quartz - 29 to 43 percent; plagioclase - 20 to 24; k-feldspar - 26 to 36; muscovite - 3 to 9; and, tourmaline - 0 to 12 per cent.

Agglomerate and Basaltic rocks consist of a mixed mass of dark green to grey basic rock with red brown specks that contains a large variety of fragments of variable size (up to 300 mm). These are both rounded and angular pieces of quartzitic, sandstone, siltstone and hornfels (apparently of Malmesbury derivation), porphyritic granite, basic rocks and fine grained reddish granite, all with random orientation. The contact with the granite is sharp throughout. The basic igneous rock consists predominantly of chlorite, plagioclase, calcite, muscovite, iron oxide and dark minerals such as augite and clinozoisite. It has a porphyritic texture with olivine phenocrysts which are largely serpentinized and consist mainly of chlorite, calcite and iron oxide. Some basic dykes cut both the agglomerate and surrounding granite.

Cape Supergroup: The Graafwater, Peninsula and Parkhuis Formations.

The Graafwater formation, at the base of the succession, rests with distinct discordance on the granite and other pre-Cape rocks. A weathered zone ranging from a few millimetres to several metres in thickness characterizes the granite at the contact. The formation as a whole ranges in thickness from 65 m at Llandudno - Karbonkelberg to 25 m at Simonstown. It consists of alternations of distinctive red to purple siltstone, sandstone and shale, and mica rich sandy shale together with some thin bedded pink to white quartzitic sandstone. The thickness of individual units varies from 20 mm to 6 m.

---

[1] - *west, north west - east, south east.*

University of Cape Town

The lowest formation in the series, the basal shales, are distinguished from the main sandstone (overlying it) by their thinner bedding, bright red to maroon colour and prominent development of fine micaceous siltstone layers. There is a wide variety of water ripple marks, stream lineations, mud cracks, ball and pillow structures and clay pellet conglomerate lenses and there are indications of grading.

The Peninsula formation consists of a uniform light grey, medium to coarse grained quartzitic sandstone which is consistently well bedded. Massive and thinly bedded units alternate with one another. Complete development of this formation is only to be found on Table Mountain where a thickness of 600 m is reached at Maclear's Beacon. Fresh specimens usually show pale yellow or pink tints, and the upper levels are often drab grey to white throughout. There is an extensive development of channels with an erosion base in the underlying sandstone. The basal beds are predominantly coarse grained and trough cross bedding is specially well developed.
Outcrops of the Parkhuis formation[1] are confined to a small area on the summit of Table Mountain. It consists of a grey to yellow brown weathering massive, gritty sandstone, two metres thick, with a clayey matrix and similar although sometimes angular quartz, quartzite and chert pebbles. This massively bedded diamictite, averaging two metres in thickness rests on horizontal units of the Peninsula formation.

Dykes of Dolerite, Hornblende - Lamprophyre and Trachyte.

The dolerite dykes are intrusive into both Malmesbury rocks and the granite, and usually have a west - north westerly strike, a steep dip and outcrops are confined to the beach zones because of the scree slopes. Dolerite dykes weather with typical spheroidal exfoliation and give rise to poor outcrops. The majority are medium grained dark grey melanocratic rocks containing augite and plagioclase, as the most important minerals, and biotite and olivine are present as well as quartz, ilmenite, magnetite and glass. The rocks become paler on weathering and assume a grey-green colour as chlorite is developed.

The hornblende - lamprophyre dykes occur in several locations north of Bellville. The rock consists of dark brown to green hornblende phenocrysts up to 10 mm in length and 1mm wide which are reasonably regularly scattered in a fine grained[2] grey coloured, feldspatic groundmass. Trachyte dykes generally weather to grey and green, dense compact hard rocks with pale feldspar and dark mica phenocrysts.

---

1 - parts of the Glacial Band.
2 - less than 1 mm in size.

University of Cape Town

Surface Deposits.

A large variety of surface deposits, of which the age and mutual relationships are generally difficult to ascertain, cover the older rocks.
Alluvial deposits, consisting largely of dark coloured organic sand, border the larger river courses and gradually merge into adjoining light grey sandy soil.
Extensive scree deposits consist mainly of angular blocks of sandstone, from several centimetres to a few metres in diameter, with interstitial gravel and sand. Table Mountain sandstone, granite and Malmesbury rocks are covered by this layer which may exceed 10 m in thickness.
Along the coast as well as over large portions of the Cape Flats up to 17 km inland, extensive shell bearing light grey sands occur which may attain 50 m in thickness. The sand varies from fine to coarse grained - the silica grains have quite a high degree of rounding and a restricted number are characterized by a red brown, iron rich pellicle[1].
Dunes of various ages are present which have originated since the last Würm ice age under the influence of the prevalent south-east wind on all southerly directed sandy beaches during the dry summer months.

Inland of the shell bearing dune sands there is light grey to pale red sand soil underlying large areas of the southern suburbs of Cape Town. It streches to the slopes of the Tygerberg and Bottelaryberg hills and fringes the upper reaches of the Kuils and Mosselbank Rivers in the Kraaifontein - Durbanville area. The deposit consists of interwoven sandstone lenses older than the shell bearing dune sands. Thin clay lenses are irregularly distributed.

The predominant soil formed on Malmesbury rocks is yellow, red or brown. It is clayey and often contains small nodules of ferricrete and fragments of vein quartz plus a variable amount of sand grains. Extensive mappable exposure of this loamy soil is largely confined to the Tygerberg - Durbanville area as a relatively thin cover. The loam may rest directly on Malmesbury rocks, on a partly cemented layer containing ferricrete or on a clay layer of variable thickness which grades into weathered rock. Raised beach terraces and/or deposits of a former higher sea level are confined to the Peninsula. There is evidence of a beach at 17 to 20 m above sea level as well as one at 5 to 8 m.

Silcrete and ferricrete are widely distributed in isolated strips, specially north of Durbanville and near Phesantekraal. Silcrete outcrops consist at surface of typical hard, well silicified rock that weathers into massive, smooth, partly rounded blocks with conchoidal fracture. The ferricrete either occurs in the soil as loose nodules a few milimetres to several centimetres in diameter, or as more compact zones of variable thickness.

---

[1] - *that is, skin.*

University of Cape Town

Typical surface calcrete, composed of a hard irregular layer up to a few metres thick, often covered by sand, constitutes more than 90 percent of all outcrops. Calcrete varies from typical massive, grey, sandy surface limestone to cemented, well bedded sandy limestone and friable partly cemented calcareous sand. Sandy, massive and cross-bedded, medium grained limestone builds cliffs more than 60 m in height.
In contrast to the highly folded and cleaved Malmesbury rocks, the Cape Supergroup displays only minor deformation. On the Peninsula the Table Mountain Group is characterized by comparatively wide open folds. Whereas the pre-Cape structural grain is predominantly north-westerly, the north-east - south-west orientation also attains prominence in the Table Mountain sandstone. The joint systems and faults display a similar pattern. As a whole Malmesbury outcrops form part of the south westerly tectonic area lying to the west of the so called Saldanha Franschhoek main fault zone.
The most important mineral resources of the area are glass sand, kaolin and construction materials, of which rock aggregate, building sand, brick clay and road material are the most important.
At several localities between Fish Hoek, Noordhoek and Kommetjie, kaolin has been actively exploited since 1953. The white to cream coloured clay consists of kaolin with quartz, sericite and also tourmaline. The kaolin represents in situ weathered granite in which quartz and tourmaline veins and weathered Malmesbury inclusions are often present.

Construction Materials: Stone aggregate, building sand and clay.

Malmesbury hornfels is the most used aggregate - their good quality is derived from dense, hard, fine grained rock that breaks into irregular angular fragments.
The predominantly fine to medium grained quartz sand usually consists of fairly well sorted grains.
The clay is yellow to green brown with a high silt content. The uppermost part is generally flecked red brown but in depth becomes pale coloured or even white bleached material, such as just south of Fisantekraal. Small patches of ferricrete or silcrete quite often form a surface layer on the clay occurrences and may locally contain pieces of quartz, ferruginized nodules or even rock fragments.
The clay itself consists of variable amounts of sericite, montmorillonite, quartz and sometimes even a little vermiculite.
Ferricrete, weathered Malmesbury rocks and surface limestone are used for gravel roads or as foundation material for tarred roads.
Geochemical studies have confirmed that Table Mountain sandstone is characterized by a relatively high manganese content when compared to other arenaceous rocks.

University of Cape Town

1.3 GEOLOGY OF THE DURBAN AREA

Introduction to the area and its topography:-

The subtropical climate is pleasant all the year round. Normal day temperatures are between 18°C and 24°C, about 30°C on the warmest days and 10°C in the coldest nights. Mean annual rainfall is 1050 mm, and maximum rainfall occurs in summer. The central city and the harbour lowland between the Bluff and Berea Ridges, are flat; however, the hinterland rises rapidly to over 335 m, and is deeply dissected in the vicinity of the Mgeni and Mlazi rivers. Because of late drowning, the lower reaches of these rivers show aggradational features.
The area is covered by the Geological Map of Durban and Environs, sheet 2930DD (scale of 1:50000) to accompany the Bulletin 42, published by the Geological Survey[1].
The area extends from the sea westwards to longitude 30 (deg) 45 (min) East, and between latitudes 29 (deg) 45 (min) and 30 (deg) 0 (min) South.

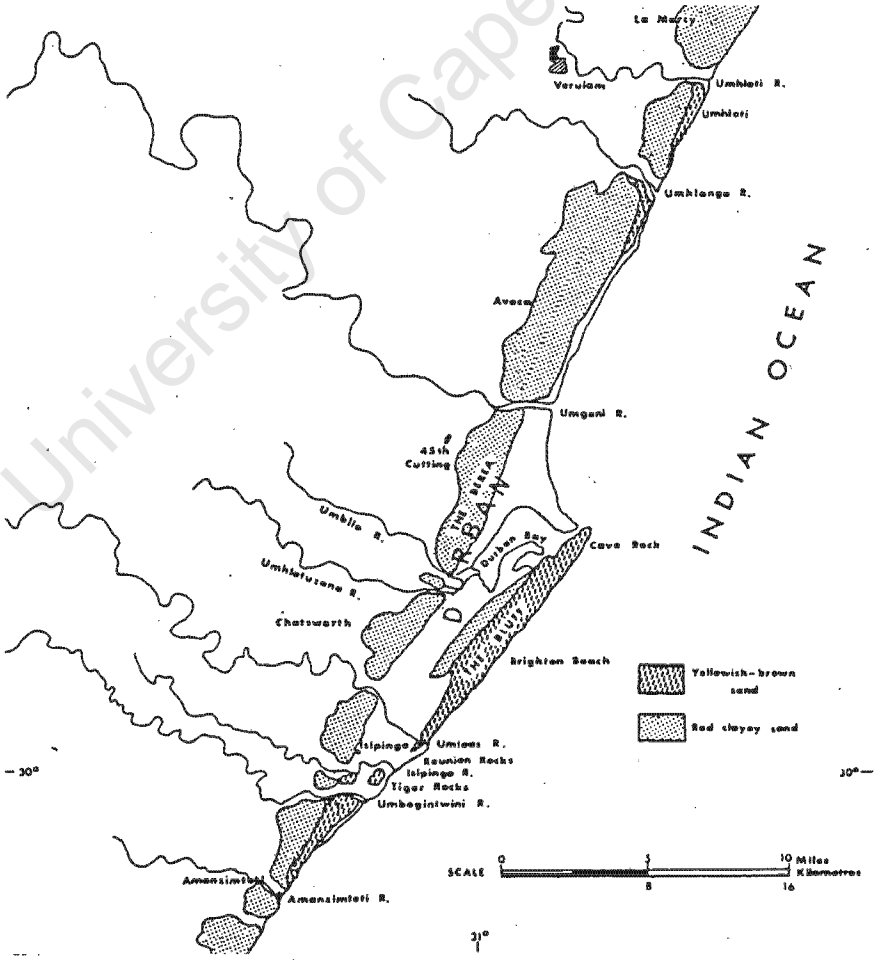

Figure 1.02: The Durban area - includes the location of the Berea Red Sand formation[2].

---

1 - *Reference 5.*
2 - *refer to subsequent section of this chapter.*

University of Cape Town

Geological Formations near Durban:-

The geological units present in the area are summarized in Table 1.02.

Table 1.02: Geological units[1].

Quaternary	- Harbour Beds		- Alluvium. - Beach sand, alluvium; - Grit sand, clay, mud.
	- Berea Red Sand		- Red sand, boulders.
	- Bluff Beds		- Consolidated sand, grit, conglomerate.
Cretaceous System	- Upper Division		- Marine sandstone and mudstone.
Karroo System	- Ecca Series	- Middle Ecca Stage	- Felspatic sandstone, grit, shale.
		- Lower Ecca Stage	- Shale.
	- Dwyka Series		- Tillite, varved shale, sandstone.
Cape System	- Table Mountain Series		- Sandstone, quartzite, shale.
Intrusive rocks:-			
Karroo			- Dolerite.
Archaean complex			- Granite, granite-gneiss, aplite, with metamorphose remnants.

Archaean granite-gneiss underlies the area. It is overlaid by the arenaceous Table Mountain Series (Cape System), glacian Dwyka Series, argillaceous and arenaceous Ecca Series (Karroo System). There are several minor intrusions of Karroo dolerite. The sedimentary rocks have a general dip seaward of 10 to 15 degrees and are much broken into earth blocks by faulting (Jurassic age), and folding is absent. Subsequently, Cretaceous marine sediments were deposited in the vicinity of the present shore.

[1] - *by L. King and R. Maud, Ref. 5.*

University of Cape Town

Archaean Complex.

Typically coarse and crystalline, and displaying a marked foliation, the gneisses are composed of quartz, microline, orthoclasse and albite with varying amounts of hornblende, biotite and some muscovite. The fresh rock is usually grey in colour[1]. The detritus supplied on weathering is similarly coarse, and includes felspar crystals 20 mm in length. The constituents of the gneiss show considerable separation into bands, those of felspar and quartz being about 6 mm wide with narrower schlieren of biotite between them. The minerals could have been separated simultaneously under metamorphic agencies.
The dip is usually steep and in their present form the rocks appear to have originated as tectonic gneisses with steep laminar flow producing the foliation.
In places the granite-gneiss was injected by aplitic and pegmatific veins varying in width from < 25 mm to > 300 mm. Small dyke-like bodies of a younger reddish granite have intruded the gneiss. Weathering of the granite-gneiss yields a moderately fertile, grey, gritty soil. Erosion of the top soil often exposes a reddish yellow subsoil.

Cape System: The Table Mountain Series.

The Table Mountain Series lies unconformably upon the Archaean granite-gneiss. The series is composed mainly of sandstone, with subordinate quartzite bands, some pebble beds, and flat, discontinuous strata and lenses of shale or mudstone irregularly distributed within the sequence.
The dominant colour of the series is a pinkish lilac. Where fresh sandstone is exposed, as in quarries and deep road cuts, much of the sandstone is greyish white in colour. The sandstone is normally coarse grained and consists of quartz grains with subordinate felspar[2] cemented by secondary quartz. Stratification is often even, with individual beds averaging 300 mm in thickness.
The shale beds, often highly micaceous, are always very subordinate to the sandstone in which they occur. Fresh, unweathered exposures may be dark blue grey but the usual colour, specially upon weathering, is maroon sprangled with silvery muscovite flakes. Petrologically, the sandstone and shale differ markedly from each other, the former having a silica content exceeding 90 percent while the latter averages around 60 percent quartz. The iron and aluminium content changes from 5 to about 25 percent.
In the Durban area the Table Mountain sandstone is cut by numerous joints which help to break up the rock into blocks. Faulting often produces shatter zones through the sandstone. On breakdown the Table Mountain Series yields a light-grey sandy soil often only a few inches thick and of low fertility. The Table Mountain sandstone is extensively used in the Durban area for road making and concrete mix.

---

1 - but under weathering it often becomes reddish.
2 - mainly microline.

University of Cape Town

Karroo System: The Dwyka Series.

The Dwyka Series in the Durban area consists of former glacial deposits, tillite with a few occurrences of silicified varved shale and lenses of sandstone. The contact with the Table Mountain Series is unconformable throughout the region, the Pre-Karroo land surface being of minor relief due to Pre-Dwyka erosion having partly removed the upper portions of the underlying sandstone prior to the deposition of the tillite. In several places, the floor of the tillite exhibits a well polished and glaciated surface. The fresh tillite is an unstratified, dark blue-green mudstone with abundant inclusions of older rock types, the whole being so hard as to fracture through matrix and inclusions alike. The mudstone matrix is composed of small, angular fragments of quartz and rock embedded in a fine base of inderterminable rock flour. Many pebbles are soled and striated by passage over the rock floor while they were entrapped in the ice. Lenses of shale, sandy mudstone and sandstone, occur locally within the tillite. The thickness of these sandstone bands can be more than 1000 mm. Most of the inclusions consist of the rock types composing the terrain across which the ice sheet moved. The most abundant inclusions are those of Table Mountain sandstone and quartzite together with different varieties of granite rocks. The Dwyka tillite is very well jointed. Faults within the Dwyka tillite are often traceable as broad zones of brecciation that may be silicified or kaolinised. Soils derived from Dwyka tillite are moderately fertile, but have poor physical properties. Top Soil is a light grey sandy loam, in which are embedded the more resistant inclusions of tillite, and the clayey subsoil is bright yellow.

The Ecca Series: The Lower Ecca Stage.

The formation is a uniform succession of dark, blue-black, unfossiliferous silty shales or laminated mudstones generally of undetermined mineral composition. Within the silty shale more indurated bands frequently occur; and conversely, up to about 30 metres above the base, clayey zones are widespread. Weathering of these zones often produces troublesome ground unstable for foundations, both of buildings and of roads. The stage is often micaceous. The thickness is about 360 metres. Although the Lower Ecca shales are extensively intruded by numerous sheets and sills of karroo dolerite, injection into this stage has been less pronounced than in the overlying Middle Ecca Stage. In contact with the intrusive dolerite the shales have undergone thermal metamorphism. On weathering, the dark colour of the shales alters to light brown or buff, and a deep, fertile clayey soil may be produced. Where erosion is active, however, the soils are usually shallow, shaly and only moderately fertile.

University of Durban-Westville

The Middle Ecca Stage.

Shales and sandstone of this stage crop out only in the northeast. In the Durban area this formation appears to have a thickness between 240 and 300 metres. The stage as a whole consists of felspathic grit, sandstone, flagstone, sandy shale and clayey shale. The Middle Ecca sandstone is usually greyish white in colour. The structure is partially that of a sandstone, rounded and subangular quartz and felspar grains cemented together by fine grained sericite and calcite and partly quartzitic, with interlocking sutured boundaries. The shale and flagstone are also lighter in colour, sandier, and often more clayey than those of the Lower Ecca. They also contain more mica in larger flakes. These rocks weather rapidly owing to the vulnerability of larger felspar grains. On weathering the sandstone yields light-grey sandy soils of low fertility, whereas the shale and flagstone produce more fertile, clayey soil-types.

The Karroo Dolerite.

Intrusions of dolerite of Stormberg age cut all the Pre-Cretaceous rock types of the Durban area. The number and relative amount of intrusions increase rapidly in the Lower Ecca, and reach a maximum in the Middle Ecca Stage. The dolerite altered the Lower Ecca into hard, black hornfels by contact metamorphism. The Middle Ecca shale and sandstone were injected with local formations. Abundant jointing of dolerite due to shrinkage upon cooling, creates residual spheroids when weathering. In situ, the rock may decompose into brown ferruginous residuum, fairly impervious to ground-water, and ultimately it weathers into a red, fertile clayey soil in well drained localities, although in areas of poor drainage it tends to form a black clayey soil.

The Cretaceous System.

The Late Cretaceous Stage is not visible though it occurs extensively below the harbour area where it is often found in boreholes. The inner margin of the suboutcrop trends northeast at a depth of about 23 m; eastward the Cretaceous formations thicken as a wedge between the harbour sediment above and the Karroo bed-rock below, until in the Bluff they are found at a depth of between 137 m and 239 m. The beds dip in the eastward direction. At the base there is often a boulder bed with well-worn cobbles of Table Mountain sandstone, Dwyka Tillite, Ecca shale and Karroo dolerite, with rarer samples of coarse granitic types of the Archaean. The succeeding formations of the Cretaceous are mostly semi-soft, sulphurous black, grey or yellow shales, variously sandy or clayey. Interbedded are bands of clean washed sandstone, full of shell fragments and cemented hard by redeposition of some of the calcareous material.

University of Cape Town

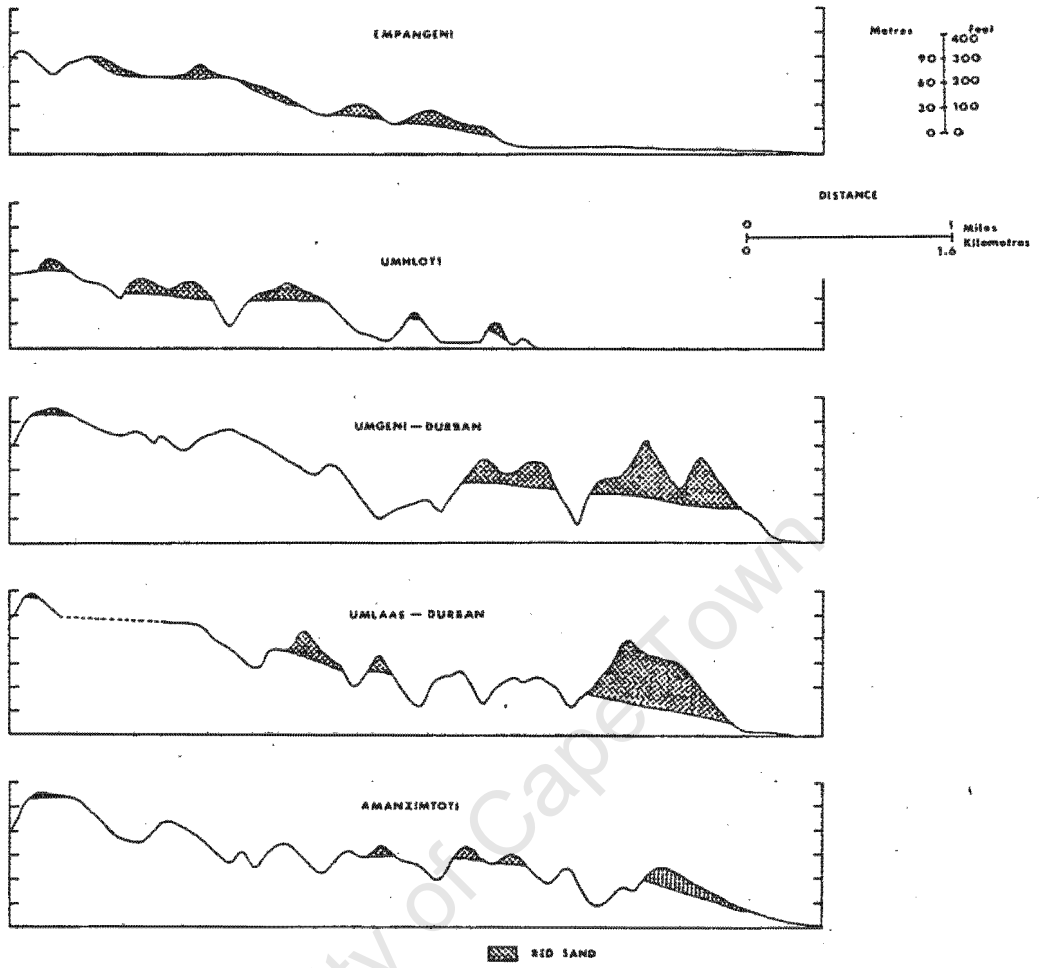

Figure 1.03: Cross sections through the areas shown in Figure 1.02 - illustrates distribution of the Red Sand[1].

The Berea Red Sand contains little felspar, though it is often clayey and cut faces stand up well. The quartz grains, subangular to rounded, vary between 0.05 and 0.8 mm in diameter, averaging 0.2 mm. The sand has considerable ilmenite and magnetite. Its red colour derives from the coating of its quartz grain with hematite or hydrated oxide. Where ilmenite is abundant a bluish purple tinge is noted. Rutile, zircon and monazite grains are present as well as felspar, pyroxene and tourmaline. Depending on the state of oxidation of its iron, the Berea Red Sand formation may range in colour from white or grey to yellow, brown, mauvish and deep or bright red. However, when reduced in acid most sand grains are of translucent quartz. Coating of grains with hematite and limonite, mainly determines the colour of each deposit. The weathering of magnetite yields other iron oxides. The red brown sand of the Bluff contains wind blown calcareous particles largely of foraminifera and calcareous algae. Red or brown sands occur at elevations up to 137 m. In places it has crept under the weathering, however, when compared to its original deposition, the sand is as in situ. Not all deposits of red and brown sand are of the same age.

---

[1] - *Reference 6.*

University of Cape Town

The Cretaceous formations encountered in the western harbour area provide problems as foundations for heavy structures: They are deep (21 - 30 m); Clayey shale and mudstone have generally little strength; and, bands of hard sandstone are seldom reliable in thickness and strength. Penetration of these contrasted and alternating types of material by borehole means that methods suitable for the one are opposite methods for penetrating the other. Thus wash boring is often sufficient for the shale, but the sandstone requires a chopping bit. Casing (cast in place of piles) is usually necessary through to the base because of caving in the shale, whereas precast piles on the other hand sometimes encounter difficulty in penetrating the shelly sandstone.

All other formations are Late Quaternary in age and include the Bluff Beds, the Berea Red Sands and boulder bed, and the Harbour Beds - they comprise a sequence of grit, sand, clay and mud which underlie the harbour and city area; also included are recent alluvia.

Quaternary System: The Bluff Beds.

The sand composing the Bluff Beds is dominantly quartzose, medium to coarse in grain size and subangular to rounded. Coarse bands usually have much fresh felspar (microline and plagioclase) in worn crystals. The bulk of the material composing the Bluff Beds has been derived from the Archaean and Table Mountain formations. Within the Bluff Beds are several layers or lenses of conglomerate including basal conglomerate. In the thicker beds are boulders (up to 150mm in diameter) of Table Mountain sandstone, Dwyka tillite, dolerite, Lower Ecca shale and more occasionally granite gneiss and earlier cemented Bluff sandstone. Beds analogous to the Bluff Beds also accur in isolated patches along the crest and eastern slopes of the Berea Ridge. The lower beds are sand from which the calcite matrix has been dissolved out by underground water, leaving them as a mere mesh of sand grains with a high proportion of voids that may at times contain a very large amount of subsurface water. Upper levels of these beds have remained highly calcareous and are sometimes cemented into hard rock. So common is the capping of red sand along the Berea Ridge as to encourage the hypothesis that it conceals further developments of the Bluff Beds thereon sandwiched between the bedrock and the red sand.

The Berea Red Sand and Boulder Bed.

Overlying the Bluff Beds upon Berea, Wentworth and Bluff Ridges are extensive developments of red brown sand that in places attains a thickness of at least 60 to 75 metres.

University of Cape Town

The boulders (in the bed at the base of the Berea Red Sand) are well rounded, percussion marked, and 75 to 225 mm in diameter. The boulders are of hard quartzite Table Mountain sandstone, derived from that formation, nearby, inland. West of the present outcrop, where erosion has taken place, relicts of the boulder bed often remain. On the Bluff the red sand rests, often without boulders at the base, on the sandstone of the Bluff Beds. The western edge of red sand outcrop shows water worn boulders with percussion marks. North of the Mgeni River, the lowest Berea Red Sand, is usually grey for some depth before grading upwards into the typical red sand. Through the western part of the metropolitan area of Durban, however, the sand is usually red from the base up, though here a characteristic rhythmic semi-stratification is present. Upon the Berea and Bluff Ridges, stone hand axes of sangoan type are found in the red sand. These are made from boulders of the boulder bed, and are now buried by metres of similar sand probably blown or crept from nearby.

The Harbour Beds.

The fullest sequence of formations is obtained from the harbour area, and may be stated in general succession above the Cretaceous or Karroo Systems. The approximate depth figures (for each formation) are as follows:

Modern subsurface sand and mud,	0 - 3 m;
Sand and grit,	3 - 9 m;
Black clay,	9 - 12 m;
Sand and grit,	10 - 24 m;
Black mud stratum,	21 - 24 m.

The Black Mud Stratum: Overlies the Cretaceous beds and extends under considerable areas of the lowland. Samples from Maydon Wharf consist of 68 percent (by weight) of decayed vegetal matter and hydrocarbons, and 31 percent of iron oxide with a few sand grains; pile driving is apt to liquify the stratum and the piles become unstable; on the other hand, for cast in place piling the stratum is apt to close-in and grip the sunken casing so tightly that it cannot be withdrawn as the pile is poured.

The bulk of sediments within the Durban area (Natal Bay - lowland) consists of clean-washed well sorted quartz sand of marine and lagoonal enviroments. Zircon, garnet, magnetite and ilmenite have been observed, and shell fragments are abundant in some layers. Redistribution of shell-lime has cemented some of these layers into strata resembling Bluff sandstone.
Widely distributed beneath the harbour at depths between 10 and 13 metres is a layer of black clay containing well preserved fossils. The clay is tough and coherent.

University of Cape Town

Above the black clay there is sand and grit similar to that below it. The true beach sand is almost entirely composed of quartz, but both ilmenite and magnetite make streaky lenses and washes, while felspar crystals tend to appear where riverine material has recently been added.

The outcrop patterns of the several older stratigraphic units in the Durban area have been largely governed by faulting of Jurassic age which was induced secondarily upon a large costal monoclinal flexure. This has resulted in most of the Pre-Cretaceous formations having a pronounced seaward dip of between 10 and 15 degrees and the downthrows are usually to the landward side. The direction of strike of the majority of faults is northeast. The Mlazi and Springfield Faults have throws in excess of 300 metres.
The effect of Quaternary tectonic activity in Plio-Pleistocene time was to induce a further seaward tilt on the rocks and on the Tertiary erosion surfaces. This resulted from a further large monoclinal flexure that had its axis in the hinterland of Natal where uplift was of the order of 1800 metres. In the Durban area the maximum amount of uplift was probably 200 to 240 metres.
Prior to the Plio-Pleistocene monoclinal tilting the terrain around Durban had been subdued and rolling in a late Tertiary cycle of erosion. Following upon the differential uplift, rejuvenation of the rivers has now obliterated the End Tertiary surface, and produced instead a maze of incised valleys. The complementary deposition of the detritus in the costal zone as the Bluff Beds, Berea Red Sand, and Harbour Beds has preserved a detailed record of events.

No exploitable deposits of minerals occur in the Durban area, but considerable amounts of stone are quarried for constructional and road making purposes. Sand and grit for similar purposes are excavated from the bed of the Mgeni River. Brick making materials are also quarried.

As the central city area is built on a series of unconsolidated sediments, difficult problems are sometimes encountered in foundation engineering. Some older formations, such as an horizon about 30 m above the base of the Lower Ecca Shale, also provide foundation problems.

University of Zululand

1.4 EXPANSIVE AND COLLAPSING SOILS.

Expansive Soils:-

The volume change behaviour of soils is very much influenced by the amounts and types of clay present in them. A clay mineral of the montmorillonoid group which includes montmorillonite, is an important constituent of the more troublesome types of expansive soils[1]. They are characterized by expanding a great deal when wetted.

Potentially expansive soils can be found almost anywhere. The enviromental conditions required (to develop problems of heave) occur readily in the semi-arid areas of the tropical and temperate zones. In each reported case of heave in these areas, swelling (or shrinking) caused serious founding problems. These problems are mostly confined to regions where there are clayey soils containing montmorillonite.

Most clays originate from the decomposition of minerals in rocks. Expansive soils can be classified as residual or transported, depending on their formation.

Residual soils result from in situ decomposition of rock. The following rock types can develop residual soils: Basic igneous rock (Norite of the Bushveld Igneous Complex, Dolerite of the Karoo Sequence, Andesite or Diabase in the Pretoria Group, or Lavas of the Ventersdorp Supergroup) - the active clay horizons are often close to the surface; Argillaceous rocks such as shales and mudrocks of the Ecca or Beaufort Groups and the Dwyka Formation (Cretaceous marine formations also fall in this category), Tillites or Varvites of the Dwyka Formation.
A considerable thickness of active soil at the top of the formation can exist before bed rock is reached.

Transported soils - sediment material is transported by a natural agency, such as water, wind, gravity or ice, as follows: Alluvium is deposited by streams from a variety of materials in the catchment and often attain considerable depth in back-swamp or flood-plain deposits; Lacustrine deposit is formed by a stream depositing from a mixed source in a pan, lake or vlei; Gulleywash is obtained from the local catchment, which may contain a variety of active soils, sometimes to considerable depth; Hillwash, or fine colluvium, is formed by sheetwash.

University of Cape Town

---

[1] - *refer to Chapter Two "Soil Structure and Clay Minerals".*

Certain parent materials can be associated with expansive soils. They can be grouped as follows:

(i) The basic igneous rocks - In these soils the felspar and pyroxene minerals of the parent rocks have decomposed to form montmorillonite and other secondary minerals;
(ii) Sedimentary rocks that contain montmorillonite and which will break down physically to form expansive soils - the shales of Ecca Series cover large parts of South Africa. For example, throughout large areas in the Orange Free State the shales and mudstones of the Karroo System have weathered to potentially expansive soils;
(iii) The residual expansive profiles developed in (i) and (ii) are complemented by transported material derived from these parent rocks and laid down as alluvial, colluvial and lacustrine deposits.
Alluvial and fluvio-lacustrine expansive soils deposited during quaternary times are widely distributed throughout South Africa, specially in the Transvaal and Orange Free State, but are restricted to level or low lying areas.

The type of volume change (that is, shrinkage versus swelling) depends upon the initial water content (wet versus dry) and the change in moisture conditions (drying versus wetting). The principal environment factors which affect the moisture conditions of the soil are:

(a) Climatic (amount of precipitation and rate of evaporation);
(b) Pedalogic (vegetation affects the moisture content);
(c) Hydrologic (location of the water table and conditions of seepage);
(d) Man-made structures.
These enviromental factors around a soil control the moisture conditions in the soil.
The more important causes of water content changes:

(a) Causes of desiccation (drying) - atmospheric evaporation (function of atmospheric climate), transpiration (function of plant type[1]), and heat reaching the soil (function isothermals[2]);
(b) Causes of moisture gain (wetting) - flow from rainfall penetration, water table and natural sources, pools of water on surface, and broken drains.
Moisture can migrate into the soil by: (i) Seepage - flow of water due to gravity; (ii) Capillary - due to suction forces developed within the voids; (iii) Vapour transfer - water vapour flow through the air voids (due to pressure differences in water vapour).

Gains or losses of water by a potentially expansive soil due to climatic and other effects are usually accompanied by heave or settlement of the ground surface.

---

1 - can extract water down to wilting point.
2 - for example, structures subjected to heat.

University of Cape Town

Swelling is most prevalent in climates where the high rate of water evaporation is high compared with that of rainfall. Buildings are often constructed on desiccated soils. These soils can subsequently take water and swelling occurs. Shrinkage on the other hand is most prevalent where climatologic and hydrologic factors are conductive to mainly wet soils, but where prolonged droughts, and consequently high evaporation rates, sometimes occur. Therefore, consideration of only mean temperatures or average yearly rainfall can be very misleading. One must consider the net effect over a given period of time. In a previous report by the present author[1] co-axial diagrams for different area/duration rainfall storms were reviewed. Moisture movements into, through and out of the soil were also discussed, and it was suggested that the diagrams could be used to estimate the depth of rainfall precipitation that goes into the soil.

The swelling behaviour of soil is dependent primarily upon the following factors:-

(1) Composition of the soil: Type and amount of clay minerals; nature and amount of exchangeable cations; proportions of sand and silt; the presence of organic matter and cementing agents.

(2) Initial water content and dry density.

(3) Internal structure: Arrangement and orientation of particles (resulting from natural or manmade processes).

(4) Chemical properties of the pore fluid before and during swelling.

(5) Confining pressure applied during swelling.

(6) Time allowed for swelling.

With the exception of (4) all the above factors are investigated in this Thesis.

It was observed by the writer that if the density of the soil is low enough, it is possible for a structure founded on potentially expansive soil to undergo consolidation settlement while the soil moisture increases. There appears to be a relationship between density and permeability which produces a rather complex situation in that a reduction in density will reduce the amount of swelling but will increase porosity, and thus permeability, which could lead to an increase in the rate of heave and degree of differential movement. Between the extremes of free swell and no volume change, there is a range of volume changes with associated swelling pressures increasing to a maximum restraining pressure for zero volume change.

---

[1] - *Reference 10.*

University of Cape Town

Collapsing Soils:-

For collapse to occur the soil must start with a structure that is open (that is, large void ratio). There are two prime requirements for collapse to be possible - a loose or open soil structure, and a partly saturated soil profile (that is, a moisture content less than saturation). Just how dry the soil must be for maximum collapse to occur is variable, however, all reports agree that moisture deficiency is a requirement.
The amount of collapse and its rate appear to be affected by the mineralogy of the materials present, the percentage of each type of clay mineral, the shape of the bulky grains and their grain size distribution, the moisture content in nature, the initial void ratio, the pore sizes and shapes, the absorbed ions and their concentration in the pore water, the cementing agents, the stress history of the materials, thickness of the soil layer involved, and the amount of added load.
Although the soil type is usually sandy, there is evidence to support collapse occuring in soils which are best described as silts or even clays or combinations of these types.

Collapse implies a radical rearrangement of particles in the soil matrix as opposed to a relatively uniform rearrangement as might occur in consolidation. The rate of collapse is often rapid - however, it is dependent on the rate of increase of moisture content, or other factors[1], which initiate the collapse. The general approach to collapse should always be such as to be aware that collapse could occur even at very low loads.

Collapsing soils have been found in soils from all types of sources, in mountainous areas and on the plains and in arid and humid areas. Soil deposits that have been identified were loessial, aeolian, subaerial, colluvial, mud flow, alluvial, residual, and man-made fills.
The deposited sands rest unconformably on rock systems. They usually have a grey or orange colour. The colour depends on whether the oxide present is one of Iron (orange) or Aluminium (grey). The darkness of the colour depends on the percentage of oxide present in the soil. All the sands display a uniformity of size, which is a direct result of the aeolian mode of transportation.
Particles which are larger and finer than the usual windblown sizes are also present in the windblown sands. The finer sizes may be deposited after travelling in suspension, or from in situ weathering after deposition of larger saltaling grains. According to Knight[2] in collapsing sands the latter can be the cause of the finer portion of the sand.

University of Cape Town

---

1 - *such as vibration.*
2 - *Reference 12.*

Initially in areas of arid climatic conditions rocks are broken down. The breaking down process is caused by the action of temperature, wind and water. When the process has continued long enough for the material to be transported, the sands will either be transported by wind for long distances, or they may be deposited locally.
Local deposition is a result of local dustbowl conditions. In the areas where the sands are deposited the climatic conditions may be different.
Kaolinite bridges are formed between the hard quartz grains. The iron oxide present covers the quartz grains and assists in the cementing together of the grains. The end result is a weakly cemented loosely packed soil mass.

The parent rock is usually granite. The sands are predominantly quartz. Small percentages of heavy minerals (such as, ilmenite and tourmaline) are present. Knight[1] uses this small percentage of heavy minerals to define the origin of the transported sands. Variable quantities of feldspar are present. The hard grains are mainly quartz and chertz. The clay content of the sands vary. Knight[1] quotes an average value of 20 percent for the clay content of collapsing sands. The sample from Sishen tested by Errera[2] had a much lower clay content - this has been confirmed by the writer (refer to Chapter One, Table 1.04, and Chapter Two).
The clay fractions of most collapsing sands consists mainly of kaolinite with minor amounts of illite. The clay is formed as a by-product of feldspar weathering. Adhering to the grains is a fine layer of iron oxide. The iron oxide is a weathering product of the mafic minerals present in wind deposited soil mass.

Aeolian sands occur in extensive areas in the Transvaal, Zimbabwe (Rhodesia), Bechuanaland and South West Africa. Aeolian or windblown sands were deposited mainly during the Pleistocene times. Pleistocene times are associated with arid climatic conditions. Areas where collapsing soils have been found, have rainfalls varying between 410 and 820 mm per annum. Underlying the transported collapsing sands a pebble-marker layer has been found. The weathering of the rock formations underlying the pebble-marker indicates the weathering that has occurred in the collapsing sand (Knight[1]).
The rapidity of in situ weathering is dependent upon climatic conditions and internal soil drainage.
In humid climates and under internal soil drainage conditions the weathering process is accelerated.

University of Cape Town

---

[1] - Reference 12.
[2] - Reference 11.

Residual decomposed granites have been found to collapse. These soils can be found near Cape Town, north of Johannesburg, northern Transvaal, Swaziland, and Zimbabwe. This soil type is formed when the feldspars and the mafic minerals of the parent rock are weathered in situ.
The resulting soil consists of a large percentage of quartz particles surrounded by finer materials. The finer material consists of fine sand particles with a thin layer of either iron oxide or aluminium oxide adhering to them. As with collapsing sands, clay bridges also link the larger sized particles in the collapsing residual granitic soils.
The colouring of granitic residual soils is either reddish brown or grey. The cause and variations in colouring is the same as for collapsing sands. The parent rock consists mainly of quartz (25% to 40%), feldspar (orthoclase, plagioclase up to 50%) and mica (light or dark).

The weathering process is divided into two main categories, mechanical weathering and chemical weathering. The weathering process usually leaves a loosely packed skeleton of unweathered products. According to Holmes[1] the unweathered products are chiefly quartz and muscovite. Mechanical weathering is the breaking down of the parent rock into smaller particles. Agents of this process are rain, frost and wind. Sudden temperature changes will cause flaking of the parent rock. Chemical weathering is the breaking down of minerals into new components by the action of chemical agents. Representative of these chemical agents are acids in the air, in the rain water and in river water. Mechanical weathering - the weathered materials may either remain in position as residual deposits or be removed by the action of wind or water. The voids in the lower soil horizons are filled with air together with water from rainfall. The jointing of the granite increases the depth of penetration of groundwater which can become acidic in passing through the soil and can under certain conditions reduce the granite to a relatively porous weak soil mass. A reduction in loading will cause a vertical expansion within the rock mass, which gives rise to the formation of sheets of rock due to the opening of joints parallel to the ground surface (a characteristic of granites). The frequency of the existence of the sheets diminishes with depth into the granite.
Once the weathering process has been completed the products that are in colloidal form are transported to other areas. The transportation process can either be due to the flow of water down a slope or by the upward movement of water. The top soil water is removed by plants and evaporation. The water below the surface is then drawn upwards. The weak solutions produced by the leaching of the rocks during the wet season, then become concentrated. Dissolved materials such as the hydroxides of aluminium and iron are then deposited (Holmes[1]).

---

[1] - *Reference 13.*

Chemical weathering - according to Holmes[1], rain water acts as a carrier for dissolved oxygen and carbon dioxide and for various acids and organic products derived from the soil. Natural water is slightly dissociated into H^+ and OH^- ions. The pH of rain water varies between four and seven (ie, it is acidic). The acidity is formed mainly from dissolved carbon dioxide which ionises the water.
The main chemical changes which occur in the soil are:
a) Solution of solubles by water; b) Oxidation of certain substances; c) Hydration of hydrolosis; d) Formation of carbonates.
The feldspars break down under the hydrolysing action of slightly carbonated waters. The main residual products of decomposition of feldspars are clay minerals and silicic acid. Most of the clay minerals initially exist in colloidal solution. Colloid particles are larger than ions but smaller than can be seen by the microscope. The particles eventually congregate into tiny scales or flakes which coat the residual grains. These clay minerals form the clay bridges.

It can be concluded that the soil is in equilibrium at its present overburden pressure and at some moisture content above the critical moisture content. Collapse of the bridges will then occur if the effective stress is increased and the soil is concurrently wetted above the critical moisture content. The effect of this is to collapse the clay bridges.

In South Africa the collapse settlement phenomenon has been identified in a wide range of Transported Soils and also in a number of residual soils other than residual granites of the Basement Complex.
Transported soils - problems with a collapsible grain structure can be encountered with the majority of the following soils:

Soil type	Agency of Transportation	Source
- Hillwash (coarse colluvium)	- Sheetwash	- Acid crystalline rock (clayey sand) - Arenaceous sedimentary (sand)
- Gulleywash	- Gulleywash	- Local catchment (gravels, sands, silts or clays)
- Aeolian	- Wind	- Usually mixed source (sand)
- Littoral deposits	- Waves	- Mixed (Beach sand)
- Biotic soils	- Termites	- The underlying soil (often a clayey or silty sand)

[1] - *Reference 13.*

University of Cape Town

Residual soils.

Residual granite soils of the basement complex, and reported occurrences in the following formations: Magaliesberg quartzite formation of the Pretoria group, Transvaal sequence - moist reddish brown very loose intact micaceous silty medium and fine sand, and residual Magaliesberg quartzite (dry density 1585 kg/m^3); Rooiberg Group of the Bushveld Complex - thin layer (1.0 m) of residual felsite of low dry density (1430 kg/m^3); Sibasa and Nzhele Formations of the Soutpansberg Group - deeply weathered residual basalt (clayey silt); Low dry density of 1200 kg/m^3; Cape Granite suite - slightly moist, grey mottled reddish brown stiff intact clayey silt, residual Cape granite (Dry density - 1440 kg/m^3); Clarens and Elliot Formations and Ecca Group of the Karoo sequence - residual felspathic sandstone; Diabase sill intrusive into shales of the Pretoria Group - dry orange loose clayey and sandy silt; Low dry density 1000 to 1300 kg/m^3; Berea Red Sands residual from Quaternary calcarenites - red or orange silty sand.

Distribution of expansive and collapsing soils:-

Figure 1.04 shows the known areas in South Africa where severe ground movement has occured due to heaving clays and collapsing sands.

University of Cape Town

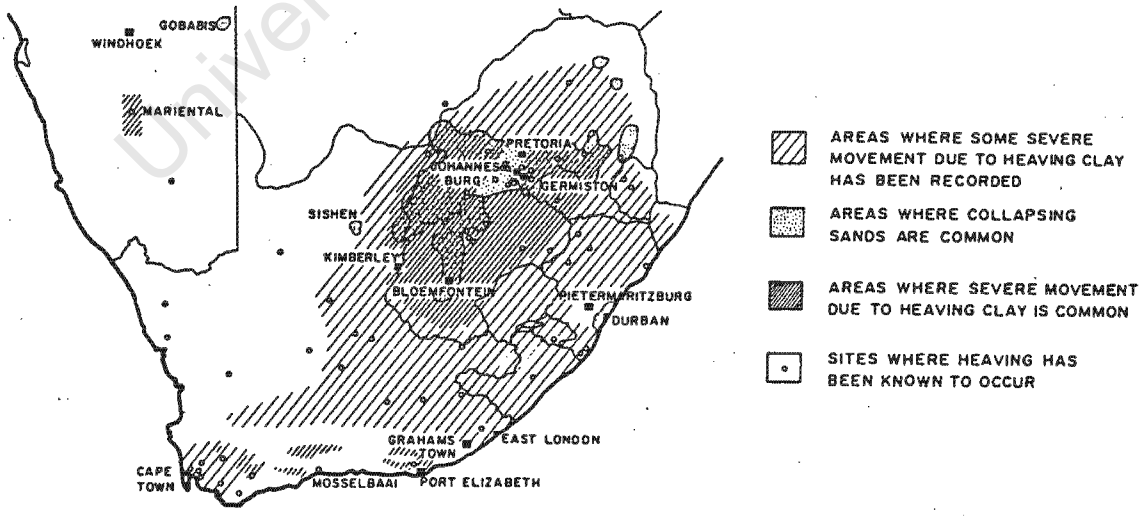

Figure 1.04: Distribution of expansive clays and collapsing sands[1].

[1] - *Reference 9.*

1.5 SOIL SAMPLES

Preliminary field investigations:-

A large number of possible sites were investigated in the Cape Peninsula. Soil samples were obtained from the known sources of expansive soils. During the field trips, the writer was always on the lookout for suitable sources of soil samples. Exposed shales in road cuts were inspected. Quarries and commercial sources of clay were visited. Ground surface cracks were looked for during dry weather. Prior to the field investigations, the writer approached the Geological Survey unit of Cape Town. Useful information was obtained concerning geological maps, decomposition of in situ rock, clays of the Cape Peninsula, and possible additional sites of expansive clays.

Factors such as geological origin, location and visual appearance were initially considered at the time of sampling each site. Natural (but disturbed) soil samples were collected, the locality of the sampling recorded and Linear Shrinkage tests[1] carried out in the Soils Laboratory. A wide range of possible sites were selected and investigated further - Atterberg Limits[1] were determined for these sites.

At the Soil Mechanics Laboratory, University of Cape Town, natural soil samples of Berea Red Soil were available in both disturbed and undisturbed states. These soil samples originating from Durban, had previously been sent to Professor Sparks. Additional Berea Red soil samples were requested by the writer - three sets of specially made boxes (wood - marine ply) and bags made of sacking were sent to Durban. Both undisturbed and disturbed samples were subsequently received (refer to the Durban area section of Table 1.03 - Berea Red soils, Sites F, G and H, and to the section on further research in chapter ten).

Laboratory tests:-

The following tests were carried out:
Linear Shrinkage; Liquid Limit; and, Plastic Limit.
The latter two are part of the Atterberg Limits (after A. Casagrande[2]). All the preliminary soil test procedures used in this thesis are detailed in Appendix A. For the purpose of this section, the following are brief definitions of the test procedures adopted.

Linear Shrinkage: The decrease in length of soil mass expressed as percentage of the original length, after the water content is reduced from the Liquid Limit (next definition) to the oven dry condition.

---

[1] - *defined in the following section, "Laboratory Tests".*
[2] - *see Reference 15.*

University of Cape Town

Liquid Limit: The water content expressed as percentage of dry soil (by weight), at the boundary between the liquid and plastic states.

Plastic Limit: The water content, expressed as percent of oven dry soil (by weight), at the boundary between the plastic and semi-solid states.

Plasticity Index: The numerical difference between the Liquid Limit and Plastic Limit.

The next section dealing with the selection of Soil Types includes a more comprehensive introduction to the test procedures adopted in this thesis.

Tabulation of Results:-

The Laboratory test results are summarized in Table 1.03 - also included are the site number, its location, and the natural colour of each soil sample obtained in the field investigation.
The abbreviations and symbols[1], used in Table 1.03, are included below.

Description:		Abbreviation:
Linear Shrinkage	-	w_{Ls}
Liquid Limit	-	w_L
Plastic Limit	-	w_p
Plasticity Index	-	I_p
percent	-	%
dark (colour)	-	dk.
light (colour)	-	lt.
reddish	-	red.
greenish	-	gre.
yellow	-	yel.
grey	-	gry.
cream	-	cre.
orange	-	ora.
chalk	-	clk.
embankment	-	emb.
trench	-	trn.
middle	-	mid.
bottom	-	bot.

Note: The colour olive refers to `green olive'.

University of Cape Town

[1] - *a complete list is included in the " Nomenclature" section of the thesis.*

Table 1.03: Summary of the test results for all the preliminary soil investigations.

Site number, Location:	w_{LS} (%)	w_L (%)	w_P (%)	I_p	Colour
Cape Peninsula					
1, Blackheath, Station rd	1.5	19.4	19.2	1	dk.brown
2, " , Industrial area	4.0	18.9	15.2	4	dk.grey
3, Durbanville, Classens Rd	8.6	36.8	19.4	17	dk.grey
4, Kenridge, Door deKraal laan	6.4	22.1	10.6	12	dk.brown
5, Mowbray, Dir.Sur. Rhodes Av	8.3	31.8	15.2	17	red.orange
6, " , " (middle)	10.8	38.5	15.7	23	red.orange
7, " , " (bottom)	11.3	48.3	17.2	31	red.brown
8, Mowbray, Cricket field emb.	13.7	45.1	22.8	22	red.brown
9, Sommerset West, Gordon Rd	7.9	29.5	10.9	19	dk.grey
10, Pinelands, Ringwood Dr	8.1	49.1	11.1	38	lt.olive
11, Rosebank, Girl's Guide hall	12.2	78.9	36.9	42	lt.red
12, Durbanville, Claasens Rd	8.3	25.0	11.7	13	lt.olive
13, Kenridge, brick factory	7.5	42.9	26.0	17	brown red
14, Mowbray, cricket field	8.6	39.2	17.3	22	yel.orange
15, Durbanville, plot 1632	7.9	53.8	27.2	27	red.brown
16, " , Wellington Rd	8.6	38.0	11.5	26	lt.olive
17, Tygerberg Quarry, entrance	2.9	22.4	17.3	5	red.brown
18, Bergvliet/Firgrove, freeway	13.7	51.1	15.5	36	lt.grey
19, Mowbray, Liesbeek Gardens	5.0	19.2	12.1	7	lt.grey
20, " , Liesbeek Flats	4.0	45.9	34.8	11	yel.olive
21, Rondebosch, Avoca Rd	8.6	47.3	24.2	23	lt.olive
22, Tygerberg Quarry, by road	8.6	46.1	15.7	30	red.brown
23, Durbanville, Wellington Rd	11.0	58.1	21.7	36	gry.orange
24, " , Barbarossa Rd	8.9	55.2	27.2	28	red.brown
25, Kenridge, Tygerberg Val. Rd	15.1	67.5	19.5	48	red.brown
26, " , " (quarry, mid.)	12.6	48.9	15.1	34	lt.yellow
27, " , " (" , bot.)	14.0	67.6	21.5	46	lt.grey
28, Wynberg, Main & Millbank Rd	6.5	55.0	29.9	25	yel.cream
29, " , " (bottom layer)	9.4	76.5	31.3	45	lt.brown
30, Hout Bay, Victoria Rd (emb)	6.1	50.6	30.9	20	cre.orange
31, " " (trn)	7.8	51.6	25.7	26	orange red
32, Kommetjie, Fish Hoek Rd	7.2	48.7	28.6	20	grey white
33, Fish Hoek, Ranger Rd (1)	7.2	46.4	22.3	24	cre.white
34, " , " (2)	8.0	53.6	29.9	24	clk.white
35, " , " (3)	8.5	45.6	22.6	23	clk.white
36, Rondebosch, Woolsach Dr (1)	8.3	46.6	23.5	23	red.brown
37, " , " (2)	10.8	64.2	29.0	35	red.brown
38, " , " (top 1)	11.9	48.5	27.5	21	dark soil
39, " , " (top 2)	5.8	42.0	28.0	24	dark soil
40, " , " (3)	3.6	22.4	14.0	12	yel.orange
41, Sishen, M&S constr.site trn.	0.1	12.8	12.2	1	pale yel.
42, Parow, Frans Conradie Dr	5.5	33.3	13.0	20	gre.grey

University of Cape Town

Site number, Location:	w_{LS} (%)	w_L (%)	w_p (%)	I_p	Colour
Cape Peninsula (continued)					
43, Bellville, La Rochelle Chr.	13.9	55.8	24.3	32	yel.orange
44, " , " (hole 1 bot)	9.6	51.2	26.1	25	yel.orange
45, " , " (hole 2)	10.5	62.8	26.5	36	yel.orange
46, " , " (hole 3 top)	5.8	42.0	23.2	19	orange
47, " , " (hole 3 bot)	4.3	38.1	20.1	18	lt.grey
49, Epping Garden Centre	15.7	76.6	15.1	62	grey
50, Wynberg Library Cape	9.2	66.8	28.1	39	lt.brown
51, Durbanville, Shop. Centre	12.2	50.2	18.9	31	dk.yellow
52, " , Brickor quarry	8.9	41.9	21.6	20	red.
53, Tygerberg Quarry (turn off)	10.1	41.6	22.3	19	dk.olive
54, Somerset West (top layer)	3.6	26.7	12.9	14	dark grey
55, Macassar Extension 4	7.0	43.0	28.0	15	dk.brown
Other areas					
48, Lady Grey Distr, Farm Unity	11.5	42.2	19.4	23	grey
56, Isando, Transvaal	10.0	51.0	28.0	23	red.brown
Durban area - Berea Red Soil					
A, Berea Road	3.7	23.4	12.4	9	red.brown
B, Francois Road	0.5	15.1	13.3	2	dk.brown
C, Margareth Mayton Ave.	1.8	20.5	16.6	4	ora.brown
D, Rose Hill	2.2	21.6	15.5	6	dk.red.
E, Yellow Wood Parkway	7.0	37.0	22.0	15	dk.red.
F, Reservoir No.3, Woodlands	4.0	33.8	16.7	17	red.brown
G, Harrison & Ronald, Glenhills	7.8	40.9	23.2	18	red.brown
H, King George V Ave., Glenwood	2.9	26.2	13.1	13	red.brown

University of Cape Town

Plasticity Index and Liquid Limit:-

Many properties of silts and clays can be correlated with the Atterberg Limits[1]. These properties include their strength, compressibility, reaction to shaking test and consistency near the plastic limit. The correlation is done by means of the Plasticity Chart (after A. Casagrande - see Ref. 15) included as Figure 1.05. In this chart, the ordinates represent the Plasticity Index and the abscissa the corresponding Liquid Limit values, taken from Table 1.03 above. The plasticity chart also includes the Casagrande A Line separating inorganic clays and silts.

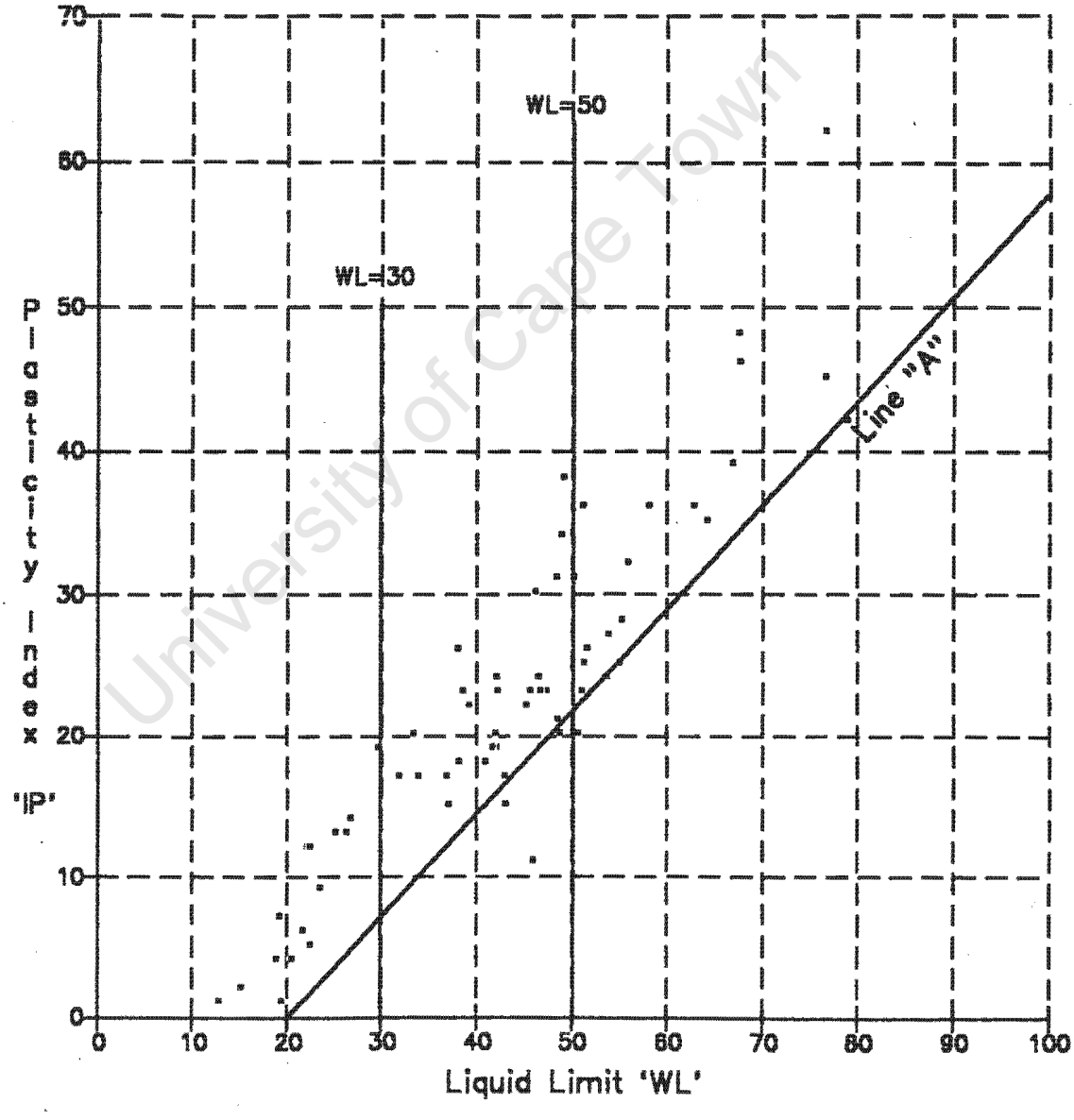

University of Cape Town

Figure 1.05: Plasticity chart - includes the plotted values of Plasticity Index and Liquid Limit, for each site listed in Table 1.03.

[1] - K. Terzaghi and R.B. Peck, Reference 15.

1.6 SELECTION OF SOIL TYPES

The Criteria adopted:-

The Linear Shrinkage results provided the initial criteria to establish potentially expansive soils. The most promising sites were investigated further (refer to previous section 1.5 "Soil Samples"). Known collapsing soil samples were available in the Soil Mechanics Laboratory of the Department of Civil Engineering. They had previously been confirmed as collapsing by various research workers, including Prof. Sparks (1963[1]) and the present writer (1974[2]).

At this stage it should be pointed out that the eventual aim was to select a number of natural soils ranging from known expansive to collapsible ones. In between these two well defined soil types, other soils (of more normal behaviour) would also be investigated. To understand the behaviour of this representative range of natural soils would ultimately enable the prediction of behaviour for similar soil types.
A study was done for each soil sample under consideration. The test results were evaluated and compared. Additional tests, including insitu testing, were carried out on some of the natural soil types initially selected (refer to `Initial Selection of Natural Soil Types', and `Insitu Tests' - which are part of this section). Soil Types were thus selected. They will provide the main source of material for virtually all the tests in this thesis.

Chapter two deals with the structure and clay minerals of the soil types selected in this chapter (refer to Table 1.06, and also Table 1.04). These soil types were selected for the purpose of part two of this thesis - that is, the soil behaviour upon wetting, while under load (refer to Chapter Three - Introduction to the Expansive and Collapsing Behaviour of Soils).

University of Cape Town

---

[1] - *Reference 17.*
[2] - *Reference 2.*

Introduction to Soil States - Consistency Limits:-

Four states can be recognized for describing the consistency of a soil: (1) The Liquid State; (2) The Plastic State; (3) The Semi-solid State; and, (4) The Solid State. These four states are related to the water content "w", and although the transition between each one is gradual, test conditions have been established arbitrarily to delineate the water content as a precise point in the transition from one stage of consistency to the next. These water contents are called the Liquid Limit "w_L", the Plastic Limit "w_P", and the Shrinkage Limit "w_S" - they are determined by oven dry procedures (defined in the next sub-section `Soil Testing Procedures'[1]).

Stages of consistency:-

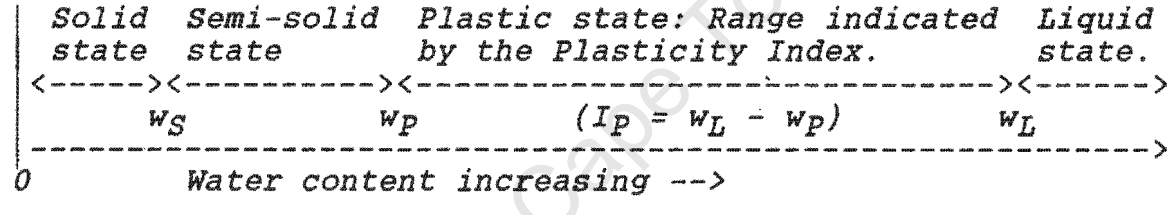

Initial selection of natural soil types:-

A Laboratory study was carried out to determine the basic engineering properties of the soil types initially selected - Table 1.04 summarizes the results of the Laboratory study. Each result is a weighted average of several tests performed on that particular soil type, in accordance with the specified test procedure. The test procedures are introduced and defined in the next section - Appendix A includes the detailed Indicator Test procedures used to determine the basic engineering properties.

Most abbreviations used in Table 1.04 (below) were previously defined for Table 1.03 - refer to section on `Soil Samples'. Additional abbreviations are defined below.

Abbreviation:		Description:
Clay	-	Particle size smaller than 0.002 mm;
Silt	-	Particle size smaller then 0.02 mm;
Sand	-	Particle size smaller than 2 mm;
G_S	-	Specific gravity.

Note: A complete list of symbols and abbreviations is included in the Nomenclature section of the thesis.

[1] - *fully described in Appendix A.*

University of Cape Town

Table 1.04: Basic engineering properties of the natural soil types - the initial selection.

Site Number, Location	w_{Ls} %	w_L %	w_p %	I_p	Clay %	Silt %	Sand %	G_s
Cape area								
11, Rosebank	11.4	69.0	30.7	38	59.0	29.0	12.0	2.755
36, Rondebosch	8.3	47.0	23.3	24	22.0	49.0	29.0	2.688
30, Hout Bay	6.4	49.0	29.0	20	23.0	34.0	43.0	2.637
7, Mowbray	10.5	47.0	22.0	25	42.0	37.0	21.0	2.759
45, Bellville	10.5	62.8	26.5	36	32.0	63.0	5.0	2.746
48, Lady Grey	11.5	42.2	19.4	23	26.0	54.0	20.0	2.750
Berea Red, Durban								
A, Berea road	3.7	25.0	13.1	12	15.0	10.0	75.0	2.665
B, Francois rd.	0.5	15.0	12.9	2	7.5	7.0	85.5	2.704
C, Margaret Mayton Av	1.8	19.7	15.9	4	12.5	4.0	83.5	2.645
D, Rose Hill	2.2	20.6	14.9	6	15.5	4.5	80.0	2.702

University of Cape Town

Definition of test procedures:-

This section provides a definition for each test procedure used in the laboratory study - Appendix A includes the detailed Indicator Test Procedures used in this Chapter.

Linear Shrinkage "w_{Ls}": The linear shrinkage of a soil is the decrease in length of a soil mass (originally moulded inside a trough), expressed as a percentage of its original length, after the water content is reduced from the Liquid Limit (defined next) to an oven dry (105 ± 5°C) condition.

Liquid Limit "w_L": It is the water content, expressed as a percentage of the weight of oven dried soil (to 105 ± 5°C), at the boundary between the liquid and plastic states. The water content at this boundary is arbitrarily defined as the water content at which two halves of a soil cake will flow together for a 12.7 mm (1/2 in) along the bottom of the groove separating the two halves, when the cup (which is part of the liquid device used) is dropped 25 times for a distance of 10 mm at the rate of 2 drops/second.

Plastic Limit "w_p": The water content expressed as a percentage of the mass of oven dried soil, at the boundary between the plastic and semi-solid states. The water content at this boundary is arbitrarily defined as the lowest water content at which the soil can be rolled into threads 3.2 mm (1/8 in) in diameter, without the threads breaking into pieces (but at which water content the threads are just about to break).

Plasticity Index "I_P": The numerical difference between the Liquid Limit and Plastic Limit values. It is expressed to the nearest whole number.

Shrinkage Limit "w_S": It is defined as the water content below which the volume (of the soil sample) remains constant for further air drying - shrinkage limit test results are included at the end of this section (refer to previous section on `Introduction to Soil States - Consistency Limits'[1]).

Particle Size Distribution.
Percentage of sand "% Sand" (with particle size smaller than 2 mm): The distribution of particles larger than 0.074 mm (that is, the amount retained on the number 200 mesh "#" sieve) is determined by sieving.
Percentage of Silt "% Silt" (of particle size smaller than 0.02 mm but larger than 0.002 mm), and percentage of clay "% Clay" (particle size smaller than 0.002 mm): The distribution of particle sizes smaller than 0.074 mm is determined by a sedimentation process, using an hydrometer to secure the necessary data.

Specific Gravity "G_S" - that is, the relative specific density of the soil particles: It is defined as the ratio of the weight in air of a given volume of a material at a stated temperature, to the weight in air of an equal volume of distilled water at a stated temperature.

Soil sampling and description of profiles:-

The location of sampling points is given for the Cape sites. Field information included was obtained during excavation[2]. The soil profile (for each excavated hole) is included as part of Figures 1.06 - 1.11. In situ soil tests were done with field investigations (for founding conditions) at two sites (refer to next subsection). The soil samples from the Berea Red sites, Durban - previously obtained for Prof. Sparks (refer to section 1.5 `Soil Samples'): A summary is included for each soil type previously tested by the writer (1974 - Ref. 2).
It should be noted that no sampling details were available for the Berea Red sites.

University of Cape Town

---

1 - and also to Chapter Four.
2 - refer to section A.2 of Appendix A.

Site 11, Rosebank - Figure 1.06.

This site is located in Alma Road, Rosebank, inside the boundary of the plot belonging to the Girl Guides.

Over a period of time several sampling holes were excavated behind the main building. Undisturbed block samples (300 x 300 x 200 mm) were carefully cut and removed from the side of the sampling holes at depths varying between 0.8 and 1.0 m. The blocks had a slightly dark, reddish brown colour, with a (medium stiff) plastic feel to it. The samples were considerably moist, appearing saturated. Disturbed samples (including the soil cuttings from the undisturbed block) were collected for consistency limits, grading and other indicator tests previously defined in `Test Procedures' - full details in Appendix A[1].

University of Cape Town

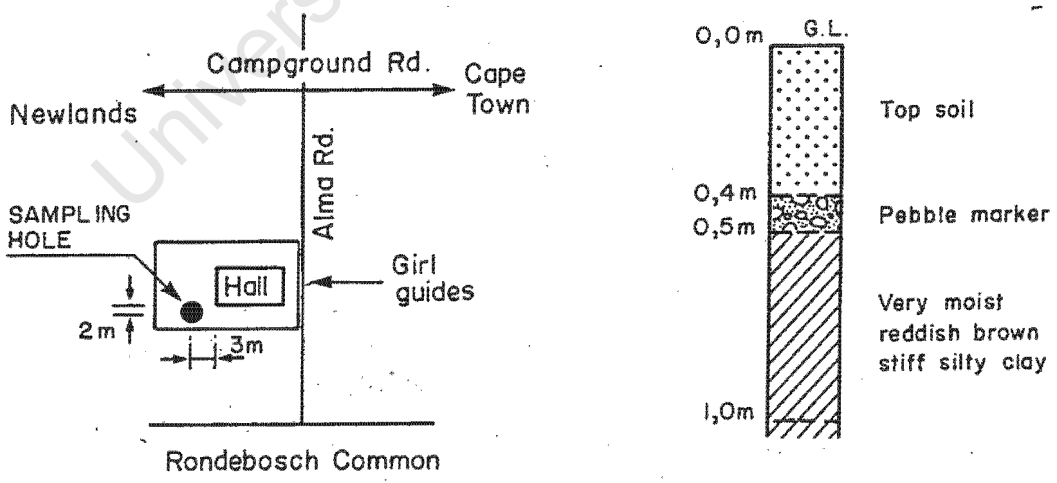

Figure 1.06: Site 11, Rosebank - (i) Location, and (ii) Soil profile.

[1] - *refer to section A.4 "Indicator and Classification Test Procedures".*

Site 36, Rondebosch - Figure 1.07.

The site is situated in Woolsack Drive, between the School of Music and the Baxter Theatre complex, Rondebosch.

A 2.0 m deep trench was previously excavated for laying pipes for the water services. Undisturbed block samples (300 x 200 x 200 mm) were cut and removed from the side of the trench at a depth of 1.5 m. Its colour was a combination of light orange and reddish brown. The soil was slightly moist. When completely moist, it felt soft and plastic. When dry, the soil felt sandy and soft. Disturbed samples were also taken.

University of Cape Town

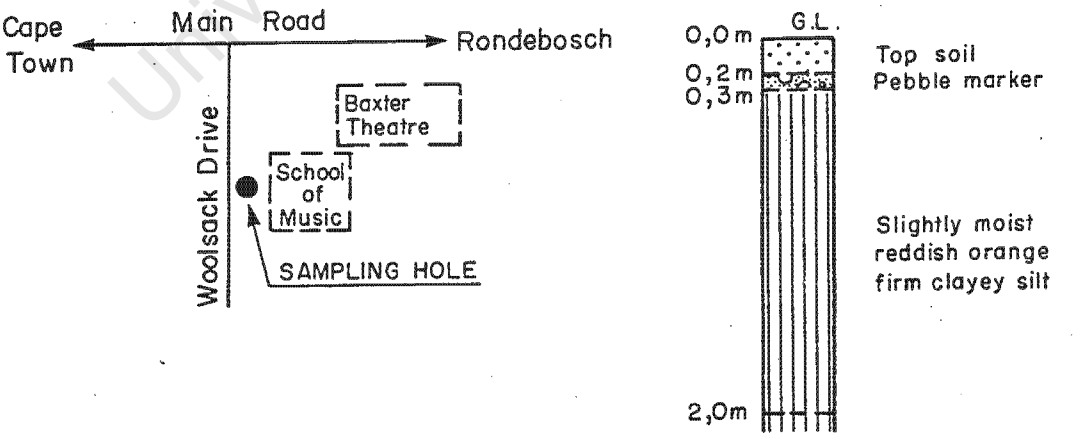

Figure 1.07: Site 36, Rondebosch - (i) Location, and (ii) Soil profile.

Site 30, Hout Bay - Figure 1.08.

It is situated off Victoria Road, Hout Bay - coming from Princess Road, turn right into Victoria Road, and then left into the fifth side street.

A 0.5 m deep hole was made 1.5 m from the top of a 2.0 m high exposed face. Undisturbed block samples (300 x 200 x 200 mm) were cut and removed. The left side of the road was also sampled (undisturbed block taken) at a place where the overburden was removed and the clay layer exposed - see Figure 1.08 (i). Disturbed samples were also taken.

University of Cape Town

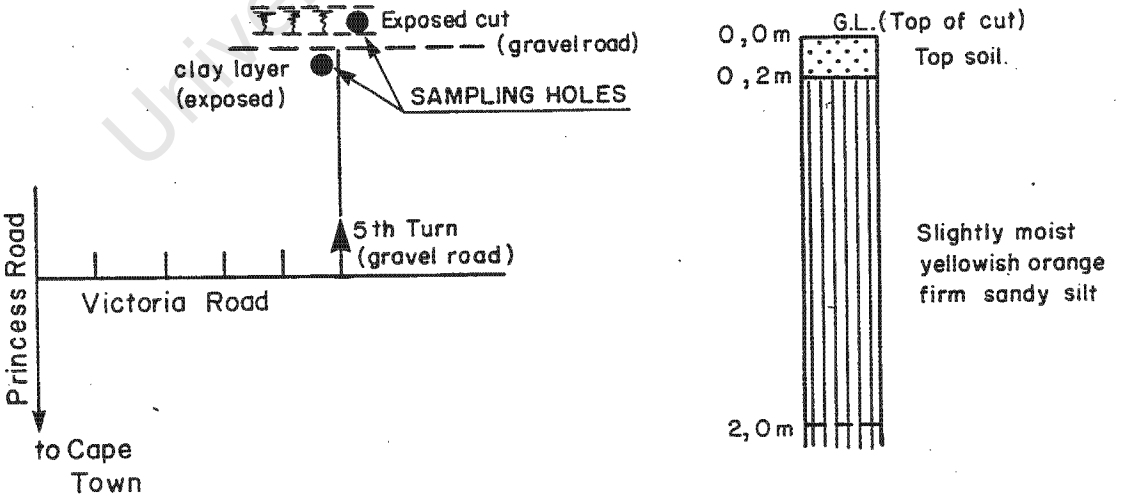

Figure 1.08: Site 30, Hout Bay - (i) Location, and (ii) Soil profile.

Site 7, Mowbray - Figure 1.09.

This site (for the proposed extensions to the Director of Surveys[1]) is situated off Rhodes Avenue, Mowbray - travelling from Cape Town, take the De Waal Drive (becomes Rhodes Drive) and turn left, at the Mowbray turn off, into Rhodes Avenue.
A 3.0 m deep hole was excavated at Test Pit 2 - refer to Figure 1.09 (i). An undisturbed block sample (300 x 300 x 200 mm) was carefully cut and removed from the side (of the sampling hole) at a depth of 2.65 metres. In addition some disturbed samples were taken for Indicator tests (previously defined[2]).

University of Cape Town

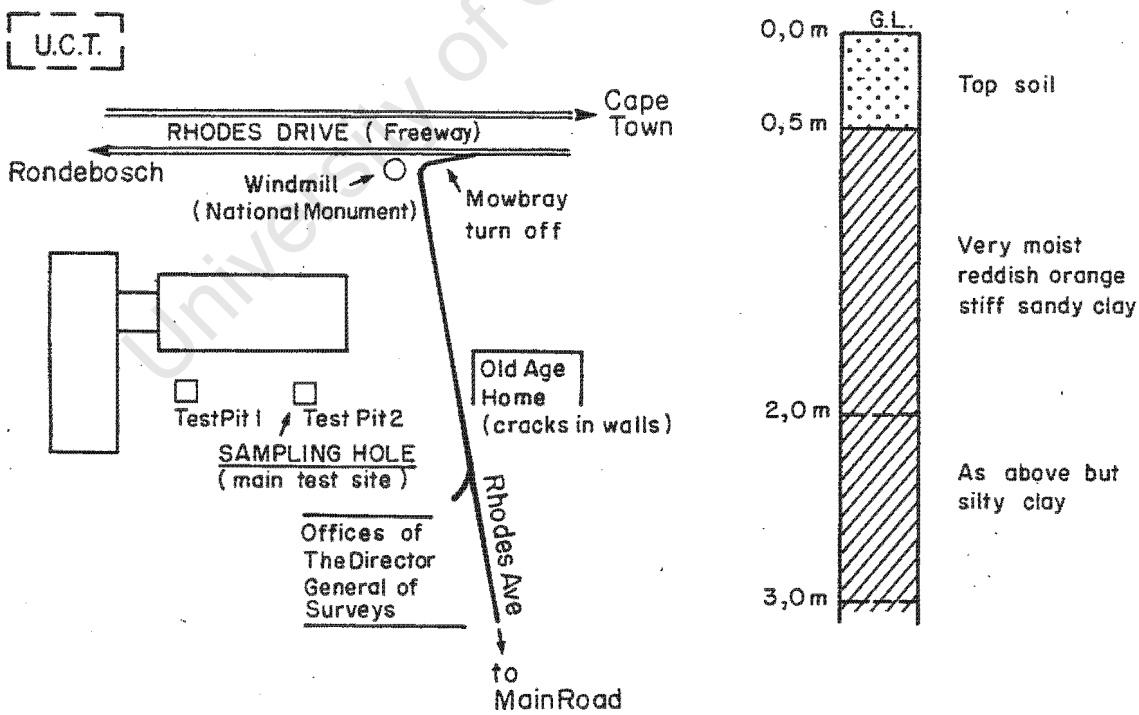

Figure 1.09: Site 7, Mowbray - (i) Location, and (ii) Soil profile.

---

1 - *refer to next section "In situ tests".*
2 - *full details in Appendix A.*

Site 45, Bellville - Figure 1.10.

This site (for the proposed church - refer to next sub-section `In situ tests') is situated in the corner of Haddley and Meerlust Streets, La Rochelle (Oakglen), Bellville - travelling from Cape Town towards Paarl (along the National Road N2), take the Bellville East turn off to Durbanville, turn right at the Old Oak Road (crossing over the N2), and about 1 km along this road turn right into Hadley Road.
A 4.0 m deep hole was excavated at Test hole 2 - refer to Figure 1.10 (i). Representative soil samples (included disturbed samples for Indicator tests, and undisturbed blocks for consolidometer tests) were taken from the side at the depth of 2.5 m. In situ tests were also carried out[1].

University of Cape Town

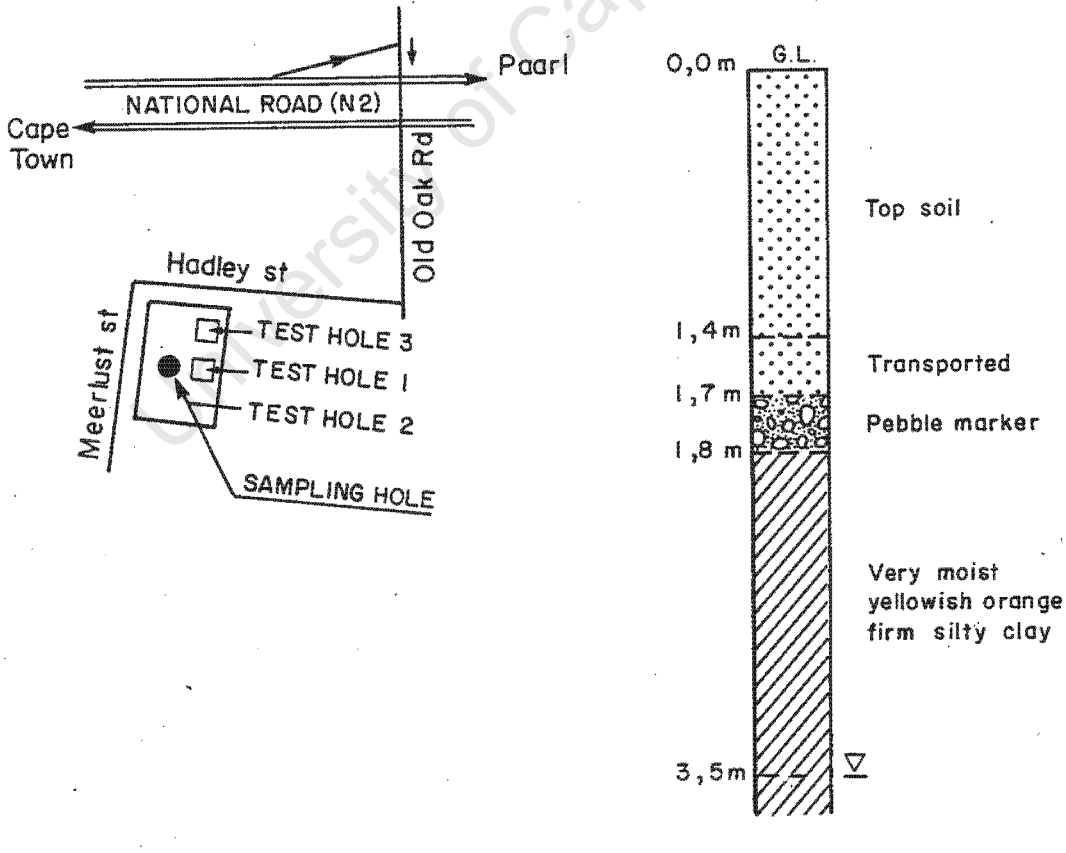

Figure 1.10: Site 45, Bellville - (i) Location, and (ii) Soil profile.

[1] - *refer to `In Situ Tests' in this section.*

Site 48, Lady Grey - Figure 1.11.

The site is situated in the farm Unity, Lady Grey district - travelling from Lady Grey the site is located on the left hand side of the road, as one faces the farm buildings.
Representative soil samples were taken from the side of the road cutting, at approximately 0.5 m depth below the grass surface on the left hand side[1].

University of Cape Town

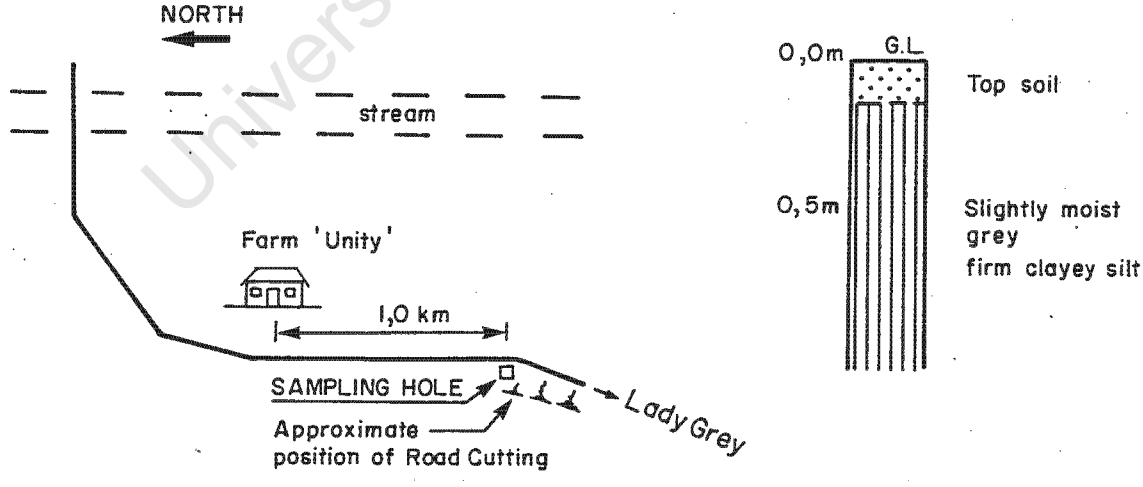

Figure 1.11: Site 48, Lady Grey - (i) Location, and (ii) Soil profile.

[1] - *refer to tests by P.A. Ballantine, Ref. 20.*

Berea Red Soil, Durban.

Site A, Berea Road:

This soil had a dark reddish brown colour, with a certain amount of shine to it; Very little organic matter was present; The size of the particles is less than 0.589 mm diameter - mainly fine sand and clay; The soil felt gritty to touch.

Site B, Francois Road:

Dark brown colour; Some very fine roots (organic matter) were visable; A few isolated particles of size greater than 0.589 mm size were present - it was mostly fine to medium sand; It also felt gritty to touch.

Site C, Margaret Mayton Avenue:

Light orange brown - the lightest colour of the Berea Red soils tested; Small amount of organic matter was visible; Particle size was less than 0.589 mm diameter - a clayey sand; Gritty to touch.

Site D, Rose Hill:

Dark reddish brown; Some small size organic matter; Particle size was less than 0.589 mm - a clayey sand; The soil felt like powder to touch.

University of Cape Town

In Situ Tests:-

In situ tests were carried out as part of the field investigations for two sites - refer to the proposed extensions to the Trigonometrical Survey Office, Mowbray (report to Architect by Liebenberg & Stander, Ref. 21), and the new church at La Rochelle, Bellville[1].
At the request of Liebenberg and Stander (the structural consultant engineers), the writer contributed to the investigation by providing a brief report based on long term tests of the soil samples, involving drying and wetting by increments. The soils report for the site of a new church, was provided directly to the Architect, as requested.

Field investigation at the Mowbray site - soil sample numbers 5 to 7, originate from the same site (refer to previous section on `Soil Samples' - Table 1.3). Six boreholes, four Dutch Probes and two test holes were sunk; Standard Penetration Tests (S.P.T.'s) were made at regular intervals in all cases.

Mowbray Site:

Description of sub-soil strata with depth:-

A) Top Soil (thickness is less than 1.5 m);

B) Sandy clay layer varies in colour from a mixture of light red and dark yellow to reddish orange with depth, and in thickness in the holes drilled, from 8.0 m to 17.5 m. X-ray diffraction of samples from the clay profile indicated that the clay is comprised mainly of hydromuscovite with small amounts of kaolinite and traces of montmorillonite. Hydromuscovite is an illite type mineral. Both kaolinite and illite are characterized by an arrangement of atoms leading up to a negative electrical charge on the flat surface of the crystals. The phenomenon of swelling is considered to be associated with the degree of dominance of these electrical charges[2].

C) Below the sandy clay layer there is a thin band of decomposed sandstone (fine to medium coarse sand grained, varying in colour from white to light yellowish orange), and bands of sandstone boulders occurring in places with decomposed shale and quartz pebbles varying in thickness from 1.0 to 3.5 m.

D) Below the sandstone the material changes from a decomposed shale to a weathered shale with depth.
Note: A water table was recorded at varying depths, in or immediately above the decomposed sandstone layer.

---

1 - soils report by the writer - Reference 22.
2 - refer to Chapter Two "Soil Structure and Clay Minerals".

University of Cape Town

The in situ test results for S.P.T. (number of blows/300 mm) and Dutch Probes (Point Resistance, KN/m^2) were plotted against depth in Figure 1.12.

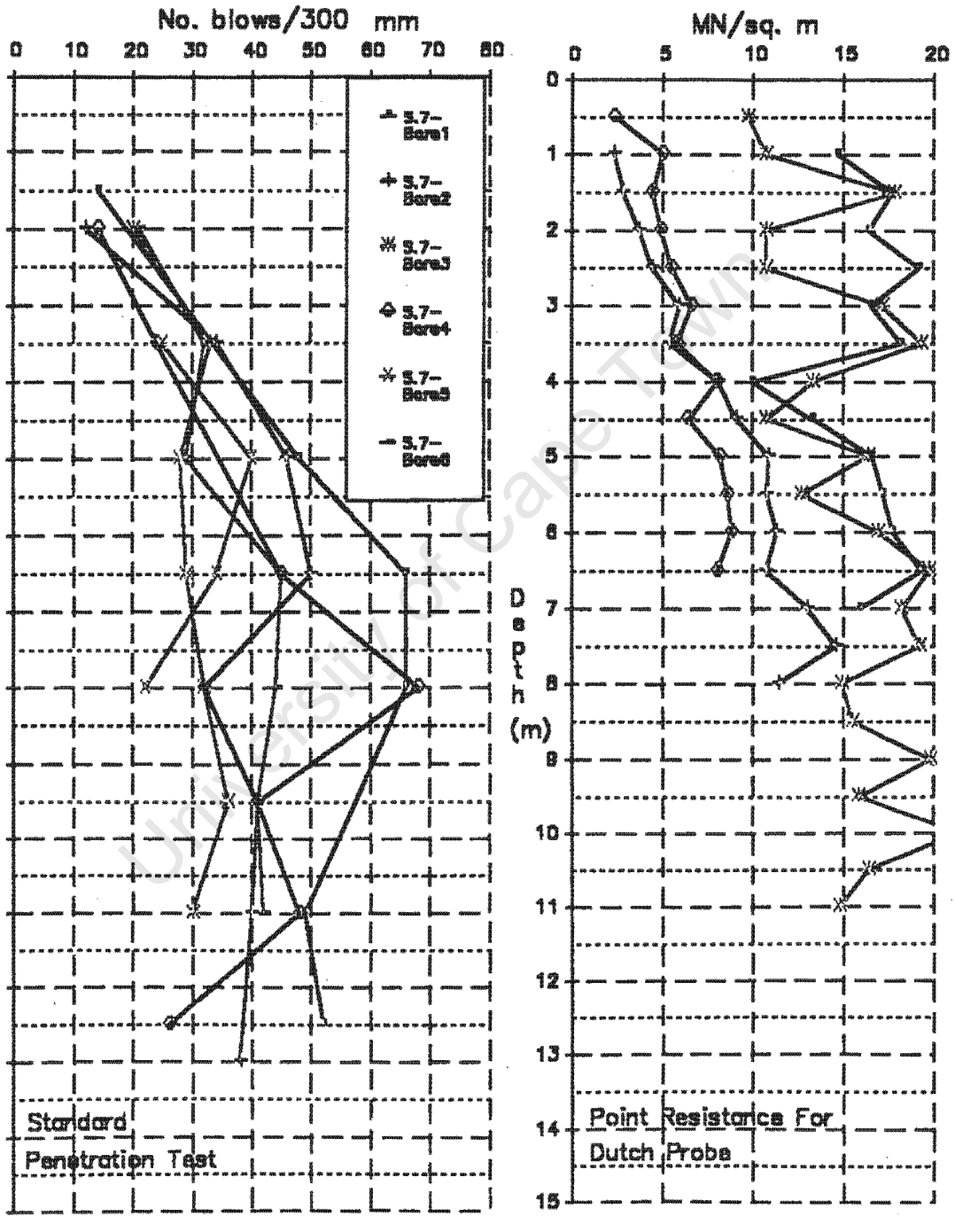

University of Cape Town

Figure 1.12: Mowbray site - in situ test results for S.P.T.'s and Dutch Probes.

La Rochelle Site:

Field investigations for the La Rochelle church site, Bellville - soil samples 43 to 47 originate from this site[1].
The following test information was obtained: Natural water content; Estimated unconfined compressive strength, and shear strength. The results are presented in Table 1.05.

Table 1.05: Results for the three test holes at Bellville[2]:

	Test Holes				
	No. 1		No. 2	No. 3	
	depth =2m	=3m	depth =2.5m	depth =1.5m	=3m
Natural water content, %	28.3	21.6	33.9	20.9	17.0
Estimated unconfined compressive strength `$q_u$' (`q_u' = 2 x cohesion `c')					
(i) From observation of consistency (KN/m^2)	25-75	25-150	25-75	50-150	100-300
(ii) Measurement with pocket penetrometer (KN/m^2)	180	(*)	110	270	400
Estimated shear strength `s' (KN/m^2)	18	(*)	40	18	33 (**)
(note: `s' = `c') Use of pocket shear vane - Pilcon direct reading hand vane tester.					

Notes:
(*) = Does not penetrate - soil too stiff
(**) = Difficult to penetrate

[1] - refer to previous section 1.5 "Soil Samples".
[2] - La Rochelle church site - Reference 22.

University of Cape Town

Natural water content of undisturbed samples:-

Undisturbed soil sample blocks were carefully removed from selected sites of the Cape area - the sample blocks were immediately sealed with wax, and safely stored for later use.
At the time of cutting a test sample (from each undisturbed block), water content measurements were made.
The following are the natural water content `w_n' for each undisturbed block[1]:

Site no.	`w_n' %	(range of w_n)	Date of sampling	Remarks
11.	28.3	(27.1 - 29.0)	27/02/77	
	30.9	(30.6 - 31.1)	11/10/77	
	35.8	(35.0 - 36.5)	16/07/77	Near top of clay layer.
	40.8	(40.6 - 41.0)	16/07/77	0.5 m below top of clay.
36.	14.8	(13.7 - 16.7)	15/06/76	
30.	13.3	(12.5 - 14.9)	15/06/76	
7.	19.8	(18.6 - 20.6)	23/08/76	
45.	33.8	(-)	22/09/77	Not available.
A.	2.0	(-)	before 1974	Air dried.

Selection of soil types:-

The soil types selected will be used throughout this thesis. They provide the basic range of soils from which test information will be obtained for the chapters that follow. Other soil types[2] will also be used in some of the chapters. The soil types selected consist of both natural and artificial soils.

The natural soil types were selected on the basis of the information obtained (refer to previous sections on `Soil Samples' and `Selection of Soil Types'), and the availability of undisturbed soil samples - the selected natural soil types provided the main source of material for most of the tests in the following chapters.

Artificial soils consist of sand (of Site A `Berea Road' particle size distribution - see chapter two) mixed with different percentages of Kaolin or Bentonite clay.
The `made up' soils were prepared in order to enable an individual control of some of the variables influencing the behaviour of a soil.

University of Cape Town

---

1 - *the date of field sampling is also included.*
2 - *from Table 1.04.*

Table 1.06 presents a summary of the measured engineering properties[1] for both the natural and artificial soil types.

Table 1.06: Soil types - summary of the measured engineering properties, as defined for Table 1.04[1].

Site No., location	w_{LS} (%)	w_L (%)	w_P (%)	I_P	w_S (%)	Clay (%)	Silt (%)	Sand (%)	G_S
Natural Soils:									
11, Rosebank	11.4	69.0	30.7	38	22.5	59.0	29.0	12.0	2.755
36, Rondebosch	8.3	47.0	23.3	24	22.0	22.0	49.0	29.0	2.688
30, Hout Bay	6.4	49.0	29.0	20	22.5	23.0	34.0	43.0	2.637
A, Berea Road	3.7	25.0	13.1	12	13.5	15.0	10.0	75.0	2.665
7, Mowbray	10.5	47.0	22.0	25	18.5	42.0	37.0	21.0	2.759
Artificial Soils:									
Kaolin No. (%)									
K.1 (13%)	0.4	12.3	11.8	1	10.0	13.0	3.5	83.5	2.667
K.2 (20%)	1.5	14.0	10.4	4	12.0	20.0	6.5	73.5	2.642
K.3 (8.5%)	0.0	NP	NP	NP	9.0	8.5	2.5	89.0	2.668
Bentonite No(%)									
B.1 (3.5%)	0.1	21.0	20.0	1	14.5	3.5	1.5	95.0	2.640
B.2 (7%)	0.5	32.0	21.0	11	26.0	7.0	2.0	91.0	2.644
B.3 (11.5%)	1.0	46.0	20.0	26	28.0	11.5	2.0	86.5	2.660
B.4 (15.5%)	1.5	59.0	19.0	40	34.0	15.5	3.0	81.5	2.682
B.5 (35%)	6.5	133.0	21.0	112	38.0	35.0	4.0	61.0	2.646

[1] - *for full Indicator Test Procedures and Results refer to Appendix A.*

University of Cape Town

1.7 CONCLUSIONS FOR CHAPTER ONE

In this chapter suitable soil types were identified on the basis of their physical and engineering properties. A number of natural soils, ranging from expected expansive to collapsible ones, were selected. Their basic engineering properties are shown in Table 1.04 of this chapter.
The plotted values of Plasticity Index and Liquid Limit for each site are included in Figure 1.13.
The artificial or `made up' soils introduced in chapter one[1] are also included in Figure 1.13.

On the basis of Figure 1.13, the soil types used in this thesis can be grouped as shown in Table 1.07.

Table 1.07: Soil types grouped according to their plasticity characteristics.

Inorganic Clays of Low Plasticity:-	Medium Plasticity:-	High Plasticity:-
Site A, Berea Rd	Site 36, Rondebosch	Site 11, Rosebank
	Site 7, Mowbray	Site 45, Bellville
	Site 48, Lady Grey	Bentonite B4
	Bentonite B2	Bentonite B5
	Bentonite B3	

Low Cohesion Soils:-	Inorganic Silts of Medium Compressibility and Organic Silts:-
Site B, Francois Rd	Site 30, Hout Bay
Site C, Margaret Av	
Site D, Rose Hill	
Kaolin K1	
Kaolin K2	
Kaolin K3	
Bentonite B1 (small clay percentage)	

The plotted results of Plasticity Index against the Liquid Limit showed that, with exception of the natural soil type for Site 30, (Hout Bay), all the soil types plot above the "Casagrande A" Line separating inorganic clays and silts.

[1] - *refer to Table 1.06.*

University of Cape Town

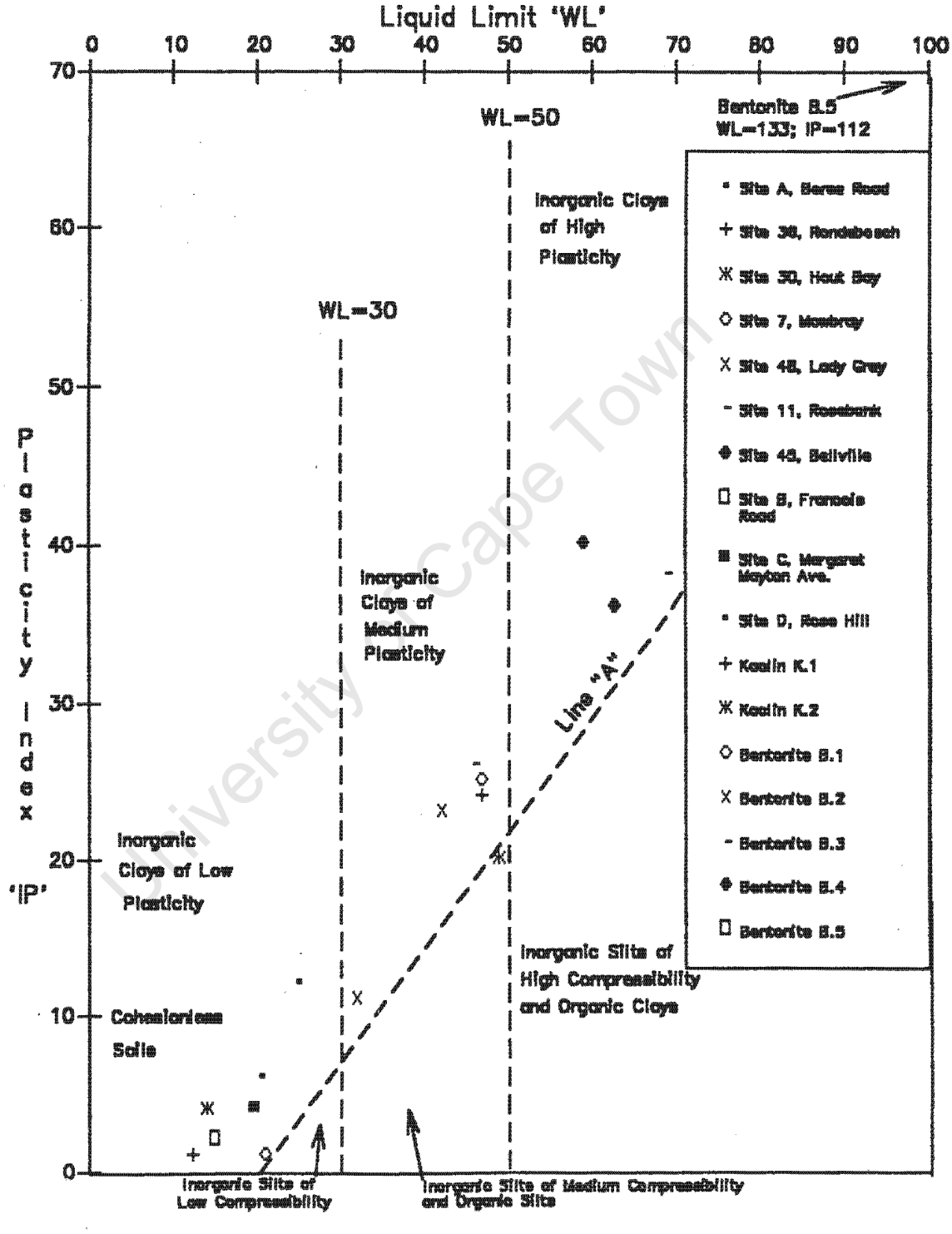

University of Cape Town

Figure 1.13: Plasticity characteristics of the soil types selected.

1.8 REFERENCES FOR CHAPTER ONE

3. CAPTOUR (1985/86): Cape Town and Hinterland - Tourist Guide. Published by the Cape Tourism Authority (Captour), Strand Concourse, Cape Town.

4. THERON, J.N. (1984). The Geology of Cape Town and Environs - Explanation for Sheet Maps (1:50000) 3318 CD, and DC, 3418 AB, AD and BA. Geological Survey (Department of Mineral and Energy Affairs), Pretoria.

5. KING, L.C. and MAUD, R.M. (1964): The Geology of Durban and Environs - Bulletin number 42. Geological Survey (Department of Mines), Pretoria.

6. MAUD, R.R. (1968): Quarternary Geomorphology and Soil Formation in Coastal Natal - Annals of Geomorphology, Neve Folge, Supplementband 7, Seite 155 - 199. Germany.

7. BRINK, A.B.A. (1979 - 1985): Engineering Geology of Southern Africa - Volumes 1 to 4. Building Publications, Pretoria.

8. Geology and Engineering of Transported Soils, Geotechnical Division (S.A.I.C.E.) and Association of Engineering Geologists (S.A. Section): Course held at the University of Stellenbosch in November 1985, to coincide with publication of BRINK, A.B.A. (1985) - Engineering Geology of Southern Africa, Volume 4 of above Reference 7.

9. Problem Soils in South Africa - Symposium held in Johannesburg, September 1985 (Geotechnical Division, S.A.I.C.E.): WILLIAMS, A.A.B., PIDGEON, J.T., and DAY, P. - "Expansive Soils"; SCHWARTZ, K. - "Collapsible Soils".

10. DE S. VINAGRE T.J.V. (1978): Postgraduate course projects for (i) Advanced Soil Mechanics, C.E. 500 (Expansive Soils: Review of the main aspects including their identification; An experimental study of potential expansive soils from the Cape Peninsula); and, (ii) Field Theory and Groundwater Flow, C.E. 529 (Water movement within the Hydrologic Cycle and its interaction with soils: An application to South African Rainfall Conditions). Department of Civil Engineering, University of Cape Town.

11. ERRERA, L.A. (1977): Stress Paths and Collapsing Soils - M.Sc. Thesis. Department of Civil Engineering, University of Cape Town.

12. KNIGHT, K. (1961): The Collapse of Structure of Sandy Sub-soils on Wetting - Ph.D. thesis. Department of Civil Engineering, University of the Witwatersrand.

University of Cape Town

13. HOLMES, A. (1970): Principles of Engineering Geology - 2nd edition. Thomas Nelson and Sons Ltd., Great Britain.

14. JENNINGS, J.E., BRINK, A.B.A., and WILLIAMS, A.A.B. (1973): Revised Guide to Soil Profiling for Civil Engineering purposes in Southern Africa - Transactions of the S.A.I.C.E., Volume 15, Number 1, January 1973.

15. TERZAGHI, K., and PECK, R.B. (1967): Soil Mechanics in Engineering Practise - 2nd edition. J. Wiley and Sons Inc.

16. DE S. VINAGRE, T.J.V. (1976/77): Masters Thesis - Diaries One, Two, Three, Four, Five, and Six.

17. SPARKS, A.D.W. (1963): Discussion in Section A - Expansive and Collapsing Soils and Soil Moisture; and, Section C - Soil Type and Soil Mapping. Proceedings, 3rd Regional Conference for Africa on Soil Mechanics and Foundation Engineering, Salisbury.

2. DE S. VINAGRE, T.J.V. (1974): The Compression of a Collapsing Soil - B.Sc. Thesis. Department of Civil Engineering, University of Cape Town.

20. BALLANTINE, P.A. (1978): Consolidometer tests to determine the stress path in a soil subject to vertical load - post B.Sc. thesis tests for Prof. Sparks. Department of Civil Engineering, University of Cape Town.

21. LIEBENBERG AND STANDER Consulting Engineers (1976): Report to the Architects J. Boyd and Associates in association with R. Nixon and A.C. Orsmond - "Subsoil Investigation carried out at the site of the proposed extension to the Trigonometrical Survey Office, Mowbray, Cape Town", dated January 1976.

22. DE S. VINAGRE T.J.V. (1977): Soils Report for Site Investigation of New Church at La Rochelle, Bellville - for Mr. A. Ellmer (Architect). Department of Civil Engineering, University of Cape Town.

University of Cape Town

CHAPTER TWO *

SOIL STRUCTURE AND CLAY MINERALS

2.1 INTRODUCTION AND OBJECTIVES

The purpose of this chapter is threefold:-

1) To define the macro structure of the soil types selected in chapter one - by macro structure the writer means the 'visible to the human eye' structure, as defined by test procedures and results for each soil (refer to Appendix A);

2) To observe their micro structure, the 'invisible to the human eye' structure, using high magnifications obtained by means of scanning electron microscopy; and,

3) To identify the clay minerals which are present in each soil type, using X-ray diffraction techniques.

The soil structure and clay minerals are of fundamental importance to characterize the behaviour of each soil type. Within the context of expansive and collapsing behaviour of soils (to be introduced in chapter three), the knowledge of soil structure and clay minerals enables the understanding of its behaviour. The basic engineering properties, previously defined in chapter one, categorized the expected range of behaviour between potentially expansive and collapsible.

The study of soil behaviour upon wetting, while under load or unrestrained, will be the main theme of the chapters that follow this one.

University of Cape Town

2.2 MACRO STUDIES

Concerning the soil types previously introduced in chapter one, the following additional aspects are included:

(i) Visual appearance of the natural and artificial soils; Particle size distribution and definition of each soil type (based on grading curves).

(ii) pH value of each soil type - that is, the degree of effective acidity or alkalinity of a soil solution.

(iii) Soil density versus water content relationships for both the standard and modified AASHTO compaction tests performed on the natural soil types.

---

* - *Observations are in Appendices A and B.*

2.2.1 Natural and artificial soil types.

The soil types were selected in chapter one. They consisted of both natural soils[1] and artificial or made up soils. The visual appearance of each soil type is summarized in this section. The origin, formation and basic engineering properties of the natural soils were dealt with in chapter one.

Artificially prepared soils were also used in order to have closer control of the physical structure arrangement, and the measurable engineering properties of the soil. The main purpose was to obtain an homogeneous soil with consistent properties. Two types of artificial soils were prepared: The first type consisted of kaolin clay mixed with sand of similar grading to that of the Berea Red soil; and in the second, Bentonite clay was mixed with the same type of sand[2]. The grading curves are included in the next section[2].

The objective of using kaolin clay was to eliminate the possible expansive capability of a soil - by using different amounts of kaolin it was hoped to exercise control of the amount of collapse. By varying the amount of bentonite clay, it was hoped to obtain collapse at low bentonite content, and expansion at high bentonite content.

Visual appearance of the Natural Soil Types.

Site 11, Rosebank: Light reddish-brown colour which feels plastic to touch; Some organic matter is present; Size of particles - all are less than 2.0 mm in diameter.

Site 36, Rondebosch: Light orange reddish brown; Plastic and soft to touch; Small amount of organic matter present; Particle size - all less than 2.0 mm in diameter.

Site 30, Hout Bay: Light cream and yellowish orange; Smooth in appearance - feels somewhat plastic, but is gritty to touch; Very little organic matter present; Size of particles - all are less than 2.0 mm.

Site A, Berea Road: Dark reddish-brown, appears soft but feels gritty to touch; Very little organic matter present; Size of particles - all are less than 0.589 mm (sieve size) in diameter.

Site 7, Mowbray: Light reddish brown; Plastic and soft to touch; Small amount of organic matter present; Size of particles - all are less than 2.0 mm in diameter.

---

[1] - *as found in situ.*
[2] - *refer to 'Particle size distribution'.*

University of Cape Town

Visual appearance of the Artificial Soil Types.

K1 (13% kaolin clay): Light cream colour; Slightly soft but gritty to touch; No organic matter; Particle size less than 0.589 mm (sieve size) in diameter.

K2 (20% kaolin clay): Light cream colour; Soft but gritty to touch; No organic matter; Particle size less than 0.589 mm in diameter.

K3 (10% kaolin clay): Light cream colour; Gritty to touch; No organic matter; Particle size less than 0.589 mm in diameter.

B1 (3.5% bentonite clay): Light cream olive colour; Gritty to touch; No organic matter; Particle size less than 0.589 mm in diameter.

B2 (7% bentonite clay): Light cream olive colour; slightly soft but gritty to touch; No organic matter; Particle size less than 0.589 mm in diameter.

B3 (11.5% bentonite clay): Cream olive colour; Soft but gritty to touch; No organic matter; Particle size less than 0.589 mm in diameter.

B4 (15.5% bentonite clay): Cream olive colour; Soft and slightly sticky (when wet) to touch; No organic matter; Particle size less than about 0.589 mm in diameter.

B5 (35% bentonite clay):Cream olive colour; Soft and sticks (when wet) to touch; No organic matter; Particle size less than about 0.589 mm (sieve size) in diameter.

University of Cape Town

2.2.2 Particle size distribution.

The percentage of sand '% Sand', silt '% Silt', and clay '% Clay', were introduced and defined in chapter one - Tables 1.04 and 1.06 listed those percentages for the natural and artificial soils.

On the basis of the particle size only, the following definitions are used: % Sand size = percentage of material with sizes between 2 mm and 0.06 mm; % Silt size = percentage of material with sizes between 0.06 mm and 0.002 mm; % Clay size = percentage of material with size equal to, or less than 0.002 mm.

This section deals with the particle size distribution for the soils previously selected.
Based on its particle size, each natural or artificial soil is described.
A representative range of particle size distribution is included for each natural soil type - refer to Figures 2.01 and 2.07. Also included with the conclusions for this chapter is a particle size grading envelope for all the natural soils[1].
Figures 2.08 and 2.09 show the range of particle size distribution for the artificial soil types.

A particle size distribution curve is obtained in two stages:
(i) hydrometer analysis; and,
(ii) sieve analysis.
The sieve analysis stage applies to particles of size equal or greater than 0.074 mm (sieve size). The hydrometer analysis stage refers to particle size less than 0.074 mm.

Various dispersing agents were used in order to find the one(s) which prevented flocculation during the hydrometer stage. Appendix A includes the particle size distribution curves obtained (for each soil type) using various combinations of dispersing agents.

University of Cape Town

---

[1] *- refer to section 2.5 'Conclusions for Chapter Two'.*

Natural Soils:-

Site 11, Rosebank - refer to Figure 2.01. Particle size distribution: The soil consisted of 59.0% clay size, 29.0% silt, and 12.0% sand size; and, 93.5% (passing) consisted of soil material with size less than 0.425 mm. Definition of material (based on particle size only) - fine silty clay, with only a small amount (± 10%) of fine sand.

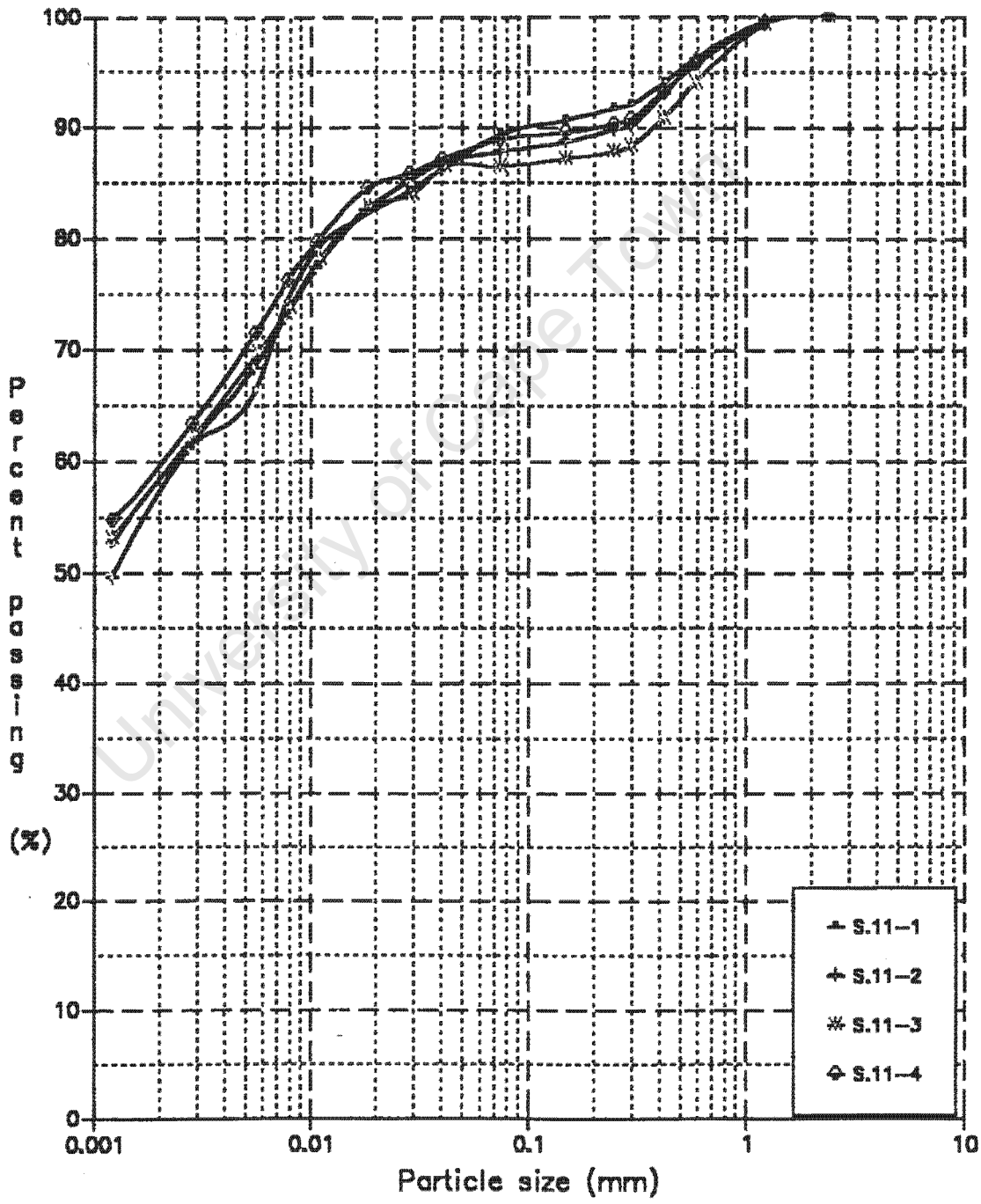

Figure 2.01: Particle size distribution - site 11, Rosebank.

Site 36, Rondebosch - refer to Figure 2.02.
Particle size distribution: 22.0% clay size, 49.0% silt, and 29.0% sand size; Noted that 97.0% (passing) consisted of -0.425 mm size material.
Definition of material - clayey silt, with fine sand (± 30%) and a small amount of medium sand.

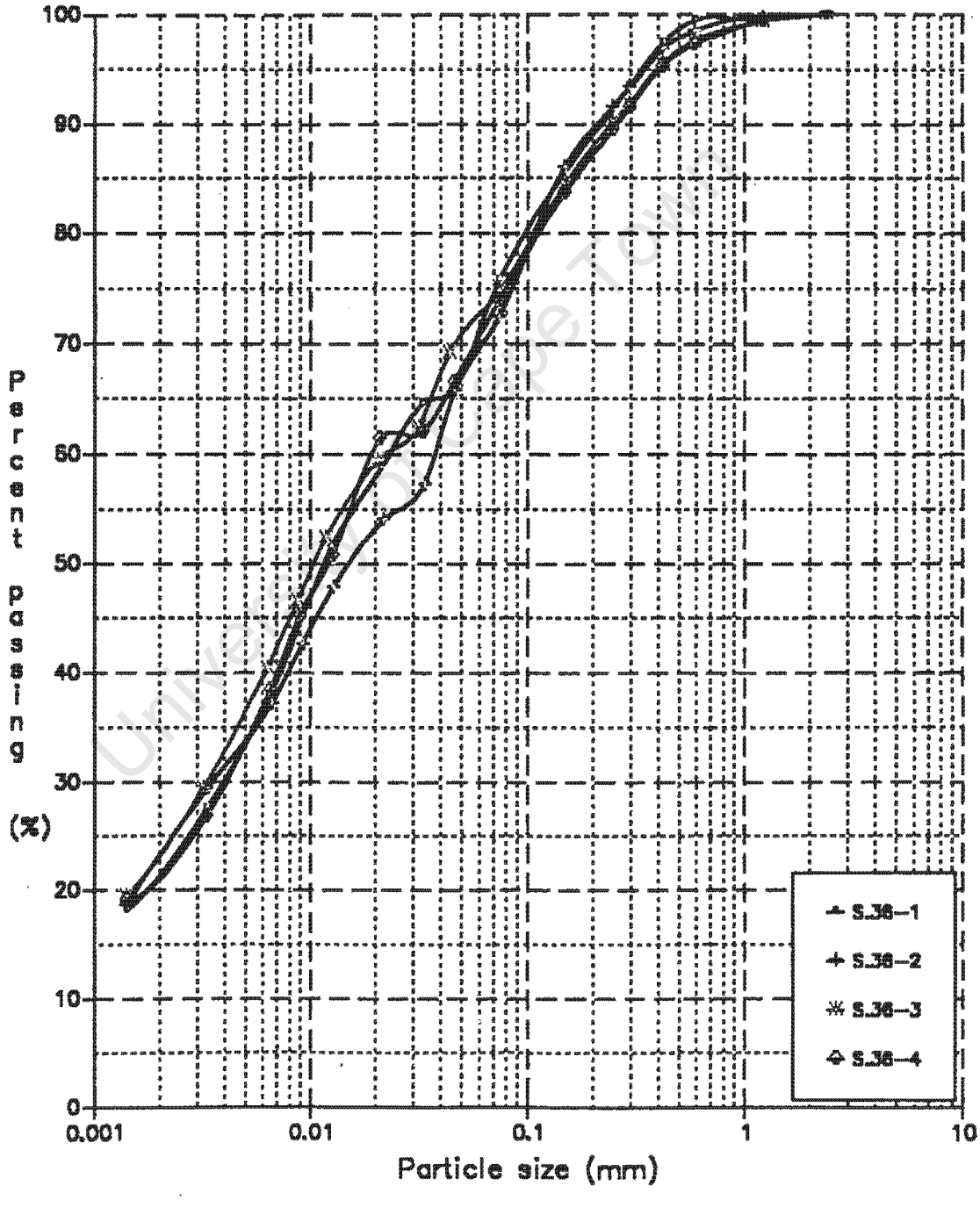

Figure 2.02: Particle size distribution - site 36, Rondebosch.

Site 30, Hout Bay - refer to Figure 2.03. Particle size distribution: 23.0% clay, 34.0% silt, and 43.0% sand size; 80.0% was -0.425 mm size material. Definition based on particle size - fine to medium sandy silt, with a small amount (± 15%) of coarse sand.

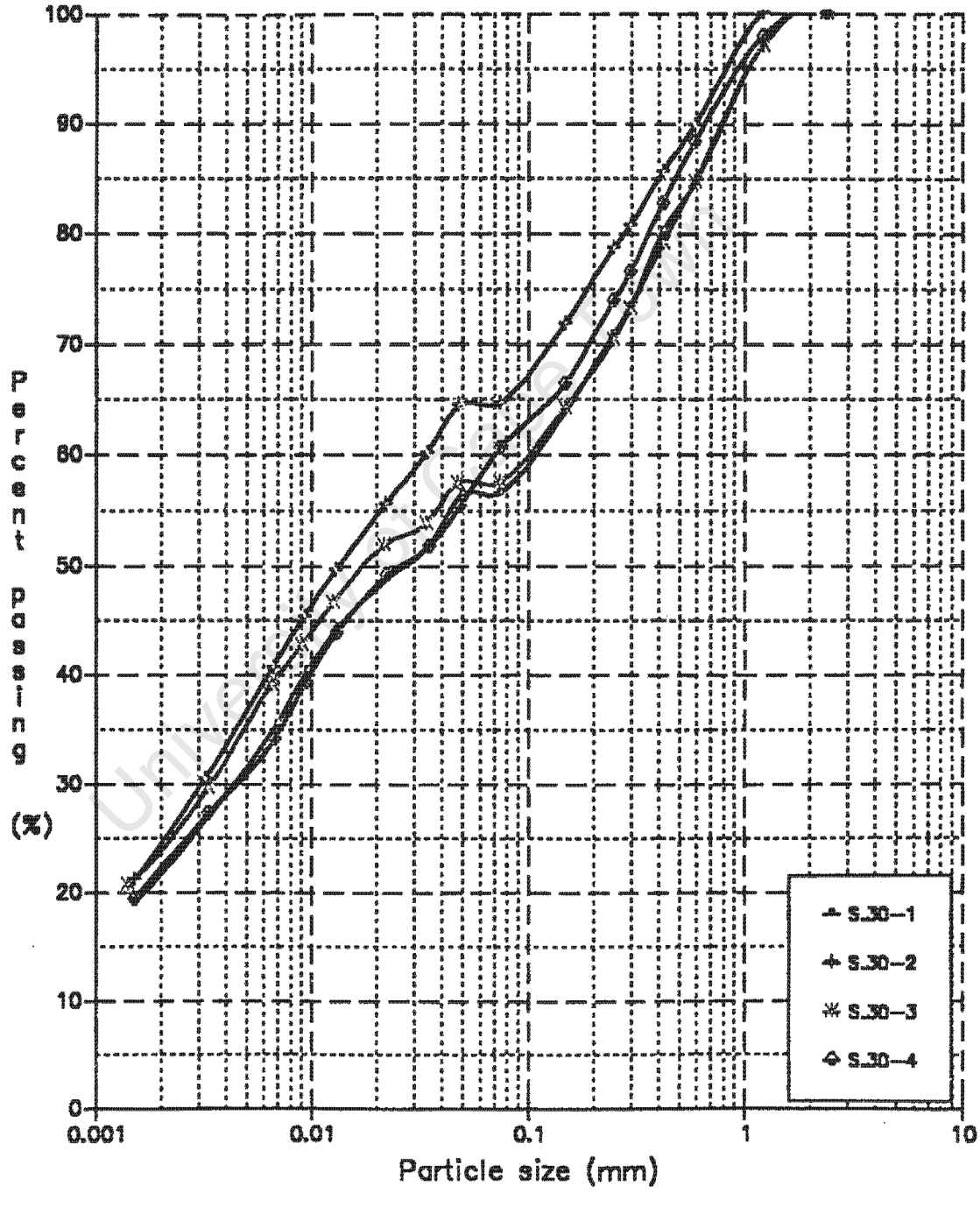

Figure 2.03: Particle size distribution - site 30, Hout Bay. (Comment: Dips in grading curves should not exist[1]).

[1] - *they are due to smoothing algorithm.*

Site A, Berea Road (Durban) - refer to Figure 2.04. Particle size distribution: 15.0% clay, 10.0% silt, and 75.0% sand size; 99.0% was -0.425 mm size material. Definition - clayey sand (fine to medium size) with a small amount of silt.

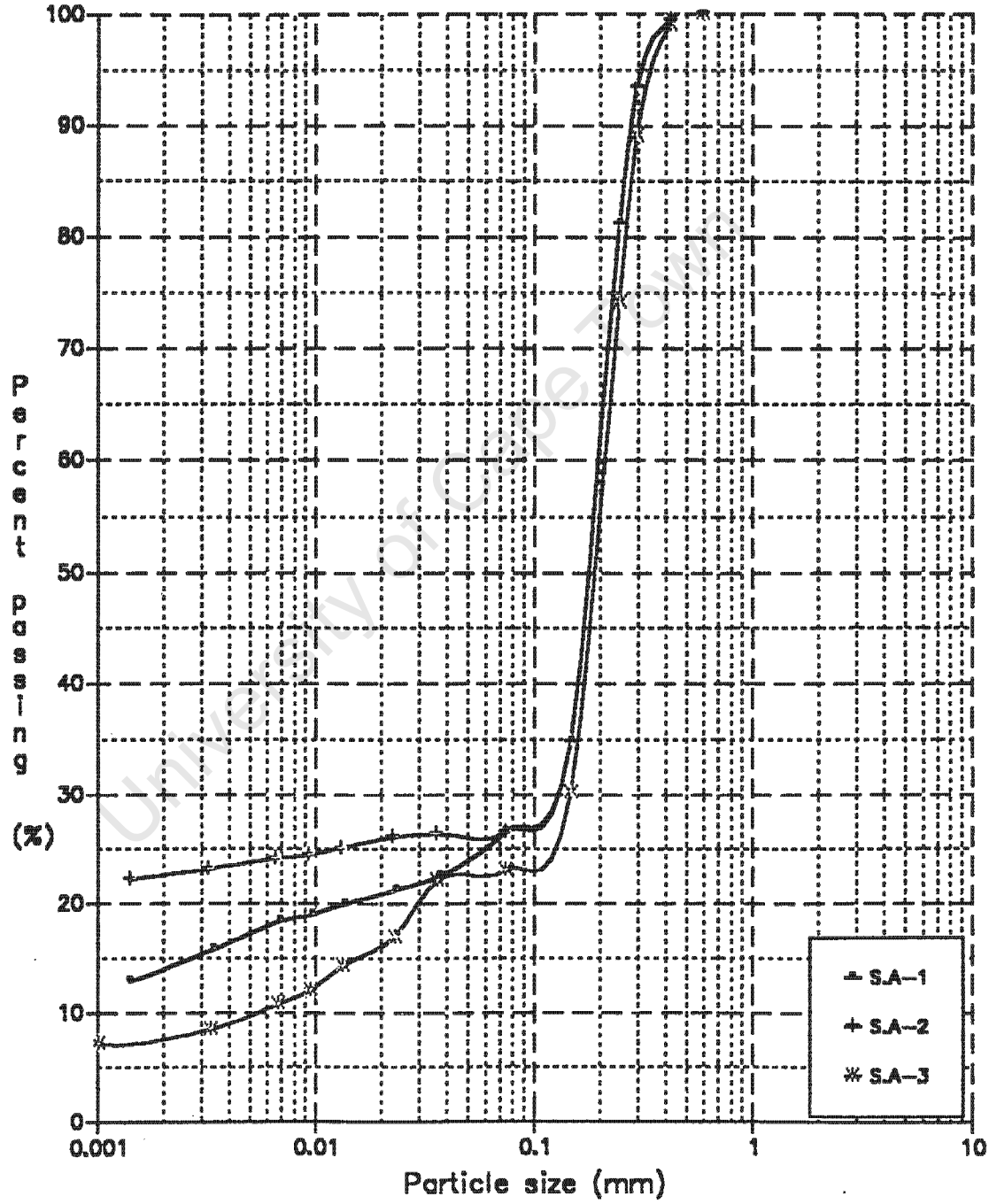

Figure 2.04: Particle size distribution - site A, Berea Road (Durban). (Comment: Dips in curves should not exist[1]).

[1] - *they are due to smoothing algorithm.*

Site 7, Mowbray - refer to Figure 2.05.
Particle size distribution: 42.0% clay, 37.0% silt, and 21.0% sand size; 95.0% was -0.425 mm size material.
Definition - fine silty clay, with a small amount of fine to medium size sand.

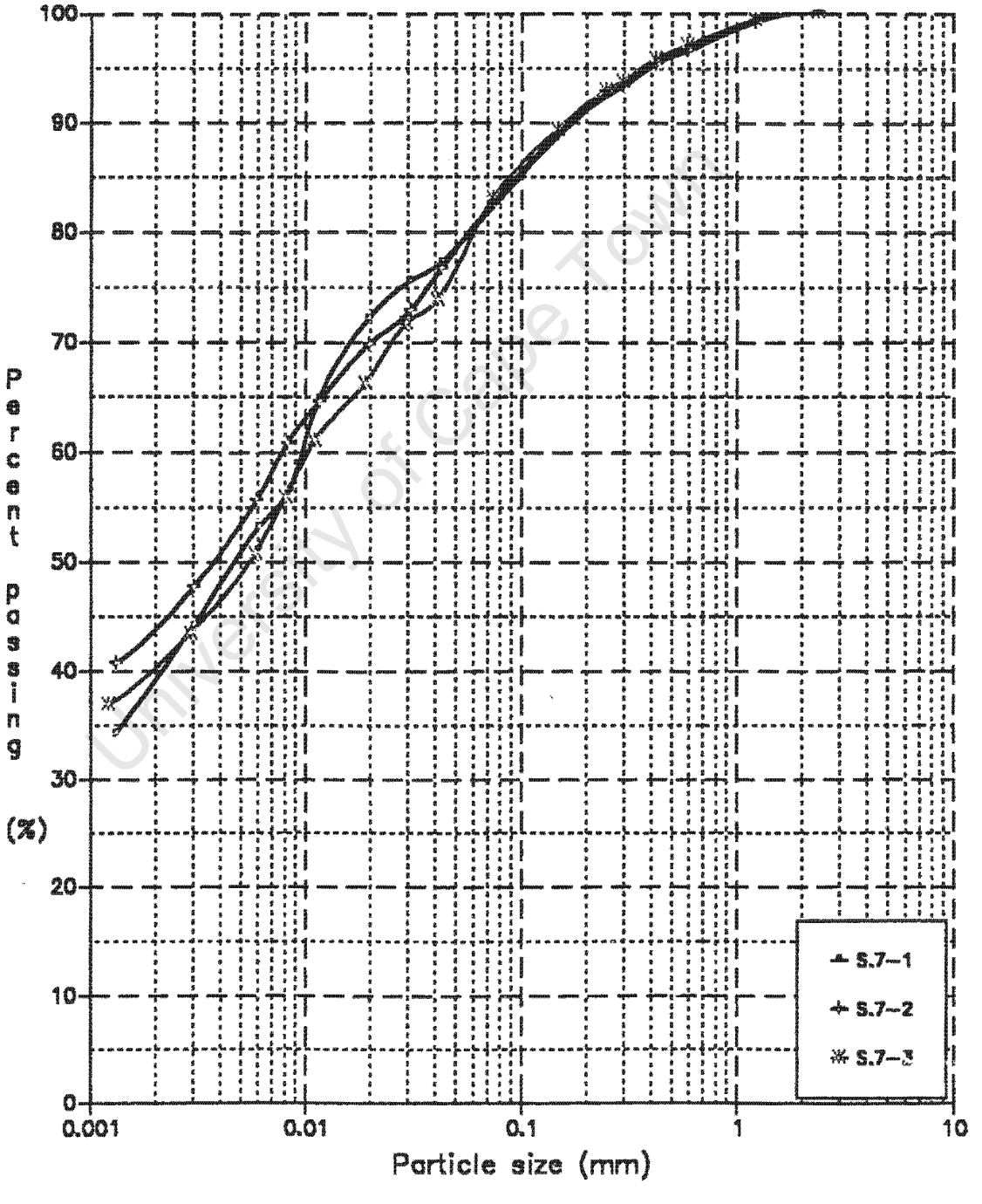

Figure 2.05: Particle size distribution - site 7, Mowbray.

Site 45, Bellville (refer to Figure 2.06): Particle size distribution - consisted of 32.0% clay size, 63.0% silt and 5.0% sand size (noted that 99% was -0.425 mm size material); Definition of material - fine to medium silty clay, with a small amount of coarse and fine sand.

Site 48, Lady Grey (refer to Figure 2.06): Particle size - 26.0% clay, 54.0% silt, and 20.0% sand (99% was -0.425 mm); Definition - clayey silt (medium to coarse), with a small amount of predominantly fine sand.

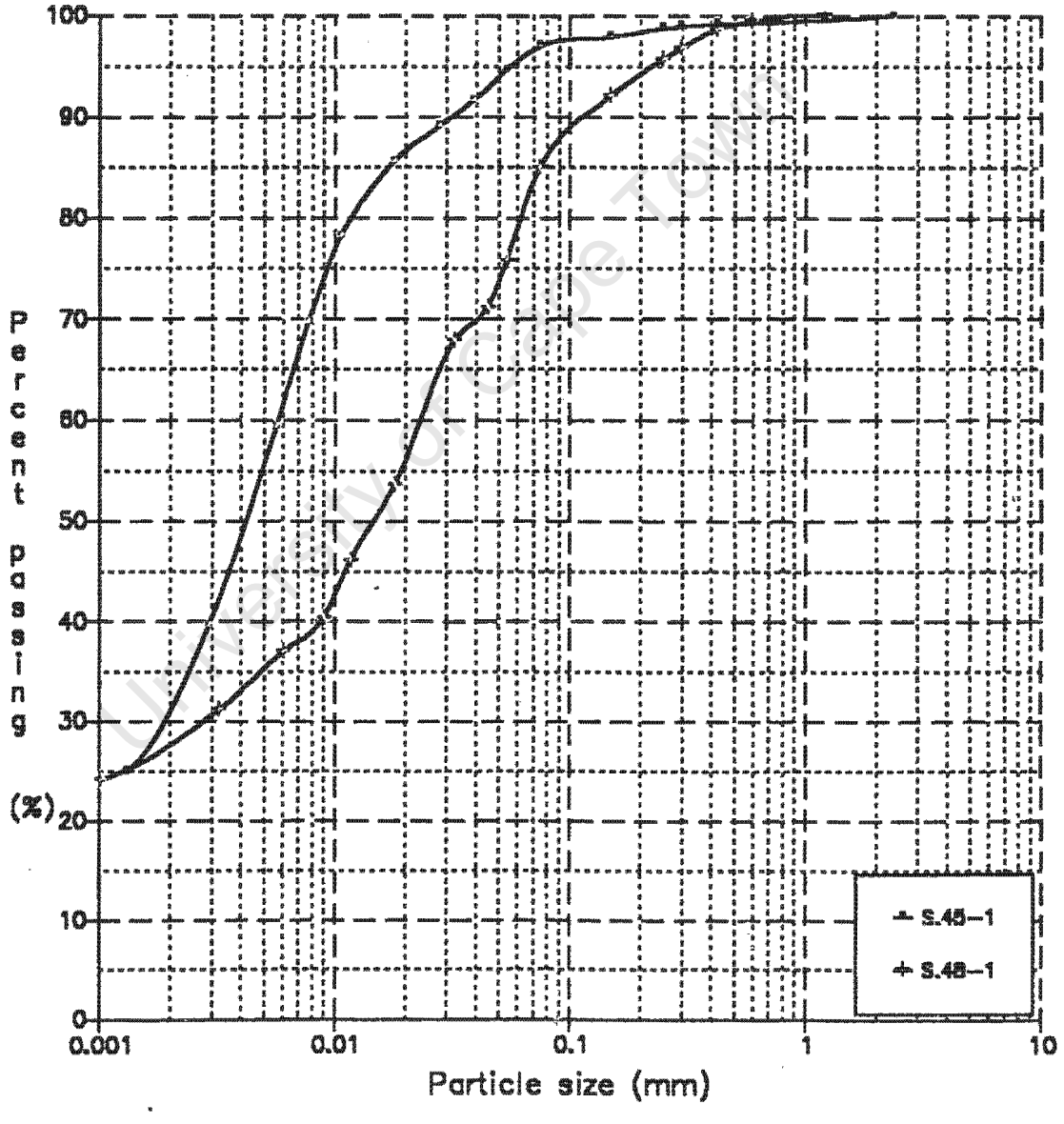

Figure 2.06: Particle size distribution - (i) site 45, Bellville, and (ii) site 48, Lady Grey.

Site B, Francois Road (refer to Figure 2.07(i)): Particle size distribution - consisted of 7.5% clay, 7.0% silt, and 85.5% sand size (noted that 99.5% was -0.425 mm size material); Definition of material - fine to medium sand containing small (but noticeable) amounts of clay and silt.

Site C, Margaret Mayton Avenue (Figure 2.07(ii)): Particle size - 12.5% clay, 4.0% silt, and 83.5% sand (99.5% was -0.425 mm size): Definition - clayey sand (fine to medium size), with a very small amount of silt.

Site D, Rose Hill (Figure 2.07(iii)): Particle size - 15.5% clay, 4.5% silt, and 80.0% sand (99.5% was -0.425 mm); Definition - clayey sand (fine to medium), with a very small amount of silt.

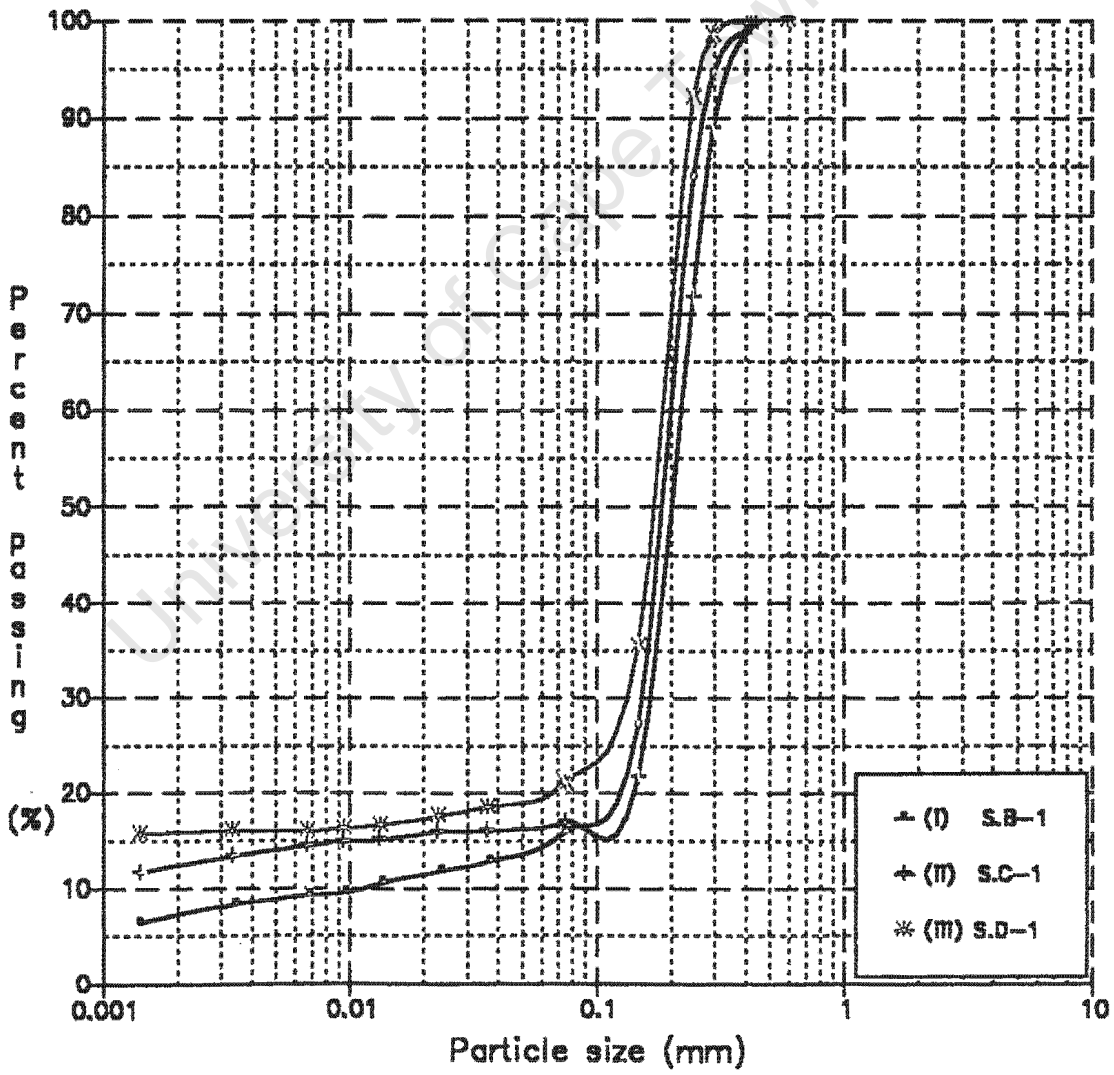

University of Cape Town

Figure 2.07: Particle size distribution - (i) Site B, Francois Road, (ii) Site C, Margaret Mayton Avenue, and (iii) Site D, Rose Hill (all sites in Durban).

Artificial soils:-

Kaolin clay (% used) - refer to Figure 2.08.

Kaolin K.1 (13%): Particle size distribution - consisted of 13.0% clay, 3.5% of silt and 83.5% sand (noted that 99.5% was -0.425 mm size material); Definition - clayey sand (fine to medium size) with a very small amount of silt.

Kaolin K.2 (20%): Particle size - 20.0% clay, 6.5% silt, and 73.5% sand (99.5% was -0.425 mm); Definition - clayey sand (fine to medium), with a small amount of silt.

Kaolin K.3 (10%): Particle size distribution - 8.5% clay, 2.5% silt, and 89.0% sand (99.5% was -0.425 mm); Definition - fine to medium sand containing a small but noticeable amount of clay, and a very small amount of silt.

Bentonite clay (%) - refer to Figure 2.09.

Bentonite B.1 (3.5%): Particle size distribution - consisted of 3.5% clay, 1.5% silt and 95.0% sand size (noted that 99.5% was -0.425 mm size material); Definition - fine to medium sand with a very small amount of clay and silt.

Bentonite B.2 (7%): Particle size - 7.0% clay, 2.0% silt, and 91.0% sand (99.5% = -0.425 mm); Definition - fine to medium sand with a small amount of clay and a very small amount of silt.

Bentonite B.3 (11.5%): Particle size - 11.5% clay, 2.0% silt and 86.5% sand (99.5% = -0.425 mm); Definition - clayey sand (fine to medium), with a very small amount of silt.

Bentonite B.4 (15.5%): Particle size - 15.5% clay, 3.0% silt, and 81.5% of sand size (99.5% = -0.425 mm); Definition - clayey sand (fine to medium size) with a very small amount of silt.

Bentonite B.5 (35%): Particle size distribution - 35.0% clay, 4.0% silt and 61.0% sand (99.5% = -0.425 mm); Defined as a clayey sand (fine to medium), with a very small amount of silt.

University of Cape Town

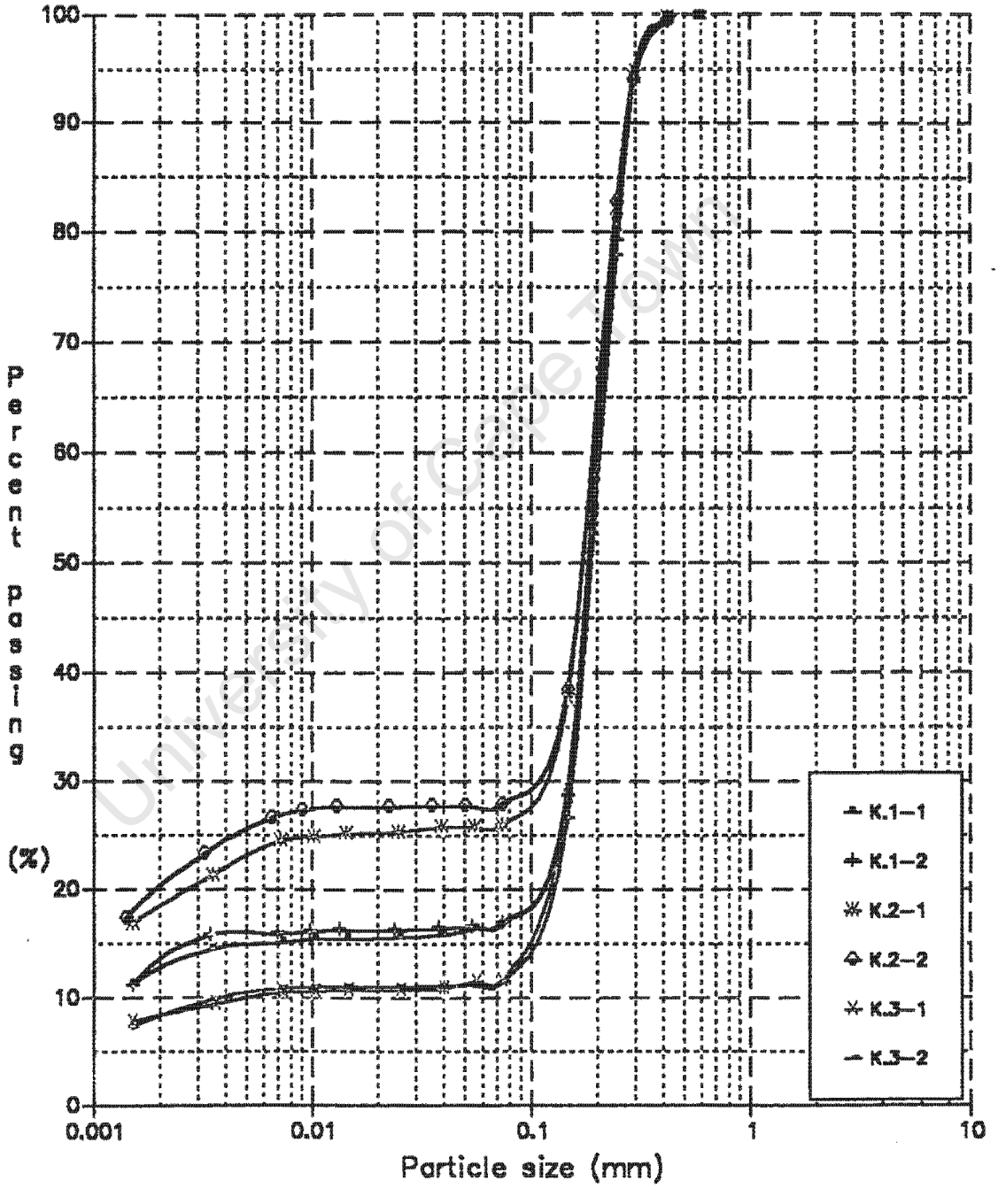

University of Cape Town

Figure 2.08: Particle size distribution - Kaolin K.1 (13%), K.2 (20%), and K.3 (10%).

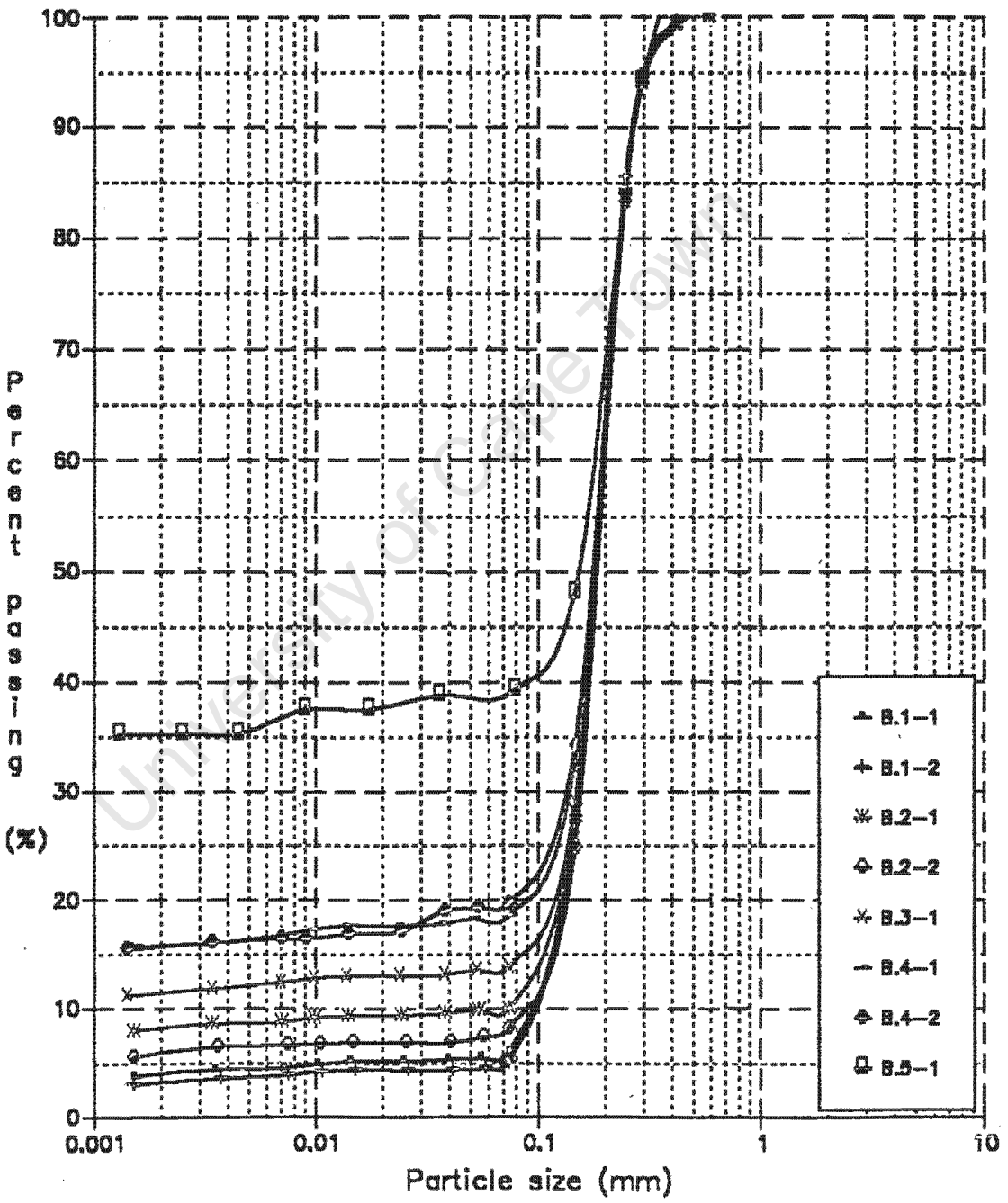

Figure 2.09: Particle size distribution - Bentonite B.1 (3.5%), B.2 (7%), B.3 (11.5%), B.4 (15.5%), and B.5 (35%).

University of Cape Town

2.2.3 'pH' Value of Each Soil Type.

The pH of the soil provides a measure of its acidity, if the pH is less than 7, the soil is called acidic, and if it is greater than 7, it is basic. The pH is determined by inserting a special probe into a mixture of soil and distilled water, previously prepared and which has been stirred gently for about half an hour - refer to test procedure in Appendix A[1].

Definition: The pH expresses the degree of effective acidity or alkalinity of a solution, and is defined as the negative Logarithm of the hydrogen ion concentration of a solution, that is, $pH = - Log(H^+)$. The practical pH range for aqueous solutions extends from 0 to 14, with 0 to 7 indicating the acidic and 7 to 14 the alkalinic range.

'pH' readings were recorded for the soil samples obtained in the preliminary soil investigations described in Chapter One. The pH measurements are included in the Appendix A[2].
Table 2.01 (below) lists the pH values of the soil types previously selected for this thesis.

Table 2.01: Soil types - pH values, as defined above (refer to Appendix A[1]).

Natural Soils:

Site No.	Location	pH	Site No.	Location	pH
[Cape area]			[Berea Red, Durban]		
11,	Rosebank	6.0	A,	Berea Road	6.0
36,	Rondebosch	5.3	B,	Francois Rd.	6.2
30,	Hout Bay	8.5	C,	Margaret Mayton	5.2
7,	Mowbray	4.5	D,	Rose Hill	4.6
45,	Bellville	6.5			
48,	Lady Grey	6.8			

Artificial Soils: (Sand plus Clay)

Clay Type	pH
Kaolin	9.4
Bentonite	9.8

1 - see section A.4.8 'pH Value of Soil Suspension'.
2 - section A.7.5 'pH Measurements'.

University of Cape Town

Table 2.02: Site 11, Rosebank - compaction tests.

[Volume of mould used, 'V_T' = 943.7 cm^3; G_S = 2.755]

Standard AASHTO:

Determination No.	1	2	3	S11/70	S11/71
Compacted soil 'M' (g)	1606	1720	1726	1709	1721
Water content 'w'	0.1807	0.2742	0.3279	0.230	0.276
Water ratio 'Ω'	0.498	0.755	0.903	0.634	0.760
Dry density 'D_D' (KN/m^3)	14.13	14.03	13.51	14.44	14.02
Oven dry soil 'M_D' (g)	1360.2	1349.9	1299.8	1389.4	1348.7
Volume solids 'V_S' (cm^3)	493.7	490.0	471.8	504.3	489.6
Void ratio 'e'	0.911	0.926	1.000	0.871	0.928
Porosity 'n'	0.477	0.481	0.500	0.466	0.481
Degree of saturation 'Sr'	0.546	0.816	0.903	0.727	0.820

Modified AASHTO:

No.	1	2	3	4	5	6	7
'M', g	1548	1675	1804	1888	1903	1859	1816
'w'	0.062	0.1068	0.144	0.1744	0.2304	0.2637	0.2818
'Ω'	0.171	0.294	0.397	0.480	0.635	0.726	0.776
'D_D', KN/m^3	15.15	15.73	16.39	16.71	16.07	15.29	14.72
'M_D', g	1457.6	1513.4	1576.9	1607.6	1546.7	1471.1	1416.8
'V_S', cm^3	529.1	549.3	572.4	583.5	561.4	534.0	514.2
'e'	0.784	0.718	0.649	0.617	0.681	0.767	0.835
'n'	0.439	0.418	0.393	0.382	0.4051	0.434	0.455
'Sr'	0.218	0.410	0.612	0.778	0.9321	0.947	0.930

University of Cape Town

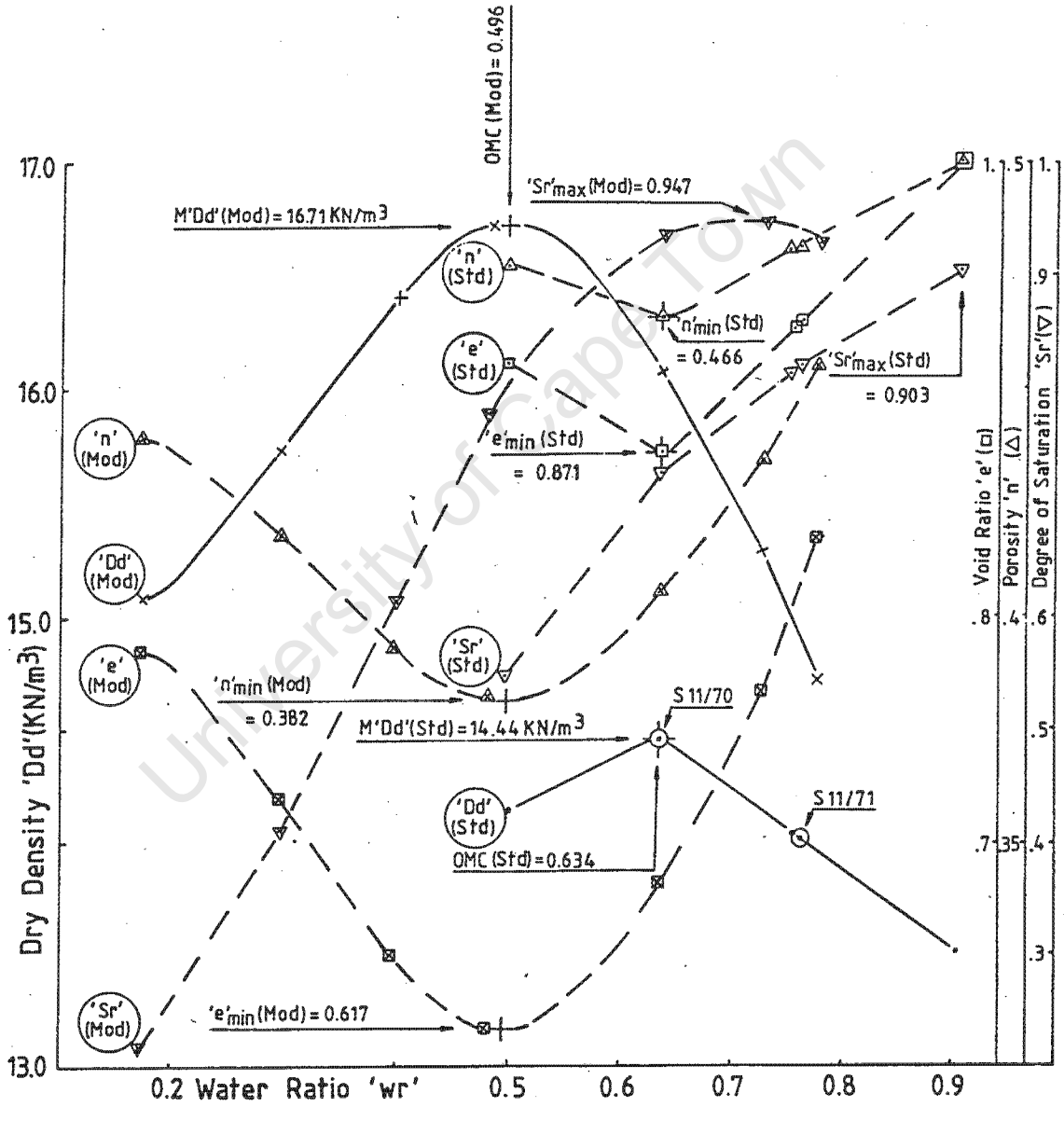

University of Cape Town

Figure 2.10: Site 11, Rosebank - relationships of water ratio versus dry density, void ratio, porosity and degree of saturation.

Table 2.03: Site 36, Rondebosch - compaction tests.

[Volume of mould used, 'V_T' = 943.7 cm^3; G_S = 2.688]

Standard AASHTO:

Determination No.	1	2	3	4	5
Compacted soil 'M' (g)	1757	1849	1923	1895	1844
Water content 'w'	0.132	0.151	0.167	0.186	0.191
Water ratio 'Ω'	0.355	0.406	0.449	0.500	0.513
Dry density 'D_D' (KN/m^3)	16.13	16.69	17.12	16.60	16.09
Oven dry soil 'M_D' (g)	1552.1	1606.4	1647.8	1597.8	1548.3
Volume solids 'V_S' (cm^3)	577.4	597.6	613.0	594.4	576.0
Void ratio 'e'	0.634	0.579	0.539	0.588	0.638
Porosity 'n'	0.388	0.367	0.350	0.370	0.390
Degree of saturation 'Sr'	0.559	0.701	0.832	0.851	0.804

Modified AASHTO:

No.	1	2	3	4	5	6	7
'M', g	1585	1635	1840	1956	2015	1963	1880
'w'	0.0156	0.0463	0.0787	0.1232	0.1624	0.2002	0.2395
'Ω'	0.042	0.124	0.212	0.331	0.437	0.538	0.644
'D_D', KN/m^3	16.22	16.24	17.73	18.10	18.01	17.00	15.76
'M_D', g	1560.7	1562.6	1705.8	1741.5	1733.5	1635.6	1516.7
'V_S', cm^3	580.6	581.3	634.6	647.9	644.9	608.5	564.3
'e'	0.625	0.623	0.487	0.457	0.463	0.551	0.672
'n'	0.385	0.384	0.328	0.313	0.317	0.355	0.402
'Sr'	0.067	0.200	0.434	0.725	0.942	0.977	0.957

University of Cape Town

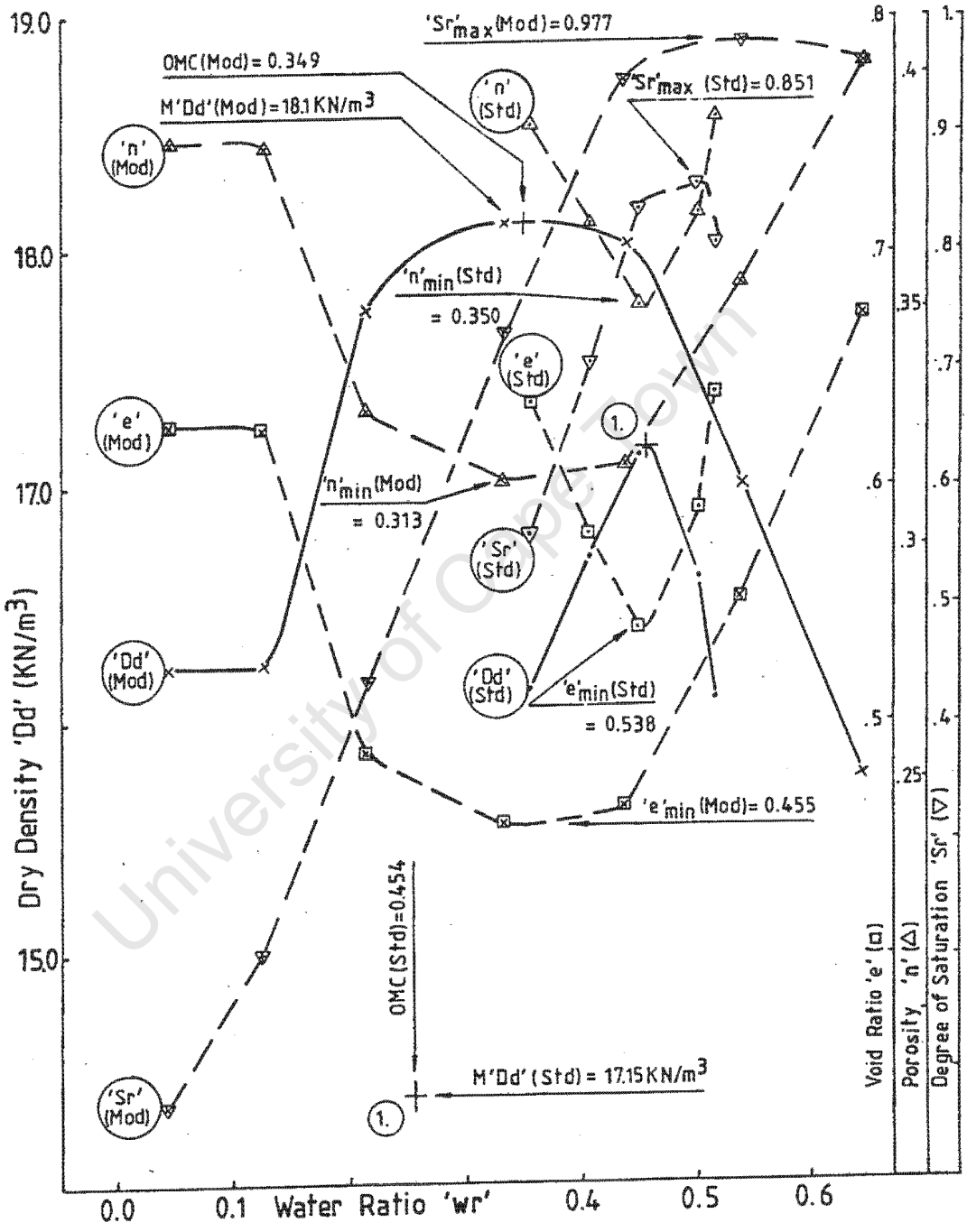

Figure 2.11: Site 36, Rondebosch - relationships of water ratio versus dry density, void ratio, porosity and degree of saturation.

Table 2.04: Site 30, Hout Bay - compaction tests.

[Volume of mould used 'V_T' = 943.7 cm^3; G_S = 2.637]

Standard AASHTO:

Determination No.	1	2	3
Compacted soil 'M' (g)	1731	1754	1685
Water content 'w'	0.2118	0.2897	0.3344
Water ratio 'Ω'	0.559	0.764	0.882
Dry density 'D_D' (KN/m^3)	14.84	14.13	13.12
Oven dry soil 'M_D' (g)	1428.5	1360.0	1262.7
Volume solids 'V_S' (cm^3)	541.7	515.7	478.9
Void ratio 'e'	0.742	0.830	0.971
Porosity 'n'	0.426	0.453	0.493
Degree of saturation 'Sr'	0.753	0.921	0.908

Modified AASHTO:

No.	1	2	3	4	5	6	7
'M', g	1575	1655	1741	1885	1915	1815	1770
'w'	0.0169	0.0608	0.1018	0.1356	0.1955	0.2587	0.2900
'Ω'	0.045	0.160	0.268	0.358	0.516	0.682	0.765
'D_D', KN/m^3	16.09	16.21	16.42	17.25	16.65	14.98	14.26
'M_D', g	1548.8	1560.1	1580.1	1659.9	1601.8	1442.0	1372.1
'V_S', cm^3	587.3	591.6	599.2	629.5	607.4	546.8	520.3
'e'	0.607	0.595	0.575	0.499	0.554	0.726	0.814
'n'	0.378	0.373	0.365	0.333	0.356	0.421	0.449
'Sr'	0.073	0.269	0.467	0.716	0.931	0.940	0.940

University of Cape Town

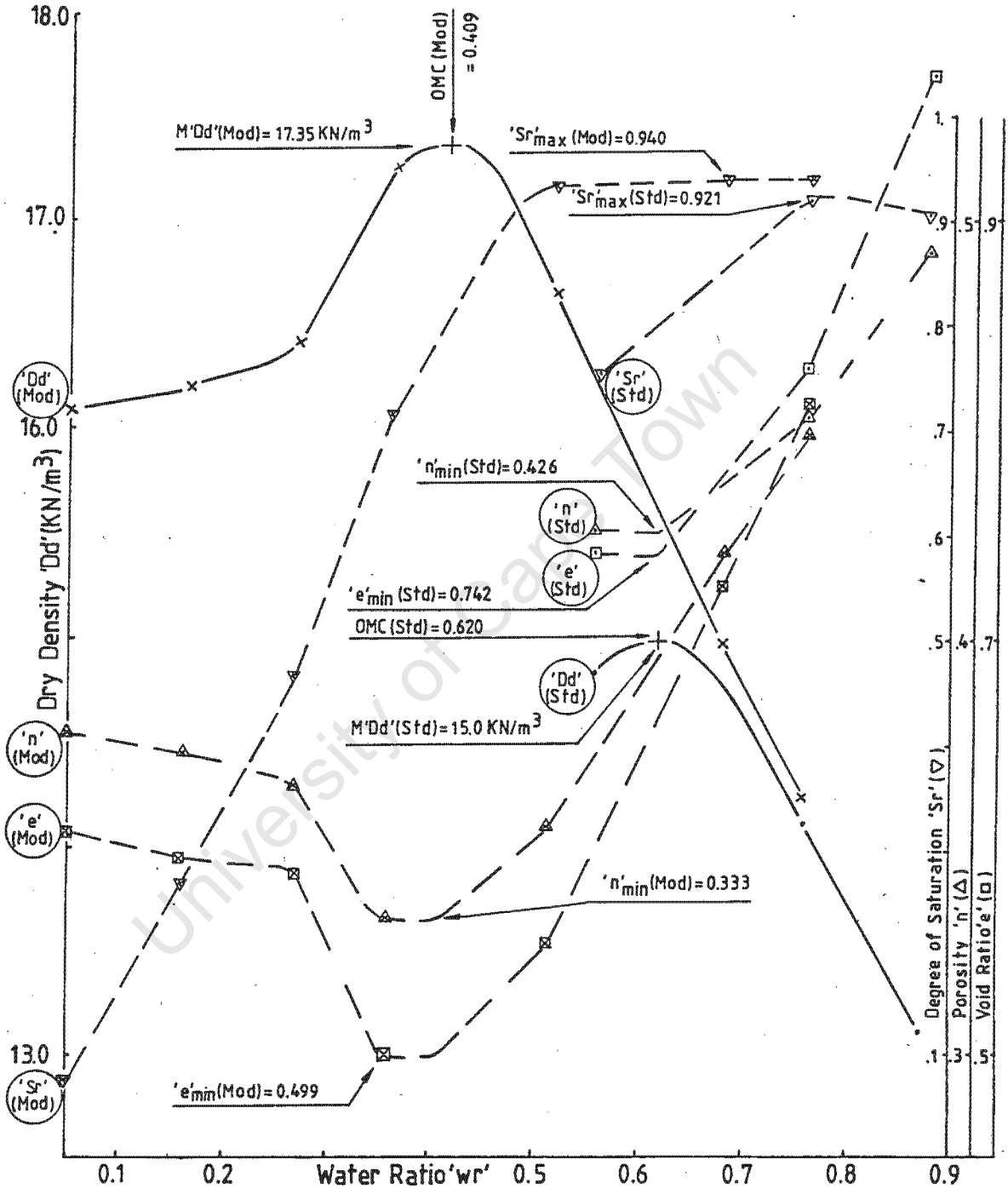

Figure 2.12: Site 30, Hout Bay - relationship of water ratio versus dry density, void ratio, porosity and degree of saturation.

University of Cape Town

Table 2.05: Site A, Berea Road - compaction tests.

[Volume of mould used 'V_T' = 943.7 cm^3; G_S = 2.665]

Standard AASHTO:

Determination No.	1	2	3
Compacted soil 'M' (g)	1947	2041	1964
Water content 'w'	0.0922	0.1222	0.1620
Water ratio 'Ω'	0.2457	0.3257	0.4317
Dry density 'D_D' (KN/m^3)	18.52	18.90	17.56
Oven dry soil 'M_D' (g)	1782.6	1818.7	1690.2
Volume solids 'V_S' (cm^3)	668.9	682.5	634.2
Void ratio 'e'	0.411	0.383	0.488
Porosity 'n'	0.291	0.277	0.328
Degree of saturation 'Sr'	0.598	0.851	0.885

Modified AASHTO:

No.	1	2	3	4	5	6	SA/9
'M', g	1661	1676	1984	2146	2089	2018	1839
'w'	0.0059	0.0350	0.0631	0.0895	0.1155	0.1316	0.0550
'Ω'	0.0157	0.0933	0.1682	0.2385	0.3078	0.3507	0.1466
'D_D', KN/m^3	17.16	16.83	19.39	20.47	19.46	18.53	18.11
'M_D', g	1651.2	1619.3	1866.2	1969.7	1872.7	1783.3	1743.1
'V_S', cm^3	619.6	607.6	700.3	739.1	702.7	669.2	654.1
'e'	0.523	0.553	0.348	0.277	0.343	0.410	0.443
'n'	0.343	0.356	0.258	0.217	0.255	0.291	0.307
'Sr'	0.030	0.169	0.484	0.862	0.898	0.855	0.331

University of Cape Town

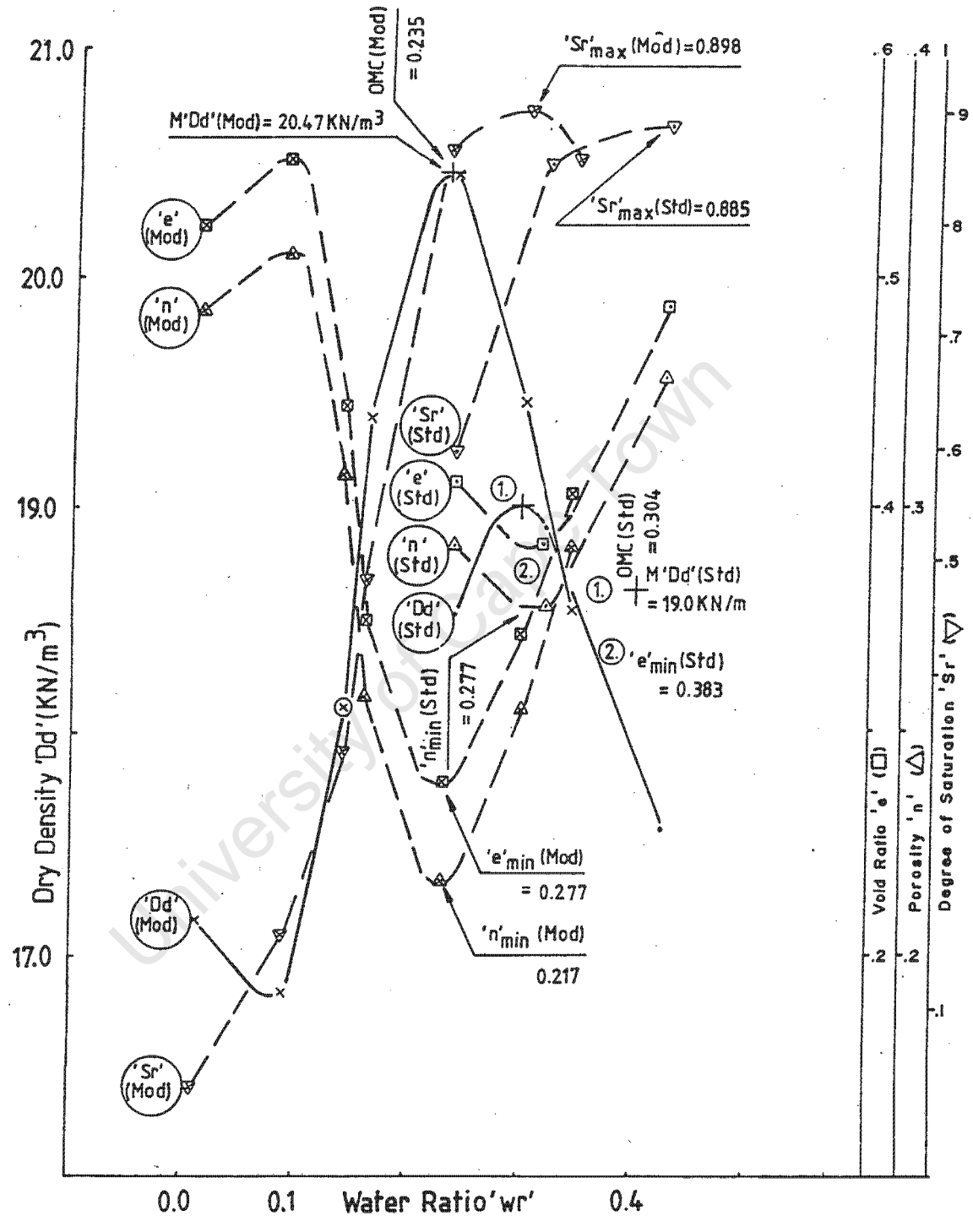

Figure 2.13: Site A, Berea Road - relationships of water ratio versus dry density, void ratio, porosity and degree of saturation.

Table 2.06: Site 7, Mowbray - compaction tests.

[Volume of mould used 'V_T' = 943.7 cm^3; G_S = 2.759]

Standard AASHTO:

Determination No.	1	2
Compacted soil 'M' (g)	1895	1880
Water content 'w'	0.1881	0.2224
Water ratio 'Ω'	0.5190	0.6136
Dry density 'D_D' (KN/m^3)	16.57	15.98
Oven dry soil 'M_D' (g)	1595.0	1538.0
Volume solids 'V_S' (cm^3)	578.1	557.4
Void ratio 'e'	0.632	0.693
Porosity 'n'	0.387	0.409
Degree of Saturation 'Sr'	0.821	0.886

Modified AASHTO:

No.	1	2	3	4	5	S7/13
'M', g	1739	1907	2045	2002	1896	1864
'w'	0.0514	0.0830	0.1279	0.1687	0.2224	0.0783
'Ω'	0.1418	0.2290	0.3529	0.4654	0.6136	0.2160
'D_D', KN/m^3	17.19	18.30	18.84	17.80	16.12	17.96
'M_D', g	1654.0	1760.8	1813.1	1713.0	1551.0	1728.6
'V_S', cm^3	599.5	638.2	657.2	620.9	562.2	626.5
'e'	0.574	0.479	0.436	0.520	0.679	0.506
'n'	0.365	0.324	0.304	0.342	0.404	0.336
'Sr'	0.247	0.478	0.809	0.895	0.904	0.427

University of Cape Town

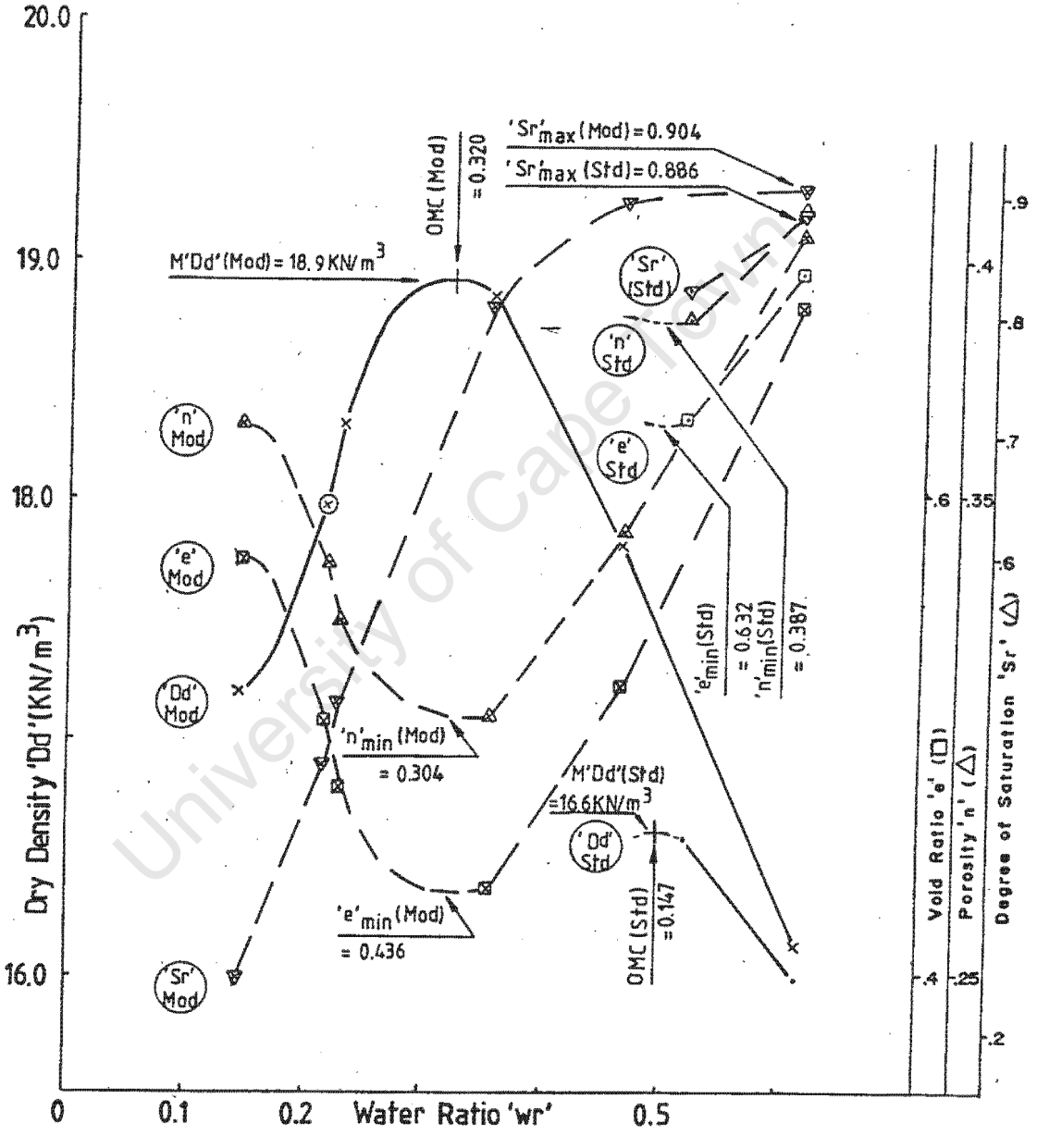

Figure 2.14: Site 7, Mowbray - relationships of water ratio versus dry density, void ratio, porosity and degree of saturation.

2.3 MICRO STUDIES - I OBSERVATIONS OF SOIL STRUCTURE BY MEANS OF SCANNING ELECTRON MICROSCOPY

2.3.1 Introduction.

Purpose - to observe the micro structure of the soil types previously selected (refer to Chapter One[1]) by means of high magnifications, of the order of 2000 diametres, obtained with the scanning electron microscope.

This section deals with Scanning Electron Microscopy 'SEM'. It is divided into four parts:

One - basic theory, modes of operation, and applications;

Two - clay separation of samples for SEM and x-ray diffraction;

Three - preparation of clay samples and SEM testing; and,

Four - the photographic plates.

2.3.2 Basic theory, modes of operation and applications.

This part deals with the basic theory, modes of operation and applications of SEM.

Brief introduction to the history of the microscope.

The magnifying lens has been around since ancient times. The compound microscope is a device which utilizes two or more lenses - it was invented in Holland during 1590. About 100 years later, a three lens compound microscope was made which was easy to use. Further improvement was made in the mid-eighteenth century by the achromatic or colour corrected lens. In 1873 Ernst Abbe wrote 'The Theory of Microscope Image Formation'[2], which resulted in bringing the design of the compound microscope to its peak. Progress in optical microscopy since that time has been mainly in the nature of refinements, in particular the use of powerful computer programs for the design of lens systems, multicoating of the optical surfaces, mass production and techniques of usage.

In the early 1900's, another possibility became available. It was seen that electrons could be guided in curved paths and thus used to magnify images.
By 1931, the first electron microscope was built in Germany - the transmission type of electron microscope.

---

[1] - *section 1.6 "Selection of Soil Types".*
[2] - *Reference 32.*

University of Cape Town

The principle for a scanning electron microscope was first described by H. Stintzing in 1927. By 1935 it was demonstrated by M. Knoll. Thirty years later in 1965, after much development by Professor Oatley (described in Reference 33) and his associates at Cambridge, England, the first commercial scanning electron microscope became available.

Comparison of the scanning electron microscope with other types of microscopes.

The maximum effective magnification of the optical (light) microscope (OM) is about 1200 diameters, whereas the effective magnification of the best transmission electron microscope (TEM) approaches 1 000 000 diameters. The scanning electron microscope (SEM) can provide a range of magnification varying from about 15 diameters to about 50 000 diameters, depending on the nature and form of the material examined. The value of expanding the low magnification range of the SEM from about '2x' to '50x' has been emphasized by Meaking and Fallon[1].
Useful pictures in this range can be obtained by increasing the working distances in order to reduce distortion.

The maximum resolution (that is, the minimum distance two objects may be separated and still be observed as distinct) of the OM is about 2000 to 3000 Å[2].
The best TEM's have a resolving power of 2 to 5 Å.
Most SEM's have a resolution of 100 to 200 Å depending on the nature and condition of the sample, as well as the operating voltage of the instrument and final aperture size.

The outstanding feature of SEM micrographs is the remarkable three-dimensional quality. The optical microscope can be focused in only one plane and, therefore, its depth of field is severely limited. It is useful for revealing the shape of specimens only at low magnification since its depth of field decreases with increasing magnification. For internal detail the OM is best used with thin or flat samples, and even thinner sections are required for the TEM. Useful sections for study in the OM commonly range from 8 to 15 µm, however, sections to be studied in the TEM generally range from 300 to 700 Å in thickness and must be cut on a special microtome. Because the specimens examined in the TEM must be so thin, the depth of field is limited and an essentially two-dimensional image is obtained. No such limits are found with the SEM.

University of Cape Town

---

1 - Reference 34.
2 - one Angstron Å unit = 0,0000000001 m.

In contrast to the OM or the TEM, in which the illuminating source (light or electrons) must pass through the specimen, in the SEM the electrons that are recorded do not pass through the specimen, but rather secondary electrons are collected from the surface of the specimen and are used to form an image. These secondary electrons need not be focused, only collected. Therefore, in the SEM there is virtually no constraint on the size of the specimen to be studied, the size being limited only by the capacity of the specimen stage.

The depth of field in the SEM, compared with the OM, is better at comparable magnifications by a factor of ≥300.

Basic theory and operation of the SEM.

In very simple terms, the scanning electron microscope, as compared with an optical one, uses electrons instead of light and its lenses are magnetic rather than glass. The SEM is used to image the surface features of objects by scanning a finely focused beam of electrons across the surface of a specimen, in a high vacuum. As the beam of electrons strikes the object's surface, it causes other electrons to be knocked out into the vacuum where they are attracted to a sensor. There the electrons are detected, converted to a data signal, processed, and then reassembled as a picture on a high resolution television monitor. At this point, the image may be viewed and photographically recorded.

In the SEM only one spot on the subject's surface need be in focus at any one time. Hence, the SEM is able to vary the focus point constantly to follow the contours of the surface and thus, in theory, produce an overall image that is entirely in focus from point to point.
As an added possibility, since the image information is carried by electronic signal after being detected, the data may be processed, enhanced, or stored in a computer if necessary.
A schematic comparison of the light optical and a transmission electron optical system with the scanning electron microscope system is illustrated in Figure 2.15.

University of Cape Town

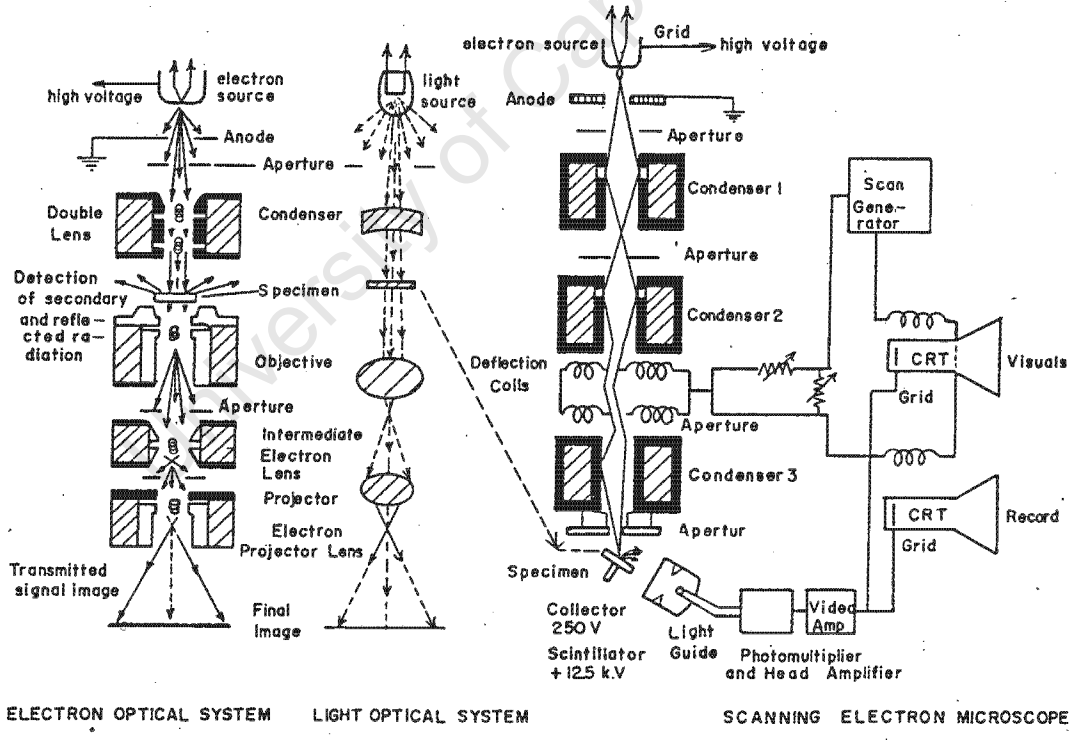

Figure 2.15: Diagram illustrating details of a transmission electron optical system, light optical system, and Scanning Electron Microscope [1].

1 - References 35 and 36.

University of Cape Town

The system, from the electron source, through the electron-optical column, to the specimen chamber, is under high vacuum[1]. This is to allow the electrons a free path so as not to collide with air molecules.

A pointed tungsten filament is generally used as the Electron Source. The electrons in a SEM are emitted by the heating of a tungsten filament (cathode) located within the gun in the upper portion of the microscope column. The cathode is generally held at 20 000 volts[2] below ground potential of the anode.
The high voltage, the heating of the filament and the tendency of a charge to accumulate at a point, all contribute to cause electrons to be emitted into the vacuum. The action of the grid tends to concentrate the emission of electrons at the filament's point; the anode helps to extrude the electrons and direct them; and, the series of holes in the grid, anode and spray aperture, help to begin the formation of the beam.
All this in combination is called the electron gun.

The electrons are directed down the electron-optical column through the three pre-aligned electromagnetic condenser lenses which serve to accelerate the electrons, form them into a beam, and focus them to a small point. The condenser lenses also serve to progressively de-magnify the electron beam into a probe, which is focused on the surface of the specimen. The electron probe thus formed may range from 10 to 50 nm in diameter. After meeting the astigmator lens, which corrects for any resultant astigmatic aberrations in the beam, the probe of electrons is deflected by scanning coils which drive the beam over the specimen surface, in a square raster comparable to that of a television screen.
This electron beam, or probe, is synchronized with the electron beam of a cathode ray picture tube.

The scanning coil assembly is located in the bore of the final or lowest condenser lens, which is sometimes referred to as an object lens. The final lens is fitted with three interchangeable apertures.
The specimen chamber is situated at the base of the microscope column in line with the electron beam.
The final aperture limits the divergence of the electron beam at the specimen surface to a tiny spot on the sample. Usually, three sizes of apertures can be selected by a control, external to the specimen chamber.

---

1 - about one millionth of an atmospheric pressure.
2 - and variable over the 1000 to 30000 volts range.

Large aperture sizes are used at high magnifications - they limit the depth of field obtainable in a focused picture. Separate diffusion pumps are provided for the column and the specimen chamber, and are backed by a single rotary pump. Column vacuum can be maintained during specimen changes and during relacement of the electron source. Both the column and specimen chamber must be under adequate vacuum[1] for operation of the instrument.

Movements of the specimen in the 'x', 'y', and 'z' directions, as well as tilting and rotation, are possible by means of controls outside the specimen chamber.

Detection and amplification.

The electron beam strikes the specimen and interacts with its surface, knocking "secondary" electrons out of the orbits of the atoms of specimen material. These secondary electrons, along with recoiled primary electrons, are emitted out into the vacuum where they are attracted to the detector by its opposite (+) charges as shown in Figure 2.16. The electrons strike the scintillator, which is coated with a phosphor; the collisions create tiny flashes of light, which are then directed out of the vacuum chamber via a light pipe, to the photomultiplier tube - a device which converts the light back to an electronic signal and amplifies it.

This signal is now further amplified, processed and enhanced as desired, after which time it is transmitted to a cathode ray tube[2] which has its own electron beam that is in synchronization with the primary beam of the electron-optical column. Both of these beams are controlled by the scan generator. The transmitted data signal modulates intensity of the C.R.T.'s beam which then writes the information upon the phosphor screen as a picture. Generally there are two C.R.T.'s - one for viewing and the other for high resolution photographic recording. Since the size of the image on the view and record C.R.T.s is constant, all that is necessary to increase magnification is to decrease the area of specimen being scanned.

---

1 - less than 10^{-4} torr.
2 - television monitor 'C.R.T.'.

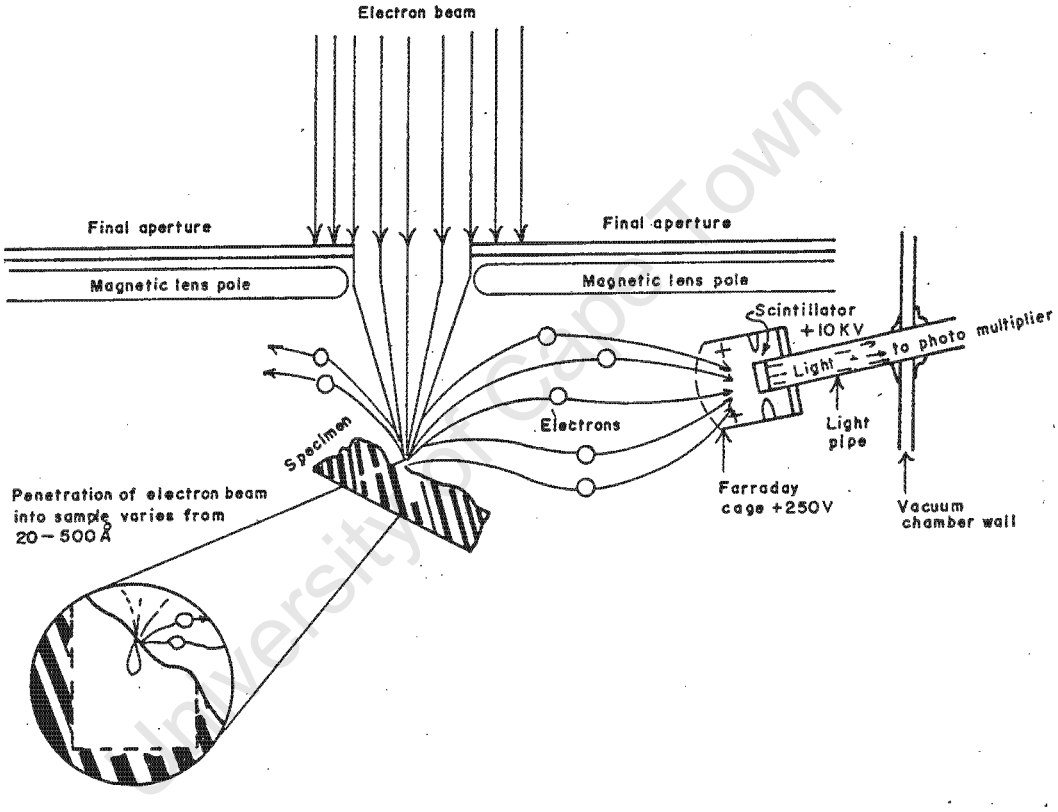

University of Cape Town

Figure 2.16: Electron sensor - the detector system for the SEM.

The following are the main components of the detector system (shown in the above illustration - Fig. 2.16): Scintillator; light guide; and, photomultiplier collector. Also included are the various types of excitations and emissions caused by the interaction of the electron beam with the specimen. Each of these excitations may be used to produce imagery when sensed by an appropriate detector.

Scanning Electron Microscopy UCT.

According to the pamphlet issued by the Electron Microscope Unit [1], "In 1976 a Cambridge S180 scanning electron microscope was installed at the University of Cape Town to complement the Philips EM300 transmission electron microscope already sited in the Physics Department. Such instrumentation, forming the basis of a facility for comprehensive microstructural and micromorphological studies of a wide range of materials, provides a service to Life Scientists, Enviromental Scientists, Materials Scientists, Chemists and Earth Scientists alike."

The following equipment was available to users:-

(1) Scanning Electron Microscopy - Cambridge S180 scanning electron microscope equipped for imaging at up to x600,000 magnification with resolution of 10 nm;

(2) Transmission Electron Microscopy - Phillips EM300 transmission electron microscope equipped for imaging at up to x600,000 magnification with high resolution imaging[2];

(3) Specimen preparation - ultramicrotomy, vacuum evaporation, ion beam thinning, sputter coating, etc.

For the purpose of this thesis, the micro structure of the soil types was observed in the scanning electron microscope shown in Photographic Plate 2.01.

University of Cape Town

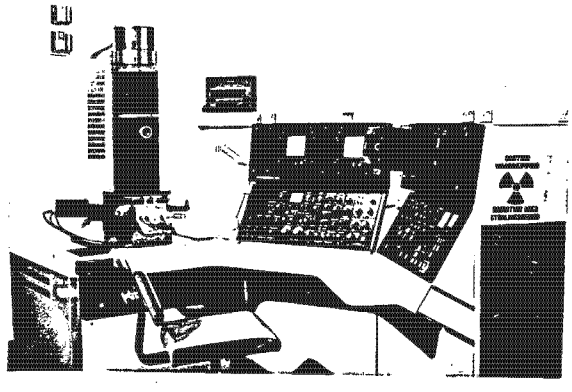

PHOTOGRAPHIC PLATE 2.01: The Cambridge S180 scanning electron microscope.

---

1 - Reference 37.
2 - 1.7 Å attainable.

The control console of the scanning electron microscope consists of two major assemblies:
The electron - optical column, with the specimen chamber, is located at the left of the photographic plate 2.01, and is mounted on a plinth containing the vacuum pumping unit;
The assembly illustrated in the right portion, included display racks with most of the operator controls, display cathode ray tube screen, processing units, meters, etc.

Modes of operation and applications of the SEM.

A scanning electron microscope system can detect, display and in some cases measure, information derived from the action of a very fine beam of electrons scanning a specimen surface in a square raster.
In general terms the information derived includes surface detail (microscopy), X-ray microanalysis, surface voltage contrast, sub-surface current, crystallographic orientation, and luminescence.
The specimen can be manipulated and its state changed during investigation. Further, the specimen can be moved linearly, rotated, and tilted. With the addition of suitable modules, the specimen can also be heated, cooled, bombarded with ions, etc.. With the addition of suitable external pattern generators, the SEM can also be used for electron-beam processing on an experimental basis.

The following are the major modes of imaging and their applications:-

(1) Emissive:- Low energy secondary electrons, emitted from the specimen by primary electron-probe excitation, are drawn usually in a curve trajectory to a positively biased scintillator - light-guide - photomultiplier collector system[1]. After amplification, this is the signal that modulates the CRT beam.
Applications of the emissive mode in the study of surface topography are virtually unlimited. In addition, it is also used to display surface voltage (generally, negative potentials appear bright and positive ones appear dark), and crystallographic orientation (large single-crystal specimens examined at low magnifications illustrate patterns of crystallographic orientation).

(2) Reflective:- Backscattered primary electrons (with a higher energy than secondary electrons) are collected. They have lower resolution than the secondary images. The resolution limit is about 500 to 2000 Å.
Information provided includes element discrimination (collected backscattered electrons can be used to obtain information regarding the kinds of atoms in a specimen), as well as topography and crystallographic orientation.

---

[1] - *refer to Figure 2.16.*

University of Cape Town

(3) Absorptive:- In this condition the signal is collected by monitoring the current flowing to earth from the specimen. Information can be obtained for topography, crystallographic orientation, surface voltage, and element discrimination.

(4) Transmission:- In this mode electrons pass through a specimen, and the electrons which have penetrated the specimen are collected. It is possible to examine thicker specimens than can be viewed with a conventional TEM. Information provided include element discrimination and crystallographic orientation.
It ought to be mentioned that previous advanced research in the electron microscope unit included high resolution transmission electron microscopy of lattice structure in exsolved minerals, and of asbestos fibres.

(5) X-rays:- The x-rays generated when the electron beam reacts with the specimen are collected, analysed, and used to form a signal. The ability to perform x-ray microanalysis of elements in the SEM is one of its most valuable assets. Applications include quantitative microanalysis (accomplished by adding to the SEM crystal diffraction spectrometers), and qualitative microanalysis (by adding energy dispersion spectrometers).

(6) Cathodoluminescence:- The one measurable phenomenon that can be displayed when a high-energy electron beam interacts with a solid specimen. When a substance that is bombarded with electrons emits light, this phenomenon can provide useful information, such as structural details, that would otherwise not be visible.
Initial applications of the luminescent mode included biological material and semiconductor work.

(7) Beam-induced conductivity:- In this condition electrical connections are made to the specimen and an external voltage is applied. The current flow that results is monitored to provide a signal. When coupled with the changes possible with the incident beam itself, the technique is of great value in the study of junction field regions in semiconductor devices.
Information provided also includes sub-surface conductivity.

The SEM's various modes of operation are summarized in Figure 2.17.

University of Cape Town

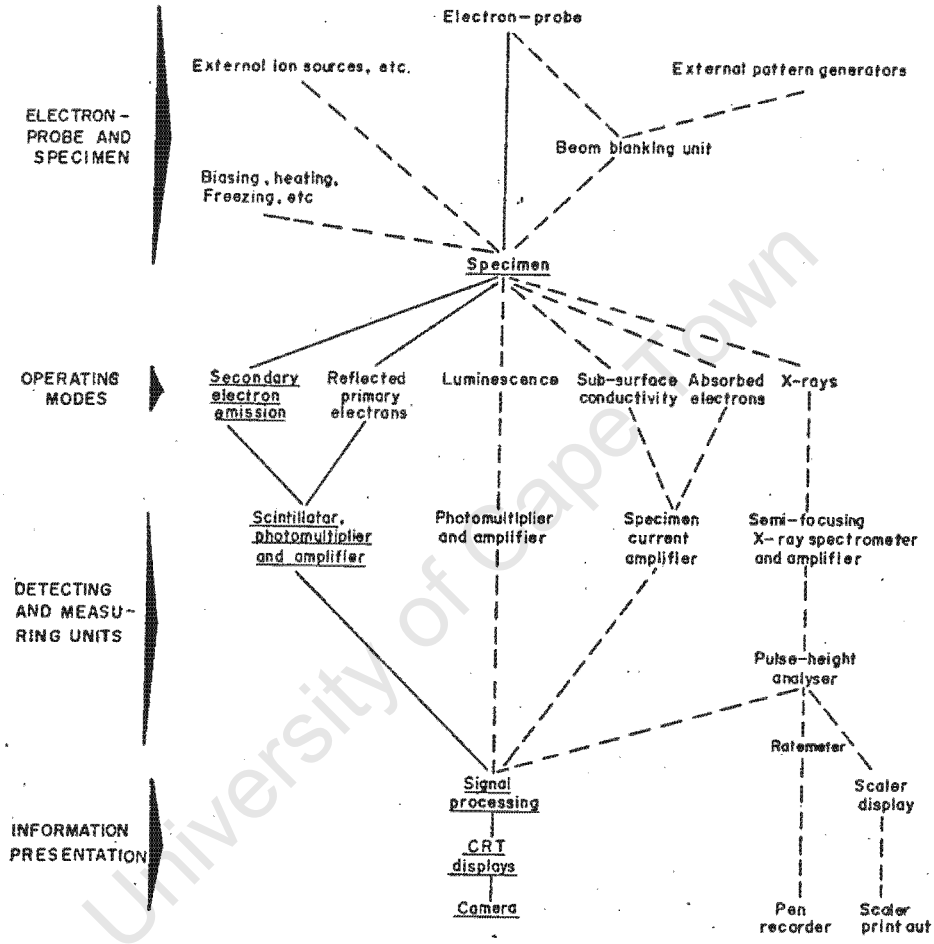

Figure 2.17: Major modes of imaging in the SEM.

There are many factors contributing to the acquisition of high-quality pictures of materials by means of the SEM. These include the following factors: (i) Specimen fixation and drying; (ii) Suitable coating of the specimen to reduce charging artifacts; (iii) Probe size and signal-to-noise ratio; (iv) Properly aligned gun; (v) Accelerating voltage of electrons; (vi) Final aperture size and its cleanliness; and, (vii) Quality of the vacuum. It should be noted that factors (i) and (ii) are mentioned in 'Preparation of the clay samples and SEM testing'[1].

[1] - *refer to section 2.3.4 of this chapter.*

University of Cape Town

2.3.3 Clay separation of samples for Scanning Electron Microscopy and X-Ray Diffraction.

This part introduces the initial preparation of the samples for scanning electron microscopy and x-ray diffraction 'X-ray D'[1] - that is the clay separation of a sample representative from each soil type.

Initial preparation of samples for SEM and X-ray D.

Representative samples were originally obtained for each soil type selected for this thesis - refer to Appendix A[2]. Soil samples were obtained for the following soil types: sites 11, 36, 30, A and 7 (natural soils); and, K and B (artificial soils).
This section introduces the subsequent initial preparation of soil samples for the purposes of both scanning electron microscopy and x-ray diffraction.
It should be noted that after this initial sample preparation stage, where the procedure adopted is the same for both SEM and X-ray D, the next stage differs between the two.
Section 2.3.4 introduces the preparation of clay samples for SEM purposes only.
As far as X-ray D is concerned, the next stage of sample preparation will be introduced in section 2.4 of this chapter.

Appendix B includes a detailed description of the procedures for the preparation of samples for SEM and X-Ray D - refer to section B.2 "Clay Separation of Samples for Scanning Electron Microscopy and X-ray Diffraction". These procedures are - "Clay separation of soil samples", and "Sediment laboratory procedure".

2.3.4 Preparation of clay samples and SEM testing.

This part introduces the preparation of clay samples for scanning electron microscopy, and the testing of the natural (sites 11, 36, 30, A, and 7), and artificial (kaolin and bentonite) soil types. Appendix B includes a detailed description of the procedure for preparation and testing of clay samples for scanning electron microscopy - refer to section B.3 "Preparation of Clay Samples and SEM Testing". The following is intended to provide an introduction to these procedures, and includes a summary of the final stage of preparation and SEM testing.

University of Cape Town

---

1 - for X-ray Diffraction refer to section 2.4.
2 - section A.3 "Preparation of Soil Samples for Testing".

Specimen preparation for scanning electron microscopy.

Specimens in an electron microscope are exposed to a vacuum pressure generally in the range of 10^{-4} to 10^{-6} torr. If a wet specimen is introduced to such vacuums, its water content will evaporate and the specimen will freeze. The surface tension forces generated during evaporation, and the resulting ice crystal formation and growth, is sufficiently harmful so as to render the resultant images almost useless.
Hard objects such as rocks, shells, and small grained materials such as clays, which have a hard exo-skeleton and plant structures including pollen grains, can still be usefully studied in the SEM without preparation. However, before viewing, the specimens are sometimes coated with a thin layer of carbon and gold-palladium to reduce charging effects in the electron beam.

Conducting samples usually need nothing more than cutting to an approximate size, sticking to a convenient metal mount while making sure there is good electrical conduction between the specimen and the mount.

The four obstacles to clear pictures which may require more complicated preparation procedures, are poor electron emission, charging, beam damage and vacuum damage. Application of a conducting layer of carbon or metal is the most popular method of suppressing charging and increasing electron emission, however, while simple to perform it has a number of drawbacks. The purpose of coating is to put on a uniform covering of conductive material, so that the surface of the coating is, as nearly as possible, an exact positive replica of the surface of the underlying material.

For scanning electron microscopy, the material may be deposited on the sample surface by vacuum deposition - commercial apparatus for this process is easily available. Production of a continuos uniform layer requires that each face of the sample is presented to the source for the same amount of time.

Amongst the metals, the noble metals have good electron emission and contouring ability. Gold is often used for coating, as it has such good electron emission, and gold palladium is used even more often, but the ability to contour accurately is such a prime consideration that many people use silver exclusively. The disadvantage of silver is that it tarnishes, and in many climates it cannot be viewed more than a few days after preparation.

University of Cape Town

Final preparation and testing of clay samples at UCT.

Preparation of samples for SEM - the final stage comprised the following steps:

(i) The clay samples were dispersed ultrasonically in acetone;

(ii) Each sample was in turn pipetted out and two drops were carefully placed on an aluminium stud; and,

(iii) The samples were coated with carbon and gold palladium.

Highlights of SEM testing (for general description, refer to 'Test procedure using the emissive mode' - Section B.3 of Appendix B) - the adjustments and recordings performed:

(i) Focus - coarse (x10 to x30), intermediate (x300 to x1000), and fine (x3000);

(ii) Reduce raster, and check astimagtism (at higher magnification than that for recording);

(iii) Wave form monitor - camera set for response to full signal variation;

(iv) Record 1600 lines/frames (800 is acceptable), and recording time (60, 120 seconds, or longer depending on noise).

It should be added that the following factors affect the quality of SEM image:
Operator; Spot size and penetration; Spherical aberration coefficient of the final lens; Distortion; Astigmatism; Noise; Vibration; Specimen damage; Focus; and, incorrect instrumental parameters.

2.3.5 The Photographic Plates.

This part includes the photomicrographs obtained during the SEM testing of the clay samples. Following an introduction to the recording of the photomicrographs themselves, the photographic plates numbers 2.02 to 2.06, are included for the natural soil types (sites 11, 36, 30, A and 7), and photographic plates 2.07 to 2.08 refer to the artificial ones (kaolin and bentonite).

University of Cape Town

Introduction to the photomicrographs.

The photomicrographs were recorded using a 'Super Rolex' camera made in West Germany, of 6 x 9 cm format (or 2½"x3¼"), and loaded with Ilford FP4 photographic film rated at 125 ASA film speed.

Each photomicrograph includes at the bottom, from left to right, the following four pieces of information: (first) The number 1 - the signal selector, which in this case means we are on Mode 1; (second) 12 kv - the voltage EHT, or extra high tension; (third) 3 µm or 12 µm - the distance in microns (10^{-6} meters) between the white markers shown along the bottom; and, (four) the numbers 01.001 to 01.007 - provide the specimen number (refer to Table 2.07 below).

Table 2.07: Correlation between the soil type, the specimen number and scale of each SEM photomicrograph.

Soil type No., Location	Specimen: number;	Scale. (µm)	Photographic plate No.
Natural Soils			
11, Rosebank (Cape)	01.001	10	2.02
36, Rondebosch (Cape)	01.003	3	2.03
30, Hout Bay (Cape)	01.006	10	2.04
A, Berea Road (Durban)	01.004	3	2.05
7, Mowbray (Cape)	01.002	3	2.06
Artificial Soils			
Kaolin 'K'	01.005	3	2.07
Bentonite 'BE'	01.007	10	2.08

The Photographic Plates - numbers 2.02 to 2.08.

Concerning the micro structure of each soil type, brief notes based on visual assessment (only) are included with each photomicrograph. A summary of these observations is included with the conclusions for this chapter[1].

[1] - *refer to section 2.5 "Conclusions for Chapter Two".*

University of Cape Town

Site 11, Rosebank.

Photographic Plate 2.02: Magnification of approximately 1300x; Fine silt surrounded by clay particles; Larger size visible particles have a thin 'platelike' appearance.

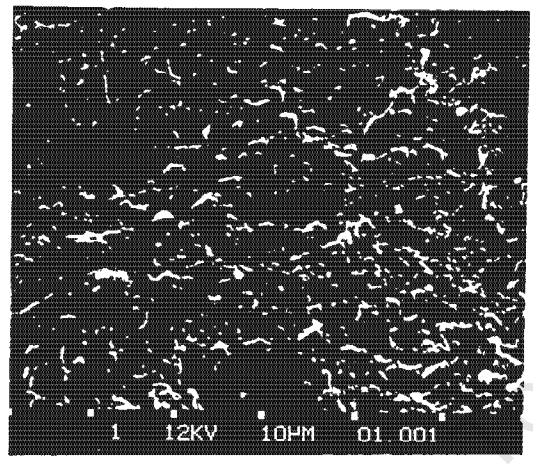

PHOTOGRAPHIC PLATE 2.02: Site 11, Rosebank - SEM photomicrograph of clay sample.

Site 36, Rondebosch.

Photographic Plate 2.03 (i): Magnification of 2300X; Fine silt and clay size particles; Flat 'plate-like' appearance of fine silt particles; Large pores between particles.

Site 30, Hout Bay.

Photographic Plate 2.03 (ii): Magnification of 1500X; Fine silt and clay size particles in fairly dense/uniform matrix.

University of Cape Town

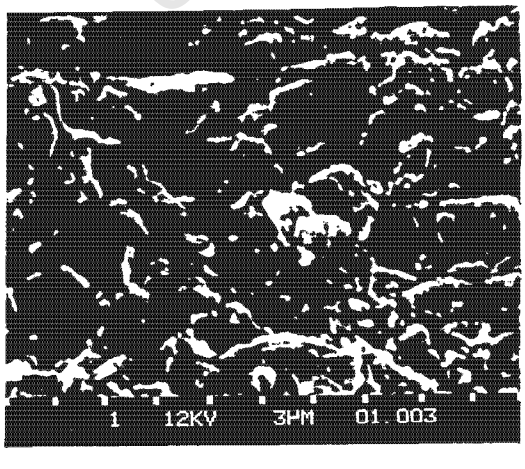

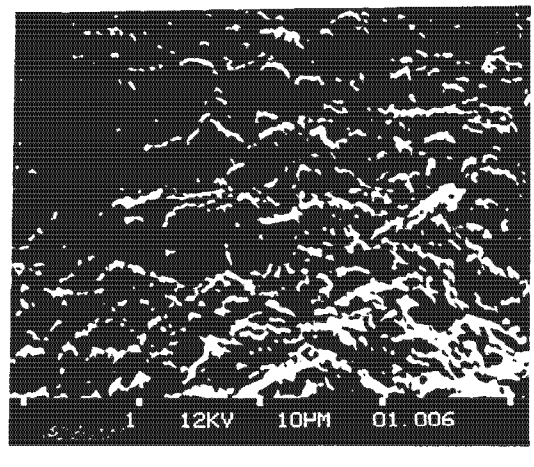

PHOTOGRAPHIC PLATE 2.03: (LHS) Site 36, Rondebosch; and, (RHS) Site 30, Hout Bay - SEM photomicrographs of samples.

Site A, Berea Road (Durban).
Photographic Plate 2.05: Magnification of 2000X; Particles of silt linked and surrounded by particles of clay size.
Site 7, Mowbray.
Photographic Plate 2.06: Magnification of 2000X; Fine silt and clay size particles in a dense arrangement.

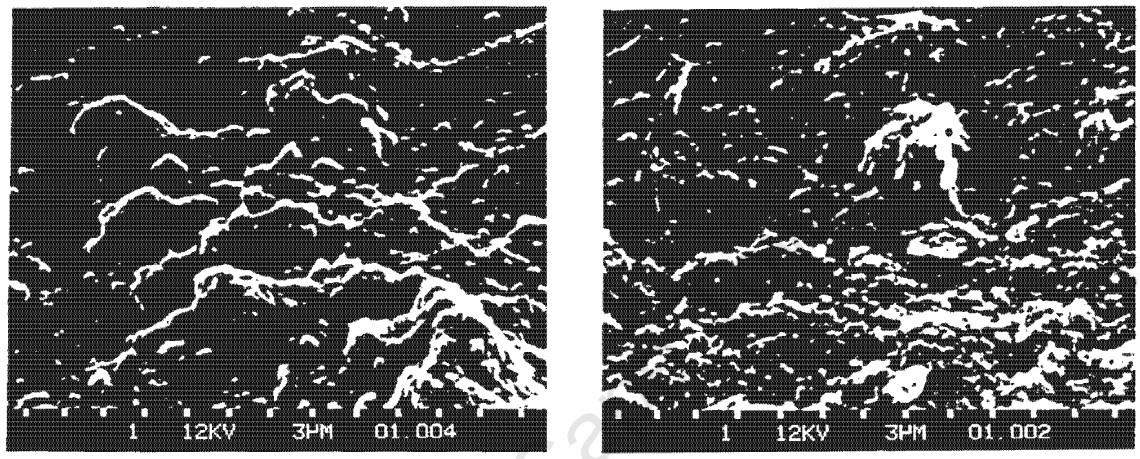

PHOTOGRAPHIC PLATE 2.04: (LHS) Site A, Berea Road (Durban); (RHS) Site 7, Mowbray - SEM photomicrographs of samples.

Kaolin Clay 'K'.
Photographic Plate 2.07: Magnification of 2000X; Very fine silt (like thin plates) and clay size particles.
Bentonite Clay 'B'.
Phoographic Plate 2.08: Magnification of approximately 1300X; Random orientation of, mostly, clay size particles.

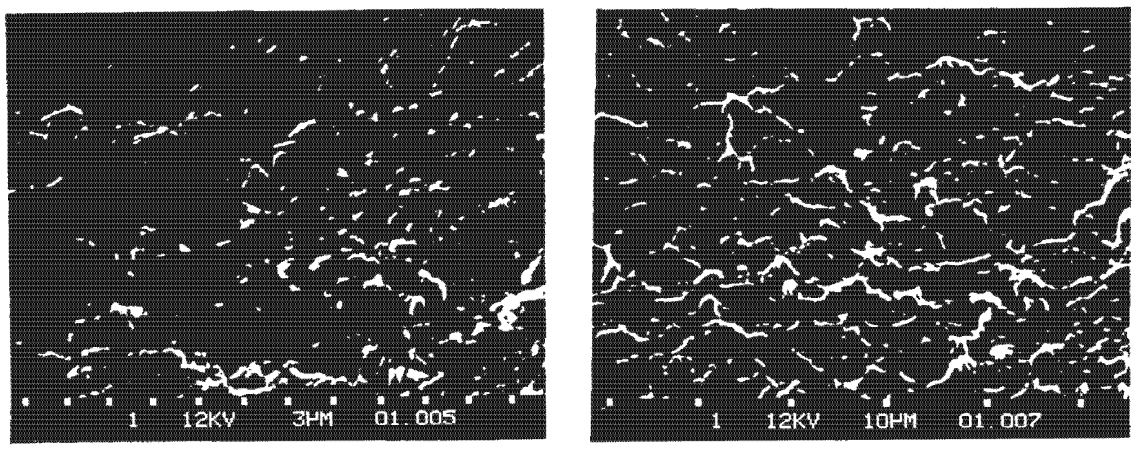

PHOTOGRAPHIC PLATE 2.05: (LHS) Kaolin Clay 'K'; and, (RHS) Bentonite Clay 'B' - SEM photomicrographs of clay samples.

2.4 MICRO STUDIES - II USE OF X-RAY DIFFRACTION DATA TO IDENTIFY THE CLAY MINERALS

2.4.1 Introduction.

Purpose - to identify the clay minerals which are present in each soil type, using X-ray diffraction techniques.

This section deals with clay minerals and their identification by means of X-ray diffraction data. It is divided into four parts, as follows:

One - Introduction to mineralogy and the clay minerals;

Two - Application of X-rays to the study of crystals;

Three - X-ray diffraction: Preparation and testing of clay samples; and,

Four - Analysis of X-ray diffraction data.

2.4.2 Introduction to Mineralogy and the Clay Minerals.

This part provides an introduction to mineralogy in general and the clay minerals in particular. Also included are references to the origin and occurence of clay minerals, their structure and the clay water-system.

Introduction to mineralogy.

Mineralogy is the study of naturally occuring, crystalline substances - minerals.
Definition of mineral: A mineral is a naturally occurring homogeneous solid with a definite (but generally not fixed) chemical composition and an ordered atomic arrangement; It is usually formed by inorganic processes.

The general term crystalline is used to denote the ordered arrangement of atoms in the crystal structure. Today, most material scientists use the term crystal to describe any solid with an ordered internal structure, regardless of whether it possesses external faces. Thus, a crystal can be broadly defined as a homogeneous solid possessing long-range, three dimensional internal order.

University of Cape Town

Crystals are formed from solutions, melts, and vapours: In general, crystals may form from a solution by evaporation of the solvent, by lowering the temperature, or by decreasing the pressure. If water is allowed to evaporate from a solution containing dissolved sodium chlorite, a point is reached when the remaining water can no longer retain all the salt solution, and solid salt begins to precipitate. If the evaporation is very slow, the ions of sodium and chlorine will group themselves together to form one, or a few crystals, with characteristic shapes and often with common orientation; if evaporation of water is rapid, many centres of crystallization will be set up usually resulting in many small, randomly orientated crystals: A crystal is formed from a melt in much the same way as from a solution - the most familiar example of crystallization from fusion is the formation of ice crystals when water freezes.

Although it is not ordinarily considered in this way, water is fused ice (when the temperature is lowered sufficiently, the H_2O molecules, which were free to move in any direction in the liquid state, become fixed and arrange themselves in a definite order to build up a solid, crystalline mass); Crystallization from a vapour - as the vapour is cooled, the dissociated atoms or molecules are brought closer together, eventually locking themselves into a crystalline solid (for example, the formation of snowflakes from air laden with water vapour).

The three-dimensional internal order of a crystal can be considered as a repetition of a motif, or a unit of pattern, in such a way that the enviroment of, and around, each repeated motif is identical. This design (in three dimensions) is referred to as a space lattice. In recent years the study of crystals by means of X-rays[1] has revealed the fact that their symmetrical forms are simply the outward expression of a perfectly organized internal structure.

A few minerals are non-crystalline in the sense that they never develop crystal forms, and for this reason they are said to be Amorphous - in such materials very tiny particles are arranged haphazardly, like the bricks in a tumbled heap, but investigations with the electron microscope[2] show that within each of the particles the atoms have a recognisable lattice arrangement. Apart from the amorphous materials, minerals are naturally occuring inorganic crystalline substances, of which each `species' has its own specific variety of crystal structure.

---

1 - see latter part of this section.
2 - refer to previous section.

University of Cape Town

It should be noted that certain substances have the capacity to occur as two or more quite different species of crystals, a phenomenon described as 'Polymorphysm' - that is, to crystallise with lattice structures appropriate to the physical conditions at the time of formation. Few minerals have the exact chemical composition corresponding to their ideal formulae - the reason is that any ion that happens to be on the spot at the time of crystallisation can act as a substitute or proxy for another without seriously disturbing the crystal lattice, provided that the ion of the proxy has nearly the same 'size' (given in Ångstrom units) as that of the ion whose place it takes in the growing crystal.

Structure and chemistry of minerals.

Many of a mineral's properties depend not only on the chemical composition but also on the geometrical arrangement of the constituent atoms, or ions, and the nature of the electrical forces that bind them together. Thus for an understanding of minerals, one must consider their structure as well as their chemistry.

Patterns of mineral distribution and assessment of our mineral wealth are directly related to the abundance and distribution of elements in the earth's crust. Geophysical investigations indicate a division of the earth into a crust, mantle and core as follows: The crust is approximately 36 km thick under the continents, and under the oceans its thickness ranges from 10 to 13 km; The boundary between the crust and the underlying upper mantle is referred to as the Mohorovicic discontinuity; The upper part of the crust is composed of a relatively large percentage of sedimentary rocks and unconsolidated materials - this cover forms but a thin veneer on an underlying basement of igneous and metamorphic rocks.

It has previously been estimated[1] that the upper 16 kilometres of the crust consists of 95% igneous rocks (or their metamorphic equivalents), 4% shale, 0.75% sandstone, and 0.25% limestone - therefore the average composition of igneous rocks would very closely approximate the average composition of the continental crust.
It turns out that this average composition is intermediate between that of granite and basalt (or its coarser grained equivalents, diabase and gabbro) which are the two most common igneous rock types - refer to Table 2.08 which lists the average amounts of the elements in crustal rocks[2].

---

[1] - *Reference 41.*
[2] - *Reference 42.*

University of Cape Town

Table 2.08: Average amounts of the elements in crustal rocks - in weight percent for the common elements (as indicated by %) and in parts per million (no unit indicated) for the less abundant ones.

Atomic No.	Weight	Element Name - symbol	Crustal average	Granite % or p.p.m	Diabase
1	1.0080	Hydrogen - H	0.14%	0.04%	0.06%
3	6.941	Lithium - Li	20	24	12
4	9.0122	Beryllium - Be	2.8	3	0.8
5	10.811	Boron - B	10	2	17
6	12.0111	Carbon - C	200	200	100
7	14.0067	Nitrogen - N	20	8	14
8	15.9994	Oxygen - O	46,60%	48.50%	44.90%
9	18.9984	Fluorine - F	625	700	250
11	22.9898	Sodium - Na	2.83%	2.46%	1.54%
12	24.305	Magnesium - Mg	2.09%	0.24%	3.99%
13	26.9815	Aluminium - Al	8.13%	7.43%	7.86%
14	28.086	Silicon - Si	27.72%	33.96%	24.61%
15	30.9738	Phosphorus - P	0.10%	0.04%	0.06%
16	32.064	Sulphur - S	260	175	135
17	35.453	Chlorine - Cl	130	50	-
19	39.102	Potassium - K	2.59%	4.51%	0.53%
20	40.08	Calcium - Ca	3.63%	0.99%	7.83%
21	44.956	Scandium - Sc	22	3	34
22	47.90	Titanium - Ti	0.44%	0.15%	0.64%
23	50.9414	Vanadium - V	135	16	240
24	51.996	Chromium - Cr	100	22	120
25	54.9380	Mamganese - Mn	0.09%	0.02%	0.13%
26	55.847	Iron - Fe	5.00%	1.37%	7.76%
27	58.9332	Cobalt - Co	25	2.4	50
28	58.71	Nickel - Ni	75	2	78
29	63.546	Copper - Cu	55	13	110
30	65.37	Zinc - Zn	70	45	82
31	69.72	Gallium - Ga	15	18	16
32	72.59	Germanium - Ge	1.5	1.0	1.6
33	74.9216	Arsenic - As	1.8	0.8	2.2
34	78.96	Selenium - Se	0.05	-	-
35	79.904	Bromine - Br	2.5	0.5	0.5
37	85.467	Rubidium - Rb	90	220	22
38	87.62	Strontium - Sr	375	250	180
39	88.9059	Yttrium - Y	33	13	25
40	91.22	Zirconium - Zr	165	210	100
41	92.906	Niobium - Nb	20	20	10
42	95.94	Molybdenum - Mo	1.7	7	0.05
44	101.07	Ruthenium - Ru	0.01	-	-
45	102.905	Rhodium - Rh	0.005	-	-
46	106.4	Palladium - Pd	0.01	0.01	0.02
47	107.868	Silver - Ag	0.07	0.04	0.06
48	112.40	Cadmium - Cd	0.2	0.06	0.3
49	114.82	Indium - In	0.1	0.03	0.08

University of Cape Town

50	118.69	Tin - Sn	2	4	3
51	121.75	Antimonium - Sb	0.2	0.4	1.1
52	127.60	Tellurium - Te	0.01	-	-
53	126.9045	Iodine - I	0.5	-	-
55	132.905	Cesium - Cs	3	1.5	1.1
56	137.34	Barium - Ba	0.04%	0.12%	0.02%
57	138.91	Lanthanum - La	30	120	30
58	140.12	Cerium - Ce	60	230	30
59	140.907	Praseodymium - Pr	8.2	20	2
60	144.24	Neodymium - Nd	28	55	15
62	150.4	Samarium - Sm	6.0	11	5
63	151.96	Europium - Eu	1.2	1.0	1.1
64	157.25	Gadolinium - Gd	5.4	5	4
65	158.9254	Terbium - Tb	0.9	1.1	0.6
66	162.50	Dysprosium - Dy	3.0	2	4
67	164.930	Holmium - Ho	1.2	0.5	1.3
68	167.26	Erbium - Er	2.8	2	3
69	168.934	Thulium - Tm	0.5	0.2	0.3
70	173.04	Ytterbium - Yb	3.4	1	3
71	174.97	Lutetium - Lu	0.5	0.1	0.3
72	178.49	Hafnium - Hf	3	5.2	1.5
73	180.947	Tantalum - Ta	2	1.6	0.7
74	183.85	Tungsten - W	1.5	0.4	0.45
75	186.2	Rhenium - Re	0.001	0.0006	0.0004
76	190.2	Osmium - Os	0.005	0.001	0.004
77	192.2	Iridium - Ir	0.001	0.006	-
78	195.09	Platinium - Pt	0.01	0.008	0.009
79	196.967	Gold - Au	0.004	0.002	0.005
80	200.59	Mercury - Hg	0.08	0.2	0.2
81	204.37	Thalium - Tl	0.5	1.3	0.13
82	207.19	Lead - Pb	13	49	8
83	208.981	Bismuth - Bi	0.2	0.1	0.2
90	232.038	Thorium - Th	7.2	52	2.4
92	238.029	Uranium - U	1.8	3.7	0.52

University of Cape Town

In a neutral atom (ie, electrically uncharged) the number of electrons swinging in their orbits around the nucleus is the same as the number of the protons in the nucleus. These electrons do not revolve in a haphazard swarm, but have orbits concentrated in a series of concentric 'shells'. The innermost shell never contains more than two electrons; The second can accommodate up to eight, but no more; The third takes up to eight for some elements, but up to eighteen for others; and, so on. The chemical properties of an element depend on the number of electrons in its atoms, and particularly on those in the outermost shell.

The outer-shell electrons, which are responsible for binding together various atoms into the molecules or crystals of a chemical compound, are called the valency-electrons. Valency is the combining power of an atom, or group of atoms, expressed numerically as the number of electrons which each atom, or group of atoms, has gained, lost or shared. Hydrogen and Sodium ions each lose one electron and their valency is 1+. Some electrons, however, like those of oxygen need two electrons to complete their outer shells. Thus an oxygen atom can combine with two atoms of hydrogen and the result is water, H_2O. But it could also combine with two valency-electrons in its outer shell, for example calcium, to make lime, CaO - in this case the valency is 2+. Where the valency is 3+, as in aluminium, the combination with oxygen requires the proportions represented by Al_2O_3; this oxide is called alumina, and as a gemstone it is familiar as ruby and sapphire. Iron is a more complicated case, as its valency can be either 2+ or 3+, and thus it makes a series of oxides and other compounds, which are distinguised as ferrous (fe^{2+}) and ferric (Fe^{3+}). For example, ferrous oxide, FeO, and ferric oxide, Fe_2O_3.

In the mineral world the most important element with a valency of 4+ is silicon. Its oxide, silica, represented by SiO_2 is well known as quartz, agate and flint. Moreover, silica combines with the other common oxides to form a group of crystalline compounds known as silicates which, together with quartz, constitute a very large majority of the minerals occuring in rocks. Carbon is another element with a valency of 4, vitally important because the latter may be either 4- or 4+. Carbon with a negative valency is the essential element in organic compounds and in all living matter. When the valency is positive, however, as in CO_2, the latter combines with other oxides to form another important group of rock-forming minerals, the carbonates, which predominate in limestones and marbles.

Although about ninety elements occur naturally in minerals (refer to Table 2.08), eight of these are so abundant that they make up approximately 99 per cent by weight of all the rocks that have been chemically analysed. Table 2.09 lists the average composition of these crustal rocks (Ref. 13).

The earth's crust can be regarded as a packing of oxgen ions, with interstitial metal ions such as Si^{4+}, Al^{3+}, Fe^{2+}, Ca^{2+}, Na^{+}, K^{+}, and so forth. The dominant minerals of the crust are thus shown to be silicates, oxides, and other oxygen compounds such as carbonates. Thus the minerals refered to as rock forming minerals are, with a few exceptions, members of these groups.

---

[1] - *Reference 13.*

University of Cape Town

Table 2.09: Average composition of crustal rocks.

In Terms of Elements:					In Terms of Oxides:	
Name	Symbol & Valency	Per cent	Ionic Rad.(Å)	Volume (%)	Name, Formula	Per cent
Oxygen	O^{2-}	46.60	1.40	93.77		
Silicon	Si^{4+}	27.72	0.39	0.86	Silica, SiO_2	59.26
Aluminium	Al^{3+}	8.13	0.51	0.47	Alumina, A_2O_3	15.35
Iron	Fe^{3+}	5.0	0.64	0.43	Ferric, Fe_2O_3	3.14
	Fe^{2+}		0.74		Ferrous, FeO	3.74
Calcium	Ca^{2+}	3.63	0.99	1.03	Lime, CaO	5.08
Sodium	Na^{+}	2.83	0.97	1.32	Soda, Na_2O	3.81
Potassium	K^{+}	2.59	1.33	1.83	Potash, K_2O	3.12
Magnesium	Mg^{2+}	2.09	0.66	0.29	Magnesia, MgO	3.46

Oxygen is by far the most abundant element in rocks. In combination with other elements it forms compounds called oxides, some of which occur as minerals. Silica, SiO_2, is the most abundant of all oxides. Silica is familiar as 'Quartz' a common mineral which is characteristic of granites, sandstones and quartz veins. The different assemblages of silica minerals that characterize igneous, sedimentary, and metamorphic rocks, are veins, pegmatites, weathered rocks, and soils. Each has the potential to tell us something of the enviroment in which it was formed. The soil, from which food is ultimately drawn, bricks, stones, concrete, and glass used in the construction of buildings are either silicates or largely derived from them.

Although each ion in a crystal affects every other ion to some extent, the strongest forces exist between ions that are nearest neighbours. These are said to constitute the first coordination shell. The geometry of arrangement for this shell and the coordination number, are dependent on the relative sizes of the coordinated ions. The relative size of ions is generally expressed as a ratio between the radius of the cation and the radius of the anion in Ångstrom units. When two or more cations are present in a structure, coordinated with the same anion, separate radius ratios must be computed for each. When coordinating and coordinated ions are the same size, the radius ratio is 1. Trial with a tray of identical spheres reveals that spherical units may be arranged in three dimensions in either of two ways, hexagonal or cubic closest packing. In either arrangement, each sphere is in contact with its 12 closest neighbours.

University of Cape Town

When the coordinating cation is slightly smaller than the anions, 8 coordination results - also called cubic coordination because the centres of the anions lie at the centre of a cube. For values of radius ratio less than 0.732, 8 coordination is not as stable as 6, in which the centres of the coordinated ions lie at the apieces of a regular octahedron. For values of radius less than 0.414, 6 coordination is not as stable as 4, in which the centres of the coordinated ions lie at the apieces of a regular tetrahedron. Calculating the limiting value of radius ratio for the condition in which four coordinated anions touch each other and the central ion, we find it to be 0.225. Therefore, we may expect 4 to be the common coordination number when the radius ratio lies between 0.414 and 0.225. Tetraheadral coordination is typified by the SiO_4 group in silicates (it can be noted that triangular or 3 coordination is stable between the limits of 0.225 and 0.155).

The radius ratio of Si^{4+} to that of O^{-2} (refer to Table 2.09) is 0.278. This radius ratio indicates that 4 coordination is the stable state of Si-O groupings. The fundamental unit on which the structure of all silicates is based consists of four ions of oxygen (O^{-2}), one at each corner of the tetrahedron, surrounded and coordinated by one ion of silicon (Si^{4+}) tucked into the intenstitial space in the middle - as illustrated in Figure 2.18(i).
The four positive charges of Si^{4+} are balanced by four negative charges, one from each of the four oxygen ions, O^{-2}, thus leaving each tetrahedron with four negative charges. By themselves these tetrahedral building units would fly appart in consequence of the resulting electrical repulsion.
To bind them strongly together, as in crystals, they must be cemented or linked so that the charges are neutralized.

The powerful bond that unites the oxygen and silicon ions is literally the cement that holds the earth's crust together. This bond may be estimated by use of Pauling's electronegativety concept[1] as 50% ionic and 50% covalent - that is, although the bond arises in part from the attraction of oppositely charged ions, it also involves sharing of electrons and interpenetration of the electronic superstructures of the ions involved. The bond is strongly localized in the vicinity of these electrons.
Although electron sharing is present in the Si-O bond, the total bonding energy of Si^{4+} is still distributed equally among its four closest oxygen neighbours. Hence, the strength of any single Si-O bond is equal to just one-half the total bonding energy available in the oxygen ion. Each O^{-2} has, therefore, the potentiality of bonding to another silicon ion and entering into another tetrahedral grouping, thus uniting the tetrahedral groups through the shared (or bridging) oxygen.

---

[1] - *References 43 and 44.*

University of Cape Town

In no case, however, are three or even two oxygens shared between two adjacent tetrahedra in nature - it would place two highly charged Si^{4+} ions close together and the repulsion between them would render the structure unstable.

Sharing of oxygens may involve one, two, three, or all four of the oxygen ions in the tetrahedron, giving rise to a diversity of structural configurations. Figure 2.18 illustrates the various structural arrangements into which SiO_4 tetrehedra can be combined.

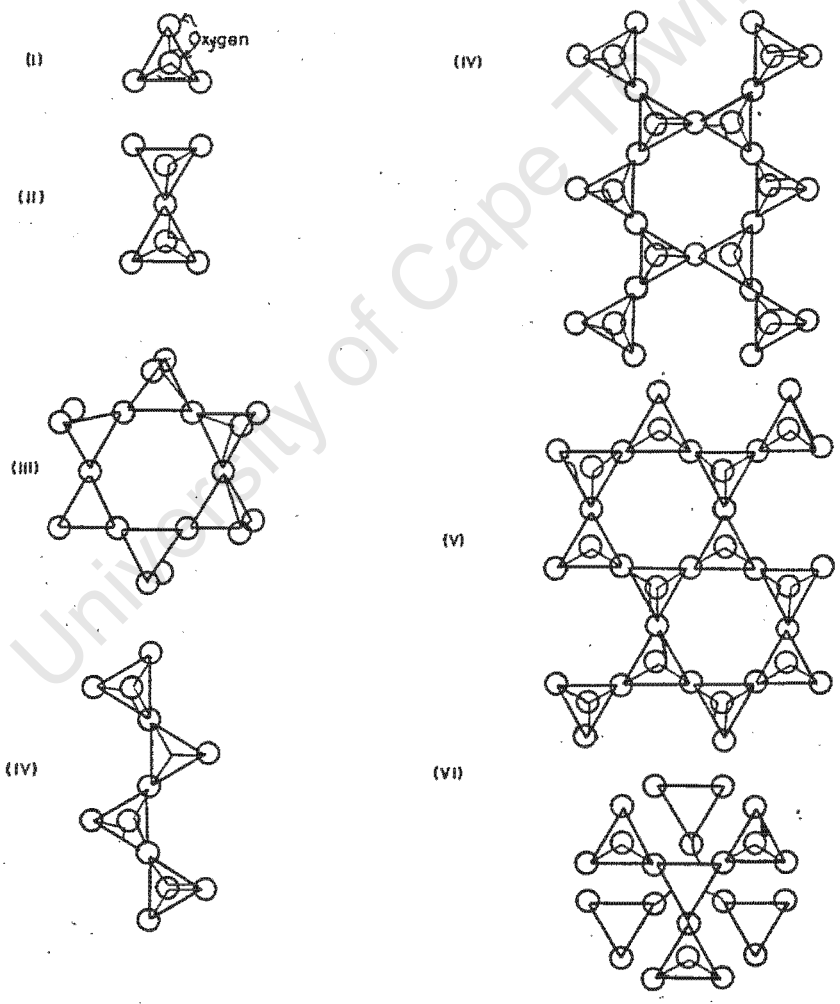

University of Cape Town

Figure 2.18: Structural arrangements of the SiO_4 tetrahedra units, as defined in Table 2.10 - (i) nesosilicates, (ii) sorosilicates, (iii) cyclosilicates, (iv) inosilicates, (v) phyllosilicates, and (vi) tectosilicates.

The resulting classification is summarized in Table 2.10, which defines the structural relationships of SiO_4- tetrahedra (structural arrangements are illustrated in Figure 2.18).

In the explanation of some of the mineral formulae it should be mentioned that Al plays a double role in crystals. It may act as one of the cementing ions between the tetrahedra, or it may replace Si inside some of the tetrahedra, as in the feldspars. Si_4 then becomes $(AlSi_3)$ or $(Al_2)Si_2$, in which cases corresponding additions of suitable ions are necessary to balance the altered charges. A further complication arises in minerals that contain ions like hydroxyl $(OH)^-$, or fluorine F^-. These may occupy relatively large 'hexagonal' spaces in the crystal lattice, as in mica, or they may substitute for oxygen.
It should be noticed that the somewhat misterious ion hydroxyl $(OH)^-$ does not imply that 'water' introduced into the crystal lattice has lost hydrogen; What happens is that the place of an hydrogen ion is taken by two hydroxyl ions - $H_2O + O^{2} - 2(OH)^-$.

Table 2.10: Classification of Silicate Structures.

Structural relationships of SiO_4-tetrahedra:-	Si:O ratio:-	Mineral examples:-
(i) Nesosilicates: Independent SiO_4 units, held together by ions such as Mg^{2+}; No oxygen shared.	SiO_4	Olivine - $(Mg,Fe)_2SiO_4$
(ii) Sorosilicates: Separate pairs of SiO_4, formed by sharing one oxygen.	Si_4O_{14} $(Al_2Si_2O)_{14}$	Melilite - $Ca_2MgSi_2O_7$ $Ca_2Al(AlSi)O_7$
(iii) Cyclosilicates: Separate closed rings of 3, 4 or 6 tetrahedra; 2 oxygens shared.	Si_4O_{12}	Beryl - $Al_2Be_3Si_6O_{18}$
(iv) Inosilicates: Continuous single chains of tetrahedra; 2 oxygens shared.	Si_4O_{12}	Pyroxenes, e.g. Hypersthene - $(Mg,Fe)SiO_3$ Diopside - $Ca(Mg,Fe)Si_2O_6$ Angites - (complex)

University of Cape Town

Continuous double chains, formed by joining 2 single ones; Alternately 2 and 3 oxygens shared; Hexagonal spaces accommodate ions of $(OH)^-$ or F^-.	Si_4O_{11}	Amphiboles, e.g. Tremolite - $Ca_2Mg_5Si_8O_{22}(OH)_2$ Hornblende - (complex)
(v) Phyllosilicates: Continuous plane sheets of hexagonal networks; Formed by sharing 3 oxygens; Resulting hexagonal spaces as for continuous double chains (above).	Si_4O_{10}	Talc - $Mg_3Si_4O_{10}(OH)_2$ Serpentine - $Mg_3Si_2O_5(OH)_4$ Clay Minerals, e.g. $Al_2Si_2O_5(OH)_A$
	$AlSi_3O_{10}$	Micas, e.g. Muscovite - $KAl_2(AlSi_3O_{10})(OH,F)_2$
(vi) Tectosilicates Continuous framework of tetrahedra in 3 dimensions; 4 oxygens shared.	Si_4O_8	Quartz SiO_2 Feldspars, e.g.
	$AlSi_3O_8$	Orthoclase - $K(AlSi_3)O_8$ Albite - $Na(AlSi_3)O_8$ Anorthite - $Ca(Al_2Si_2)O_8$
	$Al_2Si_2O_8$	Feldspathoids, e.g. Nepheline - $Na(AlSi)O_4$

University of Cape Town

Rock-forming Silicate Minerals.

Feldspars are the most abundant minerals of the earth's crust and, as previously mentioned, they consist of frameworks of SiO_4 ans AlO_4 tetrahedra, with ions of K, Na or Ca occupying the appropriate places in the structure. In alkali feldspars Na and K are interchangeable to a limited degree. Thus, potash feldspars orthoclase generally contain a small amount of albite in solid solution with orthoclase, while soda feldspar albite contains a little orthoclase with the albite-ion substitution being limited at both ends. Albite and anorthite form a continuous series of minerals, known collectively as plagioclase. Orthoclase can be recognized as pinkish or cream-coloured mineral in granite.

When feldspars are decomposed in the course of weathering, or by other processes involving solvent action of water, practically none of the aluminium is lost by solution and consequently the residual products become increasingly aluminous. The usual residues are extremely minute flakes consisting of either fine-grained micaceous material called sericite or hydromica or, when all potassium (or Na or Ca) has been lost, a clay mineral of which there are several varieties. Most clay minerals are essentially hydrons silicates of aluminium, with formulae such as $Al_2Si_2O_5(OH)_4$, as in the kaolin group[1].

Under appropriate conditions in tropical climates all silica may be removed from feldspars by weathering. Residue left is bauxite, a mixture of two aluminous minerals with compositions $Al_2O_3.H_2O$ or $AlO(OH)_3$ and $Al_2O_3H_2O$ or $Al(OH)_3$.

Micas, third in abundance amongst the minerals of granite, consist of two main varieties: Muscovite - white, silvery and glistening; Biotite - dark and bronze-like. A third variety is found in association with magnesium-rich rocks. All are hydrons alumino-silicates of potassium. Micas have perfect cleavage because their tetrahedral sheets and binding atoms are all arranged in parallel layers.

Olivine is part of a continuous solid-solution series. The common rock-forming variety contains more Mg than Fe, as expressed by the formula $(Mg,Fe)_2SiO_4$, and is called olivine because of its usual olive-green colour. Rocks in which olivine is the most abundant mineral, and usually associated with pyroxenes, are called paridotite. Serpentine is formed from olivine and other magnesium-rich silicates by a process of alteration involving adding water. Large bodies of peridotite may be replaced by serpentine, which is thus a rock as well as a mineral.
This rock consists of tough but slippery felted mesh or a network of minute crystals. Massive serpentine is usually mottled or variegated in shades of green and brown.

---

[1] - *refer to Table 2.10.*

Pyroxenes are minerals of widespread occurence in a great variety of rocks. They are second most abundant in basalts (after plagioclase) and poridotites (after olivine) and, in associated masses of rock in which pyroxenes are most abundant, are distinguished as pyroxenites.
Chemically the simplest pyroxenes (eg, hypersthene) are like members of the olivine series, but with more silica. Structurally however, they are very different - all the pyroxenes are built of innumerable single chains of SiO_4-tetrahedra with some substitution of AlO_4-tetrahedra in the more complex varieties. The chains are parallel and bound together by ions such as Mg^{2+}.
Chief aluminous pyroxene, and commonest member of the whole group, is augite which may be regarded as a solid solution of diopside with a little hypersthene and varied proportions of 'alumina' and 'ferric oxide'.

The Amphibole group is represented mainly by hornblende and its many varieties. Many rocks closely related to granite contain more hornblende than biotite. Amphiboles are abundant in the metamorphic rocks known as amphibolite. All amphiboles contain ions of hydroxyl, $(OH)^-$, which may be proxied by florine, F^-, as in mica. As in pyroxenes, the amphibole chains are bound together in long parallel bundles. These bundles can be readily split along two particular cleavage planes parallel to the length, and thus both minerals have two well developed cleavages.

The Al- and Fe- bearing ferromagnesian minerals are altered (by processes involving the addition of water) to a group of greenish minerals collectively called Chlorite. These have a double-sheet, or `sandwich', structure like the micas but the `sandwiches' are held together by (OH), Mg or Fe^3.
The particular composition depends mainly on the parent mineral. Because of its structure chlorite has an excellent cleavage. Its individual crystals are usually very small.

University of Cape Town

Rock-forming Minerals.

Although about 2000 named minerals are known, most common rocks can be adequately described in terms of a dozen series of minerals, as indicated in Table 2.11.

Table 2.11: Average Mineral Composition of some Common Rocks[1].

Minerals	Granite	Basalt	Sandstone	Shale	Limestone
Quartz	31.3	-	69.8	31.9	3.7
Feldspars	52.3	46.2	8.4	17.6	2.2
Micas	11.5	-	1.2	18.4	-
Clay Minerals	-	-	6.9	10.0	1.0
Chlorite	-	-	1.1	6.4	-
Amphiboles (mainly hornblende)	2.4	-	-	-	-
Pyroxenes (mainly angite)	rare	36.9	-	-	-
Olivine	-	7.6	-	-	-
Calcite & dolomite	-	-	10.6	7.9	92.8
Iron ores	2.0	6.5	1.7	5.4	0.1
Other minerals	0.5	2.8	0.3	2.4	0.3

By far the most abundant of the rock-forming minerals are silicates (previously described in this chapter). A few other important ones (eg, oxides, carbonates, etc) are now briefly reviewed.

Quartz previously been referred to as an oxide mineral, is classified as a mineral with a silicate structure. Chemically it could be regarded as either SiO_2 or $Si(SiO_4)$. Alumina, Al_2O_3, occurs naturally as corundum, the hardest natural abrasive after diamond. In its rarer transparent form it is familiar as ruby and sapphire.

The oxides of iron are, with the carbonate $FeCO_3$, the chief sources of iron ore. They are notable constituents in a great variety of common rocks: Magnetite, Fe_3O_4, is black and strongly magnetic; Ilmenite, $FeO.TiO_2$, is often associated with magnetite, specially in basalts and rocks of similar composition; Haematite, Fe_2O_3 is of dark red colour. Limonite, averaging about $FeO.H_2O$, is the rusty alteration product of other iron minerals.

Crystalline water, H_2O - glaciers and ice-sheets are rocks on the grand scale composed of granules of ice. After water, the next oxide in order of abundance is that of phosphorus, an element of critical importance in agriculture. Phosphates occur in ordinary rocks as the mineral apatite, $Ca_5F(PO_4)_3$, and as a related compound of organic derivation which has a similar composition, but with (OH) instead of F. If water charged with traces of fluorine passes or soaks through phosphorite, the latter gradually gives up its (OH) in exchange for F, so approaching apatite in composition and becoming more stable.

[1] - *after Holmes, Reference 13.*

University of Cape Town

The chief fluoride mineral is fluorspar, CaF_2, which characteristically occurs in association with lead and zinc ores. It appears in a variety of attractive colours and is mainly used as a flux in making iron and steel. As rock-forming minerals, however, two sulphates are outstanding - anhydrite, $CaSO_4$, and gypsum, $CaSO_4.2H_2O$. Anhydrite occurs in salt deposits, and when the brine becomes sufficiently concentrated, rocksalt or halite (the chief chloride mineral), begins to be precipitated together with anhydrite.

The chief minerals of carbonate rocks are: Calcite, $CaCO_3$, the predominant mineral of limestone; Dolomite, $CaMg(CO_3)_2$ which occurs intermixed with calcite in magnesian limestones, and by itself is the predominant mineral of the carbonate rock called dolomite; Siderite or chalybite, $FeCO_3$, an important ore of iron; and , Carbonates of lead, zinc and copper are locally prominent minerals in many of the deposits of these metals.

University of Cape Town

Introduction to the clay minerals.

According to Grim[1], "clay material is the product of weathering, has been formed by hydrothermal action, or has been deposited as a sediment". The factors which control the properties of clay materials may be classified as follows: Clay-mineral composition - identity and relative abundance of all the clay-material components, since certain clay minerals which may be present in small amounts may exert tremendous influence on the attributes of a clay material; Non-clay mineral composition - identity of the nonclay minerals, their relative abundance, and particle size distribution; Organic material - the kind and amount contained in clay-materials; Exchangeable ions and soluble salts - the relative abundance of both the exchangeable anions and cations should be determined, and the water-soluble salts[2] are frequently required to be washed out before other attributes of the clay material can be studied; Texture - refers to particle size distribution, shape, orientation, and forces tending to bind the particles together. This section deals with the clay minerals.

The clay minerals are the main constituents of the class of argillaceous sediments which, on accumulation and compaction, yields shales or mudstones. Whether in deposits or not, clays are usually products of either weathering or hydrothermal alteration, different clays resulting according to physico-chemical conditions and the nature of the parent materials - for example feldspars, micas, volcanic glasses, or ferro-magnesian minerals.

---

1 - *Reference 45.*
2 - *entrained in the clay.*

According to Holmes[1] - "Weathering is the total effect of all the various sub-aerial processes that co-operate in bringing about the decay and disintigration of rocks, provided that no large-scale transport of the loosened products is involved. The work of rain-wash and that of wind are both essentially erosional and are thus excluded. The products of weathering however, are subjected to gravity and there is consequently a universal tendency on the part of the loosened materials to fall or slip downwards, specially when aided by the lubricating action of water.
The geological work accomplished by weathering is of two kinds: (i) Physical or mechanical changes, in which materials are disintegrated by temperature changes, frost action and organisms; and, (ii) Chemical changes, in which minerals are decomposed, dissolved and loosened by the water, oxygen and carbon dioxide of the atmosphere and soil waters, and by organisms and the products of their decay. The physical, chemical and biological agents actively co-operate with one another."

The chemical processes involve rain-water acting as a carrier of dissolved oxygen and carbon dioxide, together with various acids and organic products derived from the soil. All natural waters are slightly dissociated into H^+ and $(OH)^-$ ions.
The acidity of natural waters is measured by the concentration of H^+ ions, pH as it is called[2].
If the pH value is greater than 7 the water is alkaline, and if less than 7 it is acid. Any increase in acidity increases the rate of weathering reactions.
The pH of rain-water ranges from 4 to 7.
Its acidity comes mainly from dissolved CO_2, which ionizes water:

$$CO_2 + H_2O = H^+ + (HCO_3)^-.$$

The lower values of pH may be due to lightning discharge, and values of 2,8 are also found in certain peat-bog waters.

The main chemical changes that occur during weathering are solution, oxidation, hydration or hydrolosis, and the formation of carbonates. Only a few common minerals resist decomposition, quartz and muscovite being principal examples. Limestone is scarcely affected by pure water, but when CO_2 is also present the $CaCo_3$ (calcium carbonate) of the limestone is slowly dissolved and removed as calcium bicarbonate, $Ca(HCO_3)_2$. Others, like the carbonate minerals, can be entirely removed in solution.
Most silicate minerals break down into relatively insoluble residues, such as the various clay minerals, with liberation of soluble substances which are removed in solution.

---

[1] - *Reference 13.*
[2] - *refer to section 2.2.3 "pH value of each soil type".*

University of Cape Town

Clay minerals are the main residual products of the decomposition of feldspars. Under the hydrolysing action of slightly carbonated waters the feldspars break down as follows:

$6H_2O + CO_2 + 2KAlSi_3O_8 \rightarrow Al_2Si_2O_5(OH)_4$, a clay mineral;
[water] [orthoclase]

$4SiO(OH)_2$, silicic `acid';

K_2CO_3, removed in solution.

From plagioclase the products are similar, except that Na_2CO_3 is formed from albite and $Ca(HCO_3)_2$ from anorthite. Most of the clay is probably at first in colloidal solution. Colloidal forms of clay can break down still further:

$nH_2O + Al_2Si_2O_5(OH)_4 \rightarrow Al_2O_3.nH_2O$, colloidal
[water] [clay]
aluminium hydroxide;

$2SiO(OH)_2$, colloidal silicic`acid'.

The residual products of weathering are naturally more stable in the presence of air and water than the parent minerals. They contain a larger proportion of negative ions, O^{2-} and $(OH)^-$, than the parent minerals. The source of the hydroxyl ions is not water alone, but a reaction between water and oxygen ions,

$H_2O + O_2^- = 2(OH)^-$..

Clay minerals of hydrothermal origin: Argillaceous alteration products due to hydrothermal action are frequently to be found as an aureole around metalliferous deposits - such alteration products are also found associated with hot springs and geysers, in vesicles in igneous rocks, and in fractures; All the various clay minerals have been reported in hydrothermal bodies - the various forms of kaolinite minerals are recorded, including anauxite, dickite and nacrite, as well as various smectites, and nontronite and the magnesium-rich members; A zonal arrangement of the clay minerals has been observed in many of the hydrothermal clay bodies - often there is an inner halo of sericite, an intermediate zone of kaolinite, and an outer zone of smectite and chlorite, with chlorite being most abundant on the outermost fringe.

University of Cape Town

The factors controlling the weathering process:- Parent rock - composition and texture of the parent rock are important in the initial stages of weathering, but their importance decreases as the duration of weathering increases (for example - as reported by Grim[1], soils containing either kaolinite or smectite can both develop from the same parent rock under different conditions of climate, topography, and time, also that the same type of soil with a characteristic clay-mineral composition can develop after a relatively long period of time from rocks of widely different composition and texture); Climate - temperature and rainfall, particularly its seasonal distribution, are the significant climatic factors (that is, direction of the movement of water through the weathering zone and leaching of soluble salts from the material depends on the amount of rainfall and its seasonal distribution); Topography - determines whether or not there is active vertical movement of water through the weathering material (it should be noted that topography also influences the rate of erosion at the surface); Vegetation - significant factors are its amount and kind, including the resulting products of its decay (for example, under cool, humid conditions with decidious forest growth, organic decomposition products develop in the soil which could have very drastic effects on parent silicate minerals); Time - important factor in developing alternation products because weathering processes are relatively slow (alkalies and alkaline earth may be present in the weathering zone of some rocks and an alteration product develops which, after a long time interval during which all the alkalies may be removed by leaching, will develop a different type of alteration product).

Concerning a classification and description of soil groups, the various types of soil may be considered under the three main headings of a general classification that will permit a consideration of clay-mineral composition in relation to mode of occurrence and enviroment:
(1) Zonal soils - after soil-forming processes have been at work for a considerable time, soil over wide areas underlain by rocks of varying kinds, tend to become alike in general characteristics if the climatic influences are reasonably uniform and continuous, and if erosion is not too vigorous - climate with its associated kind of vegetation and organic decomposition material, is the major factor in soil genesis;
(2) Intrazonal soil - reflect the influence of some local conditions such as poor drainage, alkali salts, or some other unique characteristic superimposed on the general characteristics resulting from the climate and vegetation factors (these soils frequently cross zonal boundaries and hence the name);
(3) Azonal soils - little or no alteration of parent material (because of their youth or enviromental setting), these are soils without profile development, such as alluvial and colluvial soil.

---

[1] - *Reference 45.*

University of Cape Town

Classification of Soil Groups of the world.[1]

I. Zonal humid soils: To be found in regions where climate varies from cold to tropical, with rainfall greater than about 625 mm/year; The vegetation is forest with grasses in warmer regions and mosses, lichens and shrubs in tundra areas; The soils are characterized by a concentration of iron and aluminium in certain horizons.

Tundra soils are characterized by an accumulation of organic matter overlying a bluish-grey sticky and compacted subsoil; The frozen subsoil causes poorly drained, boggy conditions for most of the year; The clay mineral content is often low.

Podsolic soils develop under cool and damp climatic conditions, providing an abundant surface accumulation of organic material - cover vegetation to yield on decomposition organic acids and other strong compounds, and sufficient rainfall to provide active leaching conditions; The enviroment is acid, with low pH values of 3.5 in the humus and 4.0 to 4.5 in the clay (under such conditions carbonates are quickly dissolved and alkalies and alkaline earths removed from the profile); Organic and inorganic colloidal components are translocated from the upper horizon downwards to the water table; Intense leaching conditions cause the inorganic colloidal complex to become unstable in the surface horizons, and the iron and alumina are carried away to be reprecipitated at the water table; The removal of aluminium and iron results in the development of a grey, highly siliceous, acid horizon directly beneath the surface accumulation of organic material.

Brown podsolic soils are to be found in the northern hemisphere, south of the true podsols; The siliceous grey horizon is replaced by a friable light-brown one containing considerable organic material; There is little breakdown of colloidal silicates and little translocation of these silicates or aluminium and iron.
Grey-brown podsolic soils lie further south and show mild leaching and a climate which yields a smaller quantity of such products because of more complete oxidation; The grey siliceous layer is replaced by a grey or yellow-brown horizon, and a considerable exchangeable calcium remains on the clay minerals.

Red and yellow podsolis soils are transitional with laterite soil in warm areas and have formed under mild climate, abundant rainfall, and a mixed or largely deciduous forest cover; Leaching is marked, but the breakdown of the silicates is small; There is some translocation of colloidal silicates; The relatively rapid oxidation the iron checks its downward movement, so that it tends to remain in the upper part of the profile.

---

[1] - *after Lyons and Buckman, Reference 46.*

University of Cape Town

Prairie dark and reddish brown soils form under climatic conditions similar to the grey-brown podsols but under grass instead of forest cover.
Laterite soils develop under tropical conditions of high temperatures and rainfall that is often seasonal - primary silicates are quickly broken down and the extensive rainfall causes the quick removal in solution of any alkalies and alkaline earths; Iron tends to be oxidized, particularly under seasonal rainfall, and its movement along with alumina is retarded; The organic material is very rapidly oxidized so that it does not accumulate, and downward-seeping waters carry little organic acid; The downward-moving waters are almost neutral, often slightly on the alkaline side as a result of the presence of alkalies or alkaline earths from the primary silicates - under such conditions of slight alkalinity, the silica tends to be dissolved and removed, with attendant concentration of alumina and ferric oxide in the upper part of the weathering zone.

II. Zonal aridic soils: In these regions the rainfall is less than about 625 mm per year and the vegetative cover is grass or desert plants; There is little or no disintegration of the silicates or migration of colloidal components; They are characterized by the movement of carbonate and its concentration in the horizon - with drier climate, the zone of carbonate concentration gradually comes closer to surface.
Chernozem[1] soils are to be found in areas with 300 to 625 mm of rainfall under grass cover and in a cool climate, because of which the organic material is oxidized very little, and develops a thick black surface horizon rich in organic material; There is little disintegration of the silicates, and leaching is very mild - leaching removes the carbonates from the A2 horizon, which are precipitated and concentrated in the B horizon.
The chestnut-brown aridic soils are found where rainfall is between 250 and 375 mm per year and the climate is warm; The vegetation is scant and, consequently the surface colour is grey brown; Low rainfall permits slight leaching, with the horizon of carbonate concentration being close to the surface.
Grey or red desert soils develop under conditions of high aridity, and in the general absence of a cover of vegetation - because of scant rainfall there is no downward leaching; The dominant movement of moisture through the soil is upward, because of evaporation, with the accumulation of carbonates and other salts at the surface.

University of Cape Town

---

[1] - *ie, black earth.*

The distribution of the above soil groups is presented in Figure 2.19 (from Winters and Simonson[1]) - it shows the whole of Africa, Europe, and South America, the eastern part of North America, and the western parts of Asia and Australia.

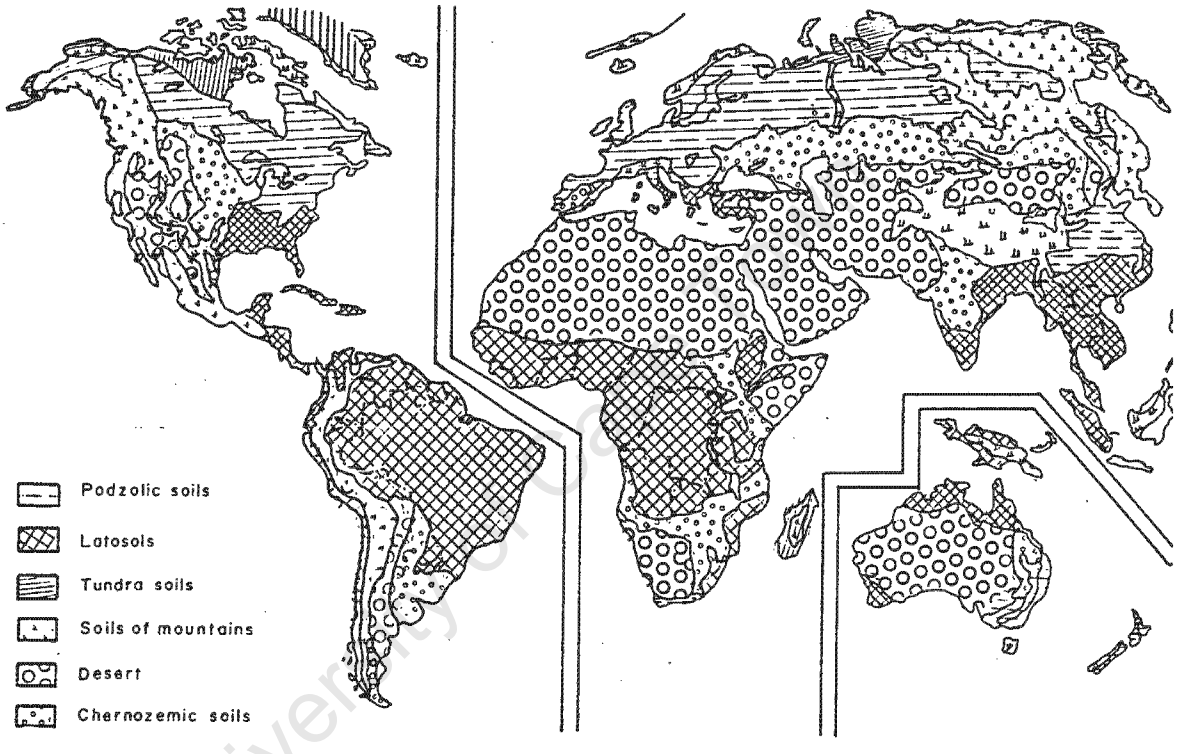

Legend:-
TUNDRA SOILS: Dwarf shrub and moss covered soils of frigid climates.
PODZOLIC SOILS: Forested soils of humid, temperate climates.
CHERNOZEMIC SOILS: Grass covered soils of subhumid, semiarid temperate climates; Includes some soils of wet-dry tropical savannas.
DESERTIC SOILS: Sparsely shrub or grass covered soils of arid, temperate and tropical climates.
LATOSOLS: Forested and savanna-covered soils of humid and wet-dry tropical and subtropical climates.
Soils of Mountains: Thin, stony soils (Lithosols) with inclusions of one or more of the above soils, depending on climate and vegetation (vary with elevation and latitude).
Note: Important areas of organic soils, saline soils, and other intrazonals are omitted as well as very important bodies of alluvial soils, along such great rivers as the Mississipi, Amazon, Nile, Niger, Ganges, Yangtze and Yellow.

Figure 2.19: Distribution of Soil Groups over Africa, Europe, South America, and parts of the other continents[2].

---

1 - *Reference 47.*
2 - *as reported by Grim, Reference 45.*

Clay-mineral composition of soils - according to Grim[1], Jackson[2] assembled data on the frequency distribution of clay minerals and provided the following conclusions:

(i) Inherited minerals such as illite, quartz, feldspar, ferromagnesian minerals, carbonates, and gypsum are most abundant in clays of little-weathered parent materials and in the zonal Desert, Brown, Chestnut, and Tundra soils (as well as intrazonal mountain groups and azonal Regosols and Lithosols);

(ii) Secondary layer-silicate minerals such as vermiculite, secondary chlorite, smectite, kaolinite, and halloysite are most abundant in clays of moderately weathered parent material in soils of zonal Chernozem, Prairie, grey-brown podsolic, Podsol, red-yellow podsolic, and low humic Latosol groups (as well as intrazonal flanosol, Rendzina, dark Magnesium soil, and Wesenboden groups);

(iii) Secondary sesquioxide minerals such as hematite, goethite, and gibbsite, and allophane, anatase, and residual resistant primary minerals such as ilmenite and magnetite, predominate in the more highly weathered materials and the zonal ferruginous humic Latosols, hydrol humic Latosols, latosolic brown, Audo soils, and laterites (as well as the intrazonal tropical savannah and ground water Podzol ortstein soils).

Significant conditions in weathering are the presence of alkalies and alkaline earths, particularly potassium and magnesium, in the envionment of alteration and the length of time they remain in the environment after their liberation from the parent minerals. The kind of alkali or alkaline earth is also important, since potash leads to the formation of illite, magnesium to the formation of smectite, and calcium probably to the formation of smectite, with an added tendency to block the formation of kaolinite. Carbonate tends to retard the disintegration of the primary silicates.

The pH of water moving through the soils is also important, particularly under conditions of active leaching and long periods of time. Under the latter conditions, acidity favours the removal of iron and alluminium and the concentration of silica, whereas neutral or alkaline conditions favour the accumulation of iron and aluminium near the surface.

University of Cape Town

---

1 - Reference 45.
2 - Reference 48.

The Clay Minerals.

The constituents of clays may be assigned to one of two groups - those called clay minerals, which by their nature give to clay its plastic properties, and the others which are accessory non-clay minerals.
The clay minerals have a number of characteristics in common. Their structures are, with a few minor exceptions, based on composite layers built from components with tetrahedrally and octahedrally coordinated cations.
Most of them occur as platy particles in fine-grained aggregates which, when mixed with water, yield materials which have varying degrees of plasticity.

Chemically, all are hydrous silicates[1] which, upon heating, lose absorbed and constitutional water, and at high temperatures yield refractory materials.
Important differences among the clay minerals however, lead to their subdivision into several main groups.
A committee on nomenclature of the Clay Minerals Group of the Mineralogical Society of Great Britain[2] previously suggested the following: That the crystalline clay minerals be divided into chain and layer structures and that the layer structures be divided into 2:1 and 1:1 families, with the names triphormic and diphormic applied to these families; That a further division be made on the basis of the dioctahedral or trioctahedral character of the minerals; and, proposed the names kandites for the kaolinite minerals, including kalloysite, and smectite for the montmorillonite minerals.

The four important layered clay mineral groups are - kandites, illites, smectites and vermiculites.
These have characteristic basal spacings of approximateely 7 Å, 10 Å, 15 Å, and 14,5 Å respectively, but for some categories (the kandite mineral halloysite, smectites and vermiculites) the layer separation is variable since swelling may occur through the intercalation of water or organic liquids, and shrinkage may result from dehydration.

The clay minerals attapulgite and sepiolite have chain-like crystal structures and are less common than the layered clay minerals. The particles of clay minerals may be crystalline or amorphous, platy or fibrous, and though nearly always small, may vary from colloid dimensions to those above the resolution of an ordinary microscope.

---

1 - *principally of aluminium or magnesium.*
2 - *Reference 50.*

University of Cape Town

Chemical composition may vary according to the extent of replacement of Si, Al, and Mg by other cations, the nature and quatity of inter-layer cations, and the water content. The clay minerals vary in their dehydration and breakdown characteristics and in their decomposition products, and they also differ in their cation exchange properties according to the nature of their inter-layer cations and residual, surface charges. Their uses are many - some, for example, being particularly suitable as components of drilling muds, some for catalysts in petroleum processing, some for fillers in paper manufacture, and some for ceramic and refractory ware.

The clay minerals are the main constituents of one class of sediments (and consequently called argillaceous) which on accumulation and compaction yield shales or mudstones. Whether in sedimentary deposits or not the clays are usually products of either weathering or hydrothermal alteration (refer to the 'Introduction to the clay minerals' part in section 2.4.2[1]), different clays resulting according to physio-chemical conditions and the nature of parent materials (for example - feldspars, micas, volcanic glasses, or ferromagnesian minerals).

University of Cape Town

The principal clay mineral groups are:

(1) Kandite group, includes kaolinite, dickite and nacrite, halloysite and meta-halloysite;

(2) Illite group, including illite, hydro-micas, phengite, brammallite, glauconite and celadonite;

(3) Smectite group, including montmorillonite, nontronite, hectorite, saponite and sauconite;

(4) Vermiculite;

(5) Palygorkite group, including palygorskite, attapulgite and sepiolite.

Grim[2] subsequently suggested the classification shown in Table 2.12, which based distinctions on the shape of the clay minerals and the expandable, or nonexpandable character of the 2:1 and 1:1 layer of silicates. The distinction between dioctahedral and trioctahedral minerals was not used as a distinguishing characteristic because of the difficulty in determining this character in many complex clay-mineral mixtures.

---

1 - *"Introduction to mineralogy and the clay minerals".*
2 - *Reference 45.*

Table 2.12: Classification of the clay minerals - according to Grim[1].

I. Amorphous
Allophane group

II. Crystalline

A. Two-layer type (sheet structures composed of units with one layer of silica tetrahedrons and one layer of alumina octahedrons).
1 - Equidimensional: Kaolinite group - kaolinite, nacrite, etc.
2 - Elongate: Halloysite group.

B. Three-layer types (sheet structures composed of two layers of silica tetrahedrons and one central dioctahedral or trioctahedral layer).
1 - Expanding Lattice
a) Equidimensional: Montmorillonite group - montmorillonite, sauconite, etc.; Vermiculite.
b) Elongate: Montmorillonite group - nontronite, saponite, hectorite.
2 - Nonexpanding Lattice: Illite group.

C. Regular mixed-layer types (ordered stacking of alternate layers of different types).
Chlorite group.

D. Chain-structure types (hornblende-like chains of silica tetrahedrons linked together by octahedral groups of oxygens and hydroxyls containing Al and Mg atoms).
Attapulgite.
Sepiolite.
Palygorskite.

Some of the important characteristics of the various clay mineral groups are briefly listed in Table 2.13.

[1] - *Reference 45.*

University of Cape Town

Table 2.13: Summary of the principal characteristics of the clay mineral groups.

	Kandites	Illites	Smectites	Vermiculites
Structure type:	1:1 tetrahedral and octahedral components (diphormic)	2:1 triphormic	2:1 triphormic	2:1 triphormic
Octahedral component:	di-octahedral	mostly di-octah.	di-cor tri-octah.	mostly tri-octah.
Principal interlayer cations:	nil	K	Ca, Na	Mg
Interlayer water:	only in halloysite (one layer H_2O mols.)	some in hydra-muscovite	Ca, two; Na, one layer H_2O mols.	two layers
Basal spacing:	7.1Å (10Å in halloysite	10Å	variable; most 15Å (for Ca)	variable; 14.4Å when fully hydrated
Glycol:	taken up by halloysite	no effect	takes two layers 17Å	takes one layer, 14Å
Chemical formula:	$Al_4Si_4O_{10}(OH)_8$	$K_{1-1,5}Al_4(Si,Al)_8O_{20}(OH)_4$	$M^+_{0,66}(Y^{+3}Y^{+2})_{4-6}Si,Al)_8O_{20}(OH)_4nH_2O$	$M^{+2}_{0,66}(Y^{+2},Y^{+3})_6(Si,Al)_8O_{20}(OH)_4 8H_2O$
Acids:	Kaolinite scarcely	readily attacked	attacked	readily attacked
Heating 200°C:	halloysite collapse to 7.4Å, others unchanged	no marked change	collapse to approximately 10Å	exfoliation; shrinking of layer spaces
Heating 650°C:	Kaolinite -> meta-kaolin. 7Å dickite -> meta-dickit.14Å	10Å	9.6-10Å	collapse to 9Å

University of Cape Town

Optics,	α	1.55-1.56	1.54-1.57	1.48-1.51	1.52-1.57
	j	1.56-1.57	1.57-1.61	1.50-1.53	1.54-1.58
	δ	≈ 0.006	≈ 0.03	0.01-0.02	0.02-0.03
	2V	24°-50°	<10°	variable	<10°
Para-genesis:		alteration of acid rocks, feldspars, etc. Acidic conditions.	alterat. of micas, felds., etc. Alkaline condit. High Al& K conc. favoura-bility.	alteration of basic rocks, volcanic material. Alkaline condit. Availabi-lity of Mg & Ca defi-ciency of K.	alteration of biotite flakes or of volcanic material, chlorites, hornblende, etc.

University of Cape Town

The Clay-Water System.

This section refers to the water which can be held by clay materials only of relatively low temperatures and is removed by heating to about 100 to 150°C. The nature of the low-temperature water and the factors that control its characteristics are of great importance, since they largely determine the plastic, bonding, compaction, suspension, and other properties of clay materials.

The water lost at low temperatures may be classed in three categories, depending on its relation to the mineral components and to the texture of the clay materials, as follows: (1) The water in pores, on the surface, and around the edges of discrete particles of the minerals composing the clay material; (2) In the case of vermiculite, smectite, and the hydrated form of halloysite, the interlayer water between the unit-cell layers of these minerals - this is the water that causes the swelling of smectite; and, (3) In the case of sepiolite-attapulgite-polygorskite minerals, the water that occurs within the tubular opening between the elongate structural units.

Type (1) water requires little energy for its removal, and drying at slightly above room temperature is adequate for its substantially complete elimination. Water of types (2) and (3) requires definite energy for its complete removal. In the case of vermiculite and smectite minerals, temperatures at least approaching 100°C are necessary for substantially complete elimination of interlayer water. These minerals rehydrate with difficulty if the dehydration is absolutely complete, but easily if a trace of water is allowed to remain between the unit layers.

In the case of the hydrated form of halloysite, drying at room temperature is adequate to remove most of the interlayer water, but higher temperatures are required for its total removal. In this case the reaction is not reversible and the hydrated mineral ordinarily cannot be formed again. The water in the channels of the sepiolite-attapulgite-palygorskite minerals is lost at about the same temperature as the interlayer water, and the layer clay minerals. The channel water is regained readily if removal is by drying only at low temperatures.

As reported in Grim (Ref. 45), many authors have presented evidence to show that the water held directly on the surfaces of the clay particles is in a physical state different from that of liquid water. The specific characteristics of this water which delimit it from ordinary water would probably be restricted ordinarily to relatively short distances from the clay-particle surfaces.

The possible thickness of nonordinary water can vary a good deal even for a given clay mineral, and the transition from nonordinary to ordinary water can be abrupt or gradual. It appears certain that the possible thickness of the nonordinary[1] water is relatively small on irregular surfaces, such as those around the edges of clay-mineral particles, and relatively large on the flat surfaces of clay minerals. The film of nonordinary water is best developed and appears to reach its greatest thickness on the basal plane surfaces of the expanding-lattice minerals of the smectite group. It follows that the water in pores would be substantially liquid water, with nonliquid water forming only a thin film on the surface of the pores and where adjacent clay-mineral particles come together.

University of Cape Town

The structure of ordinary water.

Forces between water molecules:-

The individual water molecule is well characterized, and many of its properties can be computed by quantum-mechanical calculation with the results in good agreement with experiment[2]. The O-H bond length is 0.957 Å and the H-O-H angle is 104^{o} 31^{1}. The electrons may be represented by a charge cloud which has, in addition to the appropriate density along the bonds, lobes comprising the so-called lone pairs. These lobes extend above and below the H-O-H plane and are directed somewhat backward away from the hydrogens so that the whole structure can be represented by a somewhat distorted tetrahedron, the protons directed toward two of the vertice and the lone pairs towards the other two. The dipole moment is 1.83 debye units and the quadrupole moment is -5.6×10^{-26} electrostatic unit.

---

1 - *also called nonliquid.*
2 - *Reference 51.*

The fact that the melting point, boiling point, and critical temperature of H_2O are so high relative to those of the isoelecronic species Ne and CH_4, results from the H_2O dipoles[1], and from the fact that H_2O molecules can form hydrogen bonds with each other. The hydrogen bond is a short-range interaction involving a proton of one molecule and a lone pair of another. The presence on each H_2O of two protons and two lone pairs in approximately tetrahedral geometry makes possible the fitting together of a space-filling network of hydrogen bonds in the four-coordinated structure of ice, as shown in Figure 2.20. In this structure the O-O distances are almost exactly equal at 2.76 Å, the O-O-O angles are almost exactly tetrahedral, and the protons lie almost exactly in the O-O lines, each being about 1.0 Å from the oxygen to which it, for the time being, belongs.

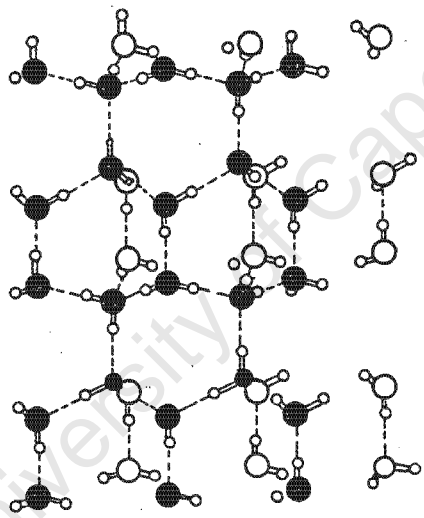

University of Cape Town

Figure 2.20: The structure of ordinary ice.

As stated above, the qualitative difference between what happens here and what happens in a pairwise encounter between two Ne atoms or two CH_4 molecules can be ascribed, to the first order, to the permanent dipole carried by an H_2O molecule. This permanent dipole attracts (on average) the permanent dipole of another H_2O and, in addition, acts on the polarizability of the other molecule to produce an induced dipole which it attracts. The effects however, are known not to be additive since values of the third virial coefficient, (describes the interaction of triplets computed on the basis of such additivity), differ from those derived from experimental data[2].

---

1 - *and higher multipoles.*
2 - *see reference 51.*

The situation becomes more complicated as vapour becomes denser and more molecules enter into simultaneous mutual interaction.

When ice melts.

The four-coordination characterizing the structure of ordinary ice is a very inefficient way of filling space. The ice structure of Fig. 2.20 contains void spaces, and the fact that water formed when ice melts is denser than ice, is to be accounted for in terms of a liquid structure in which such voids either no longer exist, were partially filled, or reduced in relative size by bond-bending or reorganization. These three alternatives have been proposed (although not in the chronological order given here) as bases for structural models of liquid water. In the explanations offered for the shrinkage that occurs when ice melts, there must be also a way to account for additional and related peculiarites, such as the phenomenon of maximum density increase of thermal expansibility when pressure is applied and the effect of increased pressure in lowering the viscosity of cold water[1]. The experimental properties of water make it look as if the structural change taking place when ice melts stops short of completion at $0^{o}C$ and 1 atmosphere pressure but can be driven farther by warming or squeezing.

The structure of cold water seems likely to consist, for most part of hydrogen-bonded four-coordinated framework regions, with interstitial monomers occupying some fraction of the cavities the framework encloses. The exact geometry of the framework has not been specified, but some evidence suggests that it is rather regular at low temperatures and becomes more random as the water gets warmer.

Adsorbed water on clay.

Introduction:-

According to R.T. Martin[2], the importance of adsorbed water to soil engineering is immediately obvious when one realizes that adsorbed water includes virtually all water at any moisture content less than approximately the liquid limit.

There is complete unanimity among different investigators that water adsorbed on clay surfaces differs in structure and physical properties from bulk liquid water. For the purpose of this thesis, adsorbed water is defined as the entire interfacial region between the oxygen or hydroxyl surface of the clay crystal and bulk liquid water. The thickness of the adsorbed water layer is a variable, ranging from only a fraction of the surface being covered by one molecular layer up to many tens of molecular layers, depending upon water content and the type of clay.

---

1 - *References 52 and 53.*
2 - *Reference 54.*

University of Cape Town

Adsorbed water density:-

Three important conclusions are shown by available adsorbed water density data for Na-montmorillonite shown in Figure 2.21: (1), at the same temperature there are no contradictory data pertaining to the density being greater or less than that of normal liquid water; (2), at water contents below 0.3g H_2O/g clay the density exceeds 1.0, while at water contents above 1.0g H_2O/g clay the adsorbed water density is within 2-3 percent of that of normal liquid water; (3), at no water content does the density approach the density required for ice (0.90) or for the hexagonal theory (0.92).

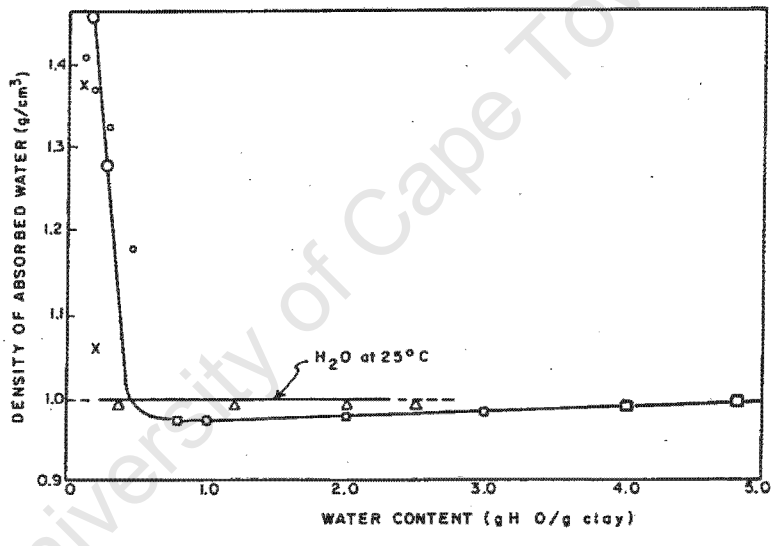

Legend :-

- • De Wit & Arens. (Ref. 55)
- X Mackenzie (Ref. 56)
- o Mooney et al (Ref. 57)
- △ Norrish (Ref. 58)
- □ Anderson & Low (Ref. 59)

Figure 2.21: Adsorbed water density on Na-montmorillonite.

Thermodynamic properties:-

For physical sorption upon an inert adsorbent, it has been demonstrated[1] that integral entropy and energy[2] are the proper thermodynamic functions to be used for interpreting the assembly of water molecules alone in terms of intermolecular interactions, configurations of assembly, rotation of molecules, etc.

---

1 - *in reference 60.*
2 - *adsorption thermodynamics.*

University of Cape Town

If adsorbent perturbations are appreciable, as for clay surfaces where exchangeable ions move out from adsorbent surface as water vapor pressure is increased, integral thermodynamic functions are well-defined quantities but extra data is necessary for elucidation of the physical significance. For dilute clay suspensions differential functions (solution thermodynamics) are appropriate. There is no clear point in the transition region between adsorption and solution where the former loses its advantage.

Entropy data showed that: On kaolinite the water in the sorbed phase have greater randomness[1] than in bulk liquid water for at least the first two molecular layers; On montmorillonite the data are inadequate to reach any definite conclusion concerning water molecules *per se*; On montmorillonite the nature of the exchangeable ion has a profound influence upon differential entropy changes which are both positive and negative; and, On montmorillonite a negative differential entropy change in the water associated with clay is measurable at a water content of 1200 percent.

Dielectric and magnetic properties.

Quirk (Ref. 61) in his review of water vapour adsorption data on clays finds that a relative humidity of 20 percent corresponds closely to a monomolecular layer and that drying four different kaolinites over P_2O_5 showed the water content to be equivalent to one-third of a monolayer. Thus it seems that Muir's dielectric loss data (Ref. 63) are for surface coverages 'θ' from 0.3 to 1.3. The low value of maximum dielectric loss is to be anticipated for such low water contents; however, any interpretation in terms of the adsorbed phase may be obscured by dielectric loss of the clay crystals themselves.

From dielectric measurements of decimeter wavelength, data of Deeg and Huber (Ref. 64) showed that dielectric properties of water in kaolinite-water can be treated as those of pure water for water contents greater than about the plastic limit (that is, about 60% for montmorillonite and 40% for kaolinite).
The dielectric dispersion[2] of kaolinite-water systems was constant at 2.5 up to a water content of 18% or at least twenty to thirty molecular layers. For the montmorillonite-water system the dielectric dispersion began increasing at a water content of 8% or less than one molecular layer - Figure 2.22.

---

1 - *that is, a positive integral entrophy.*
2 - *the real part of the complex dielectric constant.*

University of Cape Town

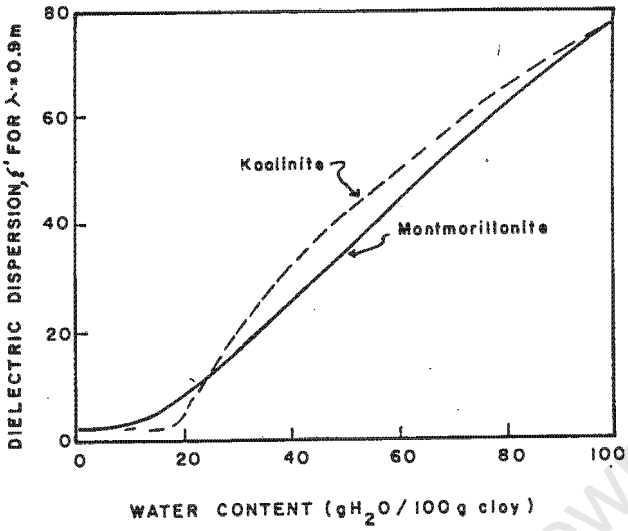

Figure 2.22: Dielectric dispersion of adsorbed water as a function of water content.

Pickett and Lemcoe[1] employed nuclear magnetic resonance for the study of adsorbed water. Figure 2.23 shows that beyond a couple of molecular layers the clay surface has only a small effect on the line width. In fact, for Na-montmorillonite at θ = 0.5, the line width is 350 milligauss, which is less than one-tenth that of ice.

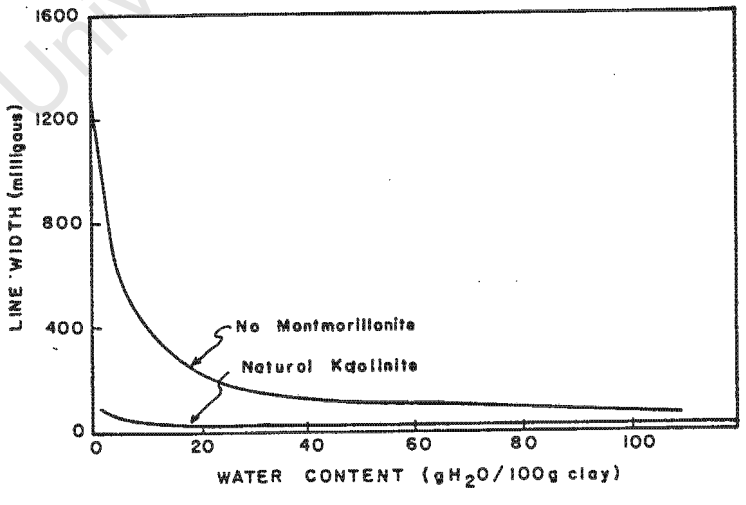

Figure 2.23: Nuclear magnetic resonance line width with water adsorbed on clay (after Pickett and Lemcoe[1]).

---

[1] - Reference 65.

University of Cape Town

From the combination of dielectric and nuclear magnetic resonance data, a two dimensional liquid model for the sorbed phase seems to allow a more consistent interpretation of the data than a fixed adsorption site model.
The meager dielectric and magnetic data available for clay-sorbed water systems would be consistent with either the two-dimentional liquid or the fixed adsorption site model.

Diffusion and fluid flow.

The interpretation of diffusion and fluid flow experiments has a great significance to clay-water systems because it requires some assumption, either explicit or implied, concerning the flow path.
The effective flow path is controlled for a given particle size by the geometrical arrangement of the particles[1].
Since clay fabric is particularly sensitive to environment, it must be either rigidly controlled or carefully considered as a possible factor that will account for experimental diffusion and fluid flow data.

Fluid flow and diffusion measurements in clay-water systems provide no clear-cut evidence concerning the nature of adsorbed water.

Freezing.

There are two aspects to the freezing of any substance: The first is supercooling, which means that upon cooling the liquid remains metastable below the melting point; The second is freezing point depression, which is a change in the temperature at which the liquid freezes or melts.
Since both occur in clay-water systems, one can conclude that the water in the clay-water systems differs from normal liquid water.

Supercooling may be very significant in fairly larger glass capillaries - Figure 2.24.
The 'spontaneous freezing temperature' of Hosler and Hosler[2] is predominantly supercooling and not freezing point depression because when freezing occurred the entire mass of water immediately changed to ice.

University of Cape Town

---

1 - *that is, the clay fabric.*
2 - *Reference 66.*

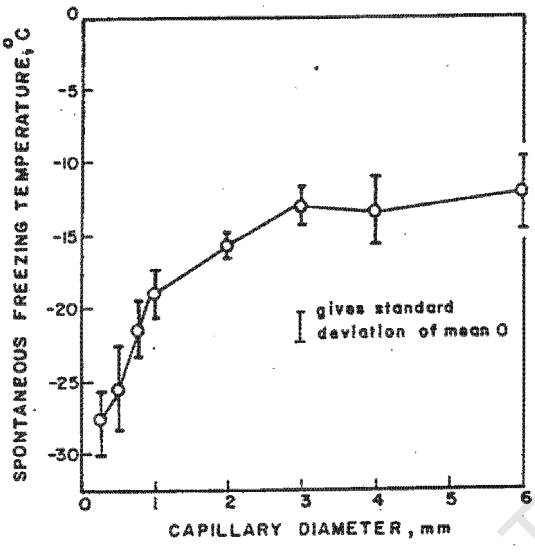

Figure 2.24: Spontaneous freezing temperature as a function of capillary diameter (from Hosler and Hosler[1]).

The fact that supercooling is very commonly observed in clay-water systems clearly indicates that the water differs from normal water. However, the direction of the change is indeterminant from supercooling data.
It is also a well documented fact that an appreciable fraction of the water in a clay-water system remains unfrozen to temperatures of at least -40°C.

Rigid water films.

Kaolinite and halloysite develop strength by air-set with little change in water content while illite and montmorillonite show no appreciable strength gain without an accompanying loss of water.
All the data from Grim and Cuthbert's[2] have been plotted on Figure 2.25. Starting at the right, the points on each curve are for time: 0; 0.25; 0.5; 1; and 3 hr, respectively.

Obviously all the clays show the same trend, from which the writer would conclude that the major factor for increase in strength with time for all the clays was the decrease in water content.

1 - Reference 66.
2 - Reference 67.

University of Cape Town

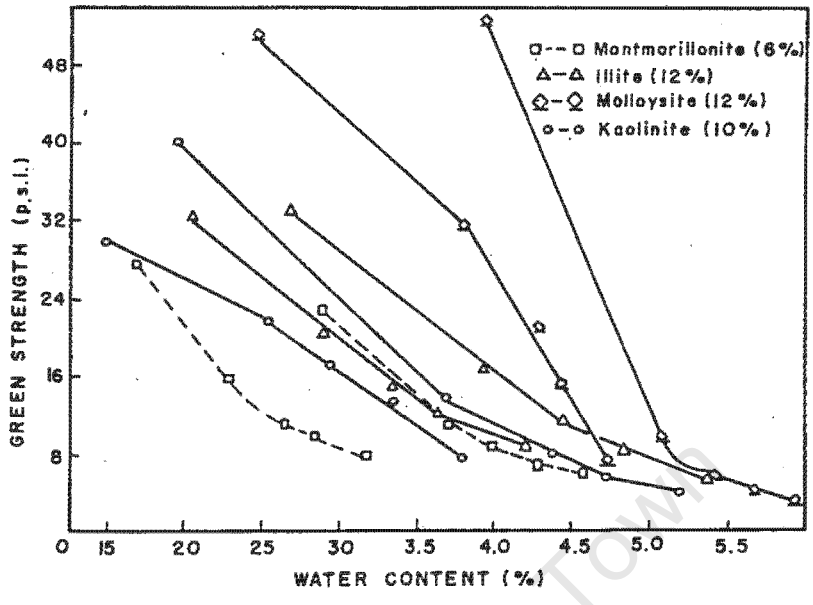

Figure 2.25: Change in strength of sand-clay mixtures with time and water content for different clays[1].

Summary and Recommendations.

Starting from normal liquid water the adsorbed water may vary in any number of ways - two models were mentioned: (1) solid; and (2) two-dimensional fluid. The solid model does not mean that water molecules are rigidly fixed into a well ordered lattice but only that there is more 'order' than in normal liquid water. The two-dimensional fluid model recognizes the constraint, due to the clay surface, slightly differently; as in the solid model each bond that forms would be stronger than in normal liquid water, however, because of surface constraint, the number of bonds that can form between the polar water molecules is considerably reduced from that in normal liquid water. The result is that two-dimensional fluid will resist appreciably normal stress but will shear more easily than normal liquid water. The available data is, for the most part, consistent with either of the two models.

Behaviour of clay-water systems below $0^{o}C$ provides additional evidence against ice structure. In addition to the evidence against ice structure and hexagonal net structure theories, there is no data to support them. The entropy of ideal two-dimensional water approximates that of normal ice; thus, an entropy less than normal liquid water does not prove that water molecules are more solidlike than normal liquid water. The water molecules may be nearly completely free to move around over the surface and the lower entropy simply results from surface constraint.

---

[1] - *after Grim and Cuthbert - Reference 67.*

University of Cape Town

Adsorbed water density data show that the water is different from normal liquid water; however, a low density can be obtained from a solid or a compressed gas. For rigid microporous solids, such as silica gel, dielectric data have provided aid toward elucidation of the molecular structure. A recurring stumbling block to the interpretation adsorbed was the problem of contaminated clay surfaces. It should be noted that the significance of any data, regardless of accuracy and precision of measurements, is limited by the sample itself. Such limitation is particularly true for clean clay surfaces because it will change spontaneously.

Therefore, there are two choices the investigator can perform his experiments using either:
(1) a clean clay surface, taking care that the surface does not change measurably during the experiment; or
(2) a clay surface in equilibrium with its enviroment which generally implies appreciable surface contamination by alumina or silica gel, or both.

University of Cape Town

The status of clay mineral structures.

Octahedral cation ordering:-

According to Bailey[1] octahedral cation order is common, but tetrahedral cation order is confirmed in only three cases. Because of ordering of Si, Al does not significantly affect the statistical tests for centrosymmetry, centrosymmetric space groups that do not permit order should be avoided during refinement. Based on theoretical grounds, Veitch and Radoslovich[2] proposed that octahedral cations of different size and valence will tend to adopt an ordered distribution. Cations with high valence will either occupy two sites, or else they occupy one site with the other two essentially filled with larger mono and divalent cations. This general tendency is confirmed in most, but not all, of the recent detailed structural studies.

The vacant site has been found to be ordered in all dioctahedral species so far investigated. In fact, heating studies at 600^{o}C on pyrophyllite, paragonite, hydrons mica, and montmorillonite by Lindgvist (Ref. 70) indicate that when two cations are distributed randomly over three octahedral sites the interplanar spacing d(060) increases to such an extent that the mineral would not be recognizable as dioctahedral.

---

[1] - *Reference 68.*
[2] - *Reference 69.*

Octahedral and tetrahedral sheet configuration and articulation.

Oversize tetrahedral sheets articulate with smaller octahedral sheets by tetrahedral rotation and, for dioctahedral species, by tetrahedral tilting around vacant octahedra. The latter mechanism influences the type and regularity of layer sequences. Undersize tetrahedral sheets articulate with larger octahedral sheets by tilting plus octahedral contraction or by inversion of some tetrahedra. The amount and direction of tetrahedral rotation and tilt, length of T-O (triclinic structure-oxygen), M-O (monoclinic structure-oxygen), and O-O (oxygen-oxygen) bonds, sheet thicknesses, and relation of cell dimensions to composition, can now be predicted with some confidence.

Octahedral sheet configuration - in an idealized dioctrahedral sheet with six Al^{3+} cations arranged in an hexagon around each vacant octrahedral site, attractive and repulsive forces within the sheet will distort it in the following ways: (i) Adjacent Al^{3+} cations will repel one another and move farther apart, as each anion is pulled in only one direction, shortening of shared edges results; (ii) Because of shortening of the shared octahedral edges, the entire octahedral sheet is thinned along the sheet normal, and is expanded along X and Y (axis) within it - typical sheet thicknesses are 2.04 to 2.10 Å for Al compositions (shown in Table 2.14); (iii) Lateral edges of the traids around the vacant site are expanded due to outward movement of these anions resulting from shared edge shortening; (iv) Direction of movement of anions on shared edges is such as to rotate the upper and lower octahedral triads in opposite directions.

For trioctahedral clays lateral cation repulsion is less than for the dioctahedral case because of smaller charge per cation. Each anion is now pulled in three directions along three shared edges. The anion cannot move directly along any shared edge, only inward along the sheet normal[1]. For this reason trioctahedral sheets are nearly as thin as dioctahedral sheets (Table 2.14).
Because of limitations on the direction of movement of octahedral anions, shared octahedral edges for trioctahedral clays are only slightly shorter than unshared edges. Observed average values for shared edges range from 2.6 to 2.9 Å and for unshared edges from 3.0 to 3.2 Å. Aside from variations due to cation ordering, the octahedra are more regular in size than their dioctahedral counterparts and do not have twisted edges.

---

[1] - *that is, the resultant of the forces.*

Table 2.14: Octahedral sheet thickness.

(A) One octahedral sheet:

Dioctahedral (Å)		Trioctahedral (Å)	
kaolinite	2.10	amesite	2.02
dictite	2.04	cronstedite	2.19
muscovite	2.09	phlogopite	2.19
paragonite	2.09	xanthaphyllite	2.15
margarite	2.07	ferri-annite	2.15
celadonite	2.46	ferriphlogopite	2.22

(B) Two octahedral sheets:

	2:1 Unit (Å)	Interlayer (Å)
prochlorite (IIb)	2.11	1.90
corundophyllite (IIb)	2.05	1.91
kammererite (Ia)	2.15	2.03
ripidolite (Ib)	2.18	1.98
dioctahedral chlorite (IIb)	2.05	2.15
vermiculite (Ia)	2.17	2.34

University of Cape Town

Importance of octahedral sheet: The size of the octrahedra and their linkage pattern are believed to have a controlling influence on the pattern of linkage of SiO_4 groups and their geometry of articulation with the octahedral network. Although the relative sizes of octahedral and tetrahedral sheets as joined together in a layer structure can be measured, it is difficult to assess their sizes in the free state.

Figure 2.26 suggests that the b parameter for an unconstrained tetrahedral sheet would be approximately 9.04 Å for composition Si_4Al_O and 9,50 Å for composition Si_2Al_2. These values can be compared with equivalent parameters of 8.65 Å measured for gibbsite and bayerite [$Al(OH)_3$] and 9.63 Å measured for brucite [$Mg(OH)_2$]. This comparison suggests that the tetrahedral sheet will be larger than the octahedral sheet for all dioctahedral Al-rich species and for trioctahedral species with appreciable tetrahedral substitution. Tetrahedral sheets with little or no substitution will be smaller than octahedral sheets containing primarily Mg and Fe.

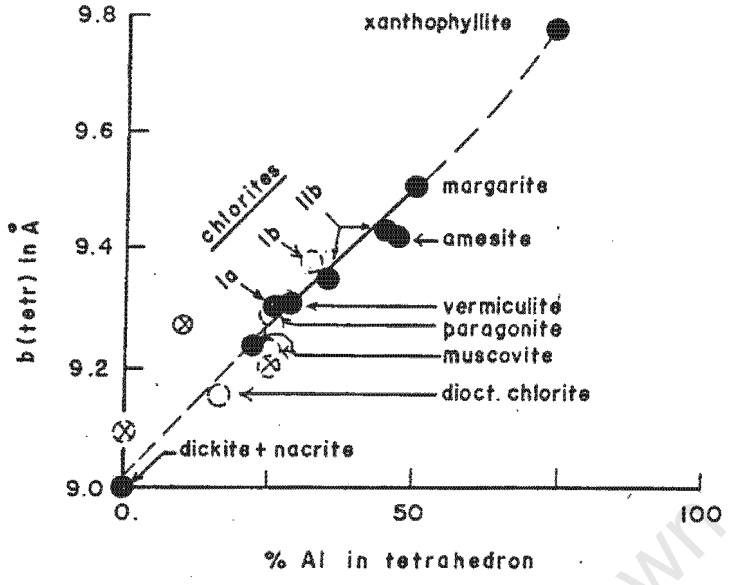

Legend:
(○) indicate no chemical analysis available;
(⊗) represent electron diffraction studies on kaolinite, celadonite, and philogopite-biotote (left to right).

Figure 2.26: Variation of lateral dimension of an unconstrained tetrahedral sheet as a function of Si, Al[1].

An alternative clockwise and anticlockwise rotation of the tetrahedra about the sheet normal will reduce the lateral dimensions according to the following expression:

'cos α = b(obs)/b(tetr)'.

Where: α - angle of rotation; b(obs) - observed or resultant b parameter; b(tetr) - initial b parameter of unconstrained sheet. The amount of tetrahedral rotation for a silicate layer can be predicted, provided b(tetr) can be estimated. Direction of rotation: In mica structures the basal oxygens in both tetrahedral sheets move toward the positions of the nearest octahedral cation in the same layer; In five chlorite and two vermiculite structures that were refined, the basal oxygens always move toward the nearest interlayer anion; In 7 Å structures the influence of octahedral cation in the next layer, considered to be below the basal oxygen surface, is the dominant factor for the trioctahedral species that were examined - basal oxygens rotate toward the octahedral cation in the layer below (direction is always away from the nearest hydroxyl below the octahedral cation and to or away from the octahedral cation, and where rotation of the basal oxygens toward the latter is physically impossible, oxygens rotate toward the nearest hydroxyl and upper octahedral cation); In the three dioctahedral kaolins, the rotation is always toward the superposed lower hydroxyl and upper octahedral cation.

---

[1] - *from Bailey, Reference 68.*

University of Cape Town

Structural adjustments: For trioctahedral layer silicates the octahedra tend to be regular and the lateral triad edges similar in size, as shown in Figure 2.27 (i), even in cases involving cation order, the deviation of individual unshared edge lengths from the mean is usually less than ± 2% - an oversize tetrahedral sheet (the common case because of tetrahedral substitution in trioctahedral clays) can fit onto this regular octahedral surface with minimum stress by the simple mechanism of uniform lateral compression as result of tetrahedral rotation; For Al-rich dioctahedral species, Figure 2.27 (ii) shows that each hexagon within the octahedral sheet is distorted (there are four short twisted edges and two elongated ones) - two short edges can adjust by tetrahedral rotation as previously described, however, the two elongated hexagon edges can only be adjusted by tilting the tetrahedra (apices of adjacent tetrahedra point away from one another on each elongated octahedral edge) and consequently the tetrahedral basal oxygen becomes non-coplanar.

University of Cape Town

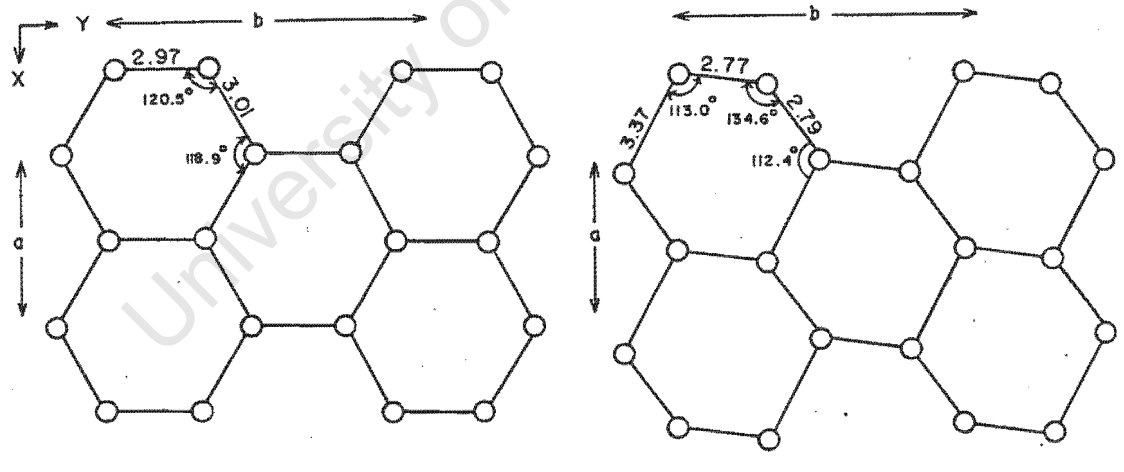

Figure 2.27: Distorted oxygen network - (i) in trioctahedral xanthophyllite, and (ii) at octahedral-tetrahedral junction in dioctahedral margarite (also included in Table 2.14)[1].

In addition to the structural adjustments due to tetrahedral rotation, tilt, and inversion, both octahedral and tetrahedral sheets can adjust their thickness considerably to achieve articulation. The variations found in octahedral thicknesses for different minerals (Table 2.14) are about two times as large as the variations in tetrahedral thicknesses (shown in Table 2.15).

---

[1] - *after Takénchi, Reference 71.*

Table 2.15: Tetrahedral sheet thicknesses.

Dioctahedral (Å)		Trioctahedral (Å)	
kaolinite	2.17	amesite	2.29
dickite	2.30	cronstedtite	2.41
muscovite	2.24	phogopite	2.17
paragonite	2.24	ferriphlogopite	2.28
margarite	2.33	ferri-annite	2.32
celadonite	2.18	xanthophyllite	2.34
dioct. chlorite	2.30	prochlorite	2.28
		corundophyllite	2.29
		kammererite	2.26
		ripidolite	2.25
		vermiculite	2.25

Variation in layer stacking[1] is common. In some cases the stabilities of different polytypes can be explained by the relative amounts of repulsion and attraction between the ions in the structures. The stabilities can be correlated with the energy available in the enviroment of crystallization.

Influence of sorbed cations and hydration on the 'a' and 'b' dimensions of montmorillonite:

Effect on the structure of aluminosilicate layers:-

According to Eirish and Tret'yakova[2], isomorphic substitutions in layer silicates result in noticeable changes in the 'a' and 'b' dimensions - studies of the effect of sorbed cations and hydration on the 'a' and 'b' dimensions, show noticeable changes in the configuration of aluminosilicate layers. The mechanism of these changes are closely similar to those in other layered silicates.

Process of cation and water sorption.

It has been established (Grim - Ref. 45) that sorption of water molecules in montmorillonite proceeds in two types of active centres: (1) through co-ordination around sorbed cations; and, (2) as a result of interaction with oxygen ions of the silicate layers with formation of hydrogen bonds. By studying the process of water desorption from various cationic forms of montmorillonite it was found that a series of separate portions of water are liberated. A portion of one molecule per exchange valency of the most strongly bound water, desorption of which usually terminates at 300 - 350 ^{o}C, was always recorded independently of the nature of the sorbed cations.

---

1 - that is, polytypism.
2 - Reference 72.

University of Cape Town

These results indicate that the first water molecule is sorbed precisely on these oxygen ions with the formation of a hydrogen bond of the long hydroxyl-bond type, as illustrated in Figure 2.28. Due to the formation of a hydroxyl bond, the hydrogen of a water molecule drawn onto an oxygen ion of the octahedron largely saturates the oxygen valency which, with subsequent hydration, may cause displacement of the sorbed cation. The second hydrogens of these water molecules form active centres in the development of hydrate layers. Under conditions of higher humidity or in water, three or four hydrate layers are formed[1].

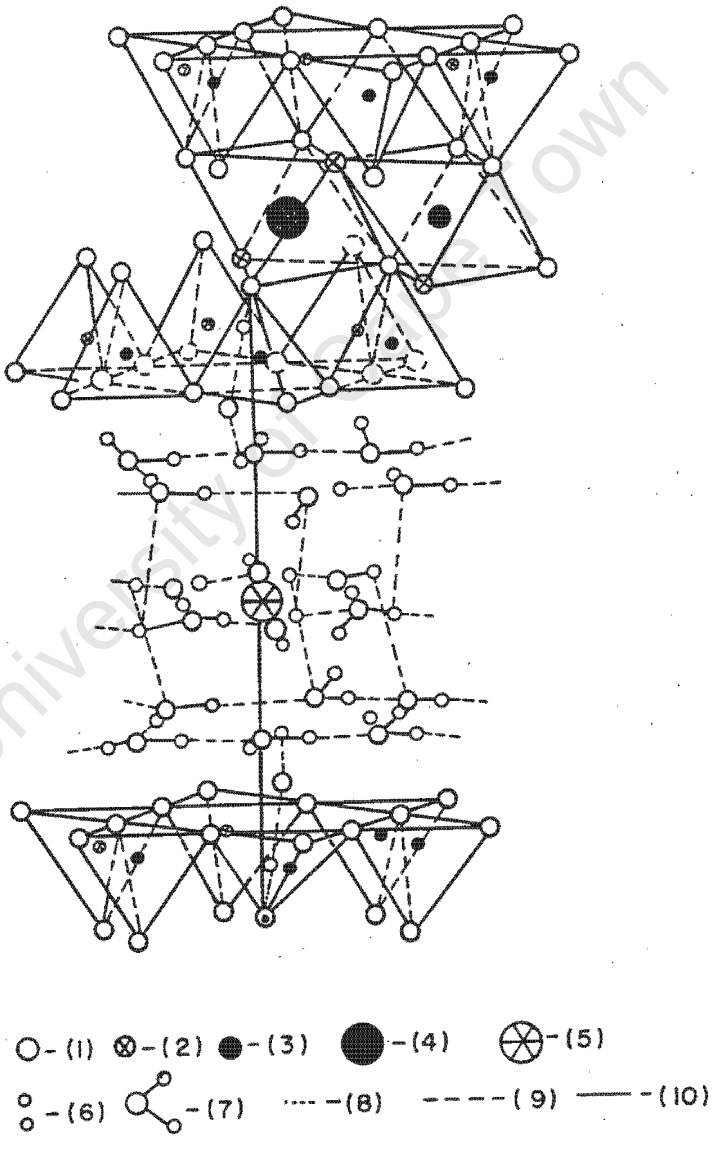

Figure 2.28: Montmorillonite structure - (1) oxygen, (2) hydroxyl, (3) alluminium, (4) magnesium, (5) sorbed cation, (6) silicon, (7) water molecule, (8) hydroxyl bond, (9) hydrogen bond, and (10) electrovalent bond[2].

---

1 - *Reference 58.*
2 - *after Eirish and Tret'yakova, Reference 72.*

When the exchange complex of montmorillonite clay contains Li^+ or Na^+ ions, disintegration of secondary particles into separate aluminosilicate layers, and formation on all basal surfaces of hydrate sheaths, occur. Consequently, X-ray diffraction analysis records interplanar spacings of over 30 Å[1]. Montmorillonite greatly swells in water.

Formation and changes of the montmorillonite structure.

Isomorphous substitutions in aluminosilicate layers determine not only the presence of a certain amount of cation neutralizers, but also predetermine the possibility of water molecule entry into the crystal structure of montmorillonite and the formation of hydrate-ionic layers. Over the entire range of conditions, from the maximum swelling of montmorillonite clay to its dehydration, even with retention of only a single sorbed water molecule the sorbed cations do not come into direct contact with oxygen ions bearing a negative charge (refer to Figure 2.28). Electrostatic interaction with changing forces takes place between these ions. At some stage of dehydration, sorbed cations enter the hexagonal holes increasing the neutralization of the oxygen ions. With change in position and bond strength of sorbed cations with valence, oxygen ions of an octahedral net should influence the interaction of silicon ions with the oxygen ions (Figure 2.28). The configuration and parameters of the tetrahedral net as well as the whole montmorillonite crystal lattice should correspondingly change.

Hydrate-ionic layers, which give rise to important properties of montmorillonite, are also the most changeable link in the structure since bonds between particles[2] within these layers are weaker than those in aluminosilicate layers. Thus, the condition necessary for forming the crystal structure (ie, the fixation of all particles), would be possible only over a somewhat small range of hydrate-ionic layer size.
It is also significant that the hydrate-ionic layers, while forming between alumino silicate layers, not only separate silicate layers but also combine them into structures of secondary particles. A more perfect mutual orientation of layers is attained in the structures of secondary particles, packets, of organo-clay complexes than in the original montmorillonite clay.

---

1 - *Reference 58.*
2 - *molecules and ions.*

Decay of the montmorillonite structure.

After heating to 250 - 350°C, montmorillonite containing sorbed cations with, strong polarizing action, lose their ability for ion-exchange reactions and intracrystalline swelling.
Patterns obtained by means of the scanning electron microscope show that disintegration usually passes through a stage of formation of crystallites containing elements with variable orientation and thickness.

Characteristically disintegrations initially occur in the 'a-b' plane due to breakage of bonds between adjacent secondary particles, and secondly only within them. In both cases, nature of the sorbed cations is the main factor. Although the basic structure of aluminosilicate layers, with opened basal surfaces, may be preserved after heating clay samples to 300 - 350°C, formation of hydrate-ionic layers becomes impossible. Thus, the crystallo-chemical structure of montmorillonite irreversible decays.

Relation between crystal-lattice configuration and swelling of montmorillonites.

According to Davidtz and Low[1], Overbeck (Ref. 74) had previously noted that for colloids in general, there is a lack of agreement between experiments and theory based exclusively on van der Waals' forces and double-layer interaction - his conclusion was that the theories were either innacurate or needed refinement.

Concerning the effect on free swelling of changes in lattice dimensions produced by isomorphous substitution, the relation between the b-dimension and isomorphous substitution in montmorillonites has been determined by Radoslovich (Ref. 75). It is,

$$b_{obs}=(8.944 + 0{,}096Mg^{2+} + 0.096Fe^{3+} + 0.037Al_{tetra})\pm 0.012\text{Å}.$$

This relation was used to obtain the b-dimension of the montmorillonites employed in Foster's (Ref. 76) and the study by Davidtz and Low[1].
The two sets of results are shown in Figure 2.29 - they indicate that swelling decreases linearly with increase in b-dimension. Differences between the two curves may relate to differences in sample preparation or method for determination of free swell. Evidently, free swelling decreases linearly with increasing b-dimension.

[1] - Reference 73.

Davidtz and Low (Ref. 73) proposed that, by virtue of the attraction between surface oxygens and adjacent water molecules, the clay surface acts as a template on which a relatively stable water structure is built.
Hence, as the b-dimension adjusts to lattice substitutions, there is a corresponding adjustment in the water structure. This adjustment takes place by changes in intermolecular bond angles and distances and, in extreme cases, by changes in coordination number. Accordingly, the relative partial molar free energy of the water $F-F^{o}$, changes.
Now, $F-F^{o}$ is related to the swelling pressure 'π', of the clay and the relative vapor pressure, p/p^{o}, of the water in it by the thermodynamic relationships[1], as follows:

$$F-F^{o} = v\pi = RT\ (\ln p/p^{o}).$$

Where: v is the partial molar volume of water in clay; R is the molar gas constant; and, T is the temperature.
Thus changes in the b-dimension lead ultimately to changes in swelling.

It was previously mentioned (refer to Figure 2.27) that the silicon tetrahedra in the clay structure rotate as the b-dimension changes. By this mechanism, the tetrahedral layers adjust to the dimensions of the octahedral layer.
If the water is bonded to the basal oxygens of the silicon tetrahedra, there should be some relation between free swelling and α, the angle through which these tetrahedra rotate. Davidtz and Low (Ref. 73) argued that rotations of silicate tetrahedra[2] influence the structure of water bonded to the basal oxygens of the tetrahedra. It was proposed that the clay surface acts as a template for the structure of the adjacent water and that, as the configuration of the surface changes, the water structure changes accordingly. This causes a change in the free energy of the water and hence, in the swelling clay.

University of Cape Town

Relation between swelling, water properties and b-dimension in montmorillonite-water systems.

According to Ravina and Low (Ref. 78) the linear relation between free swelling and b-dimension cannot be explained by the convential theory of swelling (that is, the double-layer theory. This fact was discussed in detail by Davidtz and Low (Ref. 73).
Instead of being related to the osmotic activity of the exchangeable cations, as required by that theory, free swelling is related to the dimensions of the montmorillonite lattice.

---

1 - *Low and Anderson, Reference 77.*
2 - *that accompany the changes in b-dimension.*

In their subsequent study using the same clays, Ravina and Low (Ref. 78) confirmed the relationship found by Davidtz and Low (Ref. 73) by direct measurement of b-dimensions using X-ray diffraction. The d(060) reflection was used as the basic for the measurement. Extrapolation of the data showed that for a b-dimension of 9.00 Å swelling should be zero. They also showed that as water content of a given montmorillonite increased, so also did the b-dimension, as illustrated in Figure 2.30. Interestingly, when each clay was fully swollen the b-dimension was 9.0 Å. In other words, the pressure of water evidently influenced the lattice configuration to an extent sufficient to cause a change in b-dimension.

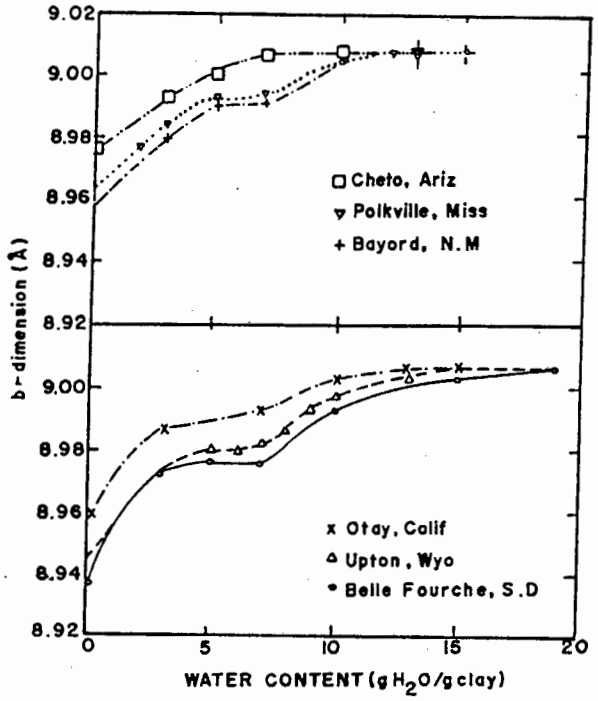

Figure 2.30: Relation between b-dimension and water content for six Na-saturated dioctahedral montmorillonites - reproducibility of b-dimension = ± 0.001 Å at low water content, ± 0.003 Å at high water content[1].

The amount of water in a fully swollen montmorillonite can be linearly related to the b-dimension it had before starting to swell provided that free swelling is proportional to the difference between the final b-dimension and the initial one - plotting of change in b-dimension for the data available[2] shows that the best-fitting line goes through the origin. Therefore, free swelling is proportional to both the initial b-dimension and the change in b-dimension.

---

[1] - *from Ravina and Low, Reference 78.*
[2] - *that is, change in b-dimension versus free swelling.*

The b-dimension of a dry montmorillonite is governed primarily by its mineralogical composition, as confirmed by the linear relation that exists between b-dimension and the amount of ionic substitution in octahedral and tetrahedral sites within the crystal (Ref. 75). However, the mineralogical composition is supposed to remain constant during swelling. Therefore, the observed increase in b-dimension must derive from changes in bond angles and/or bond lengths. These changes affect the lattice energy, and they cannot occur without the action of external forces. Since the magnitude of the force exerted by one planar crystal layer on another depends on interlayer distance, it is important to know how this distance varies with water content. Results of c-axis spacing for Na-montmorillonites, at different water contents, are shown in Figure 2.31. The results are consistent and show the expected linear relation between c-axis spacing and water content.

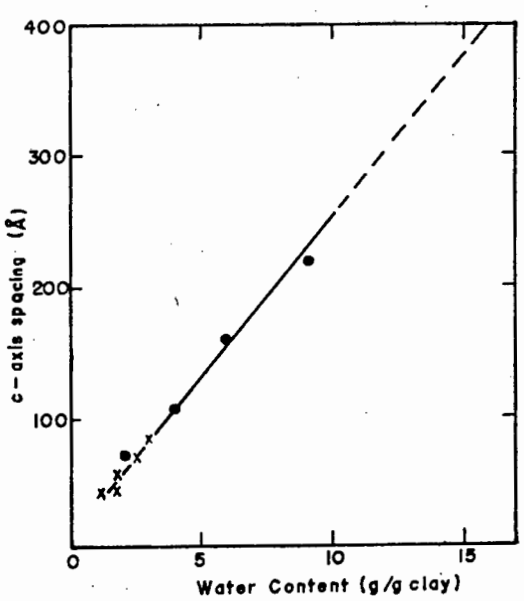

Figure 2.31: Relation between c-axis spacing and water content for Na-montmorillonite[1].

According to Ravina and Low[1], interlayer forces cannot explain the increase in interlayer distance with increasing water content, and that both electrostatic forces between the layers and van der Waal's force can be discounted. Furthermore, that neither forces emanating from exchangeable cations nor from adjacent crystal layers would be expected to impose a maximal b-dimension of ≈ 9.0 Å upon the crystal lattice of montmorillonite. However this b-dimension could be imposed by water.

---

[1] - *Reference 78.*

Pseudomorphism between water and montmorillonite.

Epitaxi is the oriented growth of one cystalline substance on a substrate of a different crystalline substance. A kind of epitaxi of special interest here is surface pseudomorphism - it is defined as the straining of an overgrowth structure to match a substrate structure. For pseudomorphism to occur between water and montmorillonite, one requirement is that the misfit between their structures is small.
As previously discussed in "The status of clay minerals structures", the structure of pure liquid water can be regarded as resembling that of ice-I-like components in it.

The structure of ice I, which is the stable crystalline state of water at below-freezing temperatures and atmospheric pressure, is diagrammed partly in Figure 2.32(A). It should be noted that the water molecules in this structure form puckered hexagons containing three molecules in one plane and three others in a closely adjacent plane - the distance between water molecules in either plane is 4.5 Å.

An unconstrained sheet of silica tetrahedra has regular symmetry, and this sheet is usually larger than the sheet of alumina octahedra in dioctahedral montmorillonites. In order for the two sheets to interconnect the misfit between them is eliminated by the alternate clockwise and counterclockwise rotation of the silica tetrahedra about their vertical axes - the angle of rotation can be calculated as previously described[1].
The crystal structures of ice I[2] and montmorillonite would match exactly if the structure of montmorillonite had regular hexagonal symmetry ($\alpha = 0$) and a b-dimension of 9.0 Å as illustrated in Figure 2.32(C).

---

[1] - *by Bailey, Reference 68.*
[2] - *or structurally similar water.*

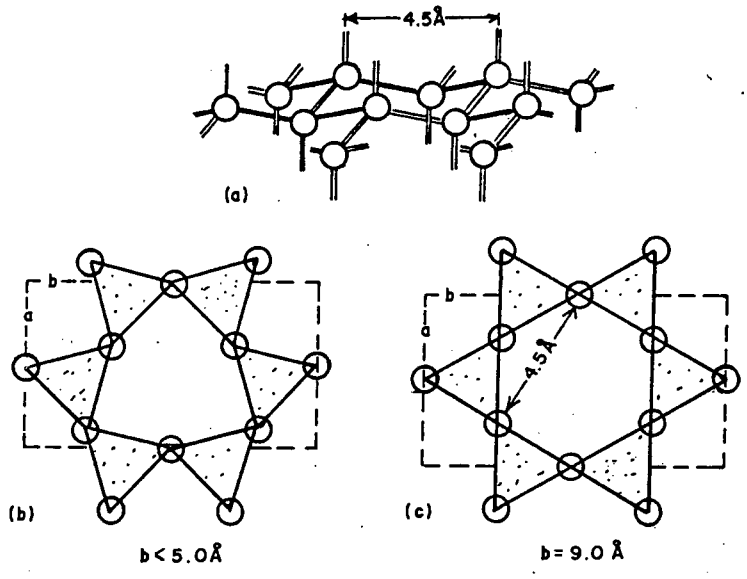

Legend: O = oxygen atoms.

Figure 2.32: (a) Diagram of the arrangement of water molecules (open circles) in ice; (b) Ditrigonal symmetry of the surface of dry montmorillonite; (c) Regular hexagonal symmetry of the surface of idealized montmorillonite.

Figure 2.30 indicates that the montmorillonite structure expands laterally with each increment of water. For pseudomorphism to occur, a concomitant adjustment must take place in the water structure.

Relation between water properties and b-dimension.

If pseudomorphism between water and montmorillonite does exist, there should be some relation between the structure-sensitive properties of water and the b-dimension of montmorillonite. According to Ravina and Low (Ref. 78), it appears that different cations enhance the b-dimension in the relative order K > Li > Na (order in which they are fixed or rendered less exchangeable in montmorillonite on drying); and that alkali metal cations effect the properties of bulk water in the order Li > Na > K; Therefore, it is reasonable to conclude that the exchangeable cations, like those proxying for Si and Al in tetrahedral sites, affect the configuration of the montmorillonite lattice and it, in turn, affects the structure and properties of the expitaxial water (as defined above).

Thermodynamic analysis.

As summarized above, Ravina and Low[1] showed that the crystal structure of montmorillonite adjusts as interlayer water is adsorbed, and expected the crystal structure of the water to undergo a simultaneous adjustment.
Figure 2.33 presents the relation between the change in free energy and the number of grams of water transferred from pure bulk water to 1g of air-dried Na-montmorillonite.

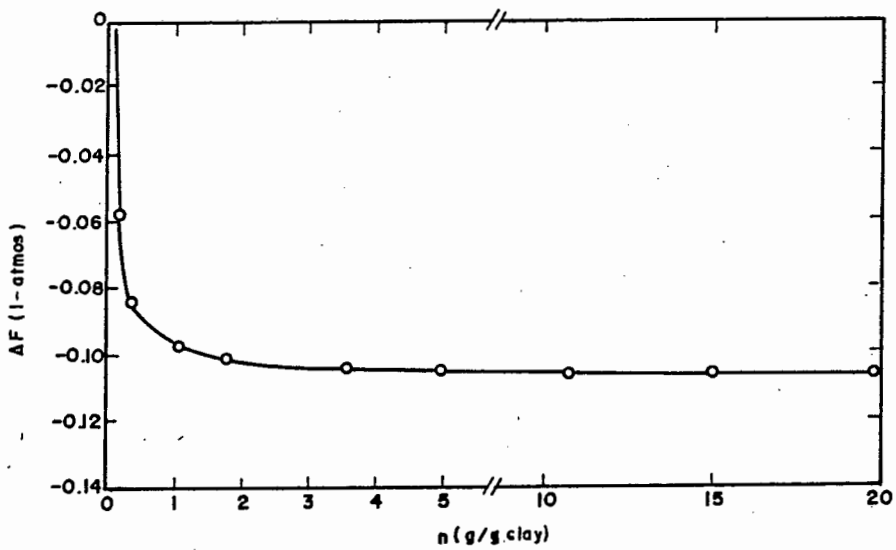

Figure 2.33: The relation between dF, the change in free energy, and n, the number of grams of water transfered from pure bulk water to 1g of air-dried Na-montmorillonite, (from Ravina and Low[1]).

---

[1] - Reference 78.

Nature of montmorillonite-water interaction.

It was proposed by Ravina and Low (Ref. 78) that the initial misfit between the montmorillonite and water structures is sufficiently small, the hydrogen-bonding between them is sufficiently strong and their elastic moduli are of such magnitudes that pseudomorphism exists at all montmorillonite-water rations.
At first, when the interlayer water is thin, it is energetically favorable for its structure to conform to that of montmorillonite. However, as the interlayer water increases, the opposite becomes true. The water structure tends to assume a preferred configuration and the montmorillonite structure adjusts accordingly. Its final value is governed by the preferred configuration of the water and, hence, is the same for all Na-montmorillonites. Alternatively, it was proposed that the crystal structure of the montmorillonite relaxes with a concomitant increase in b-dimension as stresses acting on it are relieved by the addition of water.

Regardless of which alternative is correct, the structure of water is supposed to be interlocked with, and stabilized by, that of montmorillonite whose structure, specially its surface symmetry, is indicated by its b-dimension. Therefore, the structure-sensitive properties of the water are related to the b-dimension of the montmorillonite.
Swelling stops when no further adjustment takes place, that is, when the b-dimension reaches its final value. Thus swelling is related to the change in b-dimension. The above concepts provide an explanation for the in-depth effect of montmorillonite on the properties of water in montmorillonite-water systems.

2.4.3 Application of X-Rays to the study of crystals.

This part provides a general introduction to X-ray diffraction and, in particular, to the application of X-rays to the study of crystals.

The application of X-rays to the study of crystals was the biggest single advancement that happened to crystallography. It was not until 1912[1] that, at the suggestion of Max von Lane, X-rays were used to study crystals. The original experiments were carried out at the University of Munich, where von Lane was a lecturer. Within the next few years, great strides were made as a result of the work of the father and son English physists - William Henry Bragg, and William Lawrence Bragg. In 1914 the first structure of a compound, halite 'NaCl' was worked out by them and, in the following years many more other structures were solved. They also simplified von Lane's mathematical generalizations referring to the geometry of X-ray diffraction, and popularized the results of their research through their well-written books on the subject.

X-ray spectra.

Electromagnetic waves from a continuous series varying in wavelength from long radio waves, with wavelengths of the order of thousands of meters, to cosmic radiation whose wavelengths are of the order of 10^{-2} meters. All forms of electromagnetic radiation have certain properties in common, such as propagation along straight lines at a speed of 300 000 km per second in a vacuum, reflection, refraction according to Snell's Law (Ref. 80), diffraction at edges and slits or gratings, and a relation between energy and wavelength given by Planck's Law:

$e = hv = hc/w.$

Where: 'e' is energy, 'v' is frequency, 'c' velocity of propagation, 'w' wavelength, and 'h' Planck's constant. Thus the shorter the wavelength the greater its energy and the greater its powers of penetration.

X-rays occupy only a small portion of the spectrum, with wavelengths varying between slightly more than 100 Å and 0,02 Å - refer to Figure 2.34. X-rays used in the investigation of crystals have wavelengths of the order of 1 Å. Visible light has wavelengths between 7200 and 4000 Å, more than 1000 times as great, and consequently is less penetrating and energetic than x-radiation.

---

[1] - some 17 years after the discovery of x-radiation.

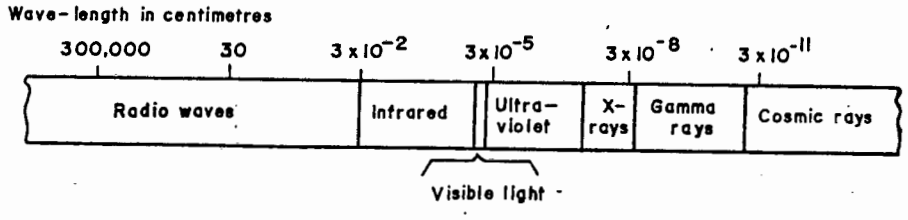

Figure 2.34: The electromagnetic spectrum.

In a modern x-ray tube there is nearly a complete vacuum. The tube is fitted with a tungsten filament as a cathode that provides the source of electrons. The anode consists of one of a number of metals such as Mo, Cu, or Fe, and acts as the target for the electrons. When the filament is heated by passage of current, electrons are emitted which are accelerated toward the target anode by a high voltage applied across the tube. X-rays are generated when the electrons impact on the target[1]. The nature of X-rays depends on the metal of the target and applied voltage. No X-rays are produced until the voltage reaches a minimum value dependent on the target material. At that point a continuous spectrum is generated.

The characteristic X-ray spectrum is produced when the bombarding electrons have sufficient energy to dislodge electrons from the inner electron shells in the atoms of the target material. When these inner electrons are expelled they leave vacancies that are filled by electrons from surrounding electron shells. The electron transitions, from outer to inner shells, are accompanied by the emission of X-radiation with specific wavelengths. The wavelengths of the characteristic X-radiation emitted by various metals have previously been accurately determined.

---

[1] - *that is, the anode.*

Diffraction effects and the Bragg equation.

Crystals consist of an ordered three-dimensional structure with characteristic periodicites, or identity periods along the crystallographic axes. When an X-ray beam strikes such a three-dimensional arrangement, it causes electrons in its path to vibrate with a frequency of the incident X-radiation. These vibration electrons absorb some of the X-ray energy and, acting as a source of new wave fronts, emit[1] this energy as X-radiation of the same frequency and wavelength.
In general the scattered waves interfere destructively, but in some specific directions they reinforce one another producing a cooperative scattering effect known as diffraction.

In a row of regularly spaced atoms that is bombarded by X-rays every atom can be considered the center of radiating, special wave shells - illustrated in Figure 2.35 (A). When the scattered waves interfere constructively, they produce wave fronts that are in phase, and diffraction will occur. Figure 2.35 (B) illustrates that rays 1 and 2 will be in phase only when distance AB represents an integral number of wavelengths, in other words when

$AB = nw = c \cos\phi.$

Where n represents whole numbers such as 0, 1, 2, 3, .., n).

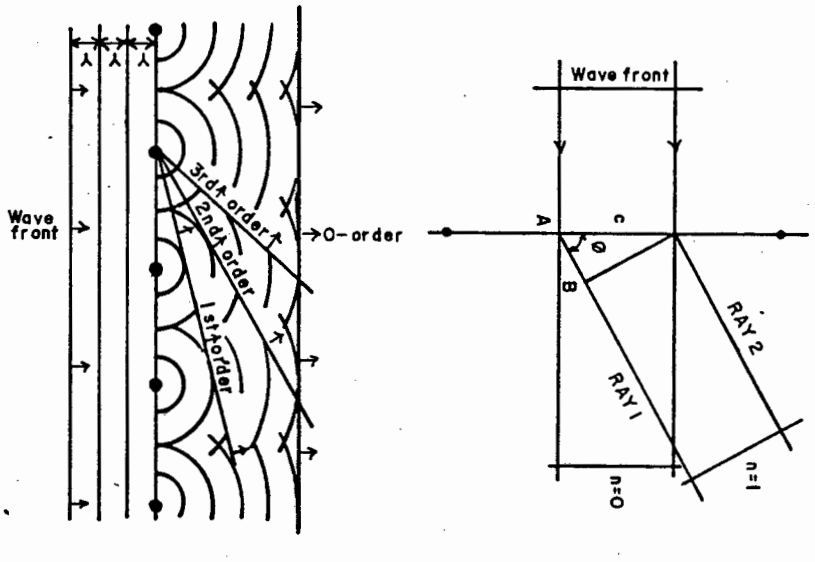

Figure 2.35: (A) Scattering of X-rays by a row of equally spaced, identical atoms; (B) Conditions for X-ray diffraction from a row of atoms.

---

[1] *- or scatter.*

For a specific value of nw, ø is constant, and the locus of all possible diffracted rays will be represented by a cone with the row of scattering points as central axis. Because the scattered rays will be in phase for the same angle ø on the other side of the incident beam, there will be another similar but inverted cone on that side - shown in Figure 2.36 (A). The two cones with n = 1 would have ø of Figure 2.35 (B), as the angle between the cone axis and its outer surface. When n = o, the cone becomes a plane that includes the incident beam. The greater the value of n the larger the value of cosø, and hence the smaller the angle ø and the narrower the cone. All have the same axis however, and all have their vertices at the same point, the intersection of the incident beam and the row of atoms.

In three dimensional lattice there are three axial directions, each with its characteristic periodicity of scattering points and capable of generating its own series of nested cones with apical angles. Diffraction cones from any three noncoplanar rows of scattering atoms may or may not intersect each other, but only when all three intersect in a common line is there a diffracted beam.
This direction, shown by the arrow in Figure 2.36 (B), represents the direction of the diffracted beam which can be recorded on a film or registered electronically.
The geometry of the three intersecting cones in Figure 2.36 (B), can be expressed by three independent equations (the Laue equation) in which the three cone angles ($ø_1$, $ø_2$, and $ø_3$) define a common direction along the path of the arrow, that is, the common intersection of the three cones.

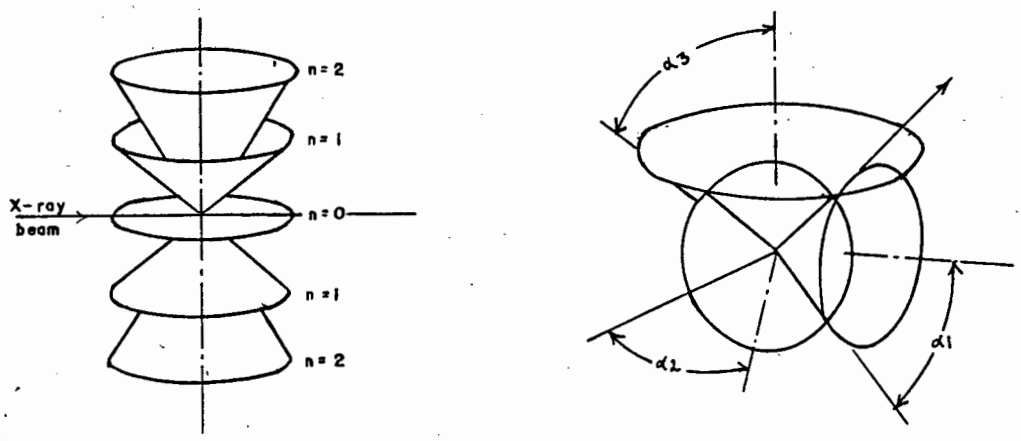

Figure 2.36: (A) Diffraction cones from row of atoms; (B) Diffraction cones from three noncoplanar rows of scattering atoms, intersecting in a common line.

Using a given wavelength, w, Bragg showed that a 'reflection' takes place from a family of parallel lines only under certain conditions. These conditions must satisfy the equation:

$nw = 2d \sin\theta$.

Where: n is an integer (1, 2, 3,...,n), w the wavelength, d the distance between successive parallel planes, and θ the angle of incidence and 'reflection' of the X-ray beam from a given atomic plane. This equation, known as the Bragg Law, expresses in a simpler manner the simultaneous fulfillment of the Three Laue equations.

We have seen that the faces most likely to appear on crystals are those parallel to atomic planes having the greatest density of lattice modes. Parallel to each face is a family of equispaced identical planes. When an X-ray beam strikes a crystal it penetrates it, and the resulting diffraction effect is not from a single plane but from an almost infinite number of parallel planes, each contributing a small bit to the total diffraction maximum. In order that the diffraction effect[1] should be of sufficient intensity to be recorded, the individual 'reflections' must be in phase with each other.

Figure 2.37 shows part of a hypothetical structure consisting of two kinds of atom, A and B. In general, although these atoms lie on separate sets of planes, the sets have the same interplanar spacings: One can picture a crystal structure as a group of simple interpenetrating, and parallel lattice-arrays of atoms, all identical in size; Diffraction from a typical structure can then be treated in terms of simultaneous reflections from this group of interpenetrating lattice arrays.

The Bragg Law states that the angle at which X-radiation is reflected by a set of planes depends only on the spacing, if the wavelength is fixed. Consequently the A and B planes reflect the same angle. However, the two sets of reflections differ in phase to an extent that depends on d, w, and s[2], and they differ in amplitude if they arise from different atoms. Hence the resultant wave from the two sets of planes differs from its constituent waves in both phase and amplitude.

---

[1] - *that is, 'reflection'.*
[2] - *the separation of A and B planes.*

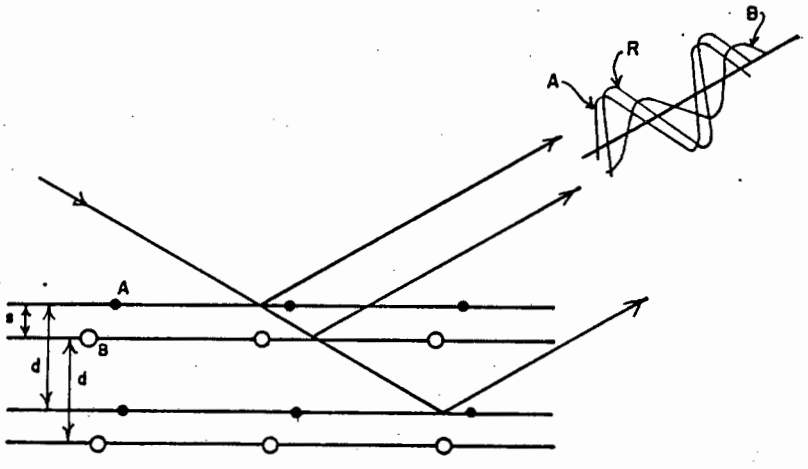

Figure 2.37: Reflection from a crystal structure[1].

The determination of crystal structures.

The orderly arrangement of atoms in a crystal is known as the crystal structure. It provides information on the location of all atoms, bond positions and types, space group symmetry, and chemical content of the unit cell.

The first step in the determination of the structure of a crystal is the determination of its space group and unit size. Next the intensities of the X-ray diffraction maxima must be determined because these intensities can be related to the electron densities of the atom.

The intensity values of X-ray diffraction maxima for use in structure determinations were, until recently, obtained from two careful intensity measurements of diffraction spots on photographic films or plates. With the advent of highly sensitive and reproducible X-ray detectors as well as computer programmed motors for simultaneous crystal and X-ray detector orientation, X-ray intensities are now measured on computer-controlled single crystal diffractometers.

The relative rarity of well-formed crystals and the difficulty of making the precise orientation required by single crystal methods led to the discovery of the powder method of X-ray investigation. The usefulness of the powder method has been greatly increased and its field of application extended by the introduction of the X-ray powder diffractometer. Part 4 of this section includes a description of the X-ray diffraction test method.

---

[1] - from Nuffield, Reference 79.

2.4.4. X-Ray Diffraction: Preparation and testing of samples.

This section introduces the following two parts:

1. Preparation of samples for X-ray diffraction analysis. This part takes up from the end of the previous sample preparation stage - refer to section 2.3.3 'Clay Separation of Samples for SEM and X-ray Diffraction'.

2. The X-ray diffraction test method adopted, and makes reference to the traces (or plots) obtained for each soil sample tested.

Preparation of clay sample for X-ray diffraction. Appendix B includes a detailed description of each procedure for the preparation and testing of the samples - refer to section B.4 "X-Ray Diffraction: Preparation and Testing of Samples". All the X-ray diffraction traces, obtained for each soil sample tested, are included in Appendix B - refer to section B.5 "X-Ray Diffraction Traces".

Representative samples were originally obtained for each soil type selected for this thesis (refer to Chapter One[1], and to Appendix A[2]). The natural soil types originate from two main areas namely: Cape Peninsula - Sites 11, 36, 30 and 7; and Durban, Natal - Site A. The Artificial soils used consist of Kaolin and Bentonite mixed with sand.

The second stage of sample preparation consisted of two parts: (A) The chemical side of the preparation of representative clay samples; and (B) preparation of slides for X-ray diffraction 'X-ray D' tests.

X-ray diffraction test method.

The X-ray diffractometer instrument is constructed in such a way as to enable the slide previously prepared (stage 2.B of the preparation of clay samples - refer to Appendix B), when clamped in place, to rotate in the path of a collimated X-ray beam. At the same time an X-ray detector, mounted on an arm, rotates about it to pick up the diffracted X-ray signals.

If the specimen was properly prepared, there will be thousands of tiny crystalline particles on the slide in random orientation. As in powder photography, all possible 'reflections' from atomic planes take place simultaneously. However, instead of recording them all on film at one time, the X-ray detector maintains appropriate geometrical relationship to receive each diffraction maximum separately.

---

1 - section 1.6 "Selection of soil types".
2 - section A.3 "Preparation of soil samples for testing".

In operation, sample, X-ray detector and paper drive of the strip chart recorder are set in motion simultaneously. If an atomic plane has an interplanar spacing 'd' such that a reflection occurs at $\theta = 20^{o}$, there is no evidence of this reflection until the counting tube has been rotated through 2θ, or 40^{o}. At this point the diffracted beam enters the X-ray detector causing it to respond. The pulse thus generated is amplified and causes a deflection on the recording strip chart.

The X-ray diffraction 'X-ray D' tests were done at the X-ray diffraction unit of the Geology Department, University of Stellenbosch.

X-ray diffraction traces.

A total of 21 slides were prepared for testing in the X-ray diffractometer using 'Cu Kα' radiation - that is, 3 slides for each soil type to be tested (the soil types are listed at the beginning of this section).

Traces (or plots) carried out for each soil type:-

Five main traces were performed in the three slides. The traces were run at the speed of 2^{o} 2θ/minute. Details for the final stages of preparation and testing, are as follows:

(i) Slide one - trace A, 3^{o} - 30^{o} 2θ Mg-saturated;
(ii) Slide one - trace C, 3^{o} - 13^{o} 2θ Mg-saturated, Ethylene glycolated;
(iii) Slide two - trace D, 3^{o} - 30^{o} 2θ Mg-saturated, previously heated to 550^{o}C for 1 hour;
(iv) Slide three - trace E, 3^{o} - 30^{o} 2θ Mg-saturated, previously heated to 105^{o}C overnight.
(v) Slide three - trace C, 3^{o} - 13^{o} 2θ Mg-saturated, Ethylene glycolated.

An additional trace was performed in slide one, in between traces A and C, at the speed of $\frac{1}{4}^{o}$ 2θ/minute to distinguish between kaolinite and chlorite:

(vi) Slide one - trace B, 24^{o} - $25\frac{1}{2}^{o}$ 2θ Mg-saturated.

A total of 42 traces (or plots) were obtained - the basic test description/sequence for each one, are included in Appendix B[1]. There are six traces per sample.

Diffractometer traces for Site 11 Rosebank, are included in this chapter as Figure 2.38 to Figure 2.42. For each trace, the position of the peaks on the chart have been identified. The interplanar spacings causing these peaks, have been determined using the equation, '$nw = 2d \sin\theta$'.

---

[1] - *refer to Table B.09.*

NATURAL SOIL TYPE.

Site 11, Rosebank.

'X-ray D' trace 1A:-

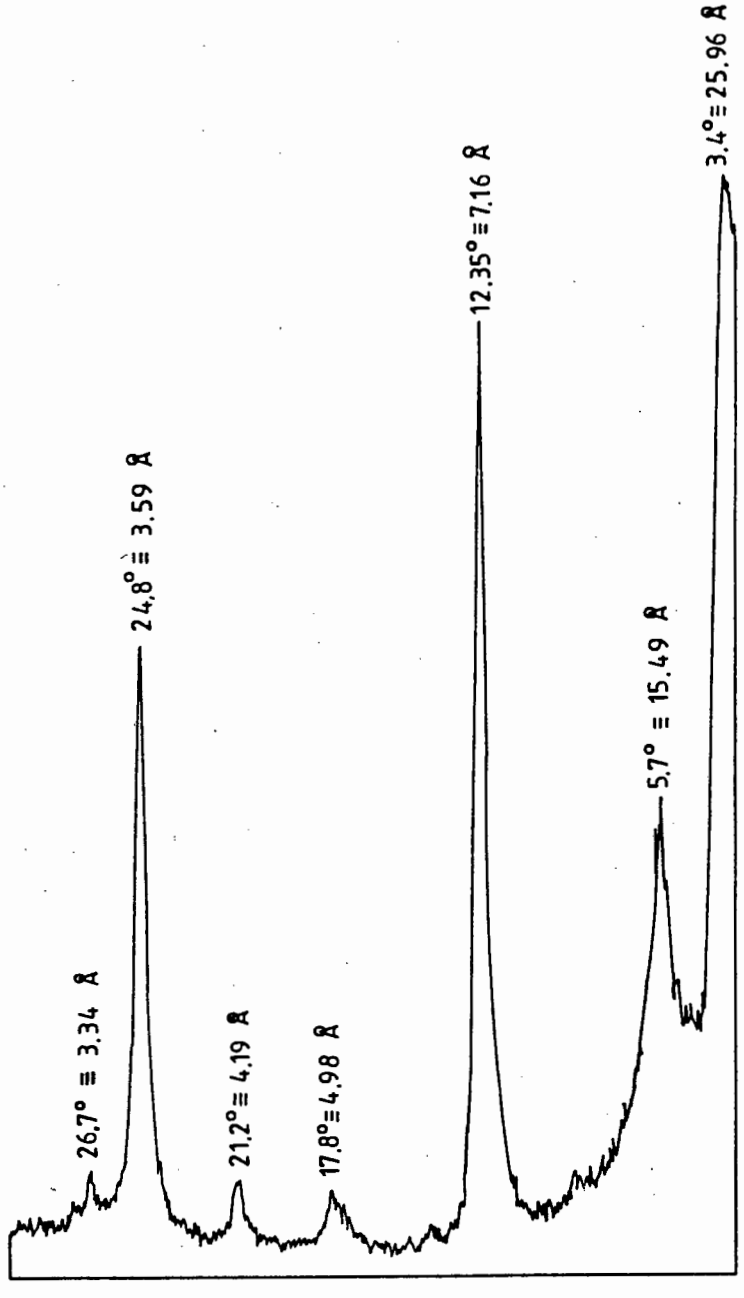

Figure 2.38: Site 11, trace 1.A - 3° 30° 2θ[1] Mg-saturated.

[1] - and speed of 2° 2θ/minute.

Site 11, Rosebank.

'X-ray D' trace 1.B and 1.C:-

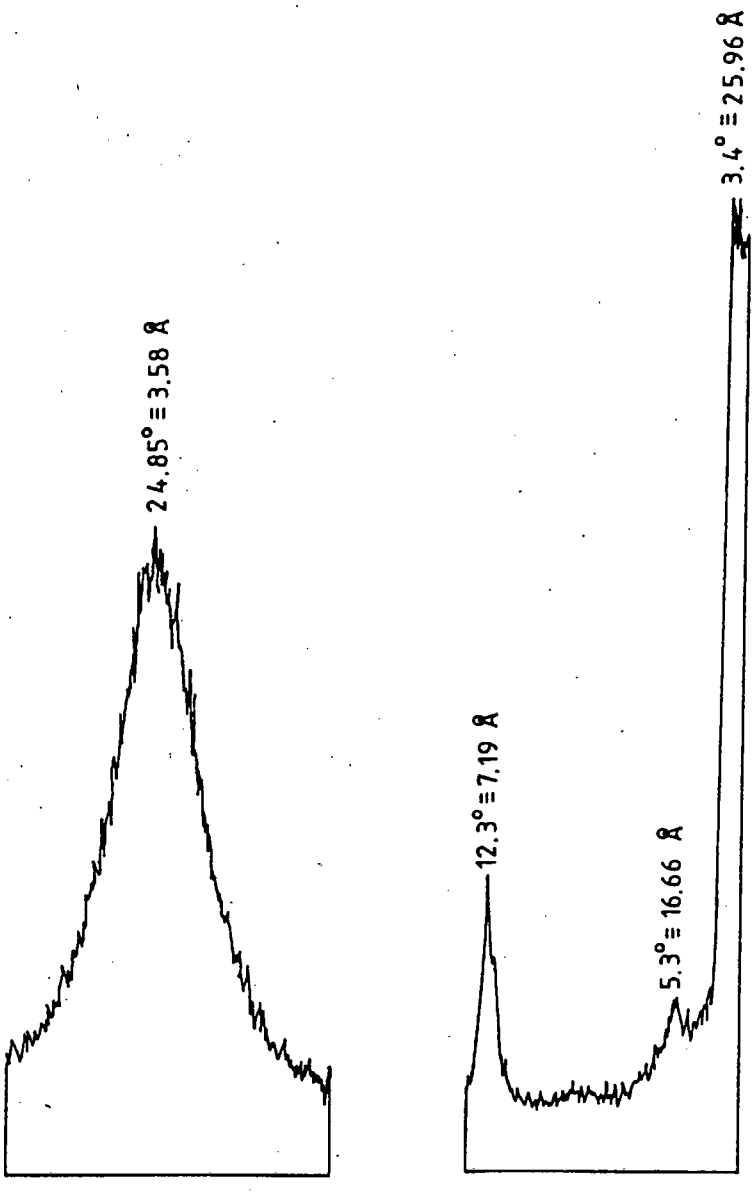

Figure 2.39: (i) Site 11, trace 1.B - 24° 25½° 2θ Mg-saturated (¼° 2θ/min.); (ii) Site 11, trace 1C - 3° 13° 2θ Mg-saturated, Ethylene glycolated (2° 2θ/min.).

Site 11, Rosebank.

'X-ray D' trace 8.D:-

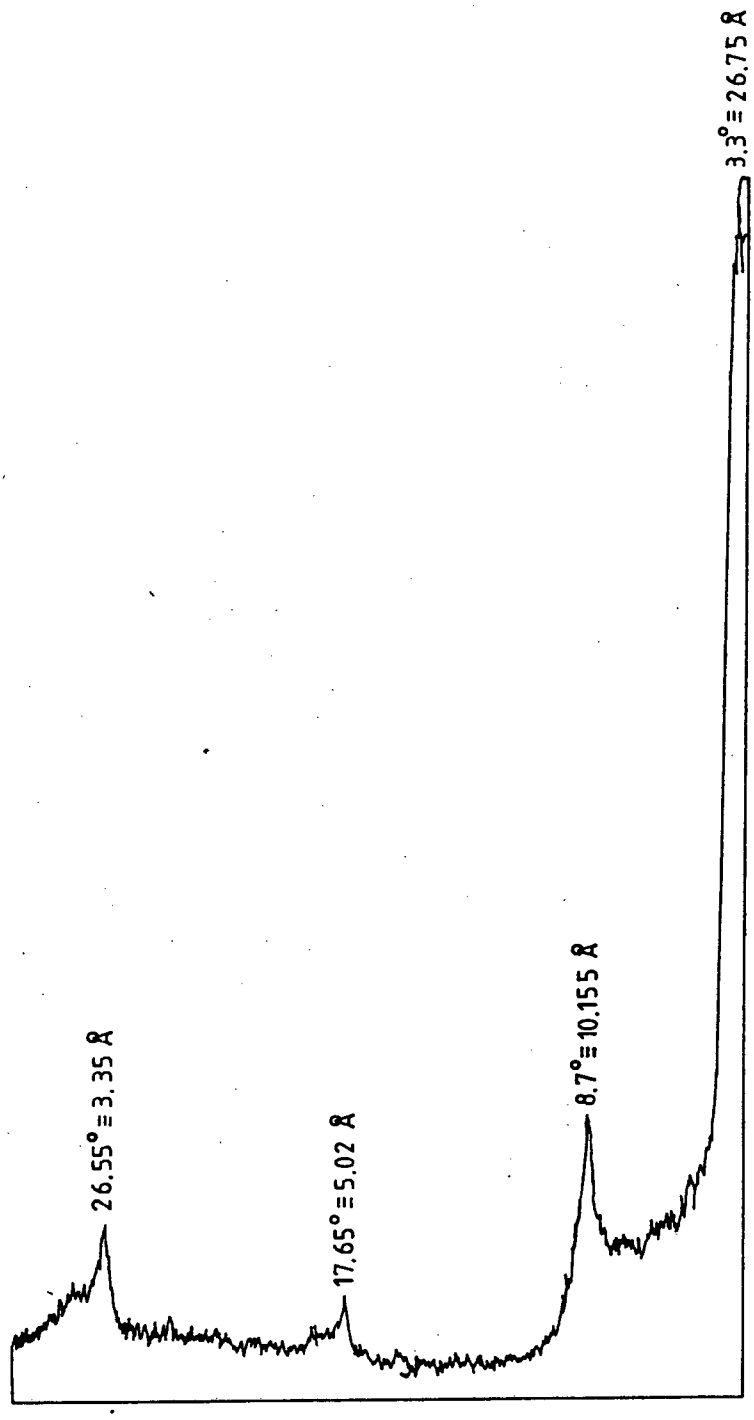

Figure 2.40: Site 11, trace 8.D - 3° 30° 2θ Mg-saturated (previously heated to 550°C for 1 hr, following which it was allowed to cool and then placed in a desiccator until testing).

Site 11, Rosebank.

'X-ray D' traces 15E and 15.C:-

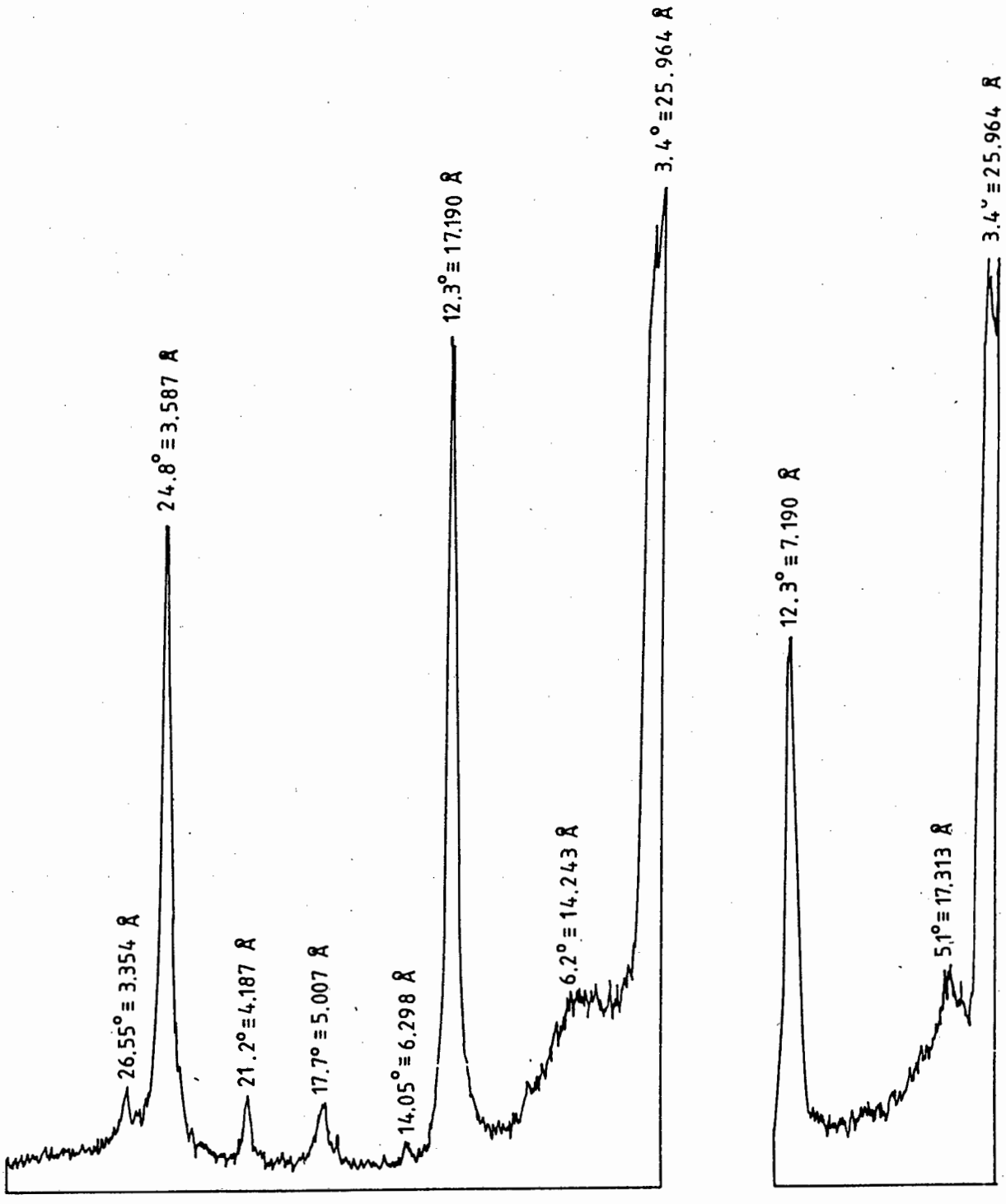

Figure 2.41: (i) Site 11, trace 15.E - 3° 30° 2θ Mg-saturated, previously heated to 105°C overnight, allowed to cool and placed in desiccator until testing; (ii) Site 11, trace 15.C - 3° 13° 2θ Mg-saturated, ethylene glycolated.

2.4.5 X-Ray Diffraction - Analysis of test data.

The 42 traces previously obtained[1] were analysed. The results are presented in Tables 2.16 to 2.22. For each trace, the main peaks observed were identified and the diffraction angle 2θ was measured. The interplanar spacing can be computed from Bragg's equation 'nw = 2d sinθ' (refer to previous section 2.4.3 'Application of X-rays to the study of crystals'). The approach adopted for the solution of Bragg's equation, was to make use of the X-ray diffraction tables by Fang and Blocs (Ref. 81).

An additional independent analysis was subsequently carried out by Specialist Chemical Investigations. The results of this analysis are included in the conclusions for this chapter[2].

Interplanar spacing 'd'.

As previously described, the interplanar spacing 'd' was determined from the diffraction angle measured in the trace of each sample. Results are given in Tables 2.16 to 2.22.

Table 2.16: Site 11, Rosebank - interplanar spacing 'd' for each main peak observed in the X-ray diffraction traces.

Trace No.	2θ (°)	d (Å)	Remarks
[Mg-saturated]			
1.A	3.4	25.96	high
	5.7	15.49	medium
	12.35	7.16	high
	17.8	4.98	small
	21.2	4.19	small
	24.8	3.59	high
	26.7	3.34	small
[Mg-saturated]			
1.B	24.85	3.58	high
[Mg-sat. Ethylene glycolated]			
1.C	3.4	25.96	high
	5.3	16.66	small
	12.3	7.19	medium
[Mg-sat., heated to 550°C]			
8.D	3.3	26.75	high
	8.7	10.16	medium
	17.65	5.02	small
	26.55	3.35	small
[Mg-sat., heated to 105°C]			
15.E	3.4	25.96	high
	6.2	14.24	small
	12.3	17.19	high
	14.05	6.298	small
	17.7	5.01	small
	21.2	4.19	small
	24.8	3.59	high
	26.55	3.54	small
[Mg-sat. Ethylene glycolated]			
15.C	3.4	25.96	high
	5.1	17.31	small
	12.3	7.19	large

1 - *refer to Appendix B, Figures B.01 to B.28.*
2 - *section 2.5 "Conclusions for Chapter Two".*

Table 2.17: Site 36, Rondebosch - interplanar spacing 'd' for each main peak observed in the X-ray diffraction traces.

Trace No.	2θ (°)	d (Å)	Remarks
[Mg-saturated]			
2.A	3.5	25.22	high
	6.0	14.72	medium
	8.8	10.04	small
	12.2	7.25	high
	17.7	5.01	medium
	21.2	4.19	small
	24.8	3.59	high
	26.7	3.34	small
[Mg-saturated]			
2.B	27.75	3.21	high
[Mg-sat. Ethylene glycolated]			
2.C	3.3	26.75	high
	5.3	16.66	medium
	8.9	9.93	small
	12.3	7.19	high
[Mg-sat., heated to 550°C]			
9.D	3.3	26.75	high
	8.7	10.16	medium
	17.6	5.03	small
	26.4	3.37	medium
	28.6	3.12	small
[Mg-sat., heated to 105°C]			
16.E	3.3	26.75	large
	8.8	10.04	medium
	12.25	7.22	high
	17.55	5.05	medium
	21.1	4.21	small
	24.7	3.60	high
	26.75	3.33	medium
[Mg-sat. Ethylene glycolated]			
16.C	3.3	26.75	high
	8.8	10.04	medium
	12.3	7.19	high

Table 2.18: Site 30, Hout Bay - interplanar spacing 'd' for each main peak observed in the X-ray diffraction traces.

Trace No.	2θ (°)	d (Å)	Remarks
[Mg-saturated]			
3.A	3.3	26.75	high
	6.0	14.72	small
	8.4	10.52	small
	9.6	9.20	small
	12.3	7.19	high
	17.8	4.98	small
	19.9	4.46	small
	21.45	4.14	small
	24.9	3.57	high
[Mg-saturated]			
3.B	24.83	3.58	high
[Mg-sat. Ethylene glicolated]			
3.C	3.4	25.96	high
	5.8	15.22	small
	7.0	12.62	small
	8.9	9.93	small
	12.4	7.13	high
[Mg-sat., heated to 550°C]			
10.D	3.3	26.75	high
	8.7	10.16	small
	26.4	3.37	small
[Mg-sat., heated to 105°C]			
17.E	3.2	27.59	high
	9.0	9.82	small
	12.4	7.13	high
	17.9	4.95	small
	21.4	4.15	small
	24.9	3.57	high
[Mg-sat. Ethylene glicolated]			
17.C	3.4	25.96	high
	8.8	10.04	small
	12.4	7.13	high

Table 2.19: Site A, Berea Road (Durban) - interplanar spacing 'd' for each main peak observed in the X-ray diffraction traces.

Trace No.	2θ (°)	d (Å)	Remarks
[Mg-saturated]			
4.A	3.3	26.75	high
	12.4	7.13	medium
	20.9	4.25	small
	25.0	3.56	medium
	26.7	3.34	medium
[Mg-saturated]			
4.B	24.87	3.58	medium
	26.66	3.34	high
[Mg-sat. Ethylene glycolated]			
4.C	3.4	25.96	high
	12.4	7.13	medium
[Mg-sat., heated to 550°C]			
11.D	3.4	25.96	high
	20.5	4.33	small
	26.4	3.37	medium
[Mg-sat., heated to 105°C]			
18.E	3.2	27.59	high
	12.4	7.13	medium
	20.9	4.25	small
	24.9	3.57	small
	26.6	3.35	medium
[Mg-sat. Ethylene glycolated]			
18.C	3.4	25.96	high
	12.4	7.13	small

Table 2.20: Site 7, Mowbray - interplanar spacing 'd' for each main peak observed in the X-ray diffraction traces.

Trace No.	2θ (°)	d (Å)	Remarks
[Mg-saturated]			
5.A	3.4	25.96	high
	8.9	9.93	medium
	12.3	7.19	high
	17.9	4.95	small
	21.4	4.15	small
	24.9	3.57	high
	26.7	3.34	medium
[Mg-saturated]			
5.B	24.88	3.58	high
[Mg-sat. Ethylene glycolated]			
5.C	3.4	25.96	high
	8.9	9.93	small
	12.3	7.19	high
[Mg-sat., heated to 550°C]			
12.D	3.4	25.96	high
	8.5	10.39	small
	17.3	5.12	small
	26.3	3.39	medium
[Mg-sat., heated to 105°C]			
19.E	3.2	27.59	high
	8.9	9.93	medium
	12.3	7.19	high
	17.8	4.98	medium
	21.3	4.17	small
	24.9	3.57	high
	26.6	3.35	medium
[Mg-sat. Ethylene glycolated]			
19.C	3.4	25.96	high
	8.9	9.93	medium
	12.3	7.19	high

Table 2.21: Artificial soil Kaolin 'K' - interplanar spacing 'd' for each main peak observed in the X-ray diffraction trace.

Trace No.	2θ (°)	d (Å)	Remarks
[Mg-saturated]			
6.A	3.3	26.75	high
	8.9	9.93	medium
	12.5	7.07	high
	17.8	4.98	small
	24.95	3.56	high
	26.8	3.32	medium
[Mg-saturated]			
6.B	24.92	3.57	high
[Mg-sat. Ethylene glycolated]			
6.C	3.3	26.75	high
	9.0	9.82	small
	12.45	7.10	high
[Mg-sat., heated to 550°C]			
13.D	3.4	25.96	high
	8.75	10.10	small
	26.4	3.37	small
[Mg-sat., heated to 105°C]			
20.E	3.5	25.22	high
	12.4	7.13	high
	8.9	9.93	medium
	17.8	4.98	small
	25.0	3.56	high
	26.75	3.33	small
[Mg-sat. Ethylene glycolated]			
20.C	3.4	25.96	high
	8.9	9.93	medium
	12.4	7.13	high

Table 2.22: Artificial soil Bentonite 'B' - interplanar spacing 'd' for each main peak observed in the X-ray diffraction traces.

Trace No.	2θ (°)	d (Å)	Remarks
[Mg-saturated]			
7A	3.5	25.22	high
	5.9	14.97	high
	17.7	5.01	medium
	26.7	3.33	medium
	29.25	3.05	medium
[Mg-saturated]			
7.B	-	-	-
[Mg-sat. Ethylene glycolated]			
7.C	3.5	25.22	high
	5.3	16.66	high
	10.3	8.58	medium
[Mg-sat., heated to 550°C]			
14.D	3.3	26.75	high
	9.1	9.71	high
	18.6	4.77	medium
	26.4	3.74	medium
	28.1	3.17	high
[Mg-sat., heated to 105°C]			
21.E	3.4	25.96	high
	6.2	14.24	high
	18.1	4.89	medium
	20.9	4.25	small
	26.6	3.35	medium
	29.8	3.00	medium
[Mg-sat. Ethylene glycolated]			
21.C	3.4	25.96	high
	5.2	16.98	high
	11.3	7.82	medium

2.5 CONCLUSIONS FOR CHAPTER TWO

Chapter two dealt with soil structure and clay minerals and, in particular with the application of this knowledge to the soil types previously selected.

Concerning these soil types, their macro structure was defined by measurement of its engineering properties, the micro structure observed by means of the scanning electron microscope, and the clay minerals were identified using X-ray diffraction techniques[1].

These conclusions are grouped into three sections, as follows:

- Engineering Properties;

- Micro Structure; and,

- Clay Minerals.

Each of the above sections will be dealt with as a separate sub-section of this chapter.

2.5.1 Engineering properties.

Particle Size Distribution.

The particle size distributions (for the natural soil types) have been combined to form a grading envelope. This grading envelope is included in the following Figure 2.43.

---

[1] - *refer to the previous sections of this chapter.*

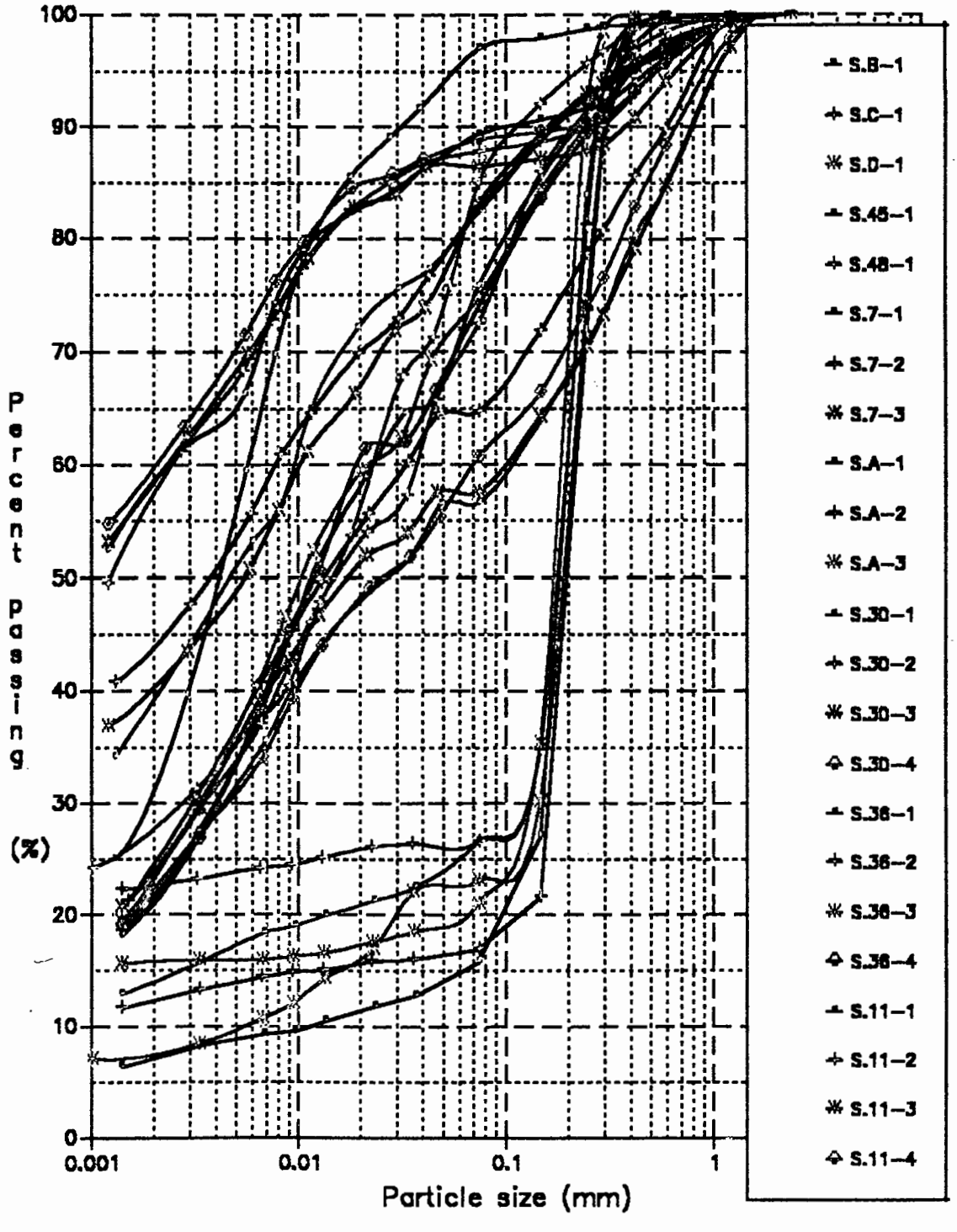

Figure 2.42: Particle size grading envelope for all the natural soil types - sites 11, 36, 30, A, 7, 48, 45, B, C and D. (Comment: Dips in grading curves should not exist[1]).

[1] - *they are due to smoothing algorithm.*

Particle size grading envelope (for all artificial soil types) is included as Figure 2.44.

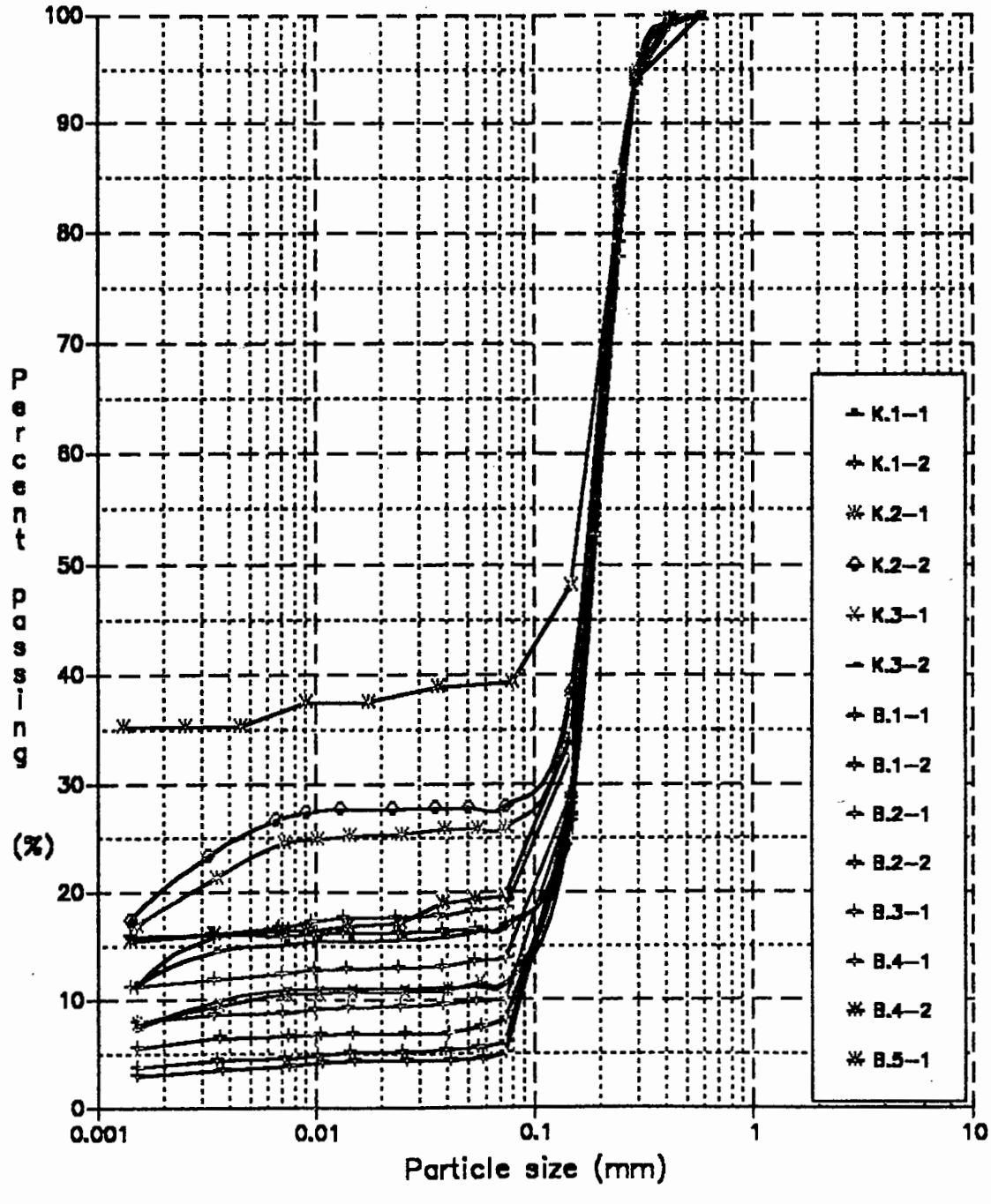

Figure 2.43: Particle size grading envelope for all artificial soil types - Kaolin K.1 (13%), K.2 (20%), and K.3 (10%), and Bentonite B.1 (3.5%), B.2 (7%), B.3 (11.5%), B.4 (15.5%), and B.5 (35%).

Soil Density versus Water Ratio.

Based on compaction tests for both the standard and modified AASHTO, Table 2.23 tabulates the maximum and minimum values of the void ratio 'e', porosity 'n' and degree of saturation 'Sr', obtained from the plot of dry density versus water ratio for each soil type[1].

Table 2.23: Soil density versus water ratio for natural soil types - includes values of void ratio, porosity and degree of saturation.

Site number, location	Dry density 'D_D' (KN/m	Water ratio 'Wr' @ OMC	Void ratio 'e'	Porosity 'n'	Degree of saturation 'Sr'
11, Rosebank					
[Modified AASHTO]	16.71	0.496	0.617	0.382	0.947
[Standard AASHTO]	14.44	0.634	0.871	0.466	0.903
36, Rondebosch					
[Modified AASHTO]	18.1	0.349	0.455	0.313	0.977
[Standard AASHTO]	17.15	0.454	0.538	0.350	0.851
30, Hout Bay					
[Modified AASHTO]	17.35	0.409	0.499	0.333	0.940
[Standard AASHTO]	15.0	0.620	0.742	0.426	0.921
A, Berea Road					
[Modified AASHTO]	20.47	0.235	0.277	0.217	0.898
[Standard AASHTO]	19.0	0.304	0.383	0.277	0.885
7, Mowbray					
[Modified AASHTO]	18.9	0.320	0.436	0.304	0.904
[Standard AASHTO]	16.6	0.147	0.632	0.387	0.886

[1] - *refer to previous Figures 2.10 to 2.14.*

2.5.2 Micro structure.

The micro structure of each soil type was observed by means of the scanning electron microscope. Based on a visual assessment of each photo micrograph, observations were noted. the following is a summary of the observations of micro structure for each soil type:-

Site 11, Rosebank - Photographic plate 2.02[1]:-

Microstructure consists of fine silt particles linked and surrounded by clay particles. Larger size of visible particles appear to have a thin 'platelet-like' appearance. Small size and low frequency of voids is also observed.

Site 36, Rondebosch - Photographic Plate 2.03[1]:-

Matrix of fine silt and clay size particles. Thin 'platelet-like' appearance of fine silt size particles. Evidence of large (of the order of 1 μm) pores are visible between the particles.

Site 30, Hout Bay - Photographic Plate 2.04[1]:-

Microstructure consists of fine silt and clay size particles in a fairly dense arrangement. No large pores are visible between the particles.

Site A, Berea Road (Durban) - Photographic Plate 2.05[1]:-

Particle of silt size linked and surrounded by particles of clay size. No prefered orientation of clay particles is apparent. Pores of 1 μm, or greater, appear to be present.

Site 7, Mowbray- Photographic Plate 2.06[1]:-

Matrix of fine silt and clay size particles in a dense arrangement. No pores appear to be visible between the particles.

Kaolin - Photographic Plate 2.07[1]:-

Microstructure is essentially dispersed. It consists of very fine silt and clay size forming thin 'platelets'. Small pores are visible between the particles.

Bentonite - Photographic Plate 2.08[1]:-

Microstructure consists essentially of a uniform matrix. Random orientation, of mainly clay size particles, is mostly visible.

---

[1] - refer to section 2.3.5.

2.5.3 Clay minerals.

Absorbed Water on Clay.

Present knowledge of crystal and surface chemistry of clay leads to the following conclusions:-

(i) Positions of the oxygen atoms of the adsorbed water molecules have been established by X-ray diffraction of vermiculite. These positions preclude both the ice structure and the Hendricks-Jefferson net structure, even after modification to accommodate the exchangeable ions.

(ii) Density of water sorbed on Na montmorillonite has a minimum value of about 0.7 g/cm^3 at a water content of 0.7g H_2O/g clay[1]. For water contents less than 0.7 the density rapidly rises to about 1.4, and for water contents greater than 0.7 the density gradually rises until about 6.5g H_2O/g clay the density of the adsorbed water equals that of normal liquid water.

(iii) The differential entropy of water adsorbed on kaolinite has a minimum value approximately that of ice, however - (a) this minimum occurs at about 0.7 of a monolayer, and (b) the integral entropy is greater than that for normal liquid water up to at least two molecular layers. The apparently contradictory entropy of sorbed water on montmorillonitic clay has not been resolved but is believed to be at least partially associated with clay swelling.

(iv) Diffusion and fluid flow phenomena are shown to be extremely sensitive to clay fabric; therefore, it appears that diffusion and fluid flow data on loosely compacted clay are of little help in ascertaining the structure of the adsorbed water phase.

(v) Adsorbed water is easily supercooled and an appreciable fraction of the adsorbed water remains unfrozen after ice was once formed.

The two major hypotheses indicate that the nature of the adsorbed water is either (1) a solid like substance, or (2) a two-dimensional fluid.

---

[1] - *approximately equal to the Plastic Limit.*

Clay water-system and relationship between free swelling and the dimensions of the montmorillonite latice:-

The water adsorbed on clay surfaces differs in structure and physical properties from bulk liquid water. Three important conclusions are shown by the adsorbed water density data for Na-montmorillonite shown in Figure 2.44[1]:

(1) at the same temperature there are no contradictory data pertaining to the adsorbed water density being greater or less than that of normal liquid water;

(2) at water contents below 0.3g H_2O/g clay the adsorbed water density exceeds that of normal water, while at water contents above 1.0g H_2O/g it is within 2 to 3 percent;

(3) at no water content does the adsorbed water density approach the density required for ice (0.90) or for the hexagonal theory (0.92).

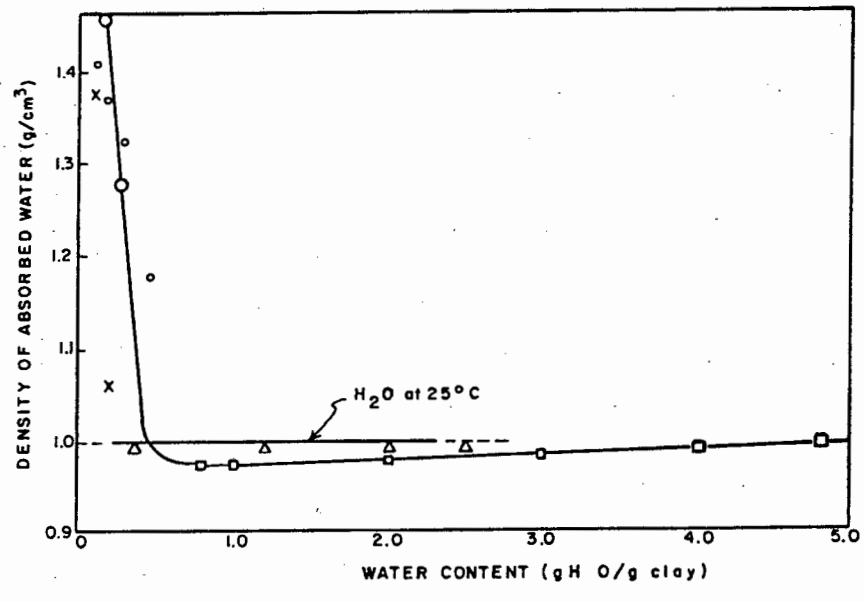

Legend :-
- • De Wit & Arens - (Ref. 55)
- X Mackenzie (Ref. 56)
- o Mooney et al (Ref. 57)
- △ Norrish (Ref. 58)
- □ Anderson & Low (Ref. 59)

Figure 2.44: Adsorbed water density on Na-montmorillonite.

Relation between crystal-lattice configuration and swelling of montmorillonites: As shown in Figure 2.45[2] swelling decreases linearly with increase in b-dimension.

---

[1] - *previously included in this chapter as Figure 2.21.*
[2] - *included in this chapter as Figure 2.29.*

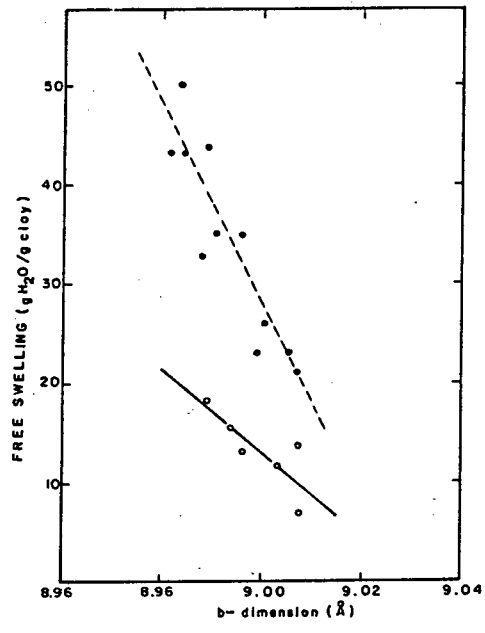

Figure 2.45: The relation between free swelling and b-dimension for Na-montmorillonites.

Elemental and mineralogical analysis.

The results obtained from the Elemental Analysis[1] are presented in Table 2.24.

Table 2.24: Elemental analysis of samples - includes all the natural soil types (sites 11, 36, 30, A, and 7), as well as the artificial ones (kaolin `K' and bentonite `B').

Element:	Soil Types / % of element present:						
	S.11	S.36	S.30	S.A	S.7	K	BE
Magnesium (as MgO)	2	1	1	-	1	-	3
Aluminium (" Al_2O_3)	29	29	32	15	30	34	18
Silicon (" SiO_2)	52	51	58	73	56	64	76
Sulphur (" SO_3)	1	2	2	1	<1	<1	-
Potassium (" K_2O)	1	2	1	<1	2	1	-
Titanium (" TiO_2)	1	2	<1	1	1	<1	-
Iron (" Fe_2O_3)	15	12	5	9	9	<1	3
Sodium (" Na_2O)	<1	<1	<1	<1	<1	<1	<1
Loss on ignition (at 850°C)	9.6	5.8	10.9	3.0	6.4	13.8	15.2

[1] - *semi-quantitative.*

2.6 REFERENCES FOR CHAPTER TWO

16. DE S. VINAGRE, T.J.V. (1976/77): Masters Thesis - Diaries One, Two, Three, Four, Five, and Six.

32. ABBE, E. (1873): The Theory of Microscope Image Formation.

33. OATLEY, C.W. (1972): The Scanning Electron Microscope. Published by the Cambridge University Press, London.

34. MEAKING, J.D., and FALLOW, L.M. (1973): Low magnification scanning electron microscopy. In Scanning Electron Microscopy/1973, O. Johari and I. Corvin, eds. IITRI 6, 145 - 150.

35. MEE, P.E. (1972): Microscopy and its contribution to computer technology. Microstructures, October/November 1972.

36. SCHARF, D. (1977): Magnifications - Photography with the Scanning Electron Microscope. Schocken Books, New York.

37. Electron Microscope Unit (1976/77) R.W. James Physics Building, University of Cape Town: Pamphlet for the electron microscopy services provided by the unit, issued in 1977, ABC press.

38. ROGERS, J. (1971): Sedimentology of Quarternary Deposits on the Agulhas Bank. Bulletin No. 1, S.A. Nat. Committee for Oceanographic Research.

39. VAN ANDEL, T.H., and FRANKLIN, K. (1968): Sediment laboratory procedure - Unpublished manual. Oceanographic Dept., Oregon State University.

40. KRUMBEIN, W.C. (1934): Size frequency distribution of sediments. J. Sediment Petrol., 4; 65-77.

41. HURLBUT, C.S., and KLEIN, C. (1977): Manual of Mineralogy - 19th Edition (after J.D. Dana). Published by J. Wiley & Sons Inc.

42. MANSON, B. (1966): Principles of Geochemistry - 3rd Edition. J. Wiley & Sons, New York.

13. HOLMES, A. (1970): Principles of Engineering Geology - 2nd edition. Thomas Nelson and Sons Ltd., Great Britain.

43. PAULING, L. (1960): The nature of the Chemical Bond - 3rd Edition. Cornell University Press, Ithaca, 644 pp.

44. COMPANION, A.L. (1964): Chemical Bonding. McGraw-Hill Book Company.

45. GRIM, R.E. (1968): Clay Mineralogy - 2nd Edition. McGraw-Hill Book Company.

46. LYONS, T.L., and BUCKMAN, H.O. (1943): The Nature and Properties of Soils. Macmillan, New York.

47. WINTERS, E. and SIMONSON, R.W. (1951): The Subsoil. Advan. Agron., 3:2-92.

48. JACKSON M.L. (1959): Frequency Distribution of Clay Minerals in Major Great Soil Groups as related to the Factors of Soil Formation. Proceedings of the 6th National Clay Conference, pp. 133-143, Pergamon Press, New York.

49. DEER, W.A., HOWIE, R.A., and ZUSSMAN, J. (1969): An Introduction to the rock Forming Minerals - 5th Impression. Longman's Green and Co. Ltd., London.

50. BROWN, G. (1955): Report of the Clay Minerals Group Sub-Committe on Nomenclature of Clay Minerals, Clay Minerals Bull. 2(13): 294-302.

51. EISENBERG, D. and KANZMANN, W. (1969): The structure and properties of Water. Oxford Univ. Press, New York.

52. Florentine Acadamy (about 1658): Saggi di Naturali Esperienze. English translations in Phil. Trans. 5, 2020 (1670); and, in Essayes of Natural Experiments, translated by R. Waler (1684); Johnson Reprint Corporation, New York, 1964.

53. BRIDGMAN, P.W. (1926): The effect of increased pressure in Lowering the viscosity of cold water. Proc. Acad. Arts Sci. 61, 57.

54. MARTIN, R.T. (1960): Adsorbed Water on Clay: A Review. Proceedings of 9th National Conference on Clays and Clay Minerals, vol.9.

55. DE WIT, C.T., and ARENS, P.L. (1950): Moisture content and density of some clay minerals and some remarks on the hydration pattern of clay. Trans. 4th Int. Cong. Soil Sci., V.2, 59-62.

56. MACKENZIE, R.C. (1958): Density of water sorbed on montmorillonite. Nature v.181, p. 334.

57. MOONEY, R.W., KEENAN, A.G. and WOOD, L.A. (1952): Adsorption of water vapour on montmorillonite. II: J. Amer. Chem Soc., v.74, pp. 1371-1374.

58. NORISH, K. (1954): The swelling of montmorillonite. Faraday Society Discussion no. 18, pp. 120-134.

59. ANDERSON, D.M. and LOW, P.F. (1958): The density of water adsorbed by Li-, Na-, and K-bentonite. Soil Sci. Soc. Amer. Proc., vol.22, pp. 99-103.

60. HILL, T.C. (1950): Statistical mechanics of adsorption, IX, Adsorption thermodynamics and solution thermodynamics. J. Chem. Phys. v.18, pp. 246-256.

61. QUIRK, J.P. (1955): Significance of surface areas calculated from water vapor sorption isotherms by use of the BET equation. Soil Sci., vol.80, pp. 423-430.

62. SIENKO, J.M. and PLANE, R.A. (1966): "Chemistry: Principles and Applications" - International Student Edition. McGraw-Hill Inc.

63. MUIR, J. (1954): Dielectric loss in water films adsorbed by some silicate clay minerals. Trans. Faraday Soc., v.50, pp. 249-254.

64. DEEG, E. and HUBER, O. (1955): Dielectric constant of clays in decimeter wavelength as a function of water content. Ber. dtch. keram. Ges., v.32, pp. 261-272.

65. PICKETT, AG and LEMCOE, M.M. (1959): An investigation of shear strength of the clay-water system by radio-frequency spectroscopy. J. Geophys. Res. v.64, pp. 1579-1586.

66. HOSLER, C.L. and HOSLER, C.R. (1955): An investigation of the freezing of water in capillaries. Trans. Amer. Geophys. Un., v.36, pp. 126-132.

67. GRIM, R.E. and CUTHBERT, F.C. (1945): Some clay-water properties of certain clay minerals. J. Amer. Crem. Soc. v.28 pp. 90-95.

68. BAILEY, S.W. (1966): The status of Clay Mineral Structures. Clay and Clay Minerals - Proceedings of xiv National Conference at Berkley, California.

69. VEITCH, L.G., and RADOSLOVICH, E.W. (1963): The cell dimensions and summetry of layer-lattice silicates. III, Octahedral ordering: Amer. Min. 48, 62-75.

70. LINDGVIST, B. (1962): Polymorphic phase changes during heating of dioctrahedral layer silicates. Geol. Foren. Forhandl. 84, 224-9.

71. TAKÉUCHI, Y. (1965): Structure of brittle micas. Clays and Clay Minerals, Pro. 13th Conf., Pergamon Press, New York.

72. EIRISH, M.V. and TRET'YAKOVA, L.I. (1970): The role of sorptive layers in the formation and change of the crystal structure of montmorillonite. Clay Minerals, v.8 pp. 255-266.

73. DAVIDTZ, J.C. and LOW, P.F. (1970): Relation between crystal-lattice configuration and swelling of montmorillonites. Clay and Clay Minerals, vol.18, pp. 325-332.

74. OVERBECK, J.Th.G. (1966): Colloid stabitity in aqueous and nonaqueous media. Discussions Faraday Society no. 42, pp. 7-13.

75. RADOSLOVICH, E.W. (1962): The cell dimensions and symmetry of layer-lattice silicates - II. Regression relations: Am. Mineralogist 47, 617-636.

76. FOSTER, M.D. (1955): The relation between composition and swelling in clays. Clays and Clay Minerals, 3, 205-220.

77. LOW, P.F. and ANDERSON, D.M. (1958): Osmotic pressure equations for determining thermodynamic properties of soil water. Soil Sci. 86, 251-253.

78. RAVINA, I. and LOW, P.F. (1972): Relation between swelling, water properties and b-dimension in montmorillonite-water systems. Clay and Clay Minerals, vol.20, pp. 109-123.

79. NUFFIELD, E.W. (1966): X-ray Diffraction Methods. John Wiley & Sons Inc., New York.

80. HALLIDAY, D. and RESNICK, R. (1970): Fundamentals of Physics. A Wiley International Edition.

81. FANG, J.H. and BLOSS, F.D. (1966): X-ray Diffraction Tables. Southern University Press.

82. CARVER, R.E. (1971): Procedures in Sedimentary Petrology. Wiley Interscience.

83. BROWN, G. (1972): The X-ray Identification and Crystal Structures of Clay Minerals. Mineralogical Society, London.

CHAPTER THREE

INTRODUCTION TO EXPANSIVE AND COLLAPSING BEHAVIOUR

3.1 INTRODUCTION AND DEFINITIONS

In general terms, any type of soil subjected to external loading may exhibit additional settlement upon being wetted. That is to say that a 'mechanical' type of collapse could be started by, or because of, the interaction of water with the inner structure of the soil.
Taking this argument further, even a potentially expansive soil can collapse if its internal structure arrangement has both a very high void ratio and deficiency in water content to begin with, and if the loading is sufficiently large.
However, for a soil to expand while under load not only are the inner structure and water content important factors but it also needs to have the type of clay which will absorb water and increase in volume.
This 'type of clay' needs to contain the clay minerals identified by the X-ray Diffraction techniques introduced in chapter two[1].

For the purpose of this thesis the following definitions of Expansive and Collapsing soils will apply:

Expansive Soil: A soil which has consolidated for at least 24 hours under a 100 kpa vertical pressure and which will increase its volume when wetted while under load.
Collapsing Soil: Conversely, a collapsing soil will decrease its volume upon wetting, that is, further settlement will occur while carrying the same load.

Three types of expansive or collapsible behaviour were investigated for controlled wetting conditions:

1) Free shrinkage and Free Swell paths while carrying no external loading;
2) Expansion or collapse under known vertical, or all round, loads; and,
3) Vertical pressure required to prevent volume changes, that is, the swell pressure.

The following types of soil samples were used to observe the expansive or collapsing behaviour:

(i) Undisturbed samples as occurring in nature;
(ii) Compacted samples prepared from disturbed soil using standard or modified AASHTO apparatus;
(iii) Remoulded samples of disturbed soil mixed with water to obtain different initial void ratios and subsequently air dried to the required water content.

---

[1] - *refer to section 2.5.3. "Clay minerals".*

Natural and Artificial Soil Types[1]:-

A large number of disturbed 'natural occurring' soil samples were originally collected. Factors such as the geological origin, location and visual appearance were considered. The initial selection of the sites was based on the linear shrinkage values obtained in the laboratory.
Preliminary tests were next performed on the soils from the selected sites. The results were compared and particular sites were finally selected to provide the soil types to be used for the purpose of this thesis. Undisturbed samples were carefully removed from the selected sites, waxed and stored for later use.

Artificially prepared soils were also used in order to have closer control of both the physical structure arrangement and the measurable properties of the soil. The main intention was to obtain an homogeneous soil with constant properties throughout.

3.2 OUTLINE OF THE MAIN TESTING METHODS

The main testing methods, used in the chapters ahead, can be briefly defined as follows:-

Free Shrinkage and Free Swell paths:
* Shrinkage and Expansion Limits.

Triaxial Tests [saturated sample, consolidated]:
* All round consolidation, drained test.

Consolidometer Test [saturated sample, consolidated]:
* Void ratio versus effective pressure relationships.

Consolidometer Test [controlled wetting under known load]:
* If soil is expansive - Swell Pressure Tests.
* If soil is collapsing - Apply known vertical pressures.

Swell Pressure Test:
* Swell pressure required for no volume change.
* Swelling against known vertical pressures.

Consolidometer Test [controlled wetting, known pressure]:
* Lateral pressure measurements.

Triaxial Test [controlled wetting, known pressure]:
* Expansive or collapsing behaviour.

---

[1] - *refer to Chapters One, Two and Appendix A.*

3.3 SUMMARY OF THE CHAPTERS AHEAD

Chapter Four 'Free Shrinkage and Free Swell Paths':-

Chapter Four describes the study of drying and swelling paths for each soil type, and in particular the relationship between volume and water content. These volume changes are due to controlled air drying or incremental wetting of the sample.

Chapter Five 'Fitting Stress Scales to Observed Data':-

The Pressure, or Stress, Scales were obtained from the void ratio versus effective pressure relationships for one dimensional consolidation, and also for isotropic consolidation.
The first type (of scales) were derived from the void ratio versus effective pressure relationship produced by the ordinary one dimensional consolidometer test for saturated soil samples. The second type (of scales) were derived from an average all round pressure under drained conditions, obtained with triaxial test equipment.

Chapter Six 'One Dimensional Expansion or Collapse':-

The one dimensional measurement of vertical movement due to incremental wetting, while supporting a known load. A standard consolidometer was used to apply a known vertical pressure, varying between 1 kpa and 400 kpa, and the soil sample expanded or collapsed while being wetted in stages.

Chapter Seven 'Swell Pressures':-

The one dimensional measurement of pressure, due to wetting, for no volume change. A modified consolidometer[1] was used to measure vertical pressure, required to prevent volume change of the soil due to incremental wetting.

Chapter Eight 'Axisymmetric Stress Behaviour of Expansive and Collapsing Soils':-

The measurement of lateral pressure developed in the soil sample due to incremental wetting, while being subjected to a known vertical load.
In the case of soils which exhibited expansive behaviour, use was made of a specially made strain gauge device[2] (April 1976) using strain gauges to measure the lateral pressures developed in the soil sample due to wetting. Another device, designed by Prof. Sparks and used by the writer, used a piston pump to provide the balancing horizontal pressure required to prevent horizontal strain.

---

[1] - suggested by Prof. Sparks and designed by the writer.
[2] - designed and constructed by Prof. Sparks and the writer.

Chapter Nine 'All Round, three-dimensional Expansion or Collapse'.

The measurement of changes in volume due to incremental wetting, while subject to known all round pressure. Triaxial equipment was used to apply all round pressure to the soil sample, and while being subjected to this pressure, the sample expanded or collapsed due to being wetted in stages.

Chapter Ten 'Concluding Summary and Further Thoughts':-

This chapter provides a concluding summary for parts one and two of the thesis. It also includes a closer look at some particular aspects, and concludes the thesis with a recommendation for future research work[1].

---

[1] - *refer to "Concluding Remark" in Chapter Ten.*

CHAPTER FOUR *

FREE SHRINKAGE AND FREE SWELL PATHS

4.1 INTRODUCTION

The work in this chapter deals with observed changes in the volume and mass of soil samples as the water content of the samples is altered, for example by allowing the sample to dry out between observations, or by the addition of measured volumes of water.
The observed sample volumes, void ratios and water contents are presented in graphical form to illustrate the trends of behaviour and to allow comparisons to be made between the paths followed by different types of soil samples. Many different types of soils were used.

Different methods of sample preparation were followed for each soil type prior to the observation of the free-shrinkage or free-swell behaviour paths. It was hoped to investigate both the unsaturated and saturated conditions of each soil sample.

4.2 DEFINITION

The words "Free-shrinkage" and "Free-swell" as used in this chapter, can be defined as follows:-
The word "Free" will in this case mean that during the process of overall volume change, the sample is neither confined by externally applied stresses nor by a fixed volume container. In other words during both the swelling and the shrinkage stages the sample is merely sitting on a flat smooth surface and is free to change its linear dimensions in all directions.
The changes in the overall volume occur due to effective stresses between the grains of the sample caused by changes in the tensions within the pore water pressure, and due to the volumetric changes of the effective soil particles.

The changes in the water content of these samples were made to happen in a controlled manner by one of the following methods:

a) In the case of a swelling increment, a limited small known volume of de-aired water was added to the whole underside of the small soil sample by means of a syringe; and, then an interval of at least six hours was allowed for this extra water to distribute itself upwards throughout the sample. At this stage the new mass and overall volume were measured, prior to the next change in water content.

---

* - *Observations are in Appendix C.*

b) In the case of a shrinkage step, the sample was permitted to lose water by evaporation to an external atmosphere which surrounded the sample. The rate of evaporation could be controlled; for example by placing the sample in a large sealed bottle or in a partly sealed one. The new water contents and the changes in overall volume were noted.

4.3 THE PARAMETERS WHICH WERE INVESTIGATED

The diagram in Figure 4.01(a) illustrates some of the parameters which were investigated. It should be noted that Figure 4.01(b) shows the use of this diagram in order to find the conventional shrinkage limit - refer to the relevant test procedure in Appendix A[1].

In this shrinkage limit test, the sample which is initially at the saturated liquid limit condition A, is permitted to lose moisture. As it loses moisture the state of the sample moves from A towards B along the saturated path AB. But air enters the sample near the state B, and if the sample were to be completely dried (ie, in oven) it would reach state C.
It will therefore be noticed that the sample state cannot normally exist below the line BC. Furthermore one would not expect the sample state to occur to the right of line AB because the soil sample would then contain a larger volume of water than the available pore volume.
The feasible locations for the state of the sample would therefore be expected to be situated above the boundary ABC in Figure 4.01(b).

Parameters related to the soil material: Other parameters relating to the soil type were measured for each one - refer to Chapters One and Two, and Appendix A. These index properties included the Linear Shrinkage; Liquid Limit 'LL'; Plastic Limit 'PL'; Plasticity Index 'PI'; Relative Specific Density of the soil particles (ie, specific gravity 'Gs'); The degree of acidity 'pH' of the soil sample; Percentage of Clay, Silt and Sand; Shrinkage Limit; Activity (PI / % Clay); Maximum dry density and optimum water content for both Standard and Modified AASHTO.

In addition a water content limit called the "Free Expansion Limit" was observed for most soils. This was the water content above which the unrestrained soil sample will not swell any further if wetted[2].

---

[1] - see section A.4.5 "Shrinkage Limit".
[2] - References 84 and 85.

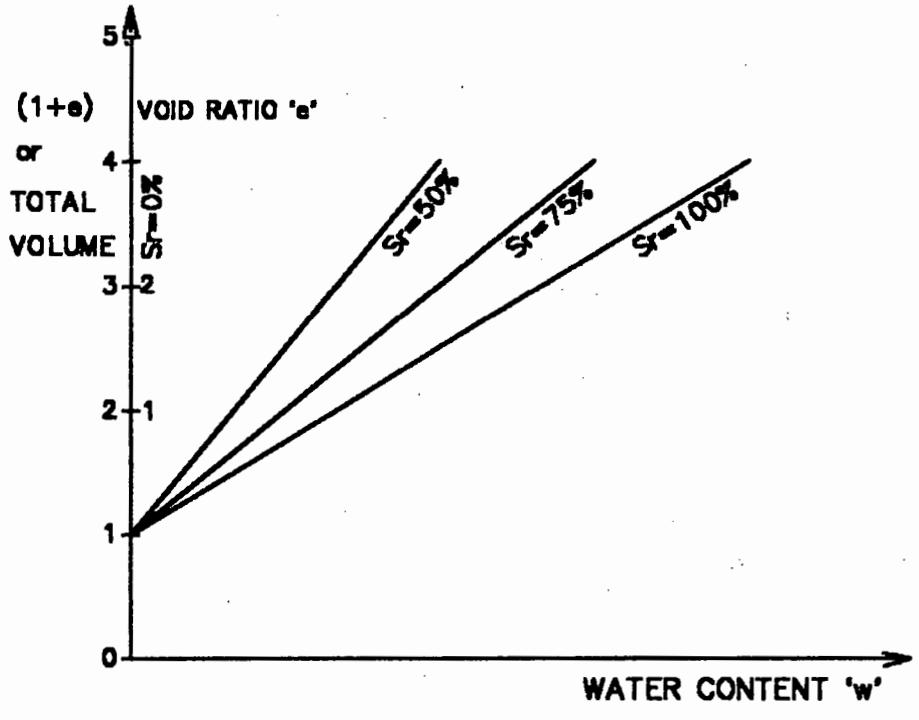

Figure 4.01(a): Relationship between void ratio (or total volume) and water content[1] - includes degrees of saturation.

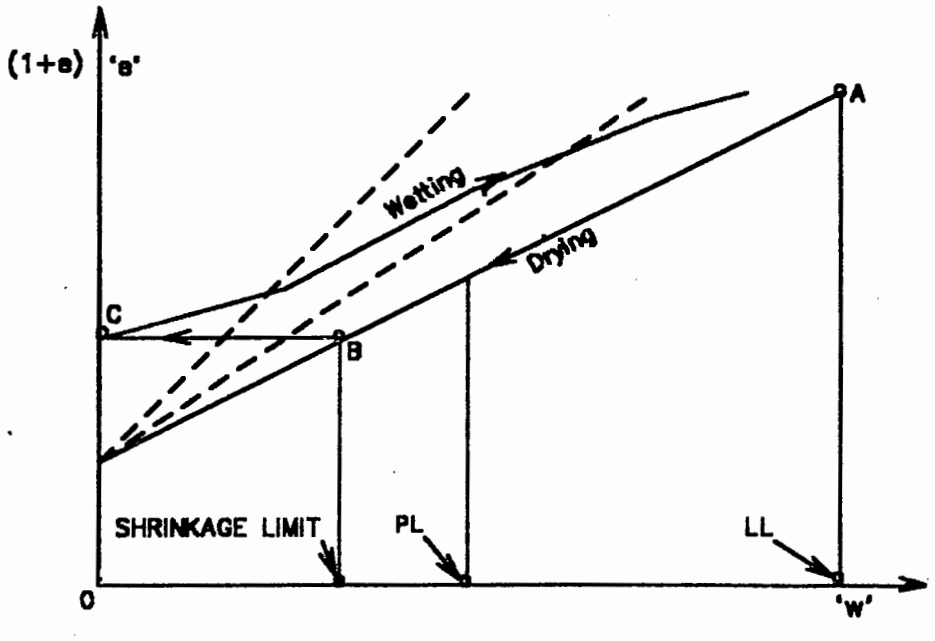

Figure 4.01(b): Relationship between void ratio and water content[1] - includes drying/wetting and shrinkage limit.

---

[1] - Models proposed by Prof. Sparks for this research.

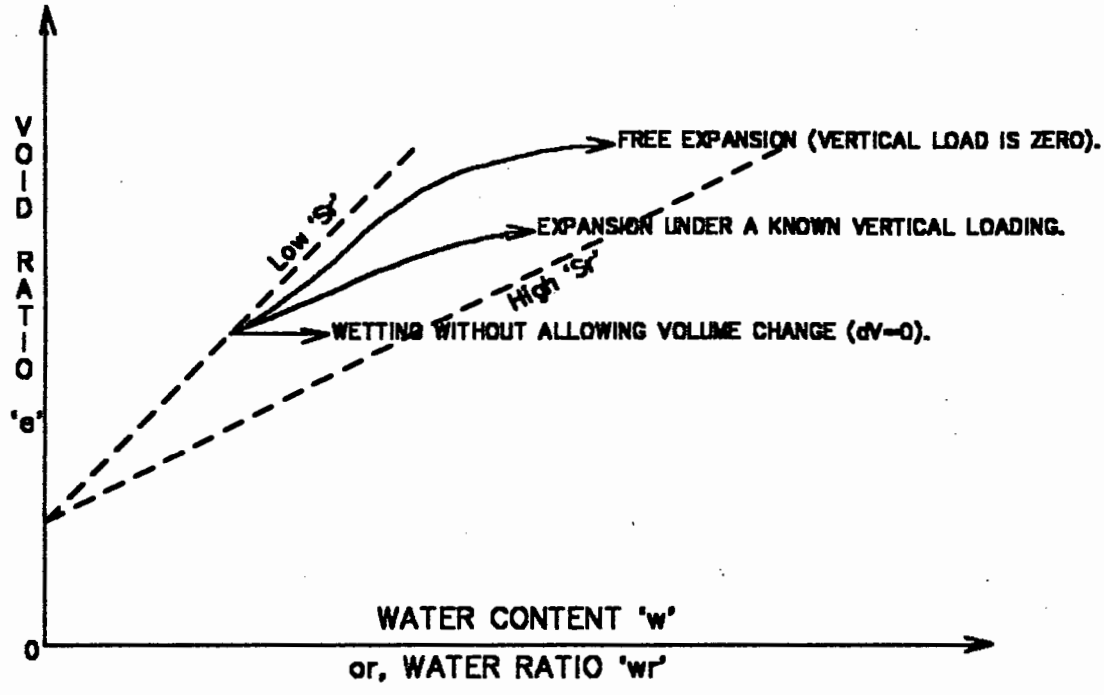

Figure 4.01(c): Relationship between void ratio and water content - includes the three types of expansion.

4.4 REASONS FOR USING THE TYPE OF PLOT SHOWN IN FIGURE 4.01

The main reasons were as follows[1]:-

A) This particular type of plot was chosen because it is easy to show a transition from a partly saturated to a saturated state. In addition an added virtue of this diagram is that it is possible to plot contours of degree of saturation as straight lines as shown in Figures 4.01(a) and 4.01(b).
Hence it is possible at a glance to notice the value or trend of the degree of saturation, even if the sample is changing its total overall volume during the change in water content.
Furthermore, this particular type of plot has been used for illustrating swelling and shrinkage paths for samples which are confined by external stresses as illustrated in Figure 4.01(c). The "confined" types of tests are dealt with in subsequent chapters.

B) It had been noticed by Sparks[1] that one of the empirical equations used by Brackley (Ref. 87, page 75 - equation 1) to describe the behaviour of expansive clays was such that it implied that a larger volume of water could be placed into a saturated clay sample than the available pore volume.

---

[1] - *This type of plot was used by Prof. Sparks (1975) to model expansive soils, Reference 86.*

It was hoped that test results plotted on diagrams such as Figure 4.01(b) could provide more clarity concerning this phenomenon.
It will be shown in the conclusion of this thesis that the above observation is valid.

C) The change in void ratio which takes place between two positions on a 'free-swell' or 'free-shrinkage' path in Figure 4.01(b) is mainly due to a change in the 'average effective stress' in the soil.
The change in the volume of the actual soil grains will normally also cause a change in the pore volume, but because these are both an increase or a decrease, the change in the value of the void ratio will be small due to this latter cause, and will be due mainly to the change in effective stresses between the grains.
The 'free-swell' or 'free-shrinkage' path can therefore be regarded as evidence of isotropic consolidation or swelling due to effective stresses which are isotropic at each point in these unconfined samples.

If a triaxial compression test can be performed on the same soil, to yield a relationship between void ratio and the isotropic effective stress, then it is possible that these results can be used to provide a stress scale on the diagram in Figure 4.01(b). Sparks had previously used such a model to predict volume changes which occur in samples which are subjected to different loading conditions. The results of his calculations were published in the proceedings of Sixth Regional Conference for Africa[1], held in Durban during 1975.

Chapter Five of this thesis "Fitting Stress Scales to Observed Data" derives 'measured' stress scales for both the one dimensional and isotropic consolidation, whereas Sparks used 'assumed' scales.
Stress contours can be superimposed on this plot as contours of stress - refer to Chapters Five[2].
Another feature of this stress scale which can be added to Figure 4.01(b) was that Sparks expressed the position and the scaling factor of the stress scale in terms of Liquid Limit and Plasticity Index of the clay. For this reason the writer measured the Liquid Limit and the other relevant properties of the soil.

D) It was desirable to try and observe the shapes of the swelling paths on the void ratio versus water content plot - See Figure 4.01(b). Similarly it was thought to be desirable to attempt to observe the paths for drying samples especially if one could start with partly saturated samples. In order to observe these swelling or wetting curves it was decided to be necessary to start the samples at conditions which lie on a grid as in Figure 4.02.

---

1 - Reference 86, Volume 2, page 68.
2 - "Fitting stress scales to observed data".

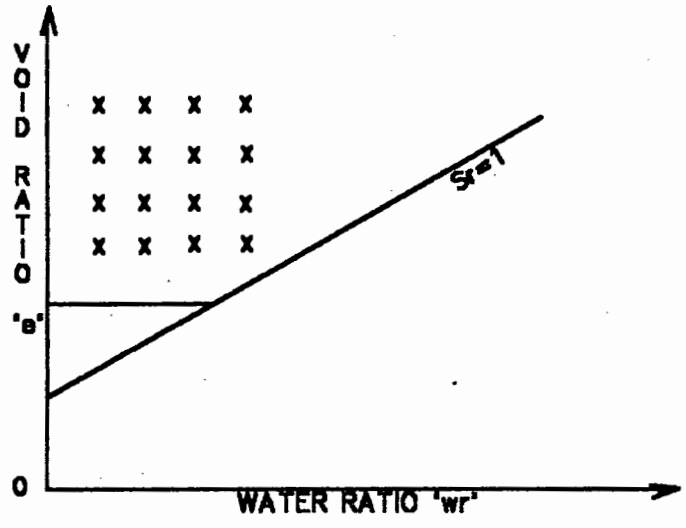

Figure 4.02: Void ratio versus water content plot - starting grid for the swelling paths.

(i) It should be noted that: In particular for the swelling curves, samples were sought which were initially very dry but which had different initial void ratios.
But when using a drying cycle (from the saturated condition) to achieve the initial dry state it was not easy to obtain a high initial void ratio prior to wetting.
Artificial compaction was one method used for obtaining the initial dry samples. But the grain structure of a dry compacted soil is not necessarily the same as that of a sample which has dried from a wet condition.
(ii) For a drying cycle, which is to be located above the line AB in Figure 4.01(b) it was necessary for air bubbles to be introduced into the initially wet sample in order that the drying curve could deviate from the line AB.
Sparks had previously designed and used a mixture like "Enos", which he mixed with a clay powdered Berea Red Soil, and then he wetted the soil to cause bubbles[1].
Another advantage of the above type of plot is that it can show the shapes of the swelling and drying paths, and also the initial, intermediate and final states of the soil on the same diagram.

E) For a sample which is expanding against a constraint, as in Figure 4.01(c) e.g. against a known isotropic loading or by preventing overall volume change, attempts were made to relate the final isotropic effective stress to the effective stress value within the free-swell sample.
It is hoped that diagrams such as Figure 4.01(c) will provide greater clarification of this connection.
Subsequent chapters[2] deal with samples which are either expanding against constraint, or being prevented from volume change.

---

[1] - *Reference 90.*
[2] - *Chapters Six to Nine.*

4.5 TYPES OF SAMPLE PREPARATION

Samples can be prepared from remoulded, compacted or undistributed soil samples. A brief description is included in this chapter for each type of preparation[1] - the detailed test procedure is included in Appendix C, "Free shrinkage and free swell - test procedure and results".

Samples prepared from remoulded soil.

The soil samples used were of fine size - no particles greater than 2.0 mm size were present. The soil was first allowed to air dry. A representative soil sample was obtained by means of a sample riffler, until the amount required is available.

(i) Method M1: The soil is thoroughly mixed with water to form a wet paste. The wet paste is then moulded into a glass dish.
It should be noted that the water content of the mixture varies between the Plastic and Liquid Limits to obtain different initial void ratios.

(ii) Method M2: In order to obtain higher initial void ratios, the soil is dry mixed together with Tartaric acid and Sodium bicarbonate (previously used by Sparks[2]).
A known amountof water is then added to the mixture which is quickly mixed and moulded into the shrinkage dish.
The present writer added lime (Calcium Hydroxide) to correct the pH of the soil (Appendix A).

Samples prepared from compacted soil.

The soil is mixed with the required amount of water in order to obtain a previously selected point on the Dry Density versus Water Content curve. The compaction of the moist soil is carried out to the required compaction specification.
The compacted block of soil is removed from the mould, and the test sample is then cut.

Undisturbed samples.

The test sample is cut from the undisturbed block of soil.

---

1 - See also Appendices C and A.
2 - Reference 90.

4.6 TEST METHOD - INCLUDES VISUAL SEQUENCE

The test sample is allowed to air-dry under controlled conditions. As the soil dries, it shrinks and reduces its overall volume and mass. The shrinkage path of the soil is obtained from the measurements of mass and volume, which are carried out at regular intervals - as illustrated in Photographic Plates 4.01 (i) to (vi).

When further air drying produces no change in total volume, a small amount of water is added to the underside of the soil. The test sample is then left for a few hours inside a closed container to allow the soil to absorb the water and to change its total volume. The mass and volume are measured and recorded, after which another wetting stage is carried out.
These wetting (with swelling) stages are repeated until the soil becomes soft - that is, the soil sample is about to deform (in shape) during the total volume measurements. The water content is at near the free expansion limit of the soil, and the soil is now hardly absorbing any water. The swelling path of the soil is obtained from the measurements of the mass and volume.

At this stage, either perform another cycle of air drying/wetting, or place the test sample inside the drying oven in order to subsequently obtain the oven dry mass of the soil sample.

The volume of the soil mass is measured by means of the mercury displacement apparatus which basically enables the measurement of the displaced mass of mercury (equals the total volume of the sample) - refer to the visual sequence of the procedure in Photographic Plates 4.01 (i) to (vi).

The detailed description of the test procedure is included in Appendix C[1] of this thesis.

---

[1] - *refer to section C.2 "Test Procedures".*

(i) (ii)

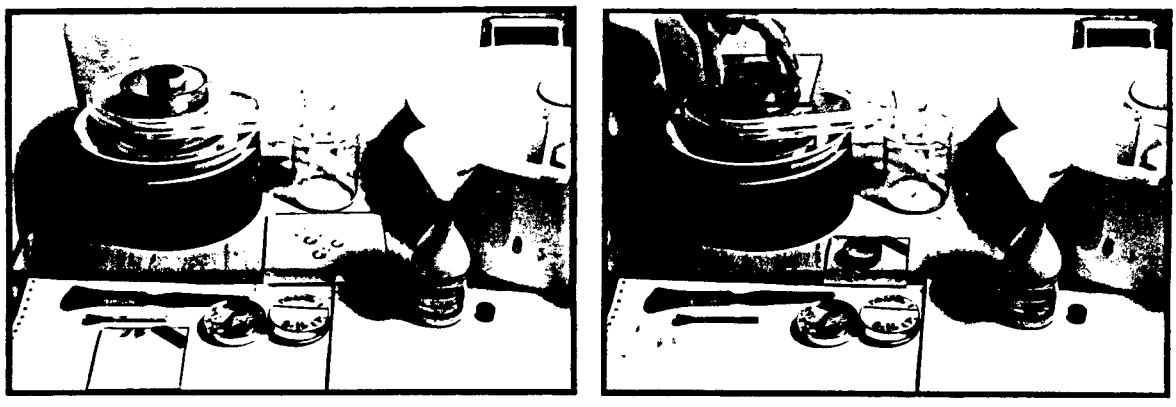

(iii) (iv)

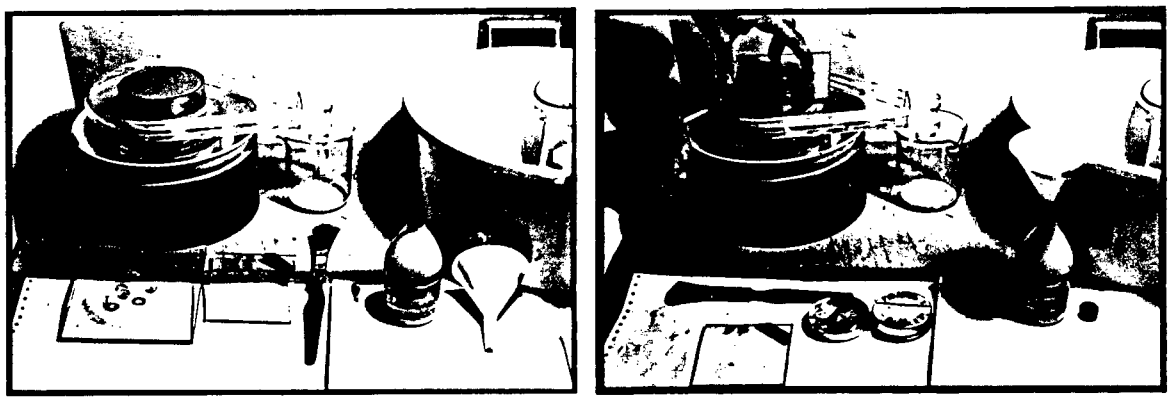

(v) (vi)

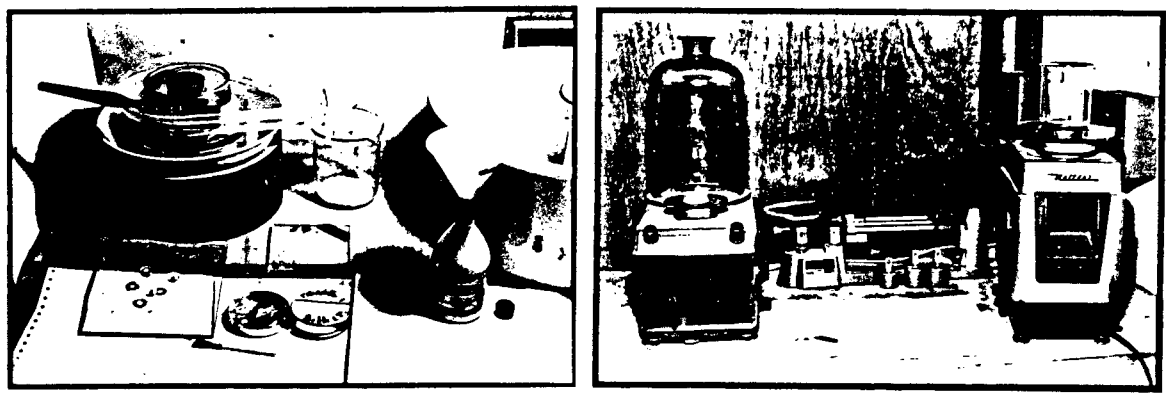

Photographic Plate 4.01: (i) Unit filled with mercury; (ii) Zero reading obtained by pressing flat plate with 3 prongs, into mercury and removing the excess; (iii) Sample is placed on top of mercury, and (iv) pressed down under it; (v) Bits of mercury are brushed into glass beaker; (vi) Masses of sample (LHS) and beaker plus mercury (RHS) are recorded.

4.7 SUMMARY OF TEST RESULTS FOR EACH SOIL TYPE

The soil types were previously defined according to the particle size and consistency limits[1].
For each soil type, its definition, particle size and the consistency limits provide the introduction to the Free Shrinkage and Free Swell paths for each soil type - refer to Figures 4.03 to 4.54.
The shrinkage path results from the plot of void ratio 'e' against water ratio 'wr' or 'Ω', for each point of the air drying portion of the cycle, and the swelling path from the plot of the wetting part.

It should be noted that: Water Ratio 'wr' = Water Content 'w' x Specific Gravity 'G_s'; and, that Appendix B includes the definitions and detailed calculations for void ratio 'e', water content 'w' and water ratio 'wr' or 'Ω'.

4.7.1 Natural Soil Types.

This section includes the relationships of free shrinkage and/or free swell paths for the following natural soil types:

(i) Site 11, Rosebank (Cape);
(ii) Site 36, Rondebosch (Cape);
(iii) Site 30, Hout Bay (Cape);
(iv) Site A, Berea Road (Durban, Natal);
(v) Site 7, Mowbray, (Cape);
(vi) Site B, Francois Road (Durban, Natal);
(vii) Site C, Margaret Mayton Avenue (Durban, Natal); and,
(viii) Site D, Rose Hill (Durban).

Free Shrinkage and Free Swell tests were carried out for the soil samples listed in Table 4.01.
The free shrinkage and free swell paths are shown in Figures 4.03 to 4.38.

---

[1] - *refer to Chapters One, Two, and Appendix A.*

Table 4.01: Natural Soils - samples used for Free Shrinkage and Free Swell tests.

Sample No.	Method of preparation [section 4.5]	Reference number	Consolidometer/Triaxial: Test No. - Chapter No.
Site 11 - Rosebank, Cape [Remoulded samples]			
S.11-42	M1 (≥LL)	III.282	92 (C) - Chp. 6
S.11-49	M1 (≥LL)	III.305	93 (C) - Chp. 6
S.11-41	M1 (≥LL)	III.278	89 (C) - Chp. 6
S.11-64	M1 (≥LL)	IV. 451	173 (C) - Chps.6 & 8
S.11-23	M1 (≥LL)	II. 253	69 (C) - Chp. 6
S.11-33	M1 (≥LL)	II. 250	74 (C) - Chp. 6
S.11-46	M1 (≥LL)	III.290	98 (C) - Chp. 6
S.11-60	M1 (≥LL)	III.384	142 (C) - Chps.6 & 8
S.11-59	M1 (≥LL)	III.394	158 (C) - Chps.6 & 8
S.11-40	M1 (≥LL)	III.276	90 (C) - Chp. 6
S.11-65	M1 (≥LL)	IV. 451	176 (C) - Chps.6 & 8
S.11-16	M1 (≥LL)	II. 231	53 (C) - Chp. 7
S.11-34	M1 (≥LL)	II. 252	75 (C) - Chp. 7
S.11-24	M1 (≥LL)	II. 253	73 (C) - Chp. 7
S.11-45	M1 (≥LL)	III.288	99 (C) - Chp. 7
S.11-63	M1 (≥LL)	IV. 421	163 (C) - Chps.7 & 8
S.11-T2	M1 (<LL)	V. 11	5 (T) - Chp. 5
S.11-50	M1 (<LL)	III.308	94 (C) - Chp. 6
S.11-11	M1 (<LL)	II. 216	47 (C) - Chp. 6
S.11-25	M1 (<LL)	II. 256	70 (C) - Chp. 6
S.11-43	M1 (<LL)	III.284	86 (C) - Chp. 6
S.11-48	M1 (<LL)	III.303	96 (C) - Chp. 6
S.11-62	M1 (<LL)	III.396	150 (C) - Chps.6 & 8
S.11-61	M1 (<LL)	IV. 416	154 (C) - Chps.6 & 8
S.11-51	M1 (<LL)	III.311	91 (C) - Chp. 6
S.11-26	M1 (<LL)	II. 256	68 (C) - Chp. 7
S.11-44	M1 (<LL)	III.286	87 (C) - Chp. 7
S.11-47	M1 (<LL)	III.301	97 (C) - Chp. 7
S.11-35	M2 (*)	II. 270	83 (C) - Chp. 6
S.11-52	M2 "	III.317	103 (C) - Chp. 6
S.11-36	M2 "	II. 272	81 (C) - Chp. 6
S.11-1	M2 "	I. 130	23 (C) - Chp. 6
S.11-4	M2 "	I. 133	30 (C) - Chp. 6
S.11-38	M2 "	II. 233	79 (C) - Chp. 6
S.11-54	M2 "	III.321	105 (C) - Chp. 6
S.11-57	M2 "	III.354	121 (C) - Chp. 6
S.11-58	M2 "	III.356	137 (C) - Chps.6 & 8
S.11-37	M2 "	II. 274	78 (C) - Chp. 6
S.11-55	M2 "	III.323	104 (C) - Chp. 6
S.11-39	M2 "	II. 237	77 (C) - Chp. 7
S.11-53	M2 "	III.319	102 (C) - Chp. 7
S.11-3	M2 "	I. 132	40 (C) - Chp. 7
S.11-2	M2 (*)	I. 131	37 (C) - Chp. 7

** - air bubbles.*

Sample No.	Method of preparation	Reference number	Consolidometer/Triaxial: Test No. - Chapter No.
<u>Site 11</u> [Compacted samples]			
S.11-8	CMod(II.162)	II. 192	31 (C) - Chp. 6
S.11-13	CMod(II.162)	II. 226	43 (C) - Chp. 6
S.11-14	CMod(II.162)	II. 239	48 (C) - Chp. 6
S.11-27	CMod(II.162)	II. 258	55 (C) - Chp. 6
S.11-70	CMod(IV.450)	IV. 458	168 (C) - Chps.6 & 8
S.11-9	CMod(II.162)	II. 224	42 (C) - Chp. 7
S.11-10	CMod(II.162)	II. 241	49 (C) - Chp. 7
S.11-28	CMod(II.162)	II. 260	56 (C) - Chp. 7
S.11-71	CStd(IV.450)	IV. 459	169 (C) - Chps.7 & 8
S.11-T4	CStd(IV.450)	IV. 459	15 (T) - Chp. 9
<u>Site 11</u> [Undisturbed samples]			
S.11-T5	U	V. 35	18 (T) - Chp. 5
S.11-6	U	II. 166	28 (C) - Chp. 6
S.11-12	U	II. 216	41 (C) - Chp. 6
S.11-15	U	II. 221	45 (C) - Chp. 6
S.11-17	U	II. 244	51 (C) - Chp. 6
S.11-19	U	II. 245	57 (C) - Chp. 6
S.11-22	U	II. 246	65 (C) - Chp. 6
S.11-7	U	II. 166	39 (C) - Chp. 7
S.11-18	U	II. 244	52 (C) - Chp. 7
S.11-20	U	II. 245	60 (C) - Chp. 7
S.11-21	U	II. 246	66 (C) - Chp. 7
S.11-31	U	II. 264	63 (C) - Chp. 7
S.11-29	U	II. 266	61 (C) - Chp. 7
S.11-30	U	II. 266	62 (C) - Chp. 7
S.11-T3	U	V. 28	14 (T) - Chp. 9
<u>Site 36 - Rondebosch, Cape</u> [Remoulded samples]			
S.36-14	M1 (≥LL)	IV. 452	172 (C) - Chp. 6
S.36-15	M1 (≥LL)	IV. 452	174 (C) - Chp. 6
S.36-3	M1 (≥LL)	III.331	110 (C) - Chp. 6
S.36-9	M1 (≥LL)	III.376	135 (C) - Chp. 6
S.36-2	M1 (≥LL)	III.329	111 (C) - Chp. 7
S.36-8	M1 (≥LL)	IV. 374	132 (C) - Chp. 7
S.36-T1	M1 (<LL)	V. 5	2 (T) - Chp. 5
S.36-13	M1 (<LL)	IV. 452	170 (C) - Chp. 6
S.36-10	M1 (<LL)	III.378	136 (C) - Chp. 6
S.36-5	M1 (<LL)	III.348	129 (C) - Chps.6 & 8
S.36-12	M1 (<LL)	III.382	147 (C) - Chps.6 & 8
S.36-4	M1 (<LL)	III.346	114 (C) - Chp. 7
S.36-11	M1 (<LL)	III.380	133 (C) - Chp. 7
S.36-7	M2 (*)	III.360	125 (C) - Chp. 6
S.36-6	M2 (*)	III.358	126 (C) - Chp. 7

** - air bubbles.*

Site 11, Rosebank.

Previously defined as a fine silty clay, with only a small amount of fine sand. The soil consists of 59% clay, 29% silt, and 12% of sand size. The consistency limits are as follows: Linear Shrinkage 'w_{Ls}' = 11.4%; Liquid Limit 'w_L' = 69.0%; Plastic Limit 'w_P' = 30.7%; Plasticity Index 'I_P' = 38; and, Shrinkage Limit 'w_S' = 22.5%.

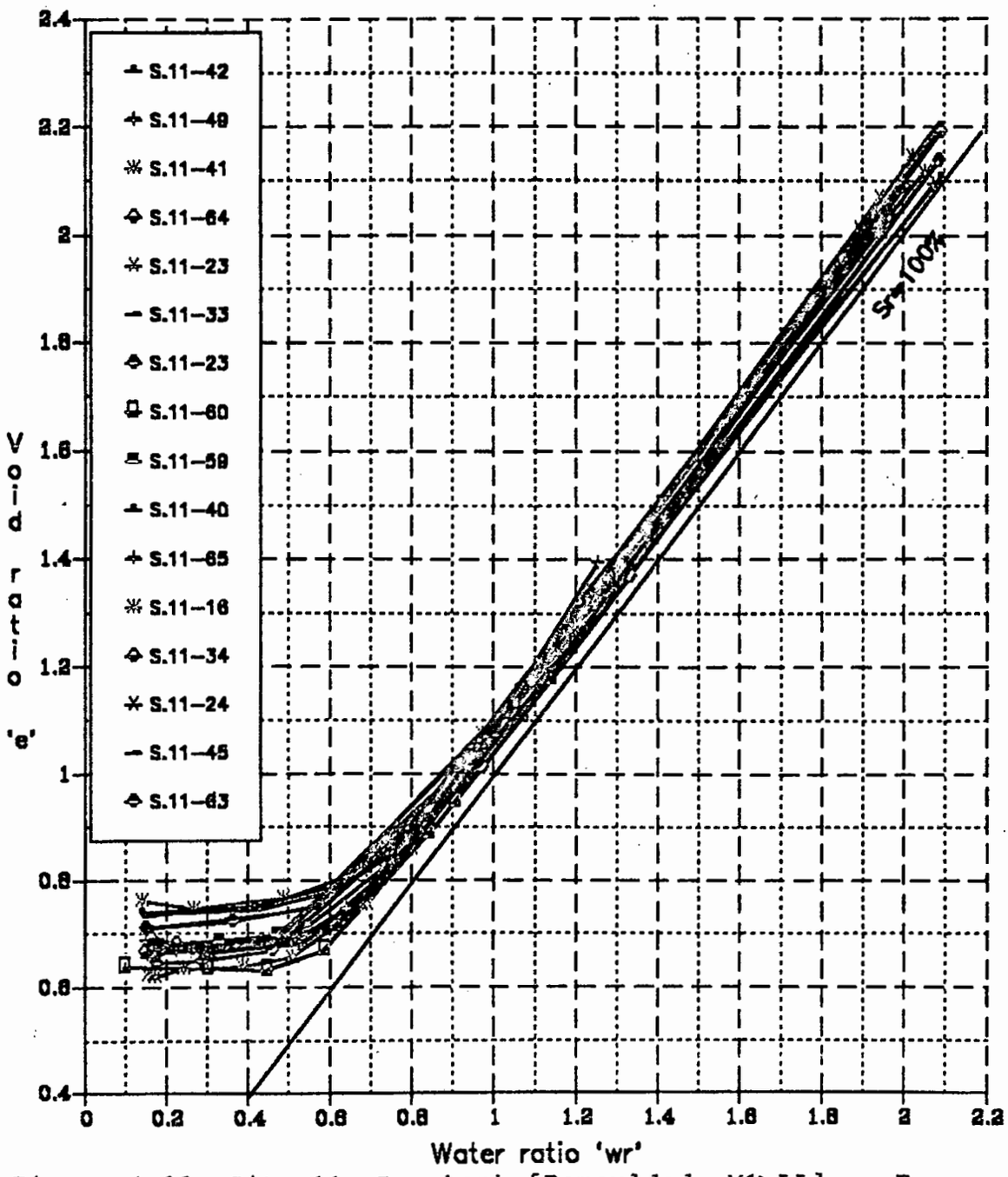

Figure 4.03: Site 11, Rosebank [Remoulded, M1≥LL] - Free Shrinkage Paths.

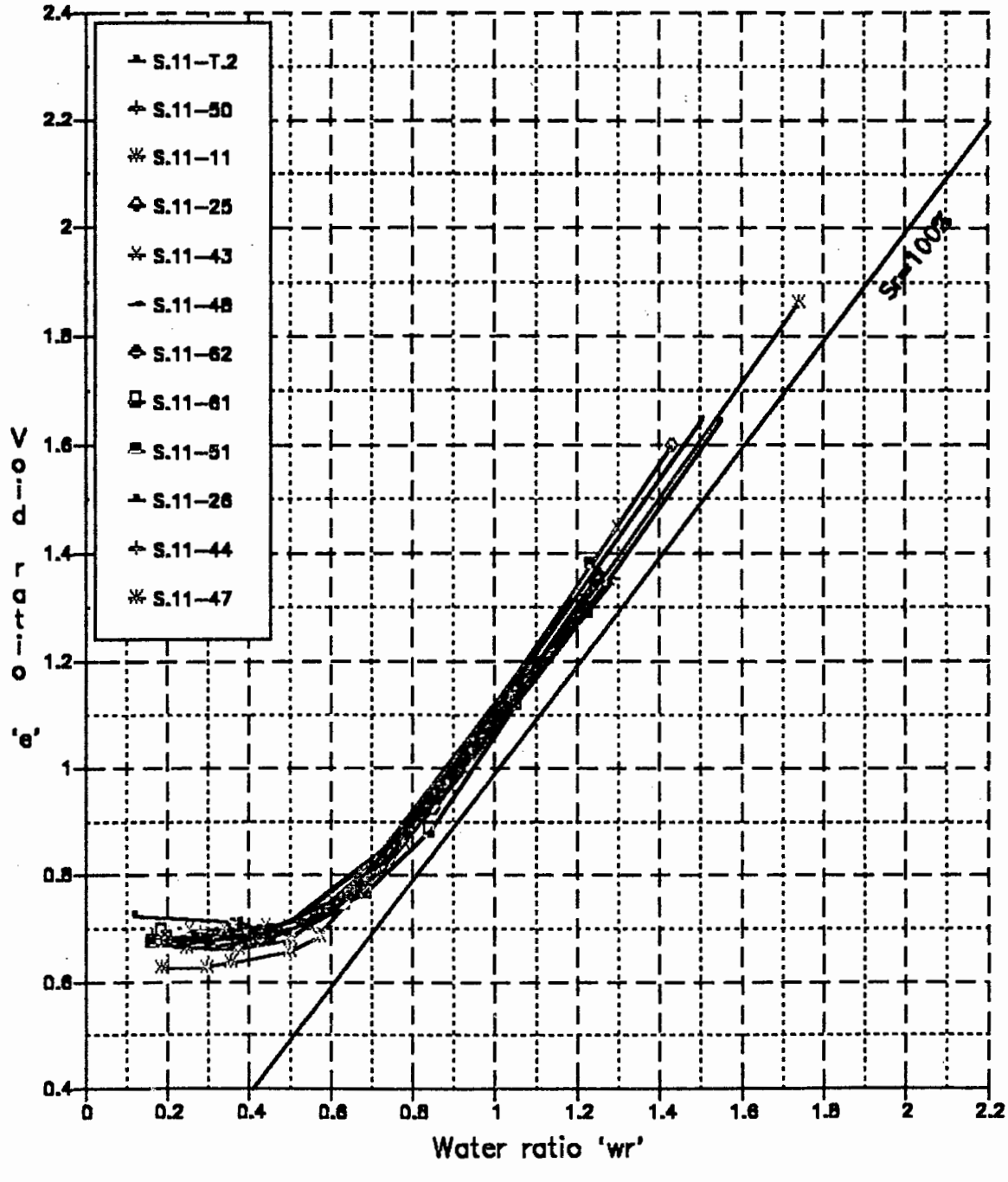

Figure 4.05: Site 11, Rosebank [Remoulded, M1<LL] - Free Shrinkage Paths.

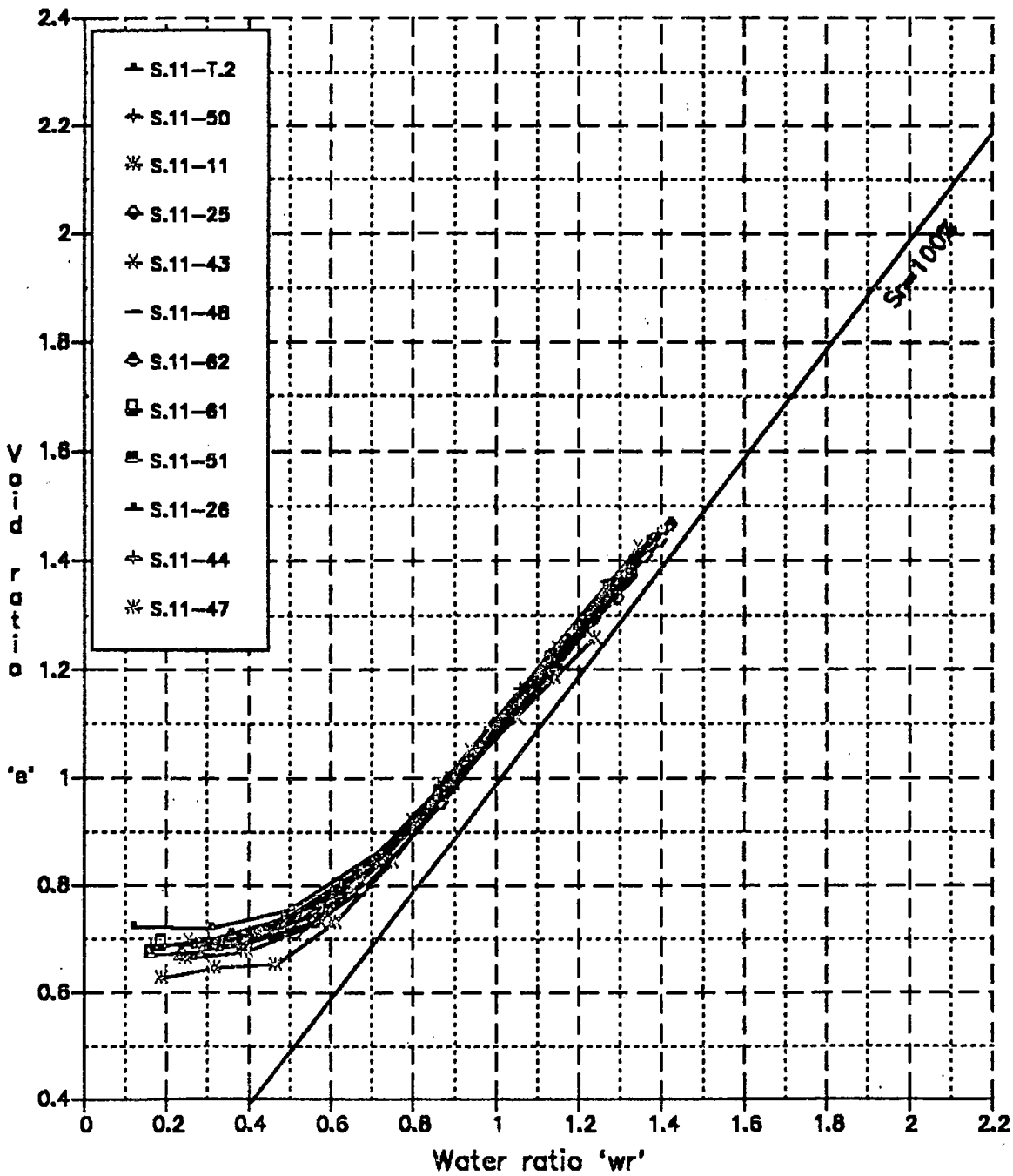

Figure 4.06: Site 11, Rosebank [Remoulded, M1<LL] - Free Swell Paths. (After shrinking to points on Figure 4.05).

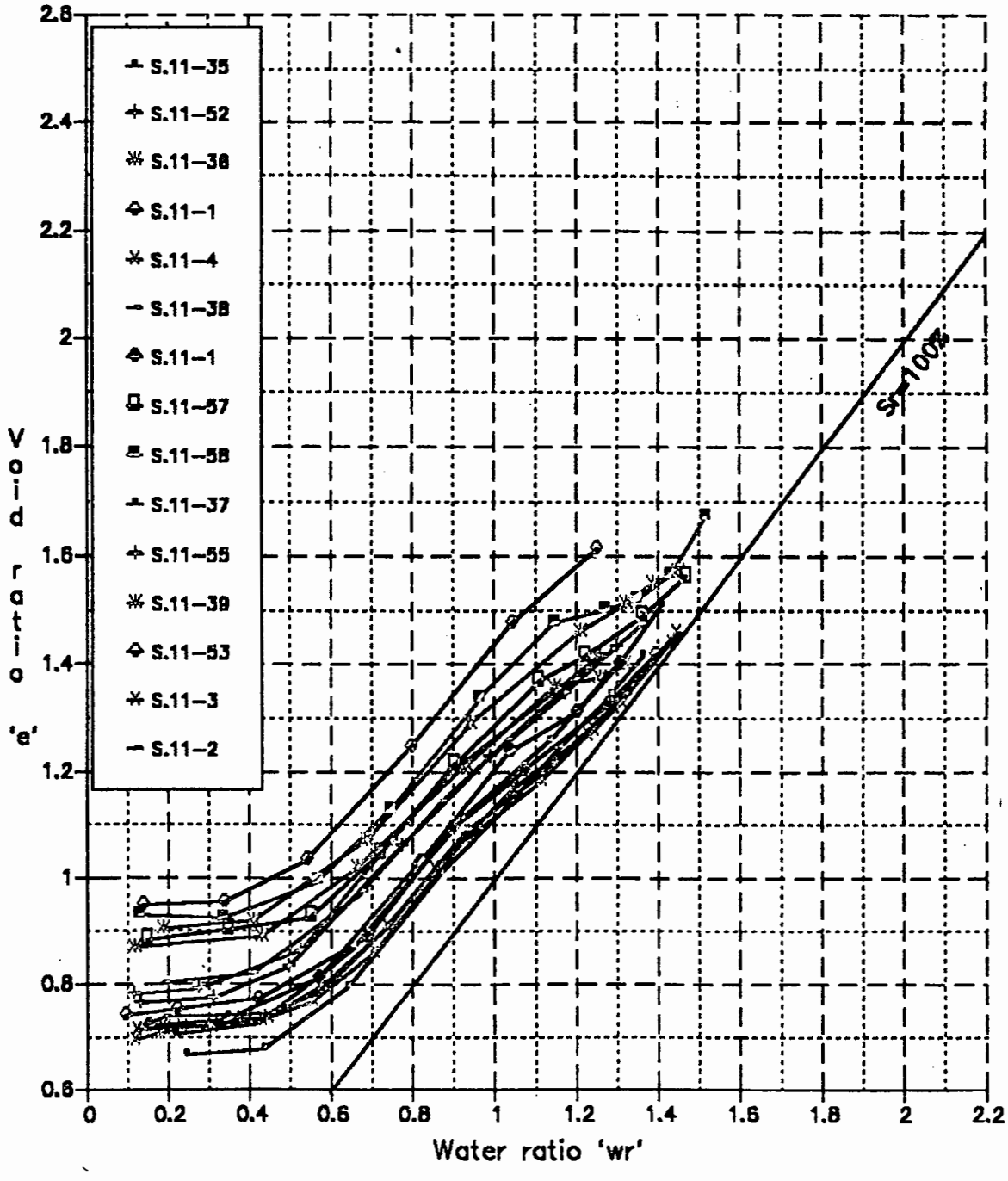

Figure 4.08: Site 11, Rosebank [Remoulded, M2] - Free Swell Paths. (After shrinking to points on Figure 4.07).

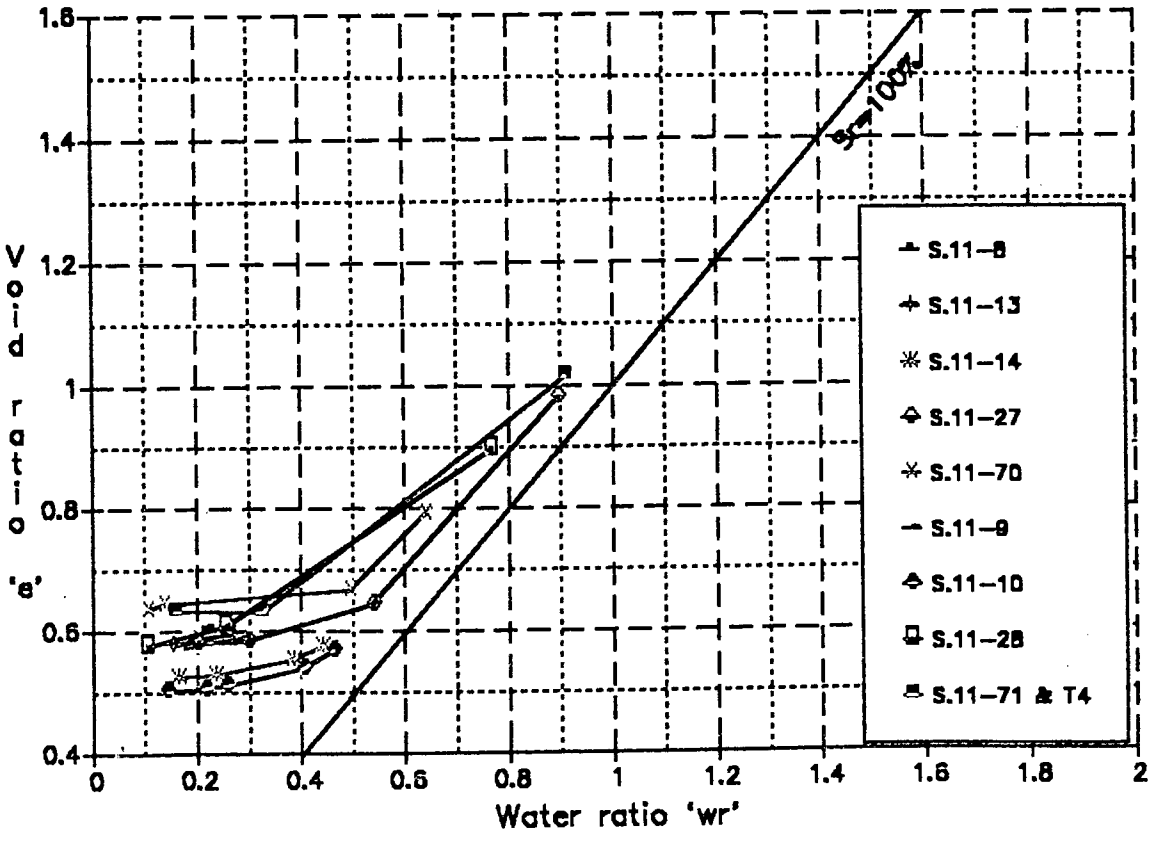

Figure 4.09: Site 11, Rosebank [Compacted] - Free Shrinkage Paths.

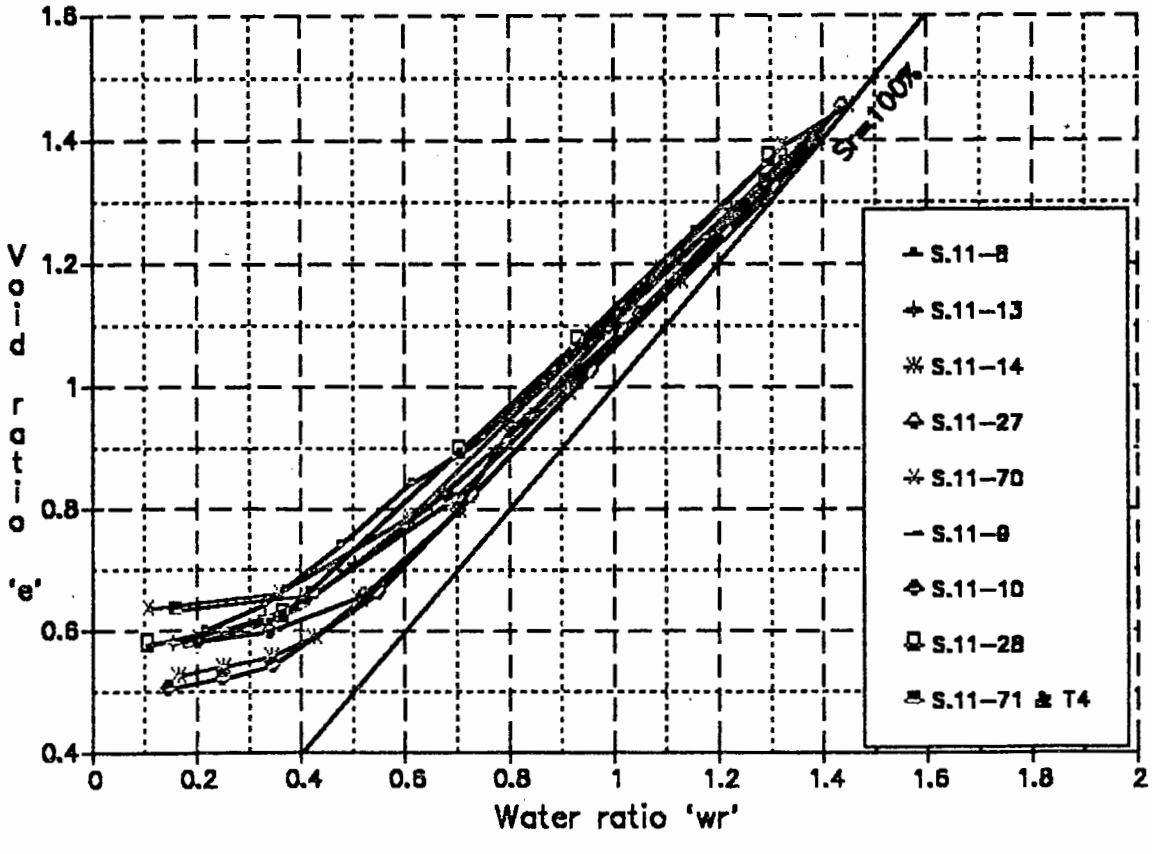

Figure 4.10: Site 11, Rosebank [Compacted] - Free Swell Paths. (After shrinking to points on Figure 4.09).

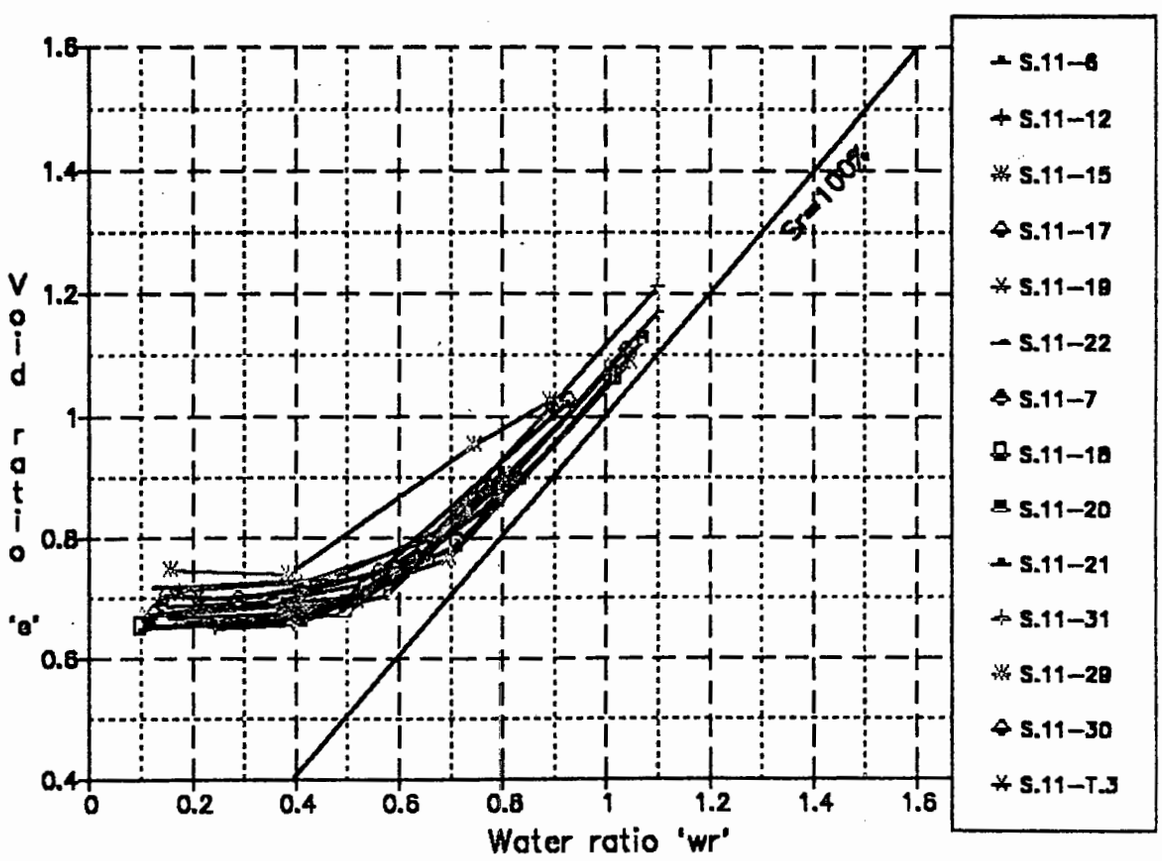

Figure 4.11: Site 11, Rosebank [Undisturbed] - Free Shrinkage Paths.

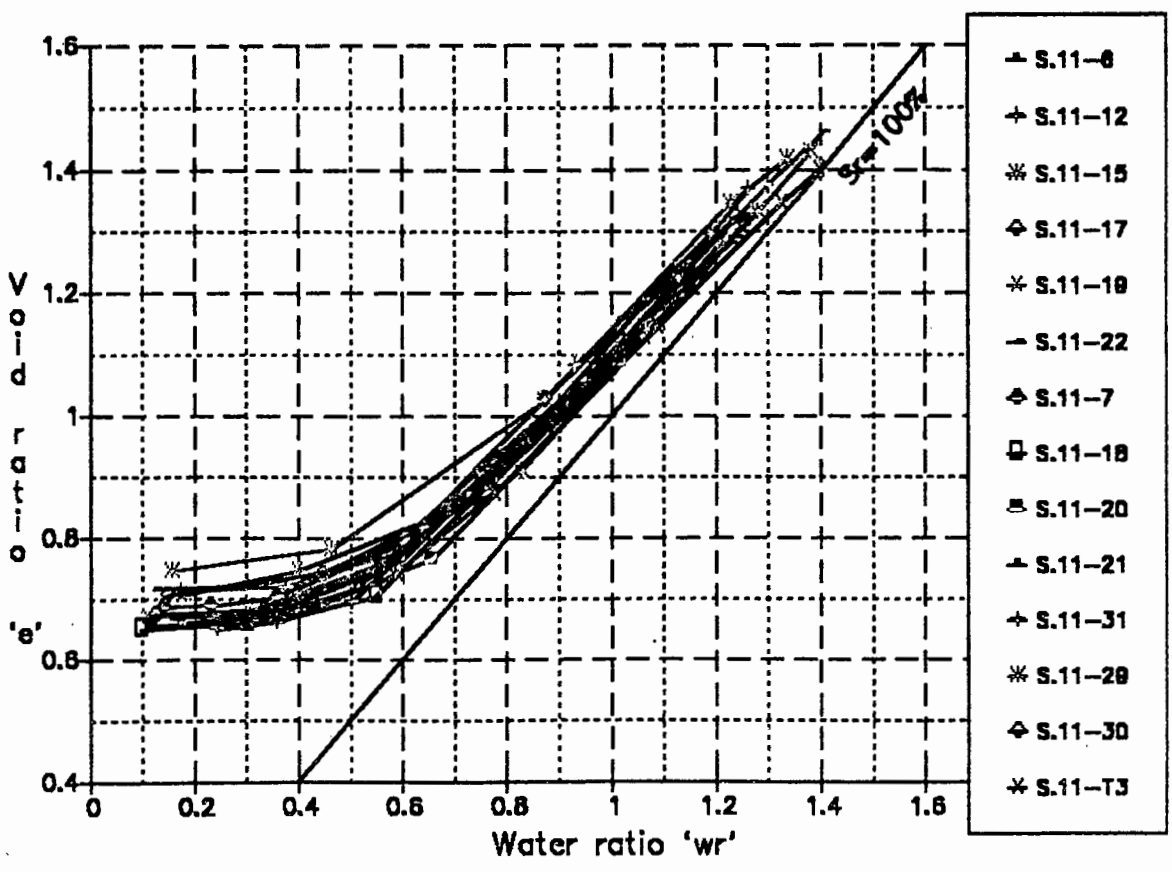

Figure 4.12: Site 11, Rosebank [Undisturbed] - Free Swell Paths. (After shrinking to points on Figure 4.11).

Site 36, Rondebosch.

A clayey silt, with fine sand and a small amount of medium sand. The soil consists of 22% clay, 49% silt, and 29% of sand size. The consistency limits are as follows: w_{Ls} = 8.3%; w_L = 47.0%; w_P = 23.3%; I_P = 24; and w_S = 22.0%.

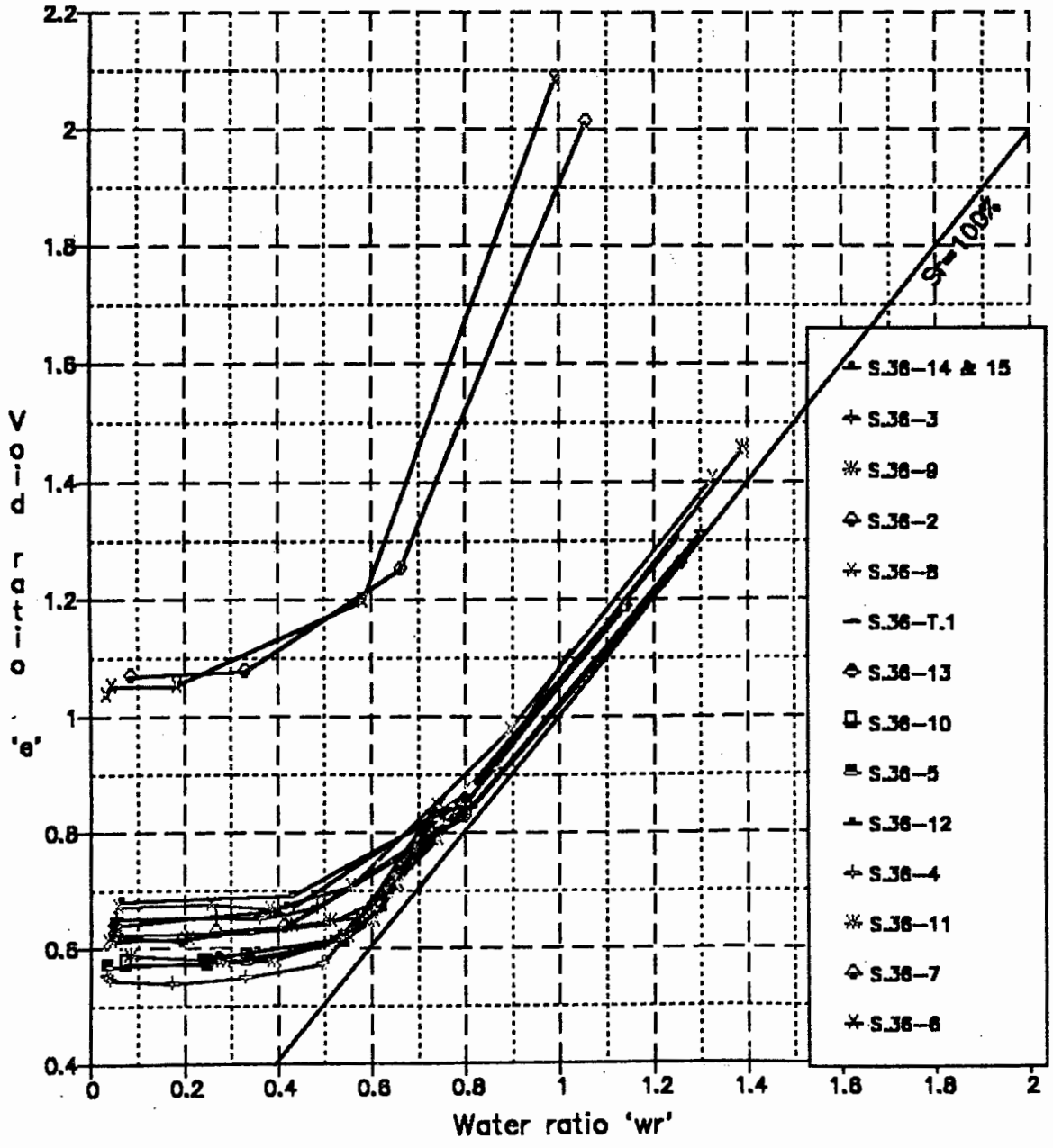

Figure 4.13: Site 36, Rondebosch [Remoulded] - Free Shrinkage Paths.

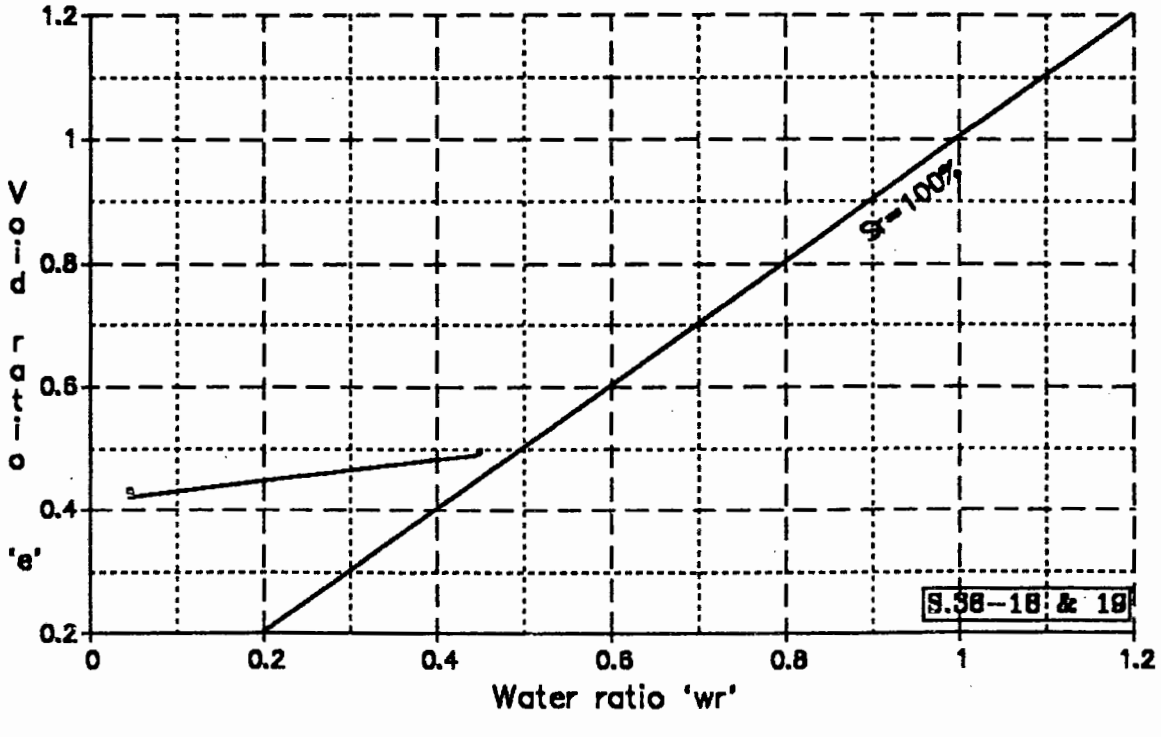

Figure 4.15: Site 36, Rondebosch [Compacted] - Free Shrinkage Paths.

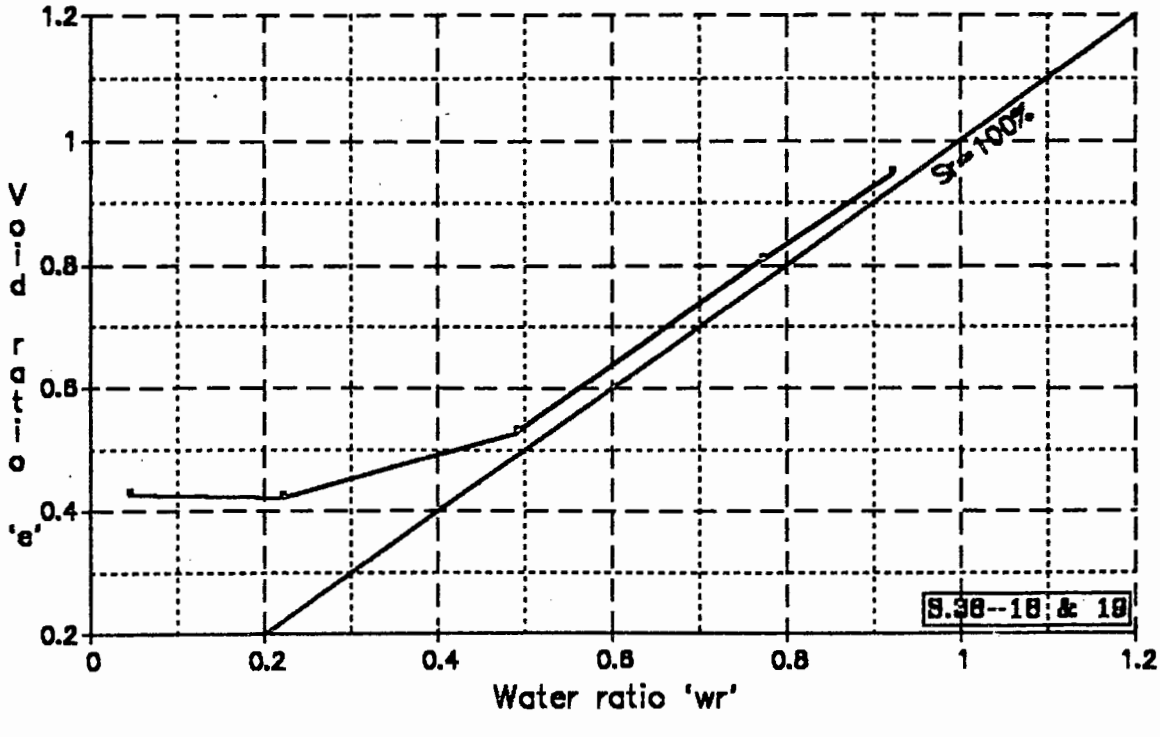

Figure 4.16: Site 36, Rondebosch [Compacted] - Free Swell Paths. (After shrinking to points on Figure 4.15).

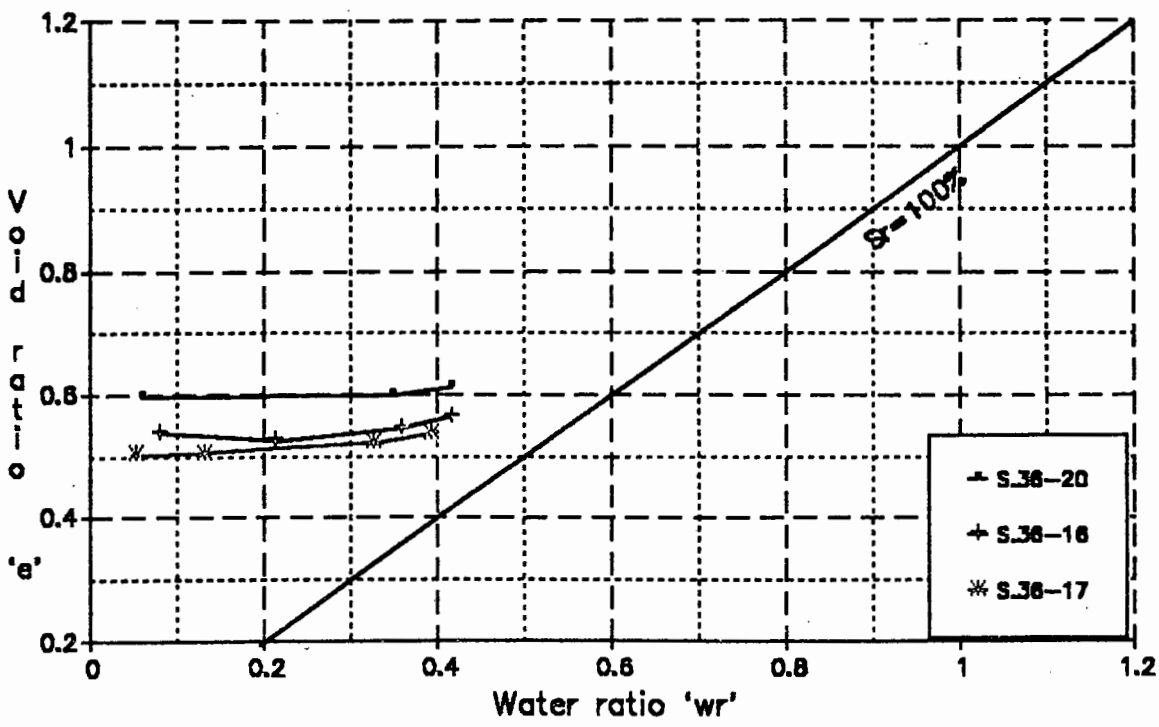

Figure 4.17: Site 36, Rondebosch [Undisturbed] - Free Shrinkage Paths.

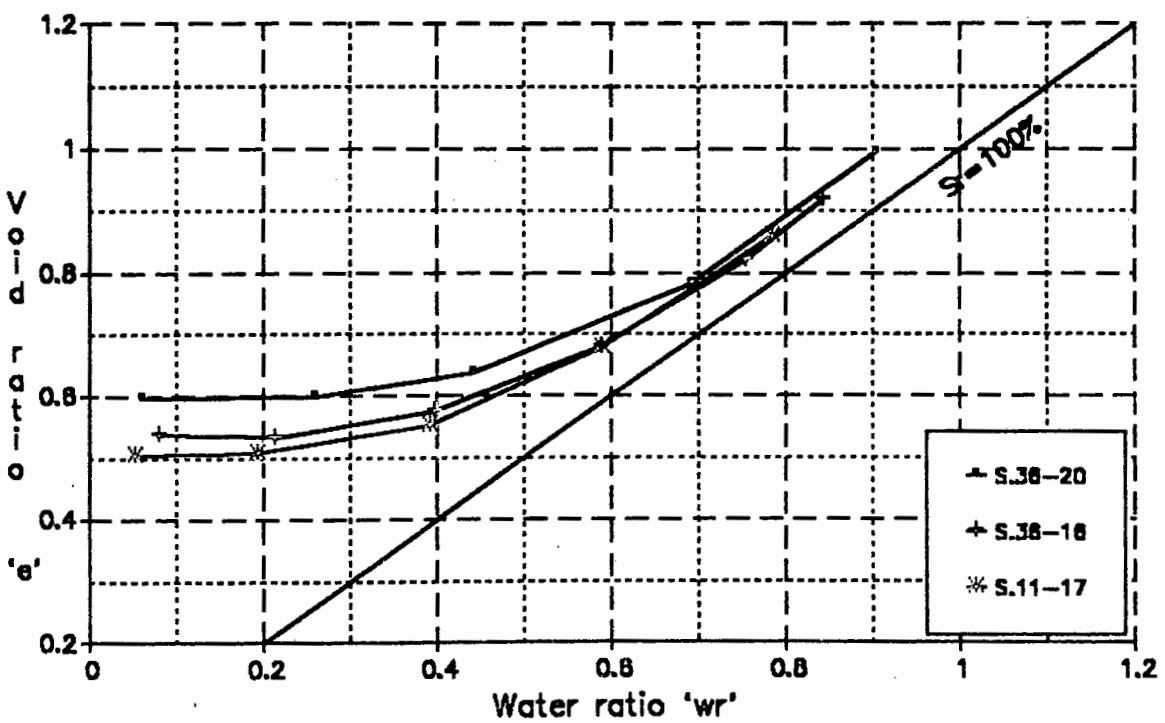

Figure 4.18: Site 36, Rondebosch [Undisturbed] - Free Swell Paths. (After shrinking to points on Figure 4.17).

Site 30, Hout Bay.

A fine to medium sandy silt, with a small amount of coarse sand. The soil consists of 23% clay, 34% silt, and 43% of sand size. The consistency limits are: w_{LS} = 6.4%; w_L = 49.0%; w_P = 29.0%; I_P = 20; and, w_S = 22.5%.

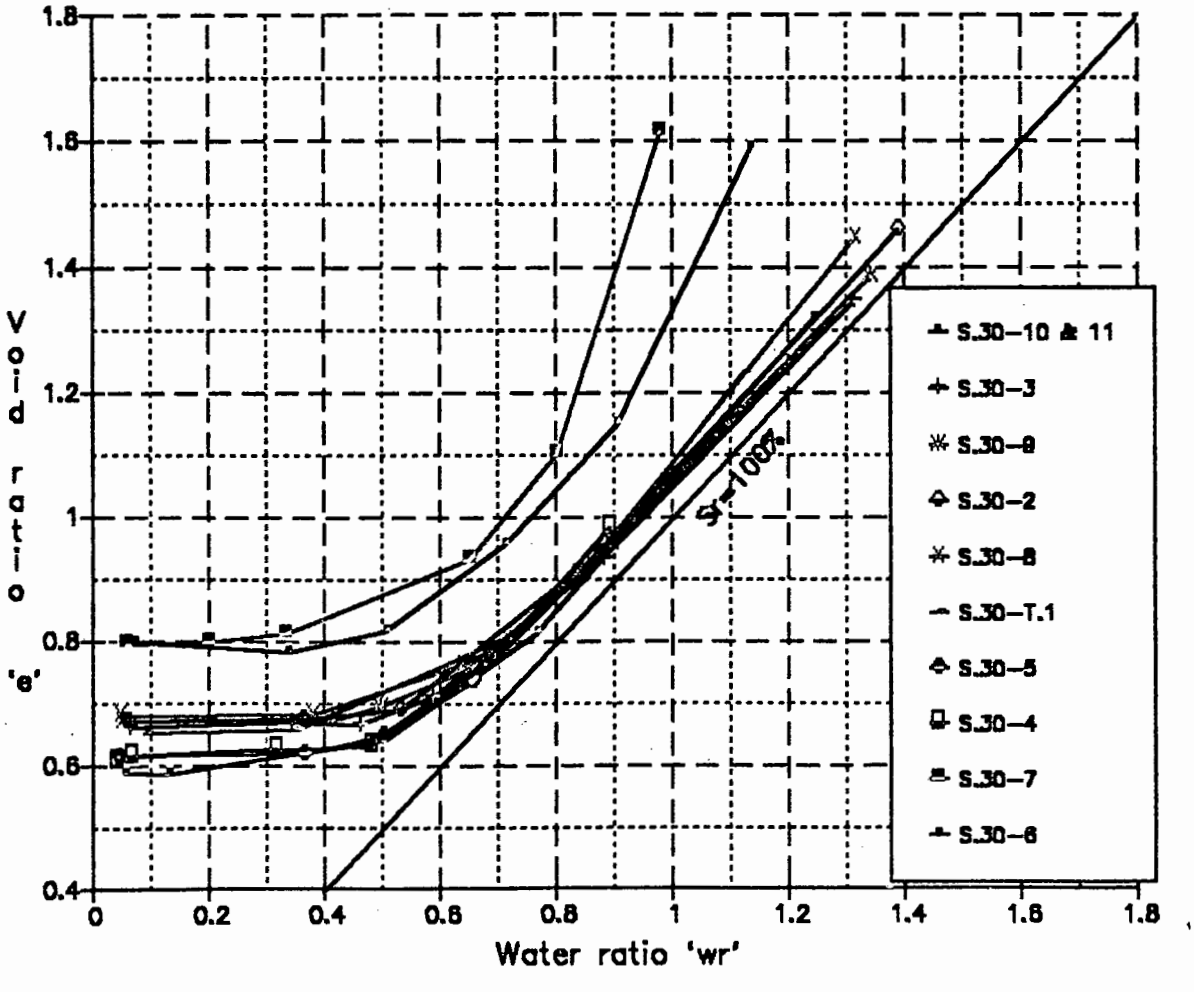

Figure 4.19: Site 30, Hout Bay [Remoulded] - Free Shrinkage Paths.

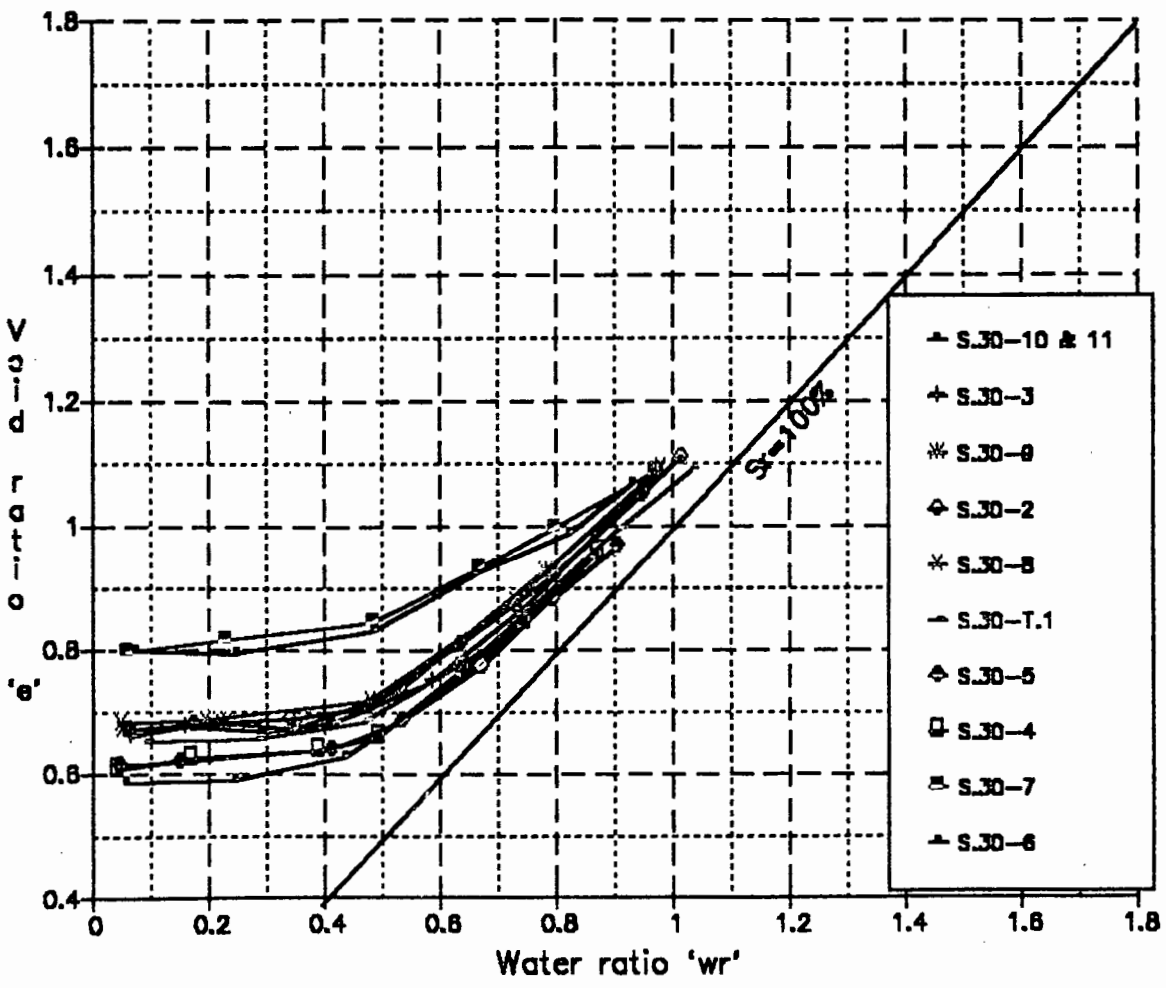

Figure 4.20: Site 30, Hout Bay [Remoulded] - Free Swell Paths. (After shrinking to points on Figure 4.19).

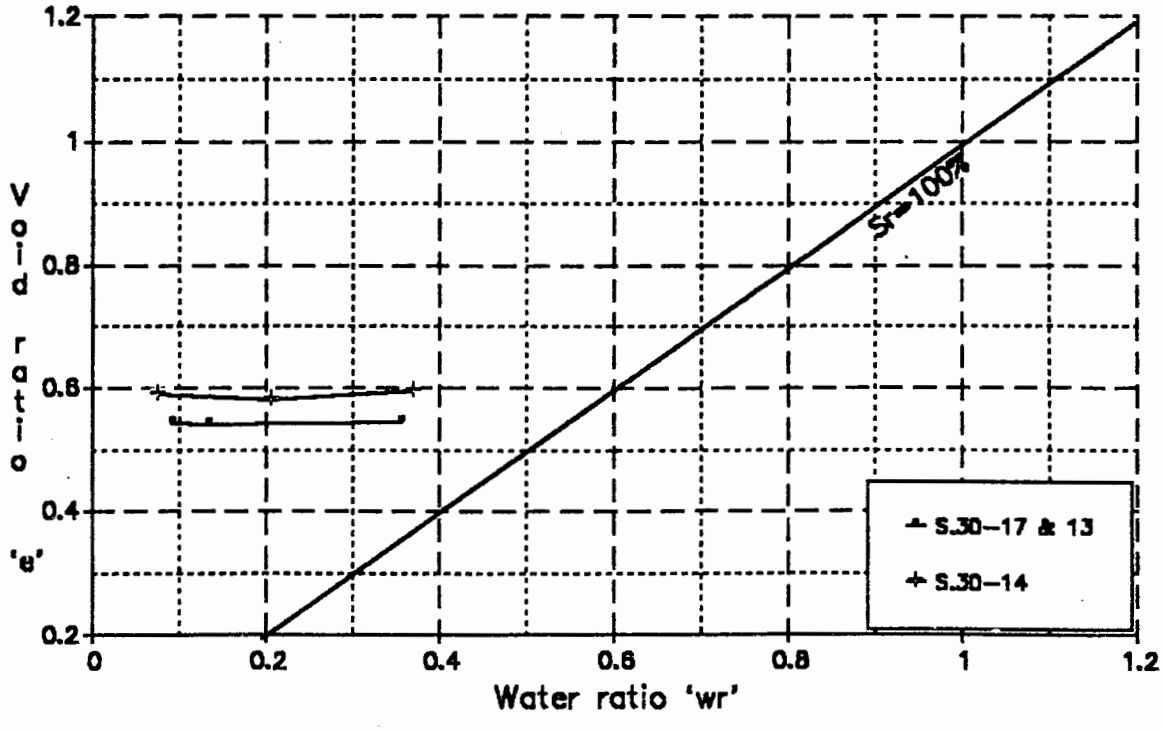

Figure 4.21: Site 30, Hout Bay [Undisturbed] - Free Shrinkage Paths.

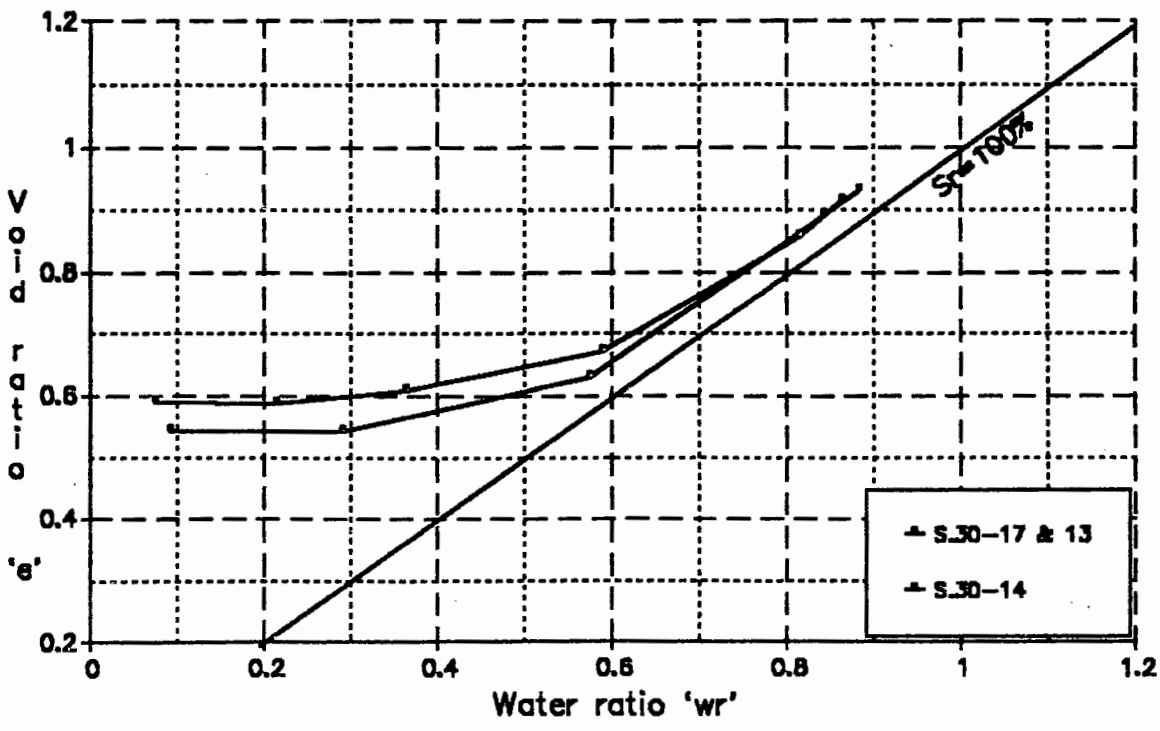

Figure 4.22: Site 30, Hout Bay [Undisturbed] - Free Swell Paths. (After shrinking to points on Figure 4.21).

Site A, Berea Road (Durban).

A clayey sand (fine to medium size) with a small amount of silt. The soil consists of 15% clay, 10% silt, and 75% of sand size. The consistency limits are: w_{Ls} = 3.7%; w_L = 25.0%; w_P = 13.1%; I_P = 12; and w_S = 13,5%.

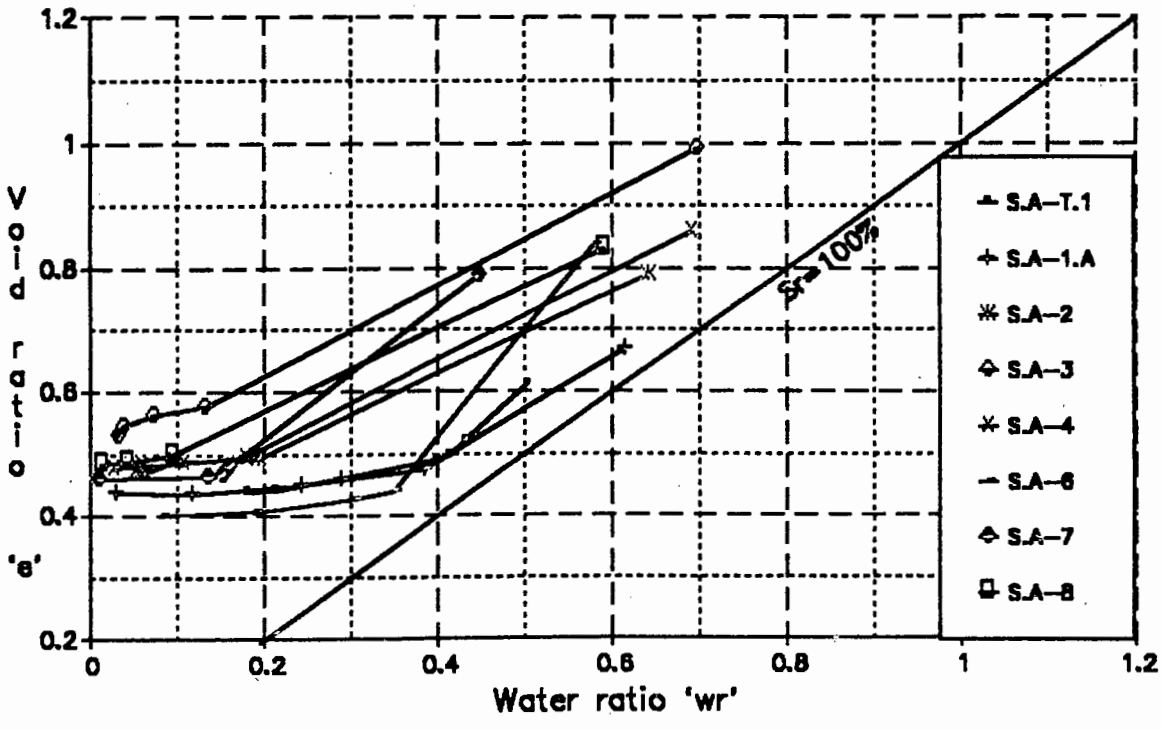

Figure 4.23: Site A, Berea Road (Durban) [Remoulded] - Free Shrinkage Paths.

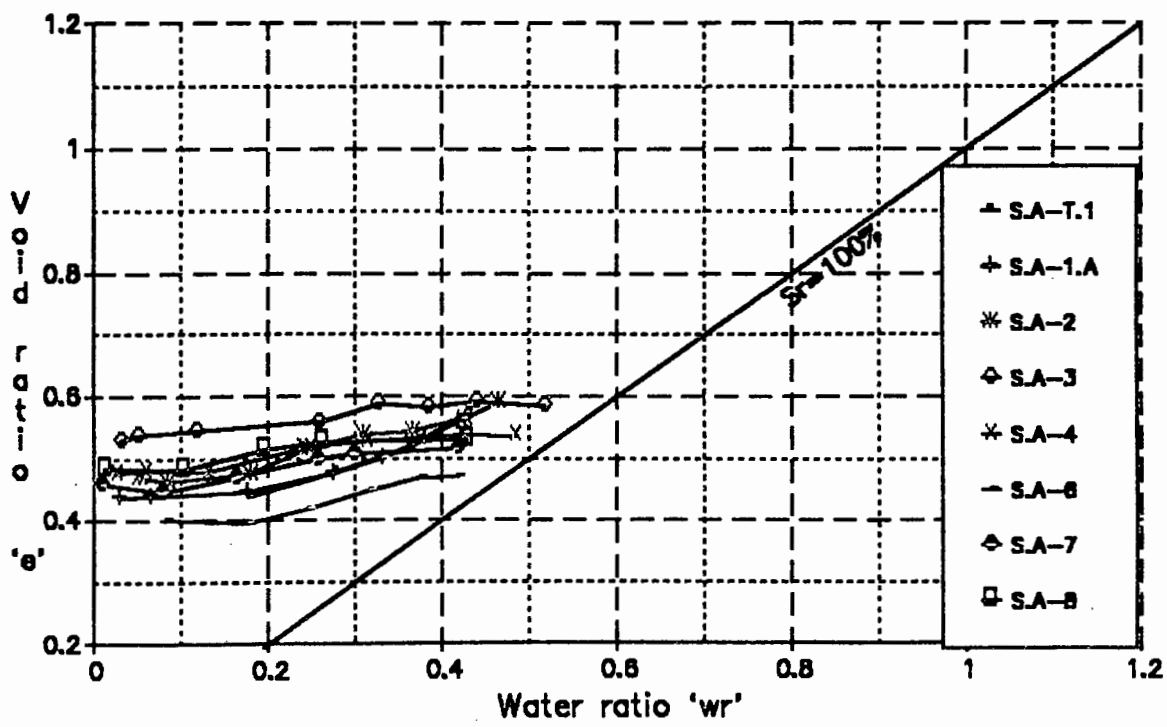

Figure 4.24: Site A, Berea Road (Durban) [Remoulded] - Free Swell Paths. (After shrinking to points on Figure 4.23).

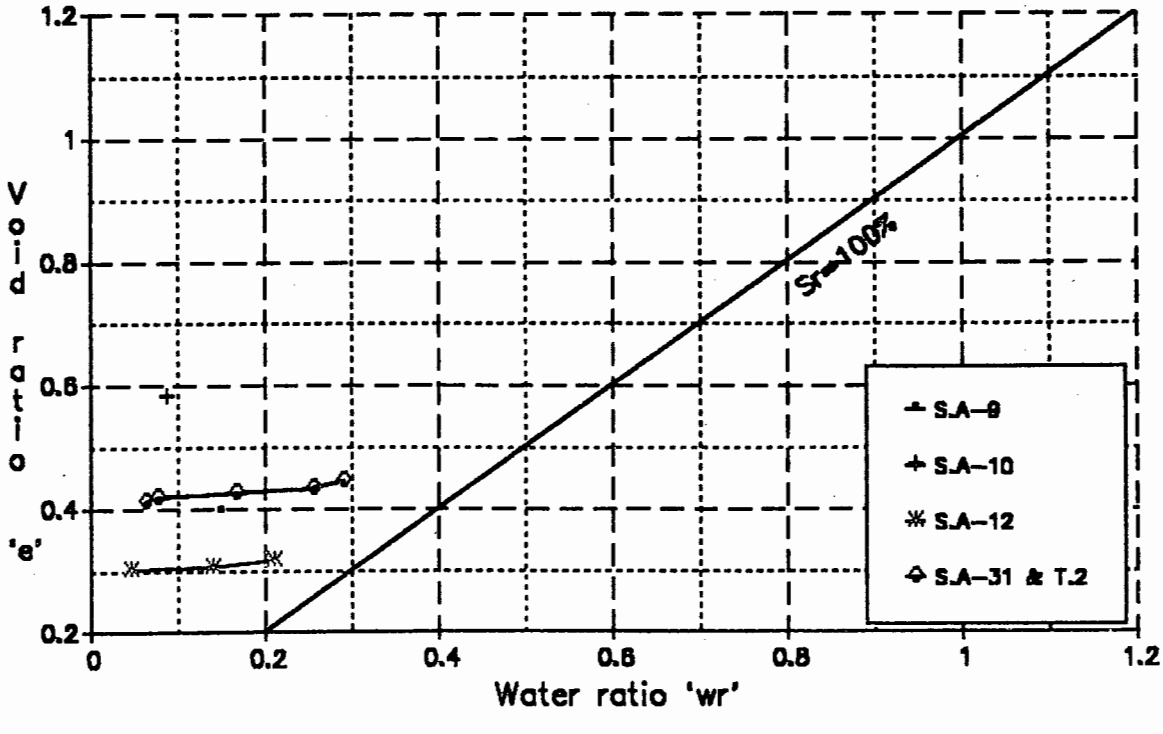

Figure 4.25: Site A, Berea Road (Durban) [Compacted] - Free Shrinkage Paths.

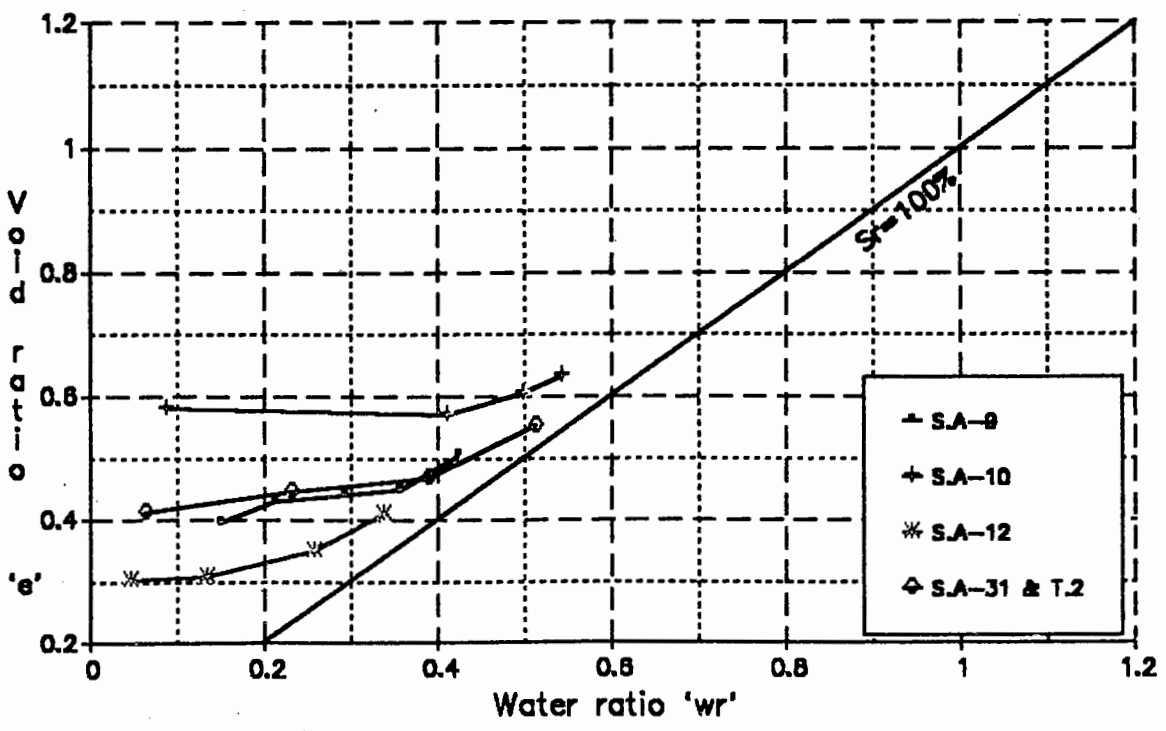

Figure 4.26: Site A, Berea Road (Durban) [Compacted] - Free Swell Paths. (After shrinking to points on Figure 4.25).

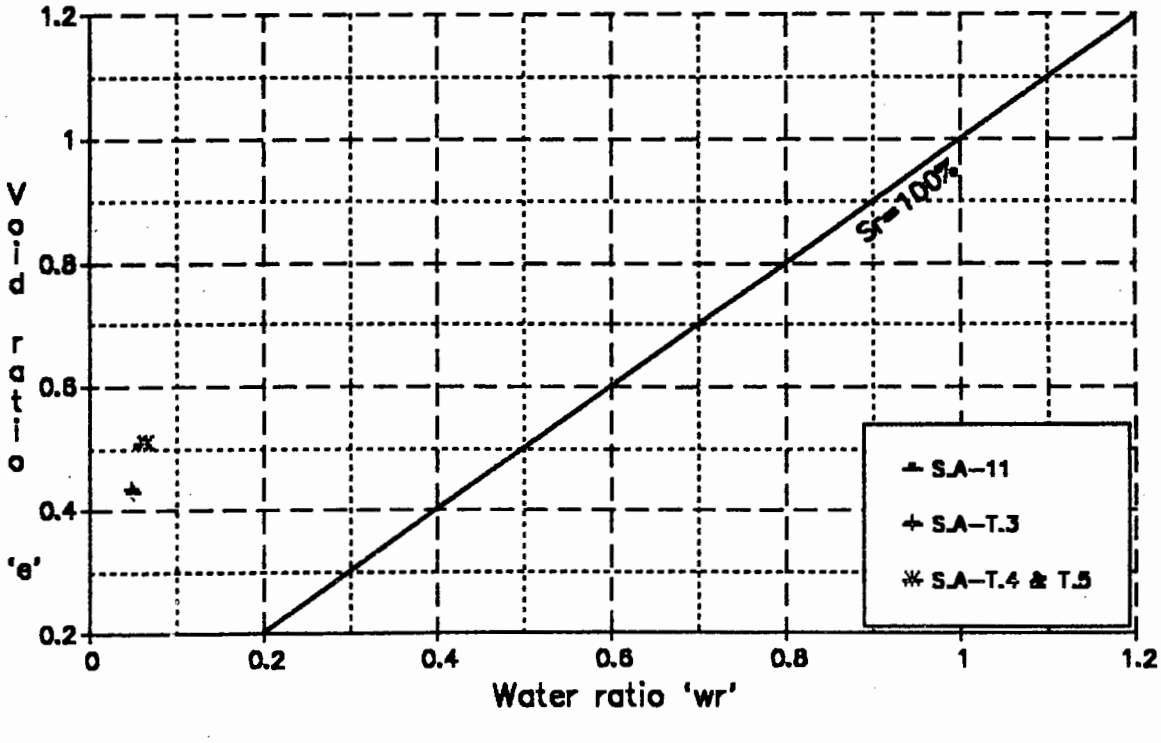

Figure 4.27: Site A, Berea Road (Durban) [Undisturbed] - Free Shrinkage Paths[1].

[1] - *Samples probably air-dry before shrinkage.*

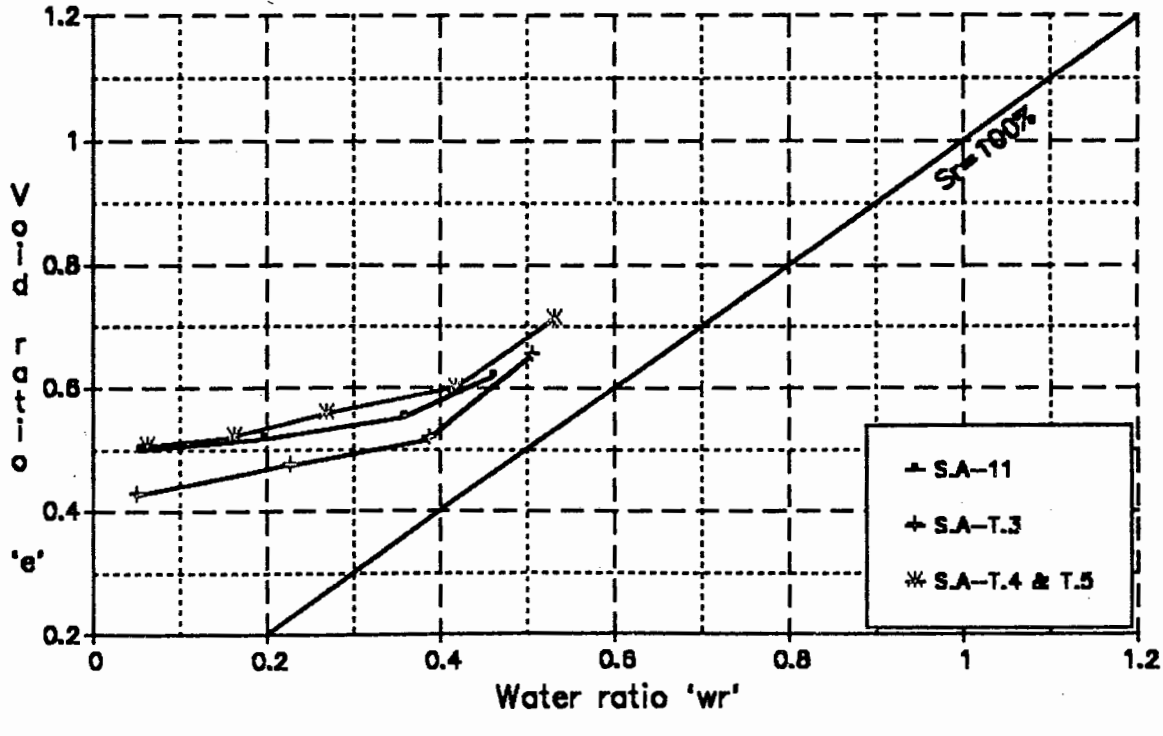

Figure 4.28: Site A, Berea Road (Durban) [Undisturbed] - Free Swell Paths. (Starts from points on Figure 4.27).

Site 7, Mowbray.

A fine silty clay, with a small amount of fine to medium sand. The soil consists of 42% clay, 37% silt, and 21% of sand size. The consistency limits are: w_{LS} = 10.5%; w_L = 47.0%; w_P = 22.0%; I_P = 25; and, w_S = 18.5%.

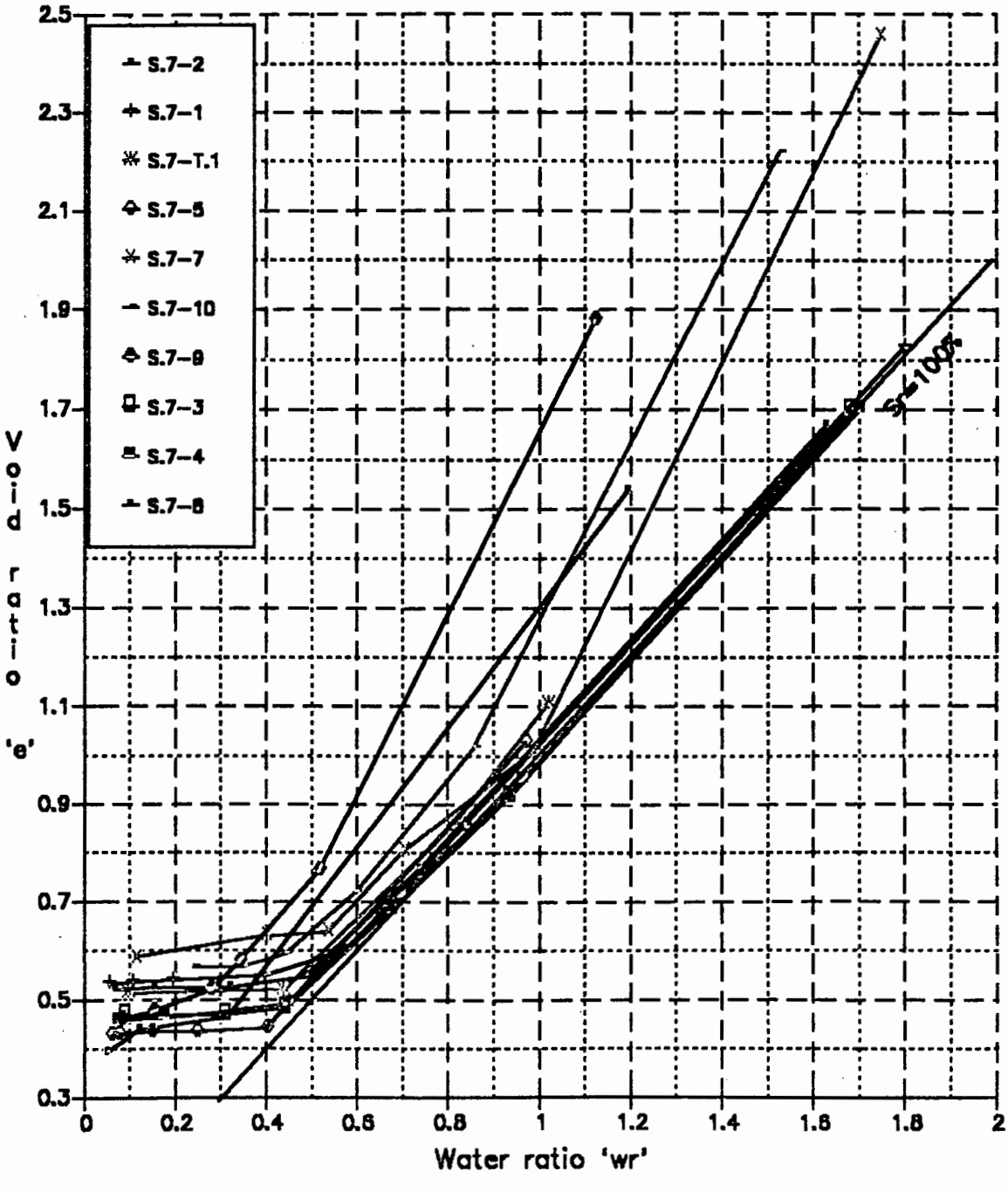

Figure 4.29: Site 7, Mowbray [Remoulded] - Free Shrinkage Paths.

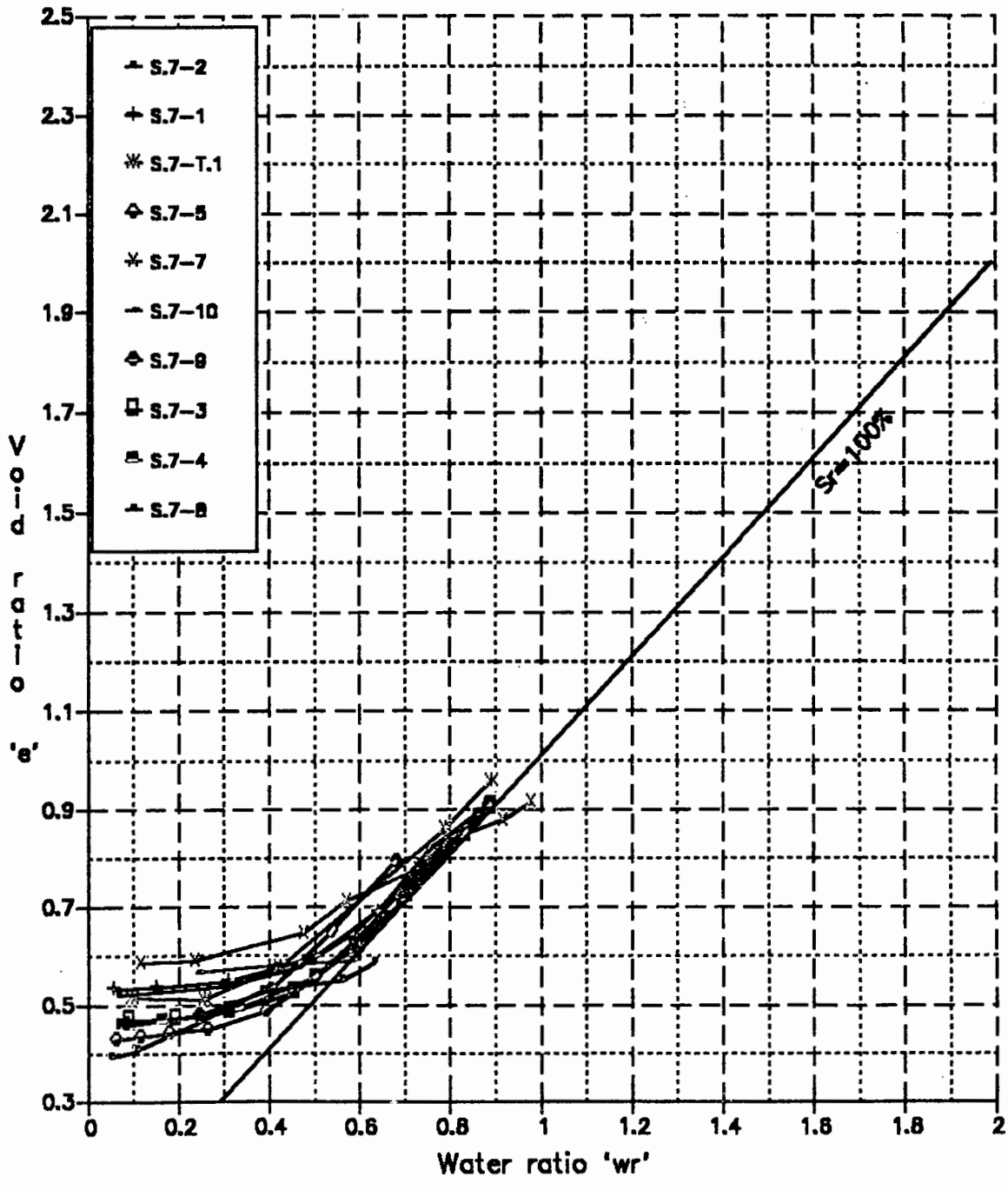

Figure 4.30: Site 7, Mowbray [Remoulded] - Free Swell Paths. (After shrinking as shown on Figure 4.29).

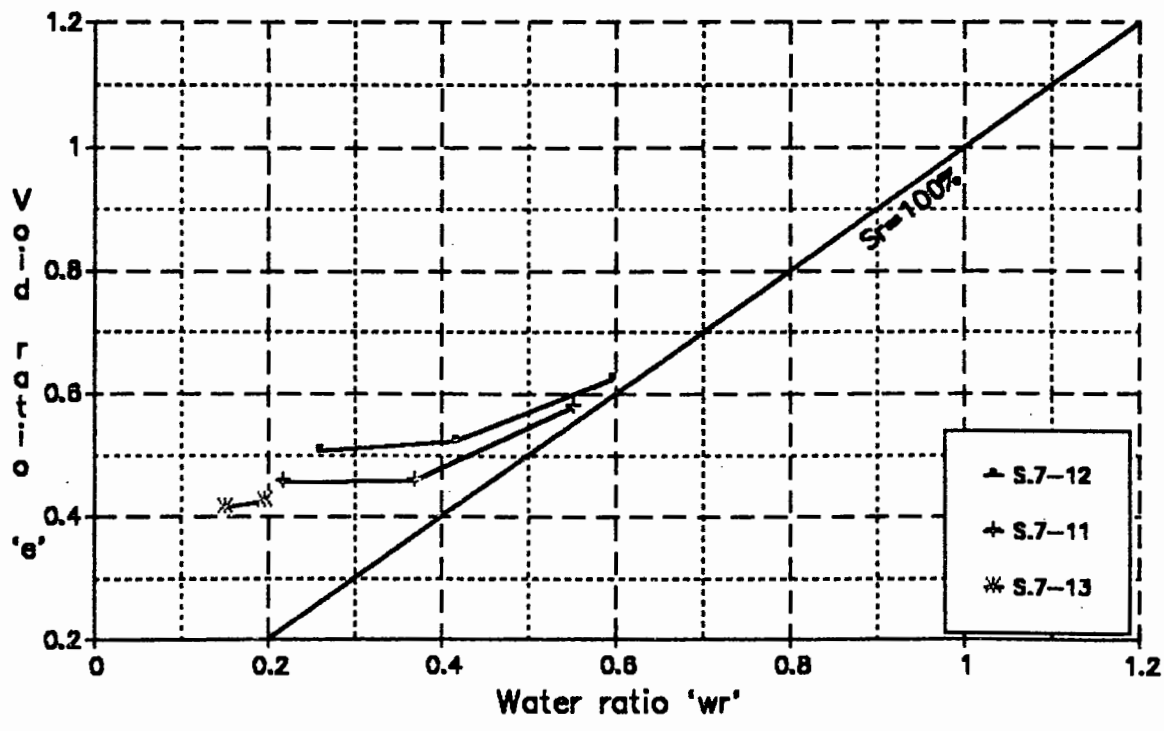

Figure 4.31: Site 7, Mowbray [Compacted and Undisturbed] - Free Shrinkage Paths.

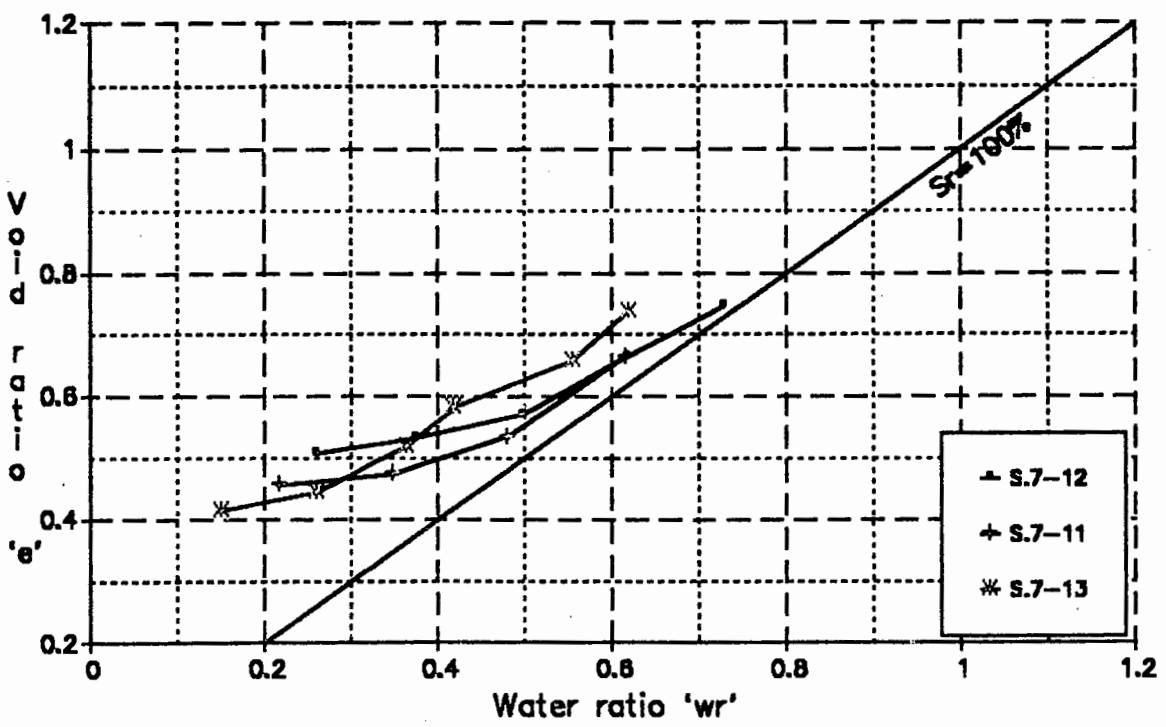

Figure 4.32: Site 7, Mowbray [Compacted and Undisturbed] - Free Swell Paths. (After shrinking to points on Figure 4.31).

Site B, Francois Road (Durban).

A fine to medium sand containing small amounts of clay and silt. The soil consists of 7,5% clay, 7% silt, and 85.5% of sand size. The consistency limits are: w_{LS} = 0.5%; w_L = 15.0%; w_P = 12.9%; I_P = 2; and, w_S = 11.0%.

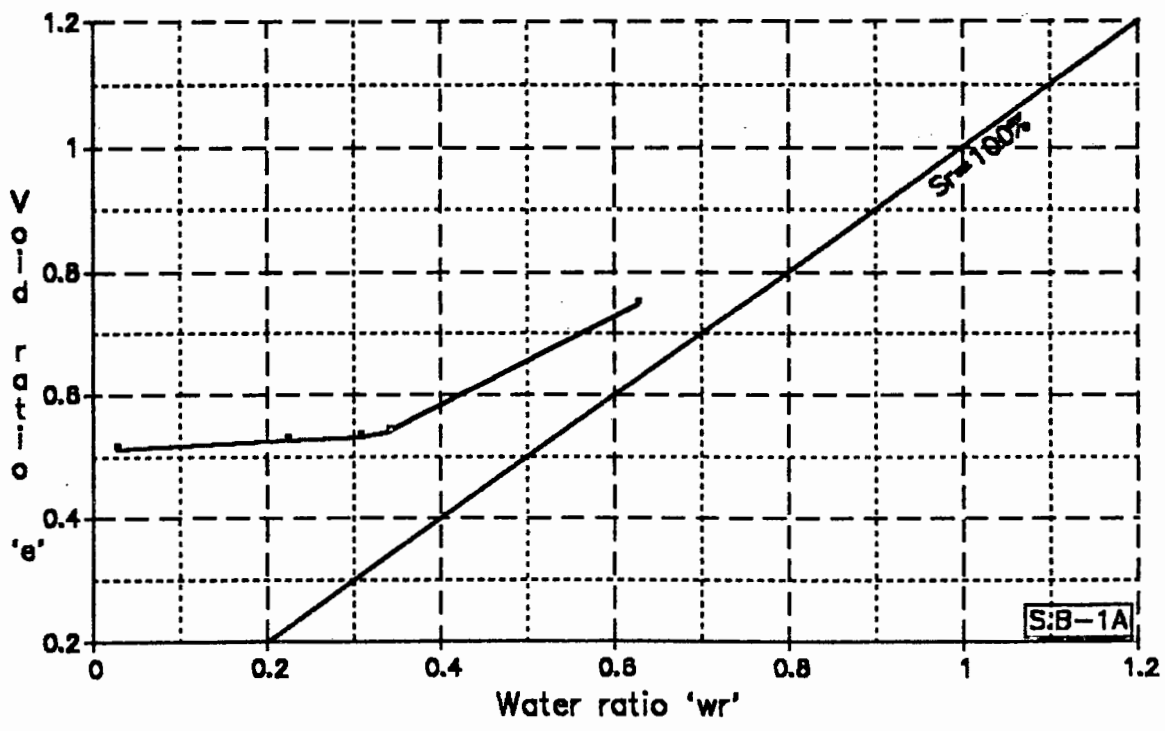

Figure 4.33: Site B, Francois Road (Durban) [Remoulded] - Free Shrinkage Paths.

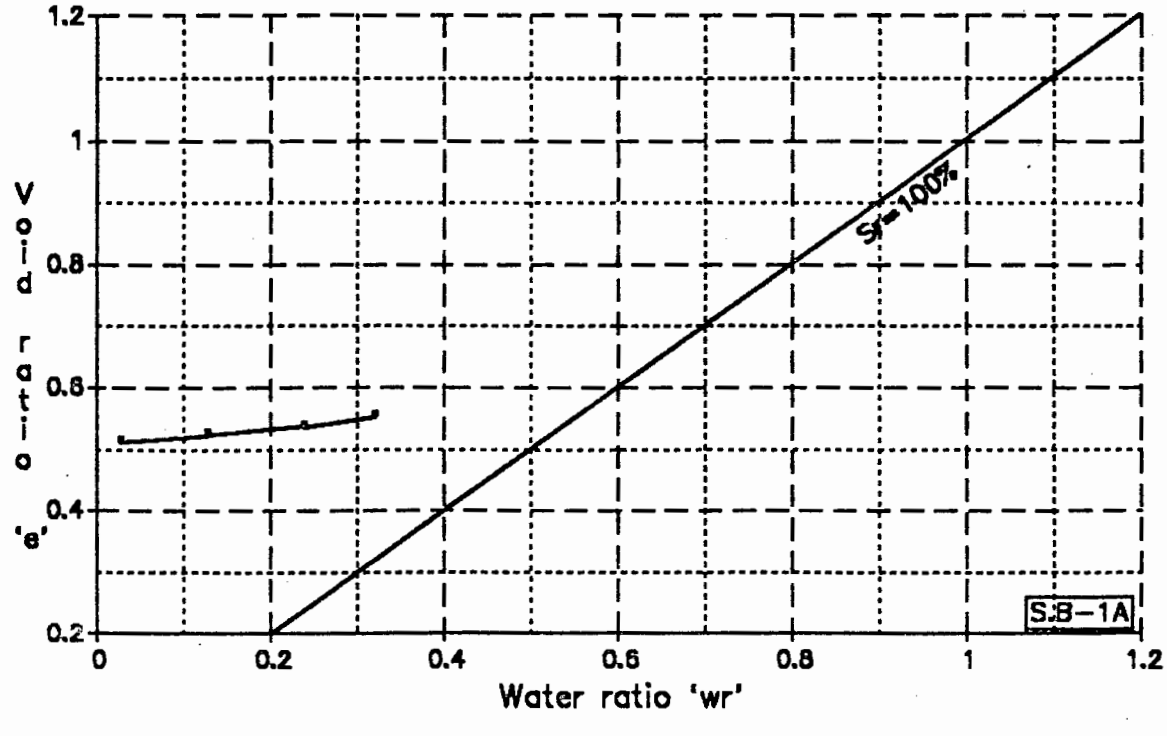

Figure 4.34: Site B, Francois Road (Durban) [Remoulded] - Free Swell Paths. (After shrinking to points on Figure 4.33).

Site C, Margaret Mayton Avenue (Durban).

A clayey sand (fine to medium size) with a very small amount of silt. The soil consists of 12.5% clay, 4% silt, and 83.5% of sand size. The consistency limits are: w_{Ls} = 1.8%; w_L = 19.7%; w_P = 15.9%; I_P = 4; and, w_S = 8.5%.

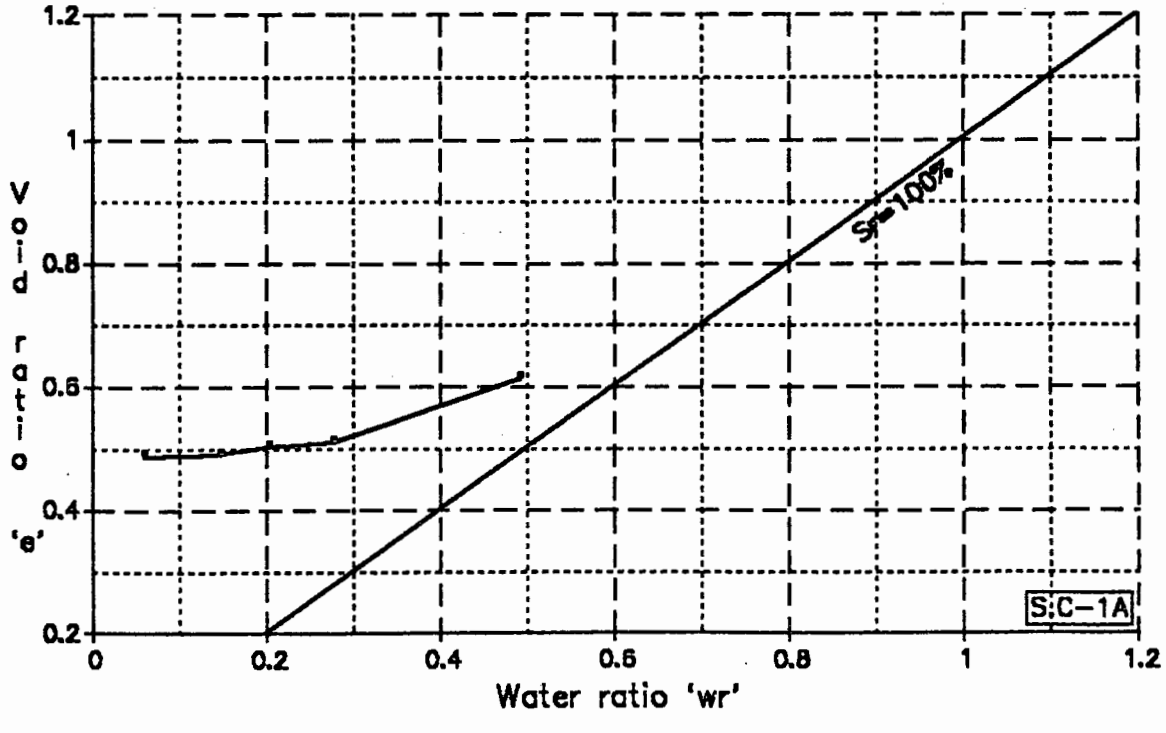

Figure 4.35: Site C, Margaret Mayton Avenue (Durban) [Remoulded] - Free Shrinkage Paths.

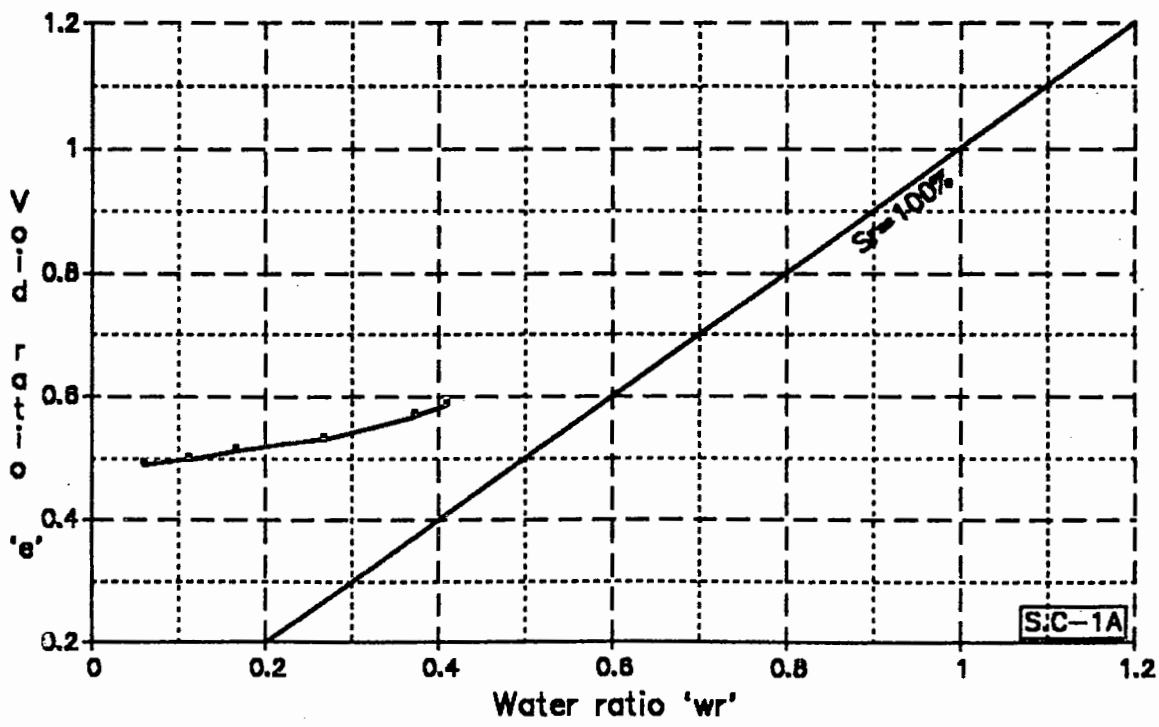

Figure 4.36: Site C, Margaret Mayton Avenue (Durban) [Remoulded] - Free Swell Paths. (After shrinking to points on Figure 4.35).

Site D, Rose Hill (Durban).

A clayey sand (fine to medium size) with a very small amount of silt. The soil consists of 15.5% clay, 4.5% silt, and 80% of sand size. The consistency limits are: w_{Ls} = 2.2%; w_L = 20.6%; w_P = 14.9%; I_P = 6; and, w_S = 12.0%.

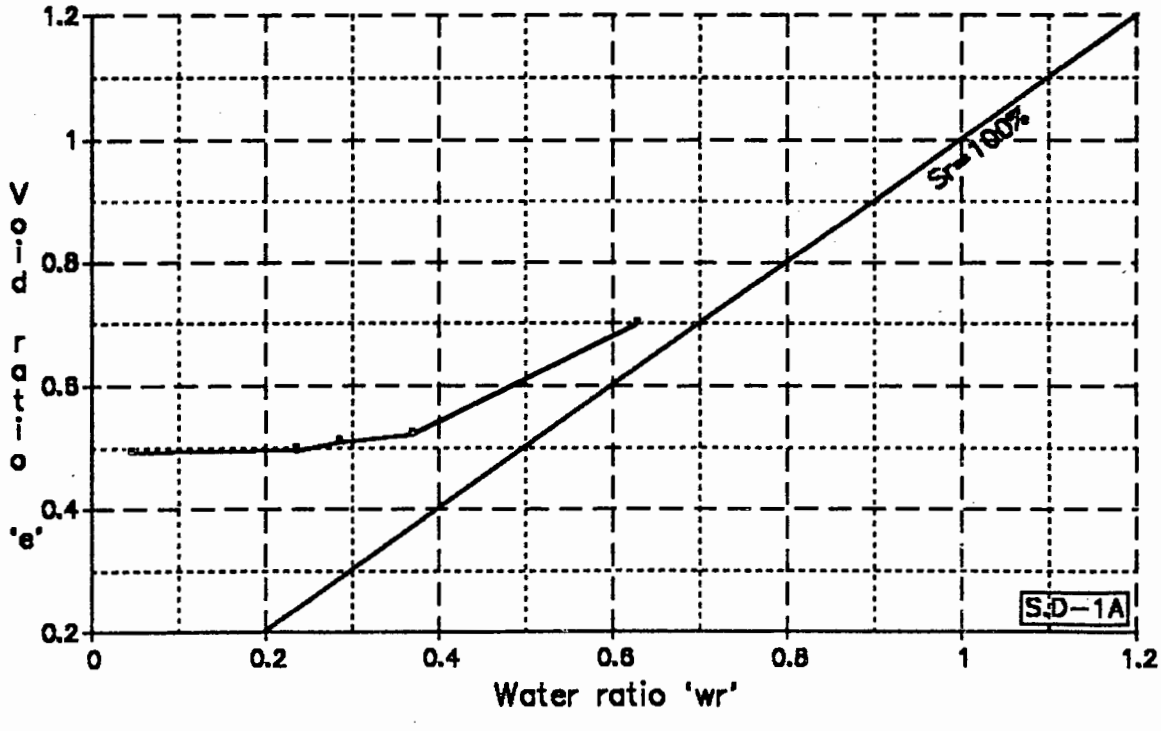

Figure 4.37: Site D, Rose Hill (Durban) [Remoulded] - Free Shrinkage Paths.

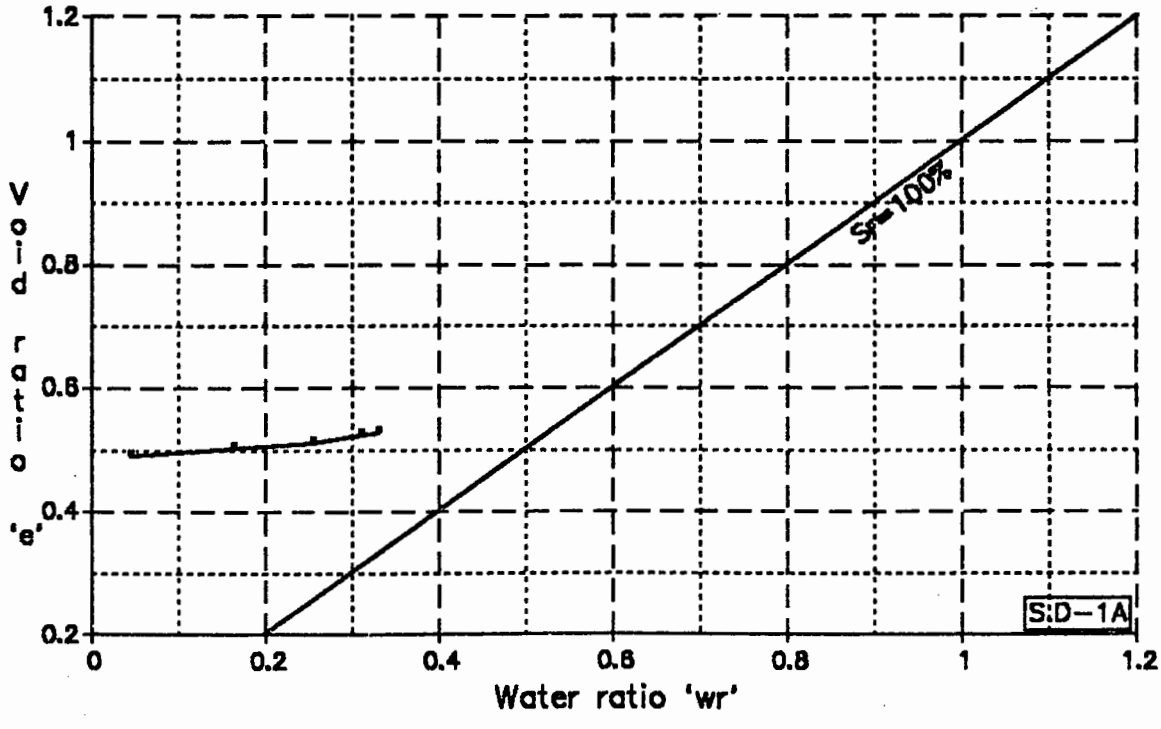

Figure 4.38: Site D, Rose Hill (Durban) [Remoulded] - Free Swell Paths. (After shrinking to points on Figure 4.37).

4.7.2 Artificial Soil Types.

This section includes the relationships of free shrinkage and free swell paths for the following artificial[1] soils:

(i) Kaolin clay mixed with sand - K.1 (13% clay size), K.2 (20% clay size), and K.3 (10% clay size); and,
(ii) Bentonite clay mixed with sand - B.1 (3.5% clay size), B.2 (7% clay size), B.3 (11.5% clay size), B.4 (15.5% clay size), and B.5 (35% clay size).

Free Shrinkage and Free Swell tests were carried out for the soil samples listed in Table 4.02.

Table 4.02: Artificial Soils - samples used for Free Shrinkage and Free Swell tests.

Sample No.	Method of preparation	Reference number	Consolidometer/Triaxial: Test No. - Chapter No.
K.1-2	M1 (≥LL)	II. 215	106 (C) - Chp. 6
K.1-3	M1 (≥LL)	II. 215	108 (C) - Chp. 6
K.2-T1	M1 (≥LL)	V. 13	6 (T) - Chp. 5
K.2-2	M1 (≥LL)	II. 219	109 (C) - Chp. 6
K.2-3	M1 (≥LL)	II. 219	112 (C) - Chp. 6
K.3-T1	M1 (NP)	V. 15	7 (T) - Chp. 5
K.3-2	M1 (NP)	II. 265	113 (C) - Chp. 6
K.3-3	M1 (NP)	II. 265	116 (C) - Chp. 6
B.1-2	M1 (≥LL)	III.338	117 (C) - Chp. 6
B.1-3	M2 (*)	III.340	120 (C) - Chp. 6
B.1-5	M2 (*)	III.362	134 (C) - Chp. 6
B.2-T1	M1 (≥LL)	V. 17	8 (T) - Chp. 5
B.2-2	M1 (<LL)	III.368	139 (C) - Chp. 6
B.2-3	M2 (*)	III.370	138 (C) - Chp. 6
B.3-2	M1 (<LL)	IV. 482	160 (C) - Chp. 6
B.3-3	M2 (*)	IV. 432	159 (C) - Chp. 6
B.4-T1	M1 (≥LL)	V. 19	9 (T) - Chp. 5
B.4-2	M1 (<LL)	III.398	151 (C) - Chp. 6
B.4-3	M2 (*)	III.400	152 (C) - Chp. 6
B.5-T1	M1 (<LL)	V. 21	10 (T) - Chp. 5
B.5-2	M1 (<LL)	IV. 446	162 (C) - Chp. 6
B.5-3	M2 (*)	IV. 446	166 (C) - Chp. 6

[1] - *or made up.*
* - *air bubbles.*

Kaolin clay mixed with sand.

Kaolin K.1.

A clayey sand (fine to medium size), with a very small amount of silt. The soil consists of 13% clay, 3.5% silt, and 83.5% of sand size. The consistency limits are: w_{Ls} = 0.4%; w_L = 12.3%; w_P = 11.8%; I_P = 1; and, w_S = 10.0%.

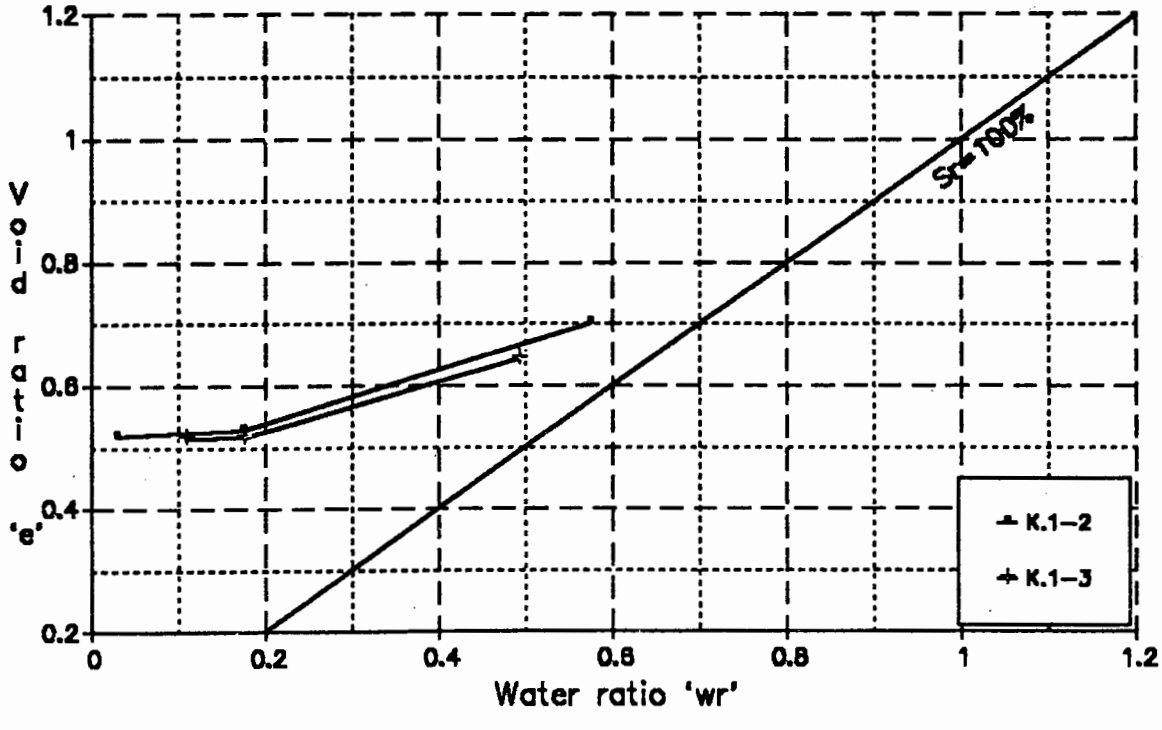

Figure 4.39: Kaolin K.1 (13%) - Free Shrinkage Paths.

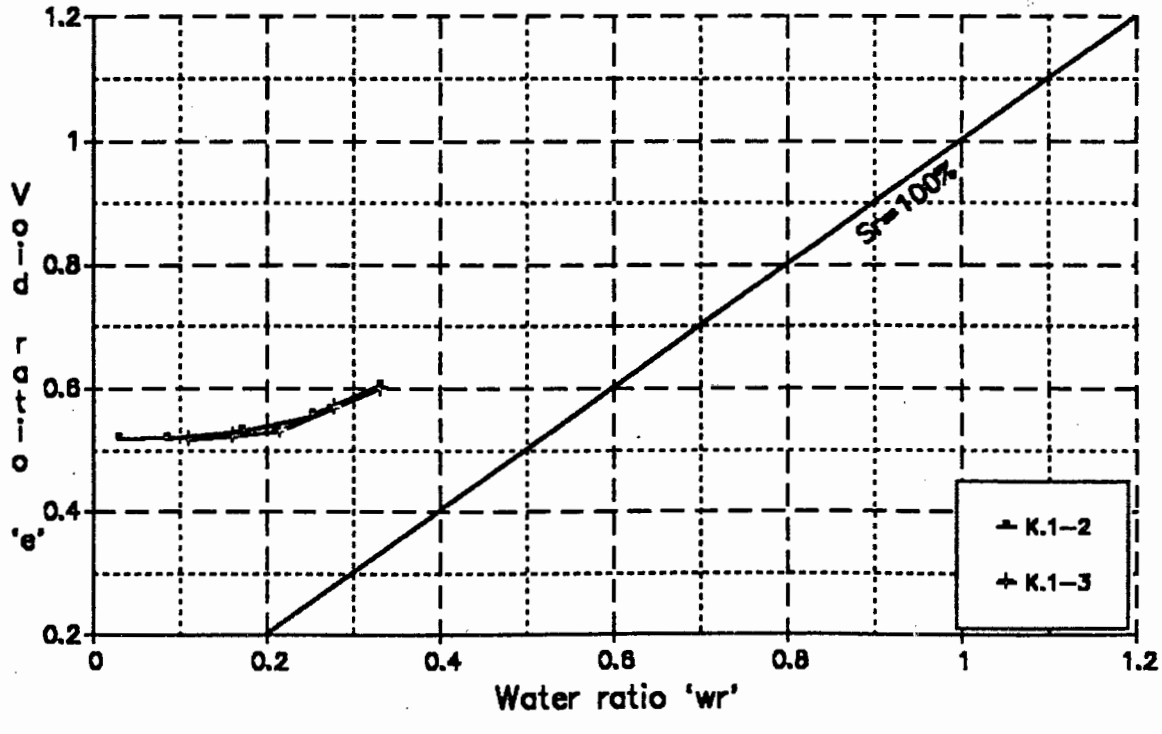

Figure 4.40: Kaolin K.1 (13%) - Free Swell Paths. (After shrinking to points on Figure 4.39).

Kaolin K.2.

A clayey sand (fine to medium size), with a small amount of silt. The soil consists of 20% clay, 65% silt, and 73.5% of sand size. The consistency limits are: w_{Ls} = 1.5%; w_L = 14.0%; w_P = 10.4%; I_P = 4; and, w_S = 12.0%.

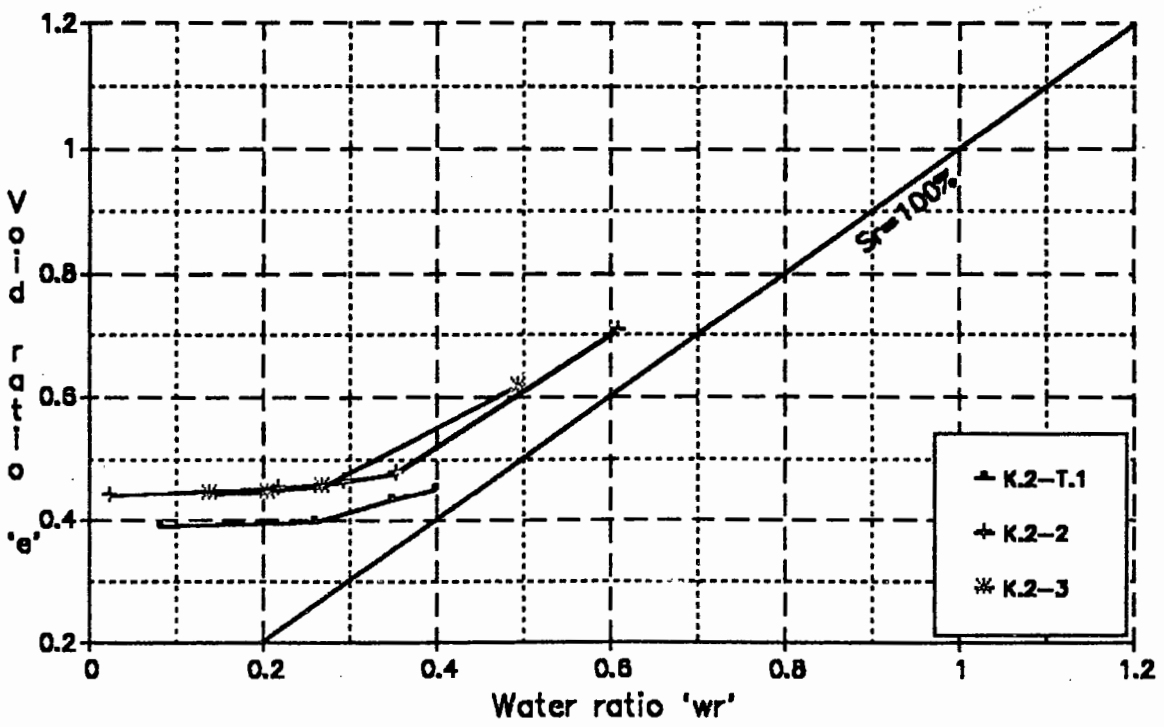

Figure 4.41: Kaolin K.2 (20%) - Free Shrinkage Paths.

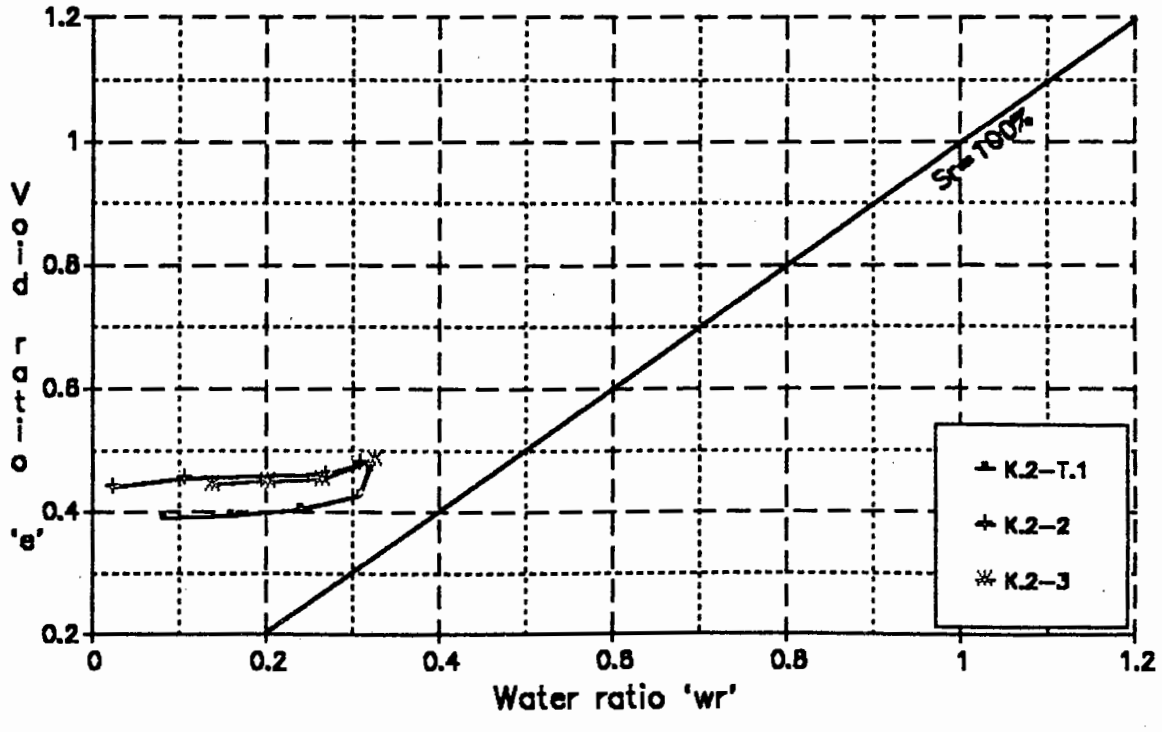

Figure 4.42: Kaolin K.2 (20%) - Free Swell Paths. (After shrinking to points on Figure 4.41).

Kaolin K.3.

A fine to medium sand containing a small amount of clay and silt (very small). The soil consists of 8.5% clay, 2.5% silt and 89% sand size. The consistency limits are: w_{Ls} = 0,0; w_L = NP; w_P = NP; I_P = NP; and, w_S = 9.0%.

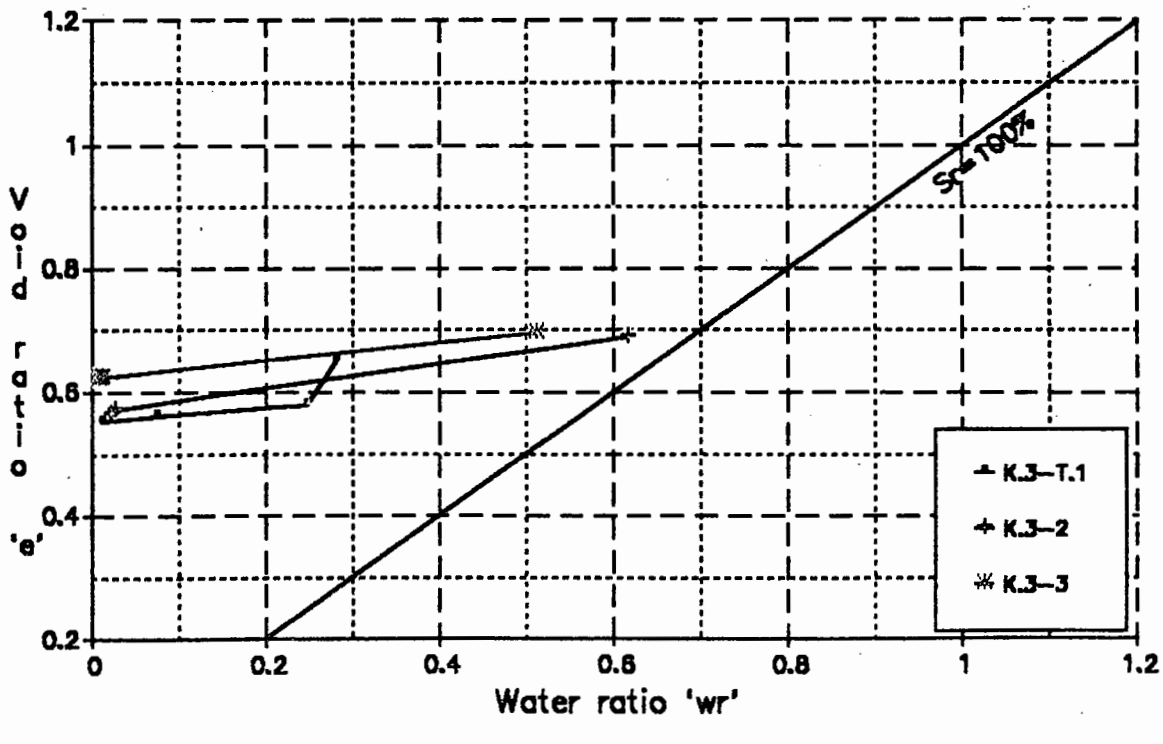

Figure 4.43: Kaolin K.3 (8.5%) - Free Shrinkage Paths.

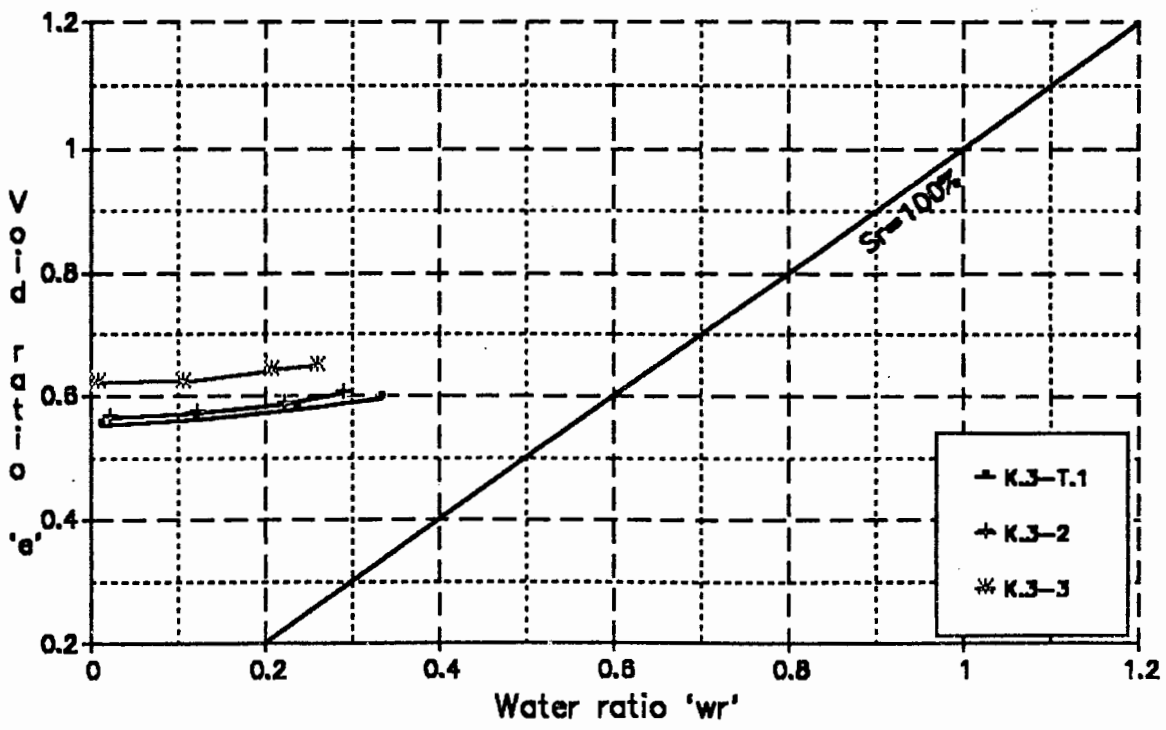

Figure 4.44: Kaolin K.3 (8.5%) - Free Swell Paths. (After shrinking to points on Figure 4.43).

Bentonite B.1 (Bentonite clay mixed with sand).

A fine to medium sand with a very small amount of clay and silt. The soil consists of 3.5% clay, 1.5% silt, and 95% of sand size. The consistency limits are: w_{LS} = 0.1%; w_L = 21.0%; w_P = 20.0%; I_P = 1; and, w_S = 14.5%.

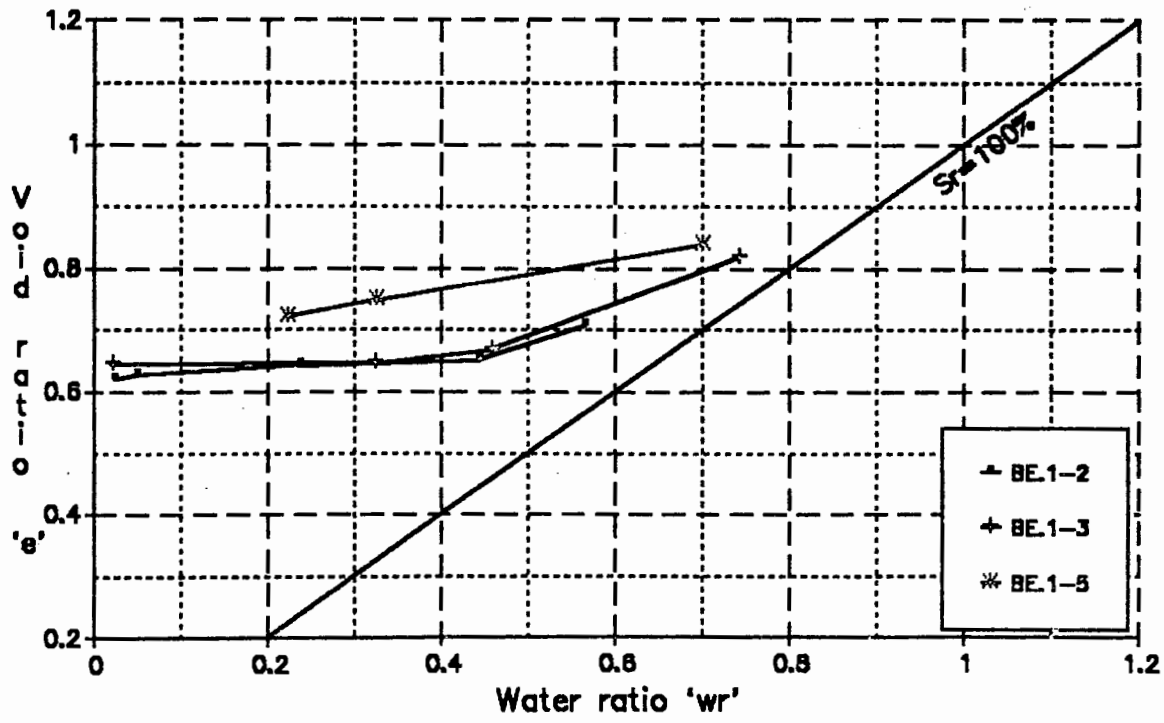

Figure 4.45: Bentonite B.1 (3.5%) - Free Shrinkage Paths.

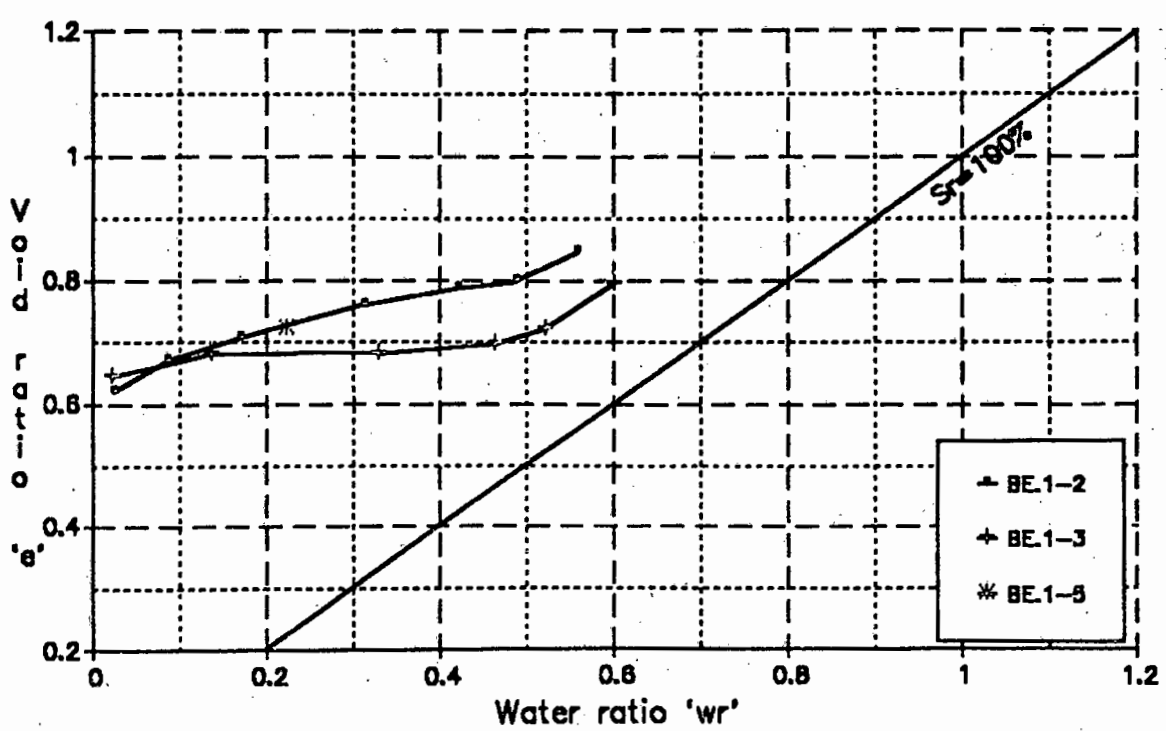

Figure 4.46: Bentonite B.1 (3.5%) - Free Swell Paths. (After shrinking to points on Figure 4.45).

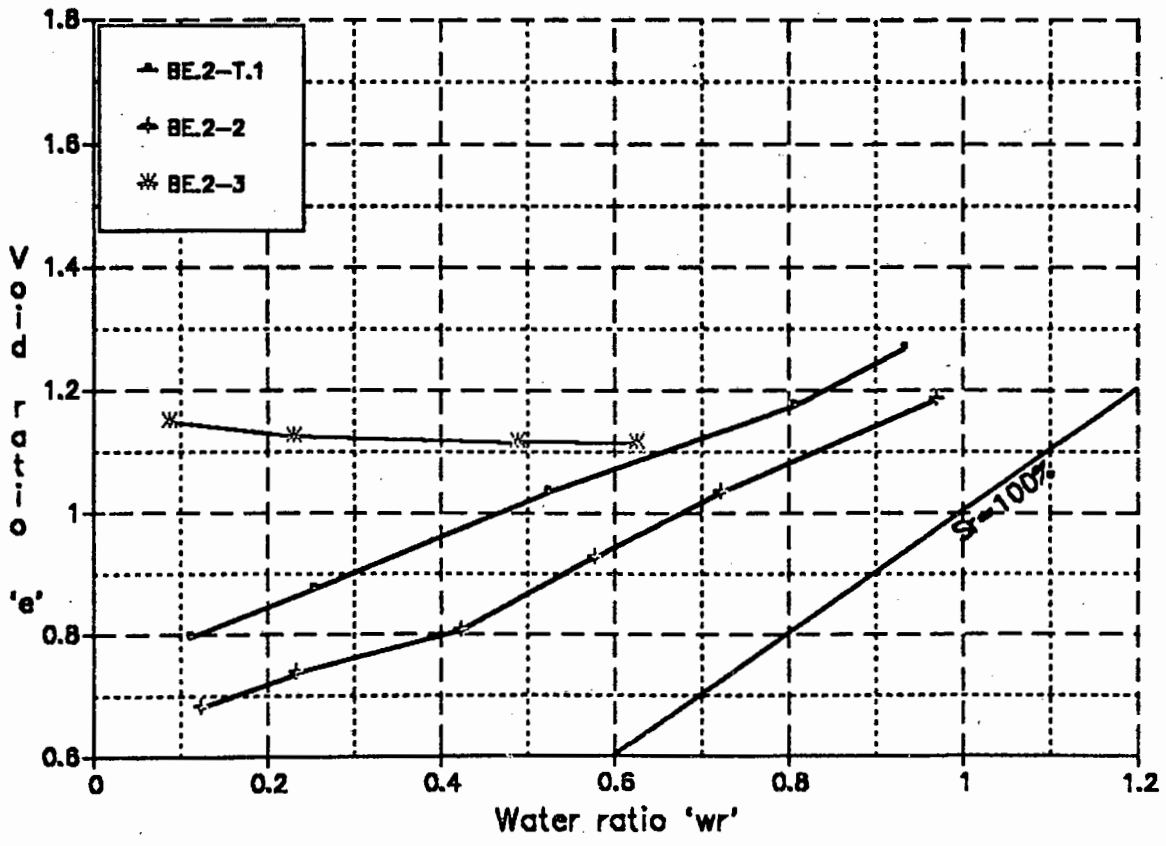

Figure 4.48: Bentonite B.2 (7%) - Free Swell Paths. (After shrinking to points on Figure 4.47).

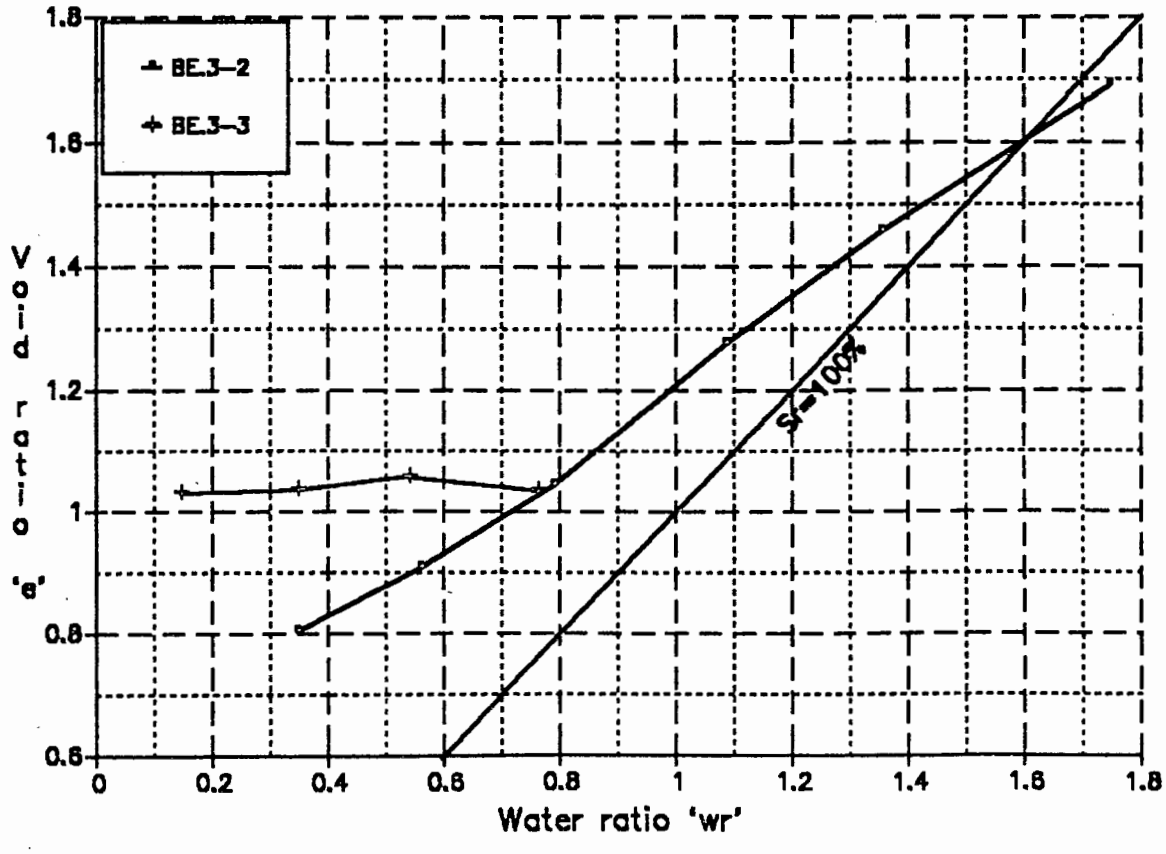

Figure 4.50: Bentonite B.3 (11.5%) - Free Swell Paths. (After shrinking to points on Figure 4.49).

Bentonite B.4 (Bentonite clay mixed with sand).

A clayey sand (fine to medium size) with a very small amount of silt. The soil consists of 15.5% clay, 3% silt and 81.5% of sand size. The consistency limits are: w_{Ls} = 1.5%; w_L = 59.0%; w_P = 19.0%; I_P = 40; and w_S = 34.0%.

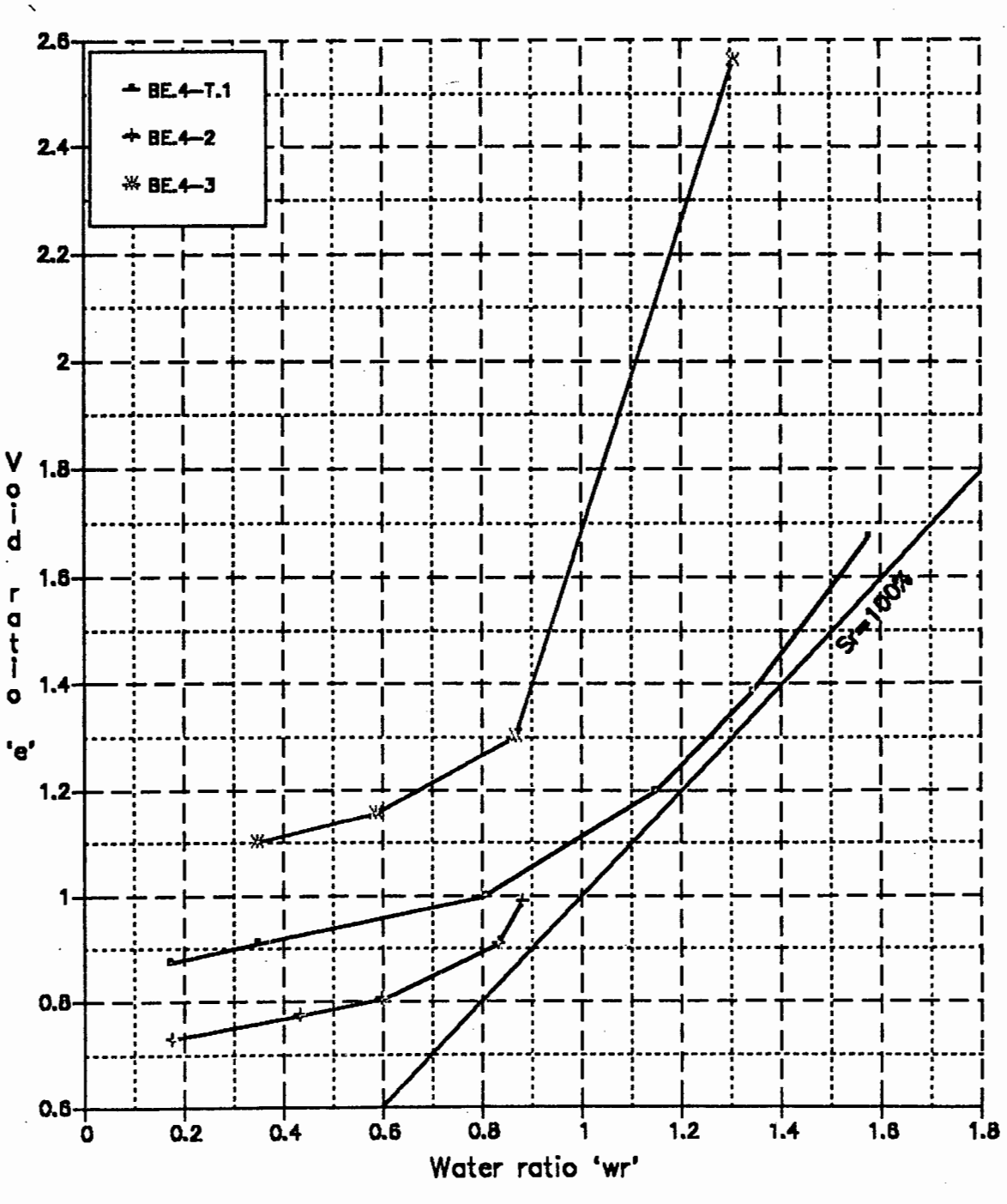

Figure 4.51: Bentonite B.4 (15.5%) - Free Shrinkage Paths.

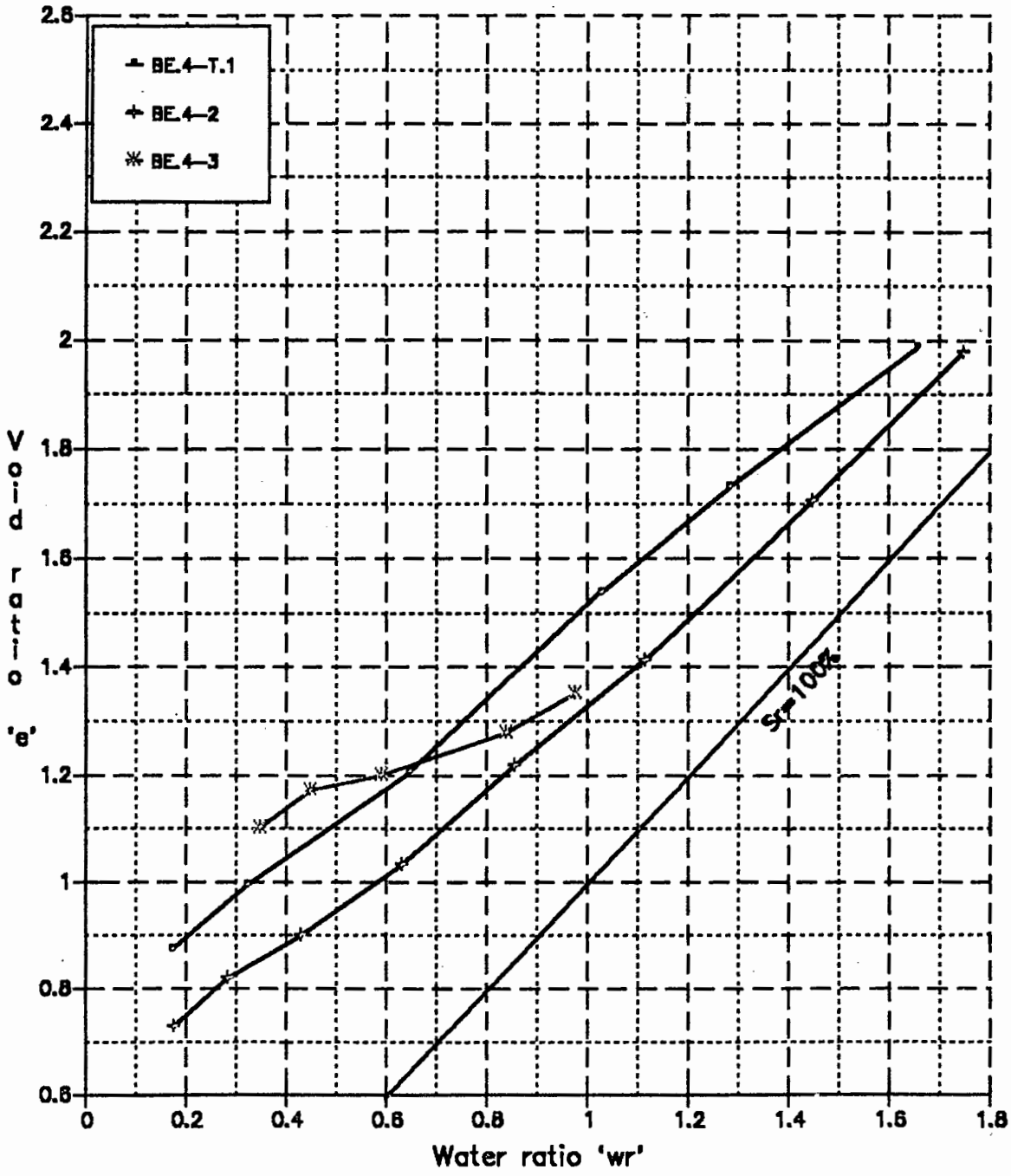

Figure 4.52: Bentonite B.4 (15.5%) - Free Swell Paths. (After shrinking to points on Figure 4.51).

Bentonite B.5 (Bentonite clay mixed with Sand).

A clayey sand (fine to medium), with a very small amount of silt. The soil consists of 35% clay, 4% silt, and 61% of sand size. The consistency limits are: w_{LS} = 6.5%; w_L = 133.0%; w_P = 21.0%; I_P = 112; and, w_S = 38.0%.

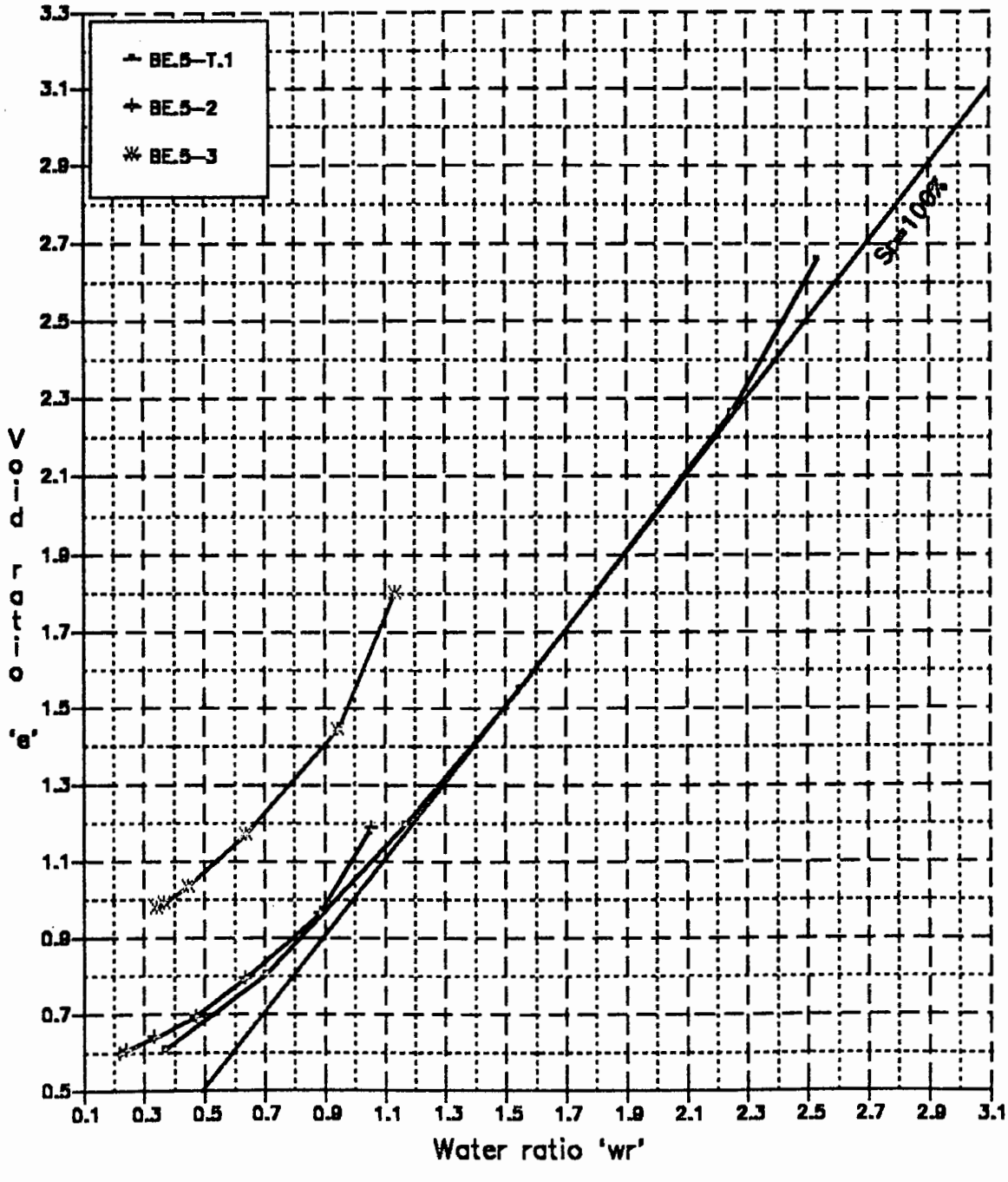

Figure 4.53: Bentonite B.5 (35%) - Free Shrinkage Paths.

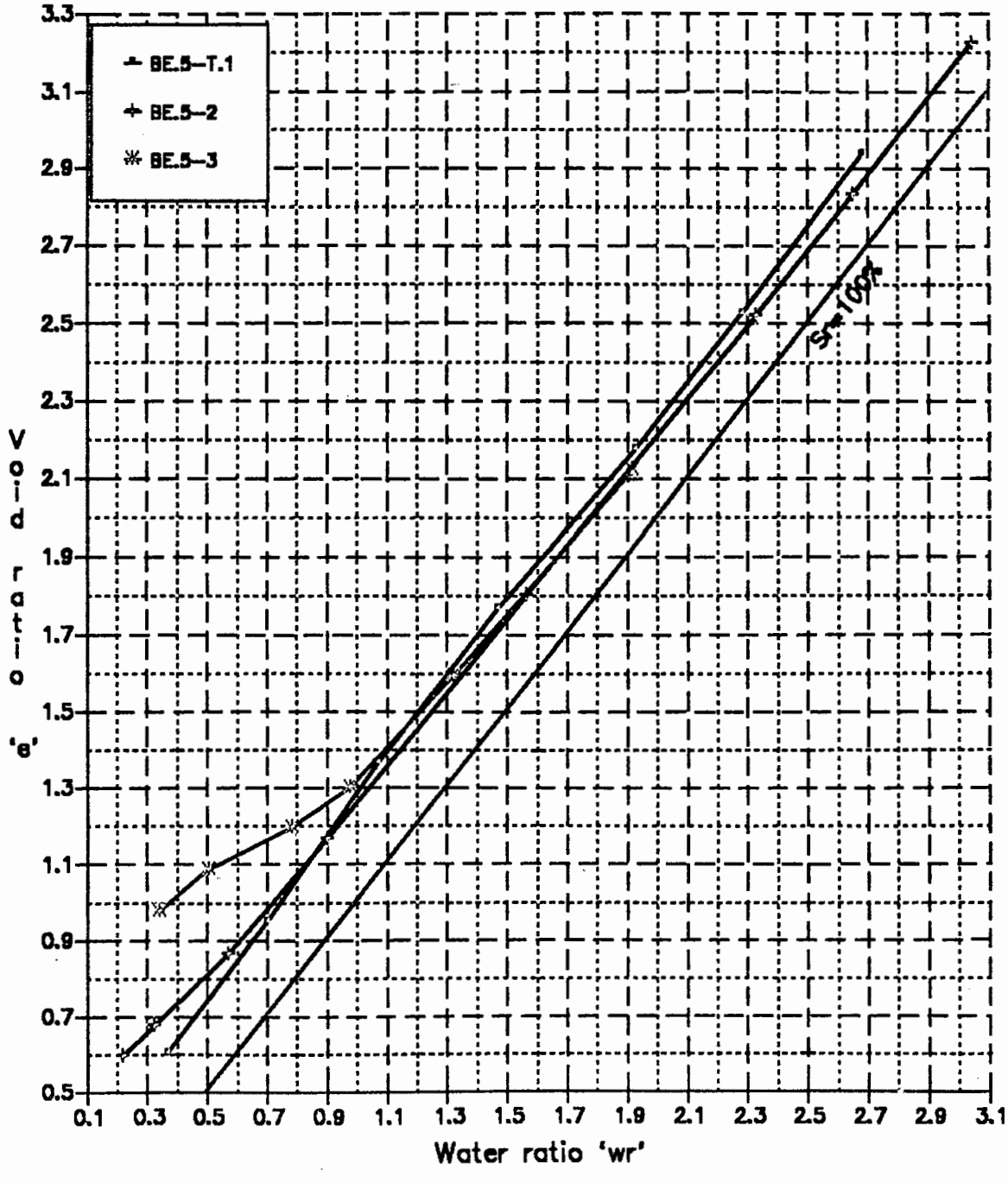

Figure 4.54: Bentonite B.5 (35%) - Free Swell Paths. (After shrinking to points on Figure 4.53).

4.8 CONCLUSIONS FOR CHAPTER FOUR

For each soil type used in this thesis, a number of samples were used to determine volumes and void ratios for a range of (measured) water contents.

4.8.1 The Free Expansion Limit.

The water content above which the unrestrained soil sample will not swell any further, was observed for the soil types. It has been expressed as water ratio, which takes into account the specific gravity of the soil particles.

The Free Expansion Limit 'FEL' has been determined for each soil type. FEL is the mean value of the results obtained. Table 4.03 includes all FEL values for natural and artificial soil, and the mean values for each soil type.

Table 4.03: Natural & Artificial Soils [Remoulded, Compacted and Undisturbed] - Free Expansion Limit 'FEL' values.

Site, Location,	Free Expansion Limit 'FEL'[1]: Remould. (R)	Compact. (C)	Mean (R+C)	Undisturb. (U)	Mean value (R+C+U)
Natural Soils					
11, Rosebank	1.365	1.342	1.361	1.246	1.335
36, Rondebosch	0.877	0.921	0.880	0.842	0.874
30, Hout Bay	0.849	-	0.949	0.848	0.932
A, Berea Road	0.454	0.418	0.442	0.478	0.449
7, Mowbray	0.822	0.618	0.803	0.671	0.783
B, Francois R	0.319	-	0.319		
C, Margaret M	0.408	-	0.408		
D, Rose Hill	0.329	-	0.329		
Artificial Soils					
Kaolin No. (%):					
K.1 (13%)	0.329	-	0.329		
K.2 (20%)	0.316	-	0.316		
K.3 (10%)	0.293	-	0.293		
Bentonite:					
B.1 (3.5%)	0.460	-	0.460		
B.2 (7%)	0.787	-	0.787		
B.3 (11.5%)	1.227	-	1.227		
B.4 (15.5%)	1.537	-	1.537		
B.5 (35%)	2.650	-	2.650		

[1] - *as a water ratio ('θ' or 'wr').*

The final water ratios were compared with both the initial void ratio and initial water ratio for each sample. Remoulded and Compacted samples were used because - (1) The preparation of the soil material is basically the same, and (2) It was used for most natural and artificial soils.

These relationships are intended to show how the initial void ratio, or water ratio (of the sample) affects the Free Expansion Limit. They are plotted in figures 4.55 to 4.80.

The final water ratio after free swelling seems to be approximately independent of the initial void ratio, but it does depend on soil type.

For all the natural soils the final water ratio, after free swell, seems to be approximately constant for a particular soil type irrespective of the method of preparation[1].

In the case of the artificial soil consisting of Kaolin and sand, only one method of preparation was used in order to try to match the void ratios for Berea Red Soils. Again the final water ratio after free swell seems to be approximately constant and does not vary with initial void ratio (see Figures 4.67, 4.68).

For artificial soils consisting of sand and Bentonite mixtures, the final water ratio after free swelling is not a constant for a particular soil but, appears to depend on the method of sample preparation and on a sample's initial void ratio and/or water ratio.

---

[1] - *see Figures 4.56, 4.58, etc.*

Natural Soil Types:-

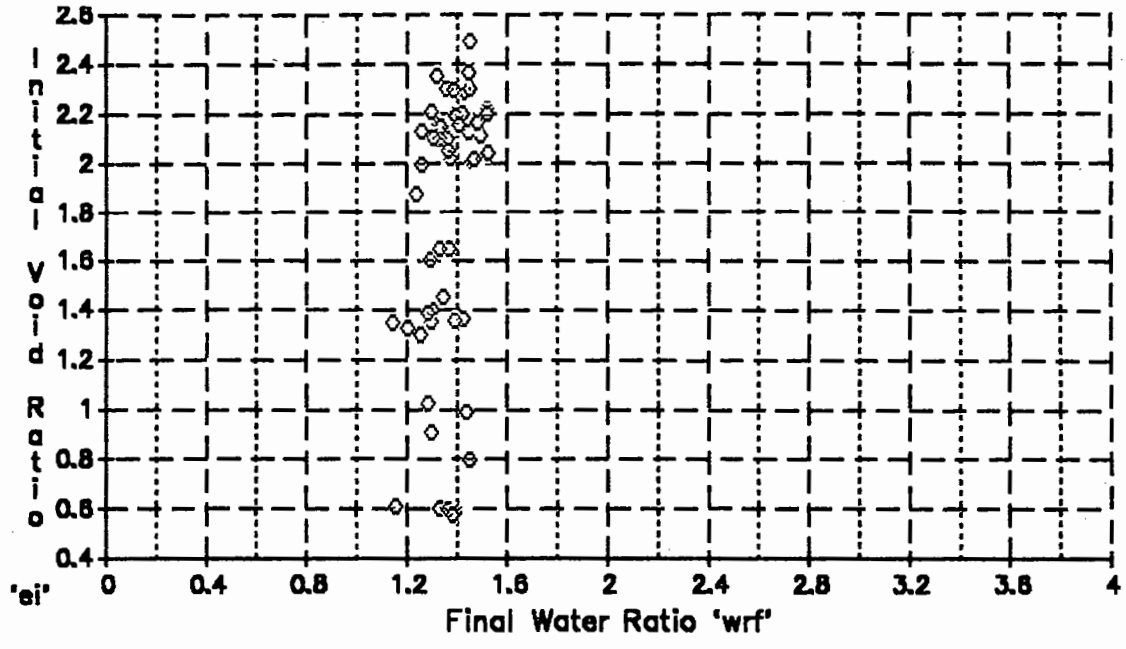

Figure 4.55: Site 11, Rosebank [Remoulded and Compacted Samples] - Initial Void Ratio 'e_i' versus final Water Ratio 'wr_f' (Free Expansion Limit).

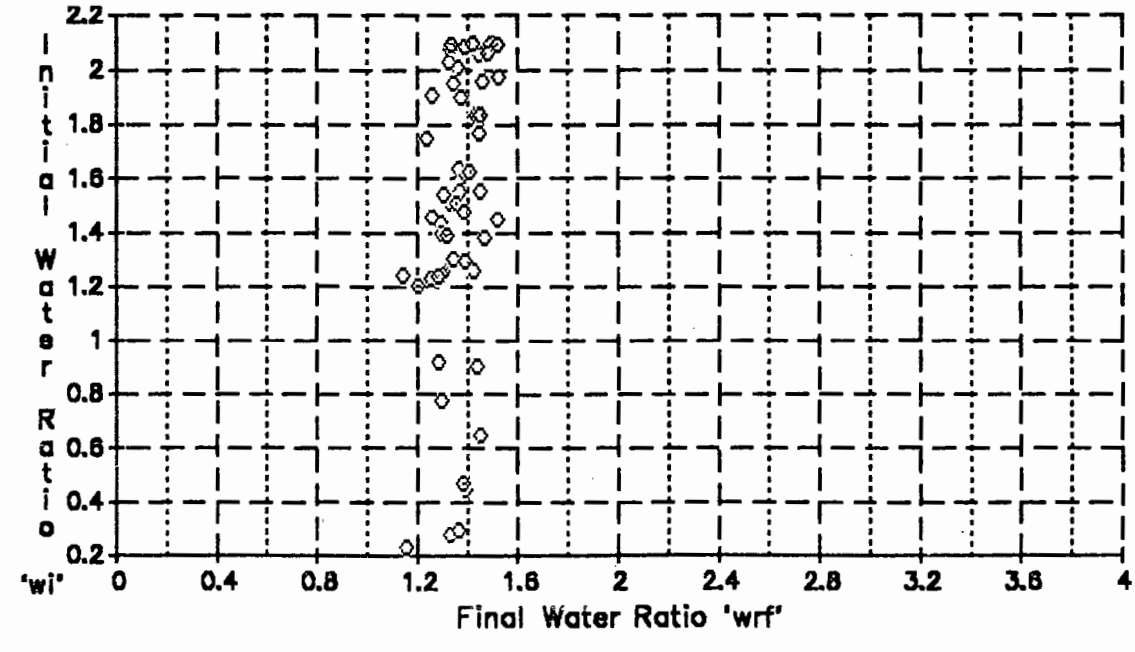

Figure 4.56: Site 11, Rosebank [Remoulded and Compacted Samples] - Initial Water Ratio 'wr_i' versus final Water Ratio 'wr_f' (Free Expansion Limit).

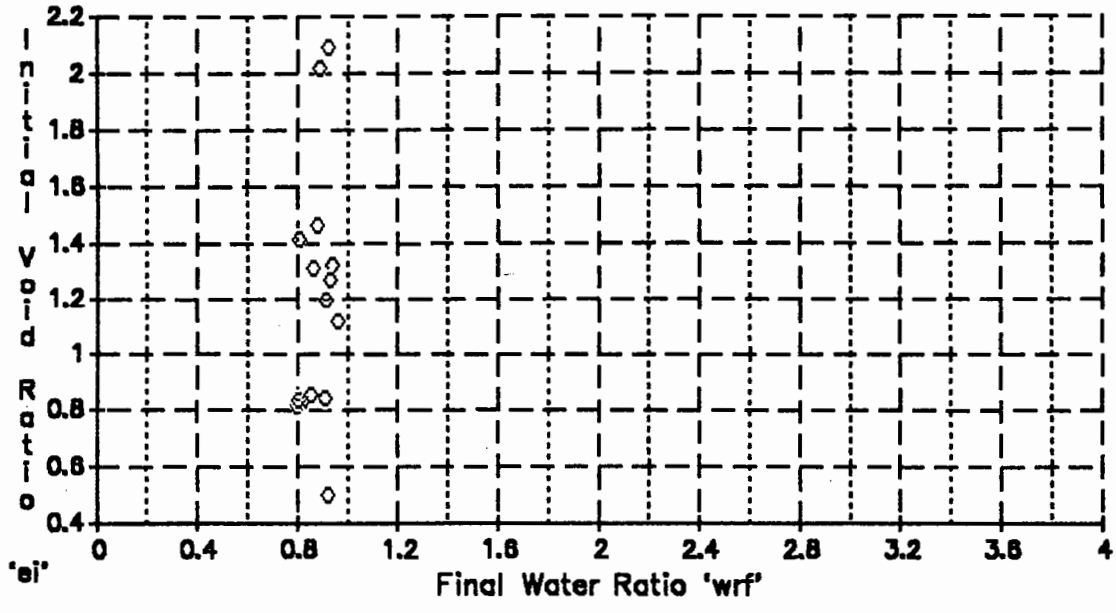

Figure 4.57: Site 36, Rondebosch [Remoulded and Compacted Samples] - Initial Void Ratio 'e_i' versus Final Water Ratio 'wr_f' (Free Expansion Limit).

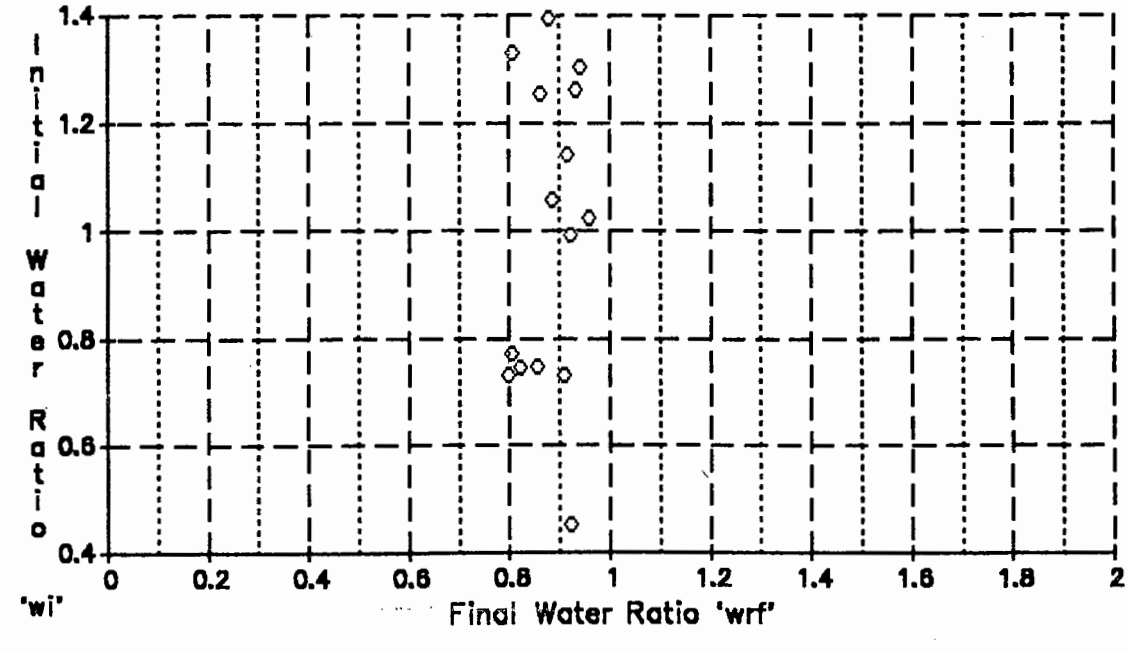

Figure 4.58: Site 36, Rondebosch [Remoulded and Compacted Samples] - Initial Water Ratio 'wr_i' versus Final Water Ratio 'wr_f' (Free Expansion Limit).

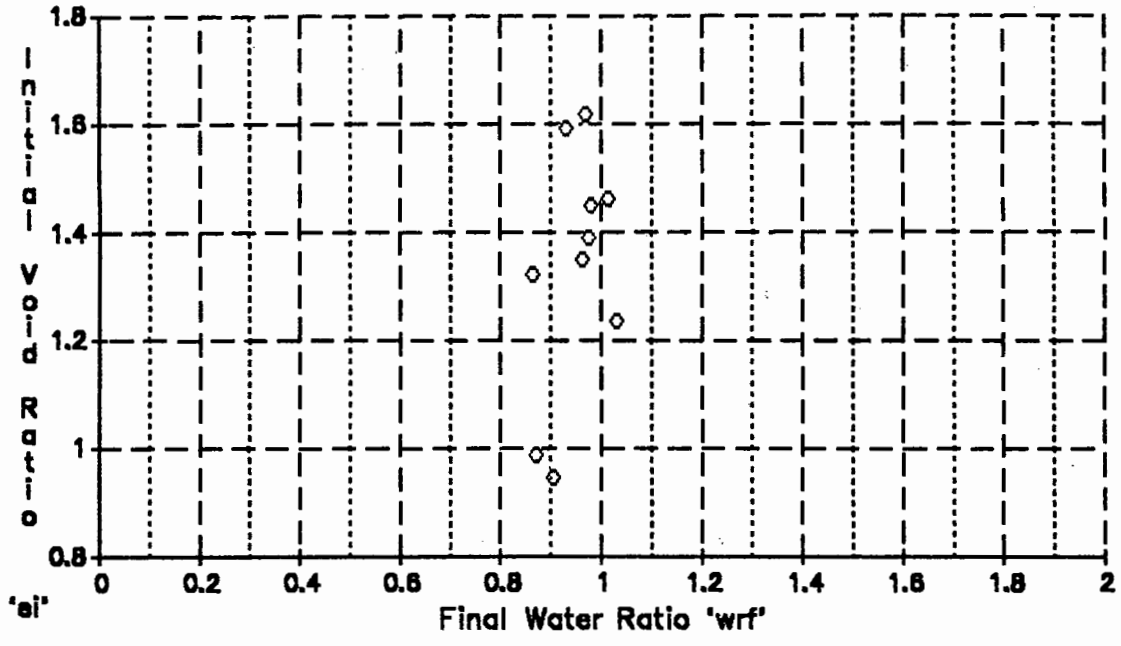

Figure 4.59: Site 30, Hout Bay [Remoulded Samples] - Initial Void Ratio 'e_i' versus Final Water Ratio 'wr_f' (Free Expansion Limit).

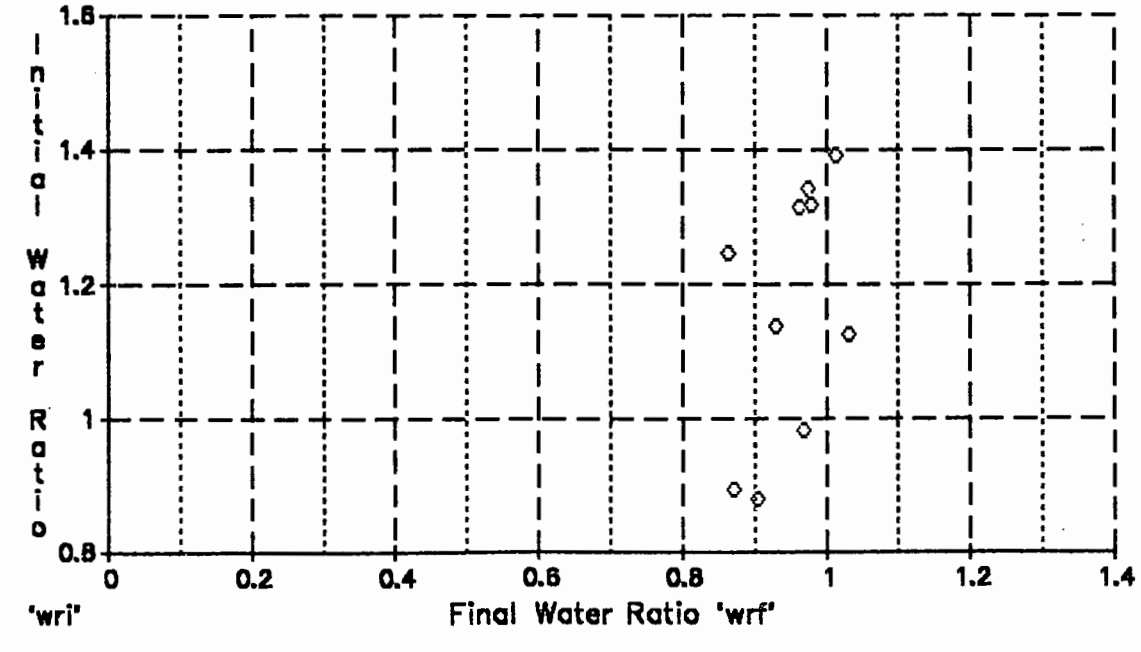

Figure 4.60: Site 30, Hout Bay [Remoulded Samples] - Initial Water Ratio 'wr_i' versus Final Water Ratio 'wr_f' (Free Expansion Limit).

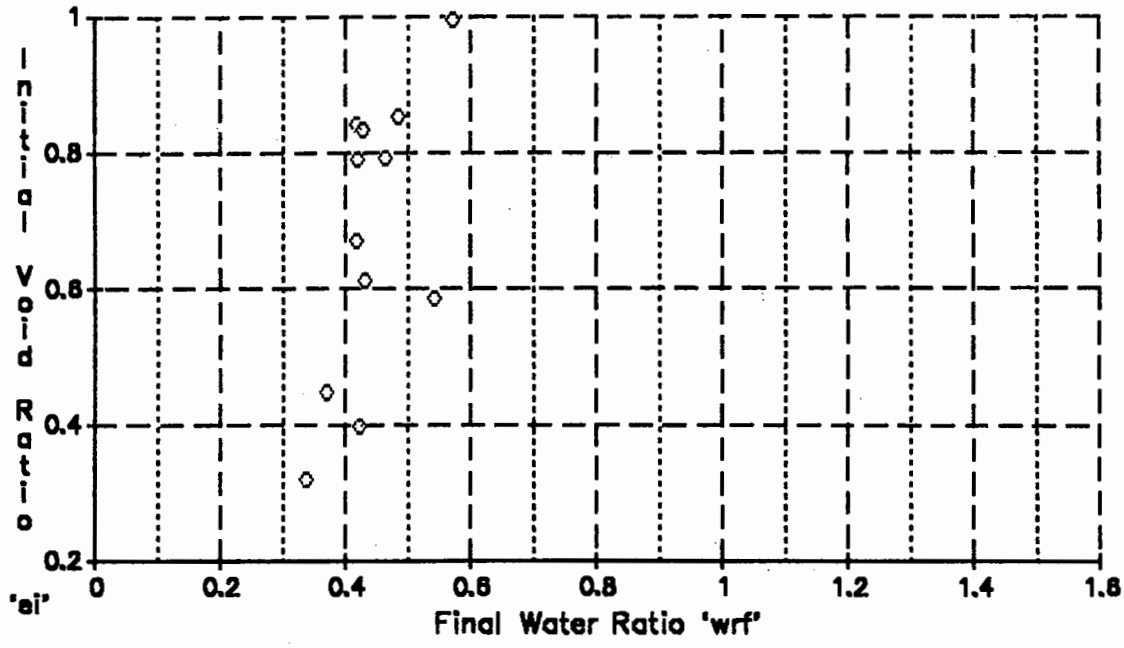

Figure 4.61: Site A, Berea Road [Remoulded and Compacted Samples] - Initial Void Ratio 'e_i' versus Final Water Ratio 'wr_f' (Free Expansion Limit).

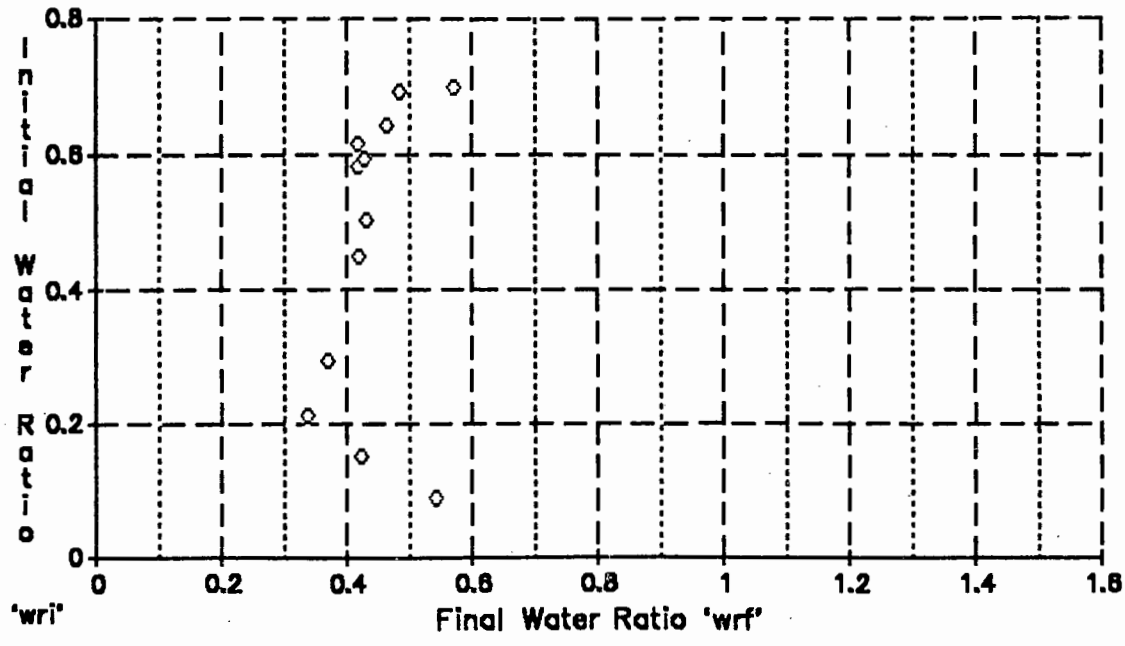

Figure 4.62: Site A, Berea Road [Remoulded and Compacted Samples] - Initial Water Ratio 'wr_i' versus Final Water Ratio 'wr_f' (Free Expansion Limit).

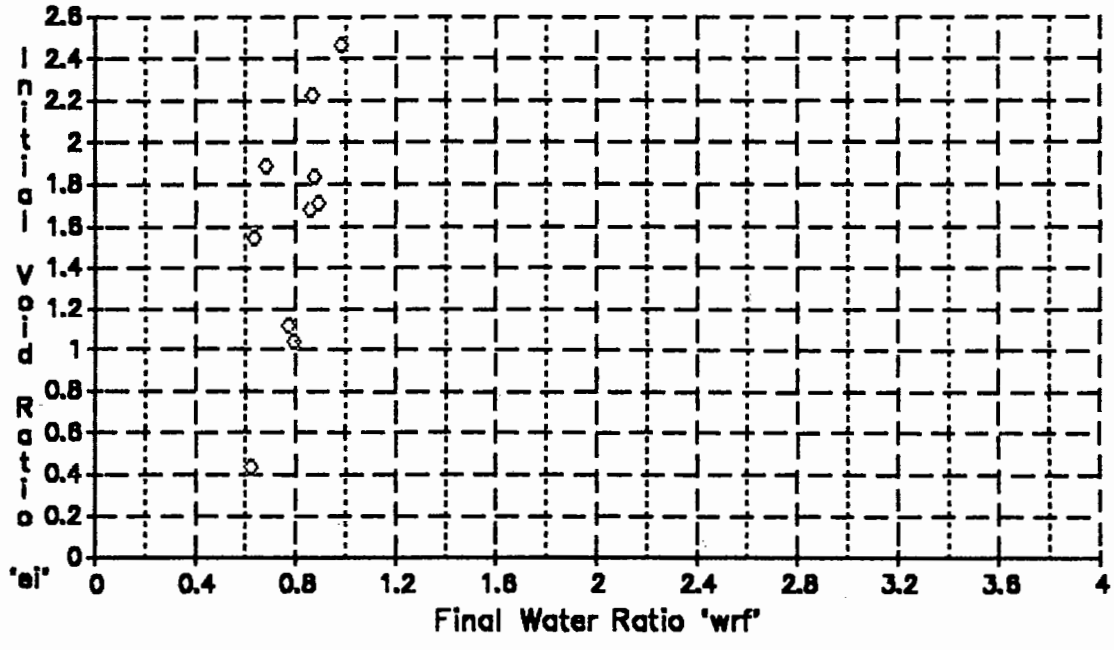

Figure 4.63: Site 7, Mowbray [Remoulded and Compacted] - Initial Void Ratio 'e_i' versus inal Water Ratio 'wr_f' (Free Expansion Limit).

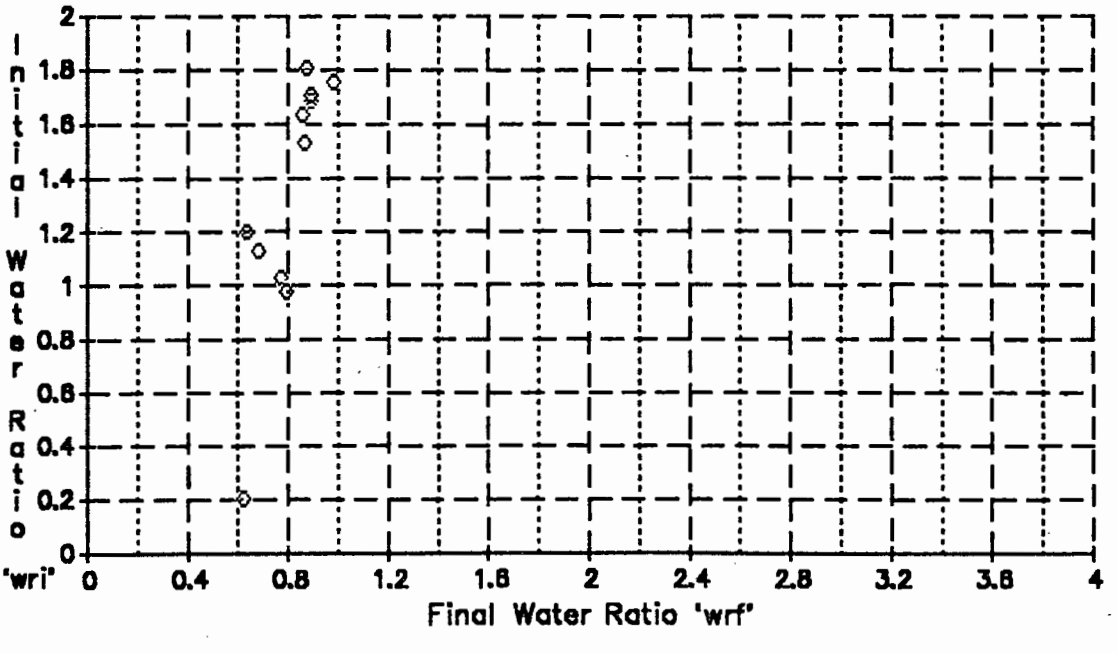

Figure 4.64: Site 7, Mowbray [Remoulded and Compacted] - Initial Water Ratio 'wr_i' versus Final Water Ratio 'wr_f' (Free Expansion Limit).

Artificial Soil Types:-

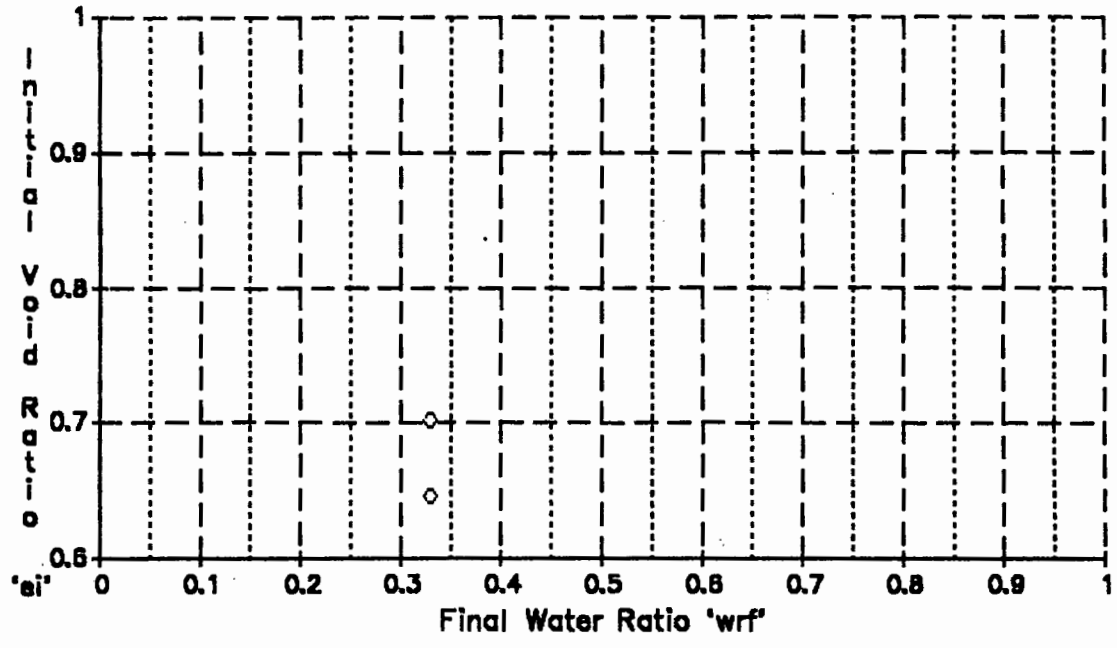

Figure 4.65: Kaolin K.1 (13% clay size) - Initial Void Ratio 'e_i' versus Final Water Ratio 'wr_f' (Free Expansion Limit).

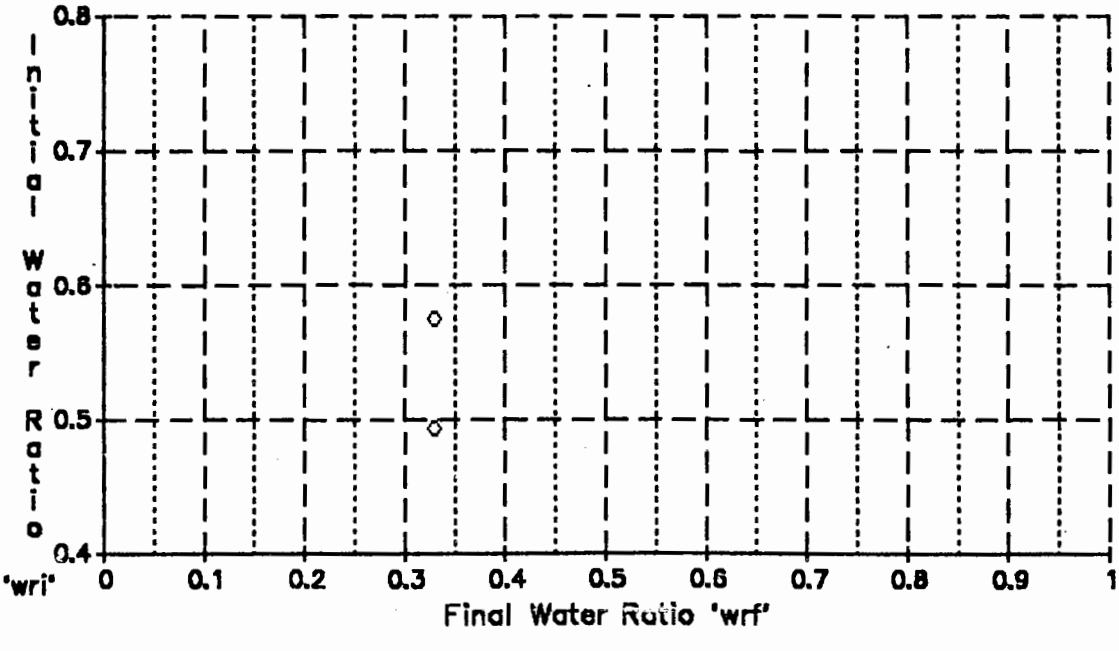

Figure 4.66: Kaolin K.1 (13% clay size) - Initial Water Ratio 'wr_i' versus Final Water Ratio 'wr_f' (Free Expansion Limit).

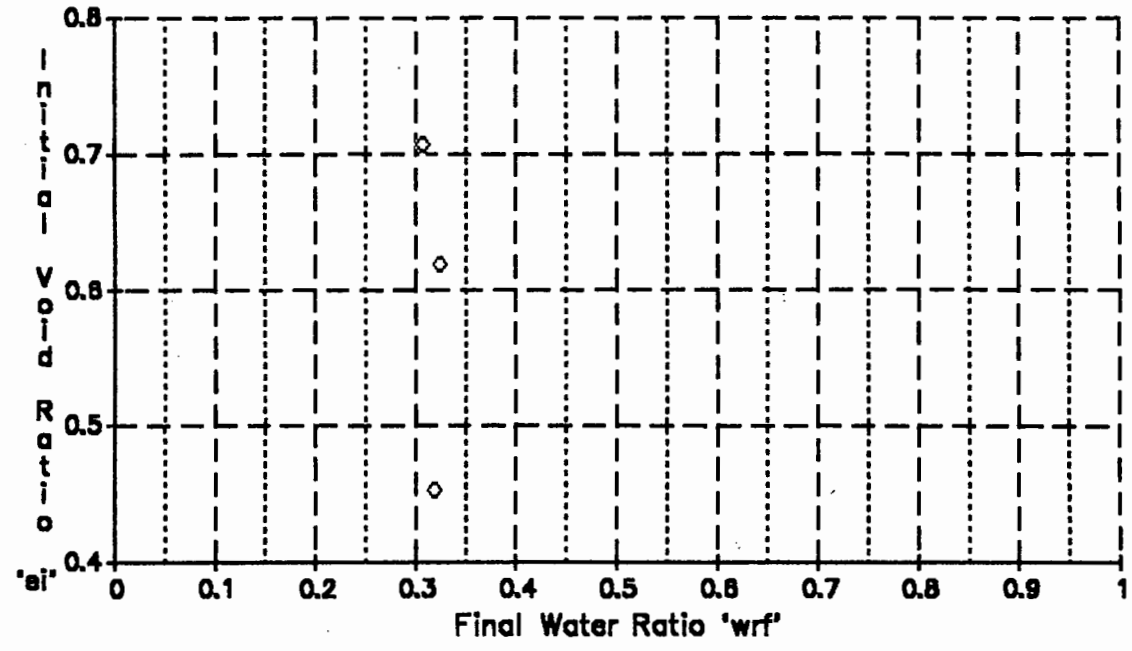

Figure 4.67: Kaolin K.2 (20% clay size) - Initial Void Ratio 'e_i' versus Final Water Ratio 'wr_f' (Free Expansion Limit).

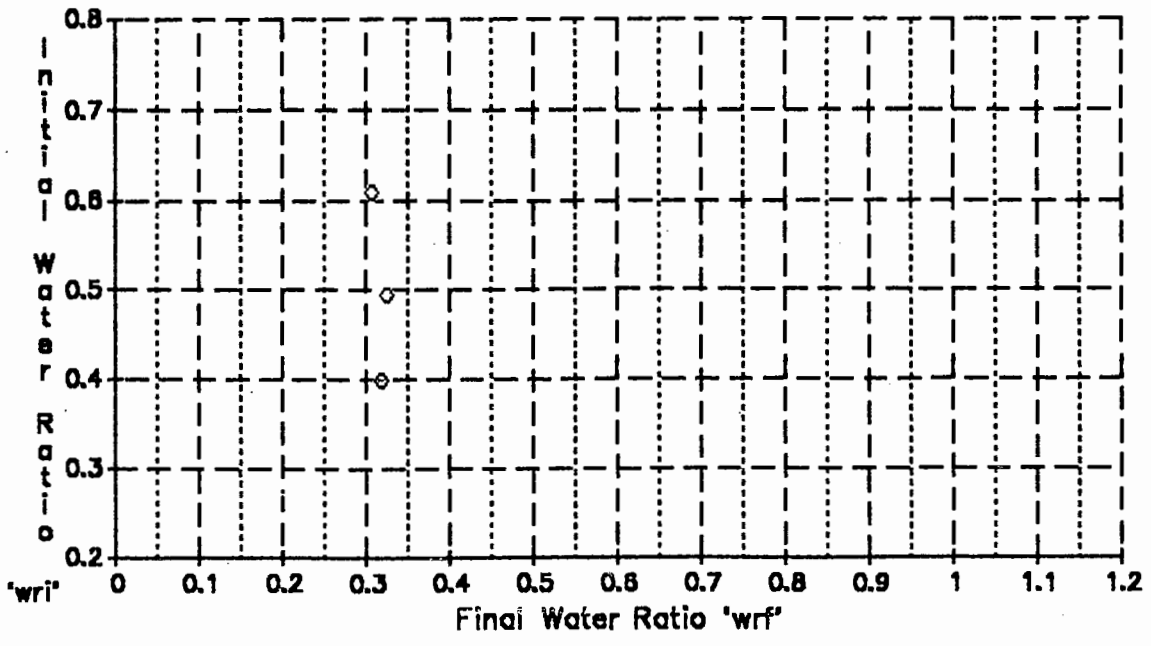

Figure 4.68: Kaolin K.2 (20% clay size) - Initial Water Ratio 'wr_i' versus Final Water Ratio 'wr_f' (Free Expansion Limit).

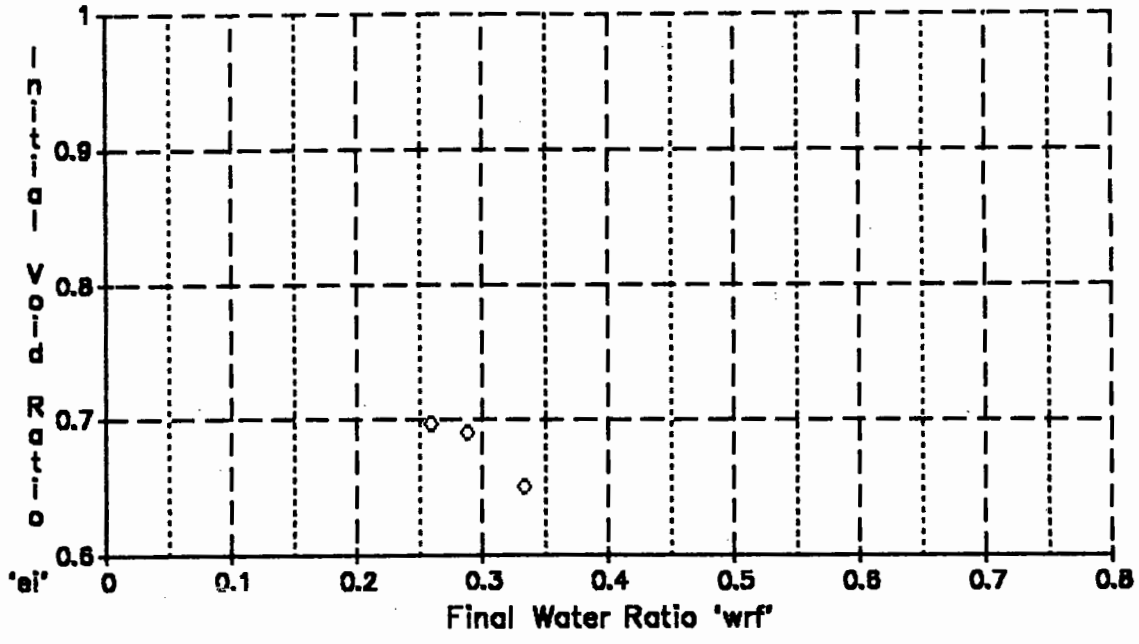

Figure 4.69: Kaolin K.3 (10% clay size) - Initial Void Ratio 'e_i' versus Final Water Ratio 'wr_f' (Free Expansion Limit).

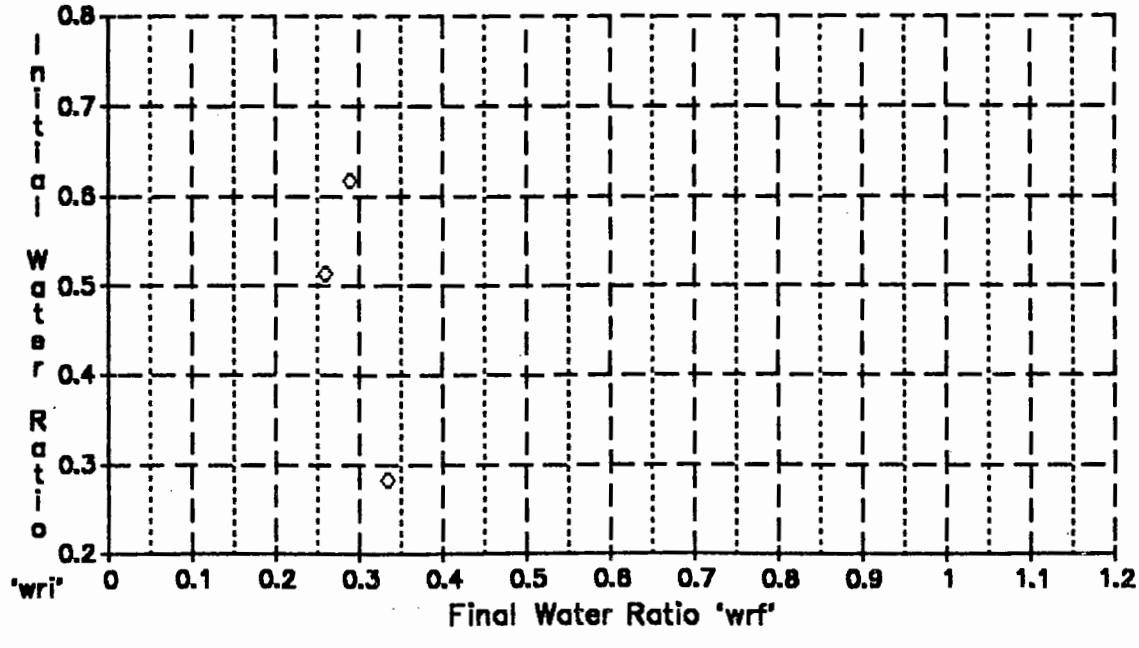

Figure 4.70: Kaolin K.3 (10% clay size) - Initial Water Ratio 'wr_i' versus Final Water Ratio 'wr_f' (Free Expansion Limit).

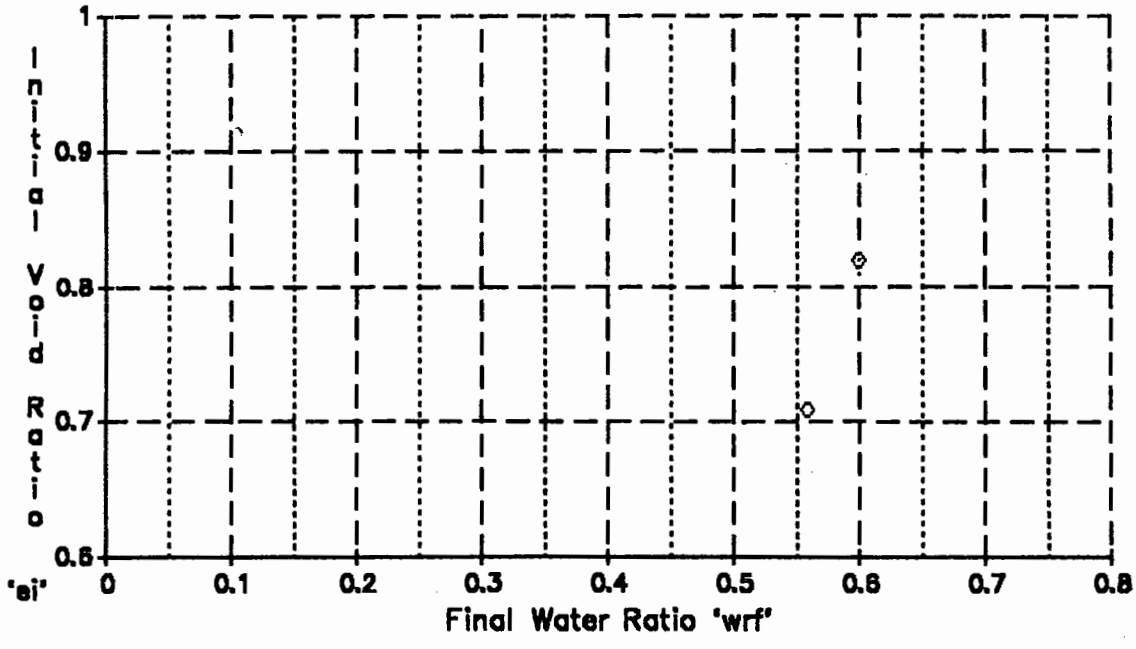

Figure 4.71: Bentonite B.1 (3.5% clay size) - Initial Void Ratio 'e_i' versus Final Water Ratio 'wr_f' (Free Expansion Limit).

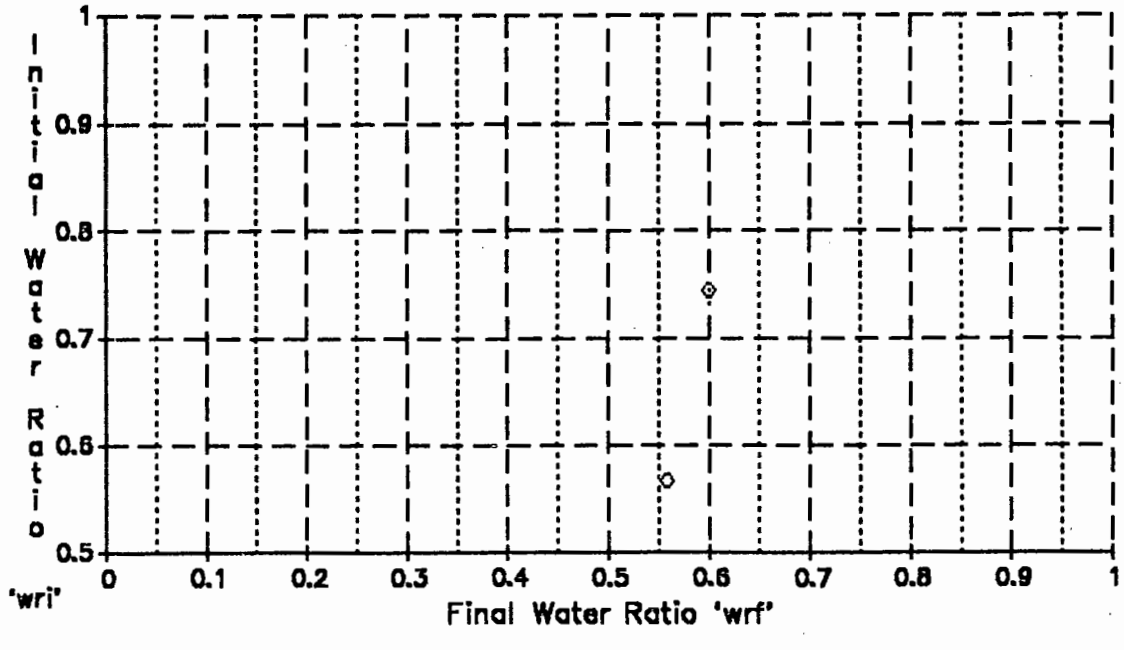

Figure 4.72: Bentonite B.1 (3.5% clay size) - Initial Water Ratio 'wr_i' versus Final Water Ratio 'wr_f' (Free Expansion Limit).

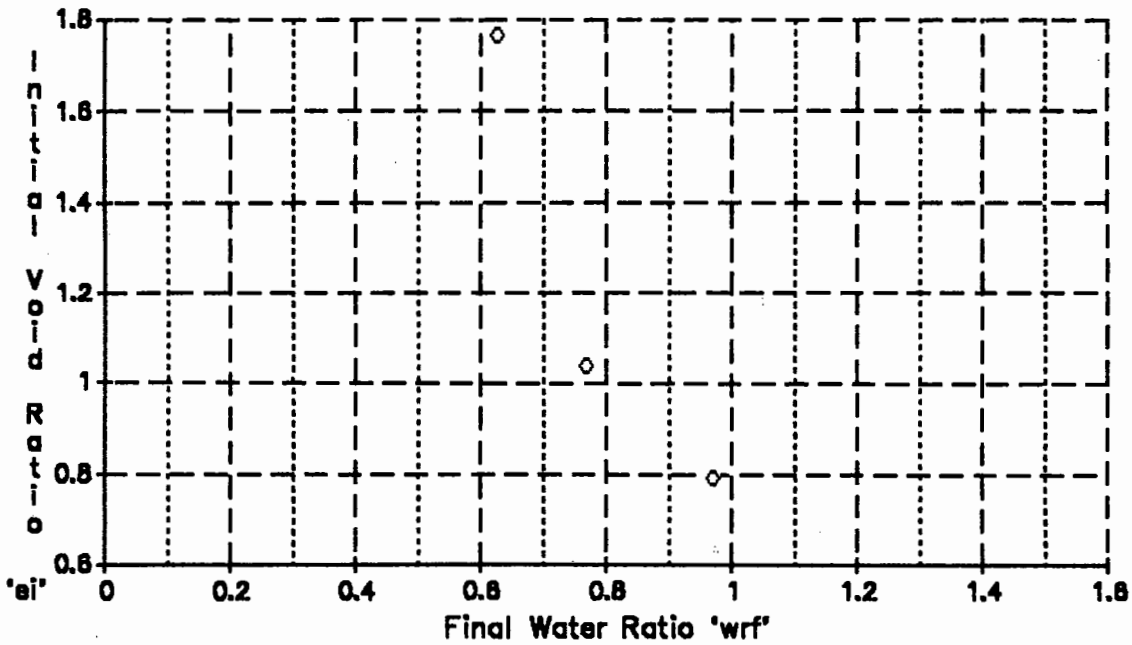

Figure 4.73: Bentonite B.2 (7% clay size) - Initial Void Ratio 'e_i' versus Final Water Ratio 'wr_f' (Free Expansion Limit).

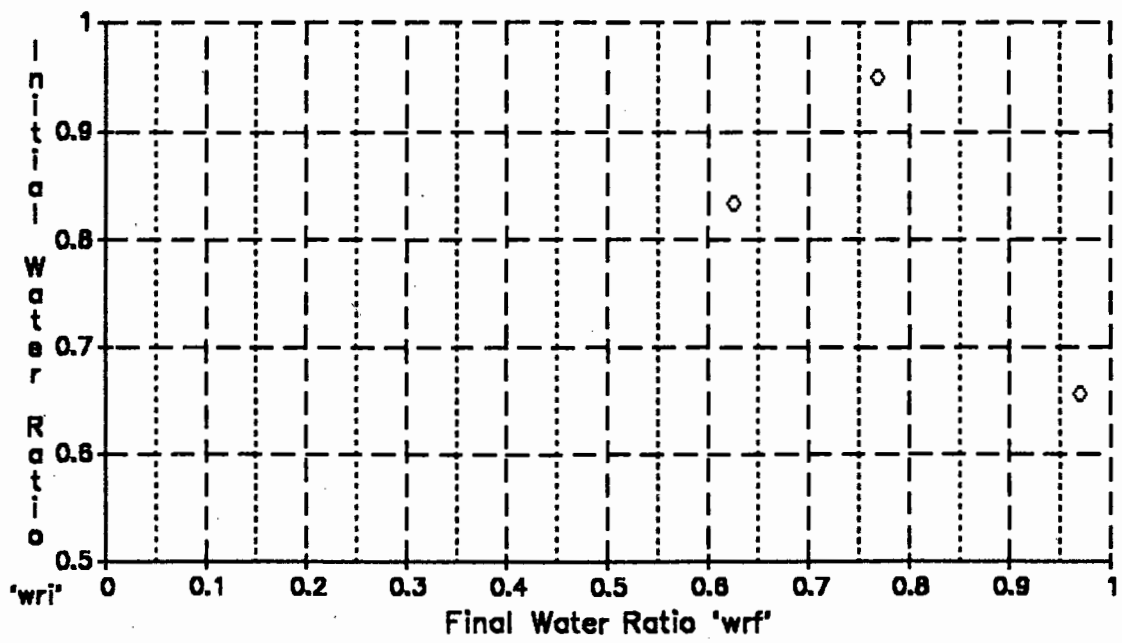

Figure 4.74: Bentonite B.2 (7% clay size) - Initial Water Ratio 'wr_i' versus Final Water Ratio 'wr_f' (Free Expansion Limit).

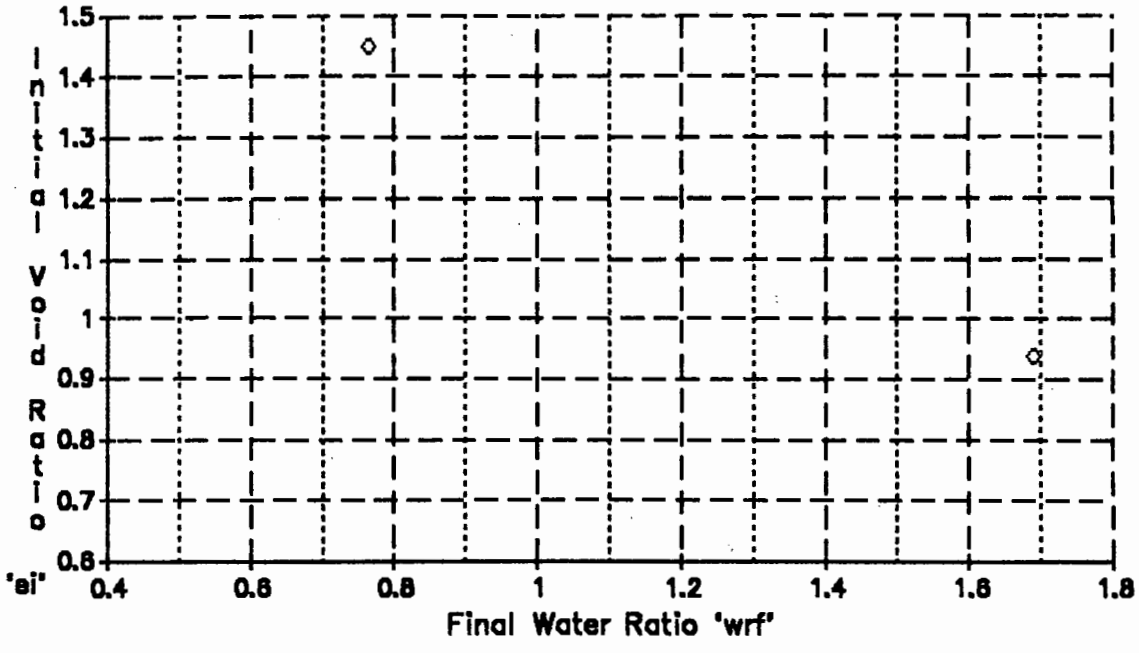

Figure 4.75: Bentonite B.3 (11.5% clay size) - Initial Void Ratio 'e_i' versus Final Water Ratio 'wr_f' (Free Expansion Limit).

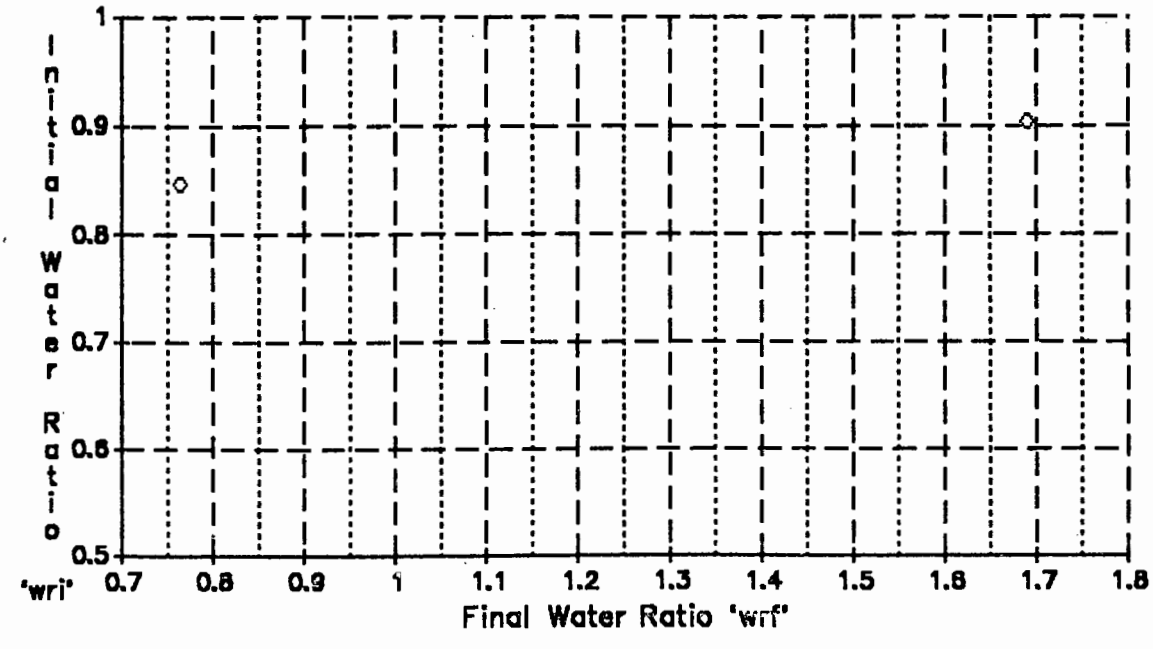

Figure 4.76: Bentonite B.3 (11.5% clay size) - Initial Water Ratio 'wr_i' versus Final Water Ratio 'wr_f' (Free Expansion Limit).

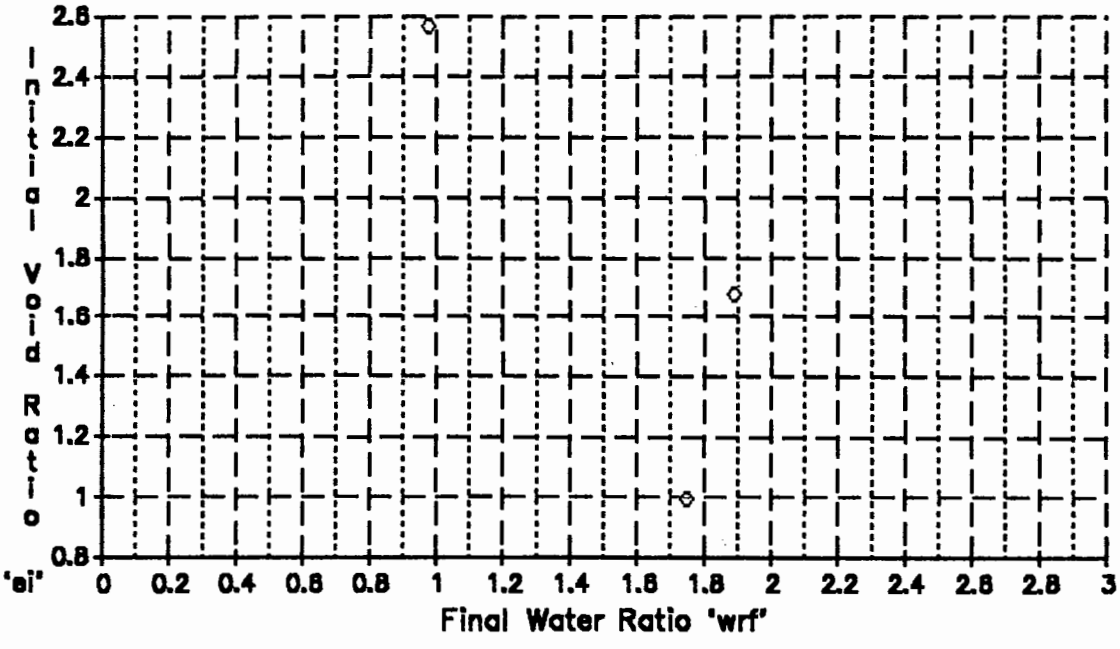

Figure 4.77: Bentonite B.4 (15.5% clay size) - Initial Void Ratio 'e_i' versus Final Water Ratio 'wr_f' (Free Expansion Limit).

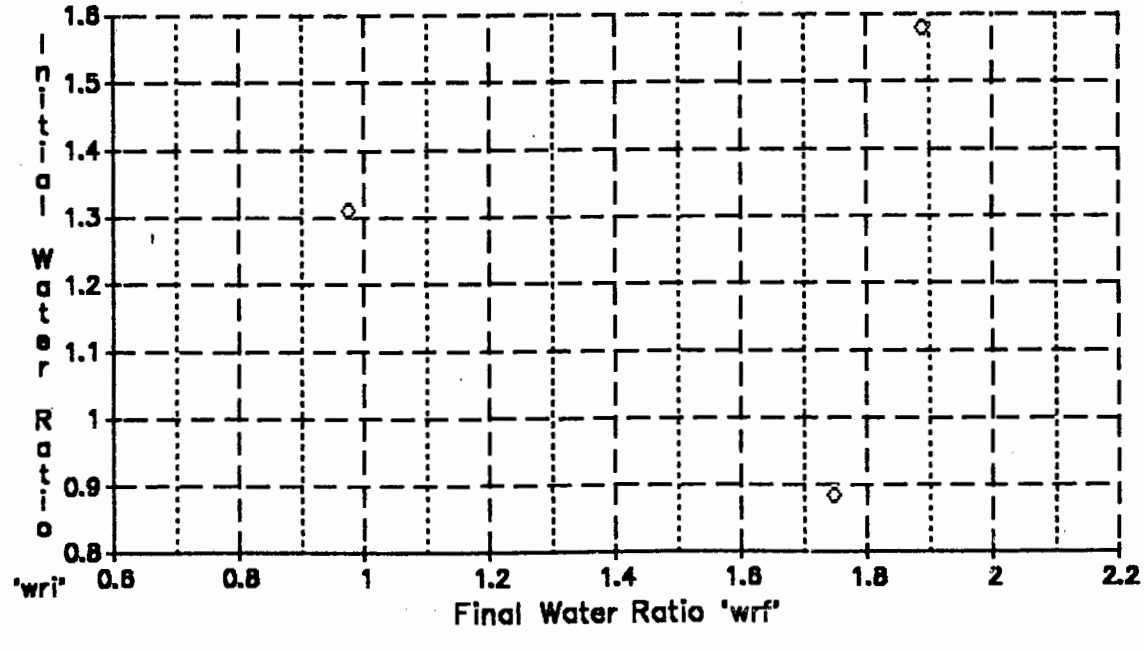

Figure 4.78: Bentonite B.4 (15.5% clay size) - Initial Water Ratio 'wr_i' versus Final Water Ratio 'wr_f' (Free Expansion Limit).

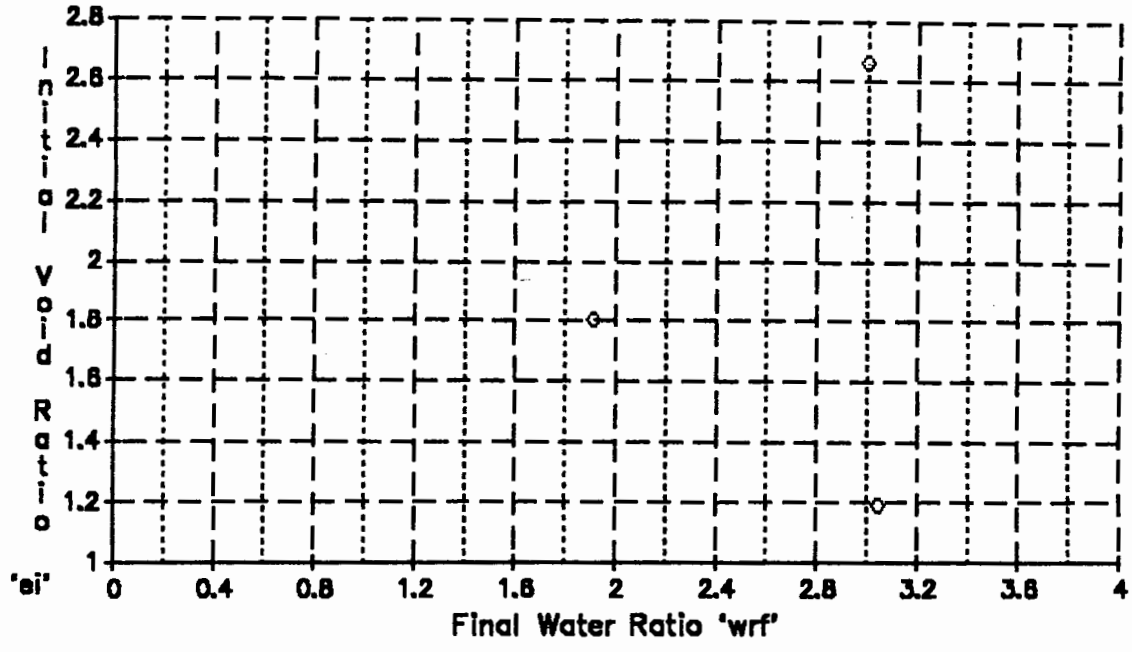

Figure 4.79: Bentonite B.5 (35% clay size) - Initial Void Ratio 'e_i' versus Final Water Ratio 'wr_f' (Free Expansion Limit).

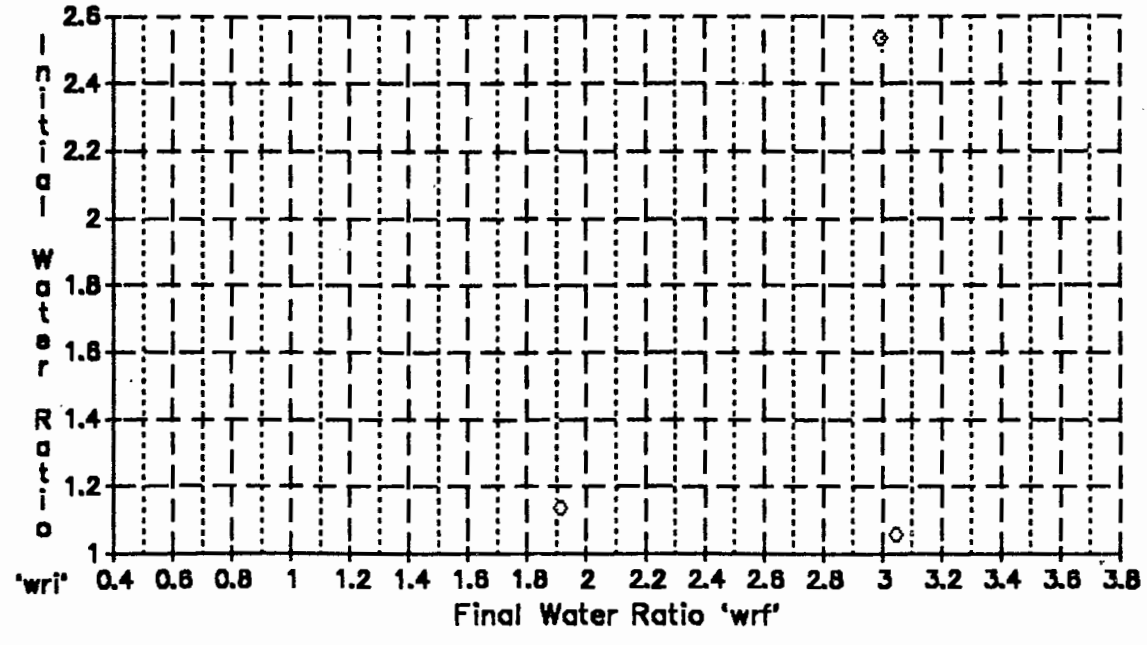

Figure 4.80: Bentonite B.5 (35% clay size) - Initial Water Ratio 'wr_i' versus Final Water Ratio 'wr_f' (Free Expansion Limit).

4.8.2 Free Swell Paths.

Upon being wetted each soil sample[1] follows a free swell path. Representative Free Swell curves were selected from all the free shrinkage and free swell paths which were carried out for the soil types used in this thesis.

The purpose is to study the relationship between void ratio 'e', or change in void ratio 'de', and water ratio 'Ω' or change in water ratio 'dΩ', at each value of degree of saturation. Plots of void ratio versus water ratio, for the free swell paths over the full range of degree of saturation relationships, are included for both natural and artificial soil types.
The following soil types were studied:

Natural Soils.

(i) Site 11, Rosebank, Cape;
(ii) Site 36, Rondebosch, Cape;
(iii) Site 30, Hout Bay, Cape;
(iv) Site A, Berea Road, Durban;
(v) Site 7, Mowbray, Cape;
(vi) Site B, Francois Road, Durban;
(vii) Site C, Margaret Mayton Avenue, Durban;
(viii) Site D, Rose Hill, Durban;

Artificial Soils.

(ix) Kaolin K.1 (13% clay size);
(x) Kaolin K.2 (20% clay);
(xi) Kaolin K.3 (10% clay);
(xii) Bentonite B.1 (3.5% clay size);
(xiii) Bentonite B.2 (7% clay);
(xiv) Bentonite B.3 (11.5% clay);
(xv) Bentonite B.4 (15.5% clay);
(xvi) Bentonite B.5 (35% clay size).

If one examines the Free Swell paths (for example in Figure 4.81) one notices that these free swell paths are all approximately parallel and that very few of these paths reach the saturated condition. All these samples had initial water ratios of about 0.2, but their initial void ratios prior to swelling were different due to different methods of sample preparation. This was the type of result which was anticipated - for example Figures 4.01 (b), (c)[2].

A few samples from Site 7 did appear to swell into the zone where 'Sr' is greater than unity. In later chapters some other soils exhibited this phenomenon, but only when they were under load during swell.

---

[1] - *for each soil type.*
[2] - *in section 4.3 "The parameters which were investigated".*

The interpretation of these relationships is further discussed in Chapter Ten of the thesis - refer to section on "Free Swell Paths".

The mixture B.3 of sand and bentonite also swelled into the region where Sr is greater than unity. The longest range of void ratio during swelling was exhibited by the sand and bentonite mixture B.5[1].

From previous tests, Prof Sparks anticipated that certain soils when saturated might appear to lie in the zone where the degree of saturation is greater than unity; he believed that this could be due to the density of the adsorbed water layer being greater than that of normal free water even when the sample is saturated.
In view of the fact that some soils have appeared to have a calculated degree of saturation which is greater than unity, it seems that Prof Sparks might be correct in his reasoning, and that the curve in Figure 2.21 (of Chapter Two[2]) can be above the normal density of water for certain clays even at high water contents.

---

1 - see Figure 4.96 at the end of this section.
2 - refer to "Adsorbed water on clay", in section 2.4.2.

Natural Soil Types:-

Site 11, Rosebank.

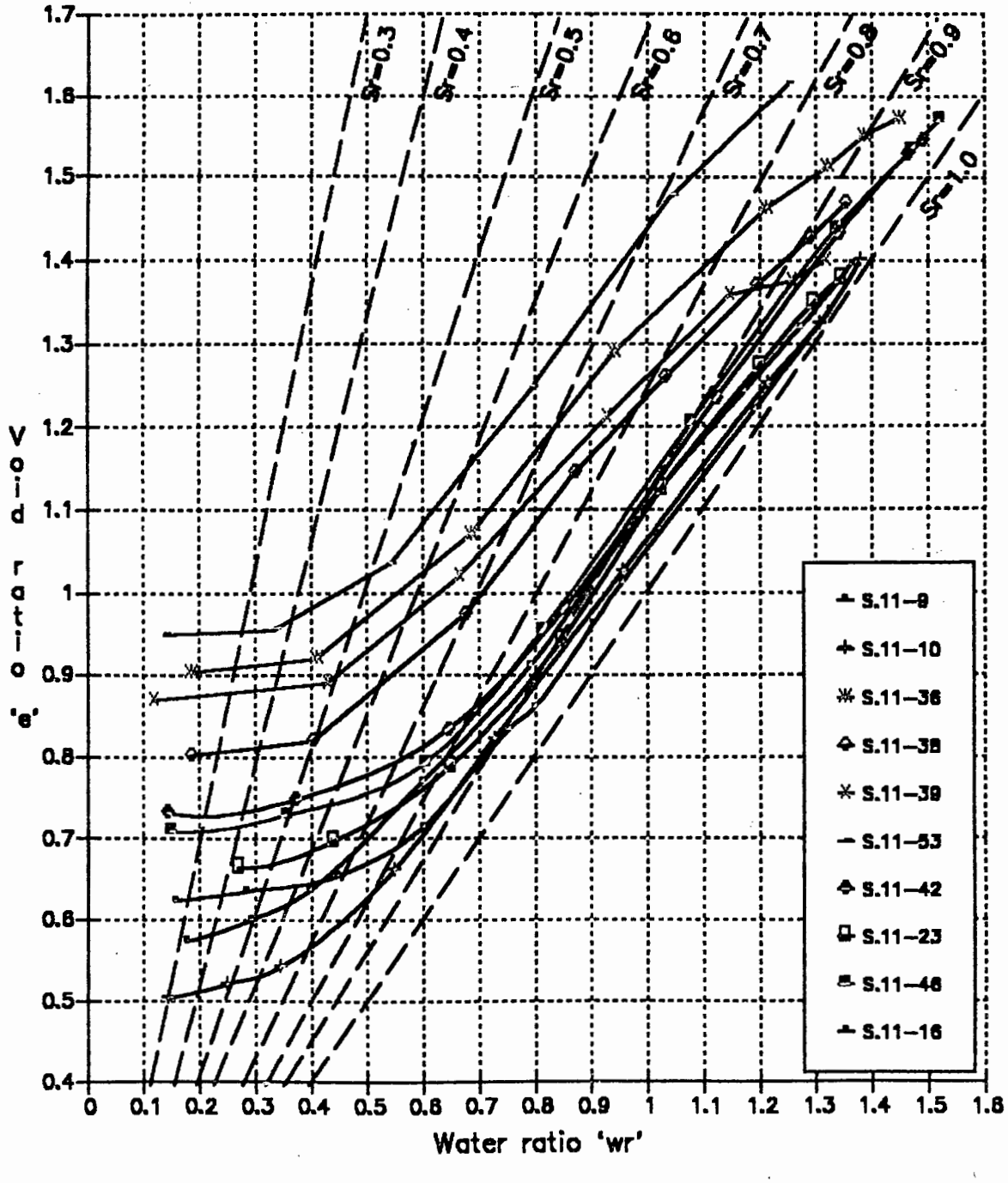

Figure 4.81: Site 11, Rosebank [Remoulded and Compacted samples] - Plots of Void Ratio 'e' versus Water Ratio 'wr' for the Free Swell Paths over the full range of Degree of Saturation 'Sr'.

Site 36, Rondebosch.

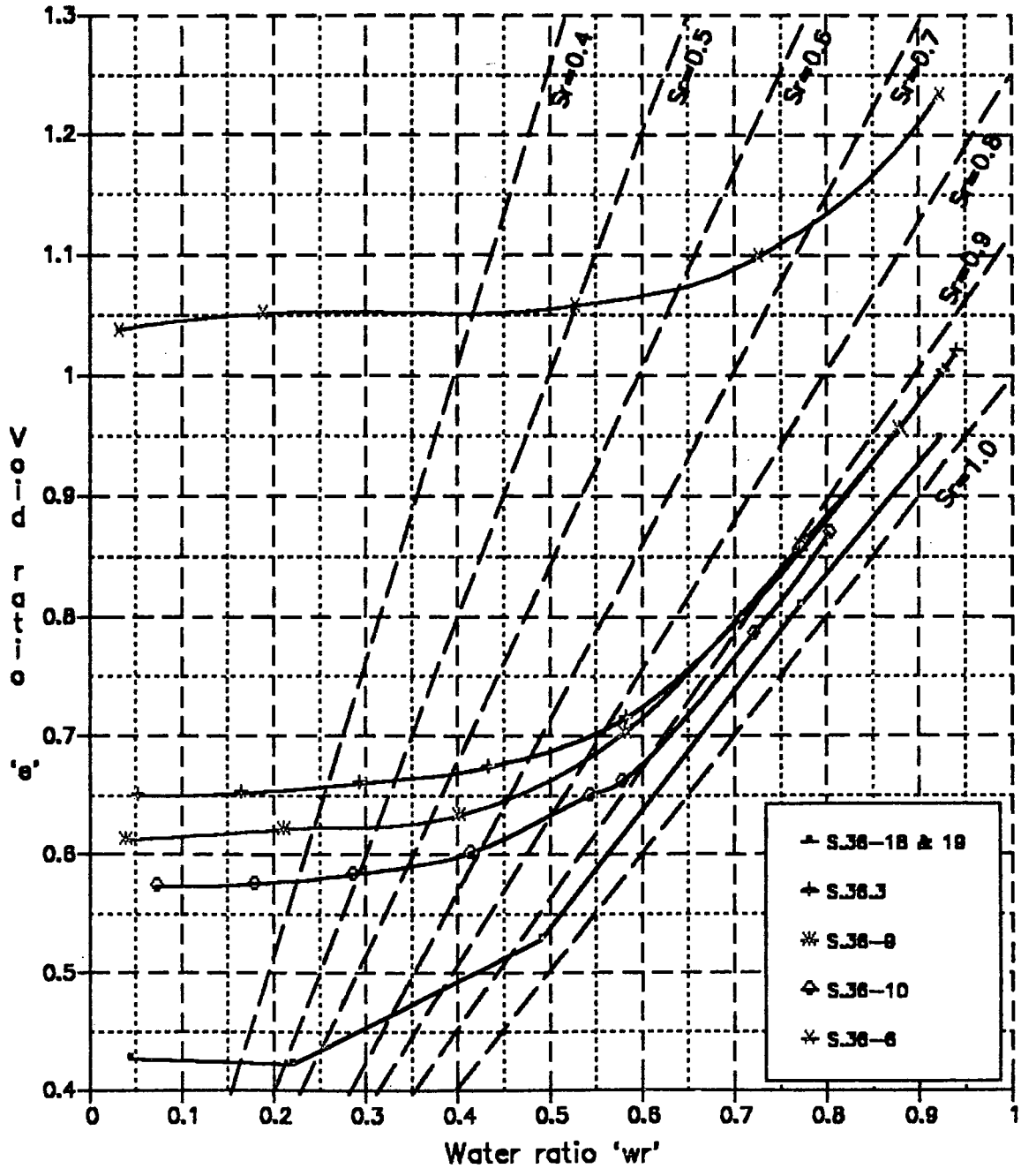

Figure 4.82: Site 36, Rondebosch [Remoulded and Compacted samples] - Plots of Void Ratio 'e' versus Water Ratio 'wr' for the Free Swell Paths over the full range of Degree of Saturation 'Sr'.

Site 30, Hout Bay.

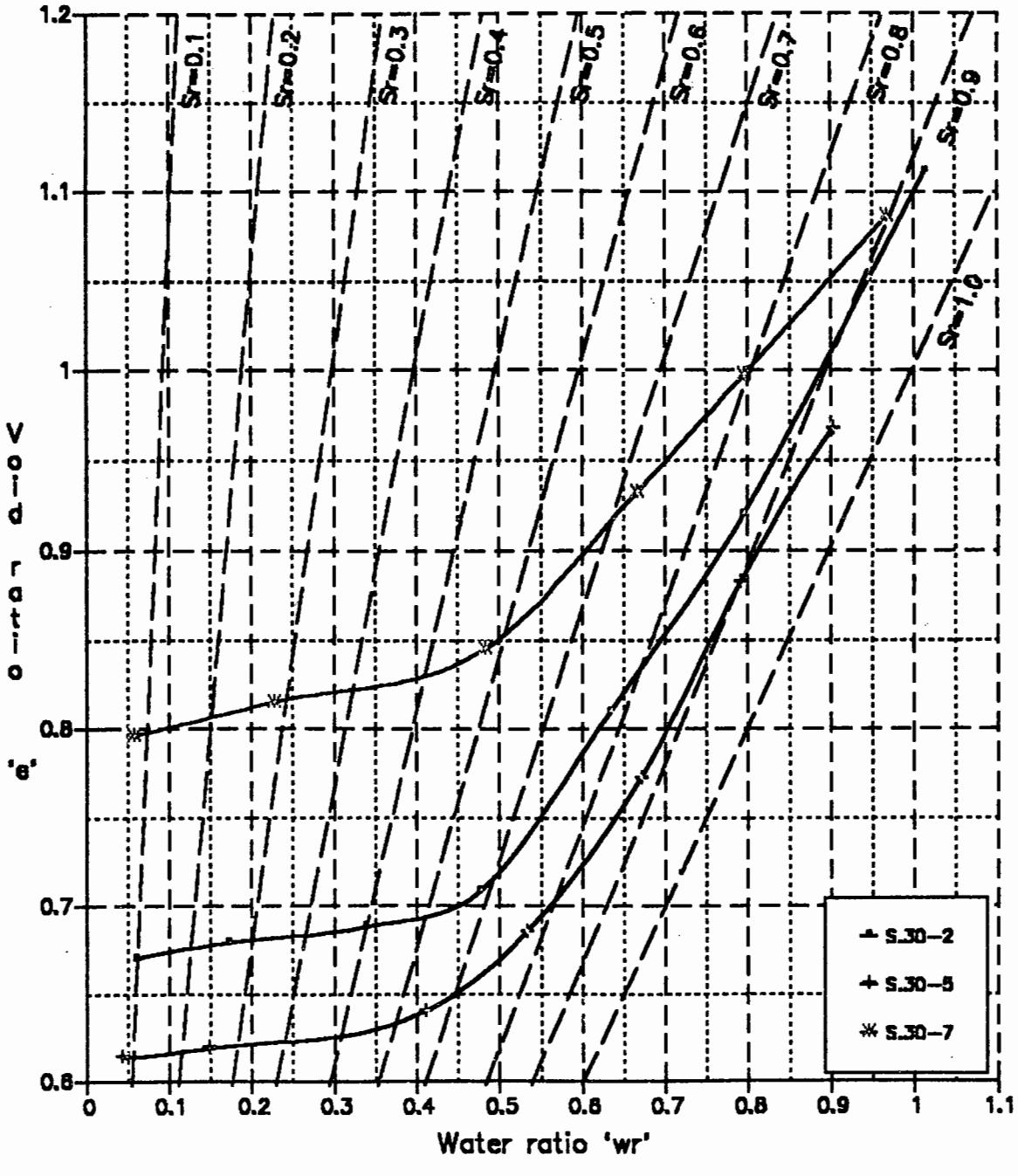

Figure 4.83: Site 30, Hout Bay [Remoulded samples] - Plots of Void Ratio 'e' versus Water Ratio 'wr' for the Free Swell Paths over the full range of Degree of Saturation 'Sr'.

Site A, Berea Road.

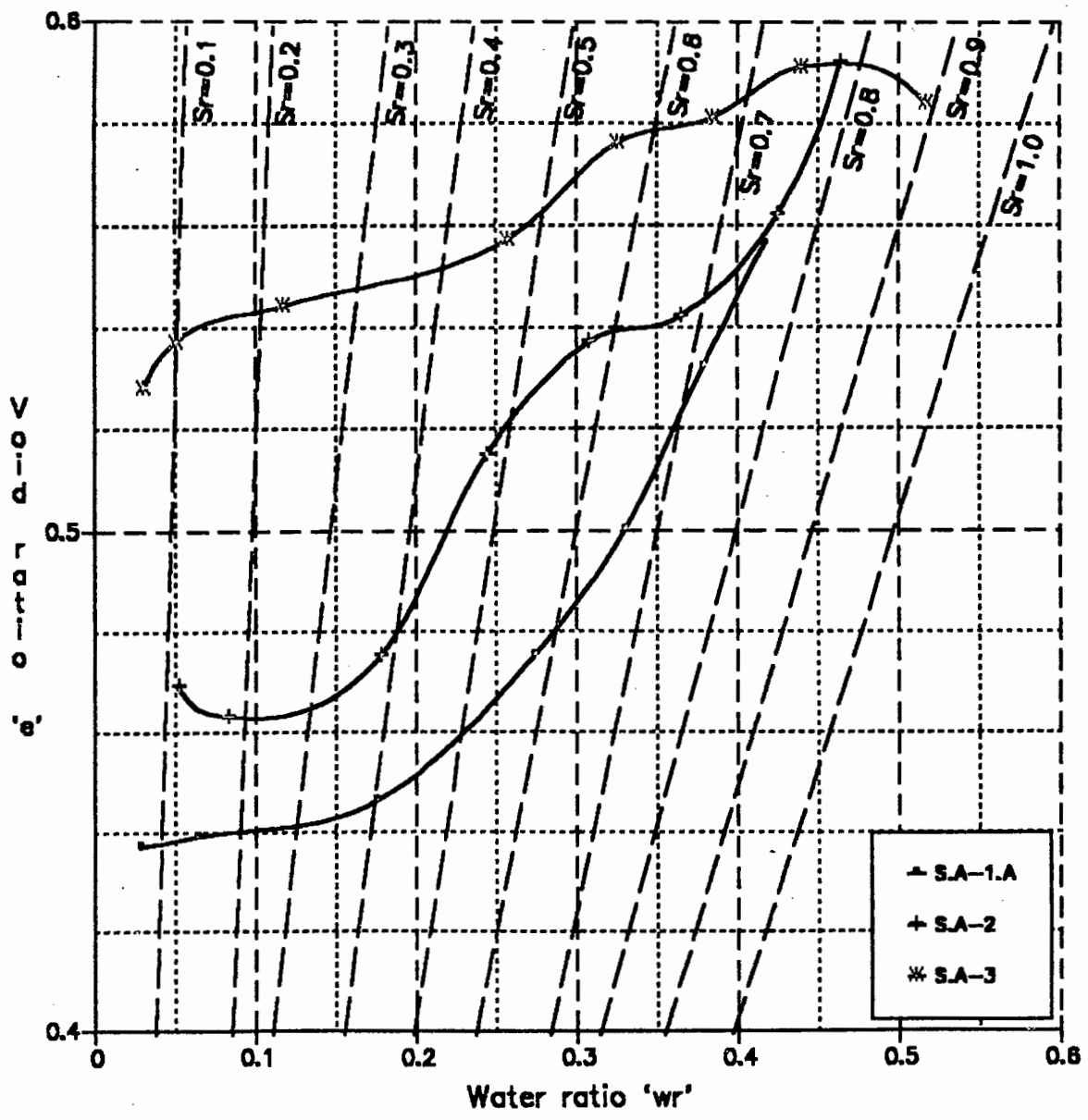

Figure 4.84: Site A, Berea Road [Remoulded and Compacted samples] - Plots of Void Ratio 'e' versus Water Ratio 'wr' for the Free Swell Paths over the full range of Degree of Saturation 'Sr'.

Site 7, Mowbray.

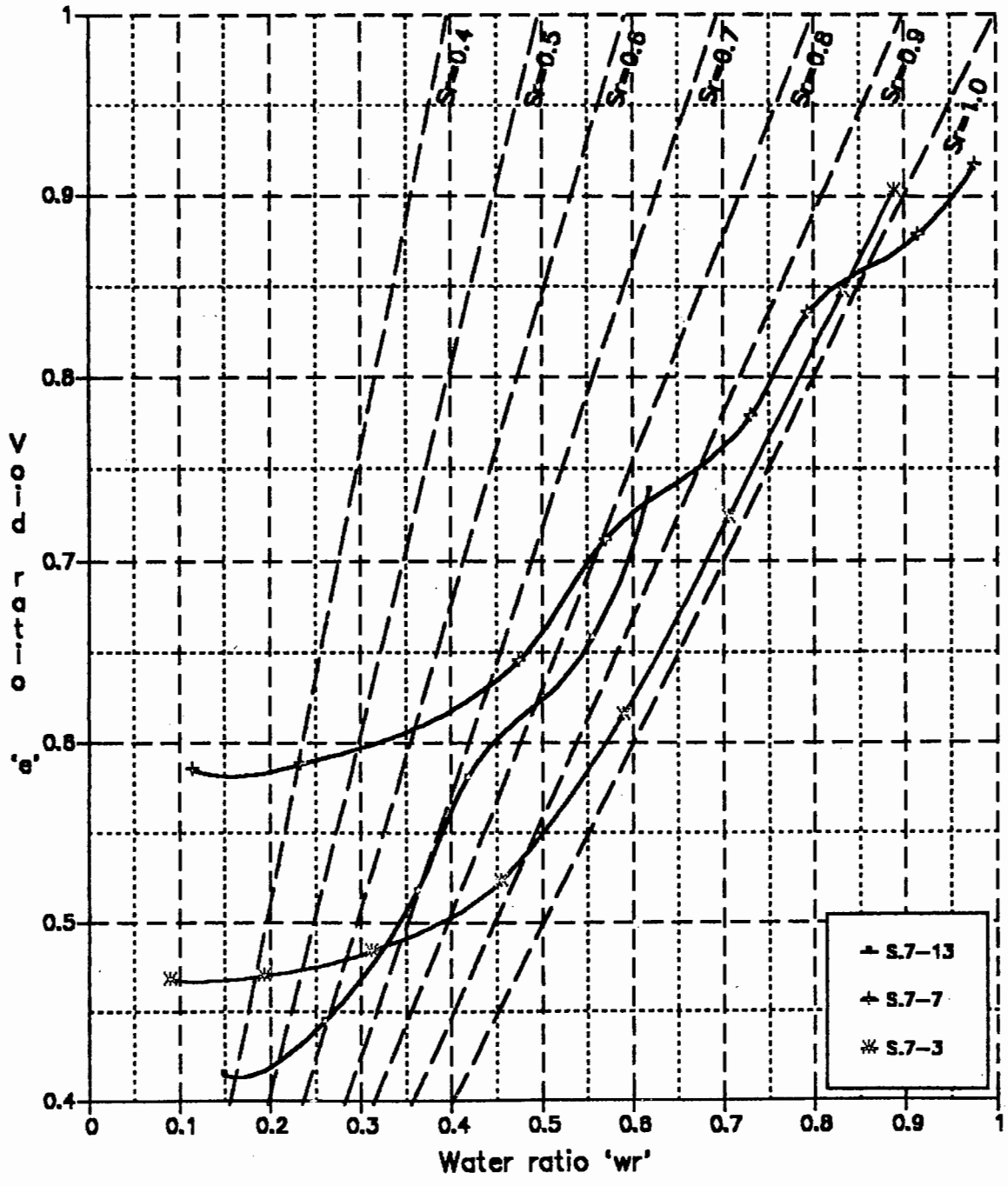

Figure 4.85: Site 7, Mowbray [Remoulded and Compacted samples] - Plots of Void Ratio 'e' versus Water Ratio 'wr' for the Free Swell Paths over the full range of Degree of Saturation 'Sr'.

Site 'B' Francois Road.

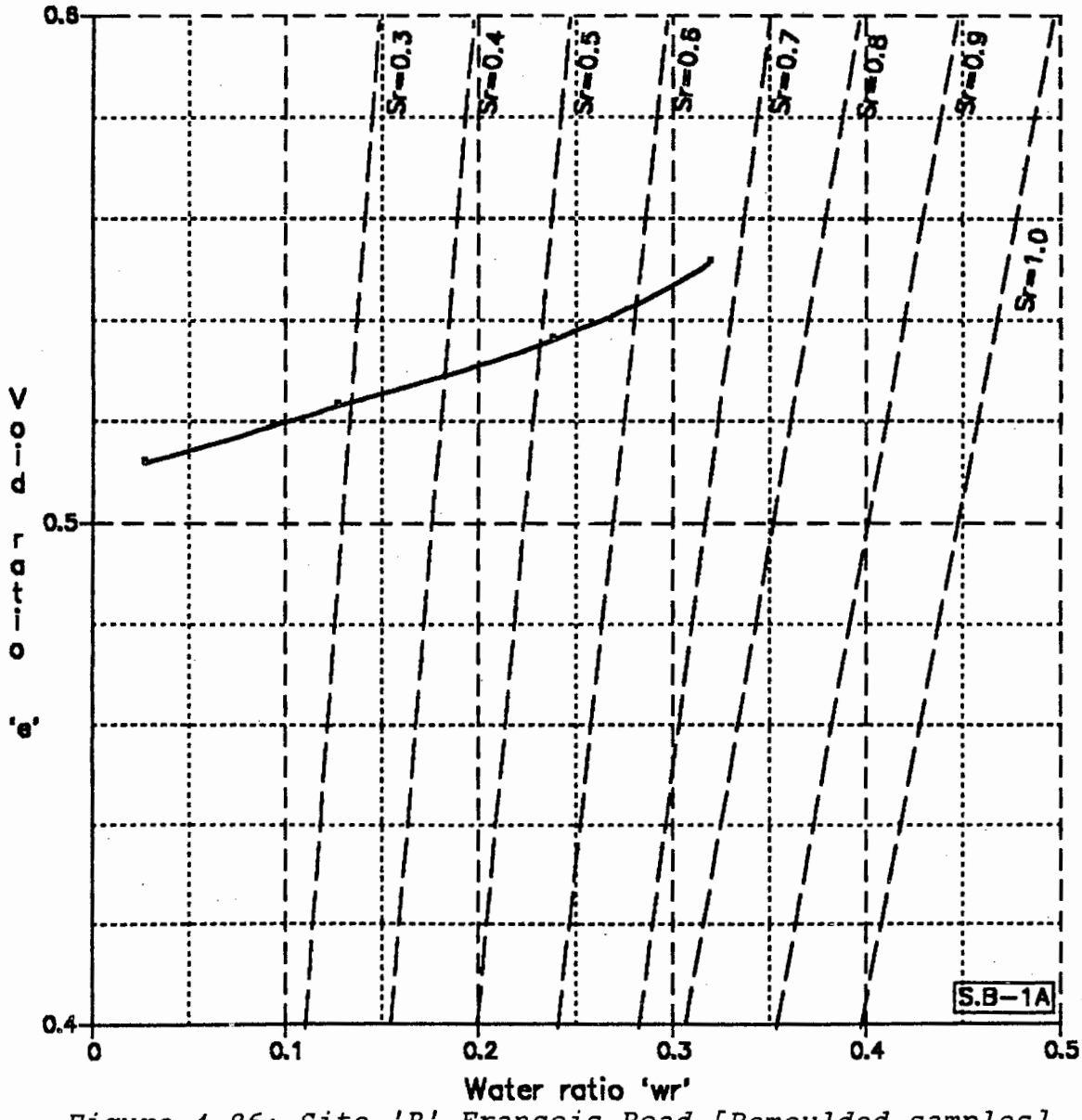

Figure 4.86: Site 'B' Francois Road [Remoulded samples] - Plots of Void Ratio 'e' versus Water Ratio 'wr' for the Free Swell Paths over the full range of Degree of Saturation 'Sr'.

Site 'C' Margaret Mayton Avenue.

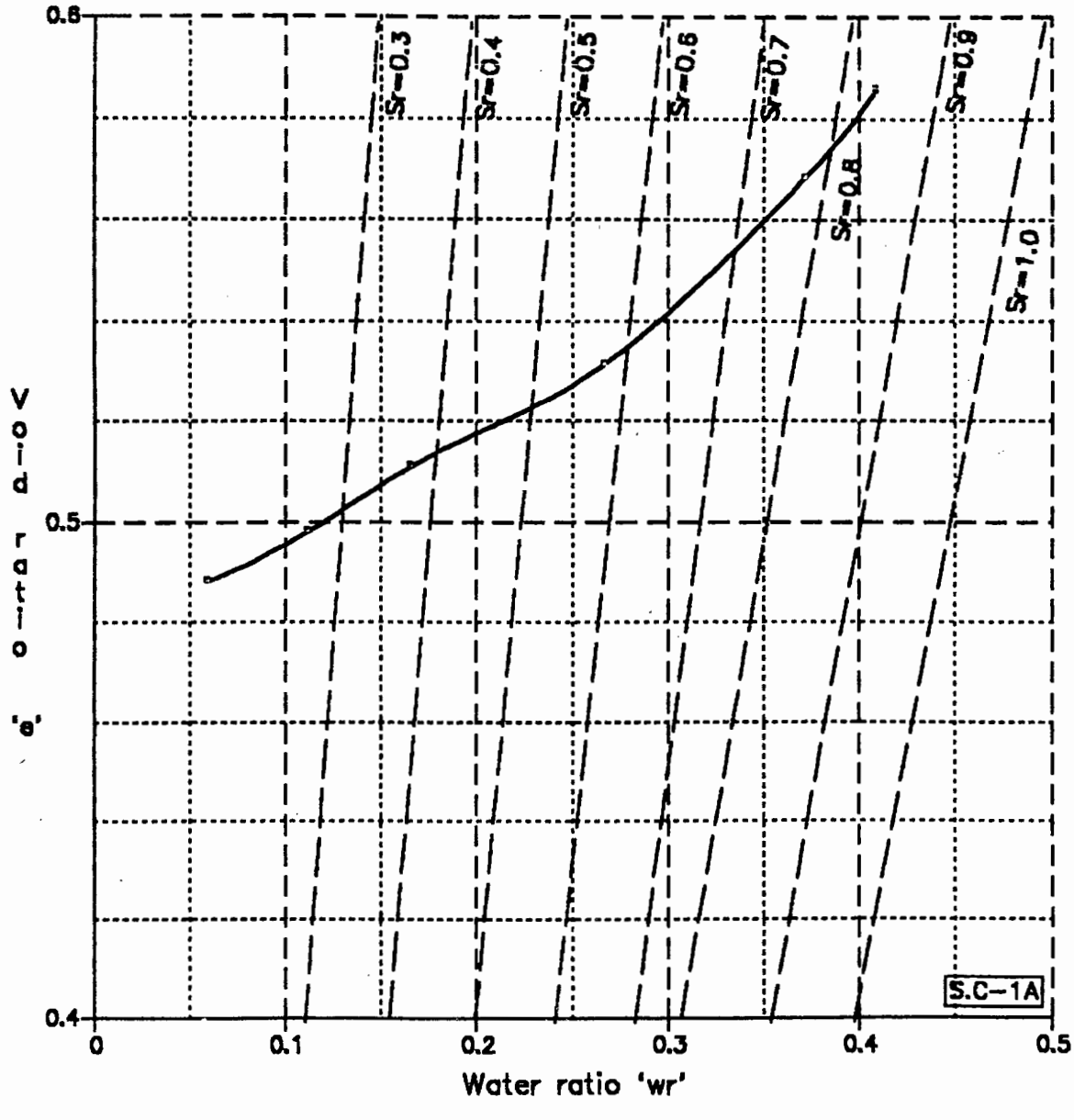

Figure 4.87: Site 'C' Margaret Mayton Avenue [Remoulded sample] - Plots of Void Ratio 'e' versus Water Ratio 'wr' for the Free Swell Paths over the full range of Degree of Saturation 'Sr'.

Site 'D' Rose Hill.

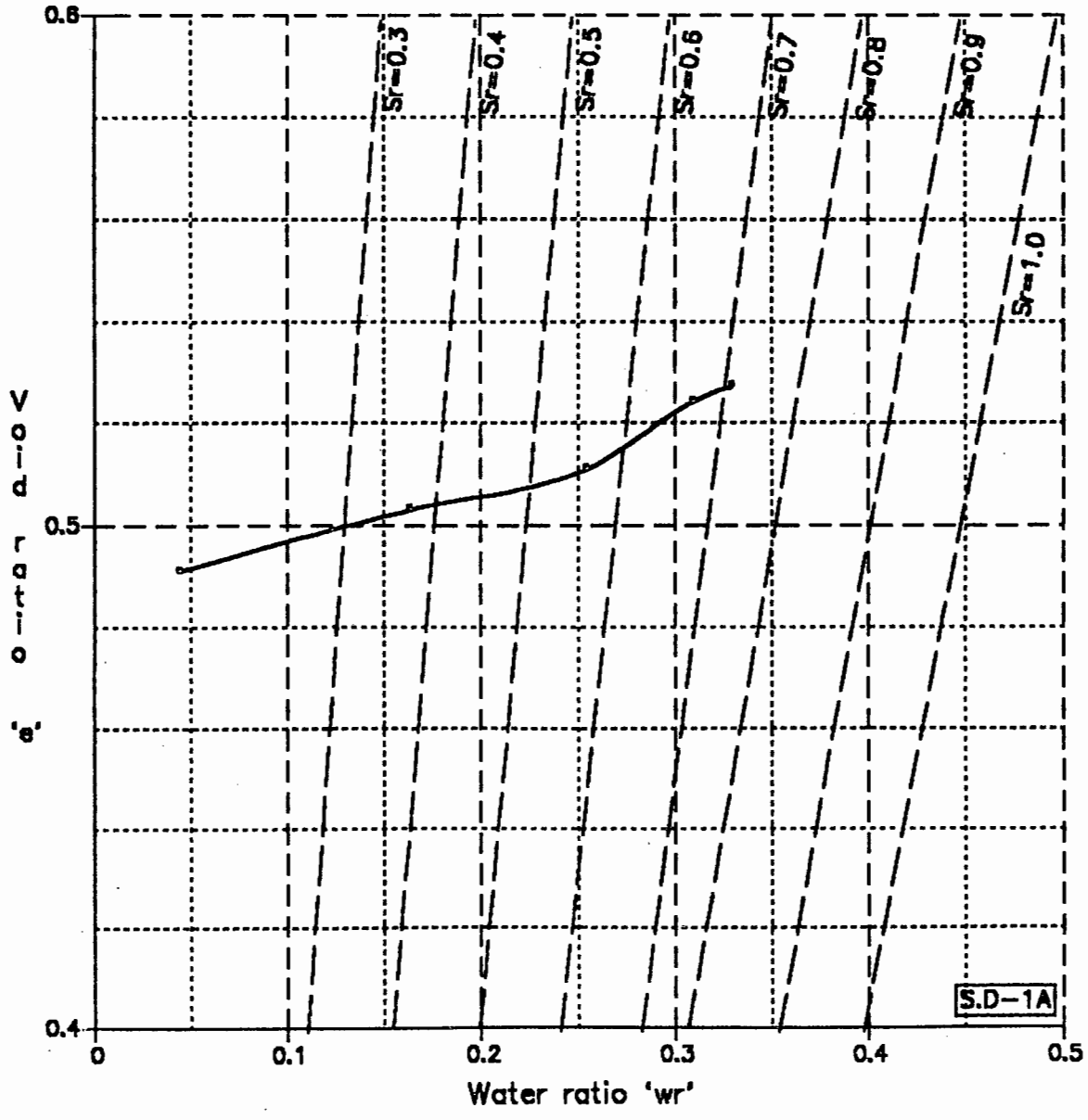

Figure 4.88: Site 'D' Rose Hill [Remoulded sample] - Plots of Void Ratio 'e' versus Water Ratio 'wr' for the Free Swell Paths over the full range of Degree of Saturation 'Sr'.

Artificial Soil Types:-

Kaolin K1 (13% clay size).

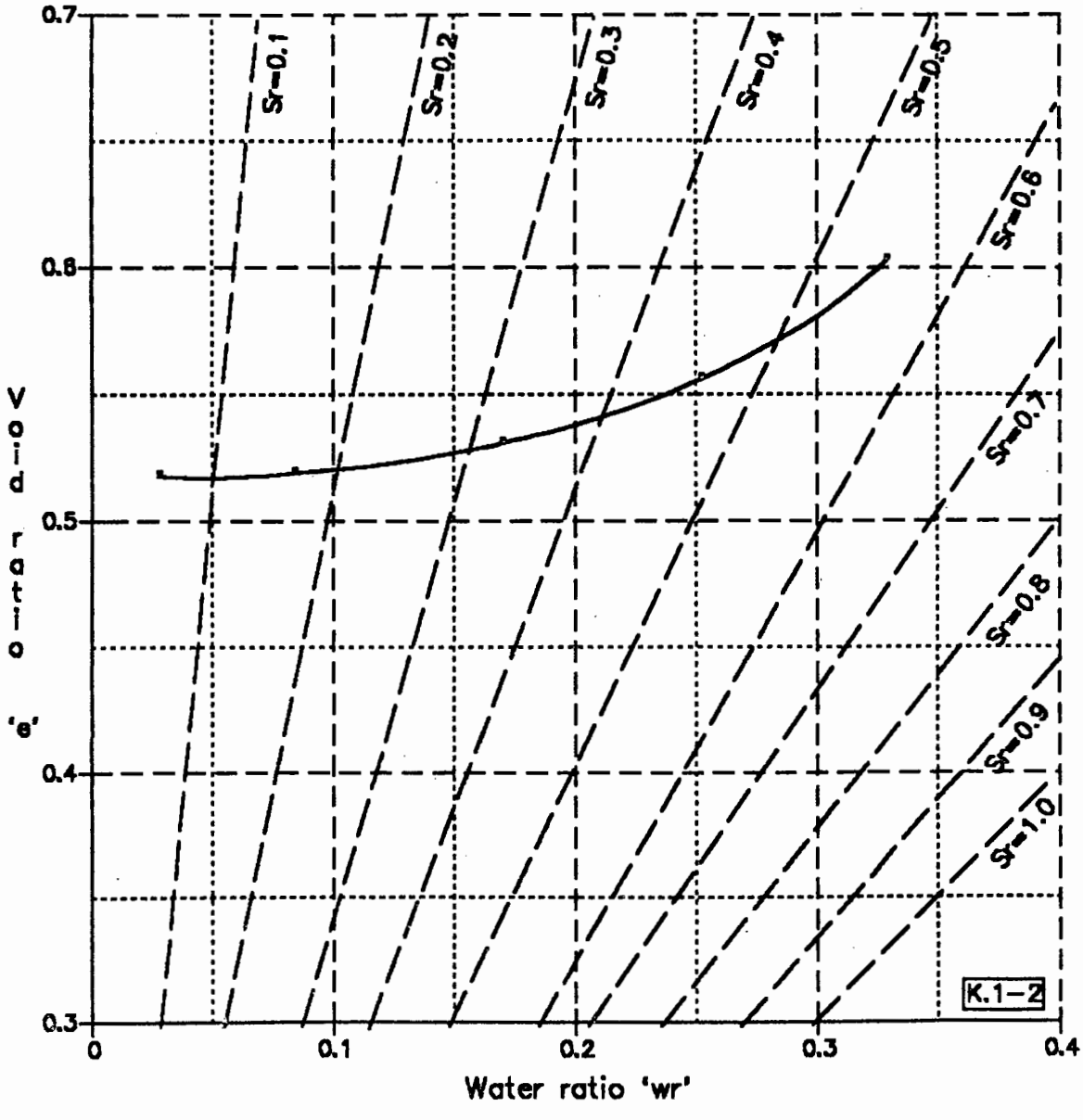

Figure 4.89: Kaolin K1 (13% clay size) - Plots of Void Ratio 'e' versus Water Ratio 'wr' for the Free Swell Paths over the full range of Degree of Saturation 'Sr'.

Kaolin K2 (20% clay size).

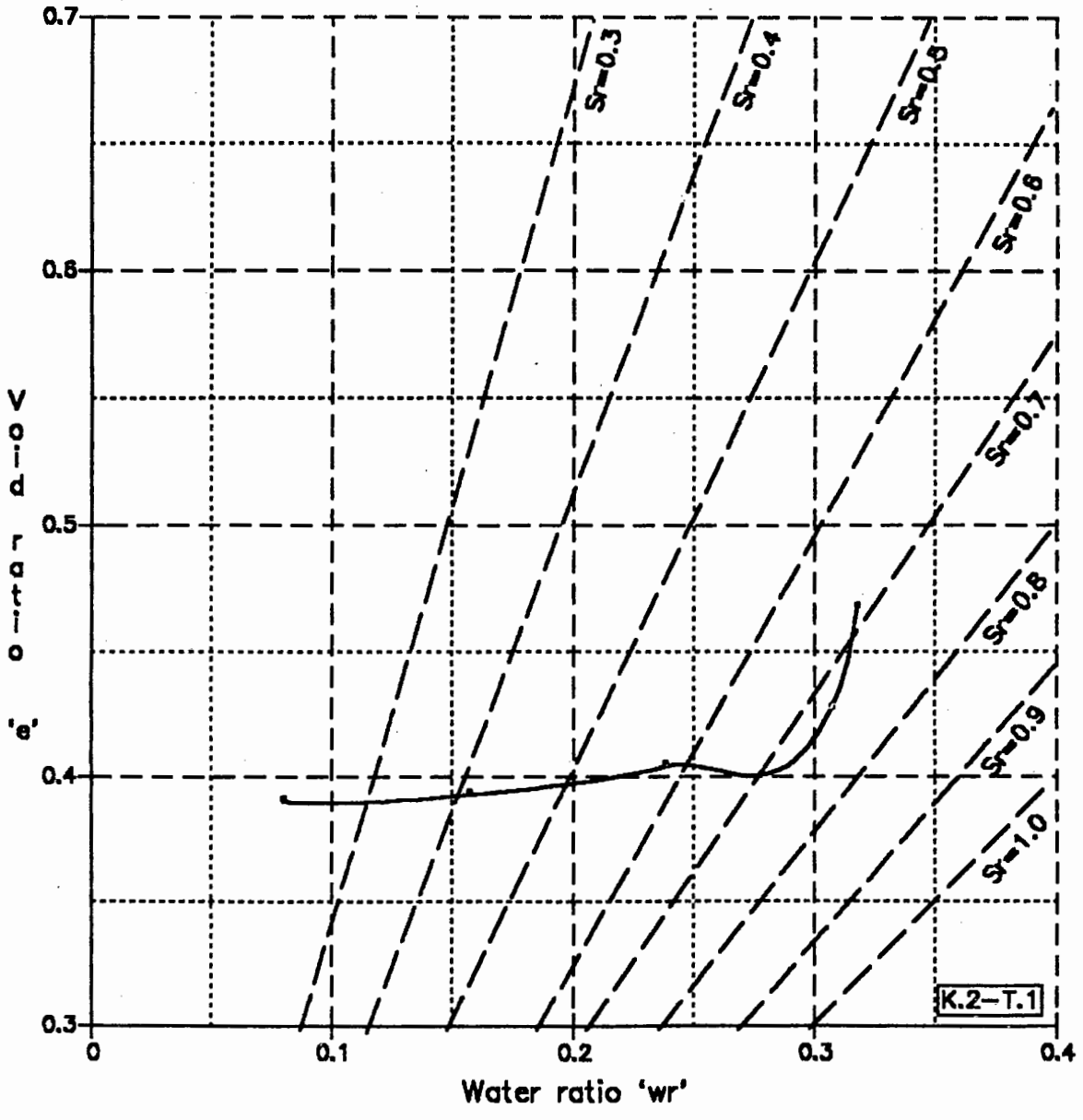

Figure 4.90: Kaolin K2 (20% clay size) - Plots of Void Ratio 'e' versus Water Ratio 'wr' for the Free Swell Paths over the full range of Degree of Saturation 'Sr'.

Kaolin K3 (10% clay size).

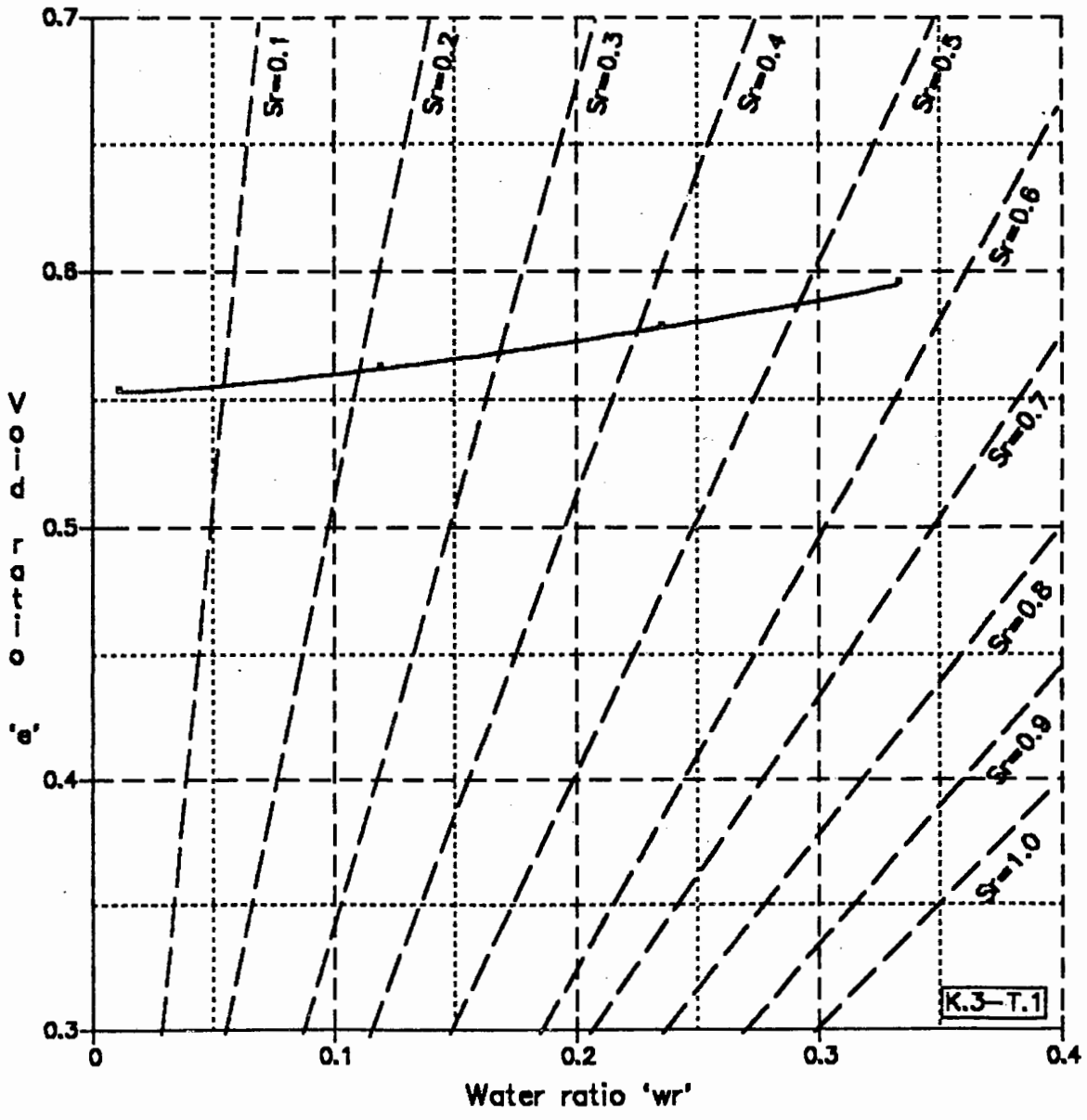

Figure 4.91: Kaolin K3 (10% clay size) - Plots of Void Ratio 'e' versus Water Ratio 'wr' for the Free Swell Paths over the full range of Degree of Saturation 'Sr'.

Bentonite B1 (3.5% clay size).

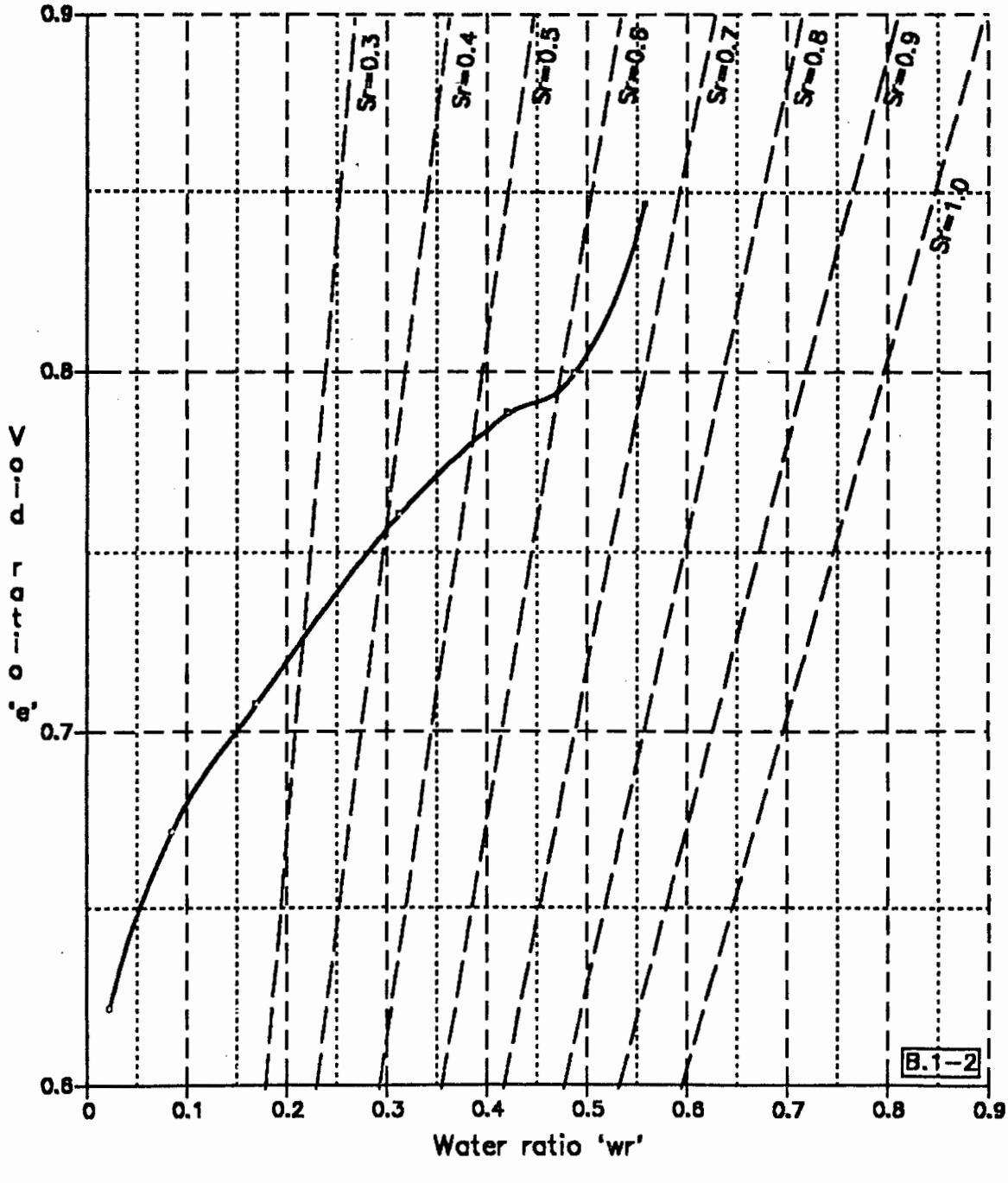

Figure 4.92: Bentonite B1 (3.5% clay size) - Plots of Void Ratio 'e' versus Water Ratio 'wr' for the Free Swell Paths over the full range of Degree of Saturation 'Sr'.

Bentonite B2 (7% clay size).

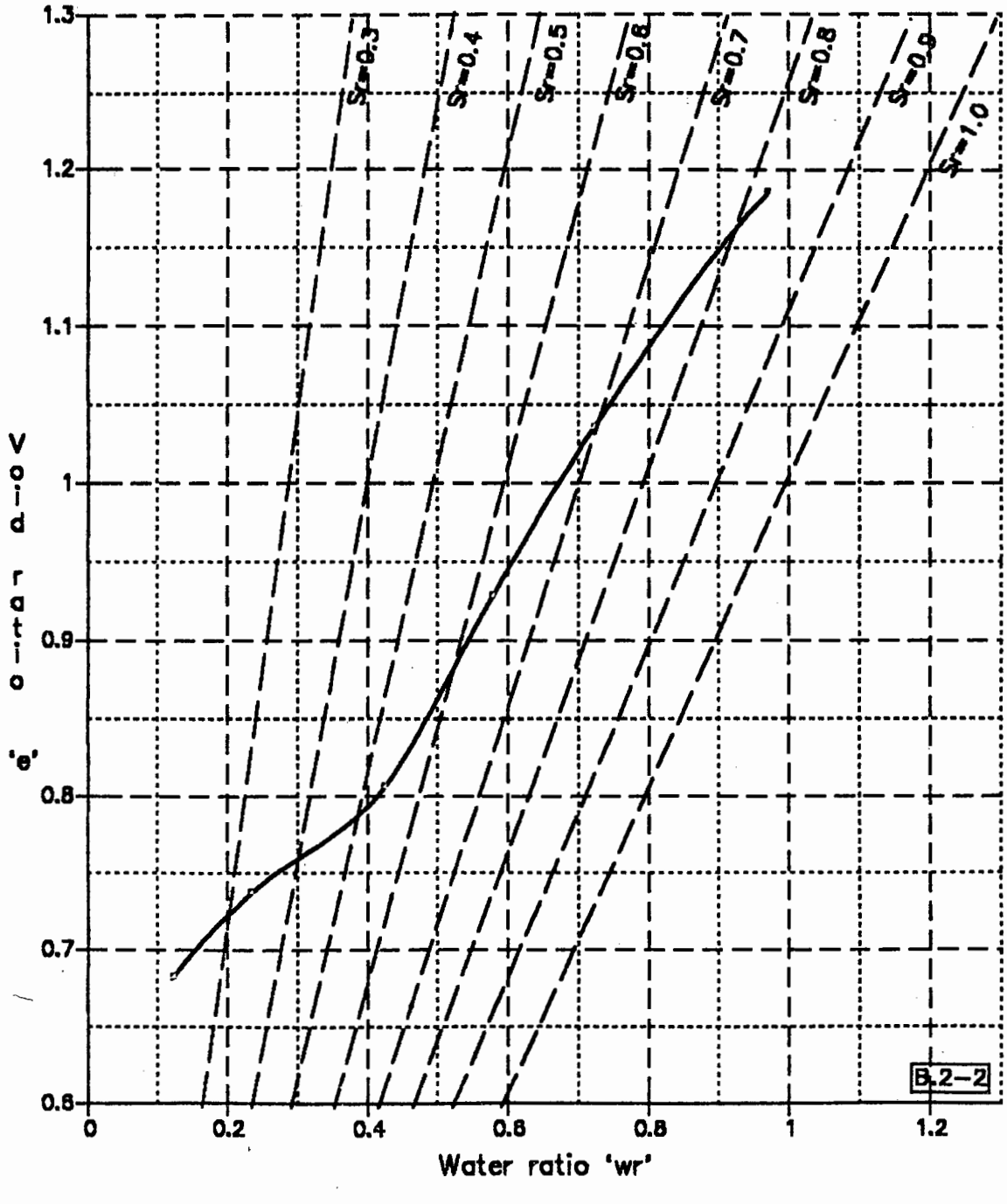

Figure 4.93: Bentonite B2 (7% clay size) - Plots of Void Ratio 'e' versus Water Ratio 'wr' for the Free Swell Paths over the full range of Degree of Saturation 'Sr'.

Bentonite B3 (11.5% clay size).

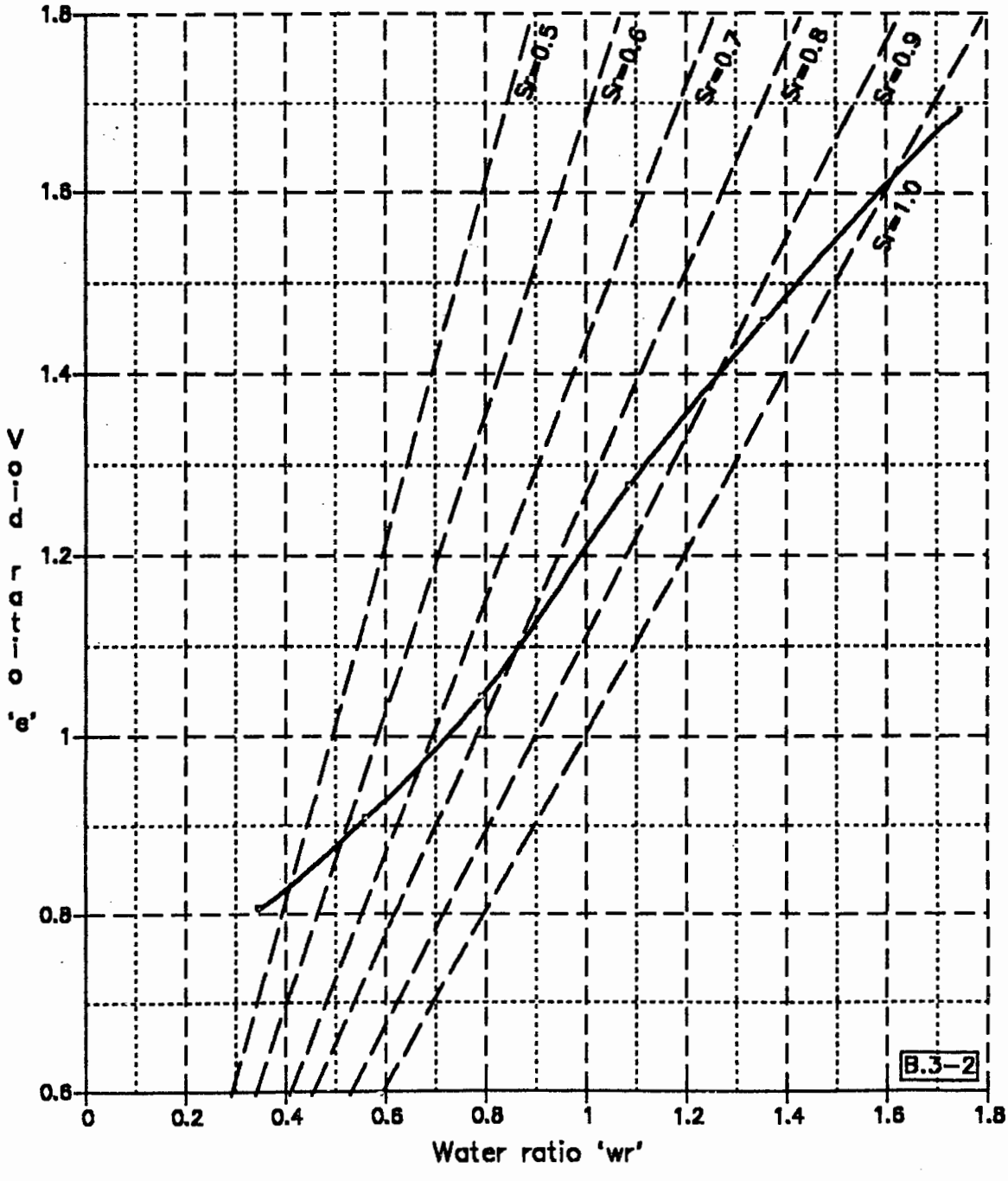

Figure 4.94: Bentonite B3 (11.5% clay size) - Plots of Void Ratio 'e' versus Water Ratio 'wr' for the Free Swell Paths over the full range of Degree of Saturation 'Sr'.

Bentonite B4 (15.5% clay size).

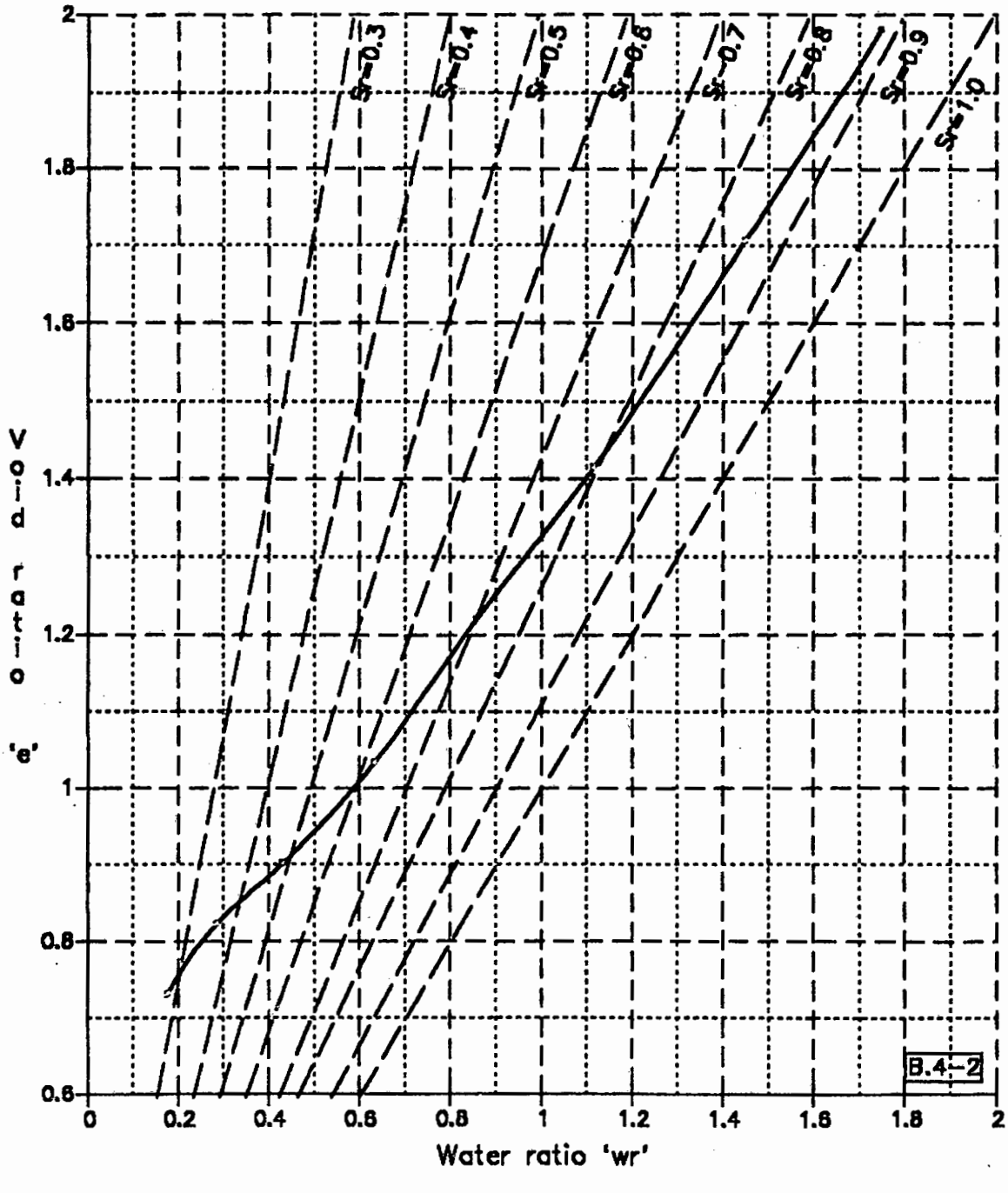

Figure 4.95: Bentonite B4 (15.5% clay size) - Plots of Void Ratio 'e' versus Water Ratio 'wr' for the Free Swell Paths over the full range of Degree of Saturation 'Sr'.

4.9 REFERENCES FOR CHAPTER FOUR

16. DE S VINAGRE, T.J.V. (1976/77): Masters Thesis - Diaries One, Two, Three, Four, Five, and Six.

84. SPARKS, A.D.W. (1961): "Partly Saturated Soils - classification; compressibility of the fluid phase; stress equations" - M.Sc. (Eng) thesis. University of the Witwatersrand.

85. SPARKS, A.D.W. (1967): A theory of consolidation for partially saturated soils. The Civil Engineer in South Africa, S.A.I.C.E., accepted October 1960, published July 1967.

86. SPARKS, A.D.W. (1975): Discussions, Vol.II, Proceedings of the Sixth Regional Conference for Africa on Soil Mechanics and Foundation Engineering; Durban, South Africa, September 1975.

87. BRACKLEY, I.J.A. (1975): A model of unsaturated clay structure and its application to swell behaviour. Sixth Regional Conf. for Africa on Soil Mech. and Foundation Eng., Durban, South Africa.

90. SPARKS, A.D.W. (1959): A Semigraphical Method for determining the Initial Compression during Consolidation in a Partially Saturated Soil. 2nd African Regional Conf. on Soil Mechanics & Foundation Eng.. Lourenco Marques.

91. SPARKS, A.D.W. (Supervisor): Discussions with the writer.

CHAPTER FIVE *

FITTING STRESS SCALES TO OBSERVED DATA

5.1 INTRODUCTION

This chapter deals with the observed changes in the void ratio of saturated soil samples as the result of either an increase, or decrease, in the amount of pressure being applied to compress the samples. The consolidation of soil samples that takes place due to the applied effective pressures (or stresses), relates to the type of test used.

The observed data was obtained from two types of tests:
(1) One-dimensional consolidation; and,
(2) Isotropic consolidation.

For each type of test, the observed void ratios (at the end of each step of applied pressure) and effective pressures are presented in graphical form in order to enable the extrapolation of stress values. A stress scale is the full set of stress values for each soil type.

The first type of scales were derived from the 'void ratio versus effective pressure (or stress)' relationship produced by the ordinary one-dimensional drained consolidometer test for saturated soil samples. The second type of scales were derived from the isotropic consolidation of the soil sample under drained conditions. This consolidation takes place as the result of an average all-round pressure (or stress) being applied by means of triaxial test equipment. The stress scales are fitted to the 'void ratio versus water content' plots used to determine the Shrinkage Limit of each soil type. These plots were previously defined in Chapter Four.

5.2 DEFINITIONS

The concepts of "Fitting stress scales to observed data", "One-dimensional consolidation", and "Isotropic or all-round consolidation", can be defined as follows:

"Fitting stress scales to observed data".

It was previously stated in Chapter Four (refer to section "Reasons for using the type of plot shown in Figure 4.01") that the free-shrinkage, or free-swell, path can be regarded as evidence of isotropic consolidation, or swelling, due to effective stresses which are isotropic at each point of unconfined soil samples.

---

* - *Observations are in Appendix D.*

Further, that it was possible that the results of the relationship between void ratio and effective stress, obtained from a triaxial compression test performed on the same soil, can be used to provide a stress scale on the diagram of Figure 4.01(b).

"One-dimensional consolidation".

One dimensional consolidation of the soil sample can be defined as the void ratio reduction that takes place as a function of time (that is, the rate and magnitude of consolidation of the soil), when the sample is restrained laterally and loaded (and drained) axially.

"Isotropic or all-round consolidation".

The all-round[1] drained consolidation test is one in which drainage is permitted throughout the test so that consolidation of the soil sample occurs under an applied all round stress. It is an attempt to satisfy the condition of zero pore water pressure.
Because the pore water pressure is zero, the effective stresses are equal to the applied stresses.
The drained test provides information on the volume changes which accompany the application of all round pressure, and on the stress-volumetric strain characteristics of the soil.

It should be noted that deformation and volume-change characteristics in drained tests are largely controlled by the sequence and sign of the stress changes.

The section on 'Macro Studies' in Chapter Two[2] includes the definitions of void ratio 'e', water content 'w', and water ratio 'Ω' or 'wr'.

5.3 THE PARAMETERS WHICH ARE BEING INVESTIGATED

The diagram in Figure 5.01 illustrates the main parameters which are being investigated. These parameters are the void ratios and the effective pressures to which the soil sample is subjected, either as one dimensional or isotropic consolidation.

The vertical axis of the diagram, in Figure 5.01, represents the void ratio of the soil sample (alternatively, the total volume may be used), and the horizontal axis represents the effective pressure being applied to the sample.

---

1 - or three dimensional.
2 - refer to section 2.2.

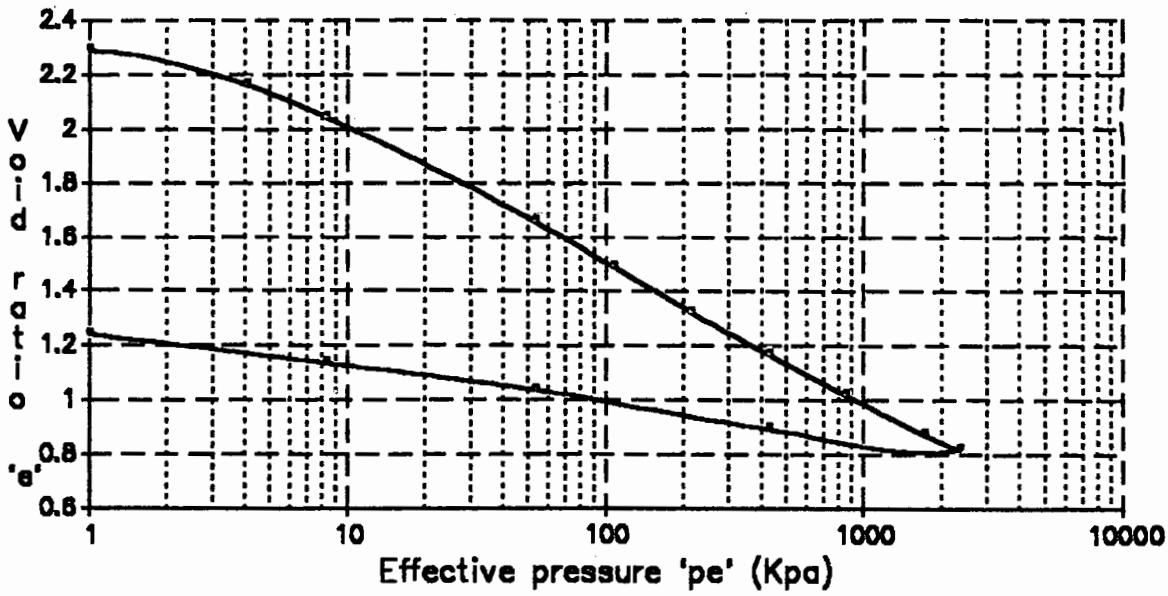

Figure 5.01: Relationship between the void ratio and the logarithm of the effective pressure (or stress).

In the case of the one dimensional consolidation test, the vertical axis represents the effective vertical pressure being applied to a sample which is restrained laterally.
And, for the isotropic consolidation test, the vertical axis represents the effective all-round (three dimensional), or average, effective pressure being applied to the sample.
Throughout the tests the water content of the soil sample remains in a saturated condition[1] as all the voids are filled with water.

In both one-dimensional and isotropic consolidation tests, the sample is initially at a saturated[2] condition. This condition was previously illustrated in Figure 4.01(b), of Chapter Four, as condition A.
As the sample is loaded in stages (that is, after the sample has consolidated under drained conditions, the effective pressure is increased to the next value) both the total volume and the void ratio decrease as the water is expelled. Throughout the test, the water content of the sample remains in a saturated condition.
The state of the sample moves towards B, along the saturated path, previously shown in Figure 4.01(b), as path AB.
The saturated path followed by the sample (Sr = 100%) is illustrated in Figure 5.02.

---

[1] - *100% degree of saturation.*
[2] - *near Liquid Limit.*

5.4 STRESS SCALES AND THE TYPE OF PLOT SHOWN IN FIGURE 5.02

Sparks[1] used several types of stress scales on a diagram such as Figure 5.02 in order to predict and model the volume changes for a soil. His stress scales include scales for isotropic consolidation and many different scales for one-dimensional consolidation. In the case of one-dimensional consolidation, Sparks used values based on different values of Poisson's ratio, and he also used a different assumption, namely that the horizontal effective stress during the compression cycle in one-dimensional consolidation could rise rapidly from a value of zero, to a value of one quarter of the vertical effective stress, other ratios were assumed for the unloading cycles.

Two of the main specific objectives in this thesis:-

(1) To obtain the void ratio for each effective pressure (or stress) applied, under drained conditions, to a soil sample whose water content remains in a saturated condition throughout the test.
These effective pressures were either applied as a vertical pressure (refer to the one dimensional consolidation of a sample being restrained laterally), or as an all round pressure (in the case of isotropic consolidation).

(2) The pressure (or stress) values for each recorded void ratio are added to the free shrinkage path (that is, the path used to determine the Shrinkage Limit) of the type of plot previously shown in Figure 4.01(b).
The resulting stress scales are illustrated in Figure 5.02.

In the Figure 5.02 the pressure values shown as the isotropic consolidation pressures, on the right of the inclined saturated line, are the cell pressures used in a triaxial apparatus to achieve isotropic consolidation to the corresponding void ratio indicated on the vertical axis of Figure 5.02.
Obviously the horizontal strain in these samples were not controlled.

The values on the left of the saturated line refer to the ordinary consolidation test, but are not the values of the vertical pressure.
These values show the average effective stress calculated from the vertical effective pressure using the assumption, previously used by Sparks, that the horizontal effective pressure is equal to one quarter of the vertical effective stress.

---

[1] - *Reference 86.*

That is,

$pe_{AV} = 1/3\ (pe_V + 2\ pe_H)$.

Where:

$pe_H = 1/4\ pe_V$; and, 'pe_{AV}', 'pe_V' and 'pe_H' are the Average, Vertical and Horizontal Effective Stresses, respectively.

This leads to a simple expression for the compression cycle in one-dimensional consolidation, namely that,

$pe_{AV} = 0.5\ pe_V$.

For example in Fig 5.02, the void ratio of 1.34 corresponding to an average pressure of 100 Kpa is the same void ratio as that corresponding to a vertical pressure of 200 Kpa in the upper curve[1] of Fig 5.03.

---

[1] - *of the two curves for one-dimensional consolidation.*

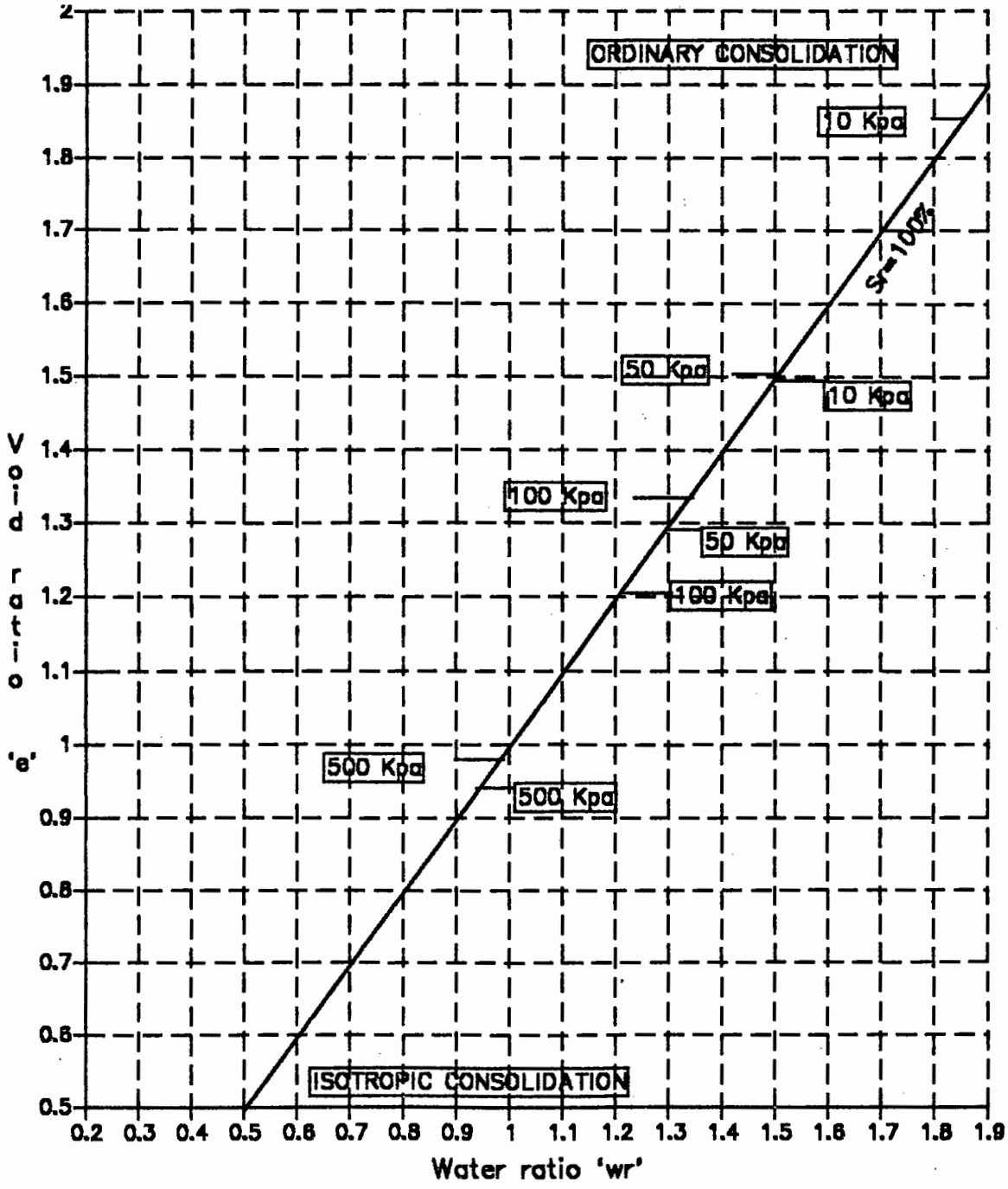

Figure 5.02: Relationship between the void ratio and the water ratio (or water content). Based on Rosebank S.11[1]. Pressure Values on the left of the line are 'average' pressures for one-dimensional consolidation, computed by assuming that the average pressure is equal to half the vertical applied pressure.

---

[1] – *See Figure 5.03.*

Reasons for using the type of plot in Figure 5.02:-

This type of Figure was used in this thesis for the following reasons:

A) It is possible to plot contours of degree of saturation as straight lines - shown in Figure 4.01 of Chapter Four.

B) One can superimpose the position and scaling factor of stress scales, whether obtained from the one dimensional or the isotropic consolidation, in terms of the Liquid Limit and Plasticity Index of the clay.

C) The stress contours can be superimposed on this plot as contours of stress.

As previously mentioned in Chapter Four, the change in the volume of the actual soil grains will normally also cause a change in the pore volume, but because these are both an increase, or decrease, the changes in the value of the void ratio will be small.
Therefore, the changes in void ratio which take place between two positions on a free shrinkage path is mainly due to a change in the average effective stress in the soil.

5.5 PREPARATION OF TEST SAMPLES

The test samples are prepared from either remoulded or undisturbed soil samples. A brief description is included in this chapter for this type of sample preparation - for more details of the test procedure refer to 'Preparation of soil samples for testing' in Appendix A[1].

Preparation of original soil sample:

(i) The samples were of fine particle size - the 2.362 mm sieve size (mesh # 8) was used to remove foreign matter, such as impurities and any odd stone;
(ii) The soil is spread over a clean surface and allowed to air dry; and,
(iii) A representative sample is obtained by quartering, or by using a sample riffler.

Known amounts of soil and water are mixed to form a wet paste. The water content at mixing should be in the Plasticity Index range, that is, between the Liquid and Plastic Limits.
The wet paste is moulded directly into either the ring used for the standard one-dimensional consolidation test - refer 'Consolidometer: One dimensional consolidation test procedure'[2], or the 1½ inches tube used to prepare the test sample for the triaxial test - refer 'Triaxial: Isotropic consolidation test procedure'[2].

---

[1] - *refer to section A.3.*
[2] - *in Appendix D.*

5.6 THE TWO MAIN TYPES OF TESTS

The two main types of tests were defined at the beginning of this chapter in the 'Definitions'[1].

The two tests are:
(1) One dimensional consolidation - use of standard consolidometer;
(2) Isotropic consolidation - use of triaxial equipment.

This section presents a summary of each test method. It also includes a 'visual sequence' illustrating the use of the triaxial test for the purpose of observing the volume changes in a sample, as the result of changes in the cell pressure - refer to Photographic Plates 5.01 (i) to (vi)[2].

5.6.1 Consolidometer test.

Test procedure for one dimensional consolidation.

Introduction:-

The soil sample is moulded directly into the standard consolidometer steel ring. The mass of the test sample plus the consolidometer ring is recorded, and the equipment is assembled for the actual test.

The sample is then loaded in stages. Settlement as a function of time is recorded during each stage of loading. In brief, the consolidometer test basically consists of recording the changes in thickness of the soil sample, after consolidation under drained conditions, as the result of each applied load.

Similarly, the soil sample is unloaded in stages, and soil recovery as a function of time is also recorded. At the end of the test, the sample is weighed and placed inside an oven to dry.

---

1 - refer to section 5.2.
2 - included at the end of this section.

Summary of consolidometer test procedure:-

Place the necessary weights on the loading platform in order to be able to apply (to the soil sample) a sequence of pressure increments similar to the following one
- 4.1 Kpa, 8.3 Kpa, 53.6 Kpa, 107.3 Kpa, 214.6 Kpa, 429.2 Kpa, 858.4 Kpa, 1716.4 Kpa, and 2360.5 Kpa.

Record the readings on the vertical deflection dial gauge before each pressure increment is applied, and at the following time intervals after each of these increments starts acting on the soil - 0.25 minutes, 0.5 min, 1.0 min, 2.25 min, 4 min, 9 min, 16 min, 30 min, 60 min, 120 min, and so on. Readings should continue until the soil has consolidated, at least until the slope of the characteristic linear secondary settlement becomes apparent. The readings of vertical deflection will enable the calculation of thickness or changes in thickness of the sample.

The recovery or unloading characteristics of the soil are observed next. Vertical deflection readings are recorded, as the external vertical pressure applied to the sample is gradually decreased, using pressure decrements similar to the following one
- 2360.5 Kpa, 429.2 Kpa, 53.6 Kpa, 8.3 Kpa, and 1.0 Kpa.

At the completion of the unloading sequence record the mass of the sample plus ring. The soil sample is carefully extracted from the steel ring, and placed inside an oven, previously set at the temperature of 105 ± 5^{o}C, for a few hours (preferably overnight). The mass of the soil sample is recorded as the oven dry mass.

The detailed description of this test procedure is included in Appendix D - refer to "One-dimensional consolidation test procedure."

5.6.2 Triaxial test.

Test procedure for isotropic consolidation.

Introduction:-

The soil sample is moulded into the required test sample for the triaxial test, and its mass, diameter and length are recorded. The sample is positioned, in place, and the triaxial equipment is assembled and made ready for the actual test. The pressure supply[1] is adjusted to the required cell pressure. Volume change as a function of time is recorded during each stage of loading the sample. Consolidation is complete when no noticeable changes occur to the reading in the volume change indicator over a period of time.

---

[1] - *in the triaxial machine.*

Similarly, the soil sample is unloaded in stages and soil recovery as a function of time is also recorded. The equipment is disassembled, and the sample is again weighed, measured and placed inside an oven to dry.

Summary of triaxial test procedure:-

Assembly of the main components of the triaxial equipment: (i) The upper part of the triaxial cell is placed over the test sample, aligned and tightened in place, and de-aired water is run into the cell; (ii) The pressure supply is adjusted to the required cell pressure - volume change as a function of time is recorded during each stage of loading; The volume change indicator (measuring device) is connected with the pressure supply and adjusted for operation.
The upper mercury cylinders are raised high enough to provide the required cell pressure. The sequence of cell pressure measurements should be similar to the following one - 10.3 Kpa, 51.7 Kpa, 103.4 Kpa, 206.8 Kpa, 620.5 Kpa, and 827.4 Kpa.

At suitable time intervals (from the start of each pressure increment stage) the volume change in the sample is measured on the volume change indicator. Consolidation is complete when no noticeable changes occur in the volume change indicator over a period of time. The readings of volume change will enable the calculation of volume or changes in volume of the sample.
The recovery or unloading characteristics of the soil are observed by means of decreasing the cell pressure as follows - 827.4 Kpa, 51.7 Kpa, 10.3 Kpa, and zero. Soil recovery is assumed to be complete when no noticeable changes occur in the volume change indicator over a period of time.
The volume and pressure supply system are isolated and the water is allowed to drain from the base of the cell.
The top of the cell is removed. The rubber membranes, `O' rings, cap and porous plate, are also removed.
The filter paper drains are taken out of the sample.

The assembly of the parts and use of the triaxial equipment is illustrated in Photographic Plates 5.01 (i) to (vi).
The soil sample is next weighed, measured and placed inside an oven (previously set at 105 ± 5^{o} C) for a few hours, preferably overnight. The sample is removed from the oven, allowed to cool down to room temperature, and its oven dried mass is recorded.

The detailed description of this test procedure is included in Appendix D[1].

---

[1] - *section D.2 'Isotropic consolidation test procedure'.*

(i)

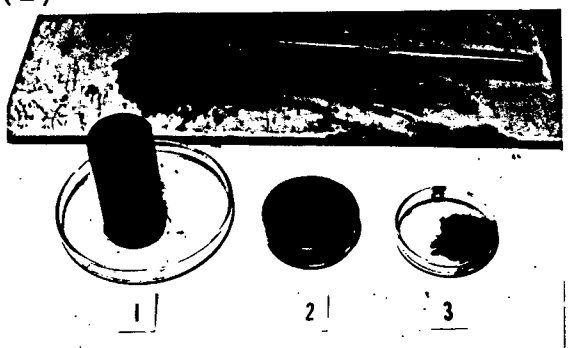

(ii)

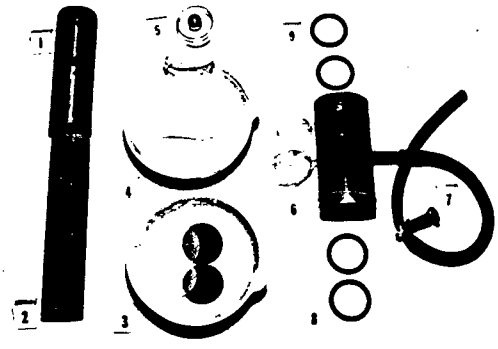

(iii)

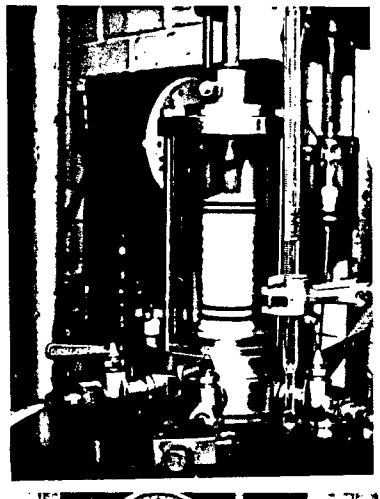

(iv)

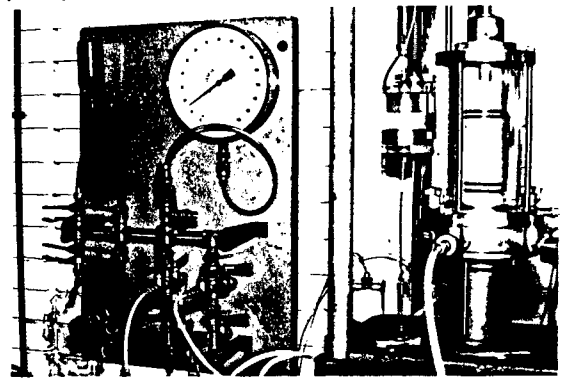

(v)

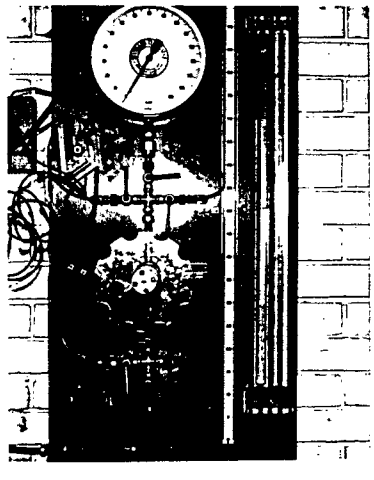

(vi)

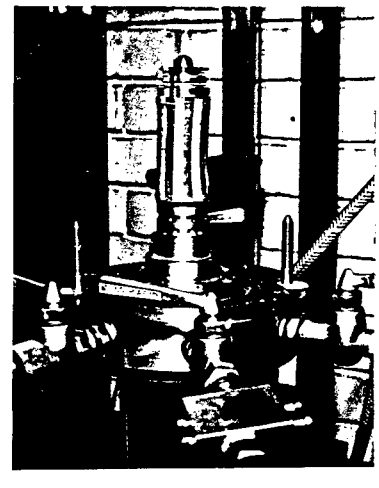

Photographic Plates 5.01: (i) Remoulded soil samples - 1. triaxial, 2. free shrinkage/swell and 3. water content; (ii) Parts for triaxial test - 1. 1½ inches diameter tube, 2. dolly, 3. filter papers and porous plates, 4. filter drains, 5. loading cap, 6. rubber membrane, 7. twin walled tube, 8. and 9. rubber 'O' rings; (iii) Ready to start test - inlet/outlet valves (left to right - cell pressure 'in', air 'out', and water 'out' - respectively); (iv) Pressure supply board; (v) Volume and pore water pressure board; (vi) At end of test - sample with filter drains.

5.7 ANALYSIS OF TEST RESULTS FOR EACH SOIL TYPE

On the basis of particle size and consistency limits, each soil type was previously defined in Chapters One and Two, and also in Appendix A.
Observations of Shrinkage Limit and Free Expansion Limit for most soils, were reported in Chapter Four[1].
These definitions, together with the reported observations for the limit values, provide the introduction to the one-dimensional and isotropic consolidation test results for each soil type.

As mentioned at the begining of this chapter, the data was obtained from two types of test - (1) One dimensional consolidation, and (2) Isotropic consolidation. The void ratios obtained from the applied effective pressures are presented in graphical form, for each of the two types of test.
These graphs result from the plot of the effective pressure 'pe' (pe = pt-u - where: pt = total pressure, or stress; and, u = pore water pressure) versus the void ratio 'e' (that is, the ratio between the volume of voids and the volume of solids).

The graph for the first type of test illustrates the void ratio reduction that takes place due to the axial compression (vertical loading) of the sample, under drained conditions, while being restrained horizontally.
Similarly, the graph for the second type of test provides the general stress-volumetric strain characteristics of the soil and, in particular, the graph illustrates the void ratio changes which accompany the application of an all round pressure under drained conditions.
These void ratios will enable the transfer of the stress values to another type of plot, for the purpose of fitting stress scales - refer to next section "Conclusions for Chapter Five".

The relationships of void ratio versus effective pressure for each soil type, either as one dimensional or isotropic consolidation, are illustrated in Figures 5.03 to 5.22.
It should be noted that Appendix D includes the detailed Consolidometer and Triaxial test procedures and results.

---

[1] - *'Free Shrinkage and Free Swell Paths'.*

5.7.1 Natural Soil Types - Remoulded Samples.

This section includes relationships of void ratio versus effective pressure for the following natural soil types:

(i) Site 11, Rosebank (Cape);
(ii) Site 36, Rondebosch (Cape);
(iii) Site 30, Hout Bay (Cape);
(iv) Site A, Berea Road (Durban, Natal);
(v) Site 7, Mowbray (Cape);
(vi) Site 45, Bellville (Cape);
(vii) Site B, Francois Road (Durban, Natal);
(viii) Site C, Margaret Mayton Avenue (Durban, Natal); and,
(ix) Site D, Rose Hill (Durban, Natal).

One-dimensional[1] and isotropic[2] consolidation tests were carried out for the soil samples listed in Table 5.01. The relationships obtained from these tests are illustrated in Figures 5.03 to 5.11.

Table 5.01: Natural Soils - Remoulded samples used for one-dimensional (consolidometer) and isotropic (triaxial) tests.

Sample No.	Test No./ Ref. Number
Consolidometer	
S.11-32	59 / II. 267
S.11-66	165/ IV. 455
S.36-1	64 / III.277
S.30-1	67 / III.283
S.A-5	12 / I. 136
S.7-6	1 / I. 94
S.45-1	84 / III.312
S.B-2	13 / II. 141
S.C-2	15 / II. 145
S.D-2	16 / II. 147
Triaxial	
S.11-T2	5 / V. 11
S.36-T1	2 / V. 5
S.30-T1	3 / V. 7
S.A-T1	4 / V. 9
S.7-T1	11 / V. 23

[1] - *Consolidometer.*
[2] - *Triaxial.*

Site 11, Rosebank.

Previously defined as a fine silty clay with only a small amount of fine sand. The soil consists of 59% clay, 29% silt, and 12% of sand size. The consistency, free shrinkage and free swell limits, are as follows: Linear Shrinkage 'w_{LS}' = 11.4%; Liquid Limit 'w_L' = 69%; Plastic Limit 'w_P' = 30.7%; Plasticity Index 'I_P' = 38; Shrinkage Limit 'w_S' = 22.5%; and, Free Expansion Limit 'w_{FE}' = 49.4%.

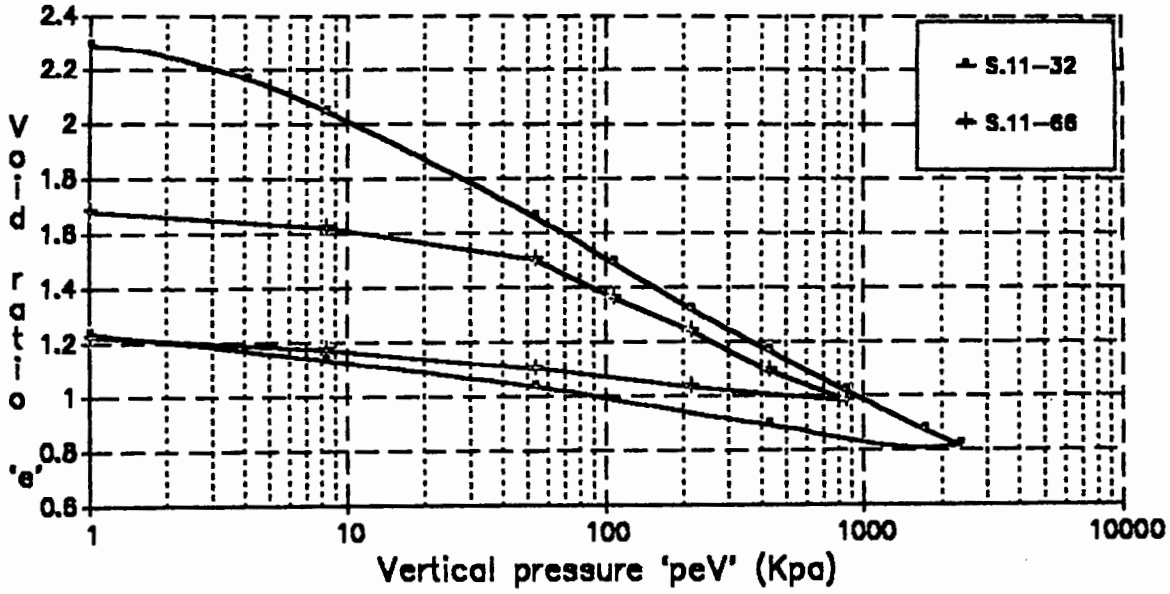

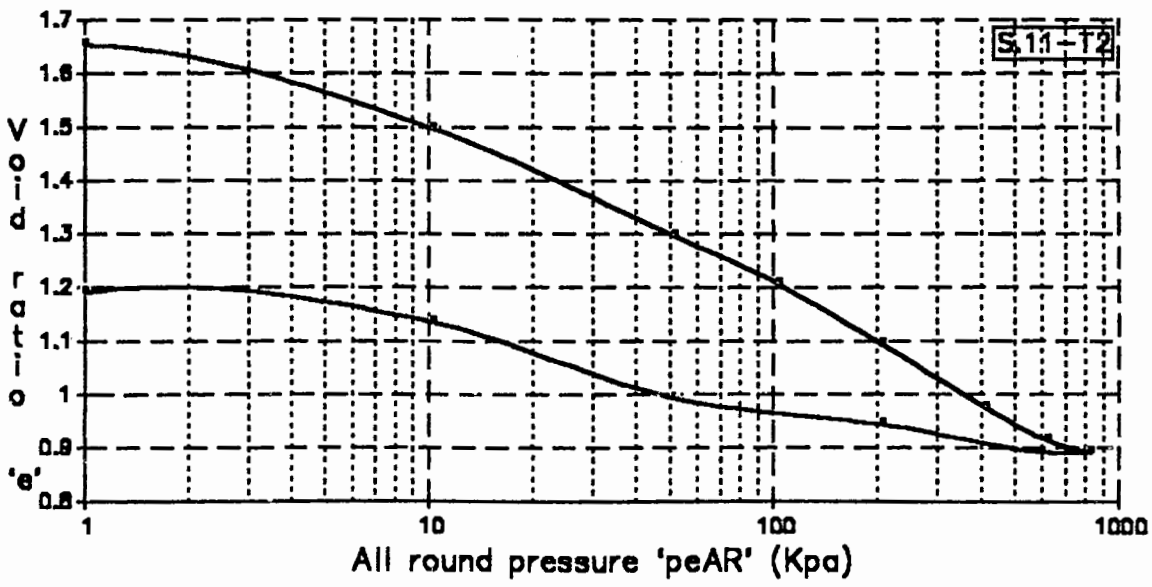

Figure 5.03: Site 11, Rosebank [Remoulded] - (Top) One-dimensional consolidation, results from two different samples[1], and (Bottom) Isotropic consolidation in triaxial.

[1] - *for S.11-66 horizontal stresses were measured but not used in above plot.*

Site 36, Rondebosch.

A clayey silt, with fine sand and a small amount of medium sand. The soil consists of 22% clay, 49% silt, and 29% sand size. The 'Limits' of the soil are: w_{LS} = 8.3%; w_L = 47.0%; w_P = 23.3%; I_P = 24; w_S = 22.0%; and, w_{FE} = 32.7%.

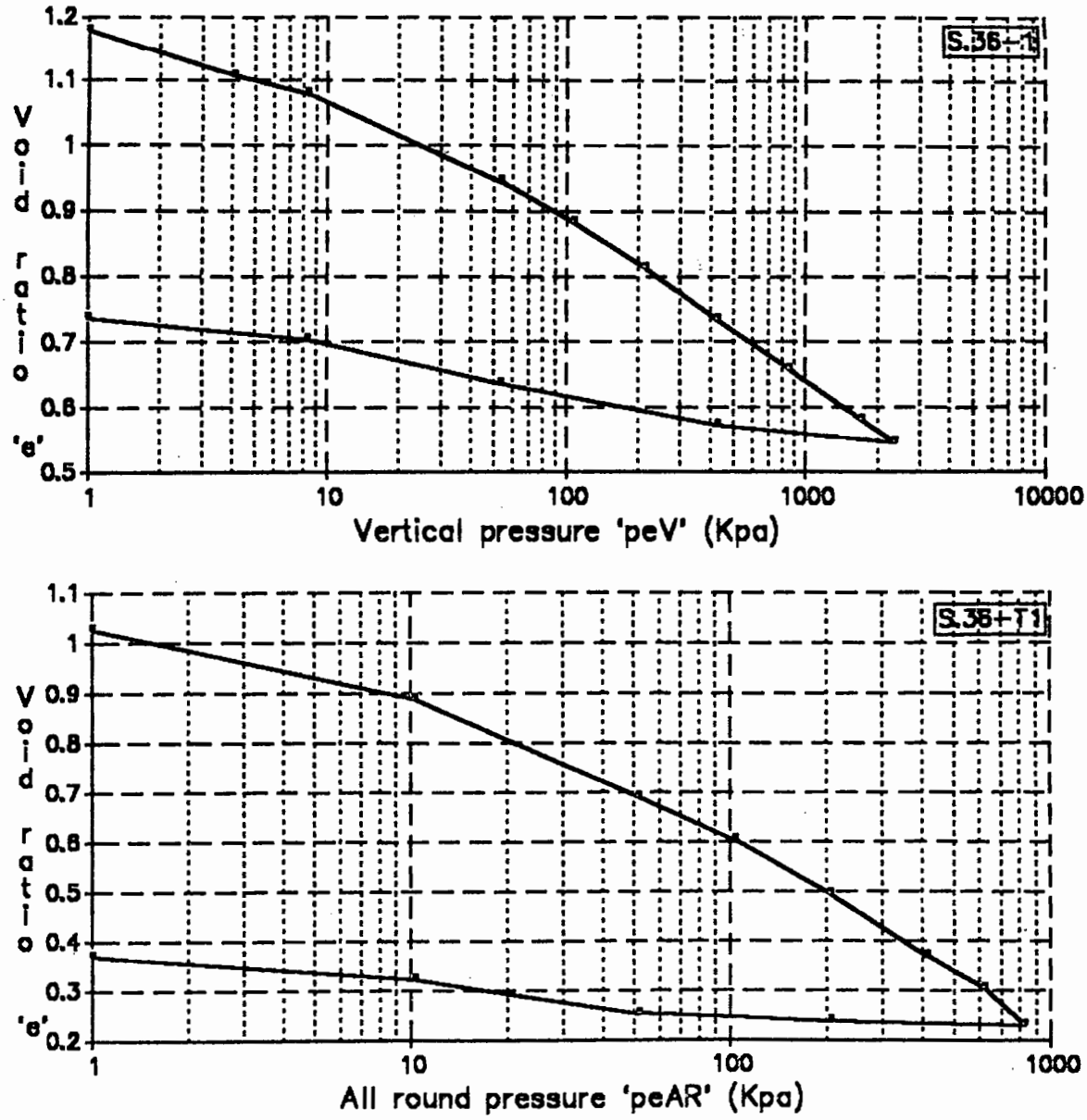

Figure 5.04: Site 36, Rondebosch [Remoulded] - (Top) One-dimensional consolidation, and (Bottom) Isotropic consolidation.

Site 30, Hout Bay.

A fine to medium sandy silt, with a small amount of coarse sand. The soil consists of 23% clay, 34% silt, and 43% sand size. The 'Limits' of the soil are: w_{Ls} = 6.4%; w_L = 49.0%; w_P = 29.0%; I_P = 20; w_S = 22,5%; and, w_{FE} = 36.0%.

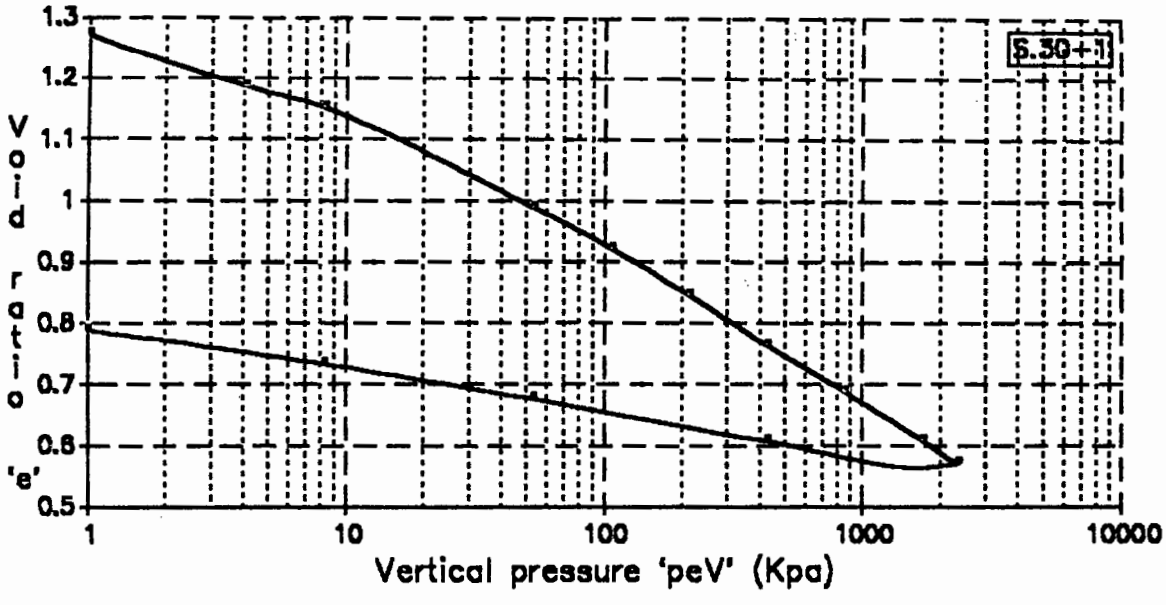

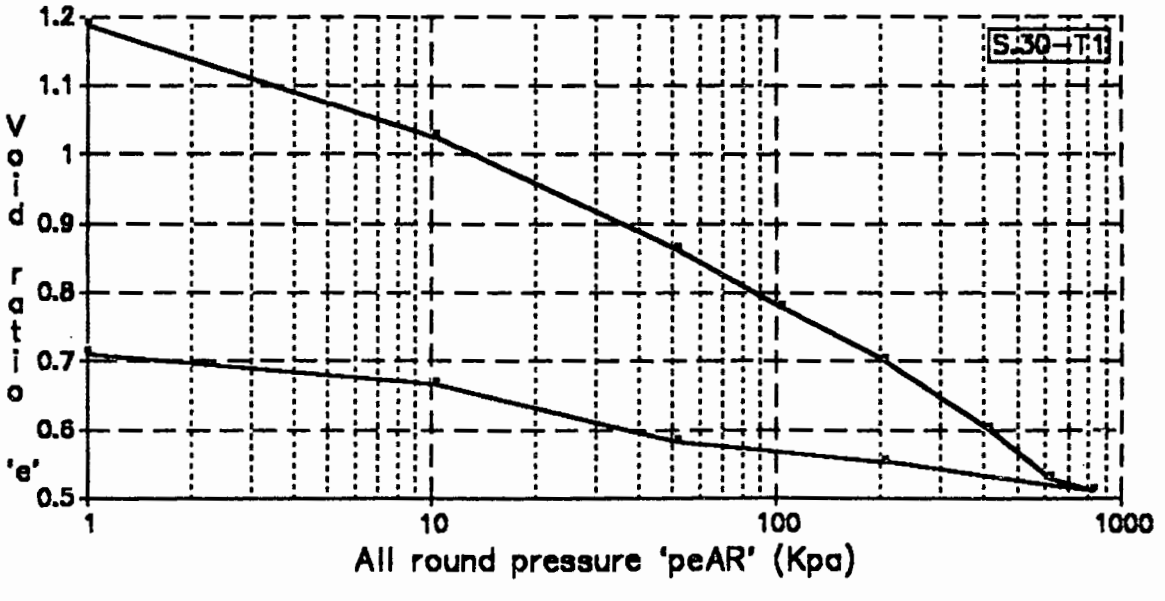

Figure 5.05: Site 30, Hout Bay [Remoulded] - (Top) One-dimensional consolidation, and (Bottom) Isotropic consolidation.

Site A, Berea Road (Durban).

A clayey sand (fine to medium size) with a small amount of silt. The soil consists of 15% clay, 10% silt, and 75% sand size. The Limits of the soil are: w_{LS} = 3.7%; w_L = 25.0%; w_P = 13.1%; I_P = 12; w_S = 13.5%; and w_{FE} = 16.6%.

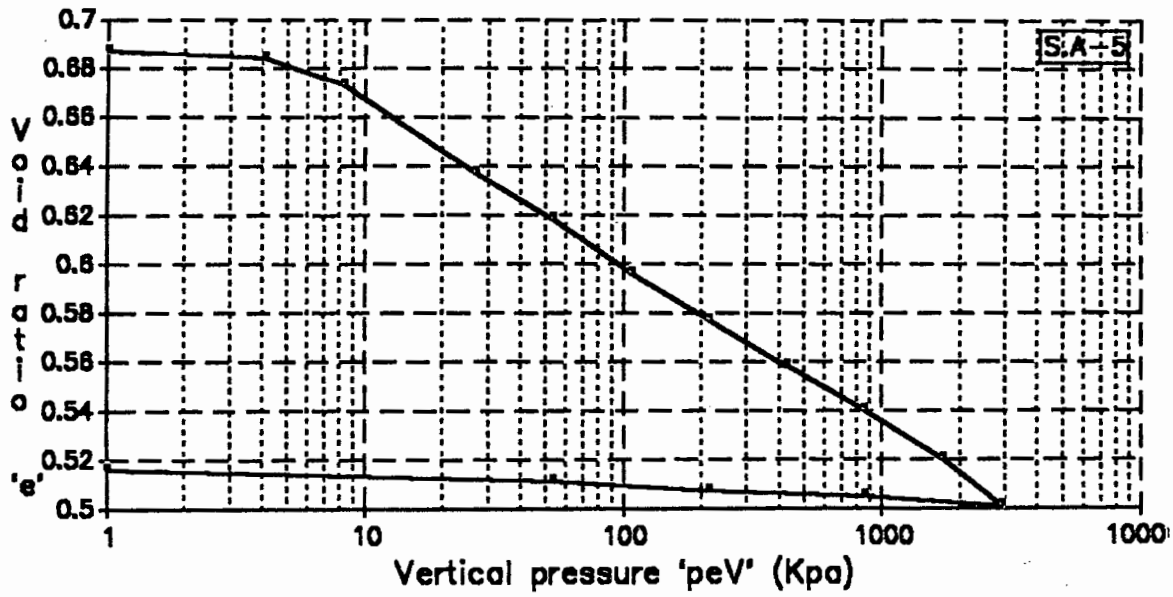

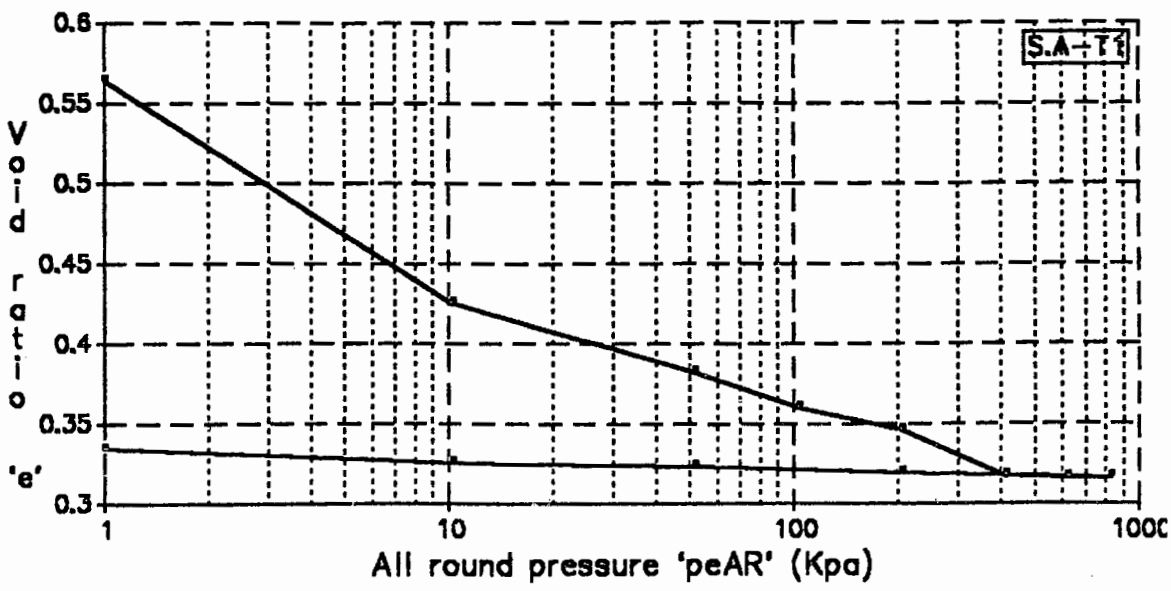

Figure 5.06: Site A, Berea Road (Durban) [Remoulded] - (Top) One-dimensional consolidation, and (Bottom) Isotropic consolidation.

Site 7, Mowbray.

A fine silty clay, with a small amount of fine to medium sand. The soil consists of 42% clay, 37% silt, and 21% sand size. The Limits of the soil are: w_{LS} = 10.5%; w_L = 47.0%; w_P = 22.0%; I_P = 25; w_S = 18.5%; and, w_{FE} = 29.1%.

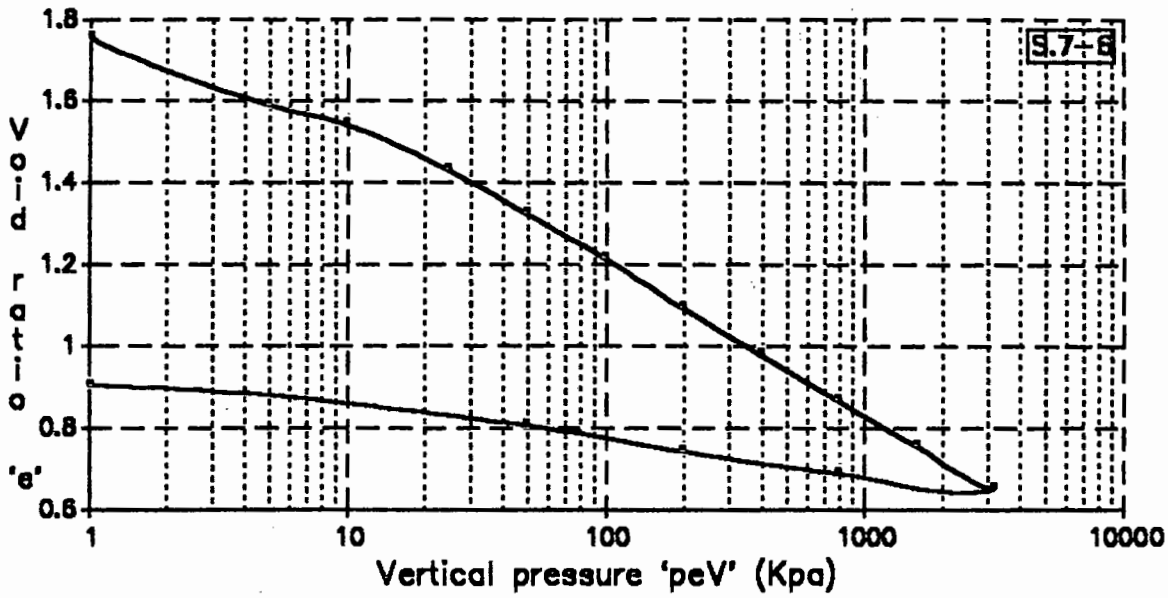

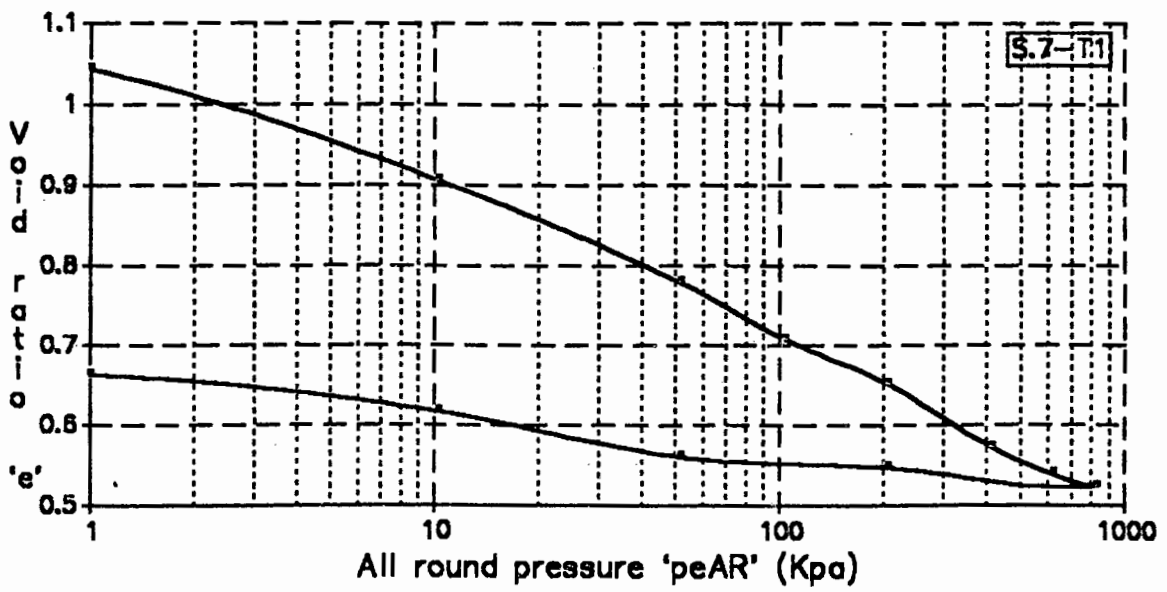

Figure 5.07: Site 7, Mowbray [Remoulded] - (Top) One-dimensional consolidation, and (Bottom) Isotropic consolidation.

Site 45, Bellville.

A fine to medium silty clay, with a small amount of coarse and fine sand. The soil consists of 32% clay, 63% silt, and 5% sand size. The Limits of the soil are as follows: w_{Ls} = 10.5%; w_L = 62.8%; w_P = 26.5%; I_P = 36.

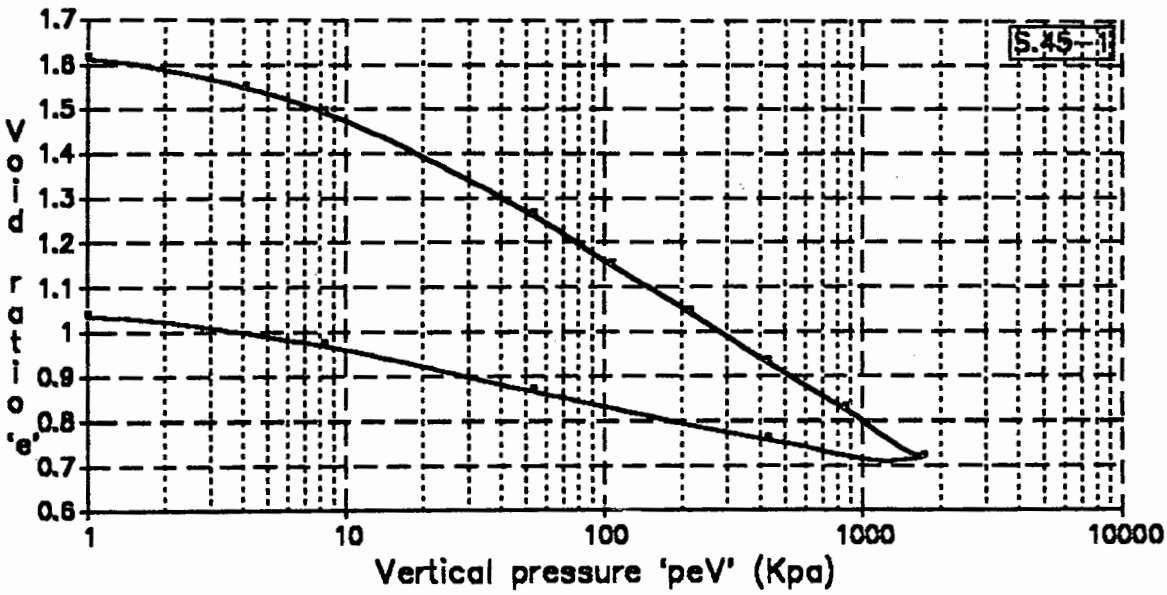

Figure 5.08: Site 45, Bellville [Remoulded] - One-dimensional consolidation.

Site B, Francois Road (Durban).

A fine to medium sand containing small amounts of clay and silt. The soil consists of 7.5% clay, 7% silt, and 85.5% sand size. The 'Limits' are: w_{LS} = 0.5%; w_L = 15.0%; w_P = 12.9%; I_P = 2; w_S = 11.0%; and, w_{FE} = 11.8%.

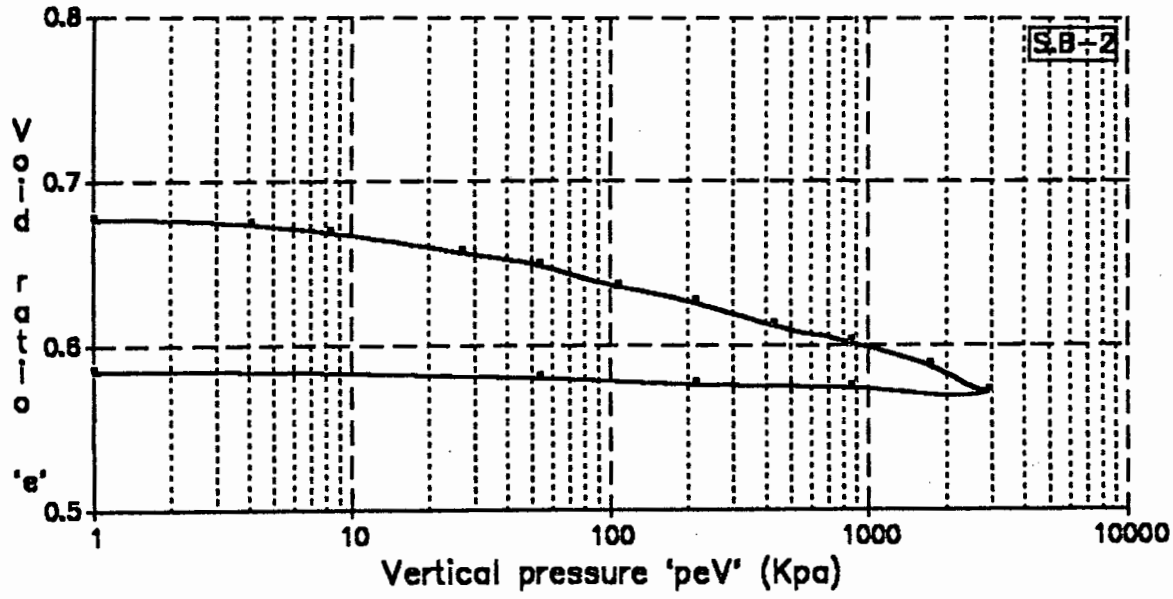

Figure 5.09: Site B, Francois Road (Durban) [Remoulded] - One-dimensional consolidation.

Site C, Margaret Mayton Avenue (Durban).

A clayey sand (fine to medium size) with a very small amount of silt. The soil consists of 12.5% clay, 4% silt, and 83.5% sand size. The 'Limits' are: w_{LS} = 1.8%; w_L = 19.7%; w_P = 15.9%; I_P = 4; w_S = 8.5%; and, w_{FE} = 15.4%.

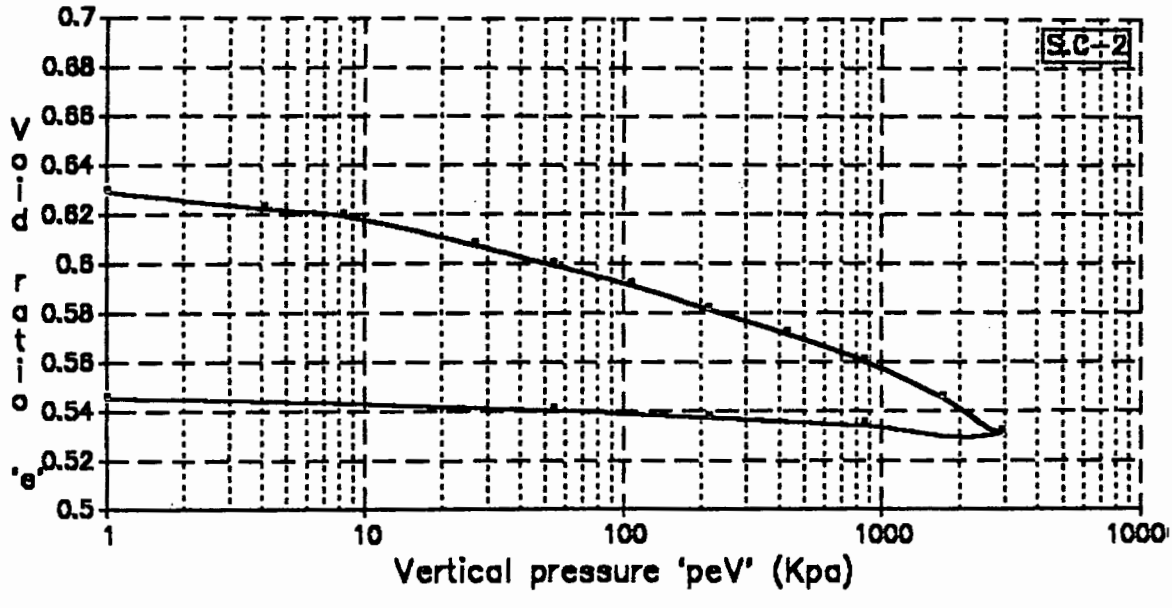

Figure 5.10: Site C, Margaret Mayton Avenue (Durban) [Remoulded] - One-dimensional consolidation.

Site D, Rose Hill (Durban).

A clayey sand (fine to medium size) with a very small amount of silt. The soil consists of 15.5% clay, 4.5% silt, and 80% sand size. The 'Limits' are: w_{Ls} = 2.2%; w_L = 20.6%; w_P = 14.9%; I_P = 6; w_S = 12.0%; and, w_{FE} = 12.2%.

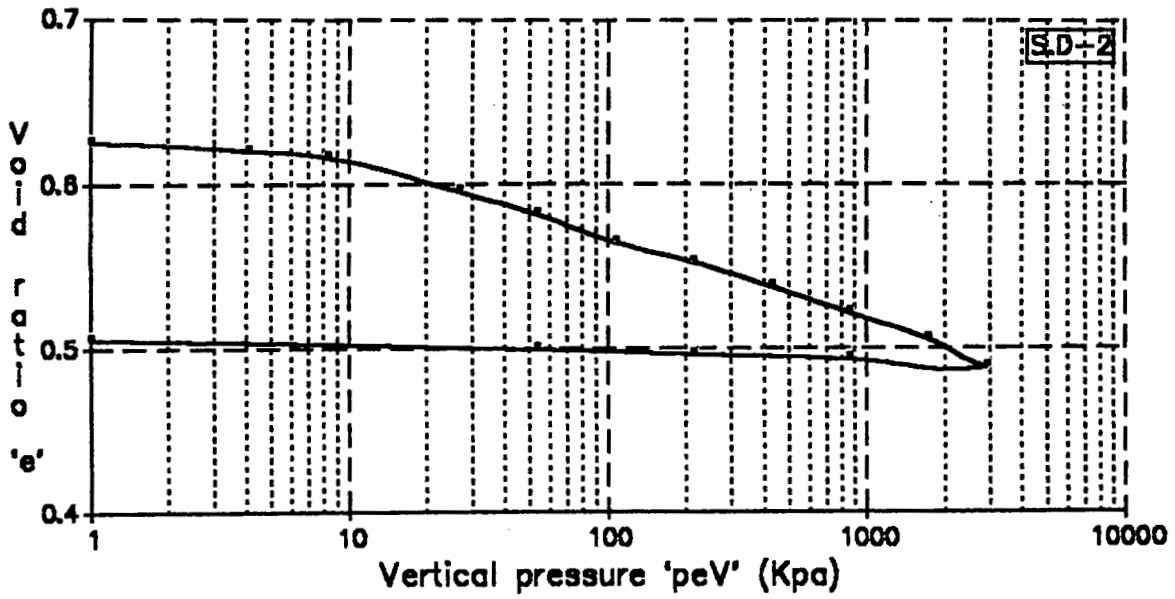

Figure 5.11: Site D, Rose Hill (Durban) [Remoulded] - One-dimensional consolidation.

5.7.2 Natural Soil Types - Undisturbed Samples.

Relationships of void ratio versus effective pressure for several undisturbed samples of natural soil types, either as one-dimensional or isotropic consolidation, are illustrated in Figures 5.12 to 5.14.
These tests were carried out for the soil samples listed in Table 5.02.

Table 5.02: Natural soils - undisturbed samples used for one-dimensional (consolidometer) and isotropic (triaxial tests.

Sample No.	Test No. / Ref. Number
Consolidometer	
S.11-56	107 / III.355
S.36-20	149 / IV. 429
S.30-17	157 / IV. 441
Triaxial	
S.11-T5	18 / V. 35

Site 11, Rosebank.

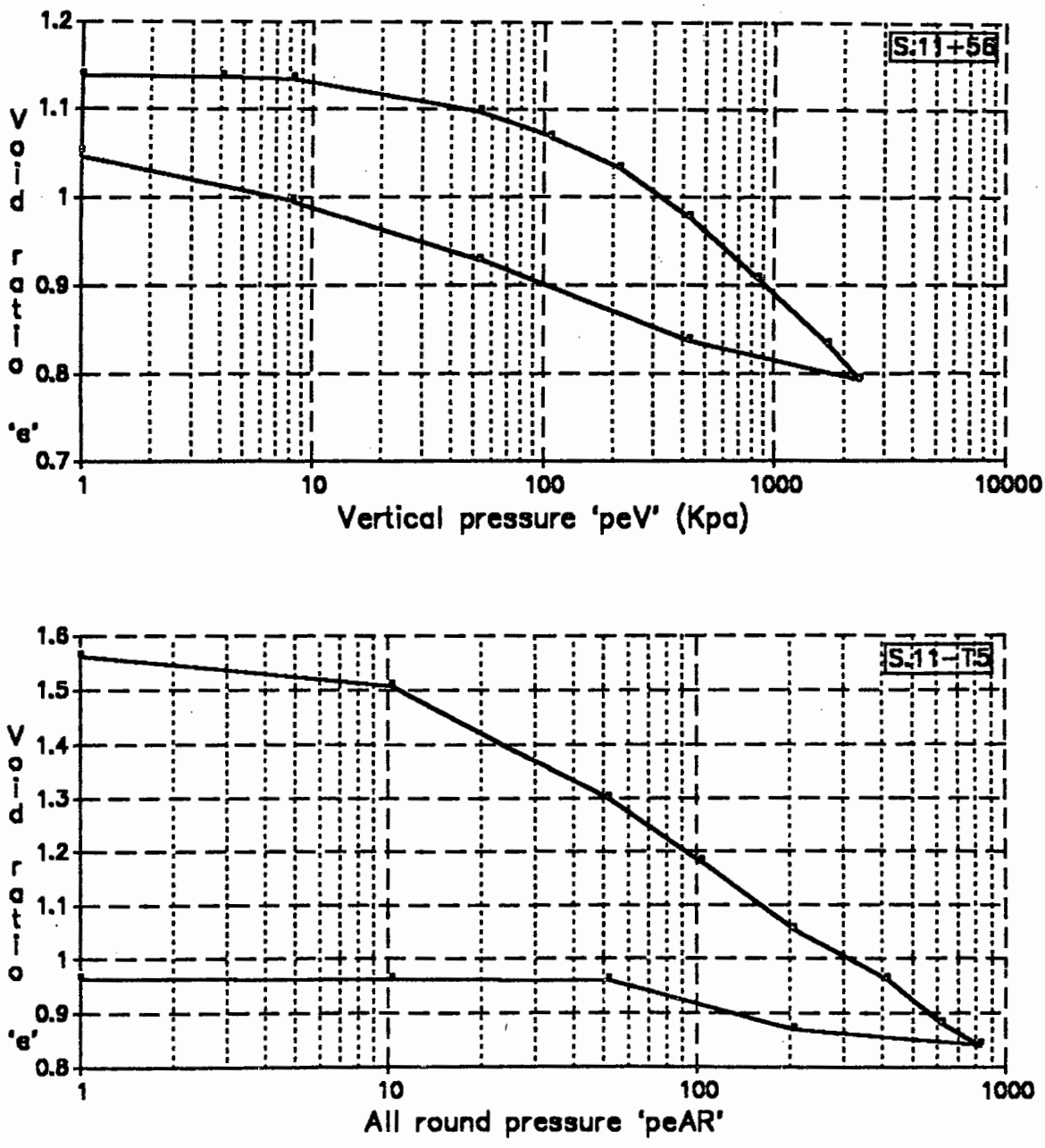

Figure 5.12: Site 11, Rosebank [Undisturbed] - (Top) One-dimensional consolidation, and (Bottom) Isotropic consolidation.

Site 36, Rondebosch.

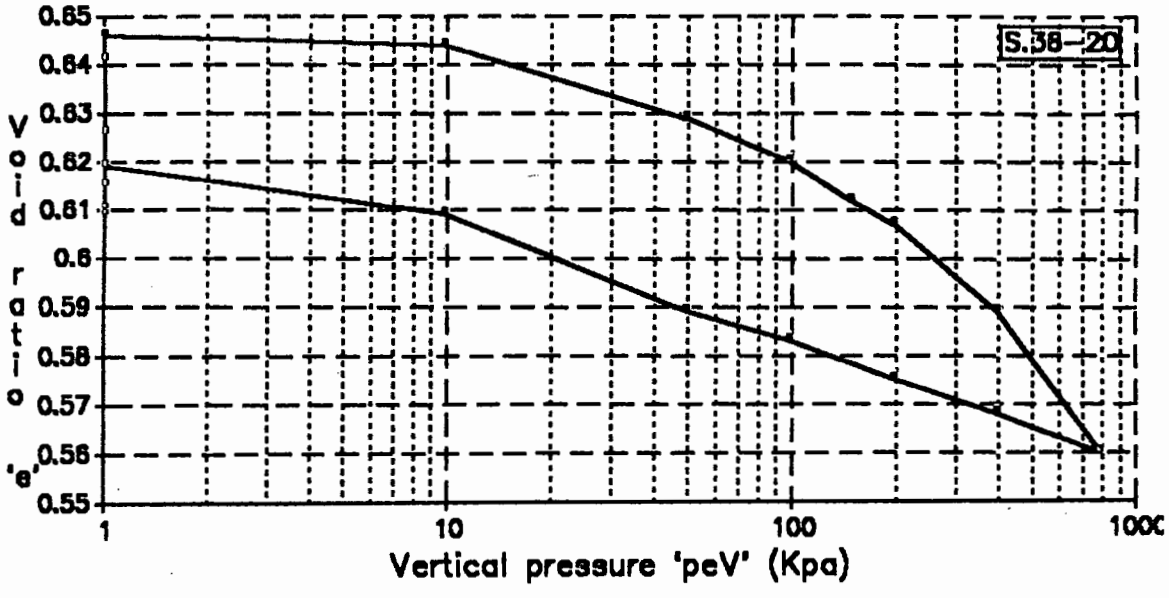

Figure 5.13: Site 36, Rondebosch [Undisturbed] - One-dimensional consolidation.

Site 30, Hout Bay.

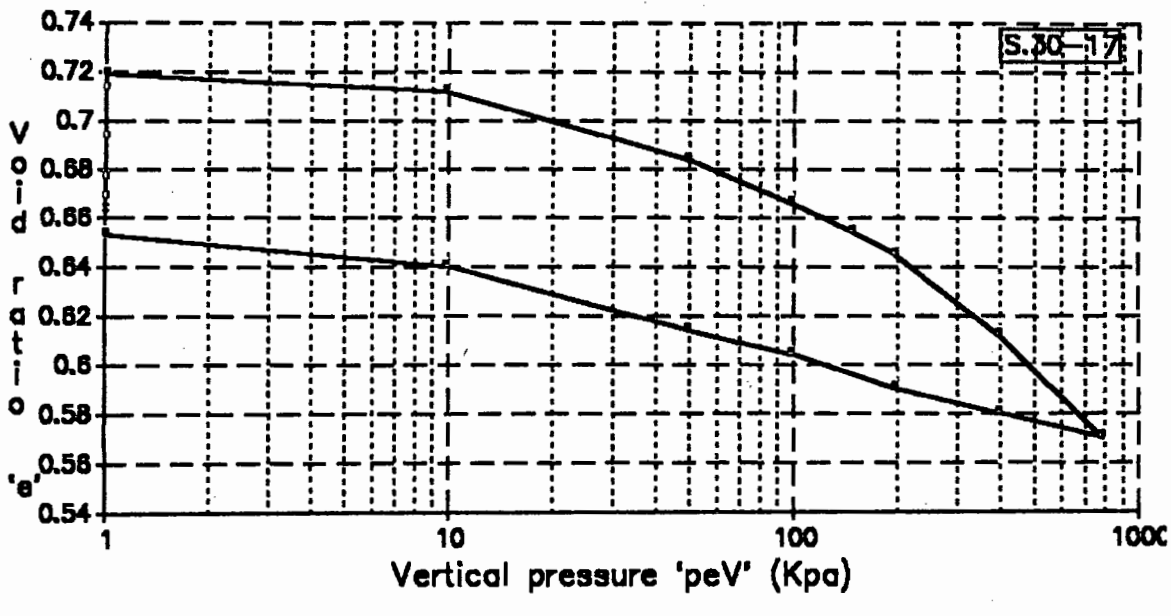

Figure 5.14: Site 30, Hout Bay [Undisturbed] - One-dimensional consolidation.

5.7.3 Artificial Soil Types.

This section includes the relationships of void ratio versus effective pressure for the following artificial (or made up) soils:

(i) Kaolin clay mixed with sand - K.1 (13% clay size), K.2 (20% clay size), and K.3 (8.5% clay size); and,

(ii) Bentonite clay mixed with sand - B.1 (3.5% clay size), B.2 (7% clay size), B.3 (11.5% clay size), B.4 (15.5% clay size), and B.5 (35% clay size).

These relationships are illustrated in Figure 5.15 to 5.22.

One-dimensional (Consolidometer) and isotropic (Triaxial) consolidation tests were performed on the samples listed in Table 5.03.

Table 5.03: Artificial soils - samples used for one-dimensional (consolidometer) and isotropic (triaxial) tests.

Sample No.	Test No. / Ref. Number
Consolidometer	
Kaolin clay mixed with sand:	
K.1-4	50 / II. 242
K.2-4	54 / II. 254
K.3-4	58 / II. 263
Bentonite clay mixed with sand:	
B.1-1	119 / III.381
B.2-1	122 / III.387
B.3-1	124 / III.391
B.4-1	127 / III.397
B.5-1	155 / IV. 439
Triaxial	
Kaolin:	
K.2-T1	6 / V. 13
K.3-T1	7 / V. 15
Bentonite:	
B.2-T1	8 / V. 17
B.4-T1	9 / V. 19
B.5-T1	10 / V. 21

Kaolin clay mixed with sand:-

Kaolin K.1.

A clayey sand (fine to medium size), with a very small amount of silt. The soil consists of 13% clay, 3.5% silt, and 83.5% of sand size. The 'Limits' of the soil are as follows: w_{Ls} = 0.4%; w_L = 12.3%; w_P = 11.8%; I_P = 1; w_S = 10.0%; and, w_{FE} = 12.3%.

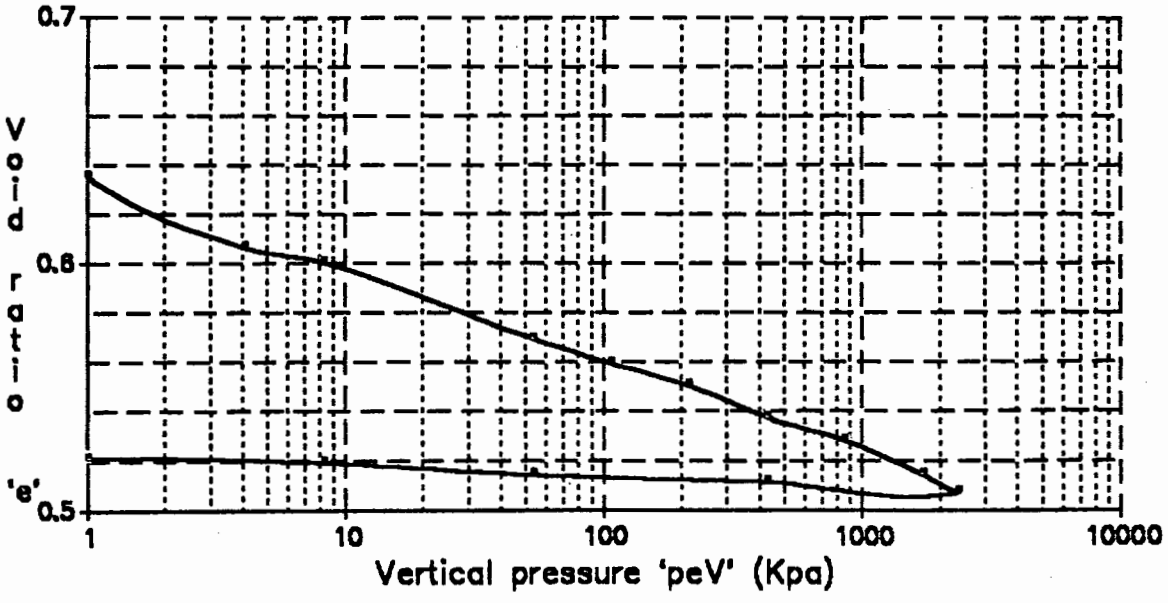

Figure 5.15: Kaolin K.1 (13% clay size) - One-dimensional consolidation.

Kaolin K.2.

A clayey sand (fine to medium size), with a small amount of silt. The soil consists of 20.0% clay, 65% silt and 73.5% sand size. The 'Limits' of the soil are: w_{LS} = 1.5%; w_L = 14.0%; w_P = 10.4%; I_P = 4; w_S = 12.0%; and w_{FE} = 12.0%.

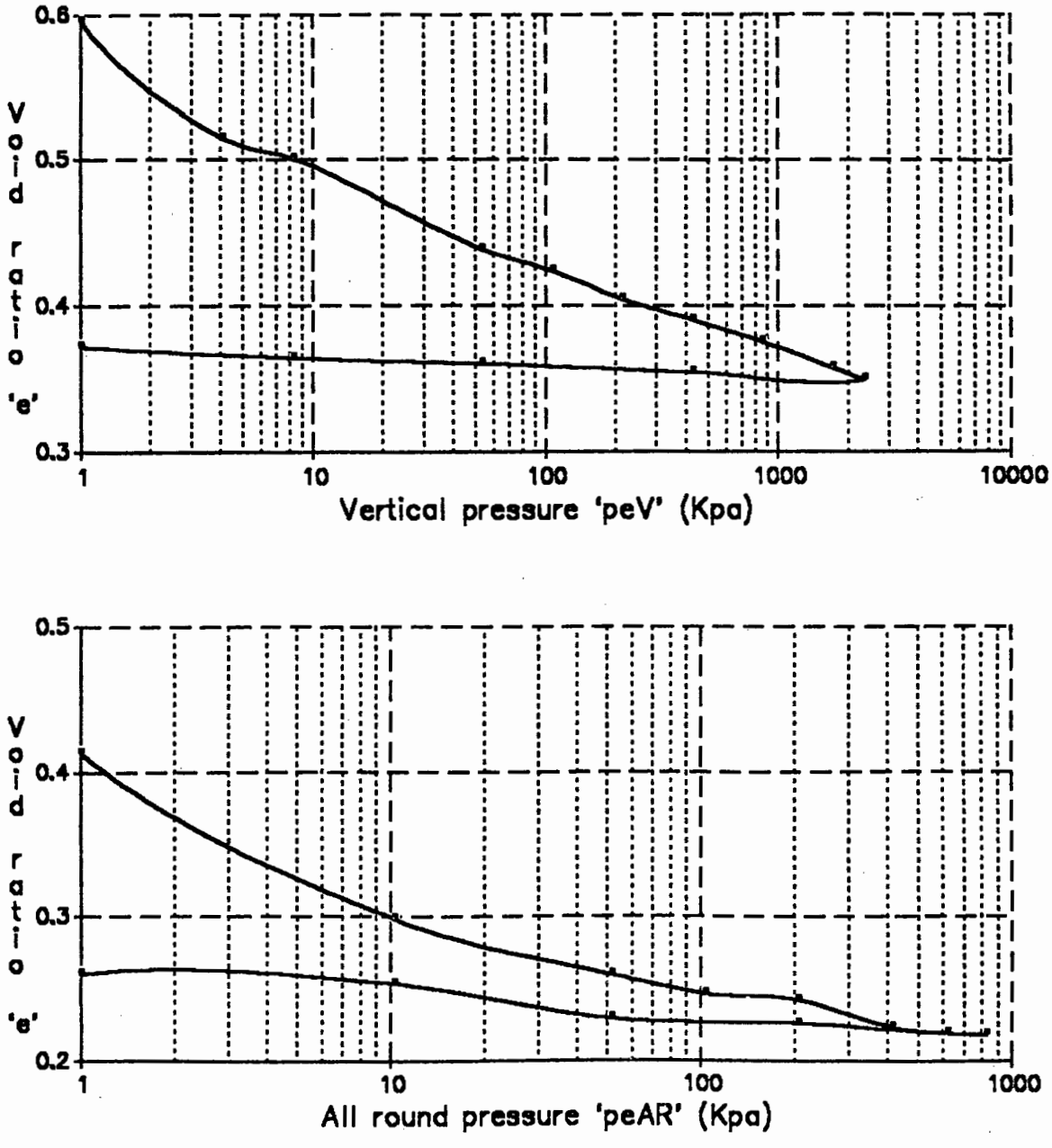

Figure 5.16: Kaolin K.2 (20% clay size) - (Top) One-dimensional consolidation, and (Bottom) Isotropic consolidation.

Kaolin K.3.

A fine to medium sand containing a small amount of clay, and a very small amount of silt. The soil consists of 8.5% clay, 2.5% silt, and 89% sand size. The 'Limits' of the soil are: w_{LS} = 0.0%; w_L = NP; w_P = NP; I_P = NP; w_S = 9.0%; and, w_{FE} = 11.0%.

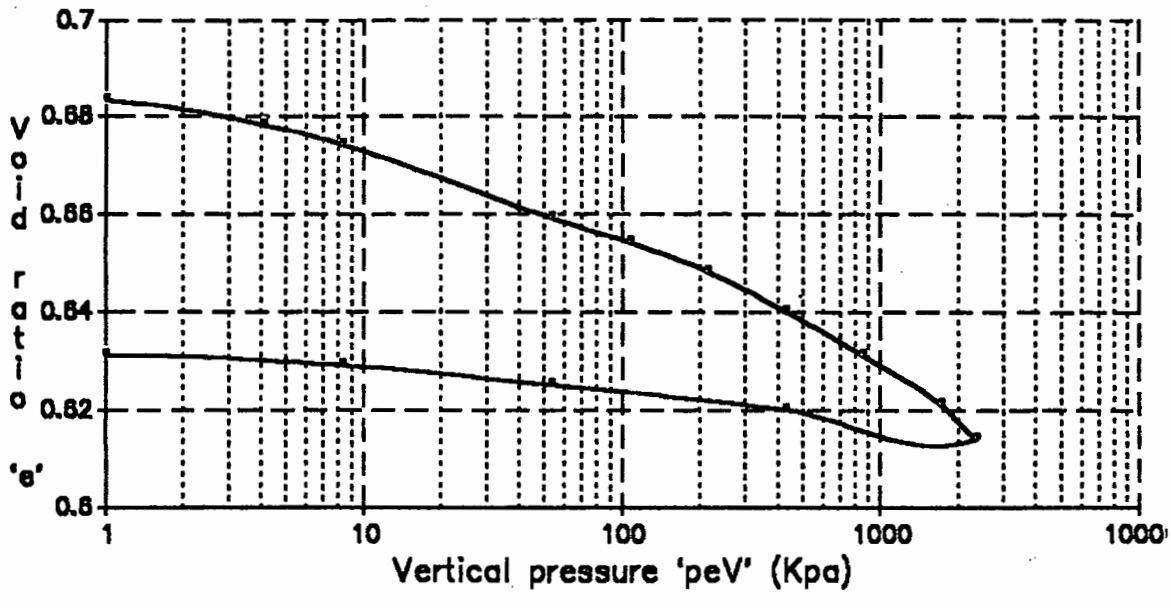

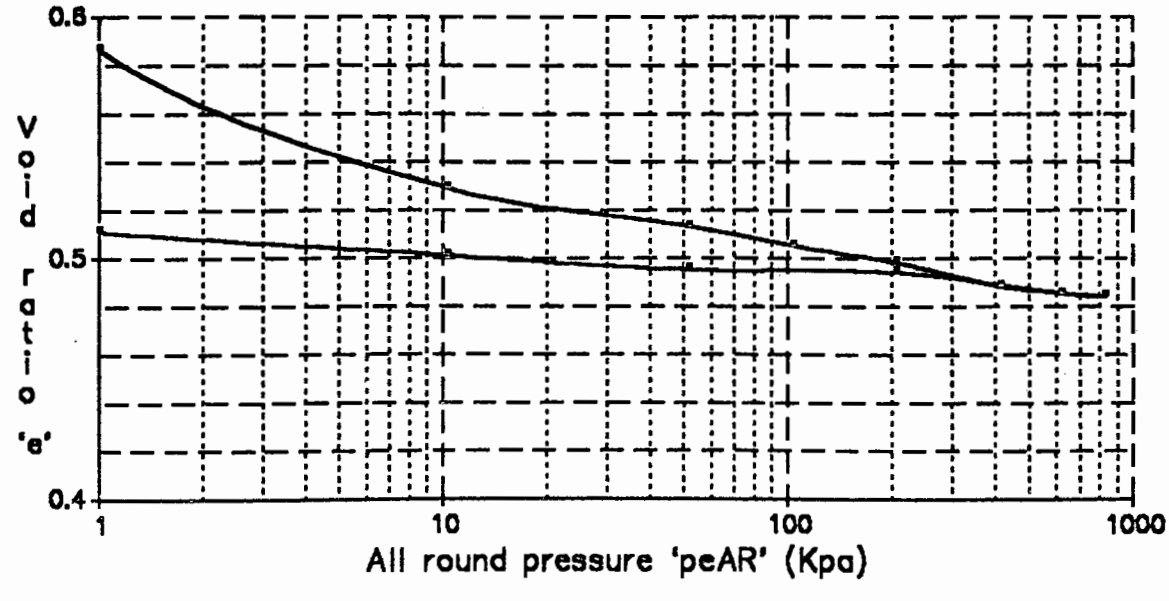

Figure 5.17: Kaolin K.3 (8.5% clay size) - (Top) One-dimensional consolidation, and (Bottom) Isotropic consolidation.

Bentonite clay mixed with sand:-

Bentonite B.1.

A fine to medium sand with a very small amount of clay and silt. The soil consists of 3.5% clay, 1.5% silt, and 95% sand size. The 'Limits' of the soil are: w_{LS} = 0.1%; w_L = 21.0%; w_P = 20.0%; I_P = 1; w_S = 14.5%; and w_{FE} = 17.4%.

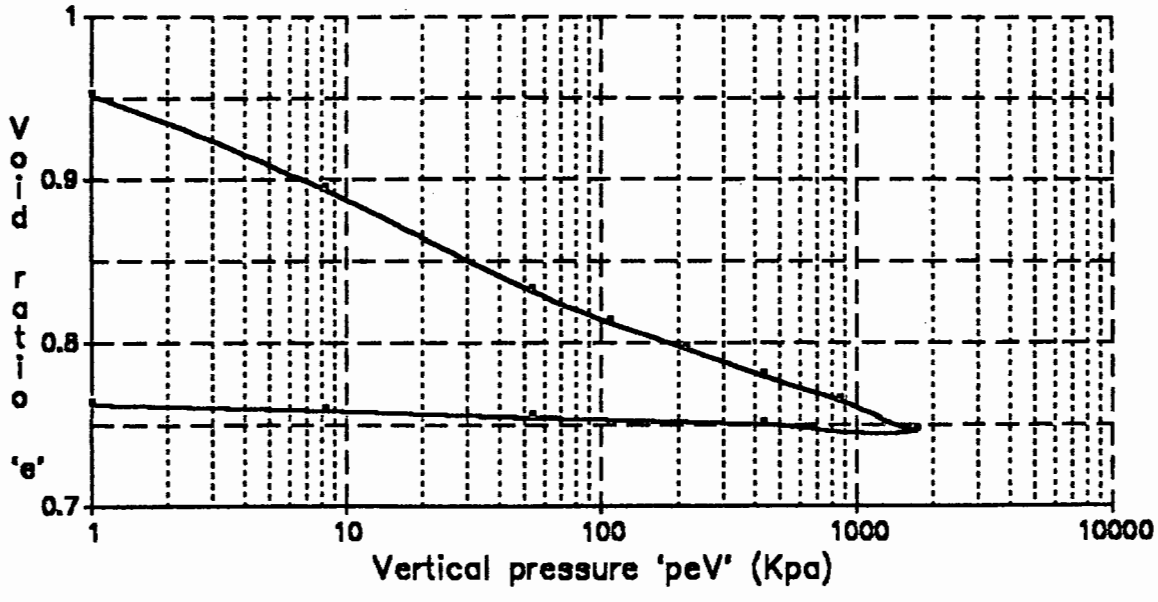

Figure 5.18: Bentonite B.1 (3.5% clay size) - One-dimensional consolidation.

Bentonite B.2.

A fine to medium sand with a small amount of clay and silt (very small). The soil consists of 7% clay, 2% silt and 91% sand size. The 'Limits' are: w_{LS} = 0.5%; w_L = 32.0%; w_P = 21.0%; I_P = 11; w_S = 26.0%; and w_{FE} = 29.8%.

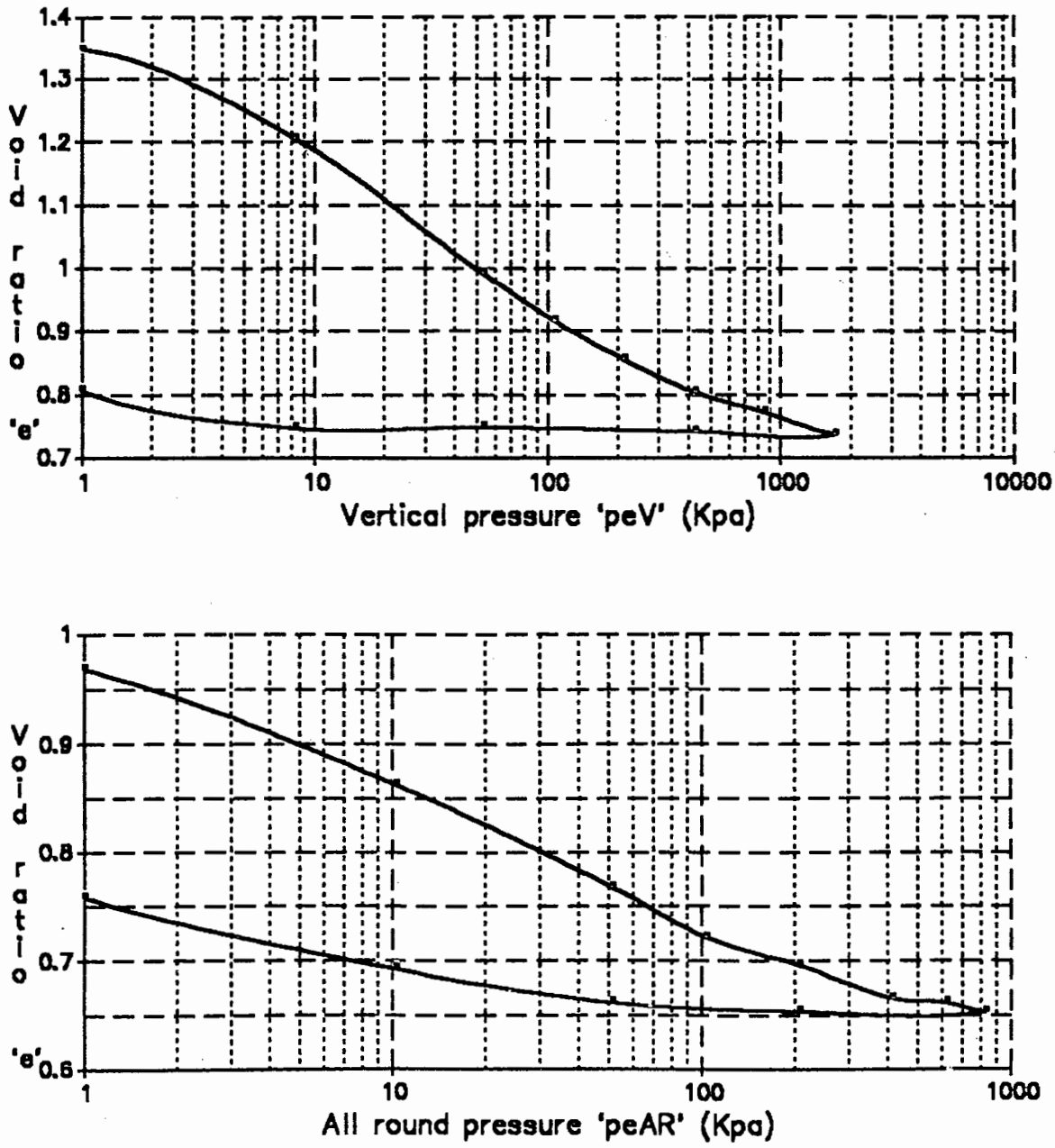

Figure 5.19: Bentonite B.2 (7% clay size) - (Top) One-dimensional consolidation, and (Bottom) Isotropic consolidation.

Bentonite B.3.

A clay sand (fine to medium size) with a very small amount of silt. The soil consists of 11.5% clay, 2% silt and 86.5% sand size. The 'Limits' are: w_{LS} = 1.0%; w_L = 46.0%; w_P = 20.0%; I_P = 26; w_S = 28.0%; and, w_{FE} = 46.1%.

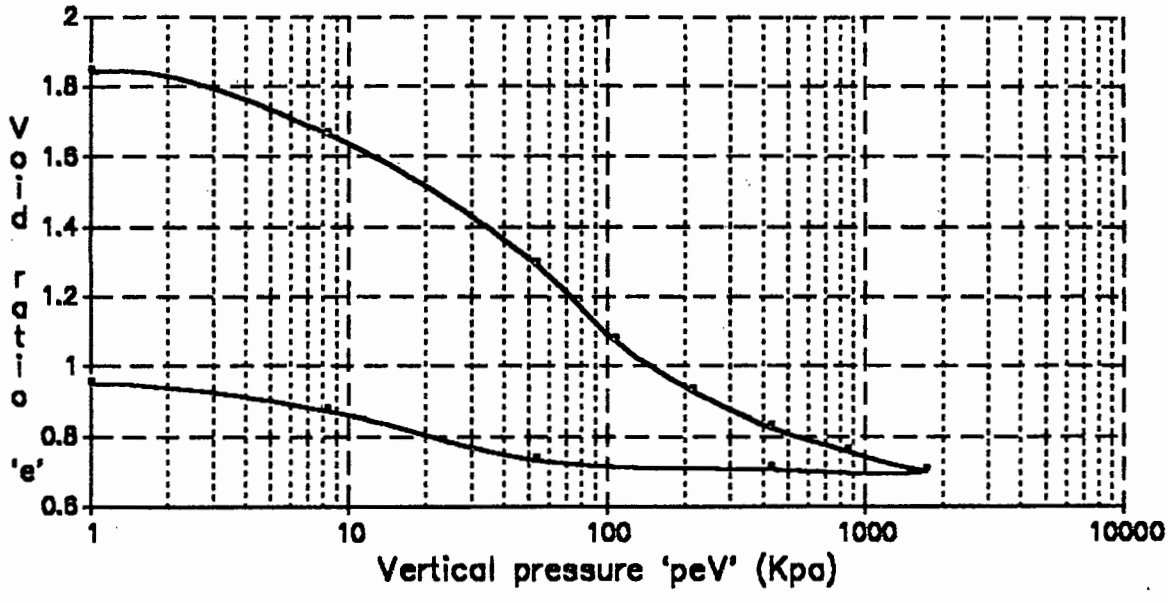

Figure 5.20: Bentonite B.3 (11.5% clay size) - One-dimensional consolidation.

Bentonite B.4.

A clayey sand (fine to medium size) with a very small amount of silt. The soil consists of 15.5% clay, 3% silt and 81.5% sand size. The 'Limits' are: w_{Ls} = 1.5%; w_L = 59.0%; w_P = 19.0%; I_P = 40; w_S = 34.0%; and, w_{FE} = 57.3%.

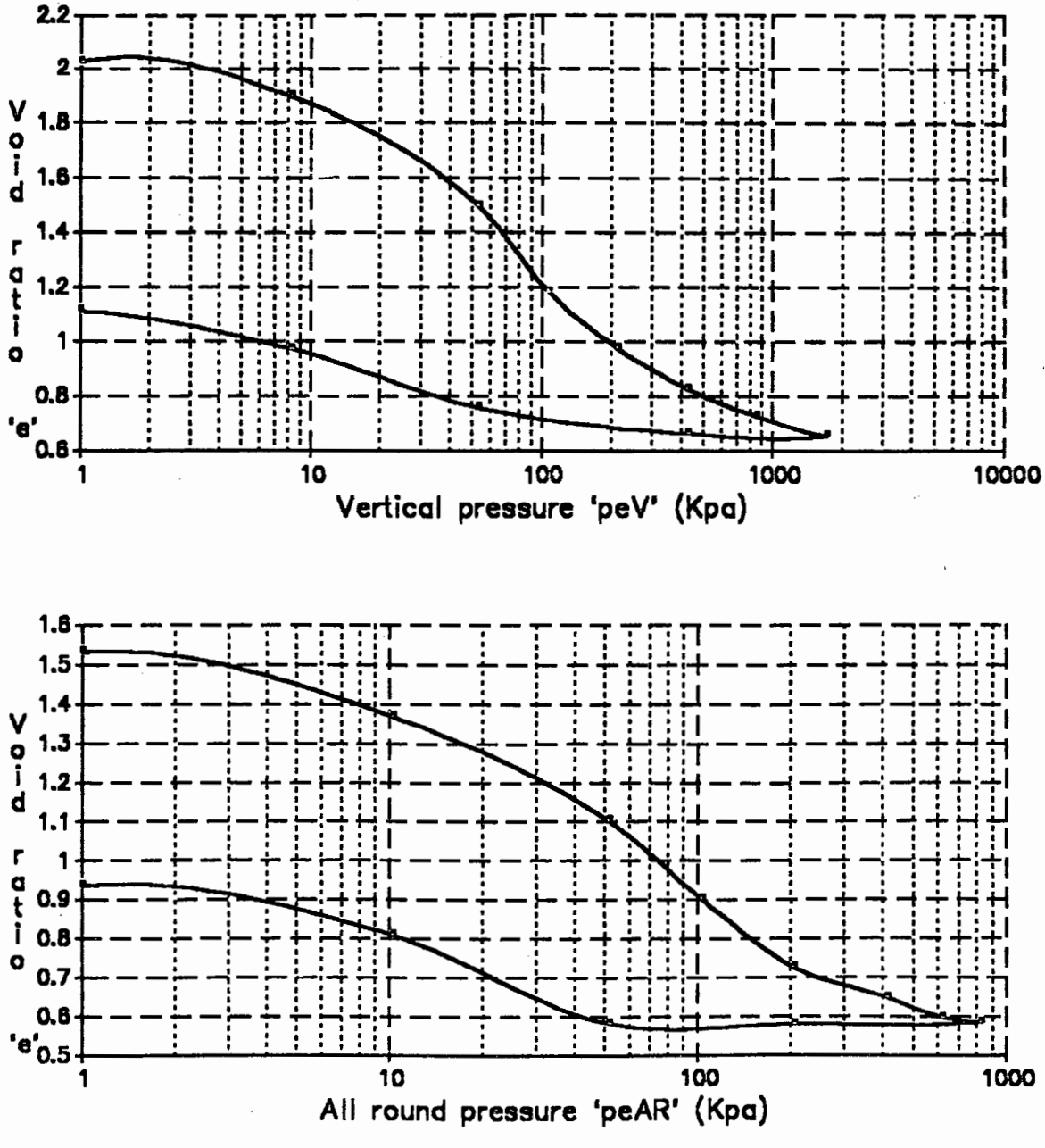

Figure 5.21: Bentonite B.4 (15.5% clay size) - (Top) One-dimensional consolidation, and (Bottom) Isotropic consolidation.

Bentonite B.5.

A clayey sand (fine to medium), with a very small amount of silt. The soil consists of 35% clay, 4% silt, and 61% sand size. The 'Limits' are: w_{LS} = 6.5%; w_L = 133.0%; w_P = 21.0%; I_P = 112; w_S = 38.0%; and, w_{FE} = 100.2%.

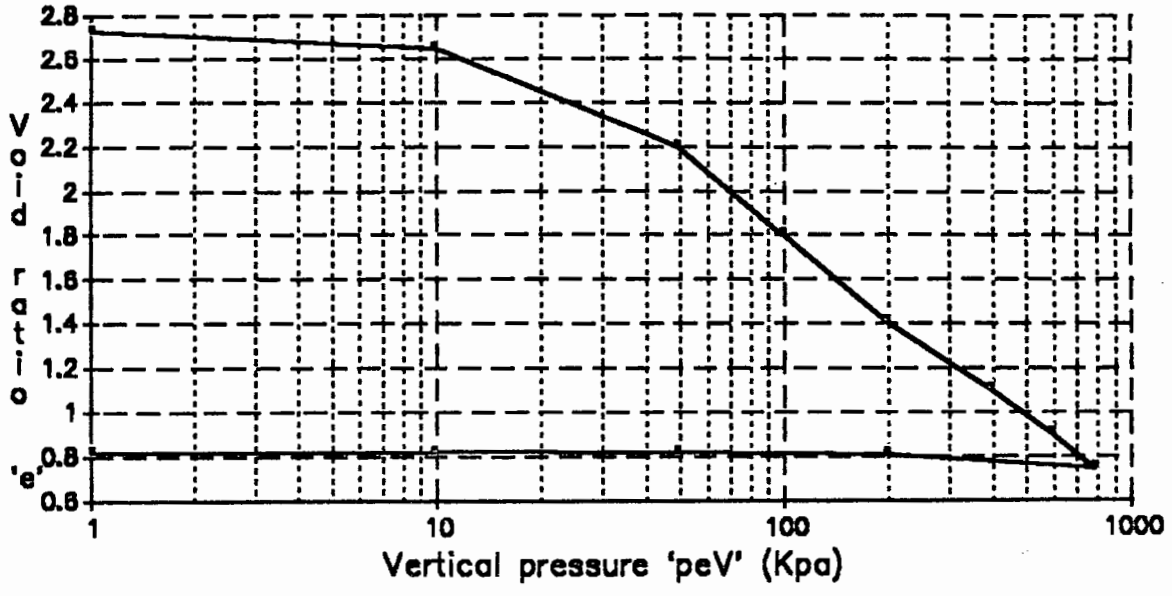

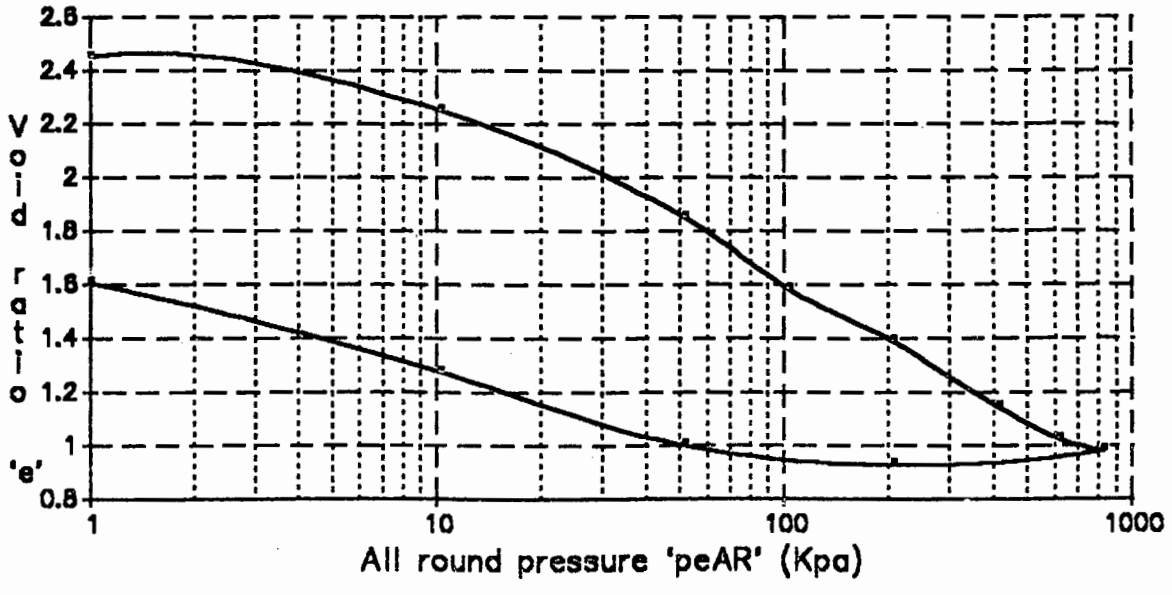

Figure 5.22: Bentonite B.5 (35% clay size) - (Top) One-dimensional consolidation, and (Bottom) Isotropic consolidation in triaxial.

5.8 CONCLUSIONS FOR CHAPTER FIVE: FITTING STRESS SCALES

The free shrinkage path under saturated conditions for each soil type was included in Chapter Four. This type of shrinkage path was defined with Figure 4.01(b), and used to obtain the Shrinkage Limit[1] of each soil.

This type of plot is ideal to use because one can express the position and scaling factor of the stress scale, whether obtained for the one dimensional or isotropic consolidation, in terms of the Consistency Limits - Liquid Limit, Plasticity Index, and so on - of the clay.

The pressure (or stress) values for each recorded void ratio are added to the free shrinkage path (that is, the Shrinkage Limit path) for each soil type.

The observed void ratios, at the end of each step of applied pressure, and the effective pressures themselves, were used to extrapolate a range of stress values characteristic for each soil type.

The relationship between the void ratio and the water ratio (or water content) were defined in a previous section of this chapter - refer to "Stress scales and the type of plot shown in Figure 5.02". The use of this type of plot for each soil type, together with the superimposed stress scales, are illustrated in Figures 5.23 to 5.42.

5.8.1 Natural Soil Types - Remoulded Samples.

This section of the conclusions includes a summary of the relationships of "Void Ratio versus Water Ratio" (alternatively the water content may be used), for the remoulded natural soil samples of the types previously defined - refer to the natural soil types[2] in "Analysis of test results for each soil type".
For each natural soil type the stress scales are superimposed on the plot of "Void Ratio versus Water Ratio".

---

1 - refer to Appendix A, section A.4.5.
2 - section 5.7.1.

Site 11, Rosebank.

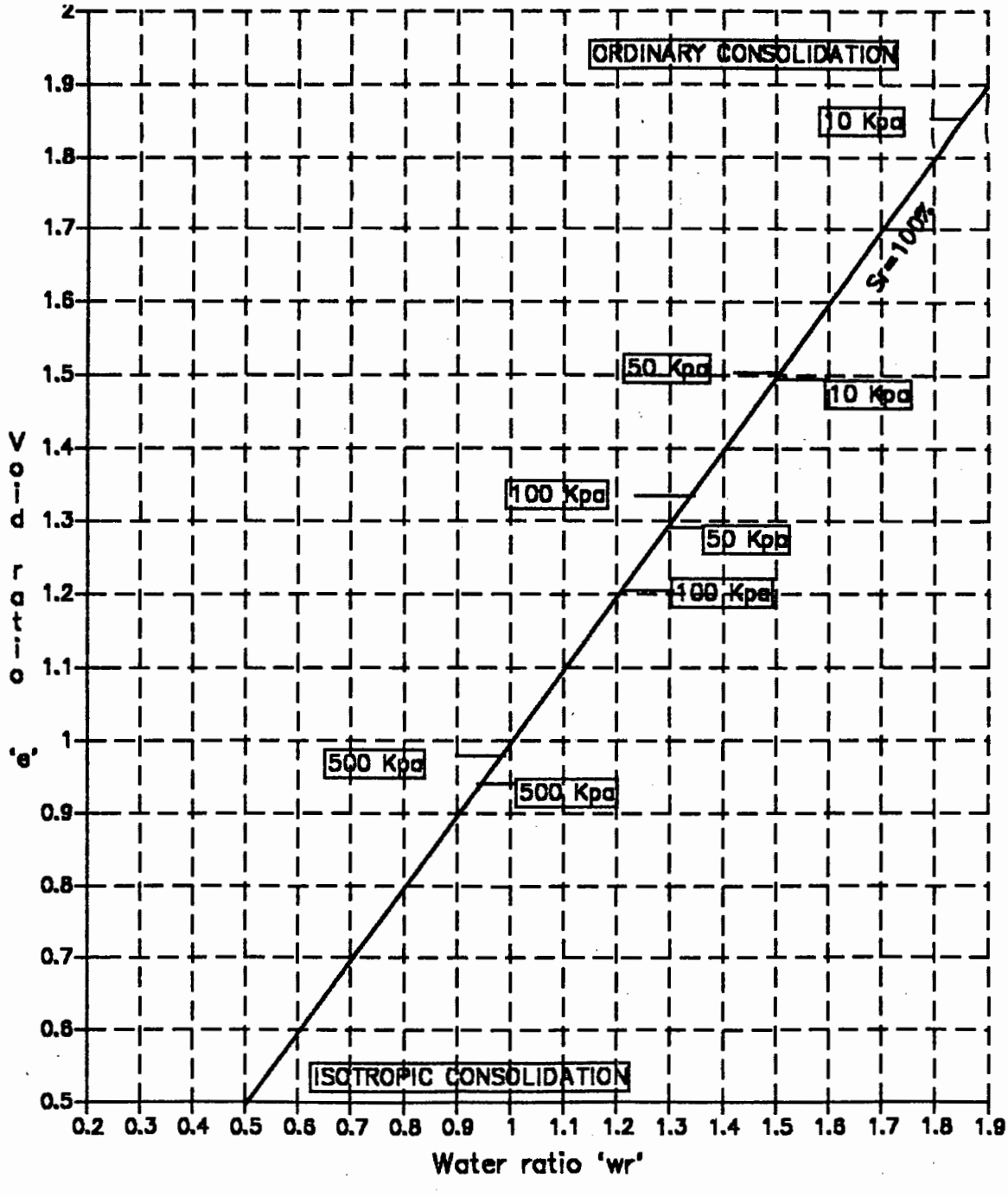

Figure 5.23: Site 11, Rosebank [Remoulded] - Stress scales. [From Figure 5.03]. Pressure values on the left of the line are 'average' pressures for one-dimensional consolidation computed by assuming that the average pressure is equal to half the vertical applied pressure.

Site 36, Rondebosch.

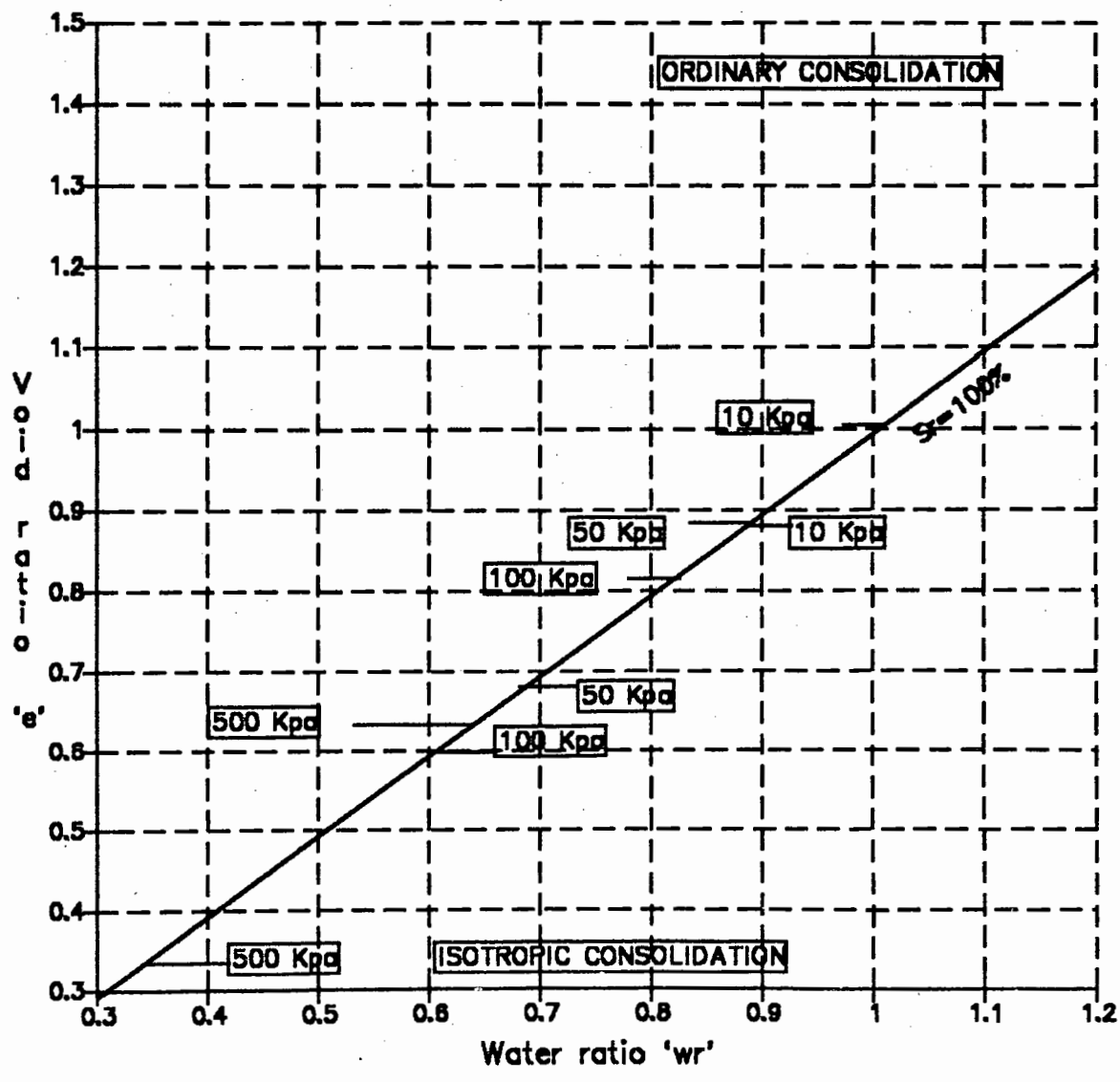

Figure 5.24: Site 36, Rondebosch [Remoulded] - Stress scales. [From Figure 5.04].

Site A, Berea Road (Durban).

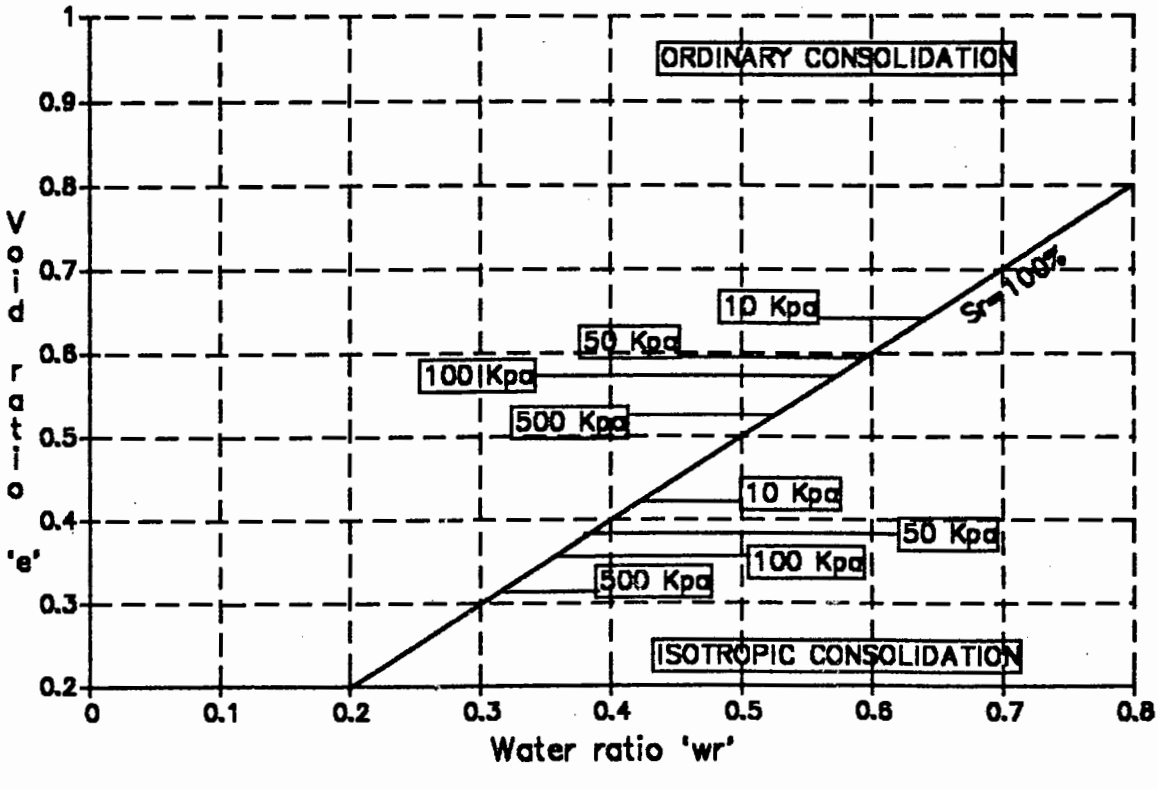

Figure 5.26: Site A, Berea Road (Durban) [Remoulded] - Stress scales. [From Figure 5.06].

Site 7, Mowbray.

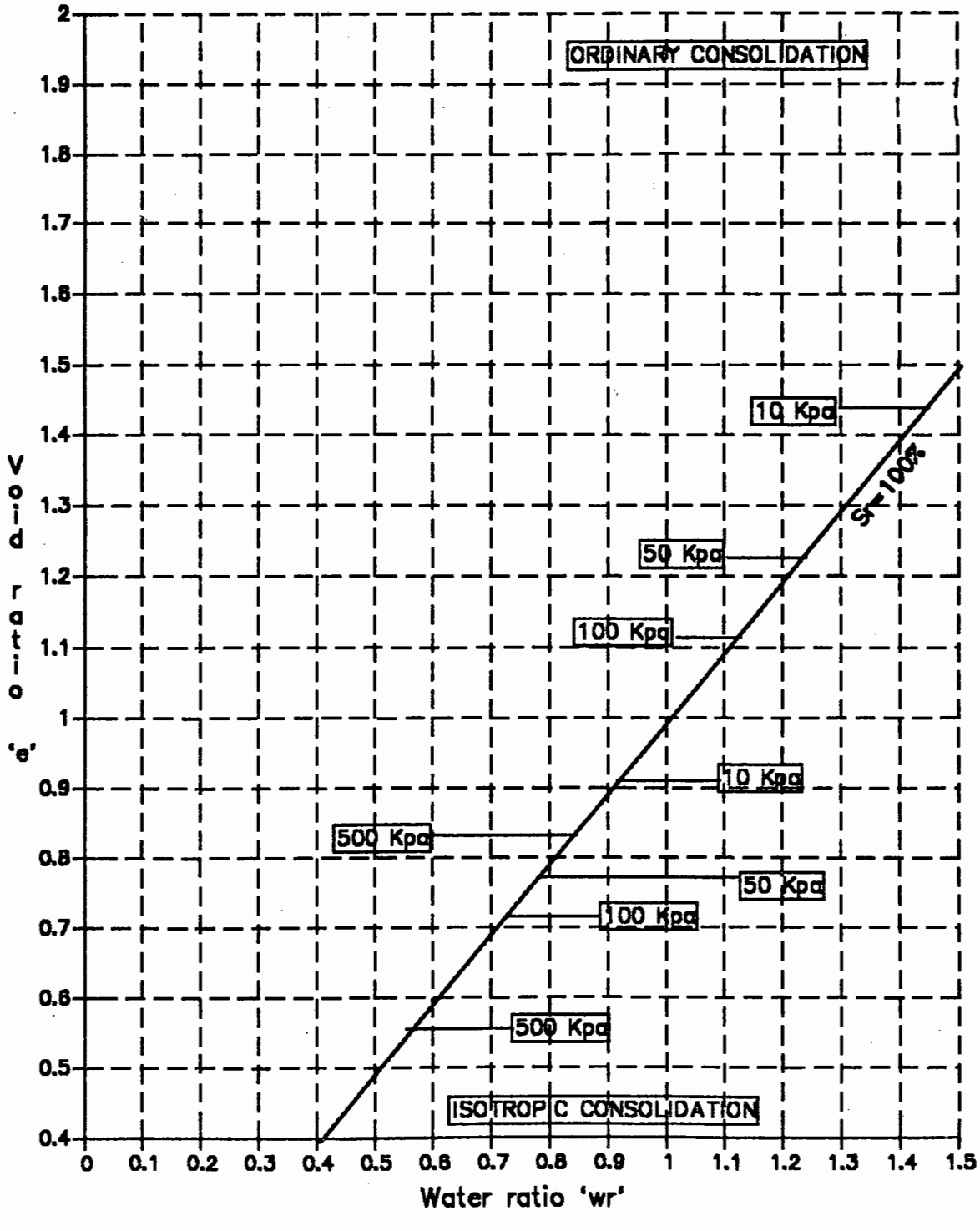

Figure 5.27: Site 7, Mowbray [Remoulded] - Stress scales. [From Figure 5.07].

Site 45, Bellville.

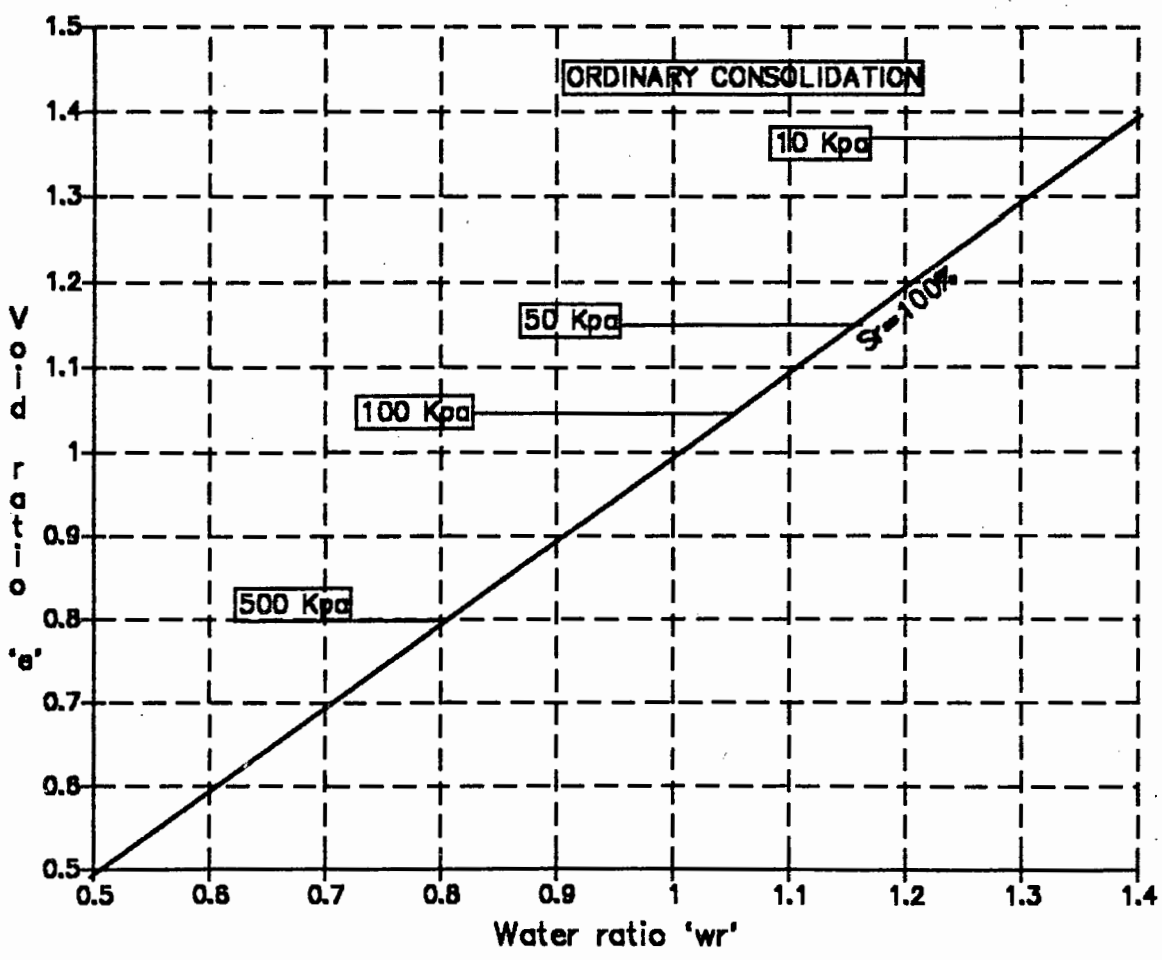

Figure 5.28: Site 45, Bellville [Remoulded] - Stress scales. [From Figure 5.08].

Site B. Francois Road (Durban).

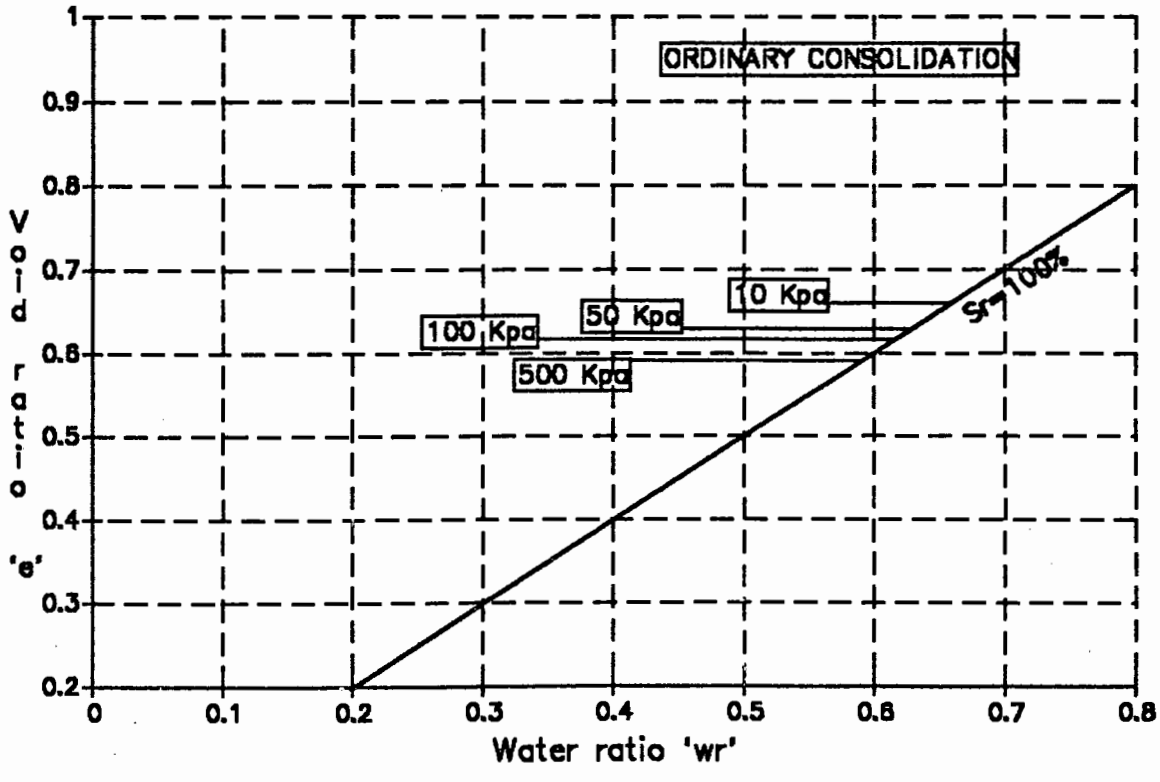

Figure 5.29: Francois Road (Durban) [Remoulded] - Stress scales. [From Figure 5.09].

Site C, Margaret Mayton Avenue (Durban).

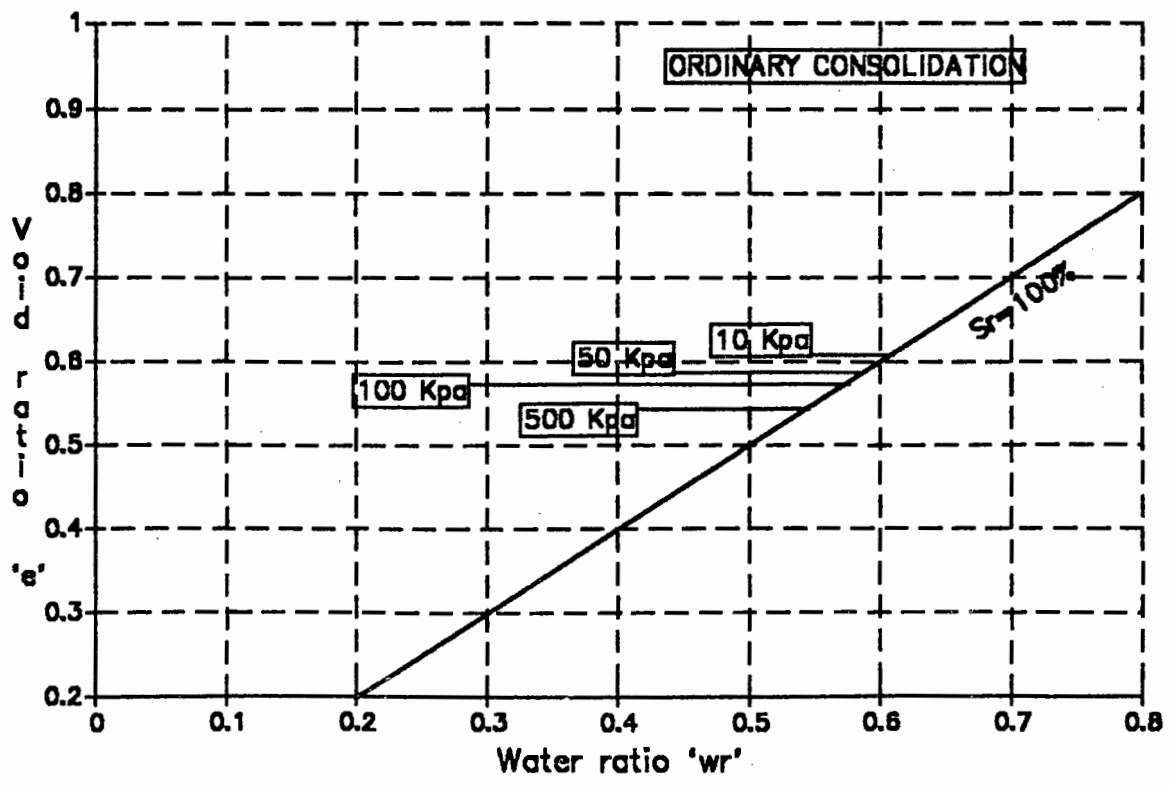

Figure 5.30: Site C, Margaret Mayton Avenue (Durban) [Remoulded] - Stress scales. [From Figure 5.10].

Site D, Rose Hill (Durban).

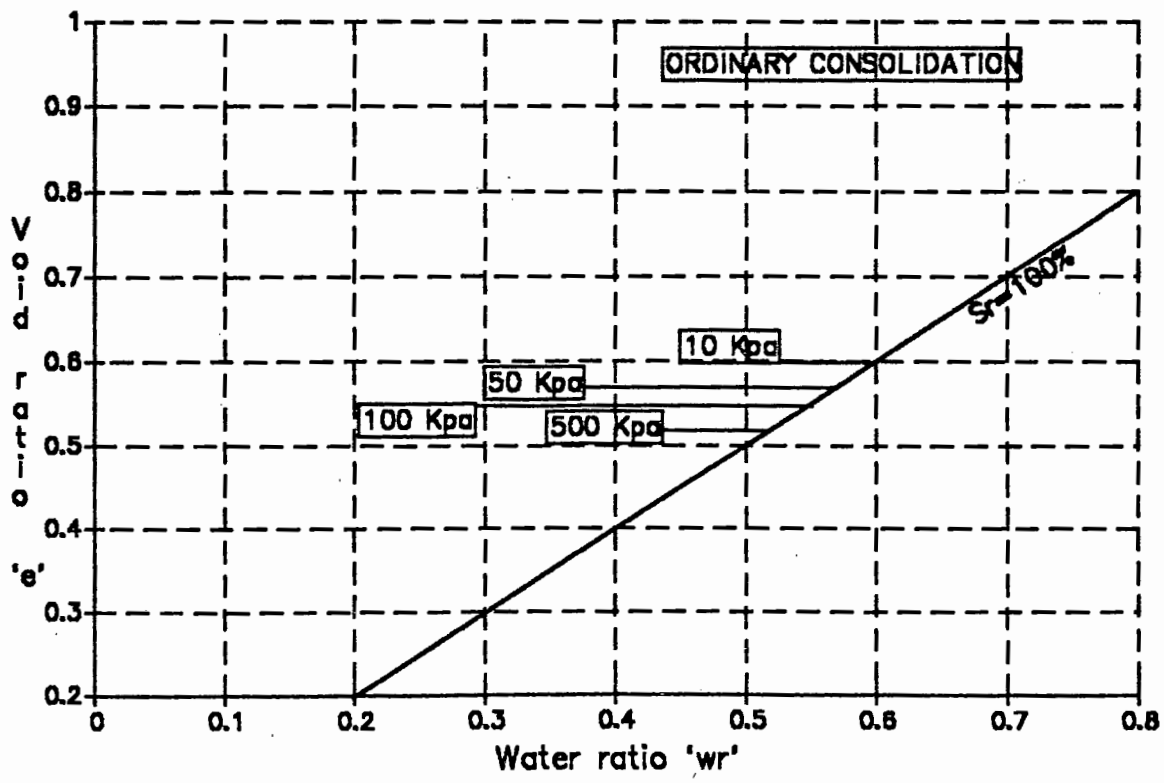

Figure 5.31: Site D, Rose Hill (Durban) [Remoulded] - Stress scales. [From Figure 5.11].
Pressure values on the left of the line are 'average' pressures for one-dimensional consolidation computed by assuming that the average pressure is equal to half the vertical applied pressure.

5.8.2 Natural Soil Types - Undisturbed Samples.

This section includes a summary of the relationships between "Void Ratio and Water Ratio" for the undisturbed samples - refer to previous section on natural soil types[1], "Analysis of test results for each soil type".

These relationships are illustrated in Figures 5.32 to 5.34. For each plot, the void ratio versus water ratio (for each applied pressure), includes the superimposition of the stress scales previously obtained in this chapter.

---

[1] - *see section 5.7.2.*

Site 11, Rosebank.

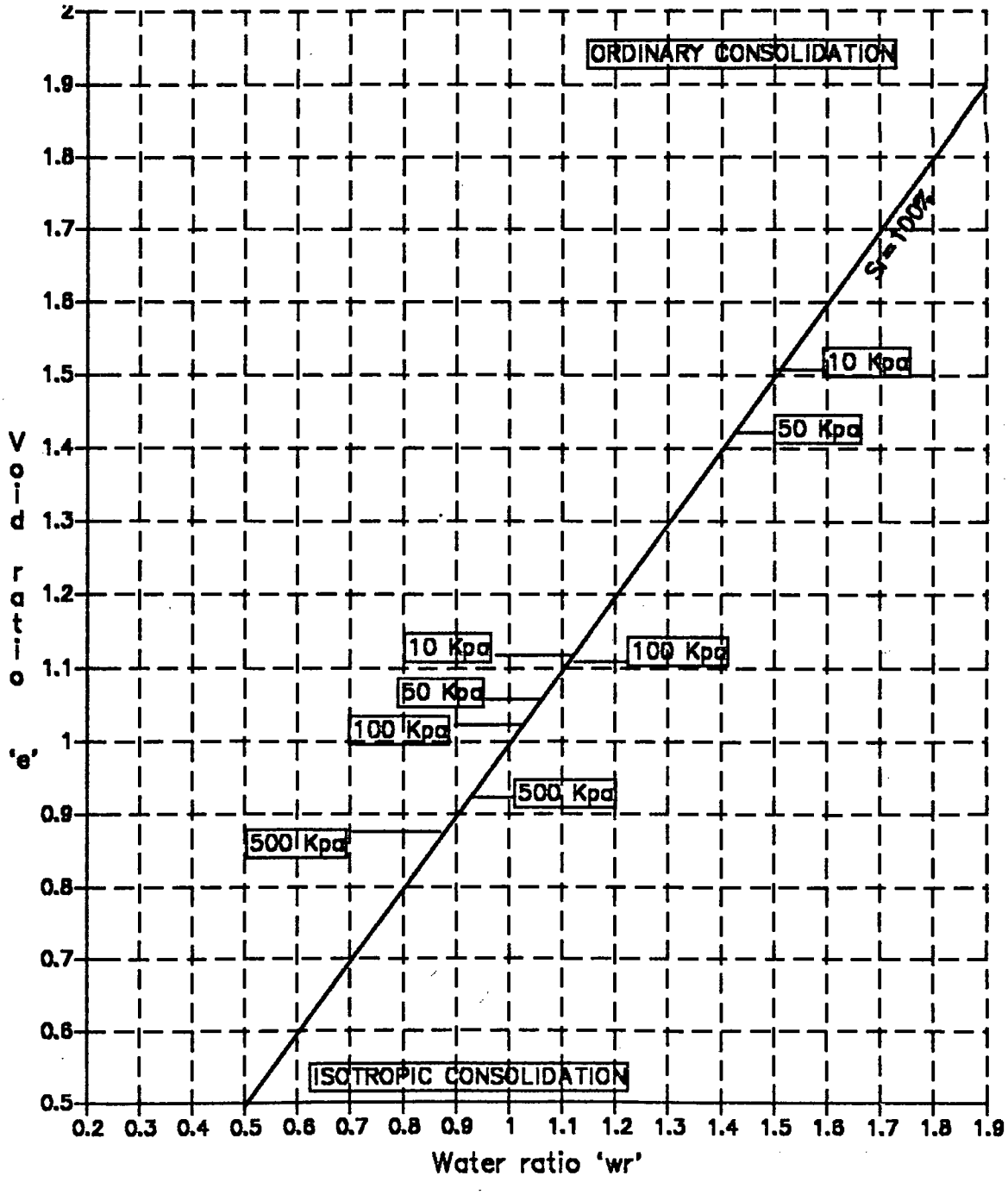

Figure 5.32: Site 11, Rosebank [Undisturbed] - Stress scales. [From Figure 5.12].
Pressure values on the left of the line are 'average' pressures for one-dimensional consolidation computed by assuming that the average pressure is equal to half the vertical applied pressure.

Site 36, Rondebosch.

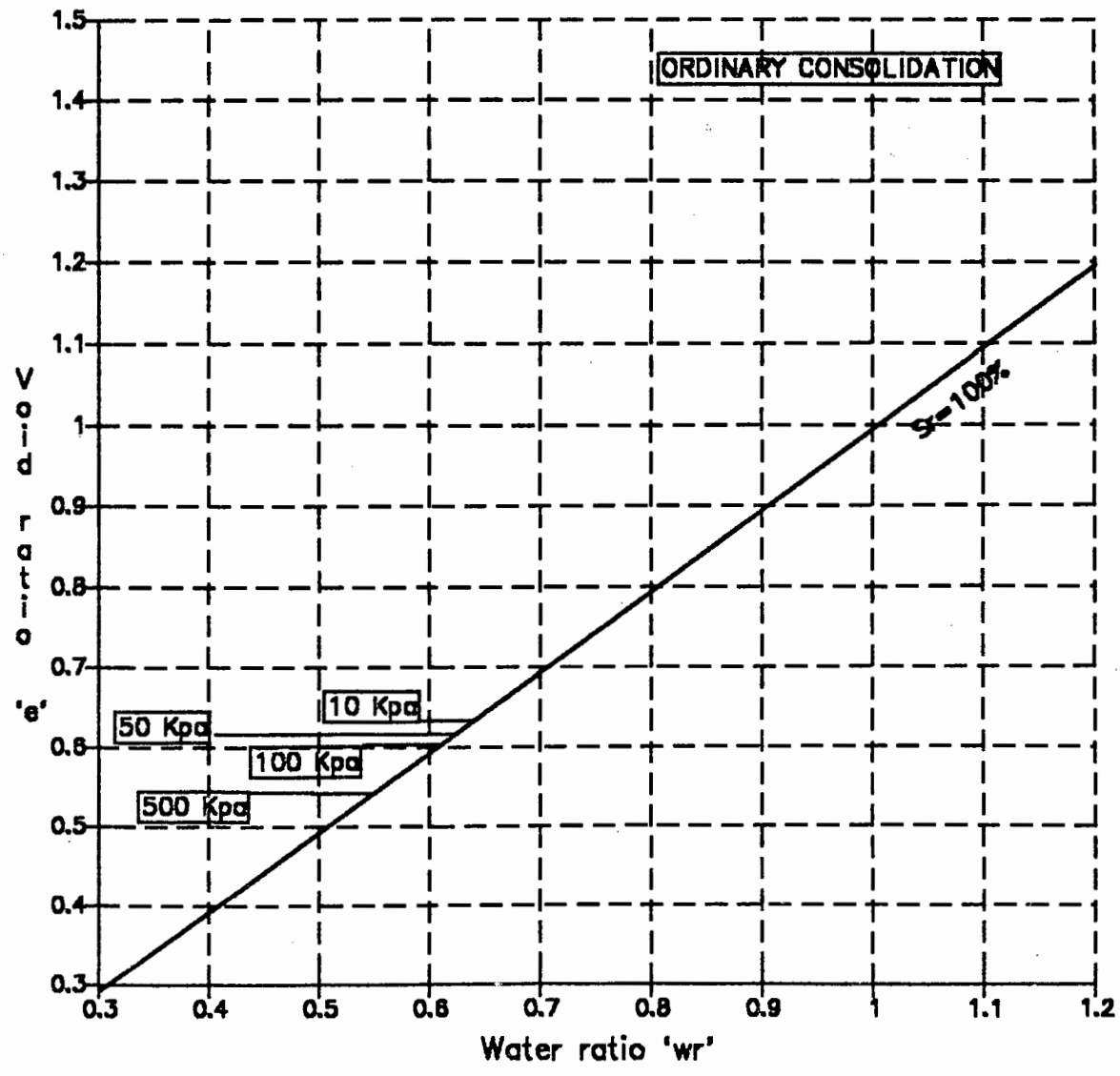

Figure 5.33: Site 36, Rondebosch [Undisturbed] - Stress scales. [From Figure 5.13].

Site 30, Hout Bay.

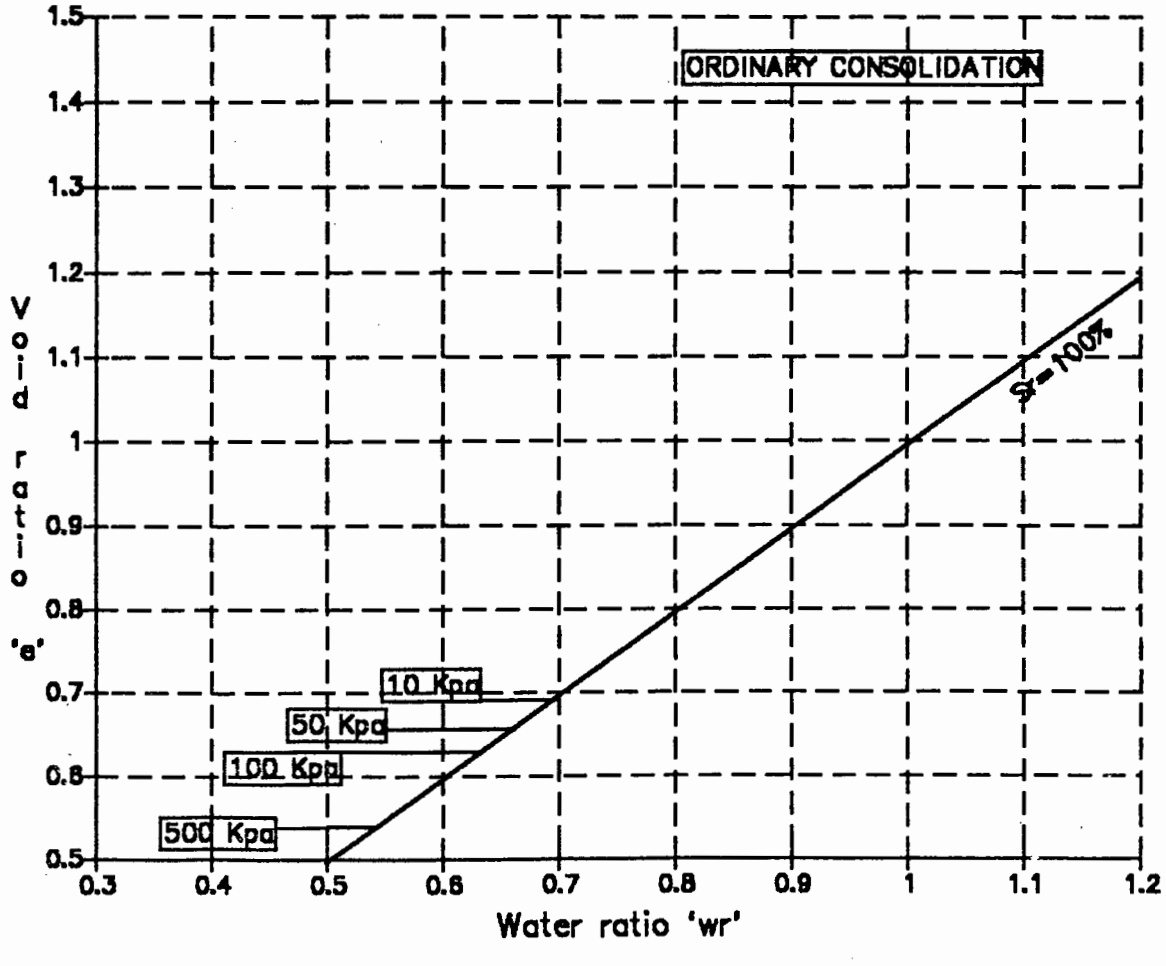

Figure 5.34: Site 30, Hout Bay [Undisturbed] - Stress scales. [From Figure 5.14].

5.8.3 Artificial Soil Types.

This section includes the relationships of "Void Ratio versus Water Ratio" for the artificial, or made up soils previously defined - refer to artificial soil types[1] in "Analysis of test results for each soil type".

Kaolin clay mixed with sand:-

Kaolin K.1.

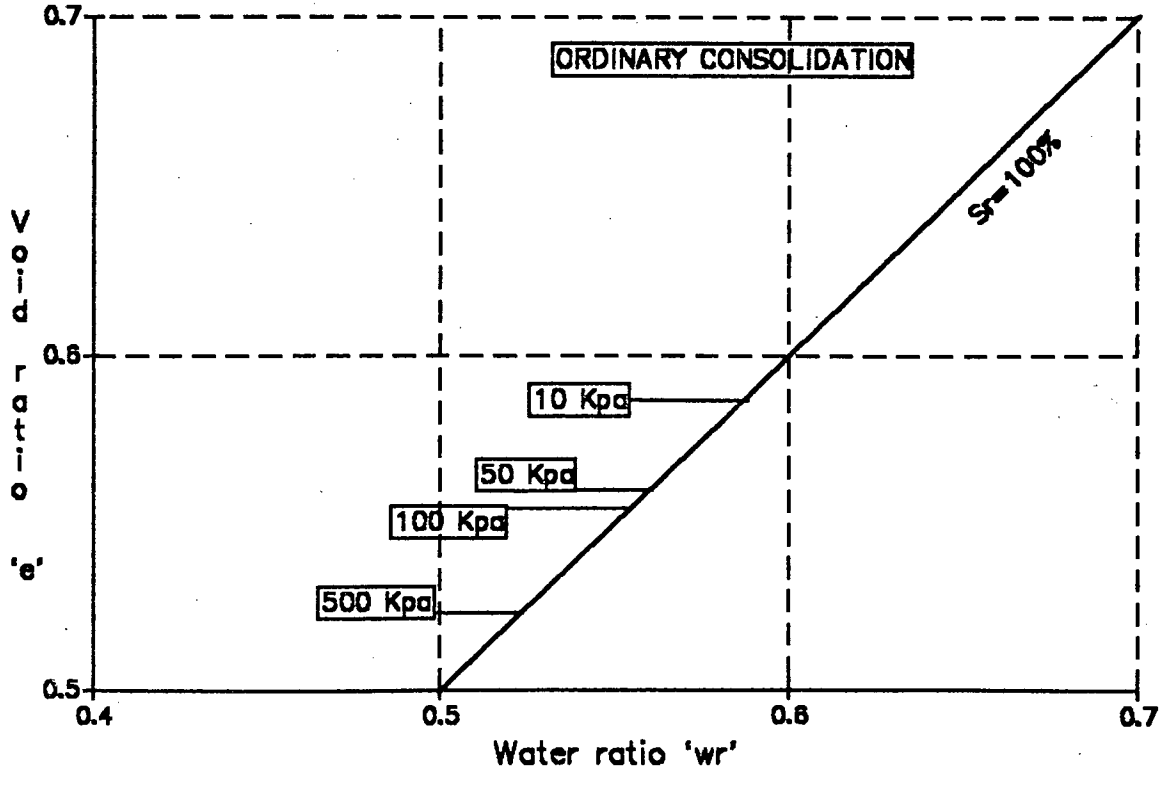

Figure 5.35: Kaolin K.1 (13% clay size) - Stress scales. [From Figure 5.15].
Pressure values on the left of the line are 'average' pressures for one-dimensional consolidation computed by assuming that the average pressure is equal to half the vertical applied pressure.

---

[1] - *see section 5.7.3.*

Kaolin K.2.

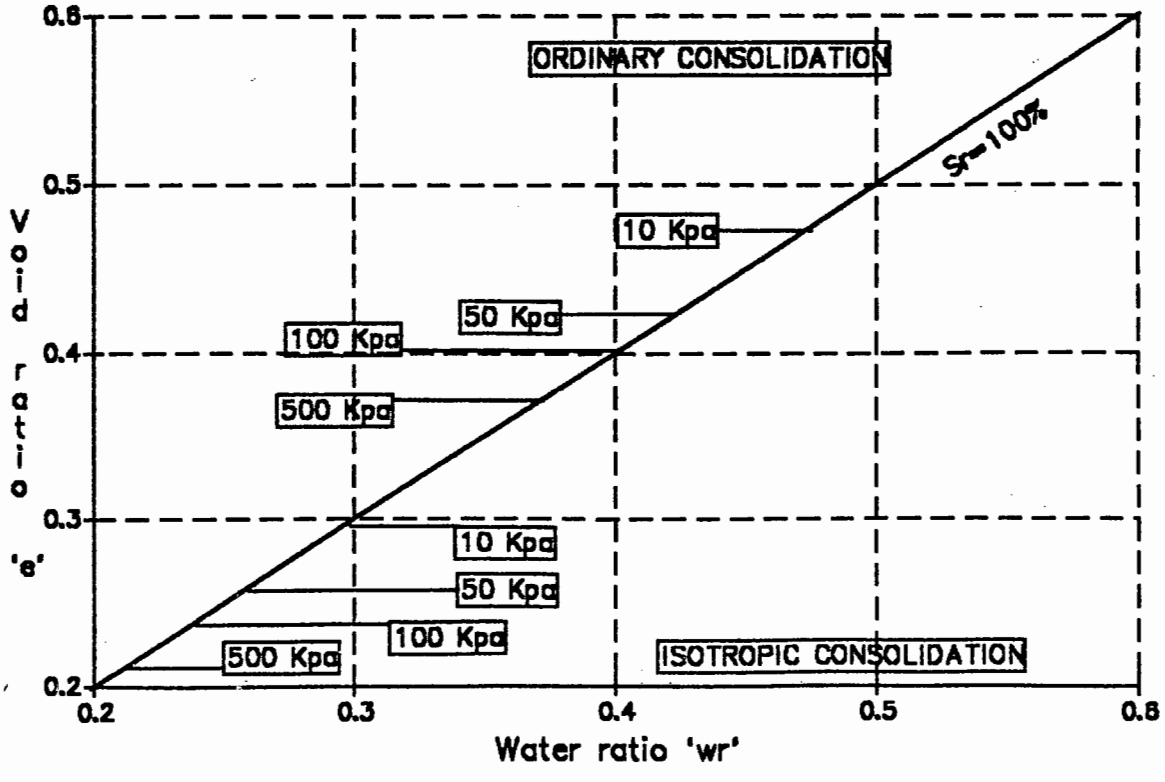

Figure 5.36: Kaolin K.2 (20% clay size) - Stress scales. [From Figure 5.16].

Kaolin K.3.

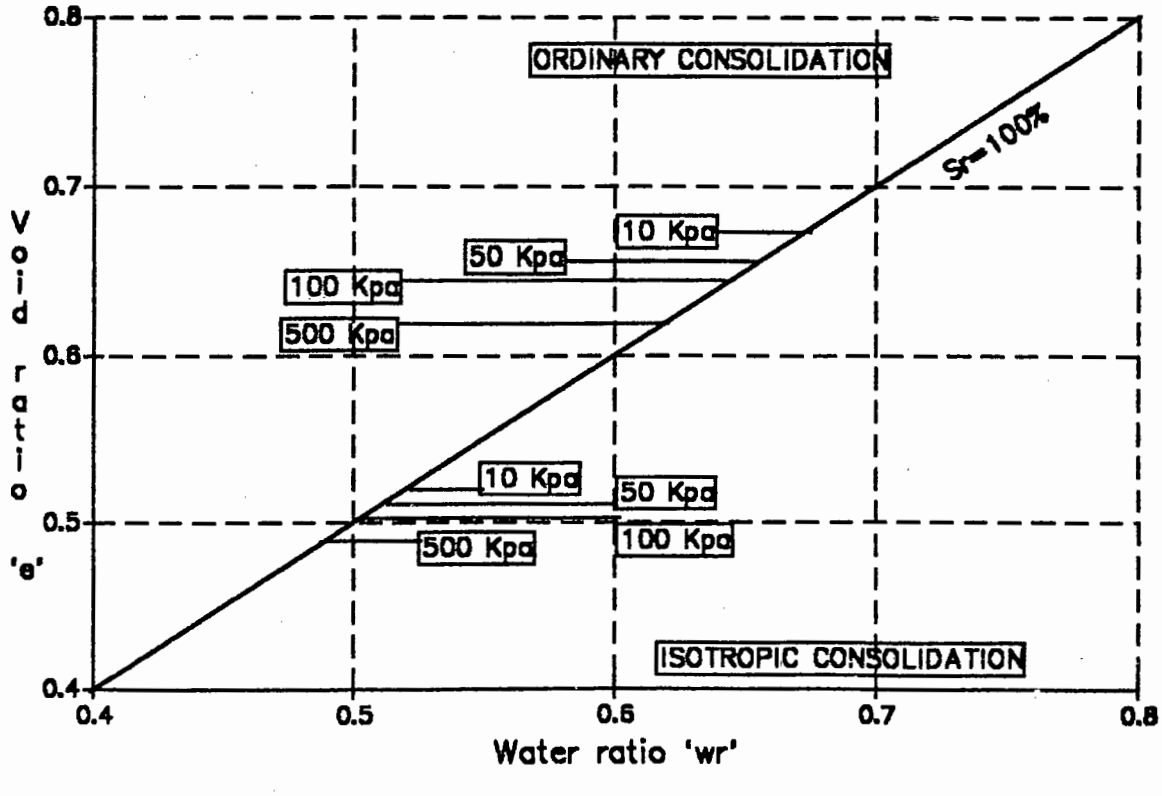

Figure 5.37: Kaolin K.3 (8.5% clay size) - Stress scales. [From Figure 5.17].

Bentonite clay mixed with sand:-

Bentonite B.1.

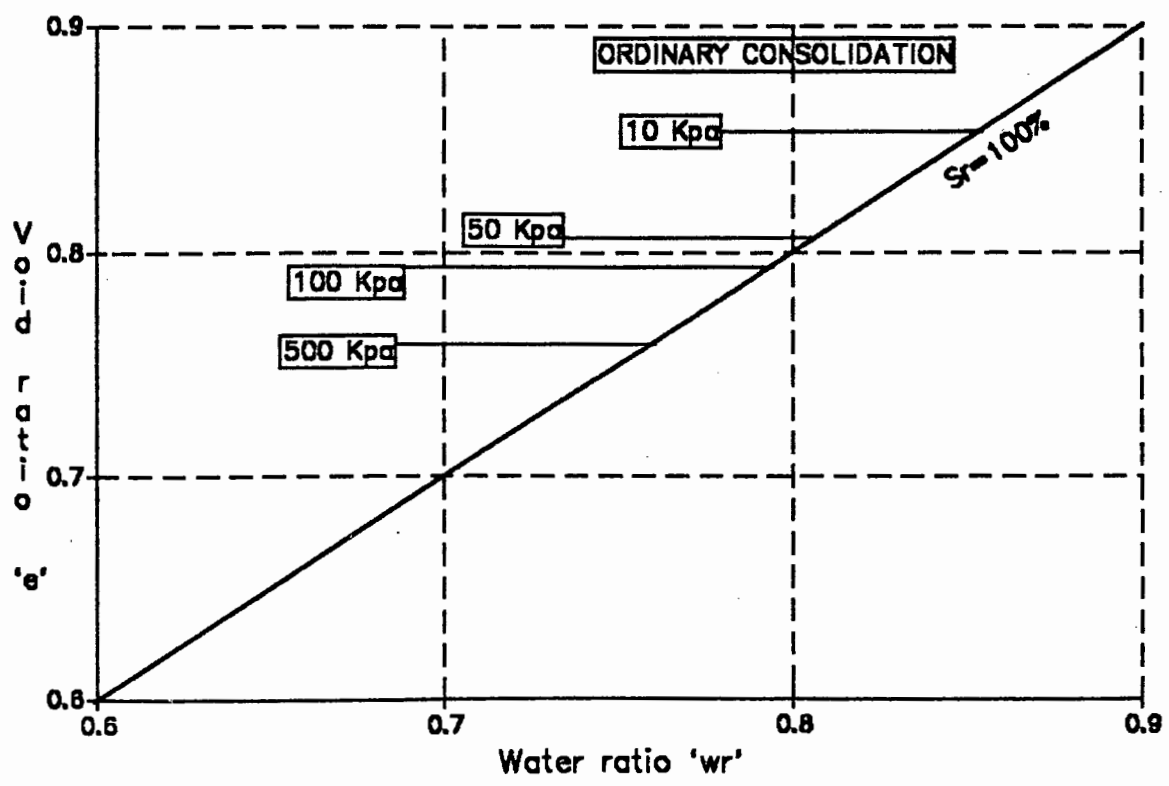

Figure 5.38: Bentonite B.1 (3.5% clay size) - Stress scales. [From Figure 5.18].

Bentonite B.2.

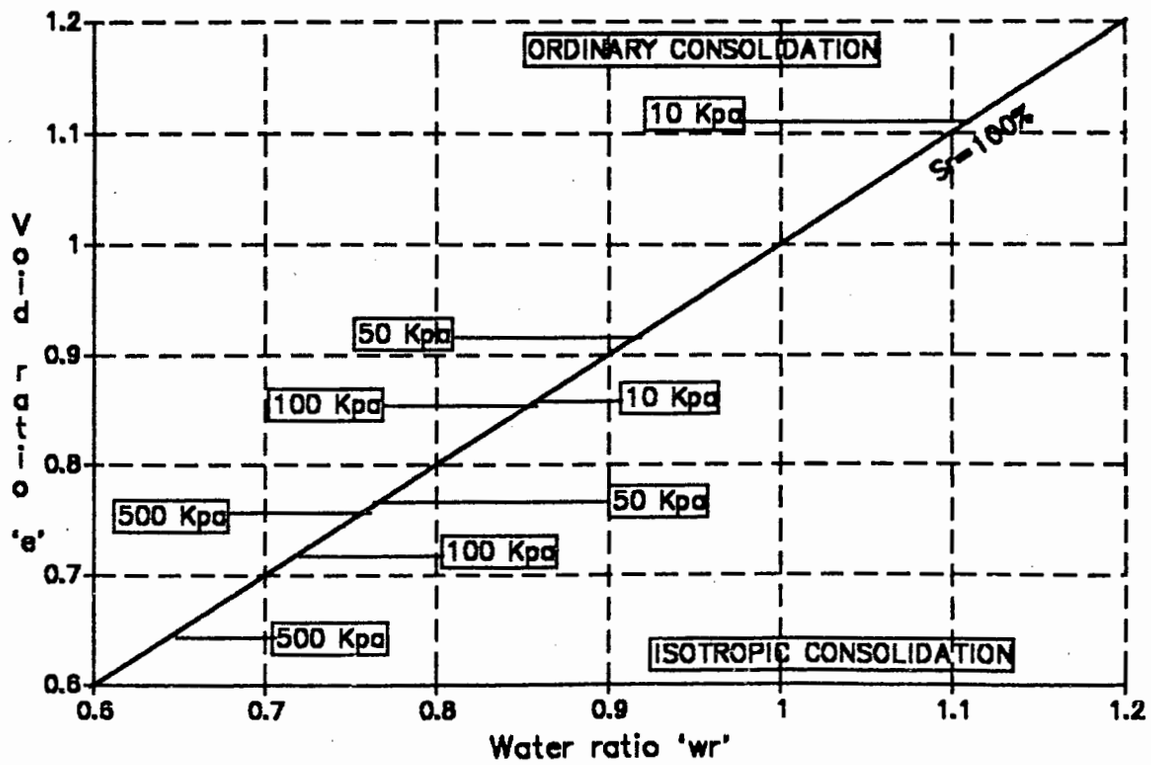

Figure 5.39: Bentonite B.2 (7% clay size) - Stress scales. [From Figure 5.19].

Bentonite B.3.

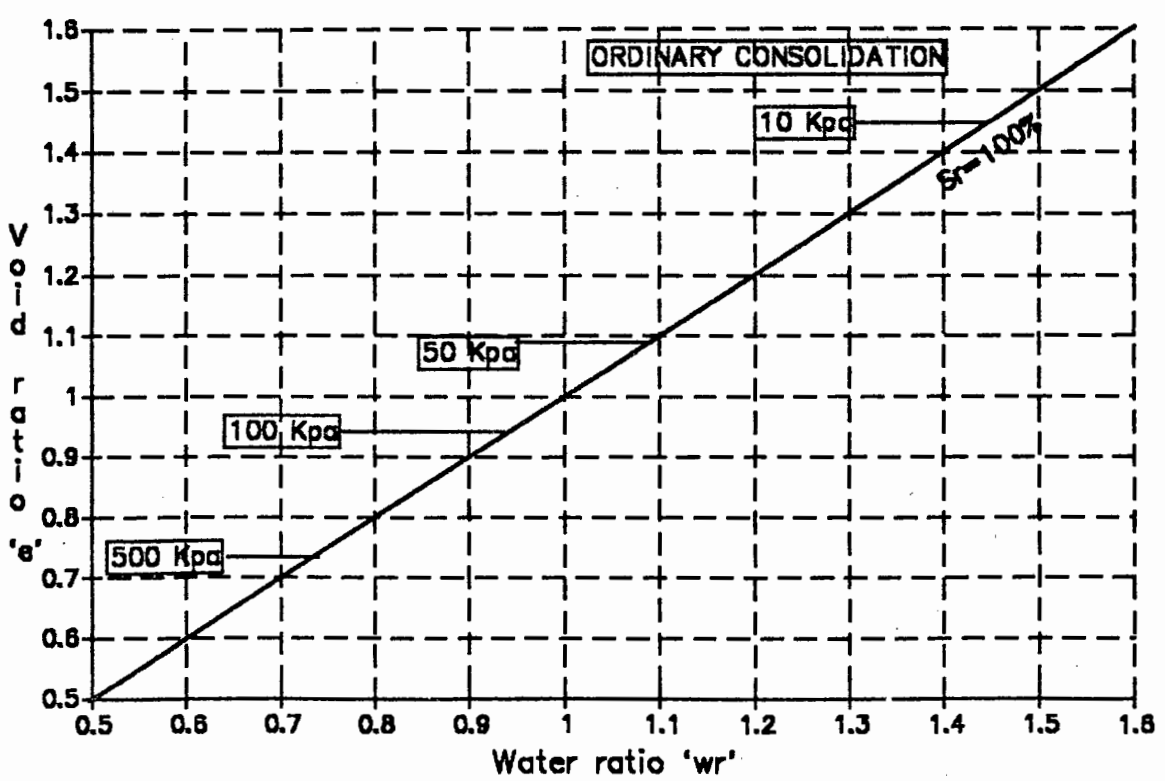

Figure 5.40 Bentonite B.3 (11.5% clay size) - Stress scales. [From Figure 5.20].

Bentonite B.4.

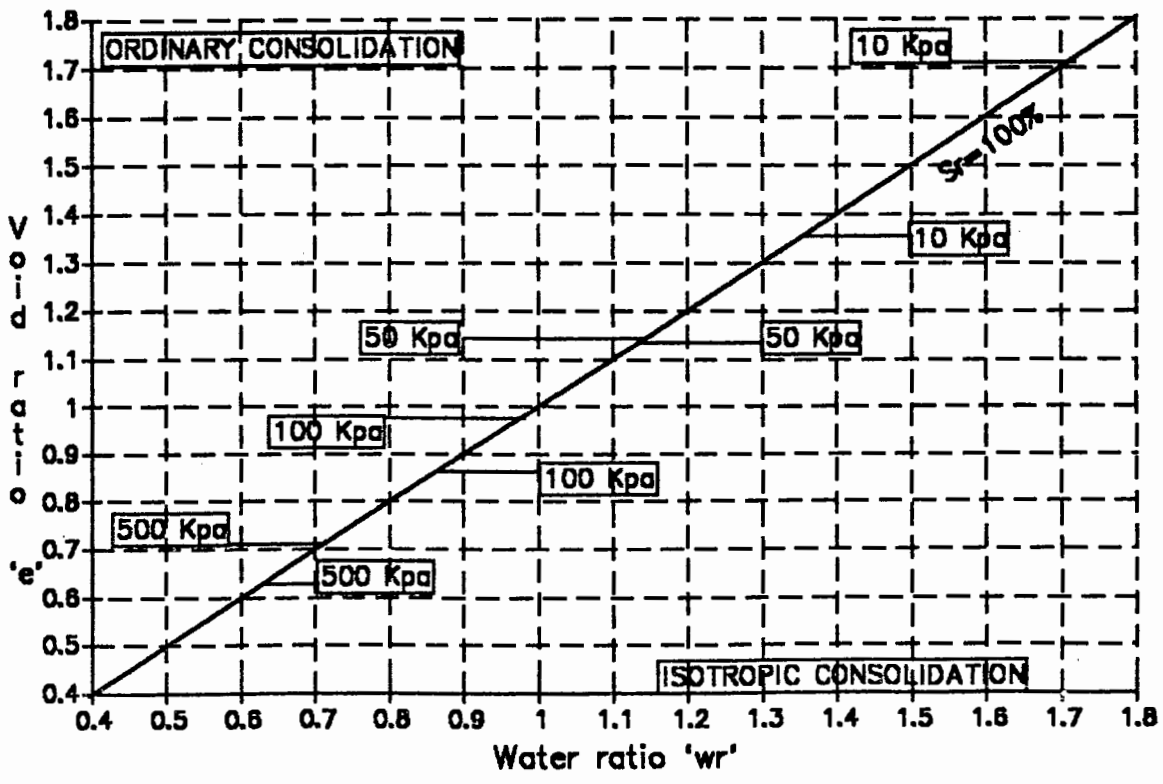

Figure 5.41: Bentonite B.4 (15.5% clay size) - Stress scales. [From Figure 5.21].

Bentonite B.5.

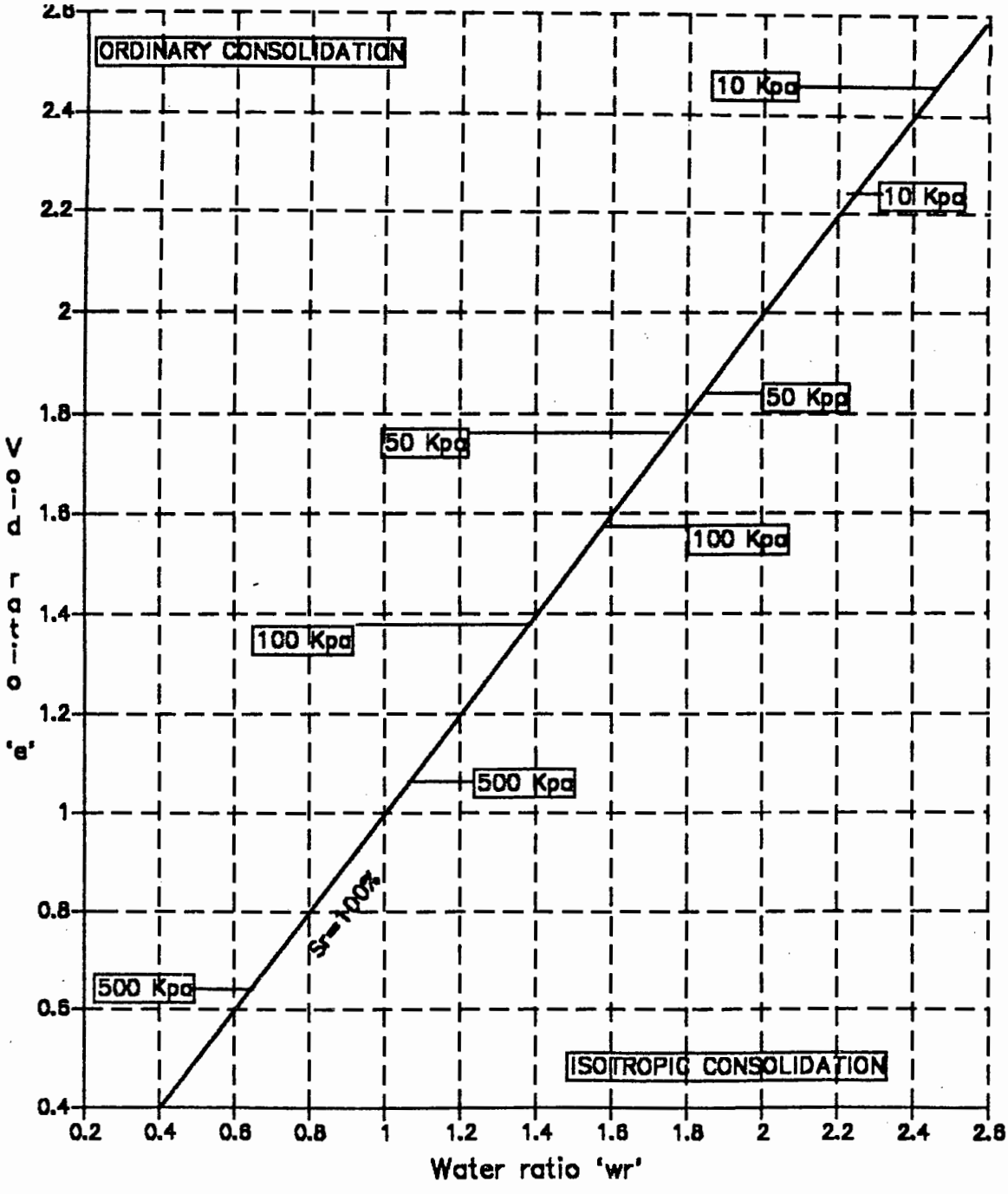

Figure 5.42: Bentonite B.5 (35% clay size) - Stress scales. [From Figure 5.22].

5.9 REFERENCES FOR CHAPTER FIVE

16. DE S. VINAGRE, T.J.V. (1976/77): Masters Thesis - Diaries One, Two, Three, Four, Five, and Six.

86. SPARKS, A.D.W. (1975): Discussions, Volume II, Proceedings of the Sixth Regional Conference for Africa on Soil Mechanics and Foundation Engineering; Durban, South Africa, September 1975.

91. SPARKS, A.D.W. Prof. (Supervisor) - Discussions with the writer.

CHAPTER SIX *

ONE-DIMENSIONAL EXPANSION OR COLLAPSE

6.1 INTRODUCTION

The work in this chapter deals with the observed one-dimensional increase (expansion) or decrease (collapse) in volume of the soil sample, while supporting a known load, as the result of the addition of measured volumes of water. The type of expansive or collapsing behaviour being investigated, under controlled wetting conditions, refers to soil samples which are confined in the horizontal directions and, while being subjected to a known vertical constraint, are allowed to increase (expand) or decrease (collapse) their volume along the vertical axis.

A standard consolidometer was used to apply the external vertical stress against which the sample expands or collapses upon being wetted. Four different external stresses were used - 1 Kpa, 50 Kpa, 100 Kpa, and 400 Kpa.

The observed water contents, void ratios, as well as the recorded vertical pressures applied (ie, the known constraint against which the sample expands or collapses), are presented in graphical form. The purpose is to illustrate trends of behaviour and to allow comparisons to be made between the 'paths' of expansion or collapse, under known vertical loads, which developed for different initial conditions and ranges of water content.

For a soil to expand while under load, not only are the inner structure and water content important factors, but it also needs to have the type of clay which will absorb water and increase in volume. This 'type of clay' needs to contain the clay minerals identified in chapter two. Various different types of soil were used. Different methods of sample preparation were followed for each soil type, prior to the measurements of one-dimensional volume change along the vertical axis. Samples were either permitted to lose or gain moisture until the required initial water content was reached. During this initial stage of free shrinkage or swell, the observed changes in the volume and mass of soil samples are recorded. It was hoped to investigate both the unsaturated and saturated conditions of each sample.

6.2 CONCEPTS AND DEFINITIONS

The concepts and definitions which together make up "One Dimensional Expansion or Collapse", as used in this chapter, can be defined as follows:-

---

* - *Observations are listed in Appendix E.*

The word "One-dimensional" refers to the one degree of freedom of the sample to increase[1] its volume along one axis, in this case the vertical axis, while being confined by a fixed consolidometer ring in the horizontal plane.

The word "expansion" refers to the increase in the overall volume of the sample caused by the interaction of water and the clay minerals in the soil sample. The addition of water causes an increase in the lattice spacing of the clay minerals which results in the overall volume increase of the sample - refer to Chapter Two[2].

The word "collapse" refers to the breakdown of soil structure resulting from the wetting up of the clay bridges which link the fine sand and silt grains, and result in loss of shear strength and decrease in the overall volume of the sample.

The words "Expansive" and "Collapsing" as used in this chapter, can be defined as follows:
The word "Expansive" refers to a soil which has consolidated for at least 12 hours, or overnight, under a known vertical pressure (or stress) being applied externally, and against which it will increase its volume when wetted; Similarly, "Collapsing" refers to a soil which will decrease its volume upon wetting - that is, further settlement will occur while the sample is being subjected to the same constant pressure.

The external vertical stresses applied to the sample vary between 1 Kpa and 400 Kpa. After consolidating under the applied pressure, the soil sample expands or collapses as the result of being (gradually) wetted by increments.

The one-dimensional measurement of the increase[1] in the volume of the sample, as the result of wetting and while being subjected to a known and constant stress, occurs under conditions in which drainage is permitted throughout. This is an attempt to satisfy the conditions of zero pore water pressure and, because the pore water pressure is zero, the effective stresses are equal to the applied stresses. The concept of zero pore water pressure was introduced in Chapter Four and its implications were also discussed in Chapter Five.

The "external vertical stress" or "constraint", will in this case mean that during the process of overall volume change, the sample is partly confined by an externally applied stress (along the vertical axis) while being fully confined by a fixed consolidometer ring (horizontal axis). Therefore, the applied vertical stress prevents the sample from increasing its volume to the full extent along the vertical axis. It should be noted that the vertical stress (or pressure) against which the sample expands or collapses, remains constant throughout the wetting stage.

---

1 - or decrease.
2 - section 2.4 "Micro Studies - II".

The changes in the water content of these samples were made to happen in a controlled manner, as follows: A small known volume of de-aired water is added to the bottom filter paper, which in turn transmits the water to the whole underside of the sample; and to wait for this extra water to distribute itself upwards into the sample while recording time measurements for one-dimensional increase or decrease in its volume - refer 'Test Method'[1].

The definitions of "Free-shrinkage" and "Free-swell" are included in Chapter Four.

The section on 'Micro Studies' of Chapter Two includes the definitions of void ratio 'e', water ratio 'Ω', or 'wr', and water content 'w'.

6.3 THE PARAMETERS WHICH ARE BEING INVESTIGATED

The diagrams in Figures 6.01 and 6.02 illustrate the three main parameters which are being investigated. These parameters are the void ratio, the water ratio (or alternatively, the water content), and the effective pressure or stress, applied along the vertical axis.

The relationship between the void ratio (that is, the ratio of volume of voids to the volume of solids) and the water ratio (the ratio of volume of water to the volume of solids), as shown in Figure 6.01, goes through the following stages:

(i) The sample is initially at condition A (that is, the condition at which the soil sample was prepared - remoulded, compacted or obtained from an undisturbed block sample);
(ii) The sample is allowed to lose moisture, and as it loses moisture the state of the sample moves from A towards B (free-shrinkage path);
(iii) At point B, the sample is prepared for the one-dimensional expansion or collapse test[2];
(iv) The "Initial loading path" BC - the loading of the sample to the required vertical stress, against which the sample expands or collapses when wetted;
(v) Starting at point C, the water content is gradually increased in steps, while the sample is confined laterally and the magnitude of vertical movement is partly restrained by the applied vertical stress - the void ratio increase (due to the expansion of the sample), or decrease (due to further settlement), is shown as the "wetting path" between points C and D;
(vi) When no further movement of the sample takes place after another increment of water, additional loading and unloading of the sample is carried out - shown as the final loading and recovery paths DE to EF.

---

[1] - *subsequent section 6.7 of this chapter.*
[2] - *see section 6.6 "Preparation of Test Samples".*

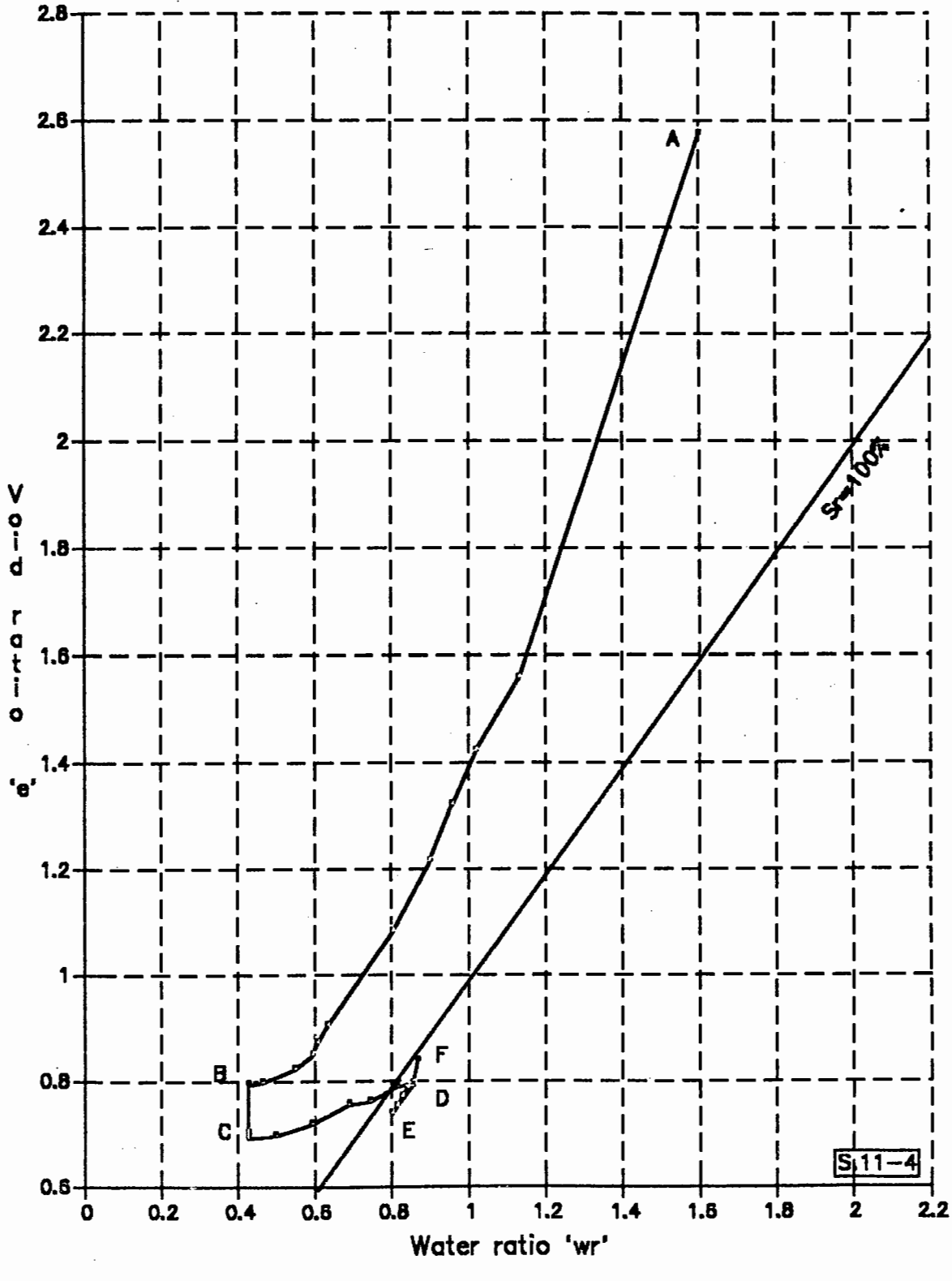

Figure 6.01: Site 11, Rosebank - Relationship between the void ratio 'e' and the water ratio 'Ω', or 'wr', for the full test path[1].

---

[1] - *described in text.*

The vertical axis of the diagram in Figure 6.01 represents the void ratio of the sample (or alternatively, the total volume), and the horizontal axis represents the water ratio[1].
Figure 6.01 is basically the same as Figure 4.01(b) combined with Figure 4.01(c), of Chapter Four.

The type of plot in Figure 6.02.

The diagram in Figure 6.02 includes the third parameter being investigated - this is the effective pressure, or stress, applied along the vertical axis.
The horizontal axis represents the effective pressure applied to the sample throughout the test.
The main differences between Figure 6.02 and Figure 6.01, are as follows:
(a) Effective pressures are plotted along the horizontal axis (water ratio values were used in Figure 6.01); and,
(b) Figure 6.02 includes water ratio values at selected points of the test path.

Other parameters relating to each soil type were also measured. These measurements are included in Chapters One, Two, and Appendix A. Chapter Four lists the main properties for each soil type used throughout the thesis.

6.4 REASONS FOR USING THE TYPES OF PLOT SHOWN IN FIGURES 6.01-02

The type of plot shown in Figure 6.01:-

(A) It is easy to show a transition from a partly saturated to a saturated state.
(B) It is possible to plot contours of degree of saturation as straight lines.
(C) To illustrate the free-shrinkage path of a sample before the one-dimensional expansion or collapse test.
(D) To illustrate the shrinkage and swelling paths for samples which are confined by external stresses.
(E) Stress contours can be superimposed on this plot as contours of stress.
(F) To express the position and scaling factor of the stress scale obtained from the one dimensional consolidation in Chapter Five, in terms of the Liquid Limit and Plasticity Index of the clay.

---

[1] - *that is, the water content 'w' multiplied by the specific gravity of the soil particles 'G_S'.*

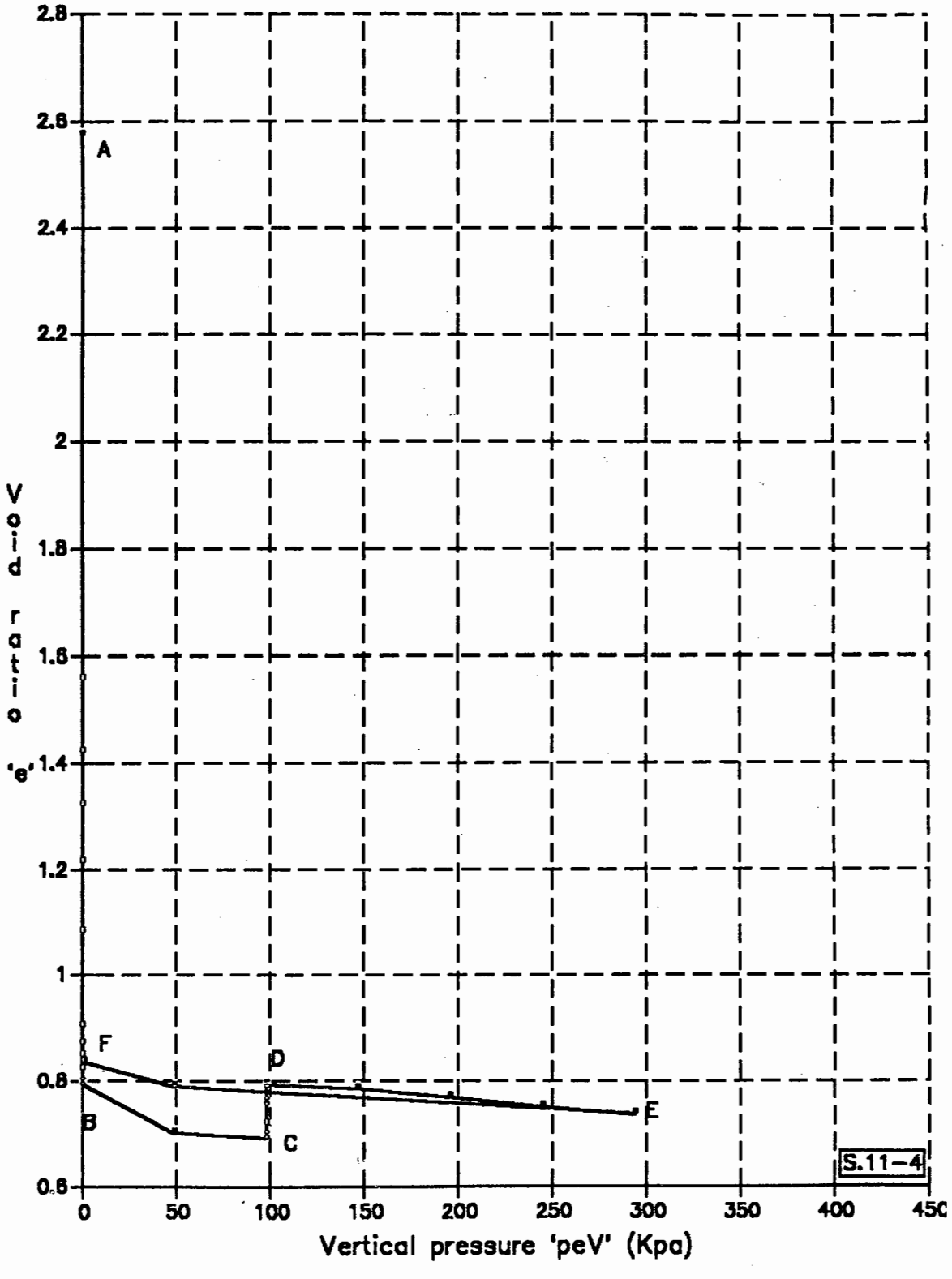

Figure 6.02: Relationship between the void ratio 'e' and effective vertical pressure (or stress) 'peV', for the full test path[1].

[1] - refer to Figure 6.01.

The type of plot in Figure 6.02:-

(A) To observe the relationship between the void ratio and the effective pressure (or stress) applied along the vertical axis, under drained conditions, to a soil sample whose water content remains in the unsaturated condition throughout the initial loading path.
(B) The void ratio changes as the result of increases in the water content of the sample, while being subjected to a constant vertical pressure.
(C) The relationship between void ratio and effective pressure (or stress) for the final loading and unloading path, under drained conditions, of a soil sample whose water content has been increased as the result of (B) above.

6.5 SOME SPECIFIC OBJECTIVES FOR THIS CHAPTER

Some of the specific objectives of this chapter:-

(i) To obtain the shrinkage path of the sample as it dries, under controlled conditions, to the initial water content required for the one-dimensional expansion or collapse test.
(ii) The void ratios for each applied effective pressure, during the "initial loading path" of the sample, to the required vertical stress against which the sample expands or collapses when wetted.
(iii) The void ratio changes determined from the one-dimensional increase (or decrease) in the volume of the sample, as the result of increases in the water content.
(iv) The measured volumes of water added to the sample.
(v) To obtain the final loading and unloading paths (to zero) of the sample.

6.6 PREPARATION OF TEST SAMPLES

Test samples can be prepared from remoulded, compacted or undisturbed soil samples. A brief description is included in this chapter for each type of sample preparation - for more details refer to either Appendix A[1], or Appendix E 'Consolidometer tests for expansive and collapsing soils - test procedures and results'[2].

Remoulded samples.

Method M1: The soil is mixed with water to form a wet paste - the water content varies between the plastic limit and a value approximately equal to the liquid limit; The wet paste is moulded into a suitable container.
Method M2: An homogeneous dry mixture is prepared by mixing known amounts of soil with tartaric acid and sodium bicarbonate - water is added to the mixture, quickly mixed and placed in a custom made container.

Compacted samples.

Select points on the 'dry density versus water content' curve for the soil type (refer to 'Compaction Tests' in Appendix A); Compact the soil to the required specification, at the selected water content; Cut the test sample from the compacted sample.

Undisturbed sample.

The test sample is cut from the undisturbed block - refer to 'Soil Sampling'in Appendix A.

6.7 TEST METHOD

The test sample is allowed to air dry under controlled conditions. The shrinkage path of the soil is obtained from the measurements of mass and volume which are carried out at various stages of drying.
This procedure is illustrated in Chapter Four - Photographic Plates 4.01 (i) to (vi).
At the required water content for the test, the sample is cut and trimmed to size until the consolidometer ring just slides over it. The top and bottom surfaces of the sample are made level. The mass of the soil sample is recorded.

The one-dimensional consolidation test can be defined in brief terms, as follows:-

The test consists of:

(1) Loading, in stages, a soil sample to the required pressure - values of settlement as a function of time are recorded for each stage of loading - and allowing consolidation under conditions of full drainage;

---

1 - section A.3 "Preparation of soil samples for testing".
2 - see section E.2 "Test procedures".

(2) Record the amounts of increase (expansion) or decrease (collapse) in volume of the sample[1] as the result of increments in its water content; and,

(3) The last stages are the final loading and unloading of the sample.

A standard consolidometer is used for two main purposes:

(1) To observe the 'one-dimensional' vertical movement resulting from the incremental wetting of the sample; and,
(2) To apply the external vertical stress against which the sample expands or collapses when wetted.

It should be noted that the external vertical stress, or constraint, remains constant throughout the duration of the 'controlled wetting' stage of the test - this stage takes place between the initial loading of the sample (to the required external stress) and the follow up loading and unloading before completion of the test[2].
Four different external stresses were used - 1 Kpa, 50 Kpa, 100 Kpa, and 400 Kpa.

The parts of the consolidometer container are assembled. The container is positioned in the loading device. The following are adjusted: Counterweight alongside the lever arm to apply a slight pressure to the sample; Micrometer dial gauge is set to its initial or zero reading. Place the necessary weights on the loading platform in order to apply, to the soil sample, the required sequence of pressure increments, as follows:

(i) The 1 kpa and 50 kpa tests - one single load increment from 'zero' pressure;
(ii) The 100 Kpa and 400 Kpa tests - 0 -> 50 -> 100 Kpa, and 0 -> 50 -> 100 -> 200 -> 400 Kpa, respectively.
Record the readings on the vertical deflection dial gauge before each pressure increment is applied, and at the following time intervals (after each of these increments starts acting on the soil) - 0.25 minutes, 0.5 min, 1.0 min, 2.25 min, 4 min, 16 min, 30 min, 60 min, 120 min, and so on, until no further settlement takes place.
The readings of vertical deflection will enable the calculation of thickness, or change in thickness, in the sample.

By means of an hypordermic syringe, add a known amount of water to the sample through the bottom filter paper. Allow the sample to expand, or to settle further, while being subjected to the same load - record the vertical deflection reading at the same time intervals given above. Repeat the procedure until no further noticeable vertical movement (increase or decrease) takes place.

---

1 - while subjected to this loading.
2 - refer to preceding summary of test method.

Support the lever arm of the consolidometer and use weights on the loading platform in order to measure the loading characteristics of the soil. Pressure increments of 50 Kpa, until a maximum of 300 Kpa is reached, are used for all cases except in the 400 Kpa test.
A bracket was incorporated in the design of the standard consolidometer, to provide support to the loading platform. The unloading, or recovery characteristics of the soil, are also recorded for the following sequence of pressure decrease: 300 (or 400) Kpa -> 50 -> 10 -> 1 Kpa, at the same time intervals given above.

At the completion of the unloading sequence, remove the assembled parts and record the mass of sample plus ring. The soil is extracted from the steel ring and placed inside the oven, previously set to 105 ± 5°C, for a few hours. The mass of the soil is recorded as the oven-dry mass.

The detailed description of this test procedure is included in Appendix E[1].

6.8 SUMMARY OF TEST RESULTS FOR EACH SOIL TYPE

The test results consist of measurements of vertical deflection observed in a sample which is confined in the horizontal axis. These changes in volume take place as a result of an increase (or decrease) in vertical pressure or water content.
An introduction to the test results will be provided by the definitions of each soil type according to particle size and the reported observations for the consistency limit values[2]. The parameters which were investigated for the full test path (at each applied vertical pressure), are presented in two basic forms:
(i) Relationship between void ratio and water ratio; and,
(ii) Relationship between void ratio and effective pressure.

6.8.1 Natural Soil Types

Relationships of void ratio versus water ratio, and void ratio versus effective pressure, are included for the following natural soil types:

(i) Site 11, Rosebank (Cape);
(ii) Site 36, Rondebosch (Cape);
(iii) Site 30, Hout Bay (Cape);
(iv) Site A, Berea Road (Durban, Natal);
(v) Site 7, Mowbray (Cape);
(vi) Site B, Francois Road (Durban, Natal);
(vii) Site C, Margaret Mayton Avenue (Durban, Natal);
(viii) Site D, Rose Hill (Durban, Natal).
(ix) Site 48, Lady Grey District - Farm Unity (Natal).

---

1 - see section E.2.
2 - refer to Chapters One, Two and Appendix A.

The relationships for the natural soils are illustrated in Figures 6.03 to 6.54 as follows:-

Void Ratio versus Water Ratio:

Site 11, remoulded samples - Figures 6.03 [1 Kpa], 6.05 [50 Kpa], 6.07 [100 Kpa], and 6.09 [400 Kpa]; Site 11, compacted samples - Figure 6.11 [100 Kpa]; Site 11, undisturbed samples - Figure 6.13 [100 Kpa];
Site 36, remoulded samples - Figures 6.15 [1 Kpa], 6.17 [50 Kpa], 6.19 [100 Kpa], and 6.21 [400 Kpa]; Site 36, compacted sample - Figure 6.23 [100 Kpa]; Site 36, undisturbed samples - Figure 6.25 [100 Kpa];
Site 30, remoulded samples - Figures 6.27 [1 Kpa], 6.29 [50 Kpa], and 6.31 [100 Kpa]; Site 30, undisturbed sample - Figure 6.33 [100 Kpa];
Site A, remoulded samples - Figure 6.35 [100 Kpa]; Site A, compacted samples - Figure 6.37 [100 Kpa]; Site A, undisturbed samples - Figure 6.39 [100 Kpa];
Site 7, remoulded samples - Figure 6.41 [100 Kpa]; Site 7, compacted sample - Figure 6.43 [100 Kpa]; Site 7, undisturbed samples - Figure 6.45 [100 Kpa];
Site B, remoulded sample - Figure 6.47 [100 Kpa];
Site C, remoulded sample - Figure 6.49 [100 Kpa];
Site D, remoulded sample - Figure 6.51 [100 Kpa];
Site 48, undisturbed sample - Figure 6.53 [100 Kpa].

Void Ratio versus Effective Vertical Pressure:

Site 11, remoulded - Figures 6.04 [1 Kpa], 6.06 [50 Kpa], 6.08 [100 Kpa], and 6.10 [400 Kpa]; Site 11, compacted samples - Figure 6.12 [100 Kpa]; Site 11, undisturbed samples - Figure 6.14 [100 Kpa];
Site 36, remoulded samples - Figures 6.16 [1 Kpa], 6.18 [50 Kpa], 6.20 [100 Kpa], and 6.22 [400 Kpa]; Site 36, compacted sample - Figure 6.24 [100 Kpa]; Site 36, undisturbed sample - Figure 6.26 [100 Kpa];
Site 30, remoulded samples - Figures 6.28 [1 Kpa], 6.30 [50 Kpa], and 6.32 [100 Kpa]; Site 30, undisturbed sample - Figure 6.34;
Site A, remoulded samples - Figure 6.36 [100 Kpa]; Site A, compacted samples - Figure 6.38 [100 Kpa]; Site A, undisturbed samples - Figure 6.40 [100 Kpa];
Site 7, remoulded samples - Figure 6.42 [100 Kpa]; Site 7, compacted sample - Figure 6.44 [100 Kpa]; Site 7, undisturbed samples - Figure 6.46 [100 Kpa];
Site B, remoulded sample - Figure 6.48 [100 Kpa];
Site C, remoulded sample - Figure 6.50 [100 Kpa];
Site D, remoulded sample - Figure 6.52 [100 Kpa];
Site 48, undisturbed sample - Figure 6.54 [100 Kpa].

Appendix E[1] includes the detailed consolidation test procedures and results for expansive and collapsing soils.

---

[1] - *refer to sections E.2 and E.4, respectively.*

One-dimensional Consolidation tests (for expansive and collapsing soils) were carried out for the soil samples listed in Table 6.01.

Table 6.01: Natural Soils - samples used for one-dimensional consolidation tests (expansive and collapsing soils).

Sample No.	Method of preparation	Free Shrinkage (Ref. number)	Expansion / Collapse (Ref./Consolidometer)
Site 11	[Remoulded samples]		
Effective pressure = 1Kpa (during wetting): Figs 6.03, 6.04			
S.11-35	M2 (*)	II. 270	III.310 / test no. 83
S.11-42	M1 (≥LL)	III.282	III.328 / test no. 92
S.11-49	M1 (<LL)	III.305	III.330 / test no. 93
S.11-52	M2 (*)	III.317	III.347 / test no. 103
Effective pressure = 50Kpa (during wetting): Figs 6.05, 6.06			
S.11-36	M2 (*)	II. 272	III.307 / test no. 81
S.11-41	M1 (≥LL)	III.278	III.322 / test no. 89
S.11-50	M1 (<LL)	III.308	III.332 / test no. 94
S.11-64	M1 (≥LL)	IV. 451	IV. 464 / test no. 173
Effective pressure = 100Kpa (during wetting): Figs 6.07,6.08			
S.11-1	M2 (*)	I. 130	II. 171 / test no. 23
S.11-4	M2 (*)	I. 133	II. 189 / test no. 30
S.11-11	M1 (<LL)	II. 216	II. 236 / test no. 47
S.11-23	M1 (≥LL)	II. 253	III.287 / test no. 69
S.11-25	M1 (<LL)	II. 256	III.289 / test no. 70
S.11-33	M1 (≥LL)	II. 250	III.295 / test no. 74
S.11-38	M2 (*)	II. 233	III.304 / test no. 79
S.11-43	M1 (<LL)	III.284	III.316 / test no. 86
S.11-46	M1 (≥LL)	III.290	III.339 / test no. 98
S.11-48	M1 (<LL)	III.303	III.335 / test no. 96
S.11-54	M2 (*)	III.321	III.351 / test no. 105
S.11-57	M2 (*)	III.354	III.385 / test no. 121
S.11-62	M1 (<LL)	III.396	IV. 430 / test no. 150
S.11-61	M1 (<LL)	IV. 416	IV. 437 / test no. 154
S.11-60	M1 (≥LL)	III.384	IV. 420 / test no. 142
S.11-59	M1 (≥LL)	III.394	IV. 442 / test no. 158
S.11-58	M2 (*)	III.356	IV. 413 / test no. 137
Effective pressure = 400Kpa (during wetting): Figs 6.09,6.10			
S.11-37	M2 (*)	II. 274	III.302 / test no. 78
S.11-40	M1 (≥LL)	III.276	III.324 / test no. 90
S.11-51	M1 (<LL)	III.311	III.326 / test no. 91
S.11-55	M2 (*)	III.323	III.349 / test no. 104
S.11-65	M1 (≥LL)	IV. 451	IV. 468 / test no. 176

** - air bubbles.*

Sample No.	Method of preparation	Free Shrinkage (Ref. number)	Expansion / Collapse (Ref./Consolidometer)
Site 11 [Compacted samples]			
Effective pressure = 100Kpa (during wetting): Figs 6.11,6.12			
S.11-8	CMod II.162	II. 192 (FS/FS)	II. 191 / test no. 31
S.11-13	CMod II.162	II. 226 (FS/FS)	II. 225 / test no. 43
S.11-14	CMod II.162	II. 239 (FS/FS)	II. 238 / test no. 48
S.11-27	CMod II.162	II. 258 (FS/FS)	II. 257 / test no. 55
S.11-70	CStd IV.450	IV. 458 (FS/FS)	IV. 458 / test no. 168
Site 11 [Undisturbed samples]			
Effective pressure = 100Kpa (during wetting): Figs 6.13,6.14			
S.11-6	-	II. 163	II. 181 / test no. 28
S.11-12	-	II. 216	II. 220 / test no. 41
S.11-15	-	II. 221	II. 229 / test no. 45
S.11-17	-	II. 244	II. 247 / test no. 51
S.11-19	-	II. 245	II. 261 / test no. 57
S.11-22	-	II. 246	III.279 / test no. 65
Site 36 [Remoulded samples]			
Effective pressure = 1Kpa (during wetting): Figs 6.15, 6.16			
S.36-13	M1 (<LL)	IV. 452L	IV. 460 / test no. 170
Effective pressure = 50Kpa (during wetting): Figs 6.17, 6.18			
S.36-14	M1 (≥LL)	IV. 452R	IV. 463 / test no. 172
Effective pressure = 100Kpa (during wetting): Figs 6.19,6.20			
S.36-3	M1 (≥LL)	III.331	III.363 / test no. 110
S.36-7	M2 (*)	III.360	III.393 / test no. 125
S.36-9	M1 (≥LL)	III.376	IV. 411 / test no. 135
S.36-10	M1 (<LL)	III.378	IV. 412 / test no. 136
S.36-5	M1 (<LL)	III.348	III.401 / test no. 129
S.36-12	M1 (<LL)	III.382	IV. 426 / test no. 147
Effective pressure = 400Kpa (during wetting): Figs 6.21,6.22			
S.36-15	M1 (≥LL)	IV. 453L	IV. 466 / test no. 174
Site 36 [Compacted sample]			
Effective pressure = 100Kpa (during wetting): Figs 6.23,6.24			
S.36-18	CStd A.55	IV. 453 (FS/FS)	IV. 457 / test no. 167
Site 36 [Undisturbed sample]			
Effective pressure = 100Kpa (during wetting): Figs 6.25,6.26			
S.36-16	-	III.390	IV. 425 / test no. 14

** - air bubbles.*

Sample No.	Method of preparation	Free Shrinkage (Ref. number)	Expansion / Collapse (Ref./Consolidometer)
Site 30 [Remoulded samples]			
Effective pressure = 1Kpa (during wetting): Figs 6.27, 6.28			
S.30-10	M1 (≥LL)	IV. 465L	IV. 469 / test no. 177
Effective pressure = 50Kpa (during wetting): Figs 6.29, 6.30			
S.30-11	M1 (≥LL)	IV. 465R	IV. 470 / test no. 178
Effective pressure = 100Kpa (during wetting): Figs 6.31,6.32			
S.30-3	M1 (≥LL)	III.336	III.373 / test no. 115
S.30-5	M1 (<LL)	III.352	IV. 418 / test no. 140
S.30-7	M2 (*)	III.366	III.404 / test no. 130
S.30-9	M1 (≥LL)	III.388	IV. 423 / test no. 144
Site 30 [Undisturbed sample]			
Effective pressure = 100Kpa (during wetting): Figs 6.33,6.34			
S.30-13	-	IV. 438 (FS/FS)	IV. 440 / test no. 156
Site A [Remoulded samples]			
Effective pressure = 100Kpa (during wetting): Figs 6.35,6.36			
S.A-1A	M1<LL(M4-75)	75. 206	I. 122 / test no. 7
S.A-2	M2 (*)	I. 113	II. 154 / test no. 18
S.A-3	M2A(*)	I. 114	II. 156 / test no. 19
S.A-4	M2B(*)	I. 115	II. 164 / test no. 20
S.A-6	M2 (*)	II. 158	II. 167 / test no. 21
S.A-7	M2 (*)	II. 159	II. 173 / test no. 24
S.A-8	M2 (*)	II. 160	II. 169 / test no. 22
Site A [Compacted samples]			
Effective pressure = 100Kpa (during wetting): Figs 6.37,6.38			
S.A-9	CMod II.163	II. 176 (FS/FS)	II. 175 / test no. 25
S.A-10	CMod II.163	II. 178 (FS/FS)	II. 177 / test no. 26
S.A-12	CMod II.163	II. 188 (FS/FS)	II. 187 / test no. 29
Site A [Undisturbed samples]			
Effective pressure = 100Kpa (during wetting): Figs 6.39,6.40			
S.A-11	-	II. 180	II. 179 / test no. 27
S.A-1	-	Ba. 78	Ba. 78 / S.A-1

** - air bubbles.*

Sample No.	Method of preparation	Free Shrinkage (Ref. number)	Expansion / Collapse (Ref./Consolidometer)
Site 7	[Remoulded samples]		
Effective pressure = 100Kpa (during wetting): Figs 6.41,6.42			
S.7-2	M1 (≥LL)	I. 91	I. 99 / test no. 2
S.7-5	M2 (*)	I. 96	I. 120 / test no. 6
S.7-7	M2B(*)	I. 116	II. 143 / test no. 14
S.7-10	M2 (*)	II. 184	II. 198 / test no. 34
Site 7	[Compacted sample]		
Effective pressure = 100Kpa (during wetting): Figs 6.43,6.44			
S.7-13	CMod II.195	II. 203 (FS/FS)	II. 202 / test no. 36
Site 7	[Undisturbed samples]		
Effective pressure = 100Kpa (during wetting): Figs 6.45,6.46			
S.7-12	-	II. 185L	II. 193 / test no. 32
S.7-1	-	Ba. 77	Ba. 77 / 6.40
Site B	[Remoulded sample]		
Effective pressure = 100Kpa (during wetting): Figs 6.47,6.48			
S.B-1A	M1<LL(M4-75)	75. 206	I. 124 / test no. 8
Site C	[Remoulded sample]		
Effective pressure = 100Kpa (during wetting): Figs 6.49,6.50			
S.C-1A	M1<LL(M4-75)	75. 206	I. 126 / test no. 9
Site D	[Remoulded sample]		
Effective pressure = 100Kpa (during wetting): Figs 6.51,6.52			
S.D-1A	M1<LL(M4-75)	75. 206	I. 128 / test no. 10
Site 48	[Undisturbed samples]		
Effective pressure = 100Kpa (during wetting): Figs 6.53,6.54			
S.48-1	-	Ba. 78	Ba. 78 / S.48-1

** - air bubbles.*

Site 11, Rosebank.

Previously defined as a fine silty clay with only a small amount of fine sand. The soil consists of 59% clay, 29% silt, and 12% sand size. The consistency, free shrinkage and free swell limits, are as follows: Linear Shrinkage 'w_{LS}' = 11.4%; Liquid Limit 'w_L' = 69%; Plastic Limit 'w_P' = 30.7%; Plasticity Index 'I_P' = 38; Shrinkage Limit 'w_S' = 22.5%; and, Free Expansion Limit 'w_{FE}' = 49.4%.

Remoulded samples.

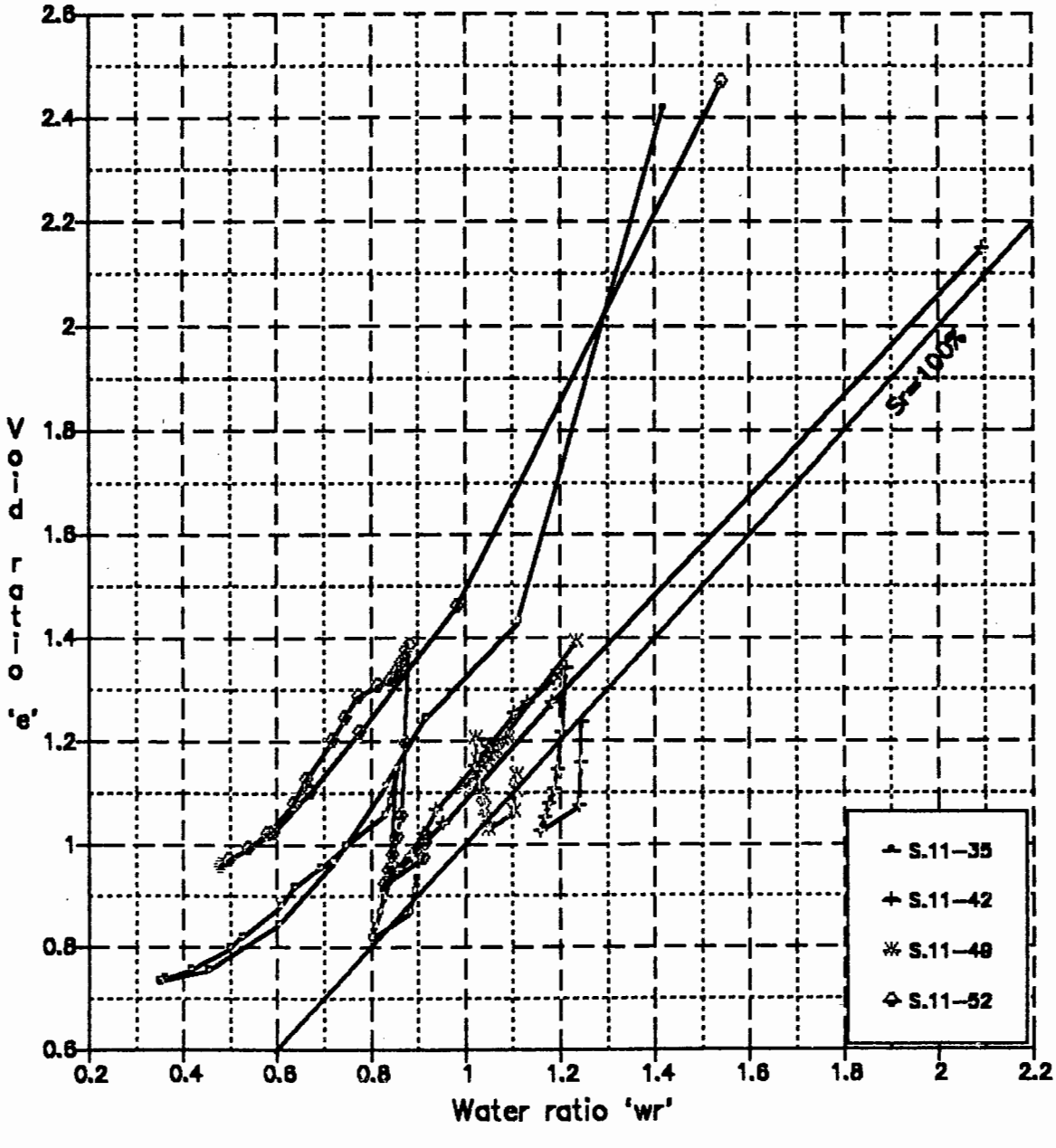

Figure 6.03: Site 11, Rosebank - [1 Kpa during wetting] Relationship between the void ratio 'e' and the water ratio 'wr'. Read in conjunction with Figure 6.04.

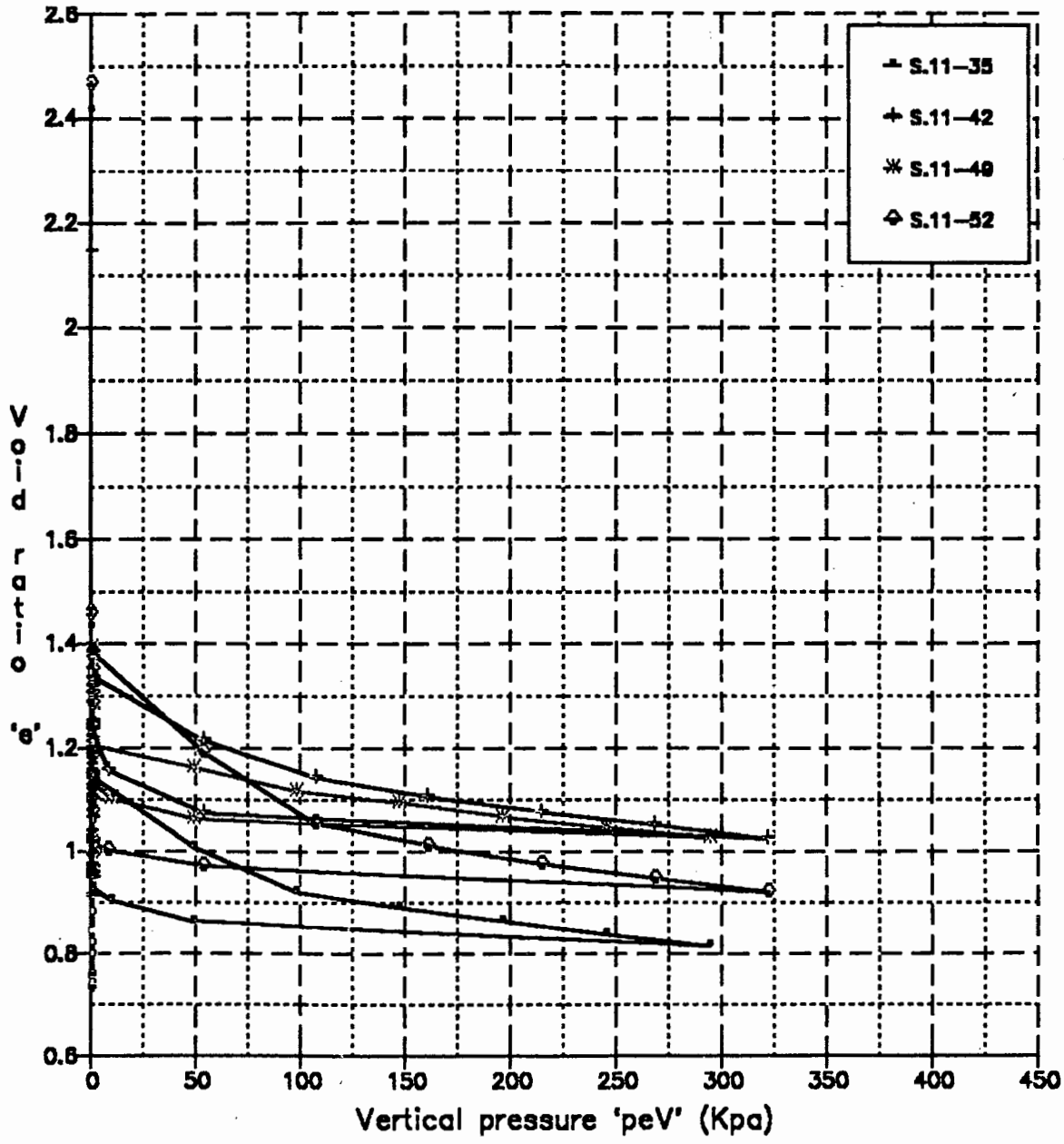

Figure 6.04: Site 11, Rosebank - [1 Kpa during wetting] Relationship between the void ratio 'e' and the effective vertical pressure (or stress) 'peV'.

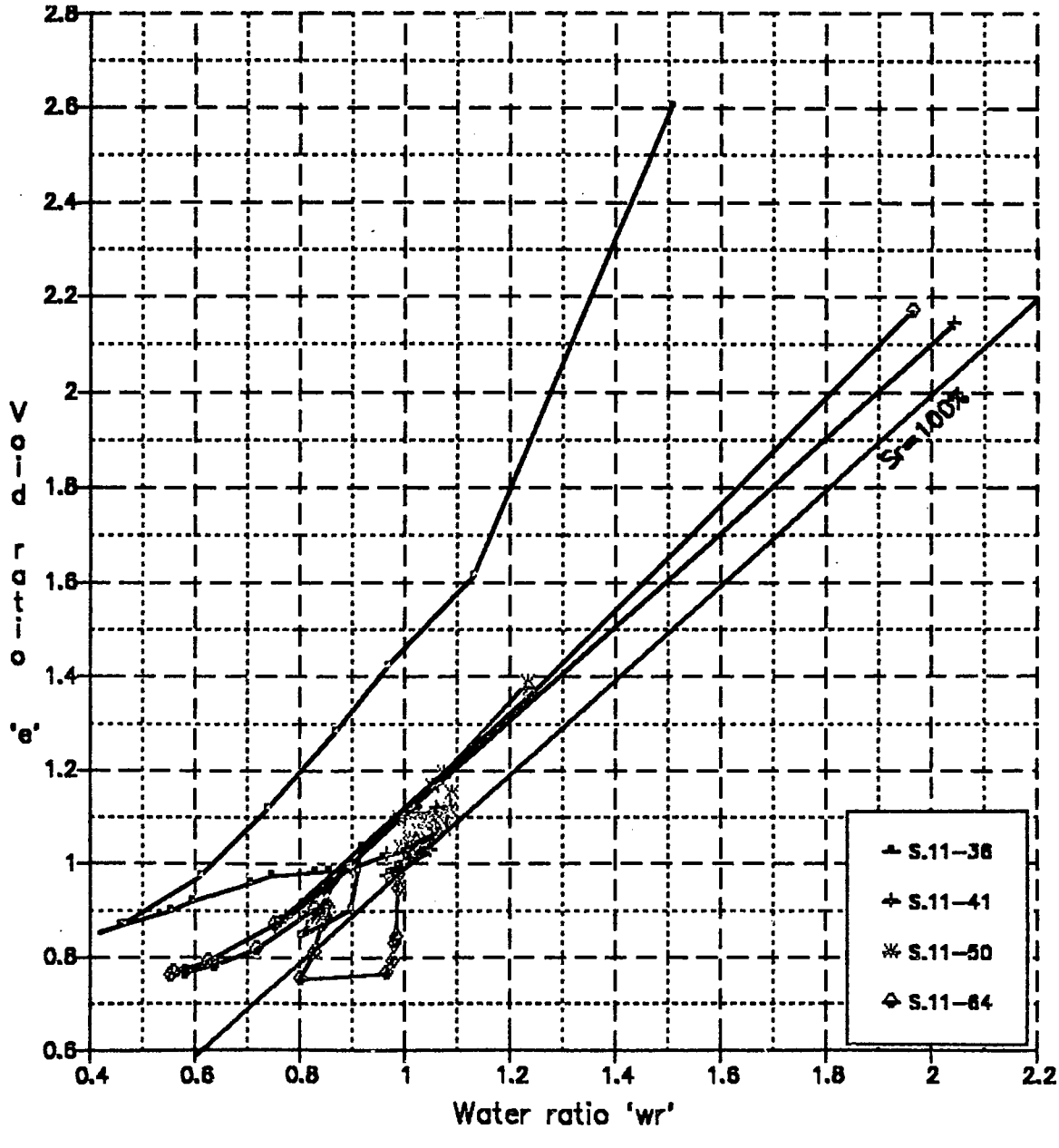

Figure 6.05: Site 11, Rosebank - [settles overnight under 50 Kpa and carries this load during wetting] Relationship between the void ratio 'e' and the water ratio 'wr'. Read in conjunction with Figure 6.06.

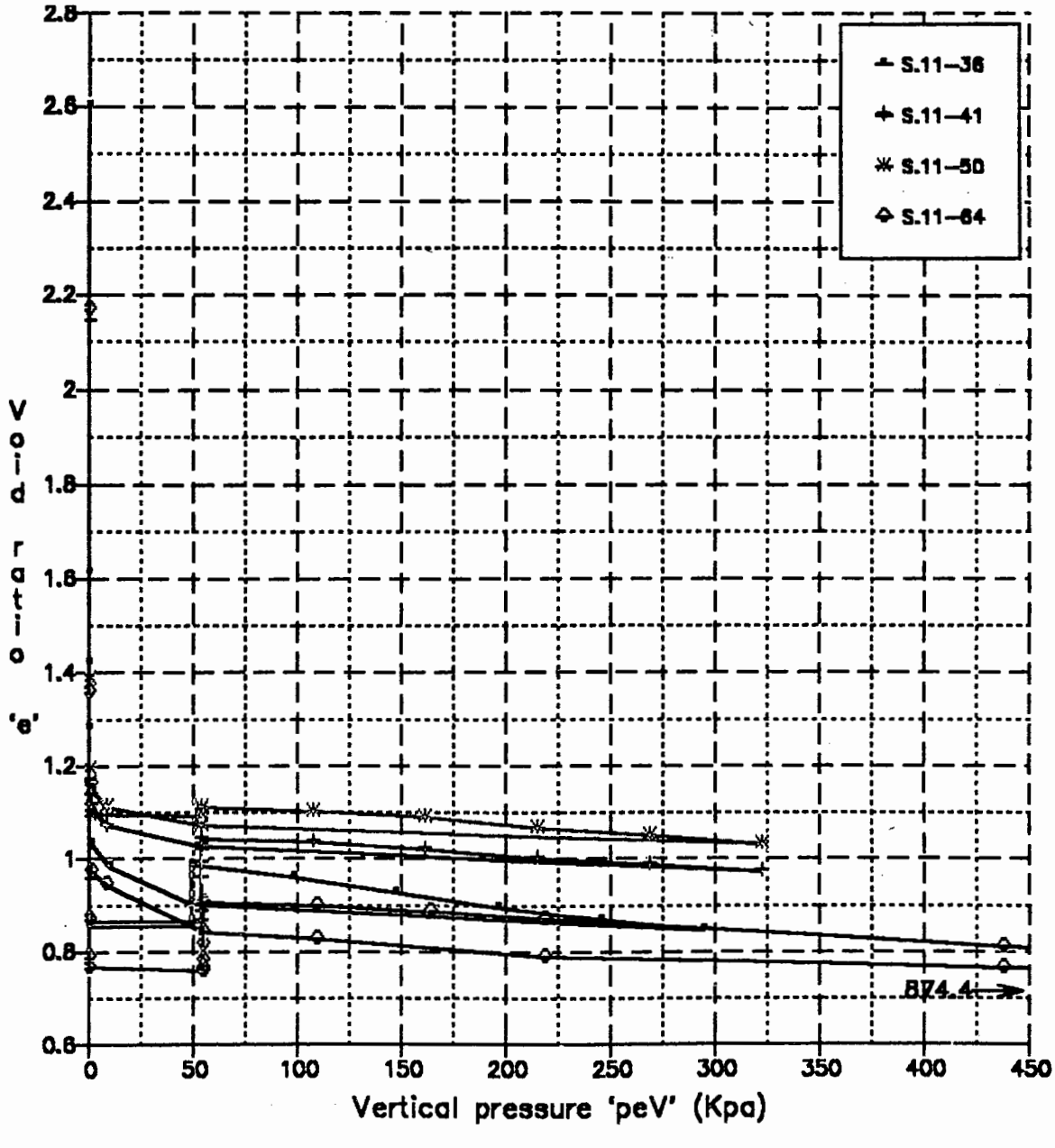

Figure 6.06: Site 11, Rosebank - [50 Kpa during wetting] Relationship between the void ratio 'e' and the effective vertical pressure (or stress) 'peV'.

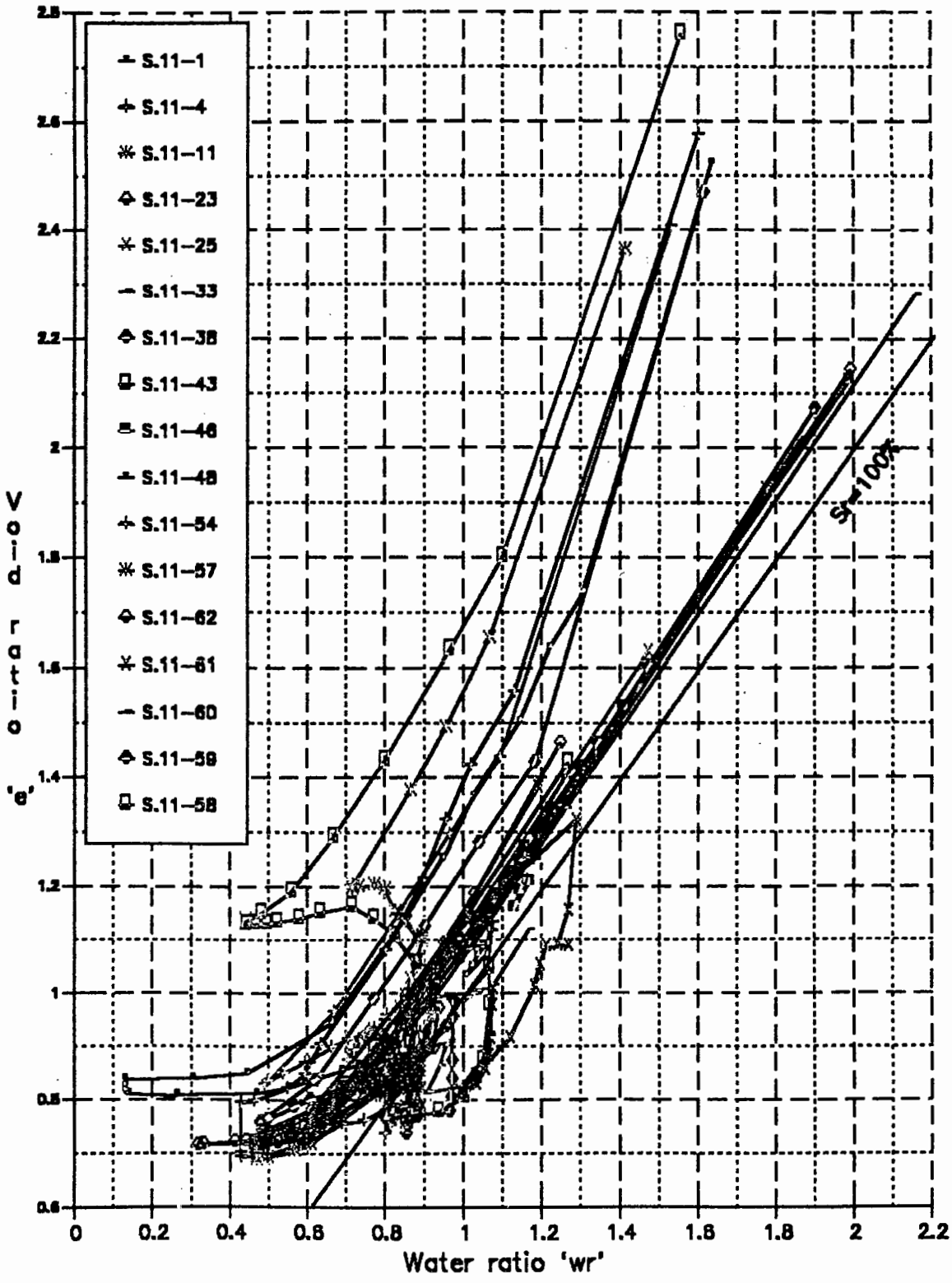

Figure 6.07: Site 11, Rosebank - [100 Kpa during wetting] Relationship between the void ratio 'e' and the water ratio 'wr'.

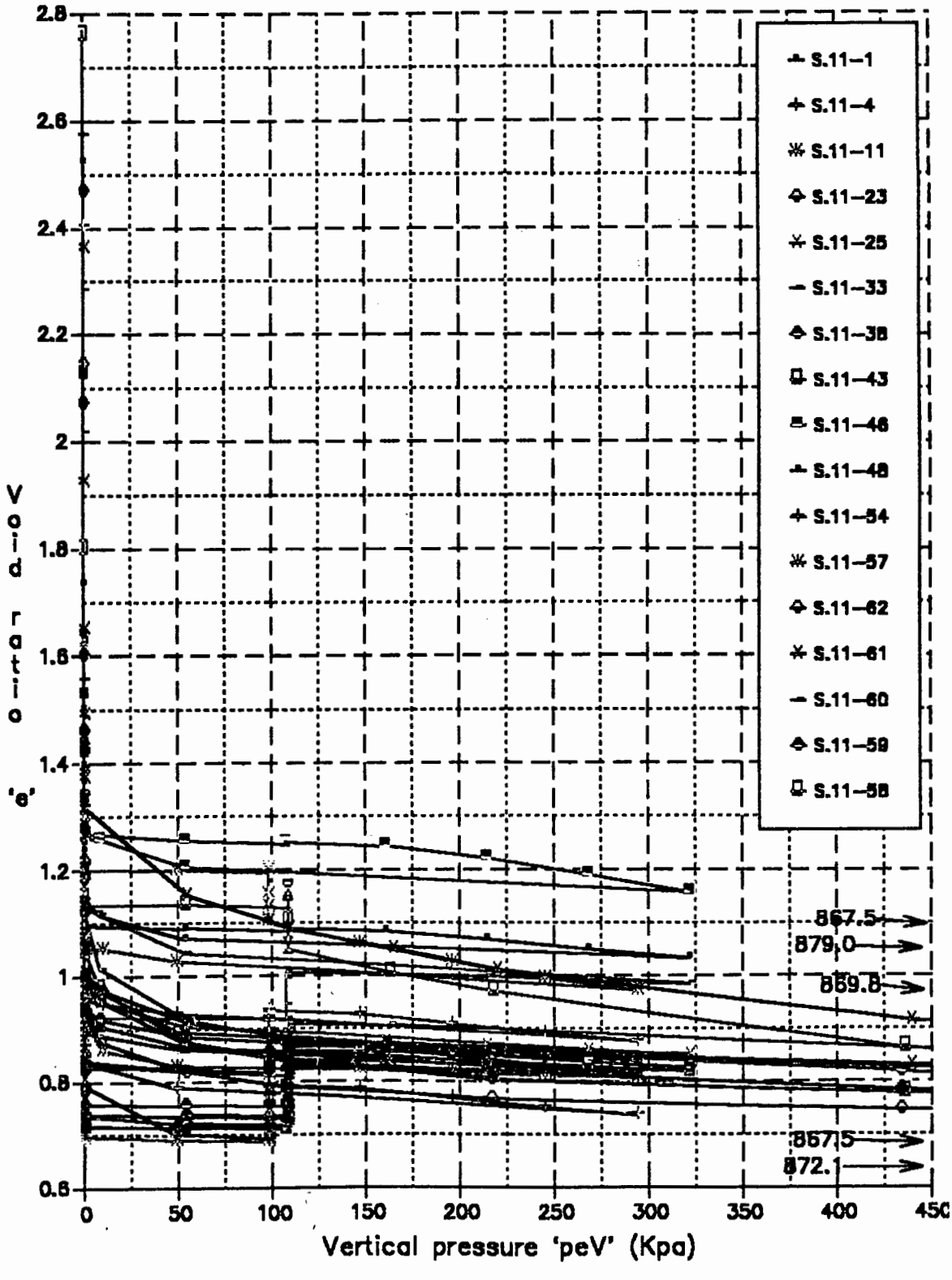

Figure 6.08: Site 11, Rosebank - [100 Kpa during wetting] Relationship between the void ratio 'e' and the effective vertical pressure (or stress) 'peV'.

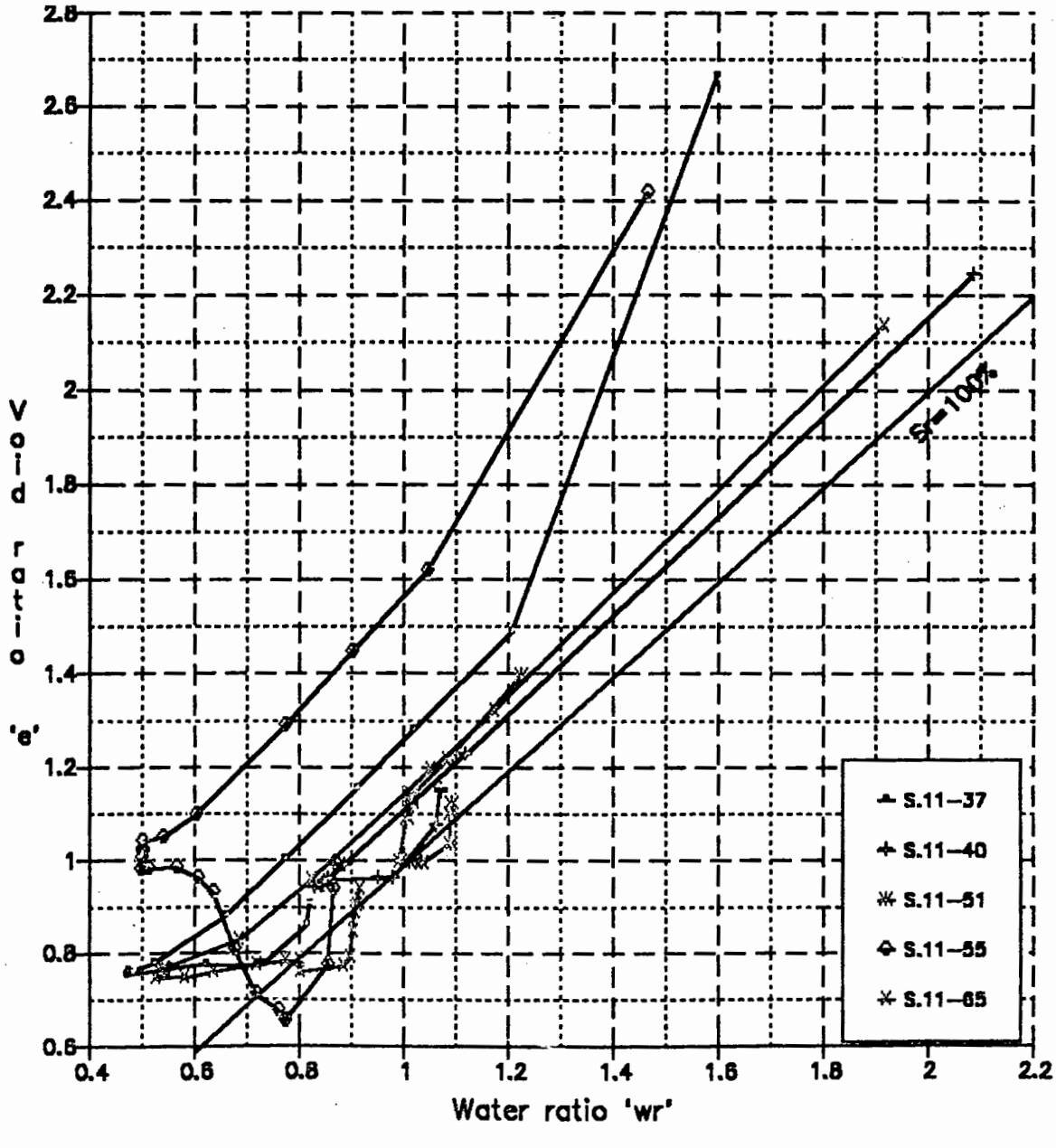

Figure 6.09: Site 11, Rosebank - [400 Kpa during wetting] Relationship between the void ratio 'e' and the water ratio 'wr'.

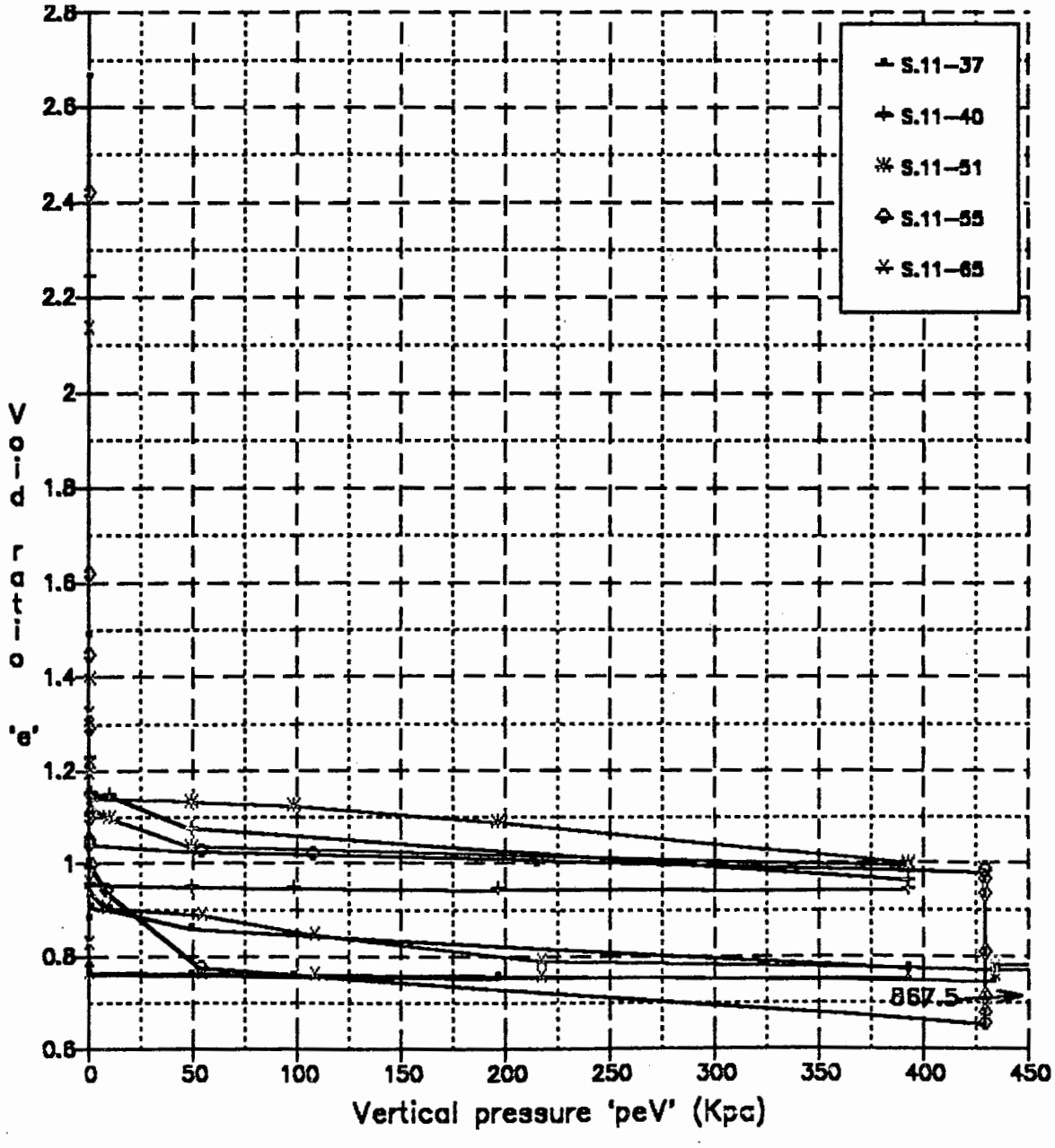

Figure 6.10: Site 11, Rosebank - [400 Kpa during wetting] Relationship between the void ratio 'e' and the effective vertical pressure (or stress) 'peV'.

Compacted samples - Mod AASHTO and Std. AASHTO.

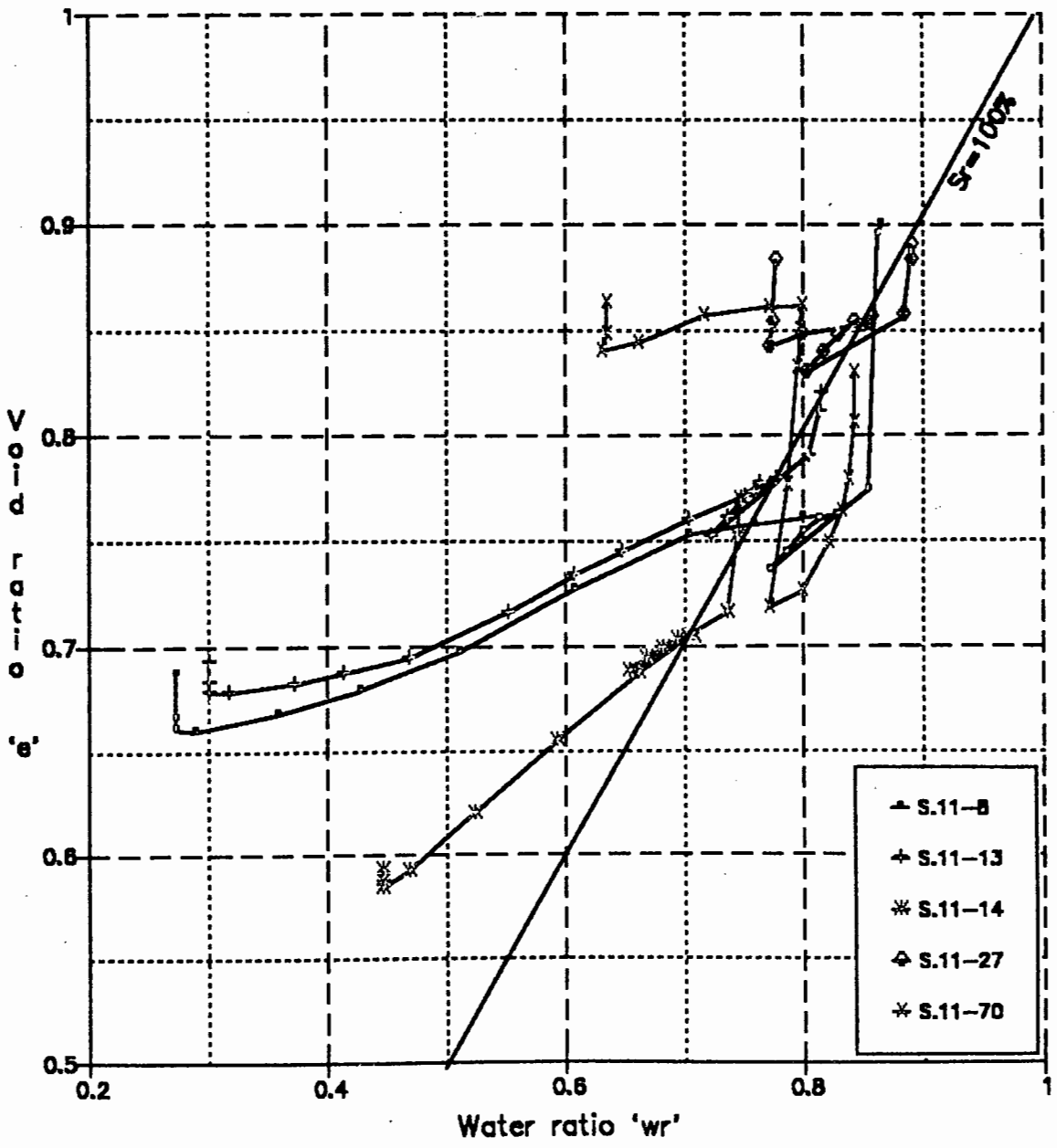

Figure 6.11: Site 11, Rosebank [Compacted] - [100 Kpa during wetting] Relationship between the void ratio 'e' and the water ratio 'wr'.

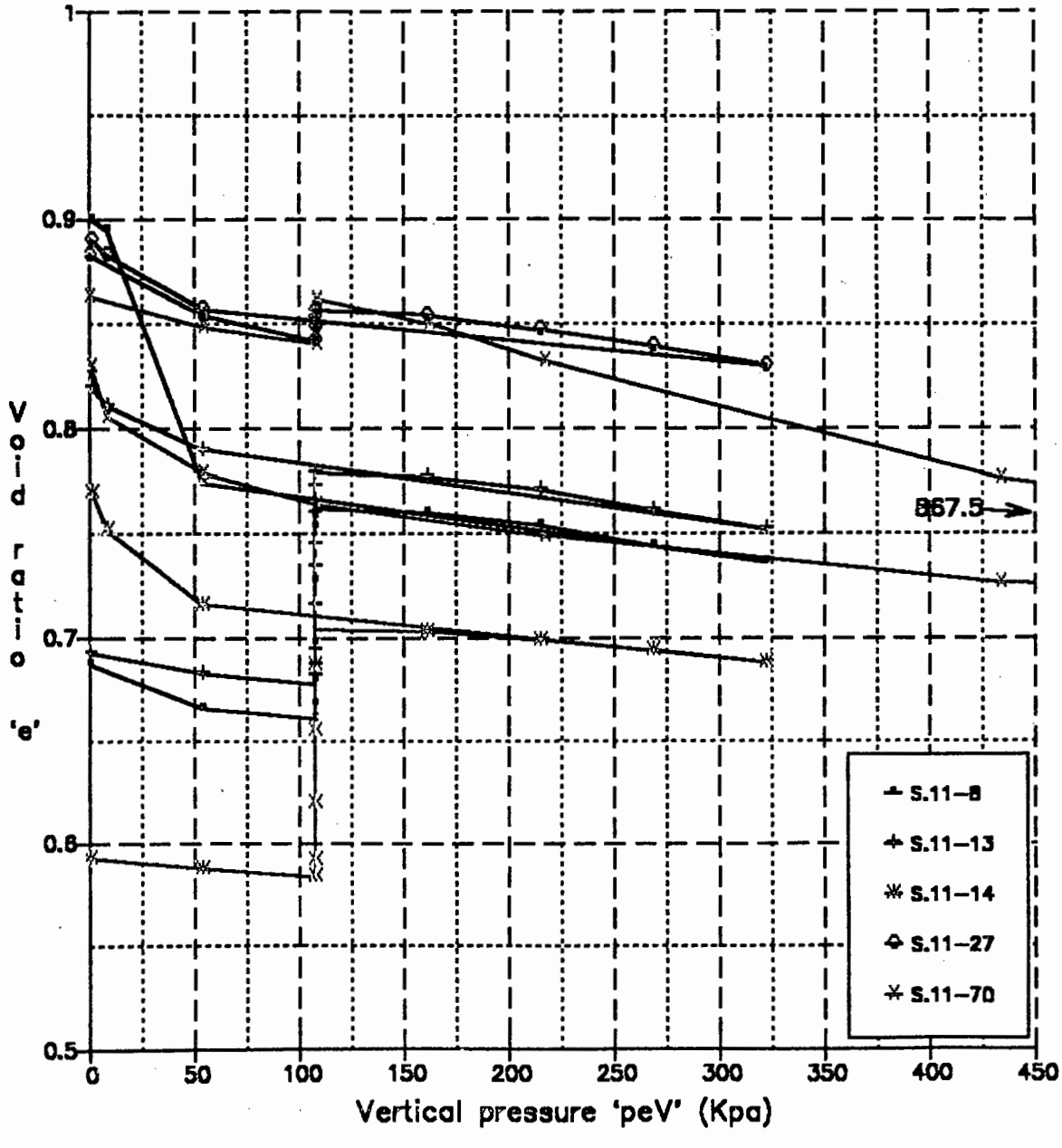

Figure 6.12: Site 11, Rosebank [Compacted] - [100 Kpa during wetting] Relationship between the void ratio 'e' and the effective vertical pressure (or stress) 'peV'.

Undisturbed samples.

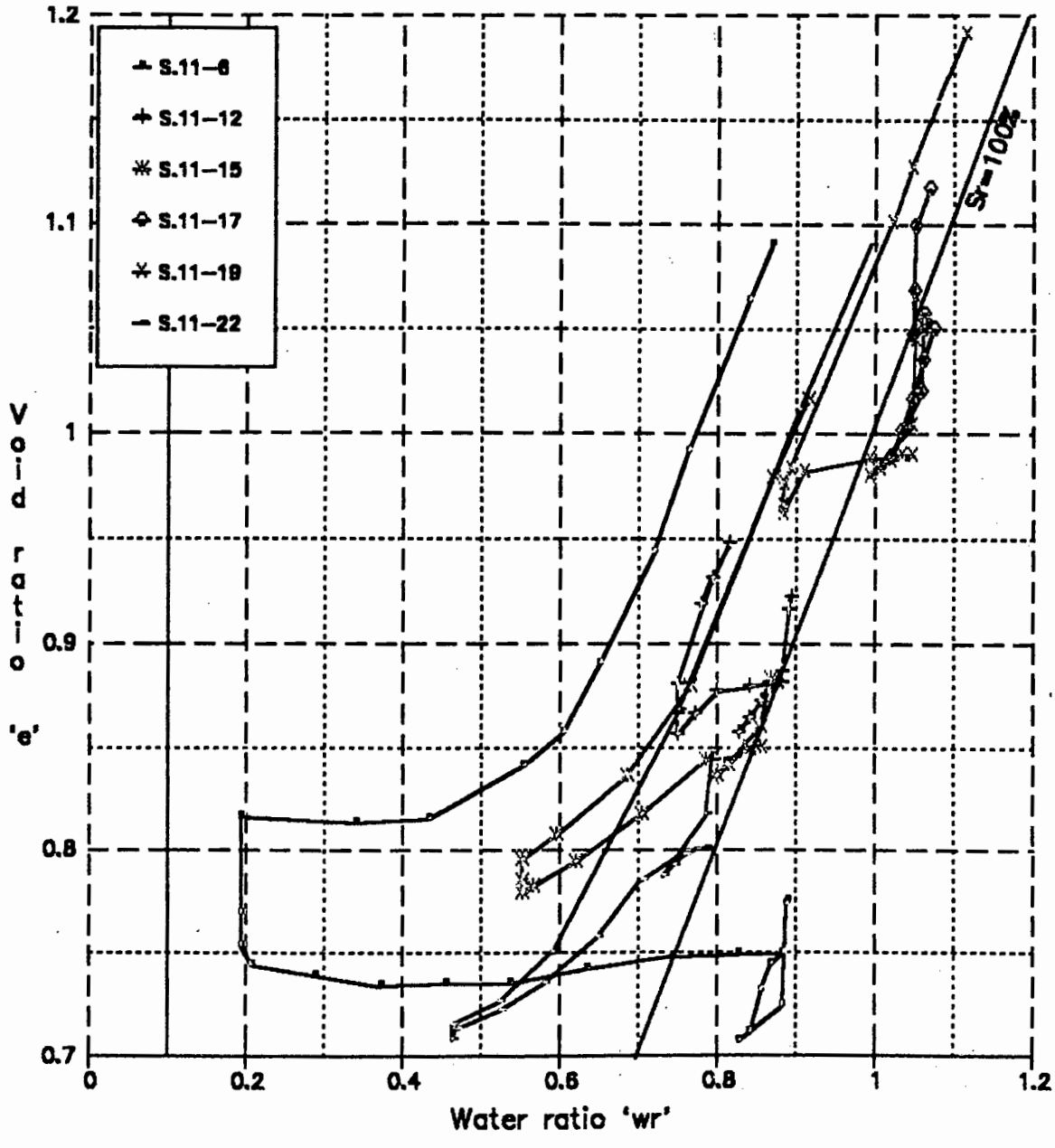

Figure 6.13: Site 11, Rosebank [Undisturbed] - [100 Kpa during wetting] Relationship between the void ratio 'e' and the water ratio 'wr'.

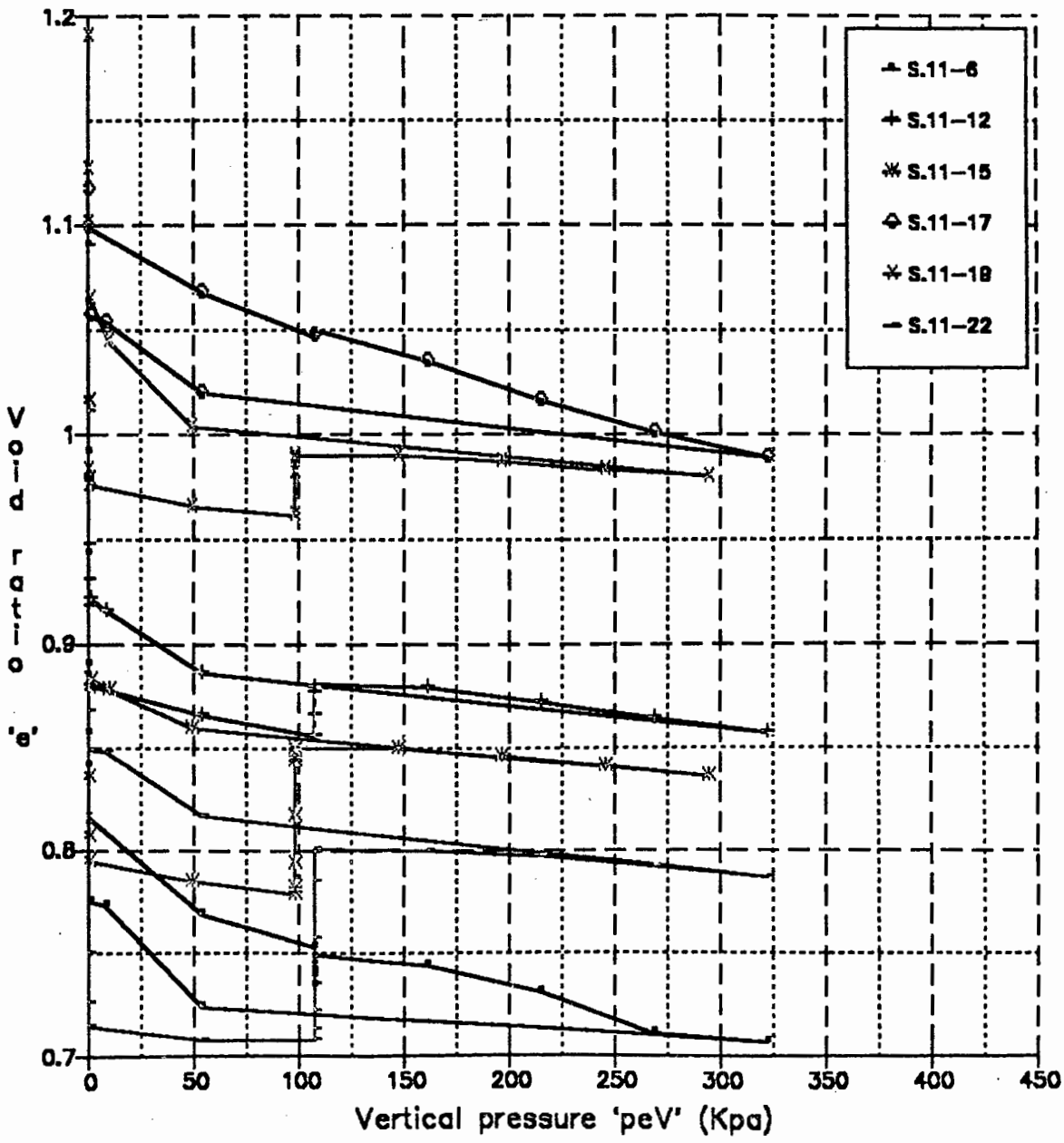

Figure 6.14: Site 11, Rosebank [Undisturbed] - [100 Kpa during wetting] Relationship between the void ratio 'e' and the effective vertical pressure (or stress) 'peV'.

Site 36, Rondebosch.

A clayey silt, with a fine sand and a small amount of medium sand. The soil consists of 22% clay, 49% silt, and 29% sand size. The 'Limits' are as follows: w_{LS} = 8.3%; w_L = 47%; w_P = 23.3%; I_P = 24; w_S = 22.0%; and, w_{FE} = 32.7%.

Remoulded samples.

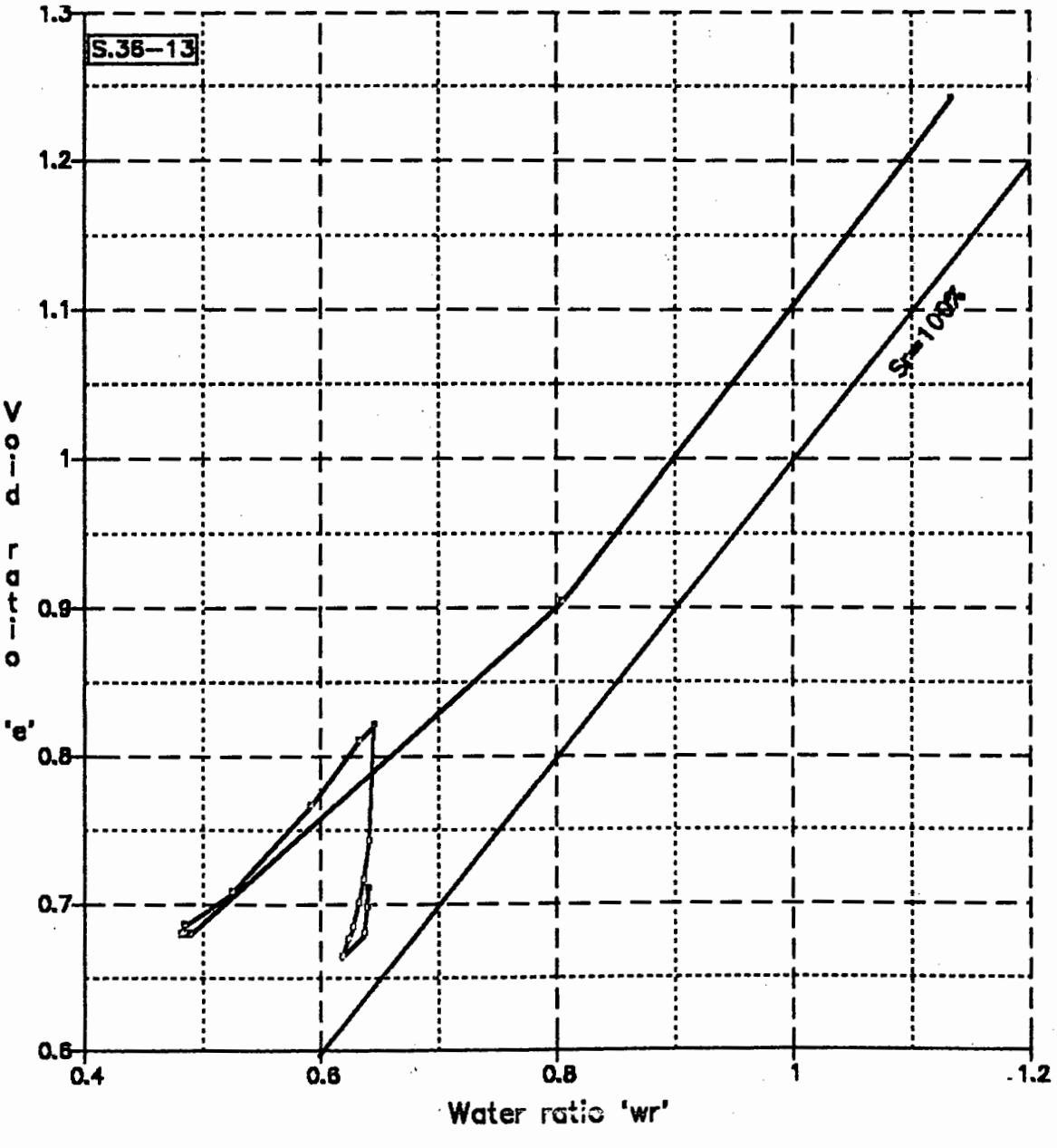

Figure 6.15: Site 36, Rondebosch - [1 Kpa during wetting] Relationship between the void ratio 'e' and the water ratio 'wr'. Read in conjunction with Figure 6.16.

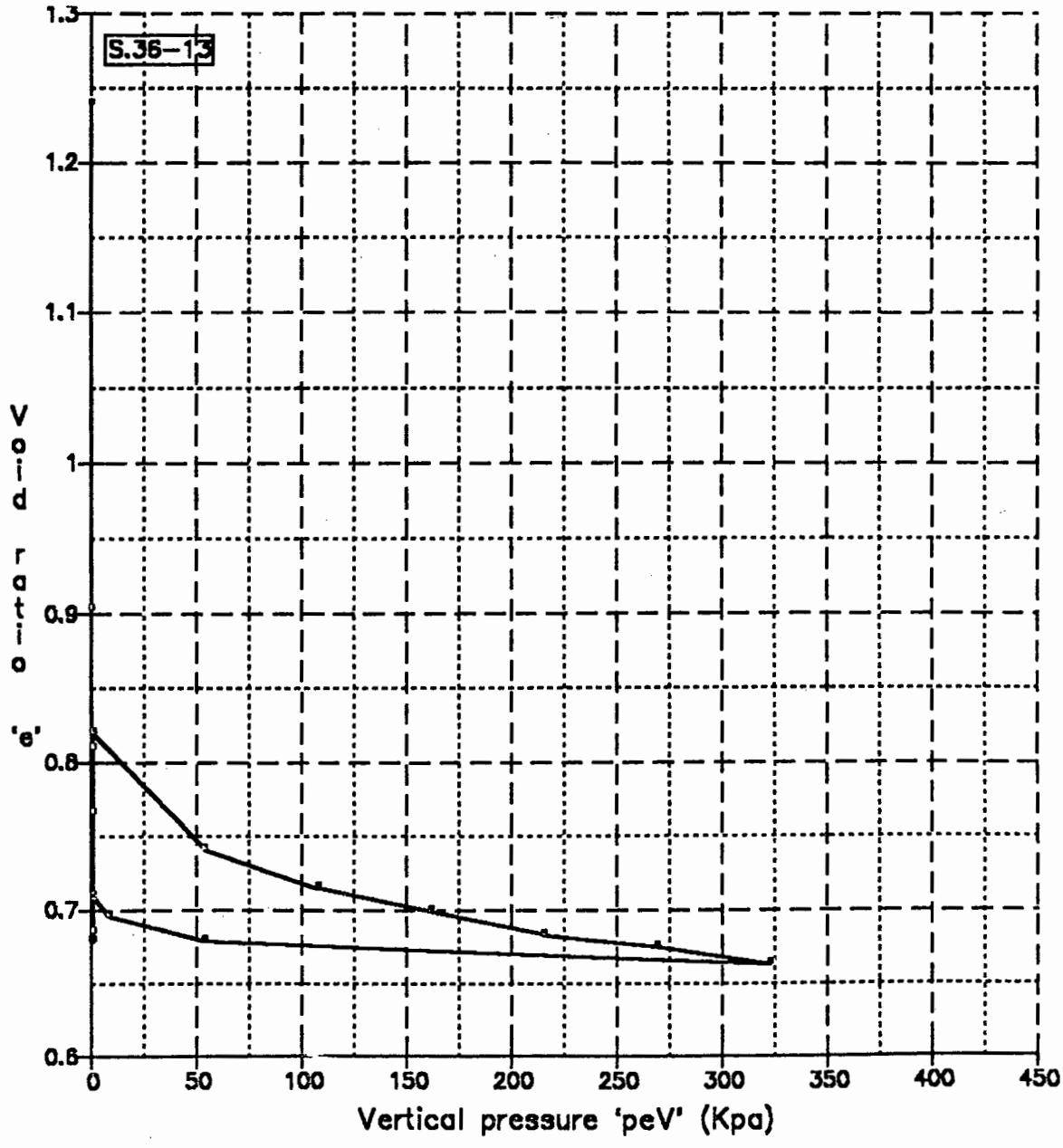

Figure 6.16: Site 36, Rondebosch - [1 Kpa during wetting] Relationship between the void ratio 'e' and the effective vertical pressure (or stress) 'peV'.

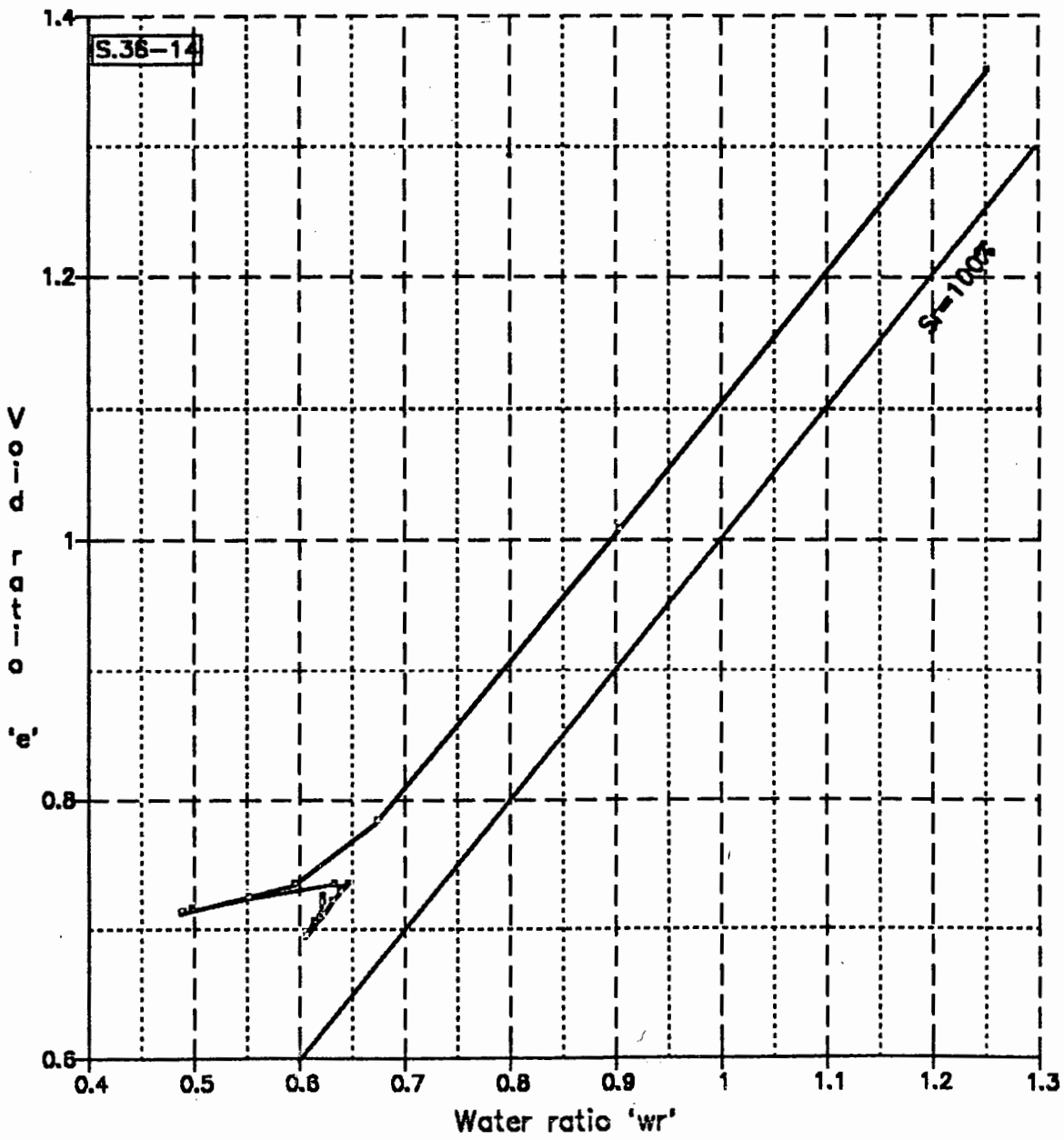

Figure 6.17: Site 36, Rondebosch - [50 Kpa during wetting] Relationship between the void ratio 'e' and the water ratio 'wr'.

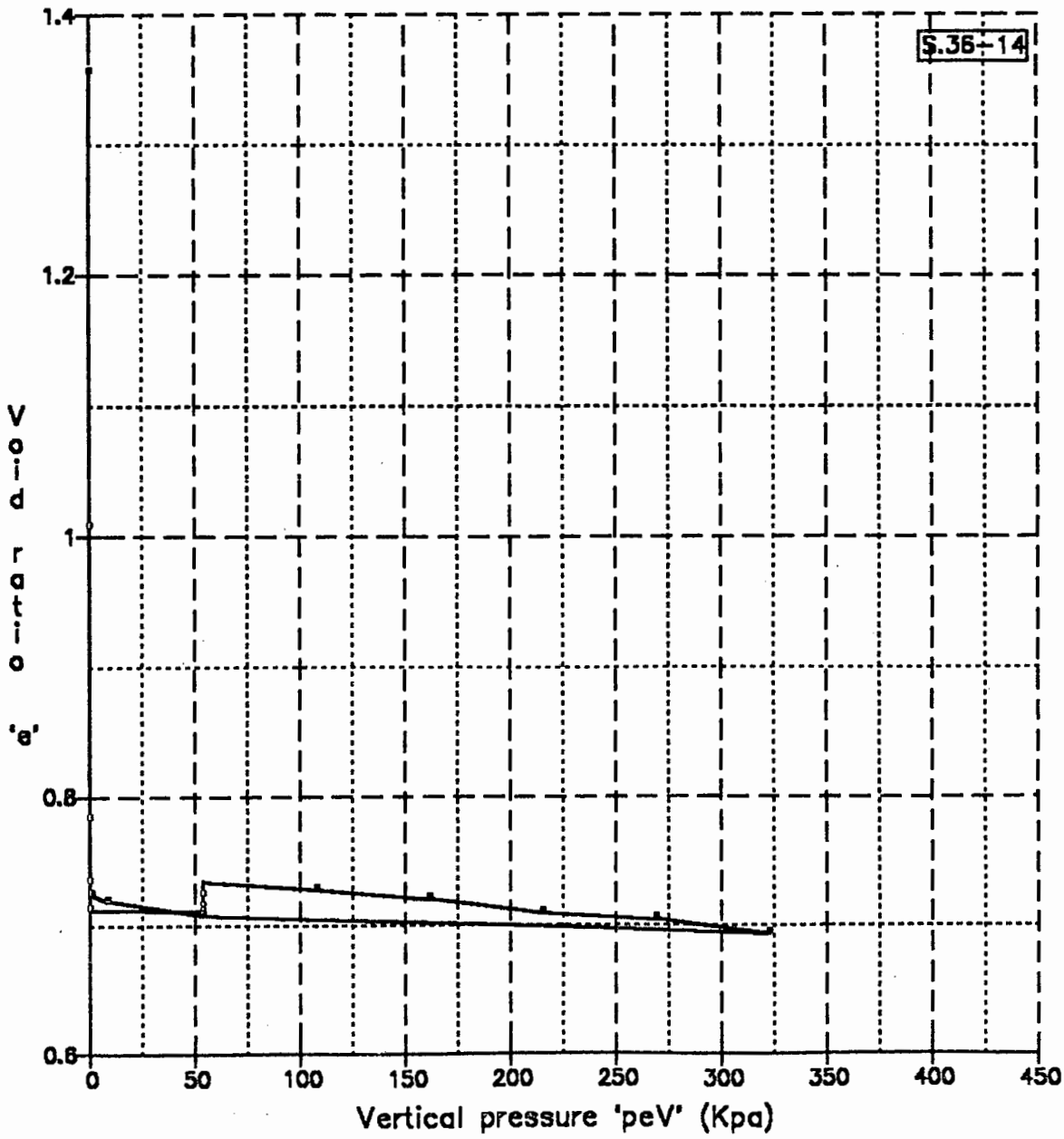

Figure 6.18: Site 36, Rondebosch - [50 Kpa during wetting] Relationship between the void ratio 'e' and the effective vertical pressure (or stress) 'peV'.

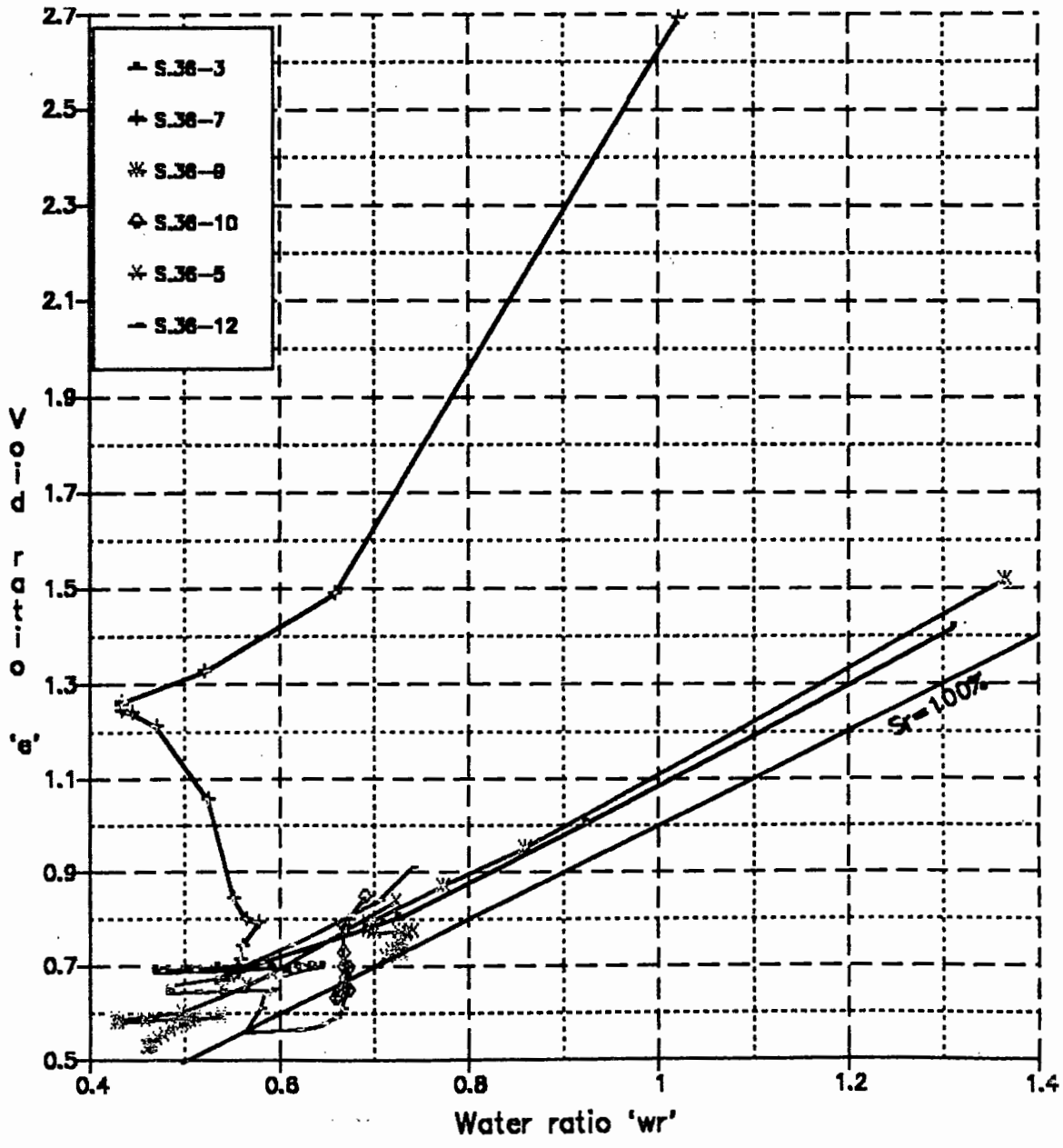

Figure 6.19: Site 36, Rondebosch - [100 Kpa during wetting] Relationship between the void ratio 'e' and the water ratio 'wr'.

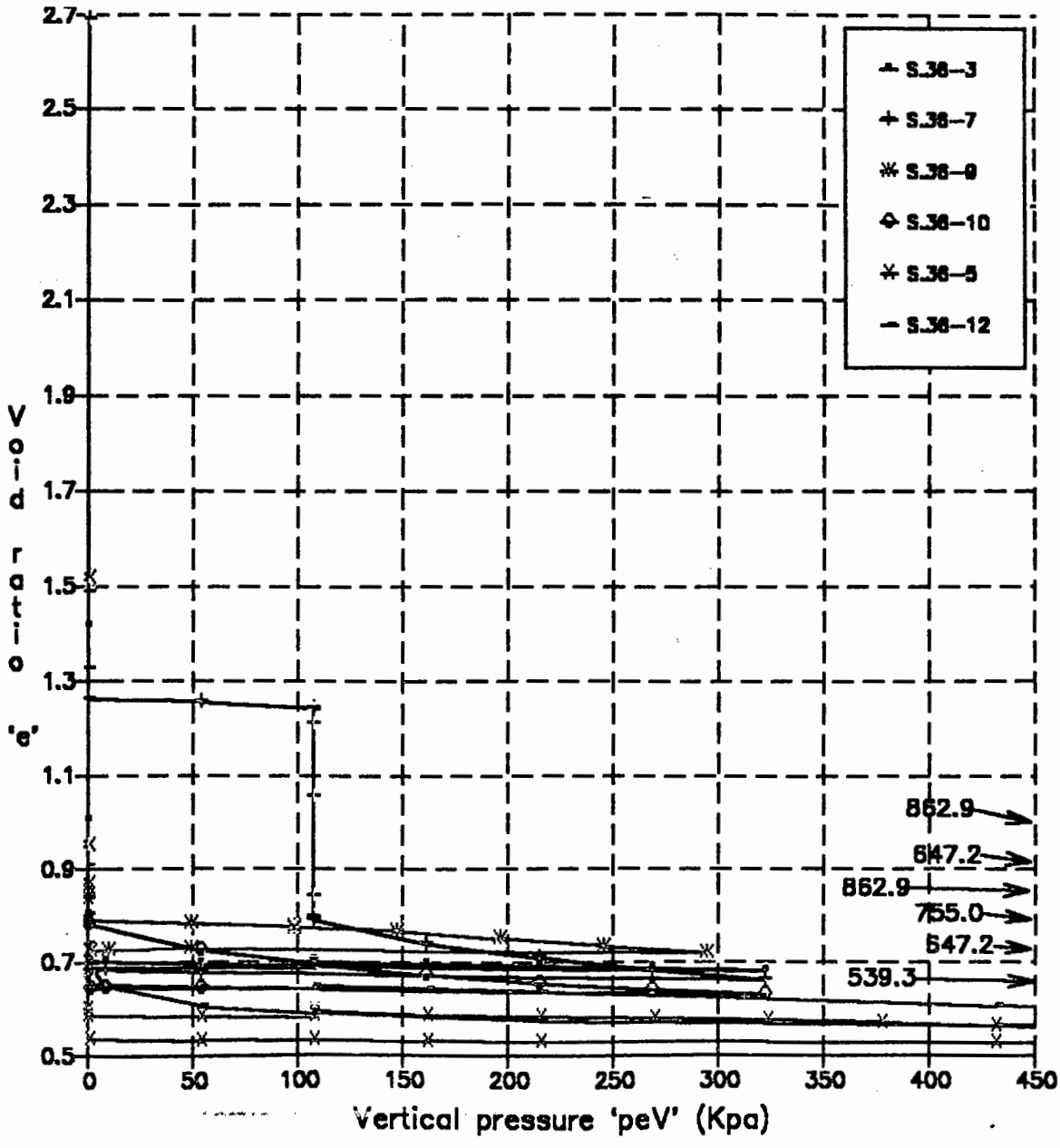

Figure 6.20: Site 36, Rondebosch - [100 Kpa during wetting] Relationship between the void ratio 'e' and the effective vertical pressure (or stress) 'peV'.

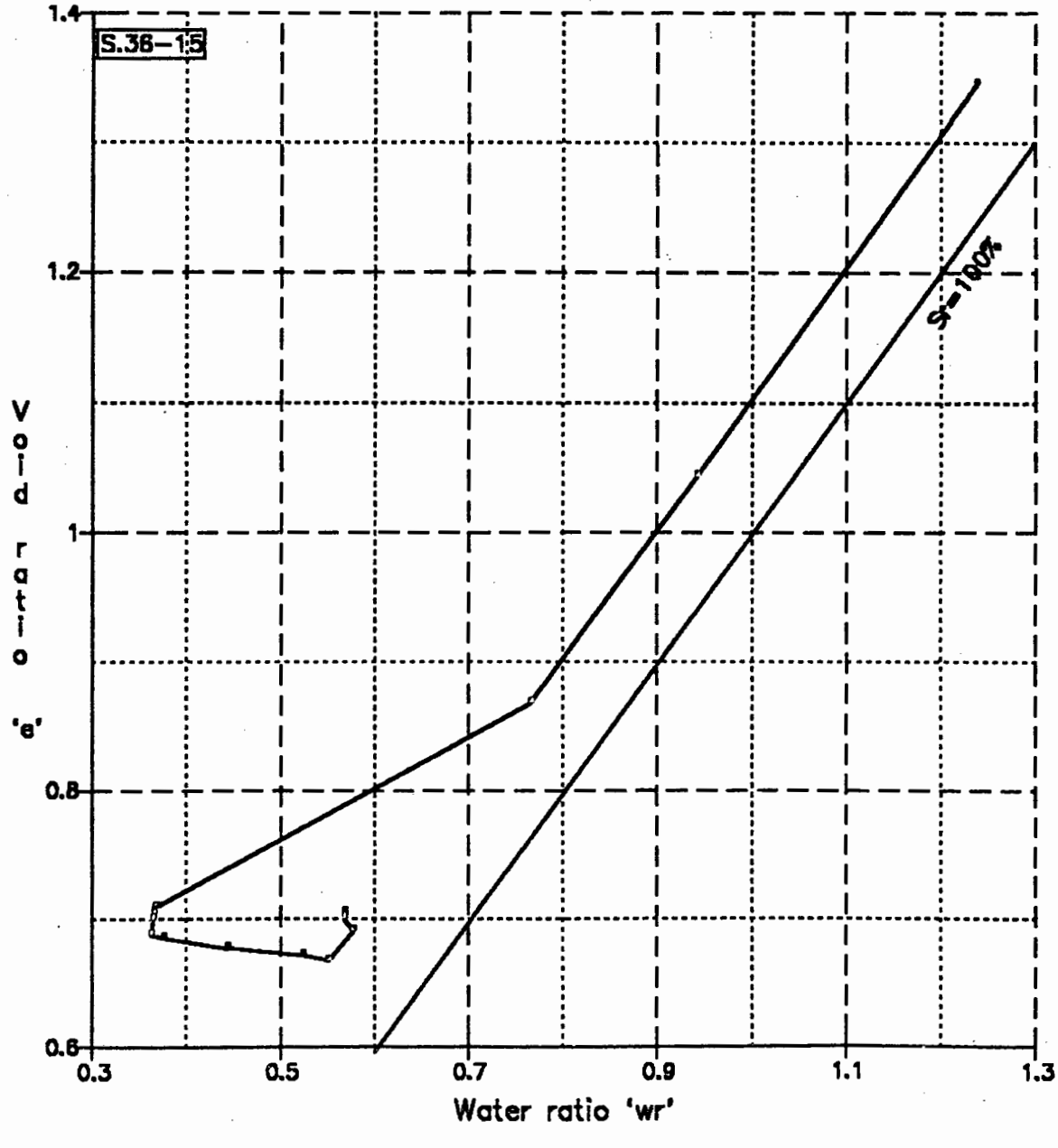

Figure 6.21: Site 36, Rondebosch - [400 Kpa during wetting] Relationship between the void ratio 'e' and the water ratio 'wr'.

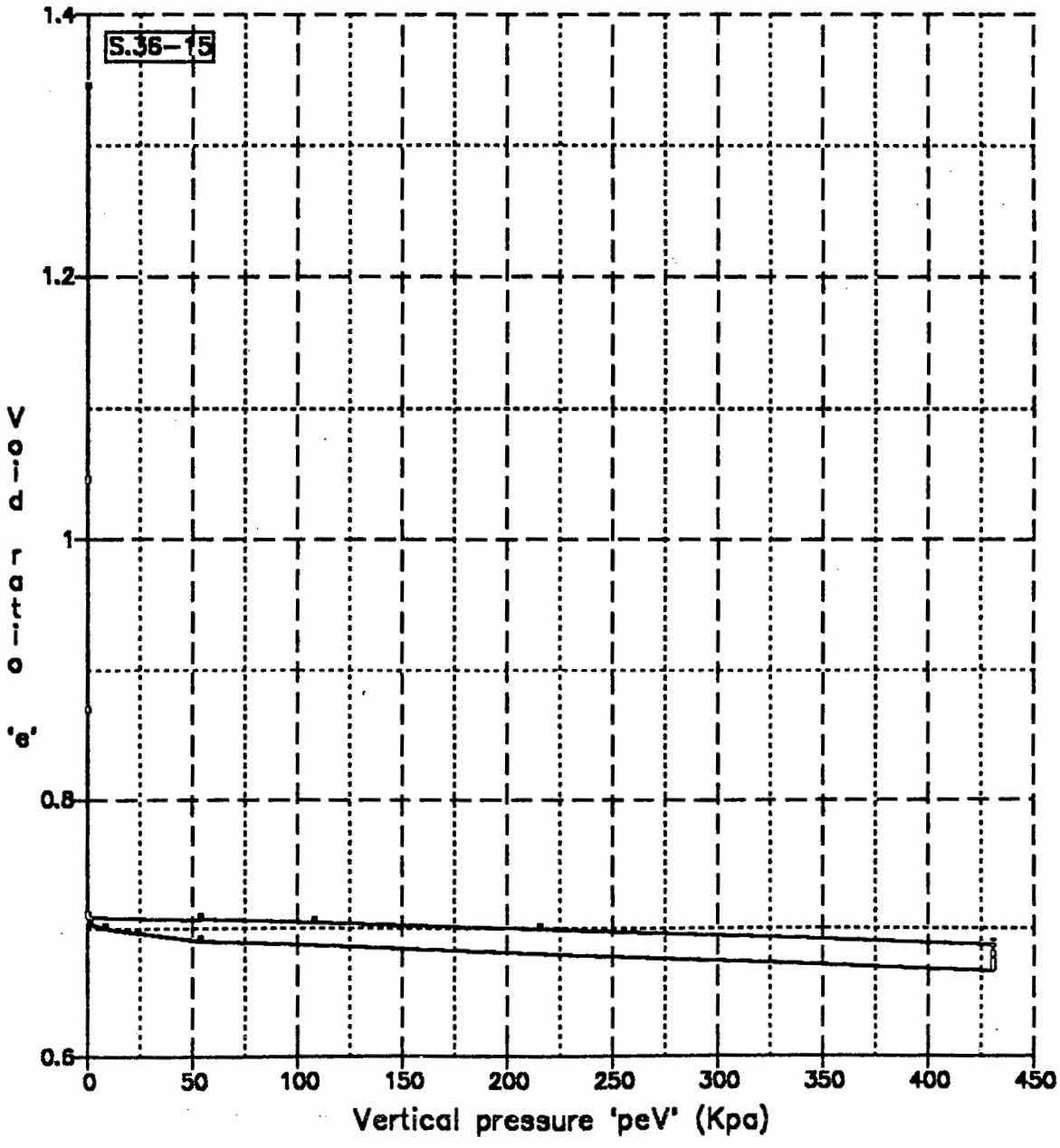

Figure 6.22: Site 36, Rondebosch - [400 Kpa during wetting] Relationship between the void ratio 'e' and the effective vertical pressure (or stress) 'peV'.

Compacted samples - Mod AASHTO.

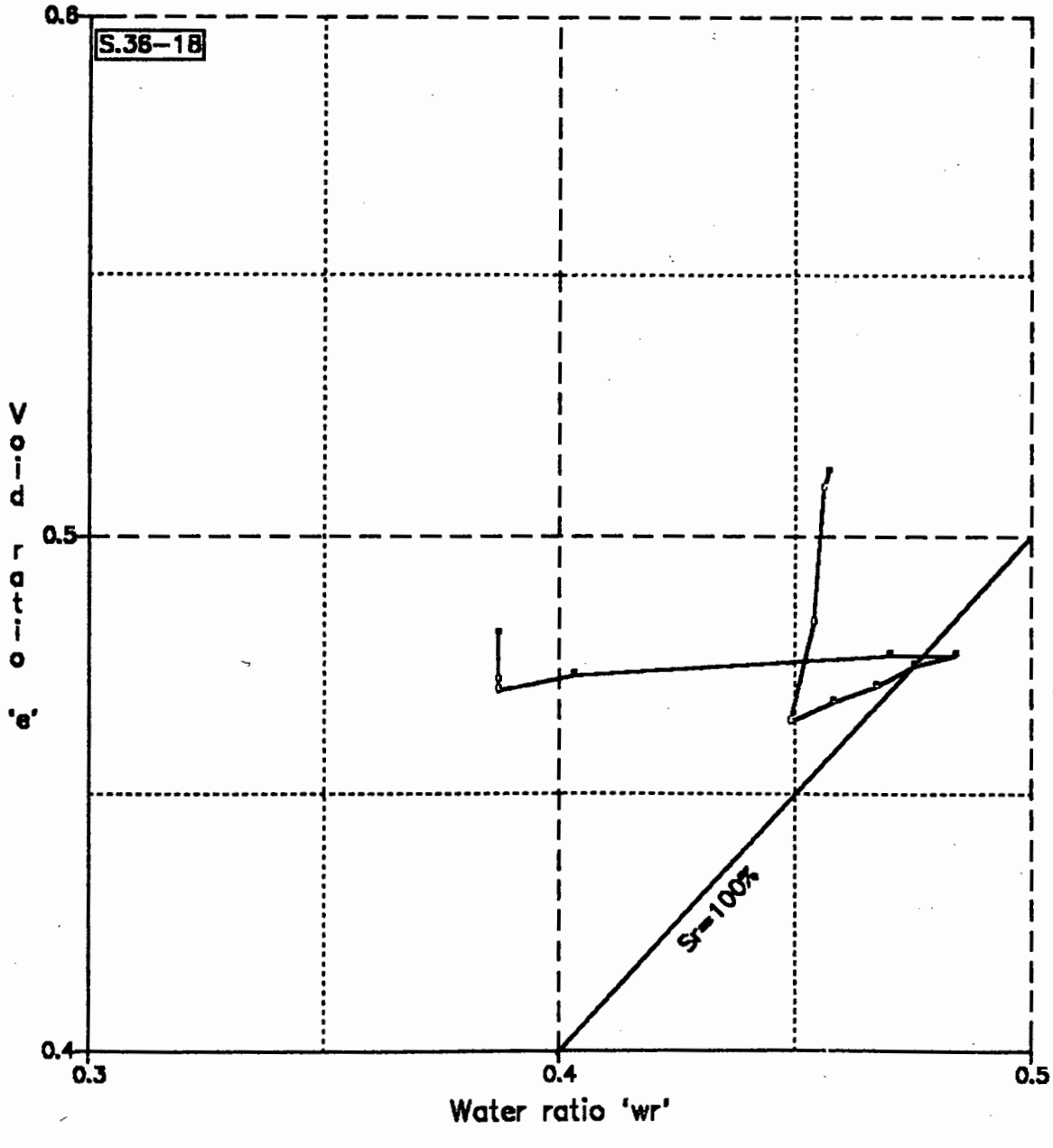

Figure 6.23: Site 36, Rondebosch [Compacted] - [100 Kpa during wetting] Relationship between the void ratio 'e' and the water ratio 'wr'.

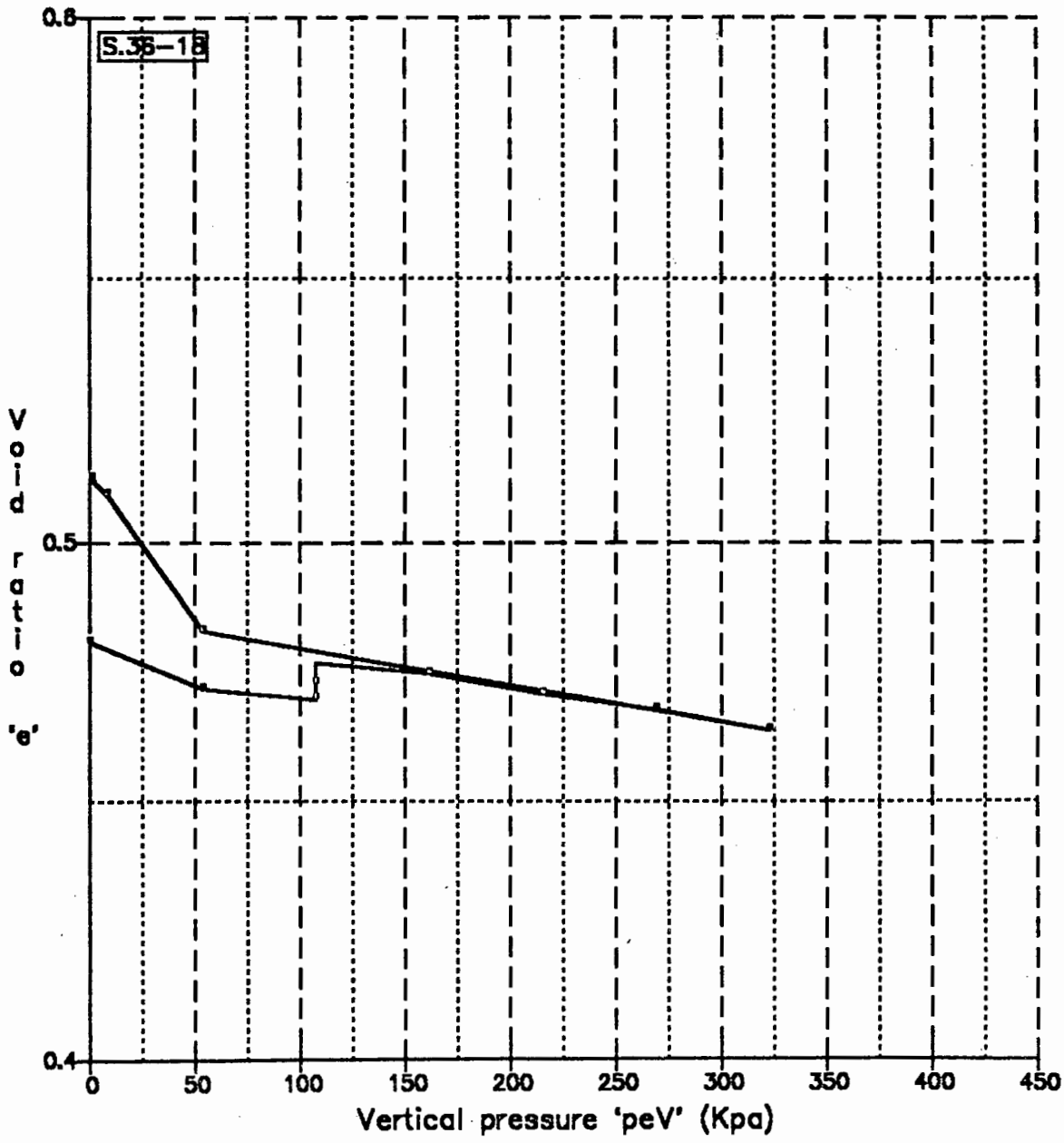

Figure 6.24: Site 36, Rondebosch [Compacted] - [100 Kpa during wetting] Relationship between the void ratio 'e' and the effective vertical pressure (or stress) 'peV'.

Undisturbed samples.

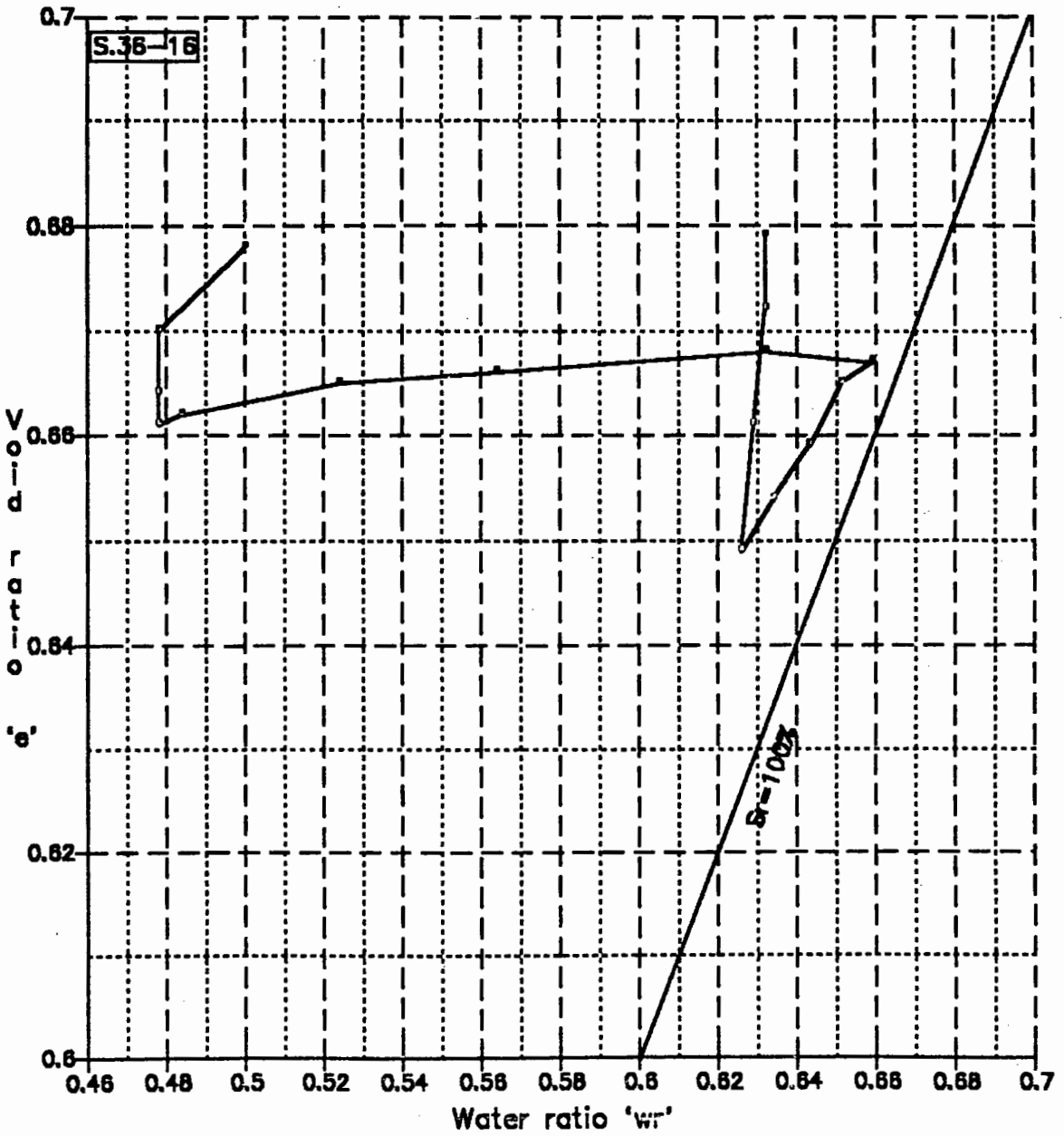

Figure 6.25: Site 36, Rondebosch [Undisturbed] - [100 Kpa during wetting] Relationship between the void ratio 'e' and the water ratio 'wr'.

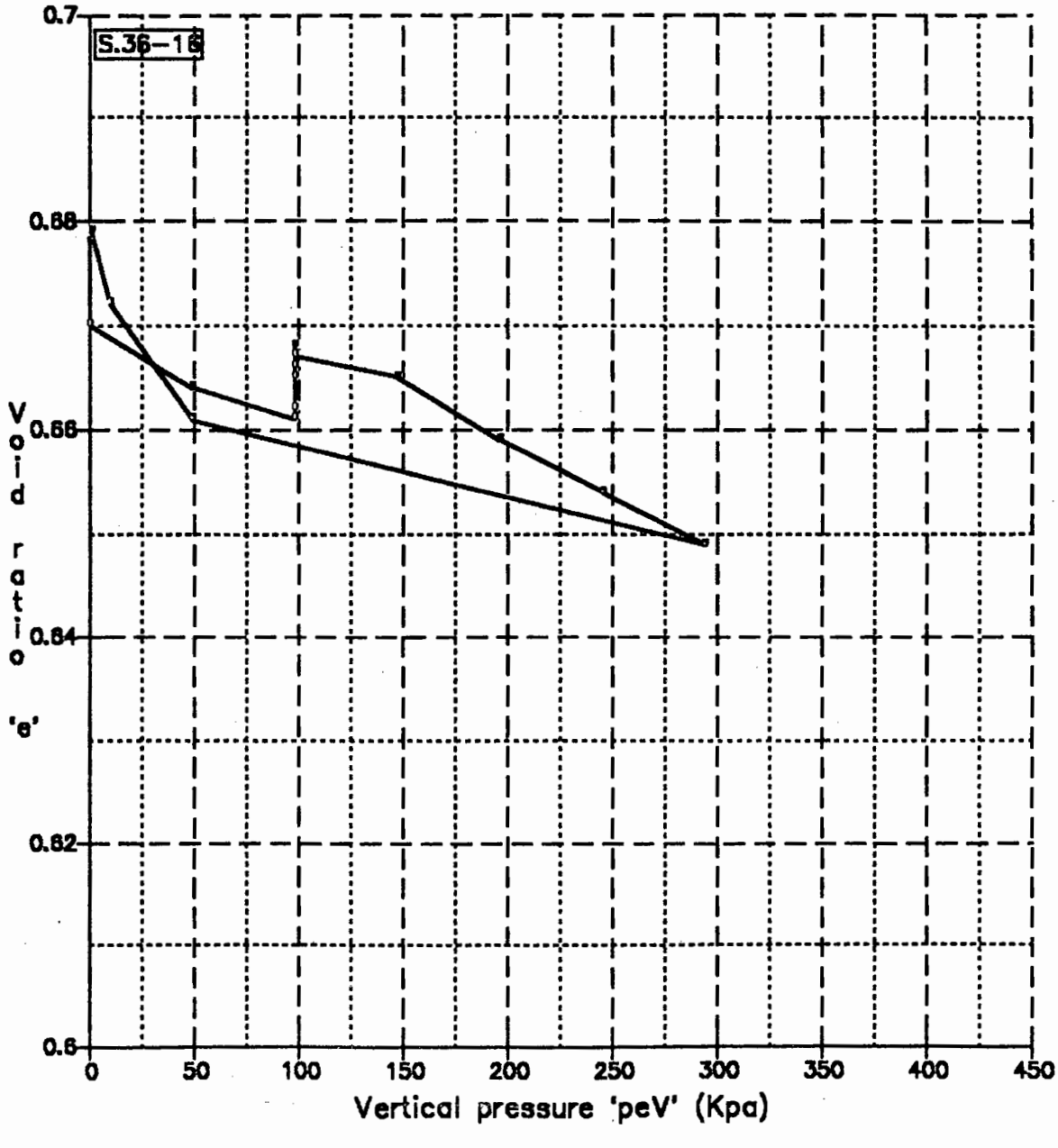

Figure 6.26: Site 36, Rondebosch [Undisturbed] - [100 Kpa during wetting] Relationship between the void ratio 'e' and the effective vertical pressure (or stress) 'peV'.

Site 30, Hout Bay.

A fine to medium sandy silt, with a saml1 amount of coarse sand. The soil consists of 23% clay, 34% silt, and 43% sand size. The 'Limits' of the soil are: w_{LS} = 6.4%; w_L = 49.0%; w_P = 29.0%; I_P = 20; w_S = 22.5%; and, w_{FE} = 36.0%.

Remoulded samples.

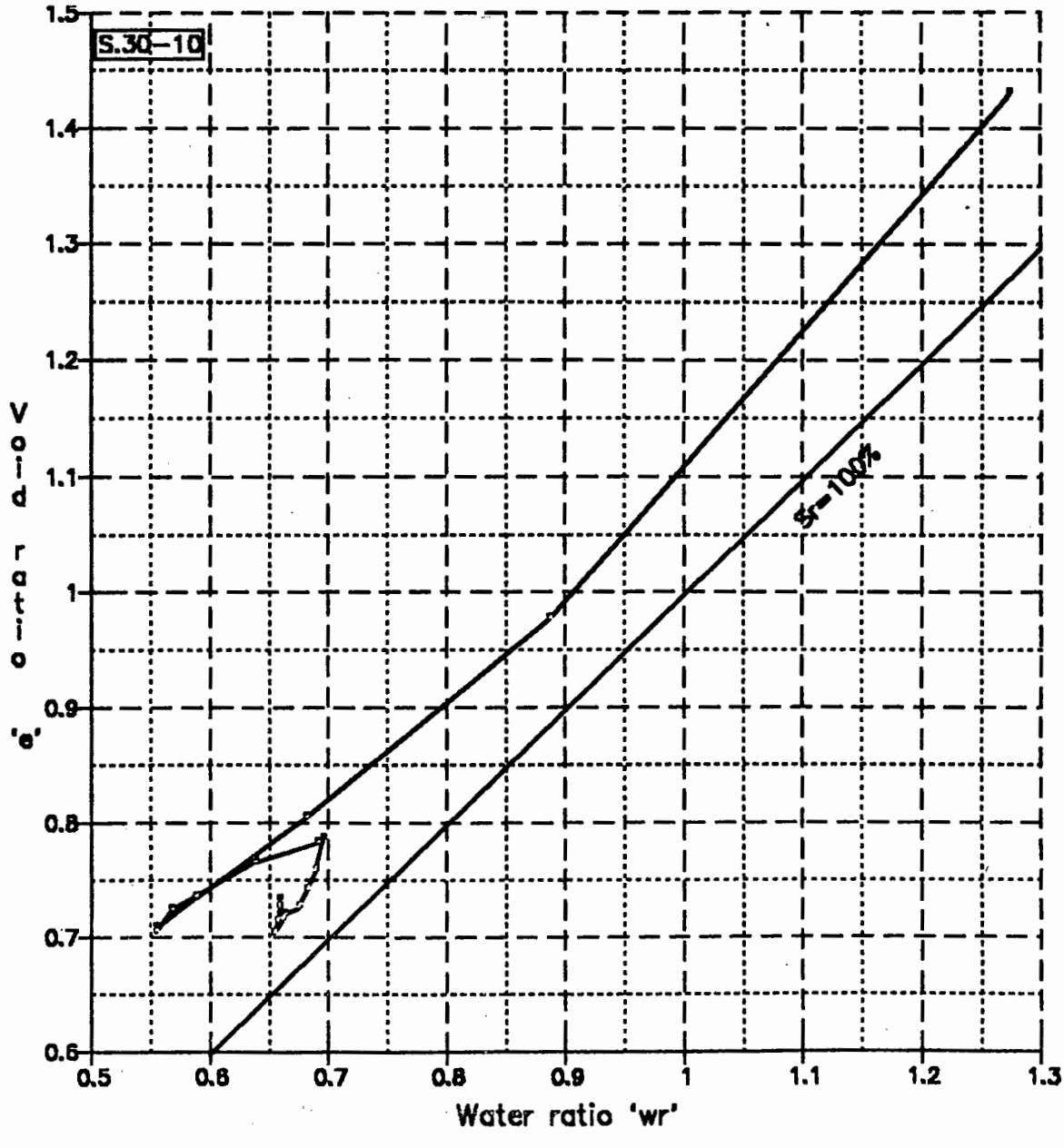

Figure 6.27: Site 30, Hout Bay - [1 Kpa during wetting] Relationship between the void ratio 'e' and the water ratio 'wr'. Read in conjunction with Figure 6.28.

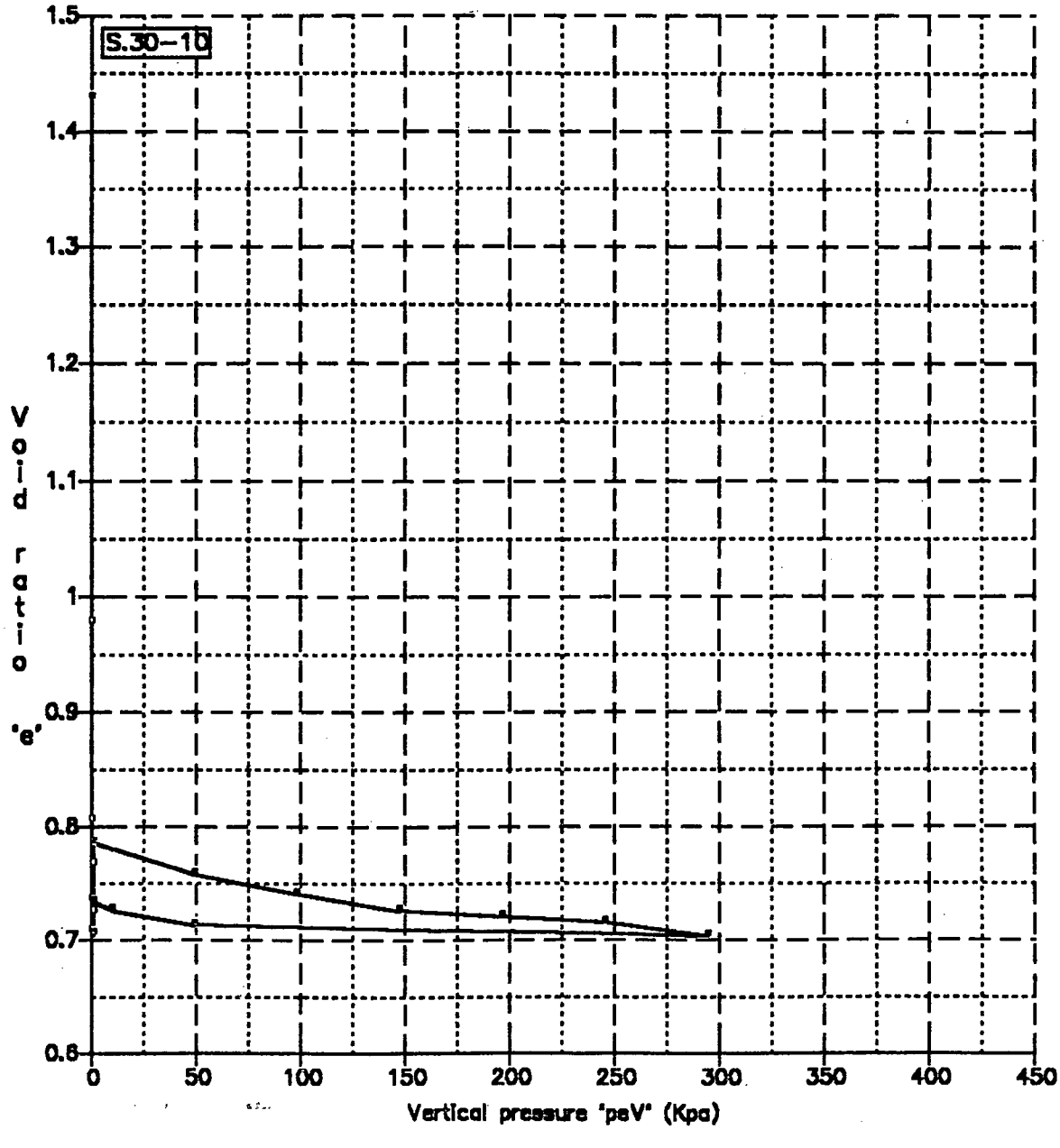

Figure 6.28: Site 30, Hout Bay - [1 Kpa during wetting] Relationship between the void ratio 'e' and the effective vertical pressure (or stress) 'peV'.

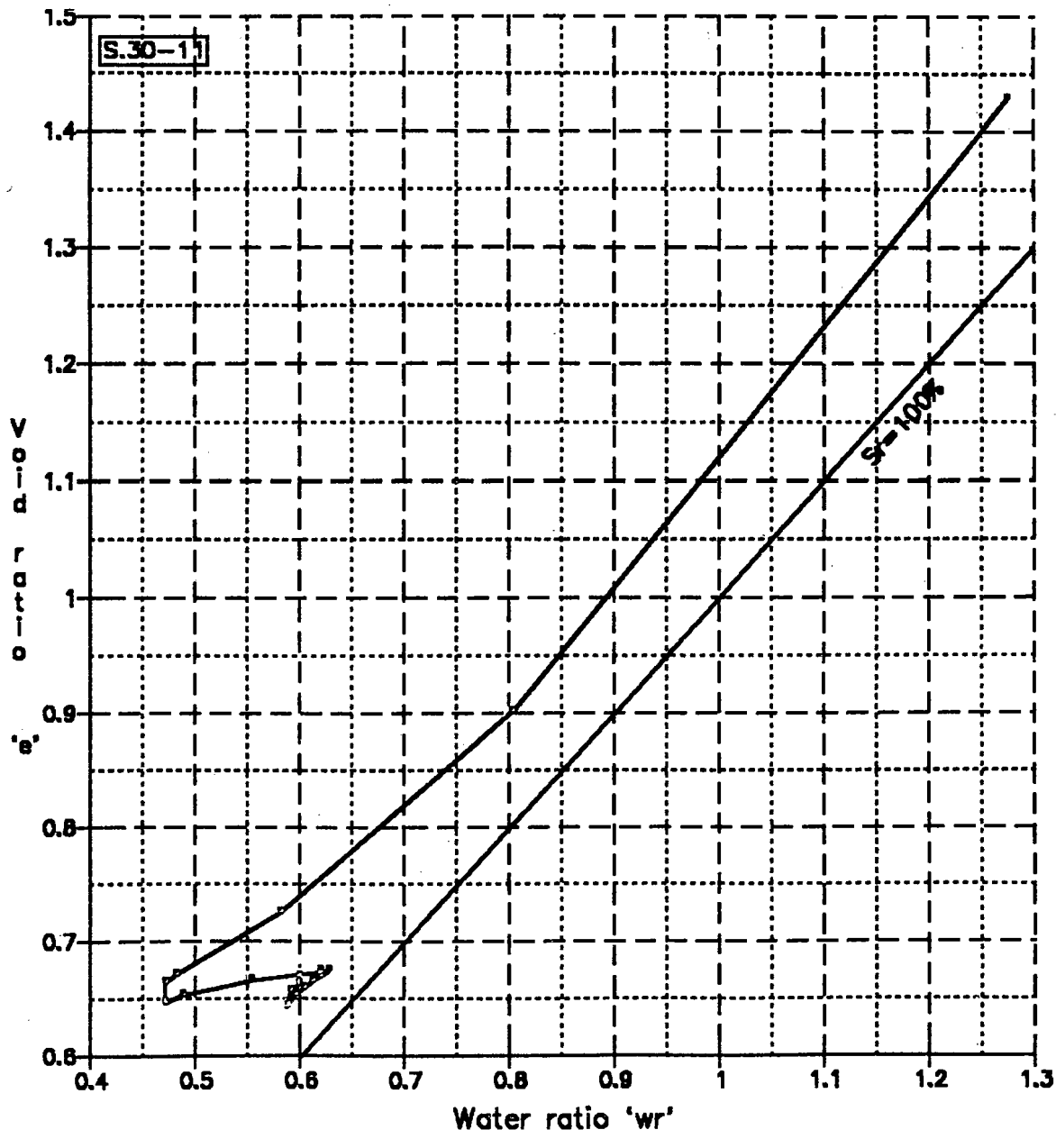

Figure 6.29: Site 30, Hout Bay - [50 Kpa during wetting] Relationship between the void ratio 'e' and the water ratio 'wr'.

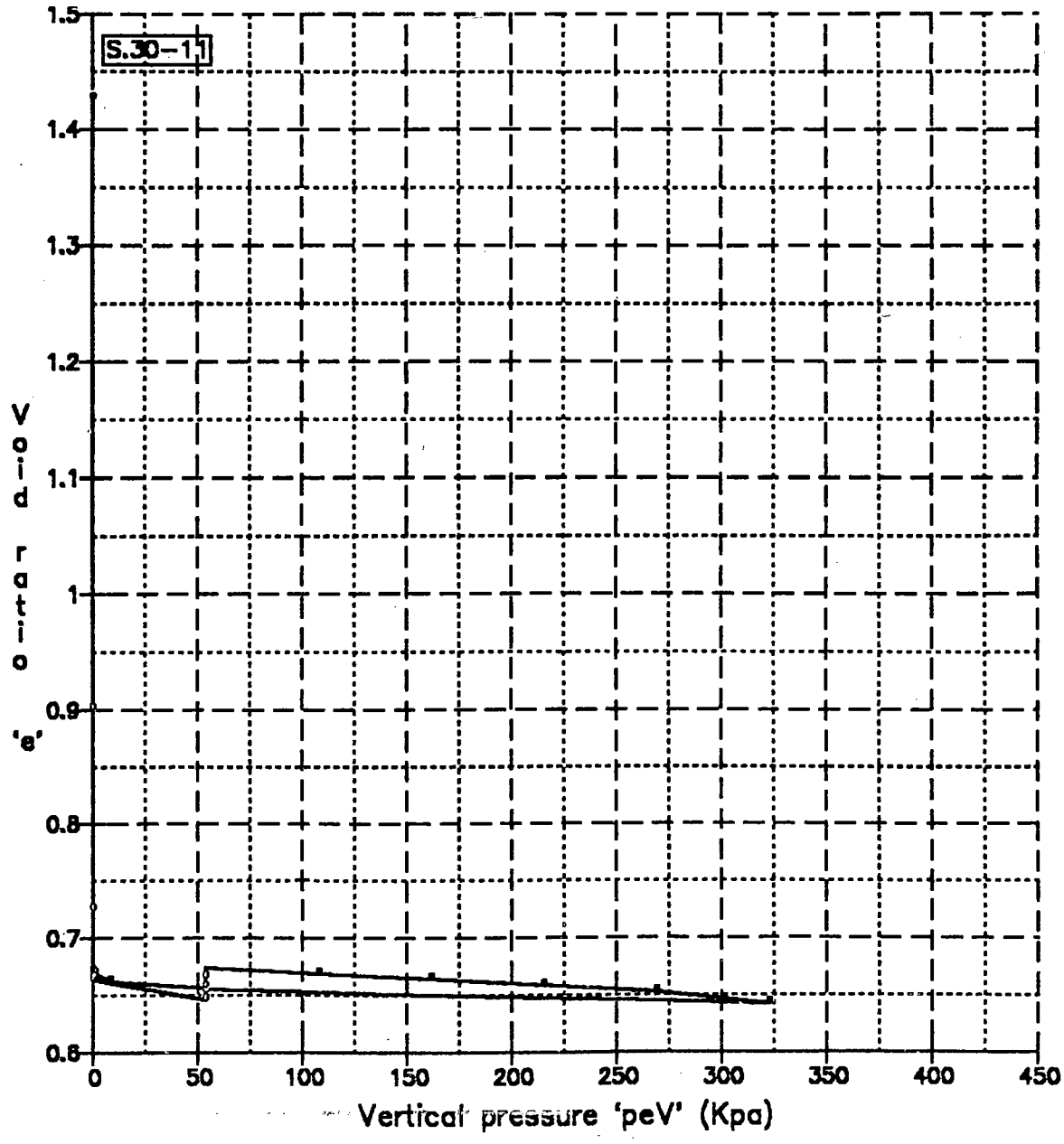

Figure 6.30: Site 30, Hout Bay - [50 Kpa during wetting] Relationship between the void ratio 'e' and the effective vertical pressure (or stress) 'peV'.

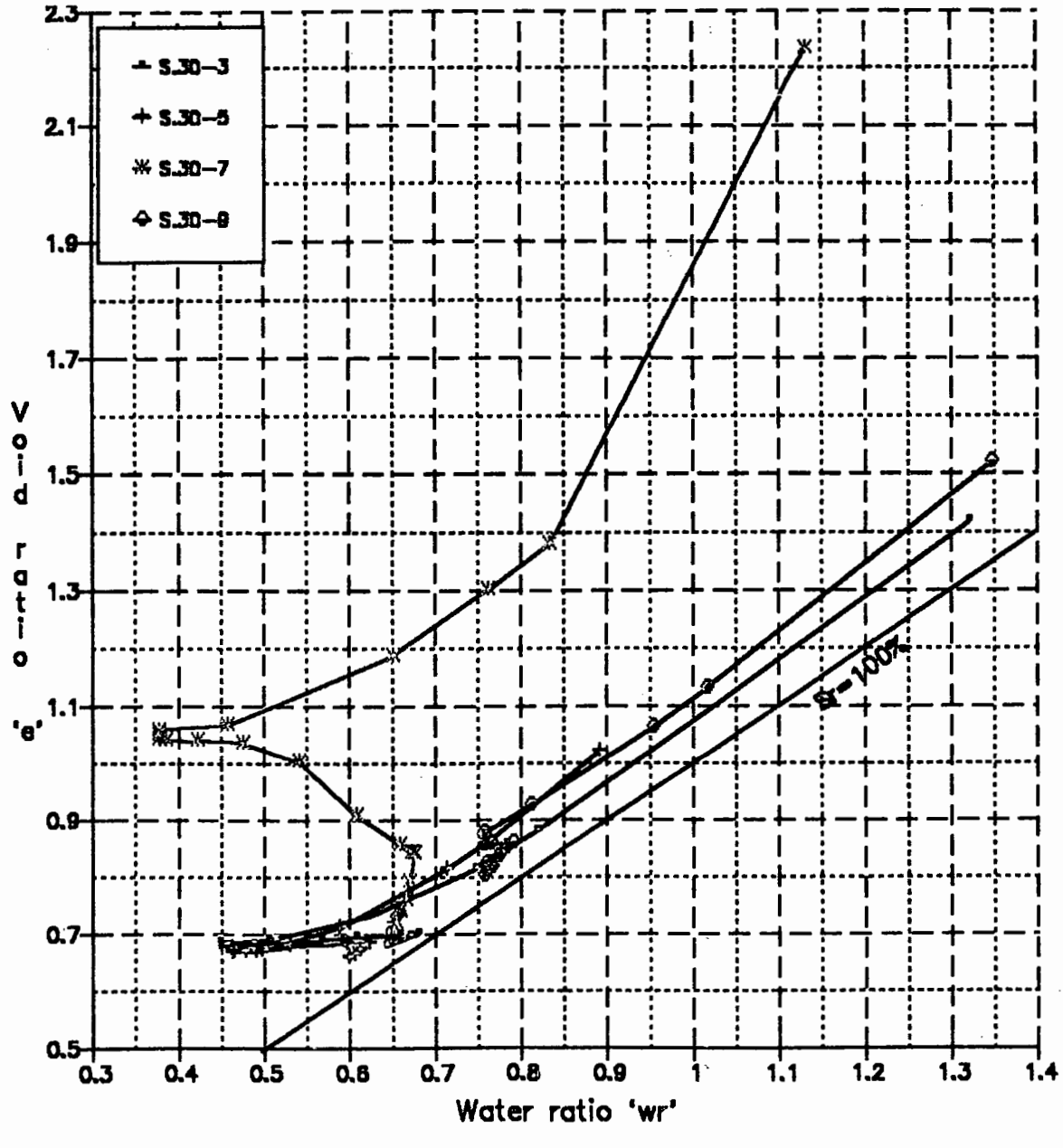

Figure 6.31: Site 30, Hout Bay - [100 Kpa during wetting] Relationship between the void ratio 'e' and the water ratio 'wr'.

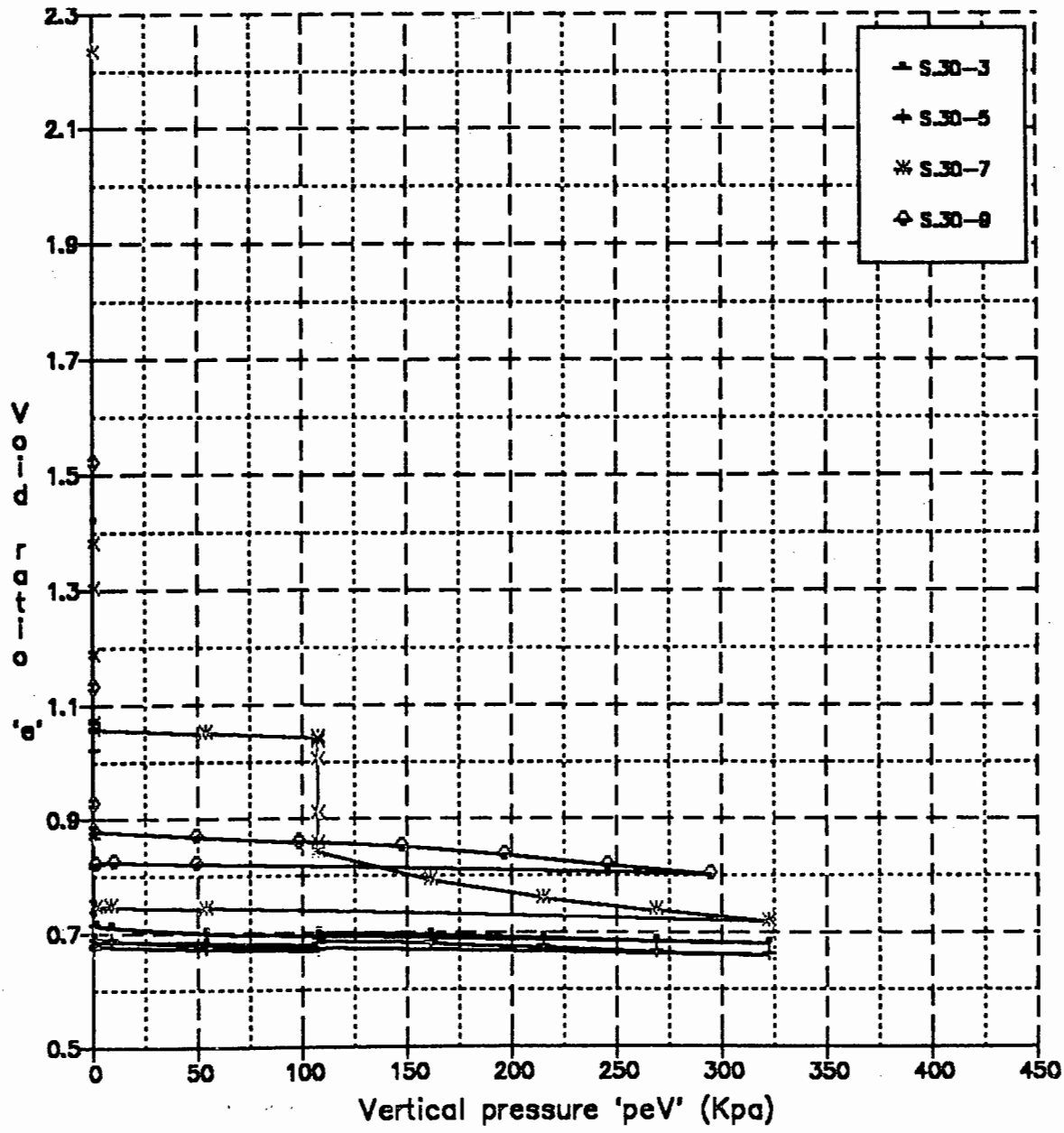

Figure 6.32: Site 30, Hout Bay - [100 Kpa during wetting] Relationship between the void ratio 'e' and the effective vertical pressure (or stress) 'peV'.

Undisturbed sample.

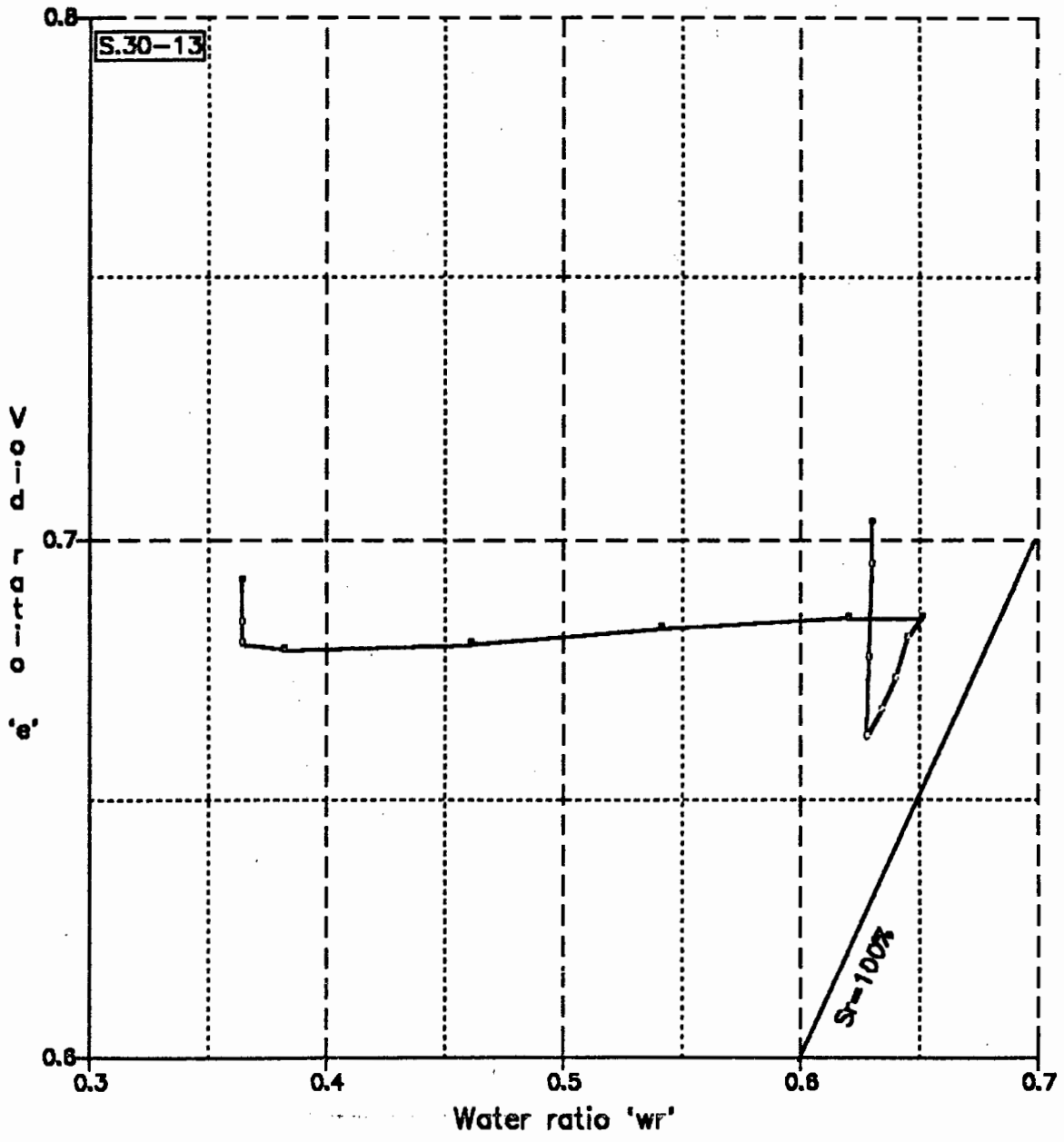

Figure 6.33: Site 30, Hout Bay [Undisturbed] - [100 Kpa during wetting] Relationship between the void ratio 'e' and the water ratio 'wr'.

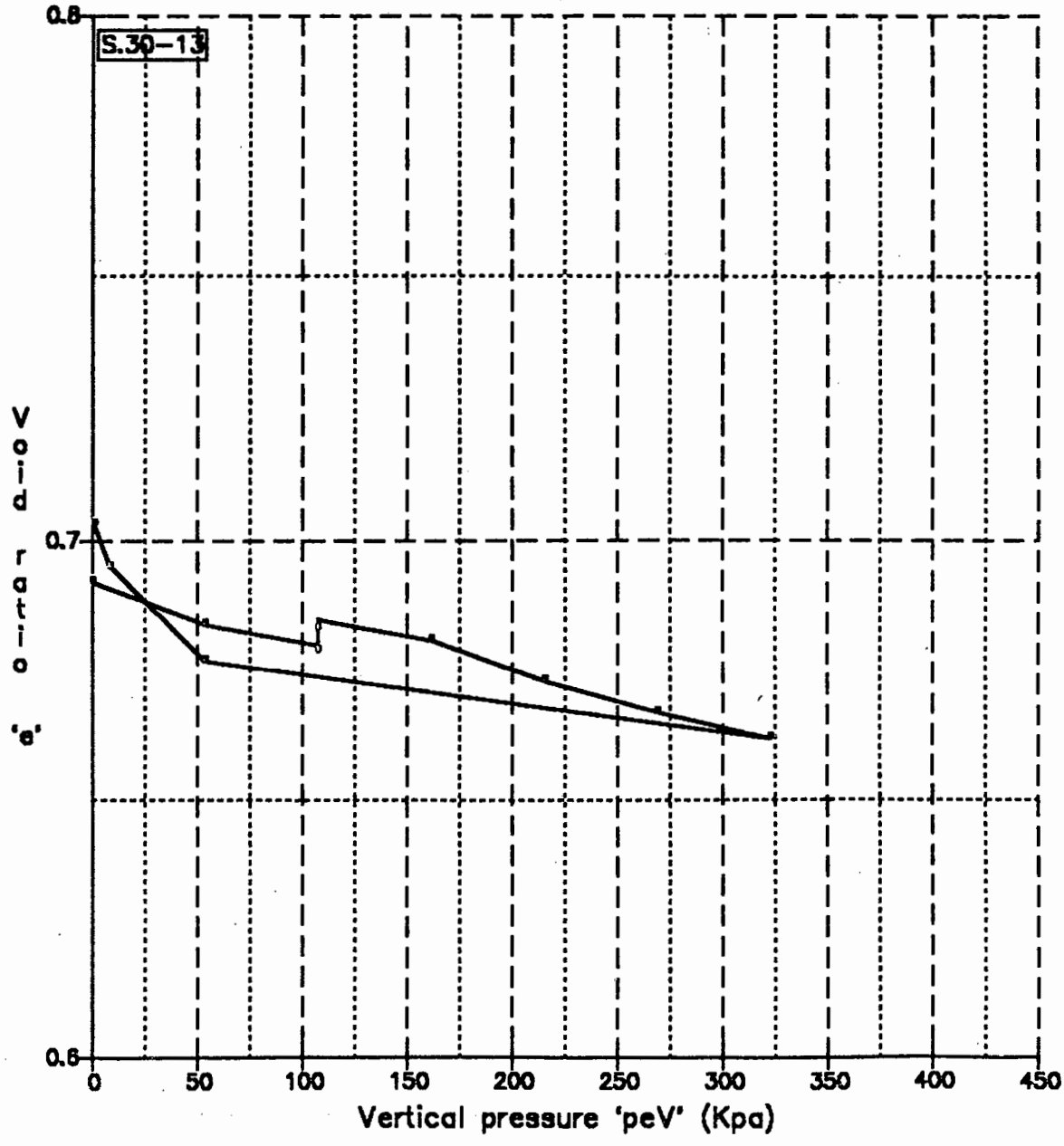

Figure 6.34: Site 30, Hout Bay [Undisturbed] - [100 Kpa during wetting] Relationship between the void ratio 'e' and the effective vertical pressure (or stress) 'peV'.

Site A, Berea Road (Durban).

A clayey sand (fine to medium size) with a small amount of silt. The soil consists of 15% clay, 10% silt, and 75% sand size. The 'Limits' of the soil are: w_{LS} = 3.7%; w_L = 25.0%; w_P = 13.1%; I_P = 12; w_S = 13.5%; and, w_{FE} = 16.6%.

Remoulded samples.

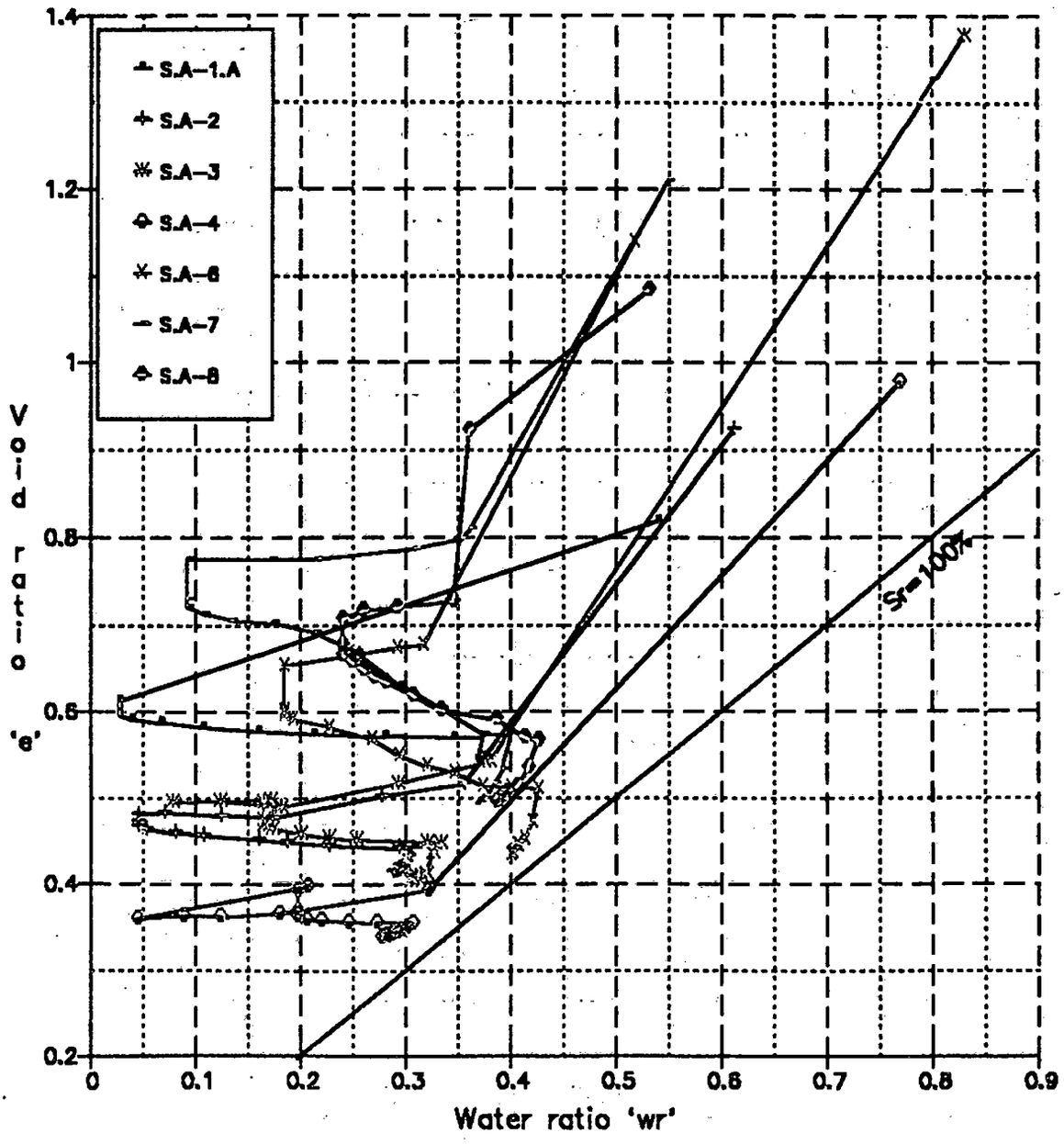

Figure 6.35: Site A, Berea Road (Durban) - [100 Kpa during wetting] Relationship between the void ratio 'e' and the water ratio 'wr'. Read in conjunction with Figure 6.36.

Undisturbed samples.

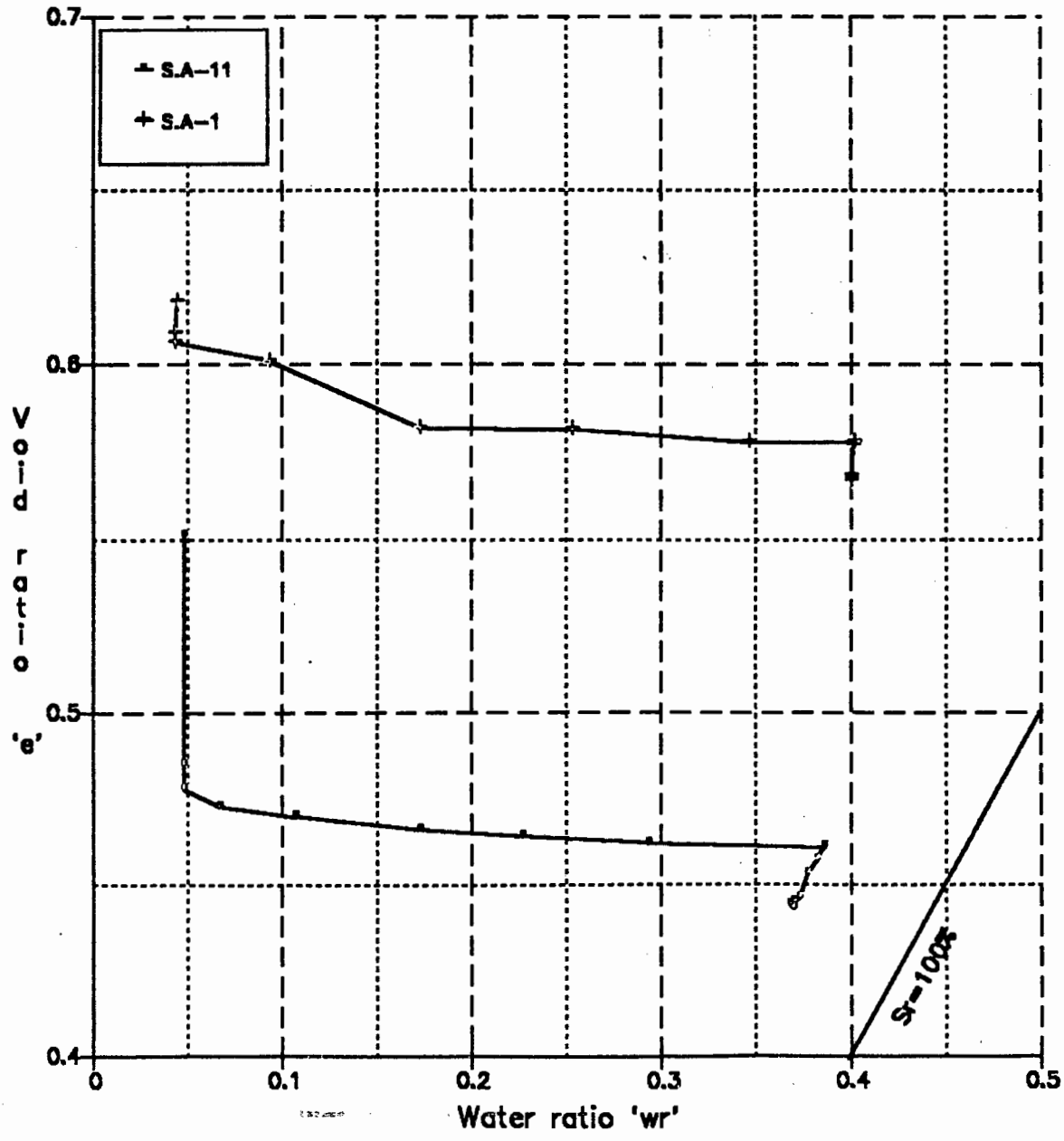

Figure 6.39: Site A, Berea Road (Durban) [Undisturbed Air dried] - [100 Kpa during wetting] Relationship between the void ratio 'e' and the water ratio 'wr'.

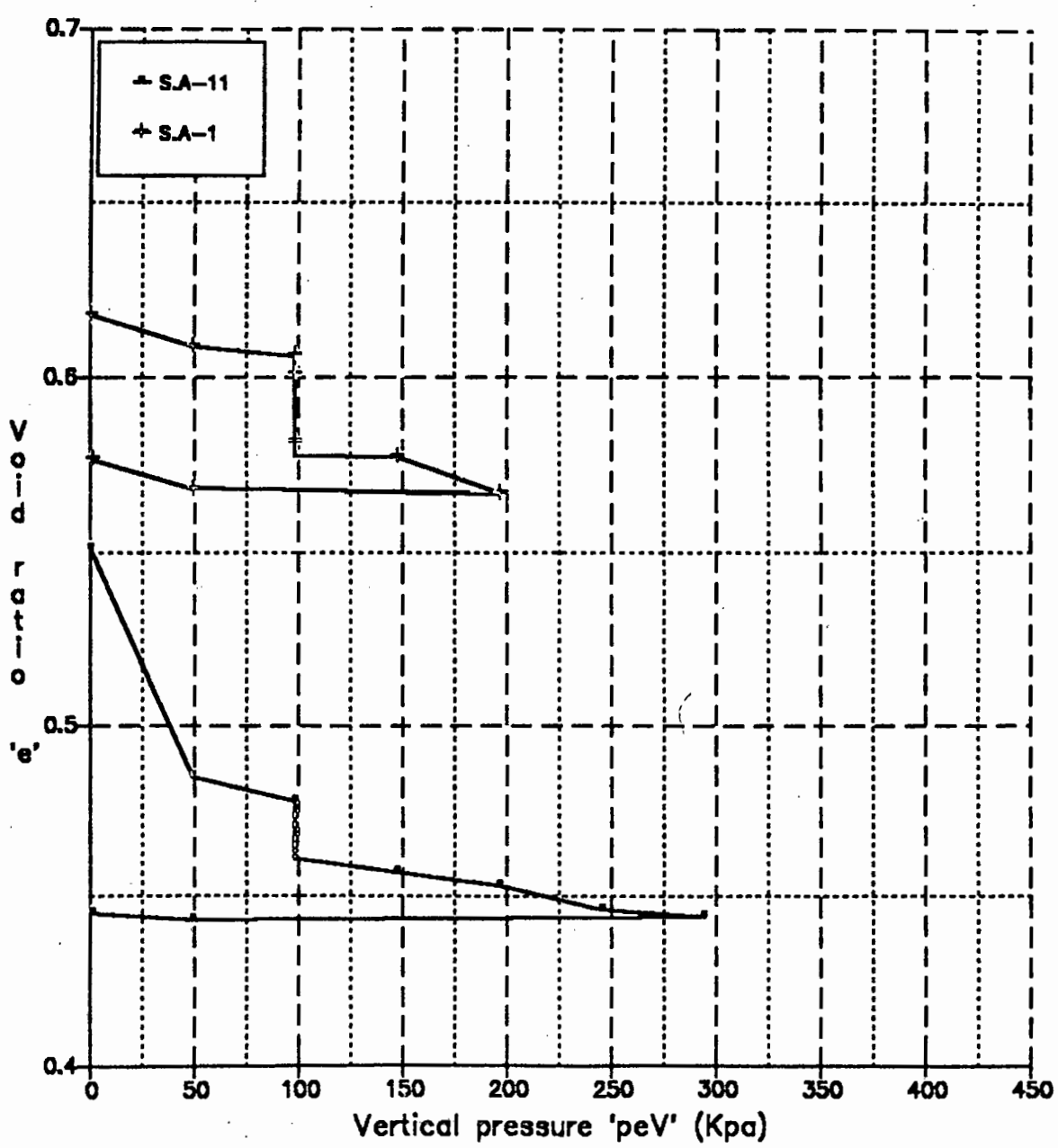

Figure 6.40: Site A, Berea Road (Durban) [Undisturbed Air dried] - [100 Kpa during wetting] Relationship between the void ratio 'e' and the effective vertical pressure (or stress) 'peV'.

Site 7, Mowbray.

A fine silty clay, with a small amount of fine to medium sand. The soil consists of 42% clay, 37% silt, and 21% sand size. The Limits of the soil are: w_{LS} = 10.5%; w_L = 47.0%; w_P = 22.0%; I_P = 25; w_S = 18.5%; and, w_{FE} = 29.1%.

Remoulded samples.

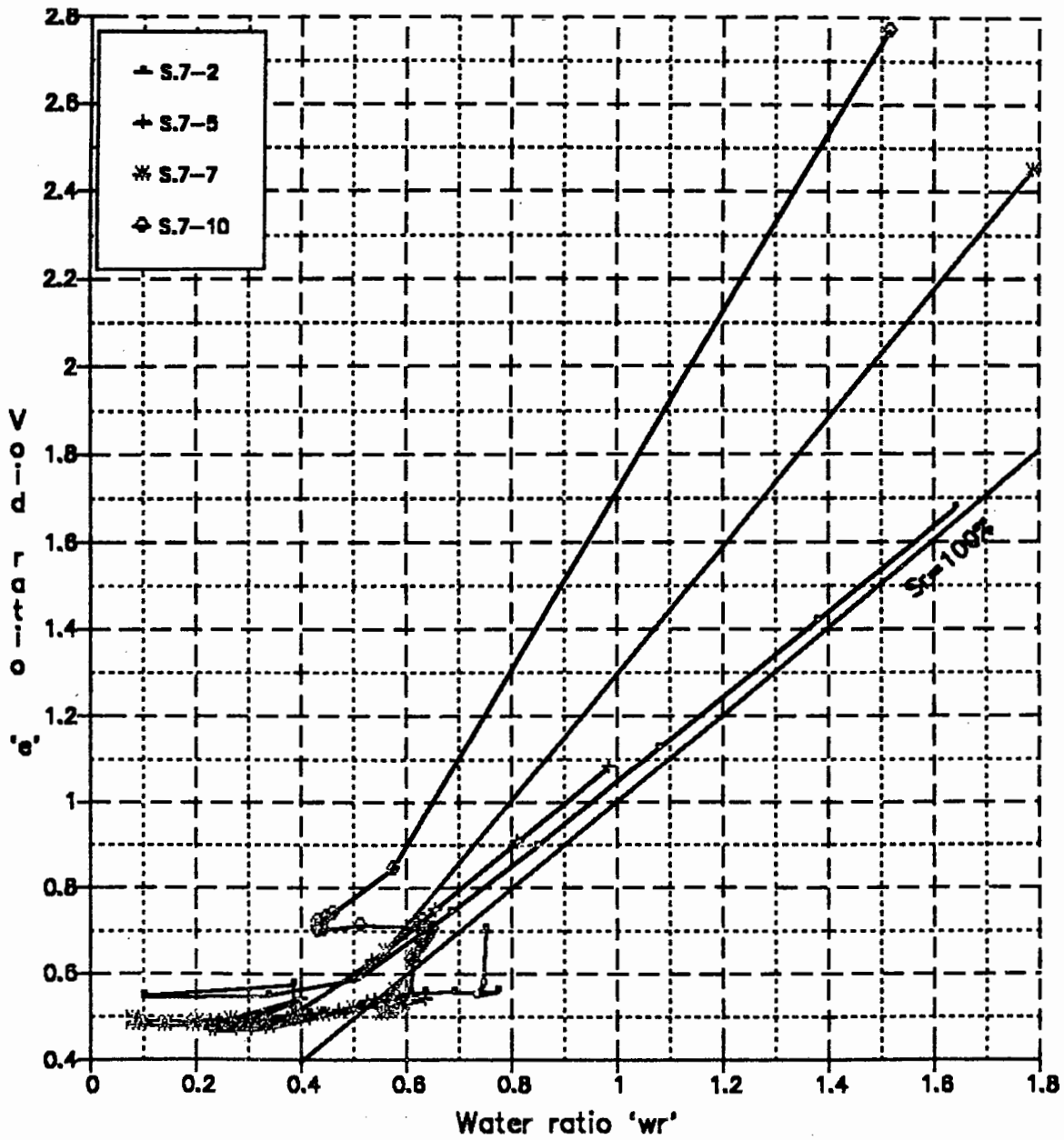

Figure 6.41: Site 7, Mowbray - [100 Kpa during wetting] Relationship between the void ratio 'e' and the water ratio 'wr'. Read in conjunction with Figure 6.42.

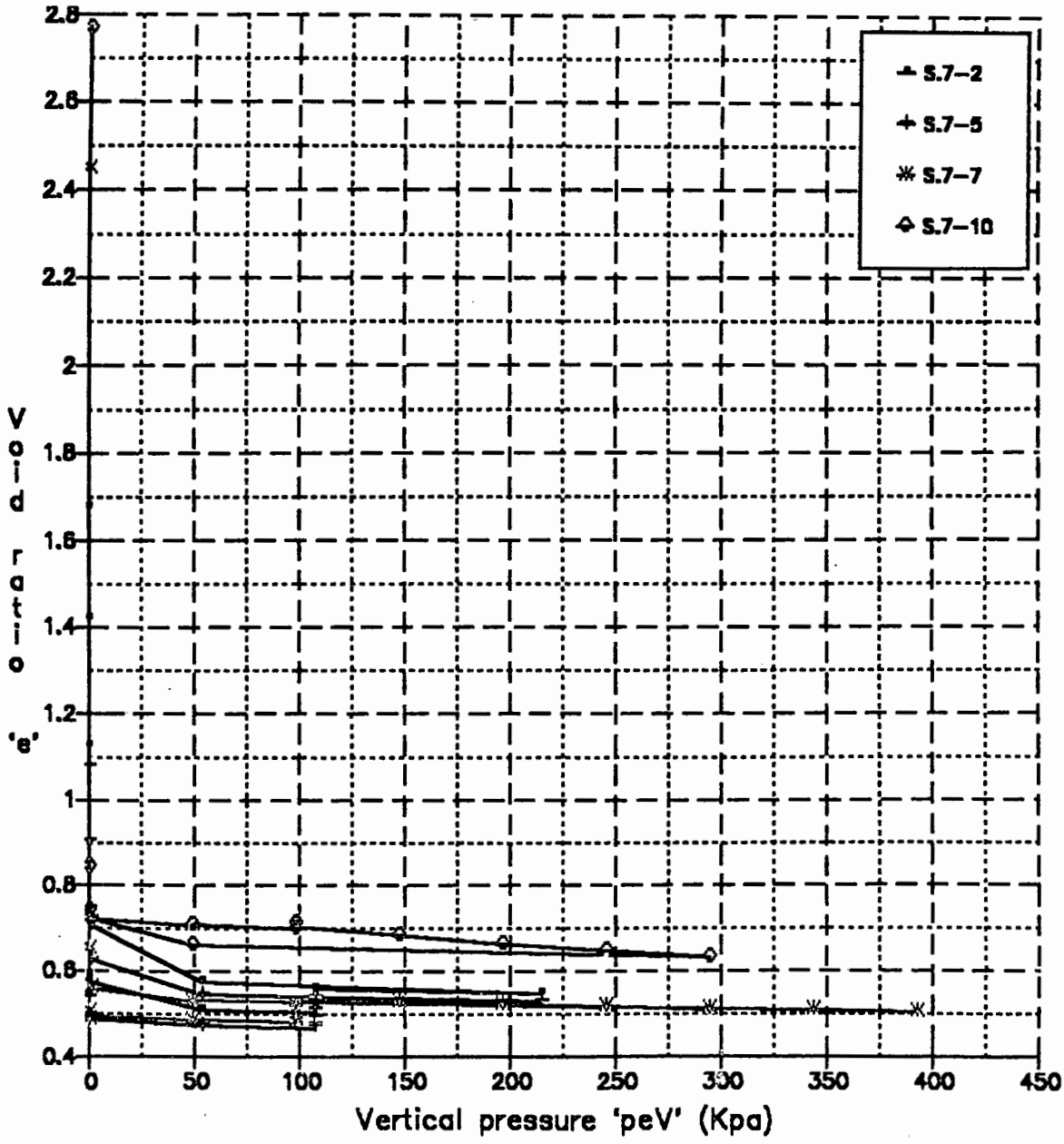

Figure 6.42: Site 7, Mowbray - [100 Kpa during wetting] Relationship between the void ratio 'e' and the effective vertical pressure (or stress) 'peV'.

Compacted samples.

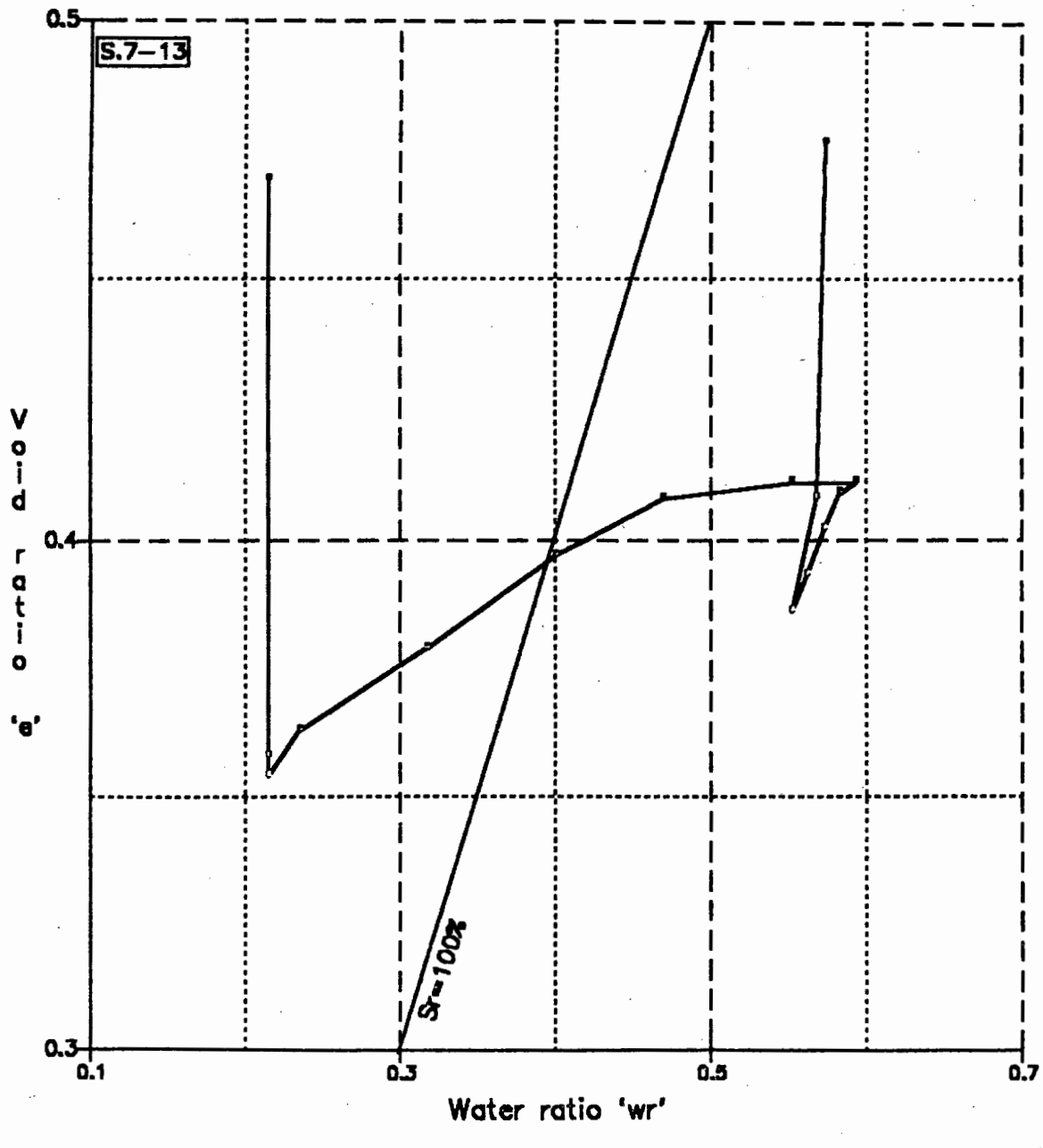

Figure 6.43: Site 7, Mowbray [Compacted] - [100 Kpa when wetted] Relationship between the void ratio 'e' and the water ratio 'wr'.

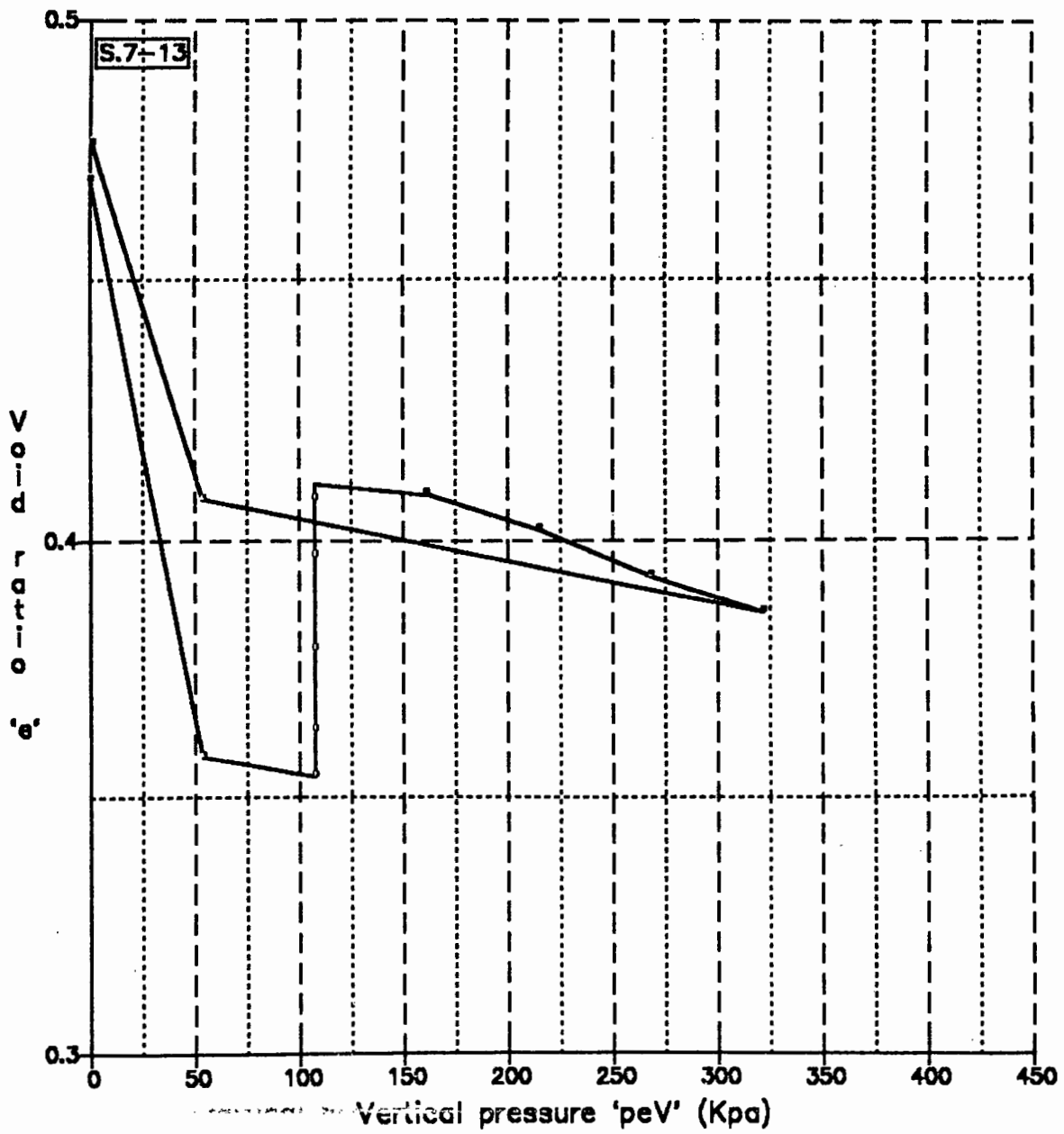

Figure 6.44: Site 7, Mowbray [Compacted] - [100 Kpa when wetted] Relationship between the void ratio 'e' and the effective vertical pressure (or stress) 'peV'.

Undisturbed samples.

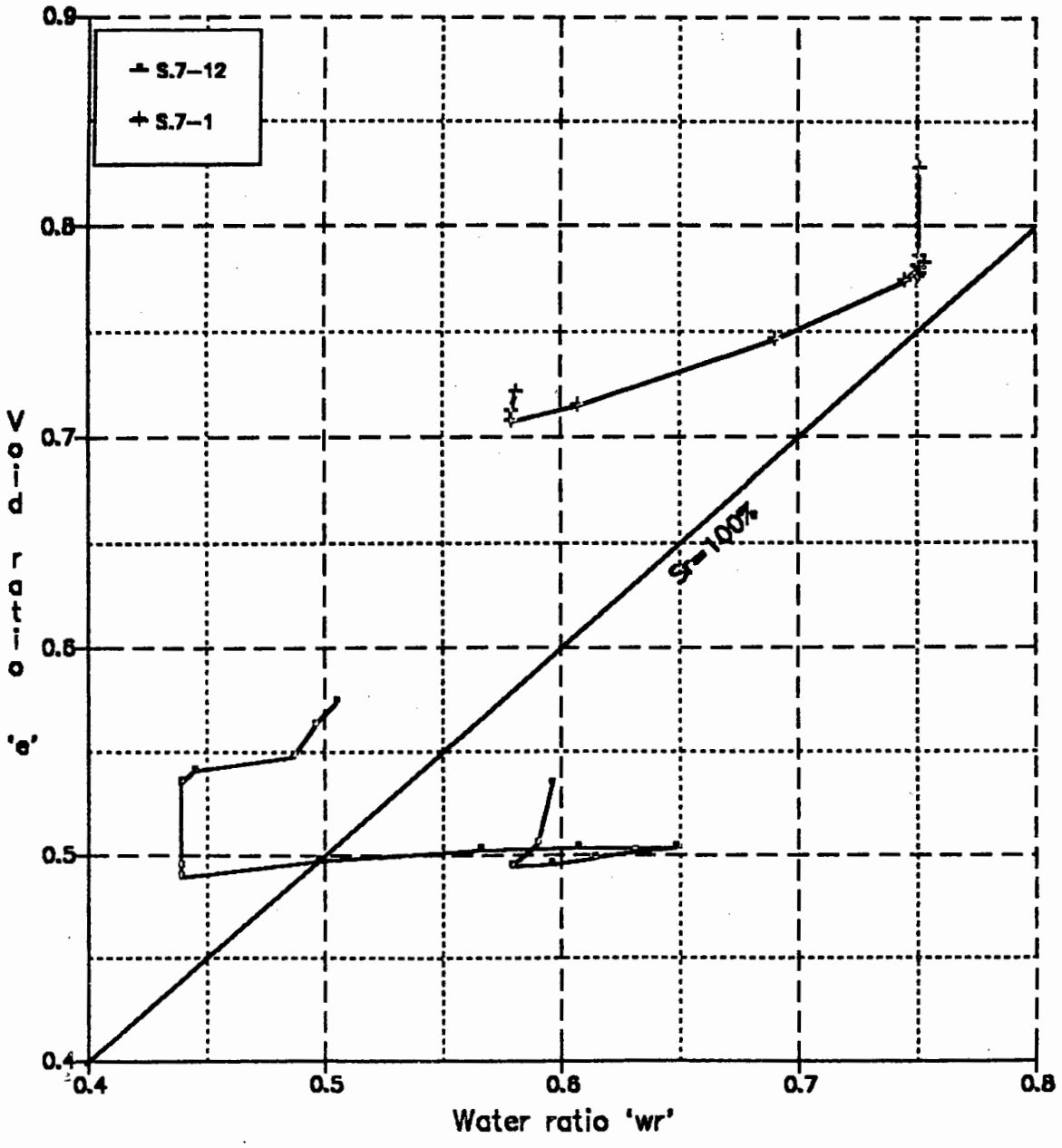

Figure 6.45: Site 7, Mowbray [Undisturbed] - [100 Kpa during wetting] Relationship between the void ratio 'e' and the water ratio 'wr'.

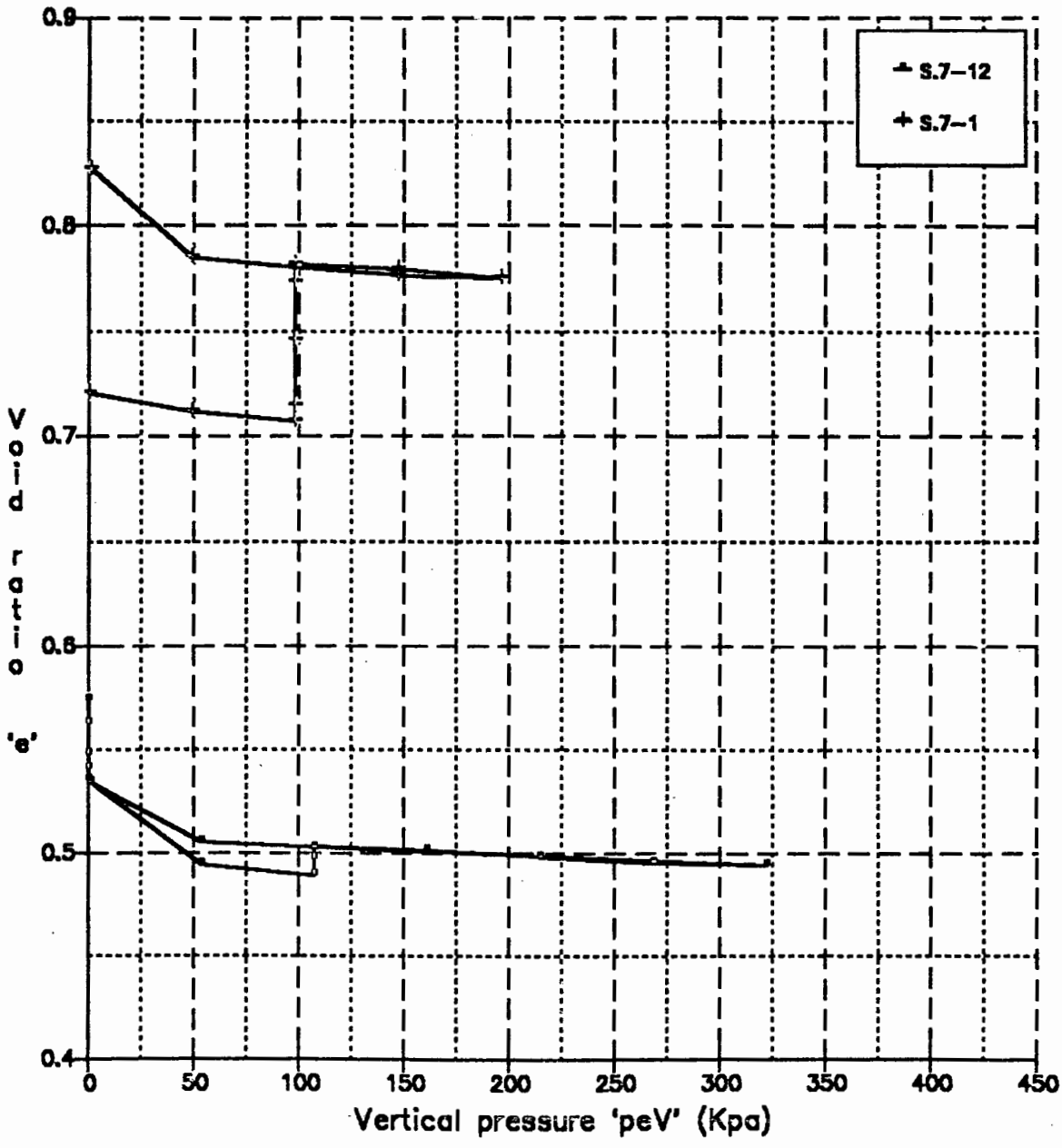

Figure 6.46: Site 7, Mowbray [Undisturbed] - [100 Kpa during wetting] Relationship between the void ratio 'e' and the effective vertical pressure (or stress) 'peV'.

Site B, Francois Road (Durban).

A fine to medium sand containing small amounts of clay and silt. The soil consists of 7.5% clay, 7% silt, and 85.5% sand size. The 'Limits' are: w_{LS} = 0.5%; w_L = 15.0%; w_P = 12.9%; I_P = 2; w_S = 11.0%; and, w_{FE} = 11.8%.

Remoulded sample.

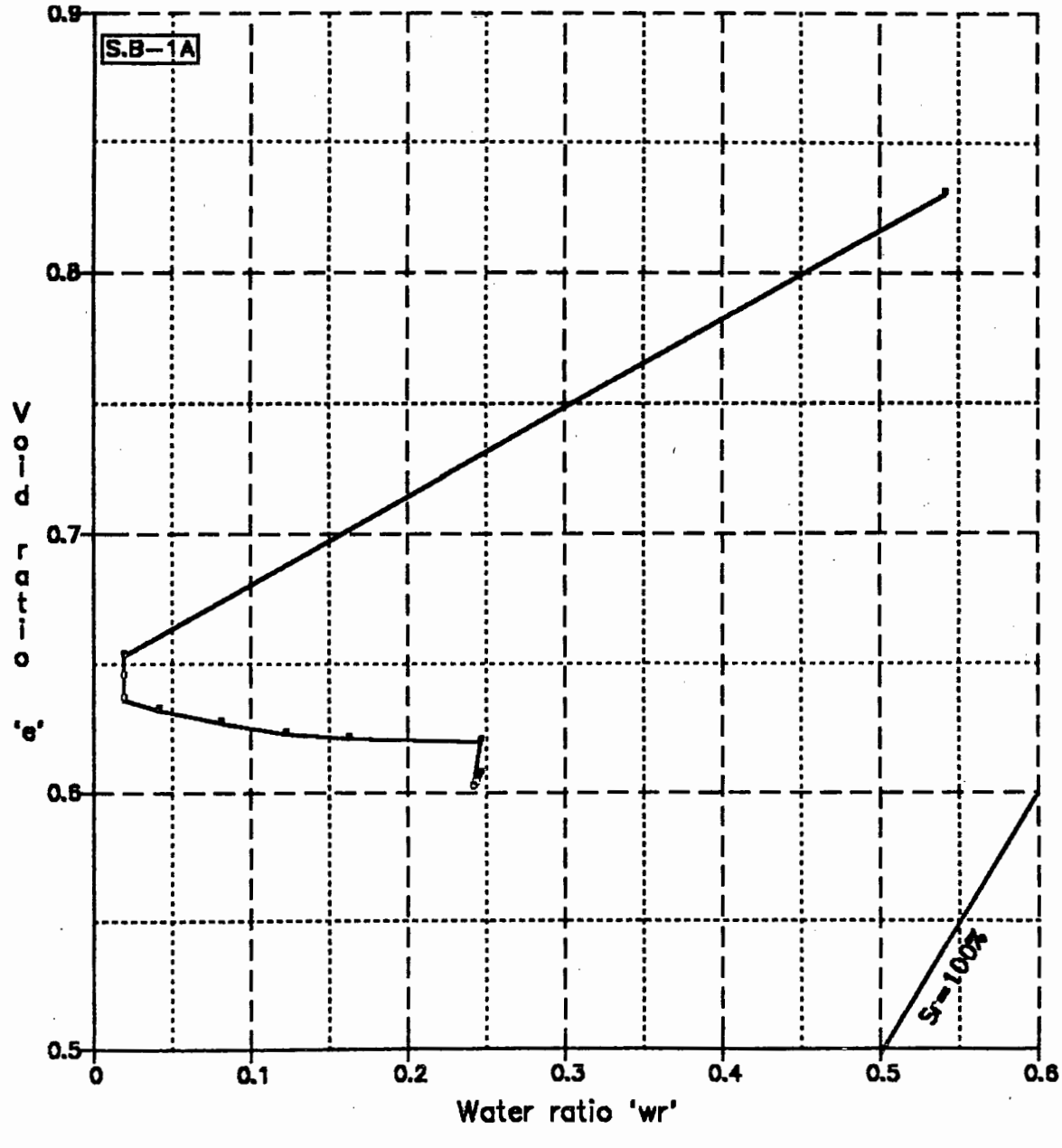

Figure 6.47: Site B, Francois Road (Durban) - [100 Kpa during wetting] Relationship between the void ratio 'e' and the water ratio 'wr'. Read in conjunction with Figure 6.48.

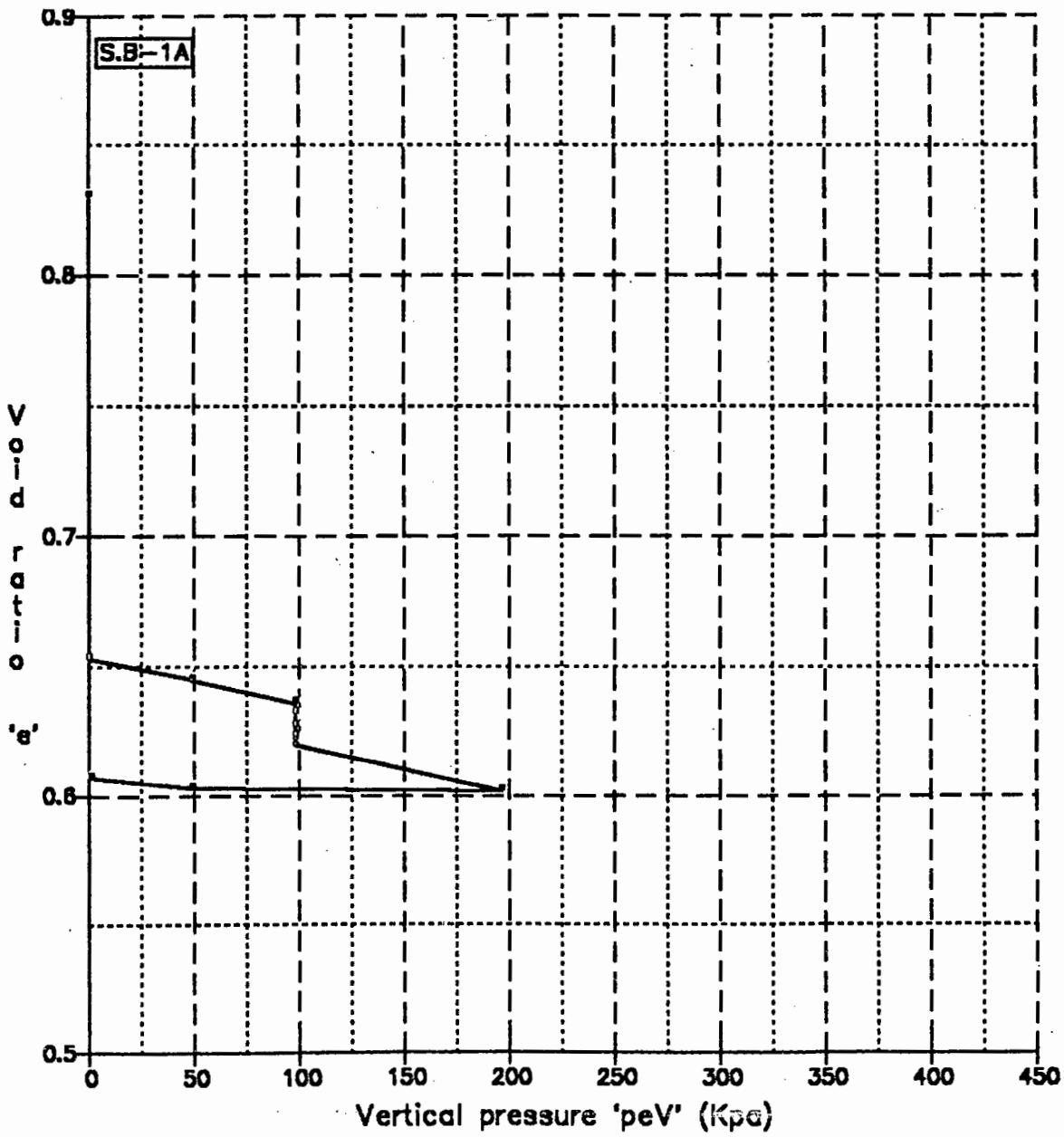

Figure 6.48: Site B, Francois Road (Durban) - [100 Kpa during wetting] Relationship between the void ratio 'e' and the effective vertical pressure (or stress) 'peV'.

Site C, Margaret Mayton Avenue (Durban).

A clayey sand (fine to medium size) with a very small amount of silt. The soil consists of 12.5% clay, 4% silt, and 83.5% sand size. The 'Limits' of the soil are: w_{LS} = 1.8%; w_L = 19.7%; w_P = 15.9%; I_P = 4; w_S = 8.5%; and, w_{FE} = 15.4%.

Remoulded sample.

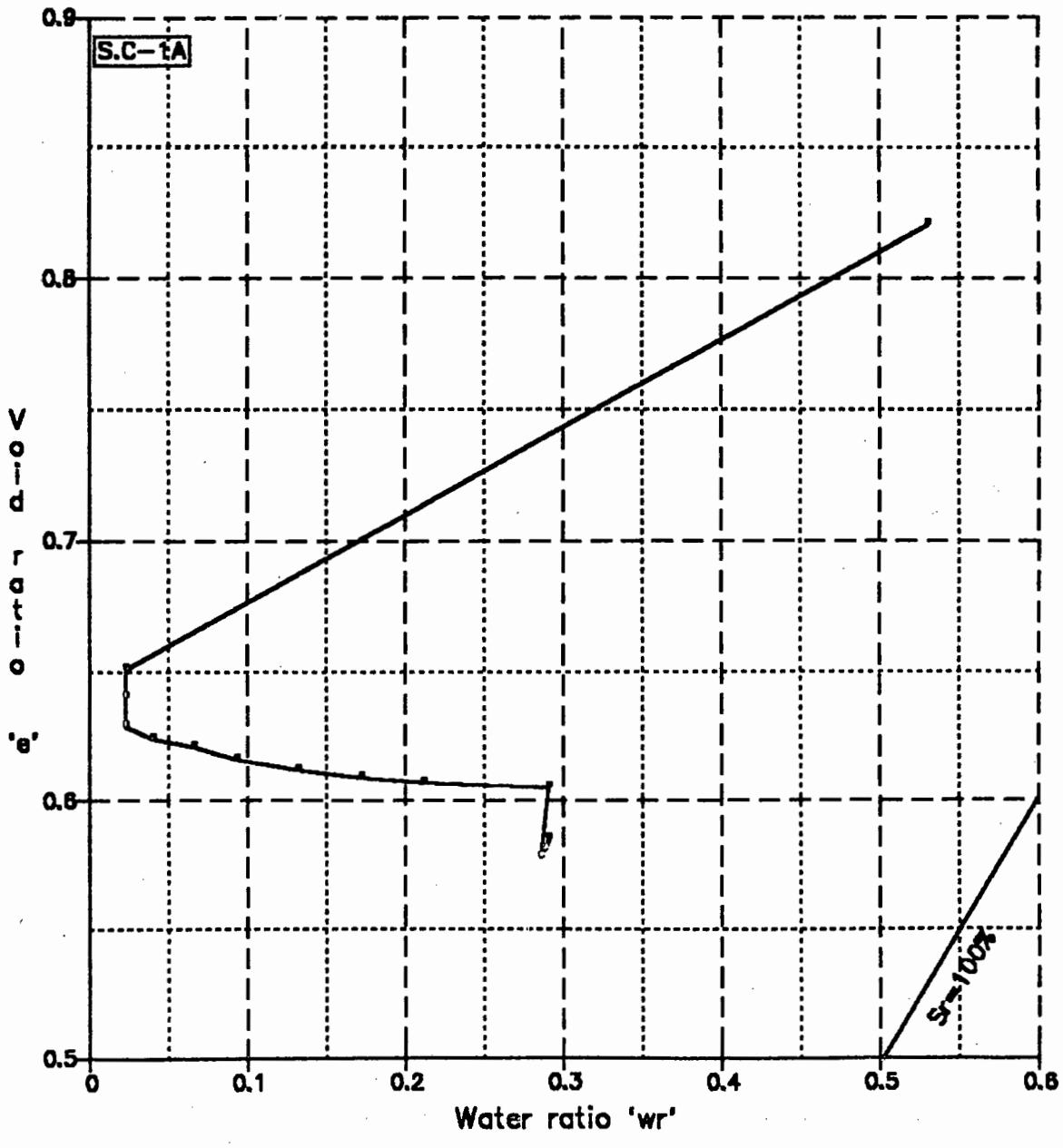

Figure 6.49: Site C, Margaret Mayton Avenue (Durban) - [100 Kpa during wetting] Relationship between the void ratio 'e' and the water ratio 'wr'.

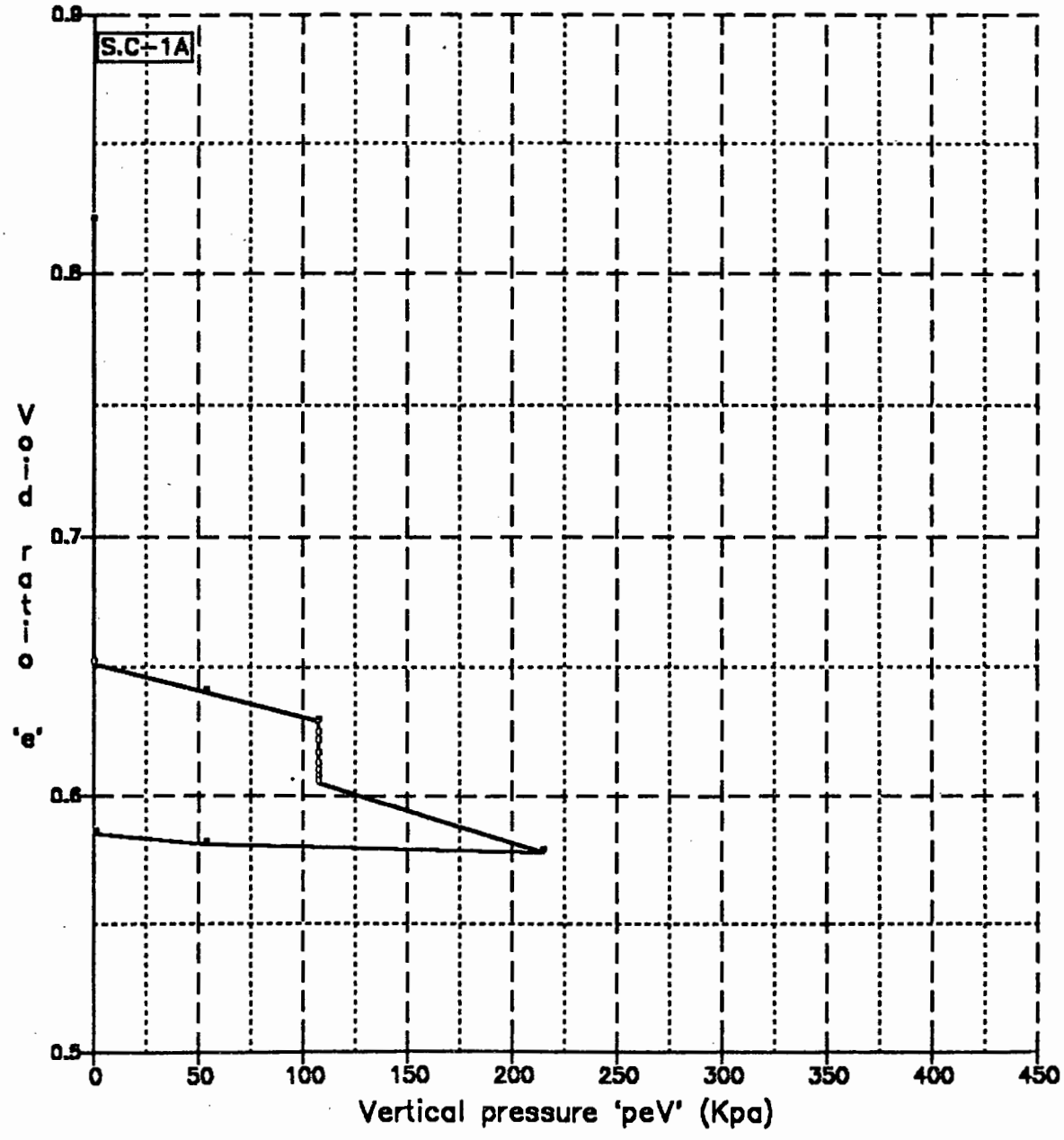

Figure 6.50: Site C, Margaret Mayton Avenue (Durban) - [100 Kpa during wetting] Relationship between the void ratio 'e' and the effective vertical pressure (or stress) 'peV'.

Site D, Rose Hill (Durban).

A clayey sand (fine to medium size) with a very small amount of silt. The soil consists of 15.5% clay, 4.5% silt, and 80% sand size. The 'Limits' are: w_{LS} = 2.2%; w_L = 20.6%; w_P = 14.9%; I_P = 6; w_S = 12.0%; and, w_{FE} = 12.2%.

Remoulded sample.

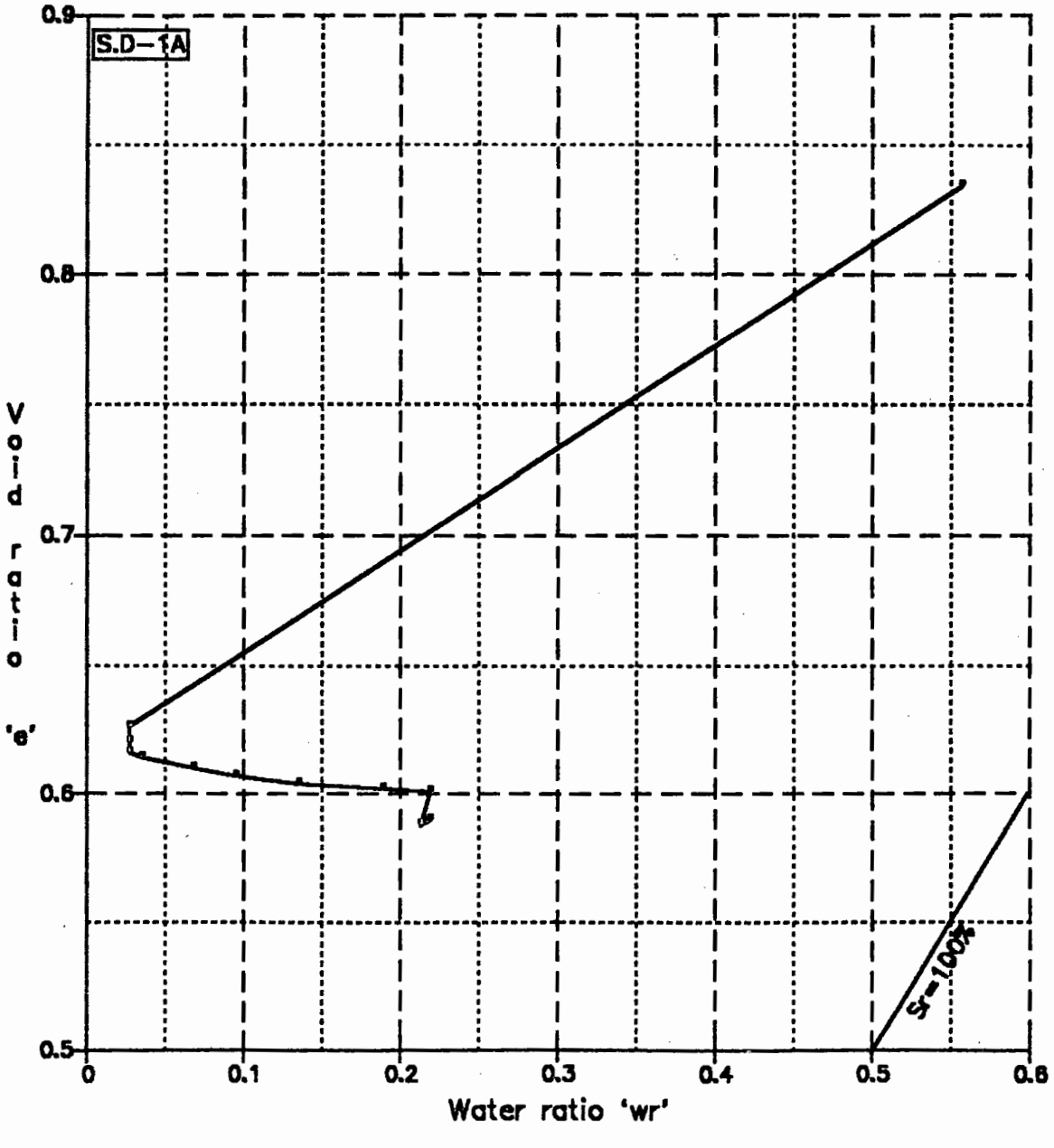

Figure 6.51: Site D, Rose Hill (Durban) - [100 Kpa during wetting] Relationship between the void ratio 'e' and the water ratio 'wr'.

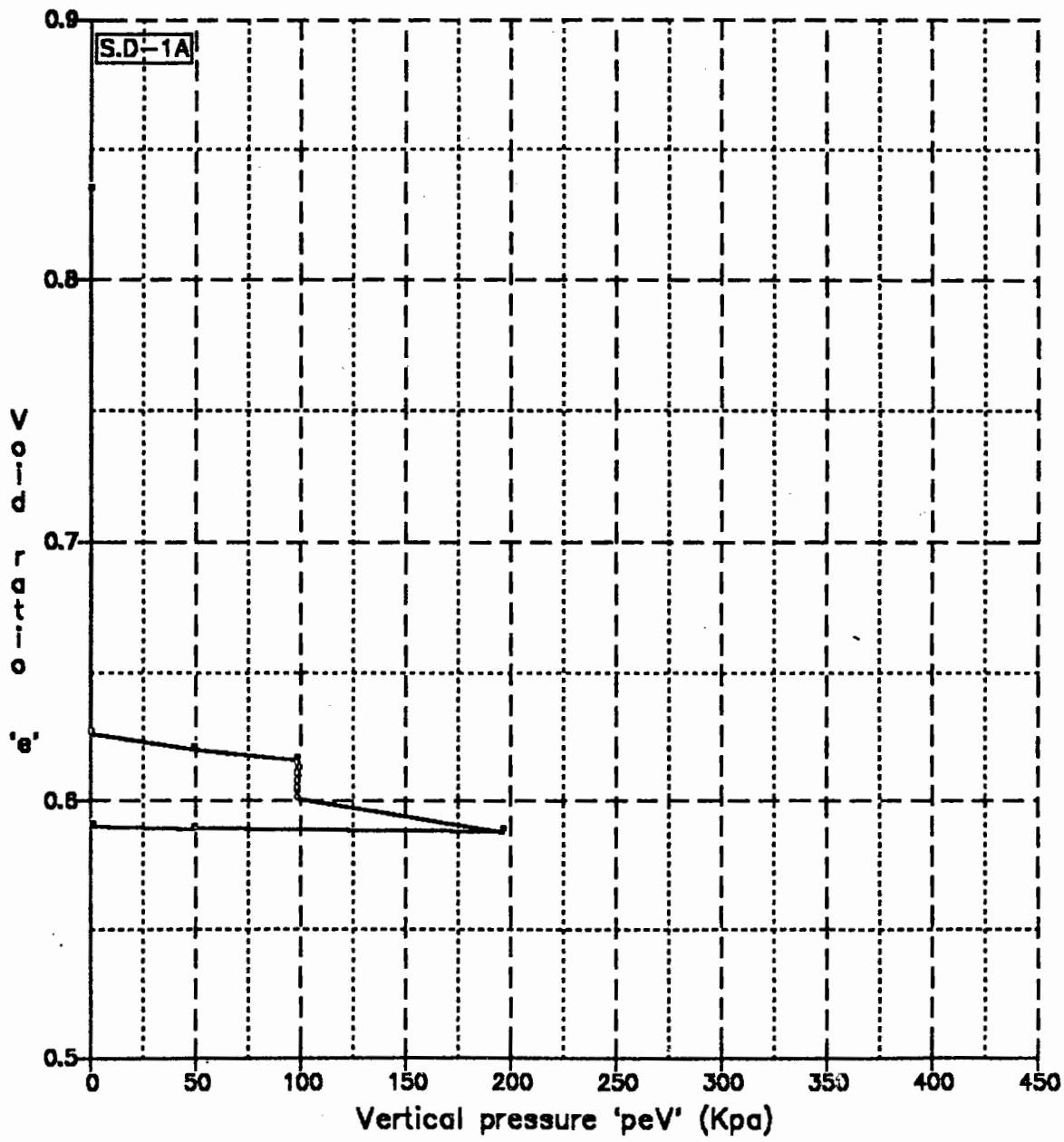

Figure 6.52: Site D, Rose Hill (Durban) - [100 Kpa during wetting] Relationship between the void ratio 'e' and the effective vertical pressure (or stress) 'peV'.

Site 48, Lady Grey District - Farm Unity (Natal).
A clayey silt (medium to coarse) with a small amount of fine sand. The soil consists of 26% clay, 54% silt, and 20% sand size. The 'Limits' are: w_{LS} = 11.5%; w_L = 42.2%; w_P = 19.4%; I_P = 23; w_S = 13.4%; and, w_{FE} = 22.1%.

Undisturbed sample.

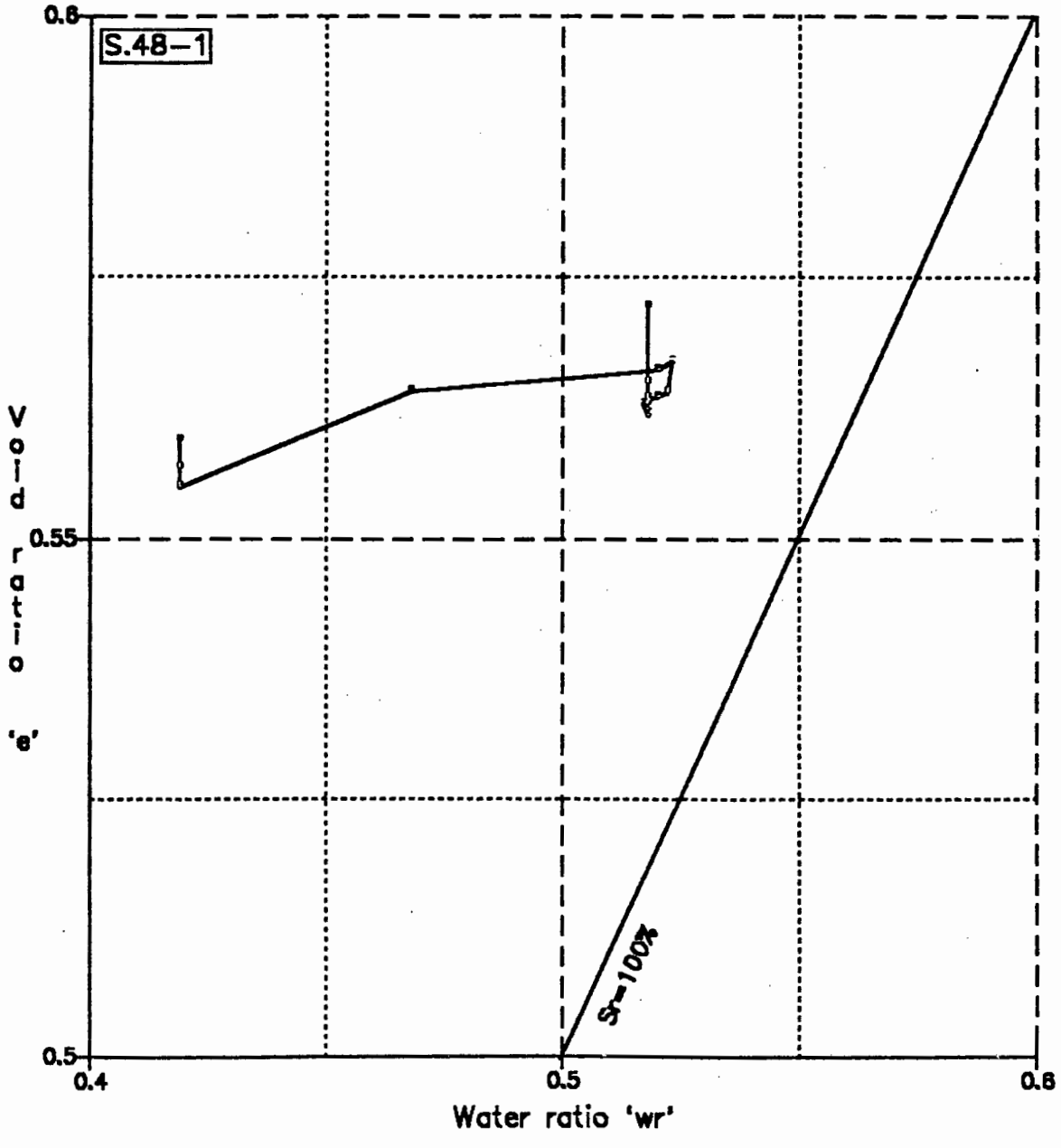

Figure 6.53: Site 48, Lady Grey (Natal) - [100 Kpa during wetting] Relationship between the void ratio 'e' and the water ratio 'wr'. Test by Ballantyne.

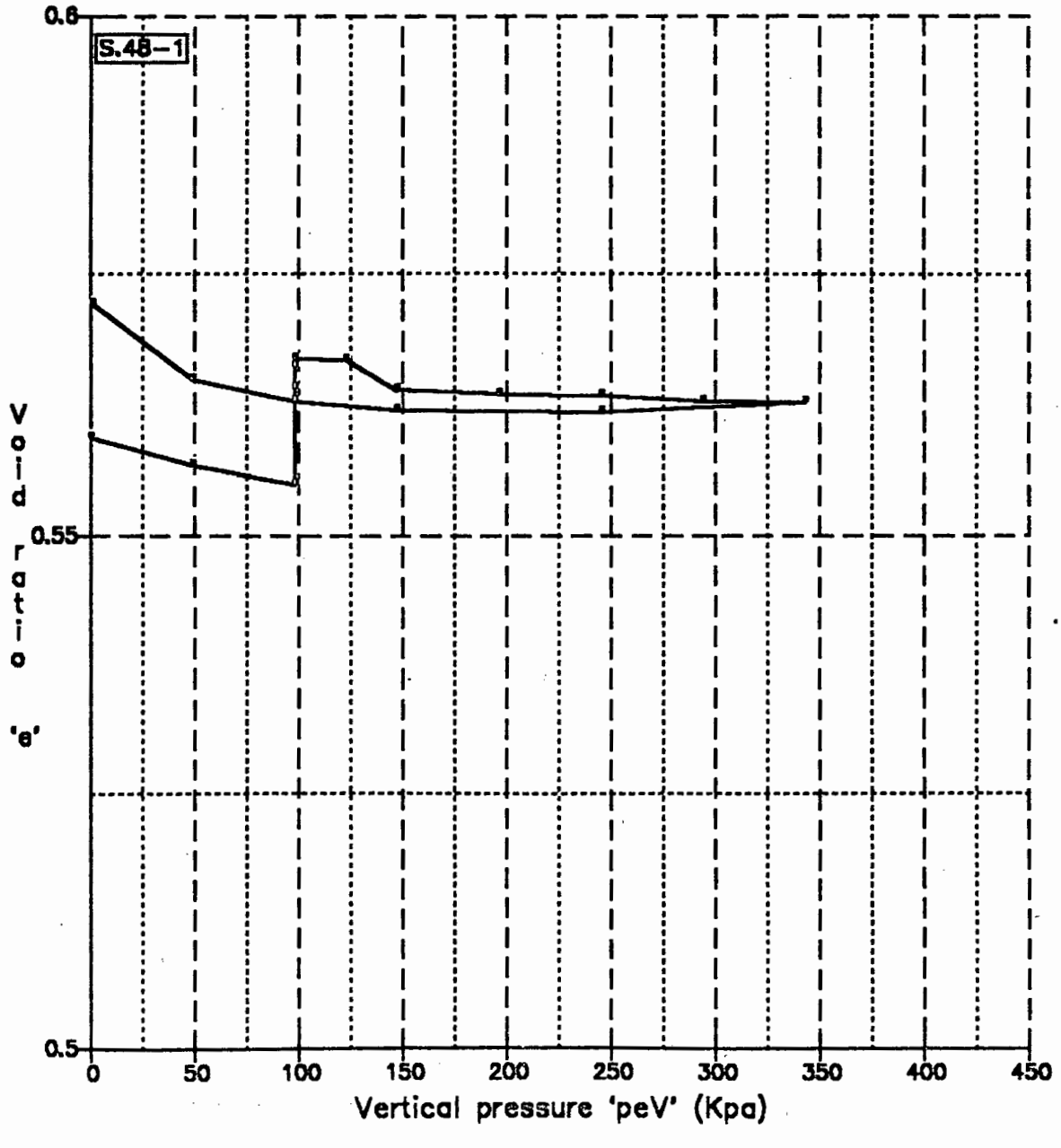

Figure 6.54: Site 48, Lady Grey (Natal) - [100 Kpa during wetting] Relationship between the void ratio 'e' and the effective vertical pressure 'peV'. Test by Ballantyne.

6.8.2 Artificial Soil Types

The relationships for the artificial soils are illustrated in Figures 6.55 to 6.70, as follows:-

Void ratio versus water ratio:

Kaolin K.1 - Figure 6.55 [100 Kpa]; Kaolin K.2 - Figure 6.57 [100 Kpa]; Kaolin K.3 - Figure 6.59 [100 Kpa]; Bentonite B.1 - Figure 6.61 [100 Kpa]; Bentonite B.2 - Figure 6.63 [100 Kpa]; Bentonite B.3 - Figure 6.65 [100 Kpa]; Bentonite B.4 - Figure 6.67 [100 Kpa]; Bentonite B.5 - Figure 6.69 [100 Kpa].

Void ratio versus effective vertical pressure:

Kaolin K.1 - Figure 6.56 [100 Kpa]; Kaolin K.2 - Figure 6.58 [100 Kpa]; Kaolin K.3 - Figure 6.60 [100 Kpa]; Bentonite B.1 - Figure 6.62 [100 Kpa]; Bentonite B.2 - Figure 6.64 [100 Kpa]; Bentonite B.3 - Figure 6.66 [100 Kpa]; Bentonite B.4 - Figure 6.68 [100 Kpa]; Bentonite B.5 - Figure 6.70 [100 Kpa].

This section includes the relationships of the void ratio versus water ratio, and void ratio versus effective pressure, for the following artificial (or made up) soils:

(i) Kaolin clay mixed with sand - K.1 (13% clay size), K.2 (20% clay size), and K.3 (8.5% clay size); and,
(ii) Bentonite clay mixed with sand - B.1 (3.5% clay size), B.2 (7% clay size), B.3 (11.5% clay size), B.4 (15.5% clay size), and B.5 (35% clay size).

One-dimensional consolidation tests (for expansive or collapsing soils) were carried out for the soil samples listed in Table 6.02. Appendix E includes the detailed test procedures and results[1].

---

[1] - *refer to sections E.2 and E.5, respectively.*

Table 6.02: Artificial soils - remoulded samples used for one-dimensional consolidation tests [100 Kpa effective pressure applied in all tests].

Sample No.	Method of Preparation	Free Shrinkage (Ref. number)	Expansion / Collapse (Ref./Consolidometer)
Kaolin K.1			
K.1-2	M1 (≥LL)	III.296	III.353 / test no. 106
K.1-3	M1 (<LL)	III.298	III.359 / test no. 108
Kaolin K.2			
K.2-2	M1 (≥LL)	III.313	III.361 / test no. 109
K.2-3	M1 (<LL)	III.315	III.367 / test no. 112
Kaolin K.3			
K.3-2	M1 (≥LL)	III.325	III.369 / test no. 113
K.3-3	M1 (<LL)	III.327	III.375 / test no. 116
Bentonite B.1			
B.1-2	M1 (<LL)	III.338	III.377 / test no. 117
B.1-3	M2 (*)	III.340	III.383 / test no. 120
B.1-4	M1A	III.342	III.399 / test no. 128
B.1-5	M2 (*)	III.362	III.410 / test no. 134
Bentonite B.2			
B.2-2	M1 (<LL)	III.368	IV. 417 / test no. 139
B.2-3	M2 (*)	III.370	IV. 415 / test no. 138
B.2-4	M1A	III.372	IV. 419 / test no. 141
Bentonite B.3			
B.3-2	M1 (<LL)	IV. 432L	IV. 445 / test no. 160
B.3-3	M2 (*)	IV. 432R	IV. 444 / test no. 159
B.3-4	M1A	IV. 433L	IV. 448 / test no. 161
Bentonite B.4			
B.4-2	M1 (<LL)	III.398	IV. 434 / test no. 151
B.4-3	M2 (*)	III.400	IV. 435 / test no. 152
B.4-4	M1A	III.405	IV. 428 / test no. 148
Bentonite B.5			
B.5-2	M1 (<LL)	IV. 446L	IV.448A / test no. 162
B.5-3	M2 (*)	IV. 446R	IV. 456 / test no. 166
B.5-4	M1A	IV. 447L	IV. 461 / test no. 171

** - air bubbles.*

Kaolin clay mixed with sand:-

Kaolin K.1.

A clayey sand (fine to medium size) with a very small amount of silt. The soil consists of 13% clay, 3.5% silt and 83.5% sand size. The 'Limits' of the soil are: w_{LS} = 0.4%; w_L = 12.3%; w_P = 11.8%; I_P = 1; w_S = 10.0%; and w_{FE} = 12.3%.

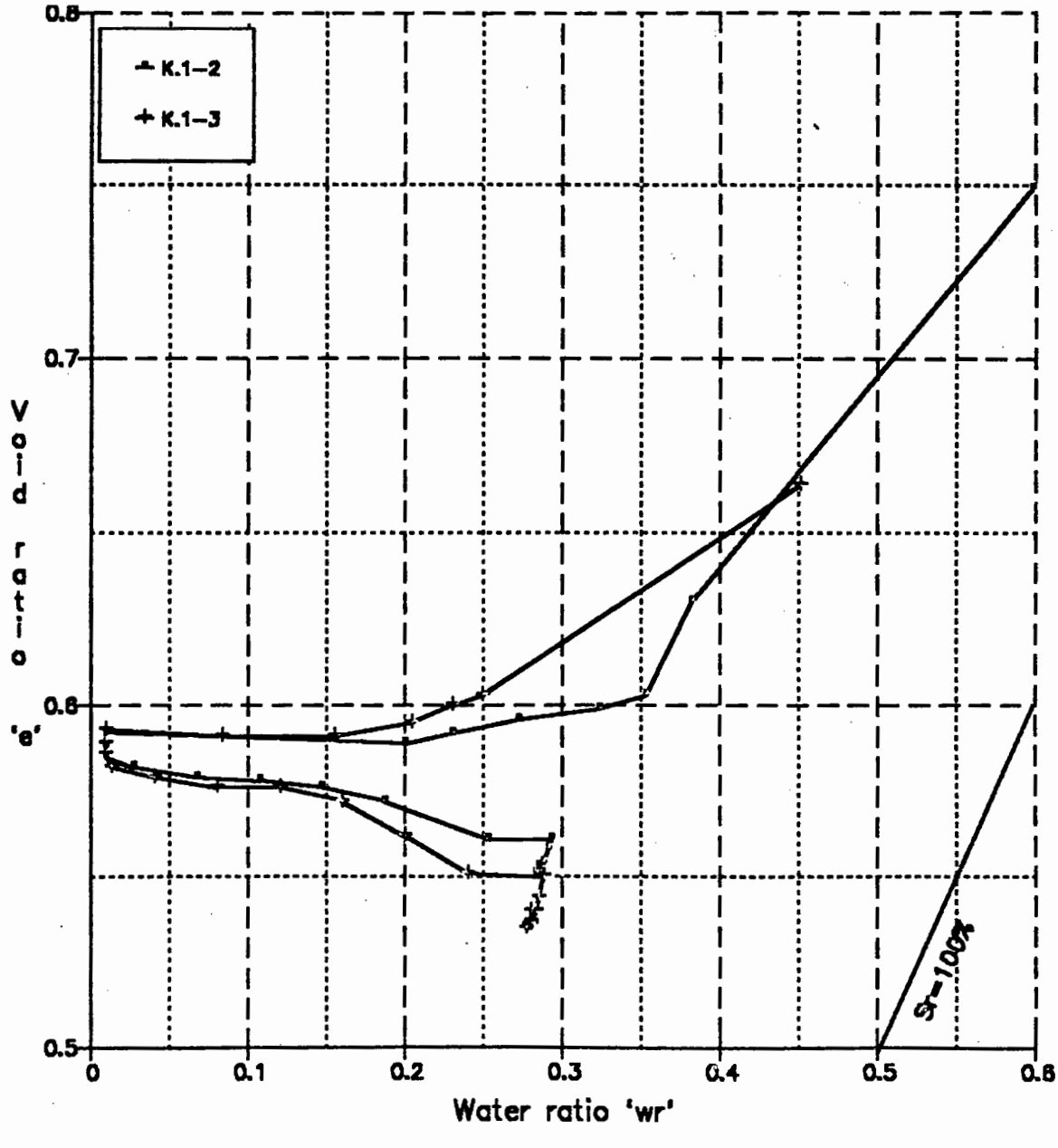

Figure 6.55: Kaolin K.1 (13% clay size) - [100 Kpa during wetting] Relationship between the void ratio 'e' and the water ratio 'wr'. Read in conjunction with Figure 6.56.

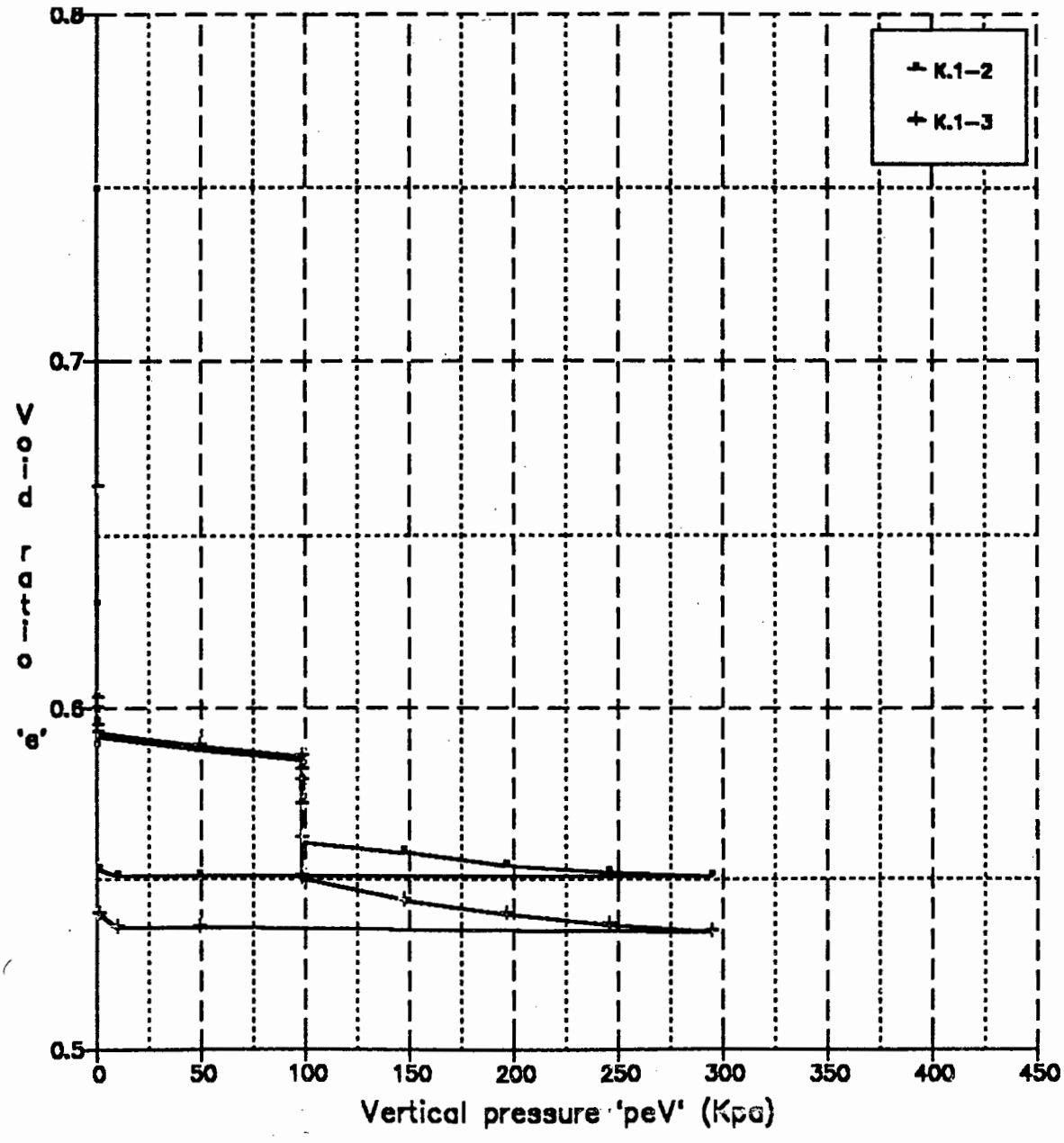

Figure 6.56: Kaolin K.1 (13% clay size) - [100 Kpa during wetting] Relationship between the void ratio 'e' and the effective vertical pressure (or stress) 'peV'.

Kaolin K.2.
A clayey sand (fine to medium size), with a small amount of silt. The soil consists of 20% clay, 65% silt, and 73.3% sand size. The 'Limits' of the soil are: w_{LS} = 1.5%; w_L = 14.0%; w_P = 10.4%; I_P = 4; w_S = 12.0%; and w_{FE} = 12.0%.

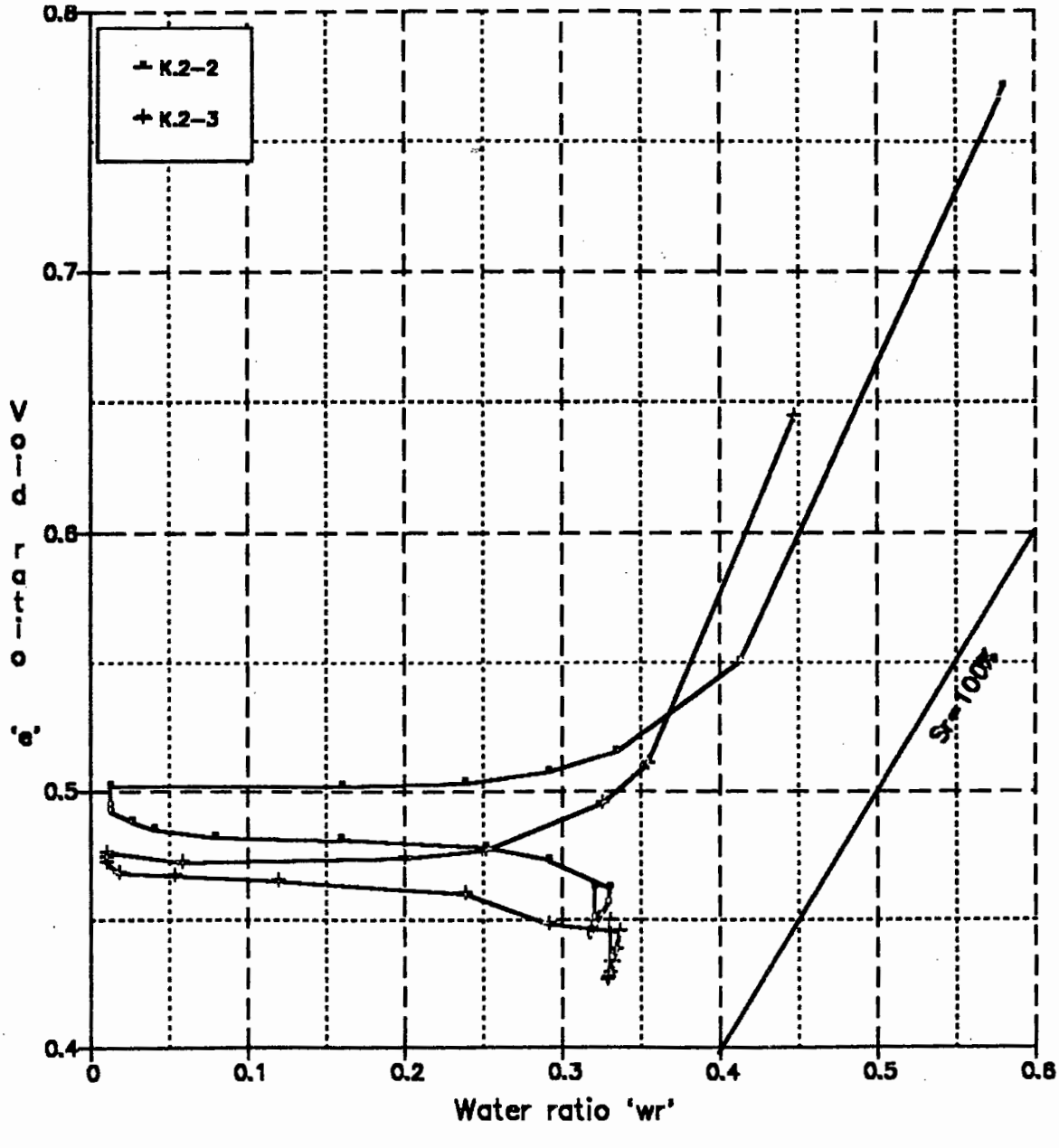

Figure 6.57: Kaolin K.2 (20% clay size) - [100 Kpa during wetting] Relationship between the void ratio 'e' and the water ratio 'wr'.

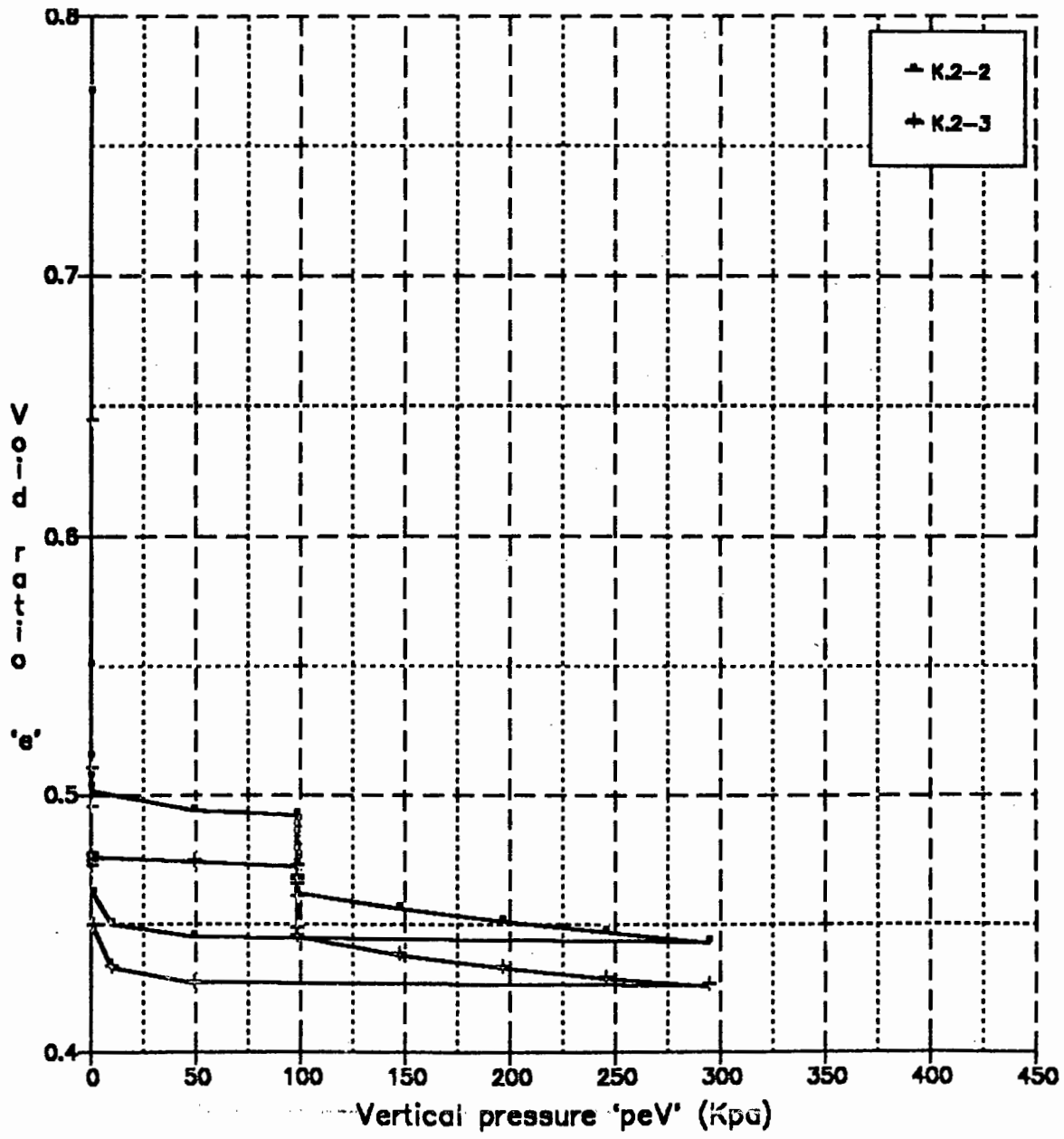

Figure 6.58: Kaolin K.2 (20% clay size) - [100 Kpa during wetting] Relationship between the void ratio 'e' and the effective vertical pressure (or stress) 'peV'.

Kaolin K.3.

A fine to medium sand containing a small amount of clay and very small amount of silt. The soil consists of 8.5% clay, 2.5% silt and 89% sand size. The 'Limits' of the soil are: w_{Ls} = 0.0%; w_L = NP; I_p = NP; w_S = 9.0%; and w_{FE} = 11.0%.

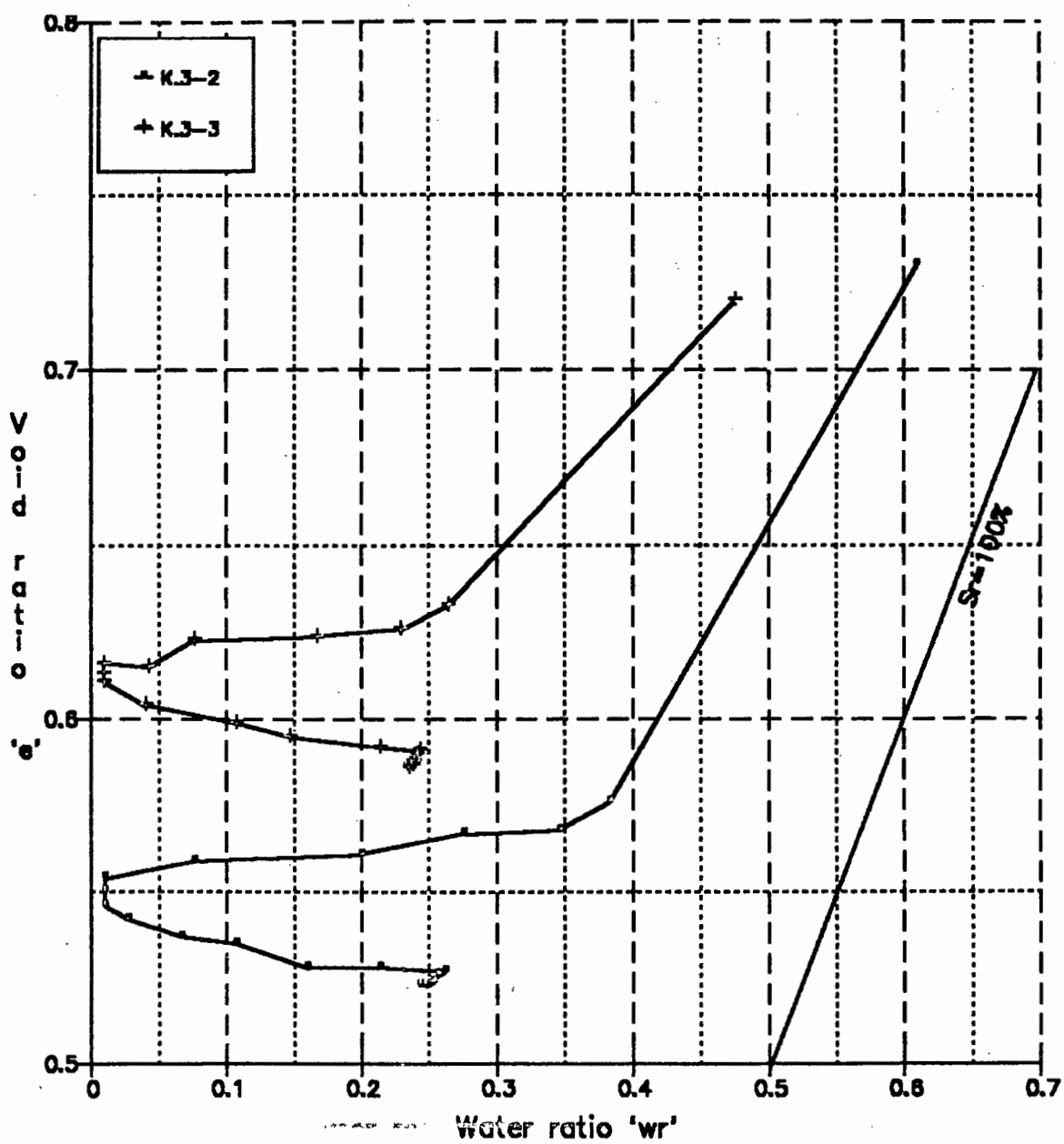

Figure 6.59: Kaolin K.3 (8.5% clay size) - [100 Kpa during wetting] Relationship between the void ratio 'e' and the water ratio 'wr'.

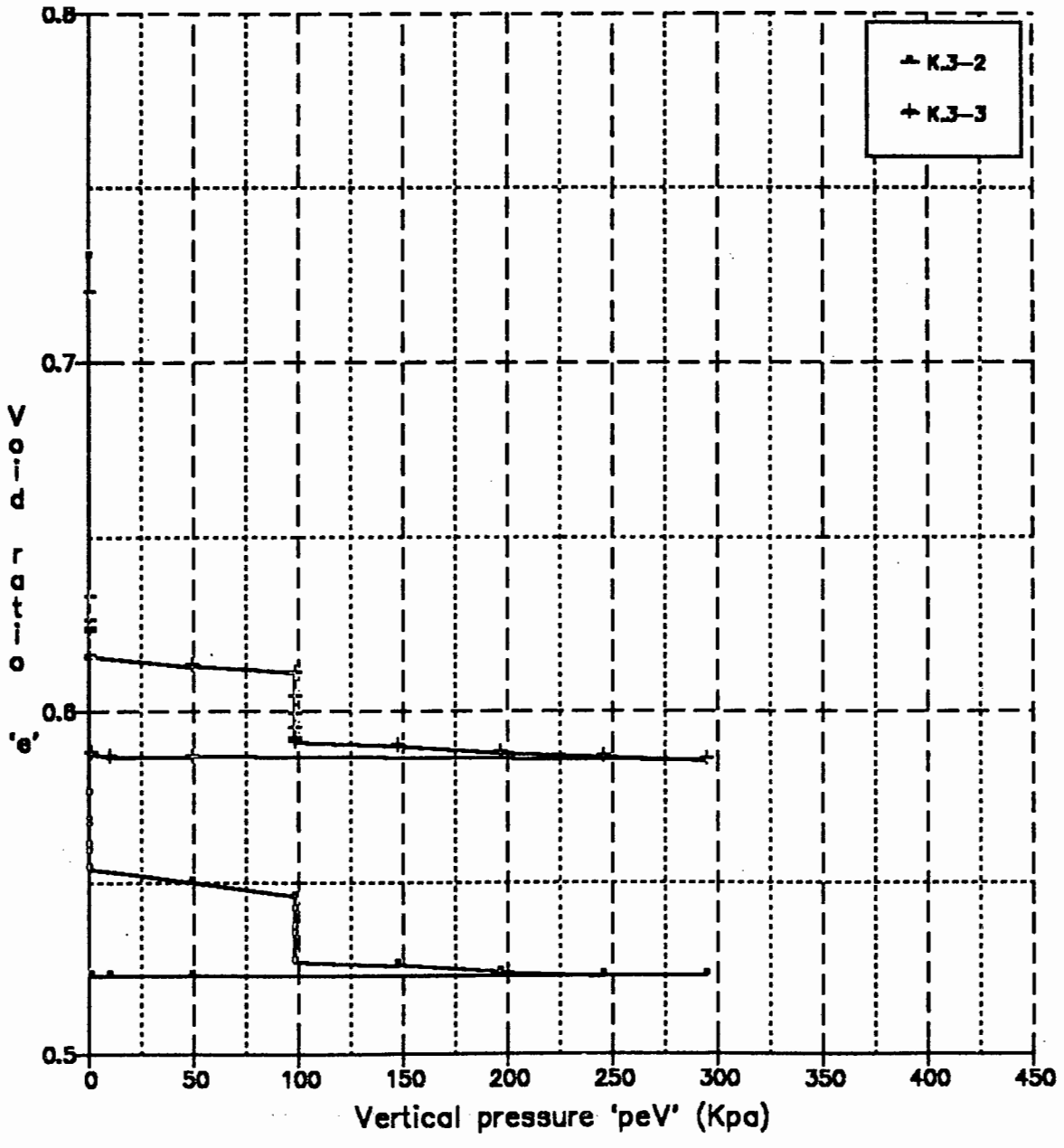

Figure 6.60: Kaolin K.3 (8.5% clay size) - [100 Kpa during wetting] Relationship between the void ratio 'e' and the effective vertical pressure (or stress) 'peV'.

Bentonite clay mixed with sand:-

Bentonite B.1.

A fine to medium sand with a very small amount of clay and silt. The soil consists of 3.5% clay, 1.5% silt, and 95% sand size. The 'Limits' of the soil are: w_{LS} = 0.1%; w_L = 21.0%; w_P = 20.0%; I_P = 1; w_S = 14.5%; and w_{FE} = 17.4%.

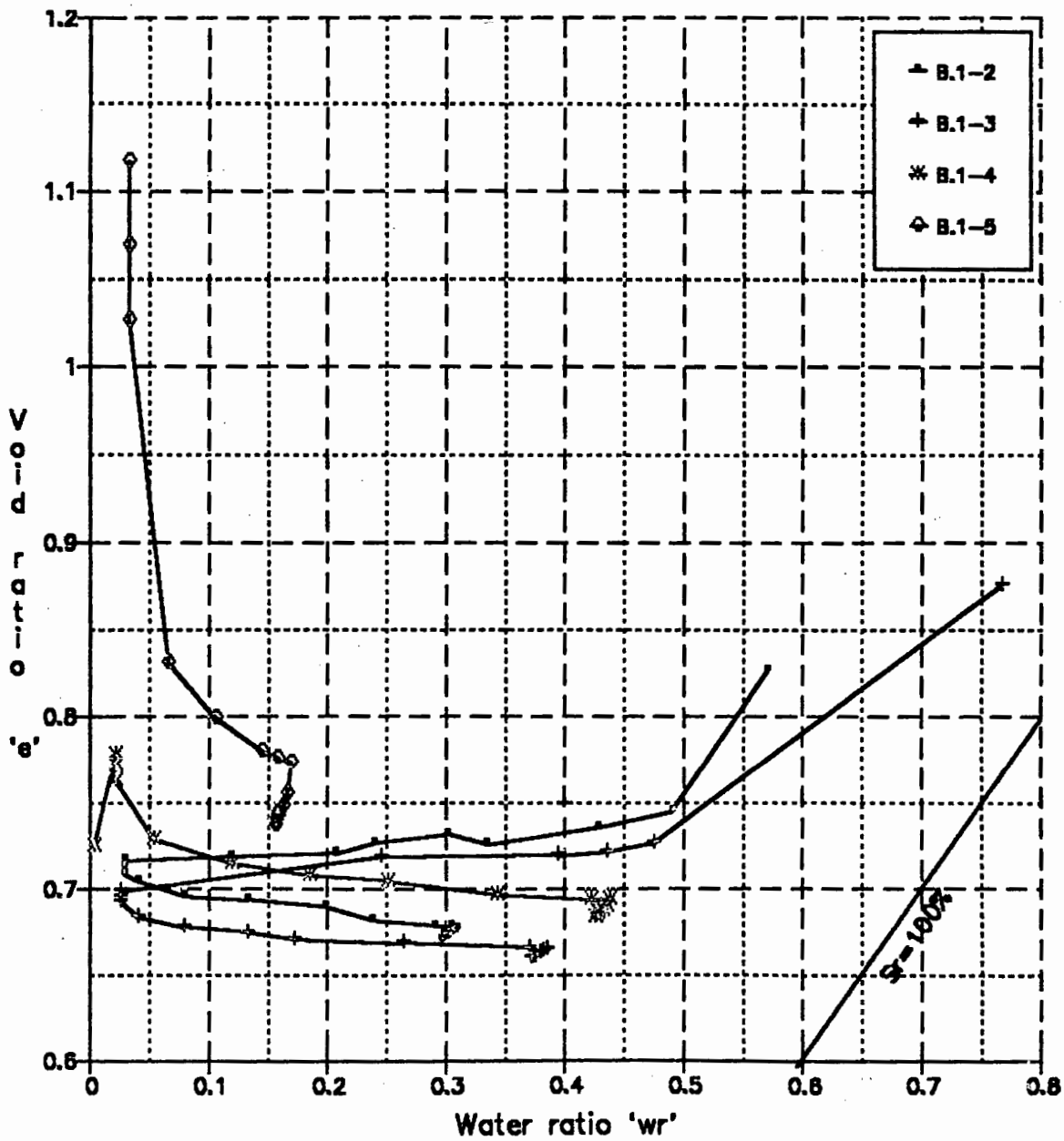

Figure 6.61: Bentonite B.1 (3.5% clay size) - [100 Kpa during wetting] Relationship between the void ratio 'e' and the water ratio 'wr'. Read in conjunction with Figure 6.62.

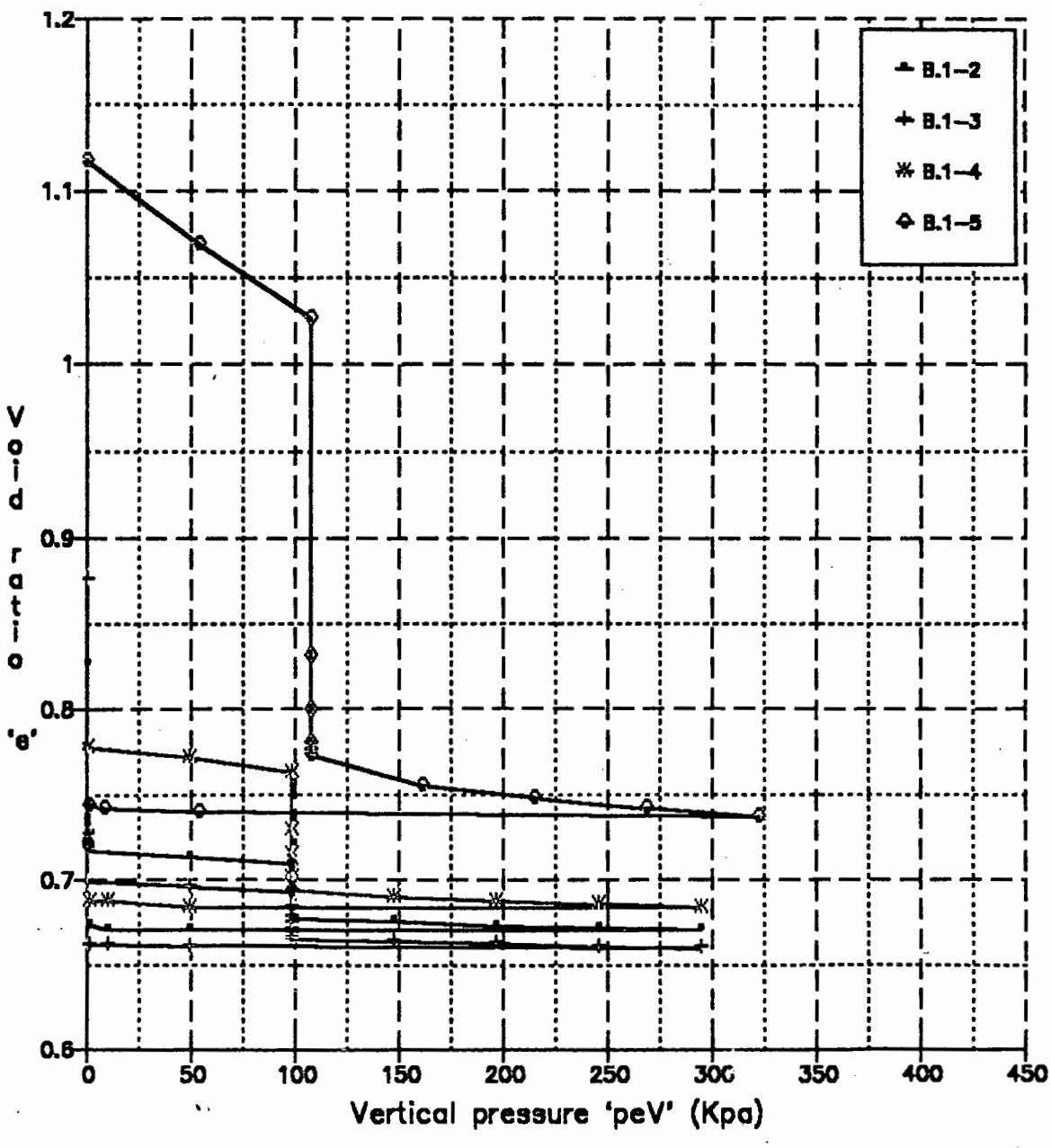

Figure 6.62: Bentonite B.1 (3.5% clay size) - [100 Kpa during wetting] Relationship between the void ratio 'e' and the effective vertical pressure (or stress) 'peV'.

Bentonite B.2.

A fine to medium sand with a small amount of clay and silt (very small). The soil consists of 7% clay, 2% silt and 91% sand size. The 'Limits' are: w_{Ls} = 0.5%; w_L = 32.0%; w_P = 21.0%; I_P = 11; w_S = 26.0%; and w_{FE} = 29.8%.

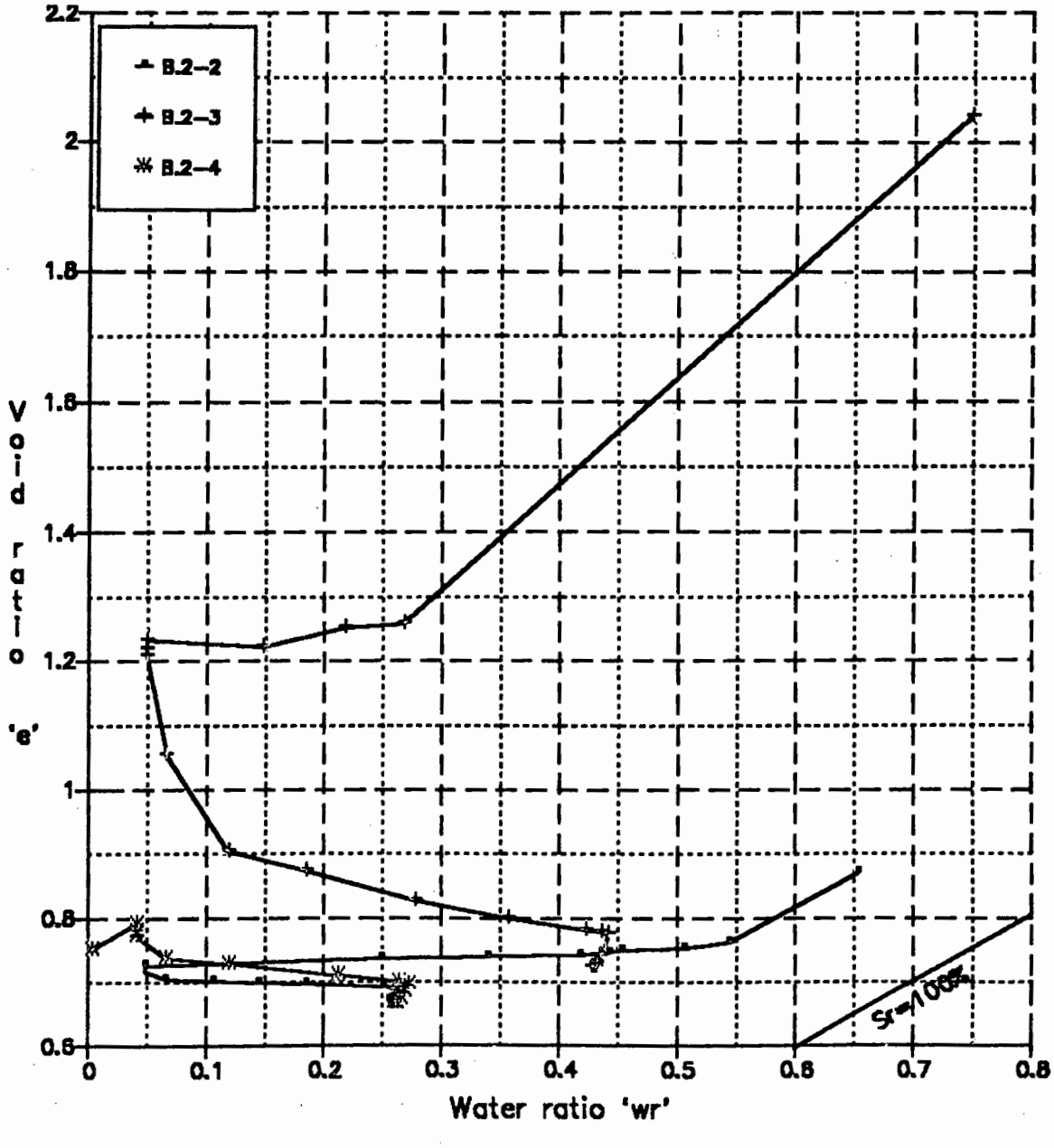

Figure 6.63: Bentonite B.2 (7% clay size) - [100 Kpa during wetting] Relationship between the void ratio 'e' and the water ratio 'wr'.

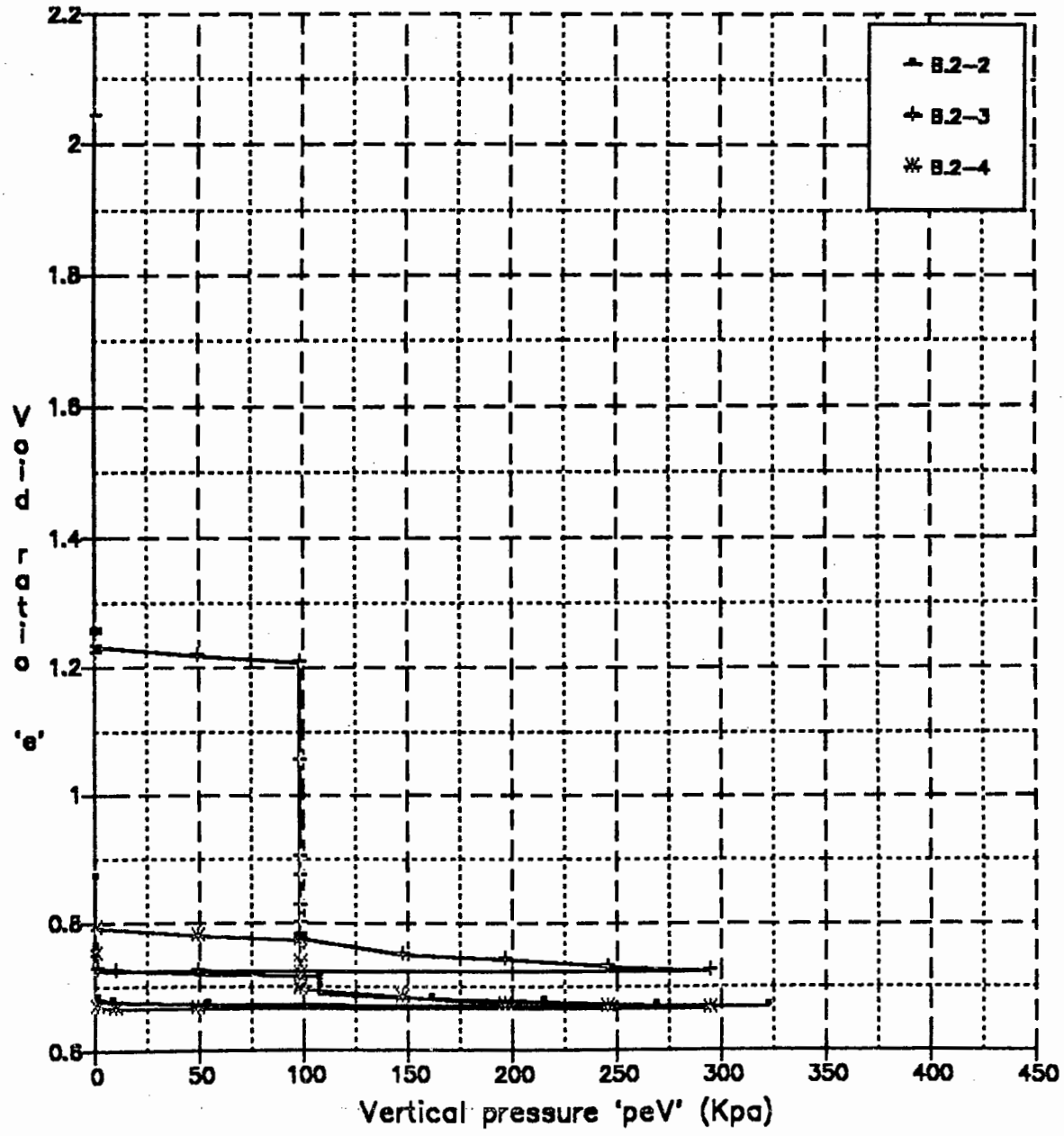

Figure 6.64: Bentonite B.2 (7% clay size) - [100 Kpa during wetting] Relationship between the void ratio 'e' and the effective vertical pressure (or stress) 'peV'.

Bentonite B.3.

A clayey sand (fine to medium size) with a very small amount of silt. The soil consists of 11.5% clay, 2% silt and 86.5% sand size. The 'Limits' are: w_{Ls} = 1.0%; w_L = 46.0%; w_P = 20.0%; I_P = 26; w_S = 28.0%; and, w_{FE} = 46.1%.

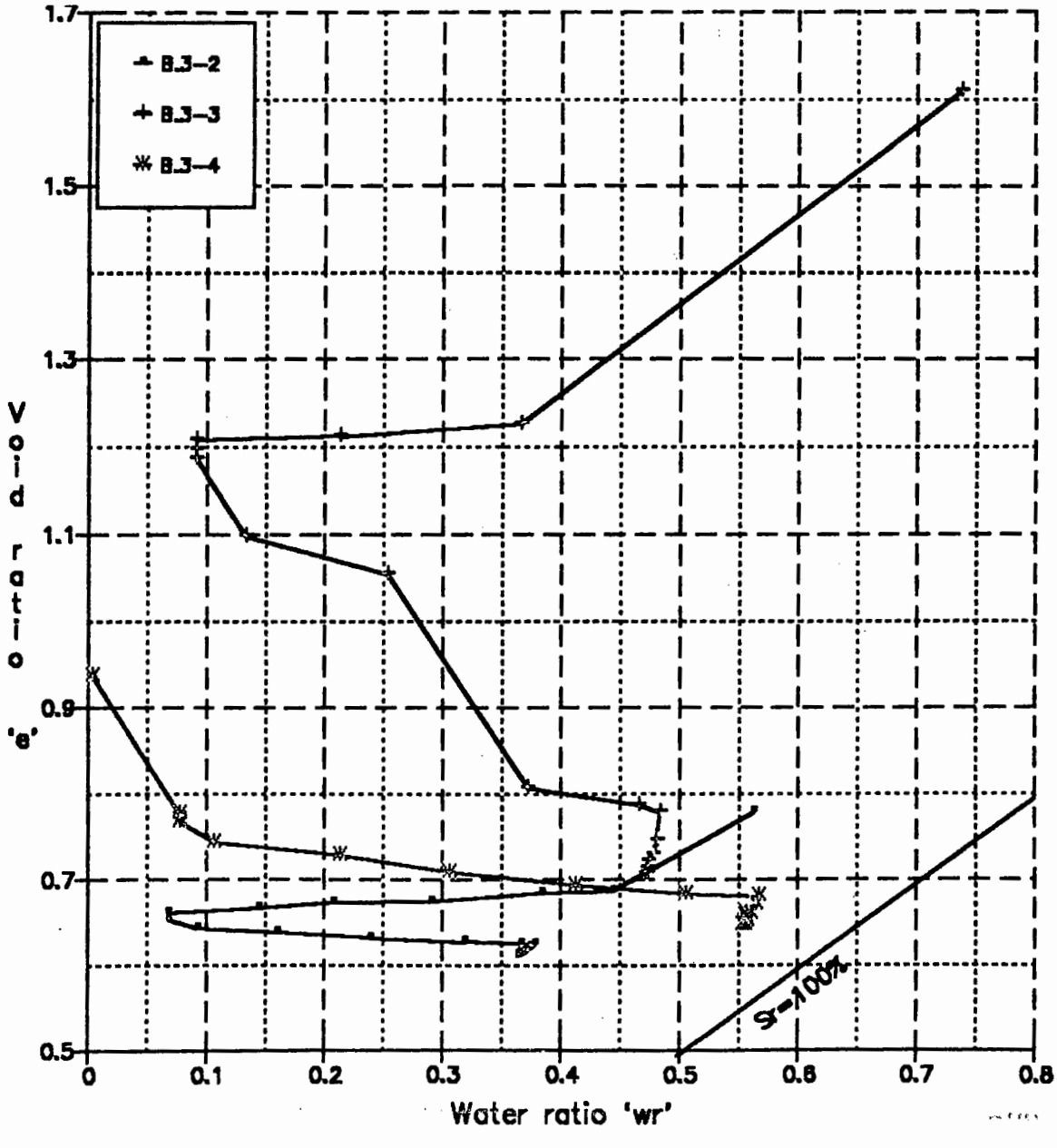

Figure 6.65: Bentonite B.3 (11.5% clay size) - [100 Kpa during wetting] Relationship between the void ratio 'e' and the water ratio 'wr'.

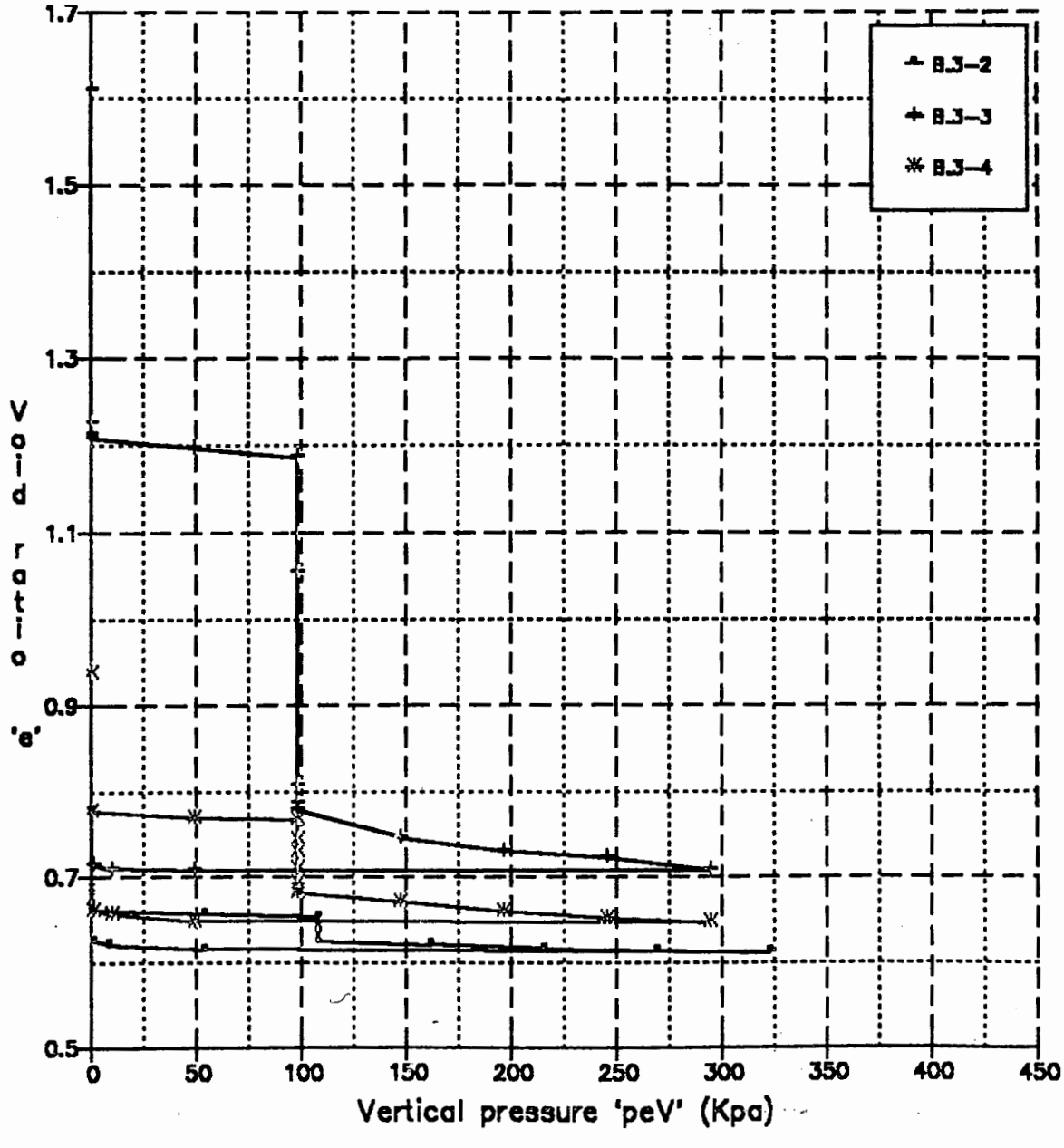

Figure 6.66: Bentonite B.3 (11.5% clay size) - [100 Kpa during wetting] Relationship between the void ratio 'e' and the effective vertical pressure (or stress) 'peV'.

Bentonite B.4.

A clayey sand (fine to medium size) with a very small amount of silt. The soil consists of 15.5% clay, 3% silt and 81.5% sand size. The 'Limits' are: w_{LS} = 1.5%; w_L = 59.0%; w_P = 19.0%; I_P = 40; w_S = 34.0%; and w_{FE} = 57.3%.

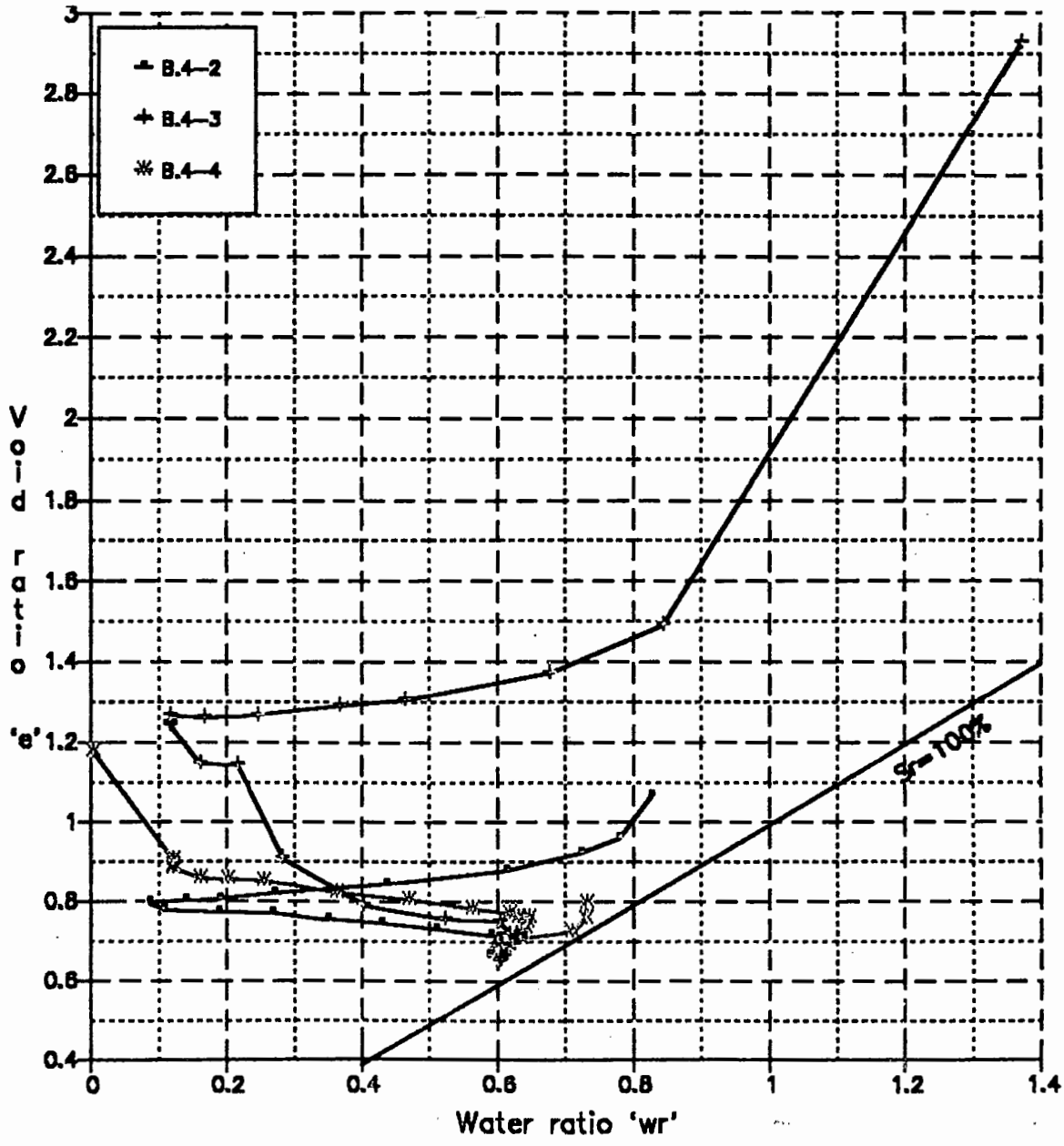

Figure 6.67: Bentonite B.4 (15.5% clay size) - [100 Kpa during wetting] Relationship between the void ratio 'e' and the water ratio 'wr'.

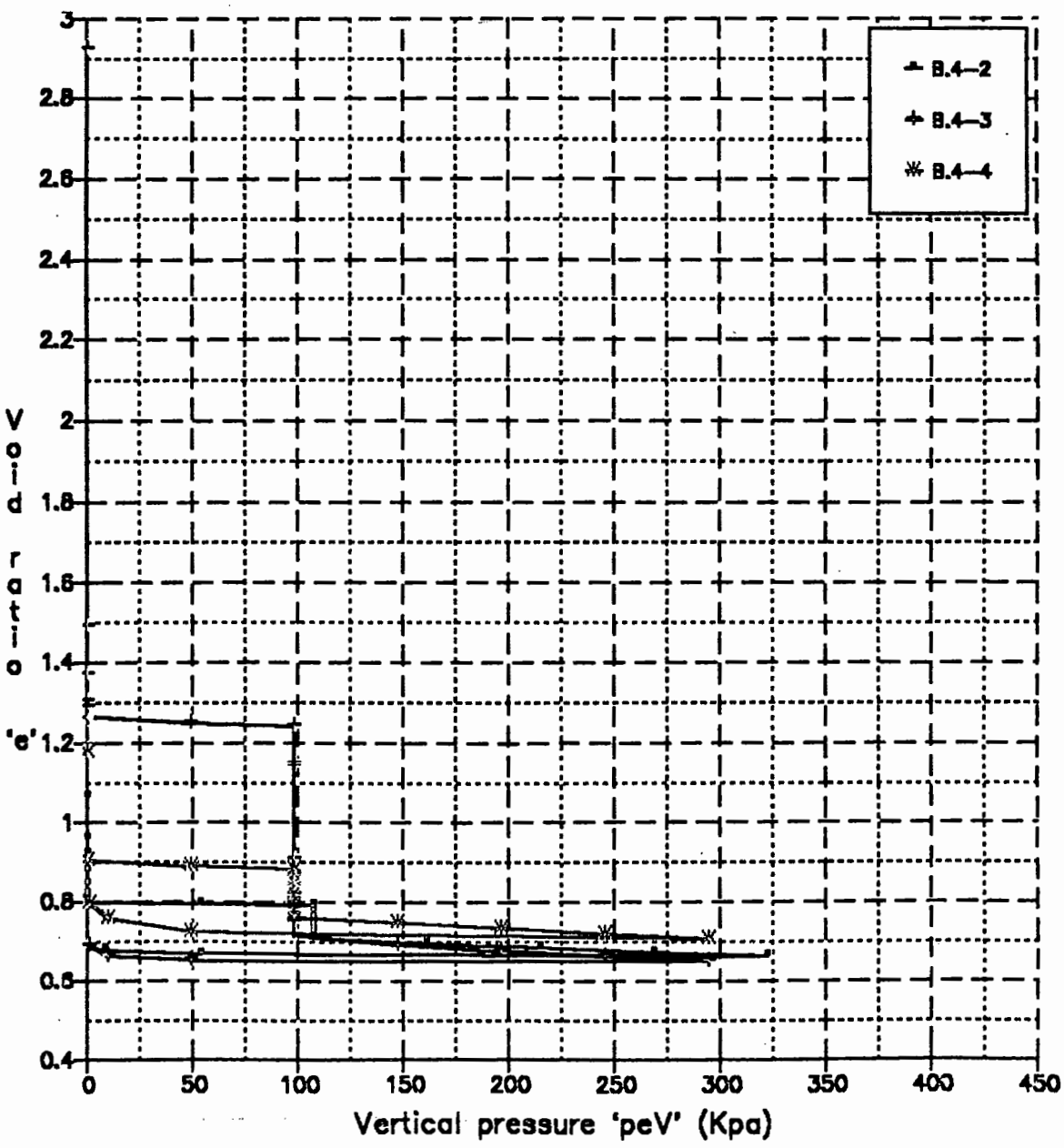

Figure 6.68: Bentonite B.4 (15.5% clay size) - [100 Kpa during wetting] Relationship between the void ratio 'e' and the effective vertical pressure (or stress) 'peV'.

Bentonite B.5.

A clayey sand (fine to medium), with a very small amount of silt. The soil consists of 35% clay, 4% silt, and 61% sand size. The 'Limits' are: w_{LS} = 6.5%; w_L = 133.0%; w_P = 21.0%; I_P = 112; w_S = 38.0%; and, w_{FE} = 100.2%.

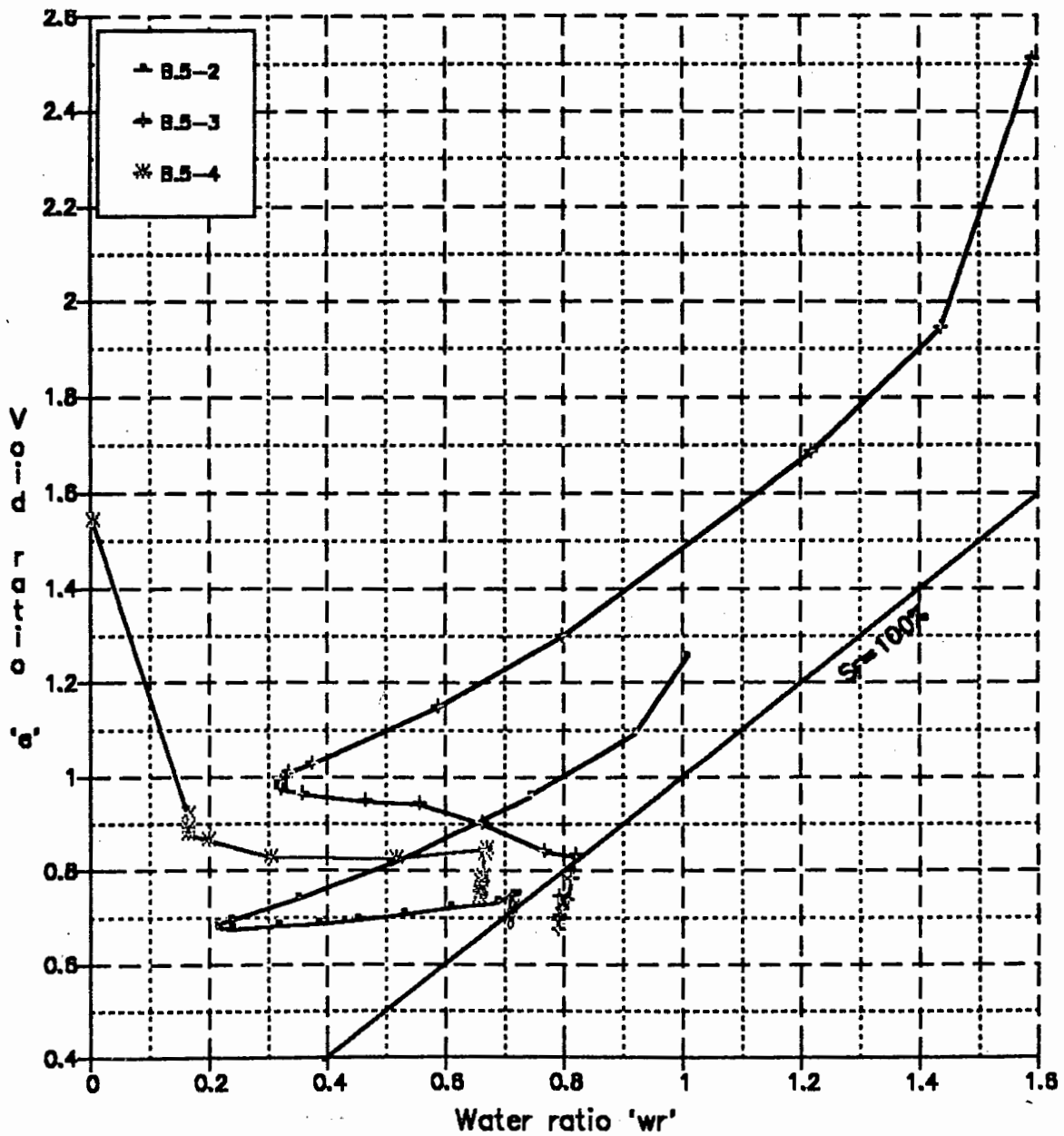

Figure 6.69: Bentonite B.5 (35% clay size) - [100 Kpa during wetting] Relationship between the void ratio 'e' and the water ratio 'wr'.

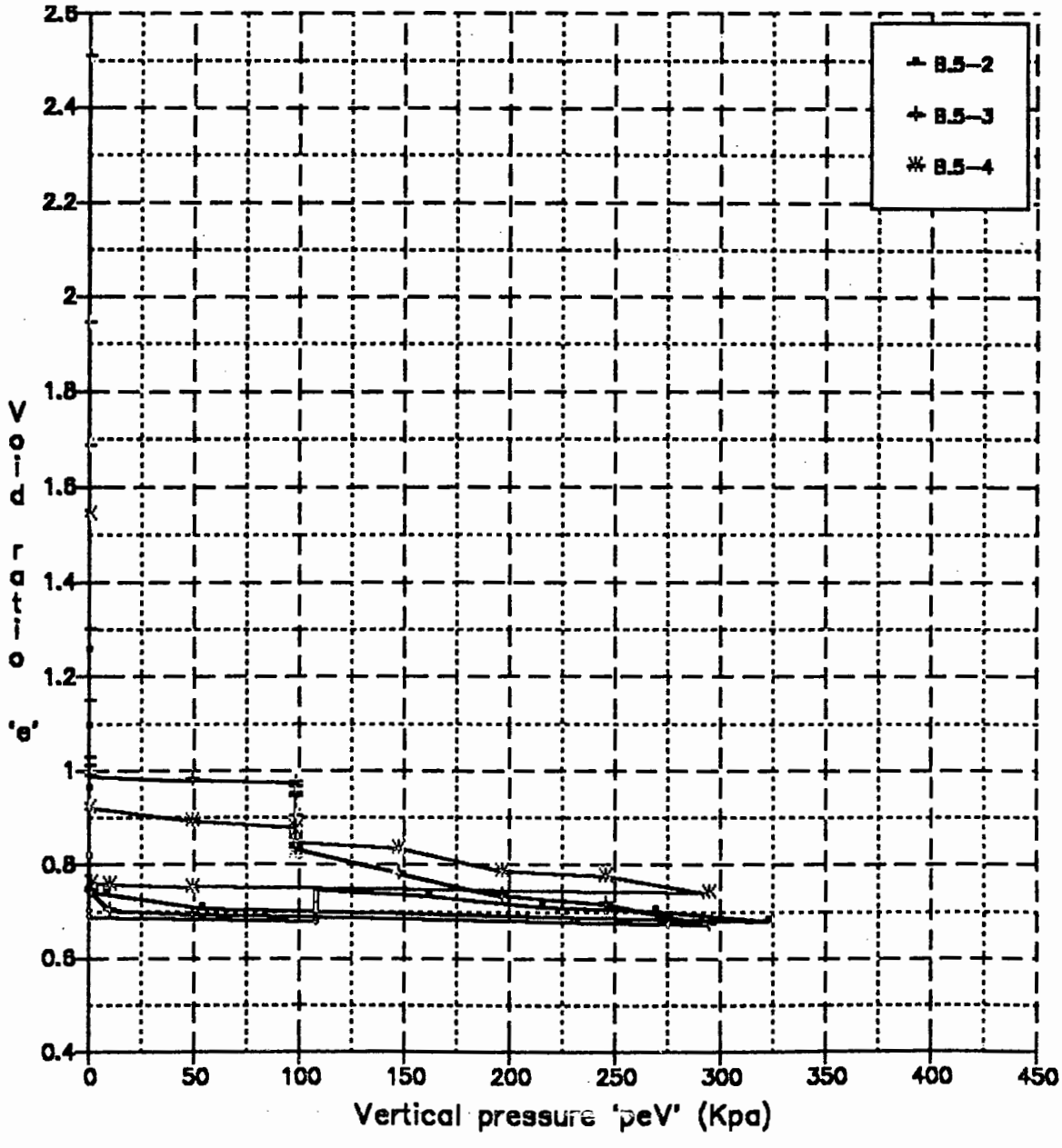

Figure 6.70: Bentonite B.5 (35% clay size) - [100 Kpa during wetting] Relationship between the void ratio 'e' and the effective vertical pressure (or stress) 'peV'.

6.9 ANALYSIS OF TEST RESULTS

The test results and their inter-relationships are analysed in two parts:

1) Stress Scales - superimposition of stress scales on the plots of 'Void Ratio' versus 'Water Ratio'; and,

2) 'Void Ratio' versus 'Effective Vertical Pressure' versus 'Water Ratio'.

These relationships are illustrated in Figures 6.71 to 6.129, as follows:

Figures 6.71 to 6.95 - Void ratio versus water ratio[1], includes the stress scales obtained in chapter five; and,

Figures 6.96 to 6.129 - Void ratio versus effective vertical pressure versus water ratio for the full test path[2].

---

1 - for each applied pressure.
2 - three dimensional plots.

6.9.1 Stress Scales: Void Ratio versus Water Ratio.

Natural Soil Types: Site 11, Rosebank.

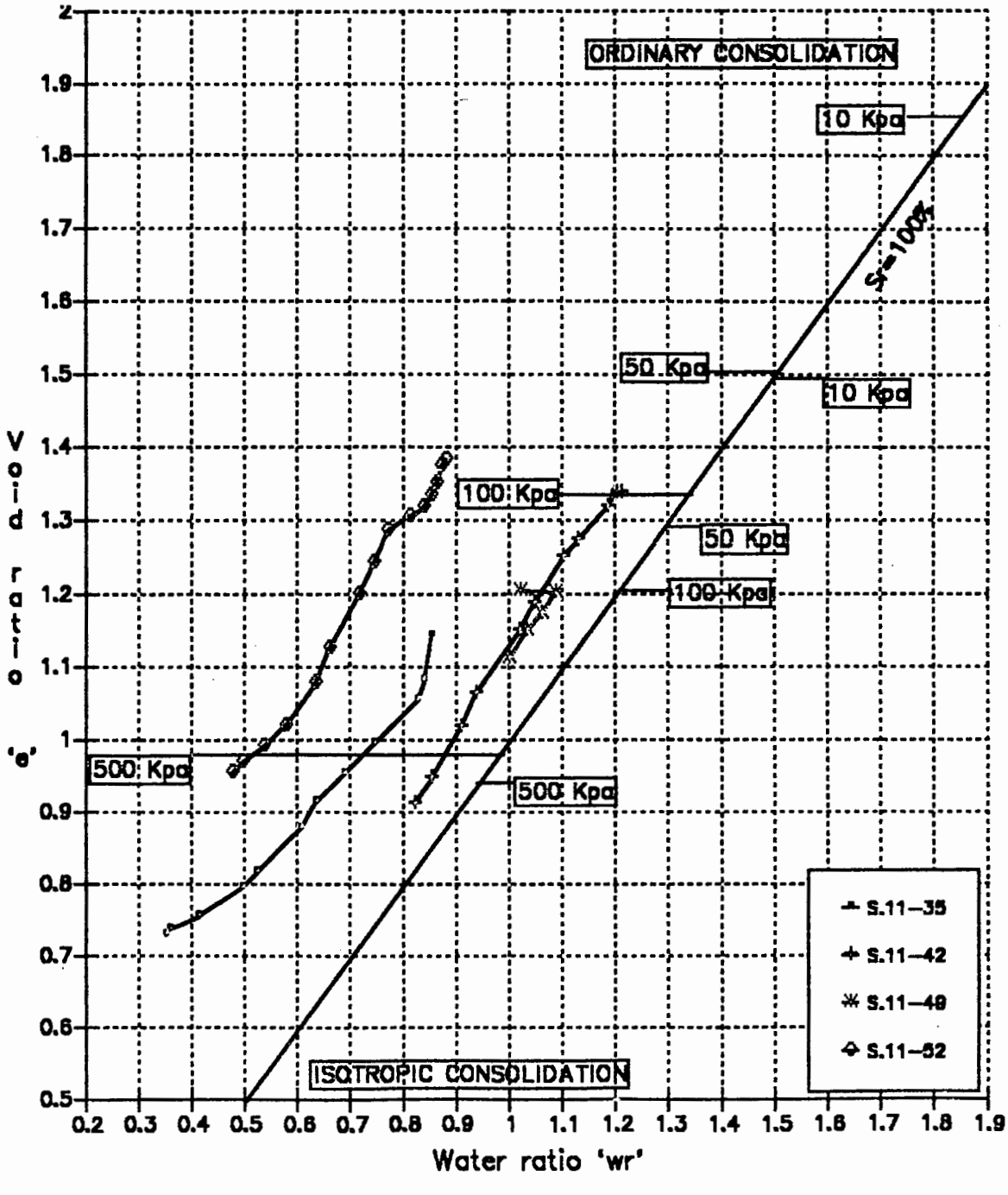

Figure 6.71: Site 11, Rosebank [Remoulded] - Void ratio 'e' versus water ratio 'wr'.
Volume change, due to wetting, shown while carrying 1 Kpa only. Scales are from other tests (Chapter 5) .

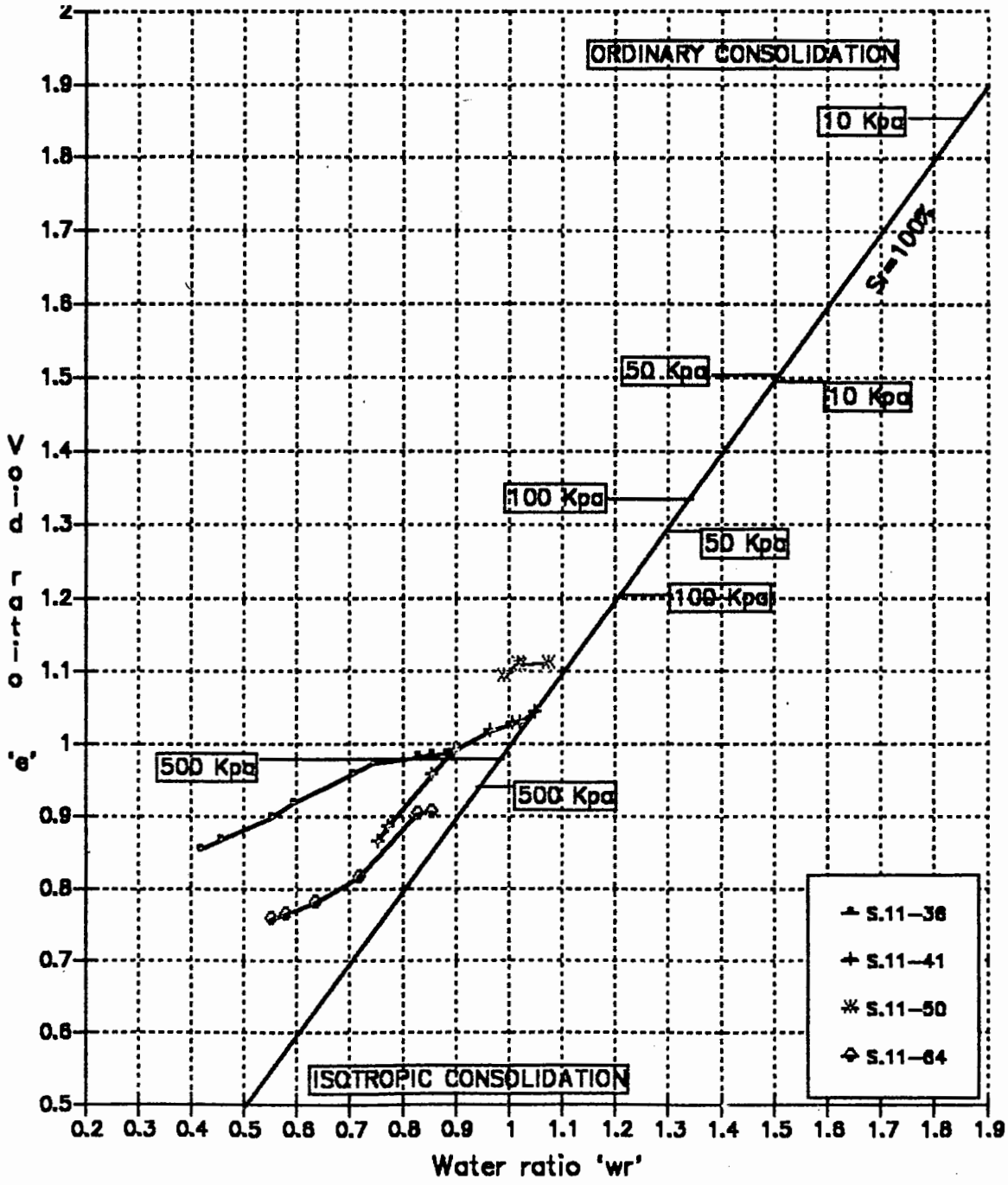

Figure 6.72: Site 11, Rosebank [Remoulded] - Void ratio 'e' versus water ratio 'wr'.
Volume change, due to wetting, shown while carrying 50 Kpa only. Scales are from other tests (Chapter 5) .

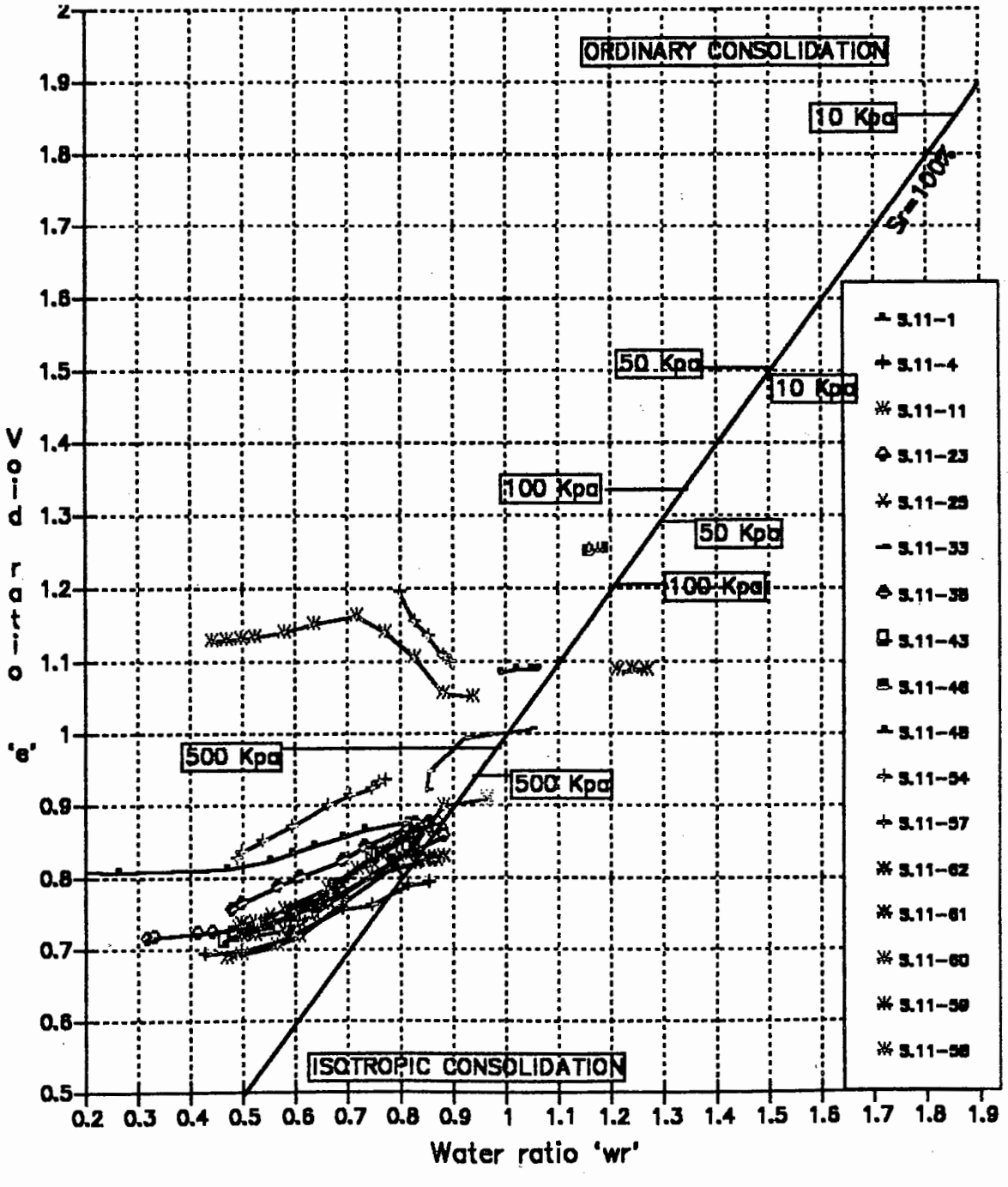

Figure 6.73: Site 11, Rosebank [Remoulded] - Void ratio 'e' versus water ratio 'wr'.
Volume change, due to wetting, shown while carrying 100 Kpa only. Scales are from other tests (Chapter 5) .

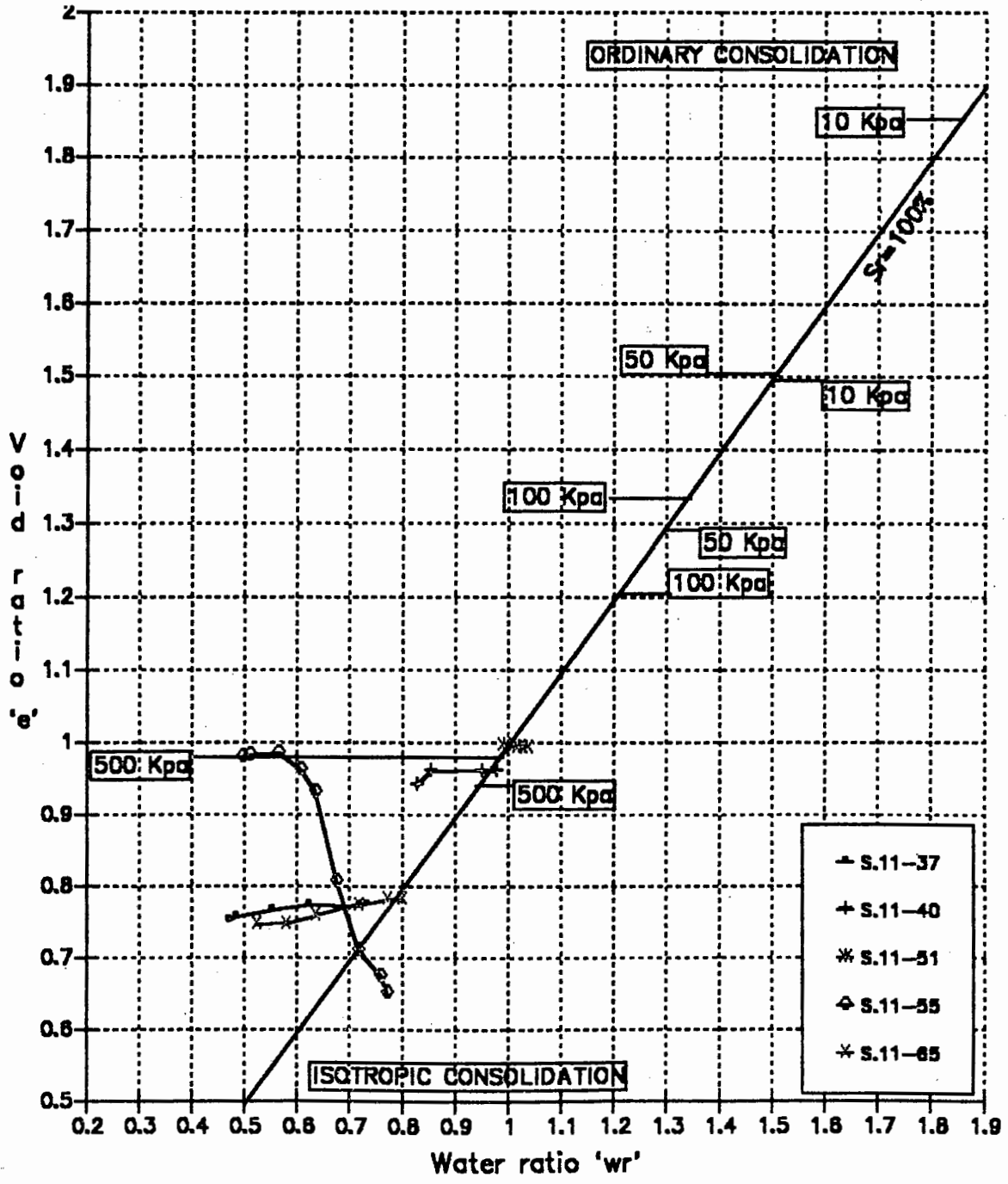

Figure 6.74: Site 11, Rosebank [Remoulded] - Void ratio 'e' versus water ratio 'wr'.
Volume change, due to wetting, shown while carrying 400 Kpa only. Scales are from other tests (Chapter 5) .

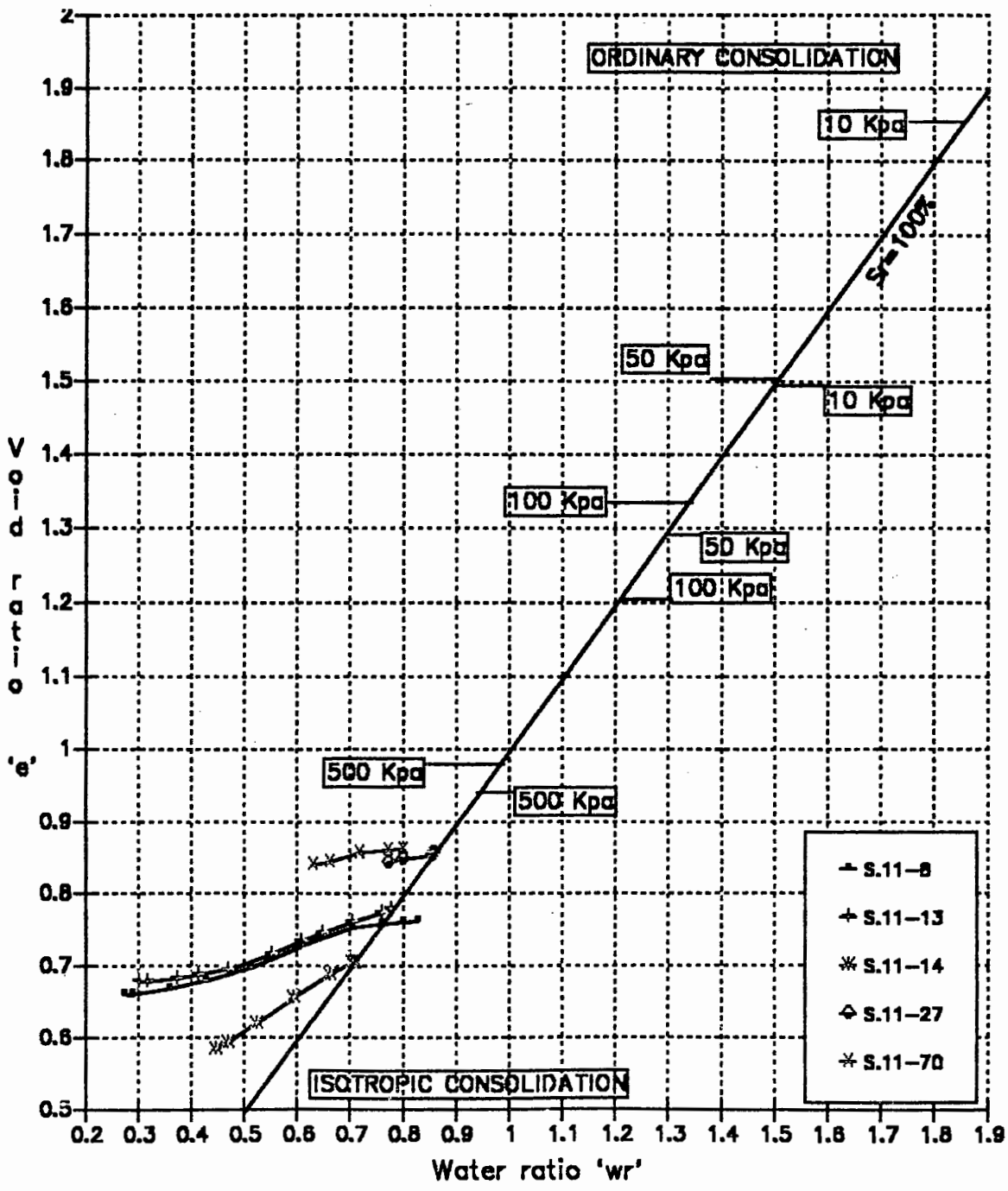

Figure 6.75: Site 11, Rosebank [Compacted] - Void ratio 'e' versus water ratio 'wr'.
Volume change, due to wetting, shown while carrying 100 Kpa only. Scales are from other tests (Chapter 5) .

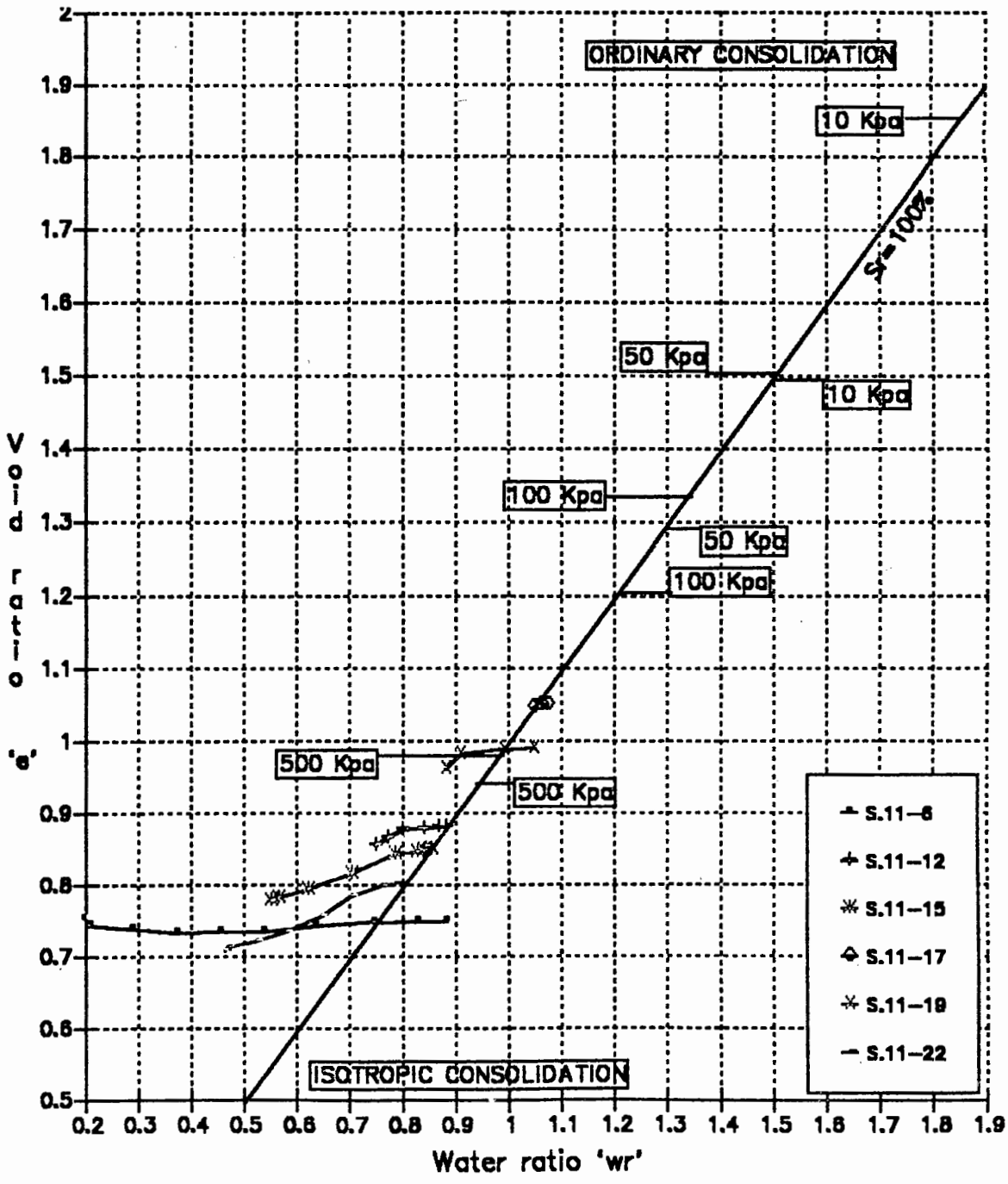

Figure 6.76: Site 11, Rosebank [Undisturbed] - Void ratio 'e' versus water ratio 'wr'.
Volume change, due to wetting, shown while carrying 100 Kpa only. Scales are from other tests (Chapter 5) .

Site 36, Rondebosch.

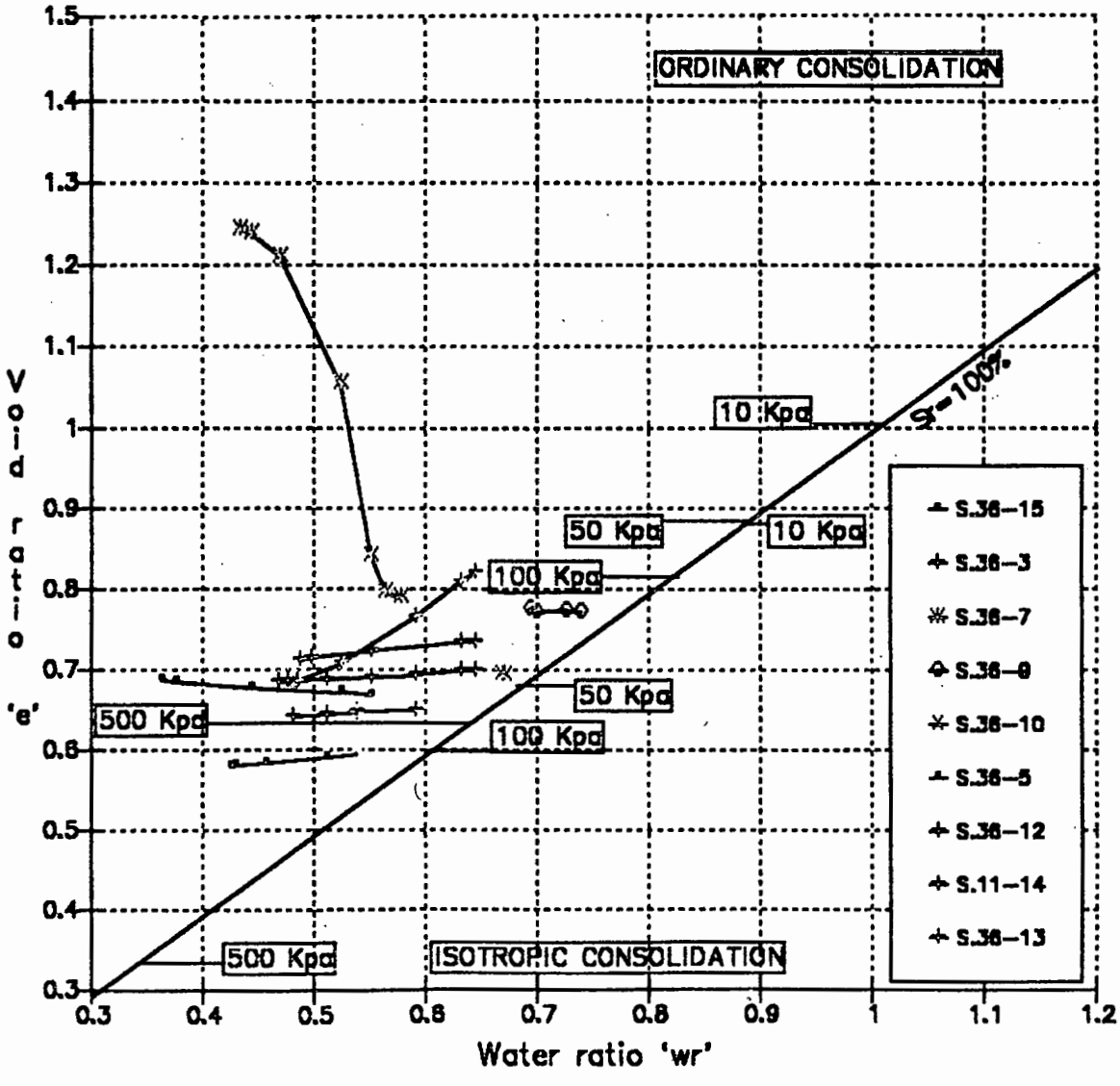

Figure 6.77: Site 36, Rondebosch [Remoulded] - Void ratio 'e' versus water ratio 'wr'. Volume change due to wetting shown while carrying 1 Kpa, 50 Kpa, 100 Kpa, and 400 Kpa. Scales are from other tests (Chapter 5).

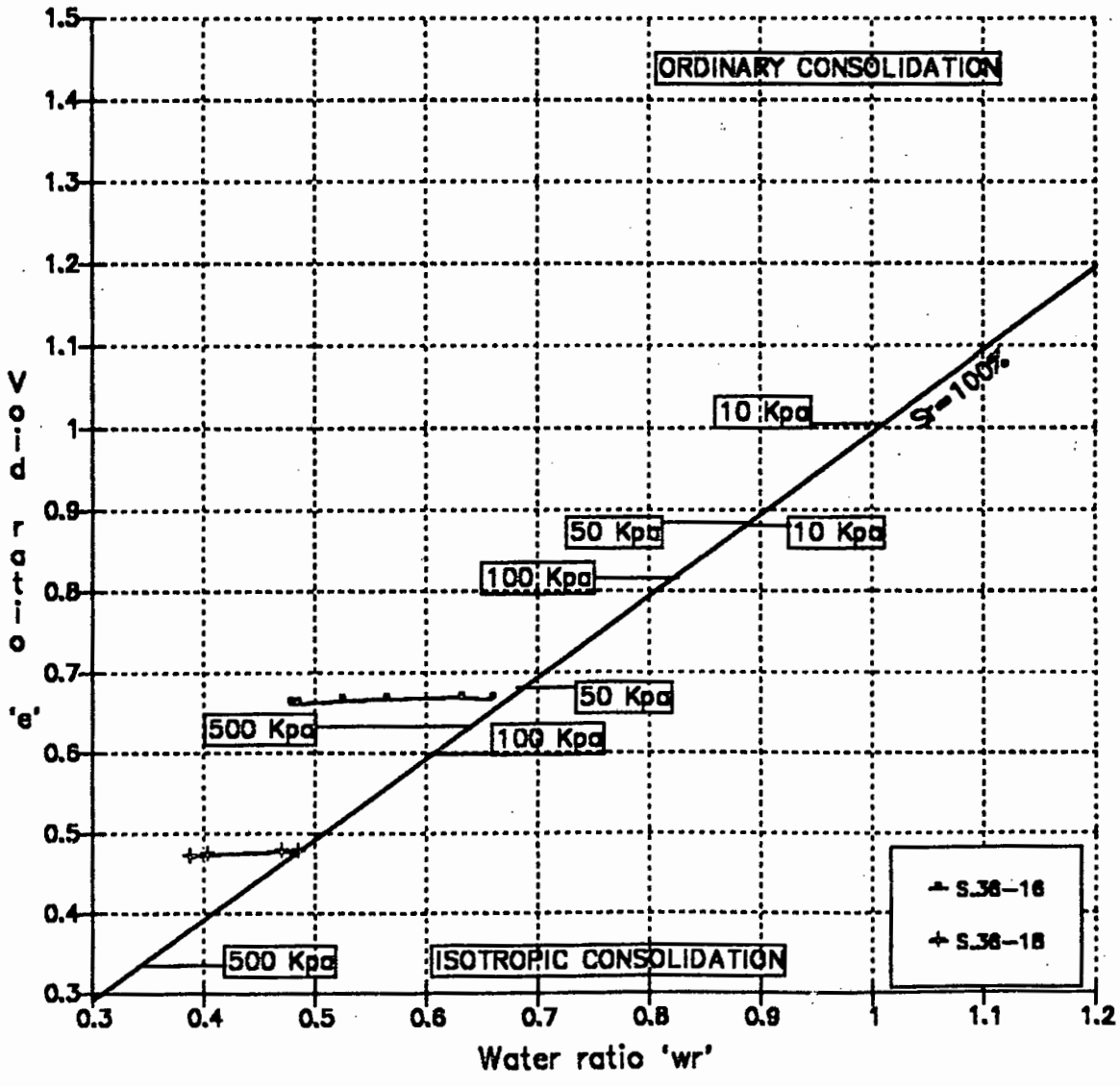

Figure 6.78: Site 36, Rondebosch [Compacted and Undisturbed] - Void ratio 'e' versus water ratio 'wr'.
Volume change due to wetting shown while carrying 100 Kpa only. Scales are from other tests (Chapter 5).

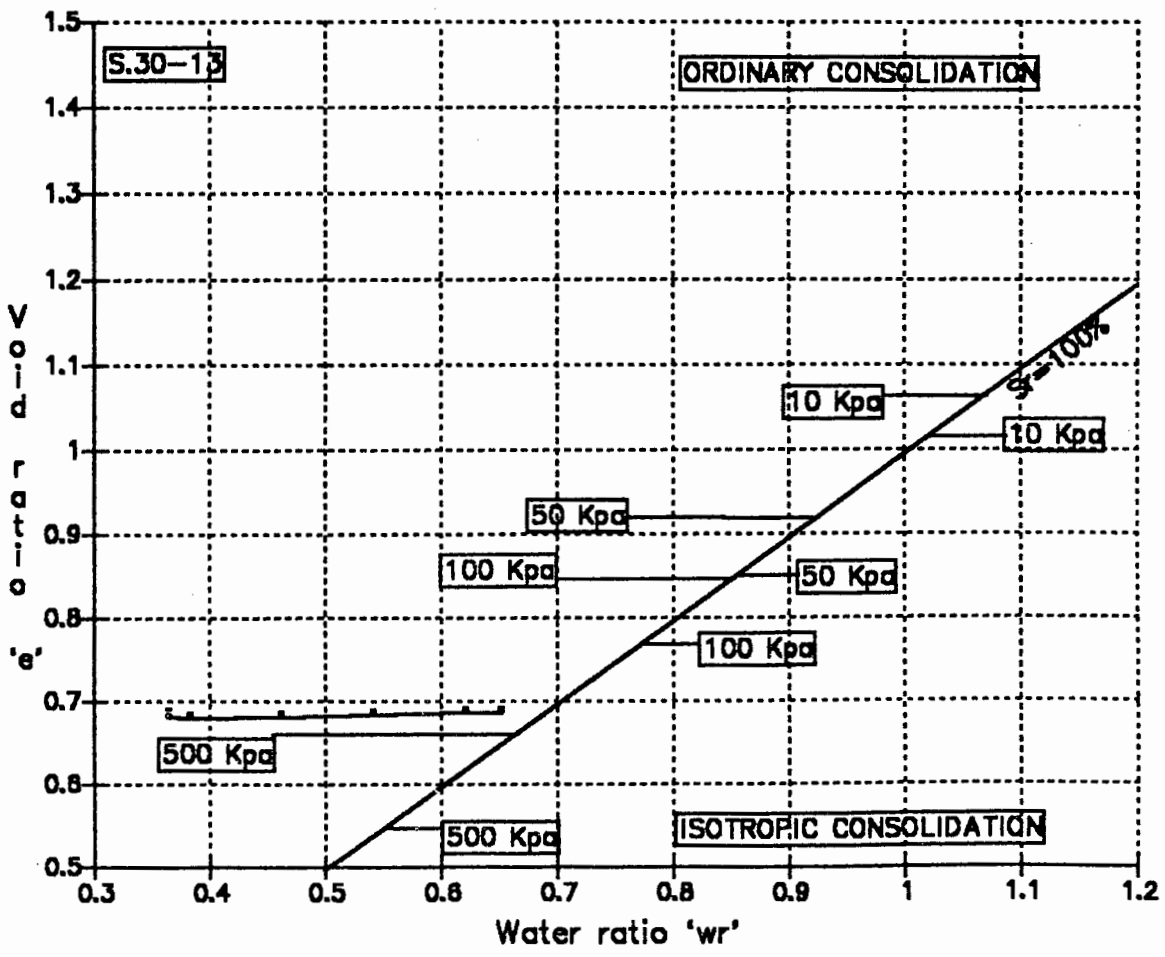

Figure 6.80: Site 30, Hout Bay [Undisturbed] - Void ratio 'e' versus water ratio 'wr'.
Volume change due to wetting shown while carrying 100 Kpa only. Scales are from other tests (Chapter 5).

Site A, Berea Road (Durban).

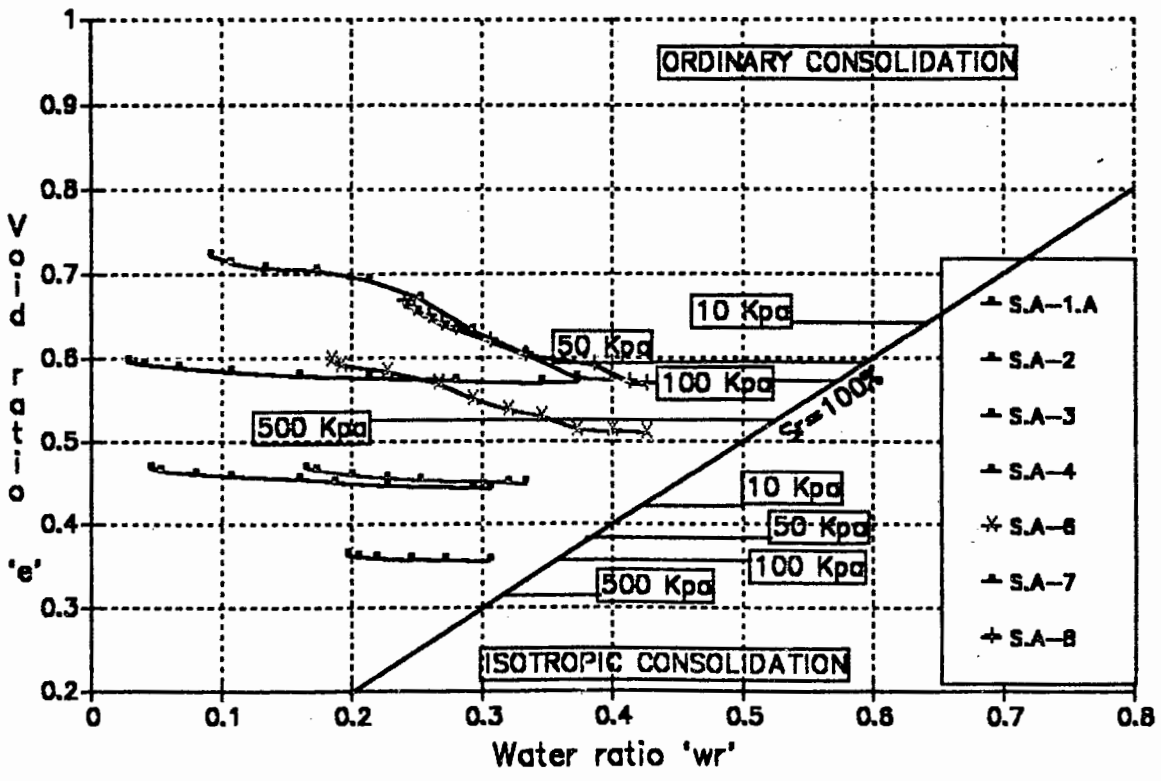

Figure 6.81: Site A, Berea Road (Durban) [Remoulded] - Void ratio 'e' versus water ratio 'wr'.
Volume change due to wetting shown while carrying 100 Kpa only. Scales are from other tests (Chapter 5).

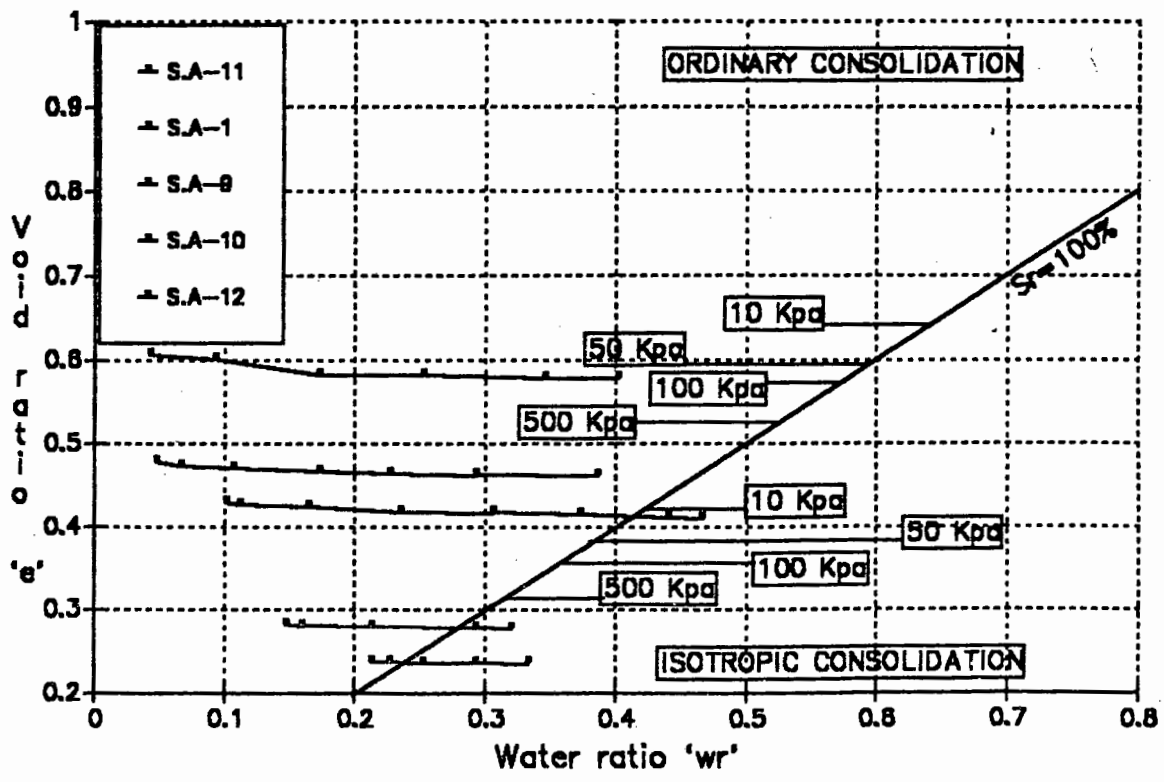

Figure 6.82: Site A, Berea Road (Durban) [Compacted and Undisturbed] - Void ratio 'e' versus water ratio 'wr'. Volume change due to wetting shown while carrying 100 Kpa only. Scales are from other tests (Chapter 5).

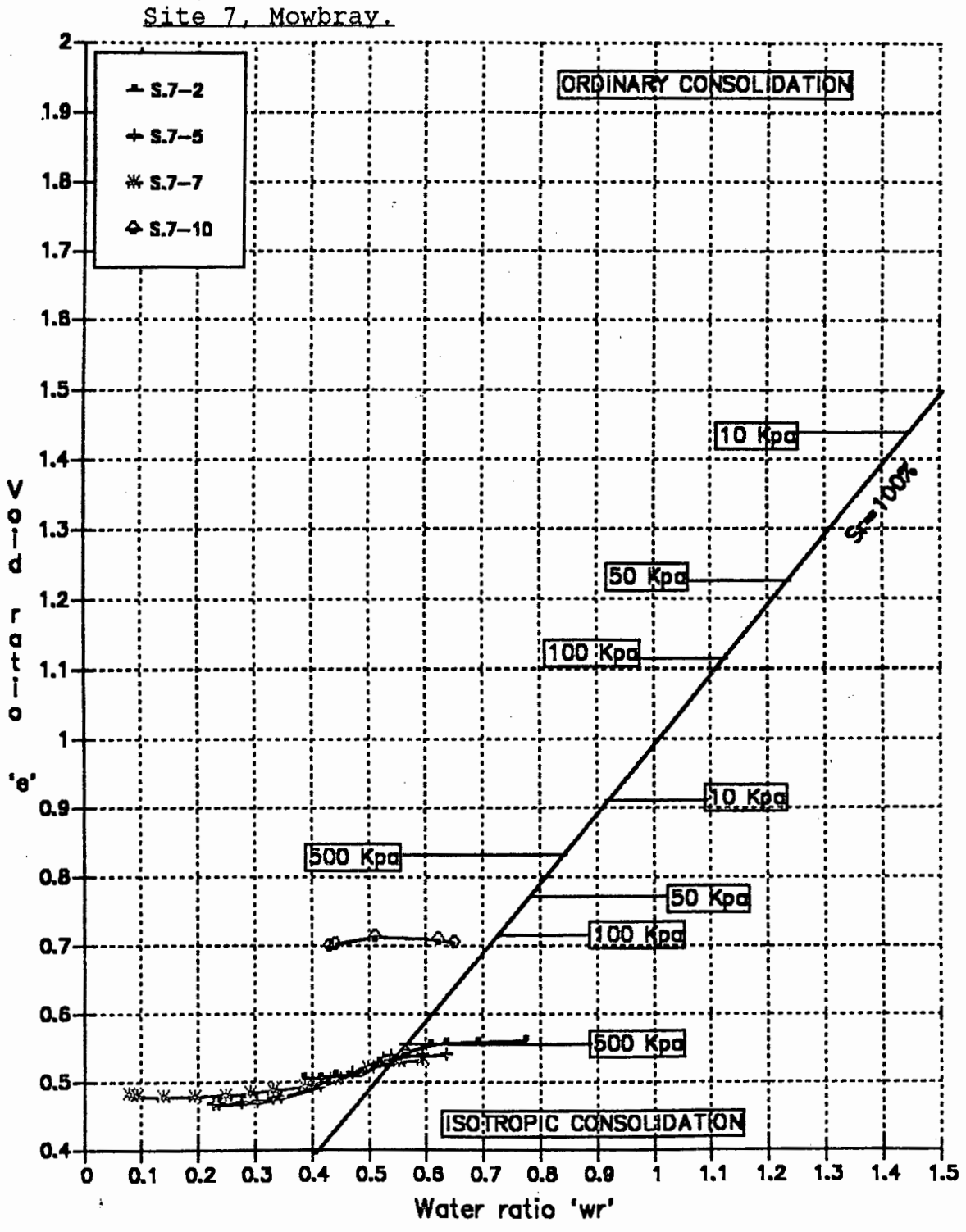

Figure 6.83: Site 7, Mowbray [Remoulded] - Void ratio 'e' versus water ratio 'wr'.
Volume change due to wetting shown while carrying 100 Kpa only. Scales are from other tests (Chapter 5).

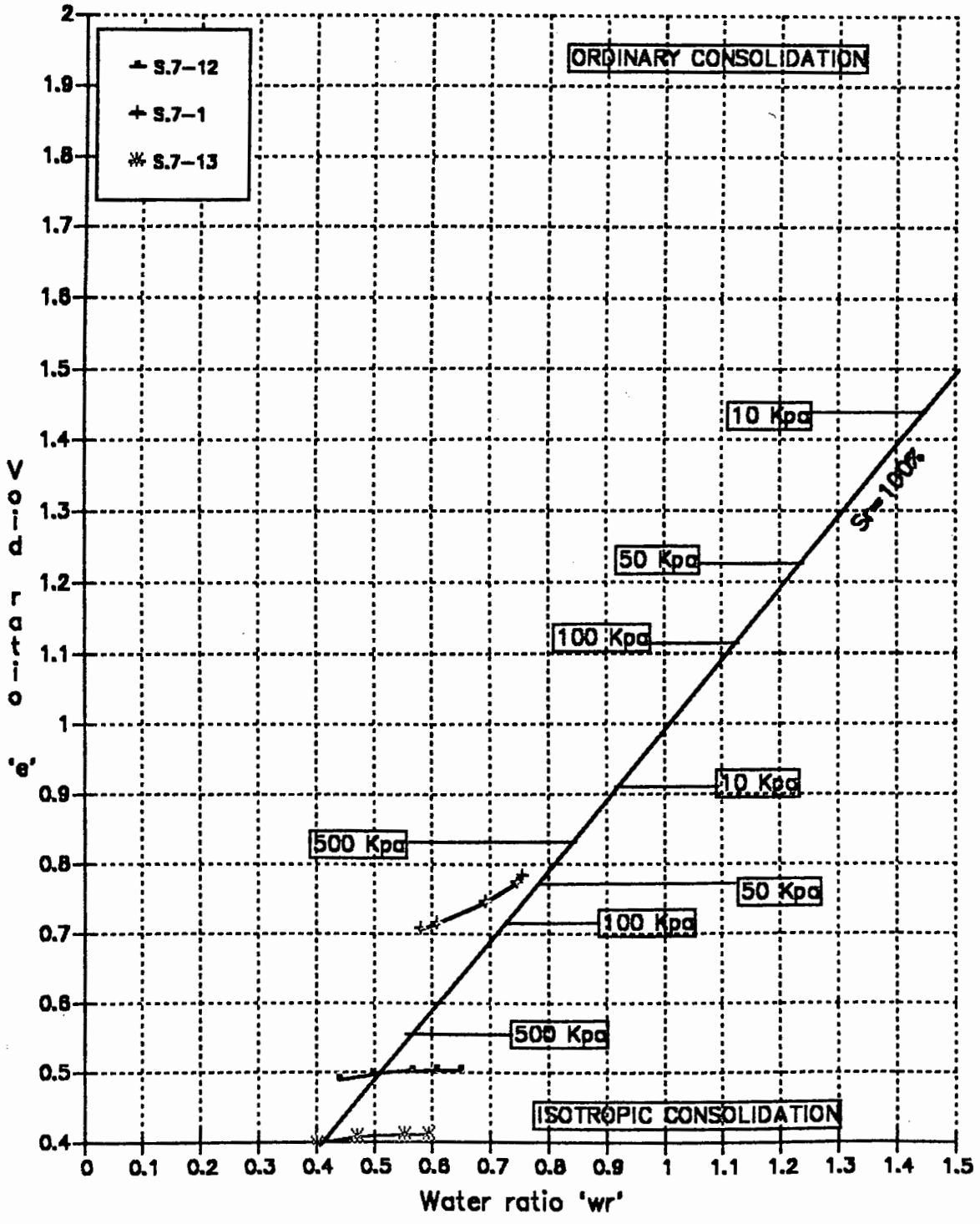

Figure 6.84: Site 7, Mowbray [Compacted and Undisturbed] - Void ratio 'e' versus water ratio 'wr'. Volume change due to wetting shown while carrying 100 Kpa only. Scales are from other tests (Chapter 5).

Site B, Francois Road (Durban).

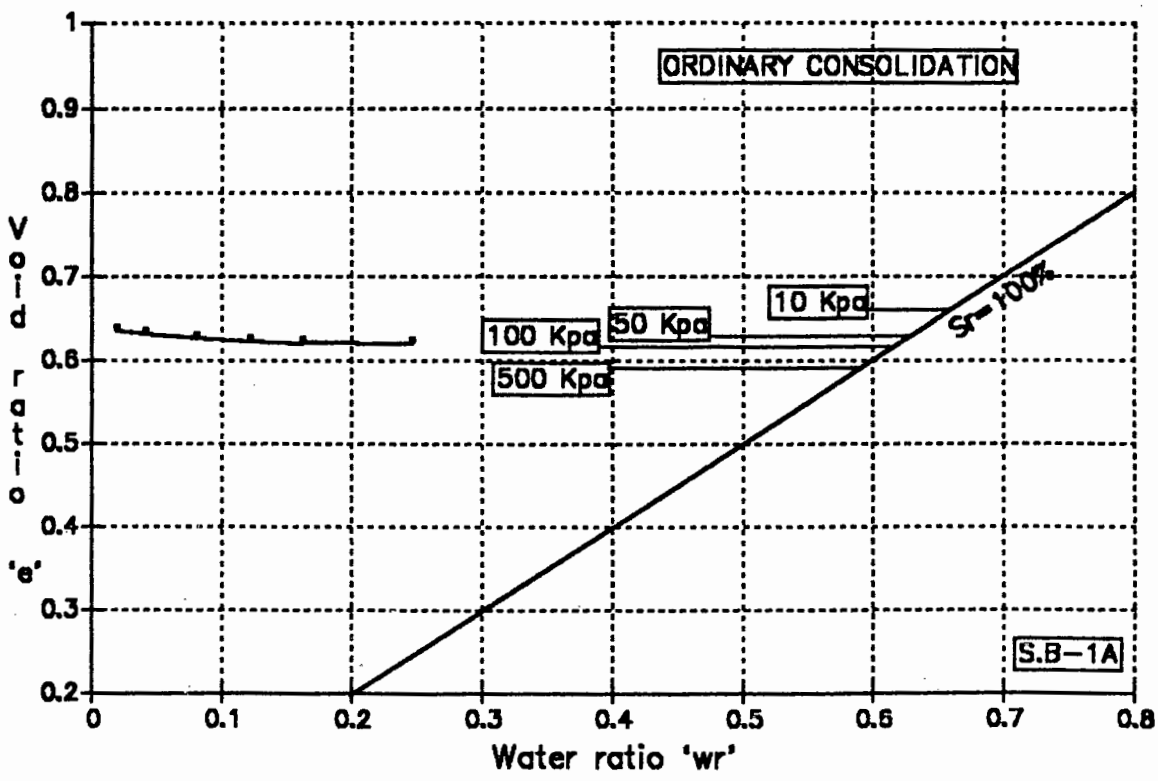

Figure 6.85: Site B, Francois Road (Durban) [Remoulded] - Void ratio 'e' versus water ratio 'wr'. Volume change due to wetting shown while carrying 100 Kpa only. Scales are from other tests (Chapter 5).

Site C, Margaret Mayton Avenue (Durban).

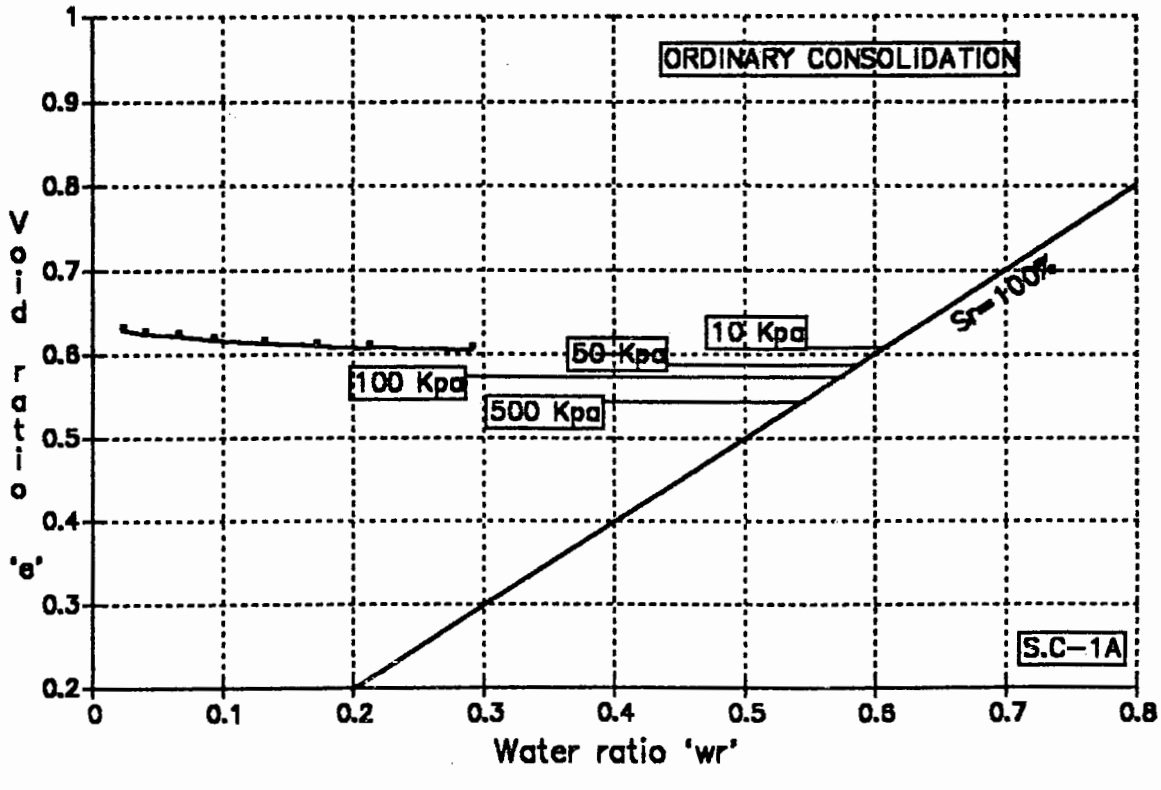

Figure 6.86: Site C, Margaret Mayton Avenue (Durban) [Remoulded] - Void ratio 'e' versus water ratio 'wr'. Volume change due to wetting shown while carrying 100 Kpa only. Scales are from other tests (Chapter 5).

Site D, Rose Hill (Durban).

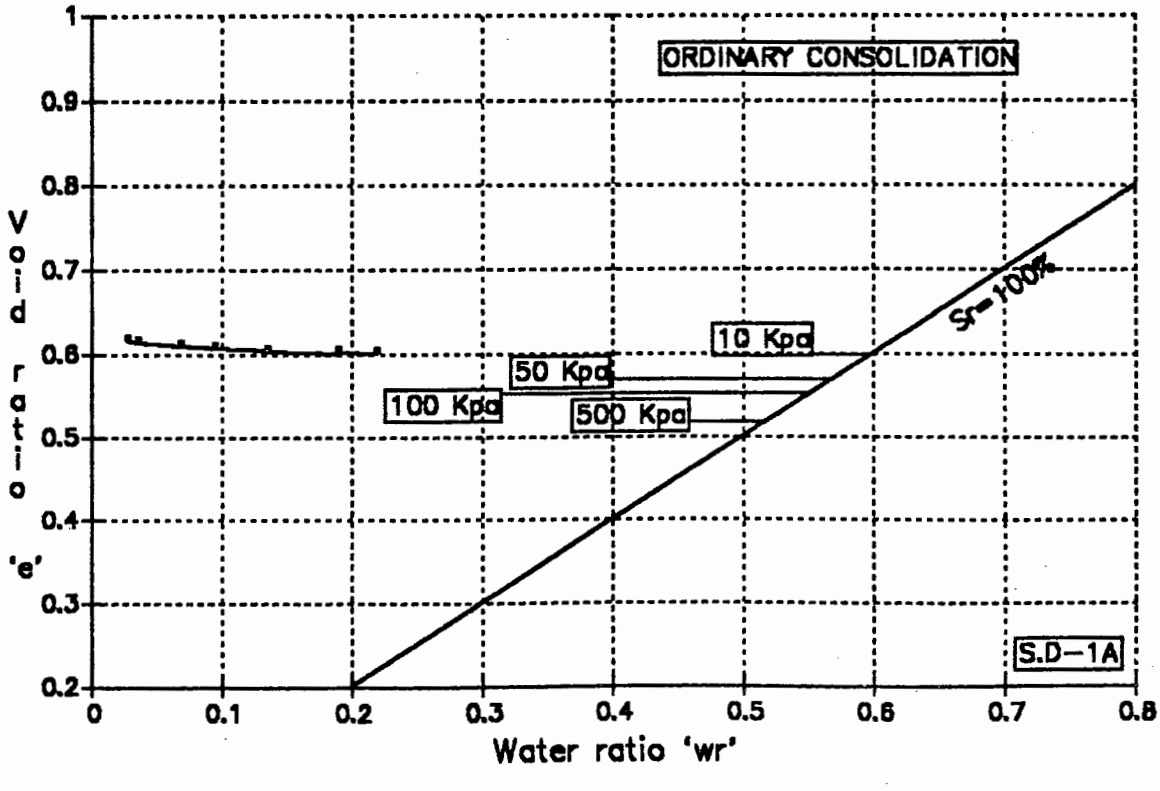

Figure 6.87: Site D, Rose Hill (Durban) [Remoulded] - Void ratio 'e' versus water ratio 'wr'.
Volume change due to wetting shown while carrying 100 Kpa only. Scales are from other tests (Chapter 5).

Artificial Soil Types: Kaolin clay mixed with sand.

Kaolin K.1:-

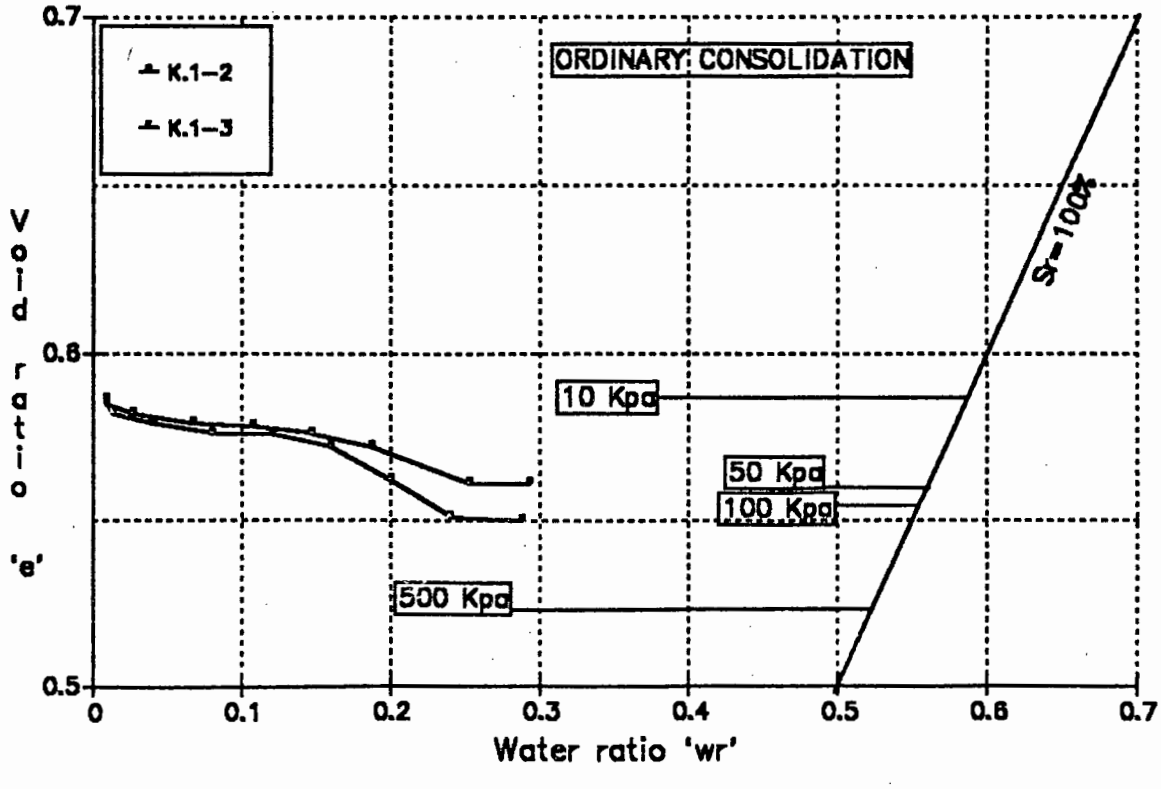

Figure 6.88: Kaolin K.1 (13% clay size) [Remoulded] - Void ratio 'e' versus water ratio 'wr'.
Volume change due to wetting shown while carrying 100 Kpa only. Scales are from other tests (Chapter 5).

Kaolin K.2:-

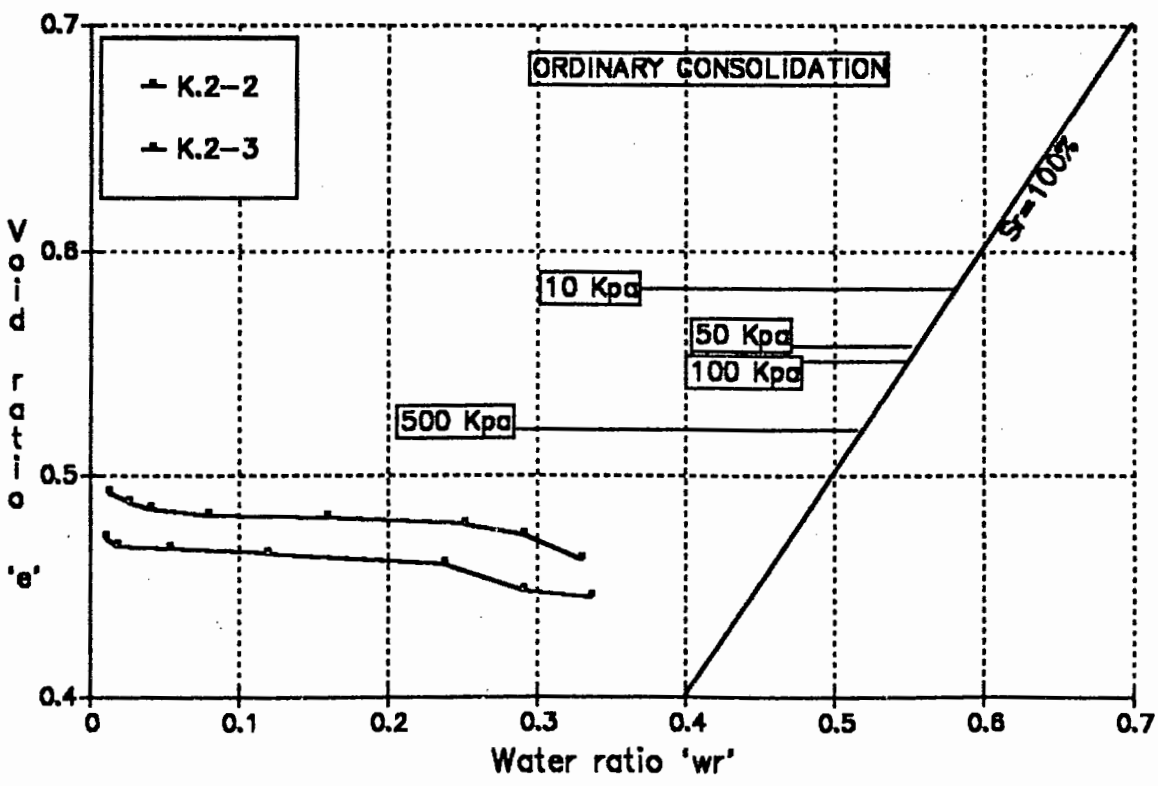

Figure 6.89: Kaolin K.2 (20% clay size) [Remoulded] - Void ratio 'e' versus water ratio 'wr'.
Volume change due to wetting shown while carrying 100 Kpa only. Scales are from other tests (Chapter 5).

Kaolin K.3:-

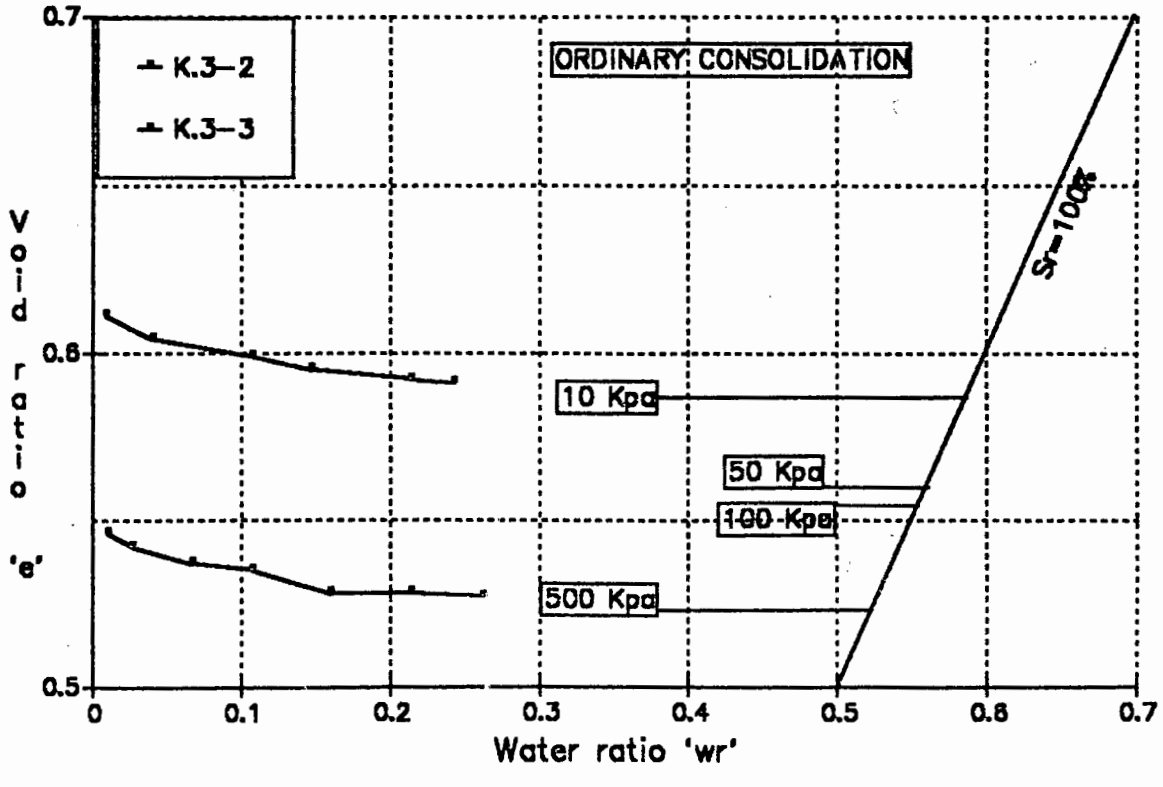

Figure 6.90: Kaolin K.3 (8.5% clay size) [Remoulded] - Void ratio 'e' versus water ratio 'wr'.
Volume change due to wetting shown while carrying 100 Kpa only. Scales are from other tests (Chapter 5).

Bentonite clay mixed with sand.

Bentonite B.1:-

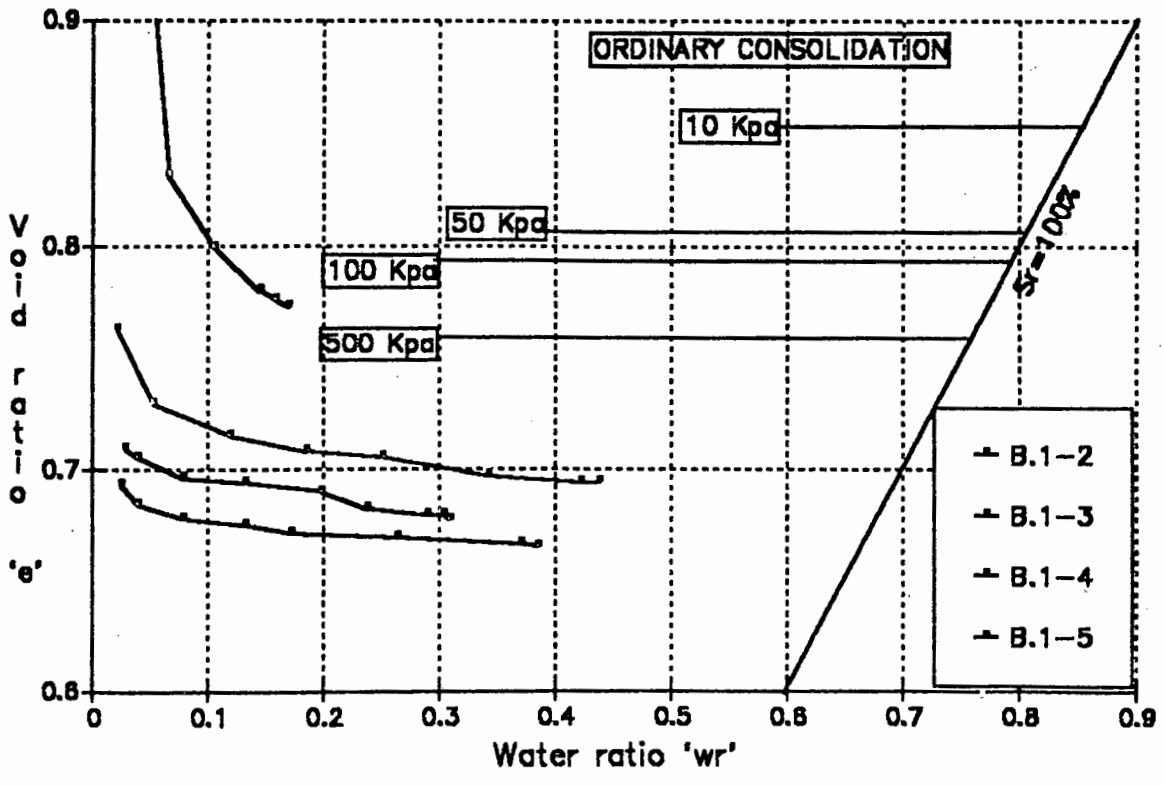

Figure 6.91: Bentonite B.1 (3.5% clay size) [Remoulded] - Void ratio 'e' versus water ratio 'wr'.
Volume change due to wetting shown while carrying 100 Kpa only, scales are from other tests (Chapter 5).

Bentonite B.2:-

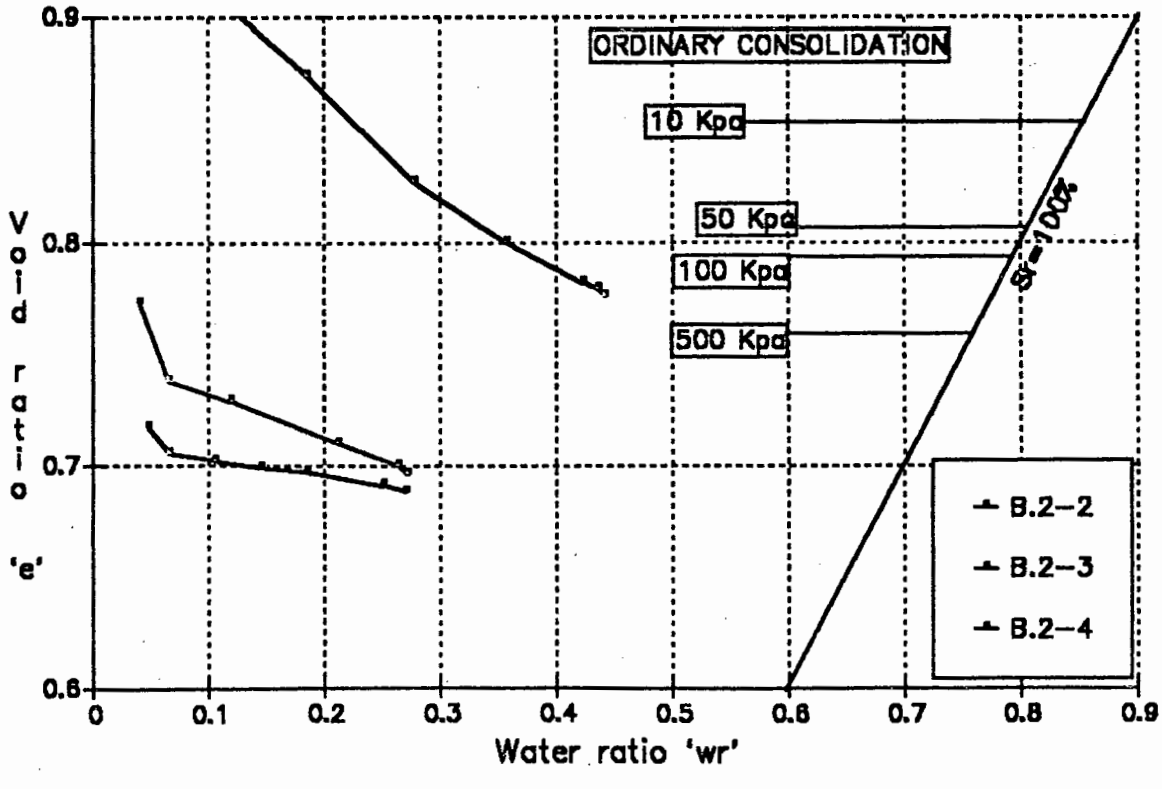

Figure 6.92: Bentonite B.2 (7% clay size) [Remoulded] - Void ratio 'e' versus water ratio 'wr'.
Volume change due to wetting shown while carrying 100 Kpa only. Scales are from other tests (Chapter 5).

Bentonite B.3:-

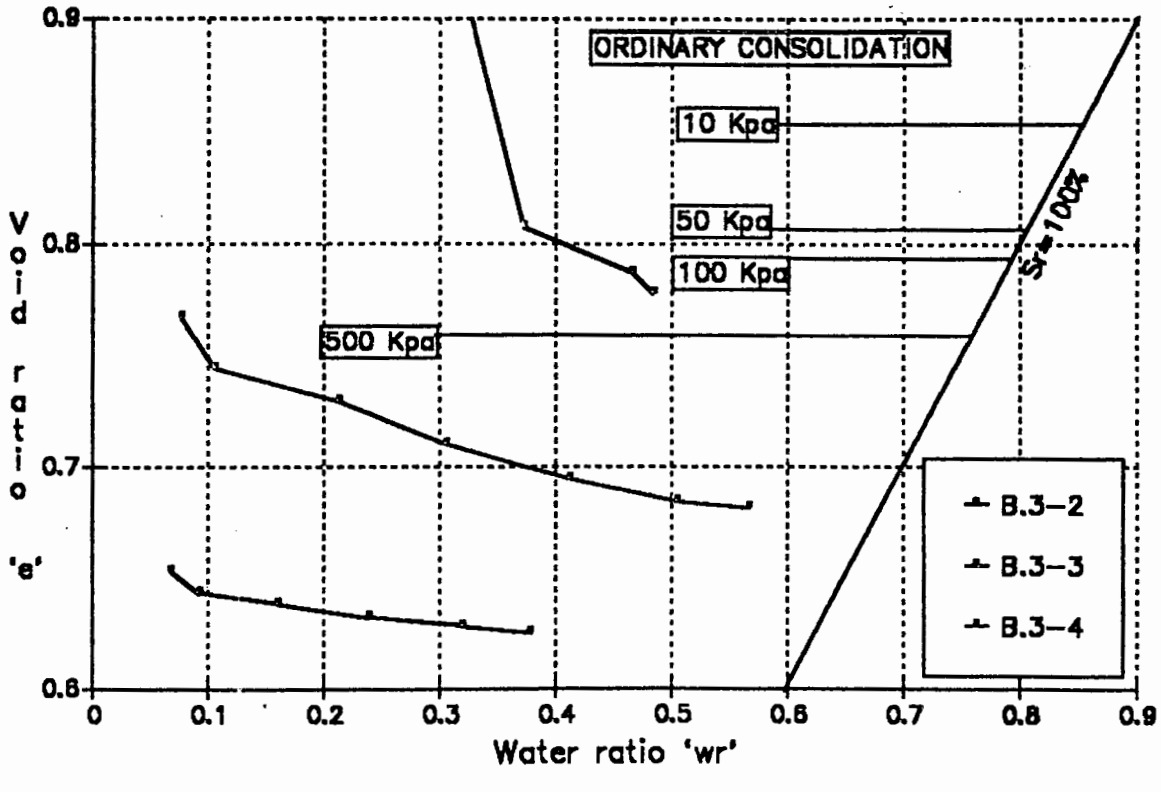

Figure 6.93: Bentonite B.3 (11.5% clay size) [Remoulded] - Void ratio 'e' versus water ratio 'wr'.
Volume change due to wetting shown while carrying 100 Kpa only. Scales are from other tests (Chapter 5).

Bentonite B.4:-

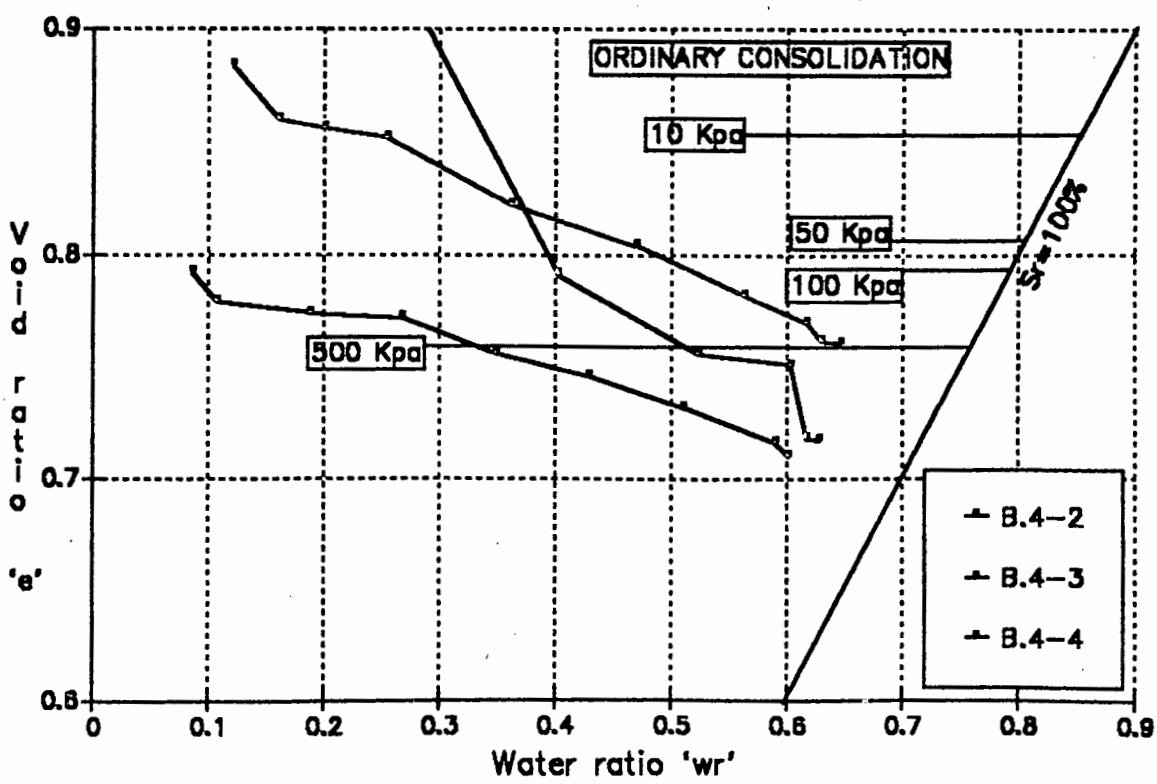

Figure 6.94: Bentonite B.4 (15.5% clay size) [Remoulded] - Void ratio 'e' versus water ratio 'wr'.
Volume change due to wetting shown while carrying 100 Kpa only. Scales are from other tests (Chapter 5).

Bentonite B.5:-

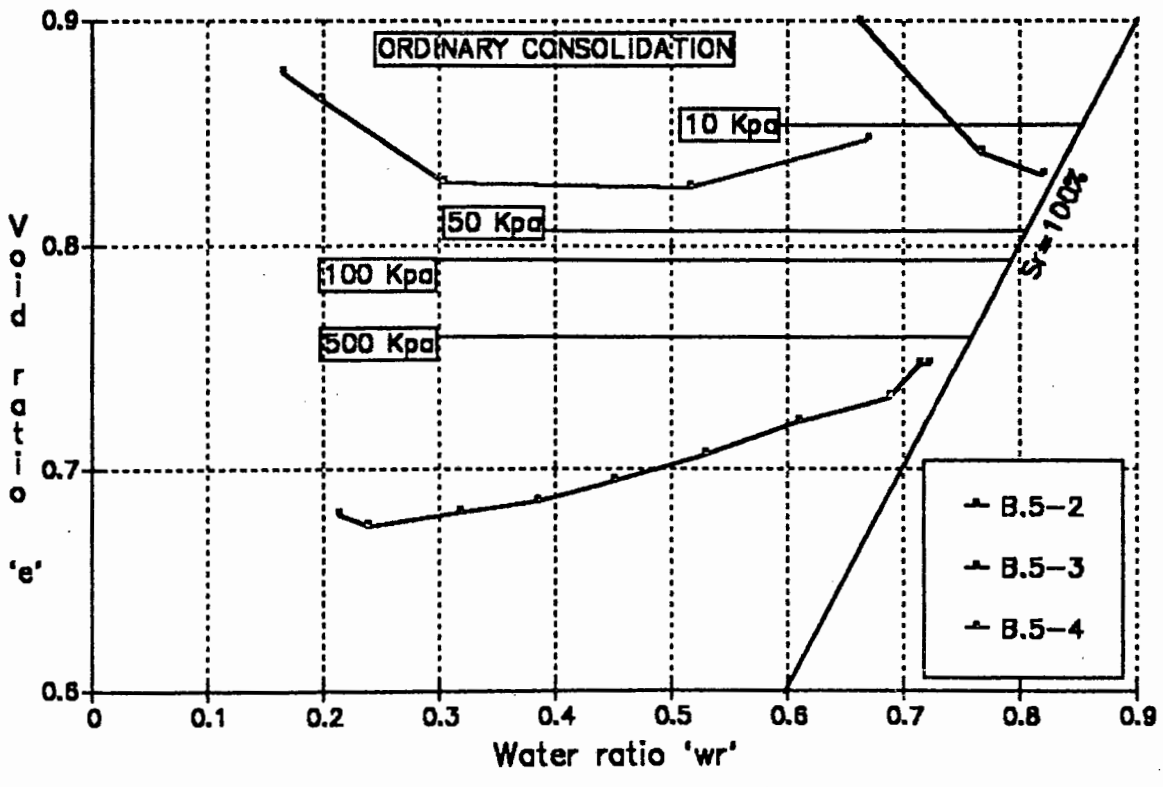

Figure 6.95: Bentonite B.5 (35% clay size) [Remoulded] - Void ratio 'e' versus water ratio 'wr'. Volume change due to wetting shown while carrying 100 Kpa only. Scales are from other tests (Chapter 5).

6.9.2 Void Ratio vs Effective Vertical Pressure vs Water Ratio.

Natural Soil Types.

Site 11, Rosebank:-

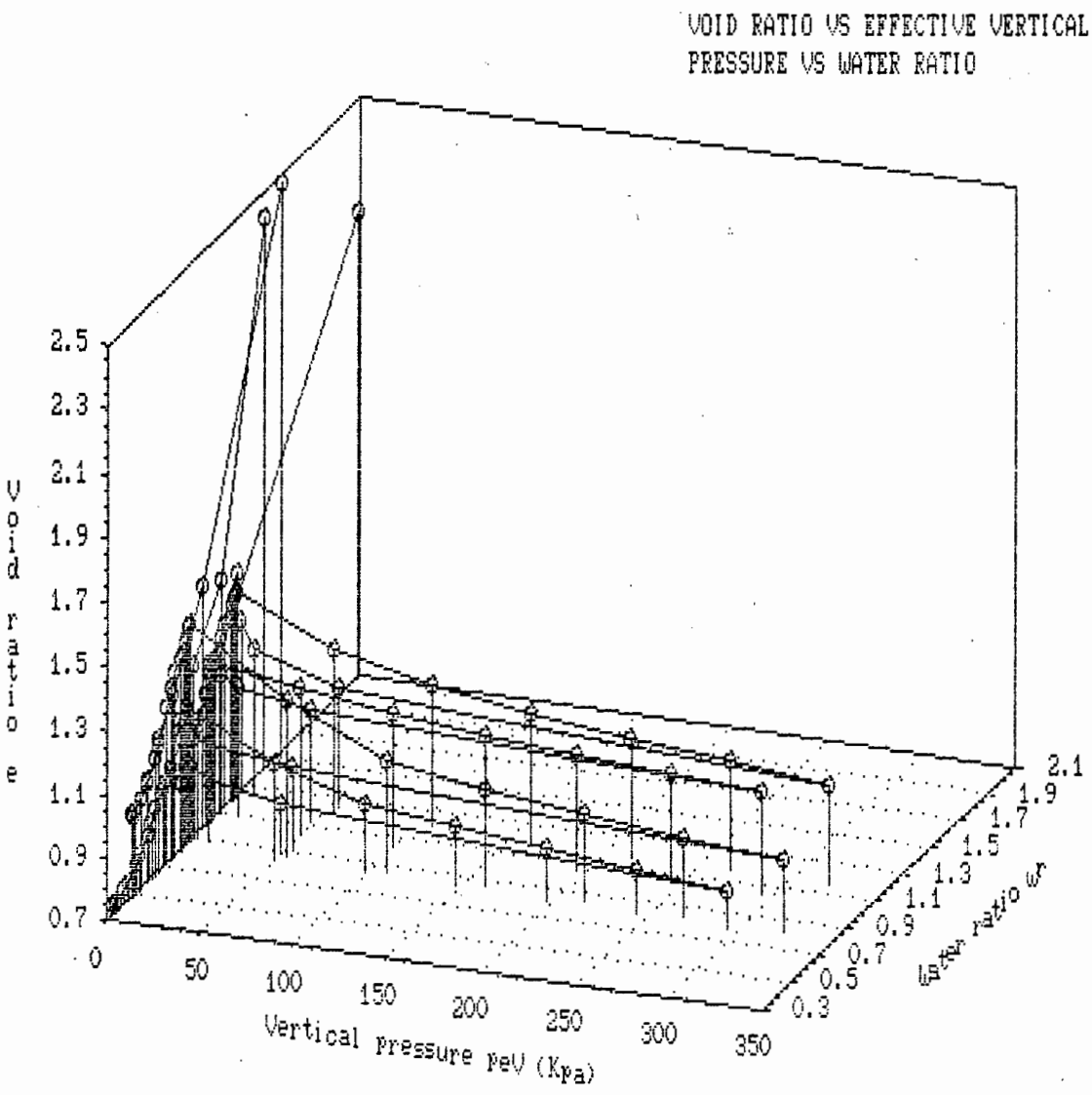

Figure 6.96: Site 11, Rosebank [Remoulded, 1 Kpa] - Void ratio 'e' vs effective vertical pressure 'peV' vs water ratio 'wr', for the full test path.

Sparks (1975)[1] has previously presented diagrams of Void Ratio versus Vertical Pressure versus Water Content.

---

1 - Reference 86.
2 - Reference 2.

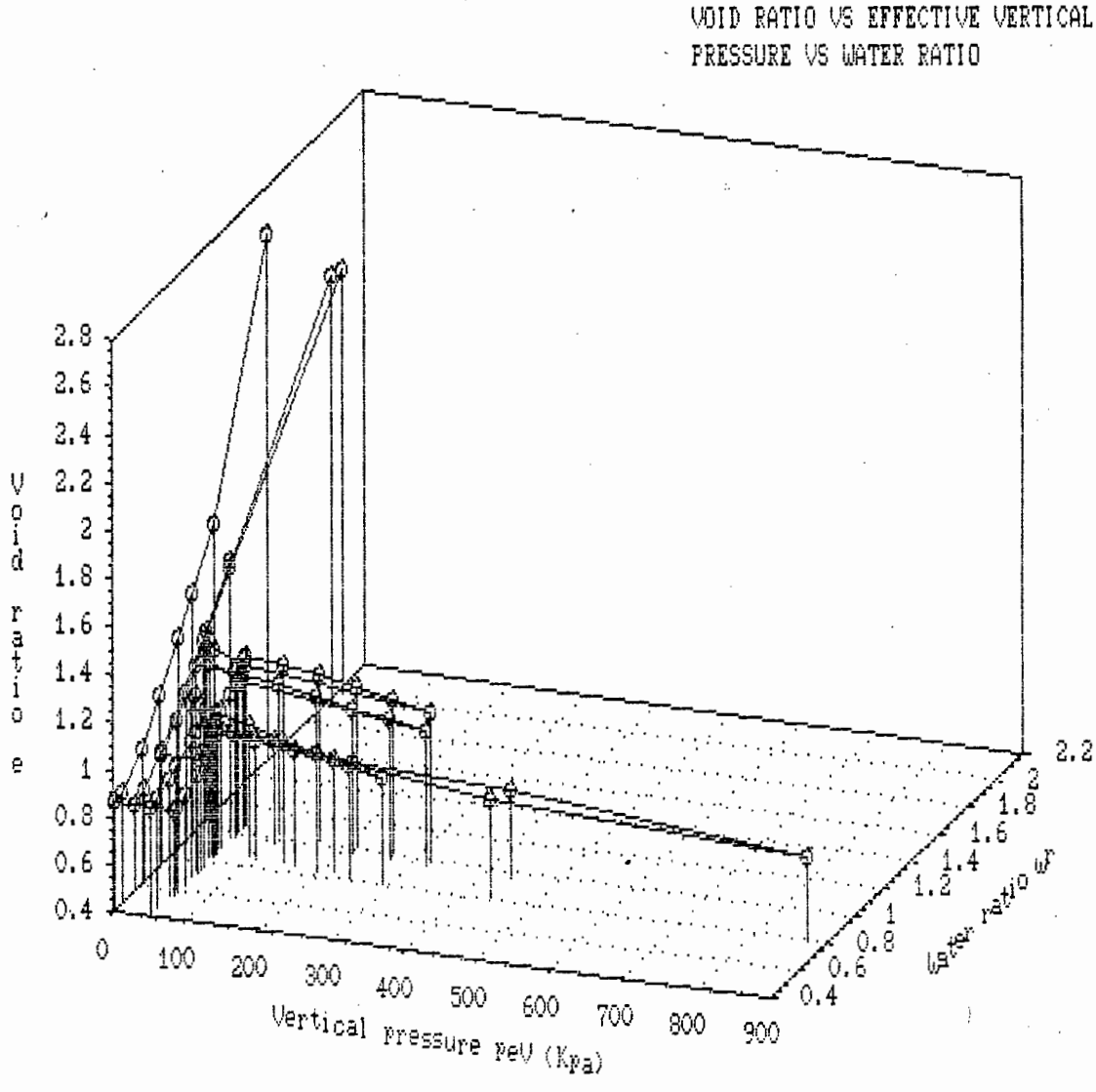

Figure 6.97: Site 11, Rosebank - [Remoulded, 50 Kpa] Void ratio 'e' vs effective vertical pressure 'peV' vs water ratio 'wr'.

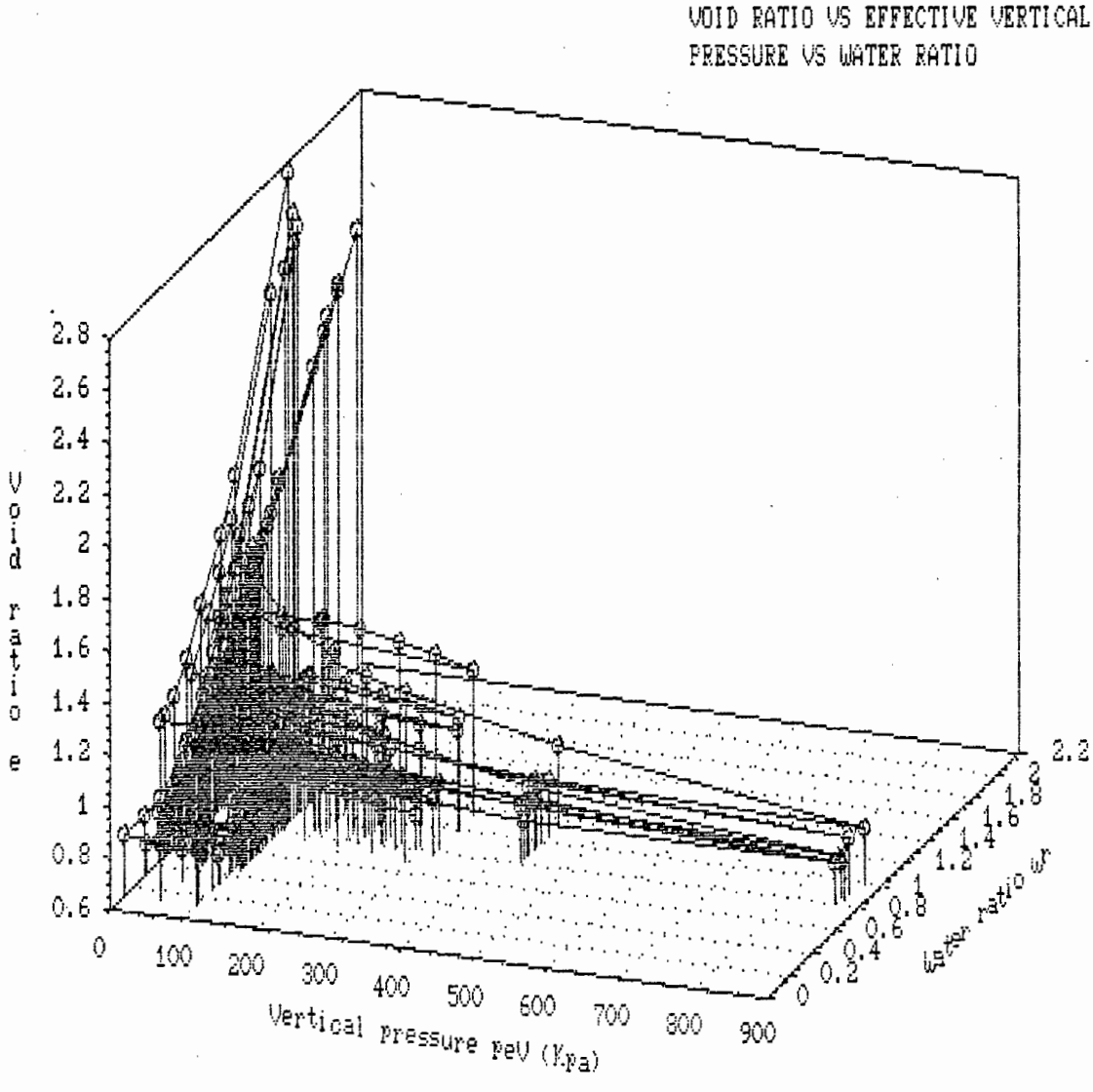

Figure 6.98: Site 11, Rosebank - [Remoulded, 100 Kpa] Void ratio 'e' vs effective vertical pressure 'peV' vs water ratio 'wr'.

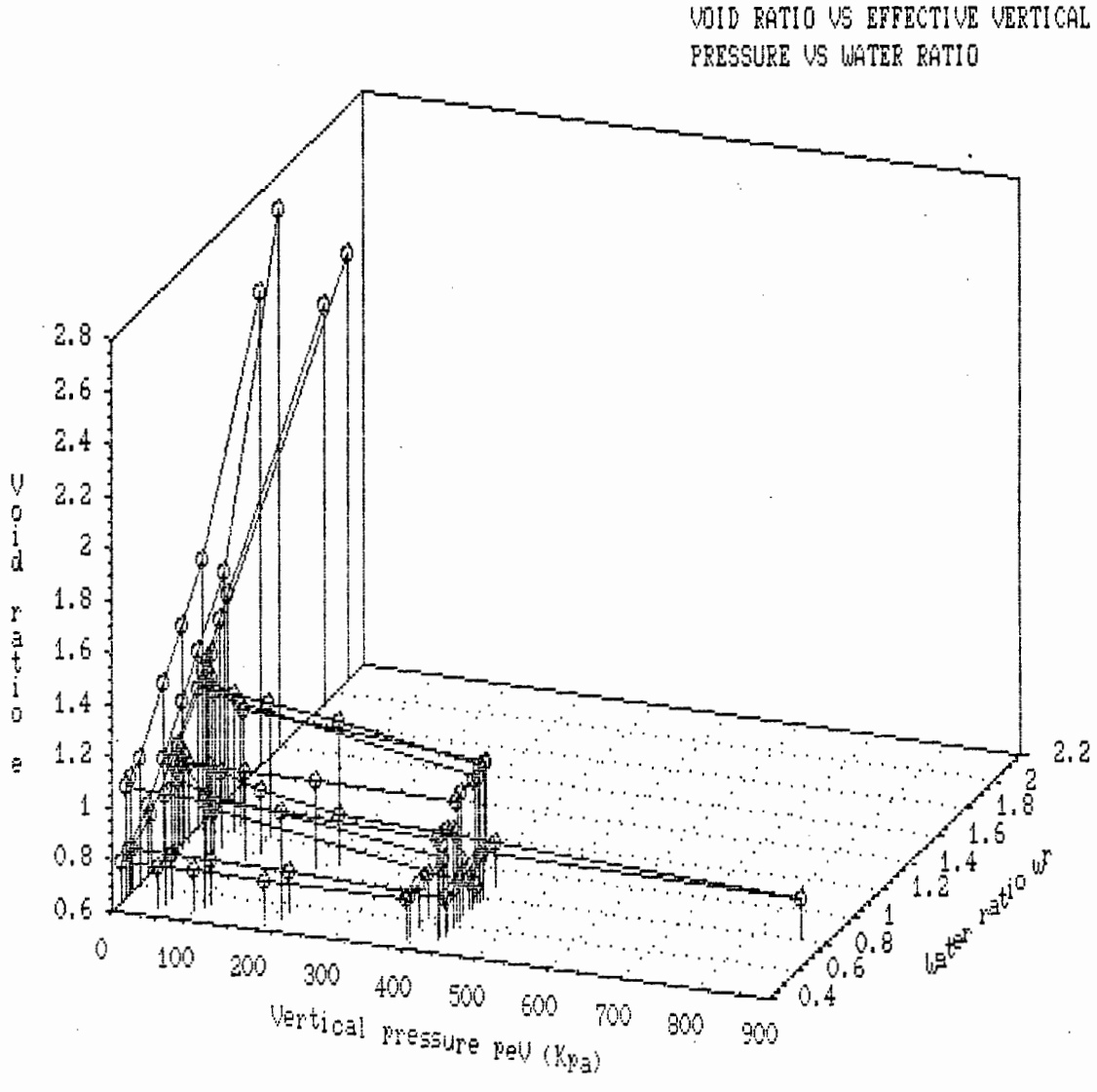

Figure 6.99: Site 11, Rosebank - [Remoulded, 400 Kpa] Void ratio 'e' vs effective vertical pressure 'peV' vs water ratio 'wr'.

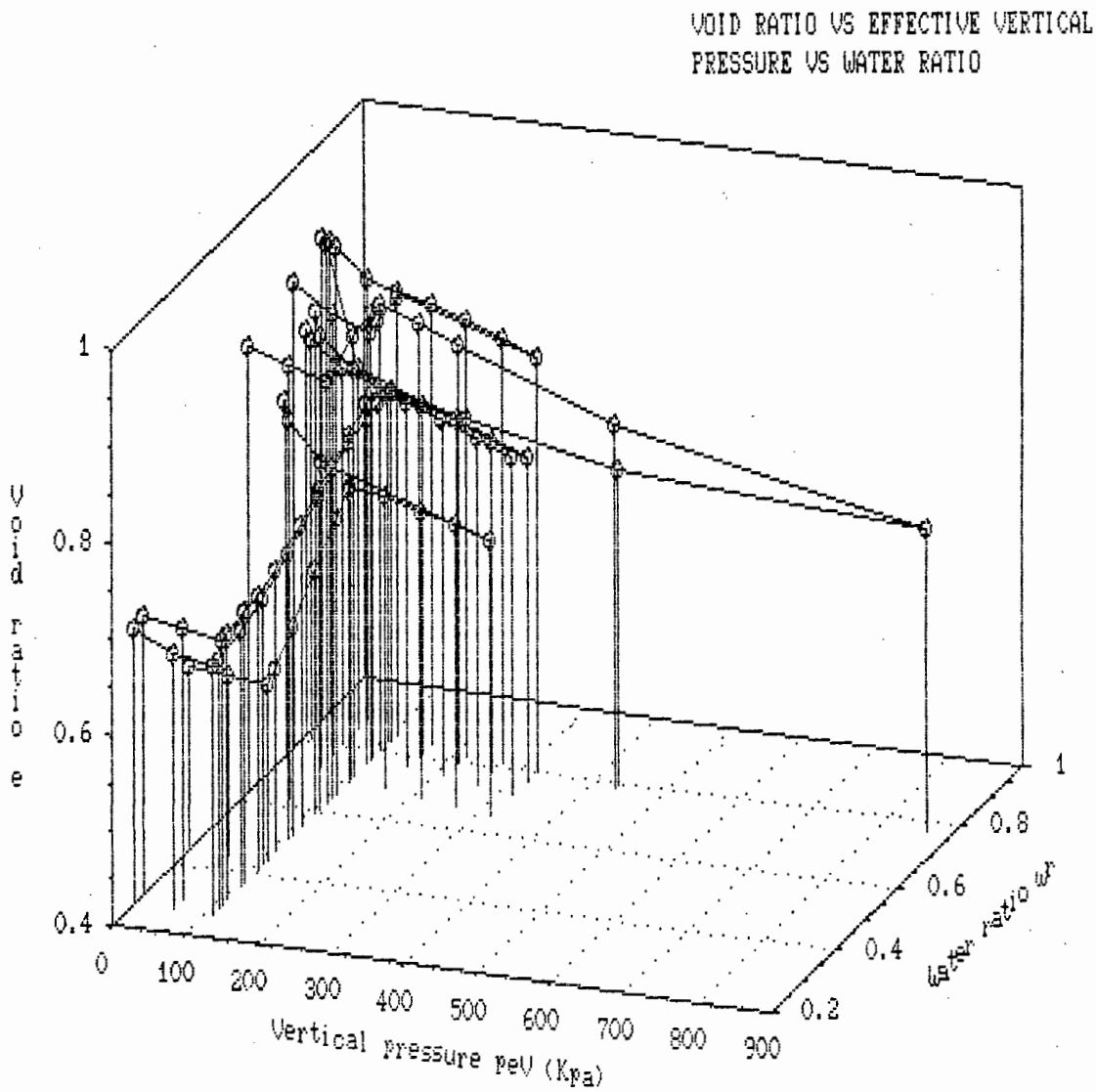

Figure 6.100: Site 11, Rosebank - [Compacted, 100 Kpa] Void ratio 'e' vs effective vertical pressure 'peV' vs water ratio 'wr'.

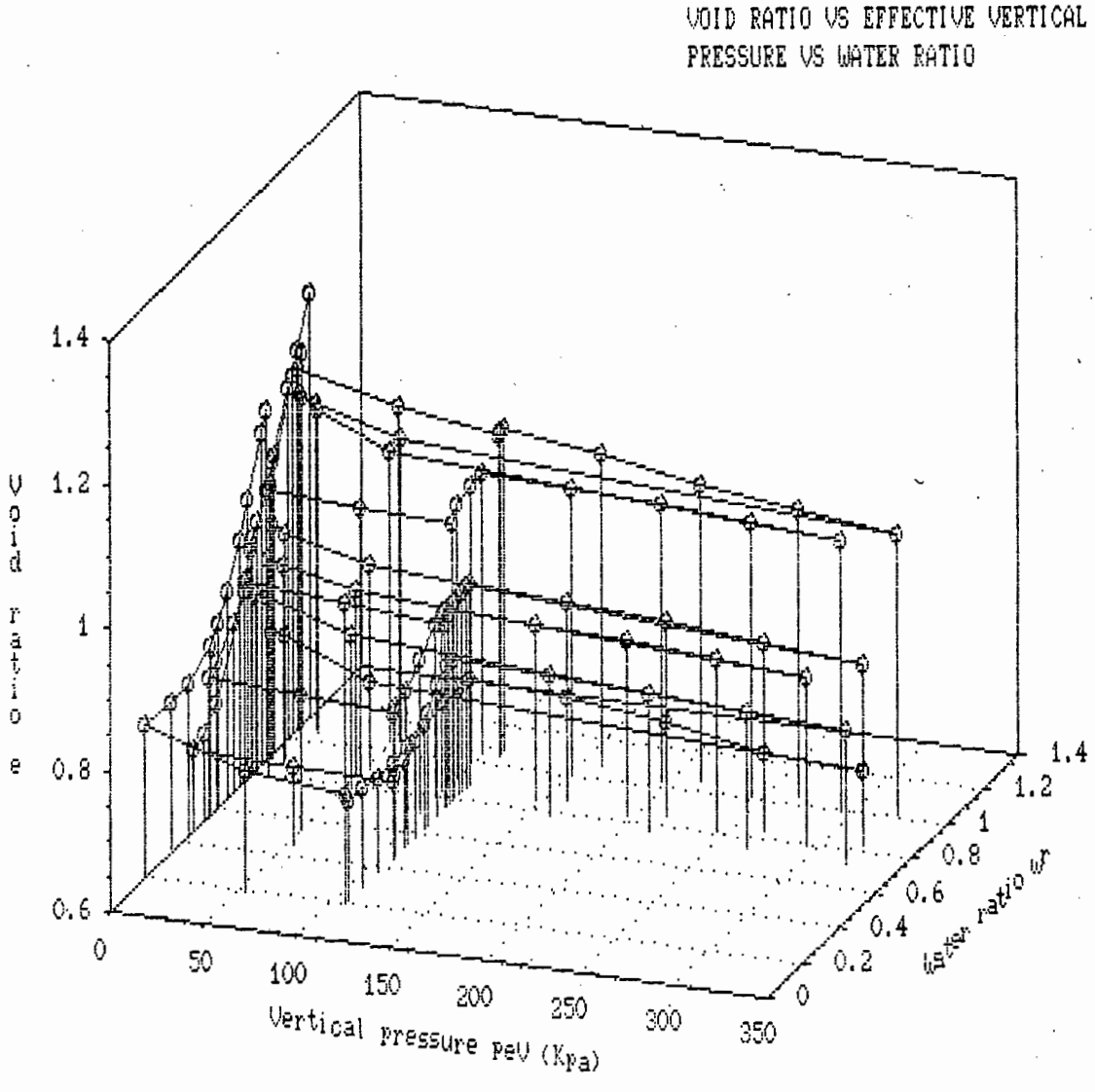

Figure 6.101: Site 11, Rosebank - [Undisturbed, 100 Kpa] Void ratio 'e' vs effective vertical pressure 'peV' vs water ratio 'wr'.

Site 36, Rondebosch:-

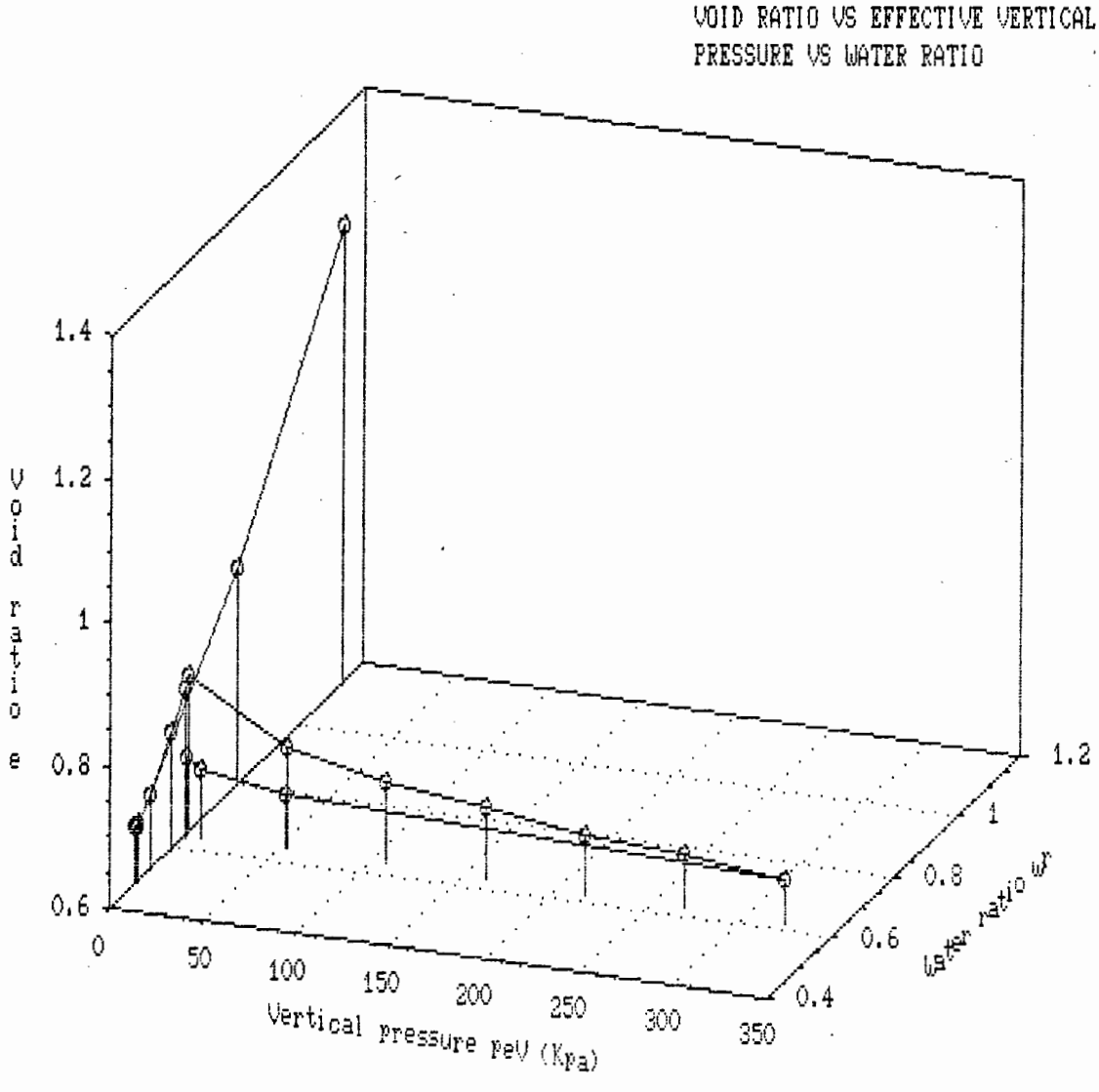

Figure 6.102: Site 36, Rondebosch - [Remoulded, 1 Kpa] Void ratio 'e' vs effective vertical pressure 'peV' vs water ratio 'wr'.

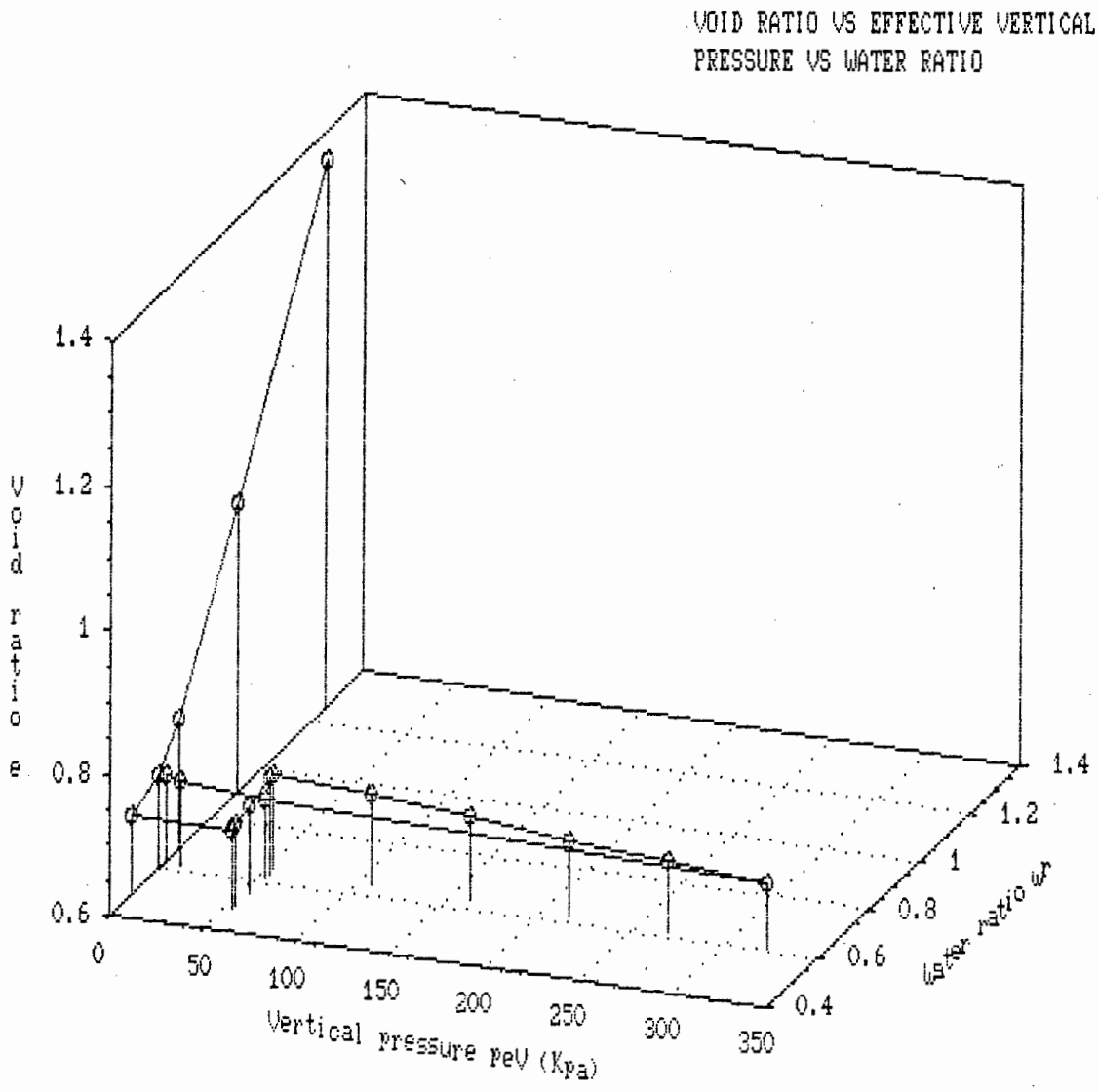

Figure 6.103: Site 36, Rondebosch - [Remoulded 50 Kpa] Void ratio 'e' vs effective vertical pressure 'peV' vs water ratio 'wr'.

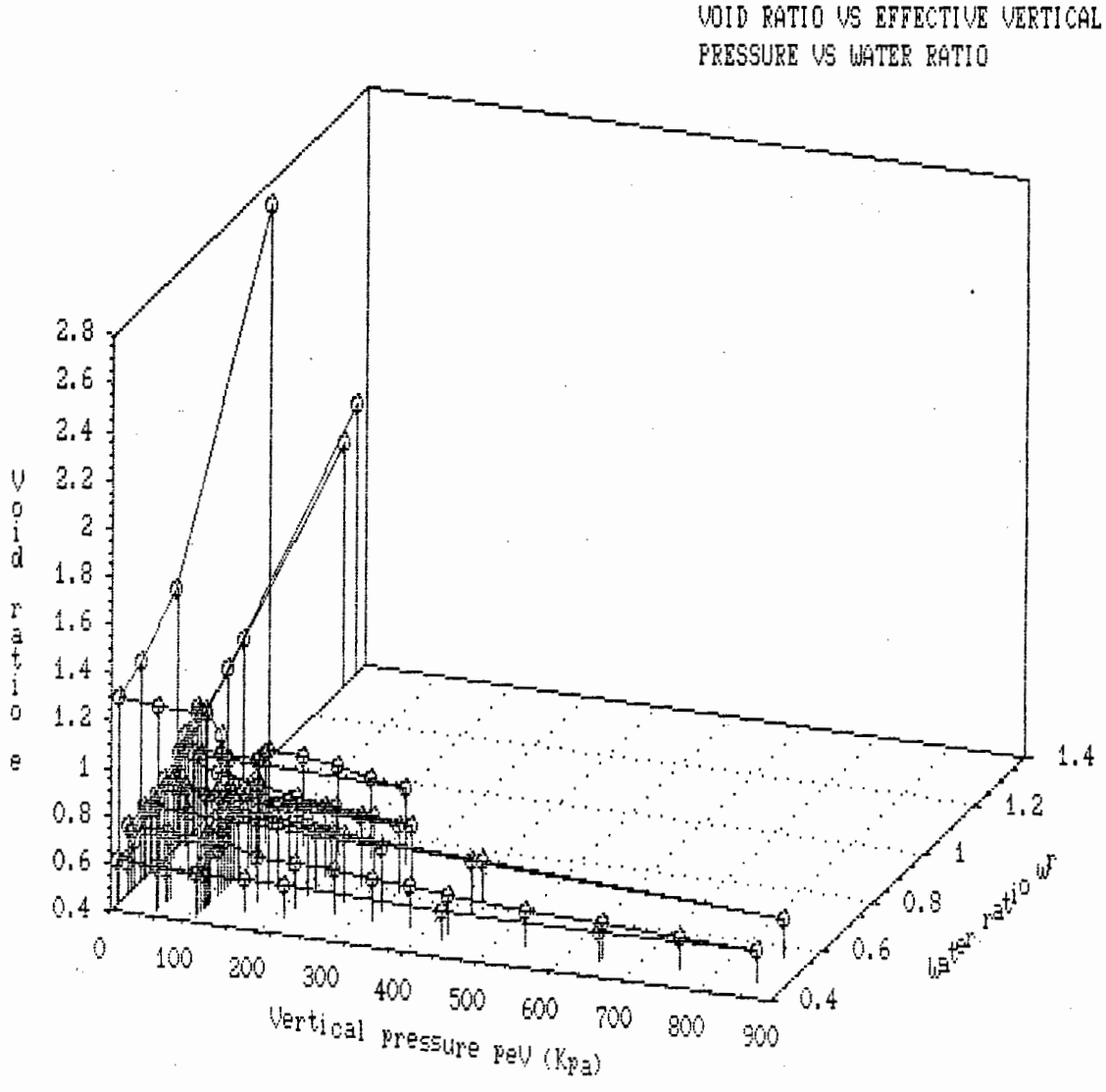

Figure 6.104: Site 36, Rondebosch - [Remoulded 100 Kpa] Void ratio 'e' vs effective vertical pressure 'peV' vs water ratio 'wr'.

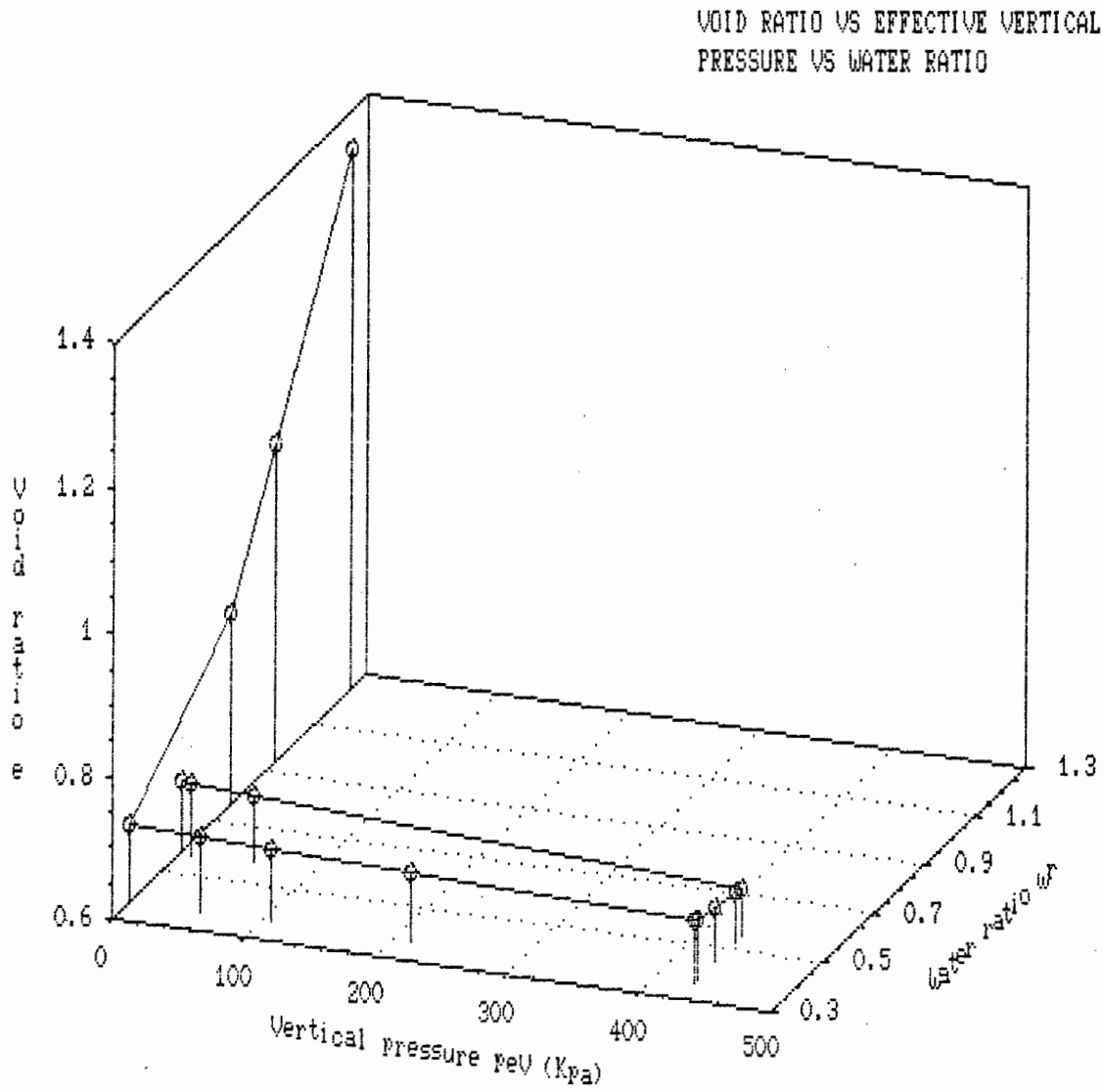

Figure 6.105: Site 36, Rondebosch - [Remoulded, 400 Kpa] Void ratio 'e' vs effective vertical pressure 'peV' vs water ratio 'wr'.

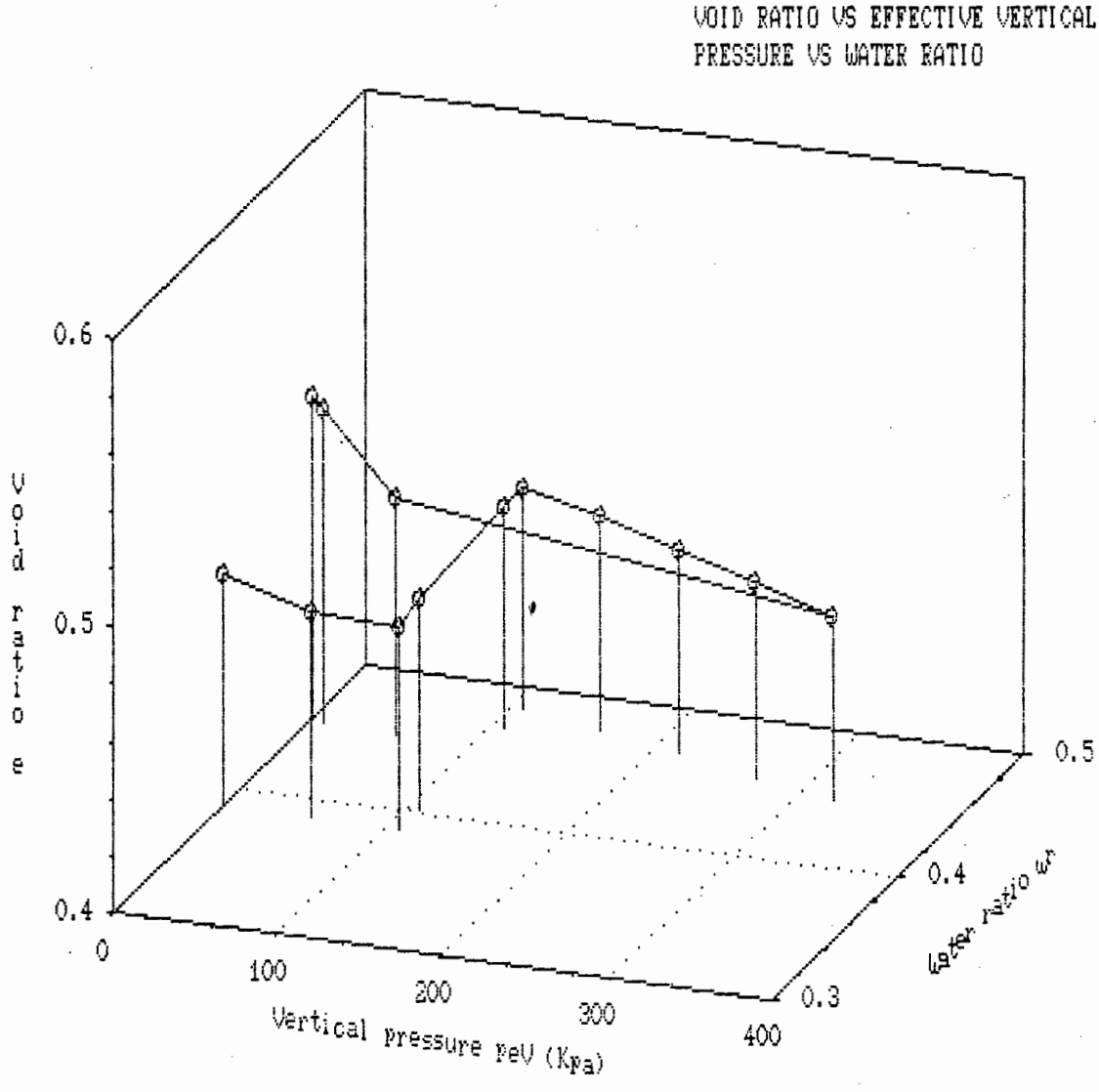

Figure 6.106: Site 36, Rondebosch - [Compacted, 100 Kpa] Void ratio 'e' vs effective vertical pressure 'peV' vs water ratio 'wr'.

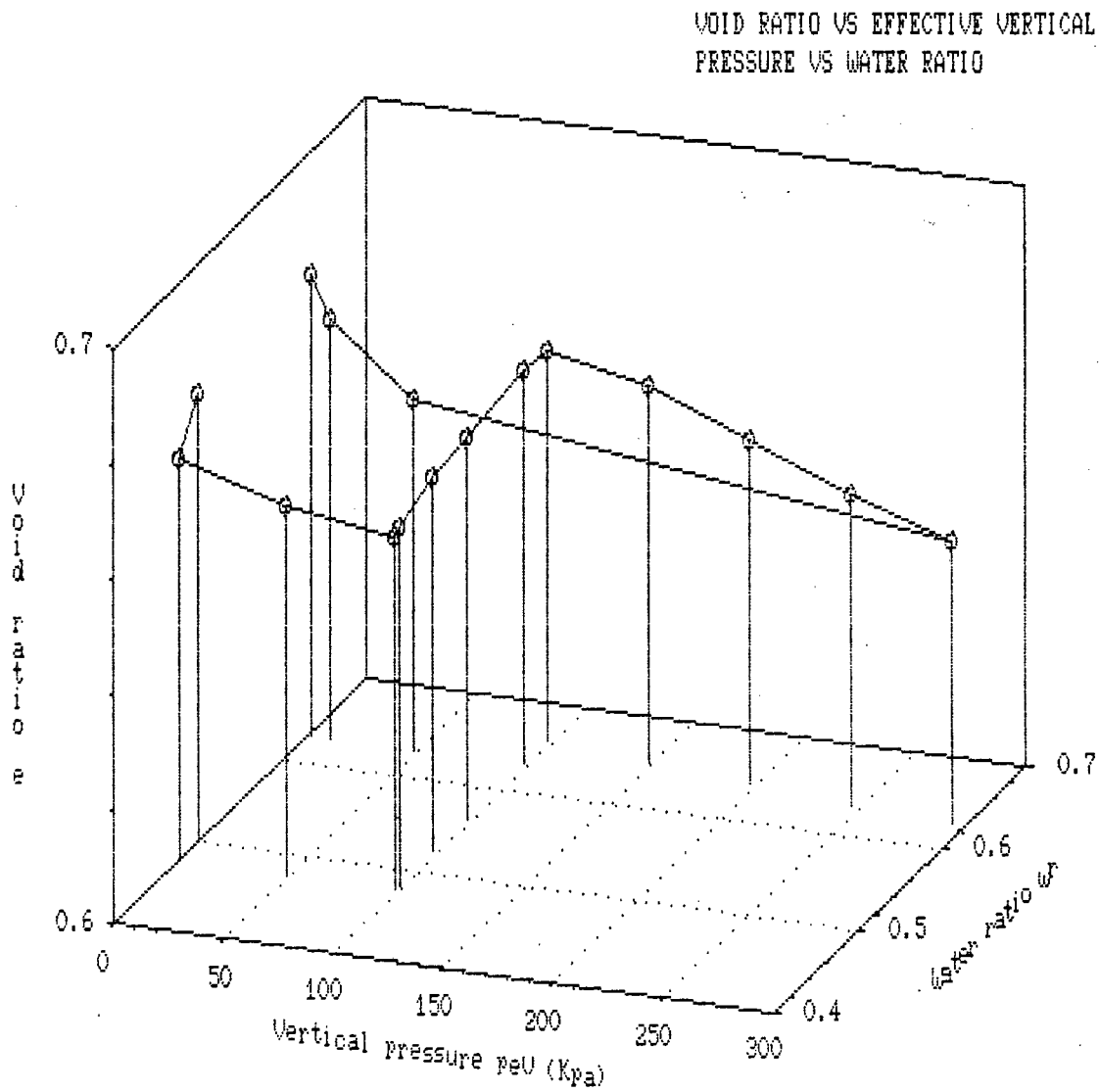

Figure 6.107: Site 36, Rondebosch - [Undisturbed, 100 Kpa] Void ratio 'e' vs effective vertical pressure 'peV' vs water ratio 'wr'.

Site 30, Hout Bay:-

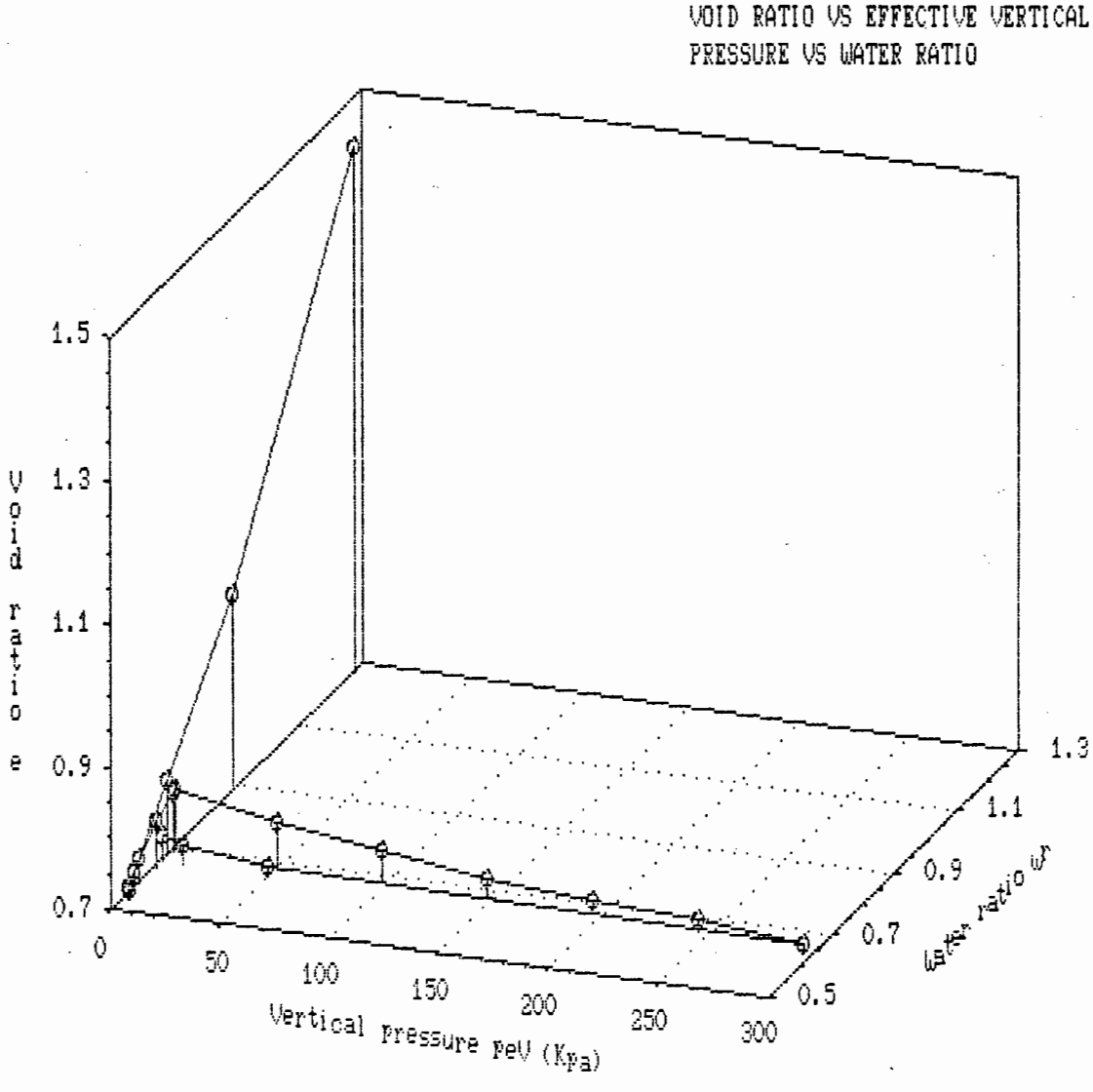

Figure 6.108: Site 30, Hout Bay - [Remoulded, 1 Kpa] Void ratio 'e' vs effective vertical pressure 'peV' vs water ratio 'wr'.

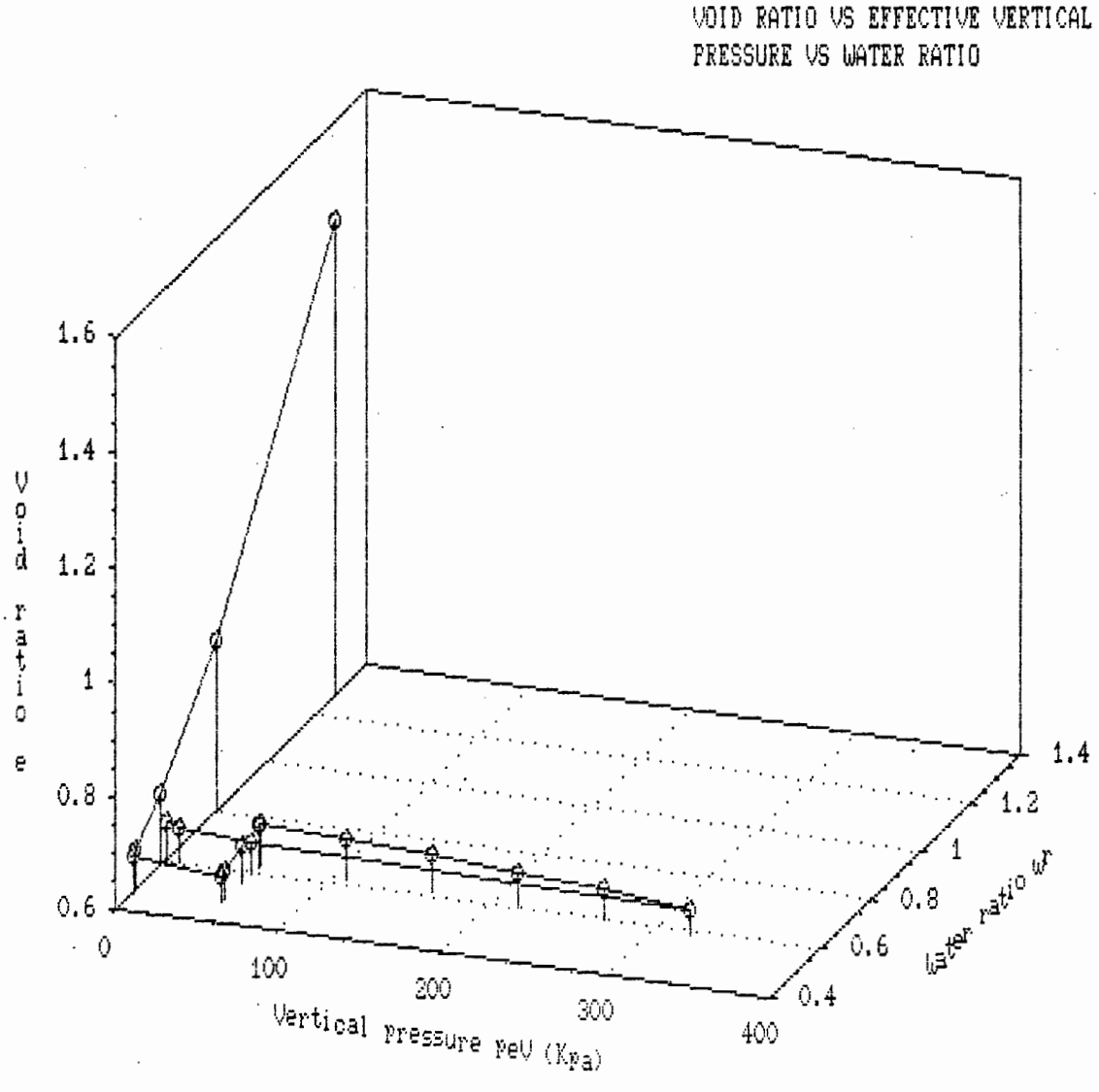

Figure 6.109: Site 30, Hout Bay - [Remoulded, 50 Kpa] Void ratio 'e' vs effective vertical pressure 'peV' vs water ratio 'wr'.

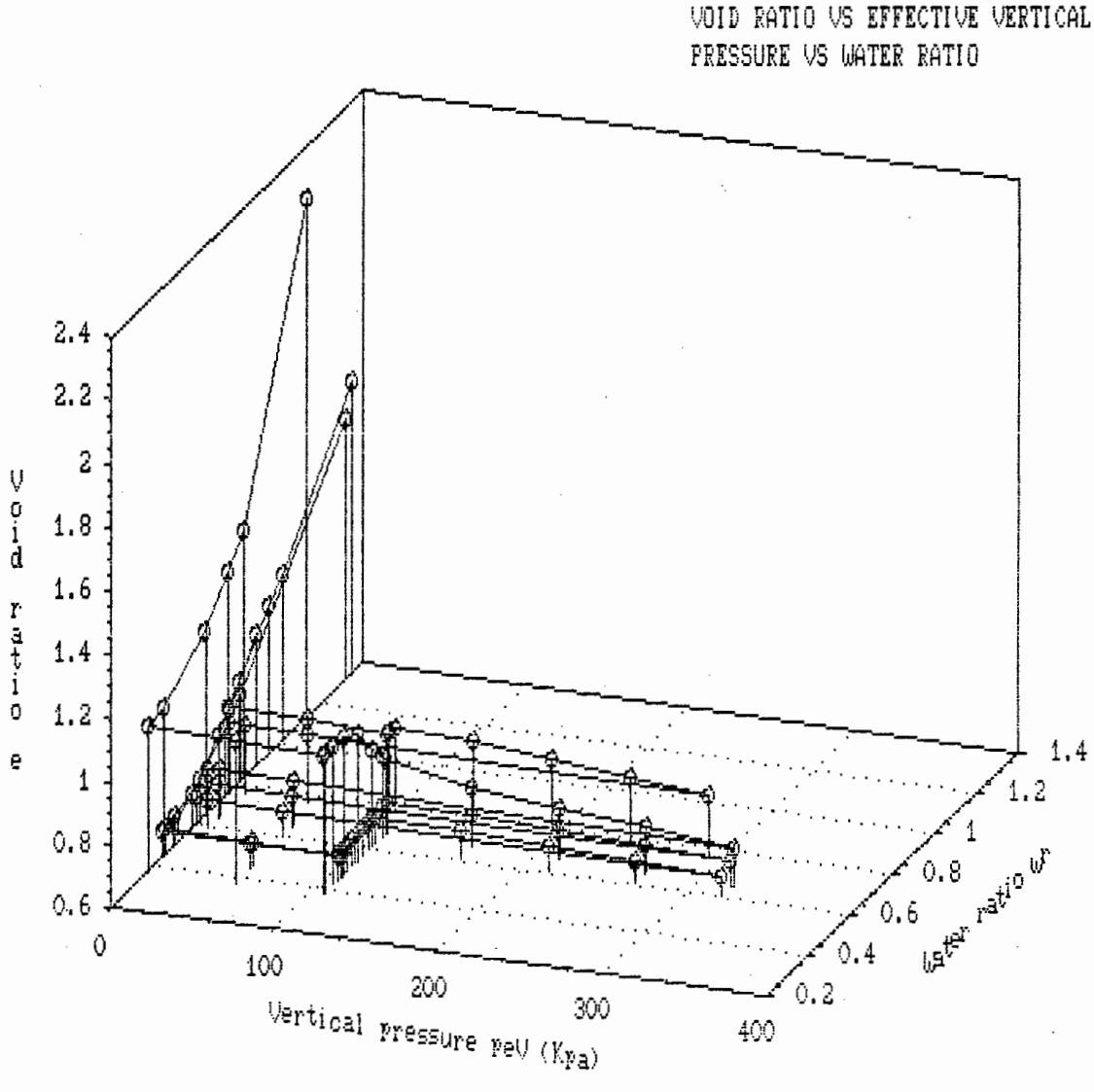

Figure 6.110: Site 30, Hout Bay - [Remoulded, 100 Kpa] Void ratio 'e' vs effective vertical pressure 'peV' vs water ratio 'wr'.

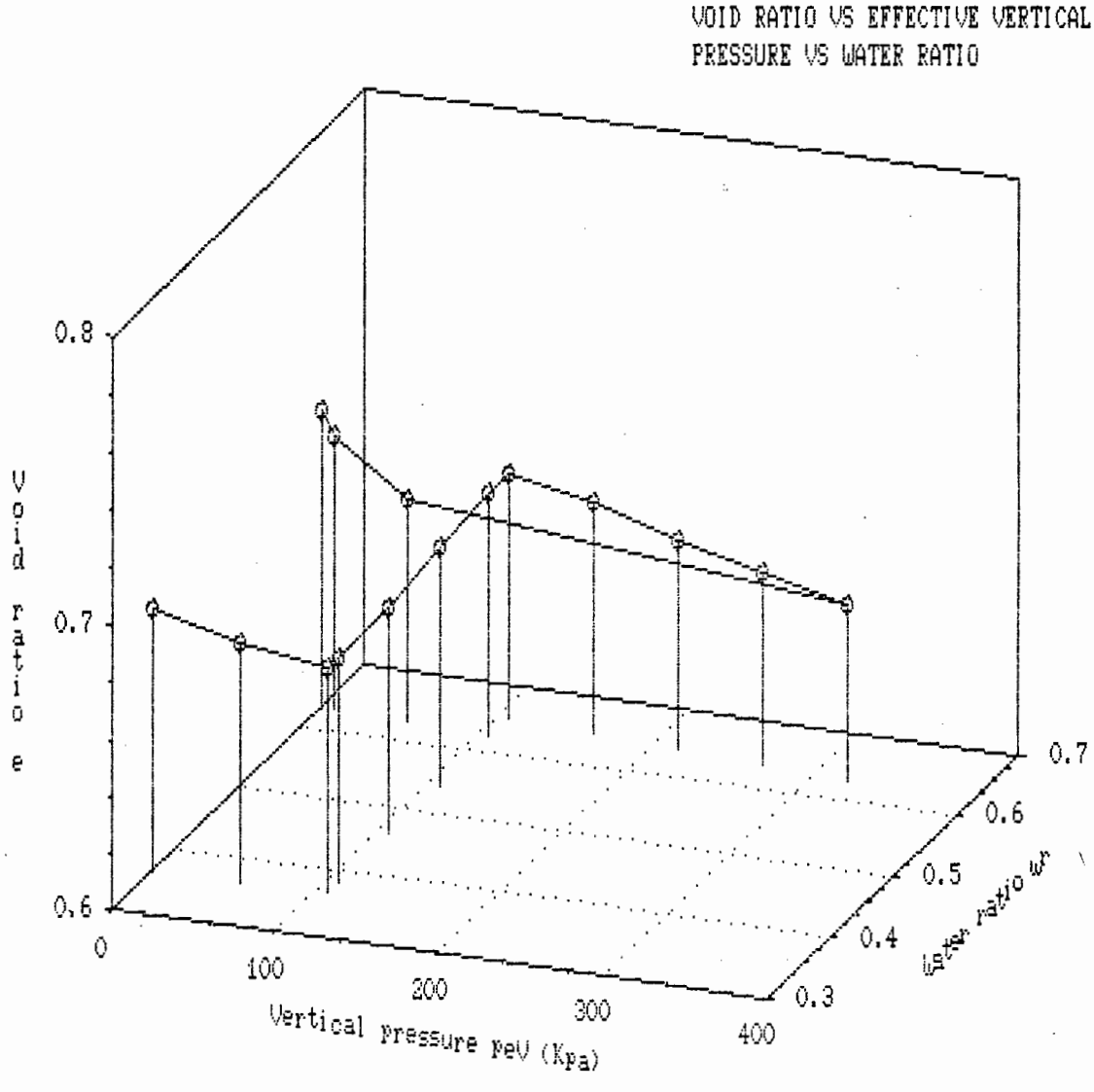

Figure 6.111: Site 30, Hout Bay - [Undisturbed, 100 Kpa] Void ratio 'e' vs effective vertical pressure 'peV' vs water ratio 'wr'.

Site A, Berea Road (Durban):-

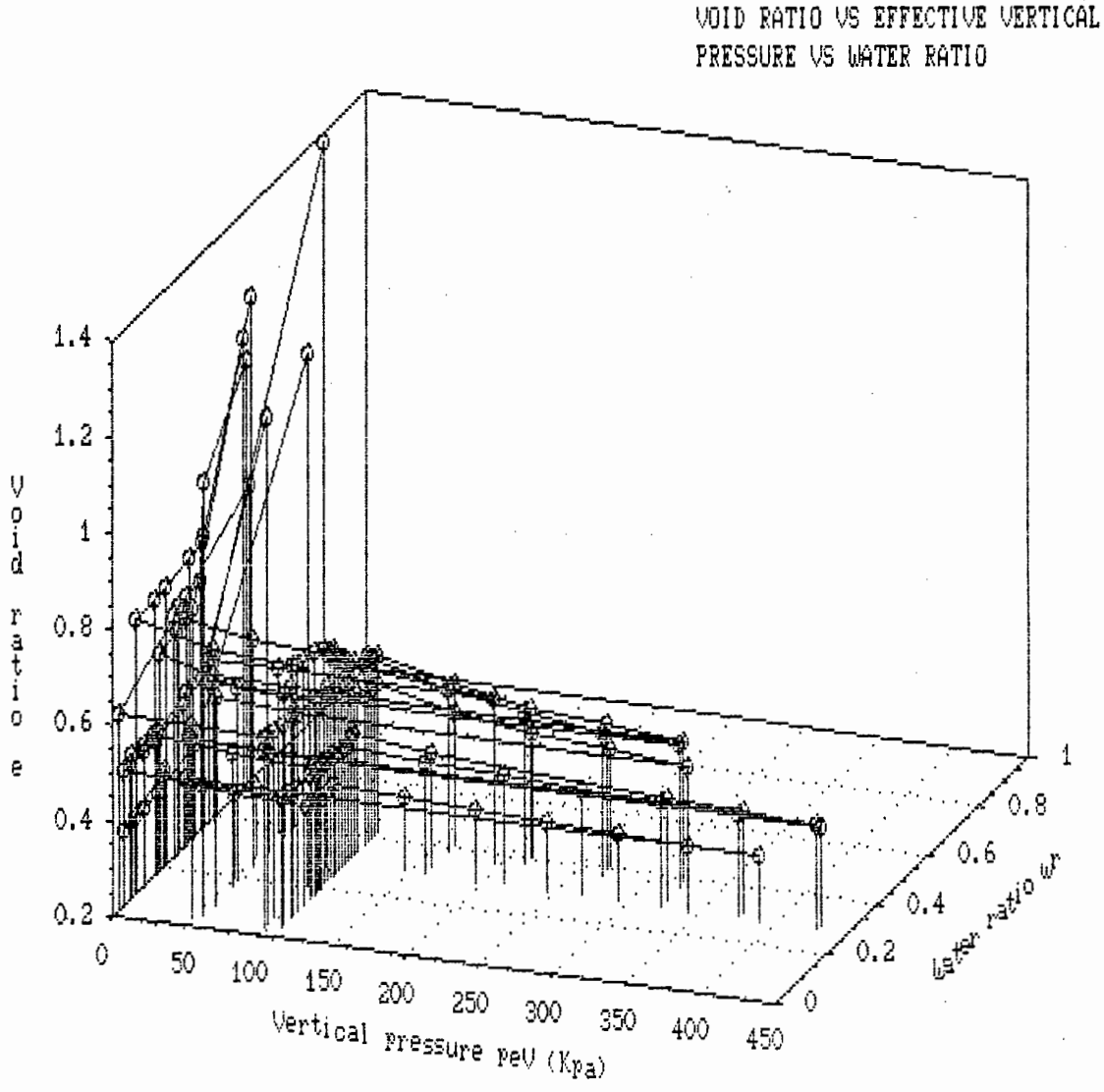

Figure 6.112: Site A, Berea Road (Durban) - [Remoulded, 100 Kpa] Void ratio 'e' vs effective vertical pressure 'peV' vs water ratio 'wr'.

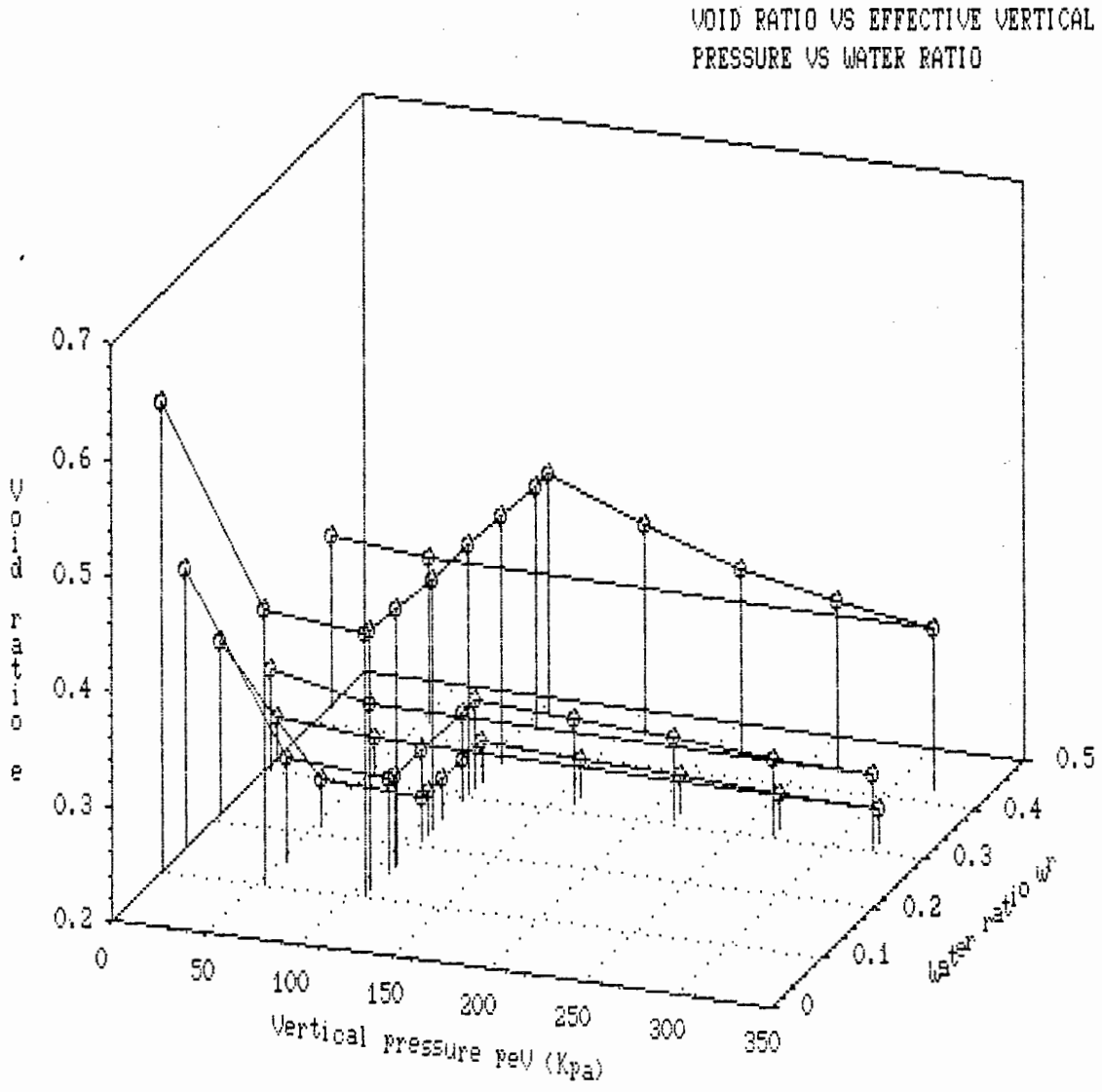

Figure 6.113: Site A, Berea Road (Durban) - [Compacted, 100 Kpa] Void ratio 'e' vs effective vertical pressure 'peV' vs water ratio 'wr'.

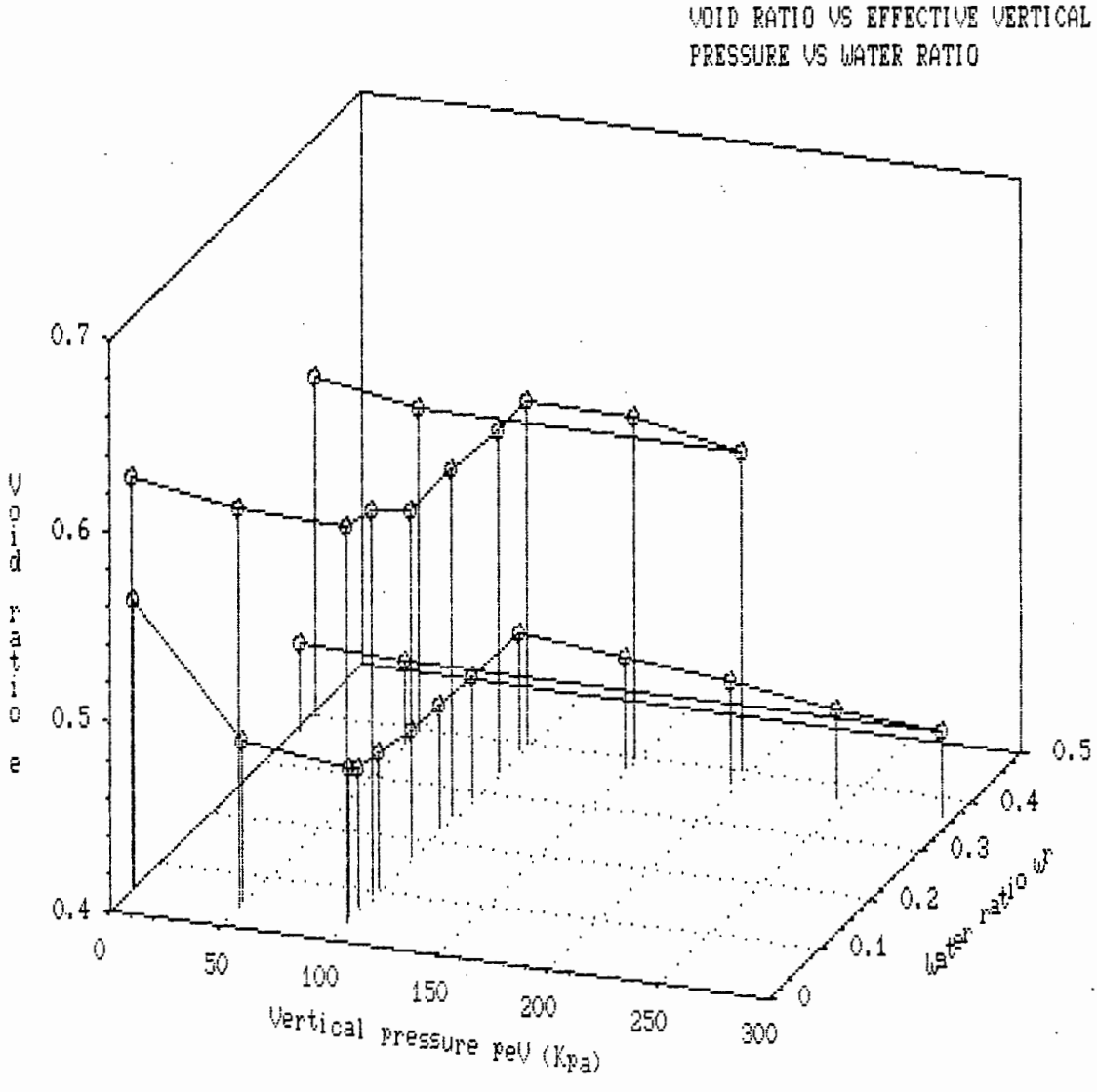

Figure 6.114: Site A, Berea Road (Durban) - [Undisturbed, 100 Kpa] Void ratio 'e' vs effective vertical pressure 'peV' vs water ratio 'wr'.

Site 7, Mowbray:-

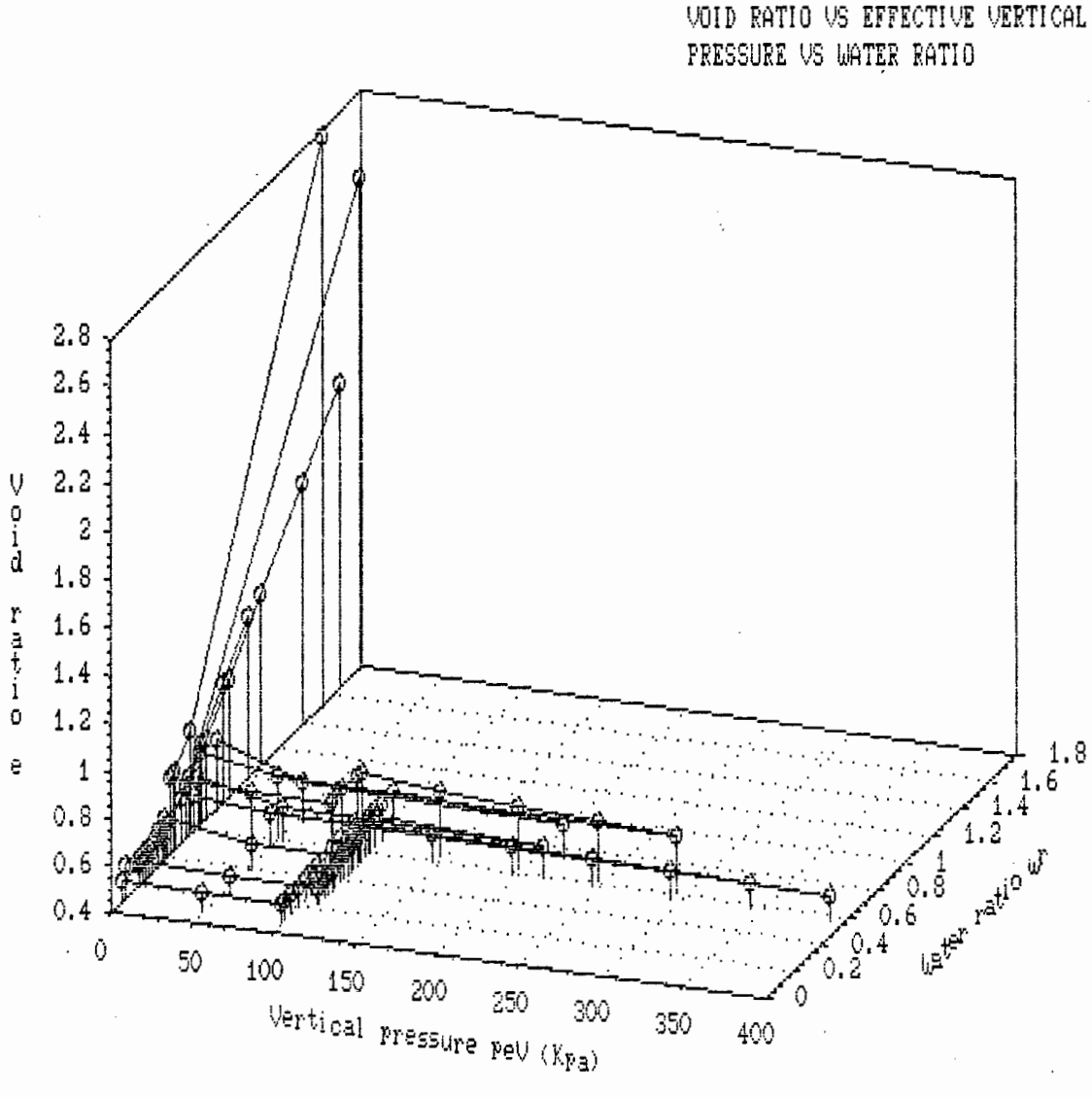

Figure 6.115: Site 7, Mowbray - [Remoulded, 100 Kpa] Void ratio 'e' vs effective vertical pressure 'peV' vs water ratio 'wr'.

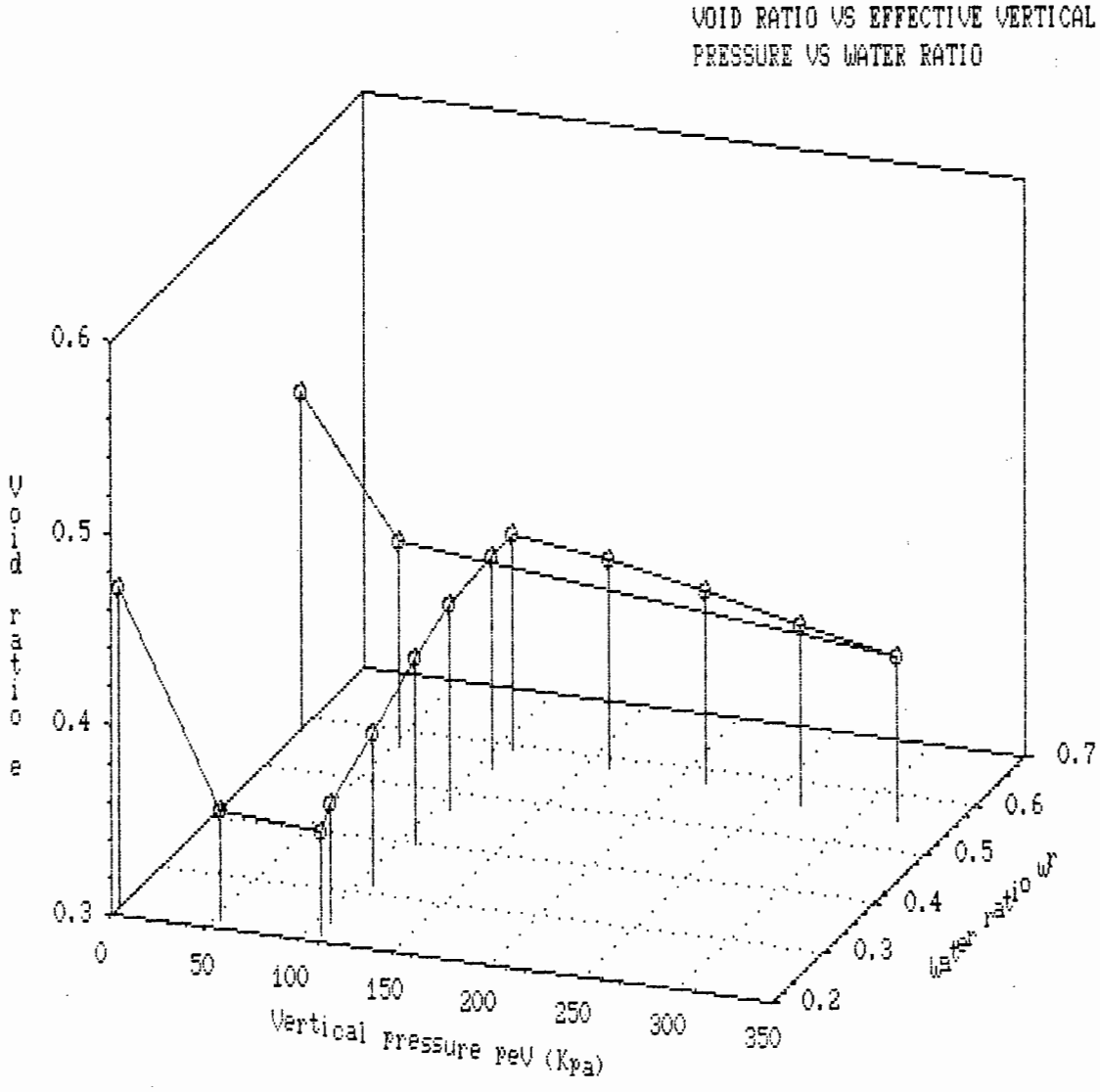

Figure 6.116: Site 7, Mowbray - [Compacted, 100 Kpa] Void ratio 'e' vs effective vertical pressure 'peV' vs water ratio 'wr'.

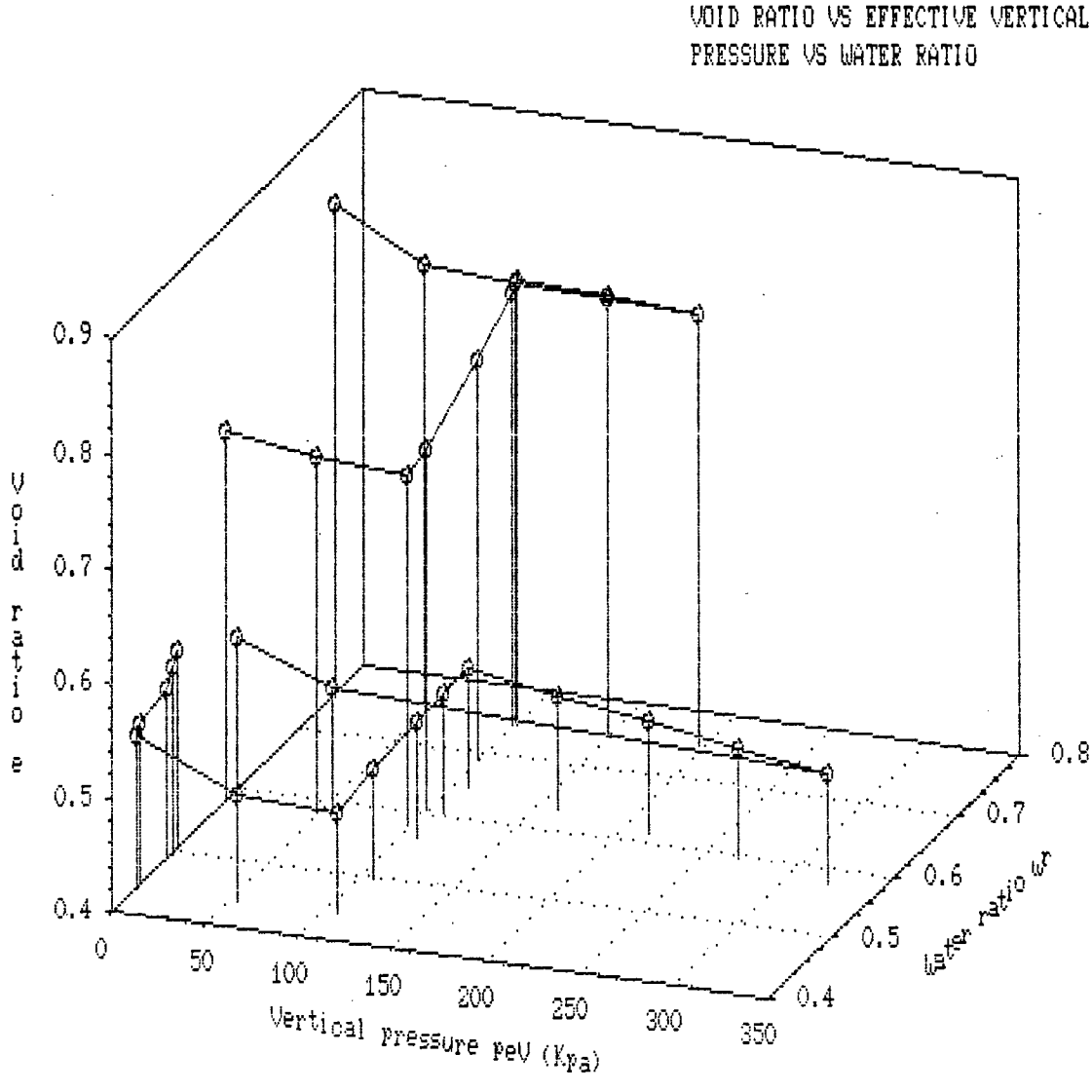

Figure 6.117: Site 7, Mowbray - [Undisturbed, 100 Kpa] Void ratio 'e' vs effective vertical pressure 'peV' vs water ratio 'wr'.

Site B, Francois Road (Durban):-

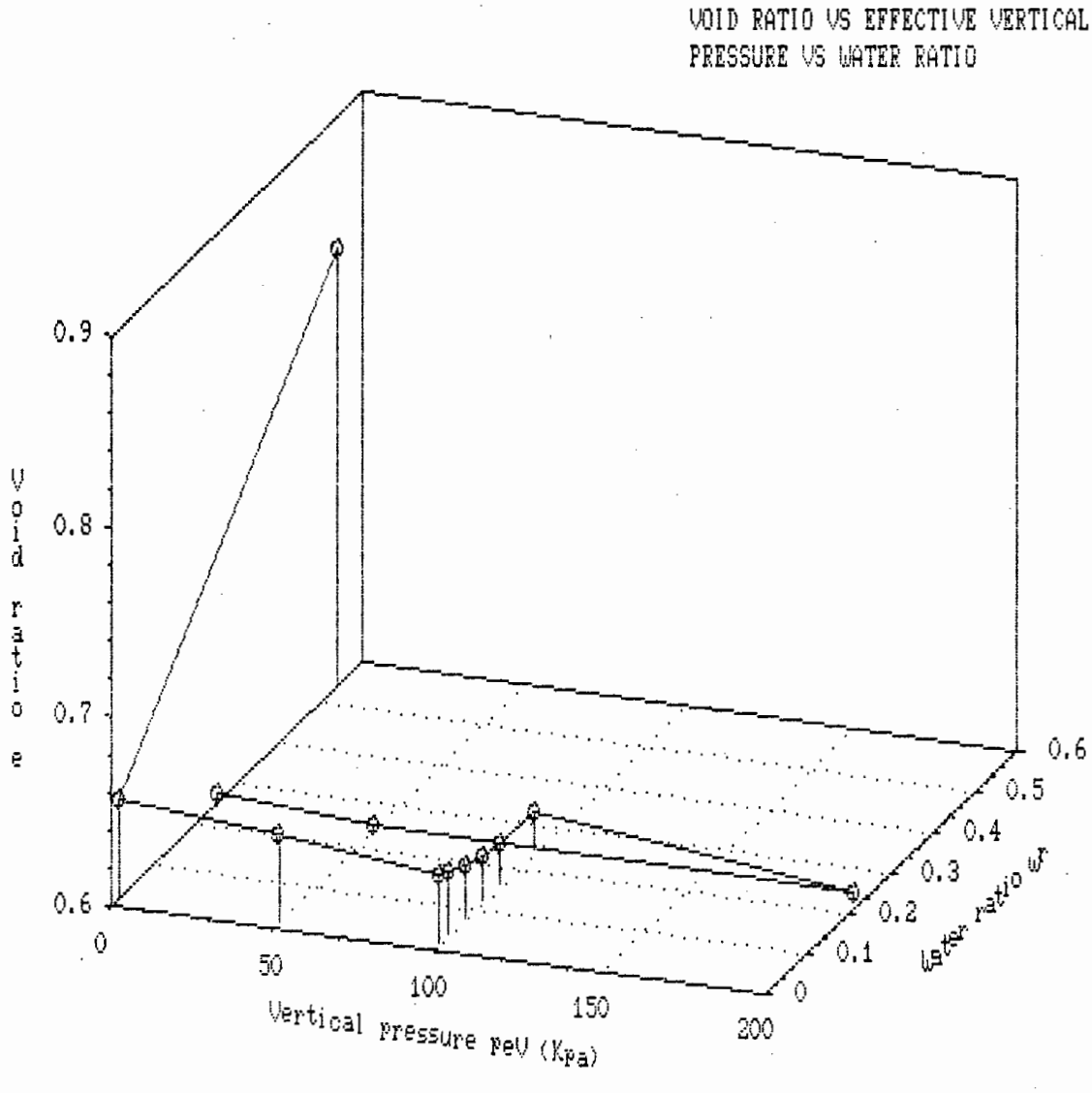

Figure 6.118: Site B, Francois Road (Durban) - [Remoulded, 100 Kpa] Void ratio 'e' vs effective vertical pressure 'peV' vs water ratio 'wr'.

Site C, Margaret Mayton Avenue (Durban):-

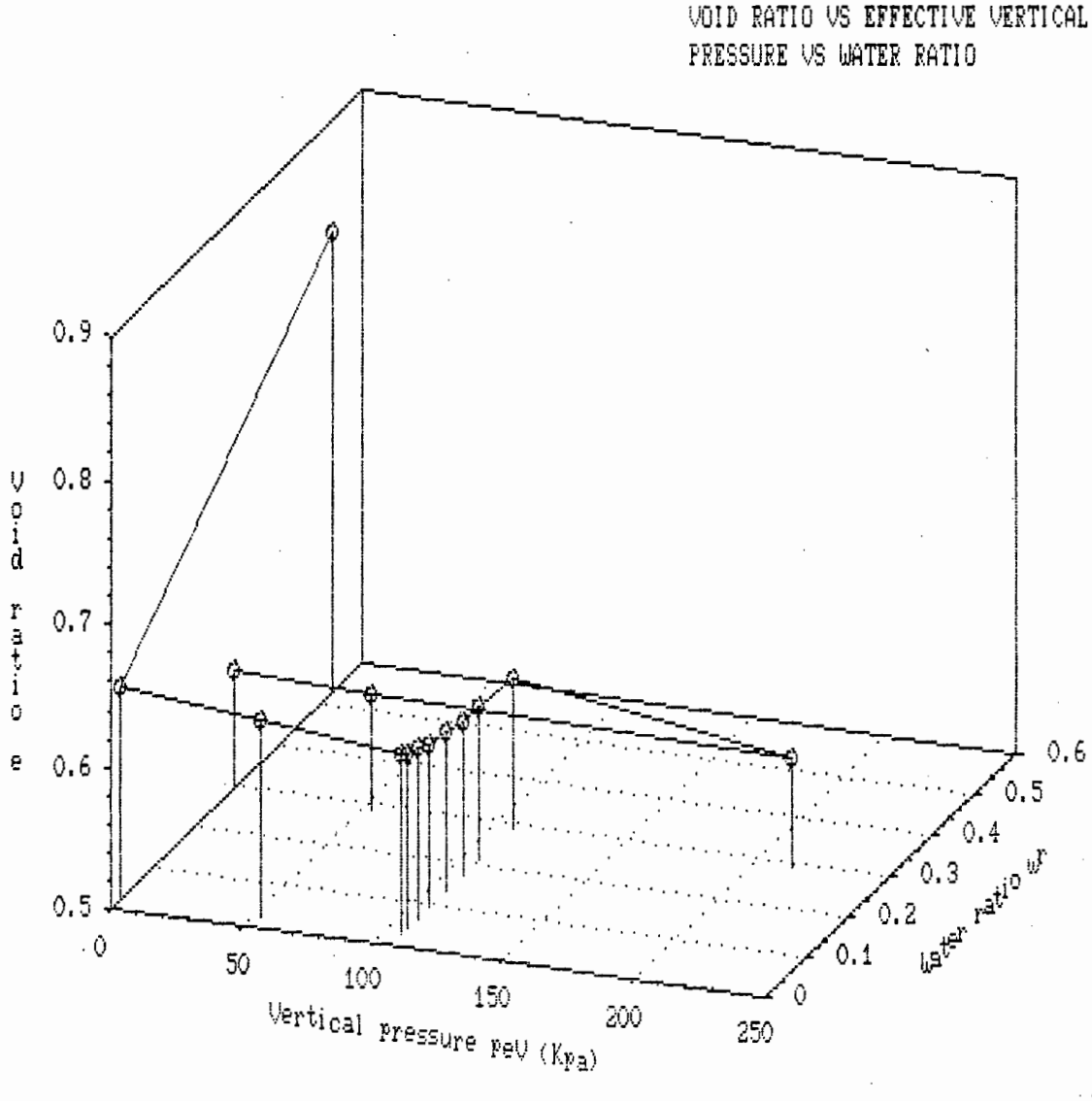

Figure 6.119: Site C, Margaret Mayton Avenue (Durban) - [Remoulded, 100 Kpa] Void ratio 'e' vs effective vertical pressure 'peV' vs water ratio 'wr'.

Site D, Rose Hill (Durban):-

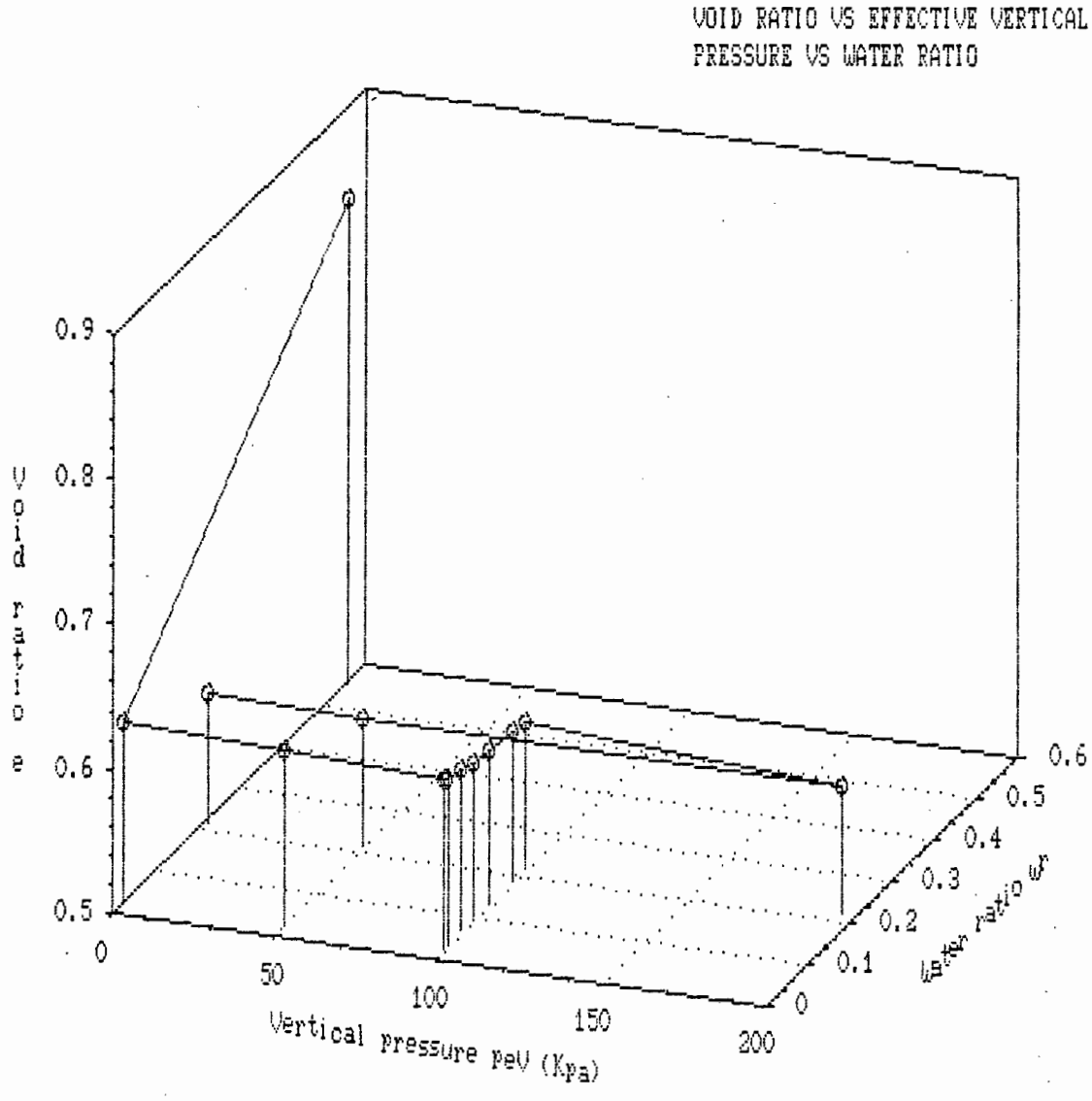

Figure 6.120: Site D, Rose Hill (Durban) - [Remoulded, 100 Kpa] Void ratio 'e' vs effective vertical pressure 'peV' vs water ratio 'wr'.

Site 48, Lady Grey District - Farm Unity (Natal):-

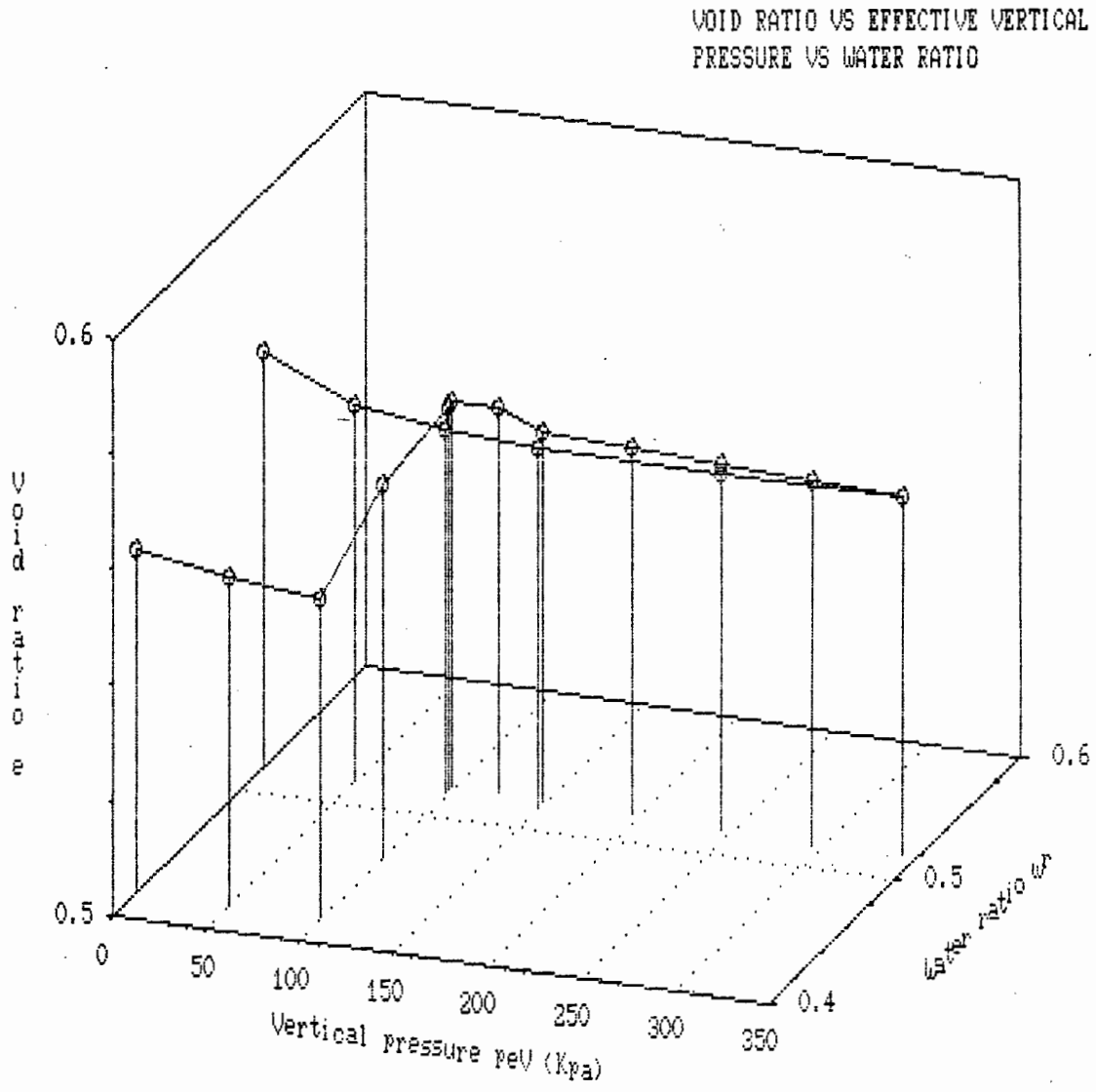

Figure 6.121: Site 48, Lady Grey (Natal) - [Undisturbed, 100 Kpa] Void ratio 'e' vs effective vertical pressure 'peV' vs water ratio 'wr'.

Artificial Soil Types.

Kaolin mixed with sand.

Kaolin K.1:-

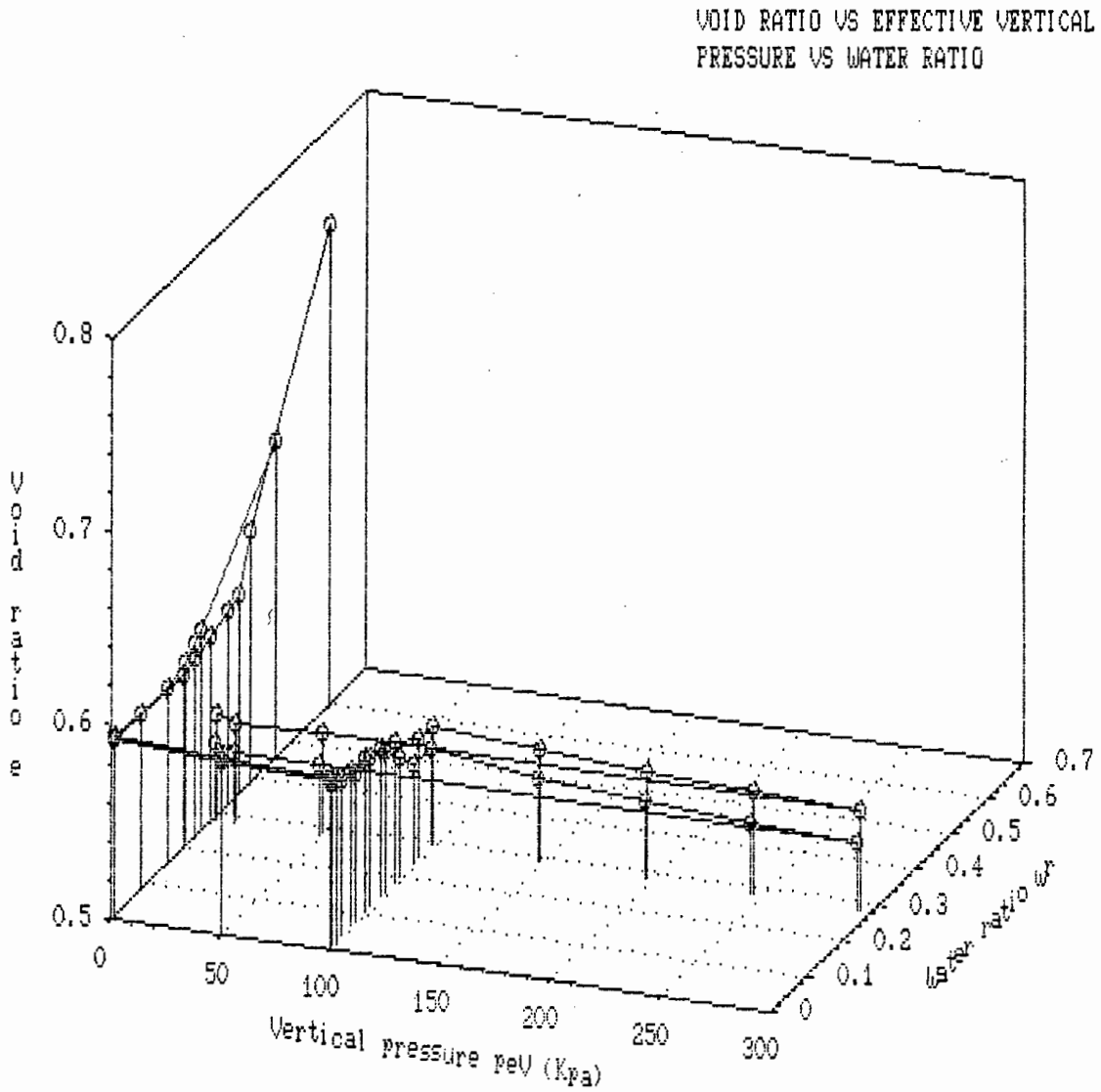

Figure 6.122: Kaolin K.1 (13% clay size) - [100 Kpa] Void ratio 'e' vs effective vertical pressure 'peV' vs water ratio 'wr'.

Kaolin K.2:-

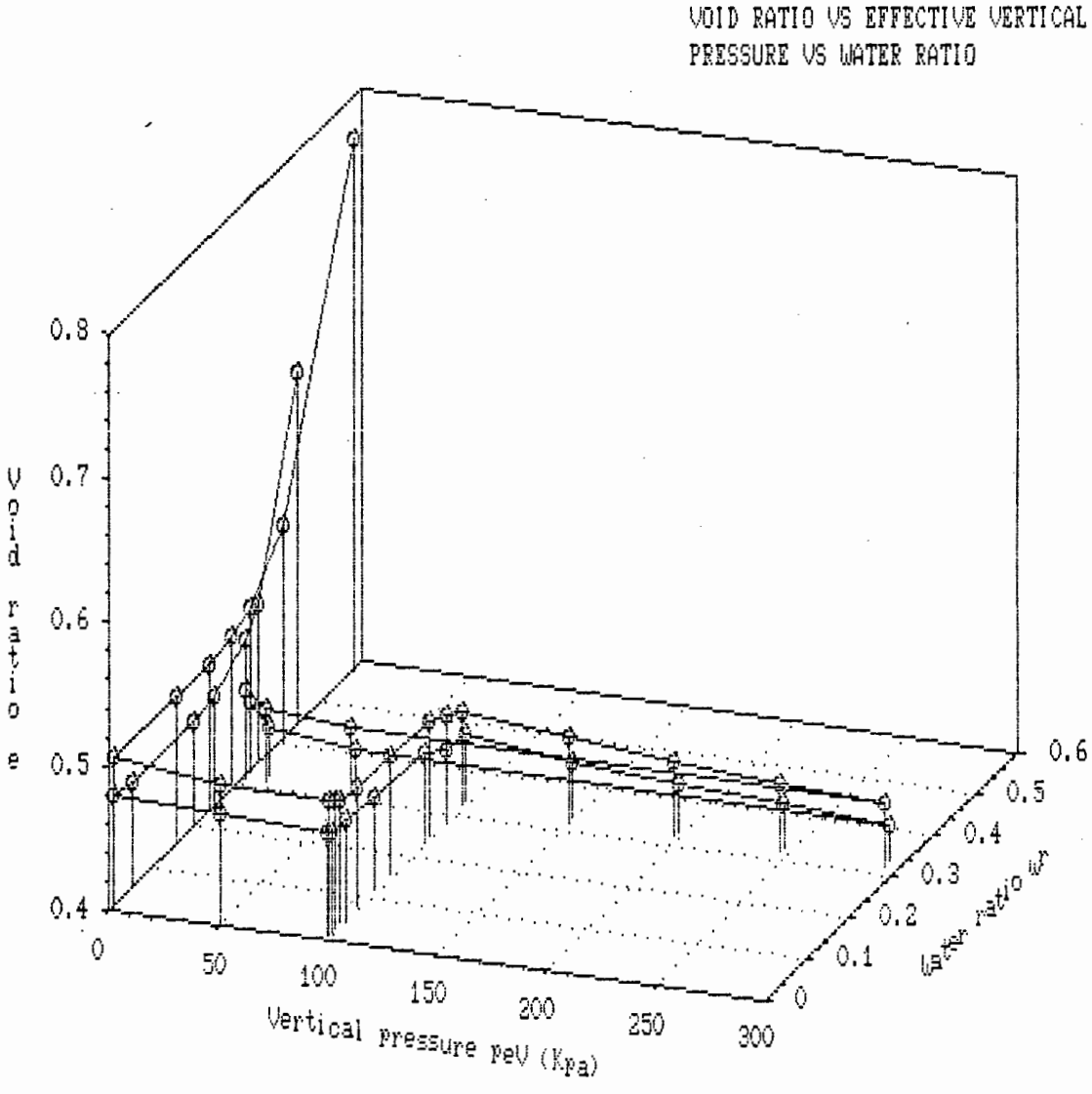

Figure 6.123: Kaolin K.2 (20% clay size) - [100 Kpa] Void ratio 'e' vs effective vertical pressure 'peV' vs water ratio 'wr'.

Kaolin K.3:-

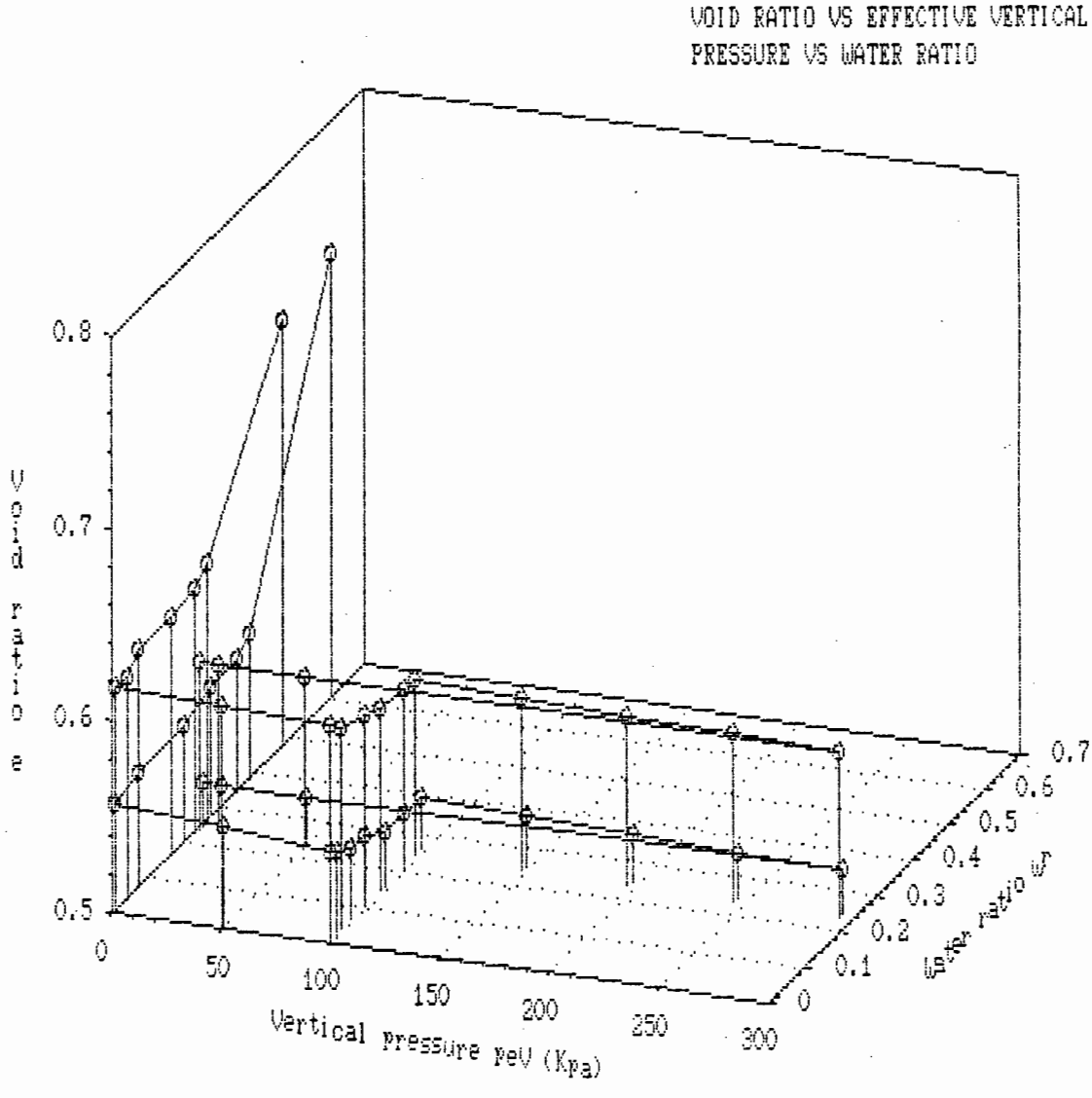

Figure 6.124: Kaolin K.3 (8.5% clay size) - [100 Kpa] Void ratio 'e' vs effective vertical pressure 'peV' vs water ratio 'wr'.

Bentonite clay mixed with sand.

Bentonite B.1:-

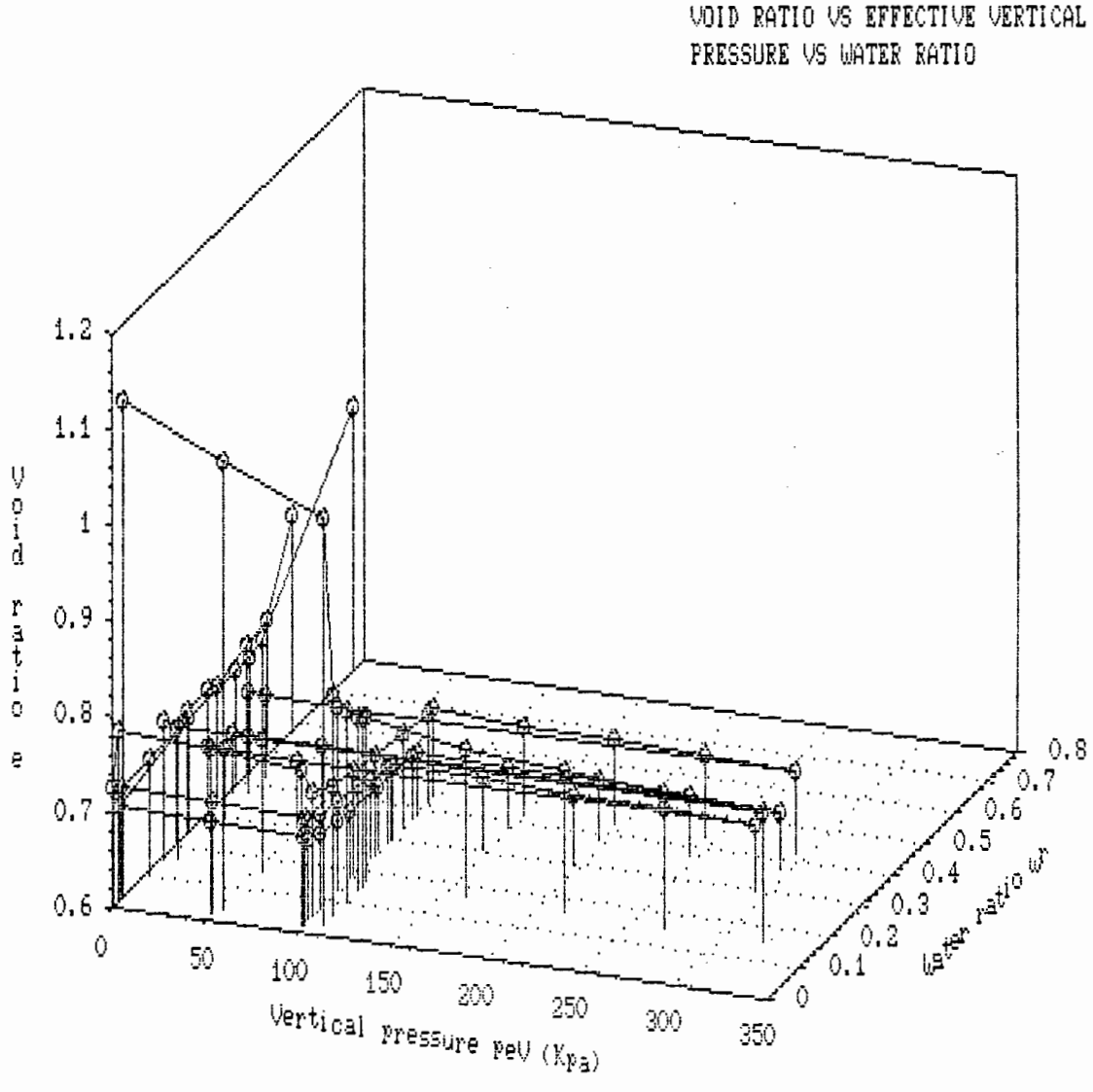

Figure 6.125: Bentonite B.1 (3.5% clay size) - [100 Kpa] Void ratio 'e' vs effective vertical pressure 'peV' vs water ratio 'wr'.

Bentonite B.2:-

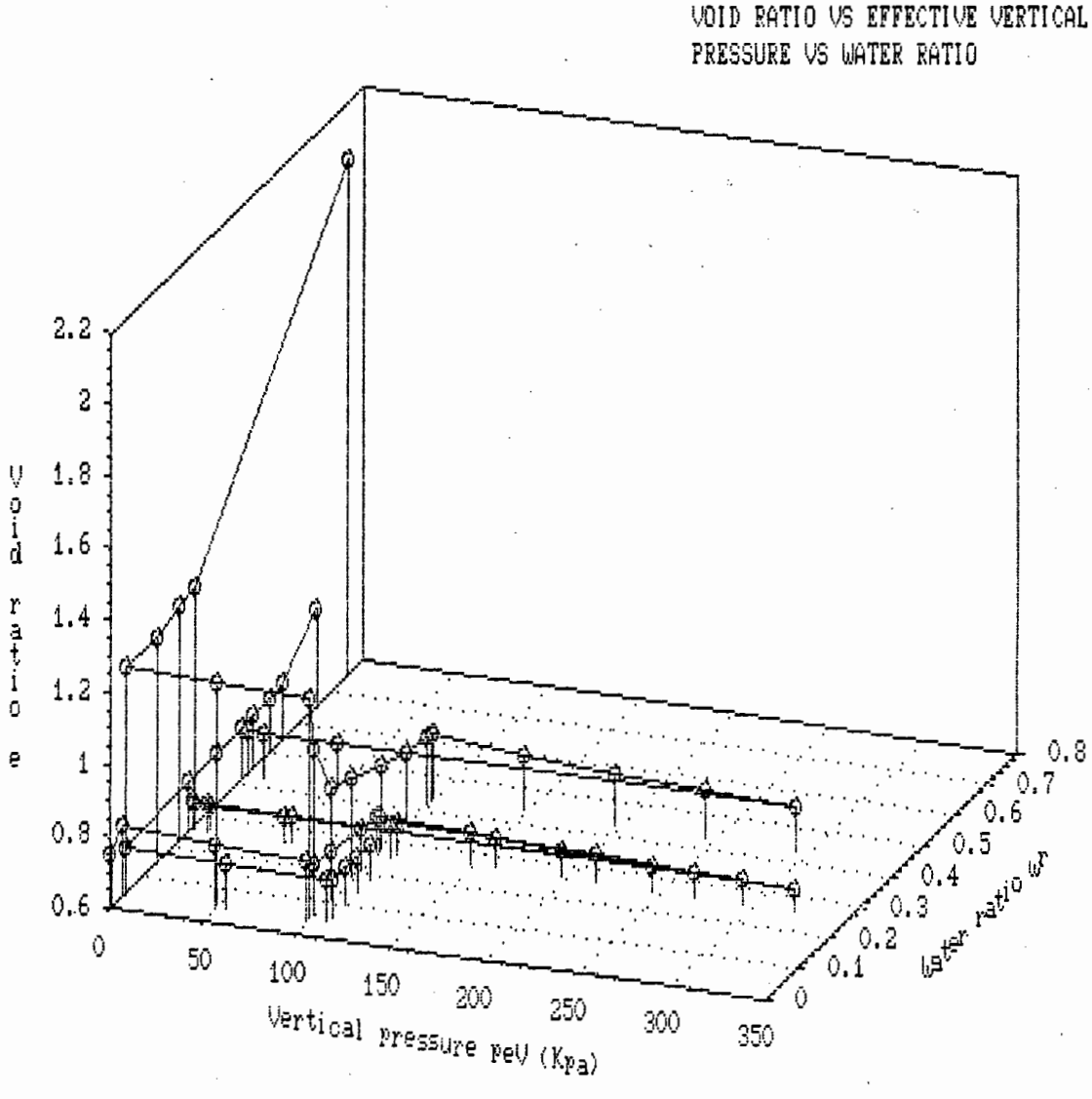

Figure 6.126: Bentonite B.2 (7% clay size) - [100 Kpa] Void ratio 'e' vs effective vertical pressure 'peV' vs water ratio 'wr'.

Bentonite B.3:-

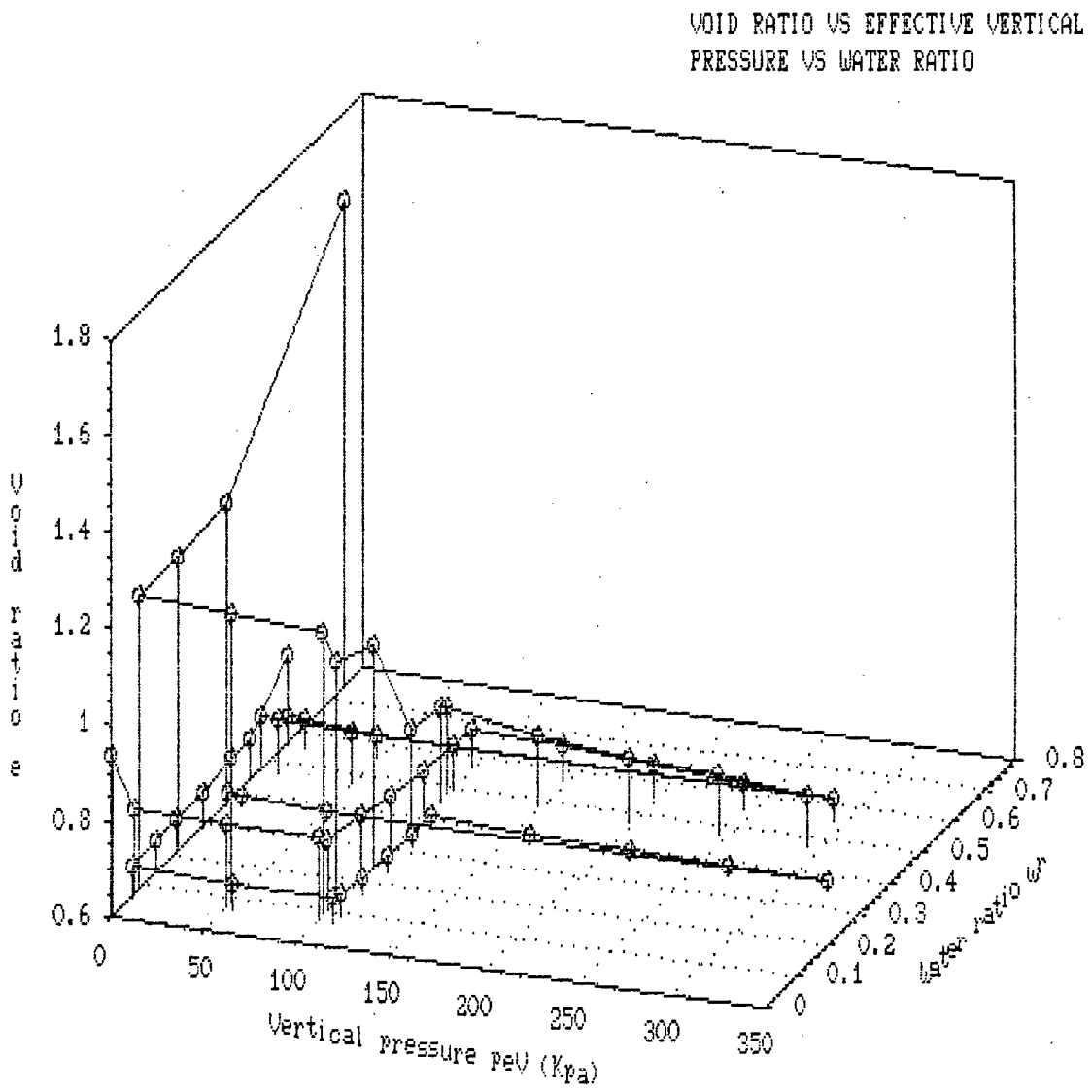

Figure 6.127: Bentonite B.3 (11.5% clay size) - [100 Kpa] Void ratio 'e' vs effective vertical pressure 'peV' vs water ratio 'wr'.

Bentonite B.4:-

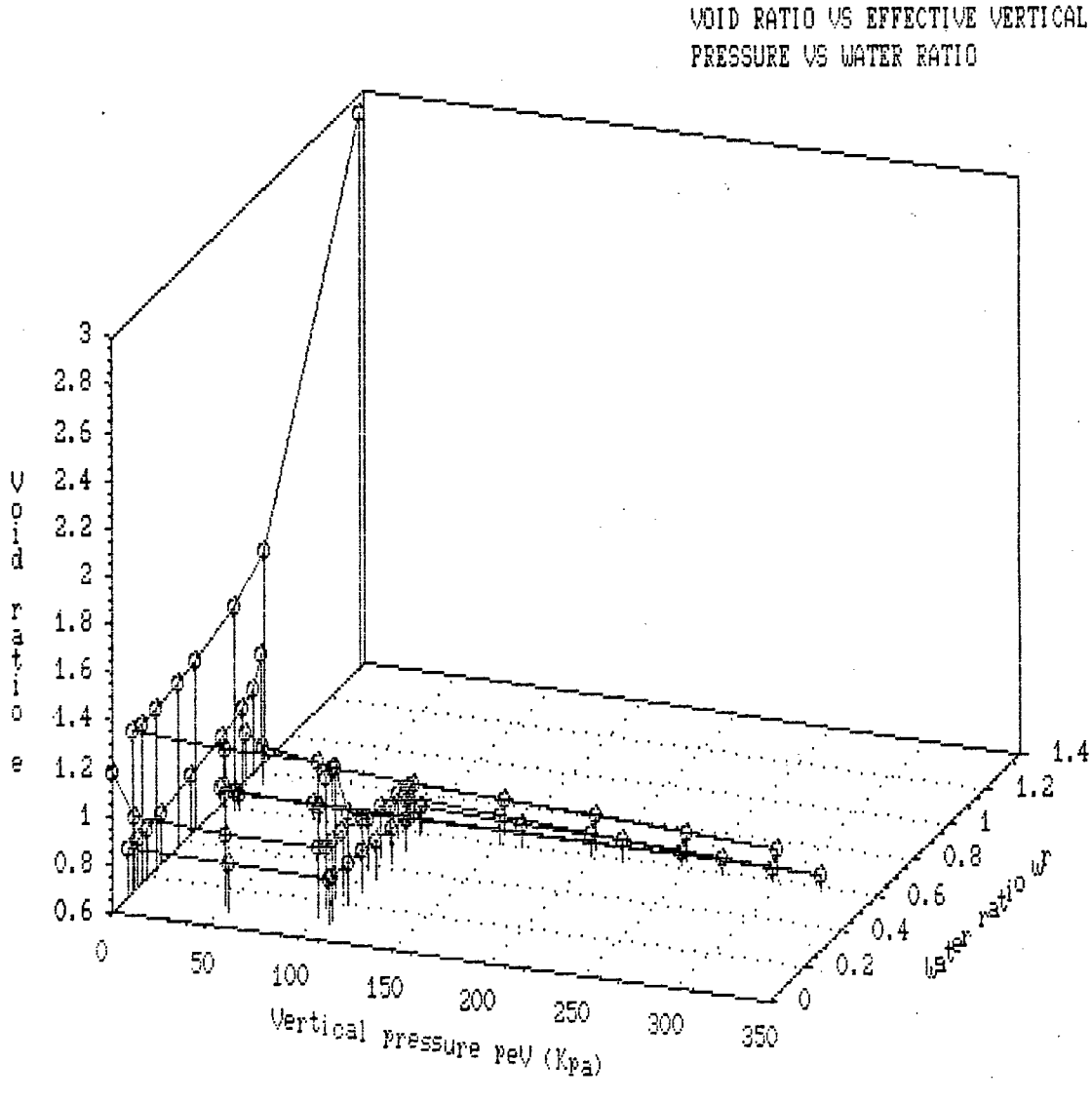

Figure 6.128: Bentonite B.4 (15.5% clay size) - [100 Kpa] Void ratio 'e' vs effective vertical pressure 'peV' vs water ratio 'wr'.

Bentonite B.5:-

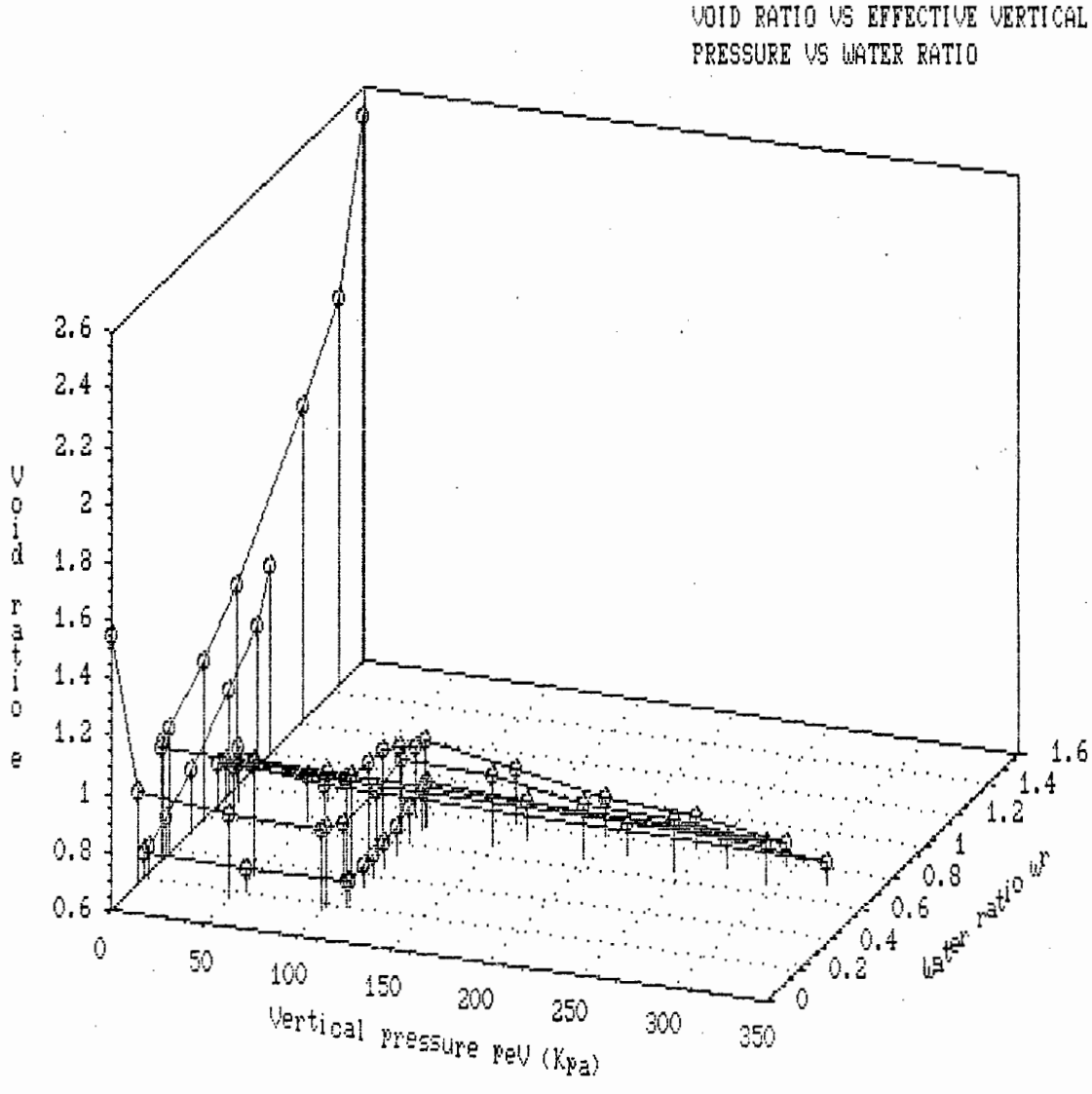

Figure 6.129: Bentonite B.5 (35% clay size) - [100 Kpa] Void ratio 'e' vs effective vertical pressure 'peV' vs water ratio 'wr'.

6.10 CONCLUSIONS FOR CHAPTER SIX

The work in this chapter dealt with the observed one-dimensional increase[1] or decrease[2] in volume of the soil sample. The type of one-dimensional increase or decrease behaviour which was investigated, under controlled wetting conditions, refers specifically to test samples which are confined in the horizontal direction and are allowed to increase[1] or decrease[2] their volume along the vertical axis while being subjected to a known vertical pressure.

Relationships between Water Content, before wetting, and Percentage Volume Change, after wetting, were determined from the observed water contents, void ratios, as well as the vertical pressures applied.
Plots of initial water content versus percentage volume change, are used to show the relationship between these two parameters. Each plotted series of values also includes the initial void ratio before wetting.
These plots have been combined for each similar range of applied pressures - they are grouped under remoulded, compacted or undisturbed samples.

Expansive and/or collapse behaviour patterns are included for the following soil types:-

Natural soil types.

(i) Site 11, Rosebank - Remoulded samples, compacted samples, and undisturbed samples.
(ii) Site 36, Rondebosch - Remoulded, compacted and undisturbed samples.
(iii) Site 30, Hout Bay - Remoulded and undisturbed samples.
(iv) Site A, Berea Road - Remoulded, compacted, and undisturbed samples.
(v) Site 7, Mowbray - Remoulded, compacted and undisturbed samples.
(vi) Sites 'B', Francois Road 'C', Margaret Mayton Avenue, and 'D', Rose Hill - Remoulded samples.
(vii) Site 48, Lady Grey - Remoulded sample.

Artificial soil types.

(viii) Kaolin K.1 (13% clay size), Kaolin K.2 (20% clay size), and Kaolin K.3 (8.5% clay size); - Remoulded samples.
(ix) Bentonite B.1 (3.5% clay size), Bentonite B.2 (7% clay size), Bentonite B.3 (11.5% clay size), Bentonite B.4 (15.5% clay size), Bentonite B.5 (35% clay size); - Remoulded samples.

---

[1] - *expansion.*
[2] - *collapse settlement.*

6.10.1 Site 11, Rosebank - Expansion or Collapse of samples due to wetting.

Remoulded samples: *Applied pressure of 0.8 - 1 Kpa.*

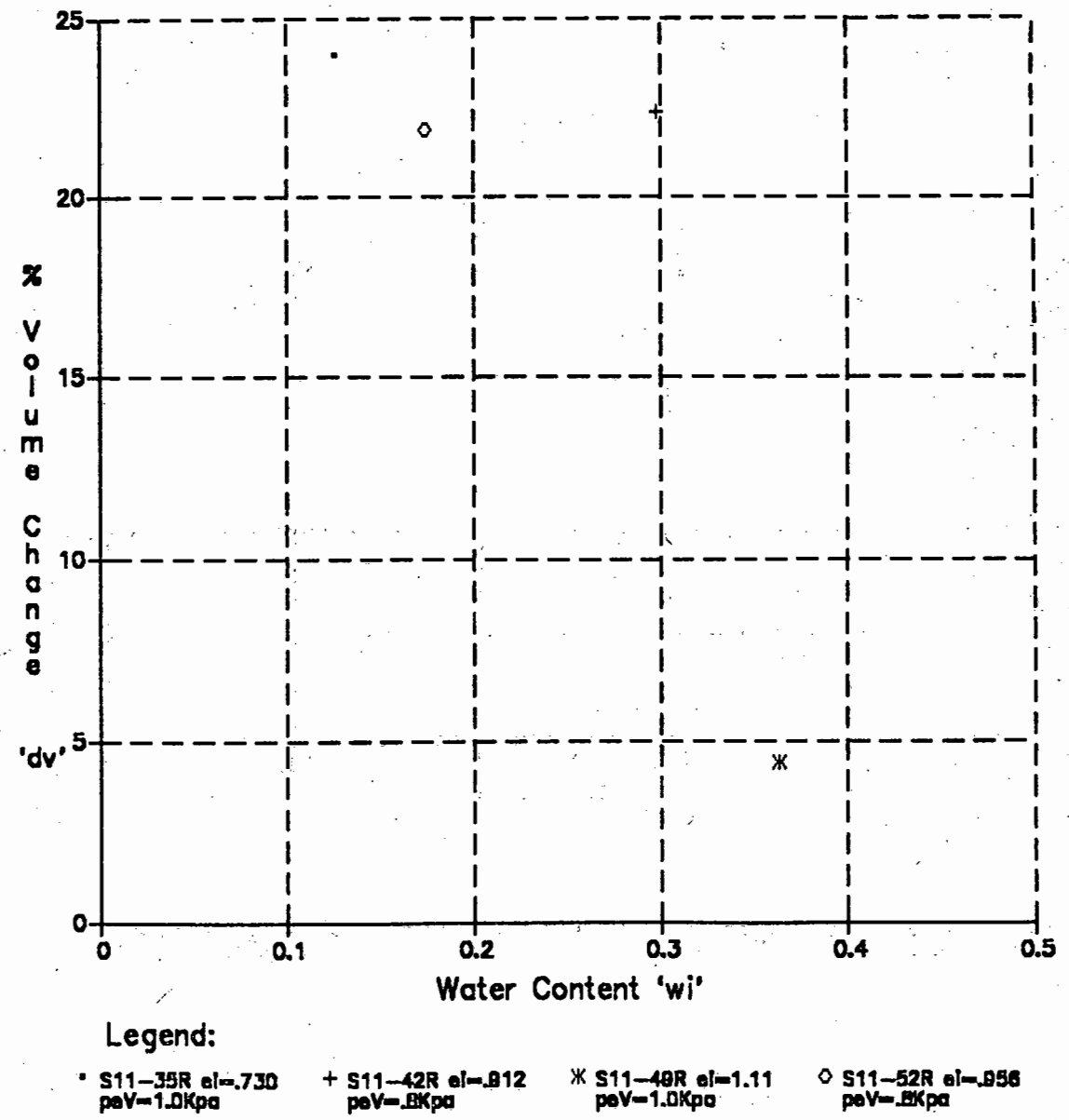

Figure 6.130: Site 11, Rosebank [Remoulded 0.8 - 1 Kpa] - Relationship between Water Content 'w_i', before wetting, and Percentage Volume Change, after wetting.

Applied pressures of 98.1 - 109.9 Kpa.

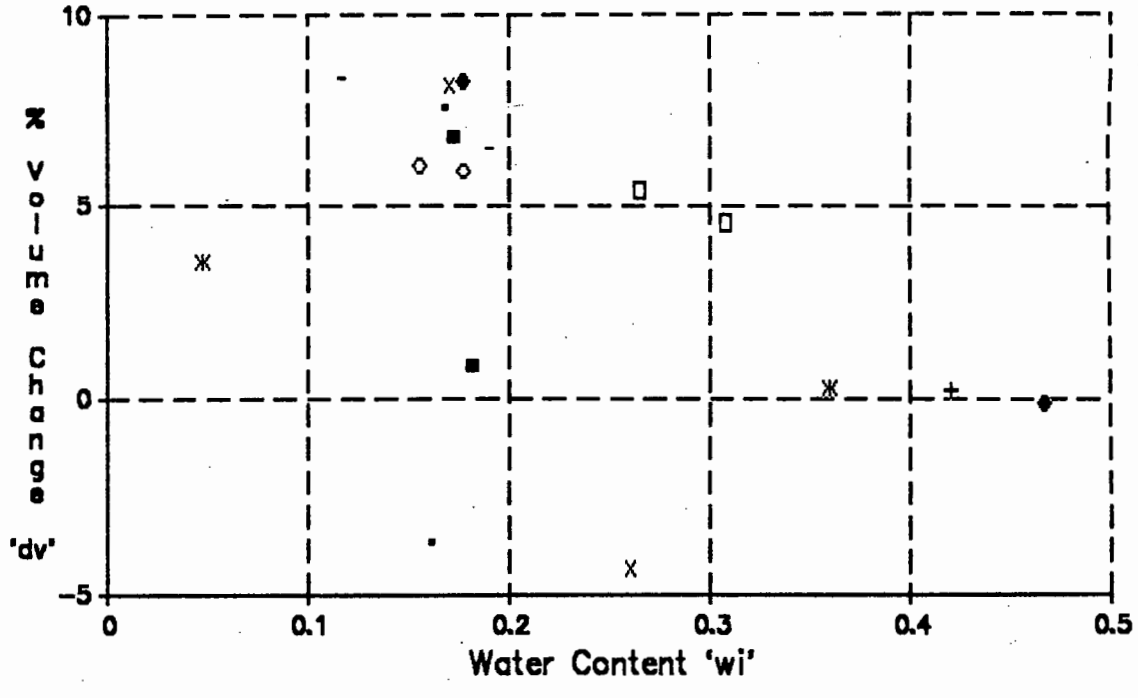

Legend:

S11−1R el=.816 peV=98.1Kpa
S11−4R el=.692 peV=98.1Kpa
S11−11R el=.688 peV=98.1
S11−23R el=.71 peV=98.1Kpa
S11−25R el=.731 peV=107.3Kpa
S11−33 el=.919 peV=107.3Kpa
S11−38R el=.754 peV=107.3Kpa
S11−43R el=.71 peV=107.3Kpa
S11−46R el=1.248 peV=107.3Kpa
S11−48R el=1.084 peV=107.3Kpa
S11−54R el=.826 peV=98.1Kpa
S11−57R el=1.194 peV=98.1Kpa
S11−62R el=.718 peV=108.4Kpa
S11−61R el=1.090 peV=109.9Kpa
S11−60R el=.812 peV=108.7Kpa
S11−59R el=.73 peV=108.4Kpa
S11−58R el=.161 peV=109.0Kpa

Figure 6.132: Site 11, Rosebank [Remoulded 98.1 - 109.9 Kpa] - Relationship between Water Content 'w_i', before wetting, and Percentage Volume Change, after wetting.

Applied pressures of 392.3 - 433.7 Kpa.

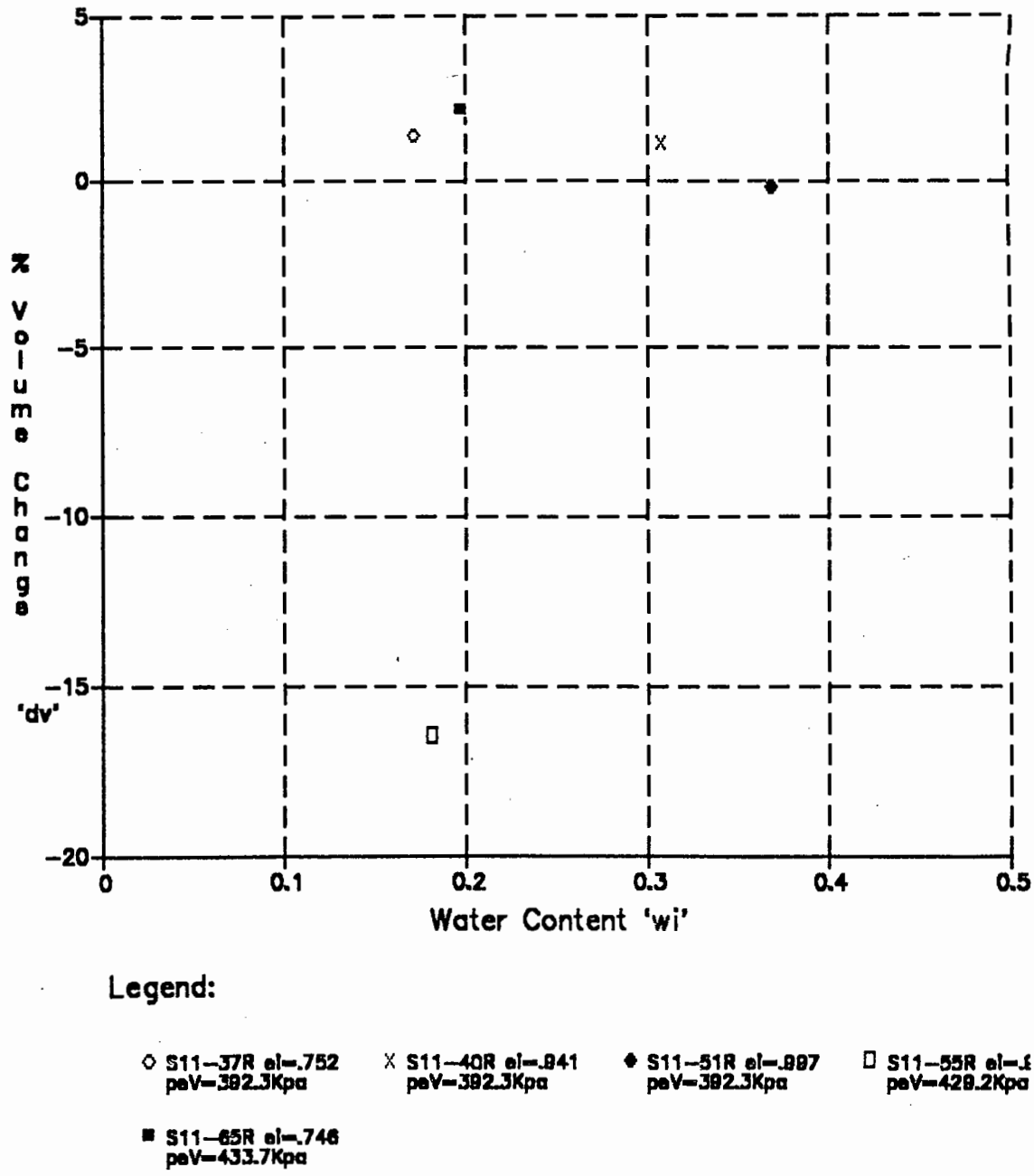

Figure 6.133: Site 11, Rosebank [Remoulded 392.3 - 433.7 Kpa] - Relationship between Water Content 'w_i', before wetting, and Percentage Volume Change, after wetting.

Compacted samples: *Applied pressures of 107.3 - 108.4 Kpa.*

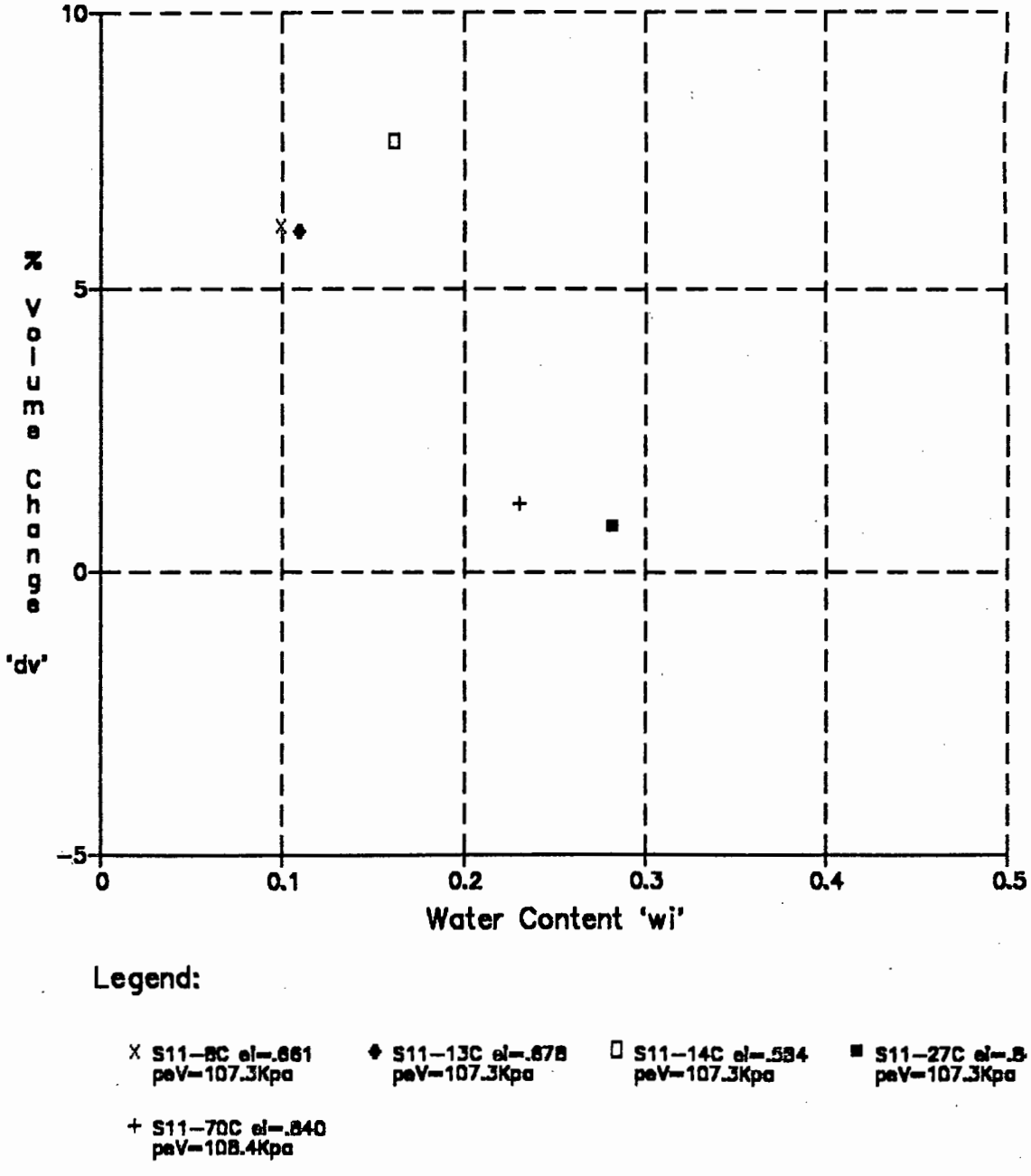

Figure 6.134: Site 11, Rosebank [Compacted 107.3 - 108.4 Kpa] - Relationship between Water Content 'w_i', before wetting, and Percentage Volume Change, after wetting.

Undisturbed samples: *Applied pressures of 98.1 - 107.3 Kpa:-*

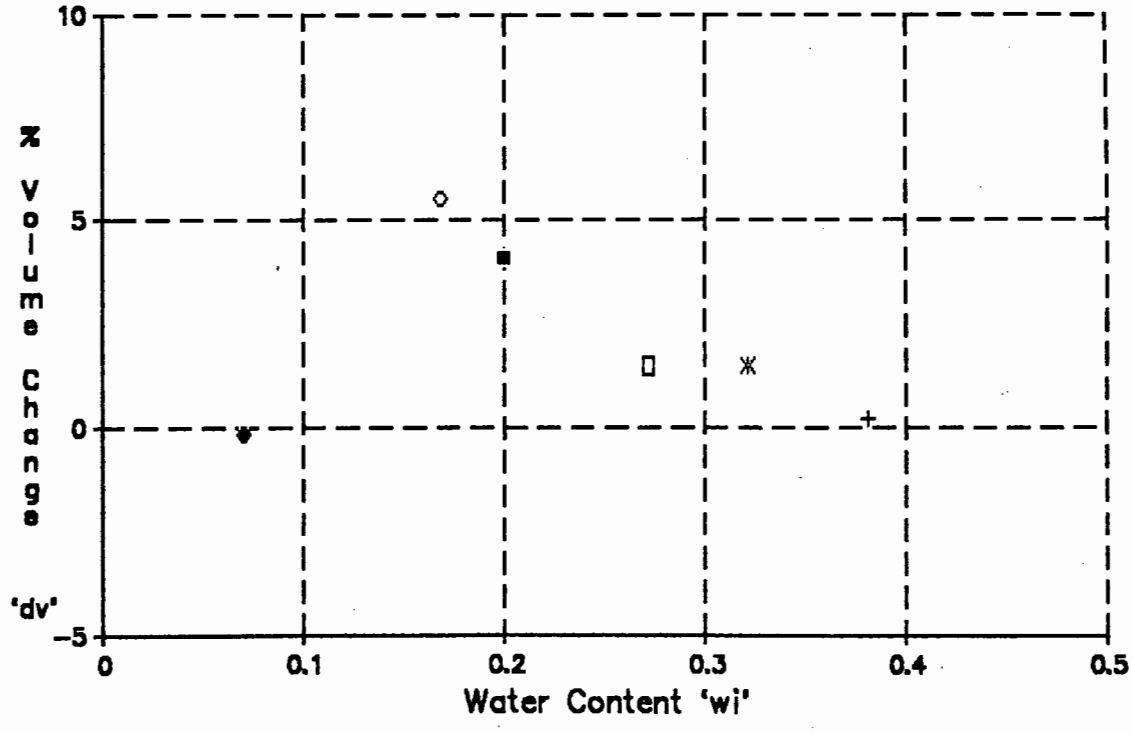

Legend:

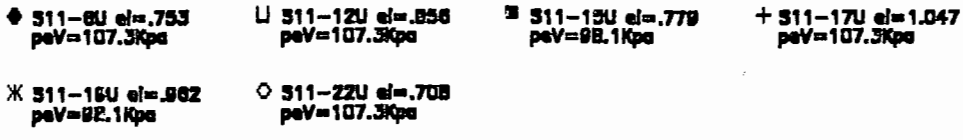

Figure 6.135: Site 11, Rosebank [Undisturbed 98.1 - 107.3 Kpa] - Relationship between Water Content 'w_i', before wetting, and Percentage Volume Change, after wetting.

6.10.2 Site 36, Rondebosch - Expansion or Collapse of samples due to wetting.

Remoulded samples: *Applied pressures of 0.8 - 430.3 Kpa.*

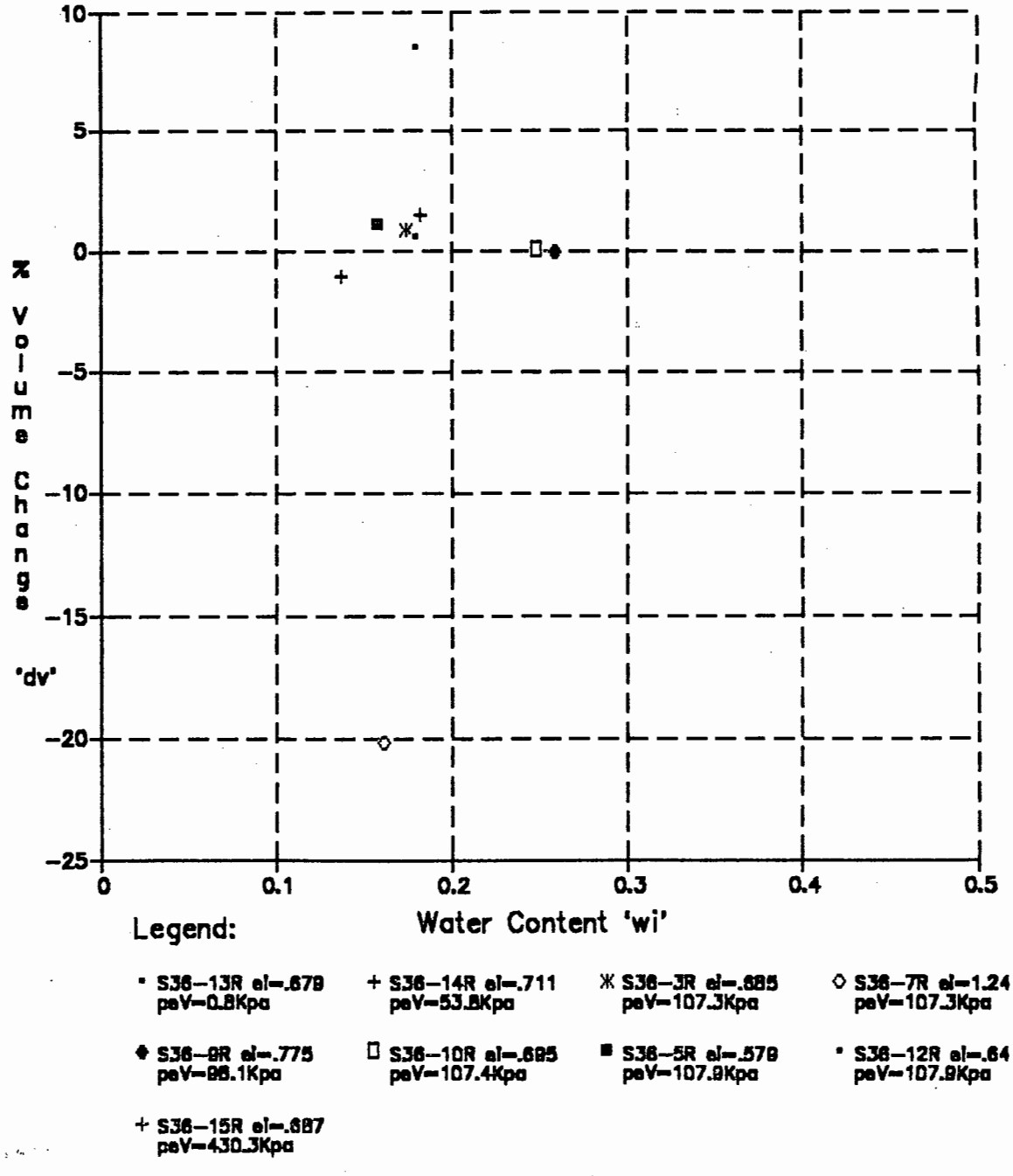

Figure 6.136: Site 36, Rondebosch [Remoulded 0.8 - 430.3 Kpa] - Relationship between Water Content 'w_i', before wetting, and Percentage Volume Change, after wetting.

Compacted and Undisturbed samples: *Applied pressures of 98.1 - 107.5 Kpa.*

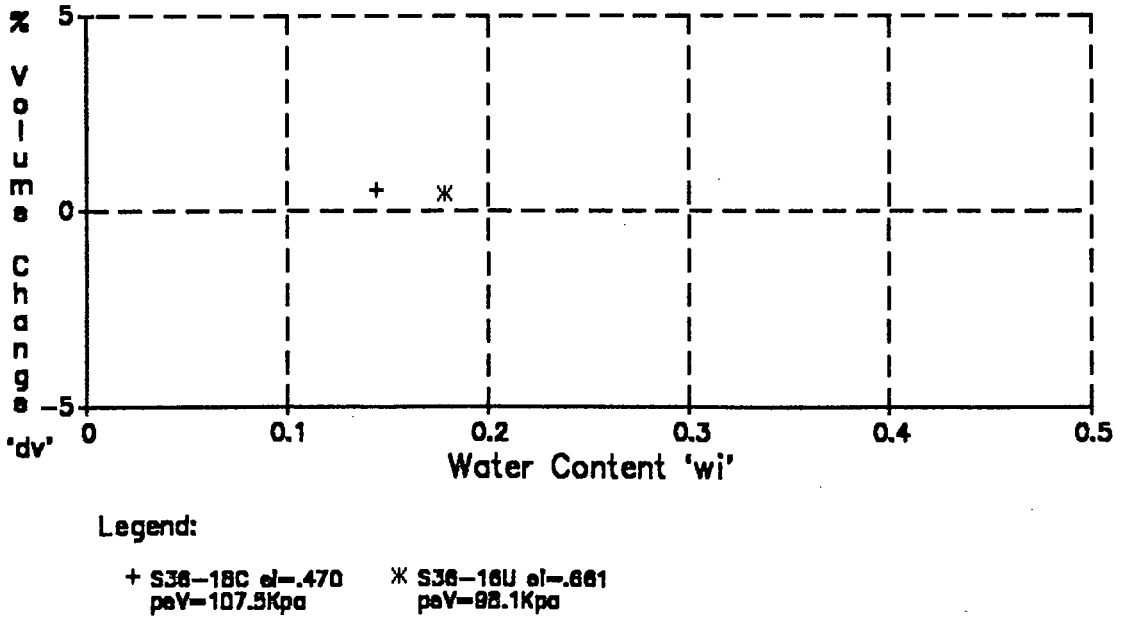

Figure 6.137: Site 36, Rondebosch [Compacted 107.5 Kpa and undisturbed 98.1 Kpa] - Relationship between Water Content 'w_i', before wetting, and Percentage Volume Change, after wetting.

6.10.3 Site 30, Hout Bay - Expansion or Collapse of samples due to wetting.

Remoulded samples: *Applied pressures of 1.0 - 107.3 Kpa.*

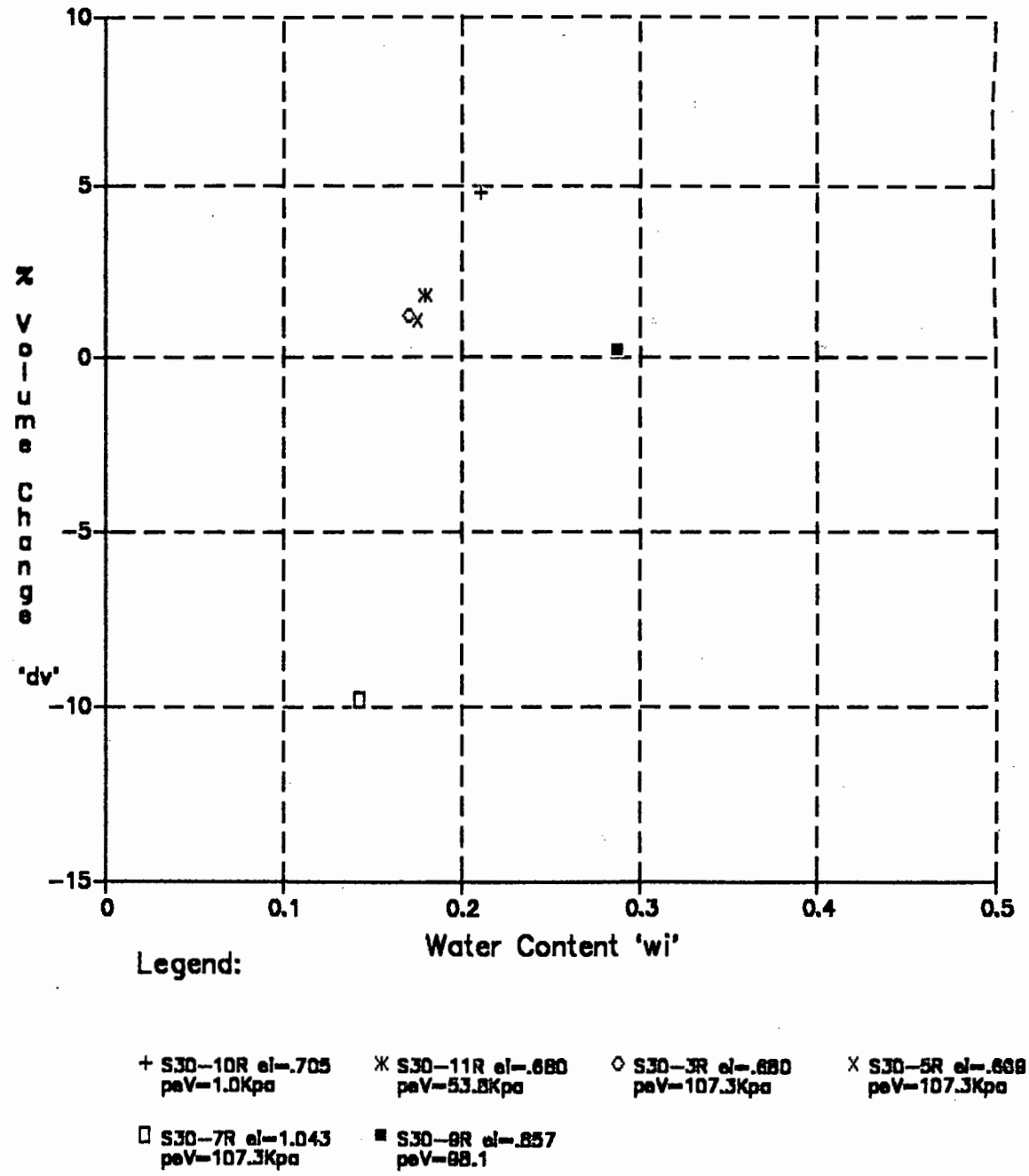

Figure 6.138: Site 30, Hout Bay [Remoulded 1.0 - 107.3 Kpa] - Relationship between Water Content 'w_i', before wetting, and Percentage Volume Change, after wetting.

Undisturbed sample: *Applied pressure of 107.6 Kpa.*

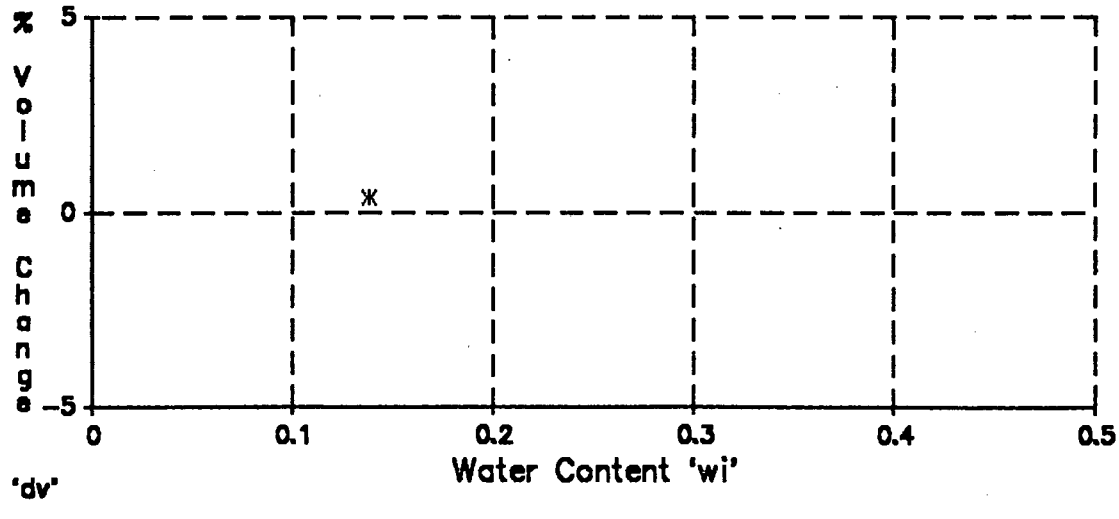

Figure 6.139: Site 30, Hout Bay [Undisturbed, 107.6 Kpa] - Relationship between Water Content 'w_i', before wetting, and Percentage Volume Change, after wetting.

6.10.4 Site A, Berea Road - Expansion or Collapse of samples due to wetting.

Remoulded samples: *Applied pressures of 98.1 - 107.3 Kpa.*

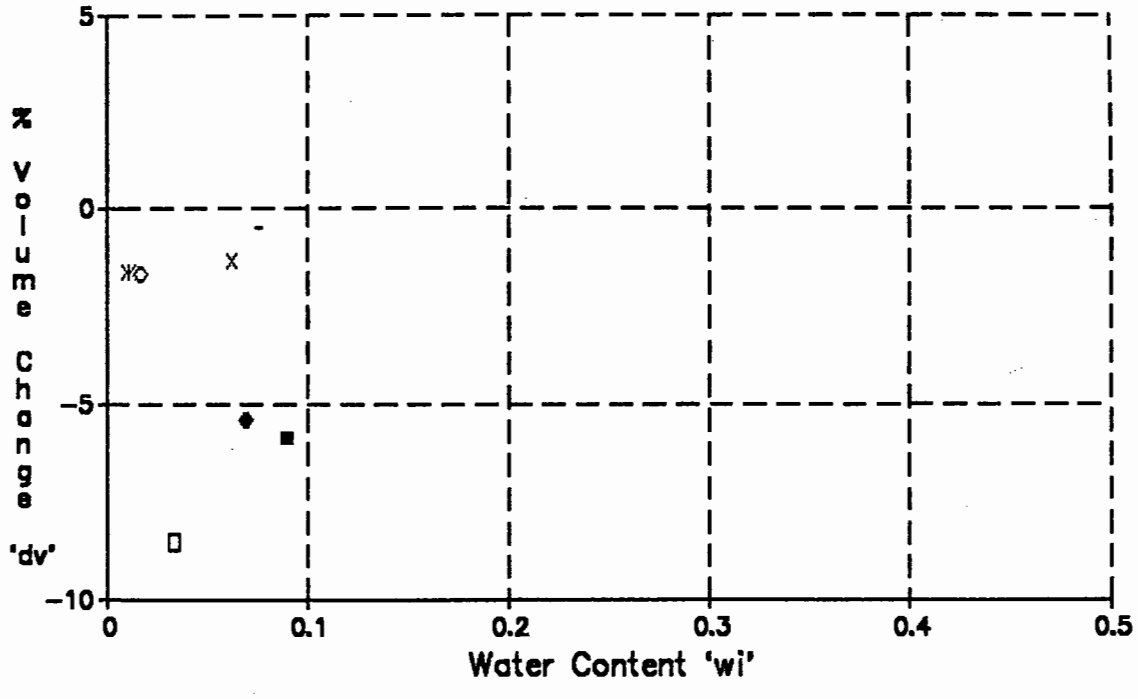

Legend:

SA–1AR el=.596 peV=98.1Kpa
SA–2R el=.467 peV=107.3Kpa
SA–3R el=.468 peV=107.3Kpa
SA–4R el=.363 peV=98.1Kpa
SA–6R el=.597 peV=107.3Kpa
SA–7R el=.721 peV=107.3Kpa
SA–8R el=.666 peV=107.3Kpa

Figure 6.140: Site A, Berea Road [Remoulded 98.1 - 107.3 Kpa] - Relationship between Water Content 'w_i', before wetting, and Percentage Volume Change, after wetting.

Compacted and Undisturbed samples: *Applied pressures of 98.1 - 107.3 Kpa.*

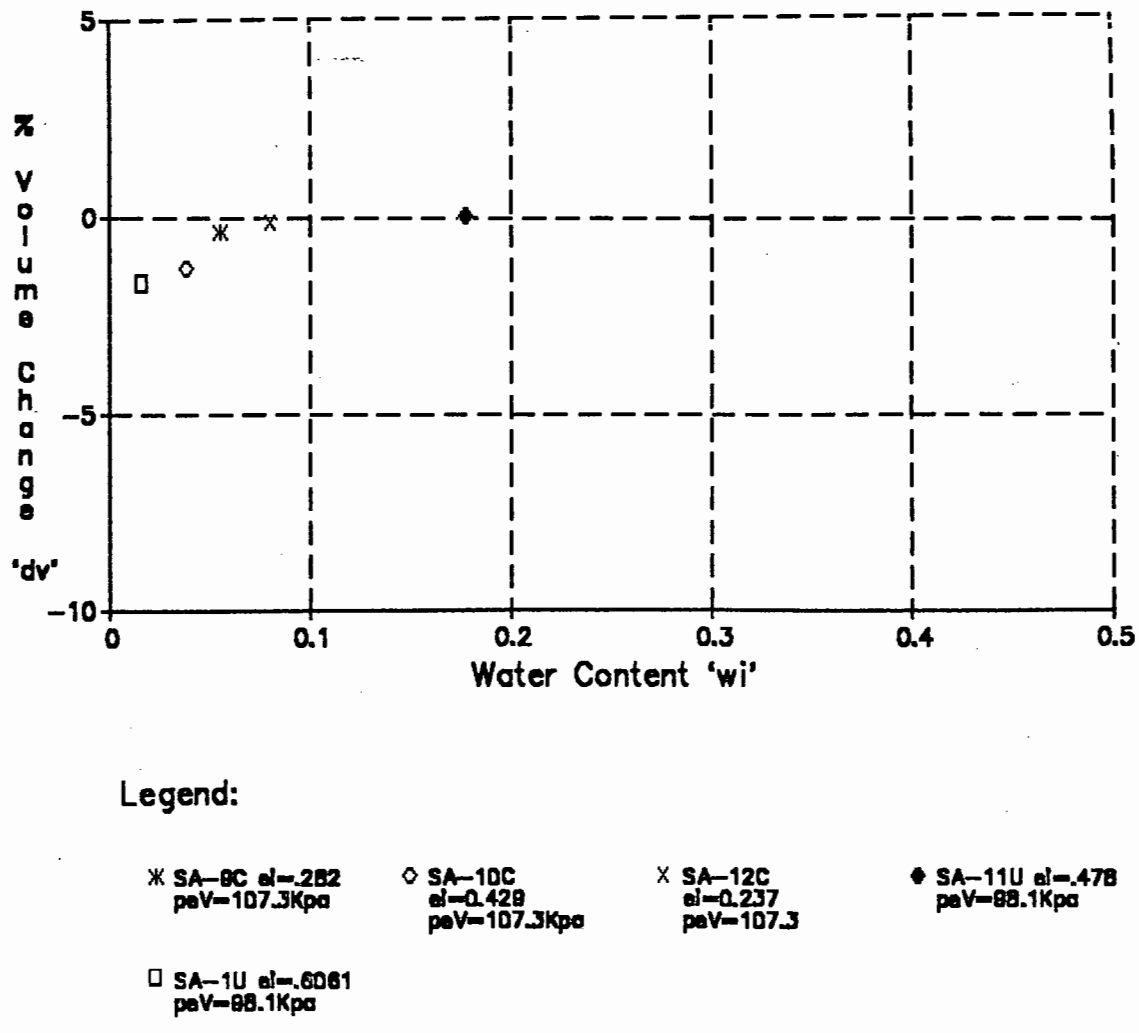

Figure 6.141: Site A, Berea Road [Compacted 107.3 Kpa, and undisturbed 98.1 Kpa] - Relationship between Water Content 'w_i', before wetting, and Percentage Volume Change, after wetting.

6.10.5 Site 7, Mowbray - Expansion or Collapse of samples due to wetting.

Remoulded samples: *Applied pressures of 98.1 - 107.3 Kpa:-*

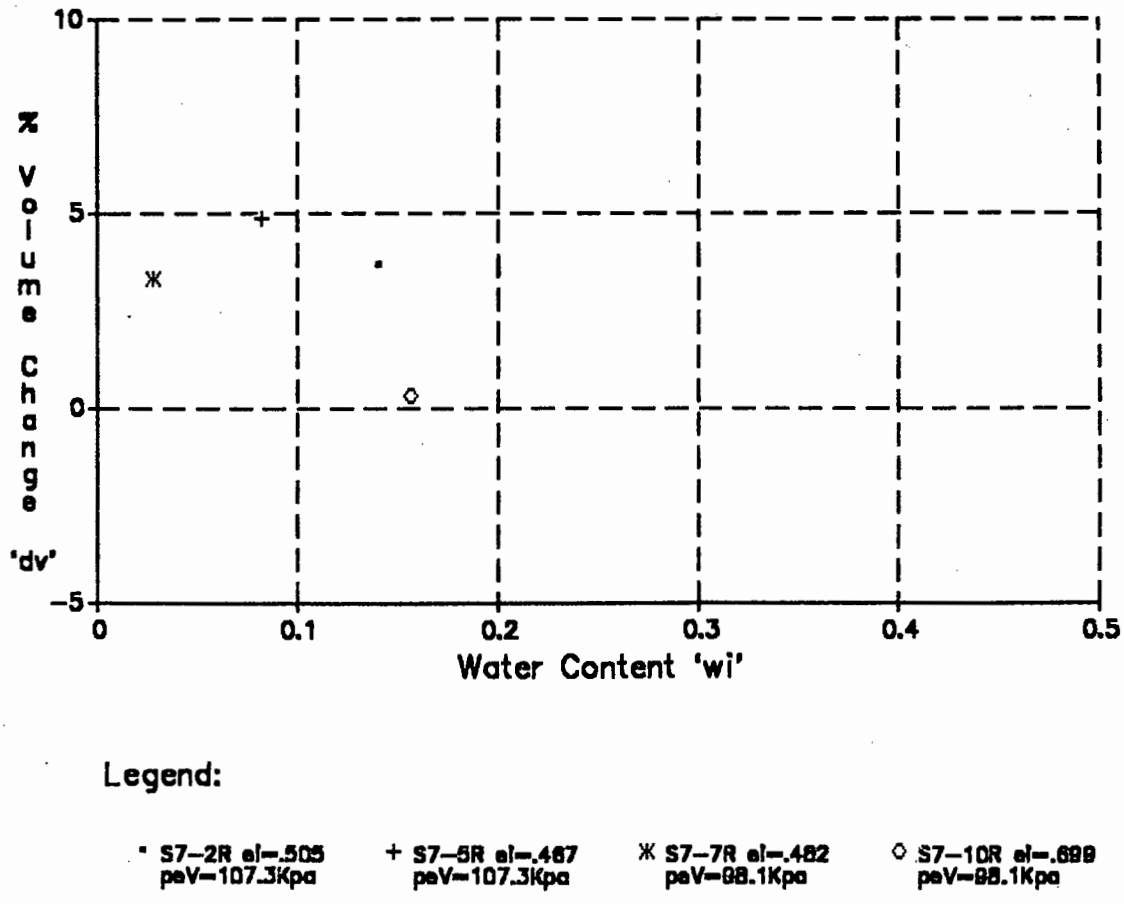

Figure 6.142: Site 7, Mowbray [Remoulded, 98.1 - 107.3 Kpa] - Relationship between Water Content 'w_i', before wetting, and Percentage Volume Change, after wetting.

Compacted and Undisturbed samples: *Applied pressures of 98.1 - 107.3 Kpa.*

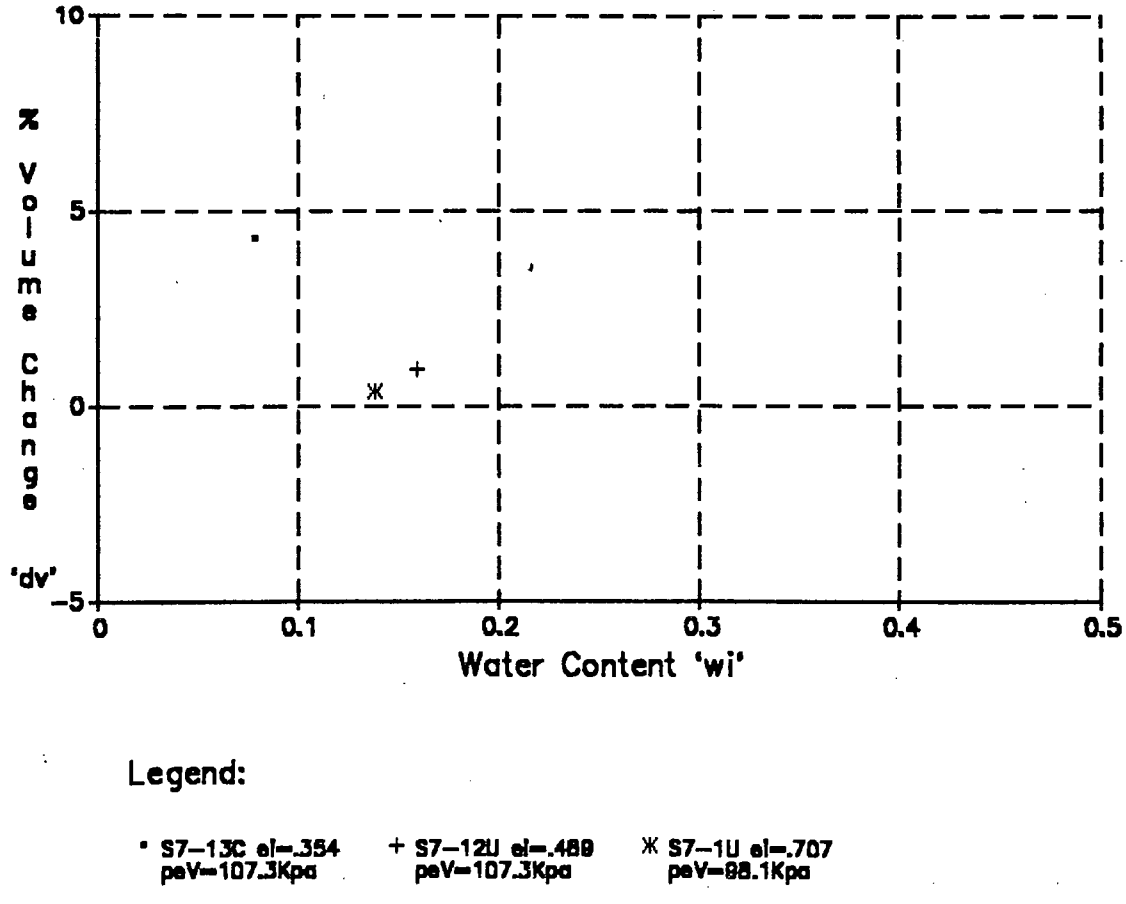

Figure 6.143: Site 7, Mowbray [Compacted 107.3 Kpa, and undisturbed 107.3 Kpa] - Relationship between Water Content 'w_i', before wetting, and Percentage Volume Change, after wetting.

6.10.6 Sites 'B' Francois Road, 'C' Margaret Mayton Avenue, and 'D' Rose Hill - Expansion or Collapse of samples due to wetting.

Remoulded samples: *Applied pressures of 98.1 - 107.3 Kpa.*

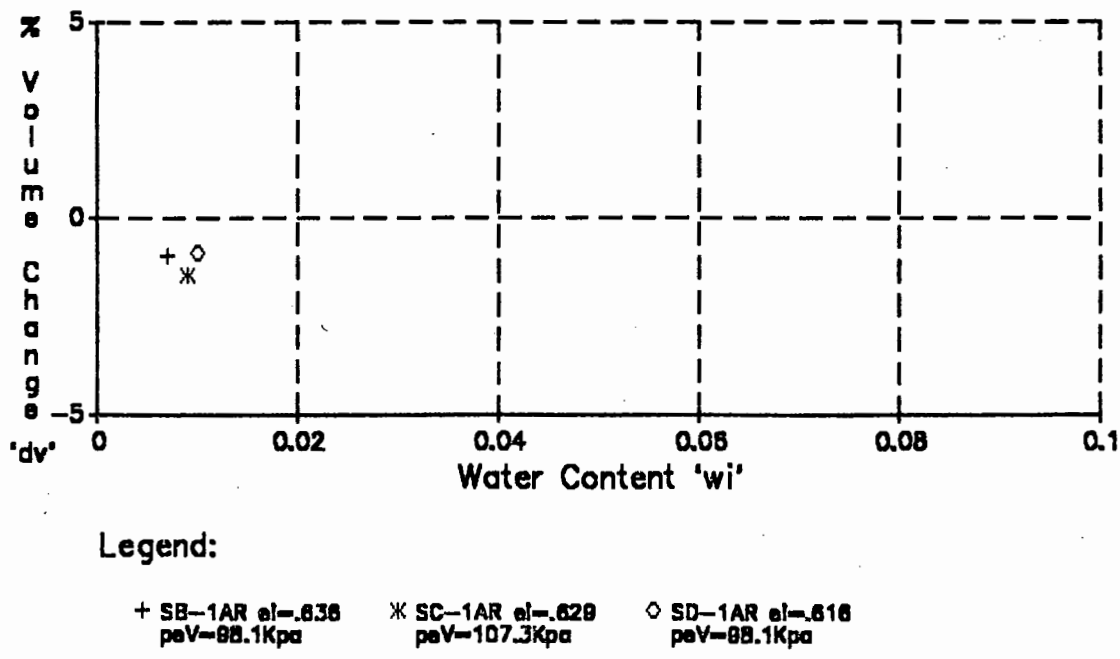

Figure 6.144: Site 'B' Francois Road, site 'C' Margaret Mayton Avenue, and site 'D' Rose Hill [Remoulded, 98.1 - 107.3 Kpa] - Relationship between Water Content 'w_i', before wetting, and Percentage Volume Change, after wetting.

6.10.7 Site 48, Lady Grey - Expansion or Collapse of sample due to wetting.

Undisturbed sample: *Applied pressure of 98.1 Kpa.*

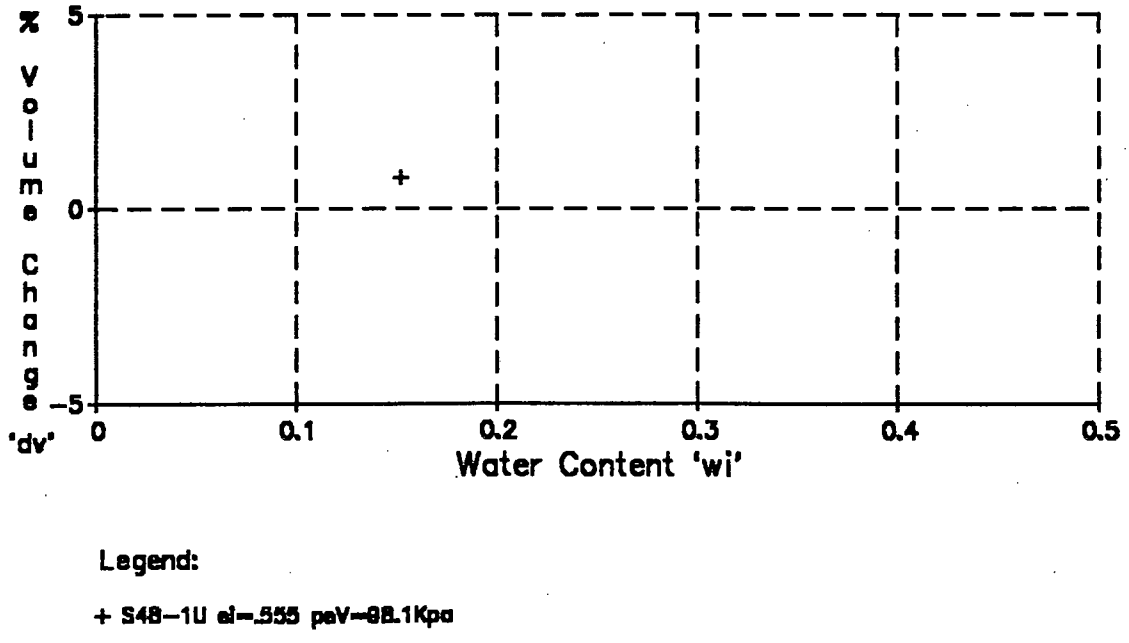

Figure 6.145: Site 48, Lady Grey [Undisturbed, 98.1 Kpa] - Relationship between Water Content 'w_i', before wetting, and Percentage Volume Change, after wetting.

6.10.8 Kaolin K.1 (13% clay size), K.2 (20% clay), and Kaolin K.3 (8.5% clay size) - Collapse of samples due to wetting.

Remoulded samples: *Applied pressure of 98.1 Kpa.*

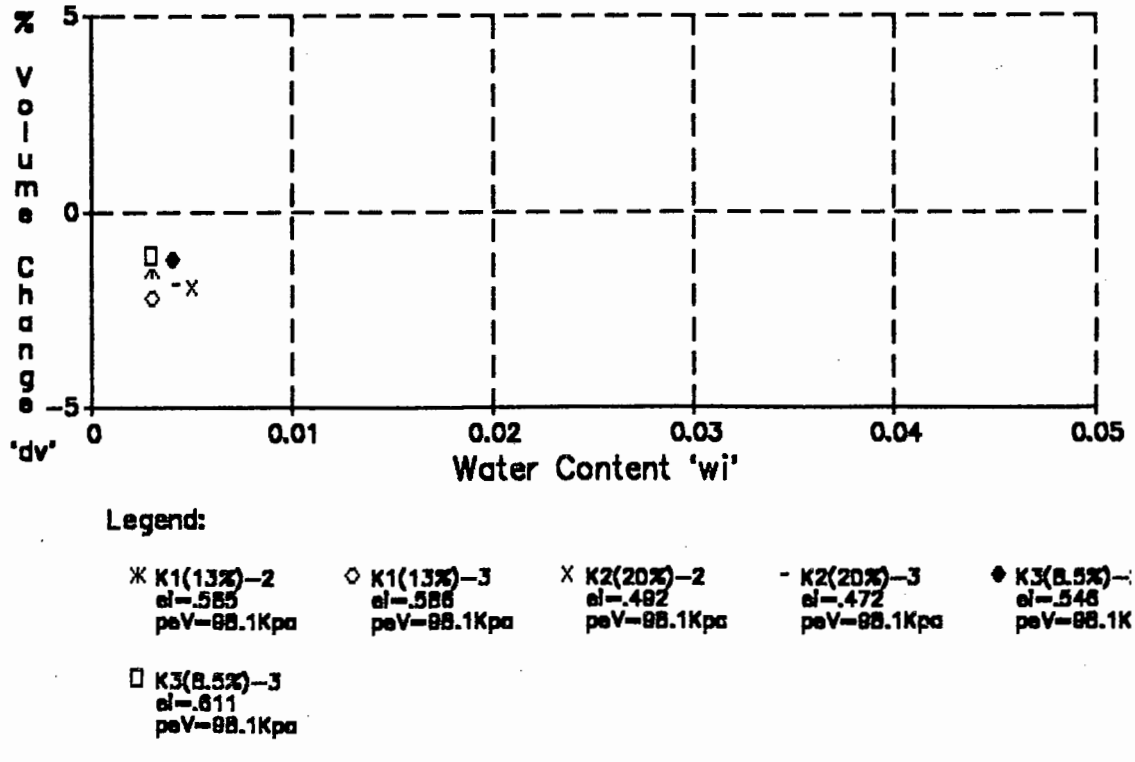

Figure 6.146: Kaolin K.1 (13% clay size), K.2 (20% clay), and Kaolin K.3 (8.5% clay size) [Artificial soil types - Remoulded, 98.1 Kpa] - Relationship between Water Content 'w_i', before wetting, and Percentage Volume Change, after wetting.

6.10.9 Bentonite B.1 (3.5% clay size), B.2 (7% clay), B.3 (11.5% clay), B.4 (15.5% clay), and Bentonite B.5 (35% clay) - Collapse of samples due to wetting.

Remoulded samples: *Applied pressure of 98.1 - 107.6 Kpa.*

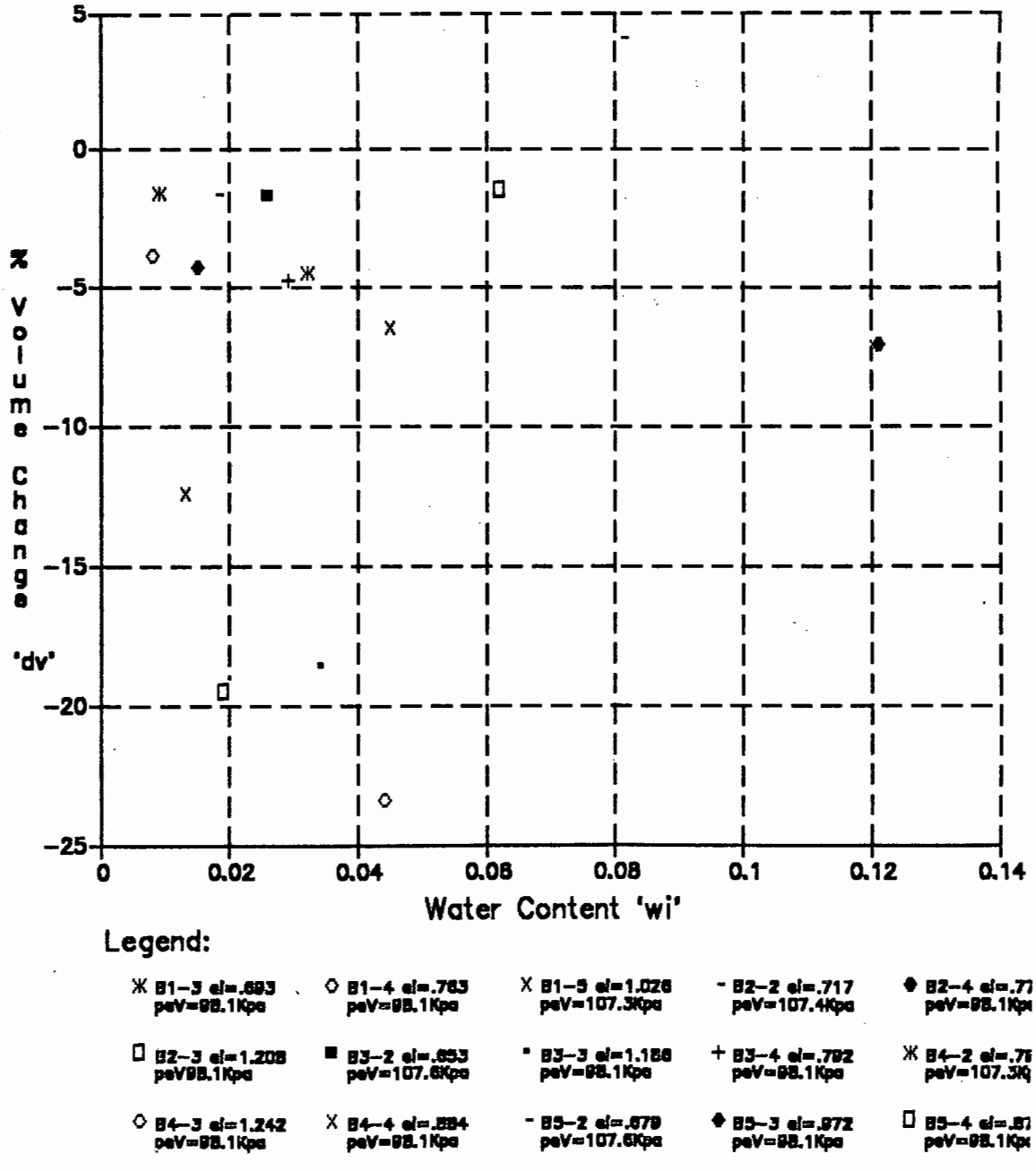

Figure 6.147: Bentonite B.1 (3.5% clay size, B.2 (7% clay), B.3 (11.5%) B.4 (15.5%), and Bentonite B.5 (35% clay size) [Artificial soil types, Remoulded 98.1 - 107.6 Kpa] - Relationship between Water Content 'w_i', before wetting, and Percentage Volume Change, after wetting.

The diagrams of sections 6.10.1 to 6.10.9 will be combined in Chapter Ten as the following Figures:-

Natural Soil Types.

Site 11, Rosebank. (Remoulded and Compacted samples)	->	Figure 10.49
Site 36, Rondebosch. (Remoulded and Compacted samples)	->	Figure 10.50
Site 30, Hout Bay. (Remoulded samples)	->	Figure 10.51
Site A, Berea Road. (Remoulded and Compacted samples)	->	Figure 10.52
Site 7, Mowbray. (Remoulded and Compacted samples)	->	Figure 10.53
Site 'B' Francois Road, Site 'C' Margaret Mayton Av., and Site 'D' Rose Hill.	->	Figure 10.54

Artificial Soil Types.

Kaolin K.1 (13% clay size), Kaolin K.2 (20%), and Kaolin K.3 (8.5%).	->	Figure 10.55
Bentonite B.1 (3.5% clay size), Bentonite B.2 (7%), Bentonite B.3 (11.5%), Bentonite B.4 (15.5%), and Bentonite B.5 (35%).	->	Figure 10.56.

6.11 REFERENCES FOR CHAPTER SIX

2. DE S. VINAGRE, T.J.V. (1974): The Compression of a Collapsing Soil - B.Sc. (Eng) Thesis. Department of Civil Engineering, University of Cape Town.

16. DE S. VINAGRE, T.J.V. (1976/77): Masters Thesis - Diaries One, Two, Three, Four, Five, and Six.

86. SPARKS, A.D.W. (1975): Discussions, Volume II, Proceedings of the Sixth Regional Conference for Africa on Soil Mechanics and Foundation Engineering; Durban, South Africa, September 1975.

91. SPARKS, A.D.W. Prof. (Supervisor) - Discussions with the writer.

CHAPTER SEVEN *

SWELL PRESSURES

7.1 INTRODUCTION

The work in this chapter deals with the observed swelling pressures developed in a soil sample, which is being prevented from overall volume change, as the result of the addition of measured volumes of water.

The observed water ratios, void ratios and swelling pressures (required to prevent the overall volume change of the sample) are presented in graphical form to illustrate the trends of behaviour and to allow comparisons to be made between the 'paths' of swell pressure developed for different initial conditions and ranges of water content.

For a soil to develop swell pressure while being restrained, it requires to have the type of clay which will absorb water and increase its volume - this type of clay needs to contain the clay minerals identified in Chapter Two.
Various different types of soils were used.

Different methods of sample preparation were followed for each soil type prior to the observations of swell pressures. Samples were either permitted to lose or gain moisture, until the required initial water content was reached. The observed changes in the volume and mass of soil samples are recorded throughout. It was hoped to investigate both the unsaturated and saturated conditions of each soil sample.

7.2 DEFINITIONS

The concepts behind "Swell Pressures" as used in this chapter can be defined as follows:-

The word "swell" will in this case mean the outward expansion of the soil sample resulting from the interaction of the (added) water and its clay minerals. As introduced in Chapter Two (refer to section 2.4 'Micro Studies - II') and described in Chapter Six of this thesis (refer to section 6.2 'Concepts and definitions'), the addition of water causes an increase in the lattice spacing of the clay minerals which leads to an increase in the overall volume of the sample.

---

* - *Observations are in Appendix F.*

The one-dimensional measurement of the swell pressure, generated within the sample by the added water, occurs under conditions in which drainage is permitted throughout. As described in Chapters Four, Five and Six, it is an attempt to satisfy the conditions of zero pore water pressure and, on the basis that the pore water pressure is zero, the effective stresses are equal to the applied stresses.
The applied stresses required to prevent an increase in the volume of the sample are the swell pressure measurements obtained by means of a proving ring, as described in 'Test Method'[1] of this chapter.

The word "pressure" will in this case mean that during the process of overall volume change, the sample is prevented from increasing its volume by an externally applied stress (along the vertical axis) while being confined by a fixed consolidometer ring (horizontal plane). Therefore, "Swell Pressures" are the measured stresses required to prevent the sample from increasing its volume along the vertical axis while being confined along the horizontal plane.

The changes in the water content of these samples were made to happen in the following controlled manner: A limited amount of de-aired water is added to the bottom filter paper, which in turn transmits the water to the whole underside of the soil sample; and, to wait for this extra water to distribute itself upwards into the sample while time measurements of swell pressure are recorded - refer to 'Test Method'[1] in this chapter.

The definitions of "Free-shrinkage" and "Free-swell" are included in Chapter Four.

A sub-section[2] of 'Macro Studies' in Chapter Two includes the definitions of void ratio 'e', water ratio 'wr', or 'Ω', and water content 'w'.

7.3 THE PARAMETERS WHICH ARE BEING INVESTIGATED

The diagram in Figure 7.01 illustrates some of the parameters which are being investigated.
These parameters are the void ratio and the water ratio (or water content).
The relationship between the void ratio and the water ratio, as shown in Figure 7.01, goes through the following stages:-

(i) The sample is initially at condition A (that is, the condition at which the soil sample was prepared as remoulded or compacted, or obtained from an undisturbed block sample).

---

[1] - *subsequent section 7.6.*
[2] - *2.2.4, "Soil density versus water content relationship".*

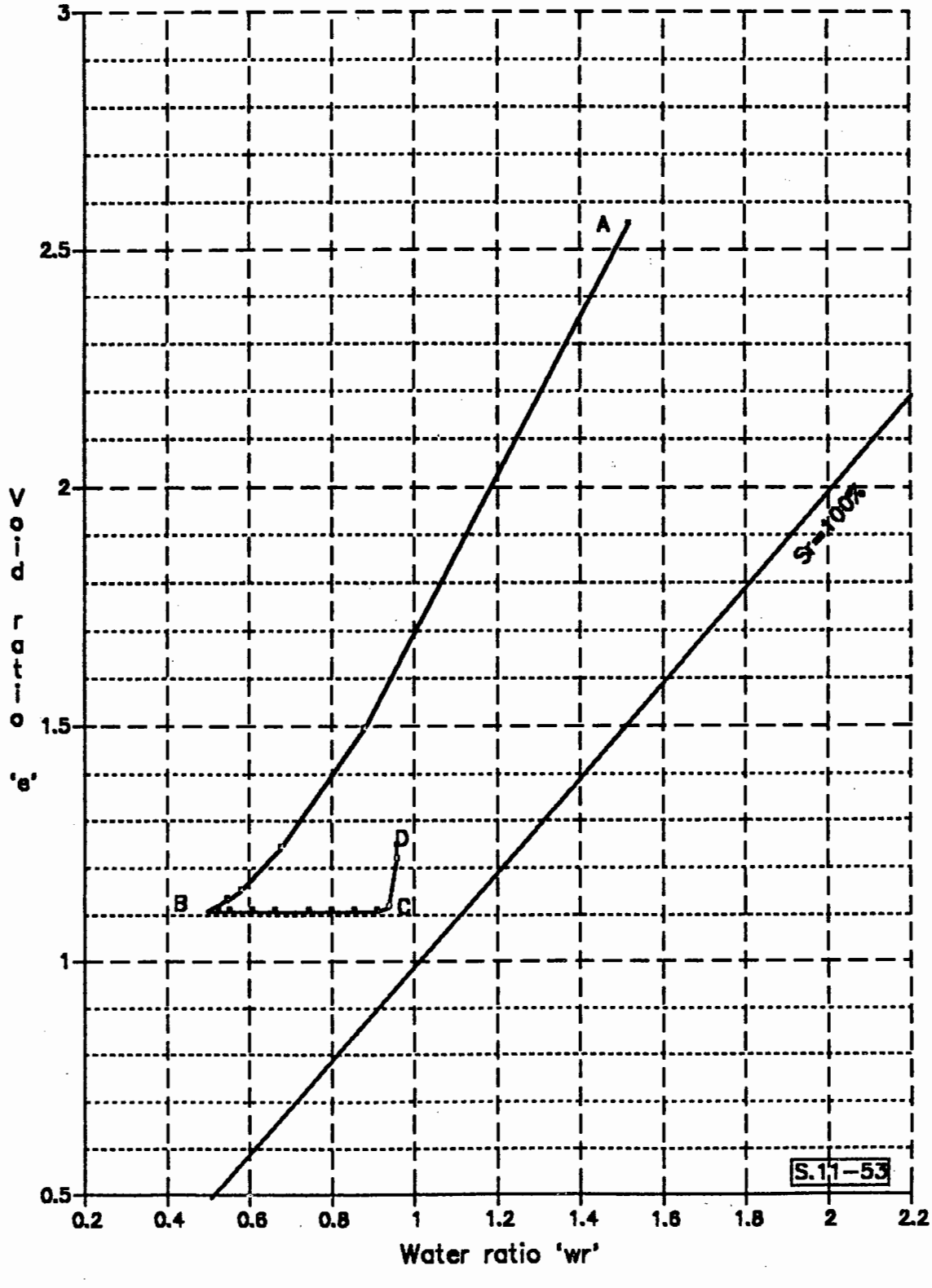

Figure 7.01: Relationship between the void ratio 'e' and the water ratio 'wr', or 'Ω' (or alternatively use the water content). For description of curve see section 7.3[1].

---

[1] - "The parameters which are being investigated".

(ii) The sample is allowed to lose moisture - as it loses moisture, the state of the sample moves from A towards B (free-shrinkage path).
(iii) At point B, the sample is prepared for the swell pressure test (refer to subsequent section `Preparation of test samples').
(iv) Starting at point B, the water content is increased in stages, while the sample is confined laterally and prevented (by applying swell pressure) from expanding upwards - the void ratio stays approximately constant between points B and C.
(v) When there is no need for a further increase in the swell pressure, after another increment of water, the sample is unloaded in stages - this is the path C to D.

The vertical axis of the diagram in Figure 7.01 represents the void ratio (the ratio of the volume of voids to the volume of solids), and the horizontal axis represents the water ratio (the ratio of the volume of water to the volume of solids - that is, the water content 'w' times the specific gravity of the soil particles 'G_S').
It should be noted that Figure 7.01 is basically the same as Figure 4.01, part (b) combined with part (c), of Chapter Four.

Other parameters relating to each soil type were also measured - refer to Chapters One, Two, and Appendix A. These index properties were listed in Chapter Four[1].

7.4 SWELL PRESSURES AND THE TYPE OF PLOT SHOWN IN FIGURE 7.02

Some of the specific objectives of this chapter:-

(i) To obtain the shrinkage path of the sample as it dries, under controlled conditions, to the initial water content required for the swell pressure test.
(ii) The swell pressures (or measured effective vertical stresses) required to prevent the sample from increasing its overall volume, as a result of increases in its water content.
(iii) The measured volumes of water added to the soil sample.
(iv) The maximum swell pressure recorded during the controlled wetting stage, as well as the pressure at the end of wetting the sample - these values of swell pressure for no volume change, and the water content at which they occur, are included in the type of plot illustrated as Figure 7.02.
(v) To obtain the recovery path of the sample due to unloading.

---

[1] - *"Free shrinkage and free swell paths".*

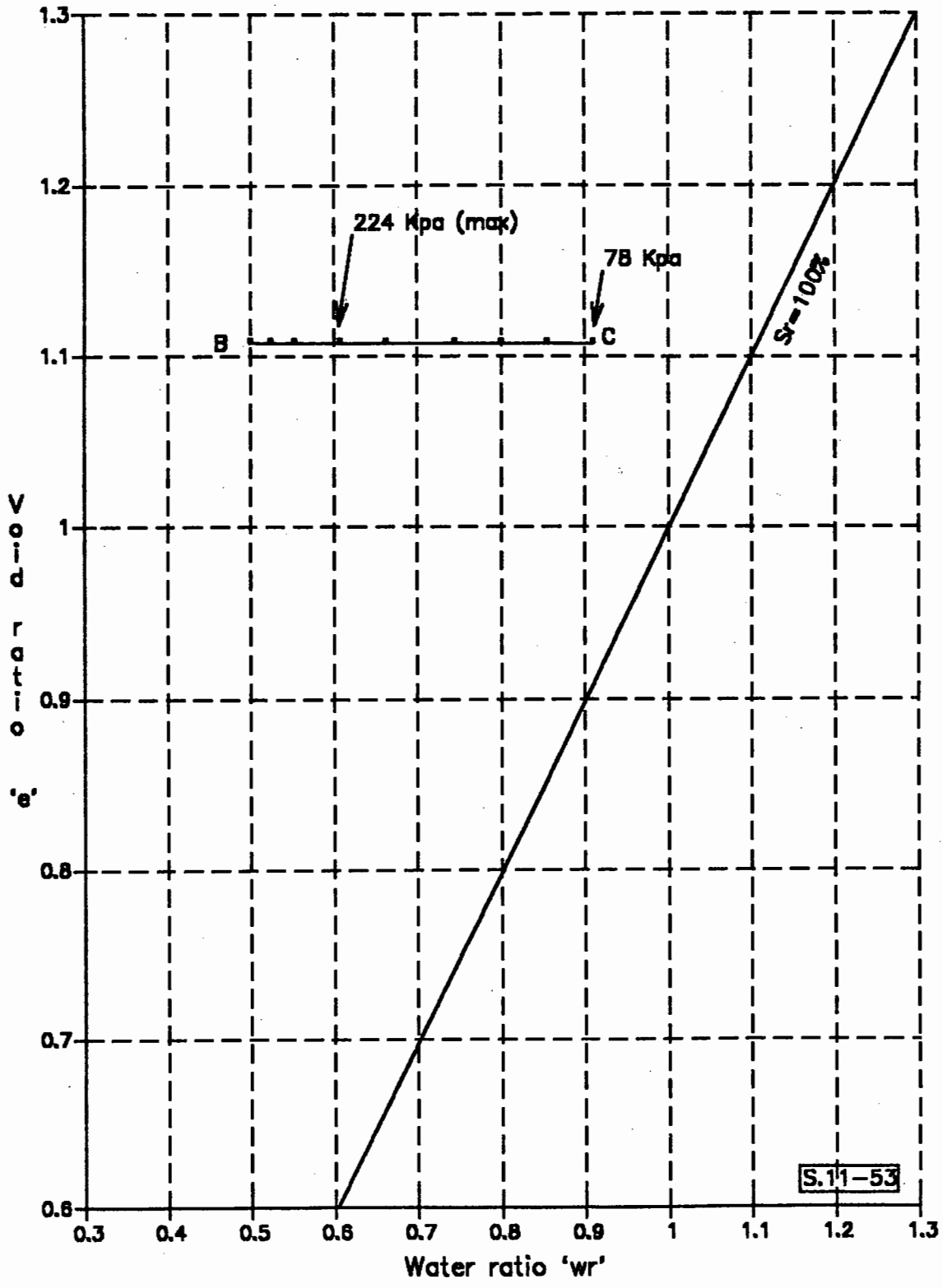

Figure 7.02: Relationship between the void ratio 'e' and water ratio 'wr', or 'Ω', for the controlled wetting stage - includes the maximum and final values of swell pressure.

The two main differences between Figure 7.01 and 7.02, are as follows:
(a) The previously defined free-shrinkage path AB and unloading path CD are omitted from Figure 7.02;
(b) The measured swell pressure values, and which are mentioned in objective (iv) described above, are included in Figure 7.02.

Reasons for using the type of plot in Figure 7.02[1]:-

(A) It is possible to plot contours of degree of saturation as straight lines.

(B) To illustrate swelling and shrinkage paths for samples which are confined by external stresses.

(C) Stress contours can be superimposed on this plot as contours of stress.

(D) To express the position and scaling factor of the stress scale obtained in Chapter Five, whether obtained from the one dimensional or isotropic consolidation, in terms of the Liquid Limit and Plasticity Index of the clay.

(E) For a sample which is prevented from overall volume change, to attempt to relate the final isotropic effective stress to the effective stress value within the swell pressure (for no strain) sample.

---

1 - This type of plot has been used previously by Sparks (Reference 86).

7.5 PREPARATION OF TEST SAMPLES

Test samples can be prepared from remoulded, compacted or undisturbed soil samples. A brief description is included in this chapter for each type of preparation - for more details refer to the preparation of test samples in Appendix F[1].

Remoulded samples.

Method 1:
The soil is mixed with water to form a wet paste, at a water content varying from about the Plastic Limit to a value equal or greater than the Liquid Limit; The wet paste is moulded into a suitable container.
Method 2:
An homogeneous dry mixture is prepared by mixing known amounts of soil, tartaric acid and sodium bicarbonate; Water is added to the mixture, quickly mixed, and placed in the container.

Compacted samples.

Select points on the 'Dry density versus Water content' curve for the soil sample (refer to Appendix A[2]); Compact the soil to the required compaction specification, at the water content for the selected point; Cut the test sample from the compacted sample.

Undisturbed sample.

The test sample is cut from the undisturbed block (refer to Appendix A - 'Soil Sampling').

7.6 TEST METHOD

The test sample is allowed to air dry under controlled conditions. The shrinkage path of the soil is obtained from the measurements of mass and volume which are carried out at various stages of drying.
This stage is illustrated in Chapter Four - Photographic Plates 4.01 (i) to (vi).
At the required water content for the test, the sample is cut and trimmed to size until the consolidometer ring just slides over it.
The top and bottom surfaces of the sample are made level.
The mass of the soil sample is recorded.

The parts of the consolidometer container are assembled. The container is positioned on the loading device of the consolidometer.

---

1 - see section F.2.
2 - section A.5 "Compaction tests".

The following parts are adjusted: Counterweight alongside the lever arm; Micrometer dial gauge; Proving ring for swell pressure measurement and its dial gauge.

By means of an hypodermic syringe, add a known amount of water to the sample through the bottom filter paper. Allow the sample to expand and record the readings of vertical movement and swell pressure with time - as the soil expands, apply vertical pressure to the sample by tightening the proving ring against the consolidometer's arm until the sample is back to its original height.
Record the reading of swell pressure for no change in height of the sample.
Repeat the above until no further noticeable vertical movement occurs.

Support the lever arm of the consolidometer and use weights on the loading platform in order to measure the unloading or recovery characteristics of the soil.
The proving ring is released, and the increase in sample thickness is recorded with time.
At the completion of the unloading sequence record the mass of the sample plus ring. The soil is extracted from the steel ring and placed inside an oven, previously set at 105 ± 5^{o}C, for a few hours.
The mass of the soil sample is recorded as the oven-dry mass.

The detailed description of this test procedure is included in the test procedure for "Swell pressure tests for expansive soils"[1].

---

[1] - *refer to Appendix F.*

7.7 TEST RESULTS FOR EACH SOIL TYPE

On the same basis as used in the previous chapters, the introduction to the swell pressure test results will be provided by the definitions of each soil type according to particle size and the reported observations for the consistency limit values[1].

In very brief terms, the test results consist of one dimensional measurement of pressure, resulting from controlled wetting, for no volume change.
A modified consolidometer was used to measure the vertical pressure required to prevent the volume change of the soil due to the incremental addition of water.

The relationships of void ratio versus water ratio are presented in two basic forms:

(1) Controlled wetting path - includes the swell pressure, and highlights its maximum and final values (it excludes the free-shrinkage and soil recovery paths);
(2) The full test path - includes the free-shrinkage and unloading paths (it excludes the swell pressures).

These relationships are illustrated in Figures 7.03 to 7.24, as follows:-

Void ratio versus water ratio for the controlled wetting paths.

Remoulded samples: Figures 7.03, 7.09, 7.15, 7.21;
Compacted: Figures 7.05, 7.11, 7.19; and,
Undisturbed: Figures 7.07, 7.13, 7.17, 7.23.

Void ratio vs water ratio for the full test path.

Remoulded samples: Figures 7.04, 7.10, 7.16, 7.22;
Compacted: Figures 7.06, 7.12, 7.20; and,
Undisturbed: Figures 7.08, 7.14, 7.18, 7.24.

It should be noted that Appendix F includes the detailed test procedure and results for the swell pressure tests.

Relationships of void ratio versus water ratio are included for the following natural soil types:

(i) Site 11, Rosebank (Cape);
(ii) Site 36, Rondebosch (Cape);
(iii) Site 30, Hout Bay (Cape);
(iv) Site A, Berea Road (Durban, Natal); and,
(v) Site 7, Mowbray (Cape).

---

[1] - *refer to Chapters One, Two and Appendix A.*

Swell pressure (consolidometer) tests were performed on the soil samples included in Table 7.01.

Table 7.01: Samples of natural soils used for swell pressure tests.

Sample No.	Method of preparation	Free Shrinkage (Ref. number)	Swell Pressure (Ref. / Consolidometer)
Site 11 (Rosebank, Cape)			
[Remoulded samples] - Figures 7.03, 7.04			
S.11-16	M1 (≥LL)	II. 231	II. 251 / test no. 53
S.11-34	M1 (≥LL)	II. 252	III.297 / test no. 75
S.11-26	M1 (<LL)	II. 256	III.285 / test no. 68
S.11-24	M1 (≥LL)	II. 253	III.293 / test no. 73
S.11-44	M1 (<LL)	III.286	III.318 / test no. 87
S.11-45	M1 (≥LL)	III.288	III.341 / test no. 99
S.11-47	M1 (<LL)	III.301	III.337 / test no. 97
S.11-63	M1 (≥LL)	IV. 421	IV. 449 / test no. 163
S.11-39	M2 (*)	II. 237	III.300 / test no. 77
S.11-53	M2 (*)	III.319	III.345 / test no. 102
S.11-3	M2 (*)	I. 132	II. 217 / test no. 40
S.11-2	M2 (*)	I. 131	II. 207 / test no. 37
[Compacted samples] - Figures 7.05, 7.06			
S.11-9	CMod,II.162	II. 224(FS/FS)	II. 223 / test no. 42
S.11-10	CMod,II.162	II. 241(FS/FS)	II. 240 / test no. 49
S.11-28	CMod,II.162	II. 260(FS/FS)	II. 259 / test no. 56
S.11-71	CStd,IV.450	IV. 459(FS/FS)	IV. 459 / test no. 169
[Undisturbed samples] - Figures 7.07, 7.08			
S.11-7	-	II. 163	II. 213 / test no. 39
S.11-18	-	II. 244	II. 249 / test no. 52
S.11-20	-	II. 245	II. 269 / test no. 60
S.11-21	-	II. 246	III.281 / test no. 66
S.11-31	-	II. 264	III.275 / test no. 63
S.11-29	-	II. 266	II. 271 / test no. 61
S.11-30	-	II. 266	II. 273 / test no. 62
Site 36 (Rondebosch, Cape) - Figures 7.09, 7.10			
[Remoulded samples]			
S.36-2	M1 (≥LL)	III.329	III.365 / test no. 111
S.36-4	M1 (<LL)	III.346	III.371 / test no. 114
S.36-8	M1 (≥LL)	III.374	III.408 / test no. 132
S.36-11	M1 (<LL)	III.380	III.409 / test no. 133
S.36-6	M2 (*)	III.358	III.395 / test no. 126

* - *air bubbles.*

Sample No.	Method of preparation	Free Shrinkage (Ref. number)	Swell Pressure (Ref. / Consolidometer)
[Compacted samples] - Figures 7.11, 7.12			
S.36-19	CStd,A.55	IV. 453(FS/FS)	IV. 454 / test no. 164
[Undisturbed samples] - Figures 7.13, 7.14			
S.36-17	-	III.392	IV. 424 / test no. 145
Site 30 (Hout Bay, Cape)			
[Remoulded samples] - Figures 7.15, 7.16			
S.30-2	M1 (≥LL)	III.333	III.379 / test no. 118
S.30-4	M1 (<LL)	III.350	III.389 / test no. 123
S.30-8	M1 (≥LL)	III.386	IV. 422 / test no. 143
S.30-6	M2 (*)	III.364	III.406 / test no. 131
[Undisturbed samples] - Figures 7.17, 7.18			
S.30-14	-	IV. 433	IV. 436 / test no. 153
Site A (Berea Road, Durban)			
[Compacted samples] - Figures 7.19, 7.20			
S.A-31	CStd,IV.450	V. 33(FS/FS)	IV. 467 / test no. 175
Site 7 (Mowbray, Cape)			
[Remoulded samples] - Figures 7.21, 7.22			
S.7-9	M2 (*)	II. 183	II. 196 / test no. 33
S.7-1	M1 (≥LL)	I. 90	I. 107 / test no. 3
S.7-3	M2 (*)	I. 92	I. 109 / test no. 4
S.7-4	M2 (*)	I. 93	I. 111 / test no. 5
S.7-8	M2 (*)	I. 117	II. 150 / test no. 17
[Undisturbed samples] - Figures 7.23, 7.24			
S.7-11	-	II. 185	II. 200 / test no. 35

** - air bubbles.*

Site 11, Rosebank.

Previously defined as a fine silty clay with only a small amount of fine sand. The soil consists of 59% clay, 29% silt, and 12% sand size. The consistency, free shrinkage and free swell limits, are as follows: Linear Shrinkage 'w_{LS}' = 11.4%; Liquid Limit 'w_L' = 69%; Plastic Limit 'w_P' = 30.7%; Plasticity Index 'I_P' = 38; Shrinkage Limit 'w_S' = 22.5%; and, Free Expansion Limit 'w_{FE}' = 49.4%.

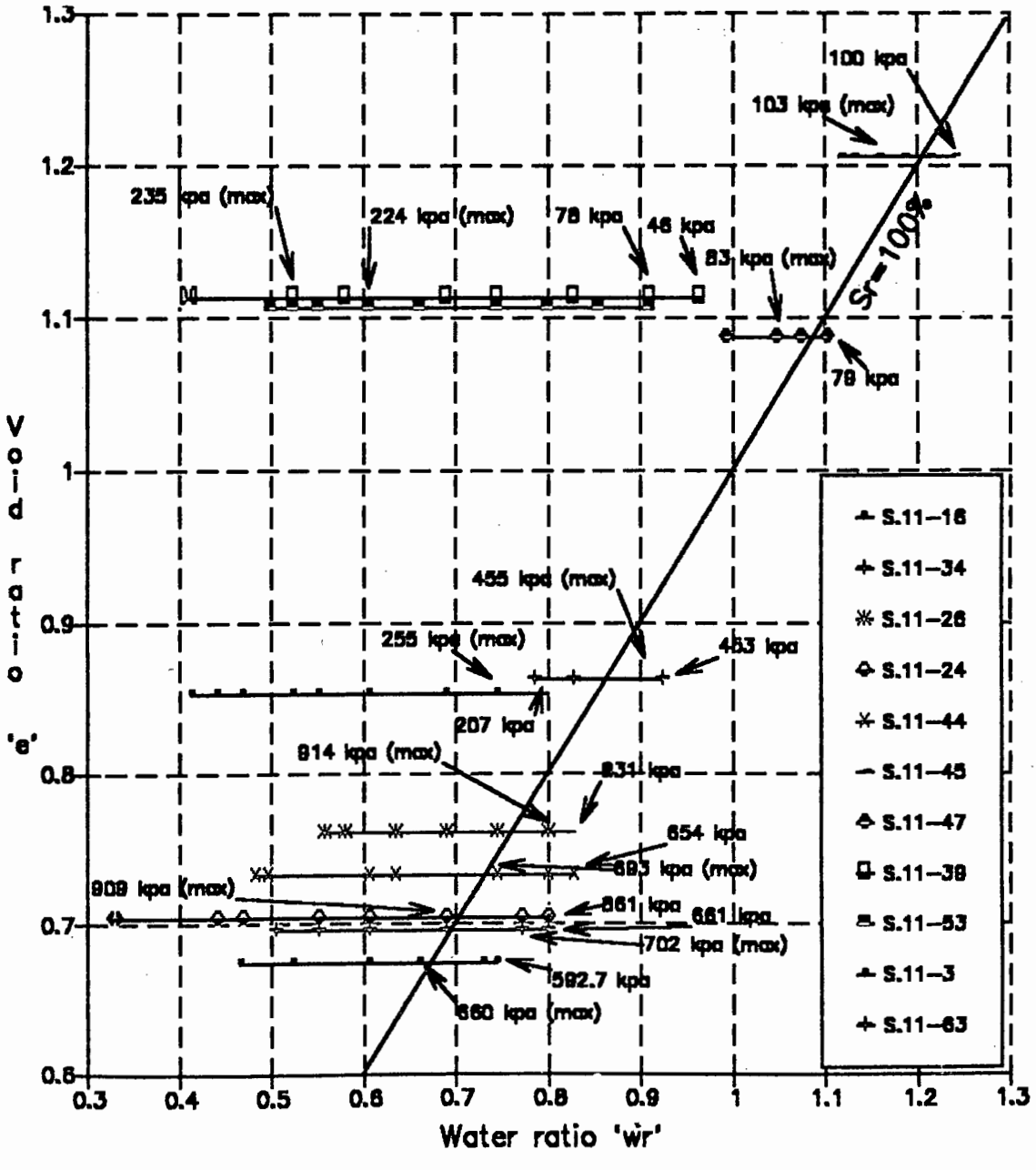

Figure 7.03: Site 11, Rosebank [Remoulded samples] - Void ratio 'e' versus water ratio 'wr', for the controlled wetting path (includes vertical swell pressures due to wetting while confined).

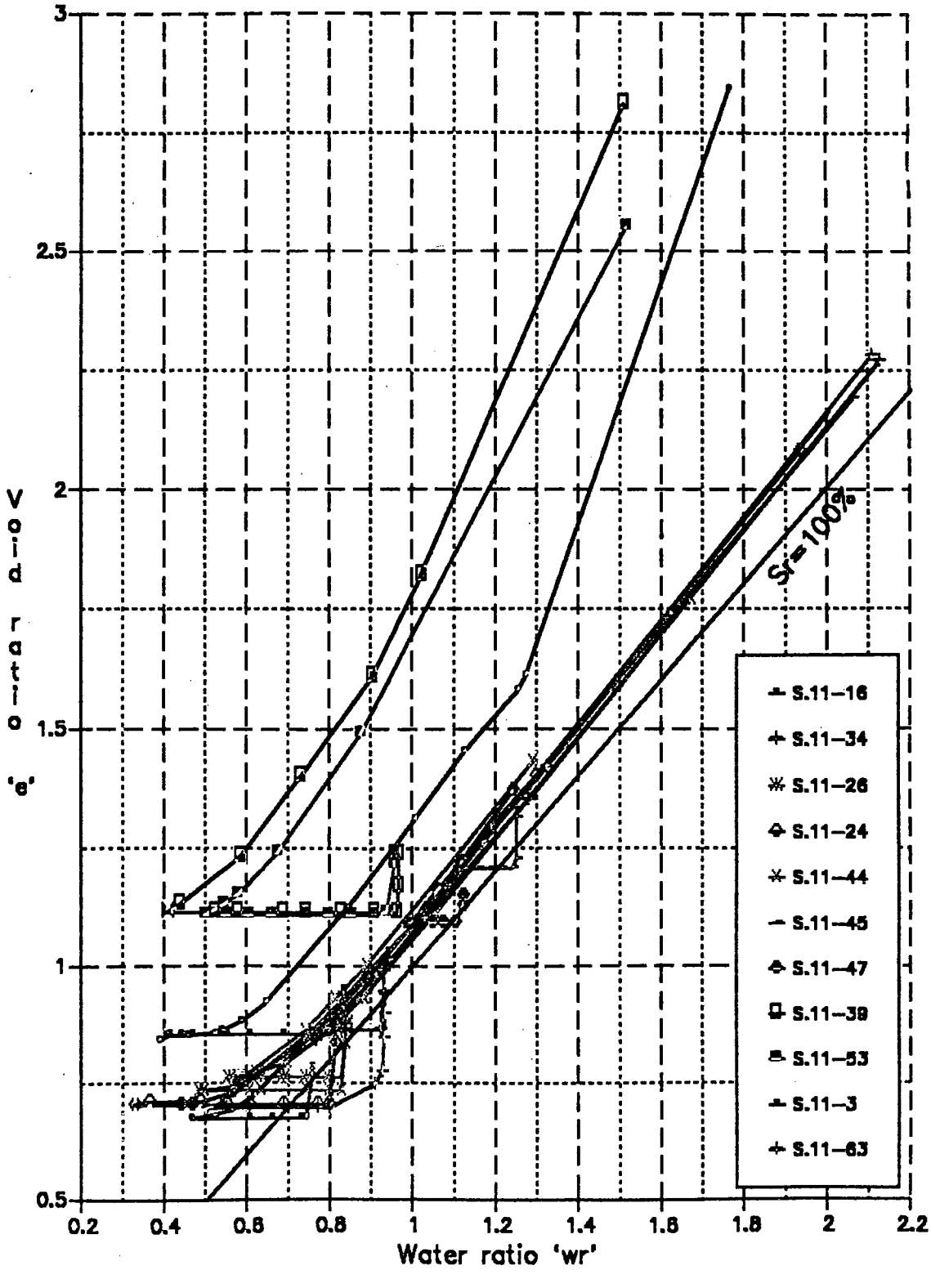

Figure 7.04: Site 11, Rosebank [Remoulded samples] - Void ratio 'e' versus water ratio 'wr', for the full test path (includes free-shrinkage and unloading paths). Horizontal portions are for wetting of confined samples.

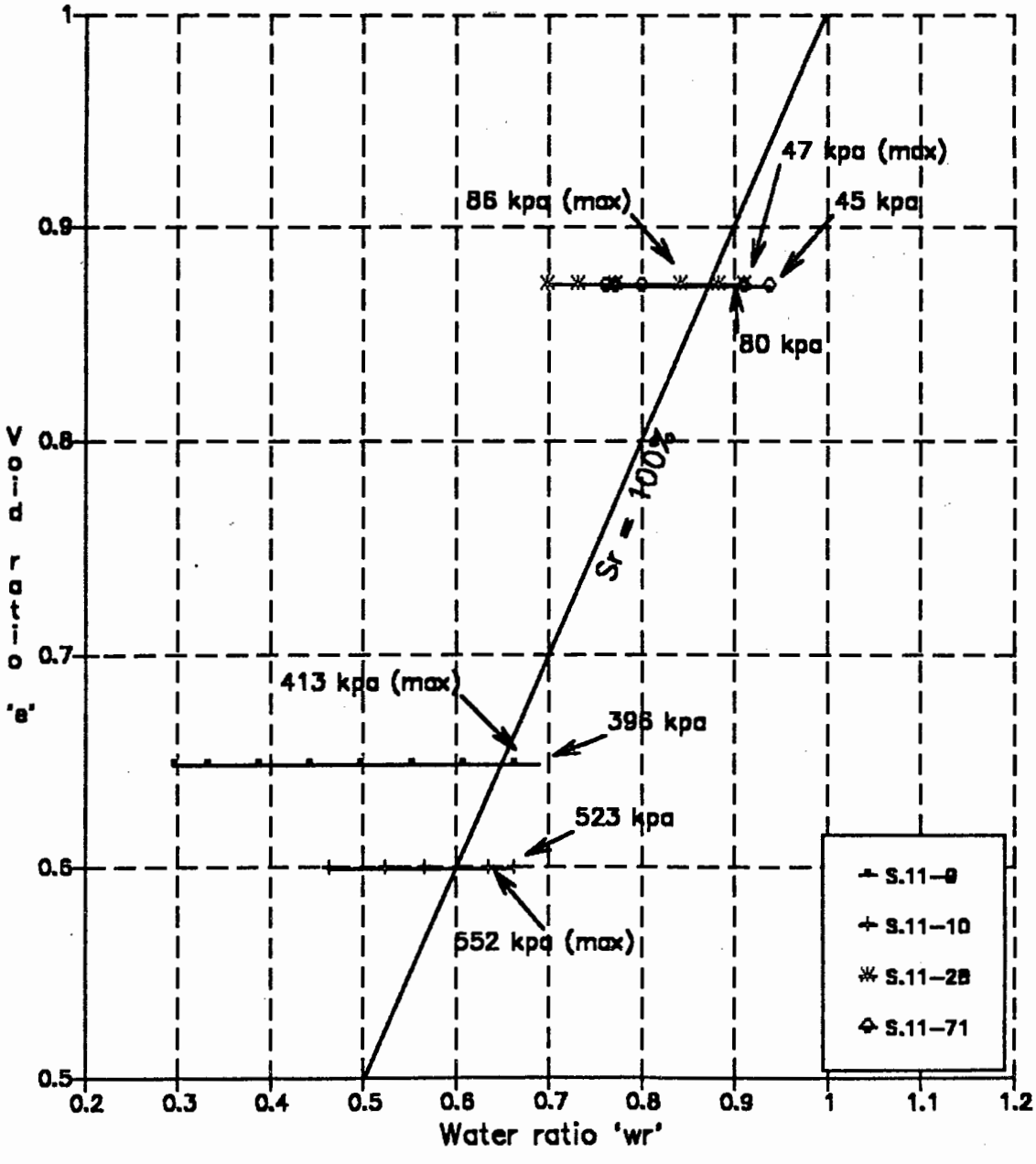

Figure 7.05: Site 11, Rosebank [Compacted samples] - Void ratio 'e' versus water ratio 'wr', for the controlled wetting path (includes swell pressures while confined).

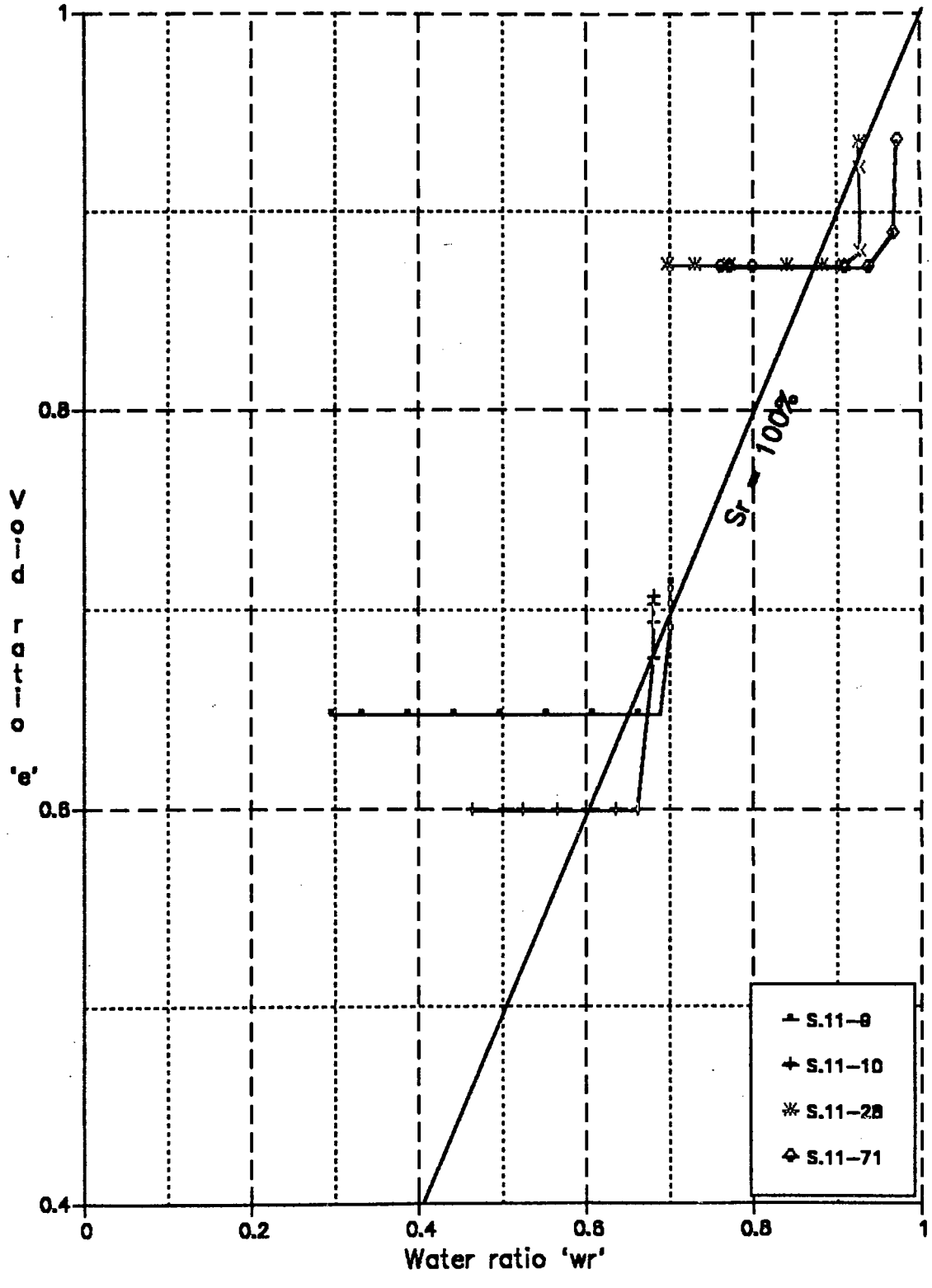

Figure 7.06: Site 11, Rosebank [Compacted samples] - Void ratio 'e' versus water ratio 'wr', for the full test path (includes free-shrinkage and unloading paths).

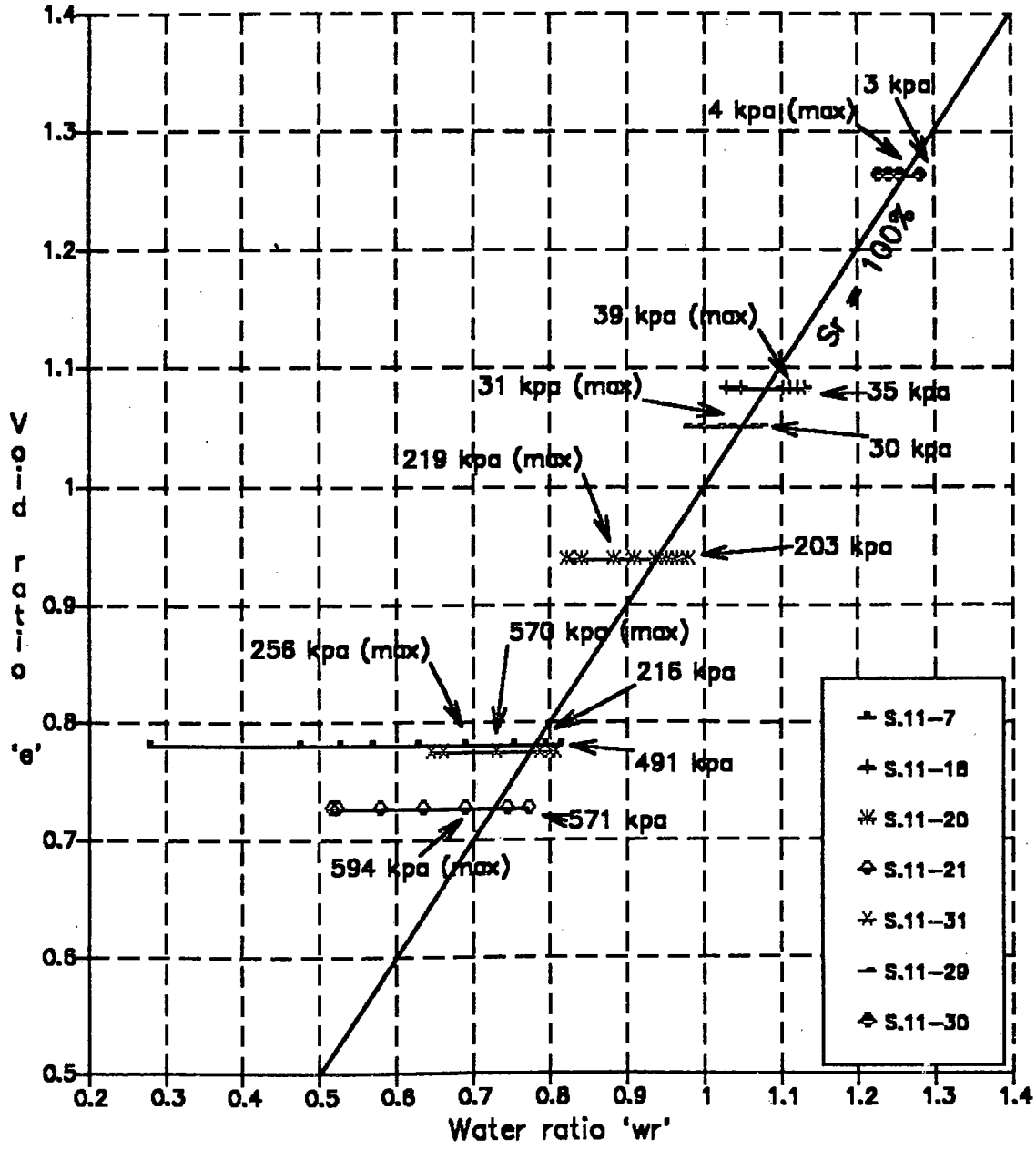

Figure 7.07: Site 11, Rosebank [Undisturbed samples] - Void ratio 'e' versus water ratio 'wr', for the controlled wetting path (includes swell pressures while confined).

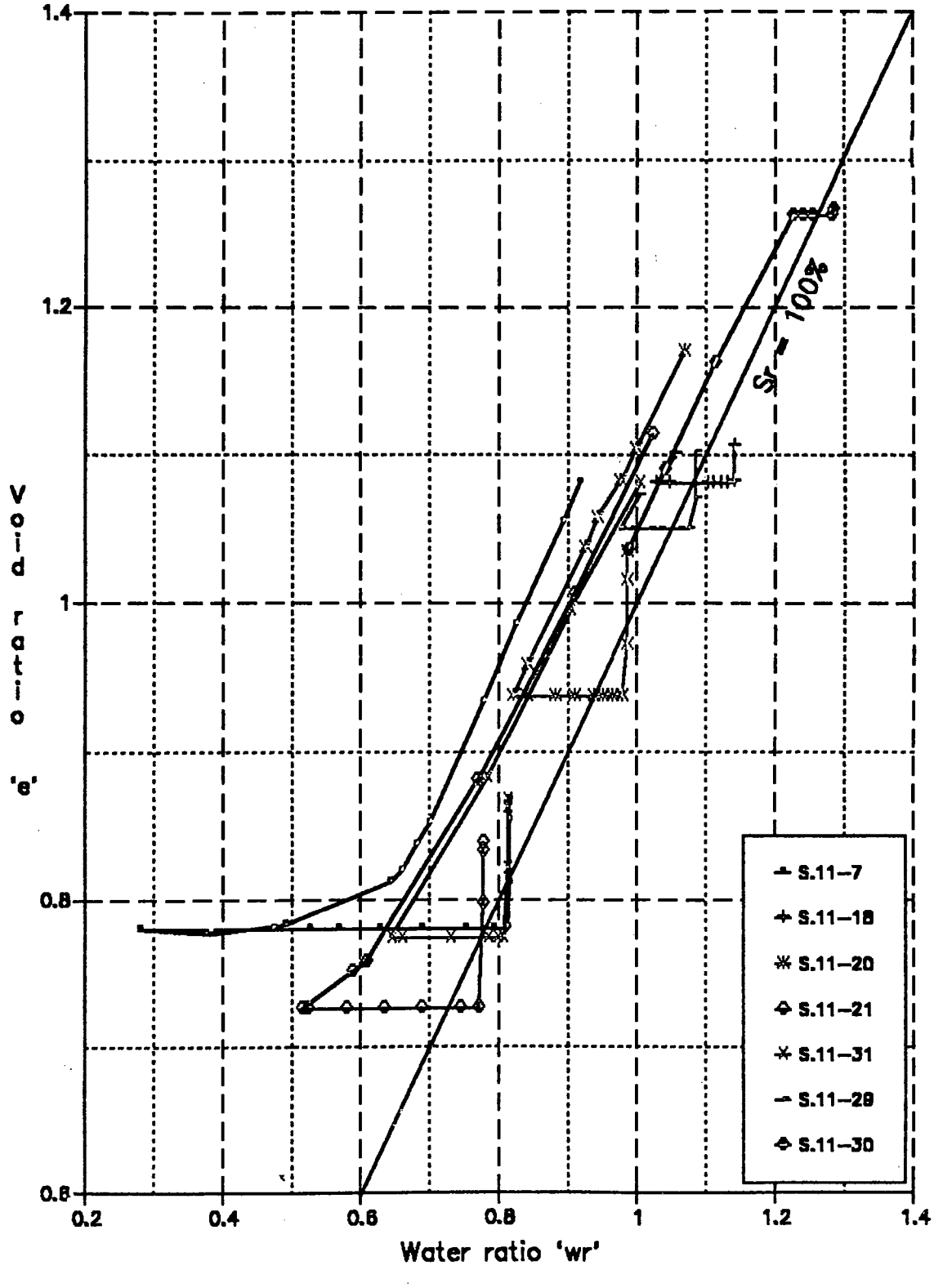

Figure 7.08: Site 11, Rosebank [Undisturbed samples] - Void ratio 'e' versus water ratio 'wr', for the full test path (includes free shrinkage and unloading paths].

Site 36, Rondebosch.

A clayey silt, with fine sand and a small amount of medium sand. The soil consists of 22% clay, 49% silt, and 29% sand size. The 'Limits' of the soil are: w_{LS} = 8.3%; w_L = 47.0%; w_P = 23.3%; I_P = 24; w_S = 22.0%; and, w_{FE} = 32.7%.

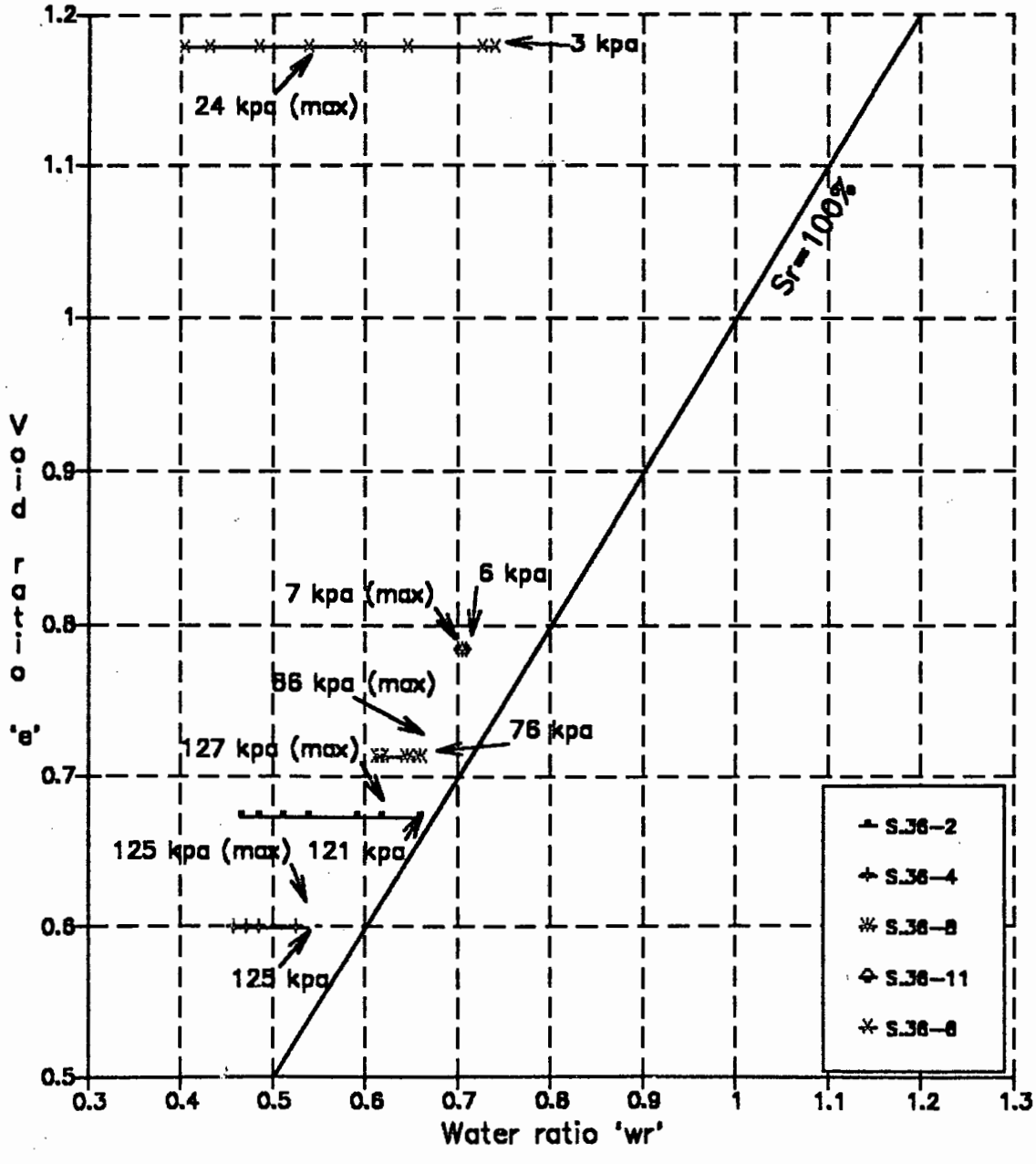

Figure 7.09: Site 36, Rondebosch [Remoulded samples] - Void ratio 'e' versus water ratio 'wr', for the controlled wetting path (includes swell pressures while confined).

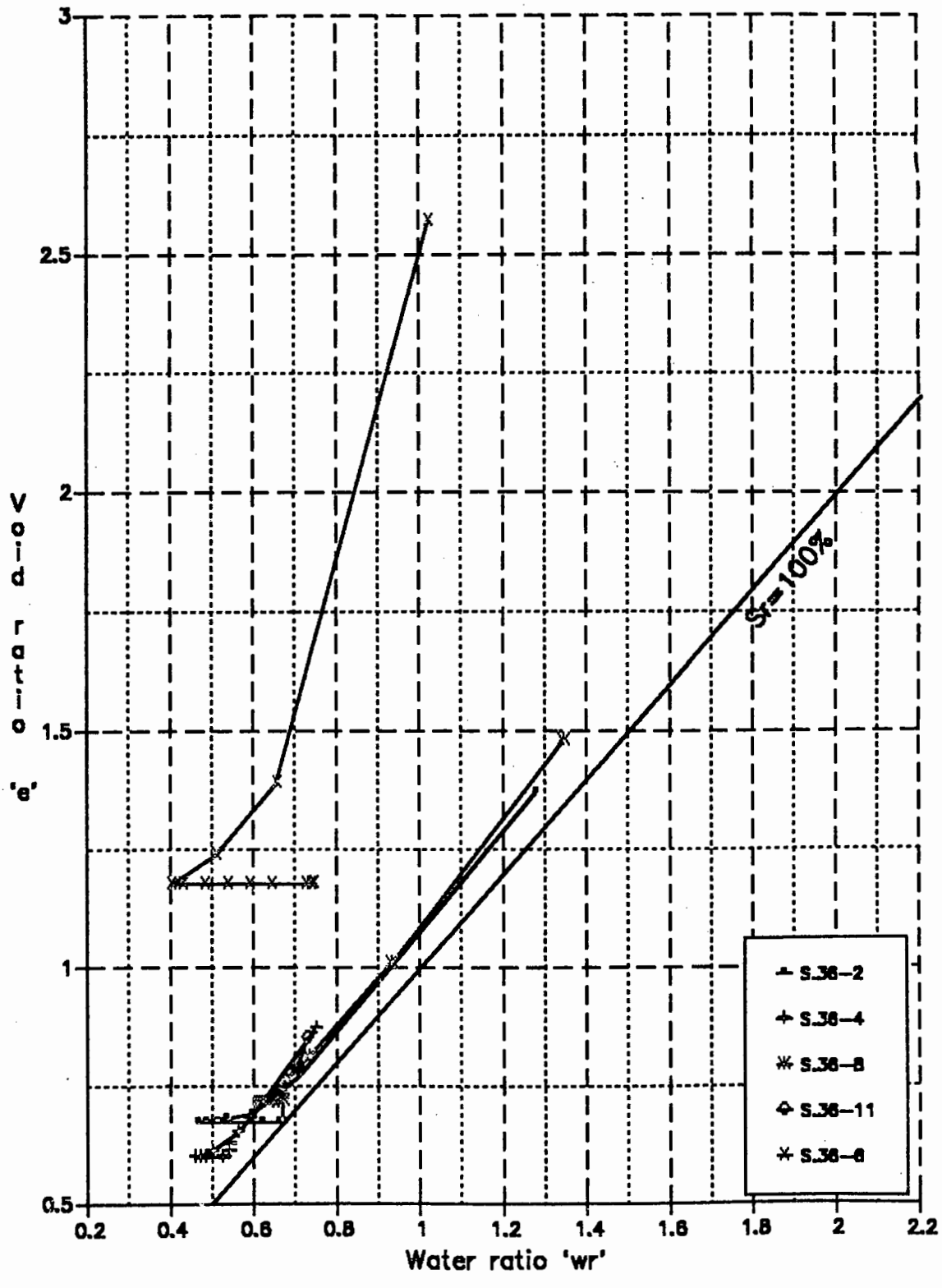

Figure 7.10: Site 36, Rondebosch [Remoulded samples] - Void ratio 'e' versus water ratio 'wr', for the full test path (includes free-shrinkage and unloading paths).

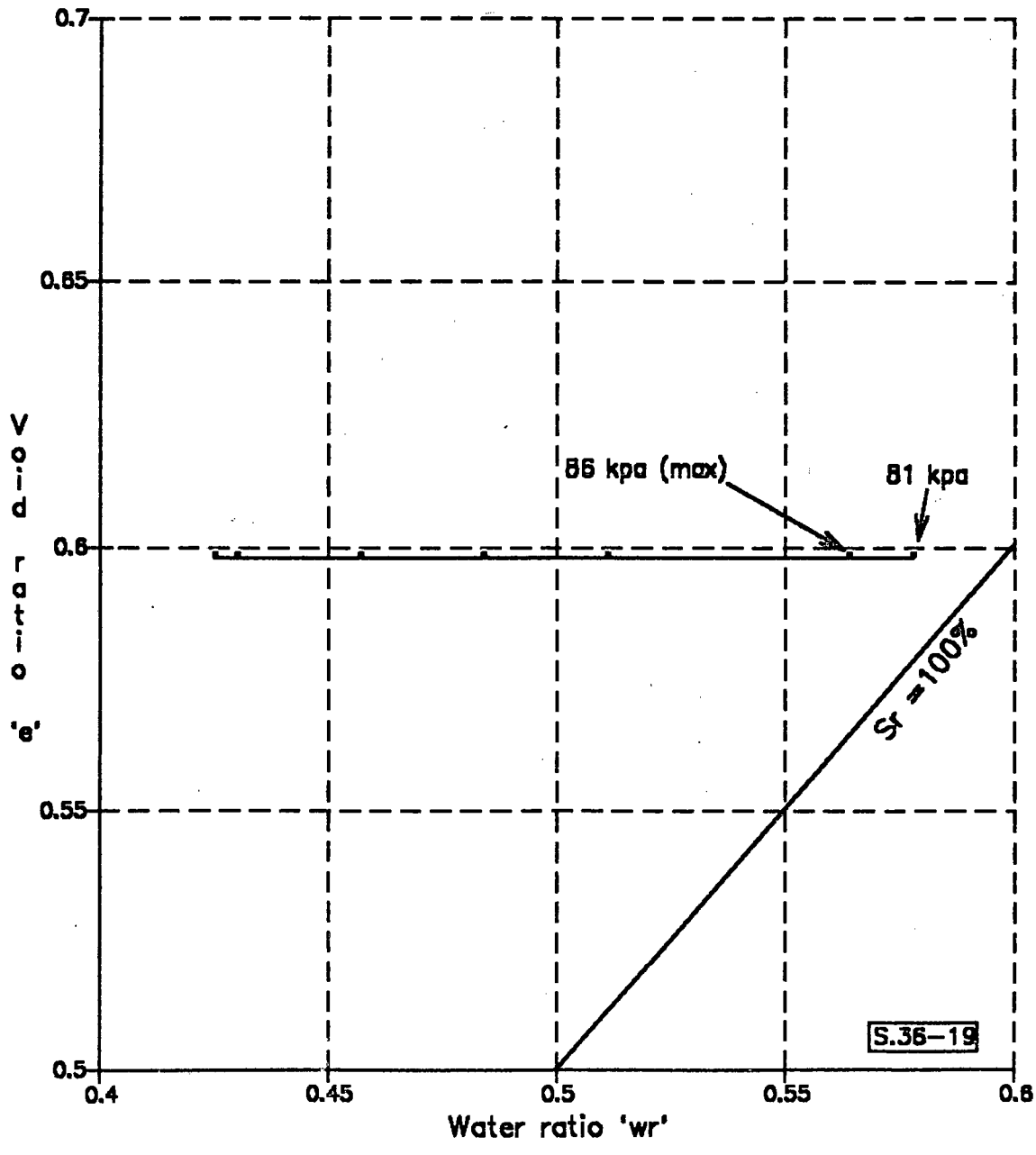

Figure 7.11: Site 36, Rondebosch [Compacted sample] - Void ratio 'e' versus water ratio 'wr', for the controlled wetting path (includes swell pressures while confined).

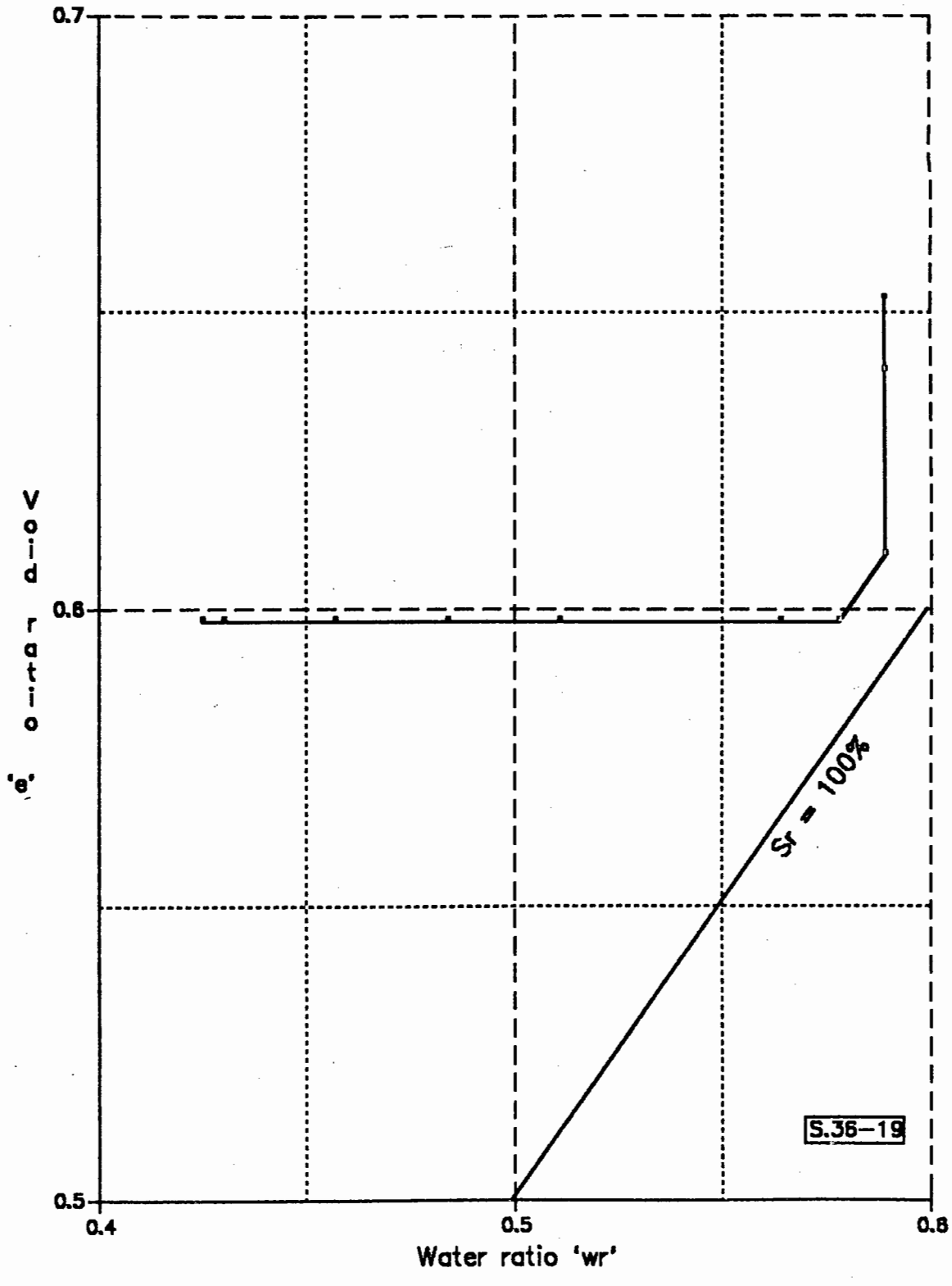

Figure 7.12: Site 36, Rondebosch [Compacted sample] - Void ratio 'e' versus water ratio 'wr', for the full test path (includes free-shrinkage and unloading paths).

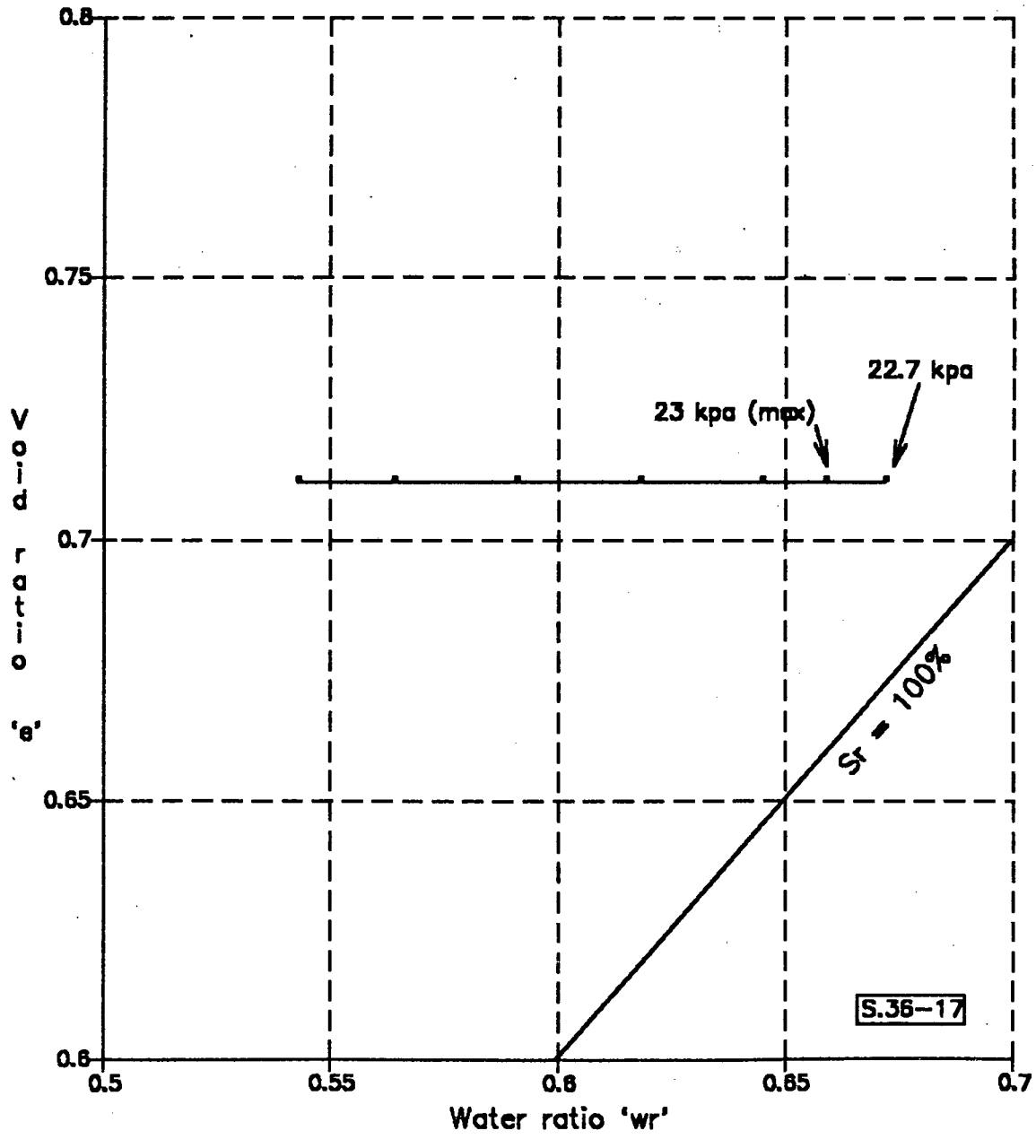

Figure 7.13: Site 36, Rondebosch [Undisturbed sample] - Void ratio 'e' versus water ratio 'wr', for the controlled wetting path (includes swell pressures while confined).

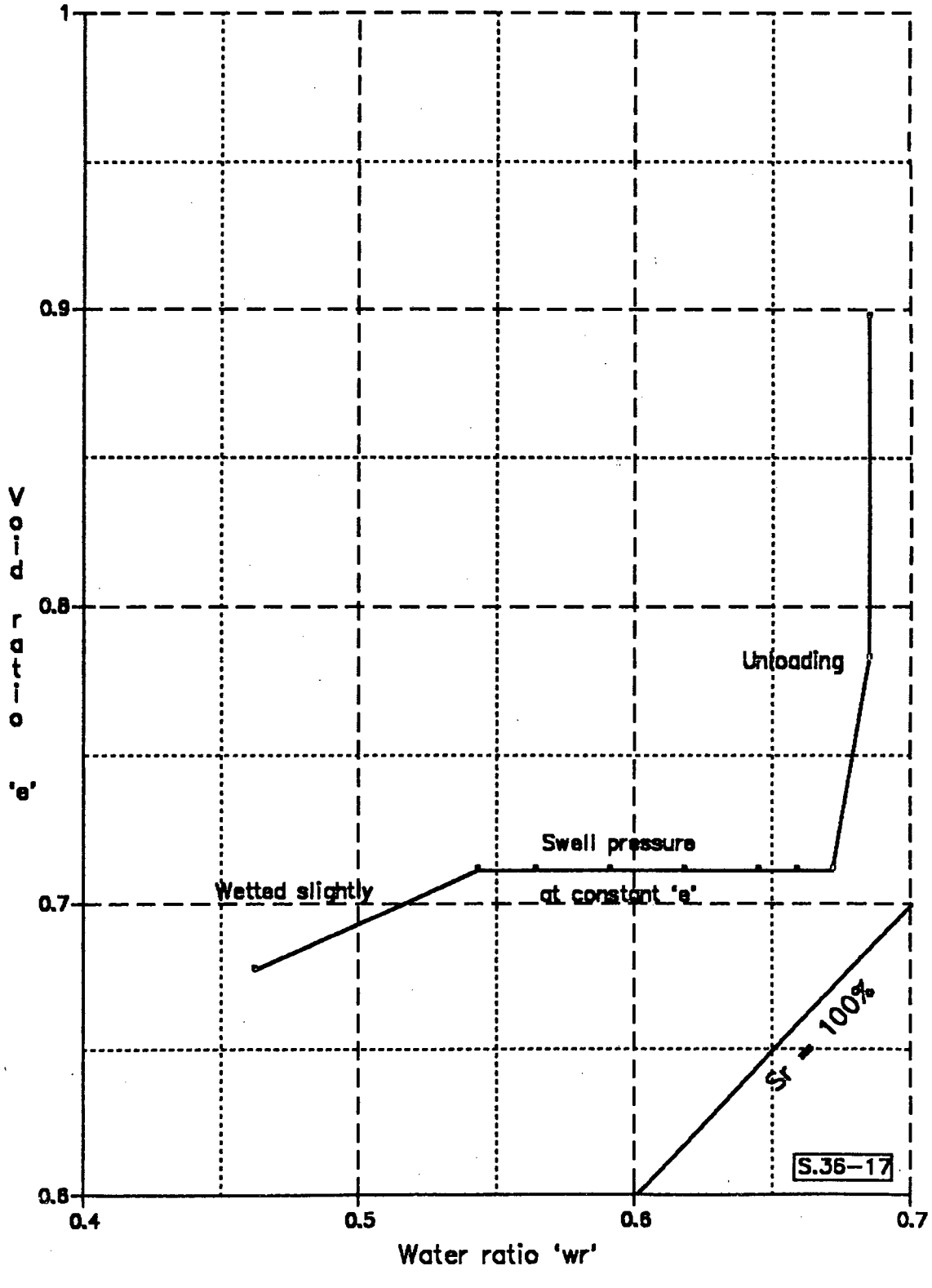

Figure 7.14: Site 36, Rondebosch [Undisturbed sample] - Void ratio 'e' versus water ratio 'wr', for the full test path (includes free-shrinkage and unloading paths).

Site 30, Hout Bay.

A fine to medium sandy silt, with a small amount of coarse sand. The soil consists of 23% clay, 34% silt, and 43% sand size. The 'Limits' of the soil are: w_{LS} = 6.4%; w_L = 49.0%; w_P = 29.0%; I_P = 20; w_S = 22.5%; and, w_{FE} = 36.0%.

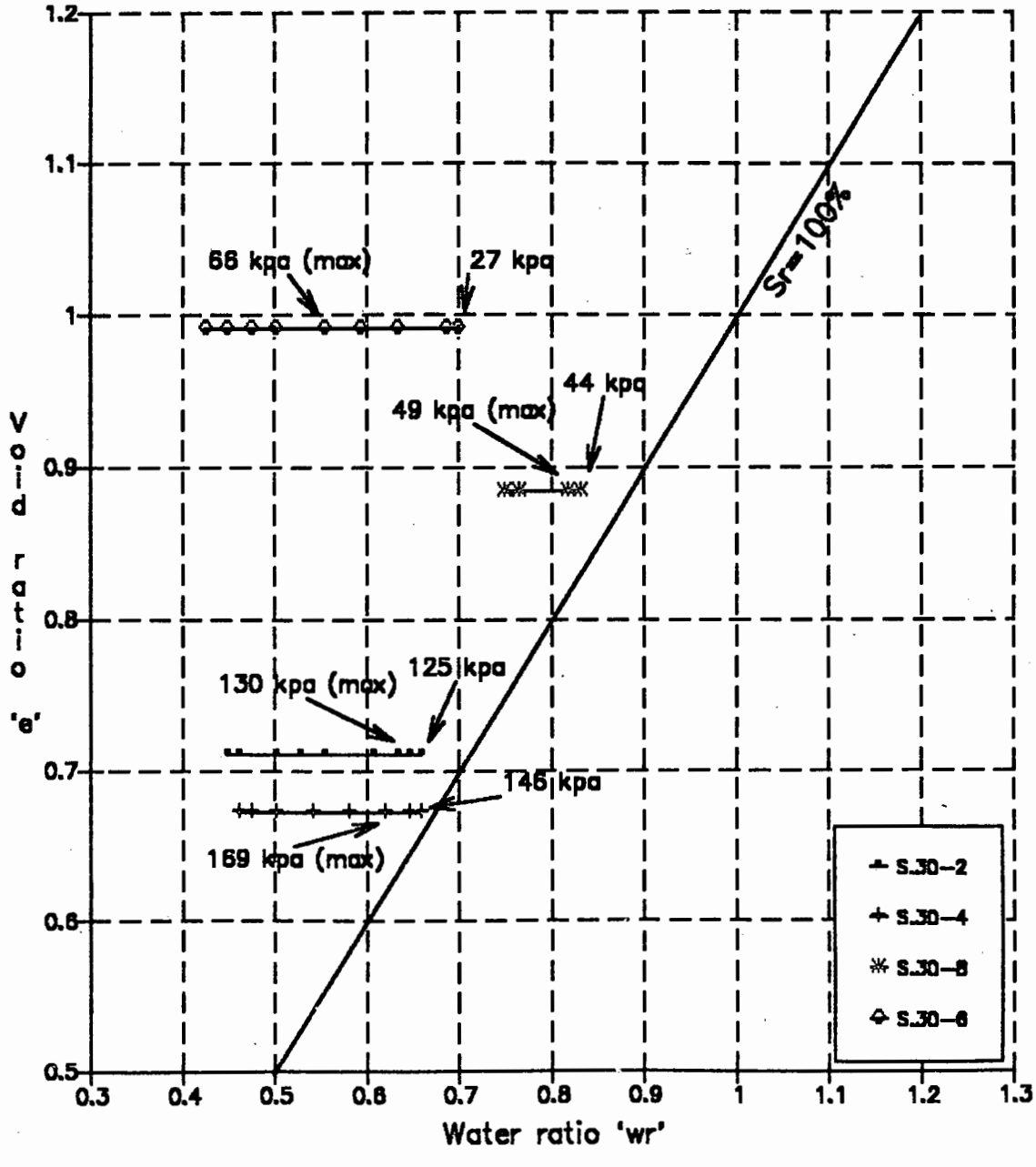

Figure 7.15: Site 30, Hout Bay [Remoulded samples] - Void ratio 'e' versus water ratio 'wr', for the controlled wetting path (includes swell pressures while confined).

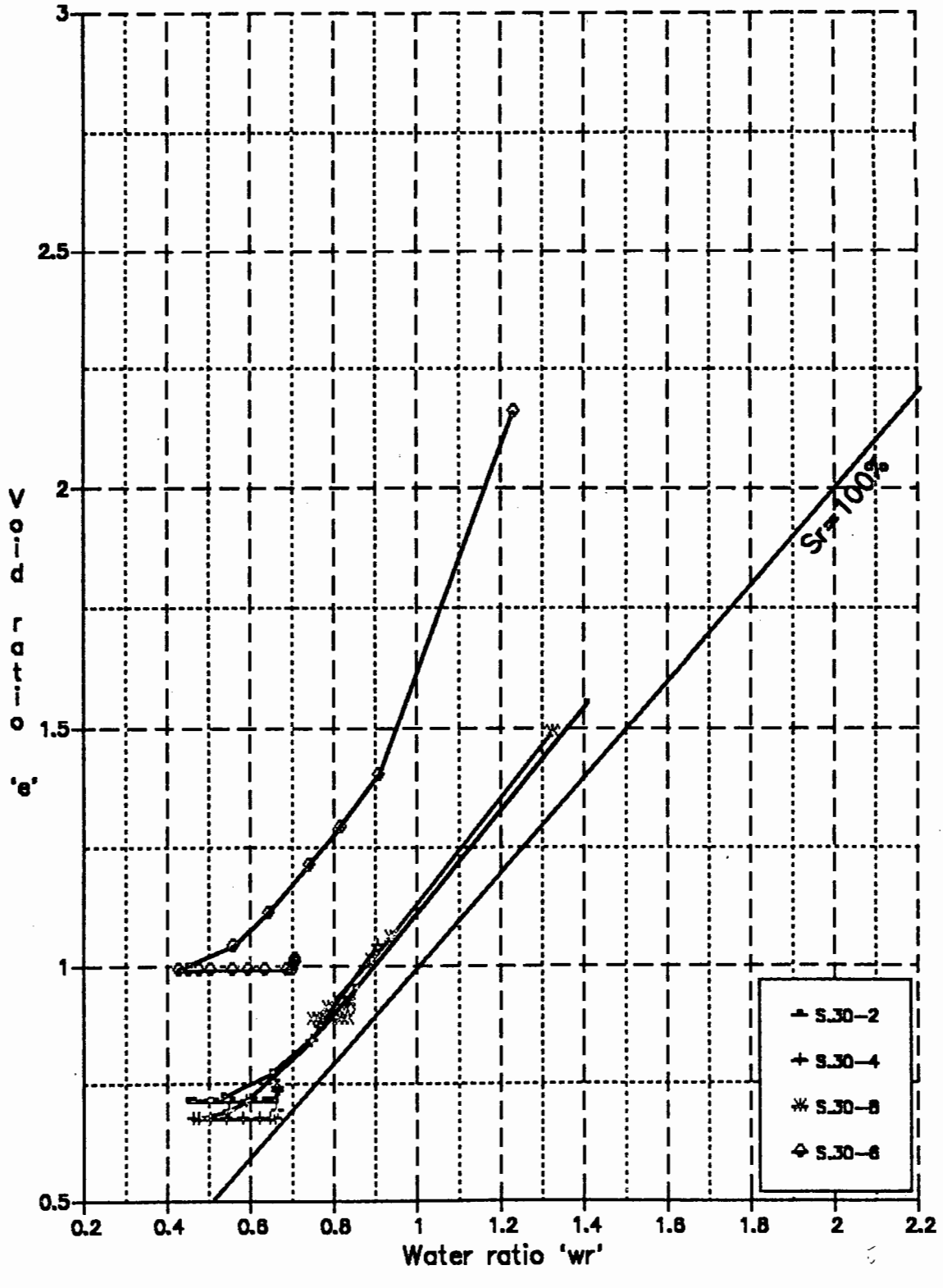

Figure 7.16: Site 30, Hout Bay [Remoulded samples] - Void ratio 'e' versus water ratio 'wr', for the full test path (includes free-shrinkage and unloading paths).

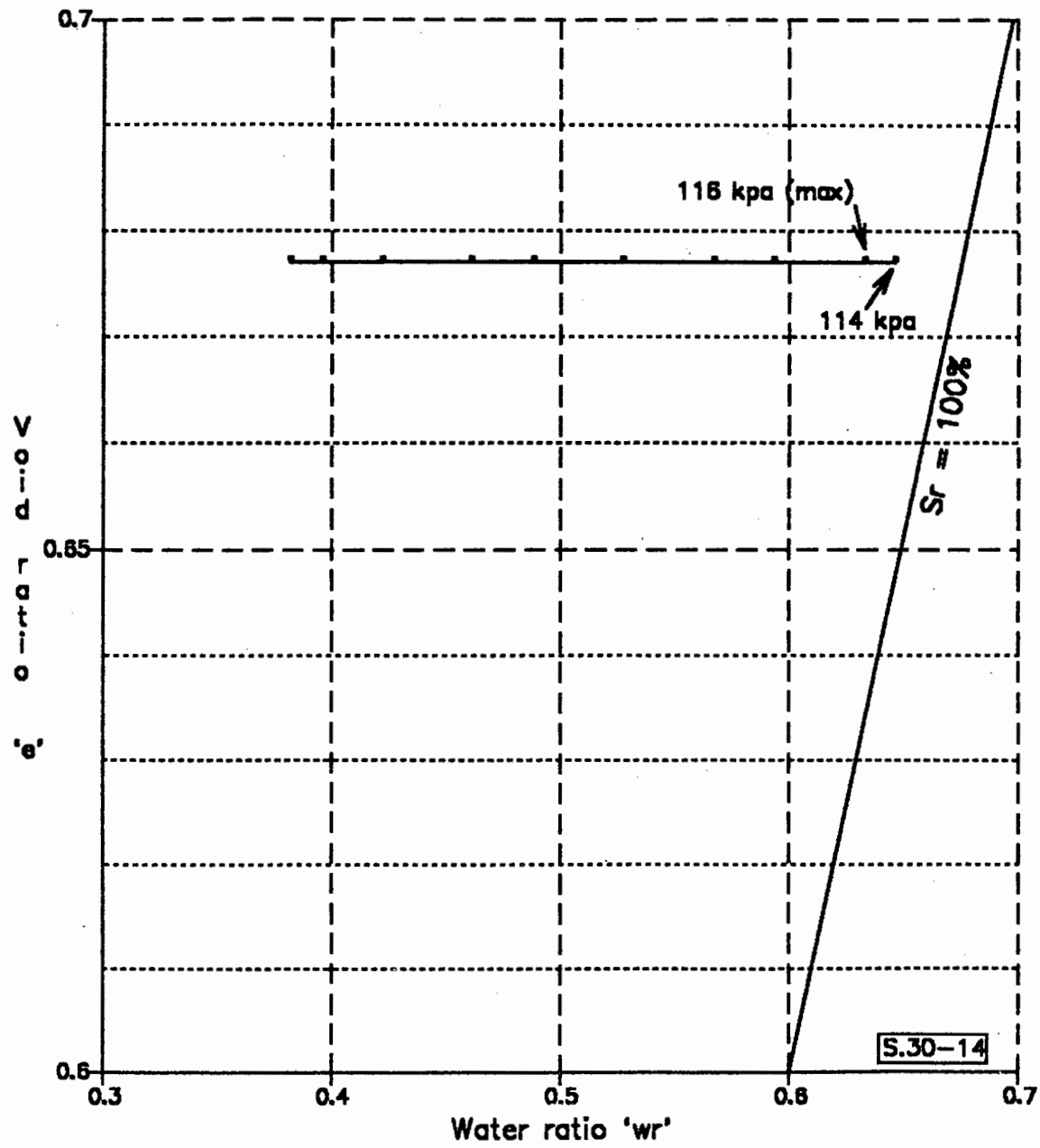

Figure 7.17: Site 30, Hout Bay [Undisturbed sample] - Void ratio 'e' versus water ratio 'wr', for the controlled wetting path (includes swell pressures while confined).

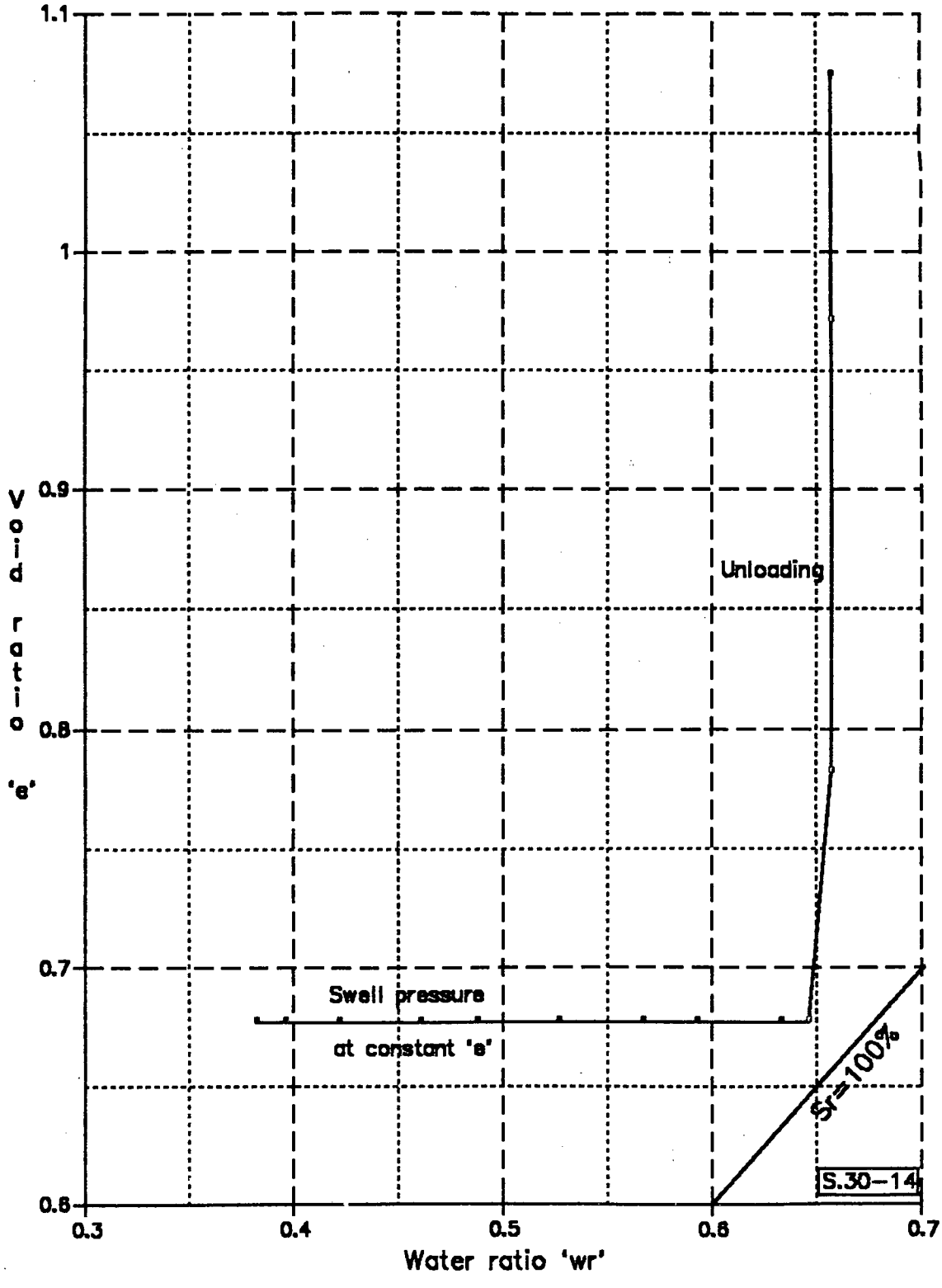

Figure 7.18: Site 30, Hout Bay [Undisturbed sample] - Void ratio 'e' versus water ratio 'wr', for the full test path (includes free-shrinkage and unloading paths).

Site A, Berea Road (Durban).

A clayey sand (fine to medium size) with a small amount of silt. The soil consists of 15% clay, 10% silt, and 75% sand size. The 'Limits' of the soil are: w_{LS} = 3.7%; w_L = 25.0%; w_P = 13.1%; I_P = 12; w_S = 13.5%; and, w_{FE} = 16.6%.

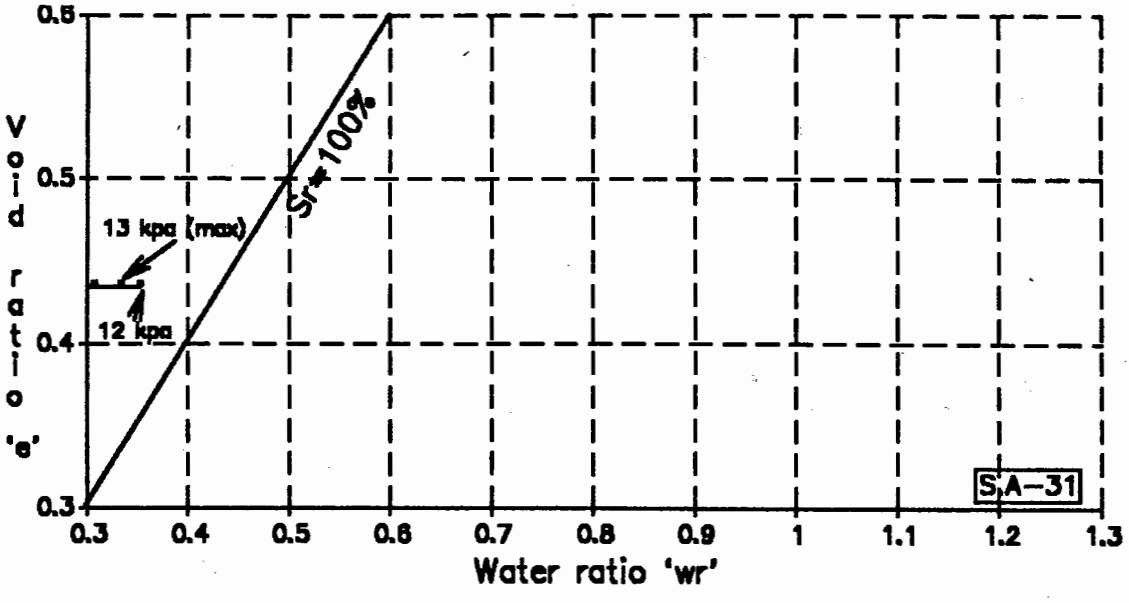

Figure 7.19: Site A, Berea Road (Durban) [Compacted sample] - Void ratio 'e' versus water ratio 'wr', for the controlled wetting path (includes swell pressures while confined).

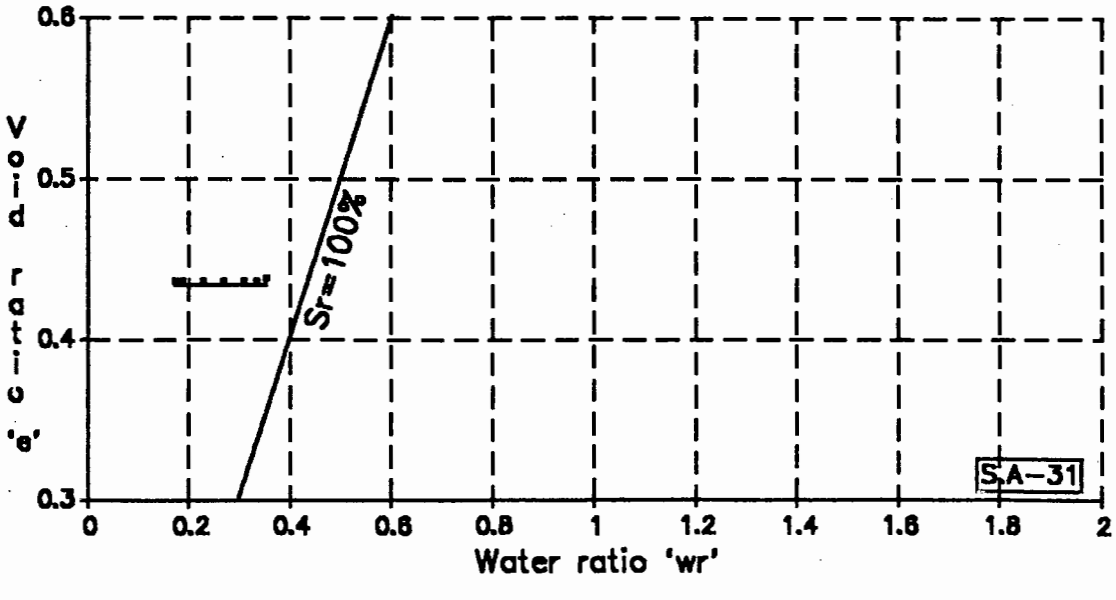

Figure 7.20: Site A, Berea Road (Durban) [Compacted sample] - Void ratio 'e' versus water ratio 'wr', for the full test path (includes free-shrinkage and unloading paths).

Site 7, Mowbray.

A fine silty clay, with a small amount of fine to medium sand. The soil consists of 42% clay, 37% silt, and 21% sand size. The Limits of the soil are: w_{Ls} = 10.5%; w_L = 47.0%; w_P = 22.0%; I_P = 25; w_S = 18.5%; and, w_{FE} = 29.1%.

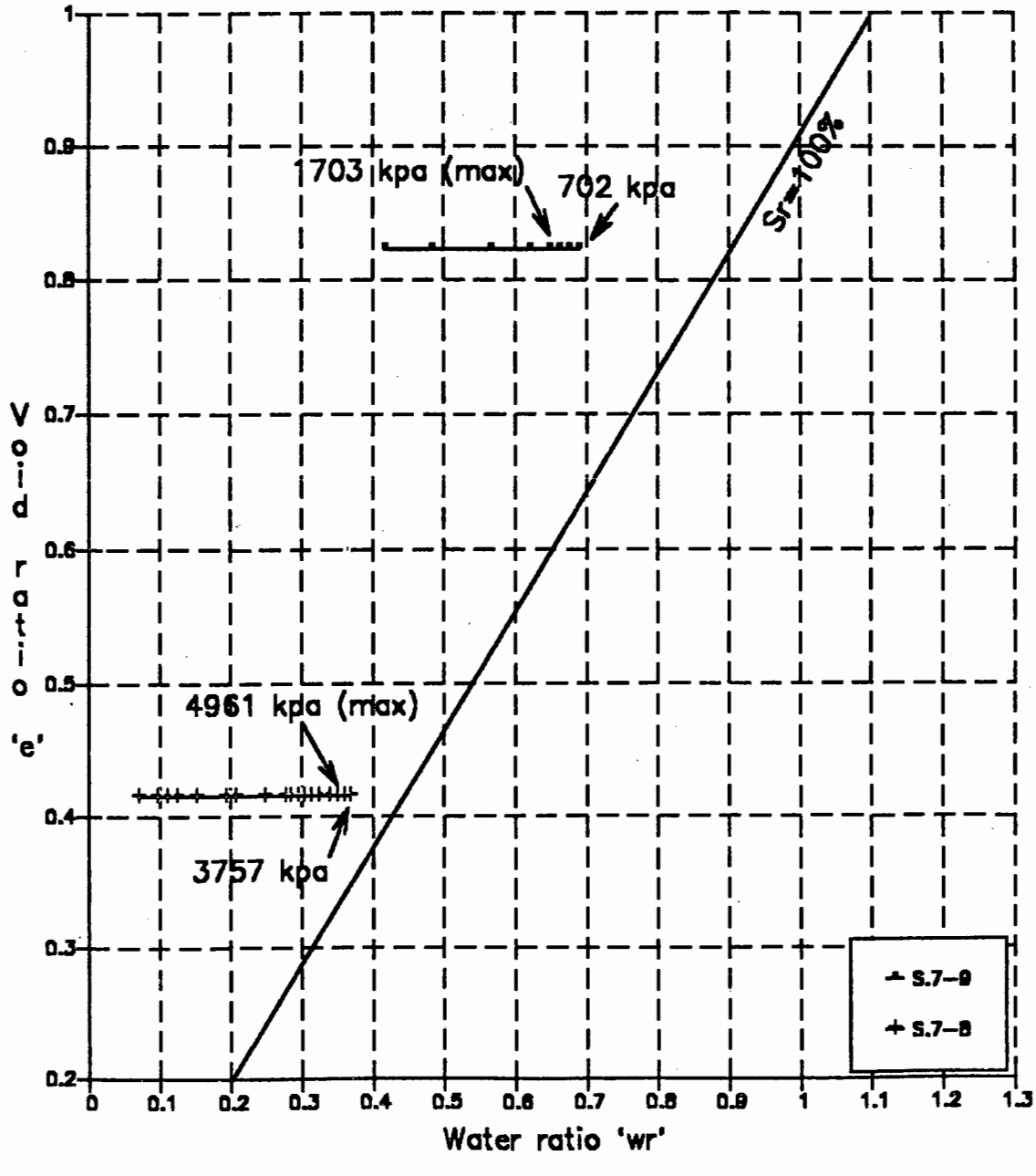

Figure 7.21: Site 7, Mowbray [Remoulded samples] - Void ratio 'e' versus water ratio 'wr', for the controlled wetting path (includes swell pressures while confined).

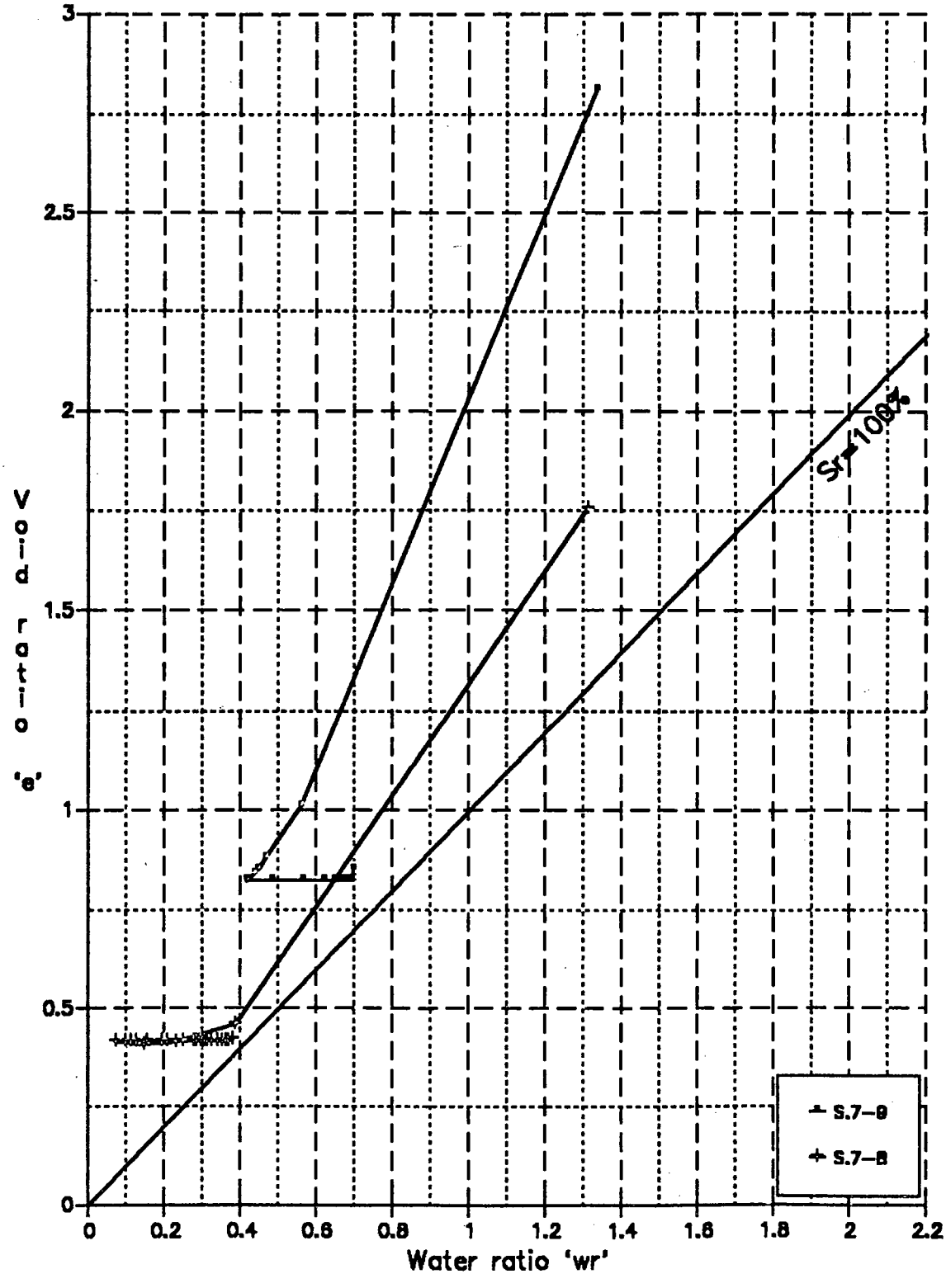

Figure 7.22: Site 7, Mowbray [Remoulded samples] - Void ratio 'e' versus water ratio 'wr', for the full test path (includes free-shrinkage and unloading paths).

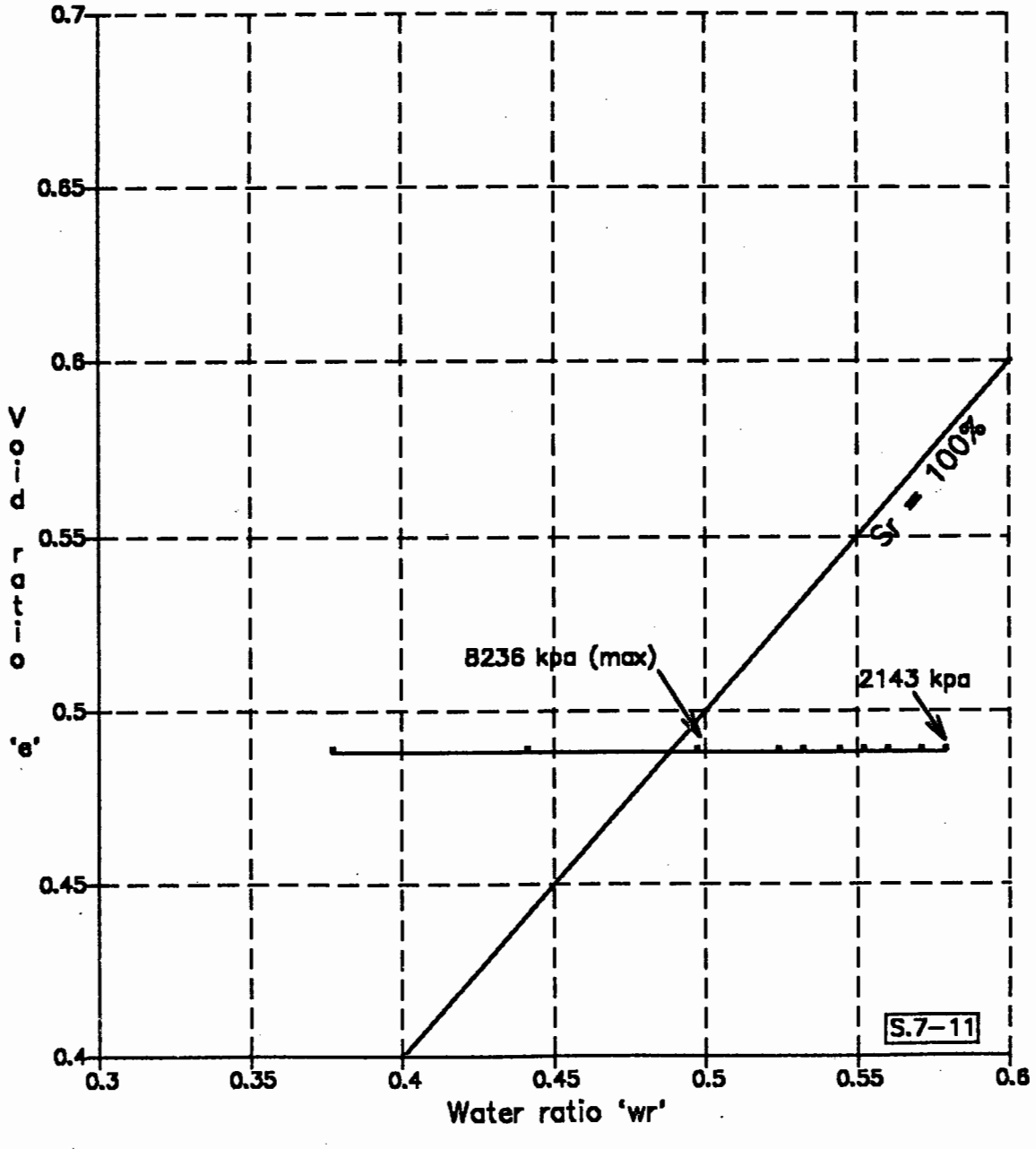

Figure 7.23: Site 7, Mowbray [Undisturbed sample] - Void ratio 'e' versus the water ratio 'wr', for the controlled wetting path (includes swell pressures while confined).

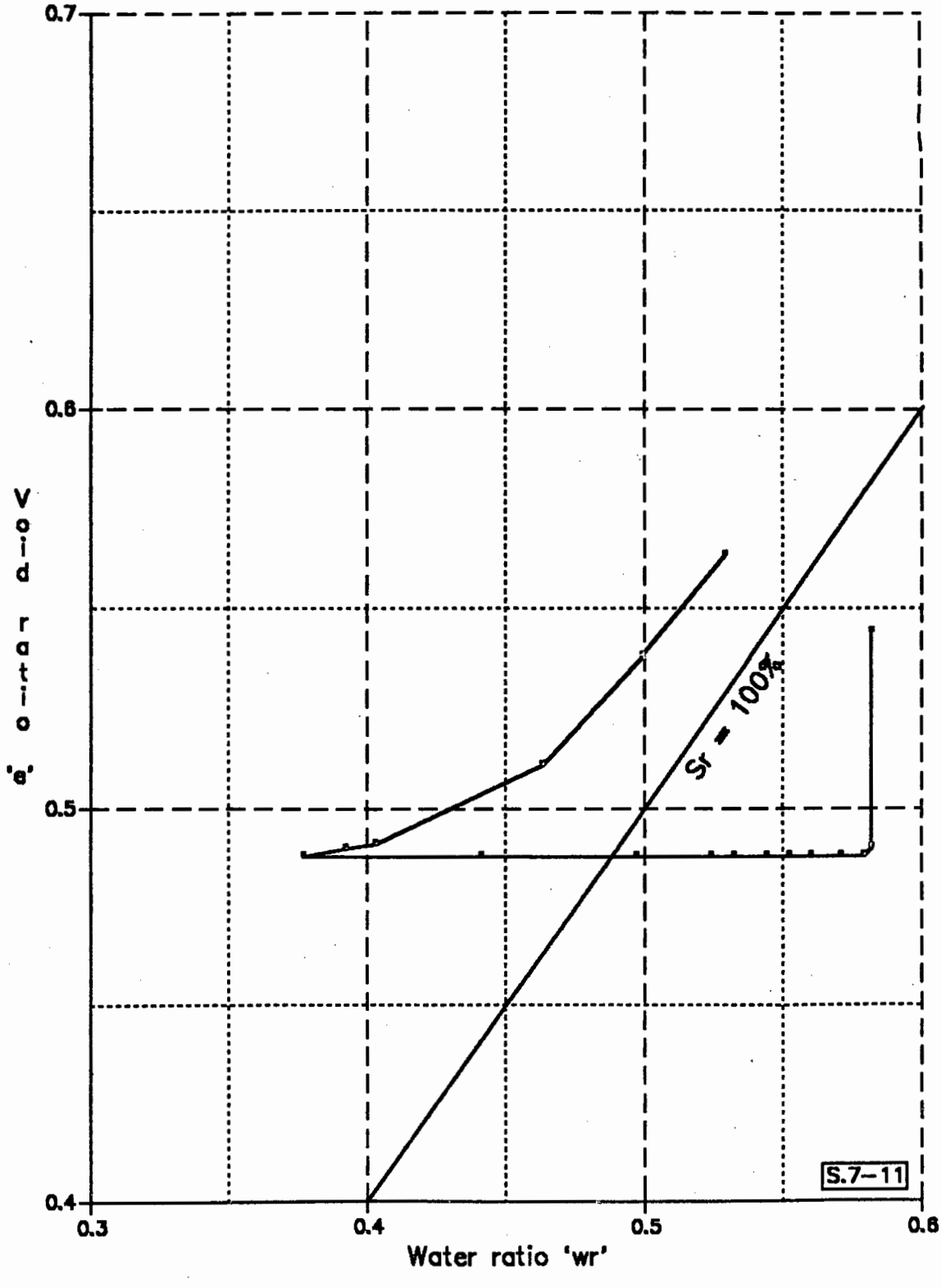

Figure 7.24: Site 7, Mowbray [Undisturbed sample] - Void ratio 'e' versus water ratio 'wr', for the full test path (includes free-shrinkage and unloading paths).

7.8 ANALYSIS OF TEST RESULTS

The test results and their inter-relationships are analysed in two parts:

1) Void Ratio versus Effective Vertical Pressure; and,

2) Void Ratio versus Effective Vertical Pressure versus Water Ratio.

These relationships are illustrated in Figures 7.25 to 7.46, as follows:

Void ratio versus effective vertical pressure for the full test path.

Site 11, Rosebank: Remoulded samples - Figure 7.25;
Compacted - Fig. 7.26; Undisturbed - Fig. 7.27.
Site 36, Rondebosch: Remoulded samples - Figure 7.28;
Compacted - Fig. 7.29; Undisturbed - Fig. 7.30.
Site 30, Hout Bay: Remoulded samples - Figure 7.31;
Undisturbed - Fig. 7.32.
Site A, Berea Road (Durban): Compacted sample - Figure 7.33.
Site 7, Mowbray: Remoulded samples - Figure 7.34;
Undisturbed - Fig. 7.35.

Void ratio vs effective vertical pressure vs water ratio for the full test path.[1]

Site 11, Rosebank: Remoulded samples - Figure 7.36;
Compacted - Fig. 7.37; Undisturbed - Fig. 7.38.
Site 36, Rondebosch: Remoulded samples - Fig. 7.39;
Compacted - 7.40; Undisturbed - Fig. 7.41.
Site 30, Hout Bay: Remoulded samples - Fig. 7.42;
Undisturbed - Fig. 7.43.
Site A, Berea Road (Durban): Figure 7.44.
Site 7, Mowbray: Remoulded samples - Figure 7.45;
Undisturbed - 7.46.

---

[1] - *three dimensional plot.*

7.8.1 Void Ratio versus Effective Vertical Pressure. Site 11, Rosebank.

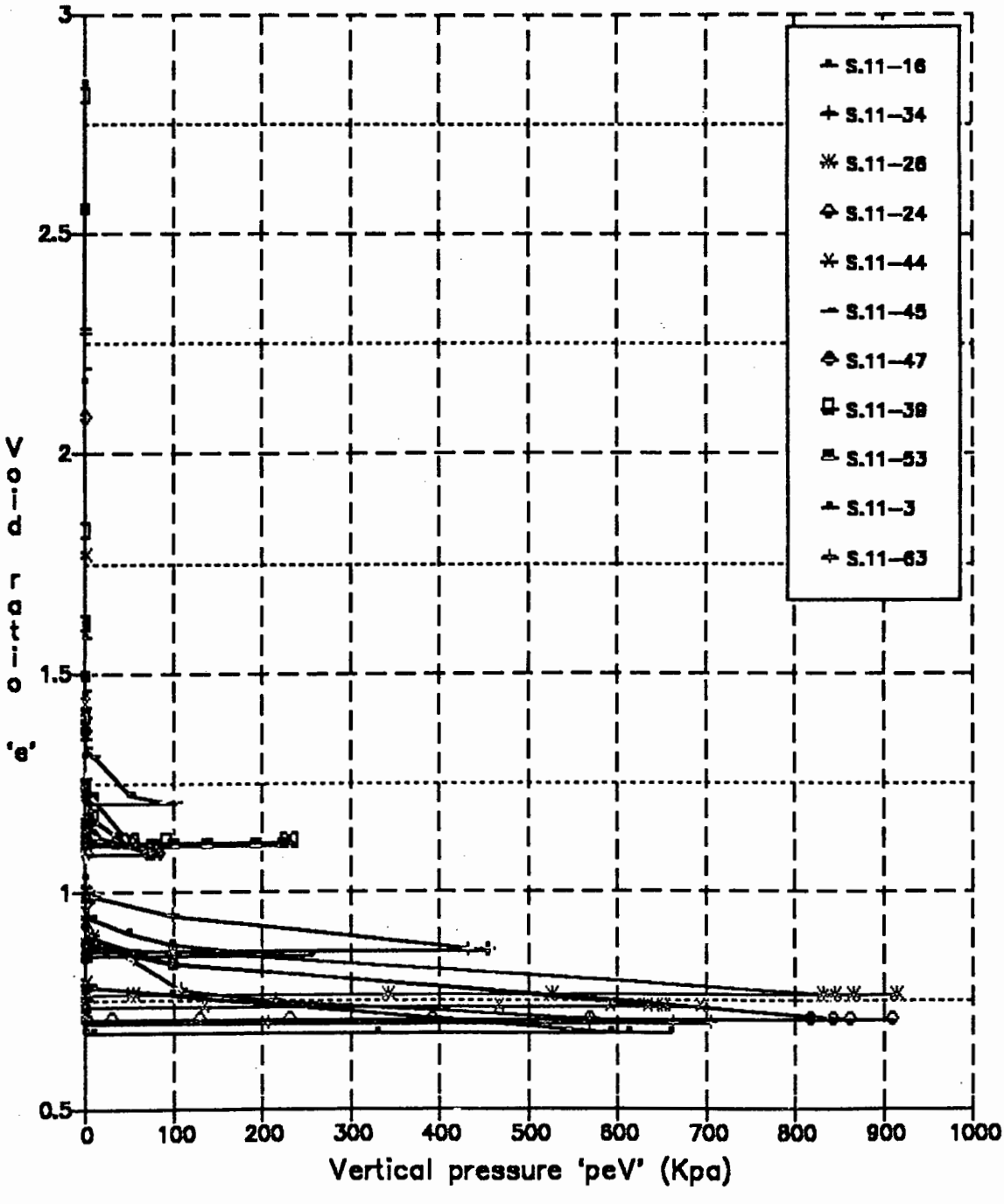

Figure 7.25: Site 11, Rosebank [Remoulded samples] - Void ratio 'e' versus effective vertical pressure 'peV', for the full test path.

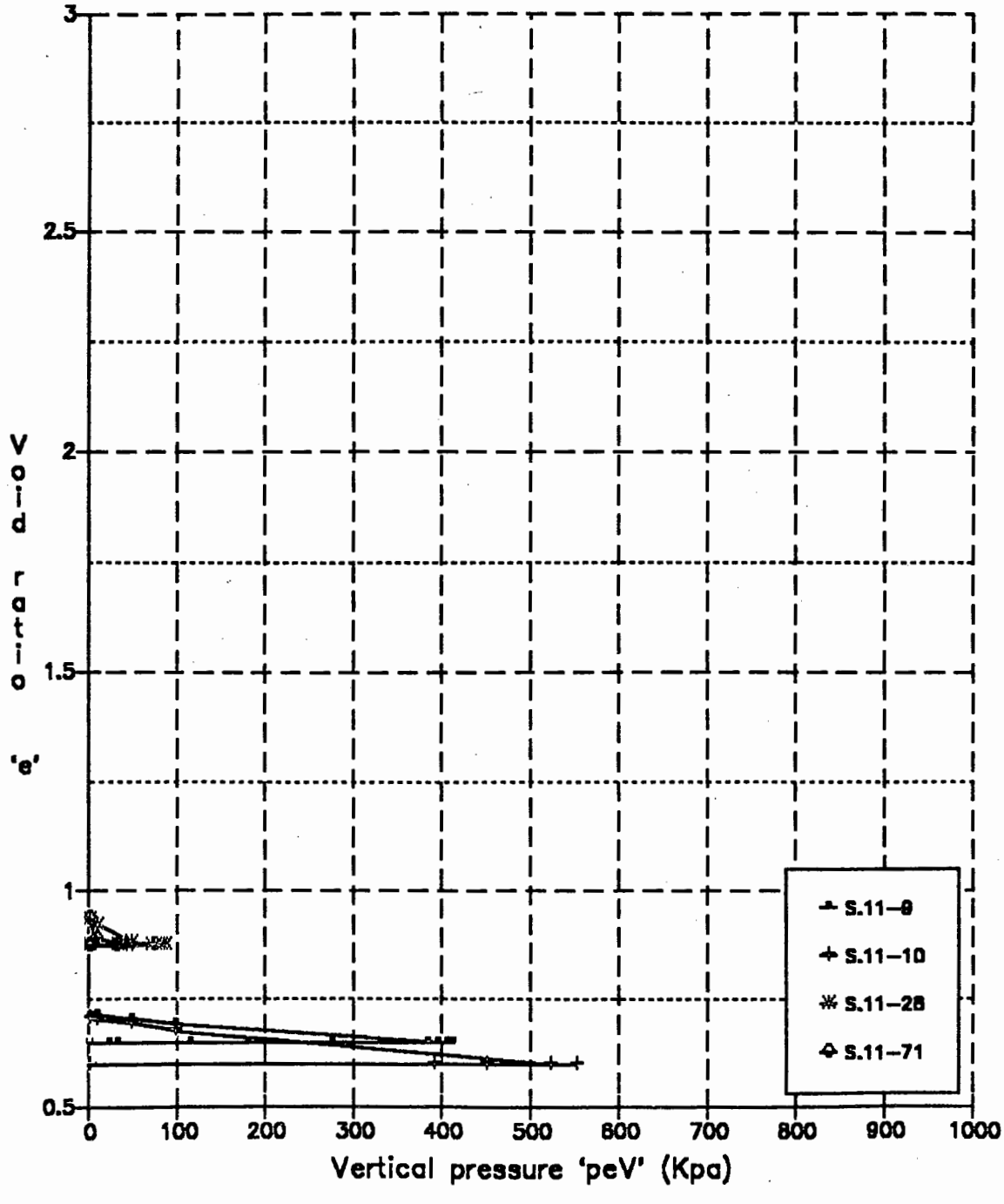

Figure 7.26: Site 11, Rosebank [Compacted samples] - Void ratio 'e' versus effective vertical pressure 'peV', for the full test path.

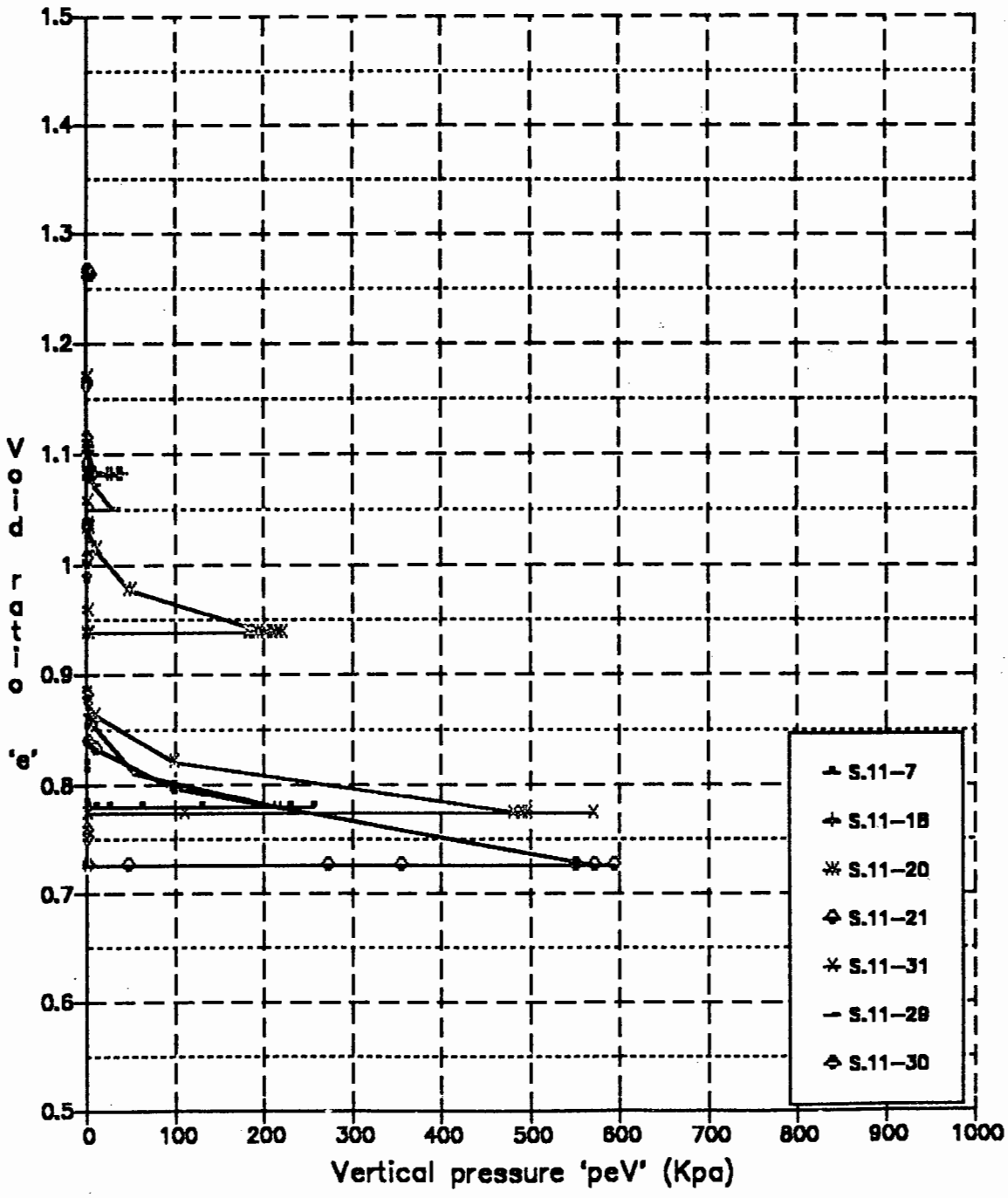

Figure 7.27: Site 11, Rosebank [Undisturbed samples] - Void ratio 'e' versus effective vertical pressure 'peV', for the full test path.

Site 36, Rondebosch.

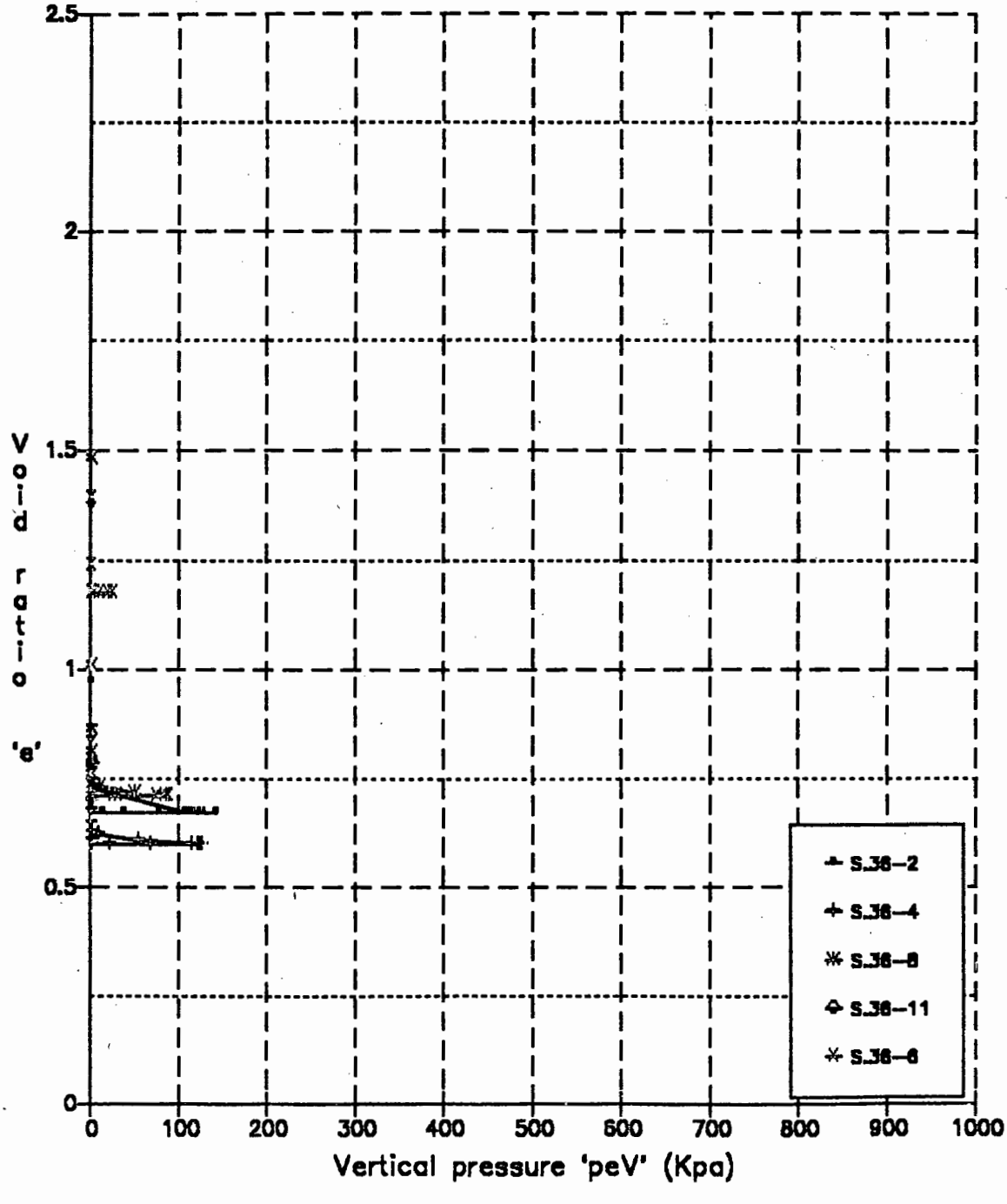

Figure 7.28: Site 36, Rondebosch [Remoulded samples] - Void ratio 'e' versus effective vertical pressure 'peV', for the full test path.

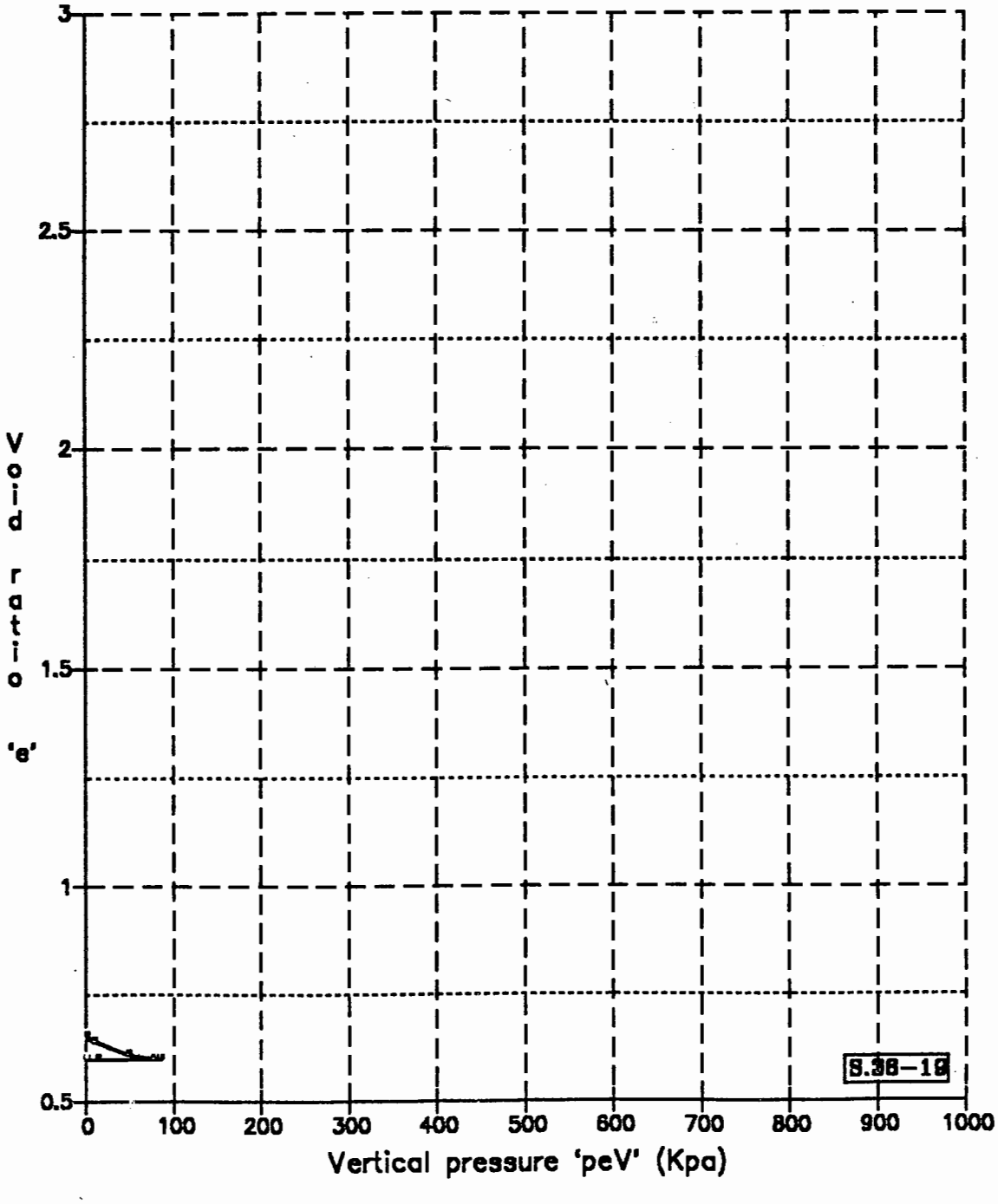

Figure 7.29: Site 36, Rondebosch [Compacted sample] - Void ratio 'e' versus effective vertical pressure 'peV', for the full test path.

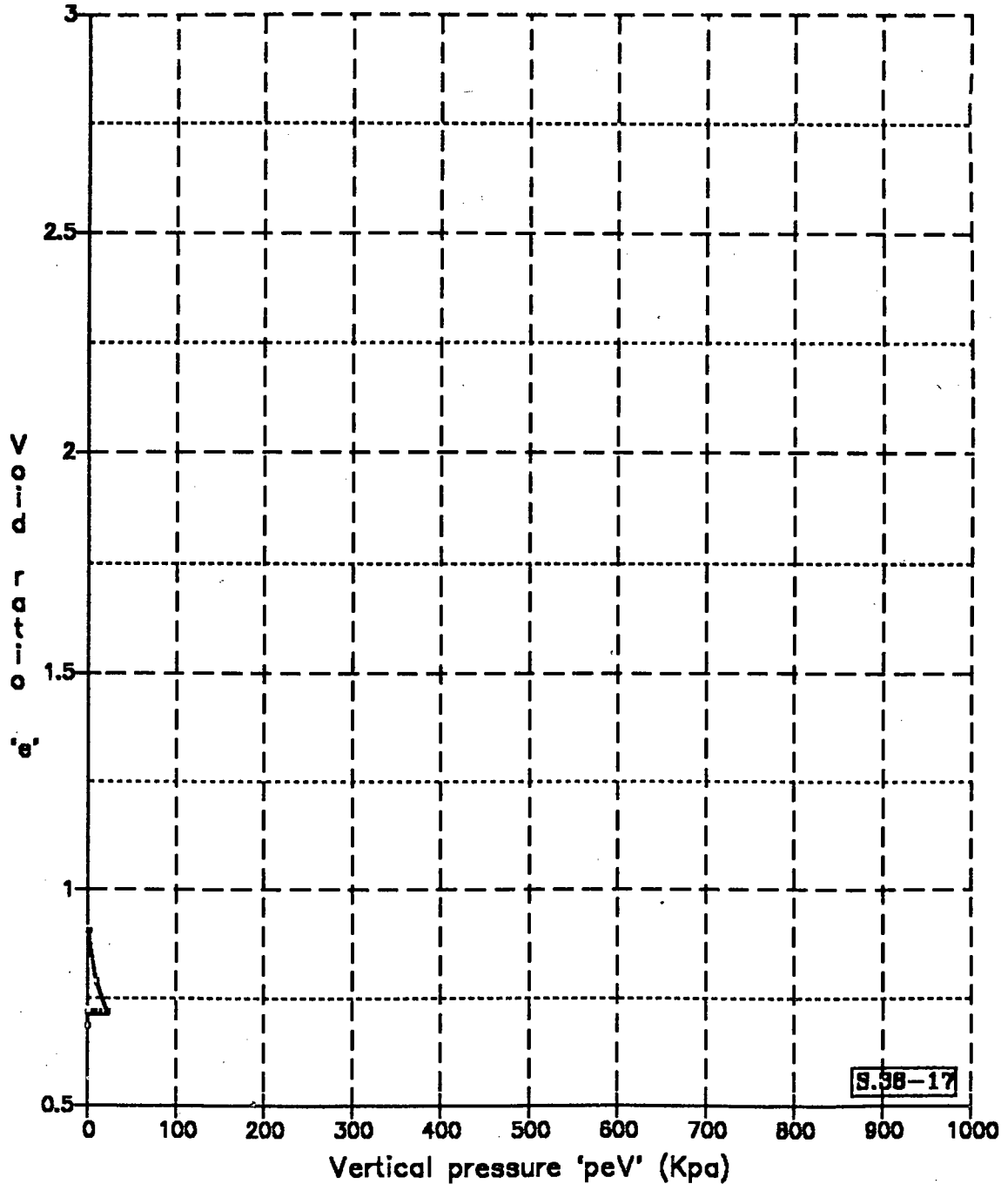

Figure 7.30: Site 36, Rondebosch [Undisturbed sample] - Void ratio 'e' versus effective vertical pressure 'peV', for the full test path.

Site 30, Hout Bay.

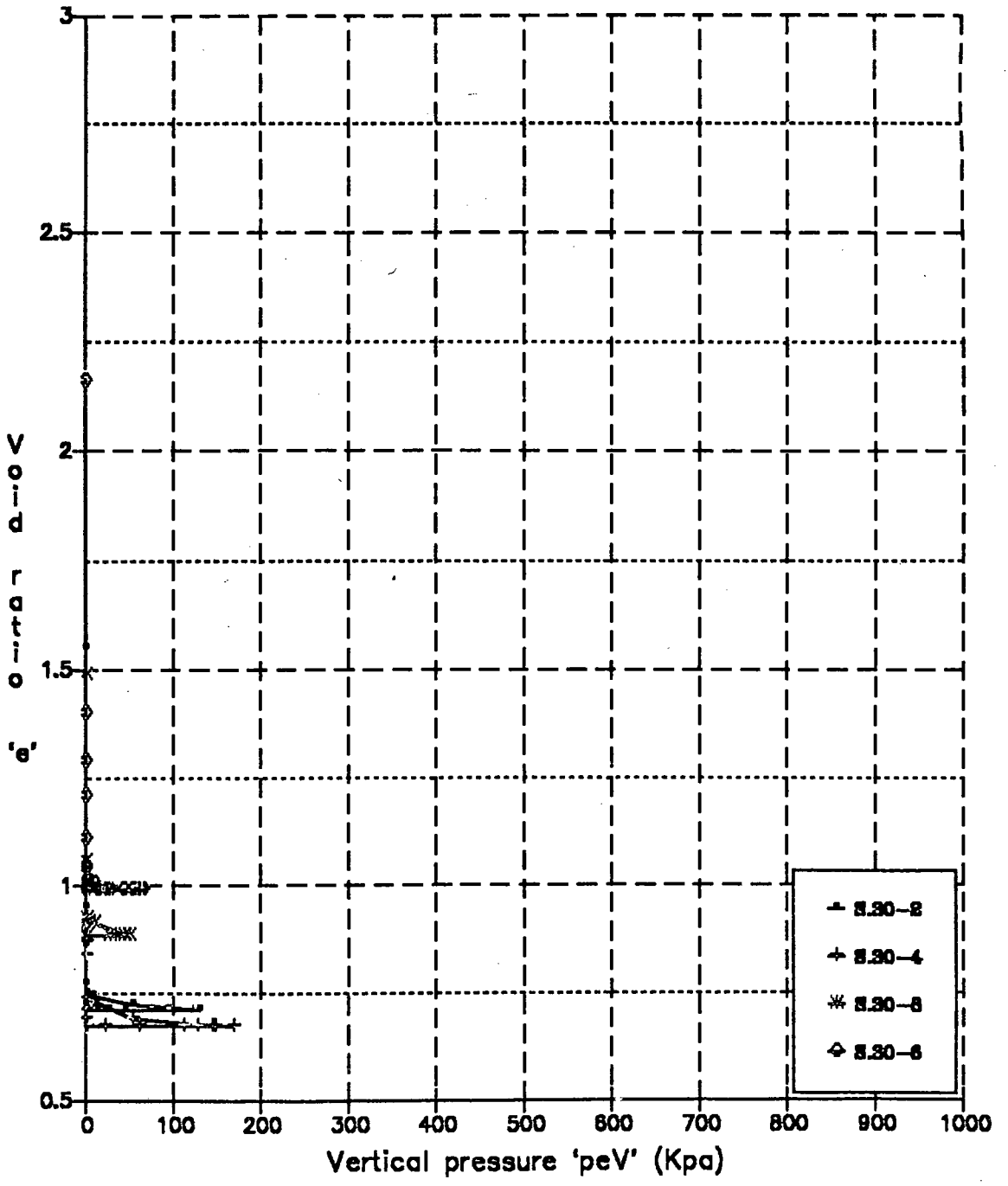

Figure 7.31: Site 30, Hout Bay [Remoulded samples] - Void ratio 'e' versus effective vertical pressure 'peV', for the full test path.

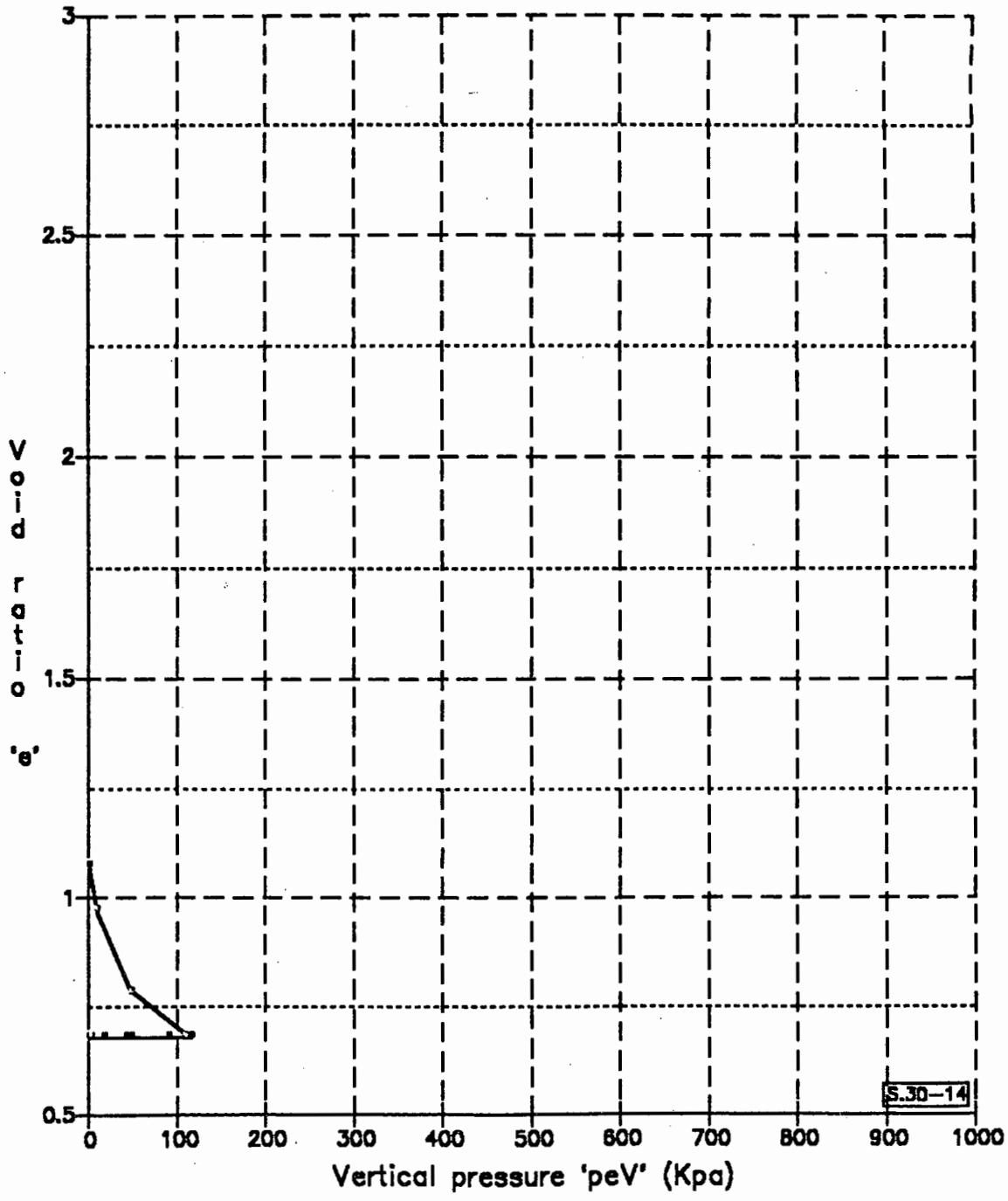

Figure 7.32: Site 30, Hout Bay [Undisturbed sample] - Void ratio 'e' versus effective vertical pressure 'peV', for the full test path.

Site A, Berea Road (Durban).

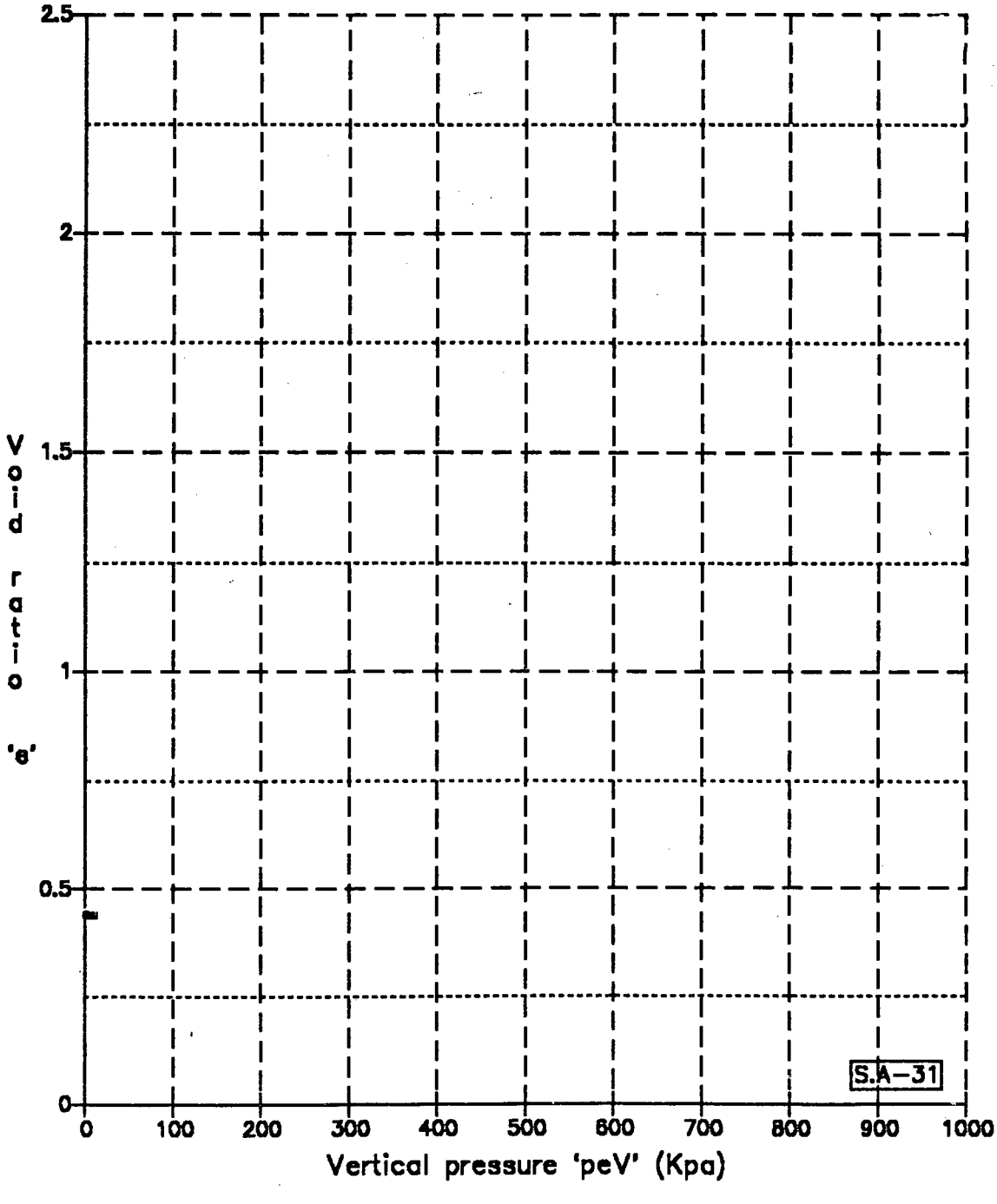

Figure 7.33: Site A, Berea Road (Durban) [Compacted sample] - Void ratio 'e' versus effective vertical pressure 'peV', for the full test path.

Site 7, Mowbray.

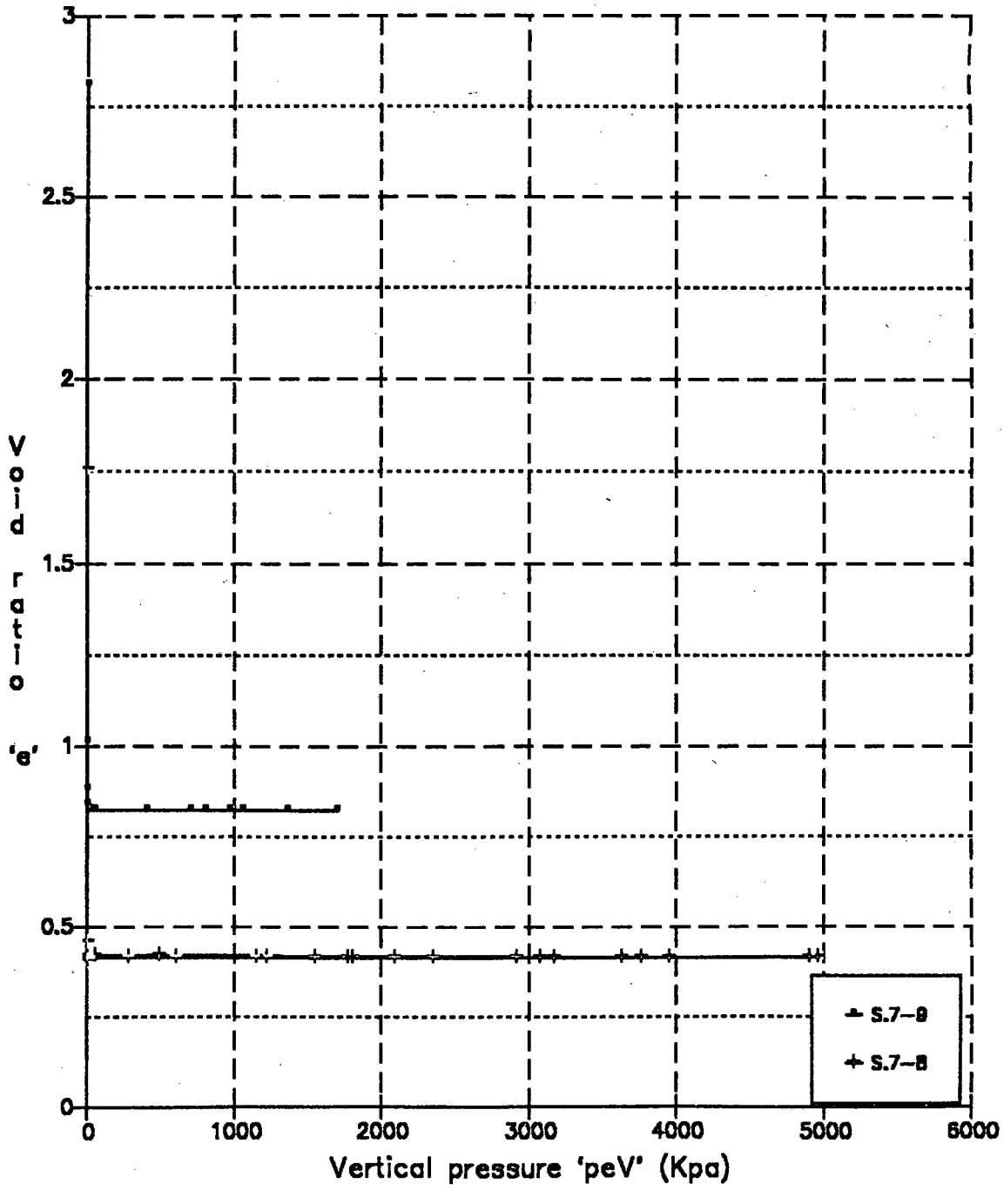

Figure 7.34: Site 7, Mowbray [Remoulded samples] - Void ratio 'e' versus effective vertical pressure 'peV', for the full test path.

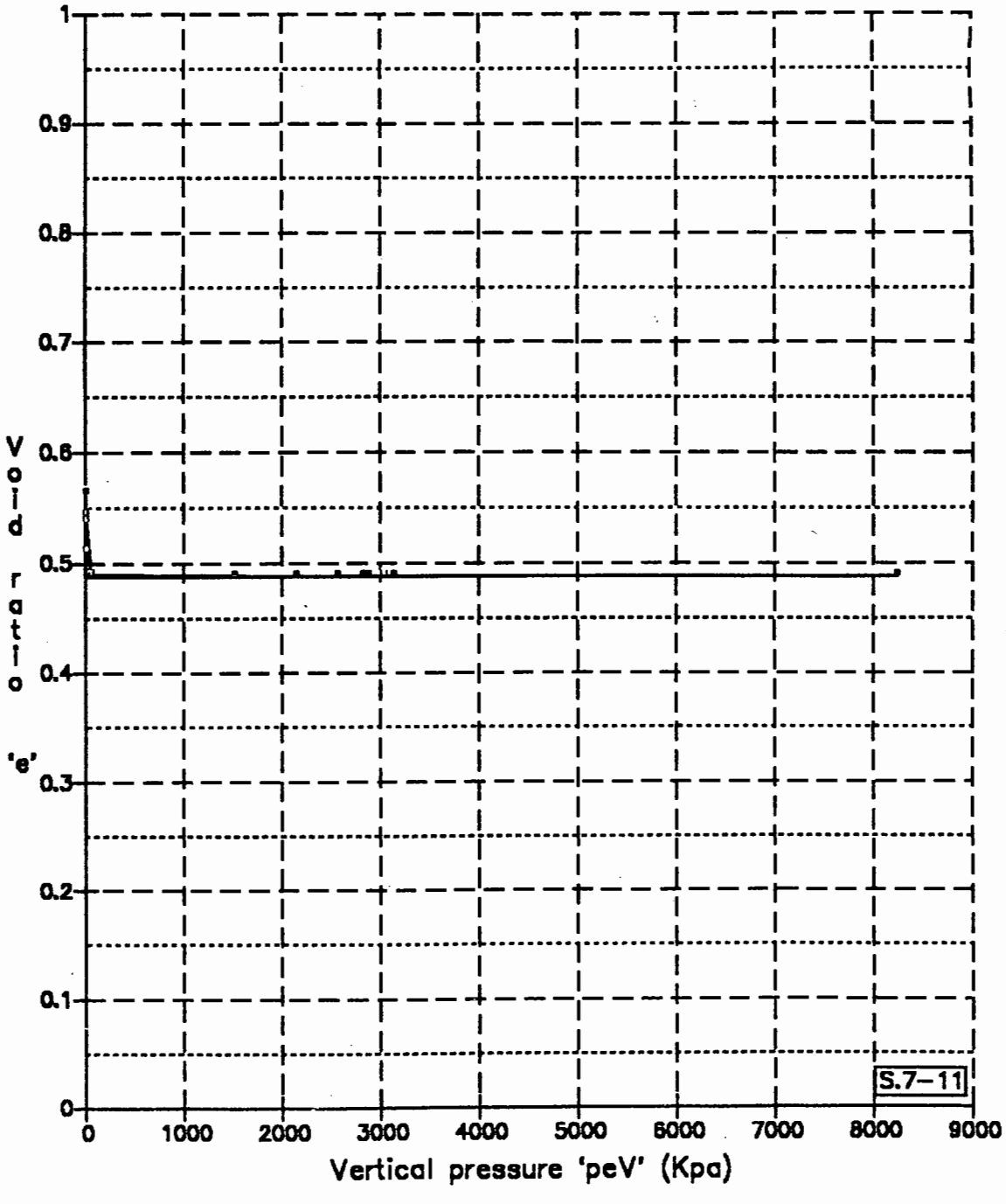

Figure 7.35: Site 7, Mowbray [Undisturbed sample] - Void ratio 'e' versus effective vertical pressure 'peV', for the full test path.

7.8.2 Void Ratio vs Effective Vertical Pressure vs Water Ratio

Site 11, Rosebank.

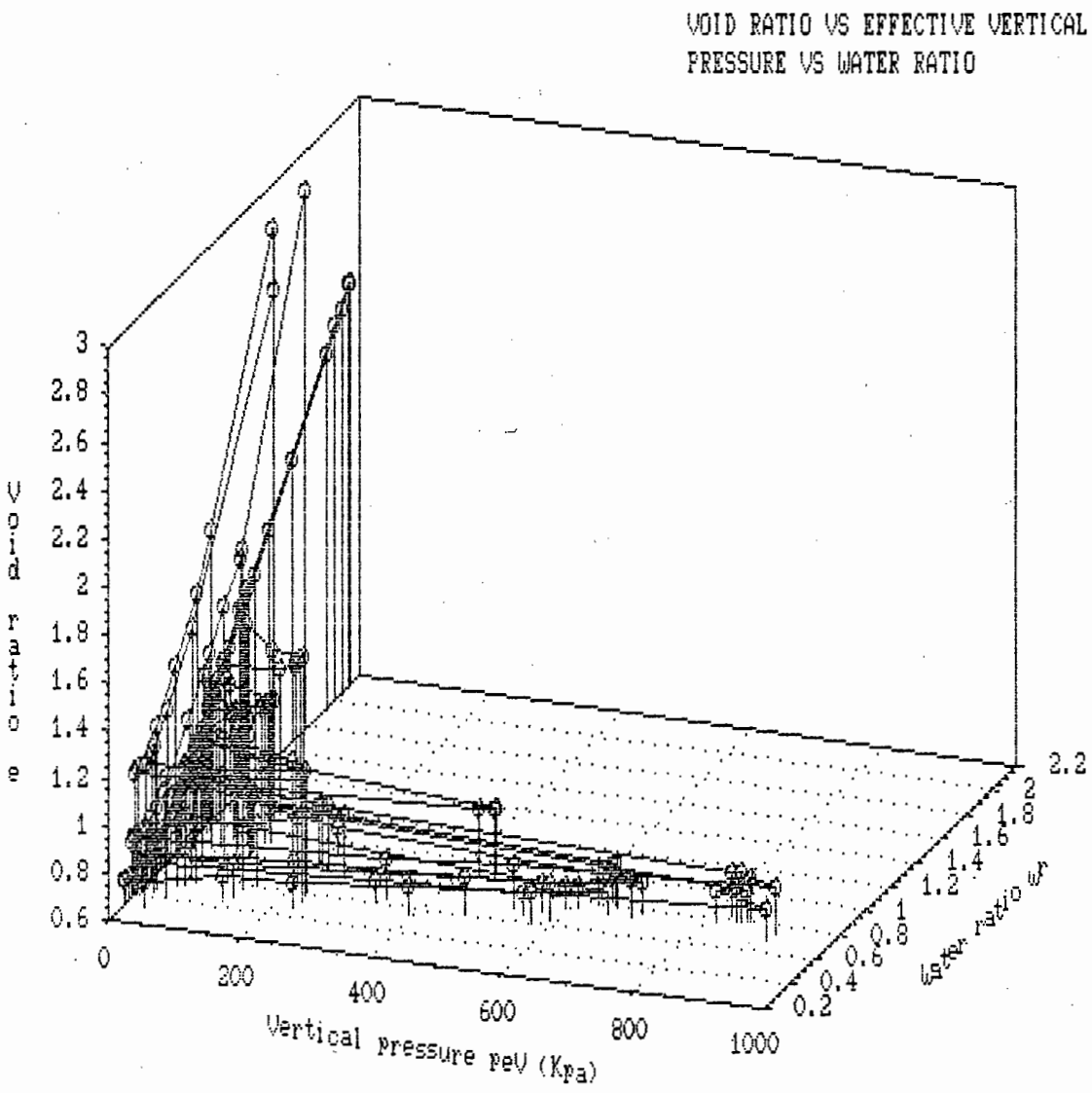

Figure 7.36: Site 11, Rosebank [Remoulded samples] - Void ratio 'e' vs effective vertical pressure 'peV' vs water ratio 'wr', for the full test path.
Sparks (1975)[1] has previously presented diagrams of Void Ratio versus Vertical Pressure versus Water Content, which had been obtained by the present writer (1974)[2].

---

1 - Reference 86.
2 - Reference 2.

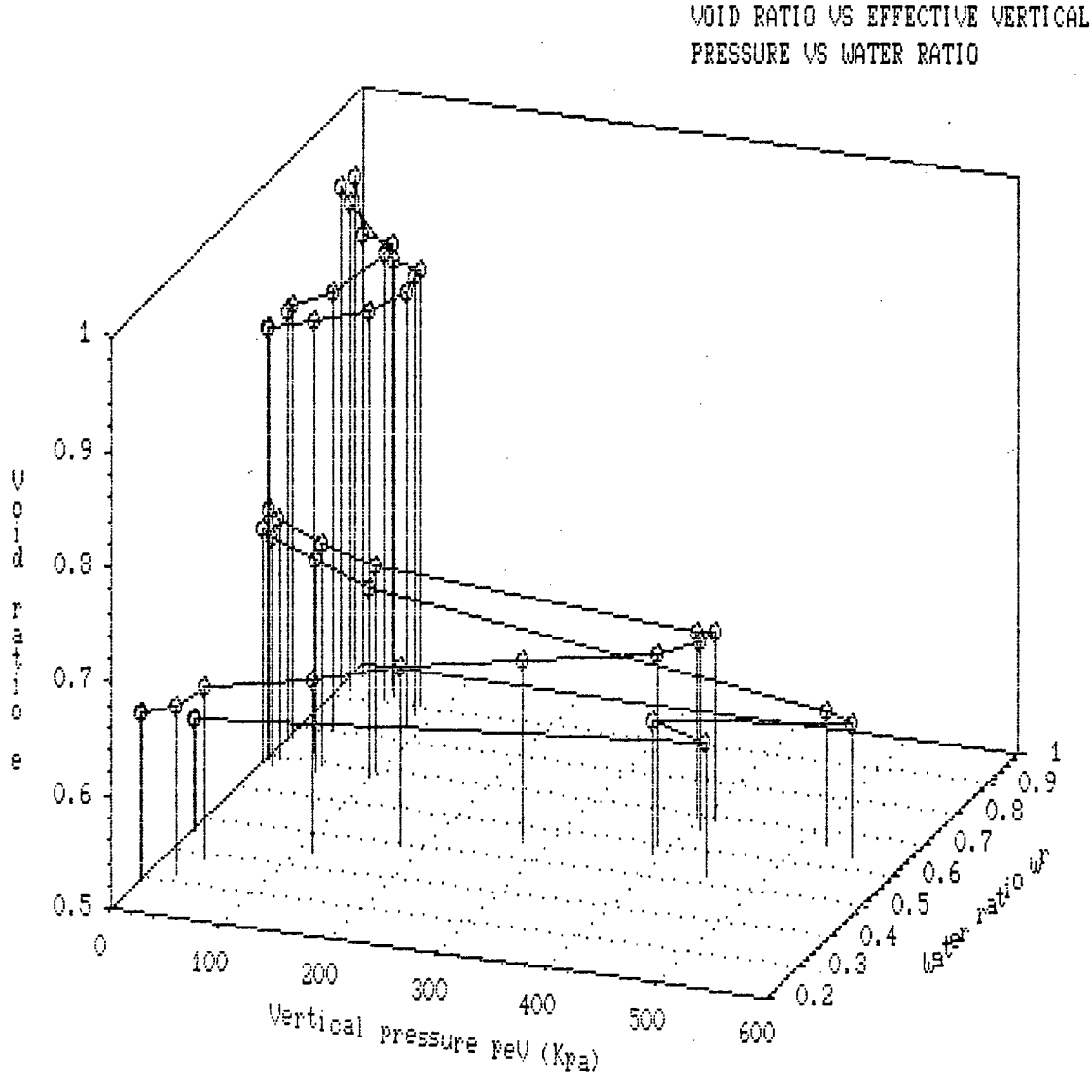

Figure 7.37: Site 11, Rosebank [Compacted samples] - Void ratio 'e' vs effective vertical pressure 'peV' vs water ratio 'wr', for the full test path.

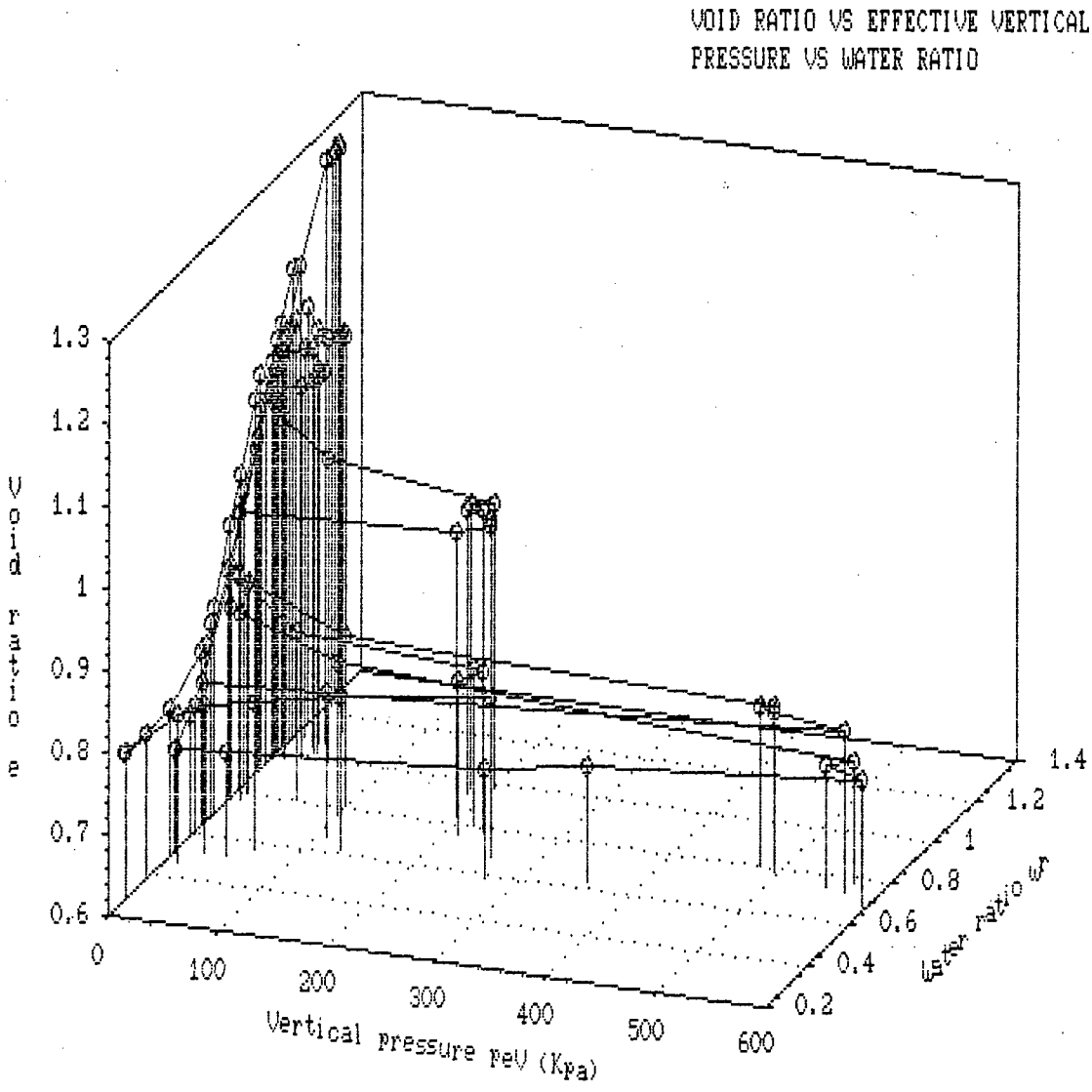

Figure 7.38: Site 11, Rosebank - [Undisturbed samples] Void ratio 'e' vs effective vertical pressure 'peV' vs water ratio 'wr', for the full test path.

Site 36, Rondebosch.

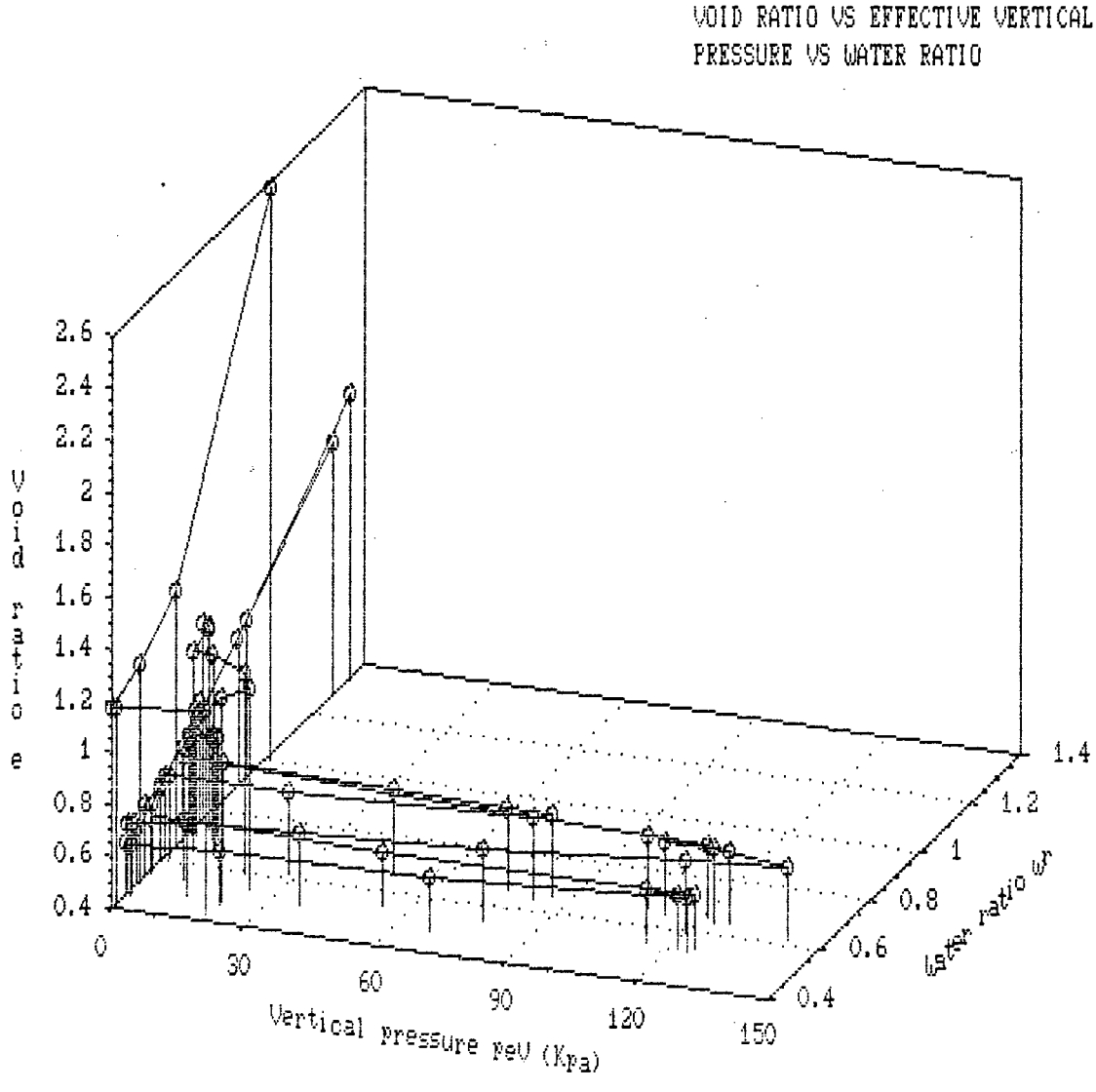

Figure 7.39: Site 36, Rondebosch [Remoulded samples] - Void ratio 'e' vs effective vertical pressure 'peV' vs water ratio 'wr', for the full test path.

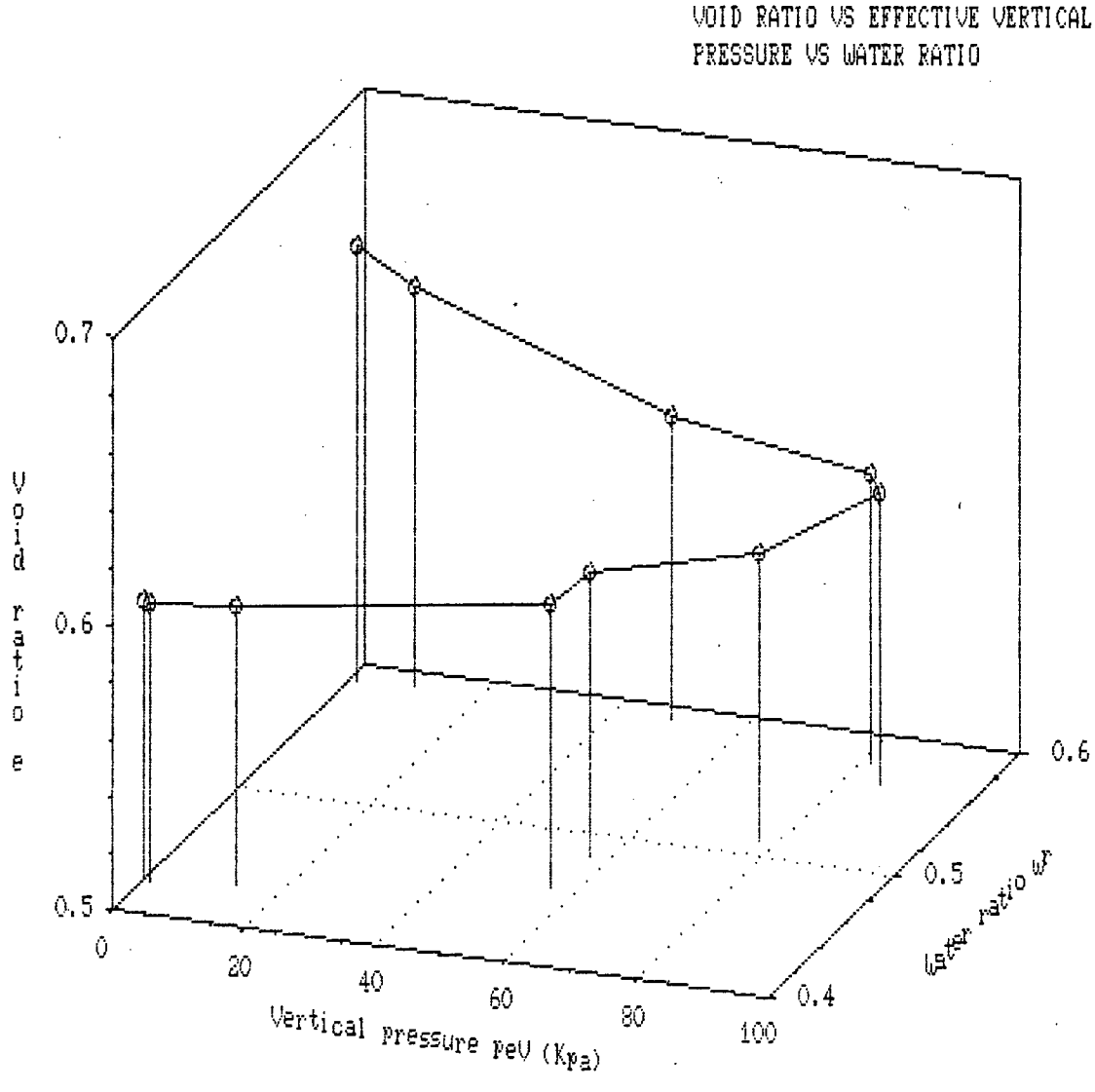

Figure 7.40: Site 36, Rondebosch [Compacted sample] - Void ratio 'e' vs effective vertical pressure 'peV' vs water ratio 'wr', for the full test path.

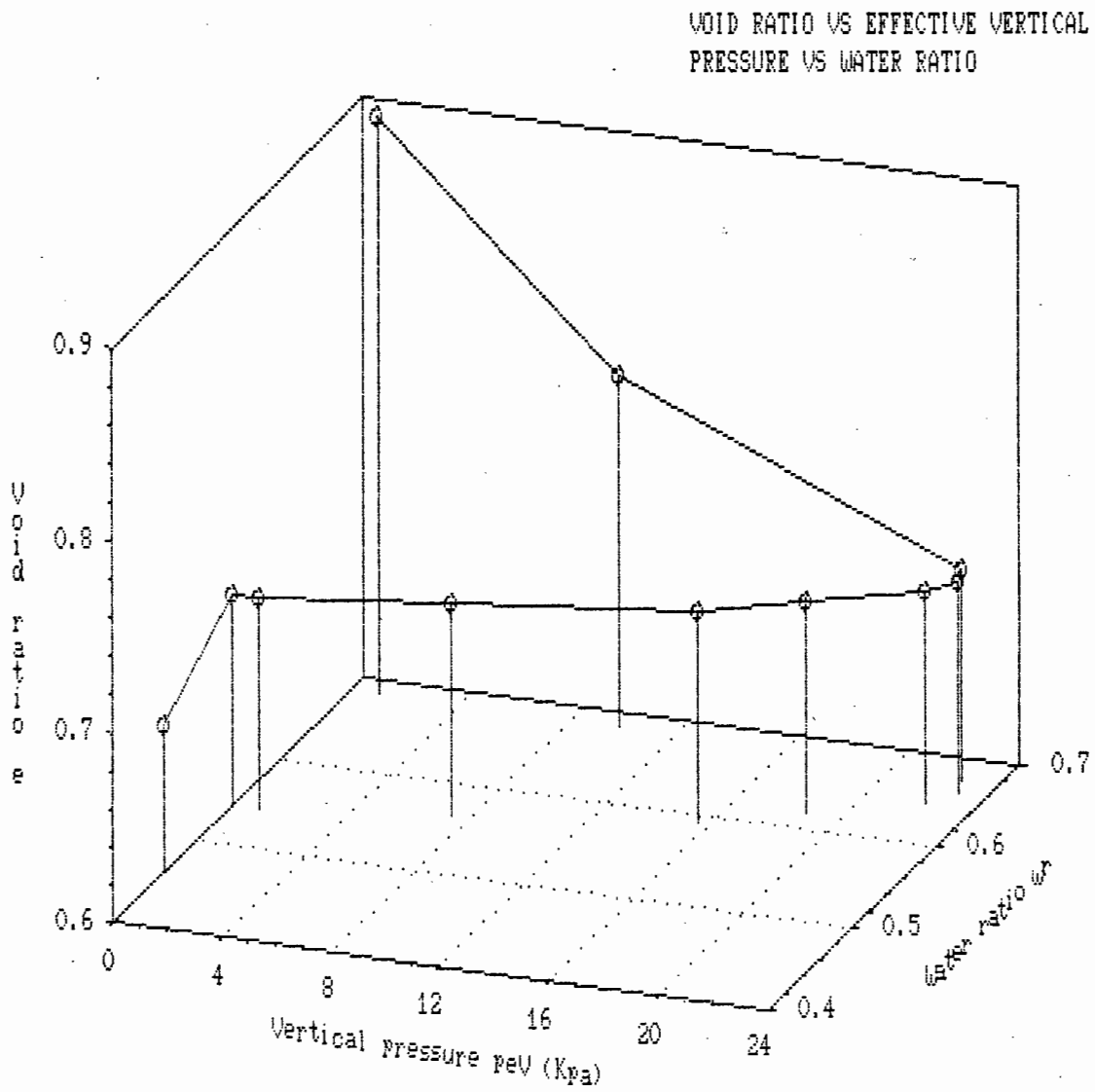

Figure 7.41: Site 36, Rondebosch [Undisturbed sample] - Void ratio 'e' vs effective vertical pressure 'peV' vs water ratio 'wr', for the full test path.

Site 30, Hout Bay.

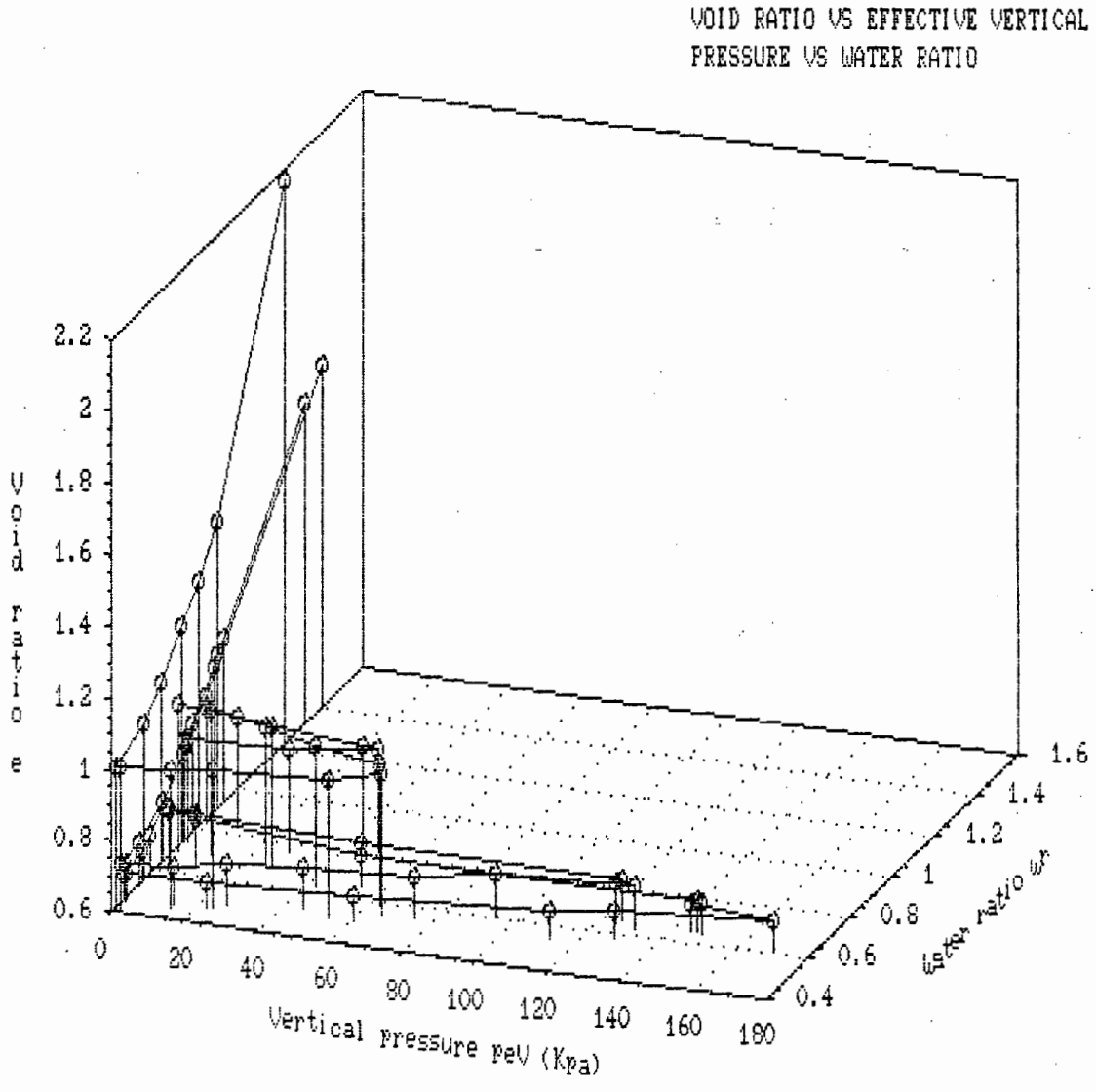

Figure 7.42: Site 30, Hout Bay [Remoulded samples] - Void ratio 'e' vs effective vertical pressure 'peV' vs water ratio 'wr', for the full test path.

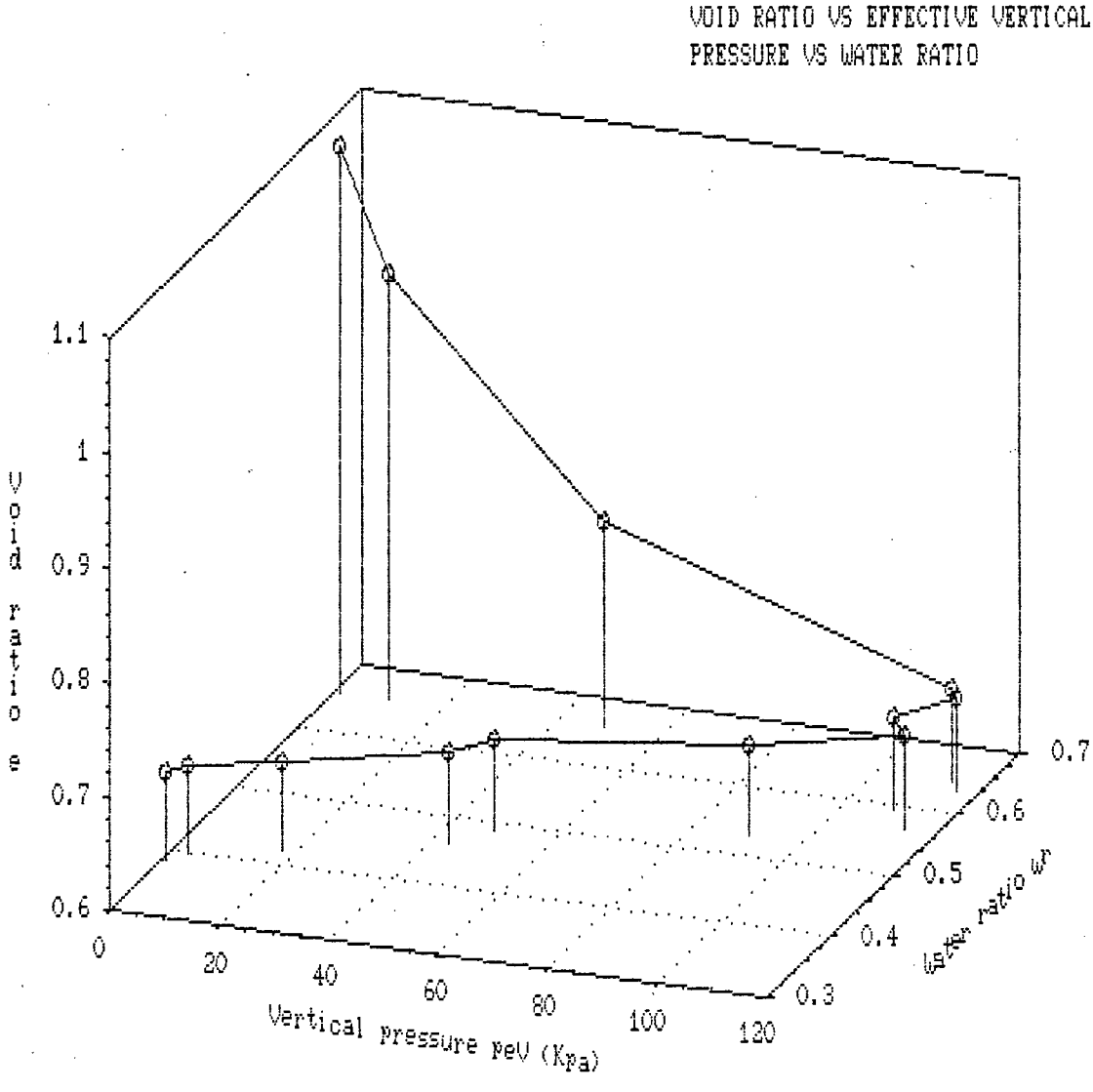

Figure 7.43: Site 30, Hout Bay [Undisturbed sample] - Void ratio 'e' vs effective vertical pressure 'peV' vs water ratio 'wr', for the full test path.

Site A, Berea Road (Durban).

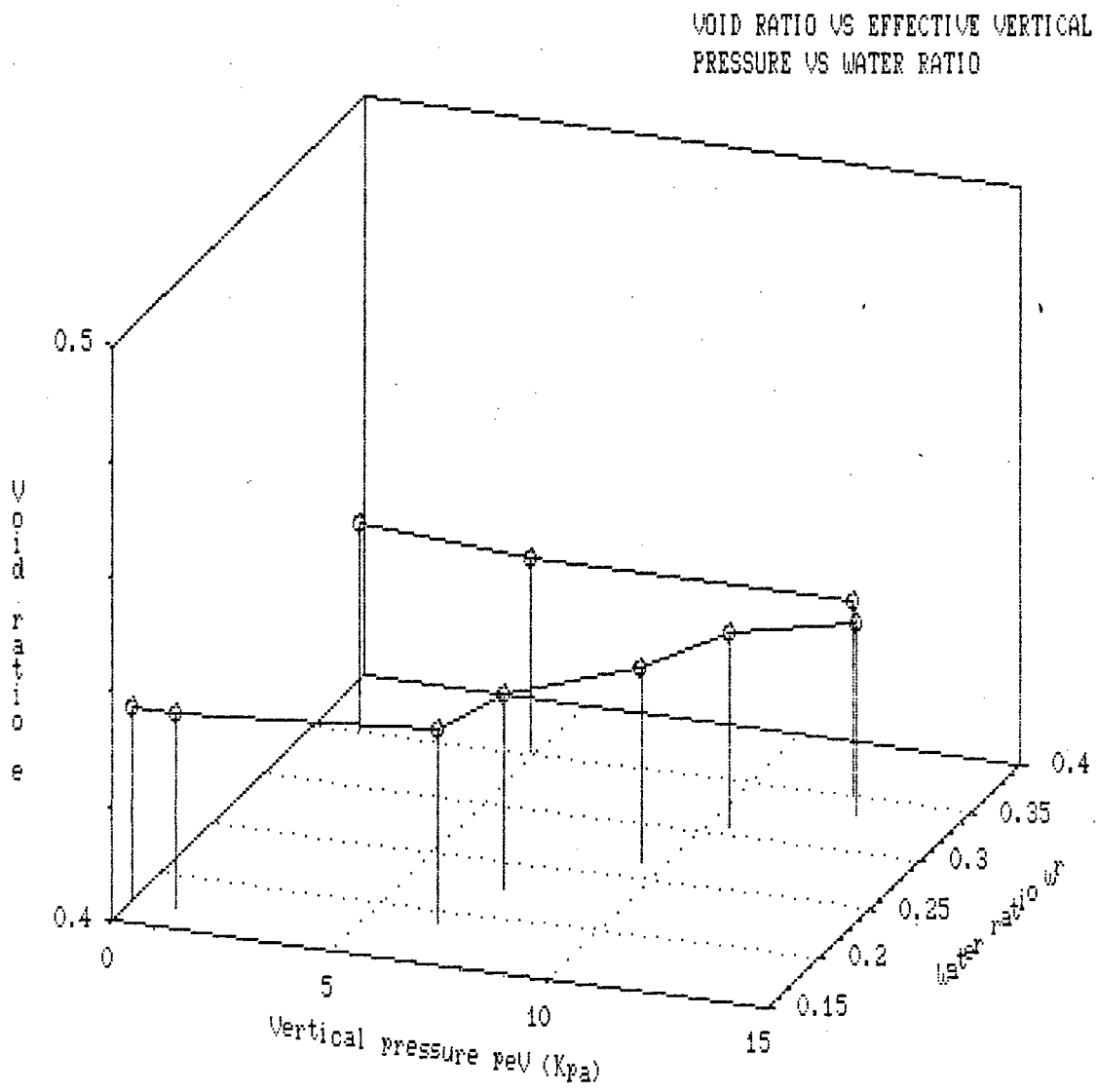

Figure 7.44: Site A, Berea Road (Durban) [Compacted sample] - Void ratio 'e' vs effective vertical pressure 'peV' vs water ratio 'wr', for the full test path.

Site 7, Mowbray.

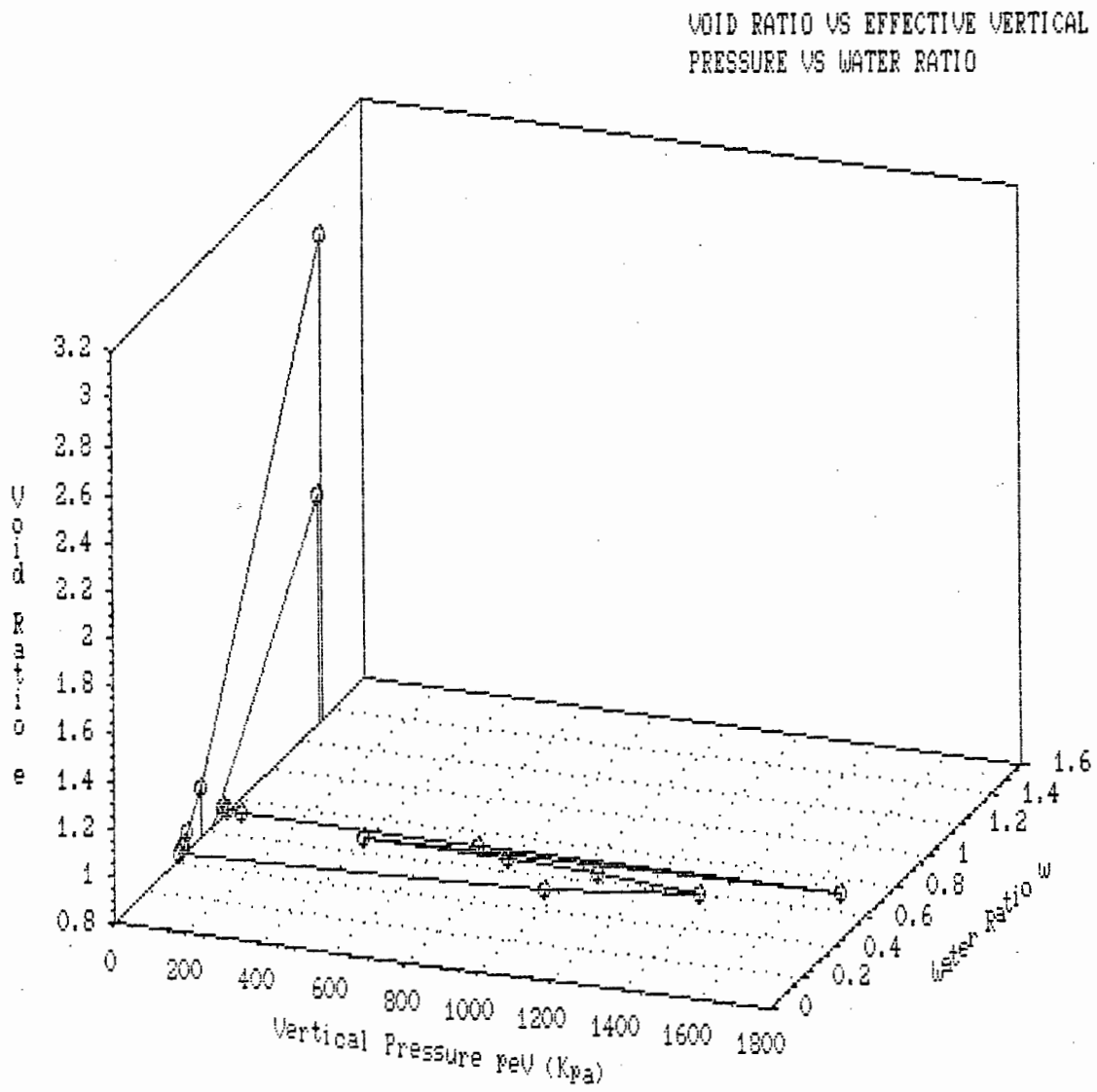

Figure 7.45: Site 7, Mowbray [Remoulded samples] - Void ratio 'e' vs effective vertical pressure 'peV' vs water ratio 'wr', for the full test path.

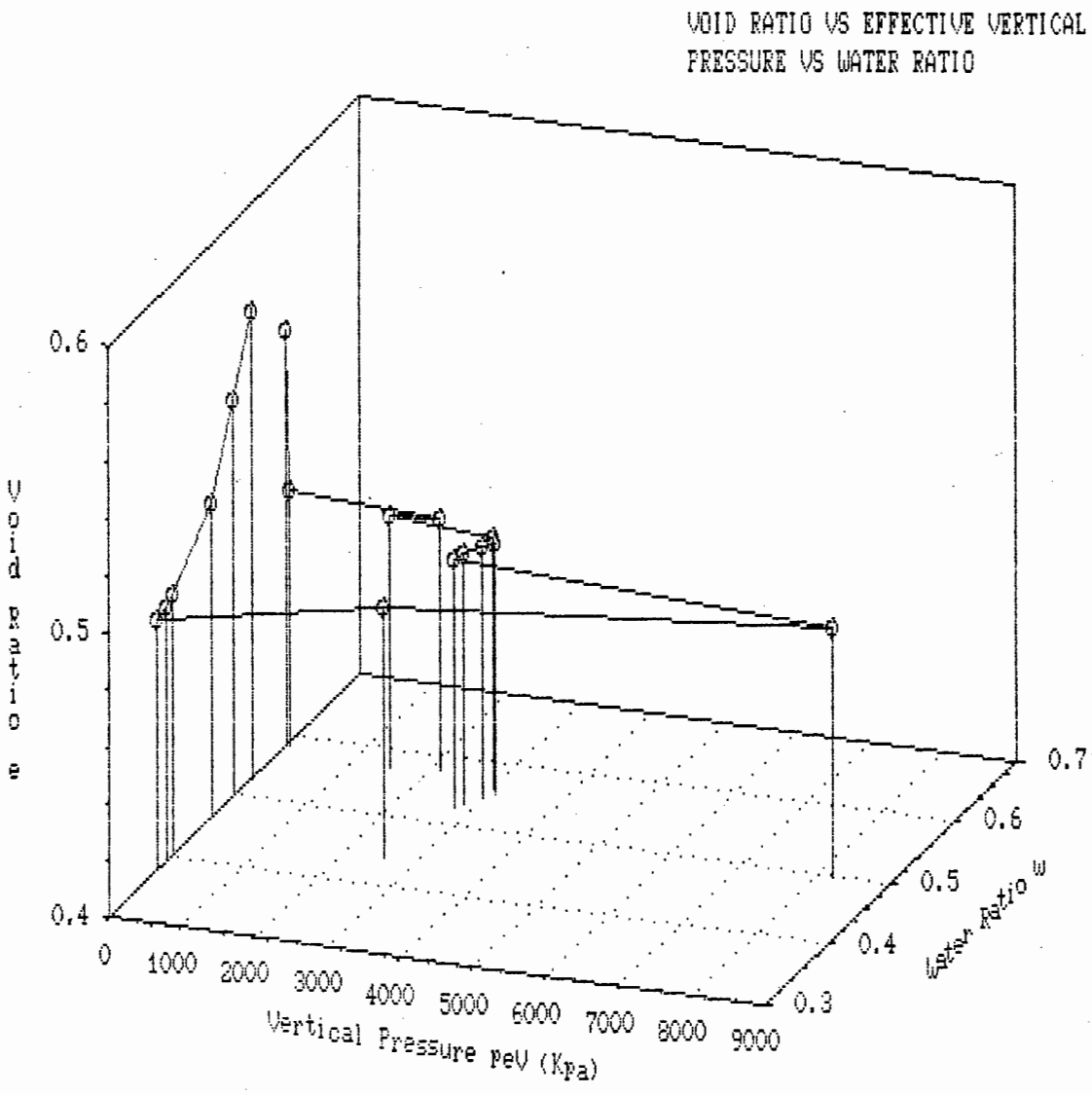

Figure 7.46: Site 7, Mowbray [Undisturbed sample] - Void ratio 'e' vs effective vertical pressure 'peV' vs water ratio 'wr', for the full test path.

7.9 CONCLUSIONS FOR CHAPTER SEVEN

The work in this chapter dealt with the observed swell pressures developed in representative samples of each main natural soil type used in this thesis.

The observed swell pressures[1] have been converted to effective average pressures, or stresses, in order to enable them to be compared to the pressure, stress scales. These stress scales were obtained for the ordinary and isotropic consolidation. Consolidation plots for each soil type were previously studied in chapter five.

Swell pressure behaviour patterns are included for the following soil types:-

1) Site 11, Rosebank - remoulded, compacted, and undisturbed samples;

2) Site 36, Rondebosch - remoulded, compacted and undisturbed samples;

3) Site 30, Hout Bay - remoulded and undisturbed samples;

4) Site A, Berea Road (Durban) - compacted sample; and,

5) Site 7, Mowbray - remoulded and undisturbed samples.

Both the unsaturated and saturated conditions were investigated. The interpretation of these relationships, over the full range of degree of saturation, are discussed in Chapter Ten of the thesis[2] - "Swell Pressures, Consistency Limits and Stress Scales".

---

1 - generated by wetting the sample.
2 - refer to section 10.3.5.

Site 11, Rosebank.

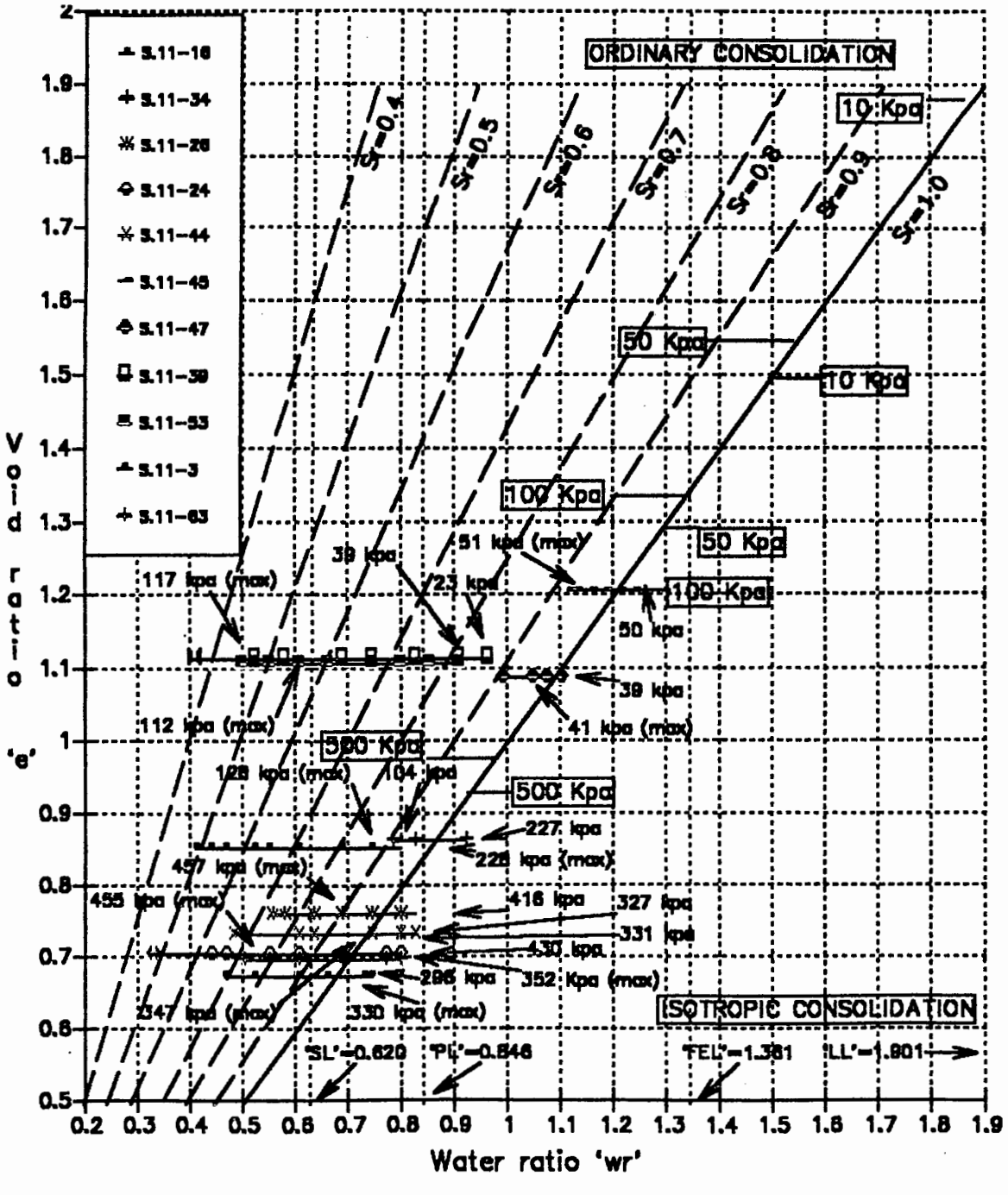

Figure 7.47: Site 11, Rosebank [Remoulded samples] - Void ratio 'e' versus water ratio 'wr' over the full range of degree of saturation, for swelling against constraint (includes stress scales, "average stresses" 'peAV' and consistency limits).
These average stresses have been taken to be half of those shown on Figure 7.03. Stress Scales on inclined line were found by other tests[1].

---

[1] - refer to Chapter Five.

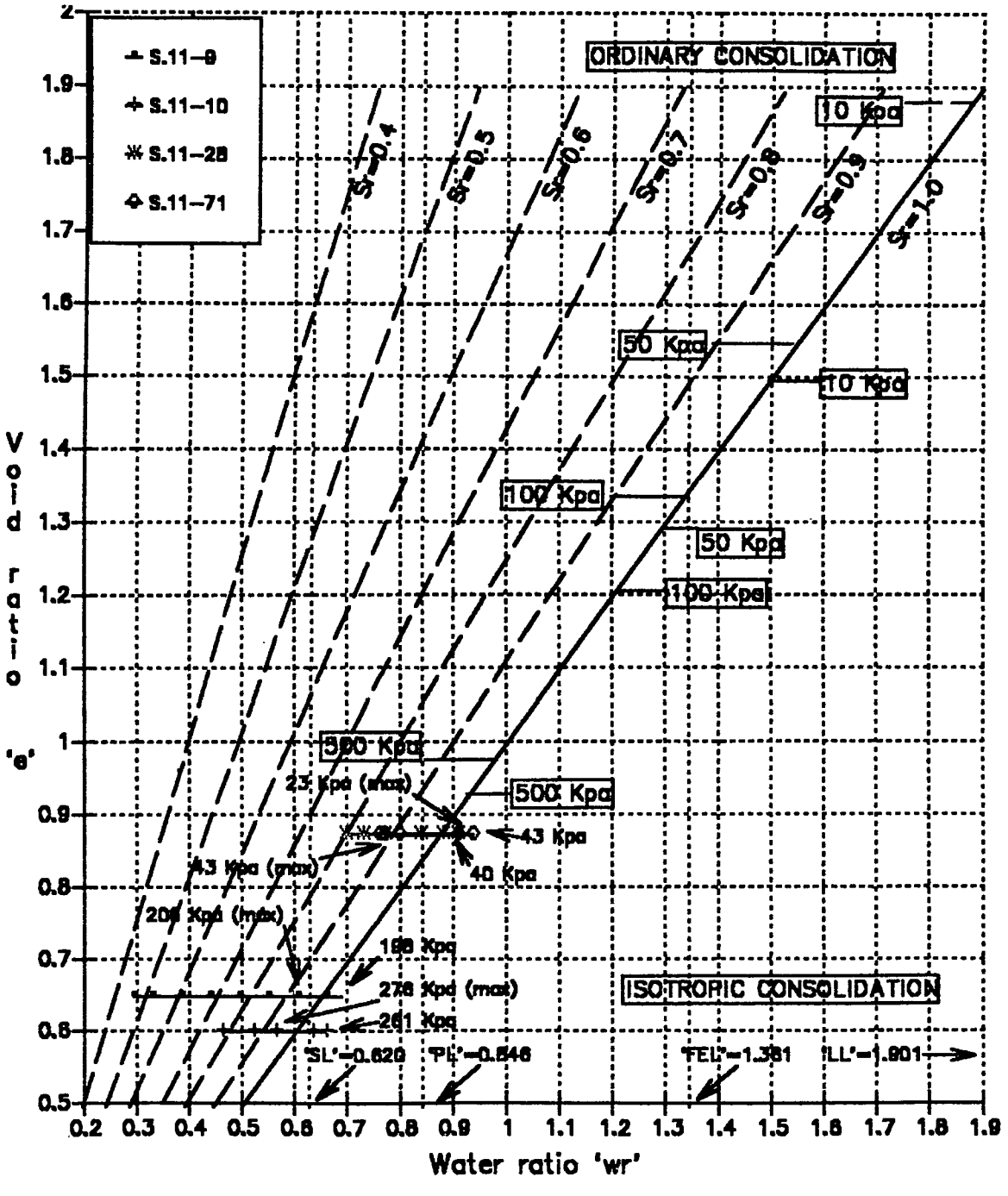

Figure 7.48: Site 11, Rosebank [Compacted samples] - Void ratio 'e' versus water ratio 'wr' over the full range of degree of saturation, for swelling against constraint (includes stress scales, "average stresses" 'peAV' and consistency limits).
These average stresses have been taken to be half of those shown on Figure 7.05. Stress Scales on inclined line were found by other tests[1].

---

[1] - *refer to Chapter Five.*

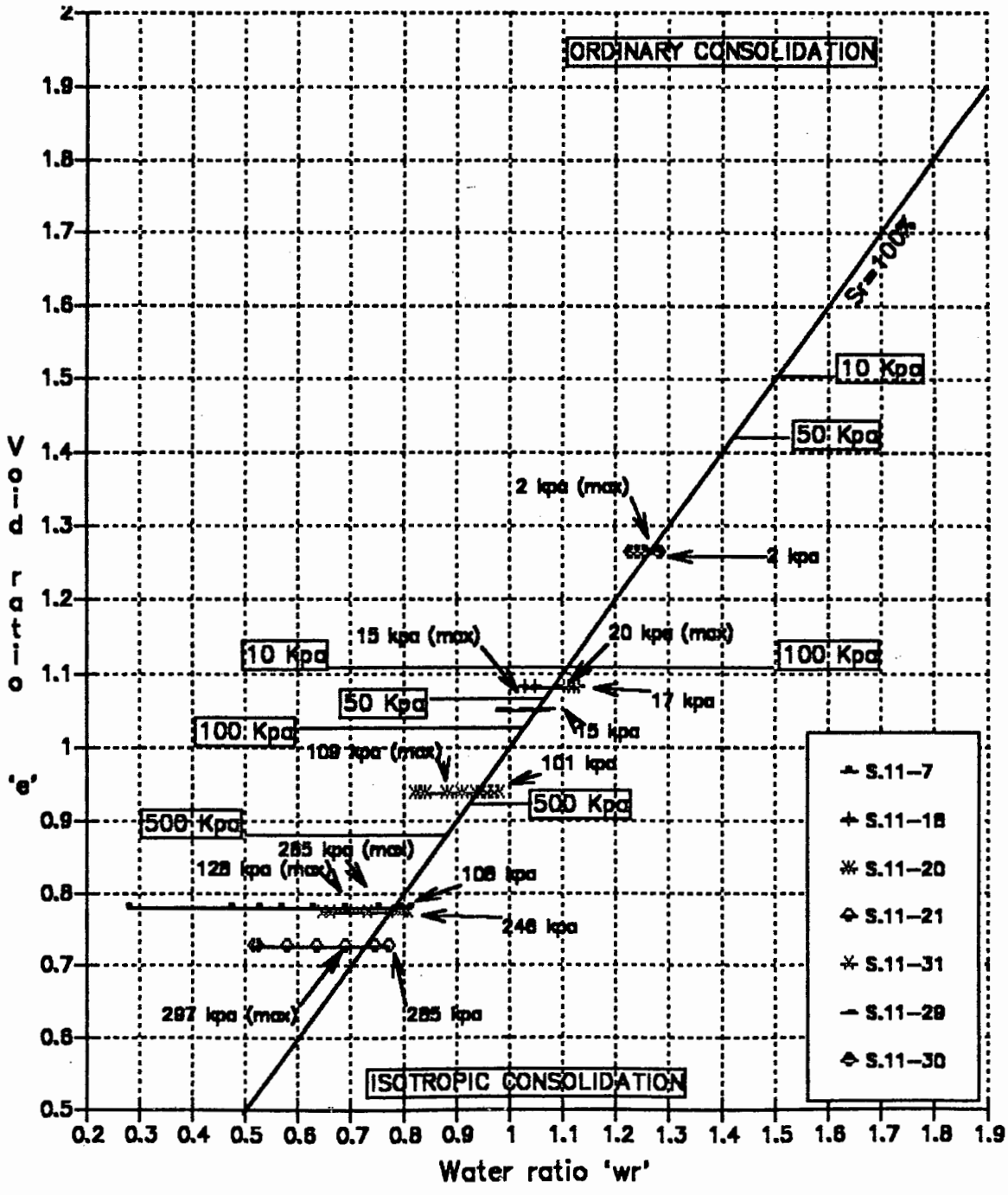

Figure 7.49: Site 11, Rosebank [Undisturbed samples] - Void ratio 'e' versus water ratio 'wr', for swelling against constraint (includes stress scales and "average stresses" 'peAV').
These average stresses have been taken to be half of those shown on Figure 7.07. Stress Scales on inclined line were found by other tests[1].

---

[1] - refer to Chapter Five.

Site 36, Rondebosch.

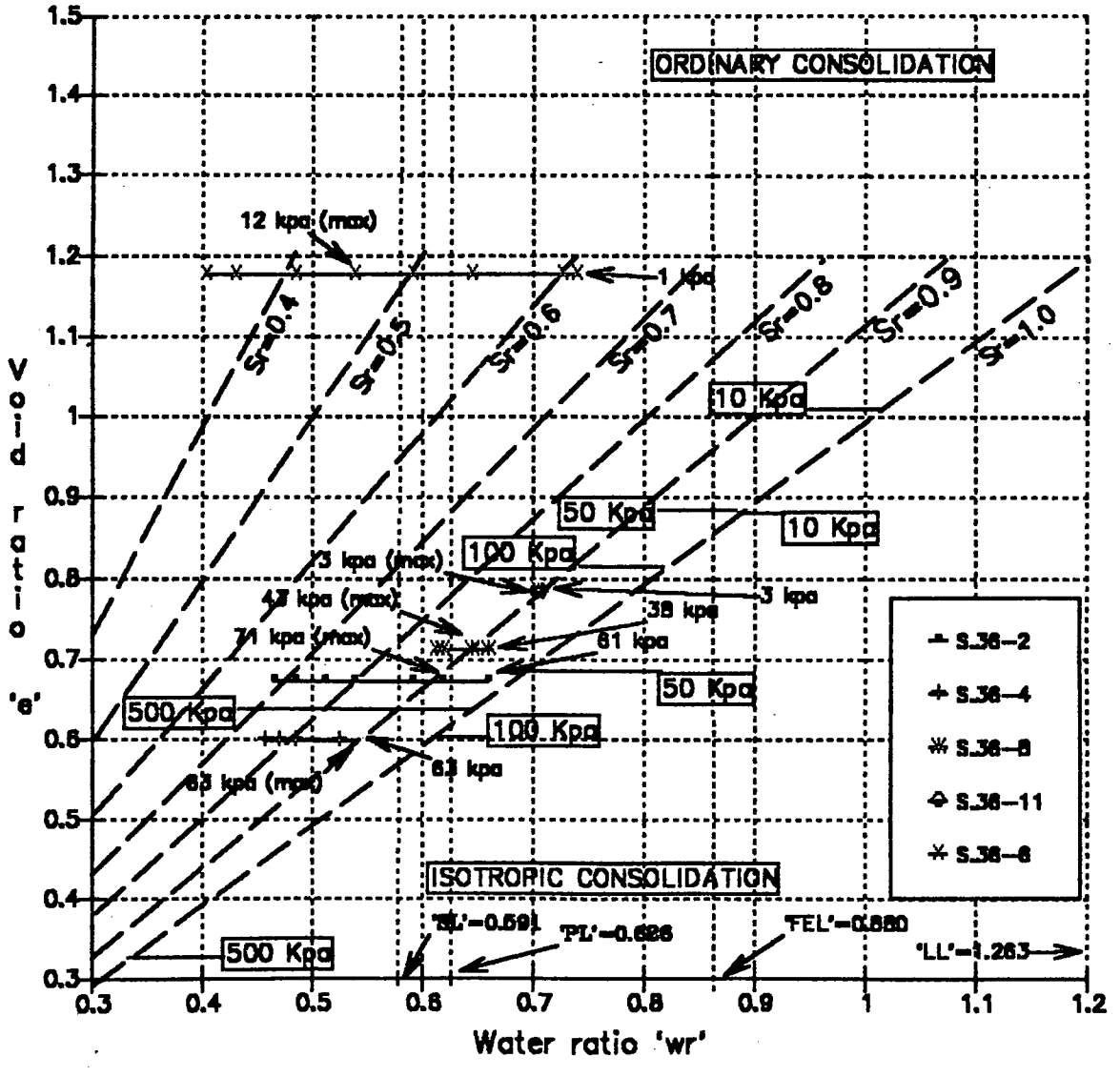

Figure 7.50: Site 36, Rondebosch [Remoulded samples] - Void ratio 'e' versus water ratio 'wr' over the full range of degree of saturation, for swelling against constraint (includes stress scales, "average stresses" 'peAV' and consistency limits).
These average stresses have been taken to be half of those shown on Figure 7.09. Stress Scales on inclined line were found by other tests[1].

---

[1] - refer to Chapter Five.

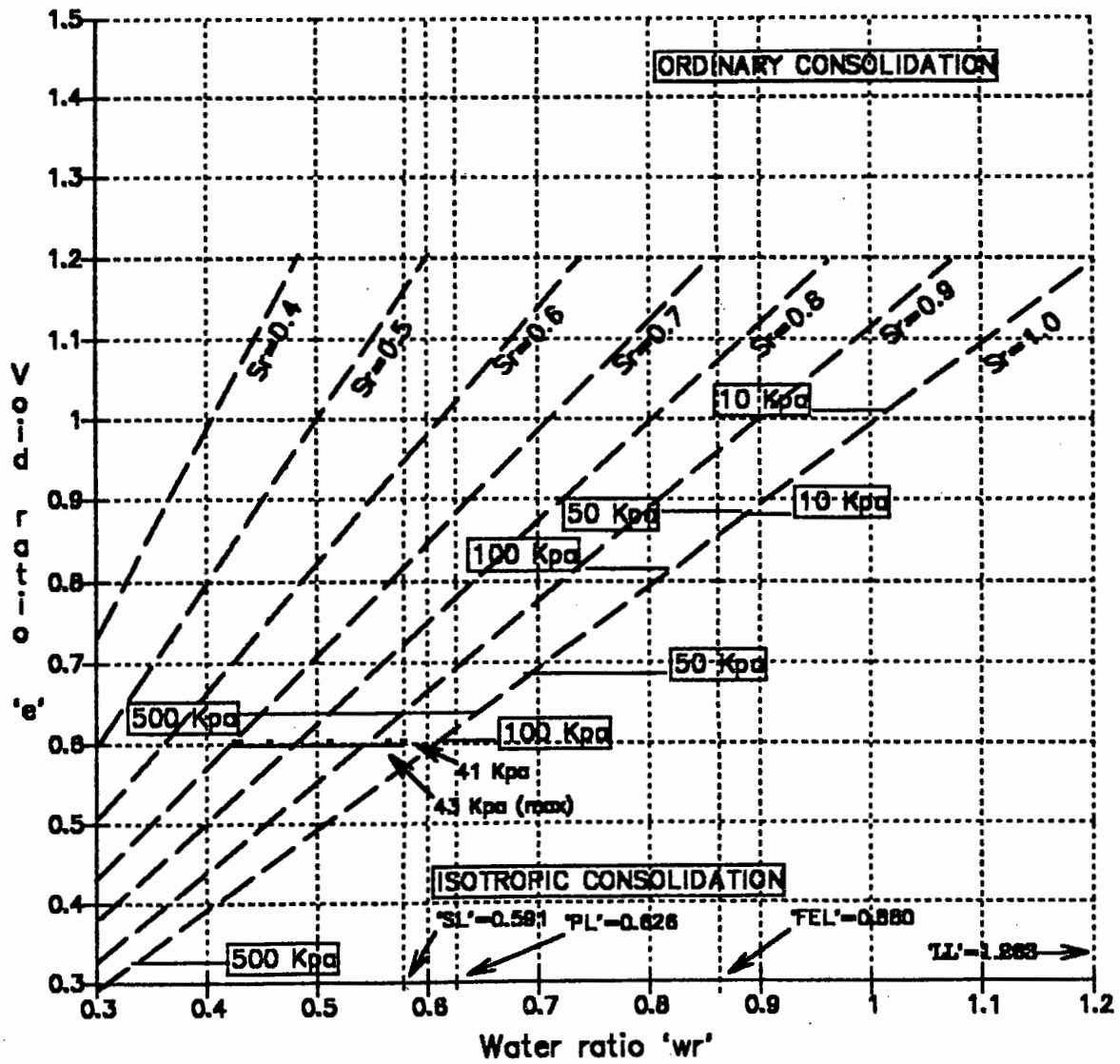

Figure 7.51: Site 36, Rondebosch [Compacted sample] - Void ratio 'e' versus water ratio 'wr' over the full range of degree of saturation, for swelling against constraint (includes stress scales, "average stresses" 'peAV' and consistency limits).
These average stresses have been taken to be half of those shown on Figure 7.11, Stress Scales on inclined line were found by other tests[1].

---

[1] - refer to Chapter Five.

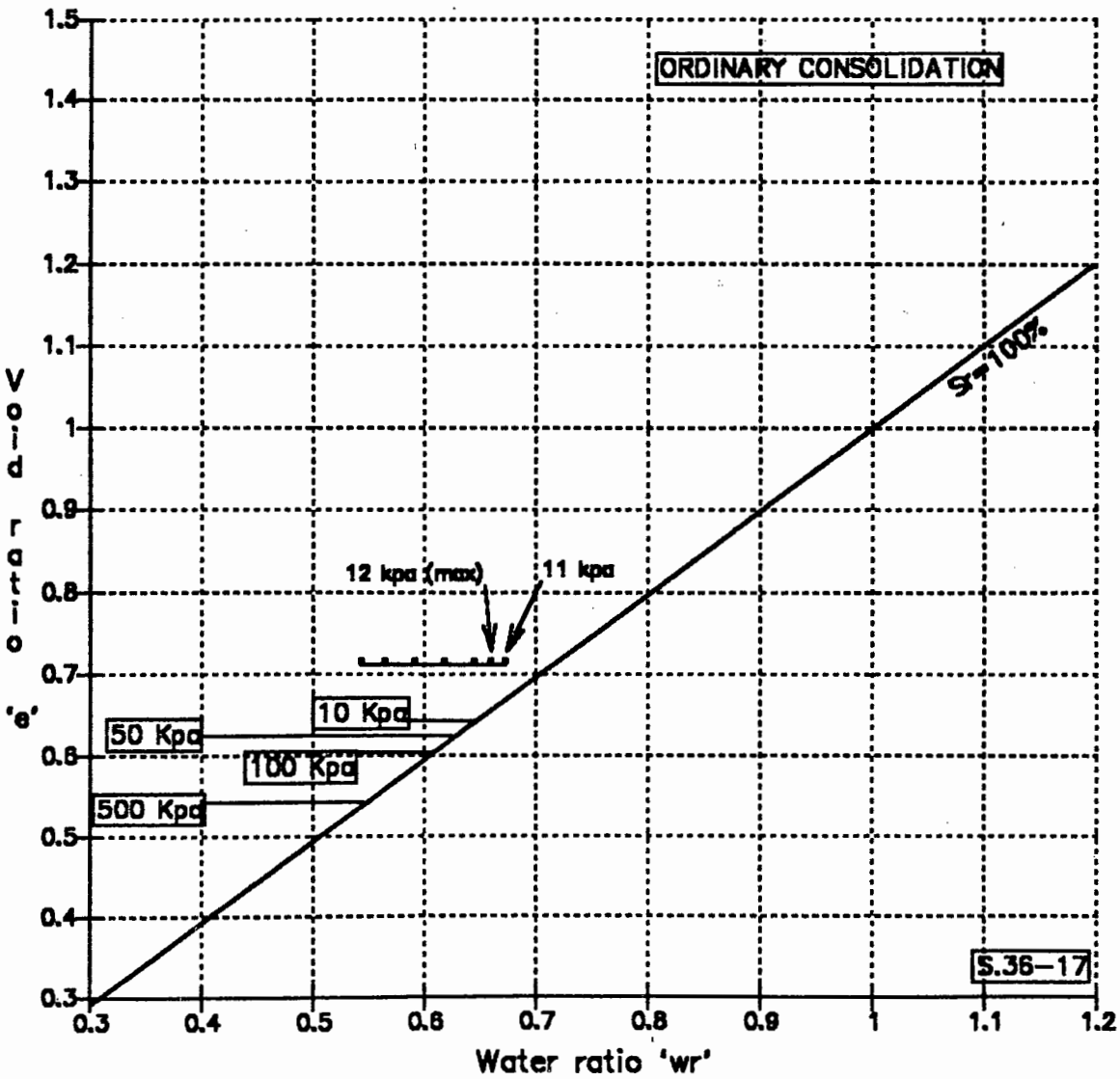

Figure 7.52: Site 36, Rondebosch [Undisturbed sample] - Void ratio 'e' versus water ratio 'wr', for swelling against constraint (includes stress scales and "average stresses" 'peAV').
These average stresses have been taken to be half of those shown on Figure 7.13. Stress Scales on inclined line were found by other tests[1].

---

[1] - *refer to Chapter Five.*

Site 30, Hout Bay.

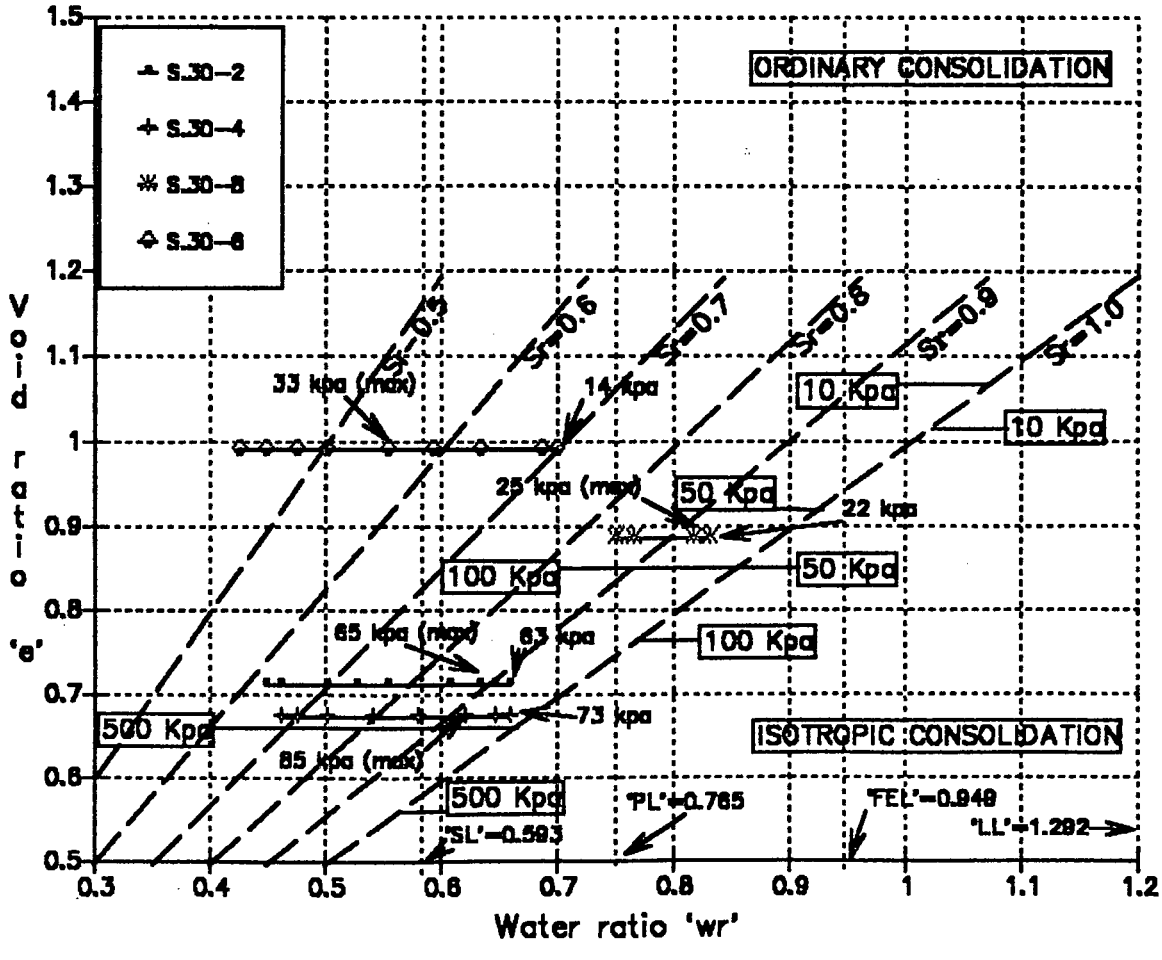

Figure 7.53: Site 30, Hout Bay [Remoulded samples] - Void ratio 'e' versus water ratio 'wr' over the full range of degree of saturation, for swelling against constraint (includes stress scales, "average stresses" 'peAV' and consistency limits).
These average stresses have been taken to be half of those shown on Figure 7.15. Stress Scales on inclined line were found by other tests[1].

[1] - refer to Chapter Five.

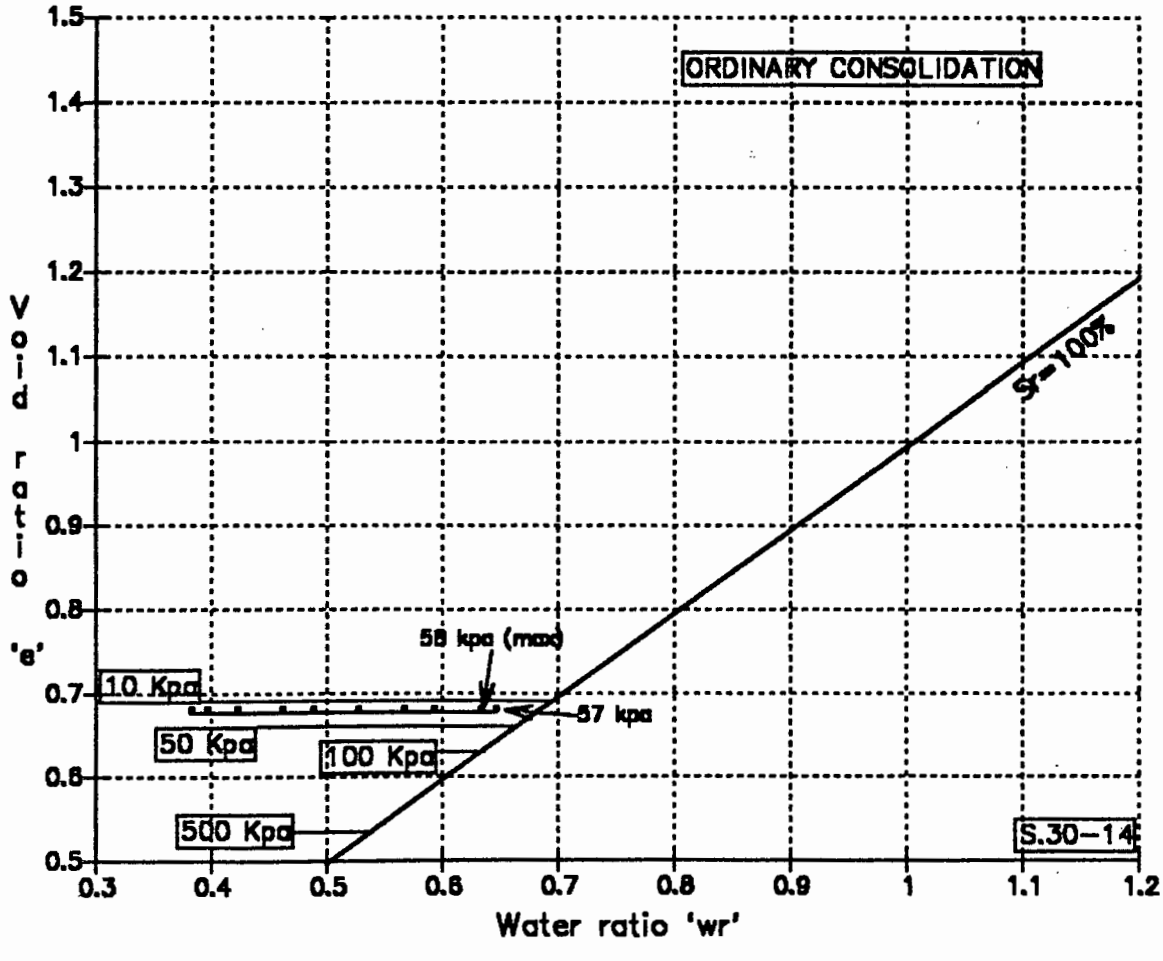

Figure 7.54: Site 30, Hout Bay [Undisturbed sample] - Void ratio 'e' versus water ratio 'wr', for swelling against constraint (includes stress scales and "average stresses" 'peAV').
These average stresses have been taken to be half of those shown on Figure 7.17. Stress Scales on inclined line were found by other tests[1].

---

[1] - refer to Chapter Five.

Site A, Berea Road (Durban).

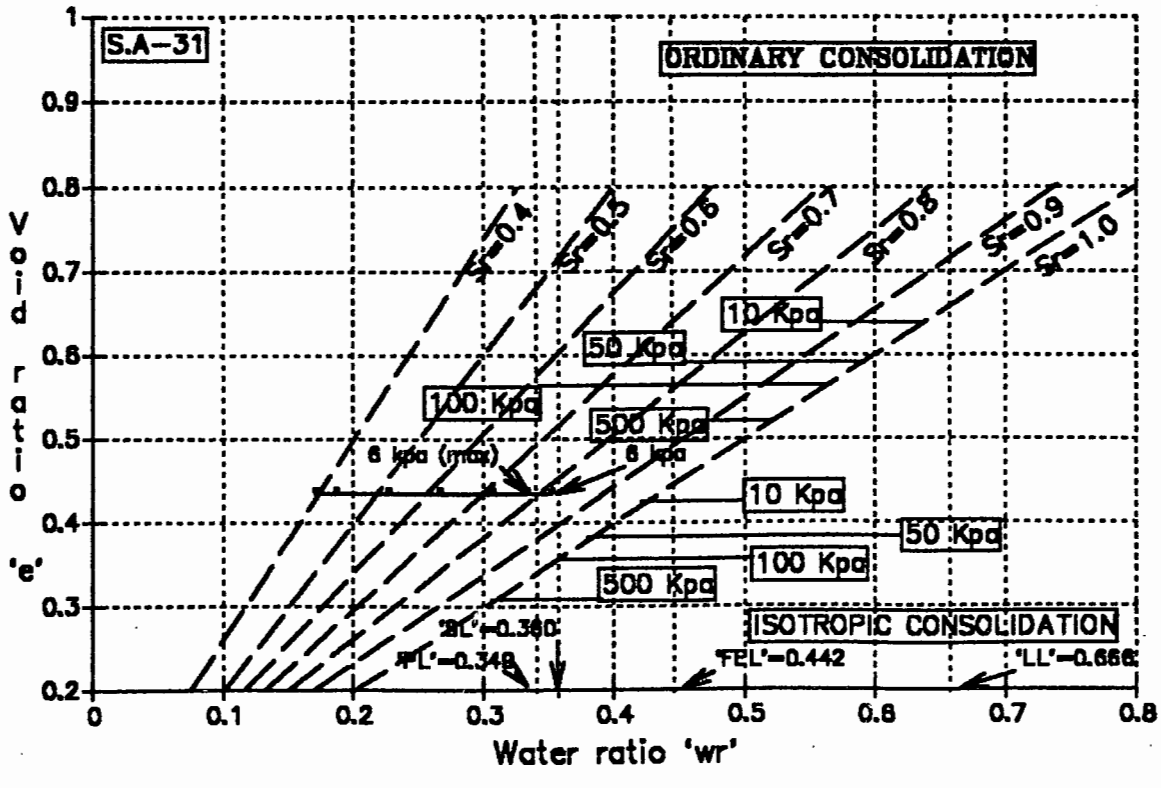

Figure 7.55: Site A, Berea Road (Durban) [Compacted sample] - Void ratio 'e' versus water ratio 'wr' over the full range of degree of saturation, for swelling against constraint (includes stress scales, "average stresses" 'peAV' and consistency limits).
These average stresses have been taken to be half of those shown on Figure 7.19. Stress Scales on inclined line were found by other tests[1].

---

[1] - refer to Chapter Five.

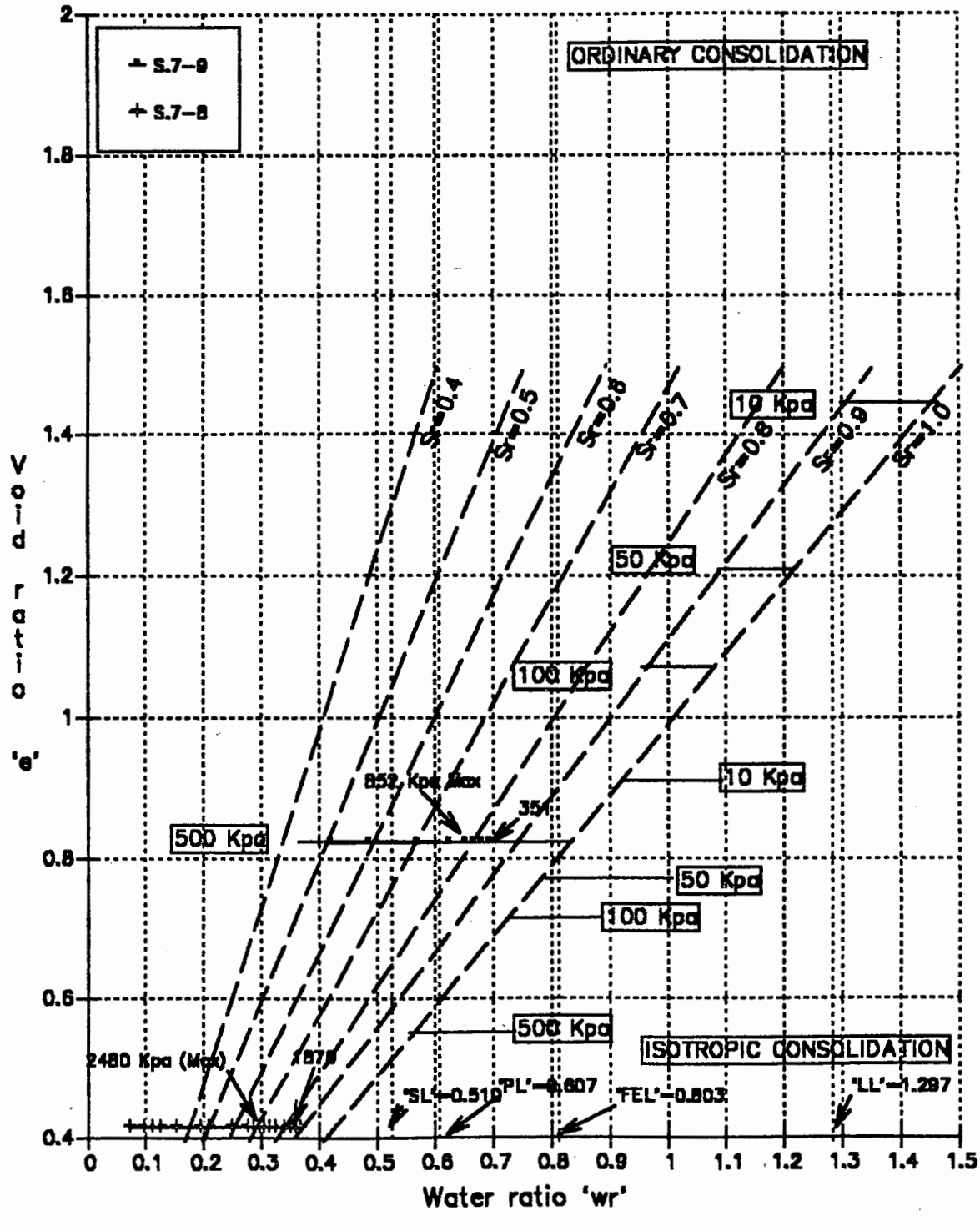

Figure 7.56: Site 7, Mowbray [Remoulded samples] - Void ratio 'e' versus water ratio 'wr' over the full range of degree of saturation, for swelling against constraint (includes stress scales, "average stresses" 'peAV' and consistency limits).
These average stresses have been taken to be half of those shown on Figure 7.21. Stress Scales on inclined line were found by other tests[1].

---

[1] - refer to Chapter Five.

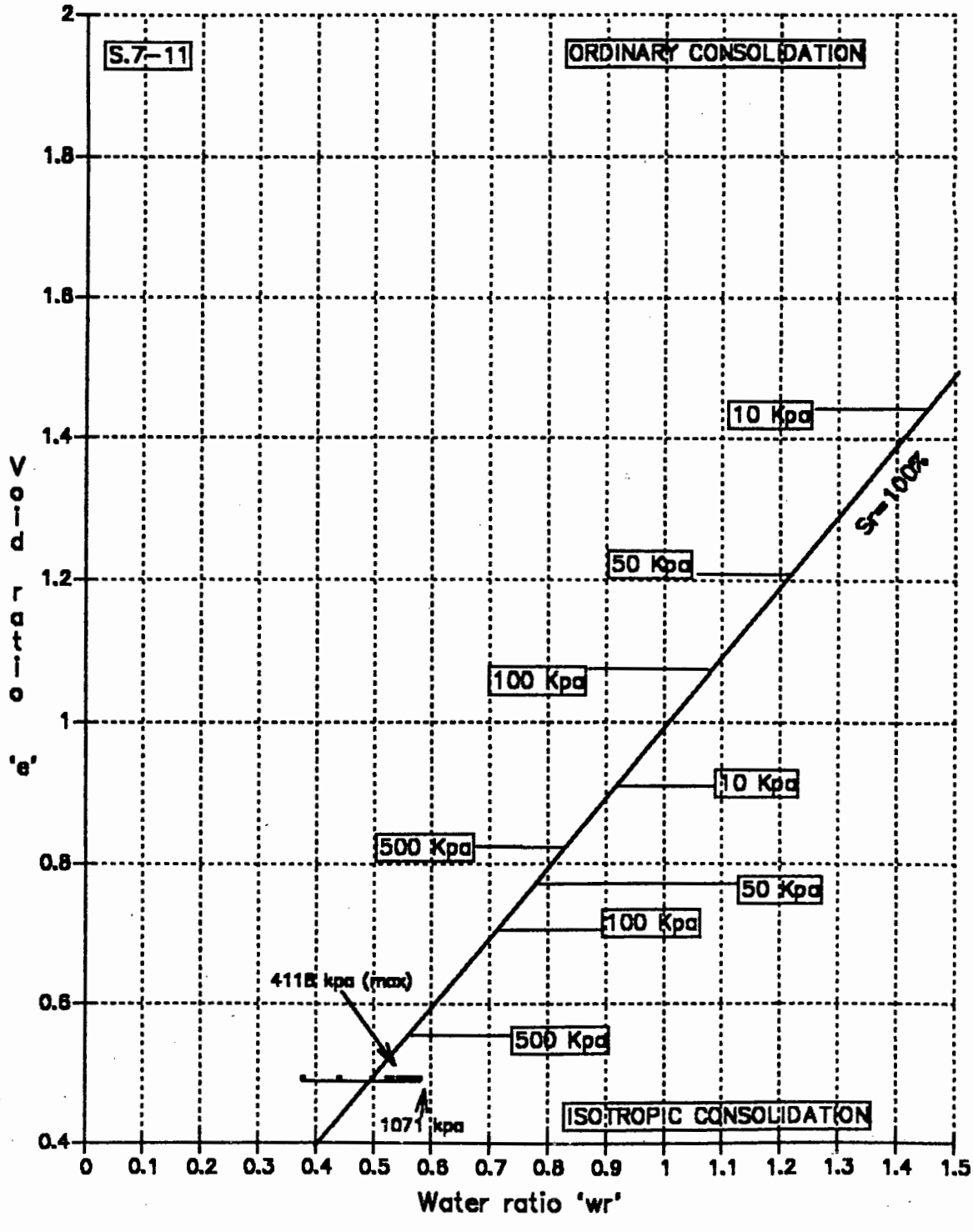

Figure 7.57: Site 7, Mowbray [Undisturbed sample] - Void ratio 'e' versus water ratio 'wr', for swelling against constraint (includes stress scales and "average stresses" 'peAV').
These average stresses have been taken to be half of those shown on Figure 7.23. Stress Scales on inclined line were found by other tests[1].

---

[1] - *refer to Chapter Five.*

7.10 REFERENCES FOR CHAPTER SEVEN

2. DE S. VINAGRE, T.J.V. (1974): The Compression of a Collapsing Soil - B.Sc. Thesis. Department of Civil Engineering, University of Cape Town.

16. DE S. VINAGRE, T.J.V. (1976/77): Masters Thesis - Diaries One, Two, Three, Four, Five, and Six.

86. SPARKS, A.D.W. (1975): Discussions, Volume II, Proceedings of the Sixth Regional Conference for Africa on Soil Mechanics and Foundation Engineering; Durban, South Africa, September 1975.

91. SPARKS, A.D.W. Prof. (Supervisor) - Discussions with the writer.

CHAPTER EIGHT *

AXISYMMETRIC STRESS BEHAVIOUR OF EXPANSIVE AND COLLAPSING SOILS

8.1 INTRODUCTION

The work in this chapter deals with the observed changes in volume and pressure that occur in soil samples as the result of external loads and increases in water content. The changes in volume refer to samples which are confined in the horizontal direction and are allowed to increase (expand) or decrease (collapse) their volume along the vertical axis, while being subjected to external vertical pressures. Because each soil sample is prevented from changing its volume in the horizontal plane, as the result of increases in water content and/or changes in the applied vertical pressures, changes in horizontal pressure, or stress, take place within the sample.

A modified consolidometer machine was used to apply the external vertical stress, or pressure, against which a soil sample expands or collapses when wetted in stages. The applied external vertical pressures ranged from 50 Kpa to 400 Kpa. The machine was equipped with either one of two specially made units for measuring strain, or changes in strain, that take place along the horizontal plane of the sample (as assembled). Chapter Six deals with the basic consolidometer tests for expansive and collapsing soils. The observed strains are used to obtain the `horizontal' stresses which develop within the soil sample being confined in its horizontal plane.

Photographic plates are included in the sections: "Test method"; and, "Measurement of horizontal strains and stresses." The photographic plates highlight the use of strain gauges for the purpose of measuring the horizontal strains developed in soil samples.

Horizontal stress measurements were also obtained for two other types of tests, as follows: (i) Swell pressure tests for expansive soils - refer to Chapter Seven; and, (ii) One-dimensional consolidation test used to obtain stress scales - refer to Chapter Five.
Concerning the observed horizontal stresses, void ratios and water contents, as well as the externally applied vertical pressures against which the sample is expanding or collapsing - they are presented in graphical form to illustrate the trends of behaviour and to allow comparisons to be made between the 'paths' of loading, unloading and expansion and collapse which develop for different initial conditions and ranges of water content.

---

* - *Observations are in Appendix G.*

For a soil to expand while under load, not only are the inner structure and water content important factors, but it also needs to have the type of clay which will absorb water and increase in volume. This 'type of clay' needs to contain the clay minerals identified in Chapter Two[1]. Various different types of soils were used.

Different methods of sample preparation were followed for each soil type prior to starting the observations of one-dimensional vertical movement and lateral stresses developed in the sample.
Samples were either permitted to lose or gain moisture until the required initial water content was reached. During this initial stage of the free shrinkage or swell of the sample, the observed changes in volume and mass are recorded.
It was hoped to investigate both the unsaturated and saturated conditions of each soil sample.

8.2 CONCEPTS AND DEFINITIONS

The words and concepts which define "Axisymmetric Stress Behaviour of Expansive and Collapsing Soils" as used in this chapter can be described as follows:

The word "Two-dimensional" refers to the observed behaviour of the soil sample along two axis, as follows:

(i) The changes in volume of the sample which is confined in the horizontal axis by a fixed consolidometer ring and allowed to increase or decrease[2] its volume along the vertical axis while either being subjected to an external vertical pressure, or stress, or as the result of increases in water content and/or vertical pressure.

(ii) The measurement of strain, or changes in strain, along the horizontal plane of the sample. The strains are the result of changes in horizontal stress developed by the sample, because it is prevented from changing its volume in the horizontal axis, as the result of either increase in its water content and/or changes in the applied vertical pressure.

The word "behaviour" means the measurable changes in the vertical and horizontal stresses observed in the soil sample, and which develop as a reaction to its water content and/or the externally applied load.

---

1 - refer to section 2.4 "Micro Studies - II".
2 - 'expand or collapse', respectively.

Behaviour of expansive and collapsing soil - within the context of two-dimensional behaviour as defined above, this concept can be described as "the additional expansion (or settlement) and development of swell pressure exhibited by a soil sample which is confined in the horizontal axis, and allowed to change its volume against an external vertical pressure, as the result of an increase in its water content and/or changes in the applied vertical pressure."

Three types of expansive or collapsing behaviour, under controlled wetting conditions, were observed in this chapter (under controlled wetting conditions):

(1) Shrinkage and Free Swell paths;
(2) Expansion or collapse under known vertical loads; and/or
(3) Vertical pressure required to prevent volume changes[1].

The measurements of "horizontal stress, or pressure" or "lateral stress, or pressure" are obtained from the observed changes in strain that take place in the horizontal plane of the sample. Two specially made units are used for the purpose of measuring the changes in strain, or stress, developed by the soil sample - refer to "Measurement of horizontal strains and stresses"[2].

The changes in volume (along the vertical axis) and the horizontal stresses developed (horizontal axis) occur under conditions in which drainage of the sample is permitted throughout. As described in the previous chapters, it is an attempt to satisfy the conditions of zero pore water pressure. Therefore, the effective stresses are equal to the applied stresses.

All the other relevant concepts and definitions, which may be needed to define the stated purpose of this chapter, are included in the previous chapters.

8.3 THE PARAMETERS WHICH ARE BEING INVESTIGATED

The diagrams in Figures 8.01, 8.02 and 8.03 illustrate the four main parameters which are being investigated in this chapter. These parameters are the void ratio, the water ratio, the effective vertical pressure (or stress) applied along the vertical axis, and the effective horizontal pressure (or stress) developed by the sample along the horizontal axis.

The diagram in Figure 8.01 illustrates two of the main parameters which are being investigated.
These parameters are the 'Void Ratio' and the 'Water Ratio'.

---

[1] - *that is, the swell pressure.*
[2] - *subsequent section 8.8.*

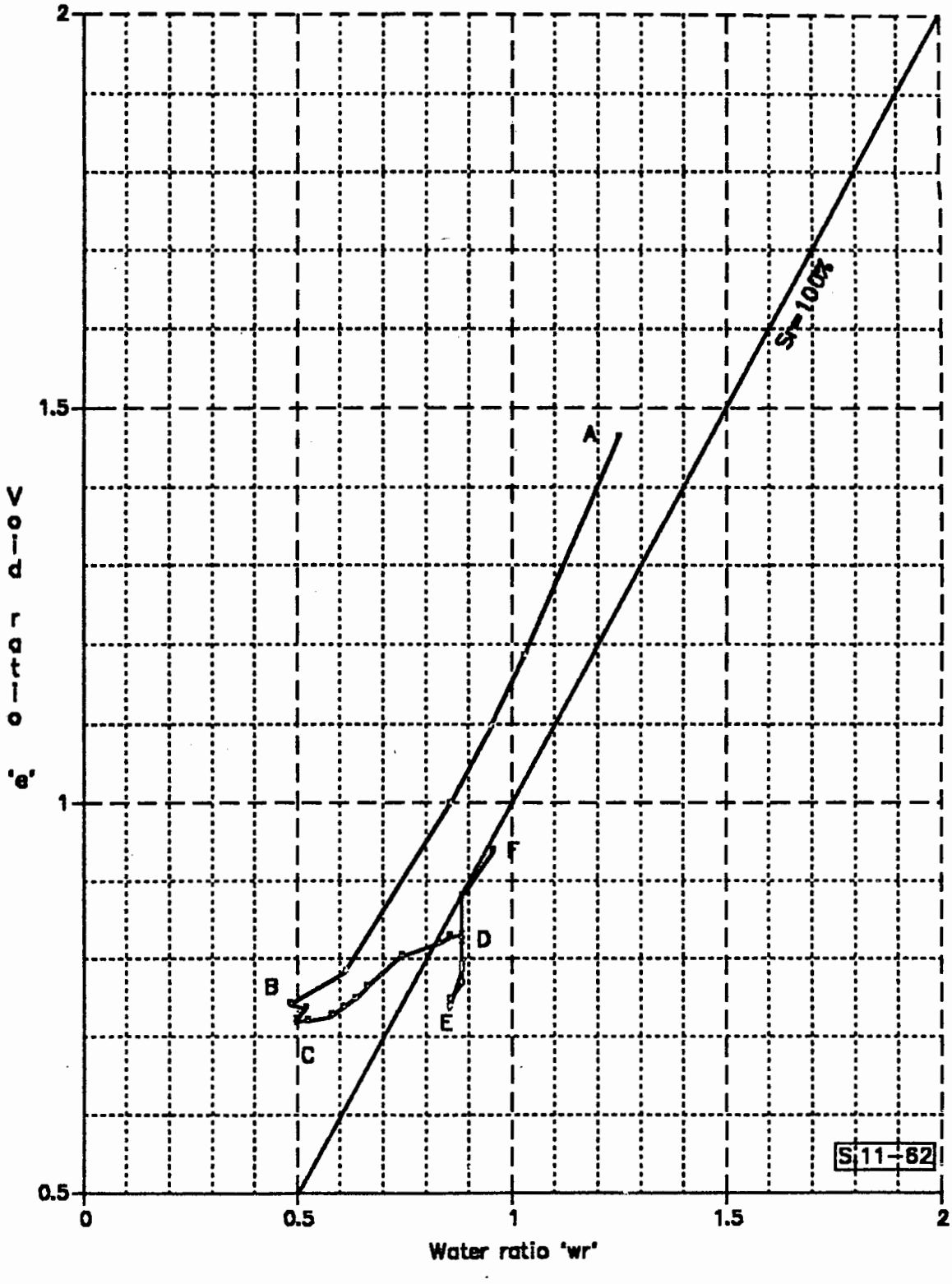

Figure 8.01: Relationship between the void ratio 'e' and the water ratio 'wr', or 'Ω', for the full test path. See Section 8.3[1] for description.

---

[1] - *"The parameters which are being investigated".*

The vertical axis of the diagram in Figure 8.01 represents the 'Void Ratio'[1] and the horizontal axis represents the 'Water Ratio'[2] (that is, the water content 'w' times the specific gravity of the soil particles 'G_S'). Figure 8.01 is basically the same as Figure 6.01 of Chapter Six.

The relationship between the void ratio and the water ratio of the sample, as shown in Figure 8.01, goes through the following stages:

The sample was prepared at condition A.
1) As it loses moisture, its state moves from A towards B - the "free shrinkage path";
2) Loading the sample to the required vertical stress, the condition of the sample moves from B to C - the "initial loading path";
3) In the next stage the water content is gradually increased in steps - the void ratio increases (due to expansion), or decreases (further settlement) is shown as CD - the "wetting path"; When another increment of water causes no further movement in the sample;
4) The final loading D to E; and,
5) Unloading from E to F.

The diagram in Figure 8.02 illustrates the relationship between the void ratio and the third main parameter which is being investigated. This parameter is the effective pressure, or stress, applied along the vertical axis. The horizontal axis represents the effective pressure applied to the sample throughout the test. The state of the sample follows the same path as described for Figure 8.01. Concerning the relationship between the void ratio and the effective vertical pressure, or stress, the condition of the sample, as it changes from condition B through to F, is illustrated in Figure 8.02.

The diagram in Figure 8.03 illustrates the relationship between the void ratio and the fourth main parameter which is being investigated. This parameter is the effective pressure, or stress, developed by the sample along the horizontal axis. The effective horizontal stress is obtained from the observed changes in horizontal strain of the confining steel ring - refer to subsequent section in this chapter "Horizontal strains and stresses".

The state of the sample follows the same path as the one described for Figure 8.01. In this case, concerning the relationship between the void ratio and the effective horizontal pressure, or stress, the condition of the sample as it changes from condition B through to F, is illustrated in Figure 8.03. It should be noted that at condition F, after the external vertical pressure has been removed, the measured horizontal stress is greater than zero due to residual or "locked-in" stresses within the sample.

---

[1] - 'ratio of the volume of voids to the volume of solids'.
[2] - 'ratio of the volume of water to the volume of solids'.

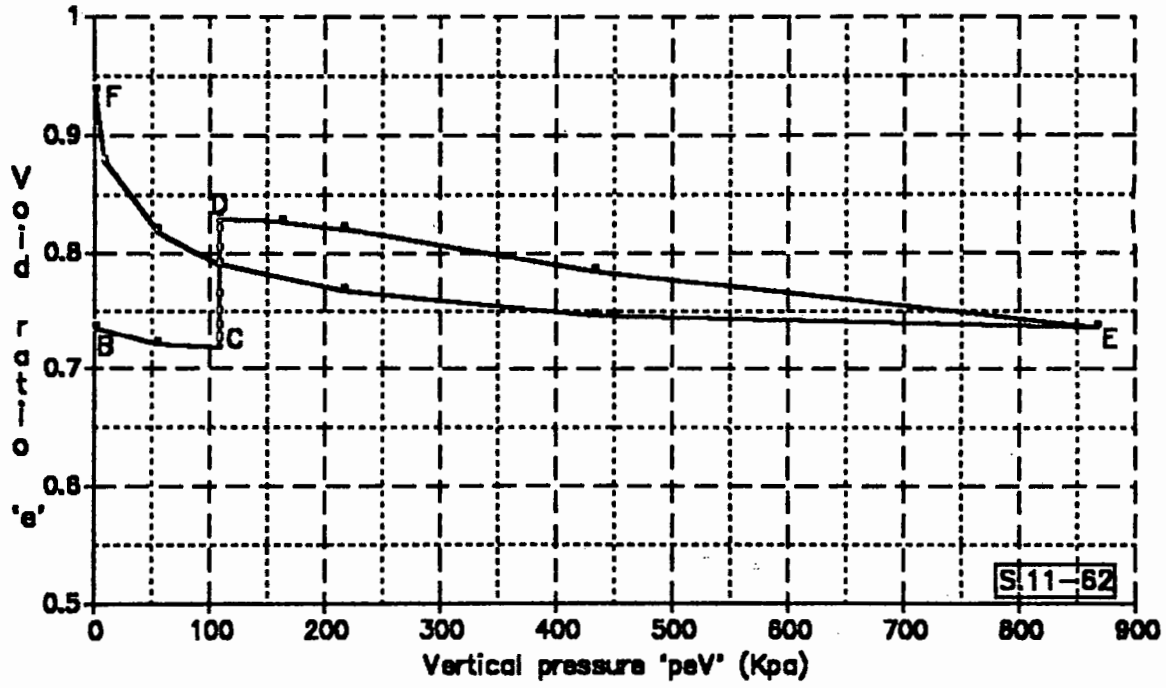

Figure 8.02: Relationship between the void ratio 'e' and the effective vertical pressure (or stress) 'peV'.

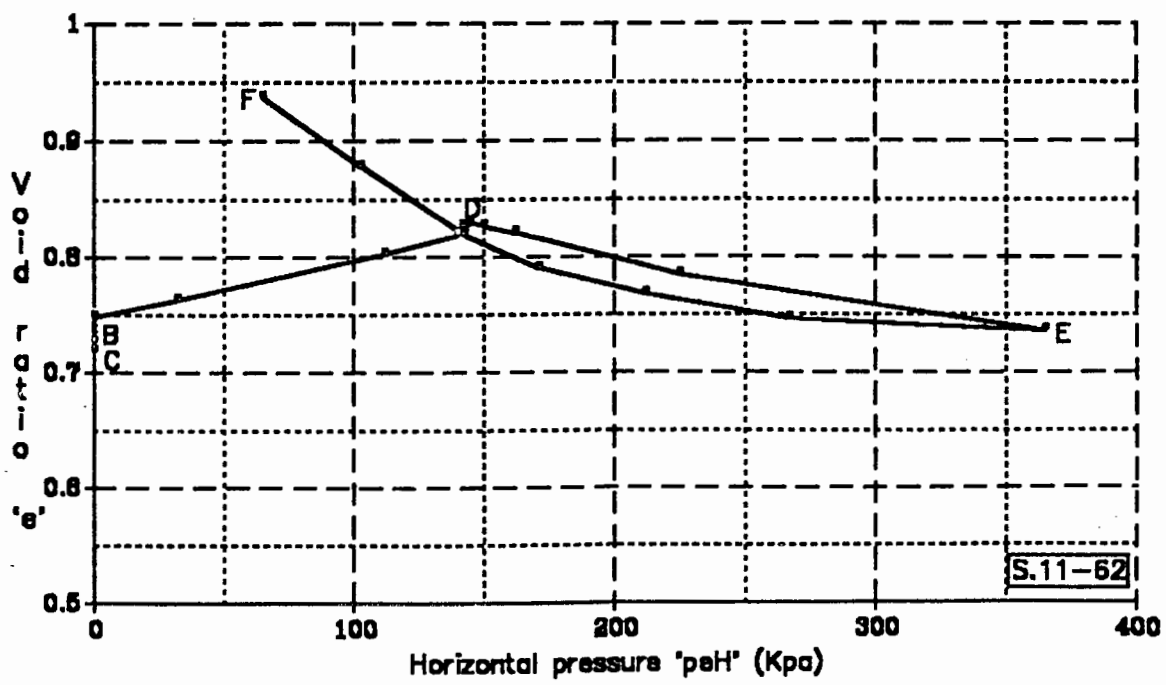

Figure 8.03: Relationship between the void ratio 'e' and the effective horizontal pressure (or stress) 'peH'.
The latter is measured by using the horizontal confining ring fitted with electrical strain gauges.

The measurements of other parameters relating to each soil type are included in Chapters One, Two, and Appendix A. The main index properties for each soil type were listed in Chapter Four.

8.4 REASONS FOR USING THE TYPES OF PLOT SHOWN IN FIGURES 8.01, 8.02, AND 8.03

The types of plot shown in Figures 8.01 and 8.02.

The type of plot shown in Figure 8.01 illustrates the relationship between the void ratio and the water ratio of the sample. This type of plot enables the position and scaling factor of the stress scale (obtained in Chapter Five) to be expressed in terms of the Liquid Limit and Plasticity Index of the soil[1].

The type of plot shown in Figure 8.02 illustrates the relationship between the void ratio and the effective pressure, or stress, applied along the vertical axis. This type of plot enables five stages, or paths (followed by the state of the sample as it changes from one condition to the next), to be observed. The five stages are: (i) Free shrinkage path; (ii) Initial loading path; (iii) Wetting path; (iv) Final loading path; and, (v) Recovery path.

All the reasons for using these types of plots were listed in the section "Reasons for using the types of plot shown in Figures 6.01-6.02", of Chapter Six.

Reasons for using the type of plot in Figure 8.03.

1) To observe the relationship between the void ratio and the effective pressure (or stress) developed by the sample along the horizontal axis, as the result of the applied vertical pressure. This stress is obtained from the observed changes in the horizontal strain.

2) The void ratio and horizontal stress changes as the result of increases in the water content of the sample. The sample is either allowed to increase (or decrease) its volume along the vertical axis, while subjected to a constant vertical pressure, or in the case of an expansive soil, it is prevented from increasing its volume by the application of an external pressure[2].

3) To establish the relationship between the void ratio and the horizontal stress, for the final loading and unloading stages (or paths) of the full test path.

---

[1] - *as used by Sparks, Reference 86.*
[2] - *that is, the 'swell pressure' - refer to chapter seven.*

8.5 SOME SPECIFIC OBJECTIVES

Some of the specific objectives of this chapter:-

The specific objectives of this chapter can be grouped in two parts. The first part provides a summary of the basic parameters obtained from the consolidometer test with horizontal strain, or stress measurements. The second part deals with the evaluation of the parameters and their inter-relationships.

Part One - Summary of the Results obtained from the full test path for the sample, shown in Figures 8.01 to 8.03, and in the following sequence:

(i) The shrinkage path of the sample as it dries to the initial water content required for the test;
(ii) The void ratios and horizontal stresses developed in the sample for its initial loading path towards the required vertical pressure, against which the sample expands or collapses when wetted;
(iii) The changes in void ratio and horizontal stress obtained from the observed increases (or decreases) in volume and horizontal strain, as the result of increases in its water content;
(iv) The measured volumes of water added to the soil sample; and,
(v) The final loading and unloading paths for the sample.

Part two - Evaluation of the Parameters and their inter relationships:

(i) The void ratio (the ratio of the volume of voids to the volume of solids) and the water ratio (the ratio of the volume of water to the volume of solids);
(ii) The void ratio and the effective vertical pressure, or stress, applied to the soil sample;
(iii) The void ratio, the vertical stress and the water ratio;
(iv) The void ratio, the effective horizontal stress (obtained from the observed changes in horizontal strain) and the water ratio; and,
(v) The void ratio, the effective average pressure, or stress (the average of the three principal stresses - assumes that the two horizontal ones are the same), and the water ratio.

8.6 PREPARATION OF TEST SAMPLES

Test samples were prepared from remoulded, compacted and undisturbed soil samples.
A brief description is included in this chapter for each type of sample preparation - for more details refer to either Appendix A ('Preparation of soil samples for testing'), or Appendix G ('Consolidometer tests with horizontal strain, or stress measurements: Test procedure and results')[1].

Remoulded samples.

Method 1: The soil is mixed with water to form a wet paste - the state of the sample is at a condition between the plastic and liquid limits; The wet paste is moulded into a suitable container.
Method 2: An homogeneous dry mixture is prepared by mixing known amounts of soil with tartaric acid and sodium bicarbonate - water is added to the mixture, quickly mixed and placed in a custom made container.

Compacted samples.

Points are selected on the 'dry density versus water content' curve for the soil sample - refer to 'Compaction Tests' in Appendix A; The soil is compacted to the required specification, and aiming for the selected water content; The test sample is cut from the compacted sample.

Undisturbed samples.

The test sample is cut from the undisturbed block - refer to 'Soil Sampling' in Appendix A.

8.7 TEST METHOD

The test sample is allowed to air dry until the required water content to start the test is reached. The shrinkage path of the soil is obtained from the measurements of mass and volume, obtained at regular intervals during the drying of the sample. The procedure (for carrying out the measurements of mass and volume) is illustrated as a visual sequence included in Chapter Four[2] - Photographic Plates 4.01(i) to (iv).
At the required water content for the test, the sample is cut and trimmed to size until the one (of two types - see below) specially made ring being used just slides over it. The top and bottom surfaces of the soil sample are made level and its mass is recorded.

---

1 - refer to section G.2.
2 - see section 4.6.

The modified consolidometer is used for three main purposee:-

1) To observe the one-dimensional changes in vertical strain, or deflection, that occur in the sample as the result of either an externally applied increase (or decrease) in the vertical pressure, and/or increases in the water content.

2) To apply the external vertical stress against which the sample expands or collapses when wetted, or alternatively, the sample is prevented from increasing its volume (for expansive soils only) by the application of swell pressure; and,

3) To enable the use of either one (or two) specially made units for measuring the changes in stress, that take place along the horizontal axis of the sample.

The normal one-dimensional consolidation test[1] for expansive and collapsing soils, basically consists of the following: Load the soil sample to the required pressure and record the values of settlement as a function of time for each stage of loading; Record the amounts of increase (expansion) or decrease (collapse) in the volume of the sample as the result of increases in the water content; and, carry out the final loading and unloading stages.

Two types of devices were used for the measurement of horizontal stresses developed by the sample as a result of increases in the water content and/or applied vertical pressure. The first type makes use of strain gauges, the 'strain unit', for measuring changes in horizontal strain, of the confining steel ring, resulting from the stresses developed in the sample - caused by increases (or decreases) in the applied effective pressure and/or water content.
The second device uses a piston pump to provide the required pressure, or stress, to get water through between the modified consolidometer ring and its built in rubber membrane, the 'ring/membrane unit'.
The two devices are described in the next section of this chapter - 'Measurement of horizontal strains and stresses'.

The strain gauge unit containing the sample is positioned on a filter paper, inside the specially built container, and all the other parts are assembled.
Photographic plates are included in the next section 'Measurement of horizontal strains and stresses'.
The total mass of the container is recorded after which it is enclosed with a plastic cover to prevent evaporation.
Position the container on the consolidometer and connect all the electrical wires of the 'strain unit' to the strain gauge measuring device - ensure that the wires are properly connected.

---

[1] - *used in chapter six.*

When using the 'ring/membrane unit' the sample is fitted within the rubber membrane which lines the ring, and its mass is recorded. The ring/membrane unit is positioned on top of a bottom plate plus filter paper, in the center of the container - refer to the 'ring/membrane unit' part of the next section. Record the mass of the container and enclose it with a plastic cover. The equipment to measure the horizontal pressure, except for the ring/membrane unit itself, is assembled next to the consolidometer. Position the container in the loading device of the consolidometer and connect the pressure tubing to the inlet of the ring/membrane unit.

The following are adjusted: (i) Counterweight alongside the lever arm to apply a firm pressure to the sample (without compressing it); (ii) Micrometer dial gauge is set to its initial, or zero, reading for the vertical deflection.

Three types of consolidometer tests were used, and each test was carried out with horizontal strain, or stress, measurements:-

1) The one-dimensional consolidation test.[1]

A) Record the initial (or zero) readings on the micrometer dial gauge (vertical deflection) and strain gauge measuring device (horizontal strain).
B) Place the necessary weights on the loading platform in order to apply to the soil sample the required sequence of pressure increments, as follows: 8.3 Kpa, 53.6 Kpa, 107.3 Kpa, 214.6 Kpa, 429.2 Kpa and 858.4 Kpa. Record the readings for vertical deflection, on the micrometer dial gauge (consolidometer), and horizontal strain (strain gauge measuring device), before each vertical pressure increment is applied, and at the following time intervals after each one starts acting on the sample - 0.25 minutes, 0.5 min, 1.0 min, 2.25 min, 4 min, 9 min, 16 min, 30 min, 60 min, 120 min, and so on. Readings should continue until the soil has consolidated or, at least, until the slope of the characteristic linear secondary settlement becomes apparent.

C) The unloading, or recovery characteristics of the soil, are observed next. The external vertical pressure applied to the sample is gradually decreased using the following sequence - 858.4 Kpa, 214.6 Kpa, 53.6 Kpa, 8.3 Kpa, and 1.0 Kpa. Readings of vertical deflection and horizontal strain, of the confining ring, are recorded before each vertical pressure decrease and, beginning immediately afterwards, at the time intervals specified above.
At the end of the unloading sequence, final readings are obtained for vertical deflection and horizontal strain.

---

[1] *- similar to the test procedure used in chapter five.*

2) The one-dimensional consolidation test for expansive and collapsing soils.[1]

A) Record the initial readings on the micrometer dial gauge (vertical deflection) and strain gauge measuring device (horizontal strain), or pressure gauge for the piston pump (horizontal stress, via the ring/membrane unit).
B) Place the necessary weights on the loading platform in order to apply to the soil sample the required sequence of pressure increments, leading up to the vertical pressure against which the sample expands or collapses when wetted. The actual values of applied vertical pressure, or stress, vary slightly between each test due to the particular consolidometer machine and ring used. The tests were performed at the following vertical pressures, or ranges of pressures: 54.6 kpa, 98.1 to 109.0 kpa, and 433.7 kpa. Record the readings for the vertical deflection and horizontal strain, or stress (*), which are observed on the respective dial gauges, before each vertical pressure increment is applied and at the time intervals, after the `new pressure' starts acting on the soil, as specified for the first type of consolidometer test with horizontal strain measurements.

C) By means of a calibrated syringe add a known amount of water to the sample and allow expansion, or further settlement, to take place - record the vertical deflection and horizontal strain (or stress) readings before each controlled water increment, and at the time intervals previously specified. Repeat the procedure until no further noticably vertical movement is observed.
D) Support the lever arm of the consolidometer and use weights on the loading platform, in order to measure the loading characteristics of the soil - pressure increments of approximately 50 kpa are used until a maximum value of about 300 kpa is reached, except for the 433.7 kpa test. As before, record the readings for vertical deflection and horizontal strain before each pressure increment and at the time intervals previously specified.
E) The unloading or recovery characteristics of the soil are also recorded, aiming for the following sequence of pressure decrease - 300 kpa, 50 kpa, 10 kpa, and 1 kpa.
Vertical deflection and horizontal strain readings are recorded as specified for the first type of consolidometer test with horizontal strain measurements.
At the end of the unloading sequence, a set of final readings are obtained for the vertical deflection and horizontal strain, or stress, measurements.

(*) - The measurement of horizontal stress refers to the water pressure between the rubber membrane and the ring, applied by means of a piston pump, at which the water just dribbles out to a drain - refer to the next section 'Measurement of horizontal strains and stresses'.

---

[1] - *similar to test procedure used in chapter six.*

3. The swell pressure test for expansive soils.[1]

A) Record the initial readings on the micrometer dial gauge (vertical deflection), strain gauge measuring device (horizontal strain), and proving ring dial gauge (swell pressure).
B) By means of an hypordermic syringe add a known amount of water to the sample through the bottom filter paper. Allow the sample to expand and record the readings, with time, for vertical deflection, horizontal strain (or stress), and swell pressure. As the soil expands, apply vertical pressure to the sample by tightening the proving ring against the consolidometer's arm until the sample is back to its original height. Record the final readings for horizontal strain (or stress) and swell pressure for no change in the height of the sample. Repeat the procedure until no further noticeable vertical movement occurs.

C) Support the lever arm of the consolidometer and use weights on the loading platform in order to measure the unloading or recovery characteristics of the soil. The proving ring is released and the increase in sample thickness and changes in horizontal strain (or stress) are recorded with time.
At the end of the unloading sequence, a set of final readings are obtained for the vertical deflection and horizontal strain, or stress, measurements.

At the completion of the unloading sequence, remove the assembled parts and carefully extract the sample from the strain gauge unit. Record the mass of the sample, after which it is placed inside an oven, previously set at 105 ± 5^{o}C, for a few hours.

Appendix G 'Consolidometer tests with horizontal strain, or stress, measurements' includes a more detailed description of the above test method.

---

[1] *- similar to test procedure used in chapter seven.*

8.8 MEASUREMENT OF HORIZONTAL STRAINS, OR STRESSES

This section deals with the measurement of horizontal strains and stresses.
The measurement of horizontal strains in the confining ring was obtained by means of strain gauges, as part of a specially made 'Strain Unit'.
The measurement of stresses was obtained by using a piston pump to provide the required pressure, or stress to overcome the horizontal stress previously developed with the sample as the result of either an increase of vertical pressure or water content.

The strain unit - Steel ring fitted with strain gauges:-

This system was designed and constructed by Prof. Sparks and the writer[1].

1. The making of the Steel Ring fitted with gauges.

The parts and tools used for fitting the strain gauges to the stainless steel ring are shown in Photographic Plate 8.01.
In brief they were used as follows: Emery (or sand) paper, cotton wool, buds and acetone - surface preparation of metal prior to placing the strain gauges; Strain gauges - type KFC-5-350-C1-16, gauge length = 5 mm and resistance = 350 Ω; Tweezers, glass plate and scotch tape - for handling the strain gauges; Cement - fixing of gauges to the stainless steel ring; Soldier plus soldier iron and tin - for soldering the electrical terminals; Electric wires, connectors, and screw driver - fitting connectors to the wires; Strain gauge cement - to provide moisture proof.

Photographic Plate 8.02 shows the stainless steel ring with strain gauges, expansion joint, and outer ring. The following is a brief description of their intended use: Stainless steel ring with strain gauges - after stage 9 of Photographic Plate 8.01; Epidermix 317, a modified epoxy, for use as a primer for Plycol 347 - contents of Activator to be mixed with Base, and applied to the surface by brush; Plycol type 347 - Polysulphide Expansion Joint Material; Outer ring to surround casted rubber (ie, expansion joint).

---

[1] - *References 16 and 90.*

Photographic Plate 8.01 [Fitting strain gauges]: 1. Emery paper; 2. Cotton wool and buds; 3. Acetone; 4. Strain gauges; 5. Tweezers, glass plate and scotch tape; 6. Cement; 7. Soldier, soldier iron and tin; 8. Electric wires, connectors and screwdriver; and, 9. Strain gauge cement.

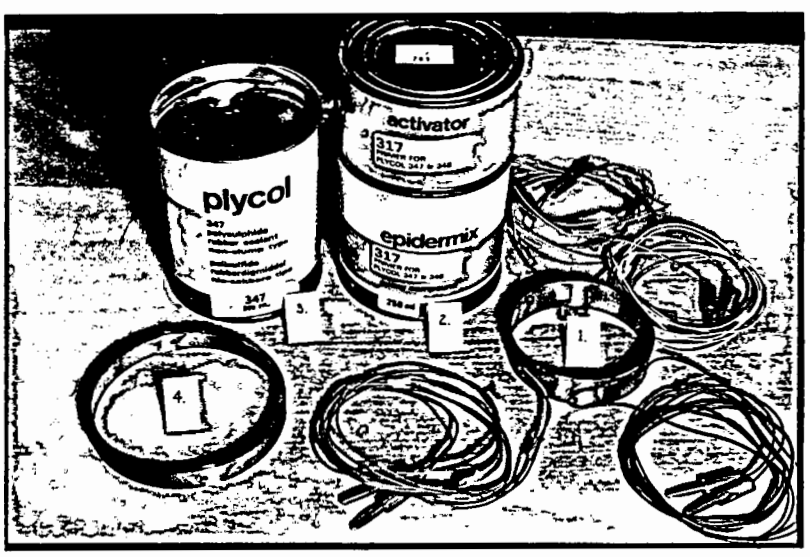

Photographic Plate 8.02 [Stainless steel ring with strain gauges and expansion joint used]: 1. Stainless steel ring with strain gauges; 2. Epidermix 317 (activator and base); 3. Plycol type 347; and, 4. Outer ring.

3. Equipment used in the consolidometer test.

The parts used in the specially made container are shown in Photographic Plate 8.04.

The various parts and their particular features, or uses, are as follows:
Base plate - slots for rubber 'O' ring and electric wire, threaded pieces for wing nuts, and centering bolts (spring loaded for holding the ring unit in position);
Filter papers - bottom (facilitates water feed into sample) and top pieces;
The strain unit - includes the stainless steel ring, electrical strain gauges, expansion joint, and outer ring;
Top loading plate - made of steel or perspex;
Top cover (provides guide to loading of sample), includes access holes (water feeding), and wing nuts (holding down of top cover);
Plastic cover - includes windows for water feed;
Rubber `O' rings - for plastic cover.

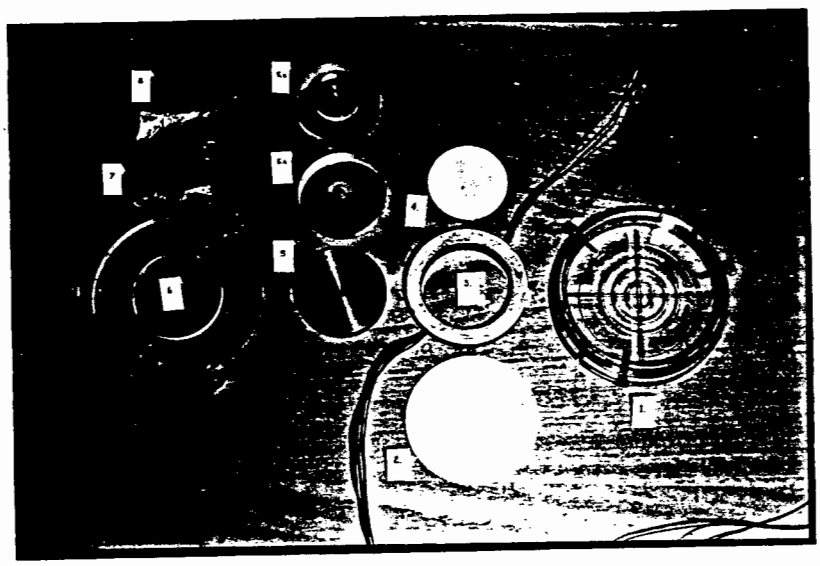

Photographic Plate 8.04 [Parts used in the specially made container]: 1. Base plate; 2. Filter paper (bottom piece); 3. The strain unit; 4. Filter paper (top piece); 5., 5A. and 5B. Top plate - steel or perspex; 6. Top cover; 7. Plastic cover; 8. Rubber 'O' ring.

The various components, as assembled and connected to the strain gauge measuring device, are shown in the Photographic Plate 8.05.
Their particular features are as follows: Strain unit plus other parts (refer to Photographic Plate 8.04) as assembled in specially built container; Board to facilitate the connection of the electrical wires between the strain unit and the strain gauge measuring device; Strain gauge measuring device (made by 'shinkoh').

The equipment, as assembled in the consolidometer, is shown in Photographic Plate 8.06.
The previously assembled container (containing the strain unit with sample) is positioned on the loading device of the consolidometer and the electrical wires are connected to the strain gauge measuring device placed next to the consolidometer machine.
Photographic Plate 8.06 shows a test in progress - the sample is being subjected to a known vertical pressure.

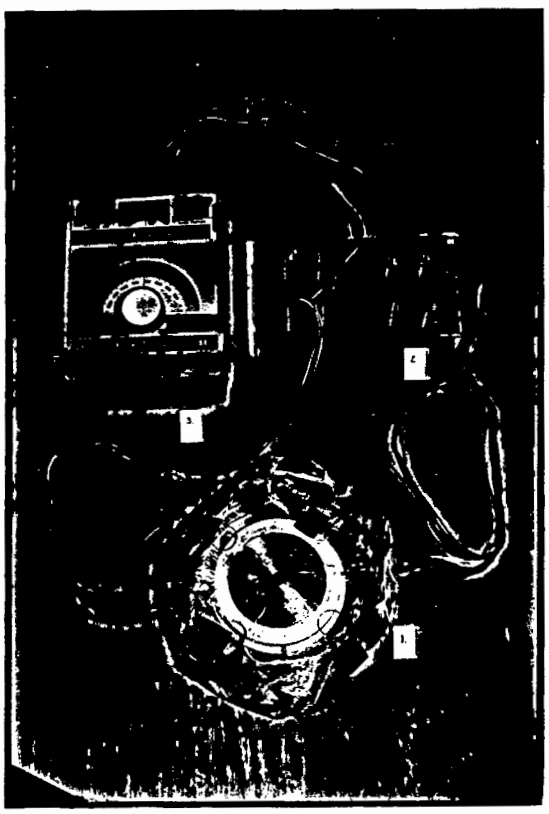

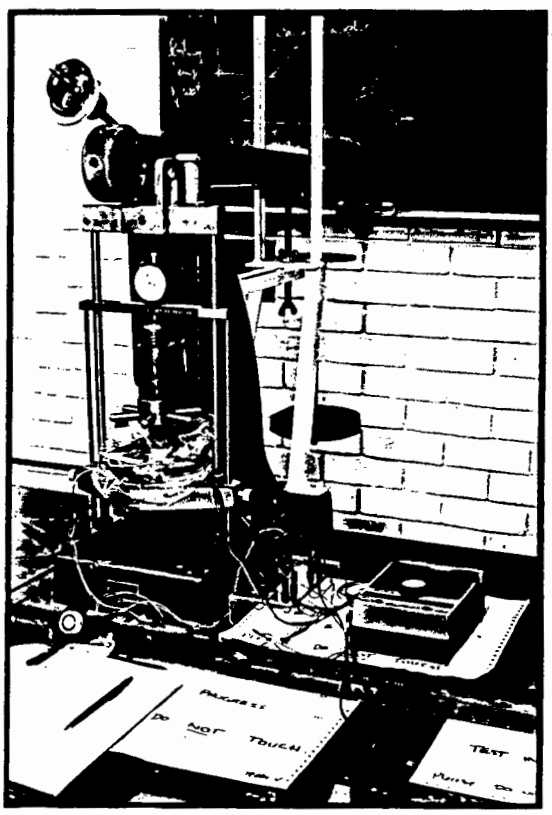

Photographic Plate 8.05 [LHS - Equipment ready to be assembled for the Consolidometer Test]: 1. Strain unit; 2. Connecting board; 3. Strain gauge measuring device.

Photographic Plate 8.06 [RHS - Consolidometer test with horizontal strain measurement]: Equipment fully assembled, and test in operation.

The Ring/Membrane Unit:-

This unit was originally designed by Prof Sparks, and used by students[1].
This unit basically consists of a special consolidometer ring which is fitted with a water tight rubber membrane around its inner surface.
The horizontal pressure developed in the soil, as the result of either an increase in vertical pressure or water content, is measured by pumping a known pressure of (water), in increments, into the inlet port of the consolidometer ring until it just starts to dribble out at the outlet point.

The equipment used to measure the horizontal stresses in the soil, consists of the following parts:
A special consolidometer ring, lined with a rubber membrane and connected to a piston pump; A water reservoir to provide water to the piston pump by means of a hose; A specially made container - the consolidometer ring fits in the centre; Filter papers; Top loading plate - provides initial pressure of about 1 kpa; Porous plate - fits into bottom of ring.

The equipment is assembled in the following order:
The sample is carefully fitted into the consolidometer ring; The bottom porous plate is positioned in the center of the container, a filter paper is placed on top, followed by the consolidometer ring containing the sample. The other filter paper and top loading plate are placed on top of the sample. The container is enclosed with a loose fitting plastic cover. The equipment used to measure the pressure applied (by means of the piston pump) is assembled on a table next to the consolidometer.

The previously assembled container is positioned on the loading device of the consolidometer, and the flexible high pressure tubing is connected to the inlet of the ring/membrane unit.
The stop cock on the water resevoir side is opened, and water is allowed into the piston pump cylinder. Close the stop cock on the reservoir side and open the other side. The water is pushed through the tubing into the gap between the ring and the rubber membrane. At a certain pressure, the water will start going through, and the sample is pushed slightly inwards by the pressure - just enough to allow through a drop or two of water.
The pressure at which the water just dribbles out (as read on the gauge fitted to the high pressure tubing) is recorded as the applied pressure which overcame the horizontal stress which had developed in the sample.

A summary of the test method is included in the previous section - for further details of the test procedures and results refer to Appendix G[2], 'Consolidometer tests with horizontal strain, or stress, measurements.'

---

[1] - *for example, Ballantine 1978 (Reference 20).*
[2] - *sections G.2 and G.3.*

8.9 ANALYSIS OF TEST RESULTS

The test results consist of measurements of vertical deflection or swell pressure (for no deflection), and horizontal stress, developed in a sample which is confined in the horizontal axis - these changes in volume, or stress, take place as a result of an increase (or decrease) in the vertical pressure or water content.
A bracket was incorporated in the design of the modified consolidometer to provide support to the loading platform. This consolidometer can also be used to measure the vertical pressure required to prevent the sample from expanding - refer to 'The swell pressure test for expansive soils'[1].

The introduction to the results for the consolidometer tests with horizontal stress measurements, will be provided by the definitions of each soil type according to particle size and consistency limit values[2].

The parameters which were investigated are analysed and presented in three basic forms:-

1) The relationship between the Void Ratio and the Water Ratio, for the full test path;

2) The relationship between the Void Ratio and the Effective Vertical Pressure, or Stress, for the full test path; and,

3) The relationship between the Void Ratio and the Effective Horizontal Pressure, or Stress, for the full test path.

These relationships are illustrated in Figures 8.04 to 8.29, as follows:-

Void ratio versus water ratio:

Site 11, Rosebank - Figures 8.06 [50 Kpa], 8.09 [100 Kpa], 8.12 [400 Kpa], 8.15 [swell pressure];
Site 36, Rondebosch - Figure 8.18 [100 Kpa];
Site A, Berea Road - Figure 8.21 [100 Kpa];
Site 7, Mowbray - Figure 8.24 [100 Kpa];
Site 48, Lady Grey - Figure 8.27 [100 Kpa].

---

1 - included in section 8.7 "Test method".
2 - refer to Chapters One, Two and Appendix A.

Void ratio versus effective vertical pressure:

Site 11, Rosebank - Figure 8.04 [one-dimensional consolidation], 8.07 [50 Kpa], 8.10 [100 Kpa], 8.13 [400 Kpa], 8.16 [swell pressure];
Site 36, Rondebosch - Figure 8.19 [100 Kpa];
Site A, Berea Road - Figure 8.22 [100 Kpa];
Site 7, Mowbray - 8.25 [100 Kpa];
Site 48, Lady Grey - Figure 8.28 [100 Kpa].

Void ratio versus effective horizontal pressure:

Site 11, Rosebank - Figure 8.05 [one-dimensional consolidation], 8.08 [50 Kpa], 8.11 [100 Kpa], 8.14 [400 Kpa], 8.17 [swell pressure];
Site 36, Rondebosch - Figure 8.20 [100 Kpa];
Site A, Berea Road - Figure 8.23 [100 Kpa];
Site 7, Mowbray - Figure 8.26 [100 Kpa];
Site 48, Lady Grey - Figure 8.29 [100 Kpa].

Appendix G includes the detailed consolidometer tests with horizontal strain, or stress, measurements - test procedures and results[1].

Relationships of void ratio versus water ratio, void ratio versus effective vertical pressure, and void ratio versus effective horizontal pressure, are included for the following natural soil types:

(i) Site 11, Rosebank (Cape);
(ii) Site 36, Rondebosch (Cape);
(iii) Site A, Berea Road (Durban, Natal);
(iv) Site 7, Mowbray (Cape); and,
(v) Site 48, Lady Grey (Natal).

Consolidometer tests with horizontal strains, or stresses, measurements (for expansive and collapsing soils) were performed on the soil samples listed in Table 8.01.

---

[1] - *see sections G.2, G.3 and G.5.*

Table 8.01: Natural soil samples used for consolidometer tests with horizontal strain, or stress, measurements.

Sample No.	Method of preparation	Free Shrinkage (Ref. number)	Expansion / Collapse (Ref./Consolidometer)
Site 11 - Remoulded 'M' & Compacted 'C':			
[One-dimensional Consolidation - Figures 8.04, 8.05]			
S.11-66	M1 (≥LL)	-	IV. 455 / test no. 165
[Effective pressure = 50 kpa - Figures 8.06, 8.07, 8.08]			
S.11-64	M1 (≥LL)	IV. 451	IV. 464 / test no. 173
[Effective pressure = 100 kpa - Figures 8.09, 8.10, 8.11]			
S.11-62	M1 (<LL)	III.396	IV. 430 / test no. 150
S.11-61	M1 (<LL)	IV. 416	IV. 437 / test no. 154
S.11-60	M1 (≥LL)	III.384	IV. 420 / test no. 142
S.11-59	M1 (≥LL)	III.394	IV. 442 / test no. 158
S.11-58	M2 (*)	III.356	IV. 413 / test no. 137
S.11-70	CStd,IV.450	IV. 458	IV. 458 / test no. 168
[Effective pressure = 400 kpa - Figures 8.12, 8.13, 8.14]			
S.11-65	M1 (≥LL)	IV. 451	IV. 468 / test no. 176
[Swell pressure - Figures 8.15, 8.16, 8.17]			
S.11-63	M1 (≥LL)	IV. 421	IV. 449 / test no. 163
S.11-71	CStd,IV.450	IV. 459	IV. 459 / test no. 169
Site 36 - Remoulded:			
[Effective pressure = 100 kpa - Figures 8.18, 8.19, 8.20]			
S.36-5	M1 (<LL)	III.348	III.401 / test no. 129
S.36-12	M1 (<LL)	III.382	IV. 426 / test no. 147
Site A - Undisturbed:			
[Effective pressure = 100 kpa - Figures 8.21, 8.22, 8.23]			
S.A-1	-	Ba. 78	Ba. 78 / S.A-1
Site 7 - Undisturbed:			
[Effective pressure = 100 kpa - Figures 8.24, 8.25, 8.26]			
S.7-1	-	Ba. 77	Ba. 77 / 6.40
Site 48 - Undisturbed:			
[Effective pressure = 100 kpa - Figures 8.27, 8.28, 8.29]			
S.48-1	-	Ba. 78	Ba. 78 / S.48-1

** - air bubbles.*

Site 11, Rosebank.

Previously defined as a fine silty clay with only a small amount of fine sand. The soil consists of 59% clay, 29% silt, and 12% sand size. The consistency, free shrinkage and free swell limits, are as follows: Linear Shrinkage 'w_{LS}' = 11.4%; Liquid Limit 'w_L' = 69%; Plastic Limit 'w_P' = 30.7%; Plasticity Index 'I_P' = 38; Shrinkage Limit 'w_S' = 22.5%; and, Free Expansion Limit 'w_{FE}' = 49.4%.

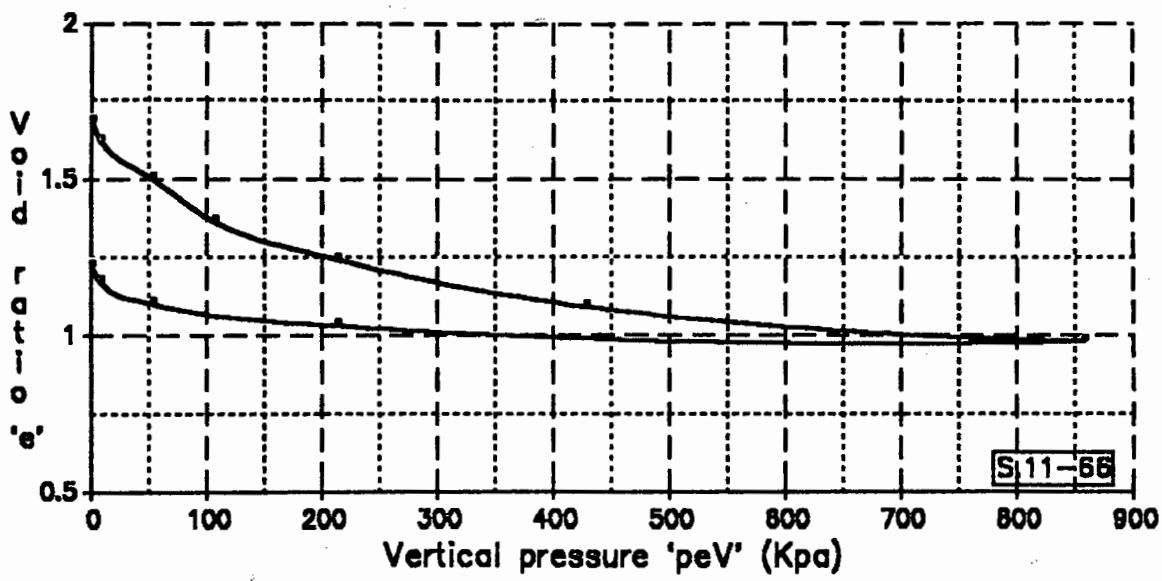

Figure 8.04: Site 11, Rosebank - [One-D Consolidation] Relationship between the void ratio 'e' and the effective vertical pressure (or stress) 'peV'.

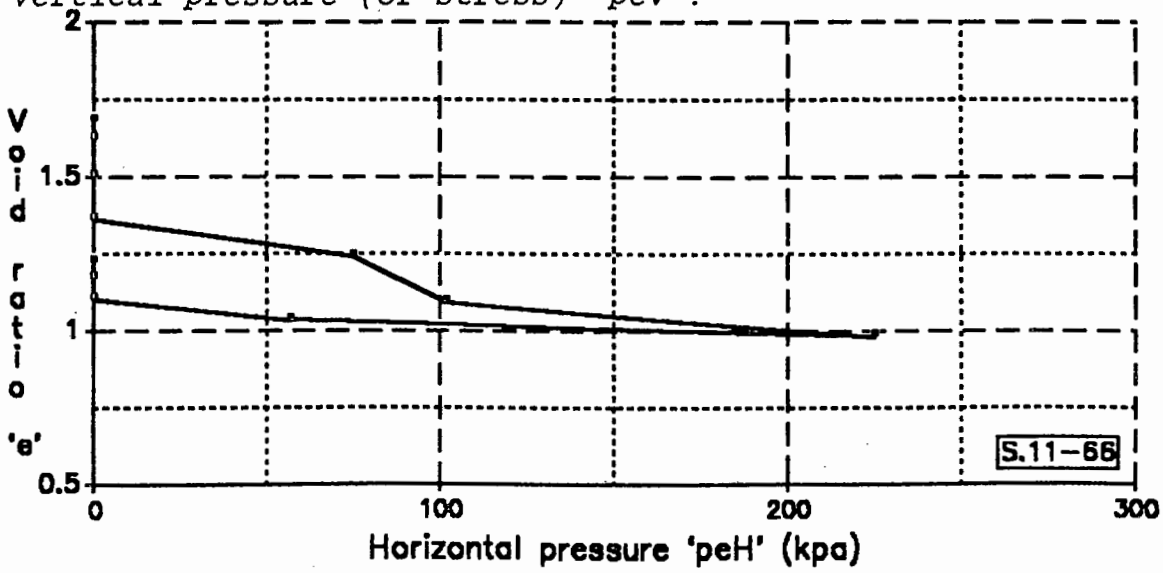

Figure 8.05: Site 11, Rosebank - [One-D Consolidation] Relationship between the void ratio 'e' and the effective horizontal pressure (or stress) 'peH'.

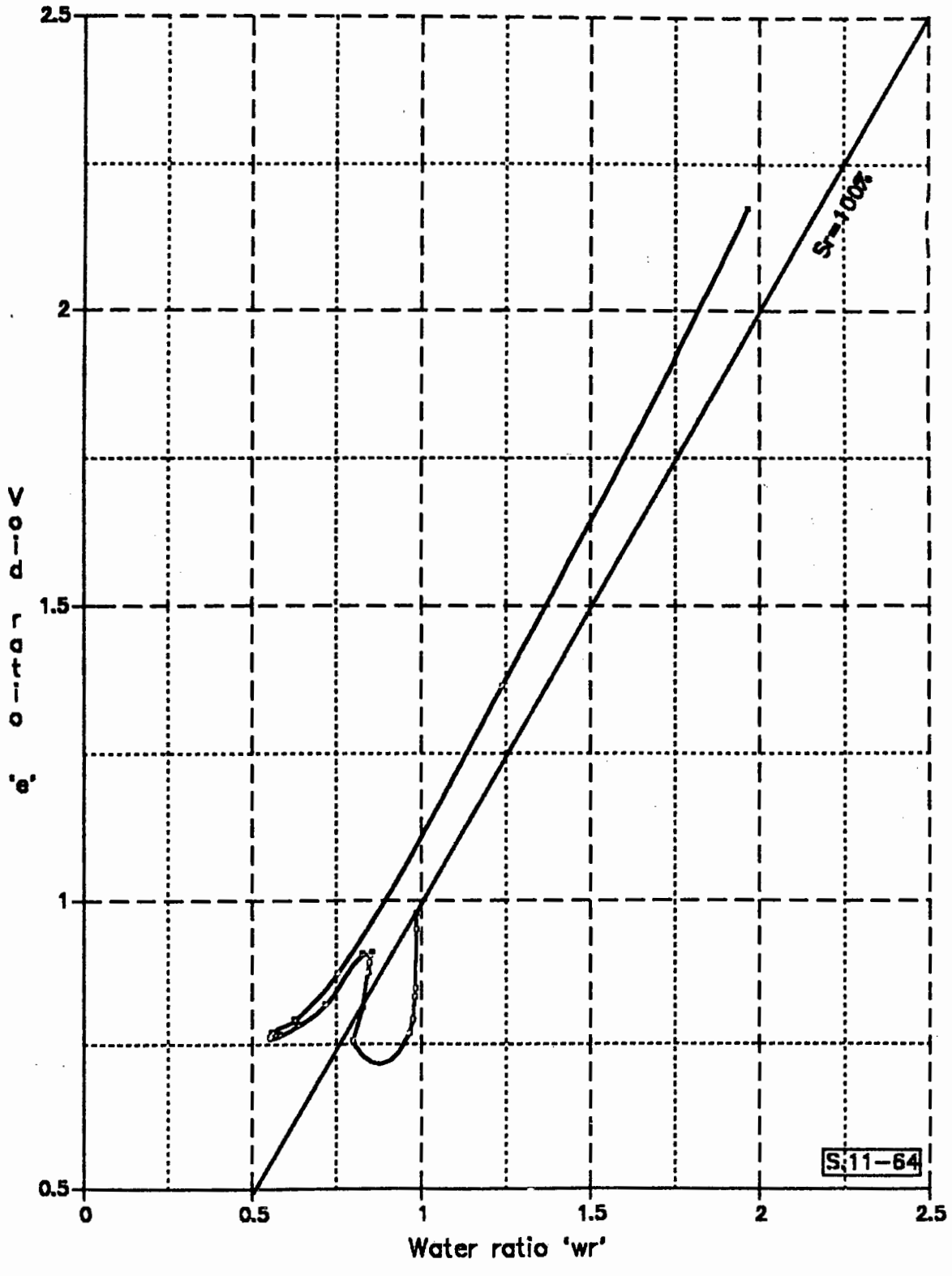

Figure 8.06: Site 11, Rosebank - [Left overnight at 50 Kpa and then wetted under this pressure] Relationship between the void ratio 'e' and the water ratio 'wr', for the full test path.

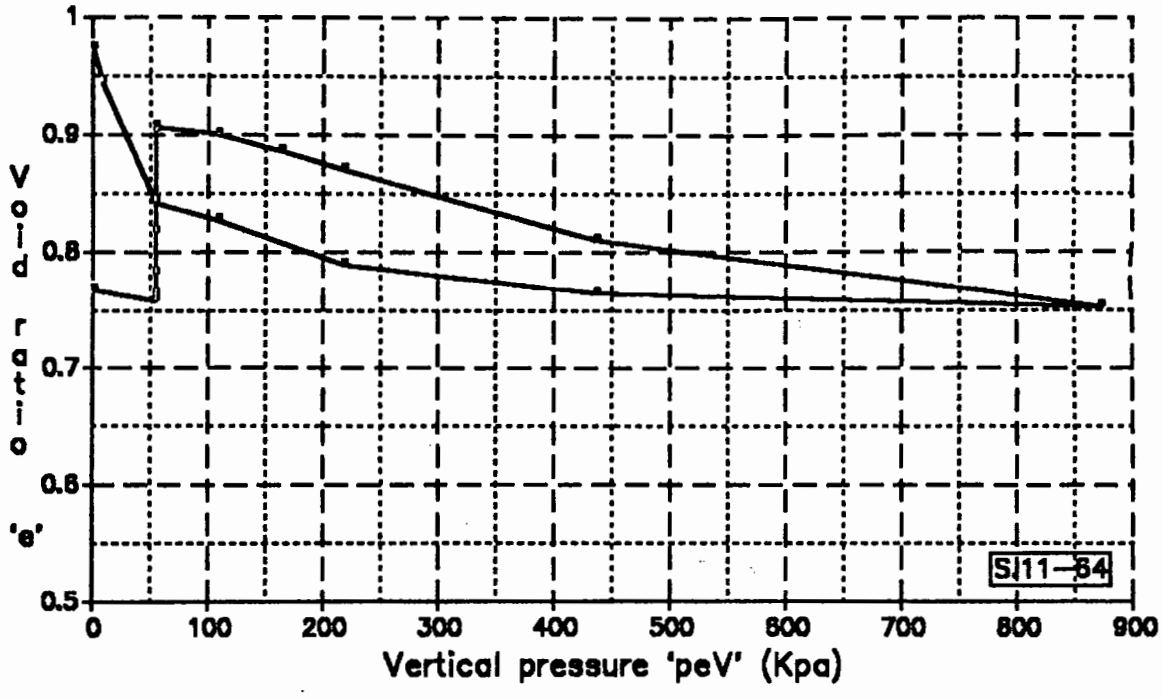

Figure 8.07: Site 11, Rosebank - [50 Kpa] Relationship between the void ratio 'e' and the effective vertical pressure (or stress) 'peV'.

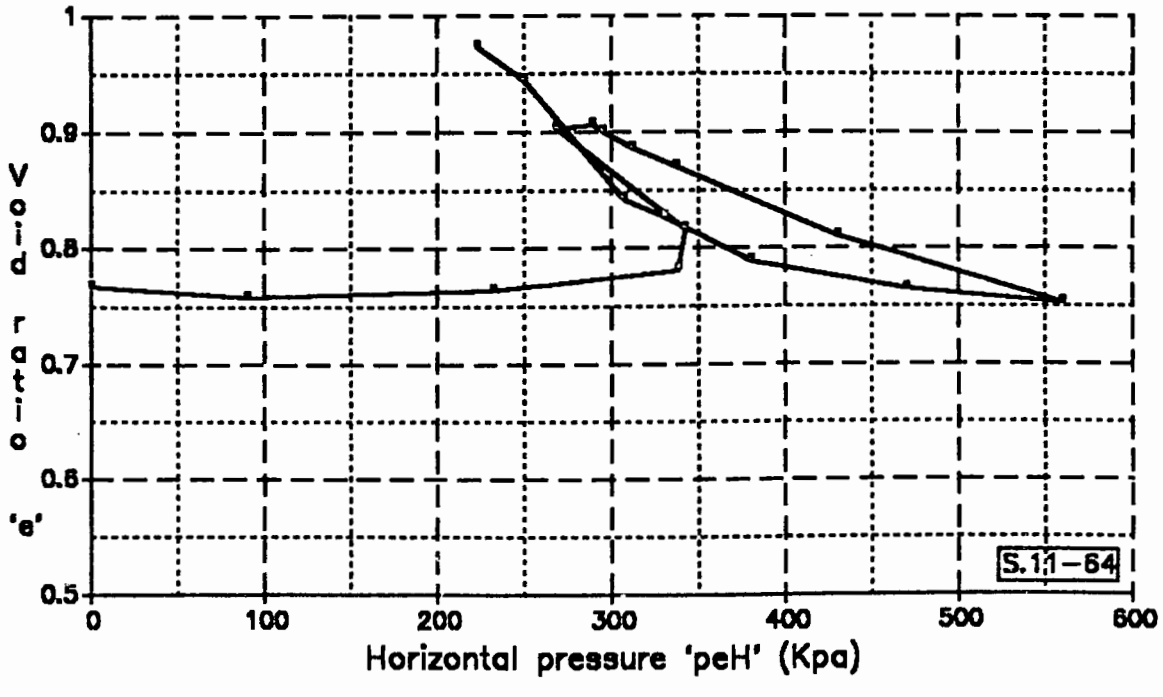

Figure 8.08: Site 11, Rosebank - [50 Kpa] Relationship between the void ratio 'e' and the effective horizontal pressure (or stress) 'peH'.

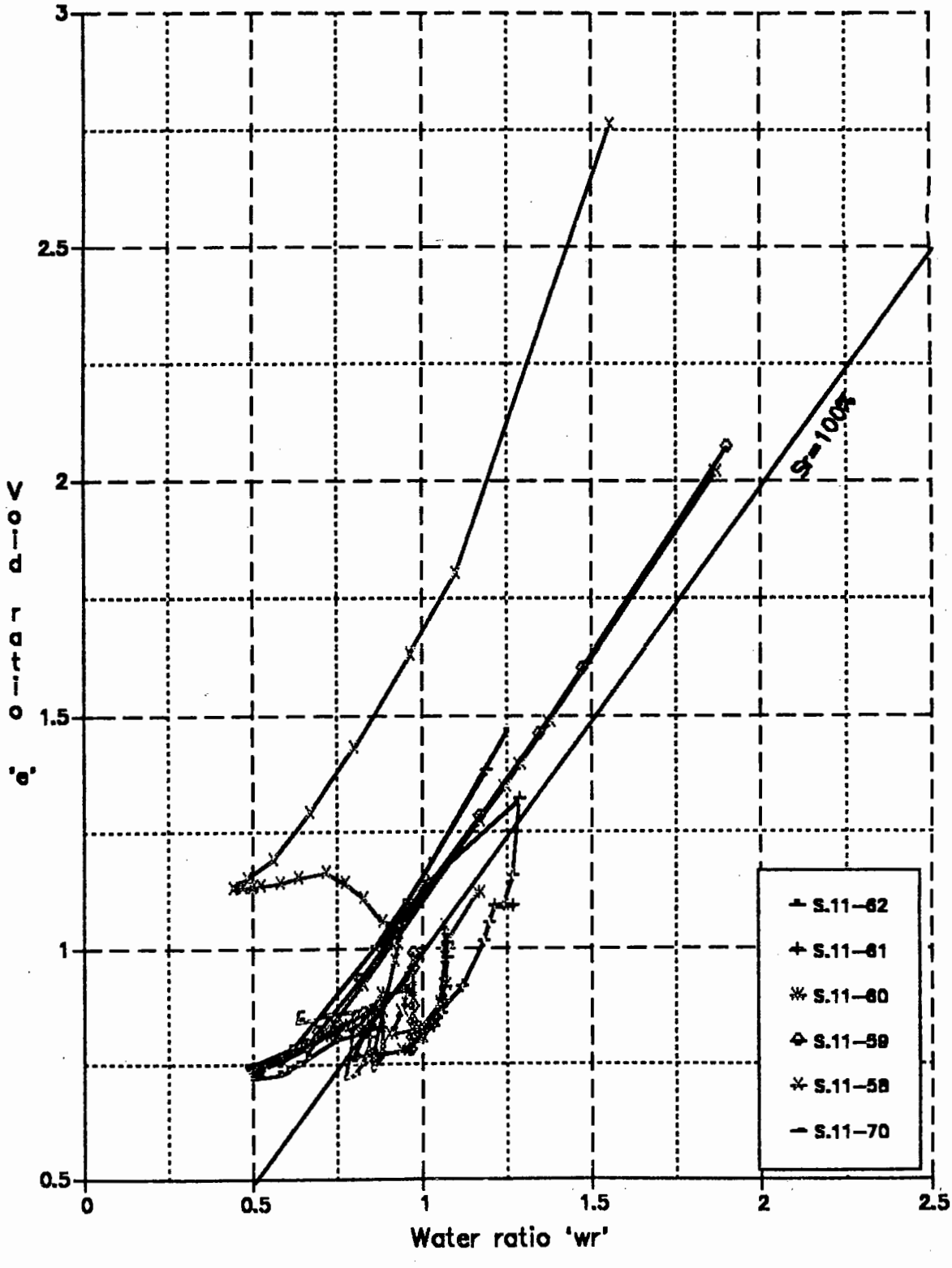

Figure 8.09: Site 11, Rosebank - [Left overnight at 100 Kpa and then wetted under this pressure] Relationship between the void ratio 'e' and the water ratio 'wr', for the full test path.

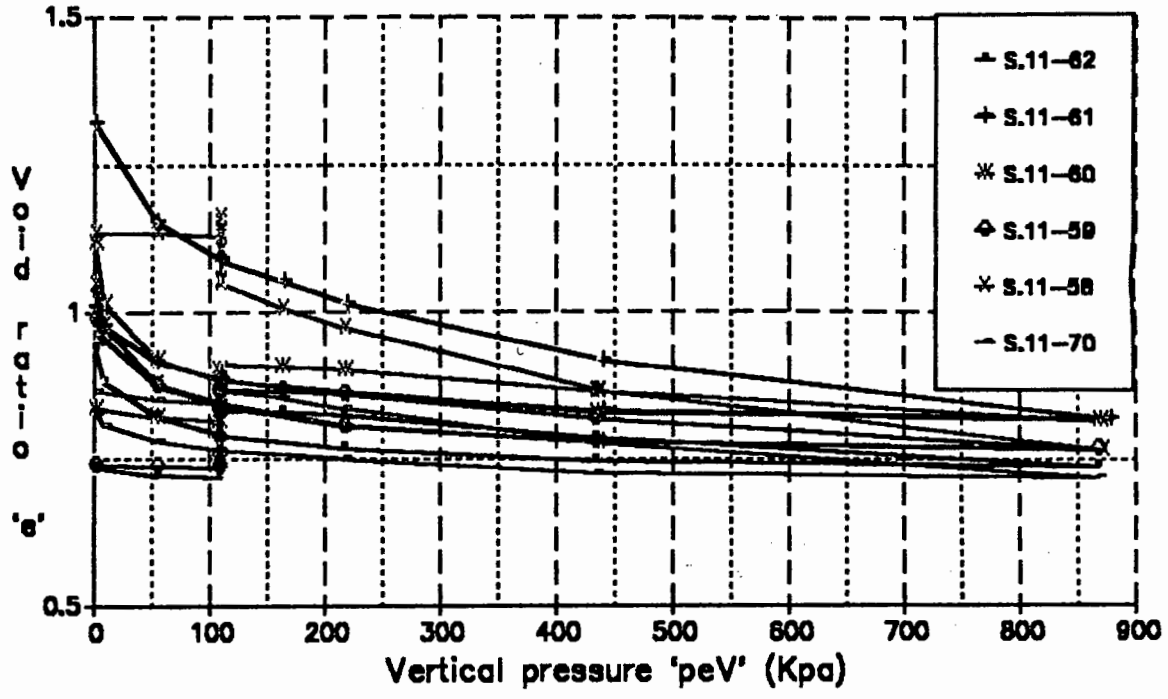

Figure 8.10: Site 11, Rosebank - [100 Kpa] Relationship between the void ratio 'e' and the effective vertical pressure (or stress) 'peV'.

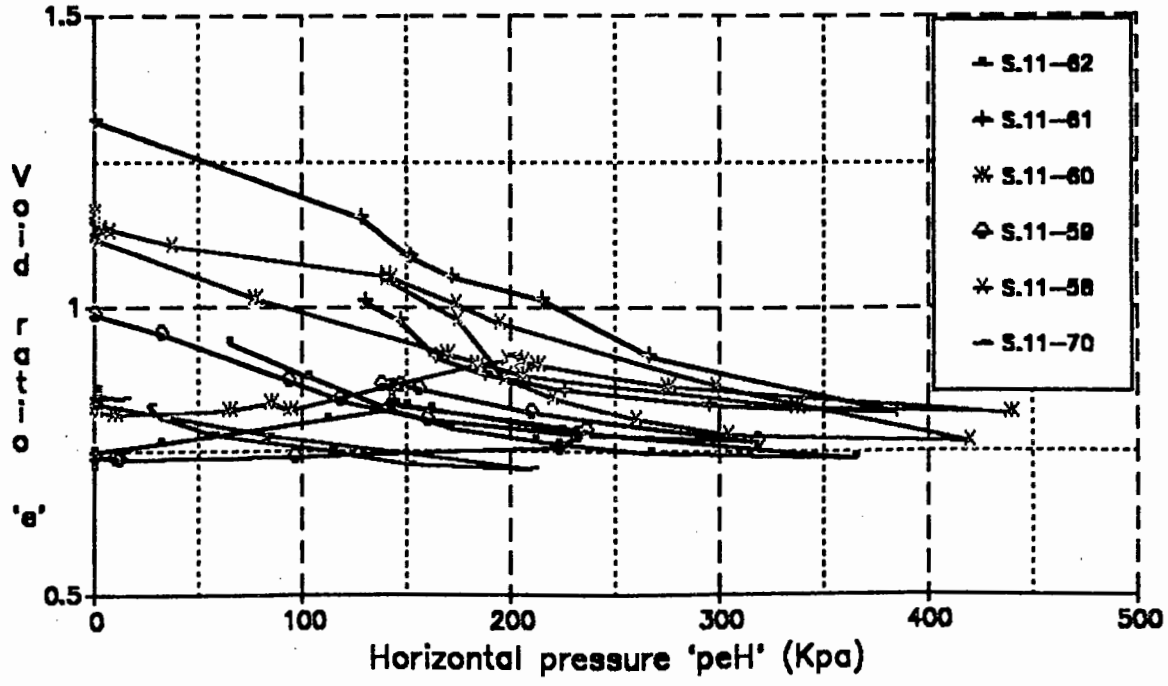

Figure 8.11: Site 11, Rosebank - [100 Kpa] Relationship between the void ratio 'e' and the effective horizontal pressure (or stress) 'peH'.

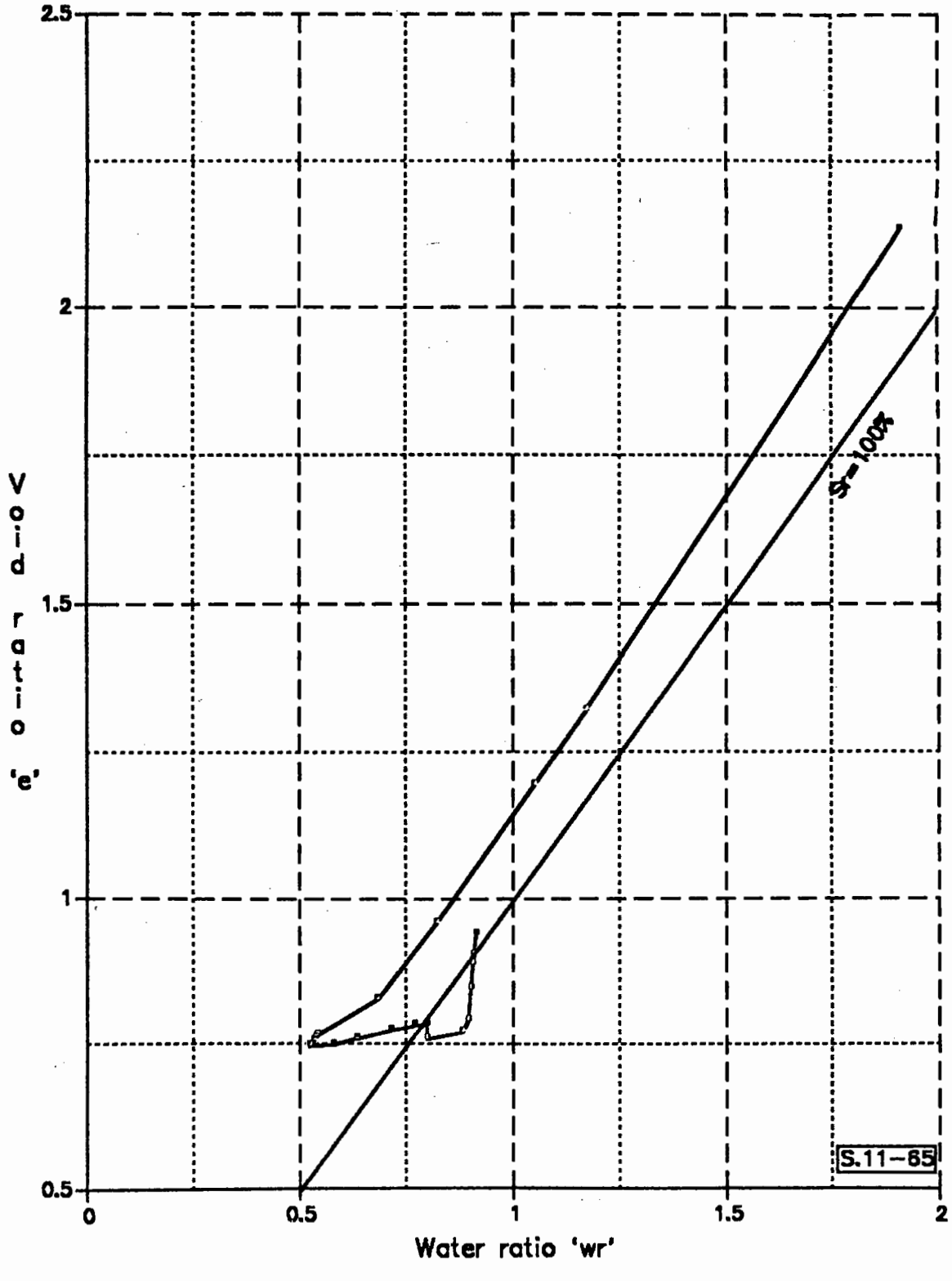

Figure 8.12: Site 11, Rosebank - [Left overnight at 400 Kpa and then wetted under this pressure] Relationship between the void ratio 'e' and the water ratio 'wr', for the full test path.

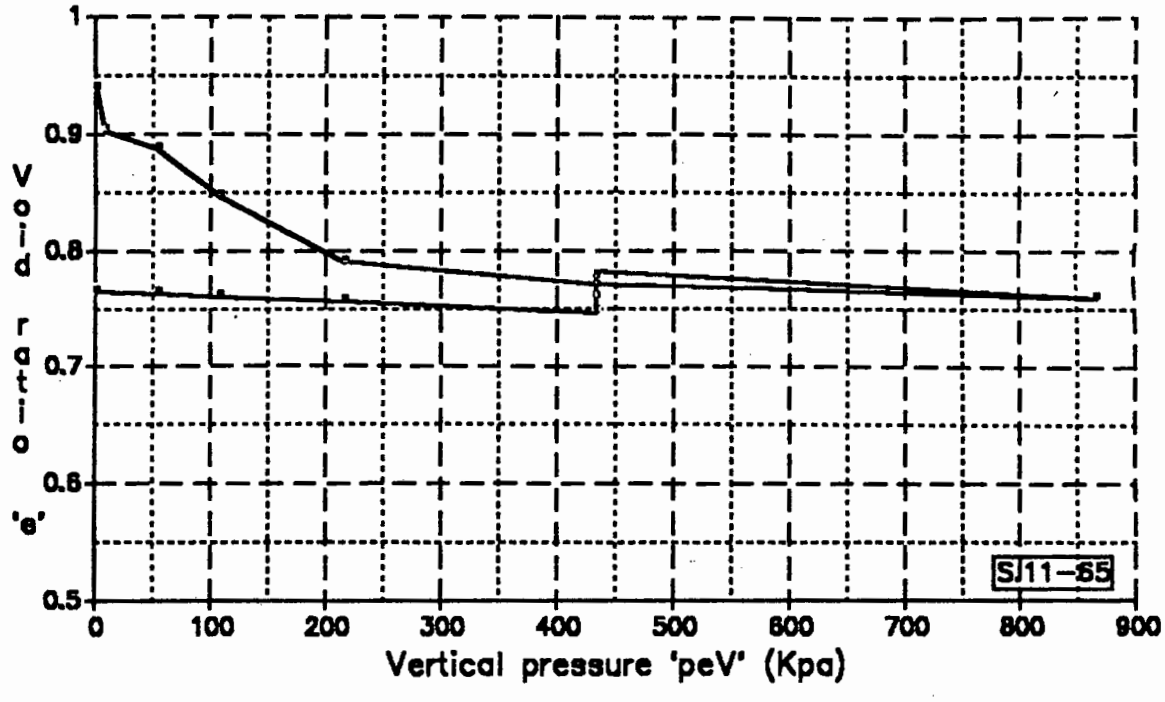

Figure 8.13: Site 11, Rosebank - [400 Kpa] Relationship between the void ratio 'e' and the effective vertical pressure (or stress) 'peV'.

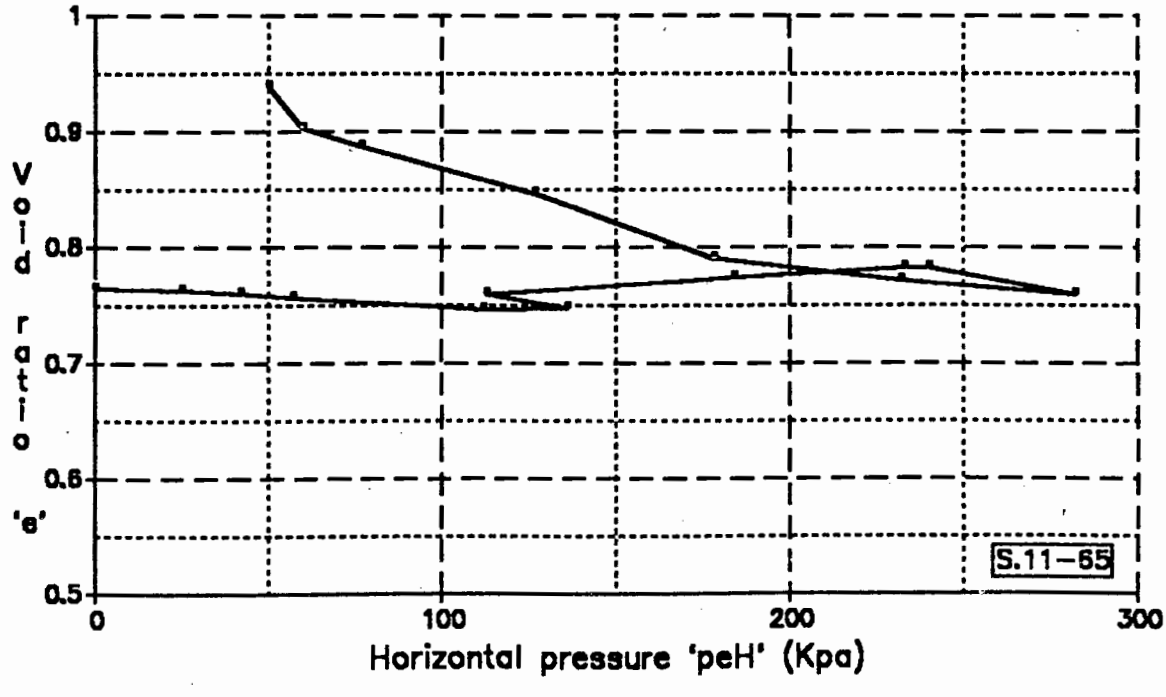

Figure 8.14: Site 11, Rosebank - [400 Kpa] Relationship between the void ratio 'e' and the effective horizontal pressure (or stress) 'peH'.

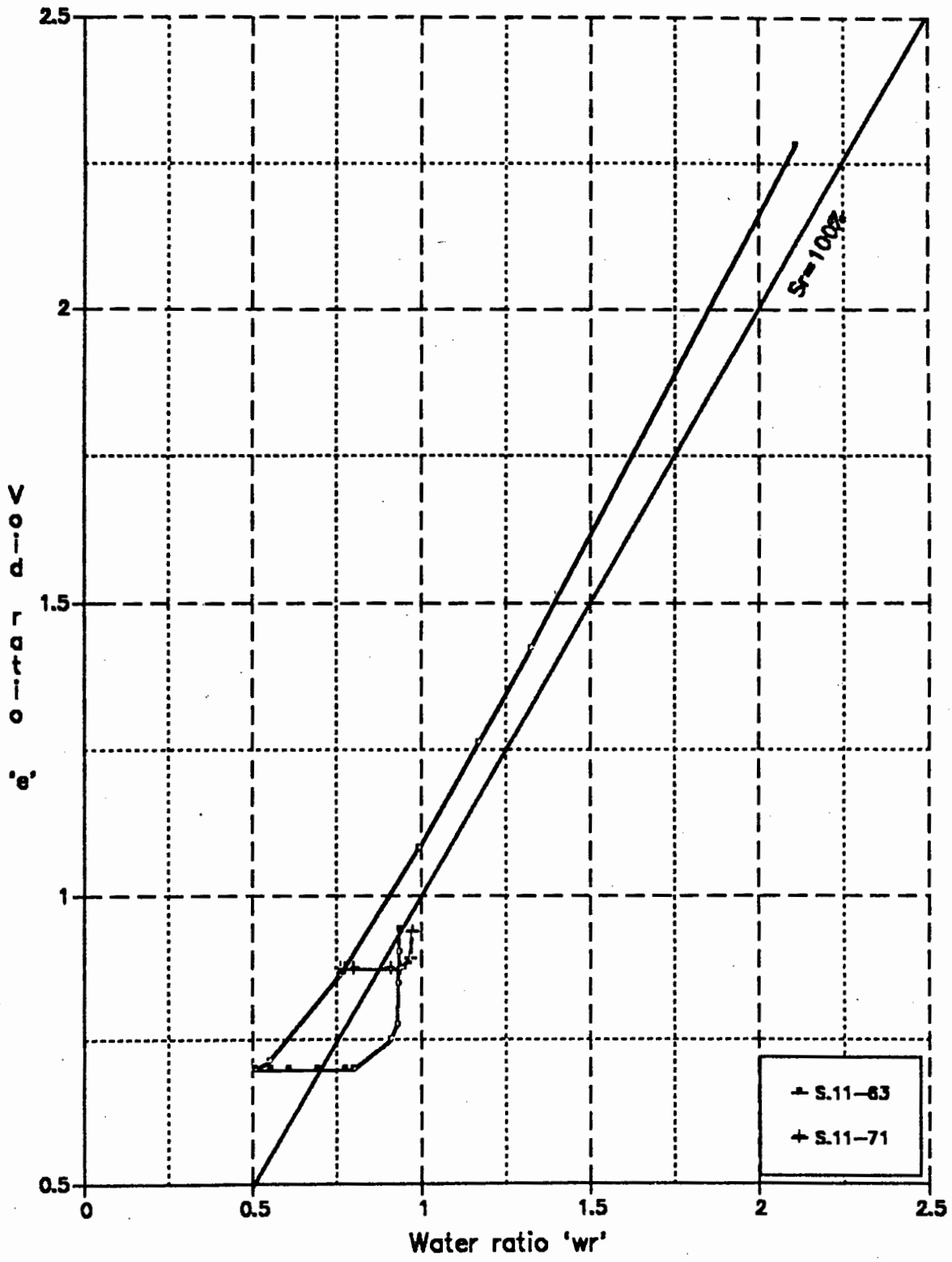

Figure 8.15: Site 11, Rosebank - [Swell Pressure] Relationship between the void ratio 'e' and the water ratio 'wr', for the full test path.

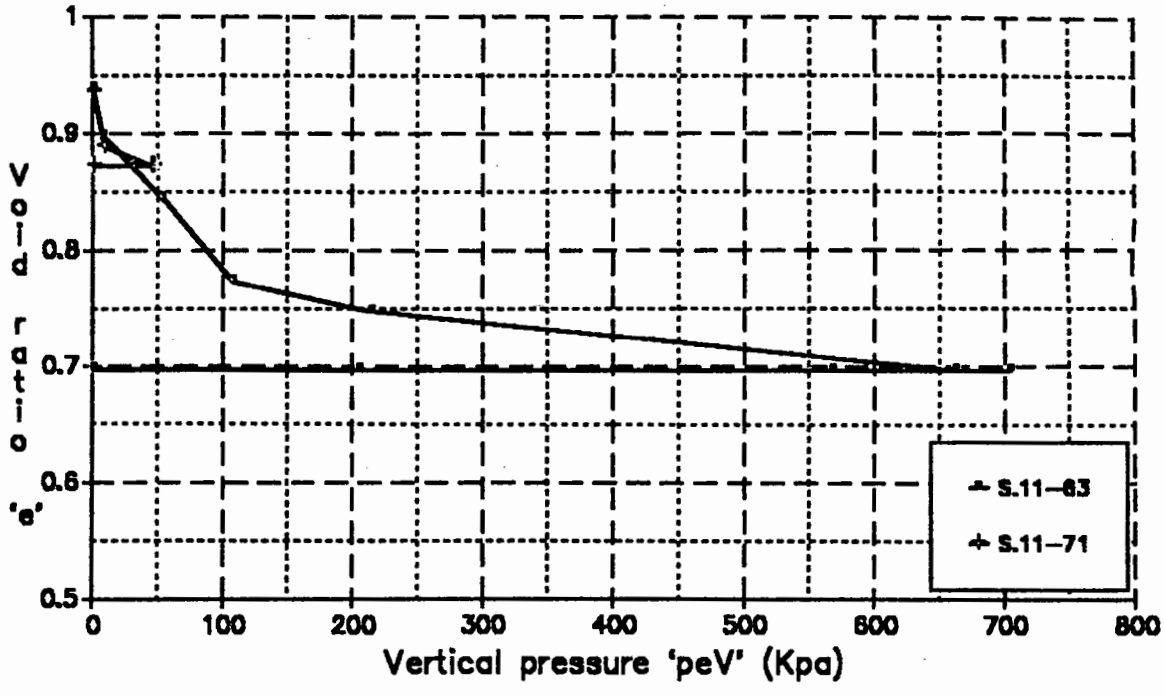

Figure 8.16: Site 11, Rosebank - [Swell Pressure] Relationship between the void ratio 'e' and the effective vertical pressure 'peV'.

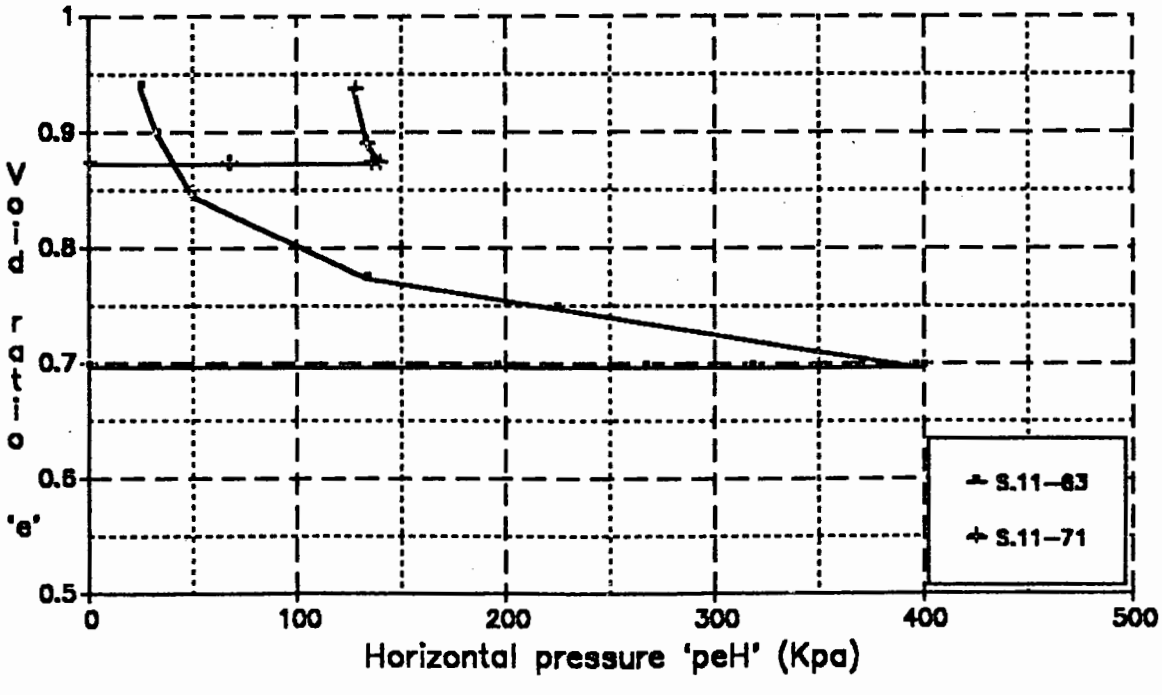

Figure 8.17: Site 11, Rosebank - [Swell Pressure] Relationship between the void ratio 'e' and the effective horizontal pressure 'peH'.

Site 36, Rondebosch.

A clayey silt, with a fine sand and a small amount of medium sand. The soil consists of 22% clay, 49% silt, and 29% sand size. The 'Limits' are as follows: w_{LS} = 8.3%; w_L = 47.0%; w_P = 23.3%; I_P = 24; w_S = 22.0%; and, w_{FE} = 32.7%.

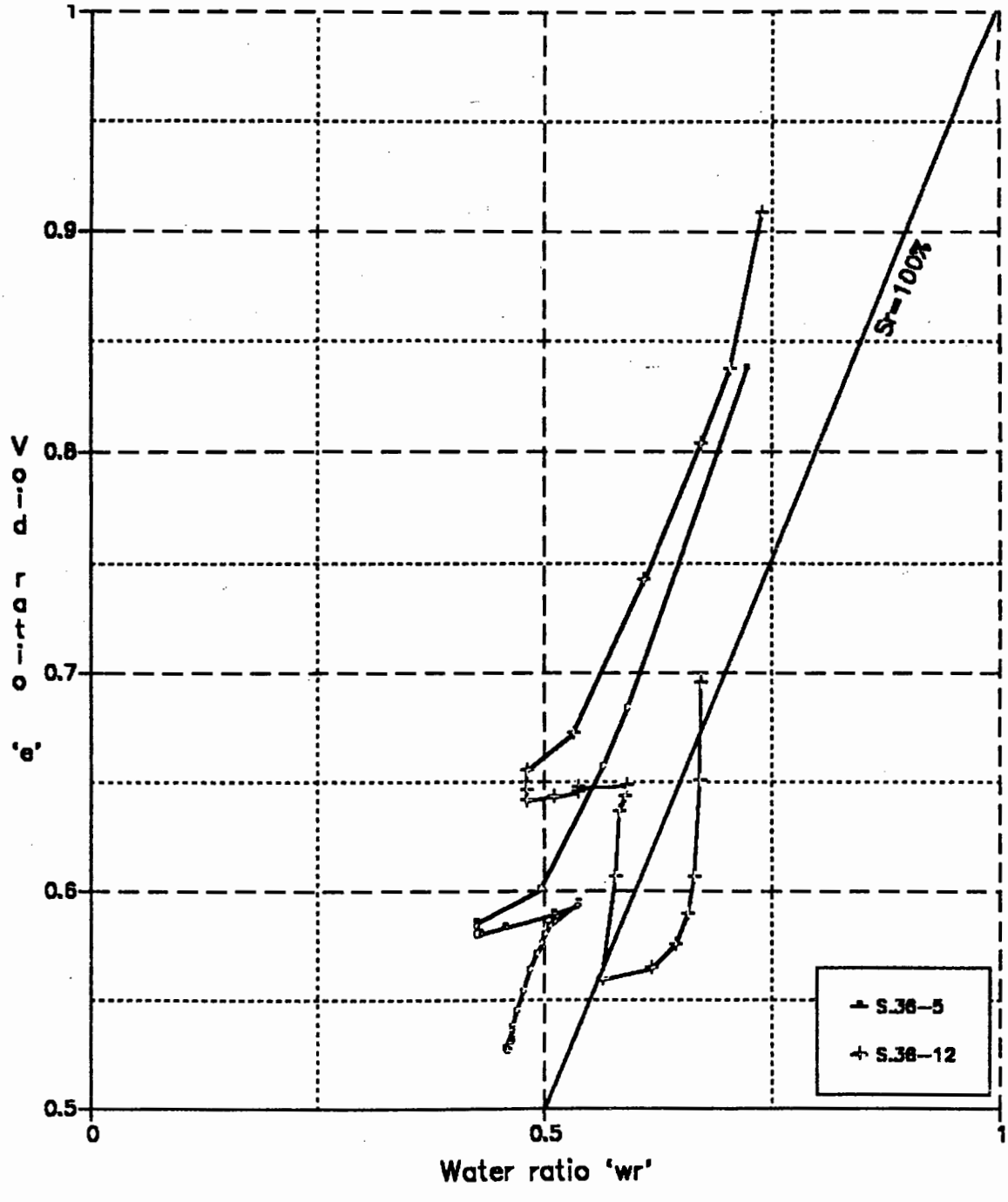

Figure 8.18: Site 36, Rondebosch - [Left overnight at 100 Kpa and then wetted under this pressure] Relationship between the void ratio 'e' and the water ratio 'wr', for the full test path.

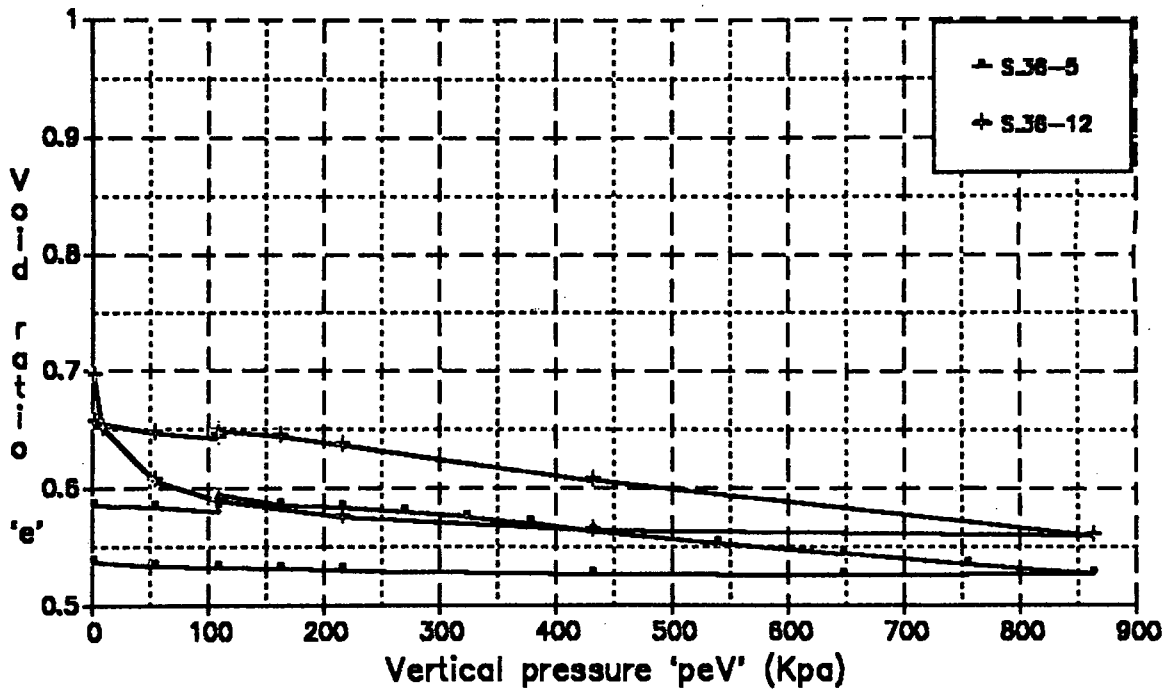

Figure 8.19: Site 36, Rondebosch - [100 Kpa] Relationship between the void ratio 'e' and the effective vertical pressure 'peV'.

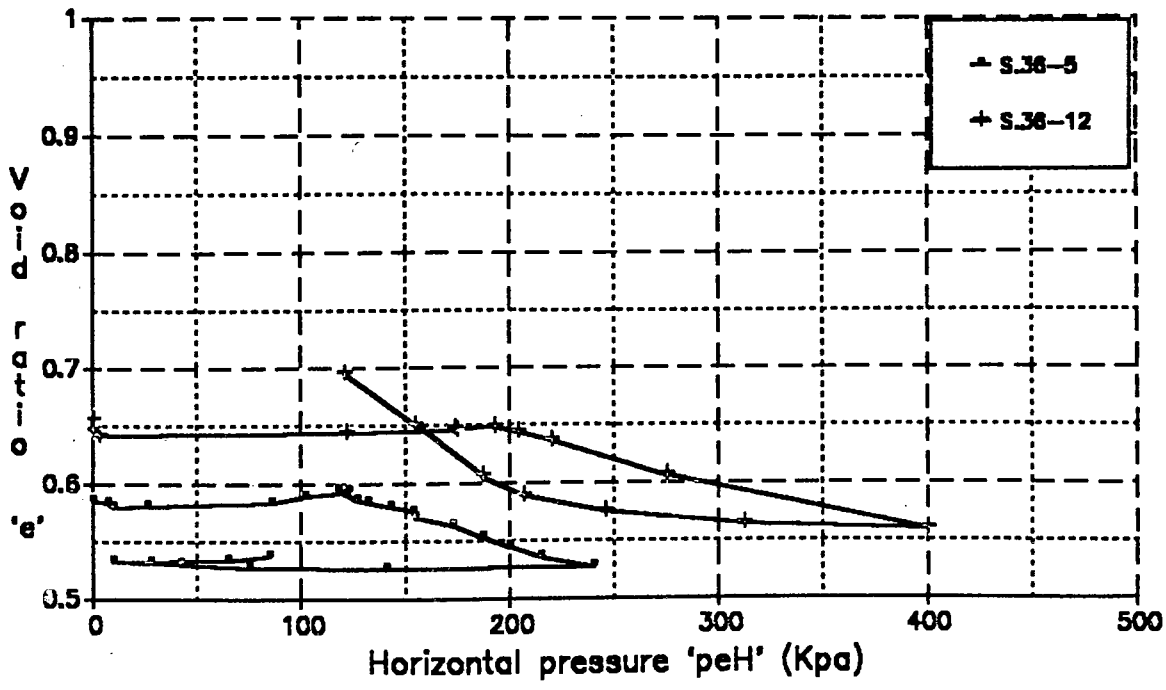

Figure 8.20: Site 36, Rondebosch - [100 Kpa] Relationship between the void ratio 'e' and the effective horizontal pressure 'peH'.

Site A, Berea Road (Durban).

A clayey sand (fine to medium size) with a small amount of silt. The soil consists of 15% clay, 10% silt, and 75% sand size. The 'Limits' are as follows: w_{LS} = 3.7%; w_L = 25.0%; w_P = 13.1%; I_P = 12; w_S = 13.5%; and, w_{FE} = 16.6%.

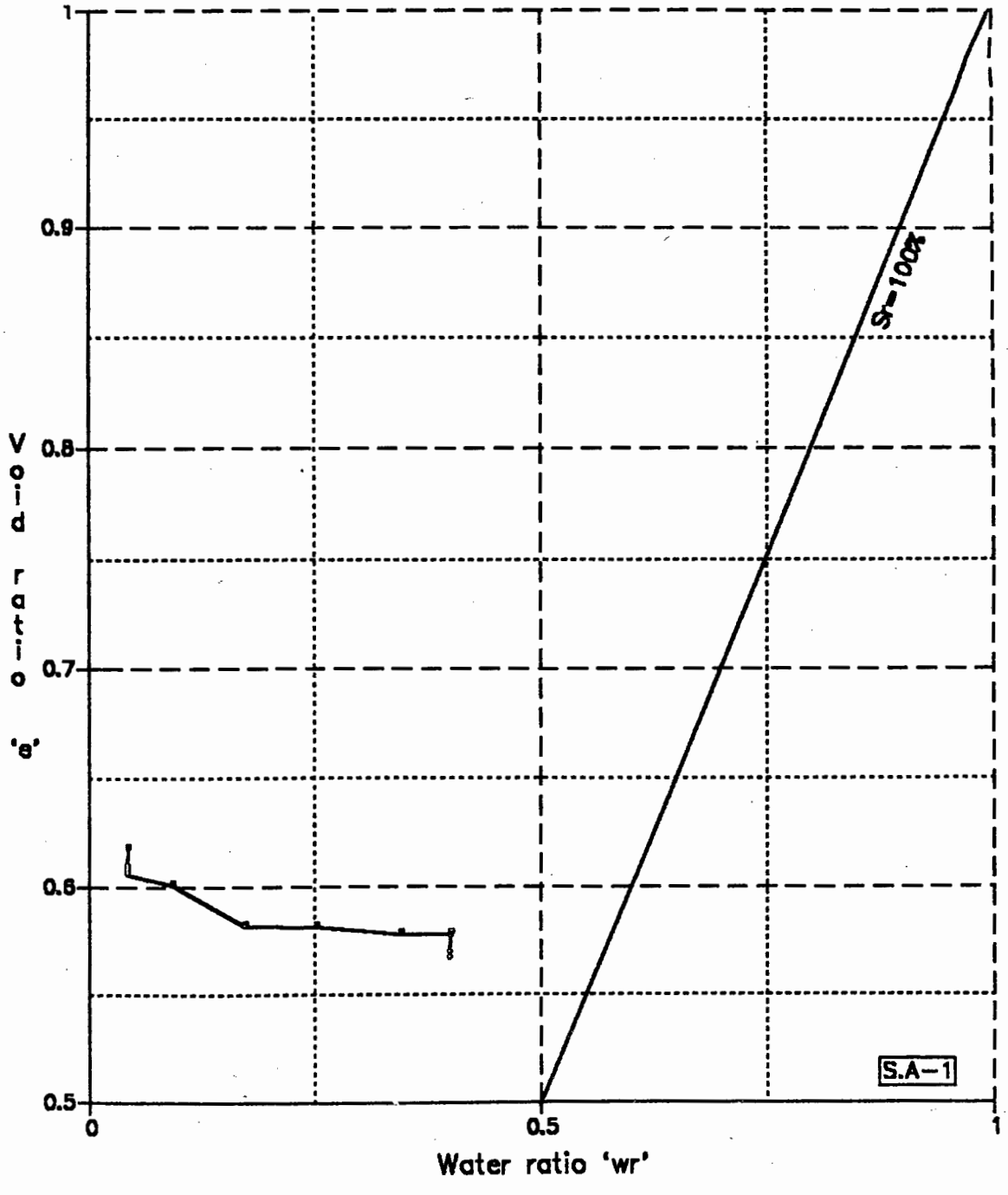

Figure 8.21: Site A, Berea Road (Durban) - [Left overnight at 100 Kpa, then wetted under this pressure] Relationship between the void ratio 'e' and the water ratio 'wr'.

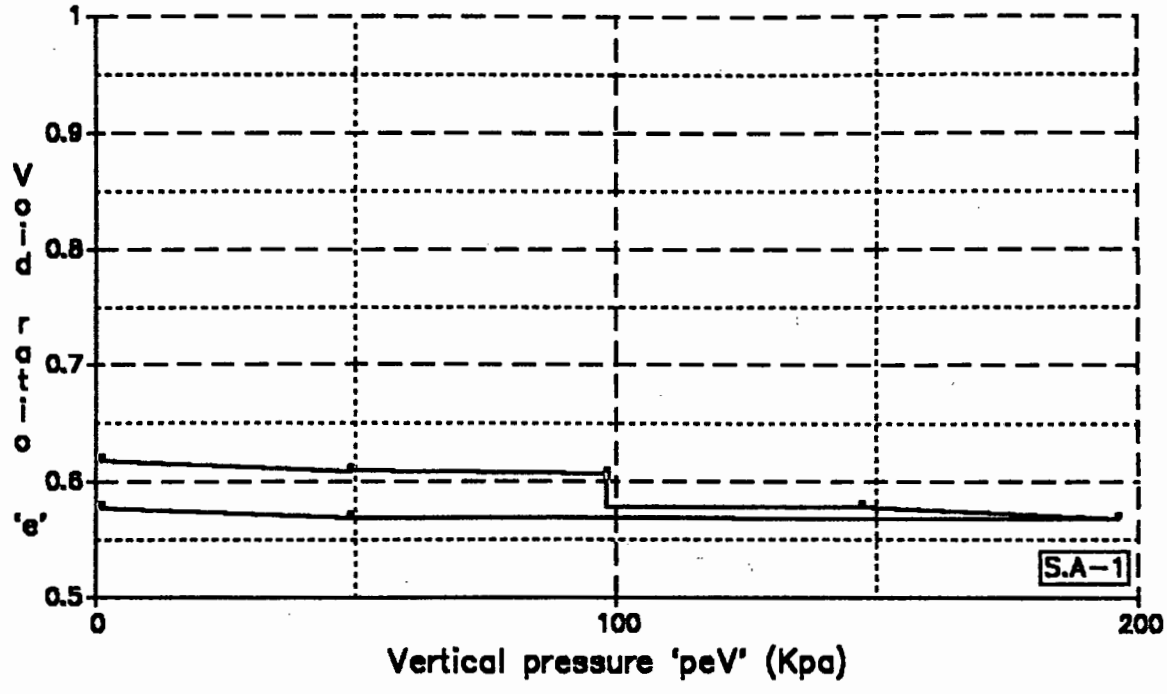

Figure 8.22: Site A, Berea Road (Durban) - [100 Kpa] Relationship between the void ratio 'e' and the effective vertical pressure 'peV'.

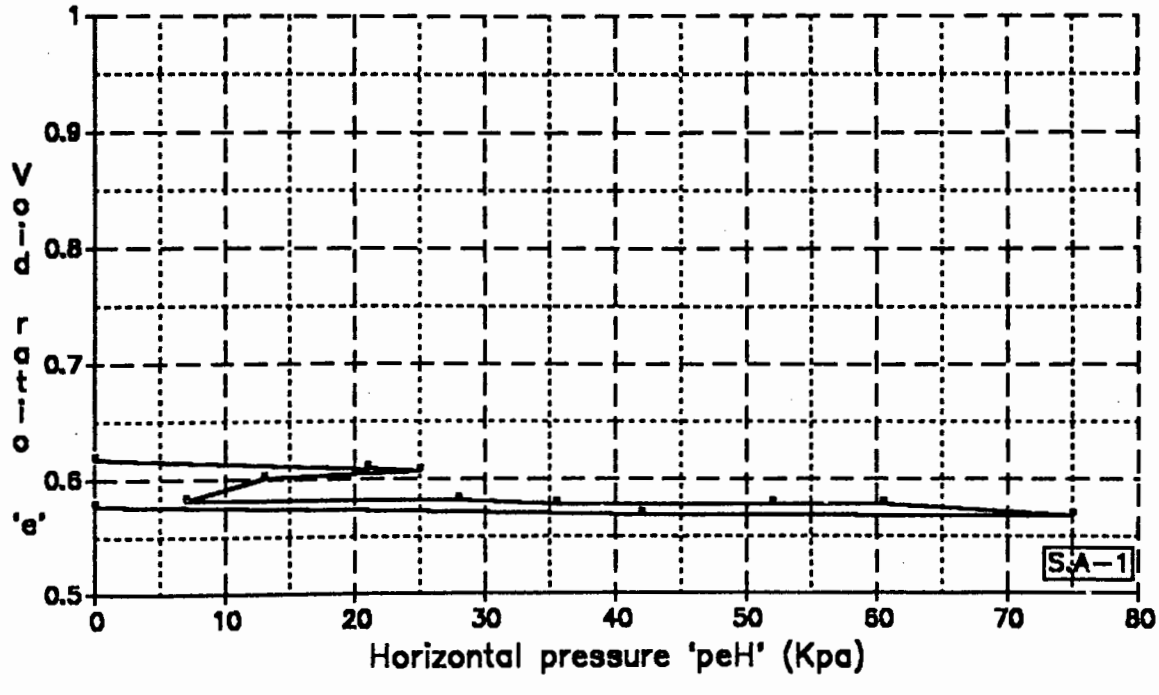

Figure 8.23: Site A, Berea Road (Durban) - [100 Kpa] Relationship between the void ratio 'e' and the effective horizontal pressure 'peH'.

Site 7, Mowbray (Cape).

A fine silty clay, with a small amount of fine to medium sand. The soil consists of 42% clay, 37% silt, and 21% sand size. The 'Limits' are as follows: w_{LS} = 10.5%; w_L = 47.0%; w_P = 22.0%; I_P = 25; w_S = 18.5%; and, w_{FE} = 29.1%.

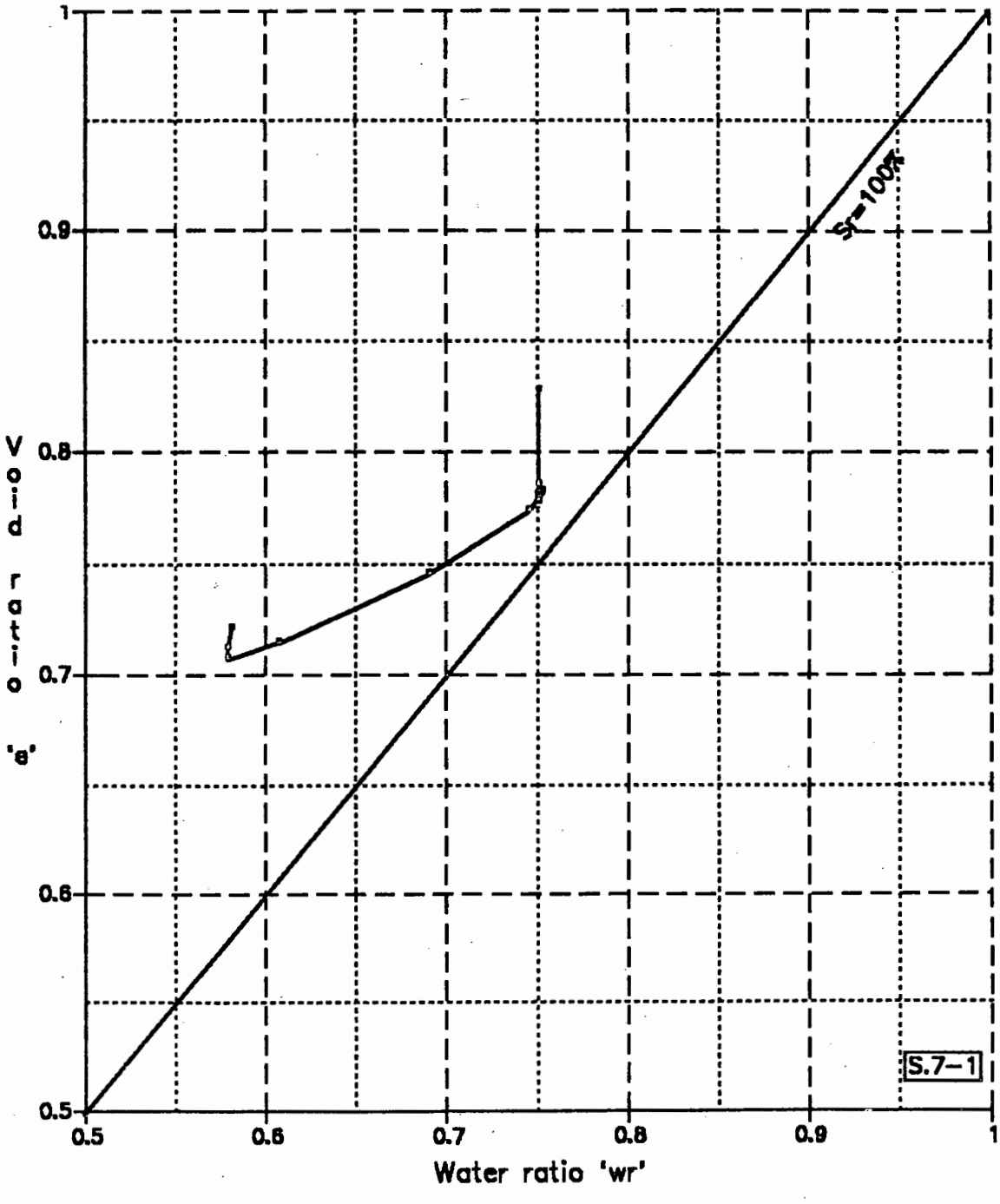

Figure 8.24: Site 7, Mowbray - [Left overnight at 100 Kpa and then wetted under this pressure] Relationship between the void ratio 'e' and the water ratio 'wr'.

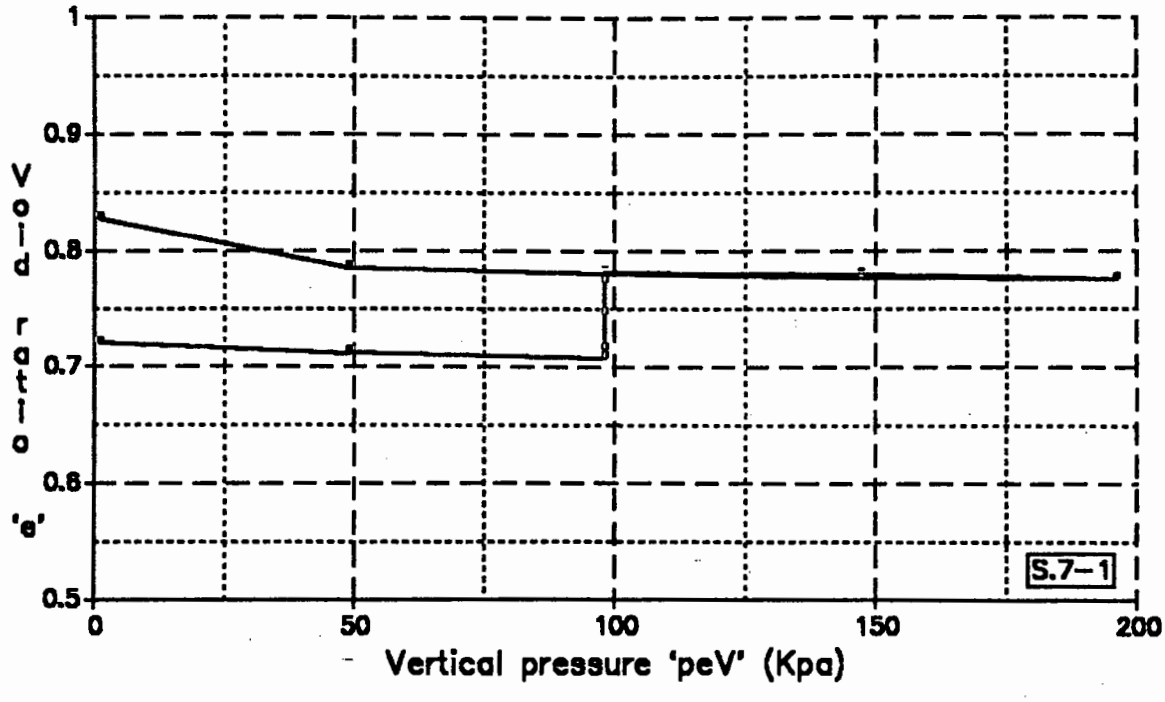

Figure 8.25: Site 7, Mowbray - [100 Kpa] Relationship between the void ratio 'e' and the effective vertical pressure 'peV'.

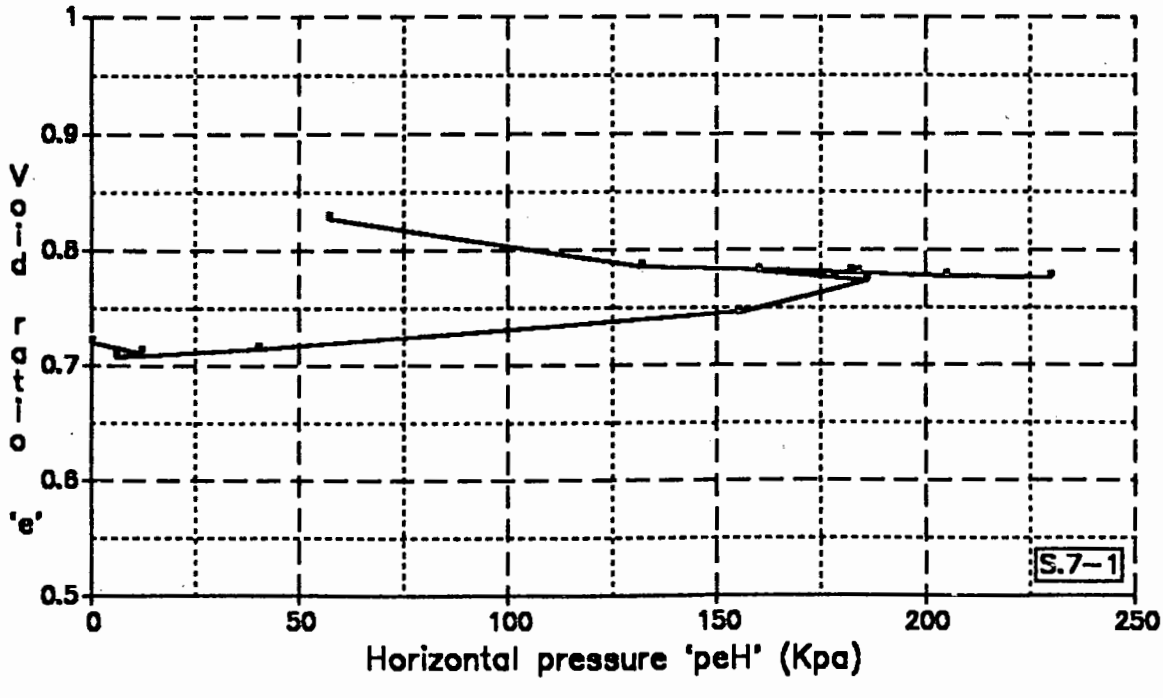

Figure 8.26: Site 7, Mowbray - [100 Kpa] Relationship between the void ratio 'e' and the effective horizontal pressure 'peH'.

Site 48, Lady Grey (Natal).

A clayey silt (medium to coarse), with a small amount of fine sand. The soil consists of 26% clay, 54% silt, and 20% sand size. The 'Limits' are: w_{LS} = 11.5%; w_L = 42.2%; w_P = 19.4%; I_P = 23; w_S = 13.4%; and, w_{FE} = 22.1%.

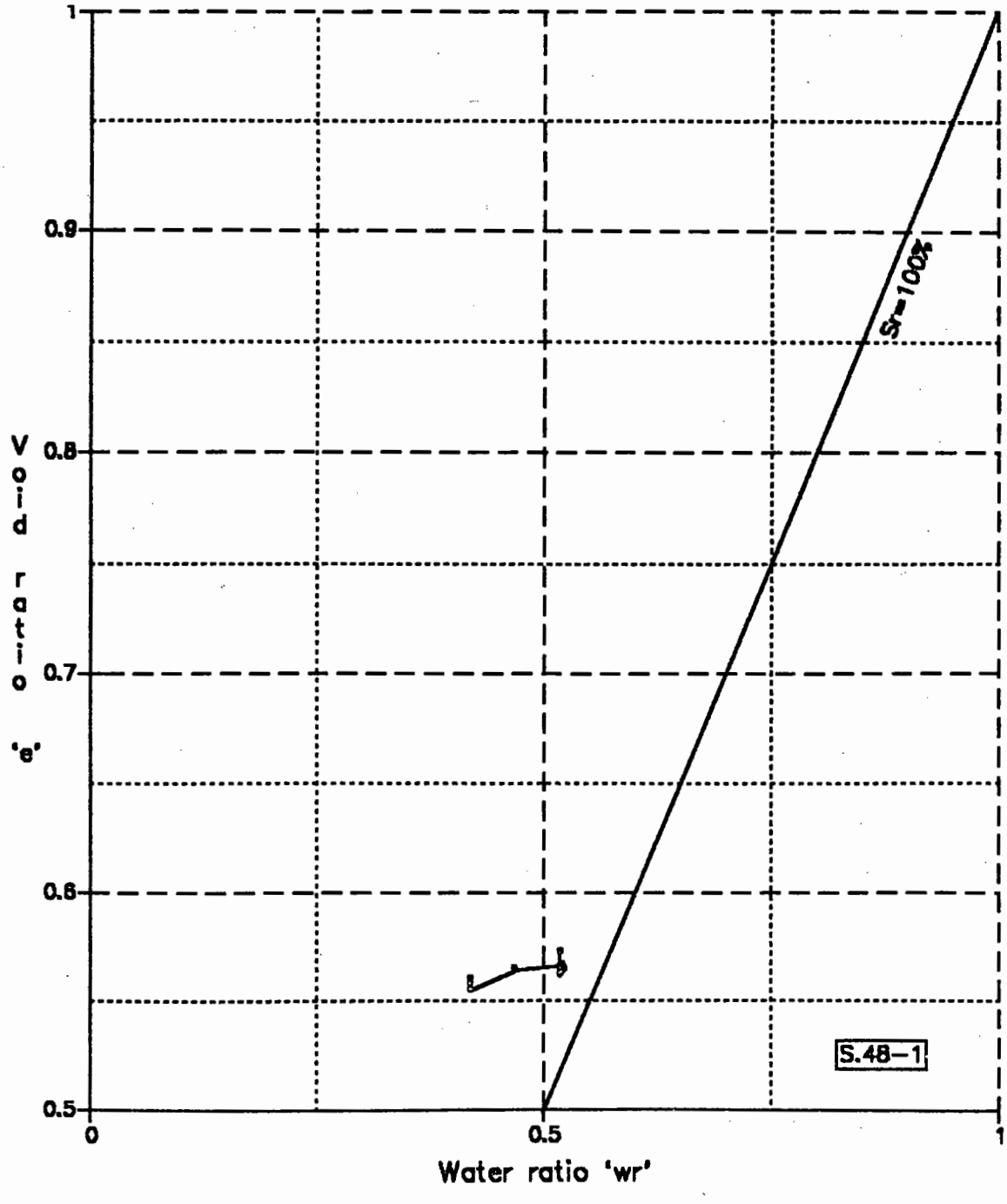

Figure 8.27: Site 48, Lady Grey (Natal) - [Left overnight at 100 Kpa and then wetted under this pressure] Relationship between the void ratio 'e' and the water ratio 'wr'.

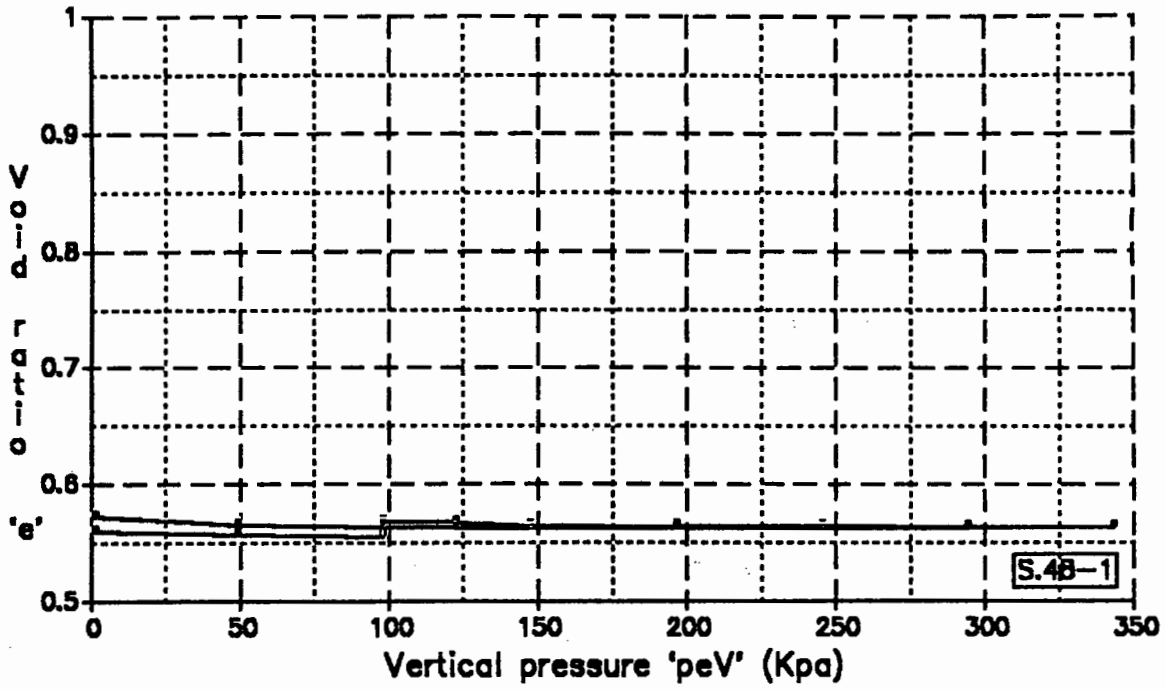

Figure 8.28: Site 48, Lady Grey (Natal) - [100 Kpa] Relationship between the void ratio 'e' and the effective vertical pressure 'peV'.

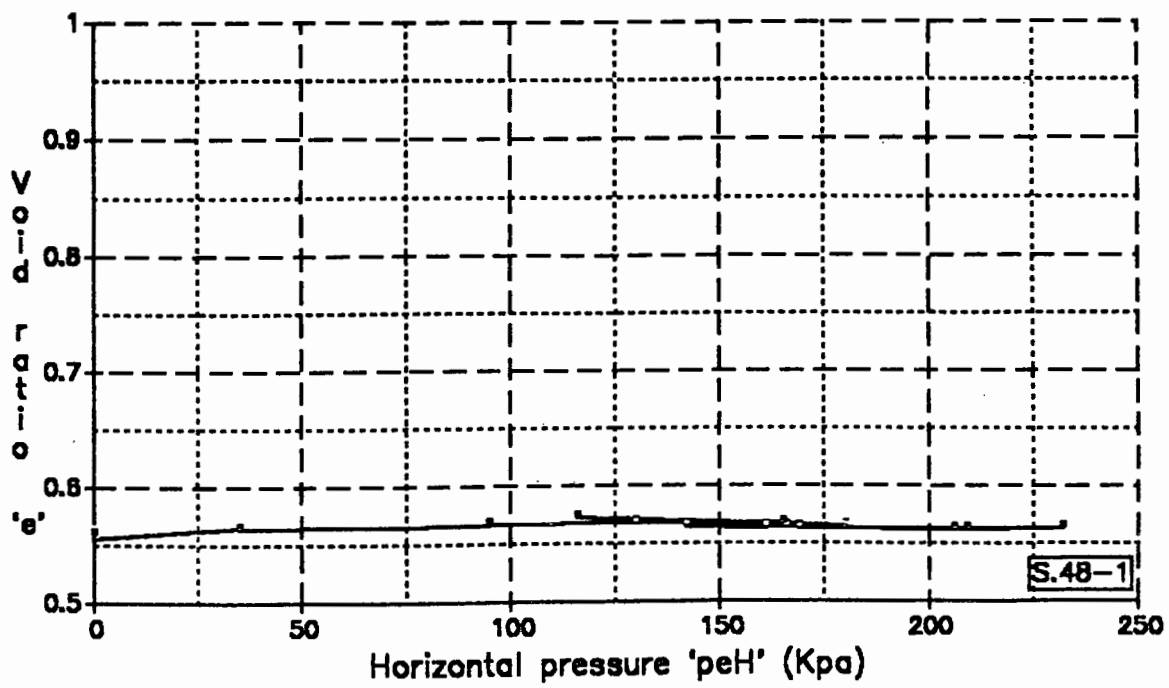

Figure 8.29: Site 48, Lady Grey (Natal) - [100 Kpa] Relationship between the void ratio 'e' and the effective horizontal pressure 'peH'.

8.10 CONCLUSIONS FOR CHAPTER EIGHT

The relationships between the parameters measured, were analysed in five parts. Plots for these relationships provide an effective means of highlighting the relationships between the various parameters.

Plots are included for the following relationships:-

1) The Stress scales previously obtained[1] are superimposed on the plot of void ratio versus water ratio;

2) The void ratio and the effective vertical pressure, or stress, applied to the sample;

3) The void ratio, the effective vertical pressure, and the water ratio;

4) The void ratio, the effective horizontal stress, and the water ratio; and,

5) The void ratio, the effective average pressure, or stress, and the water ratio.

These relationships are illustrated in Figures 8.30 to 8.59, as follows:-

Figures 8.30 to 8.34: Void Ratio versus Water Ratio - includes the stress scales obtained in Chapter Five;

Figures 8.35 to 8.39: Void Ratio versus Effective Vertical Pressure;

Figures 8.40 to 8.44: Void Ratio versus Effective Vertical Pressure, or Stress, versus Water Ratio (three dimensional plot);

Figures 8.45 to 8.49: Void Ratio versus Effective Horizontal Stress, versus Water Ratio (3 dimensional plot);

Figures 8.50 to 8.54: Void Ratio versus Effective Average Pressure, or Stress, versus Water Ratio (3-D plot).

Additional plots are discussed in Chapter Ten of the thesis[2]. These plots are for the following parameters: (i) Vertical Pressure versus Horizontal Pressure; and, (ii) Stress Paths obtained by the vertical and horizontal stresses - that is, the 'p' (vertical stress plus horizontal stress divided by 2) and 'q' (vertical stress minus horizontal stress divided by 2) diagrams.

---

[1] - refer to chapter five.
[2] - section 10.3.6 "Axisymmetric Stress Behaviour".

8.10.1 Stress Scales - Void Ratio versus Water Ratio.

Site 11, Rosebank.

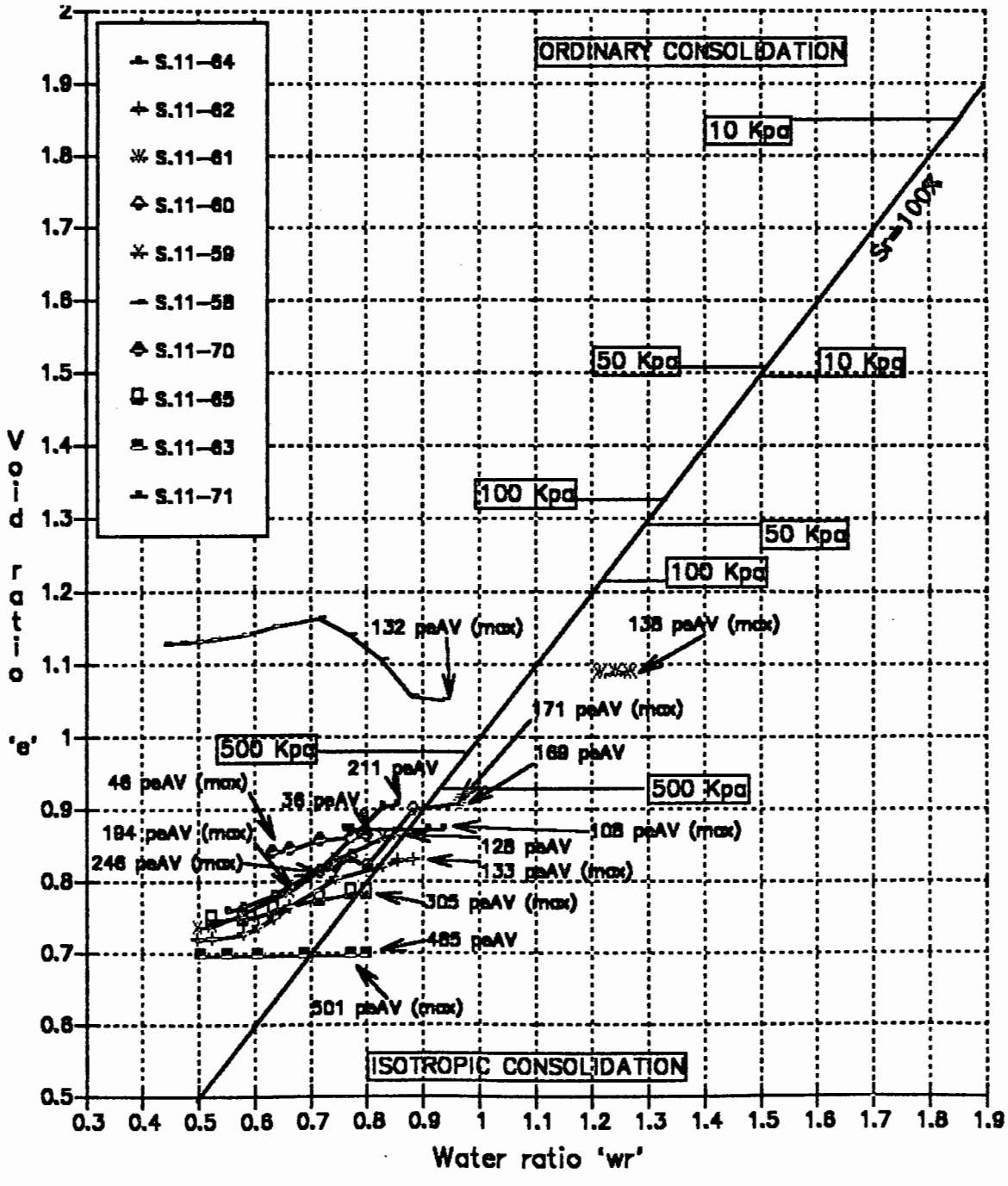

Figure 8.30: Site 11, Rosebank - [50 Kpa; 100 Kpa; 400 Kpa; Swell Pressure] Void ratio 'e' versus water ratio 'wr'[1]. The average pressures shown are the average of the vertical pressure and two equal horizontal pressures which are measured.

---

[1] - *observed values are in Appendix G.*

Site 36, Rondebosch.

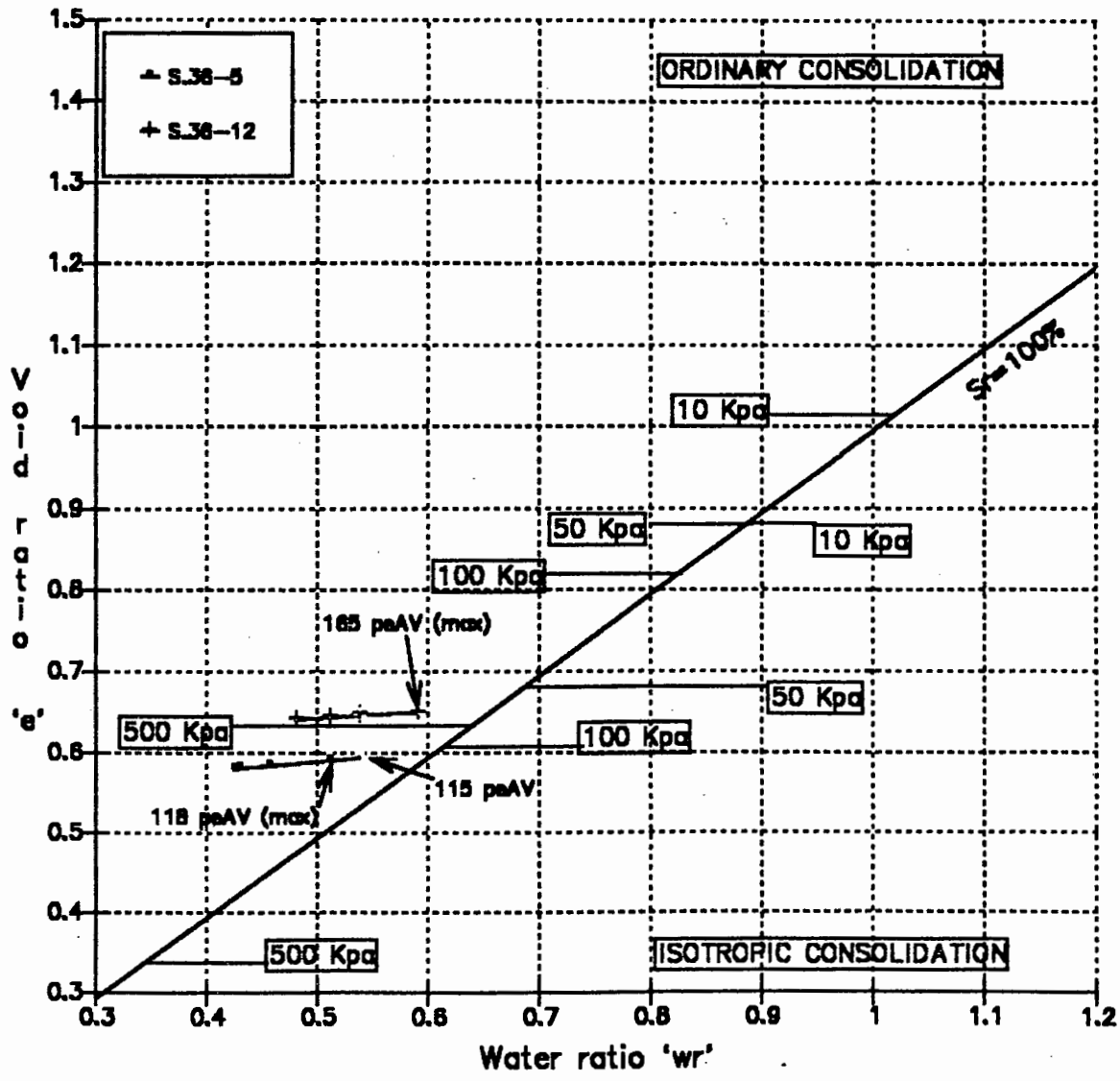

Figure 8.31: Site 36, Rondebosch - [Settled overnight under 100 Kpa and then wetted while carrying this pressure] Void ratio 'e' versus water ratio 'wr'[1]. The average pressures shown are the average of the vertical pressure and two equal horizontal pressures which are measured.

---

[1] - *observed values are in Appendix G.*

Site A, Berea Road (Durban).

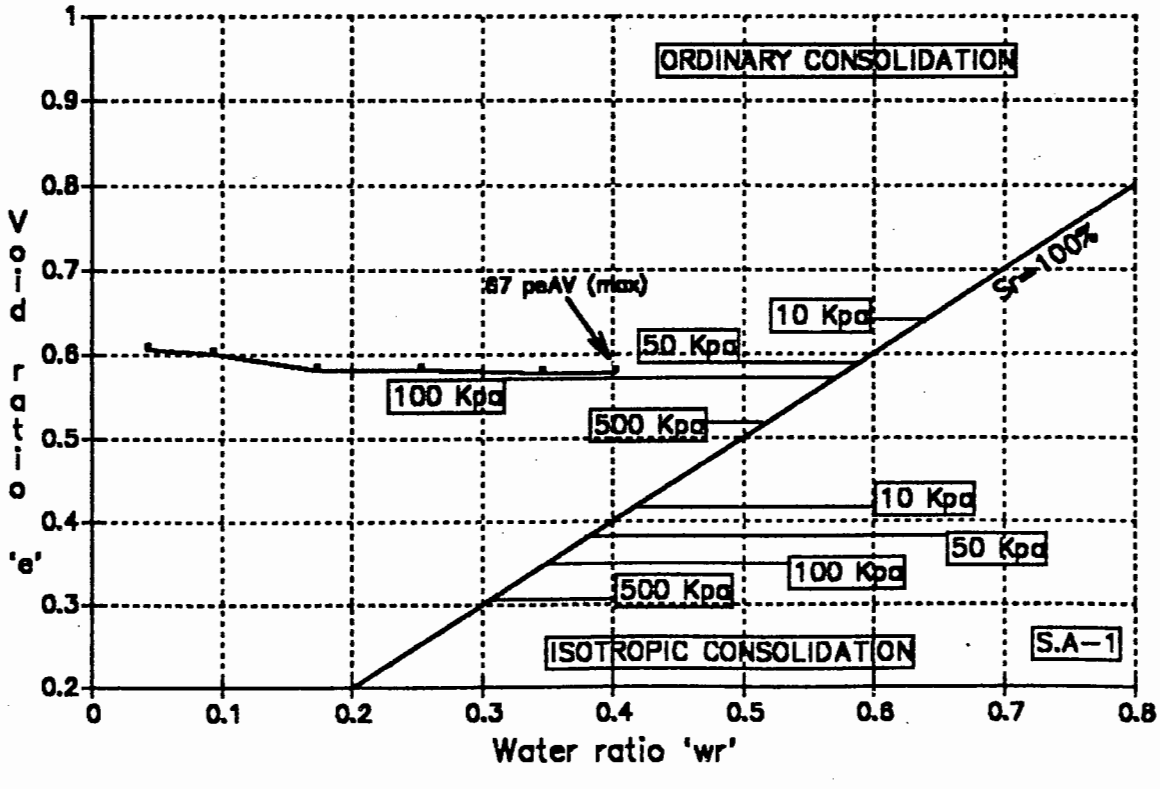

Figure 8.32: Site A, Berea Road (Durban) - [Settled overnight under 100 Kpa then wetted under this load] Void ratio 'e' versus water ratio 'wr'[1]. The average pressures shown are the average of the vertical pressure and two equal horizontal pressures which are measured.

---

[1] - *observed values are in Appendix G.*

Site 7, Mowbray.

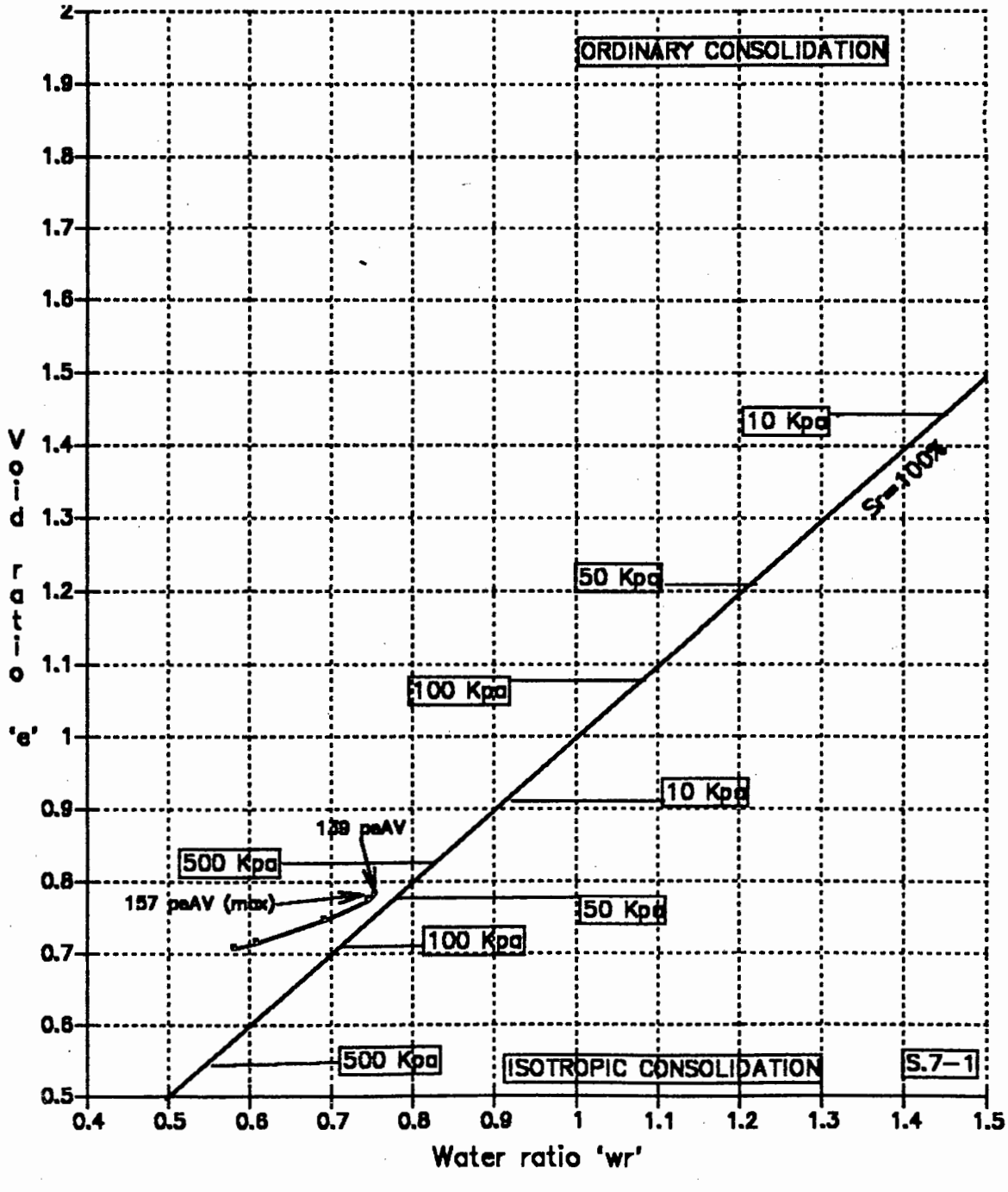

Figure 8.33: Site 7, Mowbray - [Settled overnight under 100 Kpa then wetted under this load] Void ratio 'e' versus water ratio 'wr'[1]. The average pressures shown are the average of the vertical pressure and two equal horizontal pressures which are measured.

---

[1] - *observed values are in Appendix G.*

Site 48, Lady Grey.

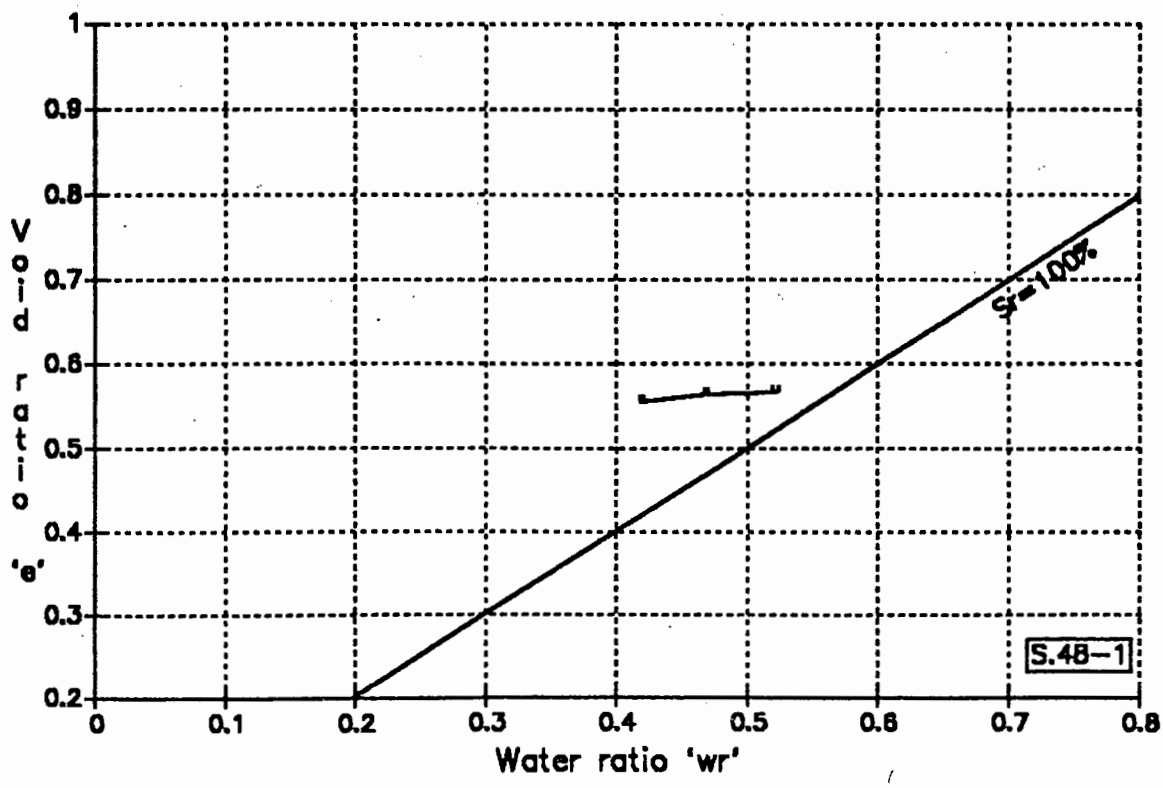

Figure 8.34: Site 48, Lady Grey (Natal) - [Settled overnight under 100 Kpa then wetted under this load] Void ratio 'e' versus water ratio 'wr'[1].
The average pressures shown are the average of the vertical pressure and two equal horizontal pressures which are measured. Test by Ballantyne - Ref. 20.

---

[1] - *observed values are in Appendix G.*

8.10.2 Void Ratio versus Effective Vertical Pressure. Site 11, Rosebank.

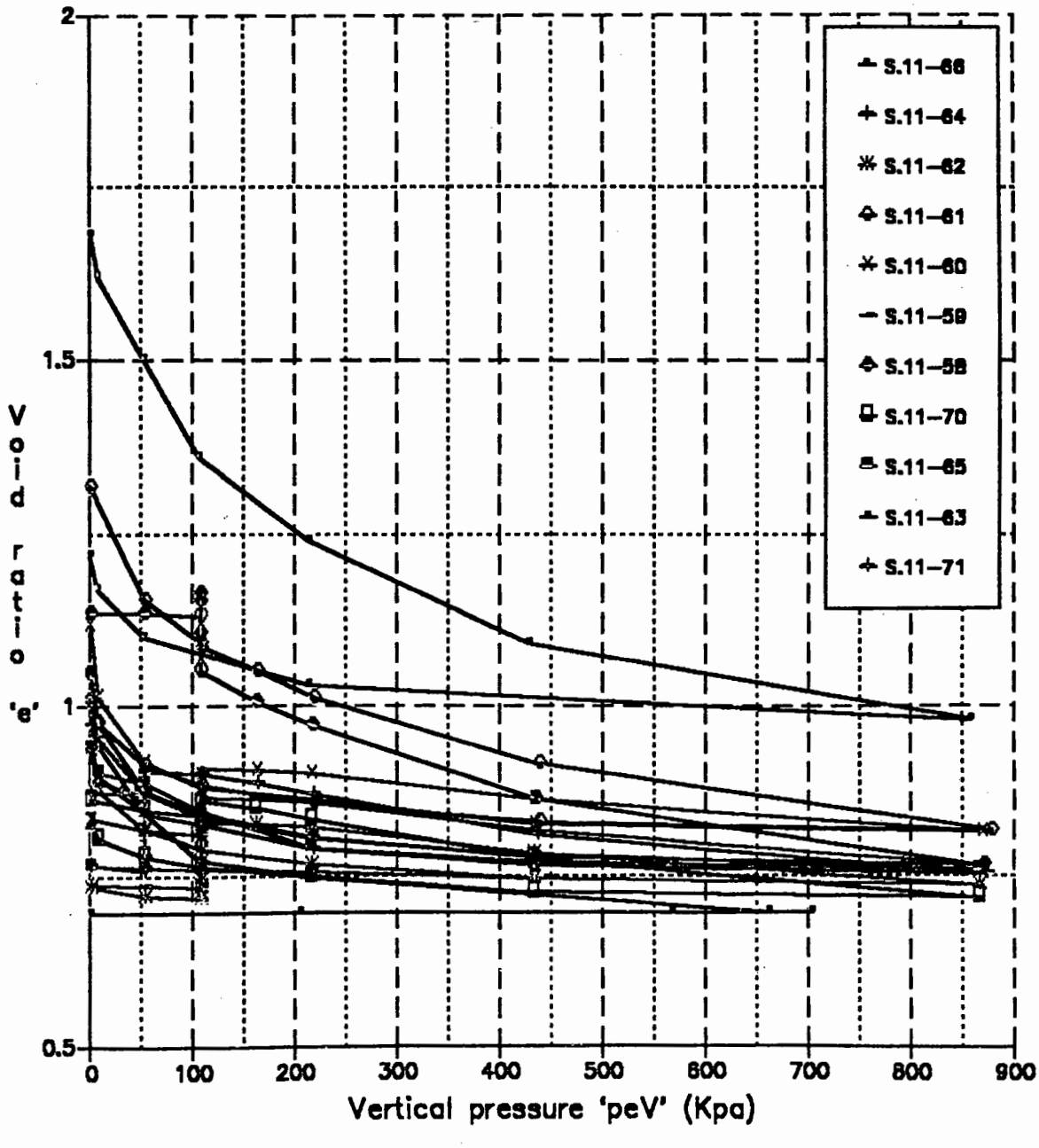

Figure 8.35: Site 11, Rosebank - [One-dimensional; 50 Kpa; 100 Kpa; 400 Kpa; Swell Pressure]. Void ratio 'e' versus effective vertical pressure 'peV'[1].

[1] - *observed values are in Appendix G.*

Site 36, Rondebosch.

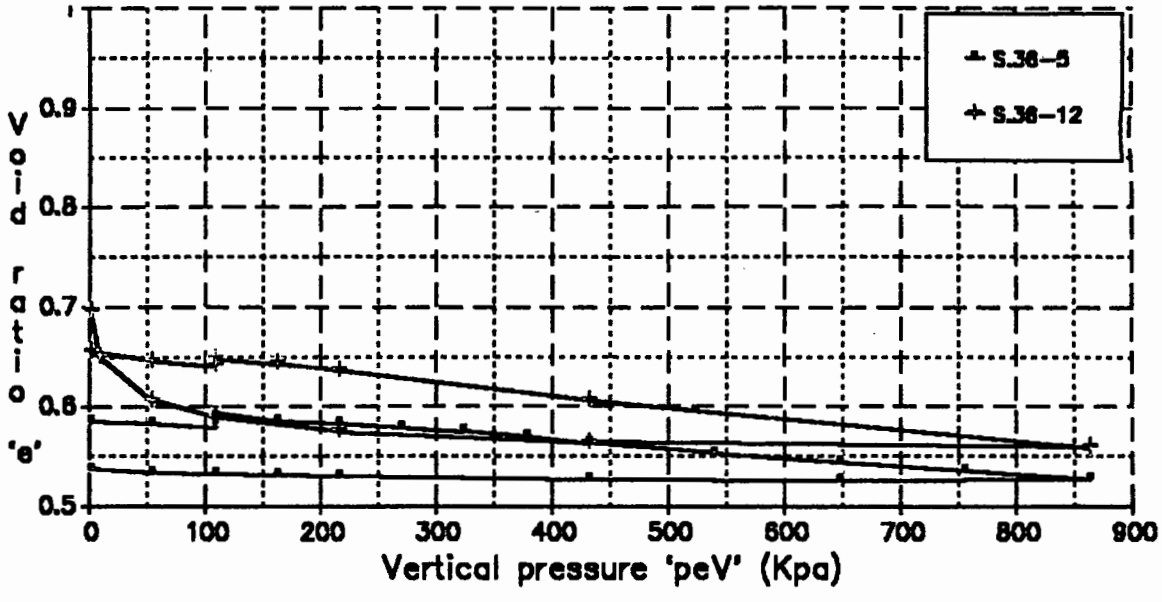

Figure 8.36: Site 36, Rondebosch - [100 Kpa] Void ratio 'e' versus effective vertical pressure 'peV'[1].

Site A, Berea Road (Durban).

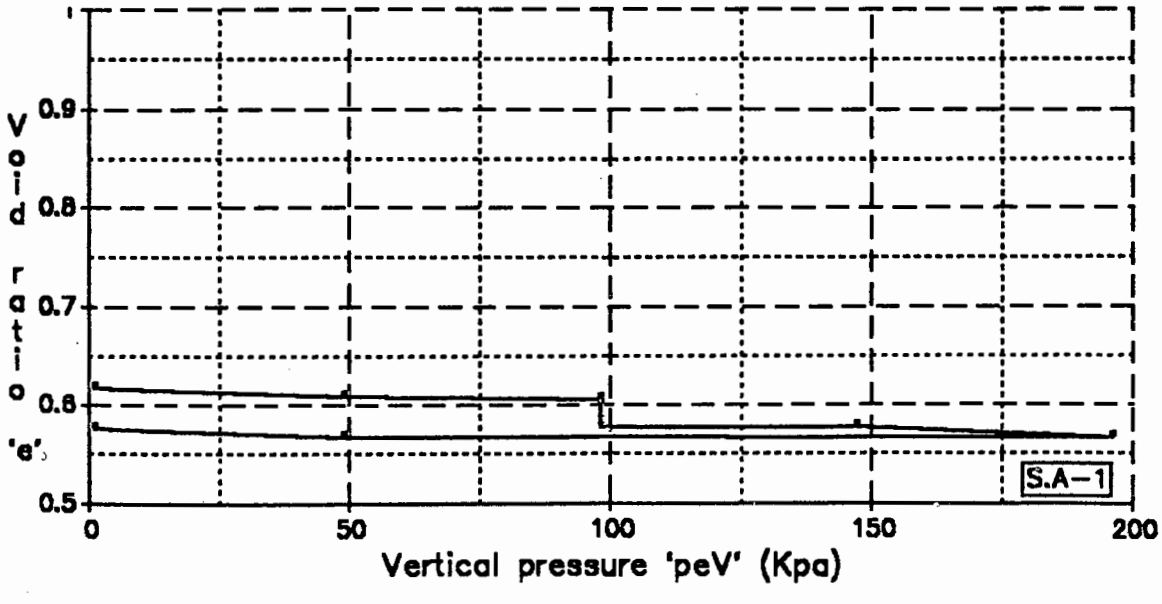

Figure 8.37: Site A, Berea Road (Durban) - [100 Kpa] Void ratio 'e' versus effective vertical pressure 'peV'[1].

---

[1] - *observed values are in Appendix G.*

Site 7, Mowbray.

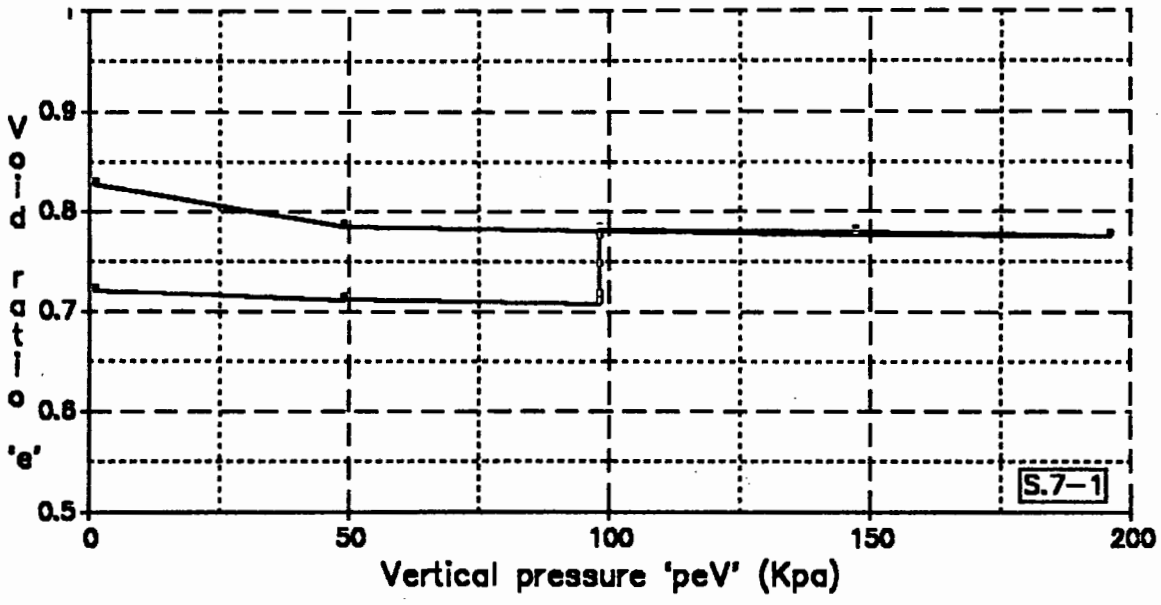

Figure 8.38: Site 7, Mowbray - [100 Kpa] Void ratio 'e' versus effective vertical pressure 'peV'[1].

Site 48, Lady Grey.

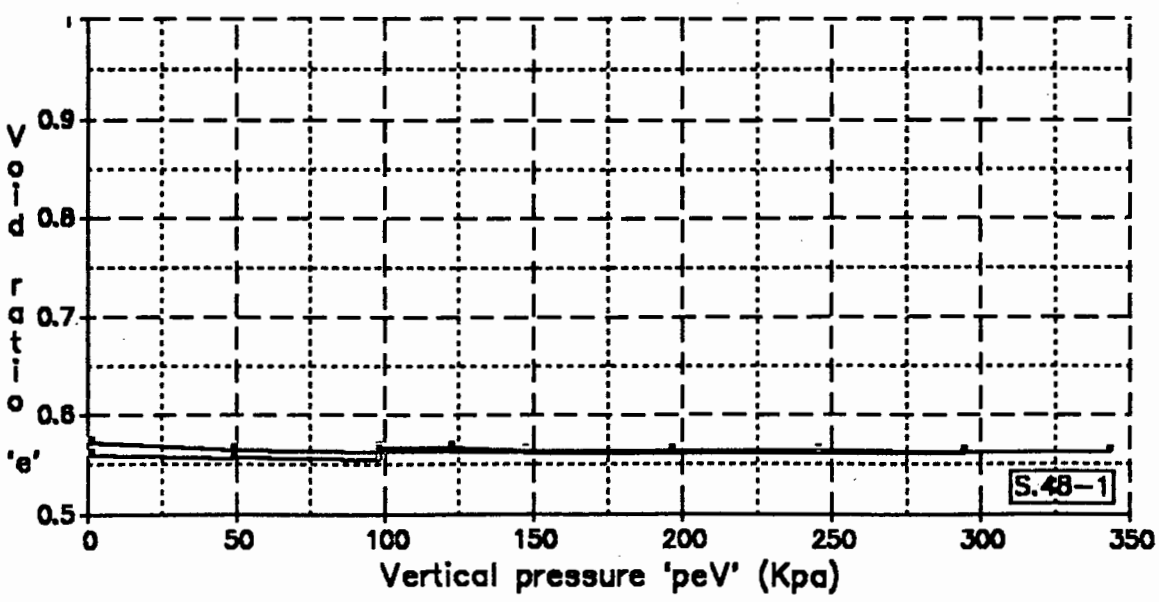

Figure 8.39: Site 48, Lady Grey (Natal) - [100 Kpa] Void ratio 'e' versus effective vertical pressure 'peV'[1].

---

[1] - *observed values are in Appendix G.*

8.10.3 Void Ratio vs Effective Vertical Pressure vs Water Ratio.

Site 11, Rosebank.

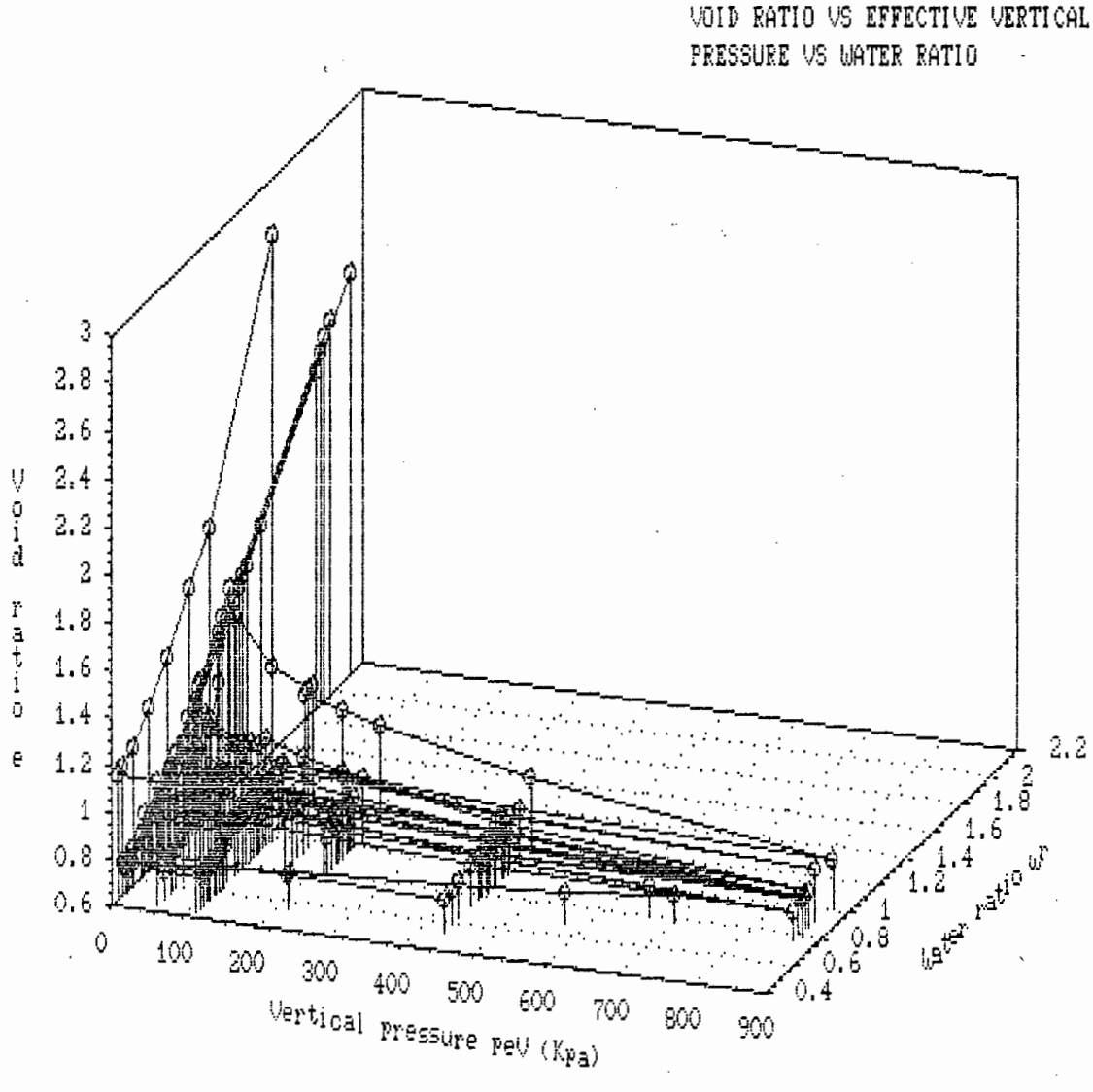

Figure 8.40: Site 11, Rosebank - [50 Kpa; 100 Kpa; 400 Kpa; Swell Pressure] Void ratio 'e' versus effective vertical pressure 'peV' versus water ratio 'wr'.

Site 36, Rondebosch.

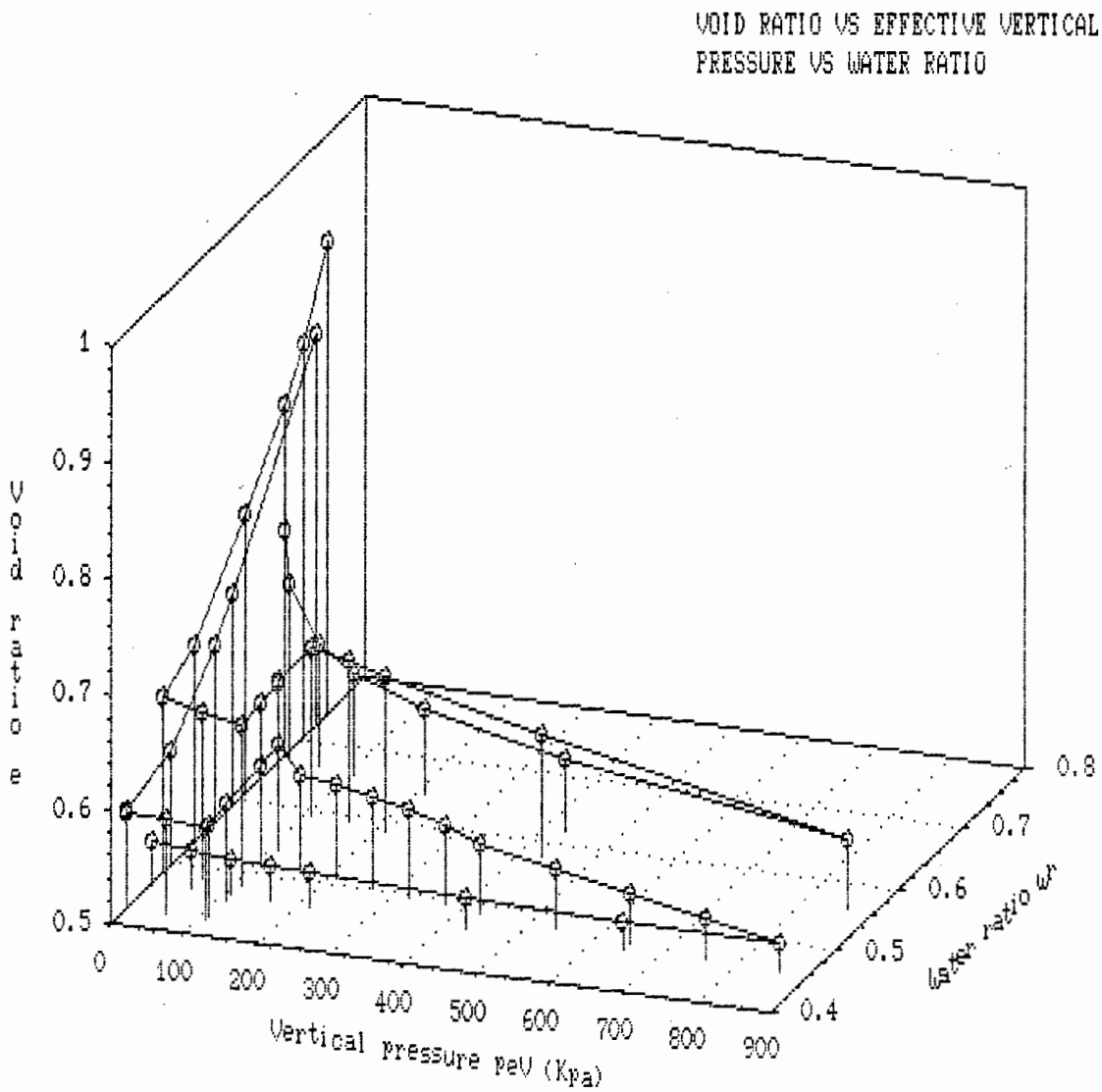

Figure 8.41: Site 36, Rondebosch - [100 Kpa] Void ratio 'e' versus effective vertical pressure 'peV' versus water ratio 'wr'.

Site A, Berea Road (Durban).

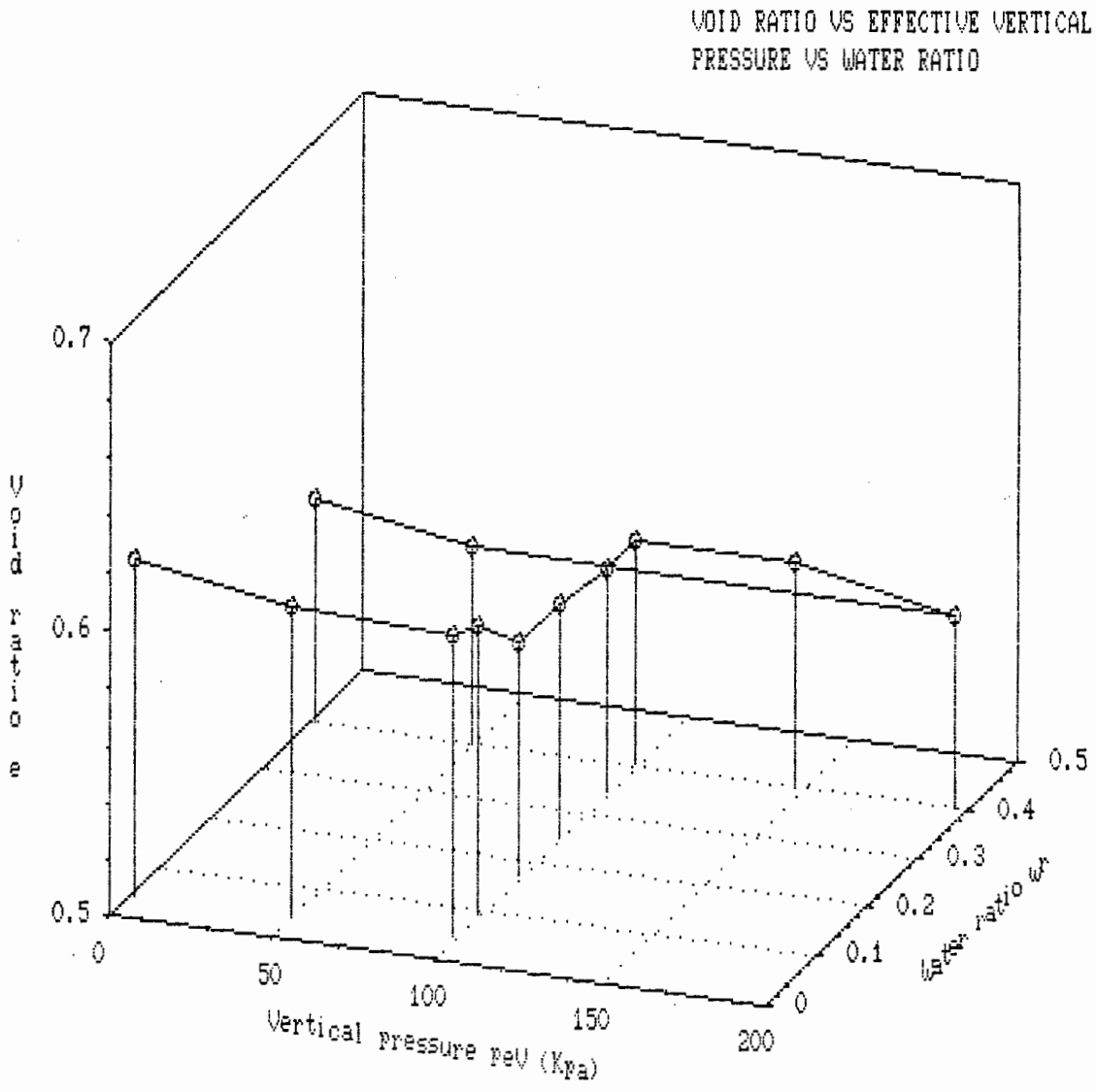

Figure 8.42: Site A, Berea Road (Durban) - [100 Kpa] Void ratio 'e' versus effective vertical pressure 'peV' versus water ratio 'wr'.

Site 7, Mowbray.

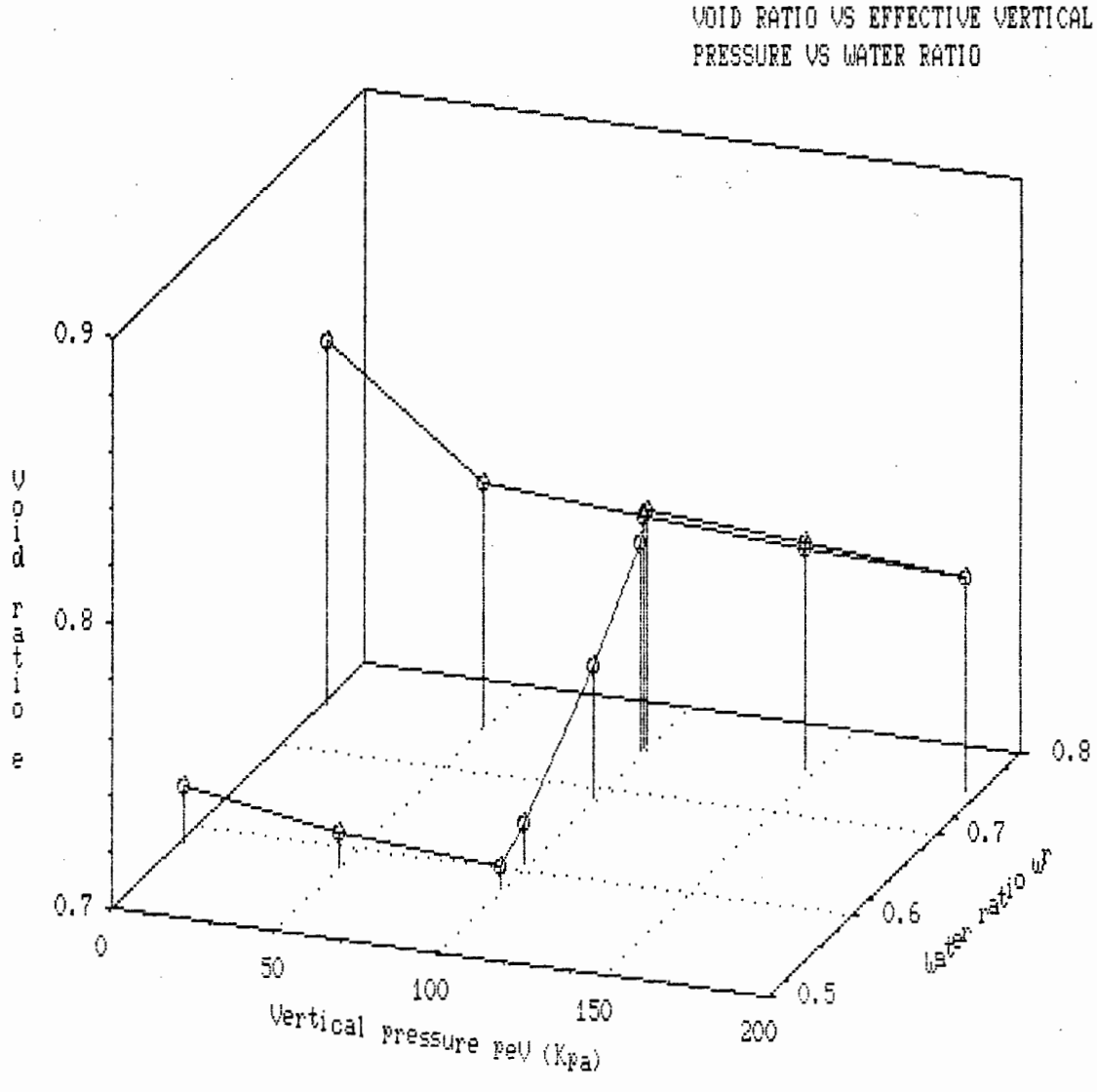

Figure 8.43: Site 7, Mowbray - [100 Kpa] Void ratio 'e' versus effective vertical pressure 'peV' versus water ratio 'wr'.

Site 48, Lady Grey.

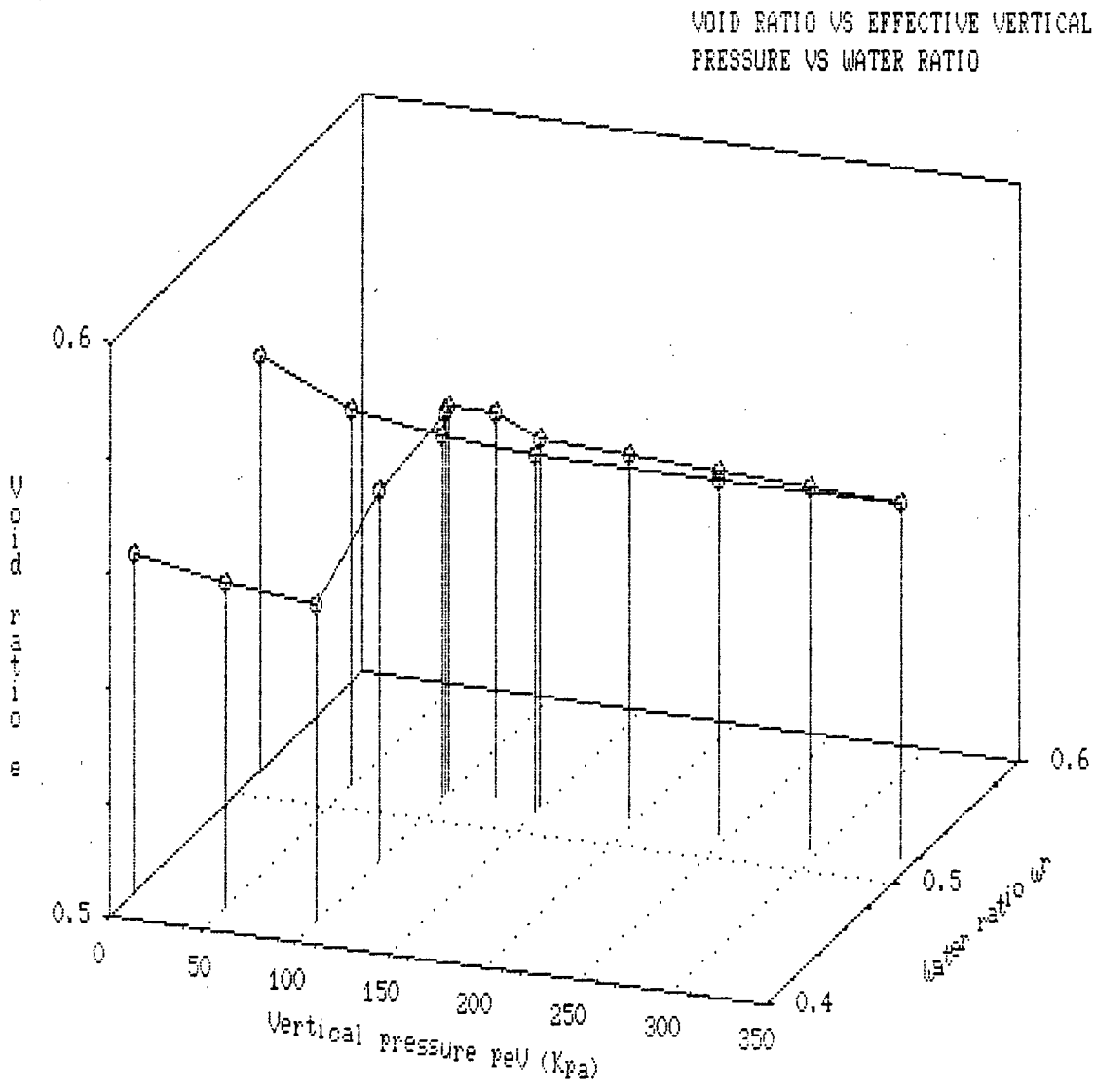

Figure 8.44: Site 48, Lady Grey (Natal) - [100 Kpa] Void ratio 'e' versus effective vertical pressure 'peV' versus water ratio 'wr'.

8.10.4 Void Ratio vs Effective Horizontal Stress vs Water Ratio.

Site 11, Rosebank.

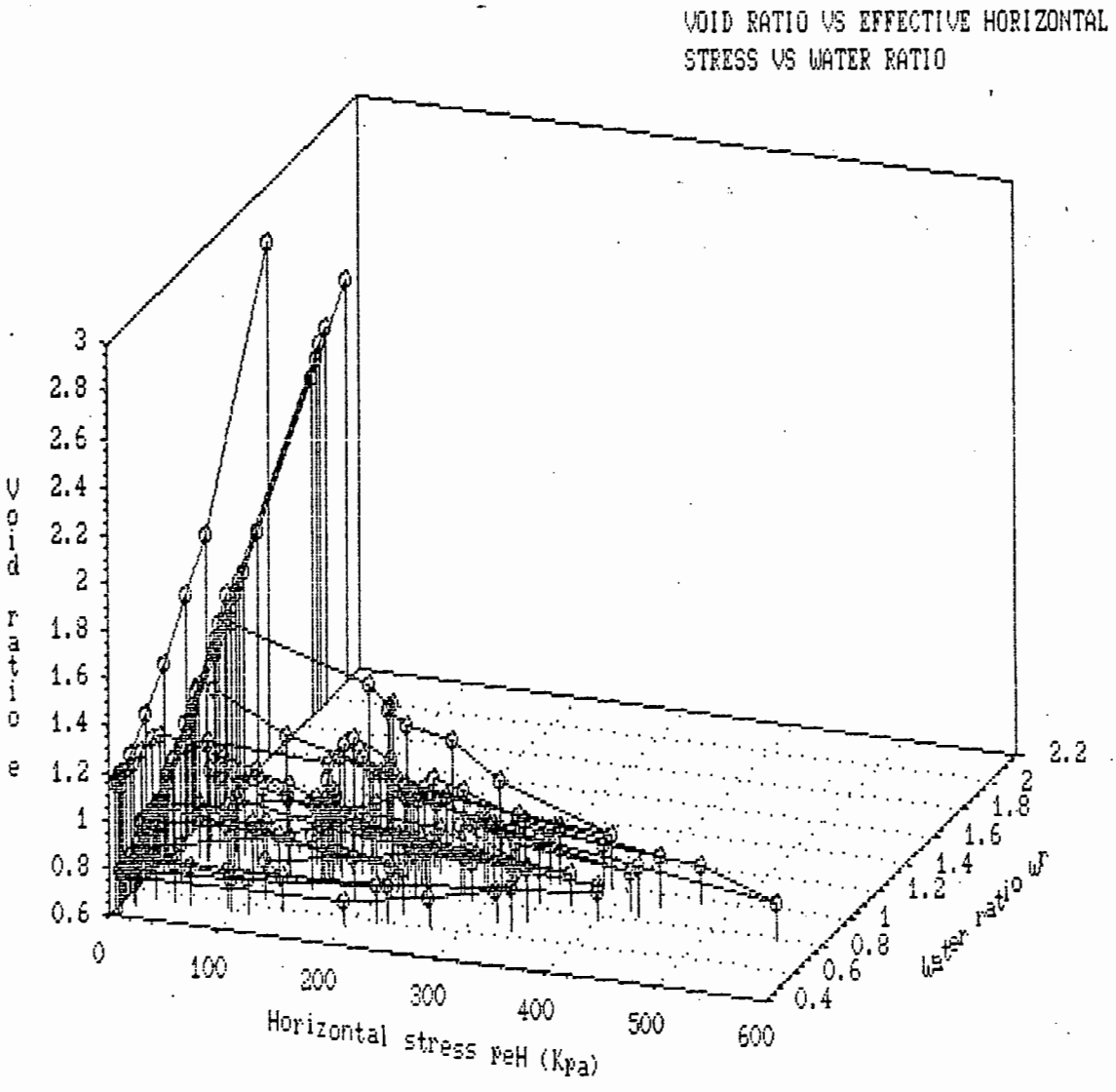

Figure 8.45: Site 11, Rosebank - [50 Kpa; 100 Kpa; 400 Kpa; Swell Pressure] Void ratio 'e' versus effective horizontal stress 'peH' versus water ratio 'wr'.

Site 36, Rondebosch.

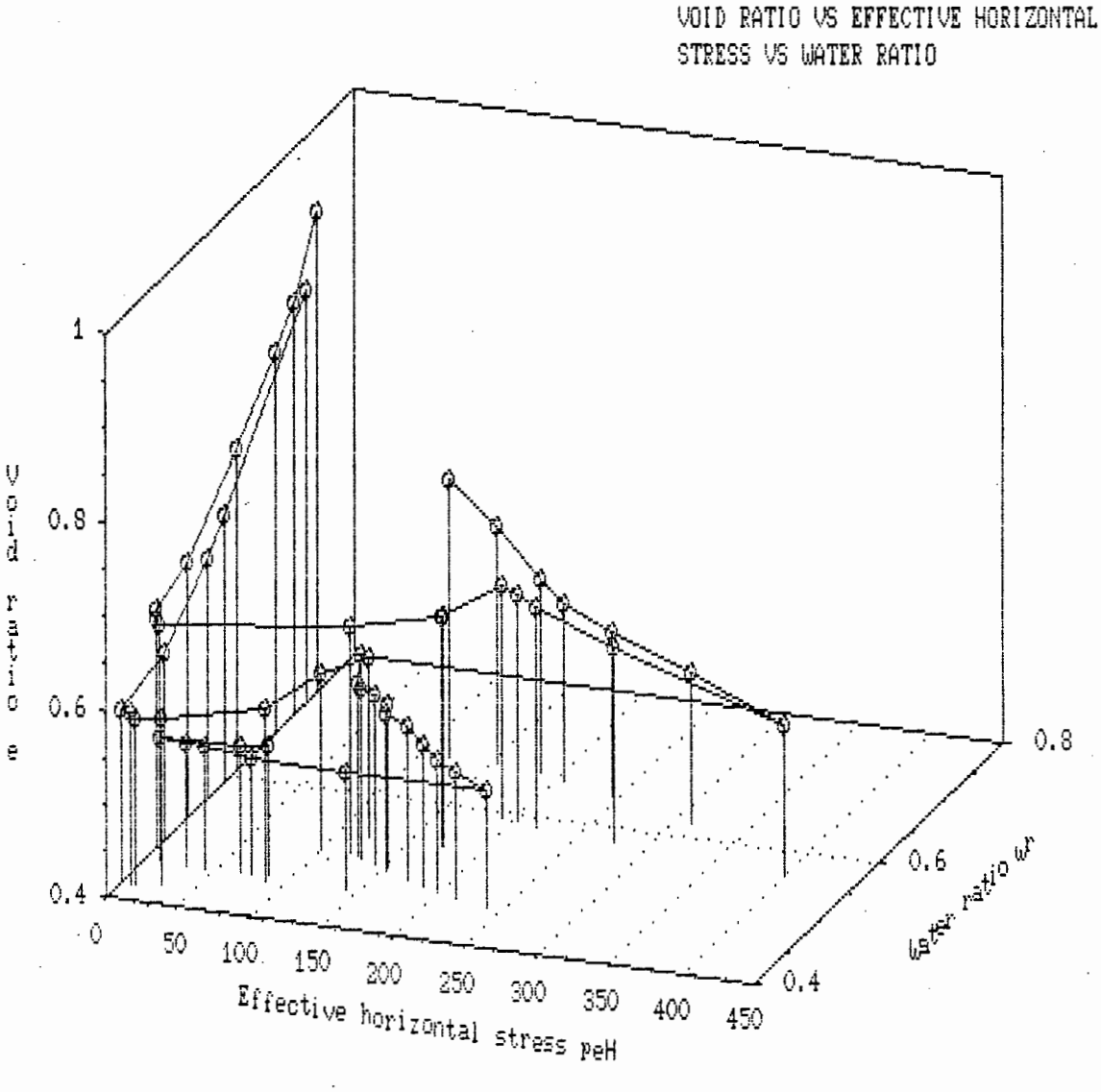

Figure 8.46: Site 36, Rondebosch - [100 Kpa] Void ratio 'e' versus effective horizontal stress 'peH' versus water ratio 'wr'.

Site A, Berea Road (Durban).

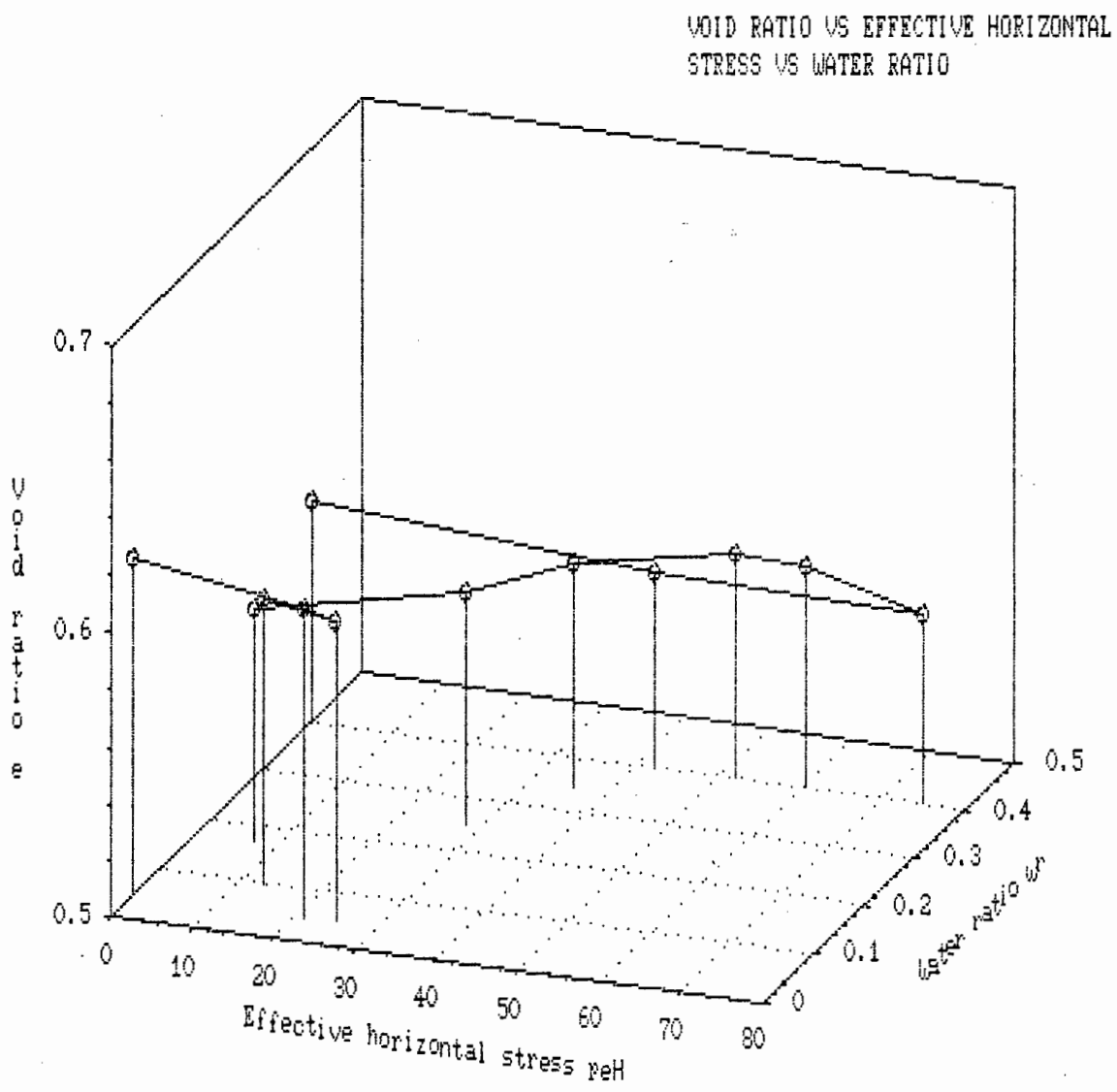

Figure 8.47: Site A, Berea Road (Durban) - [100 Kpa] Void ratio 'e' versus effective horizontal stress 'peH' versus water ratio 'wr'.

Site 7, Mowbray.

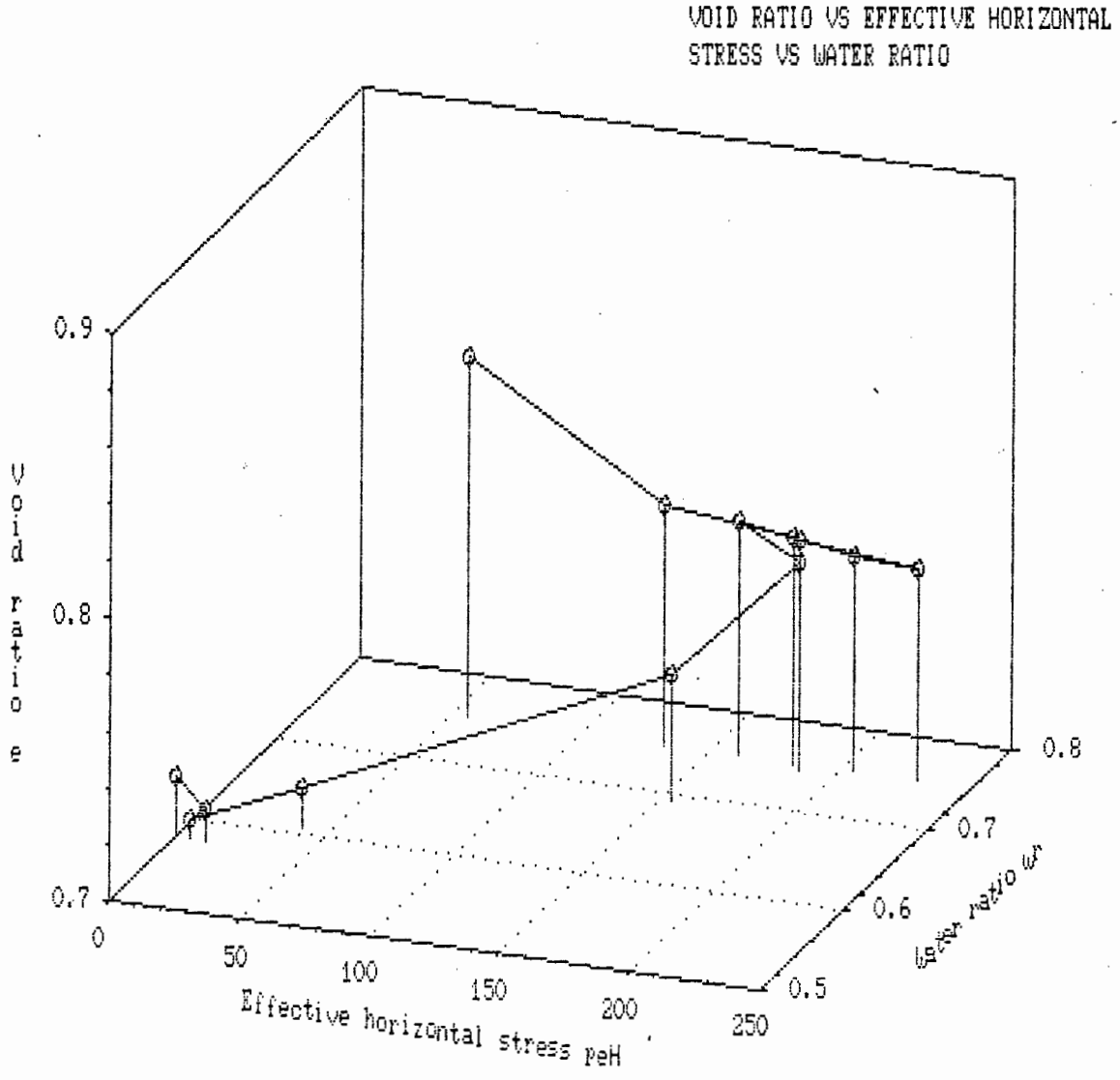

Figure 8.48: Site 7, Mowbray - [100 Kpa] Void ratio 'e' versus effective horizontal stress 'peH' versus water ratio 'wr'.

Site 48, Lady Grey.

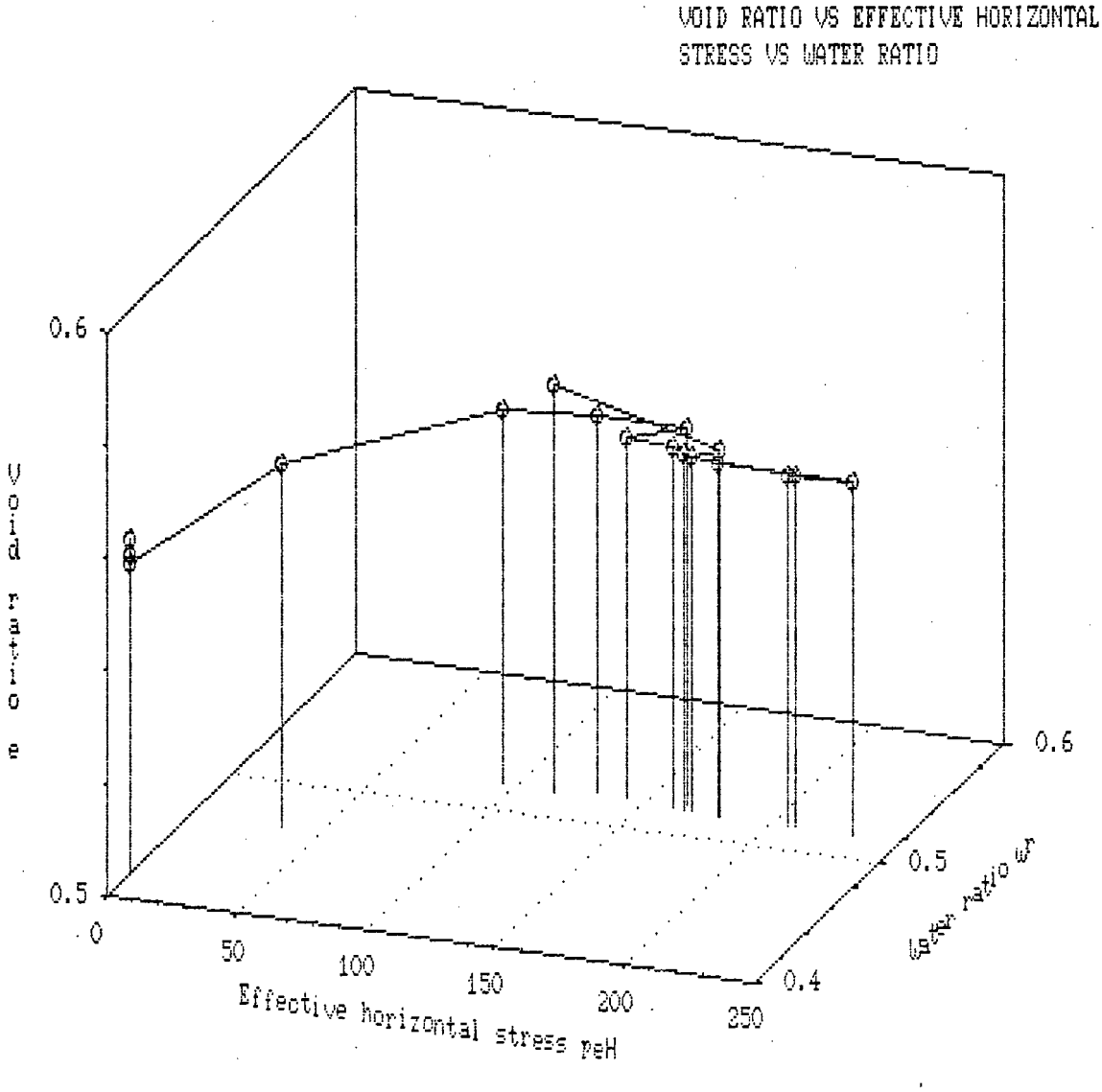

Figure 8.49: Site 48, Lady Grey (Natal) - [100 Kpa] Void ratio 'e' versus effective horizontal stress 'peH' versus water ratio 'wr'.

8.10.5 Void Ratio vs Effective Average Stress vs Water Ratio.

Site 11, Rosebank.

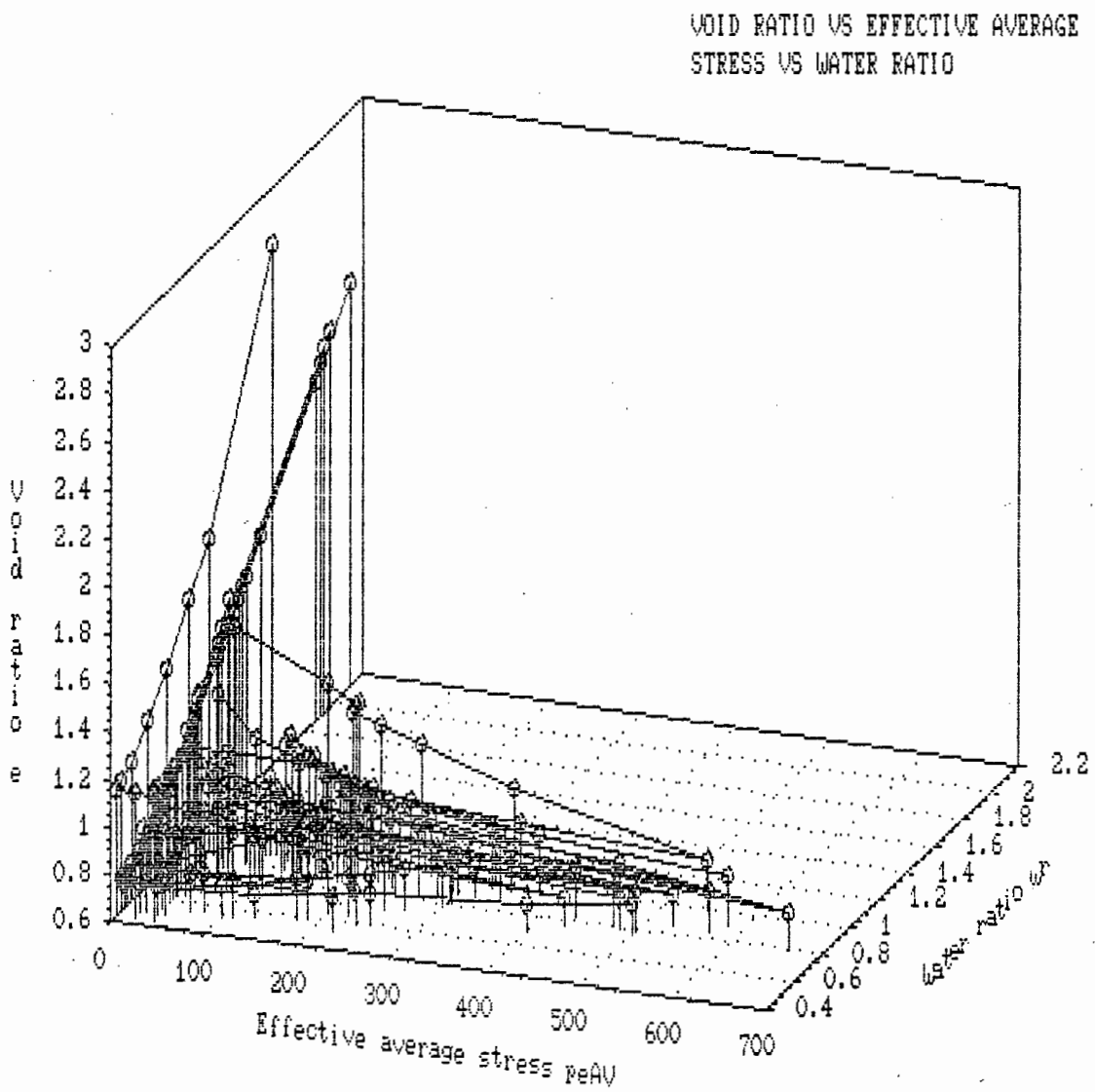

Figure 8.50: Site 11, Rosebank - [50 Kpa; 100 Kpa; 400 Kpa; Swell Pressure] Void ratio 'e' versus effective average stress 'peAV' versus water ratio 'wr'.

Site 36, Rondebosch.

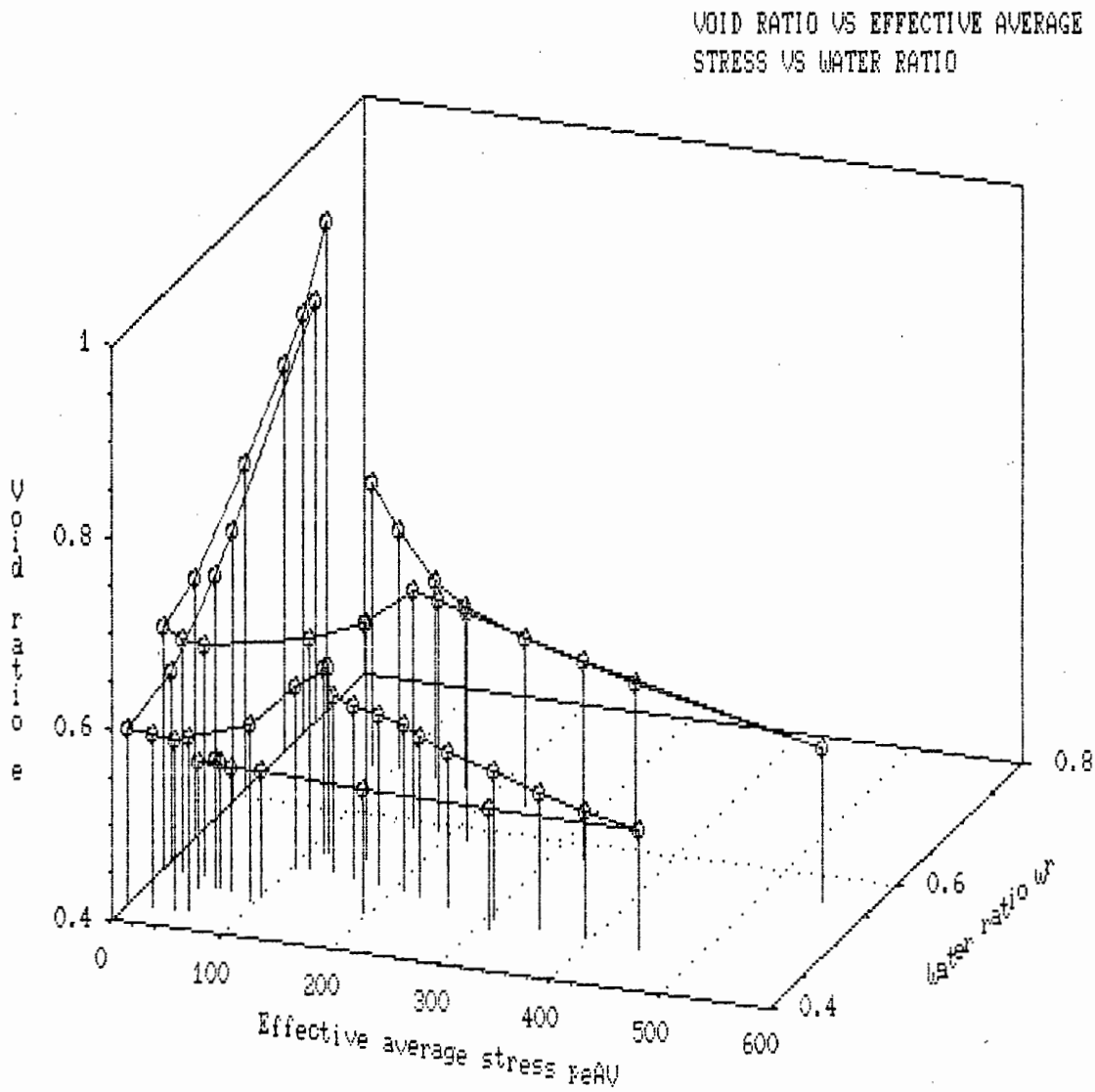

Figure 8.51: Site 36, Rondebosch - [100 Kpa] Void ratio 'e' versus effective average stress 'peAV' versus water ratio 'wr'.

Site A, Berea Road (Durban).

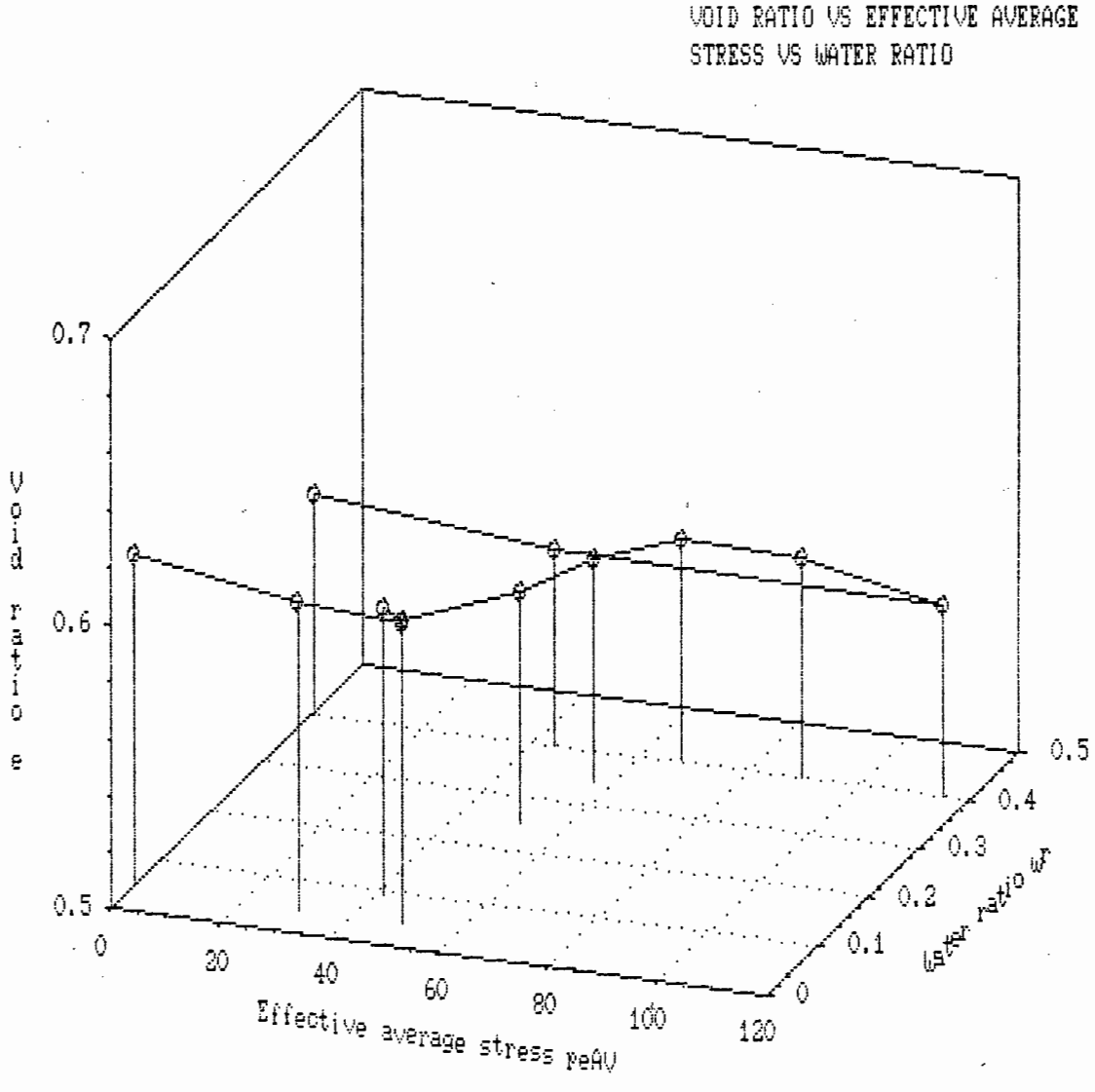

Figure 8.52: Site A, Berea Road (Durban) - [100 Kpa] Void ratio 'e' versus effective average stress 'peAV' versus water ratio 'wr'.

Site 7, Mowbray.

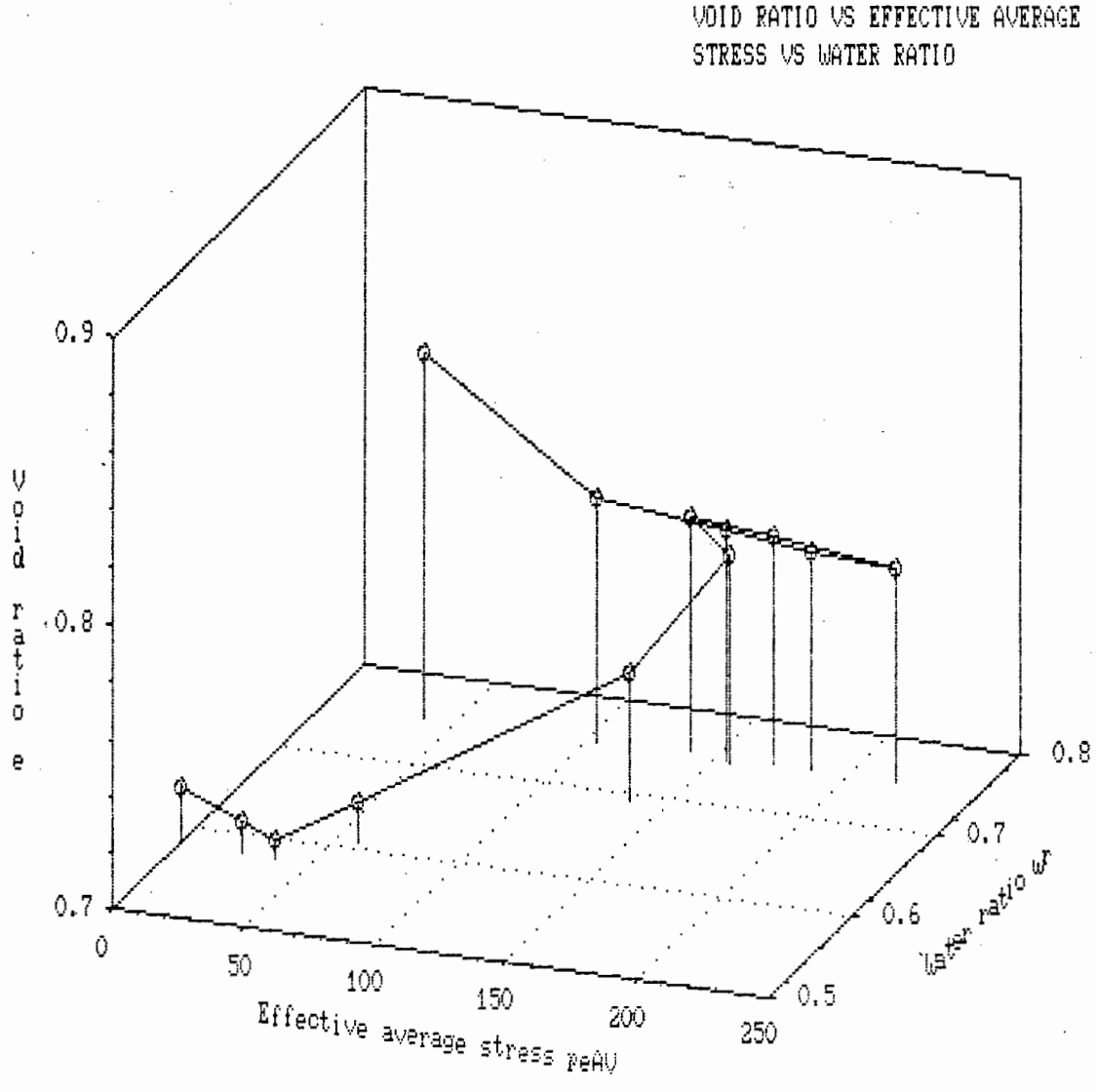

Figure 8.53: Site 7, Mowbray - [100 Kpa] Void ratio 'e' versus effective average stress 'peAV' versus water ratio 'wr'.

Site 48, Lady Grey.

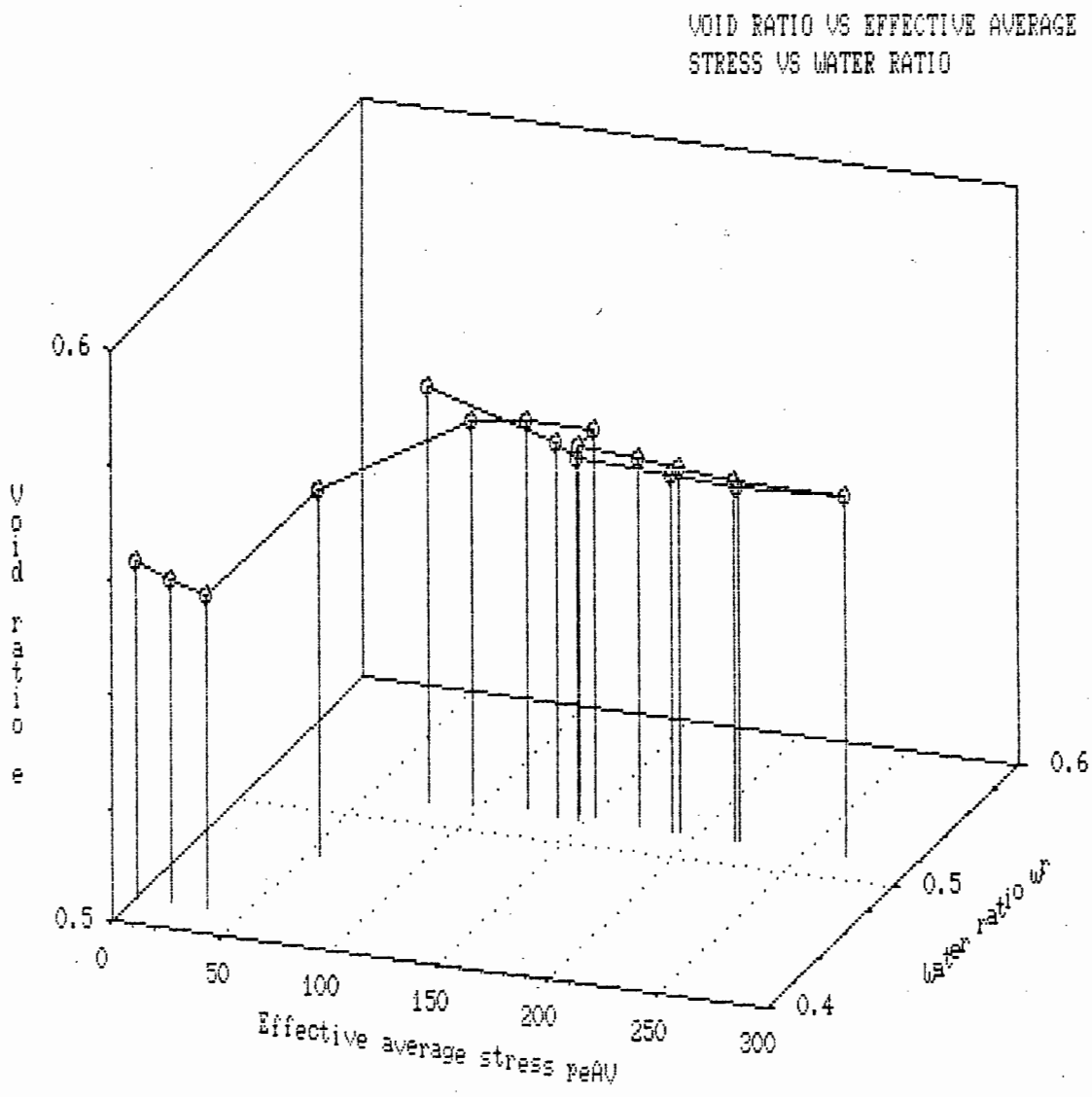

Figure 8.54: Site 48, Lady Grey (Natal) - [100 Kpa] Void ratio 'e' versus effective average stress 'peAV' versus water ratio 'wr'.

8.11 REFERENCES FOR CHAPTER EIGHT

16. DE S. VINAGRE, T.J.V. (1976/77): Masters Thesis - Diaries One, Two, Three, Four, Five, and Six.

20. BALLANTINE, P.A. (1978): Consolidometer tests to determine the stree path in a soil subject to vertical load - post B.Sc. thesis tests for Prof. Sparks. Department of Civil Engineering, University of Cape Town.

86. SPARKS, A.D.W. (1975): Discussions, Vol. II, Proceedings of the Sixth Regional Conference for Africa on Soil Mechanics and Foundation Engineering; Durban, South Africa, September 1975.

91. SPARKS, A.D.W. Prof. (Supervisor) - Discussions with the writer.

CHAPTER NINE *

ALL ROUND, THREE-DIMENSIONAL EXPANSION OR COLLAPSE

9.1 INTRODUCTION

The work in this chapter deals with the observed changes in volume of a soil sample, as the result of isotropic consolidation under drained conditions and/or the addition of measured volumes of water.

The type of expansive or collapsing behaviour being investigated refers to soil samples which are allowed to increase (expand) or decrease (collapse) their volume, as the result of increases in water content, and while being subjected to an all round pressure which remains constant throughout the wetting stage of the test.
A triaxial machine was used to apply the cell pressure, or all round pressure, against which the soil sample expands or collapses.
This all round pressure value was approximately 100 Kpa.

Initially, isotropic consolidation of the sample under drained conditions takes place as the result of applied effective pressures, or stresses.

The photographic plates included in Chapter Five (refer to section 'Test Method'), illustrate the use of the triaxial machine for the purpose of observing the volume changes that take place in a soil sample. These volume changes take place either as the result of changes in its water content, or changes in the cell pressure being applied by the triaxial machine.

The observed water contents, void ratios and cell pressures (ie, the all round pressure, or stress, applied to the sample) are presented in graphical form to illustrate the trends of behaviour and to allow comparisons to be made between the paths of expansion or collapse. The observed behaviour developed, under known loading conditions, for different initial conditions and ranges of water content. Various different types of soil were used.

Two methods of sample preparation were followed for each soil type prior to the observations of volume changes. The test samples, as used in this chapter, were prepared from either compacted or undisturbed soil samples.
It was hoped to investigate both the unsaturated and saturated conditions of each sample.

---

* - *Observations are listed in Appendix H.*

9.2 CONCEPTS AND DEFINITIONS

The words and concepts which define 'all round[1] expansion or collapse' as used in this chapter, can be defined as follows:-

The words "isotropic or all-round consolidation" refer to the initial consolidation of the sample, under drained conditions, while being subjected to an all round, or isotropic stress.
The drained consolidation test, under an all round stress, is one during which drainage is permitted throughout the test. It is an attempt to satisfy the condition of zero pore water pressure, and since the pore water pressure is zero, the effective stresses are equal to the applied stresses. The drained test provides information on the volume changes which accompany the application of the all round pressure, and on the stress-volumetric strain characteristics of the soil.

The concept of all round pressure refers to the applied stress which acts all round a sample. The sample is confined, or compressed, by the all round pressure being applied to it.

Within the context of three dimensional expansion or collapse, the concept of "three-dimensional" refers to the observed increases or decreases in the measured volume and height of a sample, as the result of changes in its water content or the applied stress.
It should be noted that the measured changes in the overall volume of the sample, are the end result of the measured changes in width, depth and height, as seen by an observer.

The words "Expansion or Collapse" refer to the observed changes in the volume of a sample which is confined by an applied initial stress, and which is allowed to increase (expand) or decrease (collapse) its volume as the result of increases in water content.

The following should also be noted:

(i) Changes in the height of the sample were also observed; and,
(ii) Drainage of the sample was permitted throughout the controlled wetting stage.

---

[1] *- or three dimensional.*

The changes in the water content of these samples were made to happen in a controlled manner, as follows:

(i) A water feeding line was established between one of the orifices in the pedestal (inside the triaxial cell) and a calibrated burette (on the outside);
(ii) By raising the burette slightly, a 'head' of water (or hydraulic gradient) is created, which causes a small flow of water from the burette towards the top of the pedestal - thus, a limited small known volume of de-aired water was added to the bottom filter paper, which in turn transmits the water to the whole underside of the soil sample; and,
(iii) Then waiting for this extra water to distribute itself upwards into the sample - during this stage, time measurements of isotropic increase or decrease (in volume of the sample), are carried out as described in 'Test Method'[1].

All the other relevant concepts and definitions, required for the stated purpose of this chapter, are defined in the previous chapters[2].

9.3 THE PARAMETERS WHICH ARE BEING INVESTIGATED

The diagrams in Figures 9.01 and 9.02 illustrate the three main parameters which are being investigated. These parameters are the void ratio, the water ratio, and the effective pressure to which the sample is being subjected as isotropic, or all-round, consolidation.

The diagram in Figure 9.01 illustrates two of the parameters which are being investigated. These parameters are the void ratio and the water ratio of the sample. The vertical and horizontal axes of the diagram in Figure 9.01 represent the void ratio (the volume of voids to the volume of solids) and the water ratio (the volume of water to the volume of solids), respectively.
Figure 9.01 is basically the same as Figure 8.01 of Chapter Eight.

The relationship between the void ratio and the water ratio, as shown in Figure 9.01, goes through the following stages:-

The sample is initially at condition A - that is, at the same condition that it will be tested.

The steps in the test are:
(1) The initial loading path AB - the loading of the sample to the required 'all round' pressure, against which the sample expands or collapses when wetted.

---

1 - refer to subsequent section 9.7.
2 - in particular chapters four to six.

(2) Starting at point B, the water content is gradually increased in stages while the sample is being confined by the all round cell pressure - the void ratio increase[1] or decrease[2] is shown as the "wetting path" between points B and C; When another increment of water causes no further change in volume of the sample, as shown in the volume change indicator (refer to subsequent section 'Test Method').
(3) The additional path of loading C to D.
(4) Unloading D to E.

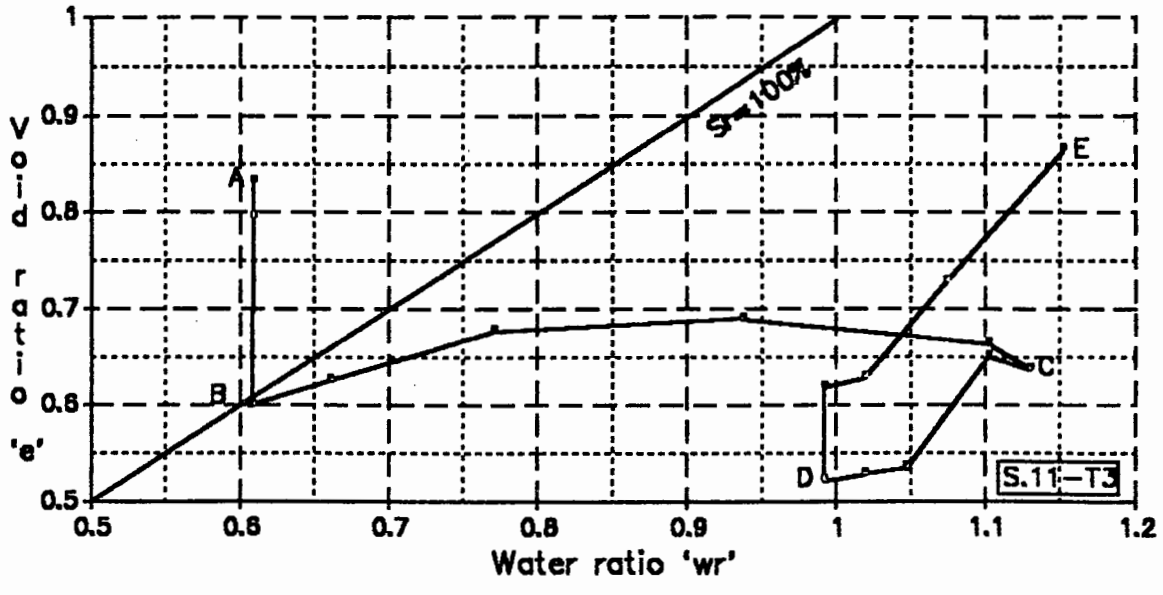

Figure 9.01: Sample S.11-T3 [Undisturbed] Drained triaxial, isotropically consolidated overnight, wetted by increments, further consolidation, then unloading. Relationship between the void ratio 'e' and the water ratio 'wr' or 'Ω', for the full test path. The above values of the water ratio are unexpecttedly high in value, but thr writer includes the data as measured values which would require further investigation.

---

[1] - *due to expansion of the sample.*
[2] - *resulting from further settlement.*

The type of plot in Figure 9.02:-

The diagram in Figure 9.02 illustrates the third parameter which is being investigated. This parameter is the effective all round pressure, or stress, which is being applied to the sample. The horizontal axis represents the all round stress throughout the test.
The state of the sample as it changes from condition A through to E, follows the same path as described for Figure 9.01.

The main difference between Figures 9.01 and 9.02 are as follows:
(a) Effective pressures are plotted along the horizontal axis (instead of the water ratio values that were used in Figure 9.01); and,
(b) Figure 9.02 includes the water ratio values at selected points along the test path.

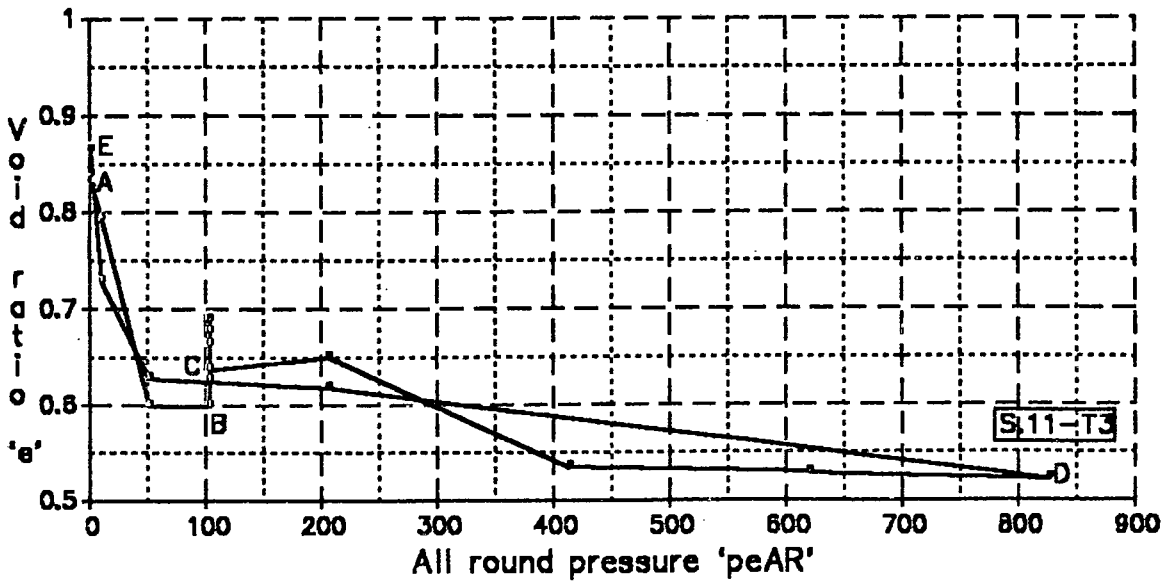

Figure 9.02[1]: Relationship between the void ratio 'e', and the effective all round pressure (or stress) 'peAR', for the full test path.

[1] - *Triaxial system. Same test as Figure 9.01.*

The measurements of the other parameters relating to each soil type are included in Chapters One, Two and Appendix A. The main index properties for each soil type were listed in Chapter Four.

9.4 REASONS FOR USING THE TYPES OF PLOT SHOWN IN FIGURES 9.01 TO 9.02

The type of plot shown in Figure 9.01 illustrates the relationship between the void ratio and the water ratio of the sample. This type of plot enables the position and scaling factor for the stress scales[1] to be expressed in terms of the Liquid Limit and Plasticity Index of the soil.

Reasons for using the type of plot shown in Figure 9.02:-

(A) To observe the relationship between the void ratio and the effective all round pressure, or stress, applied to a soil sample whose water content remains in the unsaturated condition throughout the isotropic consolidation under drained conditions.

(B) The void ratio changes as the result of increases in the water content of the sample which remains subjected to a constant all round pressure.

(C) The relationship between void ratio and effective all round pressure, or stress, for the final loading and unloading of the sample under drained conditions.

9.5 SOME SPECIFIC OBJECTIVES FOR THIS CHAPTER

The aim of this chapter is twofold - (1) to provide a summary of the results obtained, and (2) an evaluation of the parameters obtained in the triaxial test for three dimensional expansion or collapse of a sample.

Summary of the results obtained from the full test path, illustrated in Figures 9.01 and 9.02:-

(i) To obtain the void ratios for each applied all round pressure to the sample, during the initial loading path to the required all round stress against which the sample expands or collapses when subsequently wetted.

---

[1] - *obtained in chapter five.*

(ii) The changes in the void ratio of the sample obtained from the measured increase (or decrease) of its volume, as the result of increases in the water content of the sample.

(iii) The measured volumes of water added to the soil sample.

(iv) To obtain the final loading and unloading paths of the sample.

Evaluation of the observed parameters and their relationships, as follows:-

(A) The void ratio (the ratio of the volume of voids to the volume of solids) and the water ratio (the ratio of the volume of water to the volume of solids);

(B) The void ratio and the effective all round pressure, or stress, applied to the soil sample;

(C) Superimposition of stress scales on the plots of void ratio versus water ratio; and,

(D) Void ratio versus effective all round pressure versus water ratio.

9.6 PREPARATION OF TEST SAMPLES

Test samples were prepared from compacted and undisturbed soil samples.
A brief description is included in this chapter for each type of sample preparation - for more details refer to either Appendix A ('Preparation of soil samples for testing'), or Appendix H[1] ('Triaxial tests for expansive and collapsing soils: Test procedure and results').

Compacted samples.

Select points on the 'dry density versus water content' curve for the soil sample - refer to 'Compaction Tests' in Appendix A; Compact the soil to the required specification and at the selected water content; Cut the test sample from the compacted sample.

Undisturbed samples.

The test sample is cut from the undisturbed block - refer to 'Soil Sampling' in Appendix A.

---

[1] - *section H.2 "Test procedure".*

9.7 TEST METHOD

The test sample is cut and trimmed to size. The top and bottom surfaces of the sample are made level. The mass of the soil sample is recorded.

The triaxial test enables the measurement of three-dimensional 'expansion or collapse' behaviour of a sample which, while being confined by a known all round pressure, increases or decreases its volume as the direct result of changes in its water content.

The triaxial test, for expansive and collapsing soils, can be defined in brief terms.
The test basically consists of four parts:
Part 1 - To load a soil sample to the required all round pressure and to record the values of volume change from the start of each stage of loading (after the sample has consolidated under drained conditions);
Part 2 - To measure the increase (expansion) or decrease, that is collapse in volume of the sample as the result of increases in its water content;
The final loading and unloading (of the sample) - these are the last two parts of the test.

Summary of the test procedure.

The test sample is positioned in place, and the triaxial equipment is assembled and made ready for the actual test. The pressure supply is adjusted to the required cell pressure. Volume change as a function of time is recorded during each stage of loading the sample - consolidation is completed when no noticeable changes occur to the volume change indicator over a considerable period of time. At the completion of the initial loading stage, the sample is being confined by the required cell pressure, or all round stress. In this chapter the cell pressure for overnight consolidation was approximately 100 Kpa, and this pressure was also maintained during the subsequent incremental wetting.

At the start of the test, the water in the burette is kept level with the top of the pedestal; To add water to the sample, the burette is gradually raised, a bit at a time, in order to generate a slight `head' which will cause the water to slowly flow onto the top of the pedestal, be absorbed by the porous plate/filter paper, and go into the sample; The procedure is repeated until the required amount of water increment is reached (usually about 1 cc), and then waiting at least 6 hours for this extra water to distribute itself upwards throughout the sample.
The volume changes with time that take place, in the sample, from the start of wetting, are observed in the 'volume change indicator'.

The loading characteristics of the soil, under saturated conditions, are determined by adjusting the pressure supply to the required cell pressure.
The sequence of cell pressures used was as follows: 103.4 Kpa, 206.8 Kpa, 413.7 Kpa, 620.5 Kpa, and 827.4 Kpa. Volume change as a function of time is recorded during each stage of loading the sample.
The unloading, or recovery characteristics of the soil (as a function of time) are also recorded for the following sequence of pressure decrease: 827.4 Kpa, 206.8 Kpa, 51.7 Kpa, 10.3 Kpa, and 1 Kpa.

The volume and pressure supply systems are isolated, and the equipment is disassembled. The soil sample is weighed, measured and placed inside and oven (previously set at 105 ± 5°c) for a few hours. The sample is removed from the oven, allowed to cool down to room temperature, and its oven dried mass is recorded.

The detailed description of this test procedure is included in Appendix H - refer to "Triaxial Tests for Expansive and Collapsing Soils - test procedures and results". Photographic plates, which illustrate the use of the triaxial machine for observing volume changes, are included in Chapter Five[1]. It should also be noted that the basic procedure for the triaxial test is included in Appendix D[2] - 'Triaxial: Isotropic consolidation test procedure'.

---

[1] - *see section 5.6.*
[2] - *section D.2.*

9.8 TEST RESULTS FOR THE SOIL TYPES INVESTIGATED.

The test results consist of the measurements of volume, or changes in volume of a soil sample which is confined by an all round stress - these volume changes take place as the result of either an increase (or decrease) in the all round pressure or water content.
An introduction to the test results will be provided by the definitions of each soil type, according to particle size and the previously reported observations for the Consistency Limit - refer to Chapters One, Two and Appendix A.

The parameters which were investigated are presented in two basic forms:-

(i) The relationship between the void ratio and the water ratio, for the full test path; and,

(ii) The relationship between the void ratio and the effective all round pressure, or stress, for the full test path.

Relationships of void ratio versus water ratio, and void ratio versus effective pressure, are included for the two soil types used in this chapter.
The two natural soil types used were: (A) Site 11, Rosebank (Cape); and, (B) Site A, Berea Road (Durban, Natal).

These relationships are illustrated in Figures 9.03 to 9.10 as follows:-

Void ratio versus water ratio:

Site 11, Rosebank: Figures 9.03 [Undisturbed - 100 Kpa], and 9.05 [Compacted - 100 Kpa];
Site A, Berea Road (Durban): Figures 9.07 [Undisturbed - 100 Kpa], and 9.09 [Compacted - 100 Kpa].

Void ratio versus effective all round pressure:

Site 11, Rosebank: Figures 9.04 [Undisturbed - 100 Kpa], and 9.06 [Compacted - 100 Kpa];
Site A, Berea Road (Durban): Figures 9.08 [Undisturbed - 100 Kpa], and 9.10 [Compacted - 100 Kpa].

It should be noted that Appendix H[1] includes the "Triaxial tests for expansive and collapsing soils - test procedure and results".

---

[1] - *refer to sections H.2 and H.4.*

Triaxial tests to determine the volume changes (resulting from the three dimensional expansion or collapse of samples confined by an all round pressure), were performed on the soil samples listed in Table 9.01.

Table 9.01: Natural soils - samples used for triaxial tests for expansive and collapsing soils.

Sample No.	Method of preparation	Free Shrinkage (Ref. number)	Expansion / Collapse (Ref. / Triaxial)
Site 11 - Undisturbed 'U' or Compacted 'C':			
[Effective all round pressure = 100 Kpa: Figures 9.03 - 06]			
S.11-T3	U	V. 28	V.28 / test no. 14
S.11-T4	CStd(IV.450)	IV.459(S.11-71)	V.30 / test no. 15
Site A - Undisturbed 'U' or Compacted 'C':			
[Effective all round pressure = 100 Kpa: Figures 9.07 - 10]			
S.A-T3	U	V. 25	V.25 / test no. 12
S.A-T4	U	V. 26	V.26 / test no. 13
S.A-T5	U	V. 32	V.32 / test no. 16
S.A-T2	CStd(IV.450)	V. 33	V.33 / test no. 17

Site 11, Rosebank.

Previously defined as a fine silty clay with only a small amount of fine sand. The soil consists of 59% clay, 29% silt, and 12% sand size.
The consistency, free shrinkage and free swell limits, are as follows: Linear Shrinkage 'w_{LS}' = 11.4%; Liquid Limit 'w_L' = 69%; Plastic Limit 'w_P' = 30.7%; Plasticity Index 'I_P' = 38; Shrinkage Limit 'w_S' = 22.5%; and, Free Expansion Limit 'w_{FE}' = 49.4%.

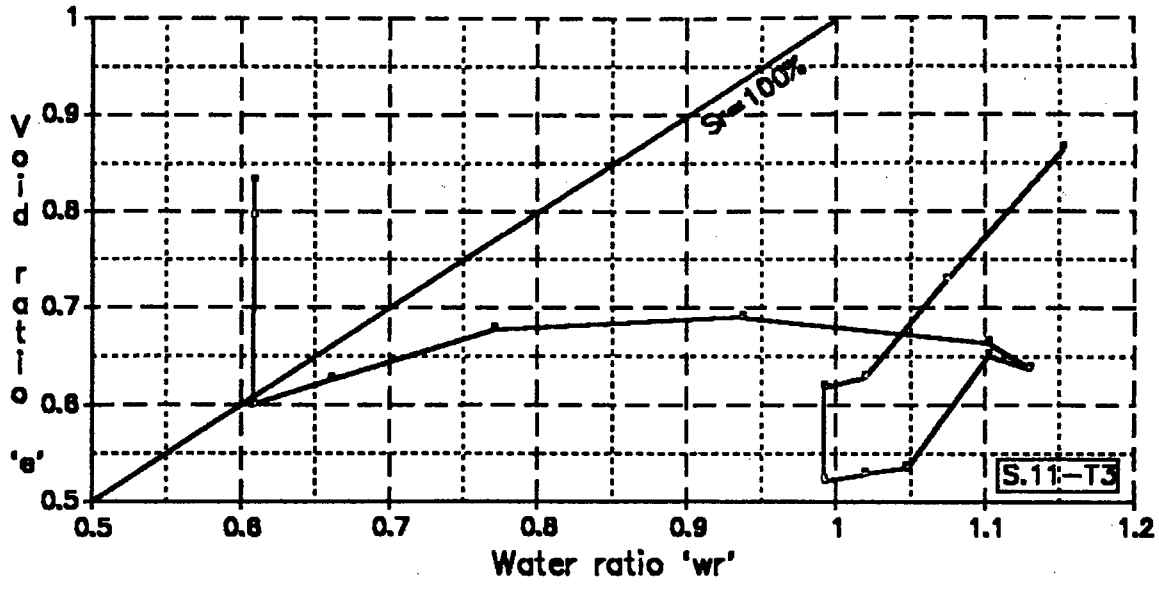

Figure 9.03: Site 11, Rosebank - [Undisturbed - 100 Kpa] Relationship between the void ratio 'e' and the water ratio 'wr'. An unusual result - See comment with Figure 9.01.

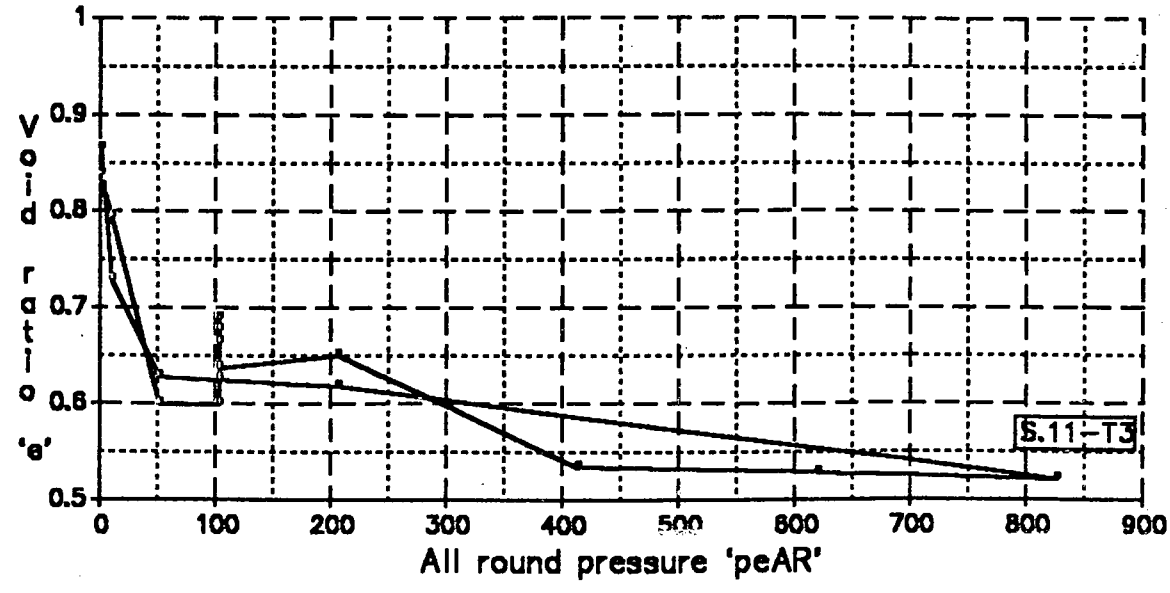

Figure 9.04: Site 11, Rosebank - [Undisturbed - 100 Kpa] Relationship between the void ratio 'e' and the effective all round pressure 'peAR'.

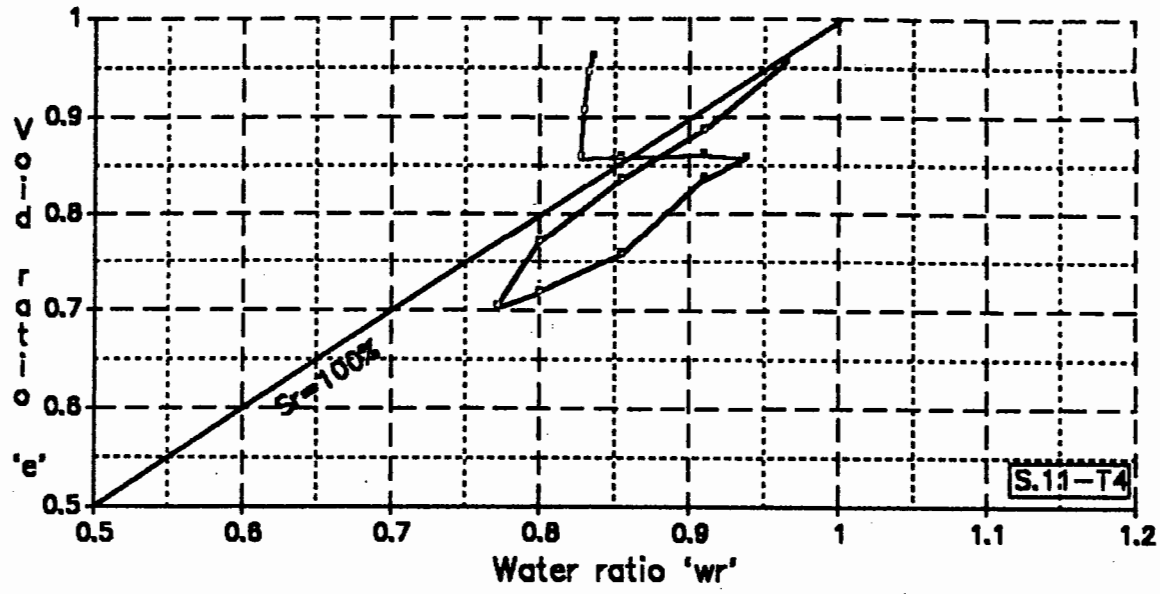

Figure 9.05: Site 11, Rosebank - [Compacted - 100 Kpa] Relationship between the void ratio 'e' and the water ratio 'wr'.

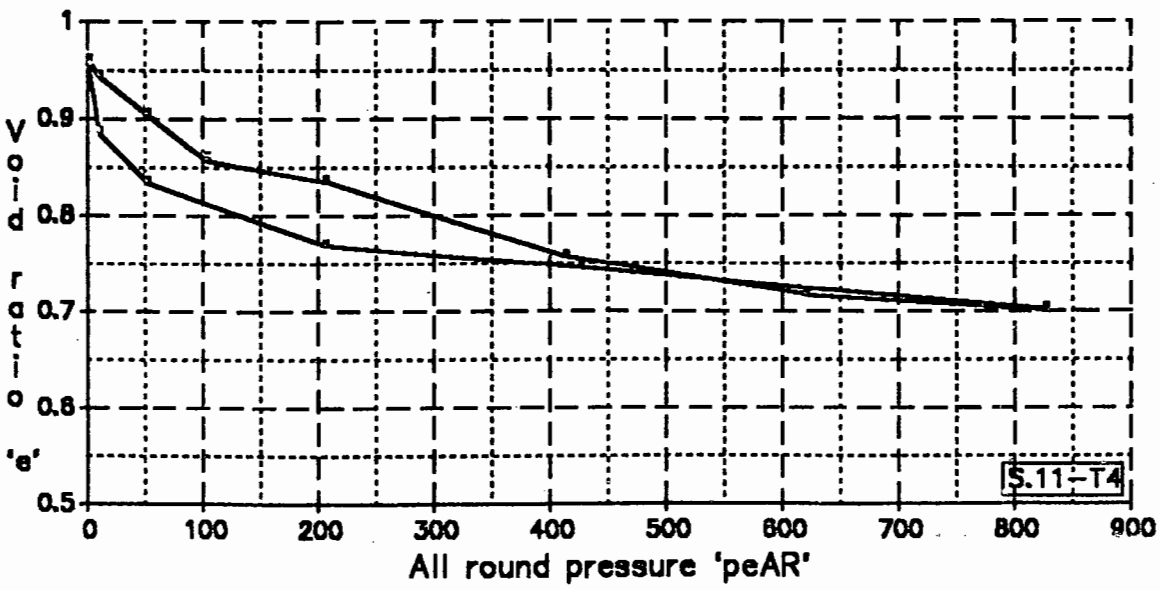

Figure 9.06: Site 11, Rosebank - [Compacted - 100 Kpa] Relationship between the void ratio 'e' and the effective all round pressure 'peAR'.

Site A, Berea Road (Durban).

A clayey sand (fine to medium size) with a small amount of silt. The soil consists of 15% clay, 10% silt, and 75% of sand size. The 'Limits' of the soil are as follows: w_{LS} = 3.7%; w_L = 25.0%; I_P = 12; w_S = 13.5%; and, w_{FE} = 16.6%.

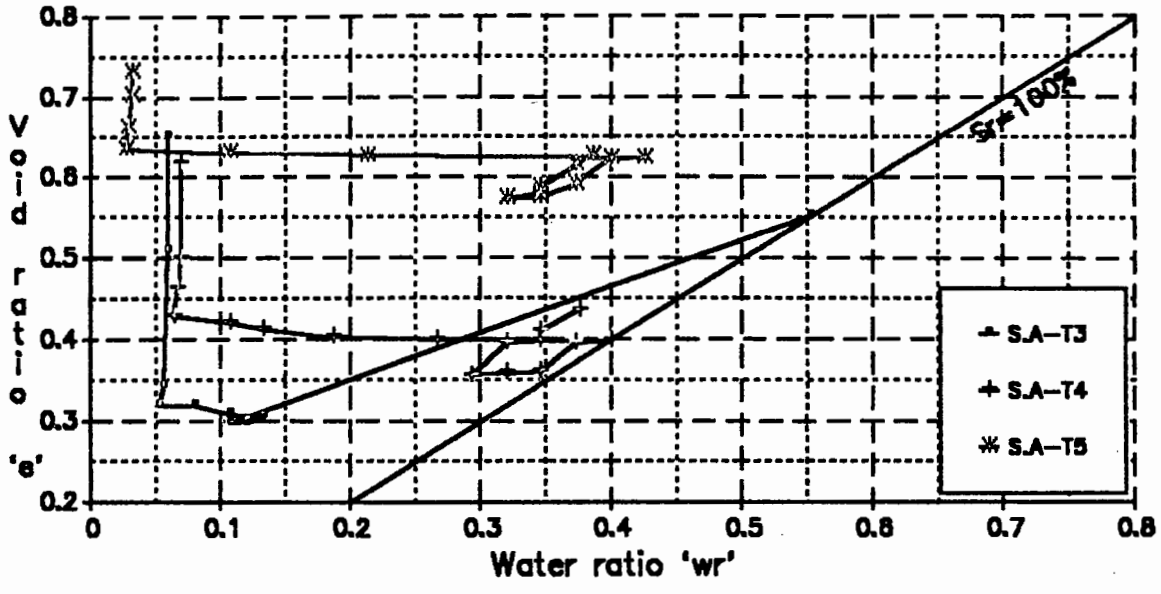

Figure 9.07: Site A, Berea Road (Durban) - [Undisturbed - 100 Kpa] Relationship between the void ratio 'e' and the water ratio 'wr'.

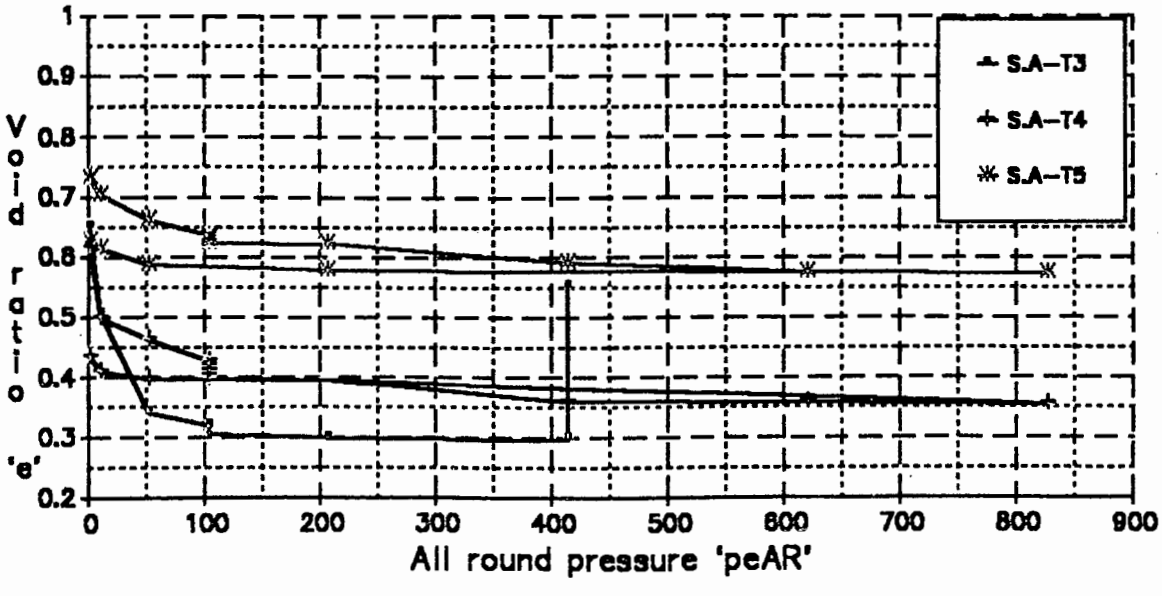

Figure 9.08: Site A, Berea Road (Durban) - [Undisturbed - 100 Kpa] Relationship between the void ratio 'e' and the effective all round pressure 'peAR'.

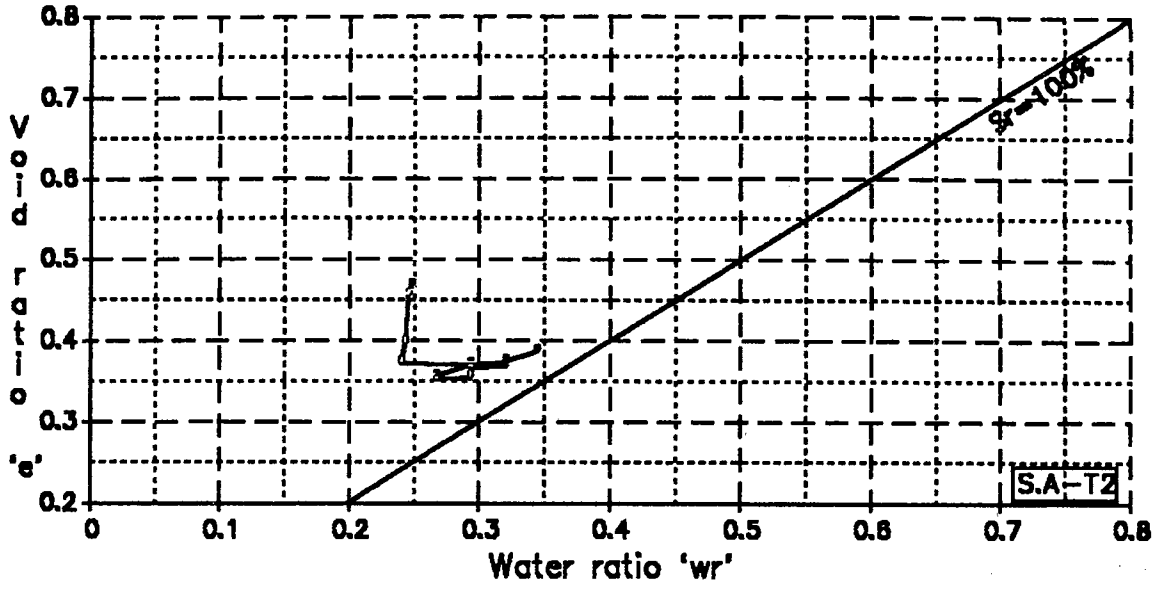

Figure 9.09: Site A, Berea Road (Durban) - [Compacted - 100 Kpa] Relationship between the void ratio 'e' and the water ratio 'wr'.

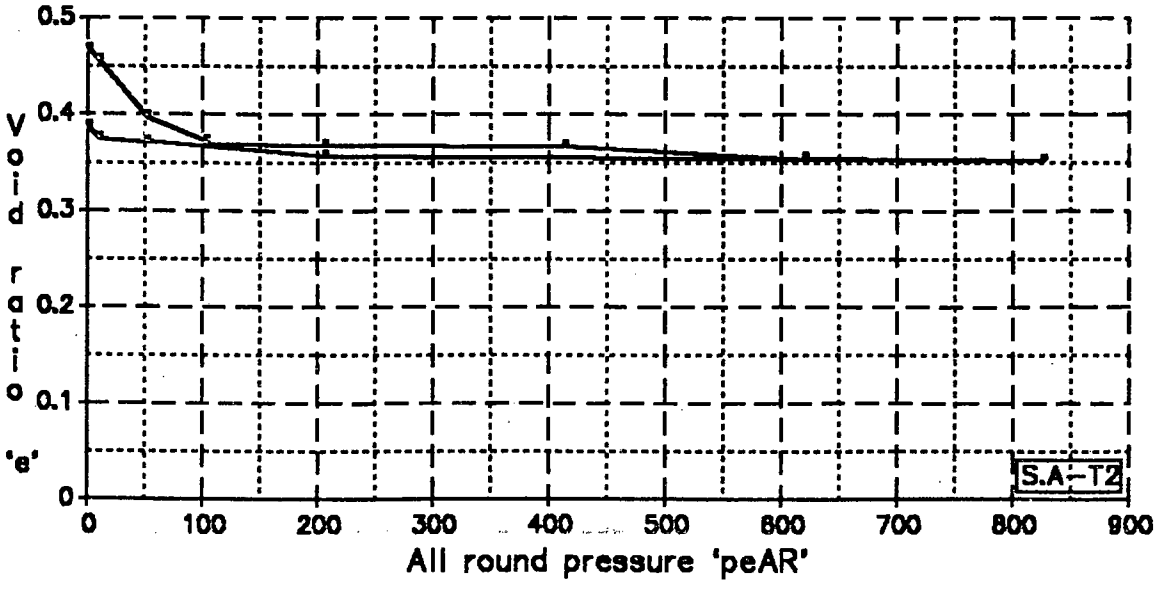

Figure 9.10: Site A, Berea Road (Durban) - [Compacted - 100 Kpa] Relationship between the void ratio 'e' and the effective all round pressure 'peAR'.

9.9 ANALYSIS OF THE TEST RESULTS

The parameters, obtained from the test results, and their inter-relationships are analysed in the plot ofVoid Ratio versus Effective All Round Pressure versus Water Ratio.

These relationships are illustrated in Figures 9.11 and 9.12 as "Void ratio versus effective all round pressure versus water ratio for the full test path"[1].

---

[1] - *three dimensional plot.*

9.9.1 Void Ratio vs Effective All Round Pressure vs Water Ratio.

Site 11, Rosebank.

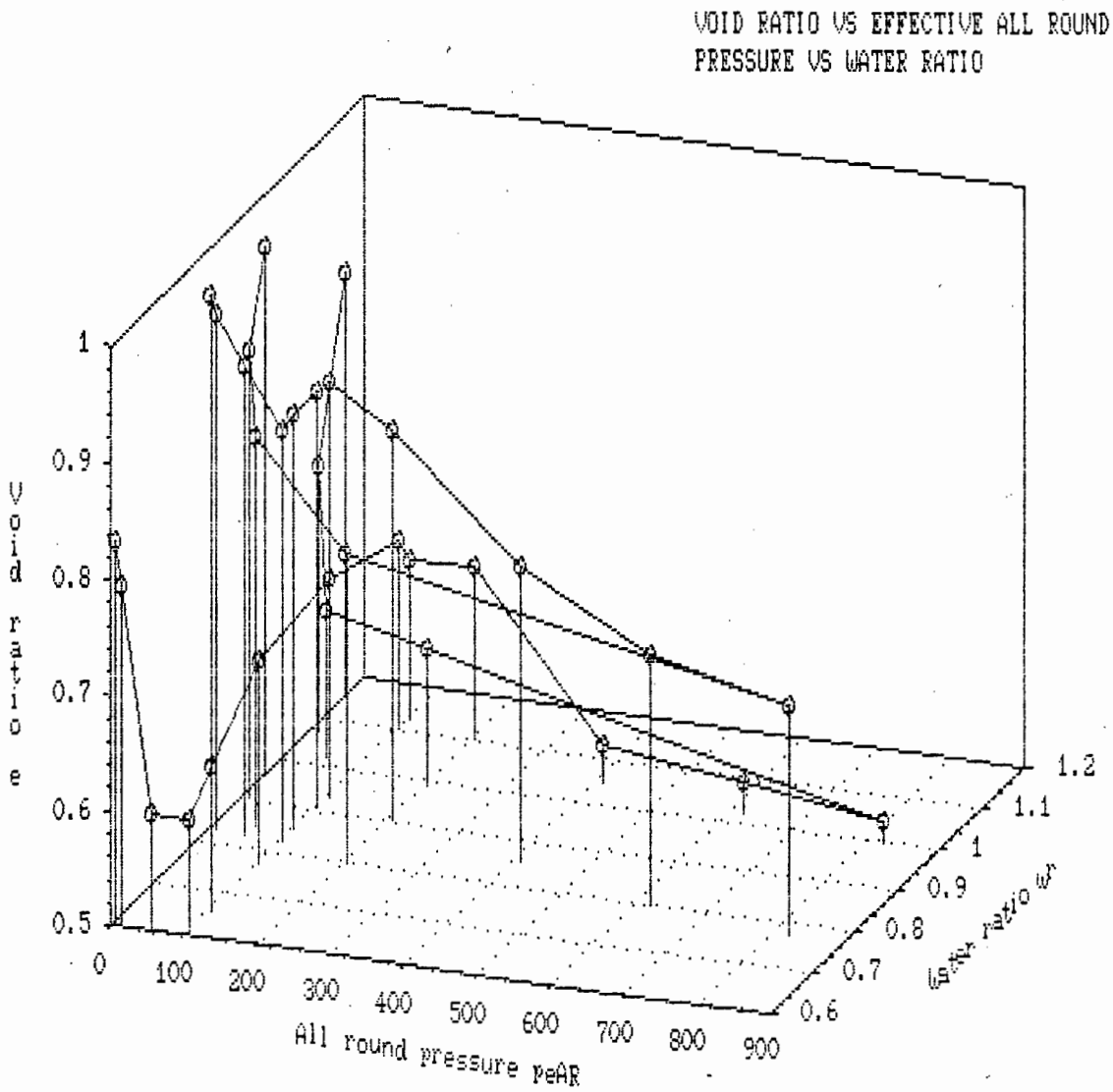

Figure 9.11: Site 11, Rosebank - [U & C[1] - 100 Kpa] Void ratio 'e' versus effective all round pressure 'peAR' versus water ratio 'wr'.

---

[1] - *Undisturbed and Compacted.*

Site A, Berea Road (Durban).

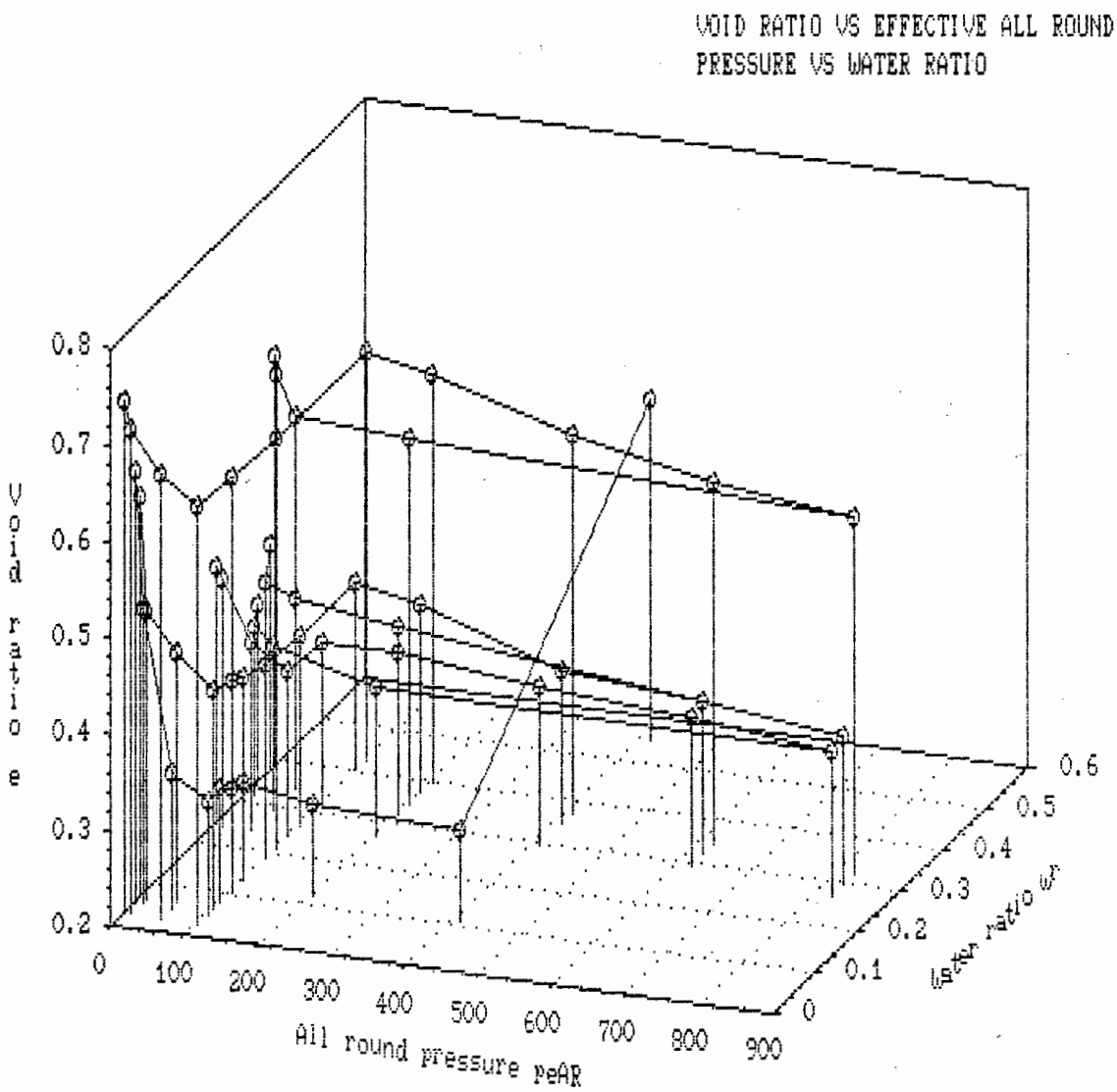

Figure 9.12: Site A, Berea Road (Durban) - [U & C[1] - 100 Kpa] Void ratio 'e' versus effective all round pressure 'peAR' versus water ratio 'wr'.

---

[1] - *Undisturbed and Compacted.*

9.10 CONCLUSIONS FOR CHAPTER NINE

The work in this chapter dealt with the observed changes in volume, as the result of the addition of measured volumes of water to a sample being subjected to isotropic consolidation under drained conditions.

The observed water ratios and void ratios of the sample, while subjected to an all round pressure of approximately 100 Kpa, have been compared with stress scales.
These stress scales were obtained for the isotropic consolidation. Isotropic consolidation for each soil type were previously studied in chapter five.

Changes in volume are included for two soil types:-

1) Site 11, Rosebank - undisturbed and compacted samples;

2) Site A, Berea Road (Durban) - undisturbed and compacted samples.

Both the unsaturated and saturated conditions were investigated.

Site 11, Rosebank.

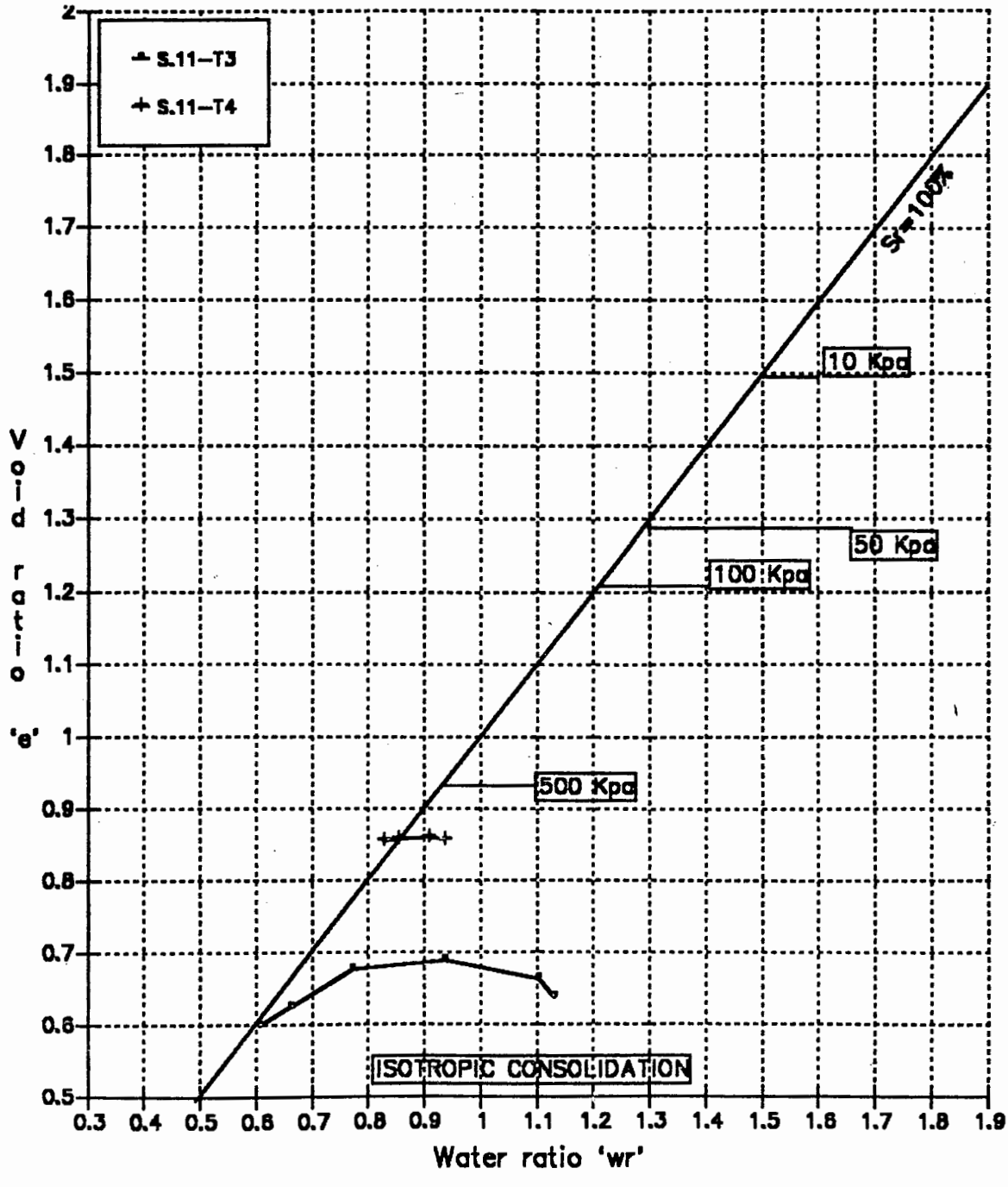

Figure 9.13: Site 11, Rosebank - [U & C[1] - 100 Kpa during wetting] Void ratio 'e' versus water ratio 'wr', under an all round pressure 'peAR' of 103.4 Kpa.

---

[1] - *Undisturbed and Compacted.*

Site A, Berea Road (Durban).

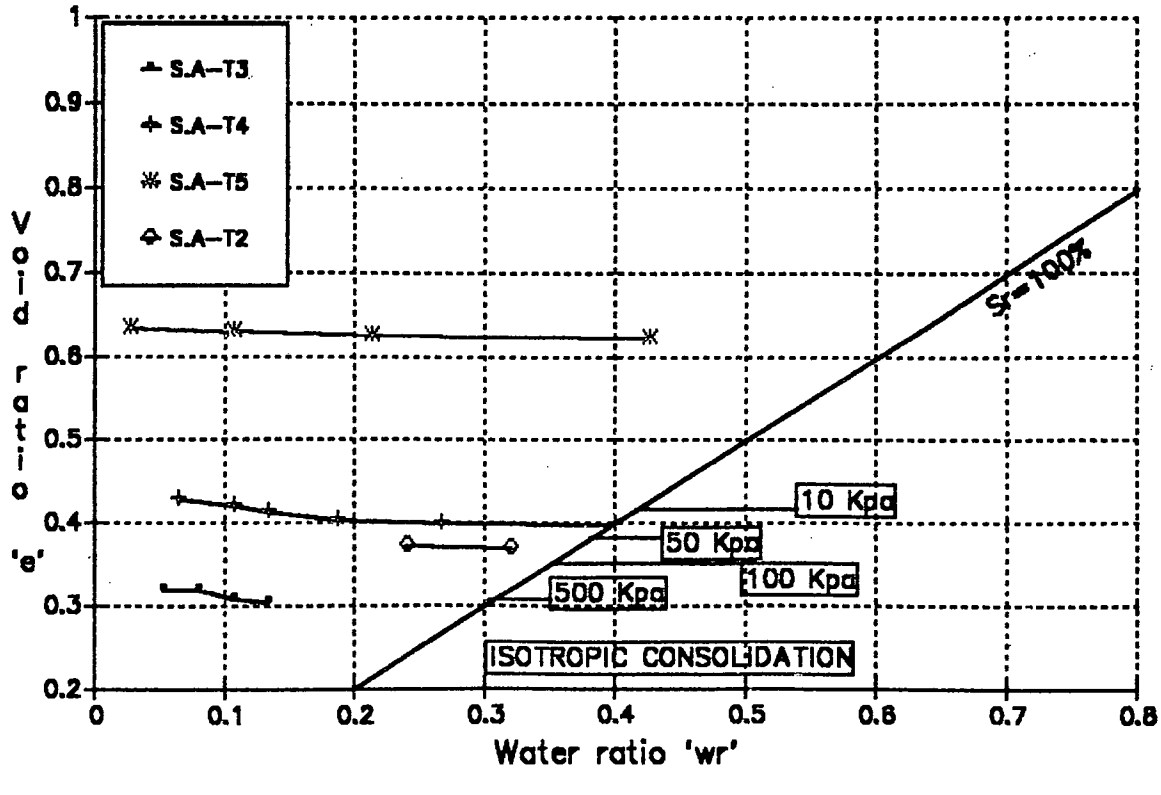

Figure 9.14: Site A, Berea Road (Durban - [U & C[1] - 100 Kpa during wetting] Void ratio 'e' versus water ratio 'wr', under an all round pressure 'peAR' of 103.4 Kpa.

---

[1] - *Undisturbed and Compacted.*

9.11 REFERENCES FOR CHAPTER NINE

16. DE S. VINAGRE, T.J.V. (1976/77): Masters Thesis - Diaries One, Two, Three, Four, Five, and Six.

CHAPTER TEN

CONCLUDING SUMMARY AND FURTHER THOUGHTS

10.1 INTRODUCTION

The original three goals set out for this thesis were achieved in the following manner:-

1) The introduction to soils exhibiting expansive and/or collapsing behaviour was provided by a literature review of the state of the art in this field. This was followed by a careful selection of suitable soil types and an in depth study of their soil structure and clay minerals.

2) The understanding, of aspects of expansive and collapsing behaviour, started to develop during the study of soil structure and clay minerals for each soil type. An in depth understanding was reached with the laboratory study of expansive or collapsible behaviour of volume change soils under controlled wetting conditions.

Three main types of expansion, or collapse, were investigated:

(i) Free Shrinkage and Free Swell paths for no load;
(ii) Expansion or collapse under known loads; and,
(iii) Vertical pressure required to prevent volume change.

3) The analysis of the test data, obtained from the extensive laboratory study, provides the basis for the conclusions of this thesis.
Chapter ten deals with the interpretation of these conclusions in the form of a concluding summary for each of the two main parts of the thesis, takes a closer look at some particular aspects of the thesis, and it also provides recommendations for future research work.

10.2 CONCLUDING SUMMARY FOR PART ONE OF THE THESIS

10.2.1 The Soil Types and their Macro Structure.

Suitable soil types were selected for this thesis. Their suitability was determined from physical structure and engineering properties. Artificial soils were also used.

The physical and engineering properties of the natural and artificial soil types, used in this thesis, can be summarized, in graphical form, as illustrated in the following section.

1) Consistency Limits.

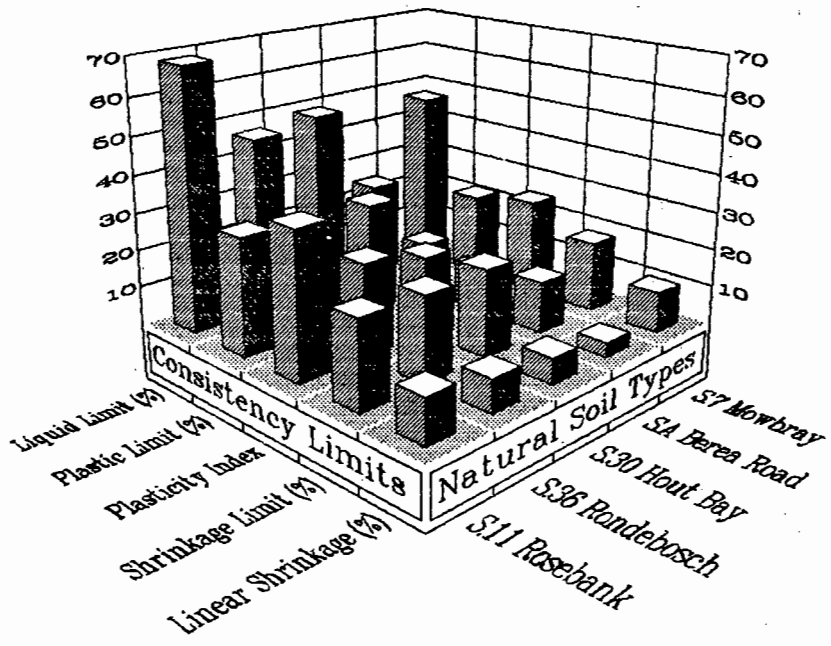

Figure 10.01: Consistency Limits - Natural Soil Types.

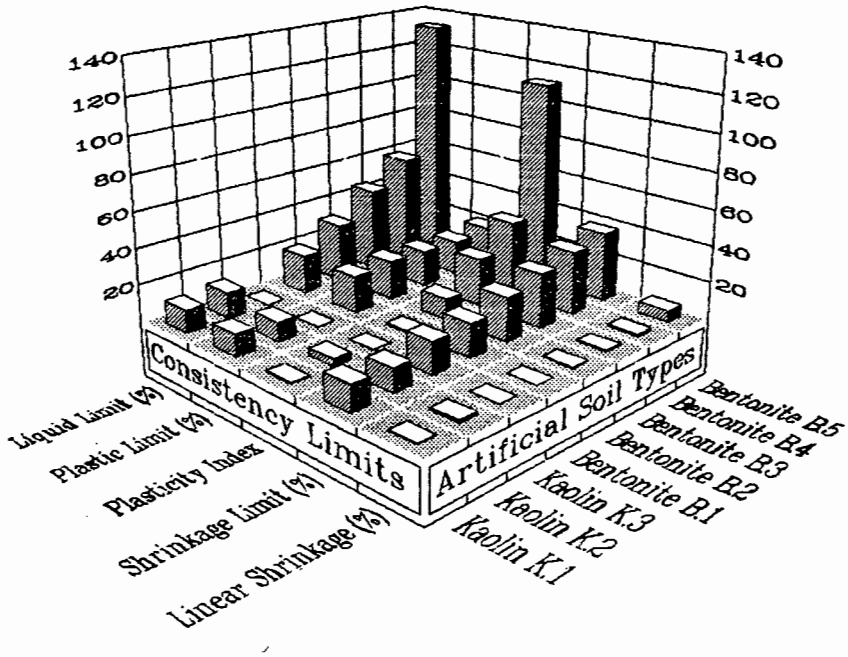

Figure 10.02: Consistency Limits - Artificial Soil Types.

Concerning the Consistency Limits for the natural soil types and the literature reviewed on this subject, it should be noted that on the basis of the definitions for Expansive and Collapsing soils introduced in Chapter Three[1], the following are preliminary conclusions which can be made at this stage:-

If we consider the normal Casagrande Plot of Liquid Limit Lw (horizontal axis) versus Plasticity Index PI (vertical axis) then the following can be stated:

1. Collapsing behaviour is more likely to be found amongst the soil types which plot to the left of the 30% Liquid Limit Line (that is, left of Line Lw = 30).

2. Expansive behaviour was observed in the soil types that had Linear Shrinkage values greater than 8%.

3. Moderate expansive behaviour is likely to happen in the soil types of medium plasticity (that is, the zone between lines Lw = 30% and Lw = 50%.

4. Highly expansive behaviour can occur in the soil types in the high plasticity zone (that is, to the right of the line Lw = 50).

It should be noted that Site 7, Mowbray, falls in the zone of Medium Plasticity as defined above - that is, between Lw=30% and 50%.

However, its subsequent measured behaviour[2] places this soil type in the highly expansive zone.

---

1 - refer to section 3.1 "Introduction and definitions".
2 - under applied load, confined or free.

2) Particle Size Distribution.

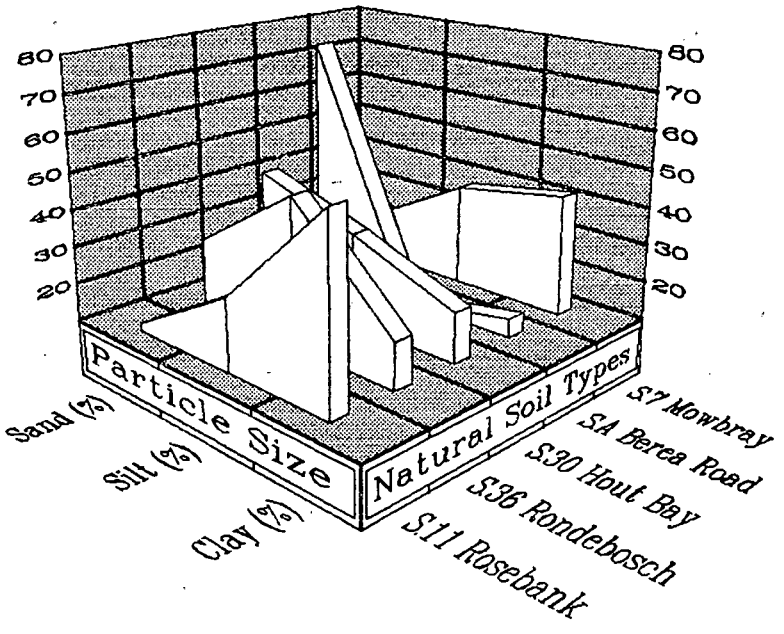

Figure 10.03: Particle Size Distribution [Percentages of sand, silt and clay] - Natural Soil Types.

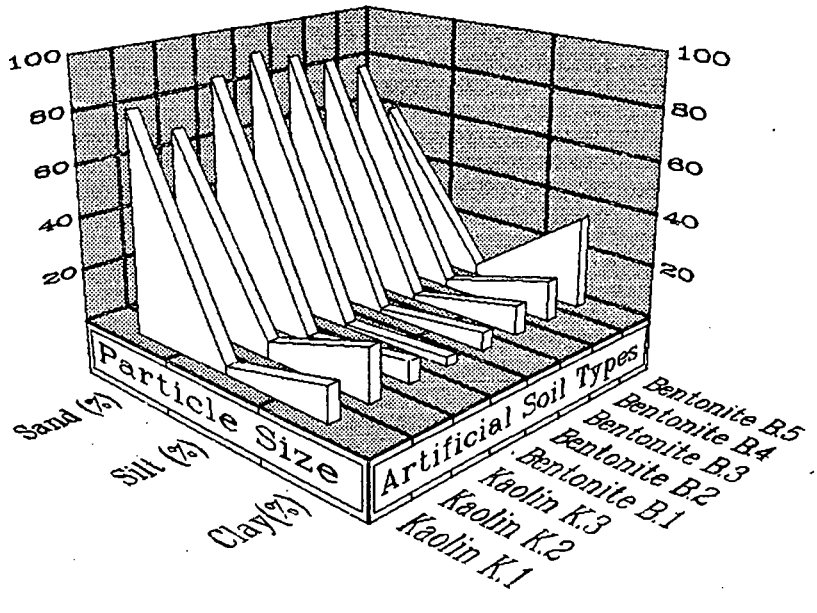

Figure 10.04: Particle Size Distribution [Percentages of sand, silt and clay] - Artificial Soil Types.

Based on particle size distribution only, the natural and artificial soil types can be defined in the following manner:-

Natural soil types.

Site 11, Rosebank (Cape): Fine silty clay, with only a small amount of fine sand.

Site 36, Rondebosch (Cape): Clayey silt, with fine sand and a small amount of medium sand.

Site 30, Hout Bay (Cape): Fine to medium sandy silt, with a small amount of coarse sand.

Site A, Berea Road (Durban): Clayey sand of fine to medium size with a small amount of silt.

Site 7, Mowbray (Cape): Fine silty clay, with a small amount of fine to medium sand.

Artificial soil types.

Kaolin K.1 (13% clay): Clayey sand of fine to medium size with a very small amount of silt.

Kaolin K.2 (20% clay): Clayey sand of fine to medium size with a small amount of silt.

Kaolin K.3 (8.5% clay): Fine to medium sand containing a small but noticeable amount of clay, and a very small amount of silt.

Bentonite B.1 (3.5% clay): Fine to medium sand with a very small amount of clay and silt.

Bentonite B.2 (7% clay): Fine to medium sand with a small amount of clay and a very small amount of silt.

Bentonite B.3 (11.5% clay), B.4 (15.5%) and B.5 (35%): Clayey sand of fine to medium size, with a very small amount of silt.

3) Relative Specific density of soil particles. [1]

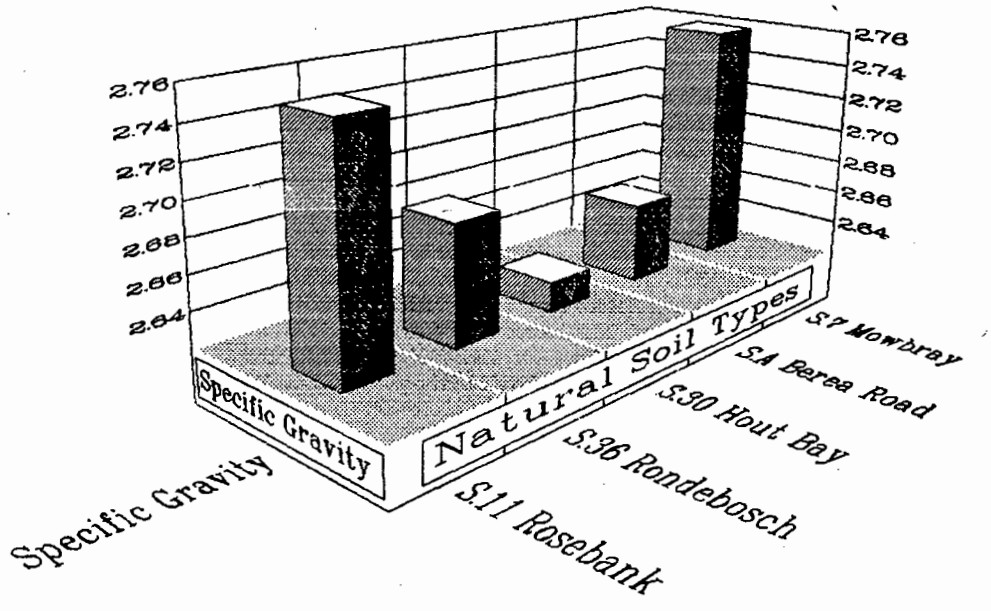

Figure 10.05: Specific Gravity - Natural Soil Types.

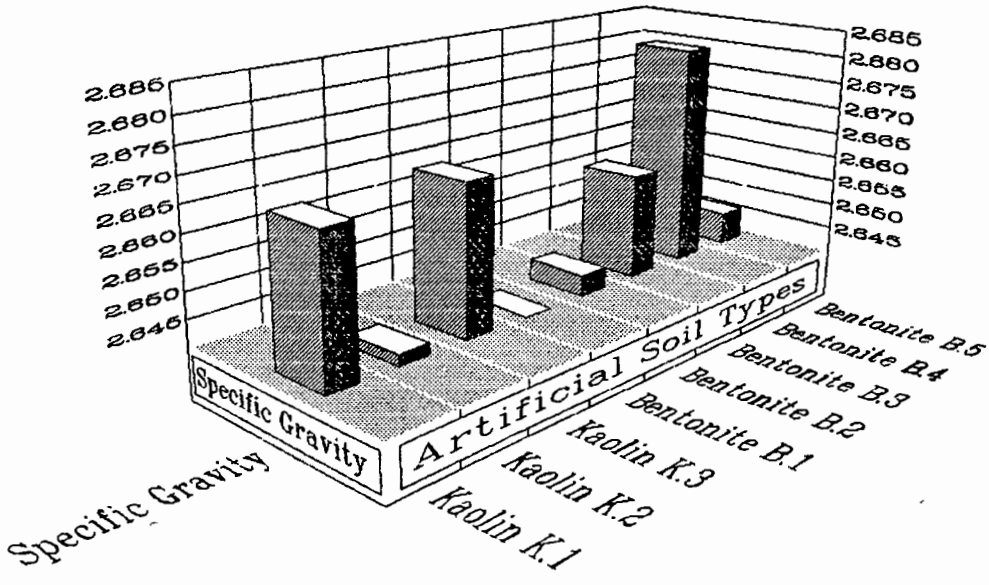

Figure 10.06: Specific Gravity - Artificial Soil Types.

---

[1] - that is, the Specific Gravity 'G_S'.

4) pH values.

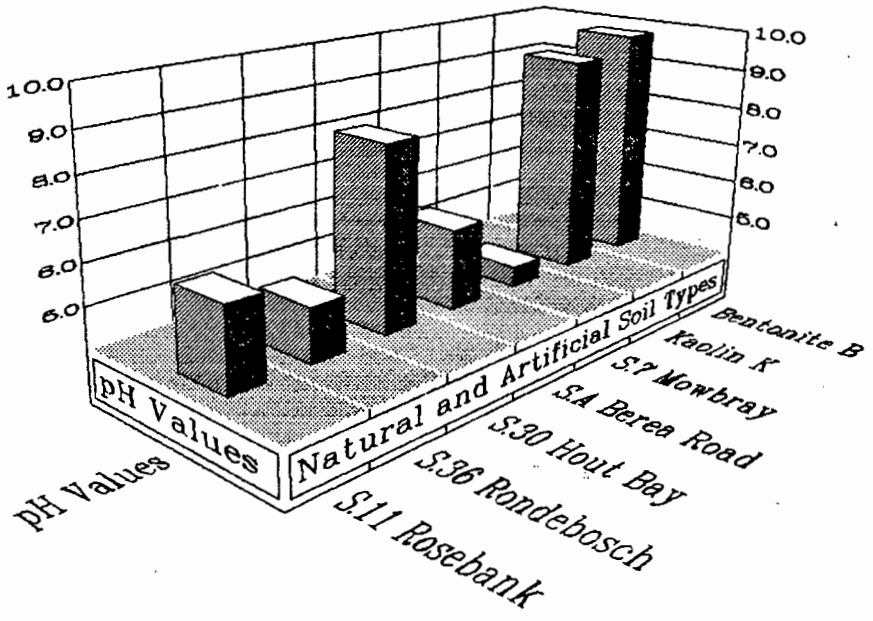

Figure 10.07: pH values - Natural and artificial soil types.

pH values for the soil types:-

With the exception of Site 30, Hout Bay (Cape), the pH values of the natural soil types fall within the acidic range (0 to 7). In the case of site 30, the pH value of 8.5 falls within the alkaline range (7 to 14).

In the case of the artificial soil types, measured pH values of 9.4 and 9.8, (for Kaolin and Bentonite respectively) fall in the alkaline range.

5) Soil Density versus Water Content.

Based on compaction tests for both the standard and modified AASHTO, Figures 10.08 and 10.09 illustrate the maximum and minimum values of void ratio 'e', porosity 'n' and degree of saturation 'Sr'.
These values were obtained from the plot of Dry density versus Water ratio for each soil type.

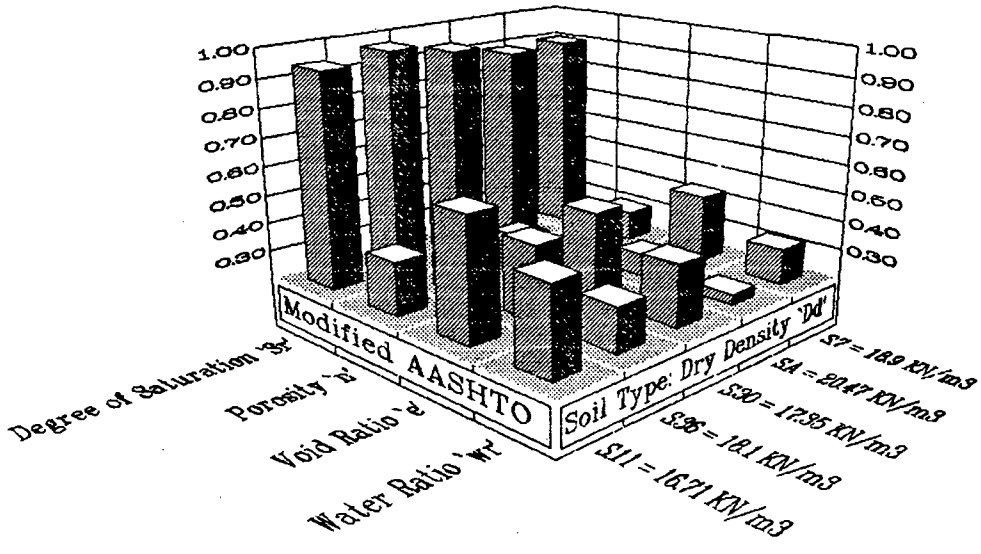

Figure 10.08: Dry Density versus Water Ratio [Mod][1] includes values of void ratio, porosity and degree of saturation.

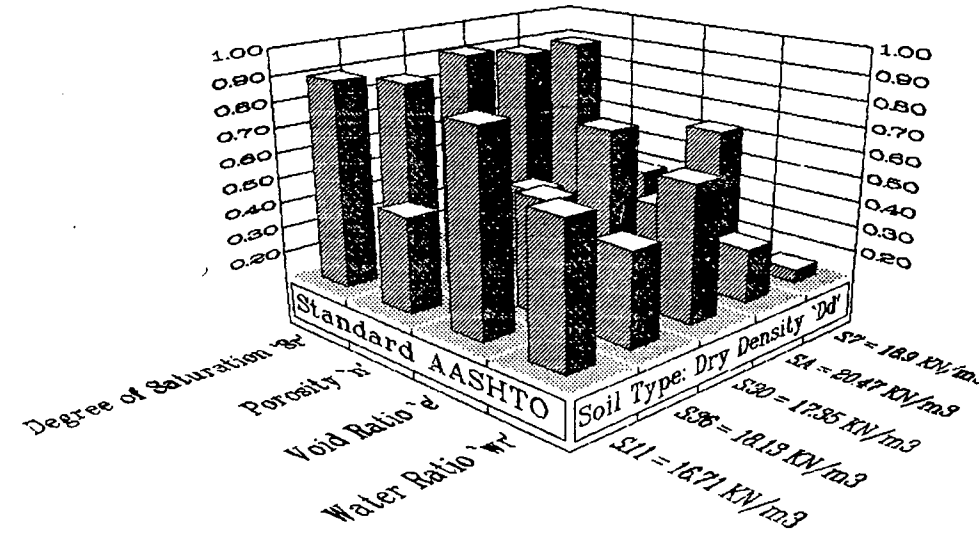

Figure 10.09: Dry Density versus Water Ratio [Std][2] includes values of void ratio, porosity and degree of saturation.

---

1 - Modified AASHTO.
2 - Standard AASHTO.

10.2.2 Micro Structure and Clay Minerals.

Previous studies have dealt with the relationship between free swelling and the b-dimension of montmorillonite lattice. It has been found that free swelling is related to the dimensions of the montmorillonite lattice, and as the water content of a given montmorillonite increases, so also does the b-dimension, as illustrated in Figure 10.10 (previously included in Chapter Two as Figure 2.30). Thus, free swelling is proportional to both the initial b-dimension and to the change in b-dimension.

For every sample studied by Ravina and Louw[1], the b-dimension increased progressively with water content from its initial value, which was characteristic of each dry montmorillonite, to a final value of ≈ 9.0A, which was common to all montmorillonites. The latter value was reached when the water content of the respective montmorillonites were equal to those at maximal swelling. It was also found that when these water contents are plotted against the corresponding changes in b-dimension a straight line that passed through the origin was obtained.

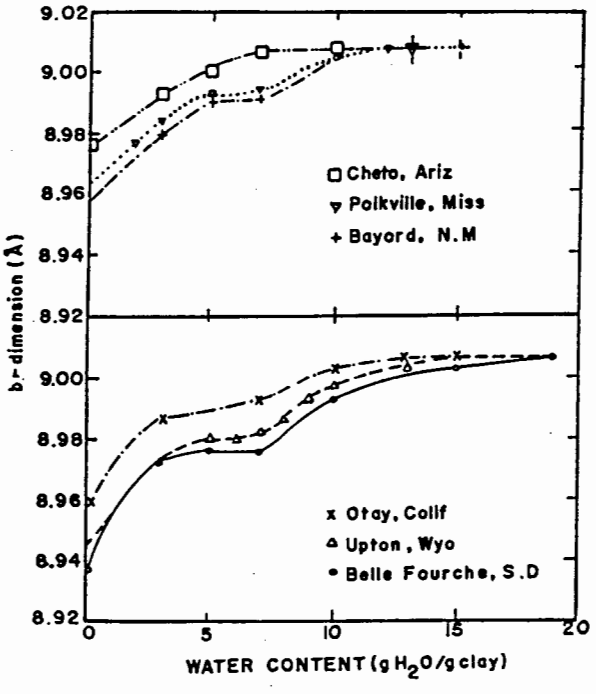

Figure 10.10: Relation between b-dimension and water content for six Na-saturated dioctahedral montmorillonites.

---

[1] - *Reference 78.*

All different structure-sensitive properties of water in montmorillonite-water systems (that is, the partial specific volume, amount remaining unfrozen at -5°C, and activation energy for ions to move through) were correlated with the b-dimension of the associated montmorillonite.

The results indicated that epitaxy exists between crystal lattice of montmorillonite and adsorbed water and that these lattices undergo mutual adjustment with each increment of water. The resulting loss of free energy causes water adsorption, that is swelling, to occur spontaneously.
Swelling stops when no further adjustment takes place. This does not happen until the adsorbed water is several angstrons thick and has achieved a preferred configuration.

The identification of clay minerals, by x-ray diffraction of the data[1], is summarized in Table 10.01.

Table 10.01: Mineralogical analysis of the natural soil types (sites 11, 36, 30, A and 7) and artificial ones (Kaolin `K' and Bentonite `B').

Sample description	Mineral identified: Names	Chemical formula.
S.11	Kaolinite	$Al_2Si_2O_5(OH)_4$
	Muscovite	$KAl_2(Si_3Al)O_{10}(OH,F)_2$
	Montmorillonite	$Na_{0.3}(AlMg)_2Si_4O_{10}OH_2xH_2O$
S.36	Kaolinite	$Al_2Si_2O_5(OH)_4$
	Muscovite	$KAl_2(Si_3Al)O_{10}(OH,F)_2$
	Hematite	Fe_2O_3
S.30	Kaolinite	$Al_2Si_2O_5(OH)_4$
	Muscovite	$KAl_2(Si_3Al)O_{10}(OH,F)_2$
S.A	Alpha-Quartz	ALPHA- SiO_2
	Kaolinite	$Al_2Si_2O_5(OH)_4$
	Hematite	Fe_2O_3
S.7	Kaolinite	$Al_2Si_2O_5(OH)_4$
	Muscovite	$KAl_2(Si_3Al)O_{10}(OH,F)_2$
	Hematite	Fe_2O_3
K	Kaolinite	$Al_2Si_2O_5(OH)_4$
	Kaolinite-Smectite	Al-Si-O-OH-H_2O
	Muscovite	$KAl_2(Si_3Al)O_{10}(OH,F)_2$
BE	Clinochlore	$Mg_5Al(Si_3Al)O_{10}(OH)_8$
	Alpha-Quartz	ALPHA- SiO_2

[1] - *refer to section 2.4.4. of chapter two.*

10.3 CONCLUDING SUMMARY FOR PART TWO OF THE THESIS

10.3.1 Free Expansion Limit.

Free Expansion Limit has previously been defined[1] as the water content (expressed as the final water ratio), above which the unrestrained soil sample will not swell any further.
The Free Expansion Limit values, shown below, are for the natural and artificial soil types used in this thesis.

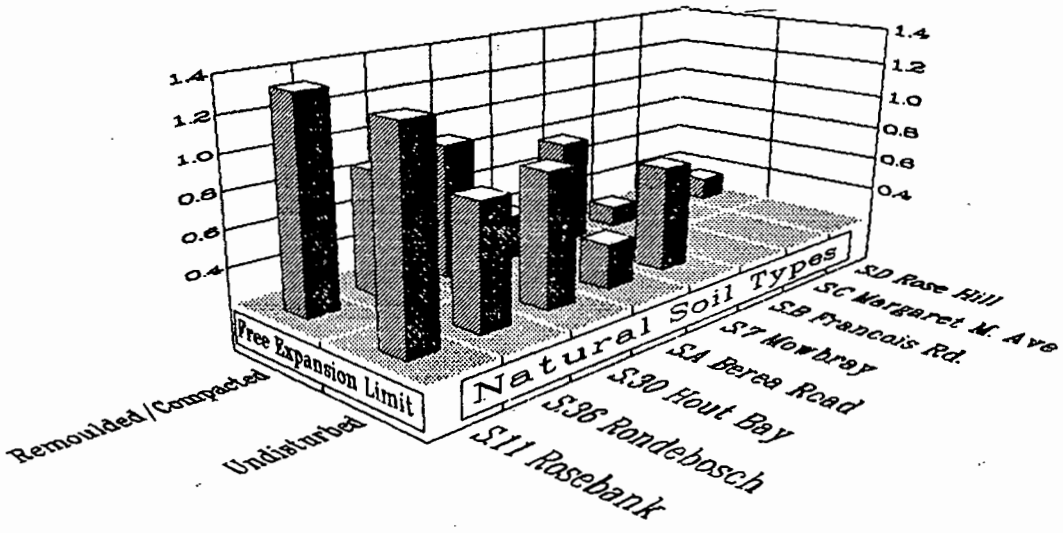

Figure 10.11: Free Expansion Limit - Natural Soil Types.

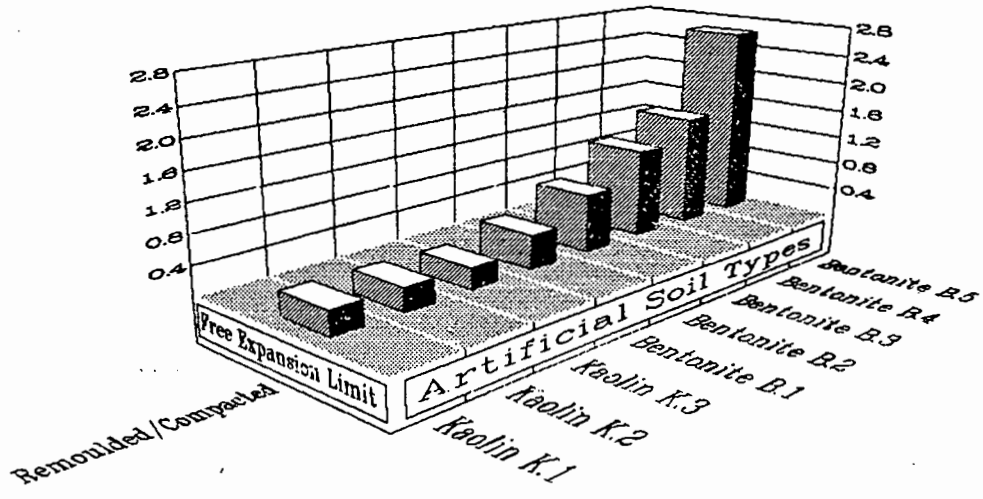

Figure 10.12: Free Expansion Limit - Artificial Soil Types.

---

[1] - refer to chapter four.

10.3.2 Relationships between Free Expansion Limit and the Consistency Limits.

Free Expansion Limit 'FEL' and Liquid Limit 'LL'.

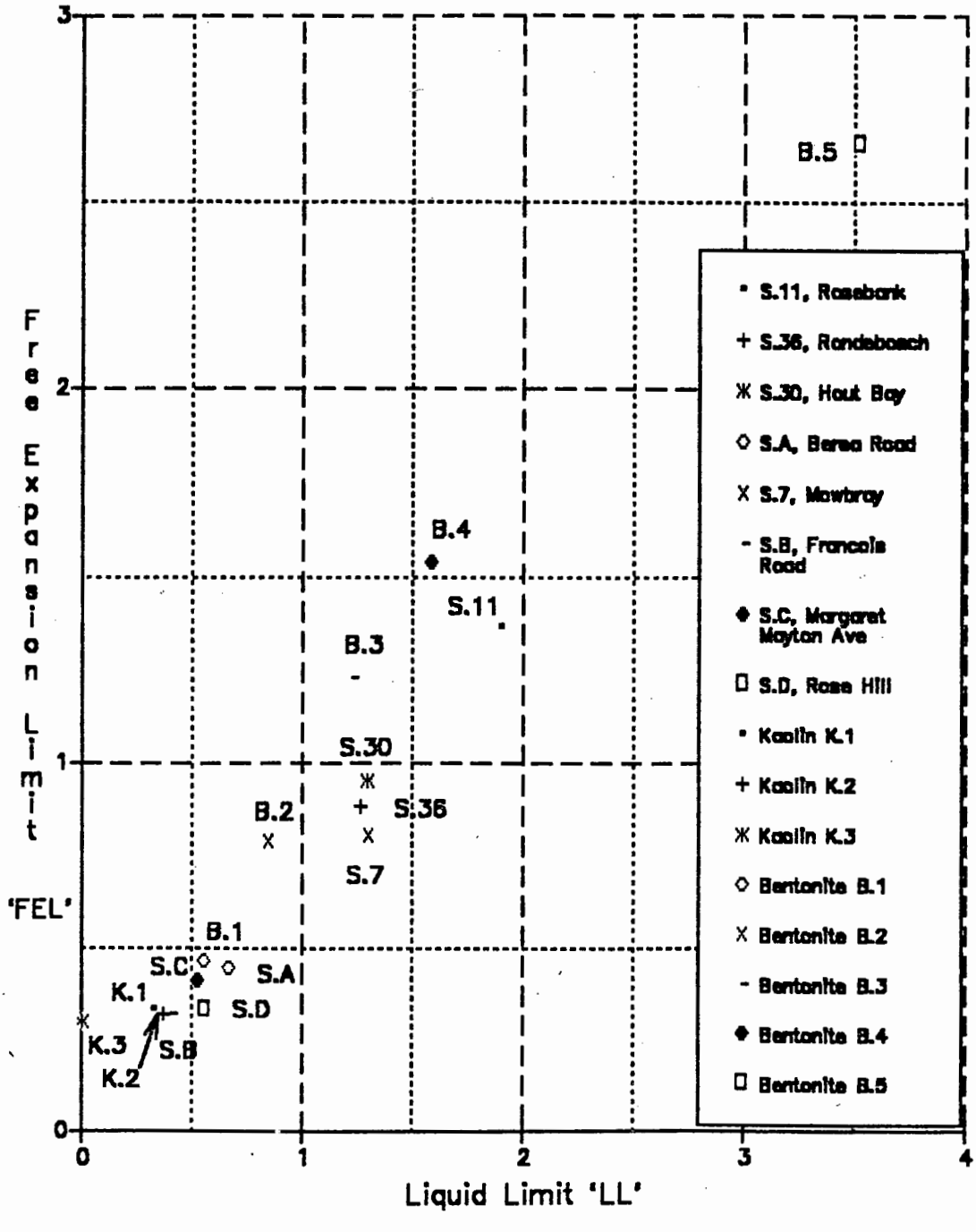

Figure 10.13: Relationship between Free Expansion Limit and Liquid Limit*.*

* - *expressed as a water ratio.*

Free Expansion Limit 'FEL'and Plastic Limit 'PL'.

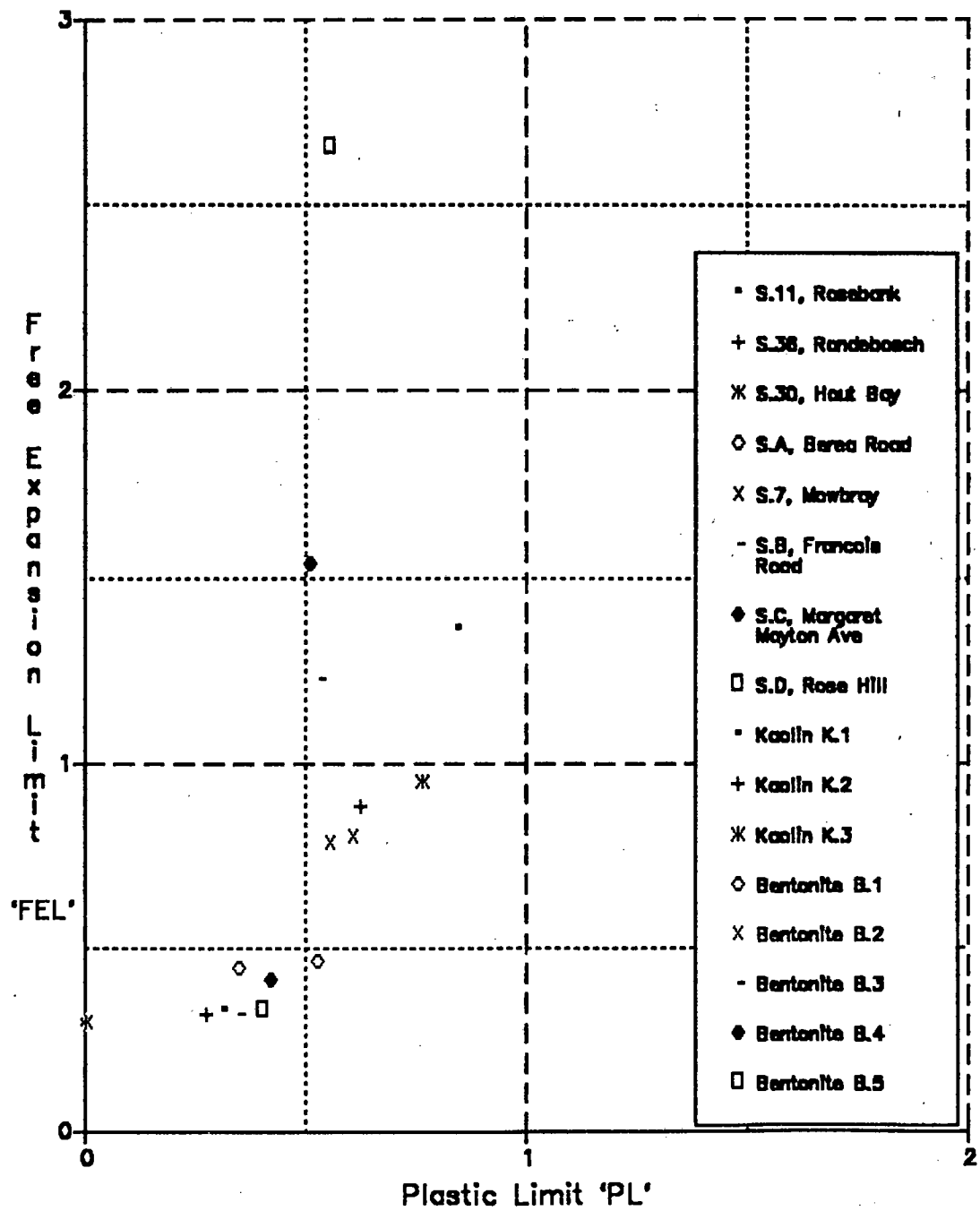

Figure 10.14: Relationship between Free Expansion Limit and Plastic Limit*.*

* - *expressed as a water ratio.*

Free Expansion Limit 'FEL' and Linear Shrinkage 'LS'.

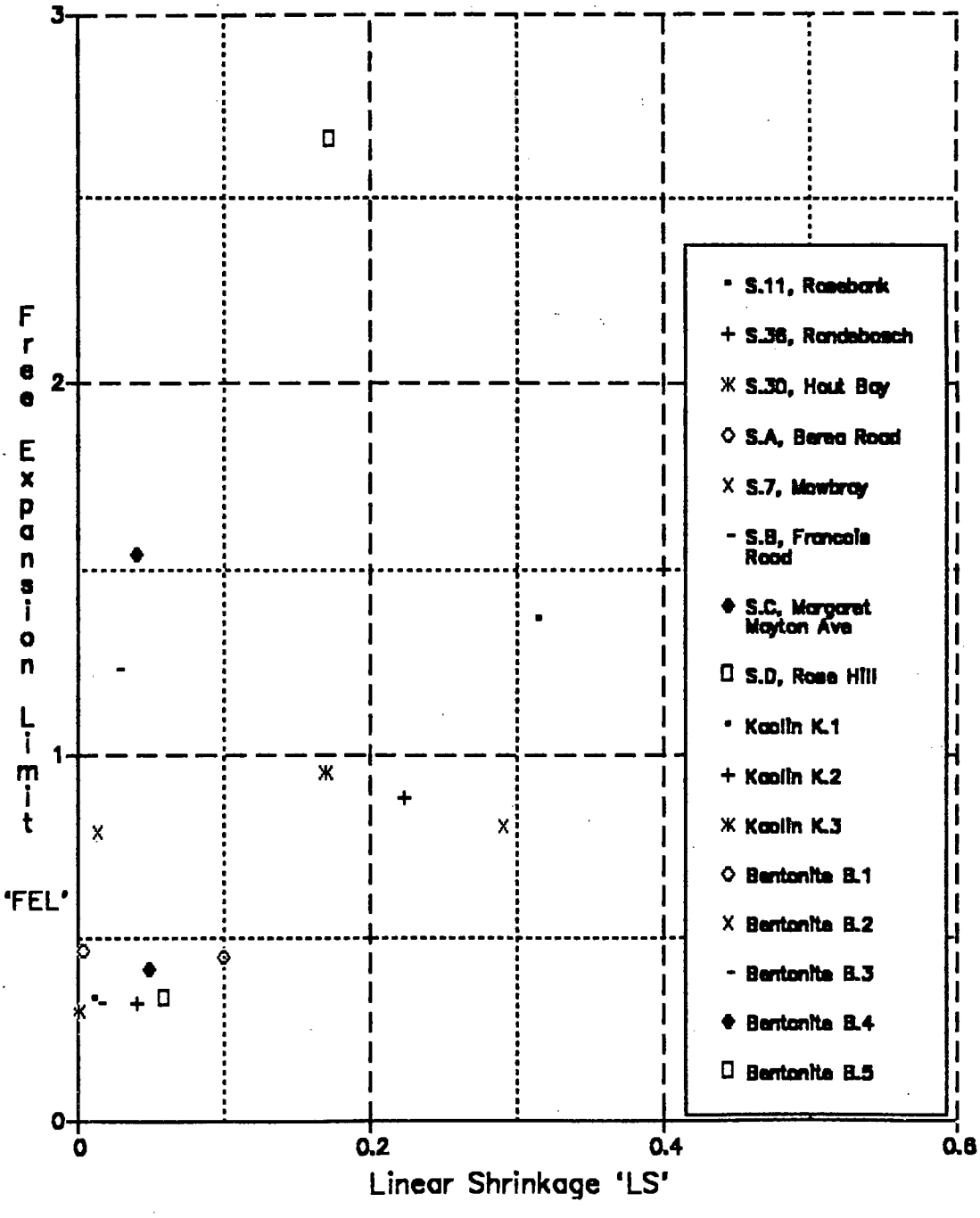

Figure 10.16: Relationship between Free Expansion Limit and Linear Shrinkage*.*

* - *expressed as a water ratio.*

10.3.3 Free Swell Paths.

The relationship between void ratio 'e', or change in void ratio 'de', and water ratio 'wr' (or 'Ω'), or change in water ratio 'dwr' (or 'dΩ'), at each value of degree of saturation, is related by a constant C which is also a function of 'e' and/or 'Sr'.

Plots of void ratio versus water ratio for the free swell paths, over the full range of degree of saturation, were studied in chapter four[1].
The purpose was to determine whether 'C' behaved like a constant, or as a function of 'Sr' and/or 'e'.
The slope of each free swell curve, at the points of intersection with known values of degree of saturation, was correlated by means of one of two equations:

$$\frac{de}{dwr} = C_{x\%\ (\text{at } Sr)} \times Sr; \qquad \ldots 10.3.3(1)$$

$$\frac{de}{dwr} = C_{x\%(Sr\ \&\ e)} \times Sr \times e \qquad \ldots 10.3.3(2)$$

The values for the constant 'C' were plotted against the void ratio 'e' for both the natural and artificial soil types used in the thesis.
These relationships are shown in the figures below - refer to Figures 10.17 t0 10.48.

It should be noted that two plots are shown for each soil type - that is, one for each of the two equations above.

---

[1] - *refer to section 4.8.3.*

Site 11, Rosebank.

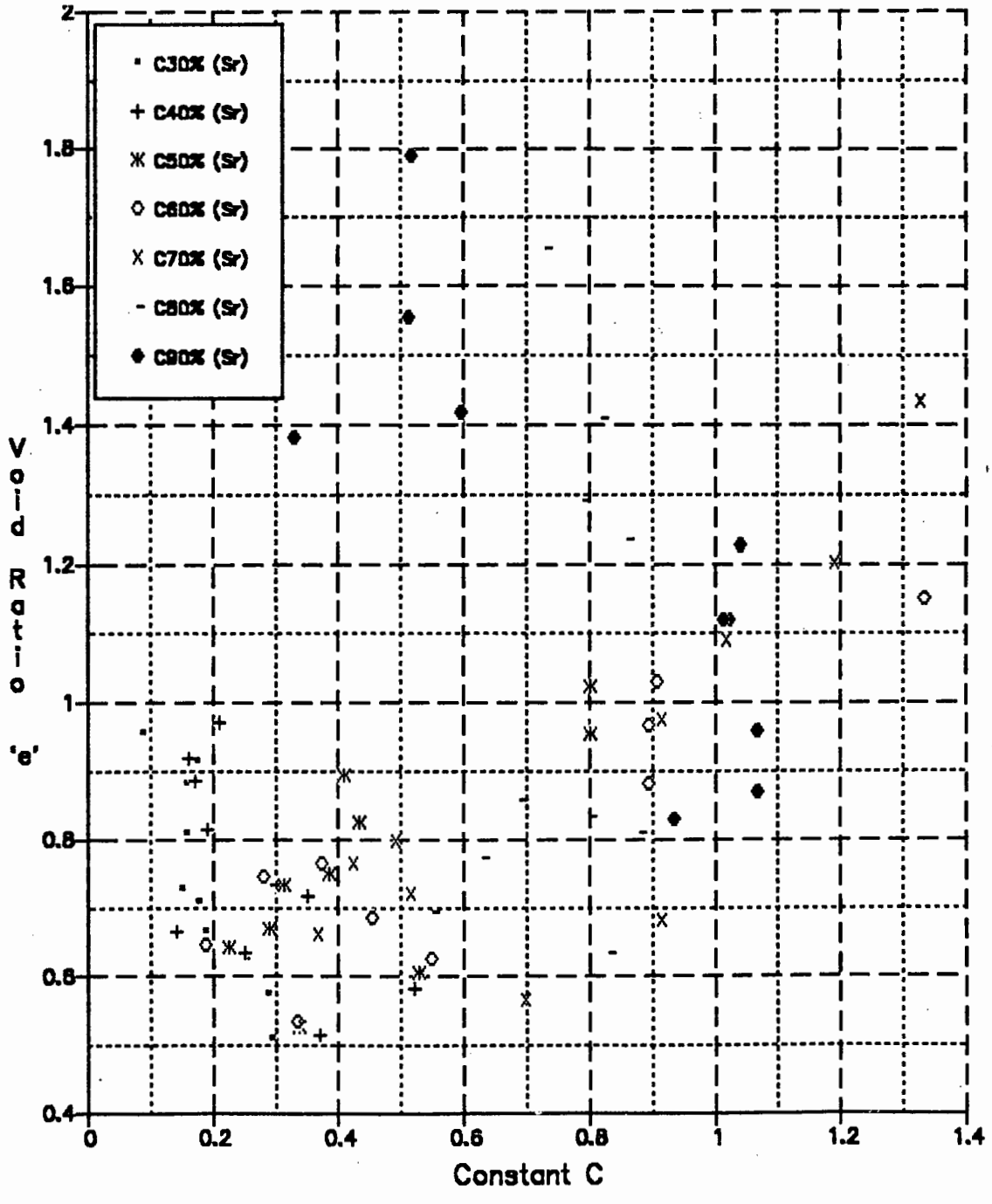

Figure 10.17: Site 11, Rosebank - Constant 'C' as function of degree of saturation 'Sr', in the Free Swell Paths[1].

[1] - *obtained in chapter four.*

Site 11, Rosebank.

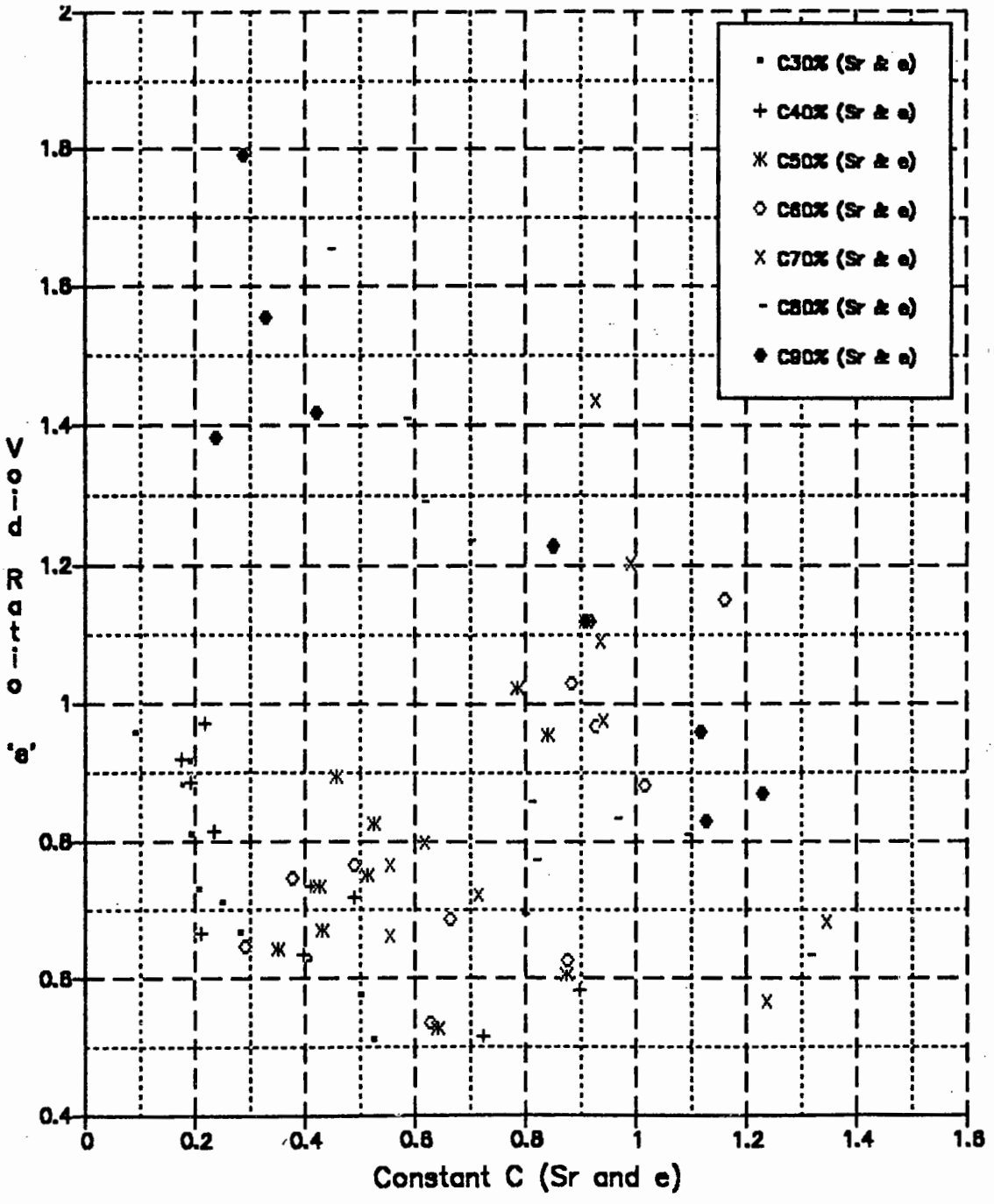

Figure 10.18: Site 11, Rosebank - Constant 'C' as function of degree of saturation 'Sr' and void ratio 'e', in the Free Swell Path[1].

---

[1] - see chapter four.

Site 36, Rondebosch.

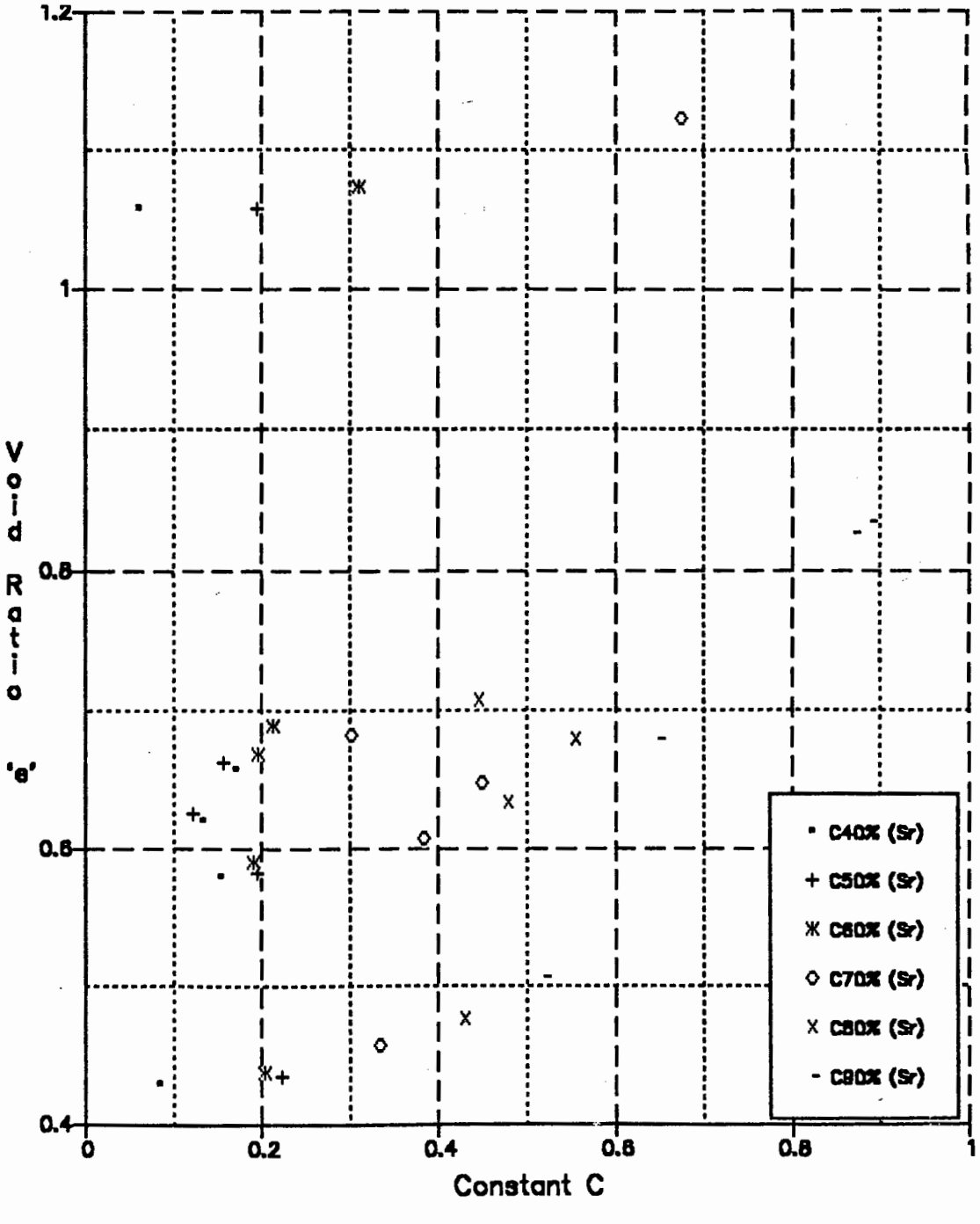

Figure 10.19: Site 36, Rondebosch - 'C' as function of 'Sr' in the Free Swell Paths[1].

---

[1] - *see chapter four.*

Site 36, Rondebosch.

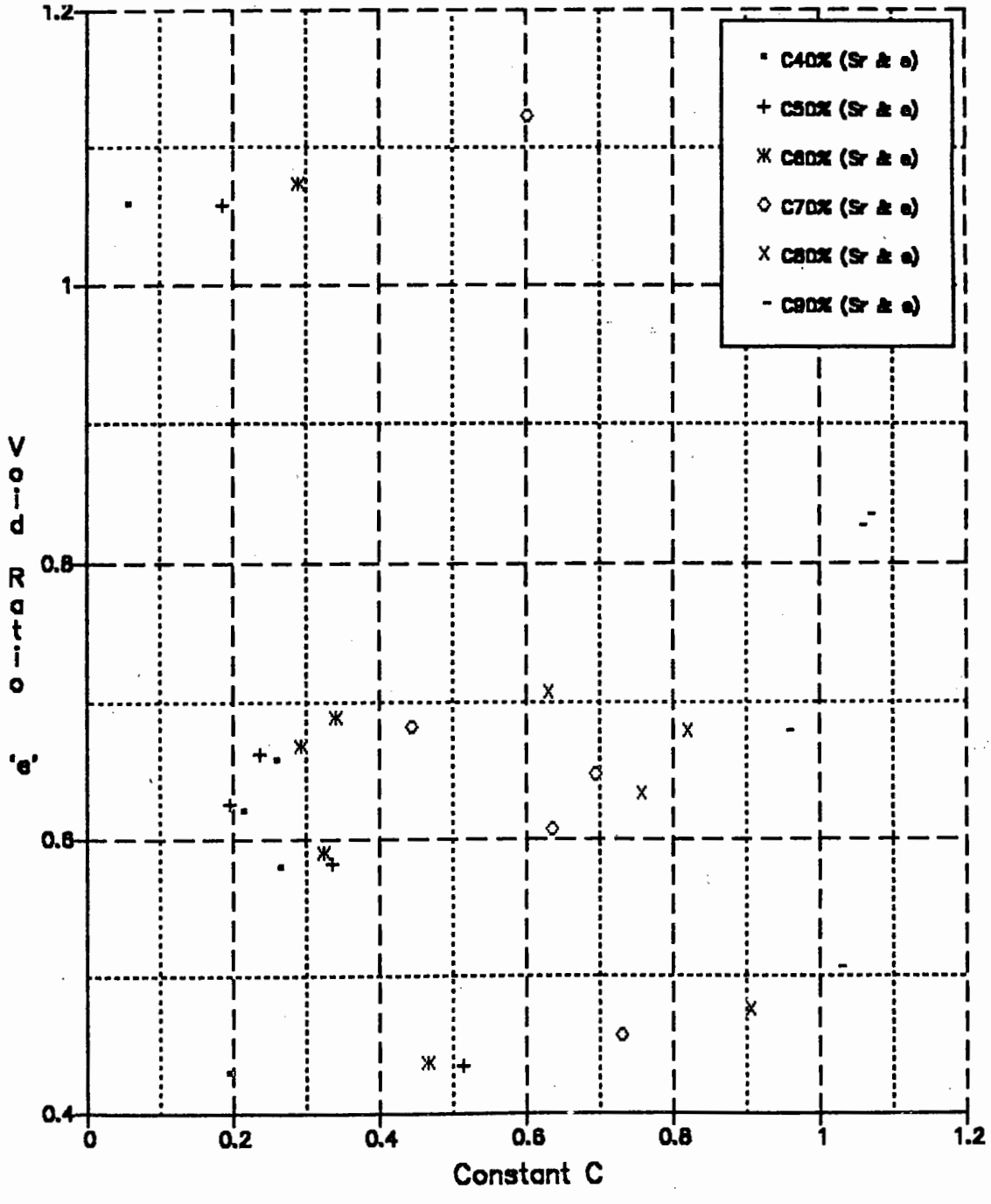

Figure 10.20: Site 36, Rondebosch - 'C' as function of 'Sr' and 'e' in the Free Swell Path[1].

[1] - *see chapter four.*

Site 30, Hout Bay.

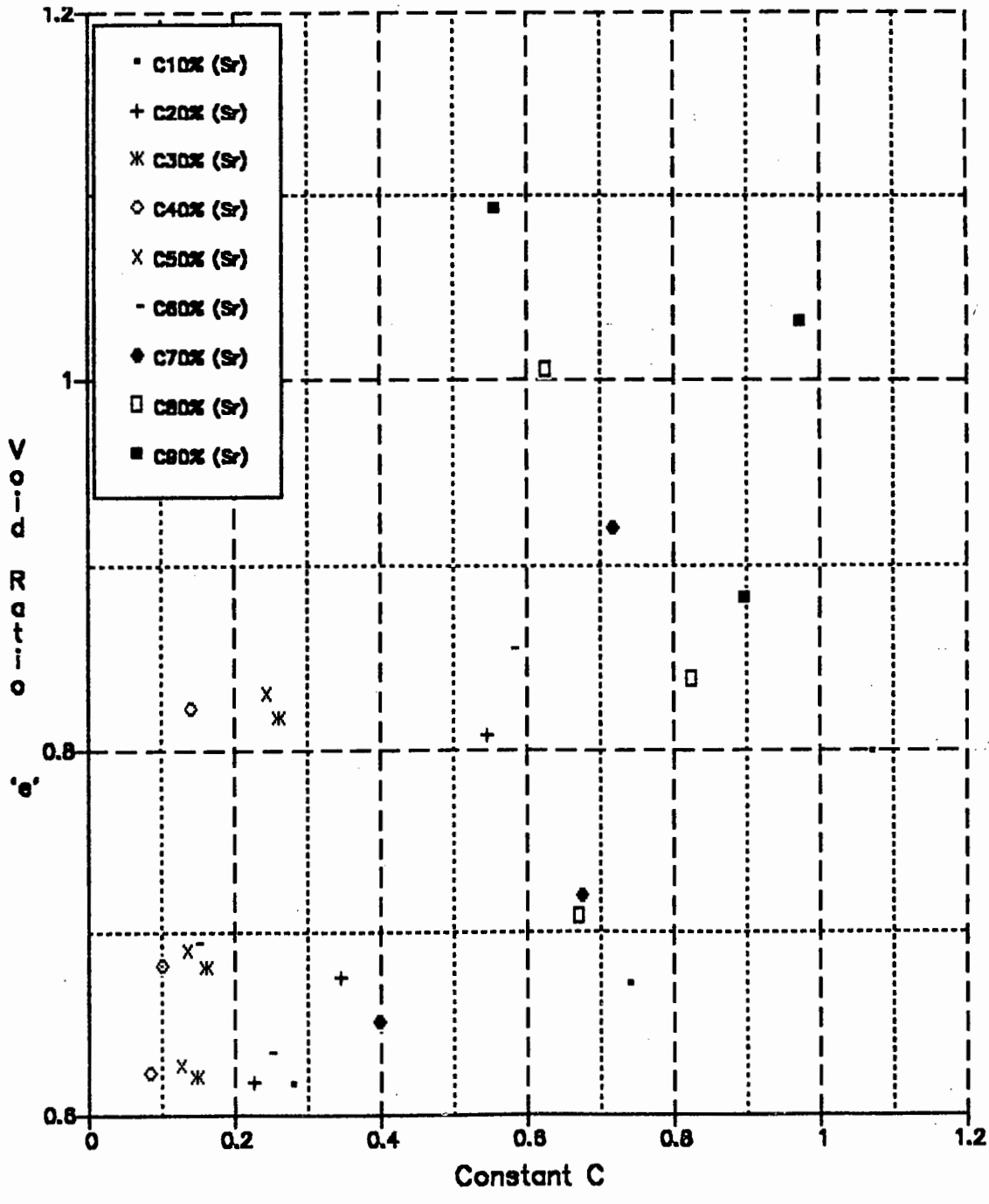

Figure 10.21: Site 30, Hout Bay - 'C' as function of 'Sr' in the Free Swell Paths[1].

[1] - *see chapter four.*

Site 30, Hout Bay.

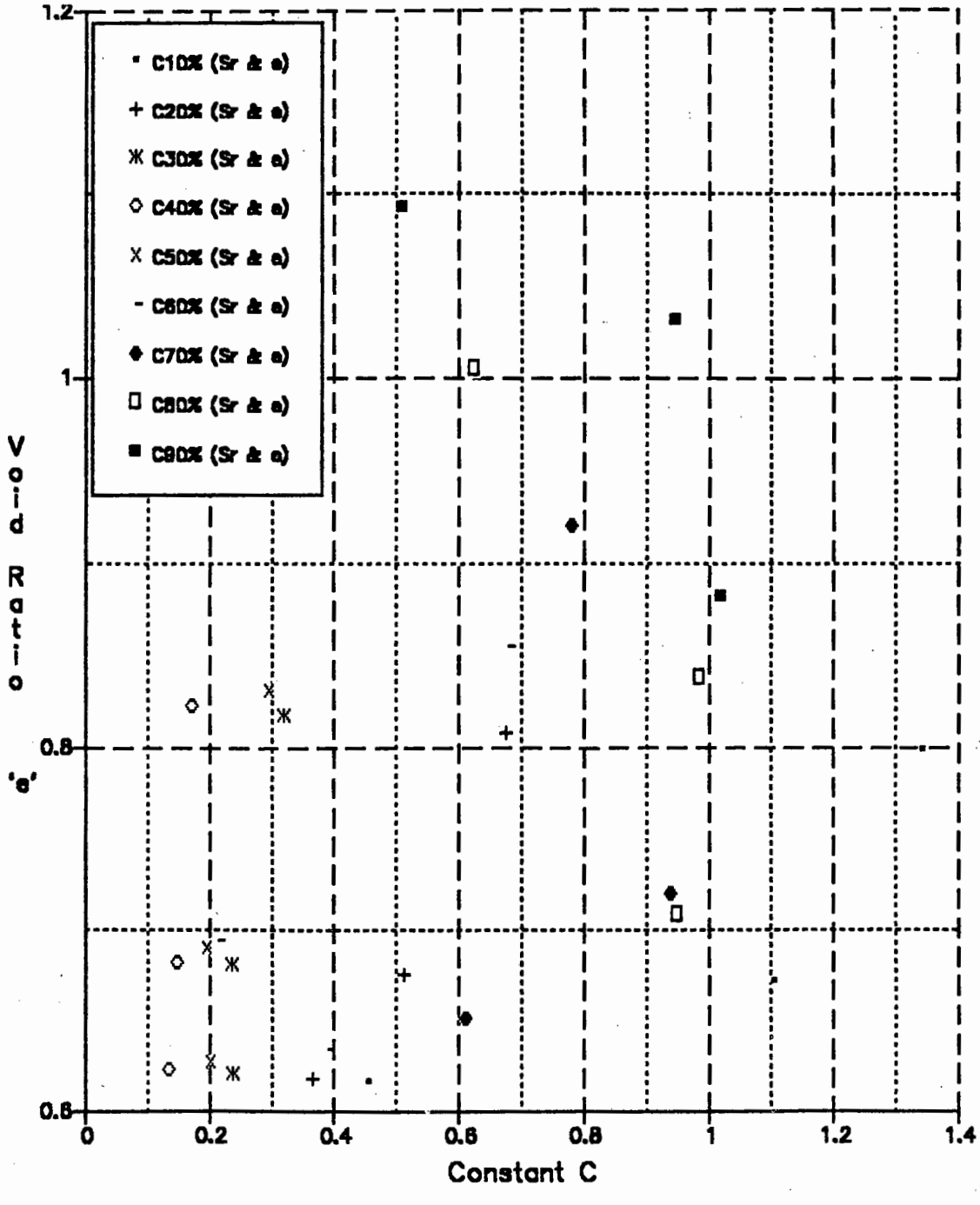

Figure 10.22: Site 30, Hout Bay - 'C' as function of 'Sr' and 'e' in the Free Swell Path[1].

---

[1] - *see chapter four.*

Site A, Berea Road.

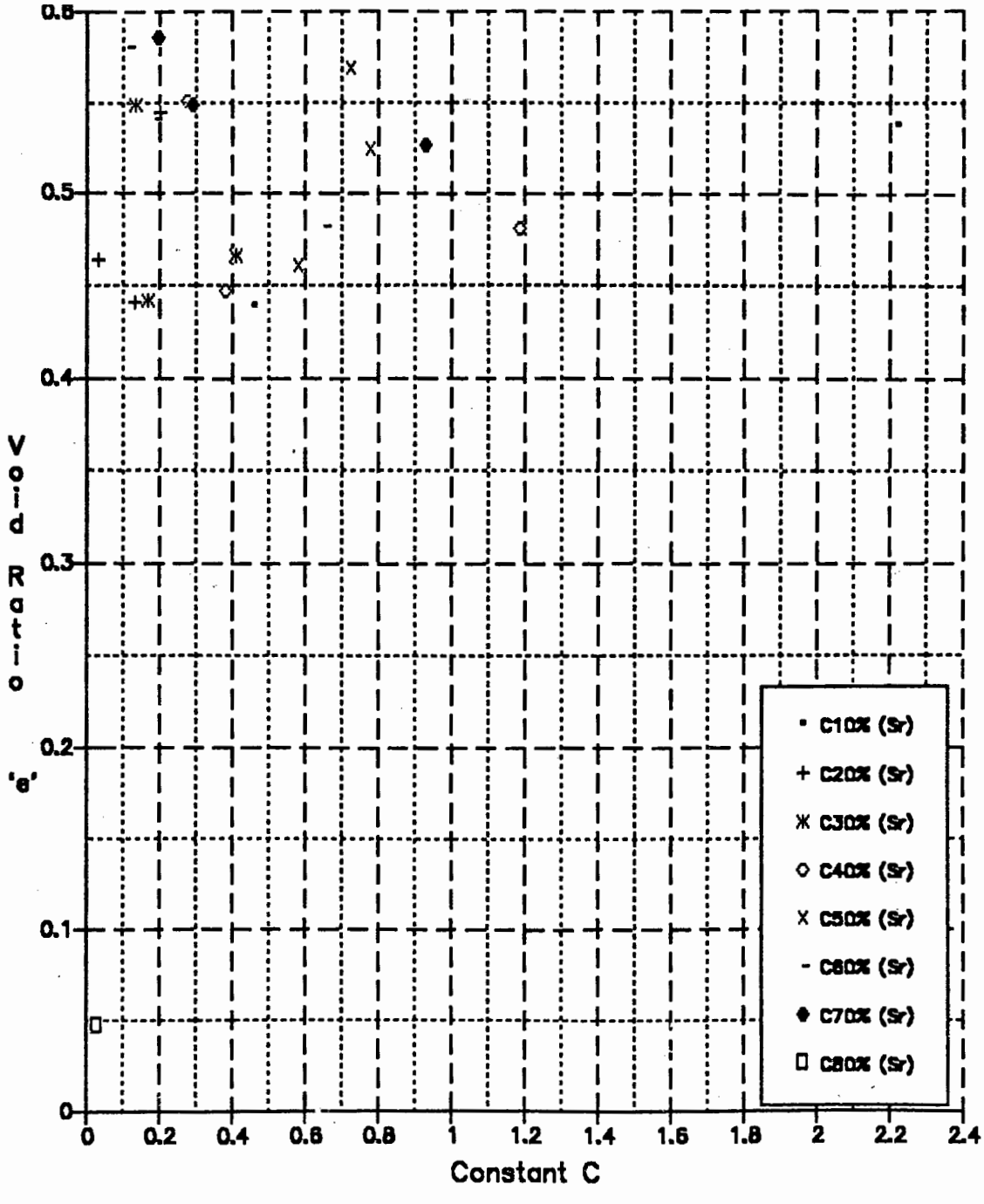

Figure 10.23: Site A, Berea Road - 'C' as function of 'Sr' in the Free Swell Paths[1].

---

[1] - *see chapter four.*

Site A, Berea Road.

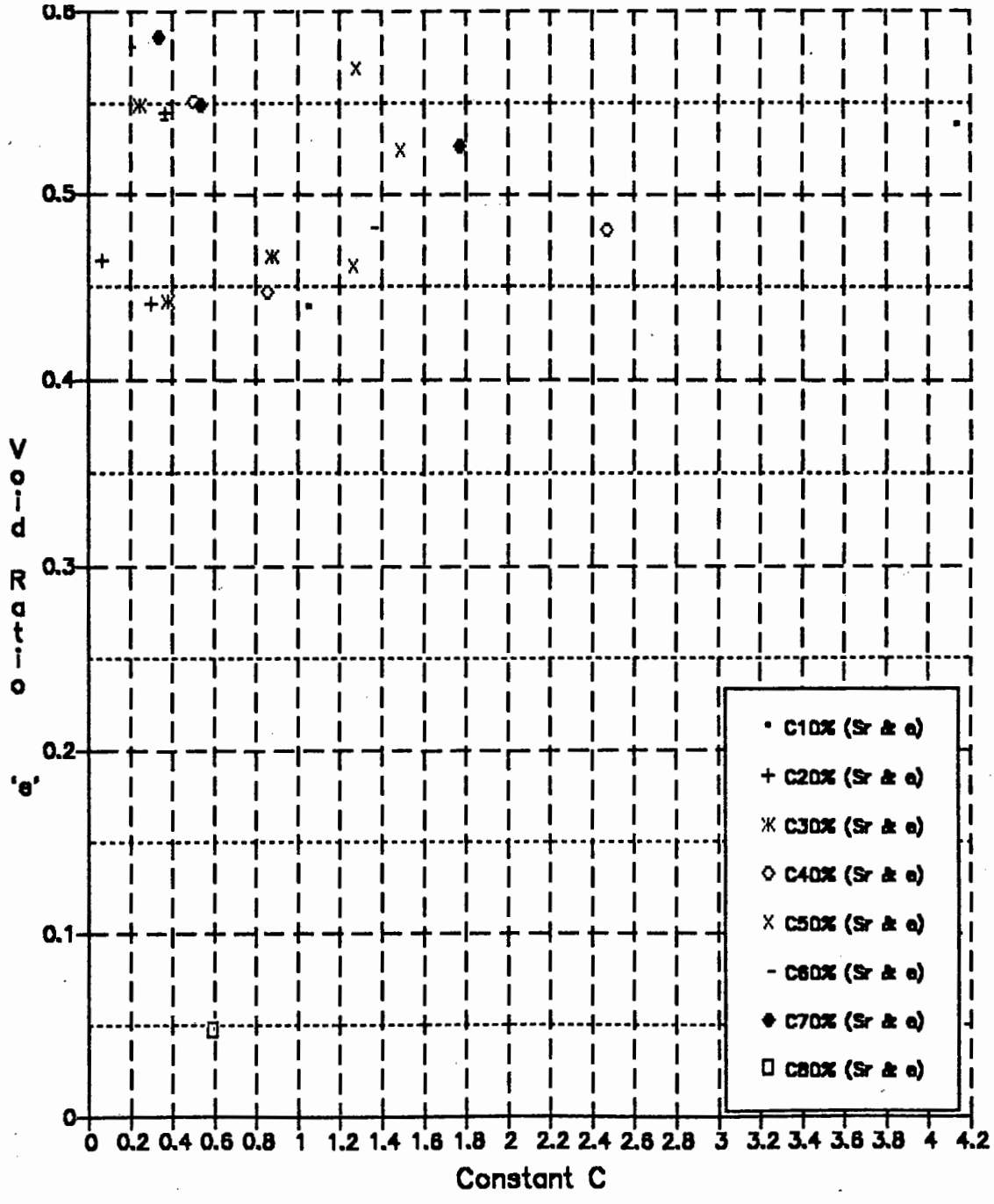

Figure 10.24: Site A, Berea Road - 'C' as function of 'Sr' and 'e' in the Free Swell Path[1].

---

[1] - *see chapter four.*

Site 7, Mowbray.

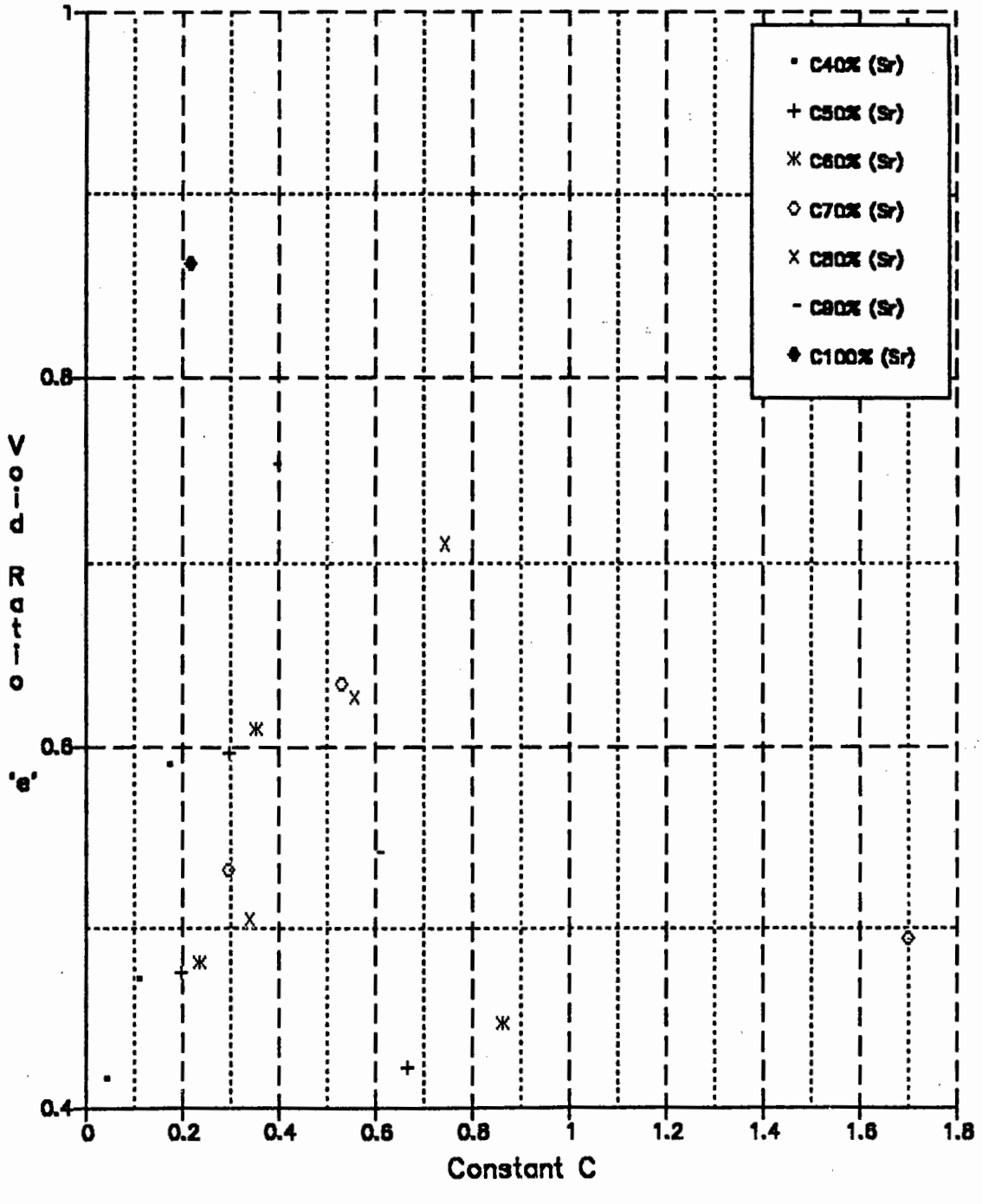

Figure 10.25: Site 7, Mowbray - 'C' as function of 'Sr' in the Free Swell Paths[1].

---

[1] - see chapter four.

Site 7, Mowbray.

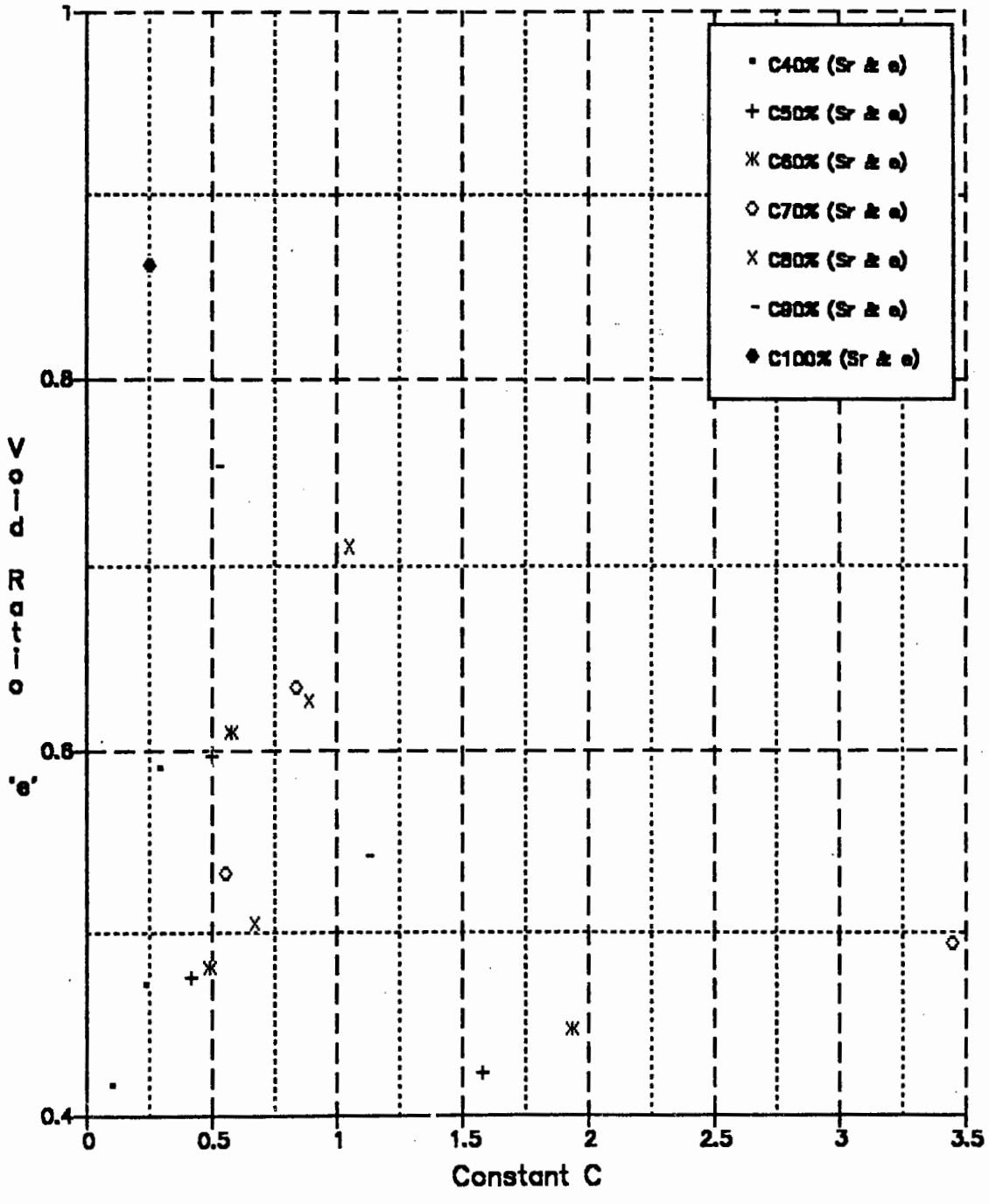

Figure 10.26: Site 7, Mowbray - 'C' as function of 'Sr' and 'e' in the Free Swell Path[1].

[1] - *see chapter four.*

Site B, Francois Road.

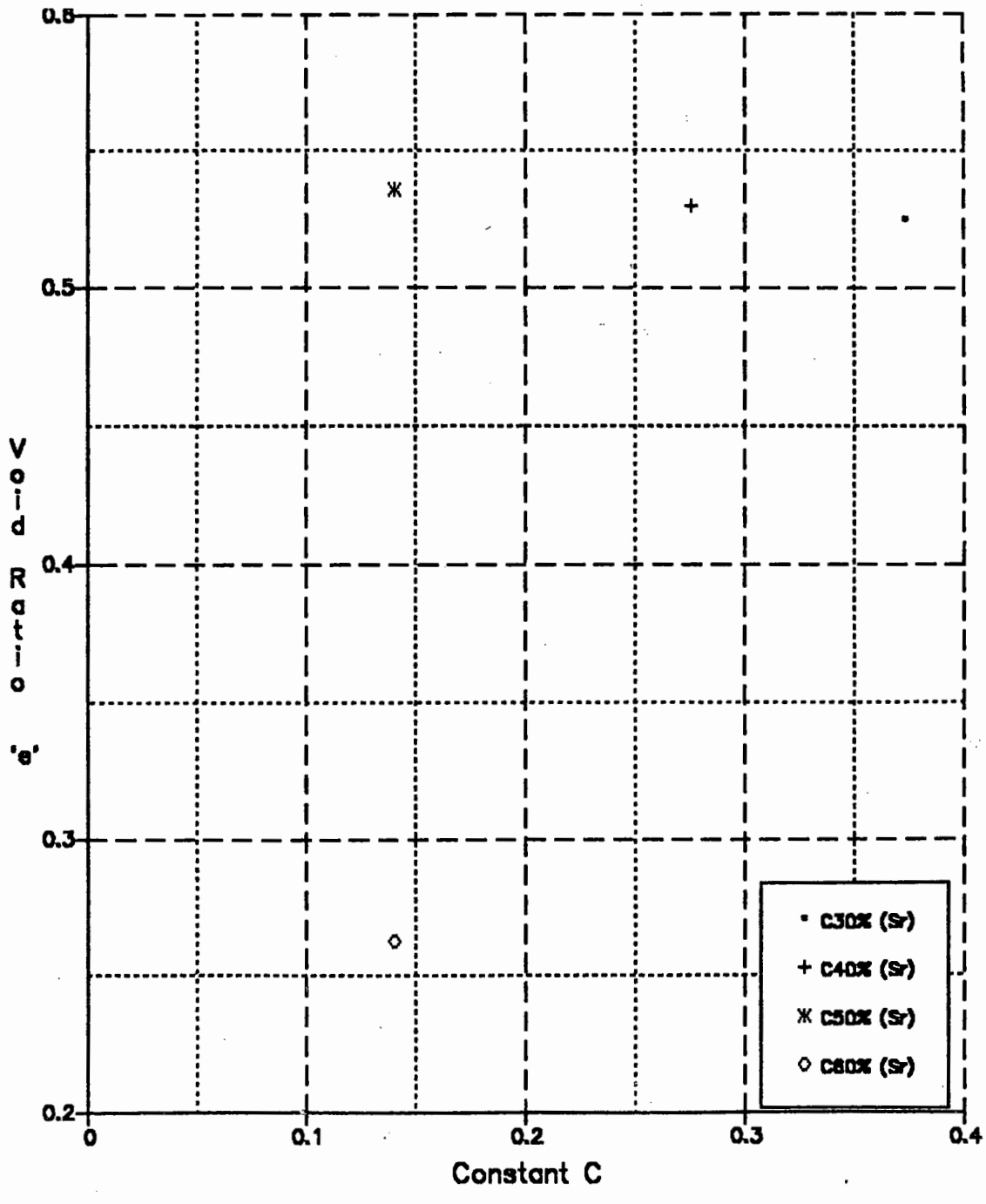

Figure 10.27: Site B, Francois Road - 'C' as function of 'Sr' in the Free Swell Paths[1].

[1] - see chapter four.

Site B, Francois Road.

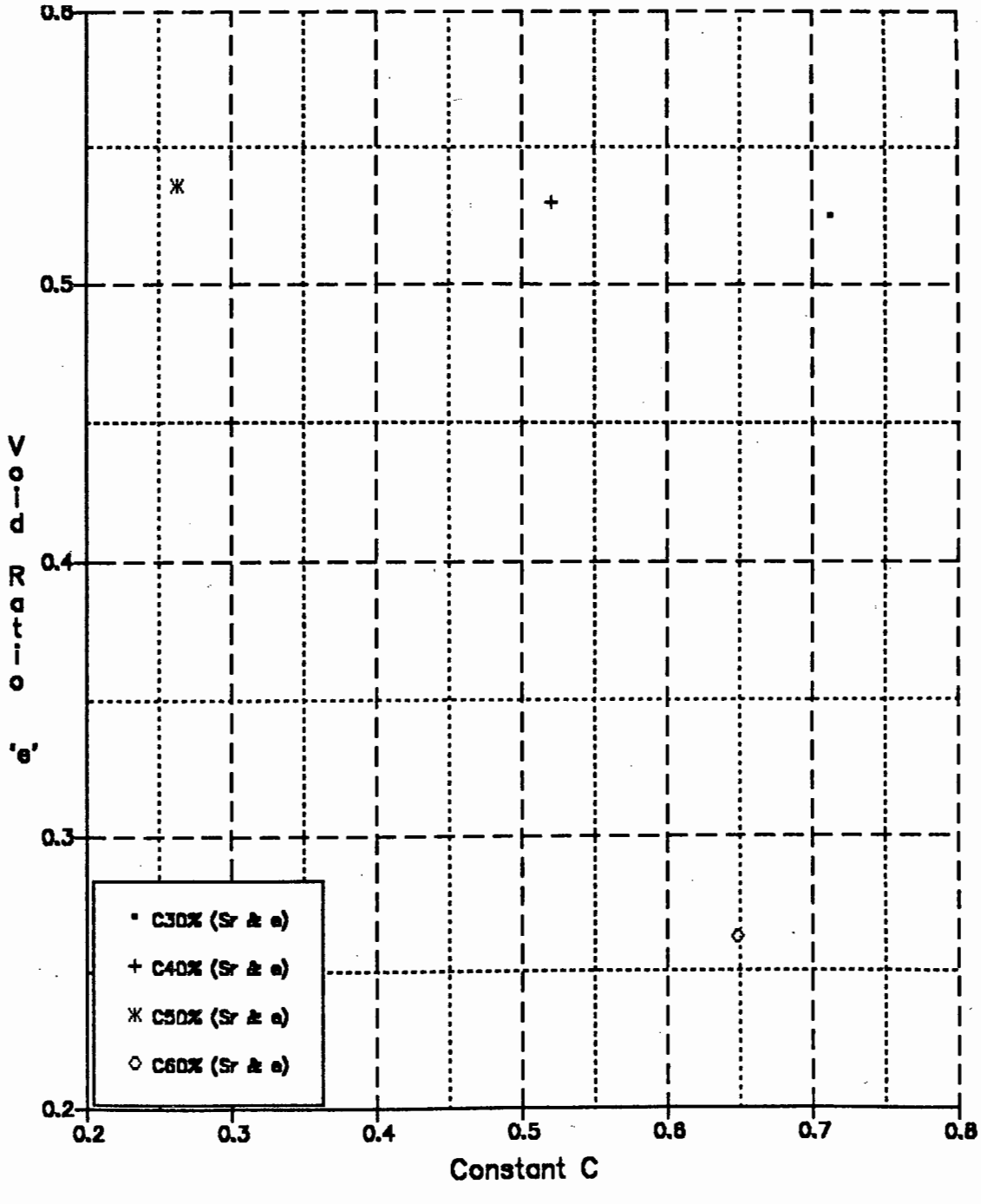

Figure 10.28: Site B, Francois Road - 'C' as function of 'Sr' and 'e' in the Free Swell Path[1].

---

[1] - *see chapter four.*

Site C, Margaret Mayton Avenue.

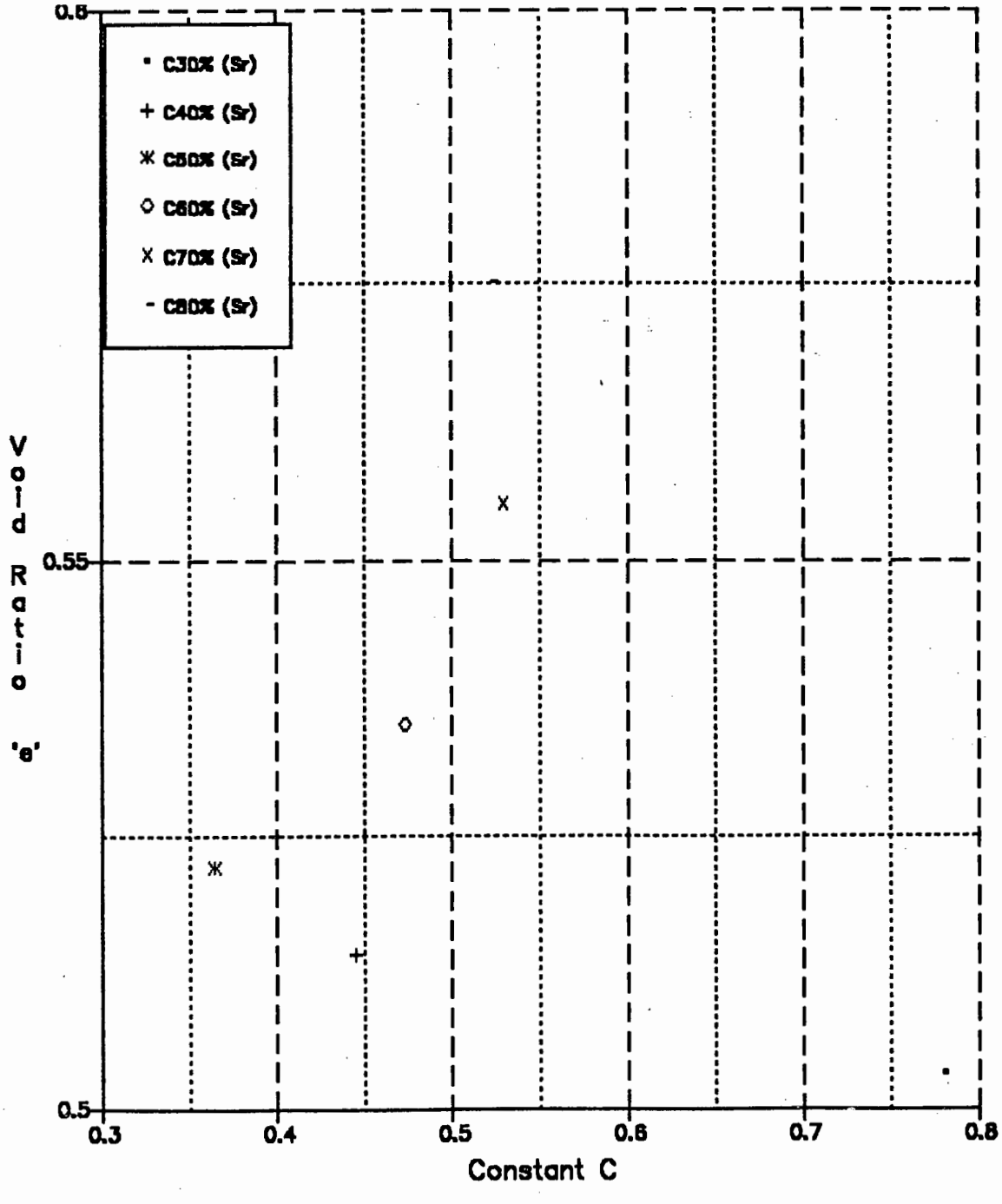

Figure 10.29: Site C, Margaret Mayton Avenue - 'C' as function of 'Sr' in the Free Swell Paths[1].

---

[1] - *see chapter four.*

Site C, Margaret Mayton Avenue.

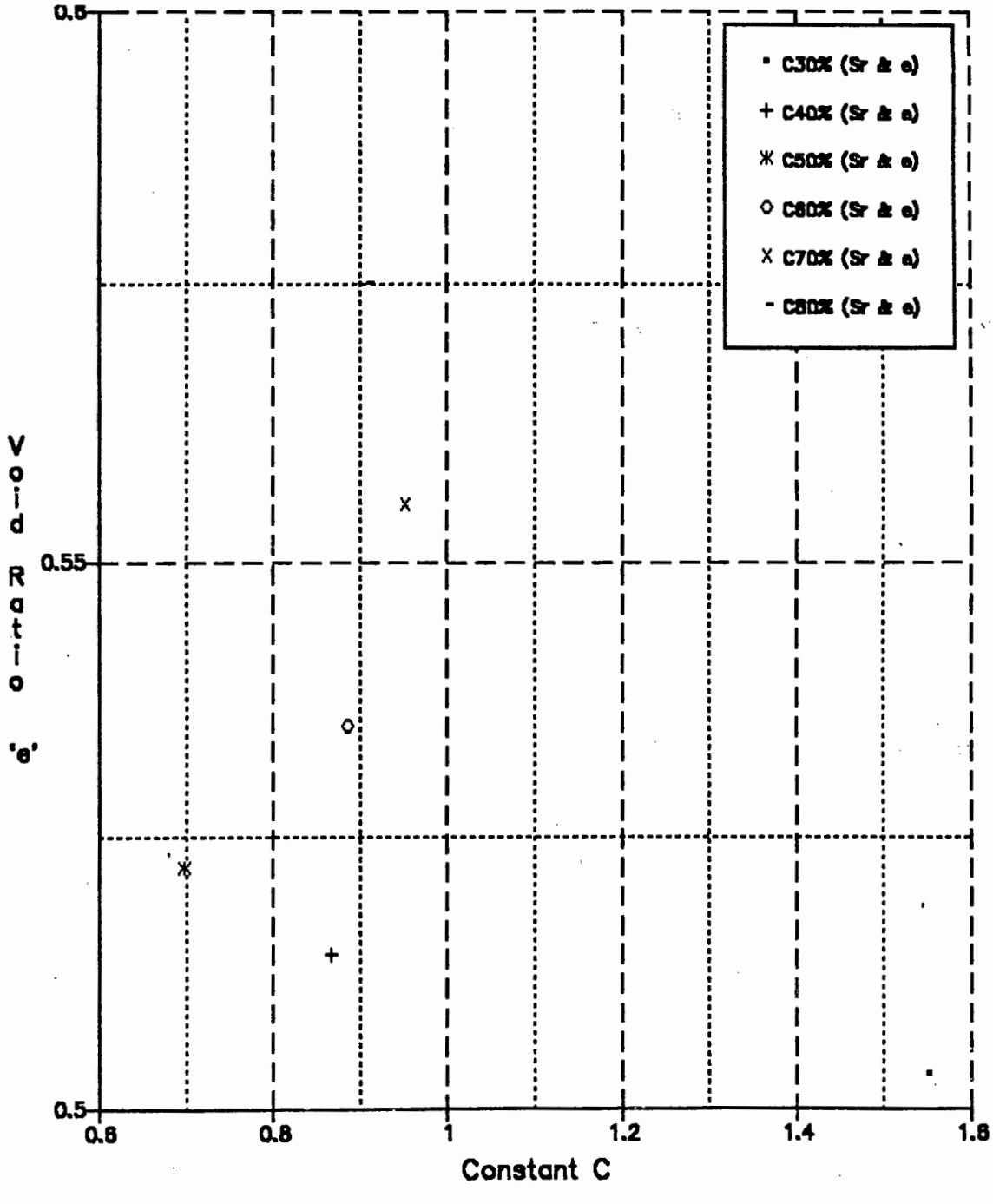

Figure 10.30: Site C, Margaret Mayton Avenue - 'C' as function of 'Sr' and 'e' in the Free Swell Path[1].

---

[1] - *see chapter four.*

Site D, Rose Hill.

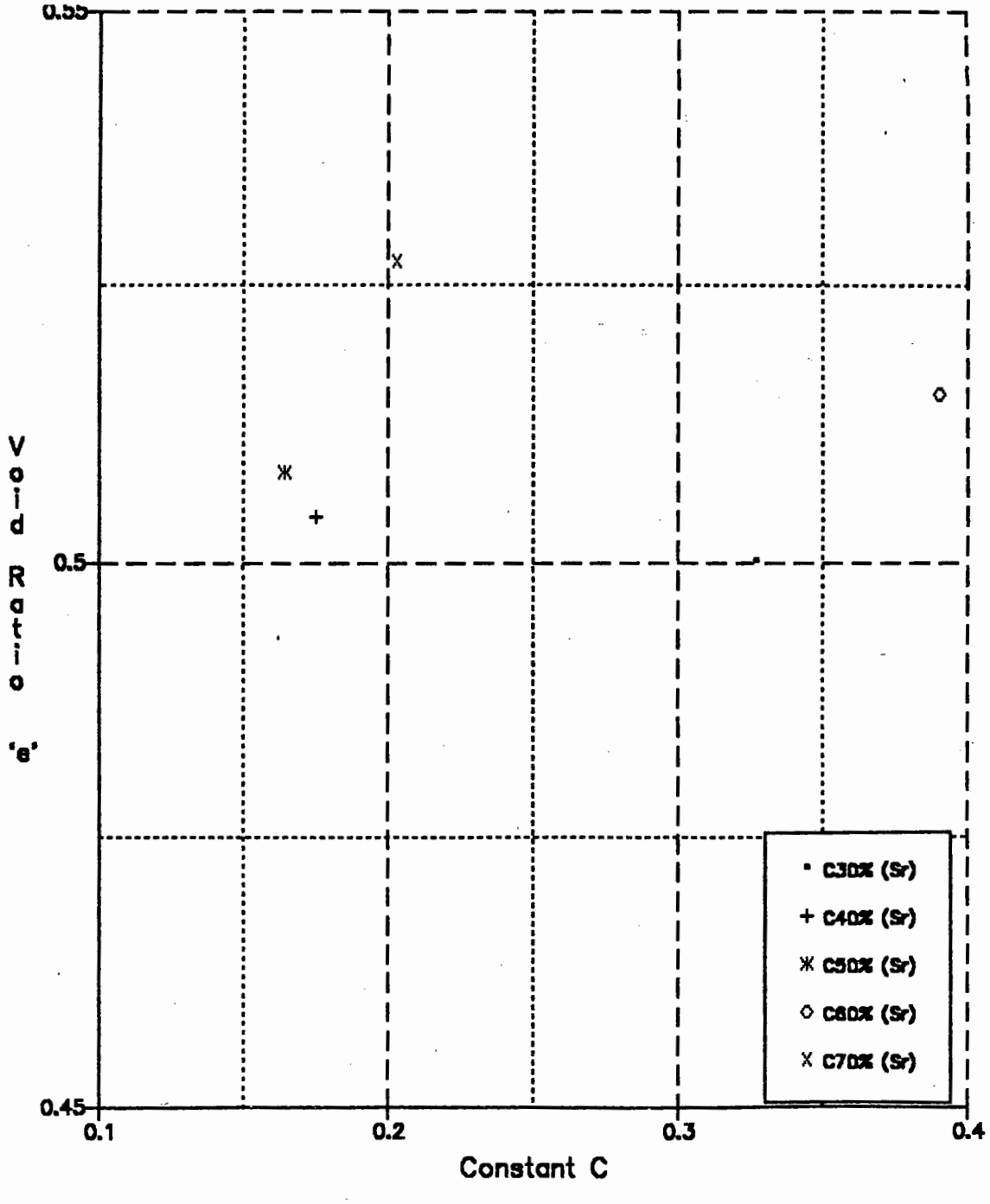

Figure 10.31: Site D, Rose Hill - 'C' as function of 'Sr' in the Free Swell Paths[1].

[1] - *see chapter four.*

Site D, Rose Hill.

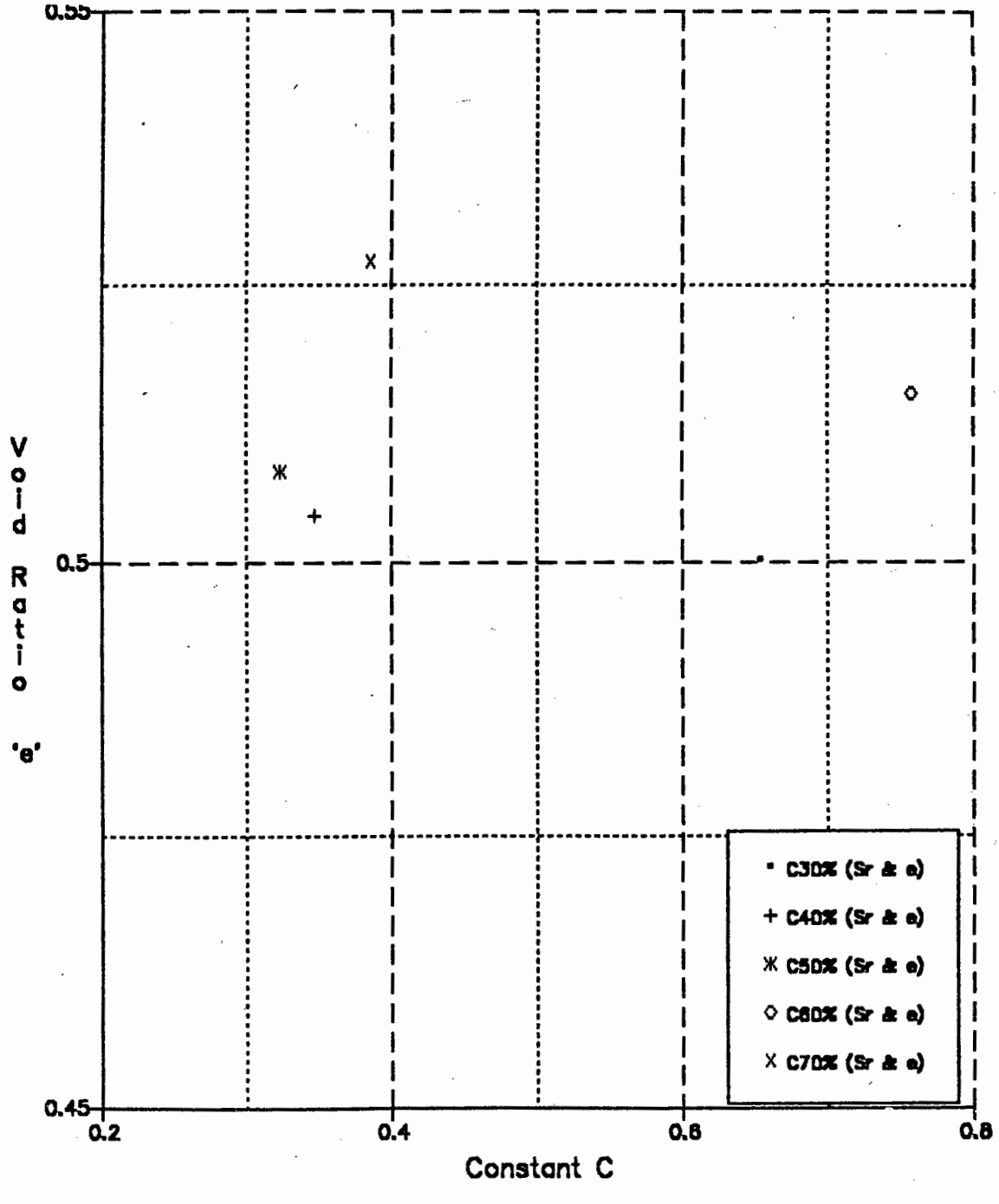

Figure 10.32: Site D, Rose Hill - 'C' as function of 'Sr' and 'e' in the Free Swell Path[1].

---

[1] - *see chapter four.*

Artificial Soil Types:-

Kaolin K.1 (13% clay).

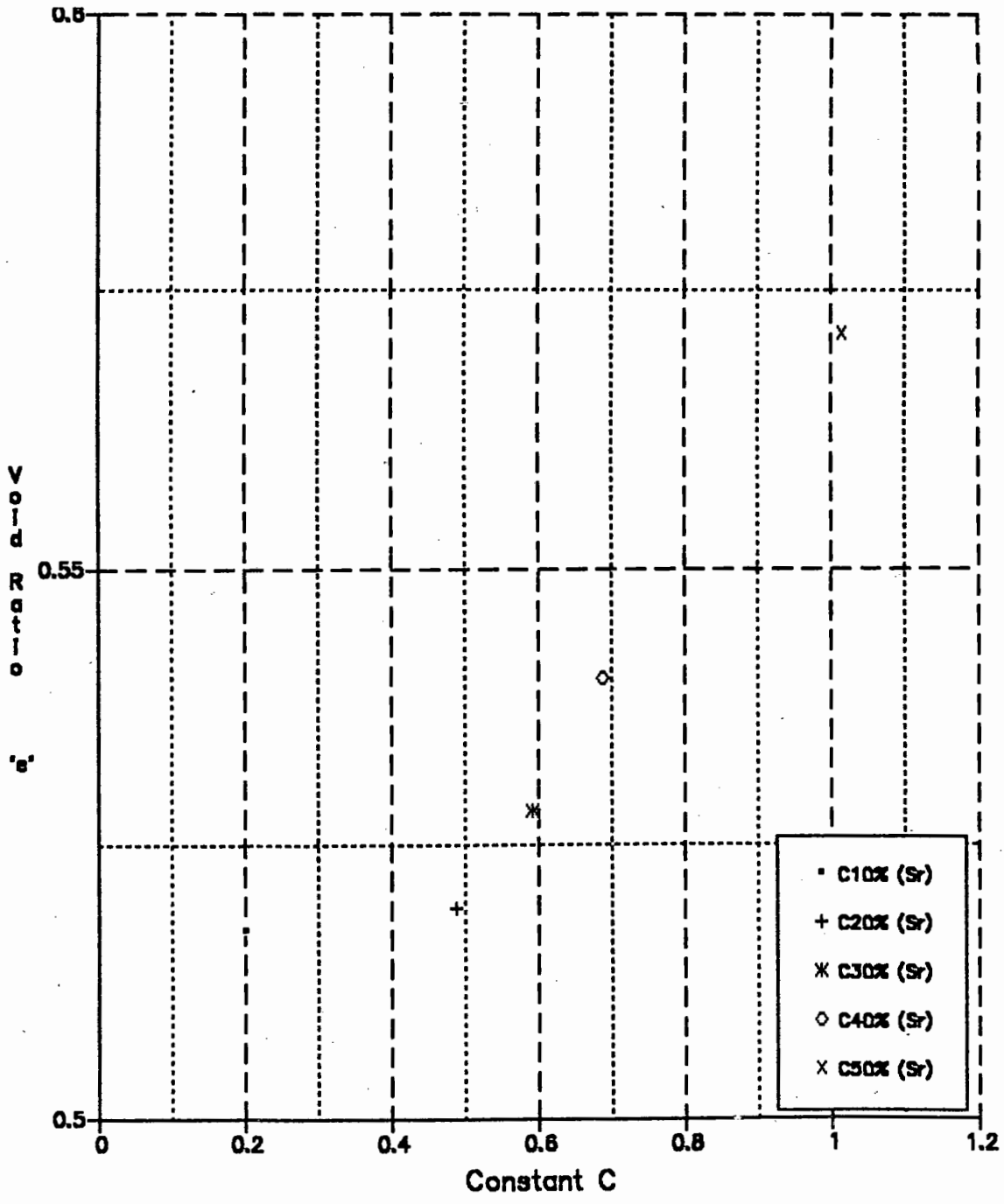

Figure 10.33: Kaolin K.1 (13% clay size) - 'C' as function of 'Sr' in the Free Swell Paths[1].

---

[1] - *see chapter four.*

Kaolin K.1 (13% clay size).

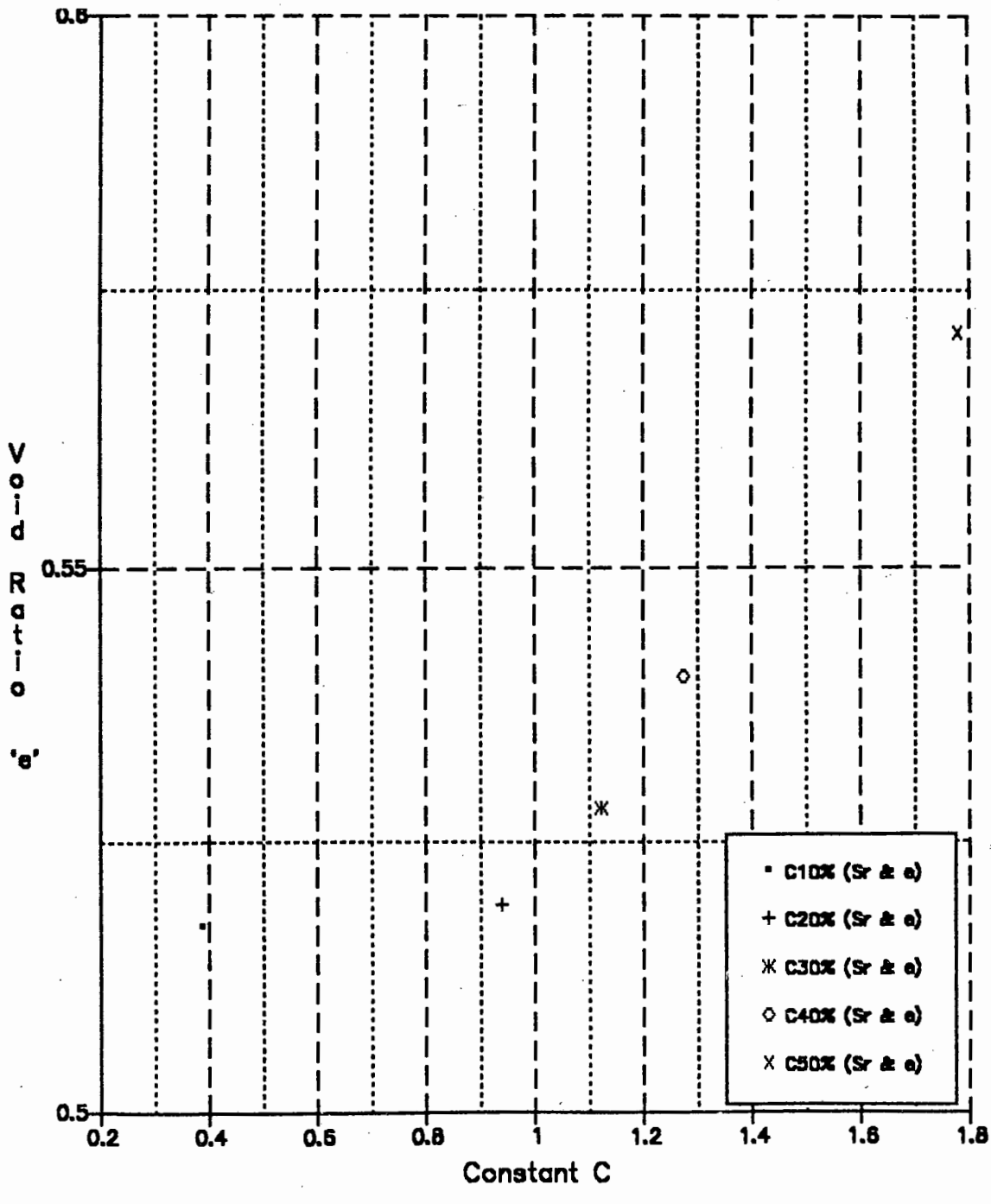

Figure 10.34: Kaolin K.1 (13% clay size) - 'C' as function of 'Sr' and 'e' in the Free Swell Path[1].

---

[1] - *see chapter four.*

Kaolin K.2 (20% clay).

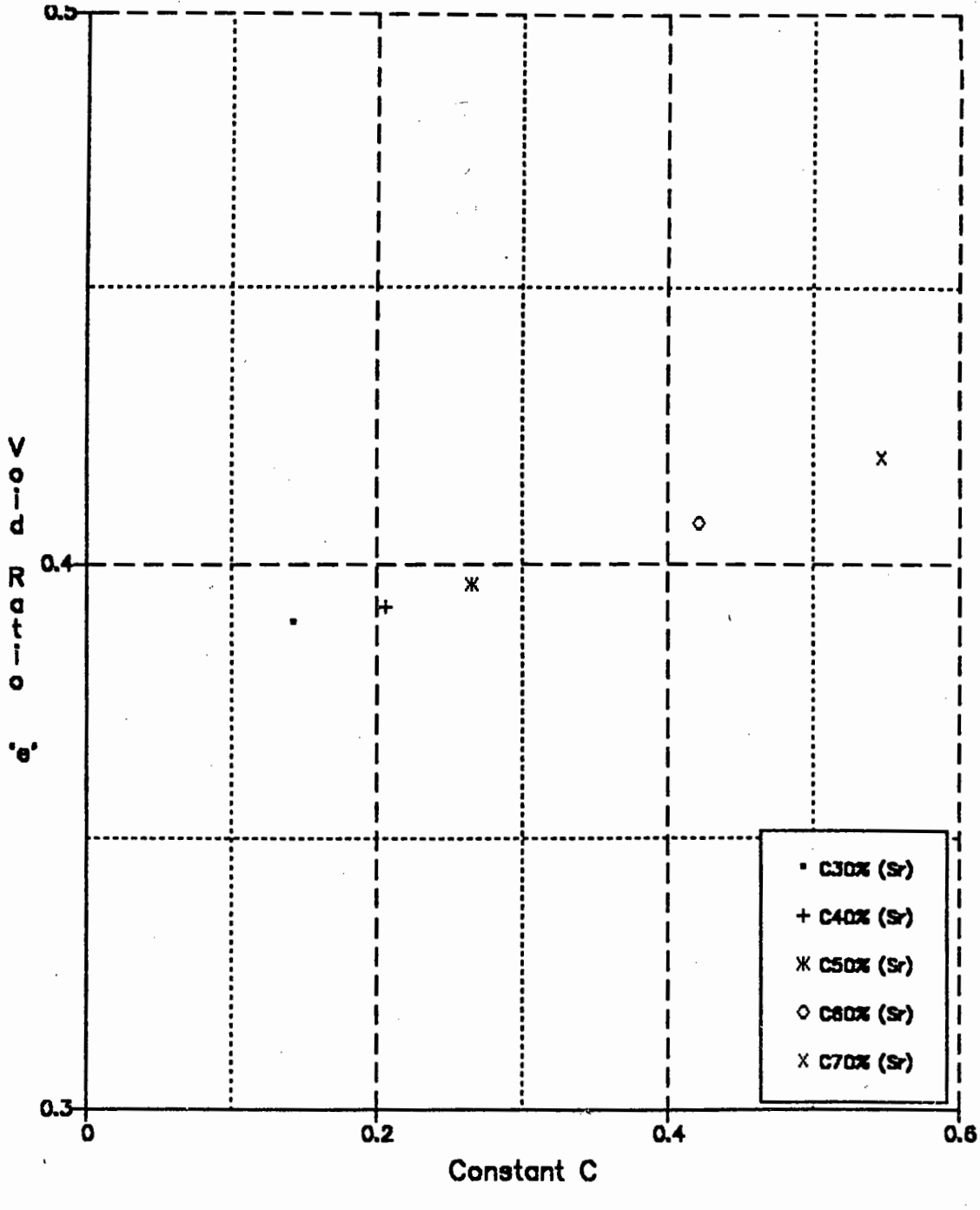

Figure 10.35: Kaolin K.2 (20% clay size) - 'C' as function of 'Sr' in the Free Swell Paths[1].

---

[1] - *see chapter four.*

Kaolin K.2 (20% clay size).

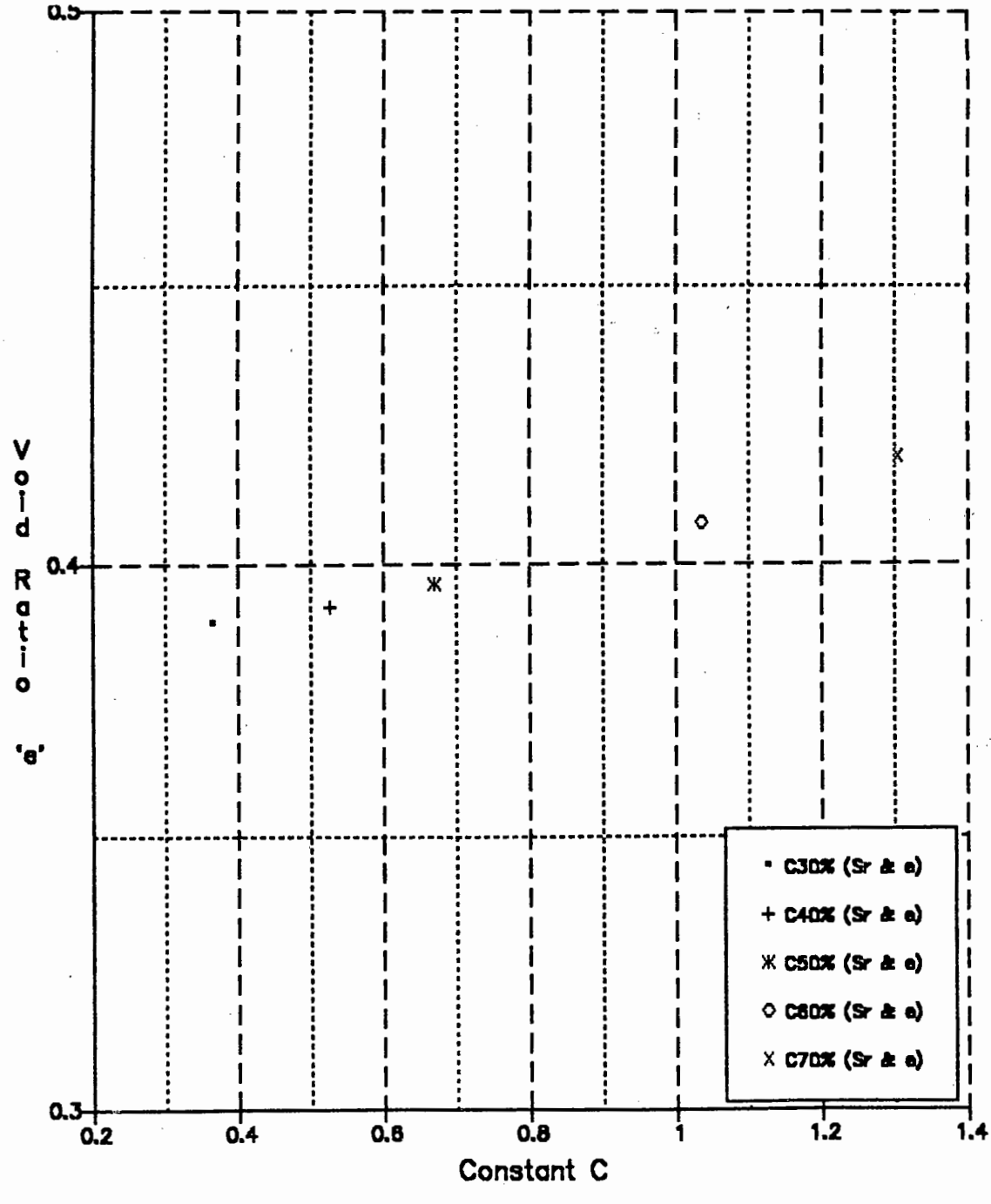

Figure 10.36: Kaolin K.2 (20% clay size) - 'C' as function of 'Sr' and 'e' in the Free Swell Path[1].

---

[1] - see chapter four.

Kaolin K.3 (8.5% clay).

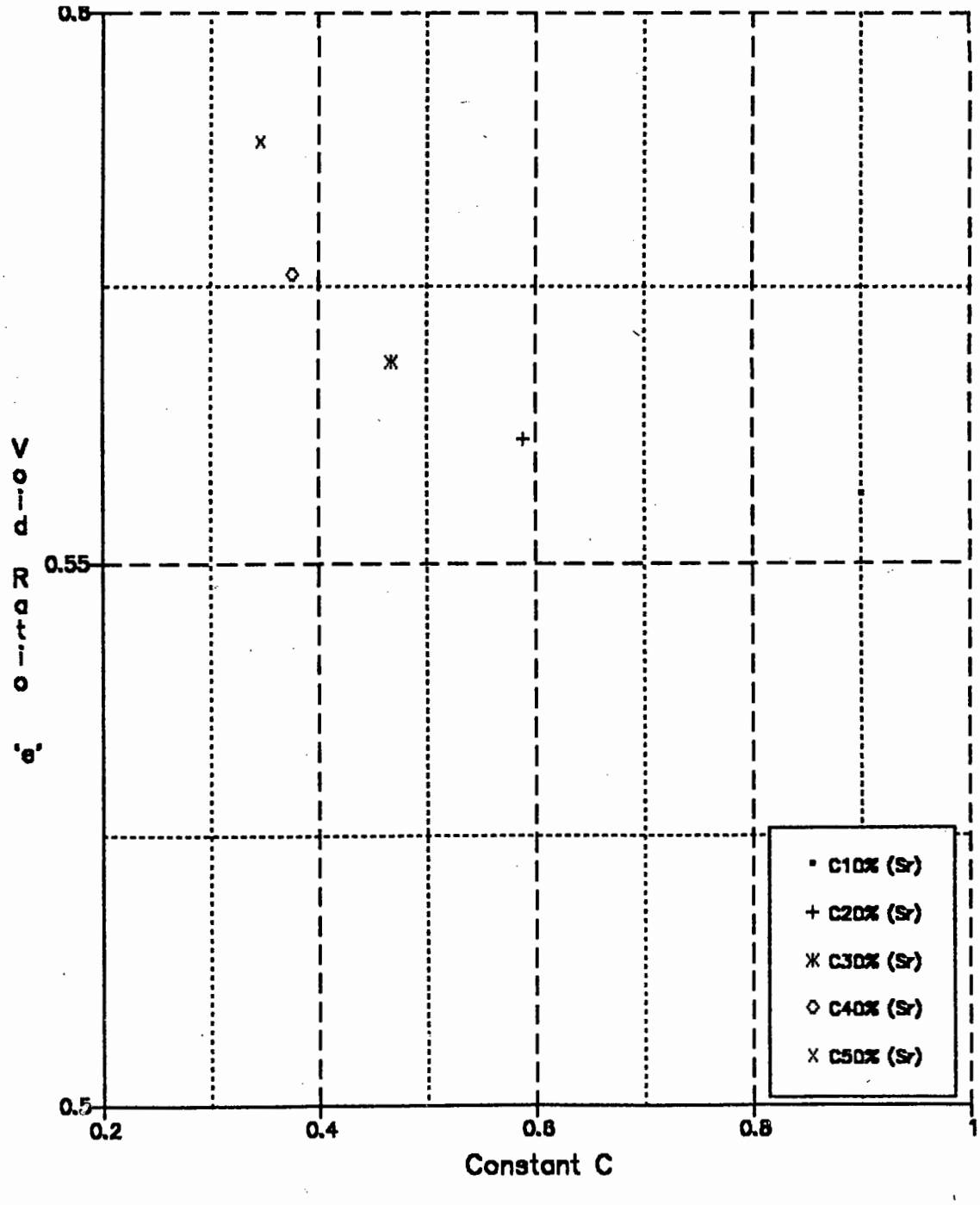

Figure 10.37: Kaolin K.3 (8.5% clay size) - 'C' as function of 'Sr' in the Free Swell Paths[1].

[1] - *see chapter four.*

Kaolin K.3 (8.5% clay size).

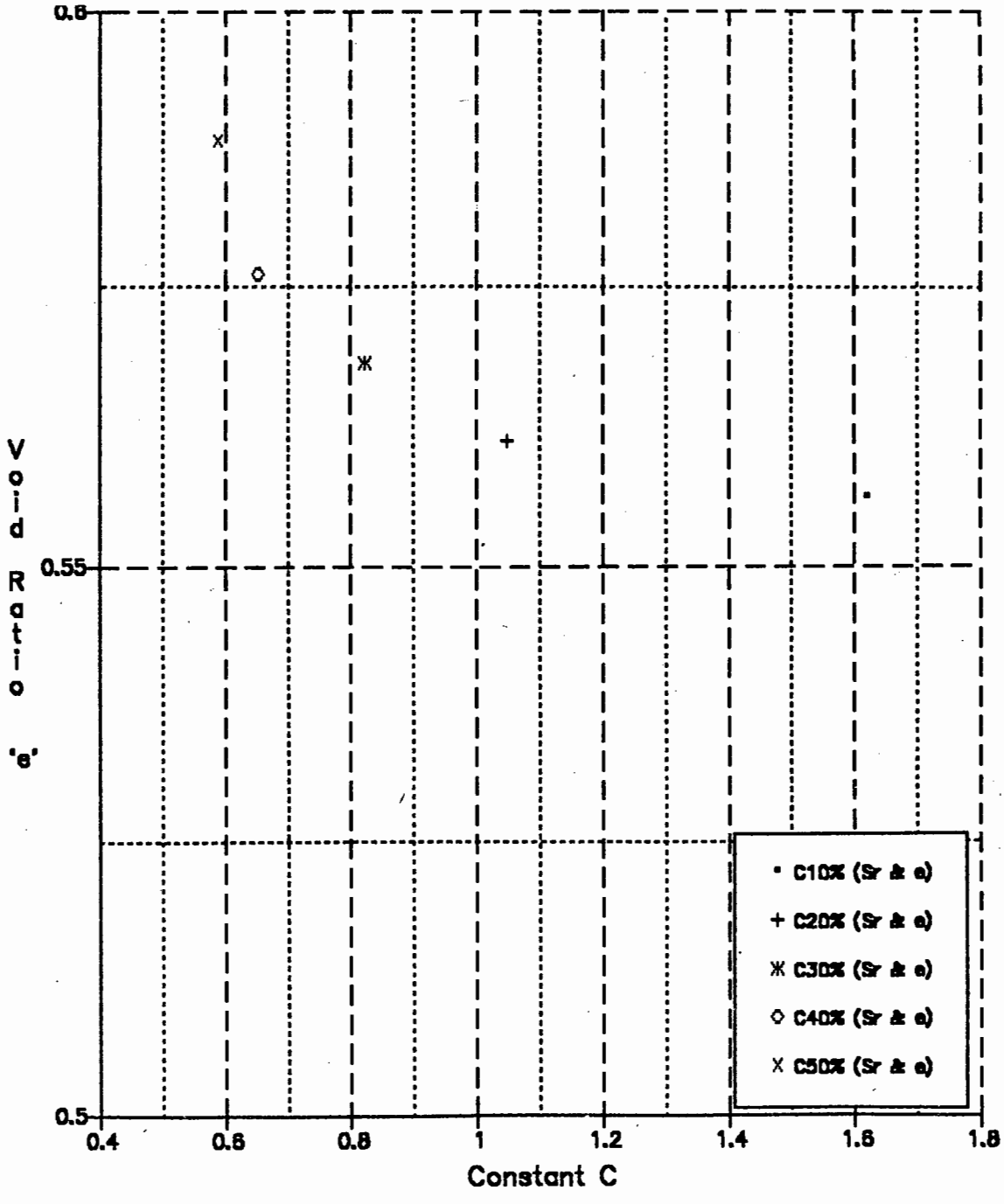

Figure 10.38: Kaolin K.3 (8.5% clay size) - 'C' as function of 'Sr' and 'e' in the Free Swell Path[1].

---

[1] - *see chapter four.*

Bentonite B.1 (3.5% clay).

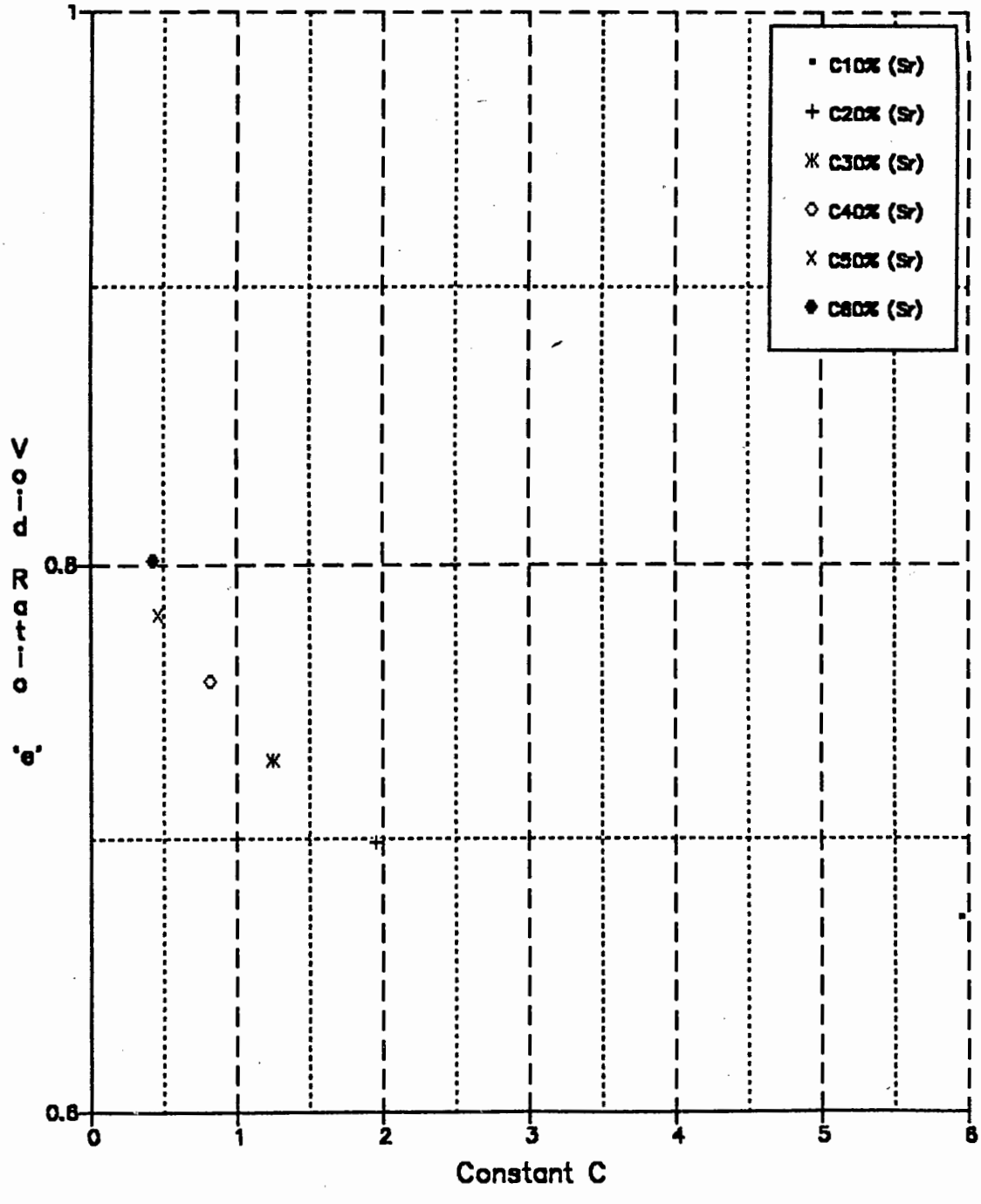

Figure 10.39: Bentonite B.1 (3.5% clay size) - 'C' as function of 'Sr' in the Free Swell Paths[1].

[1] - *see chapter four.*

Bentonite B.1 (3.5% clay size):-

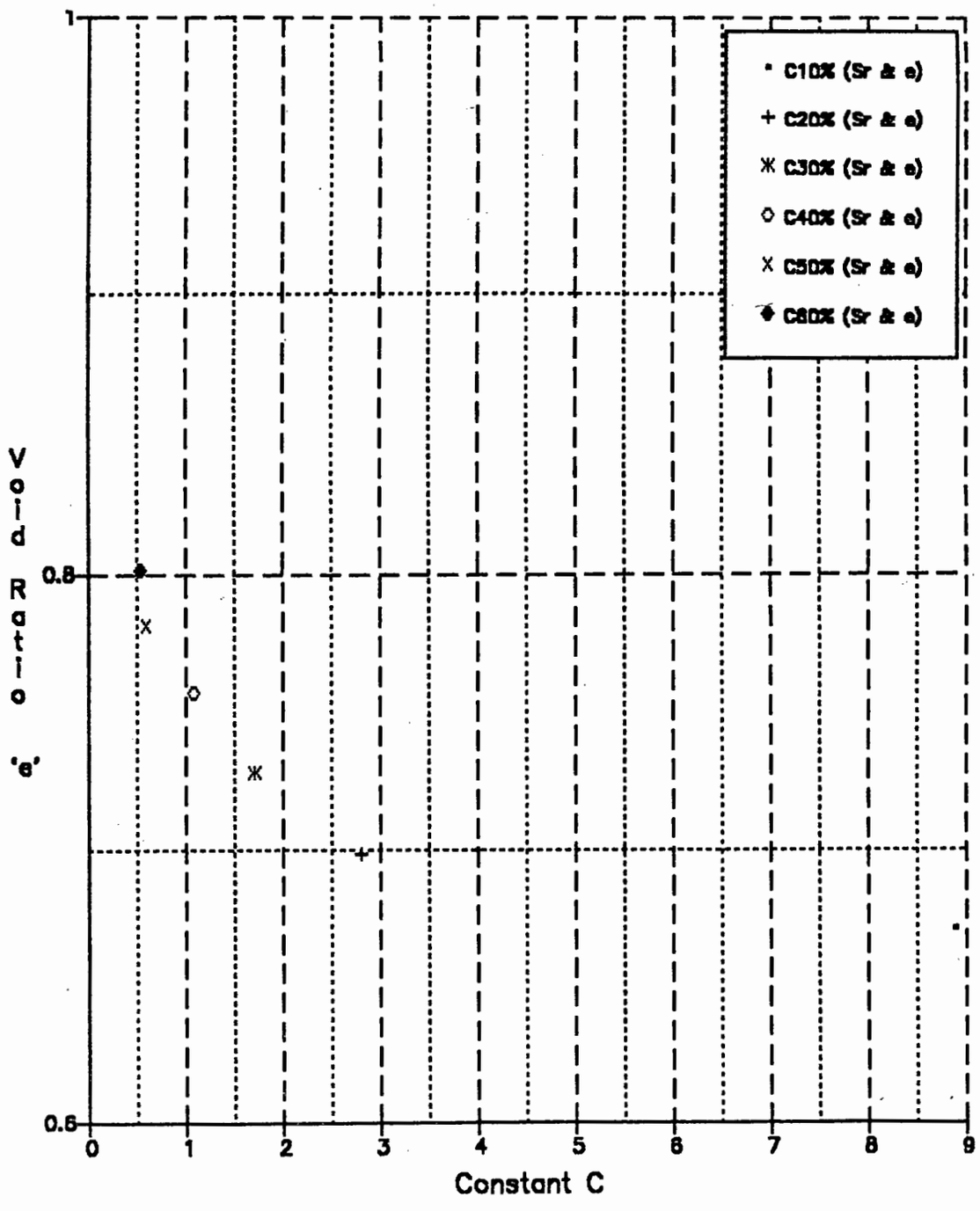

Figure 10.40: Bentonite B.1 (3.5% clay size) - 'C' as function of 'Sr' and 'e' in the Free Swell Path[1].

---

[1] - *see chapter four.*

Bentonite B.2 (7% clay).

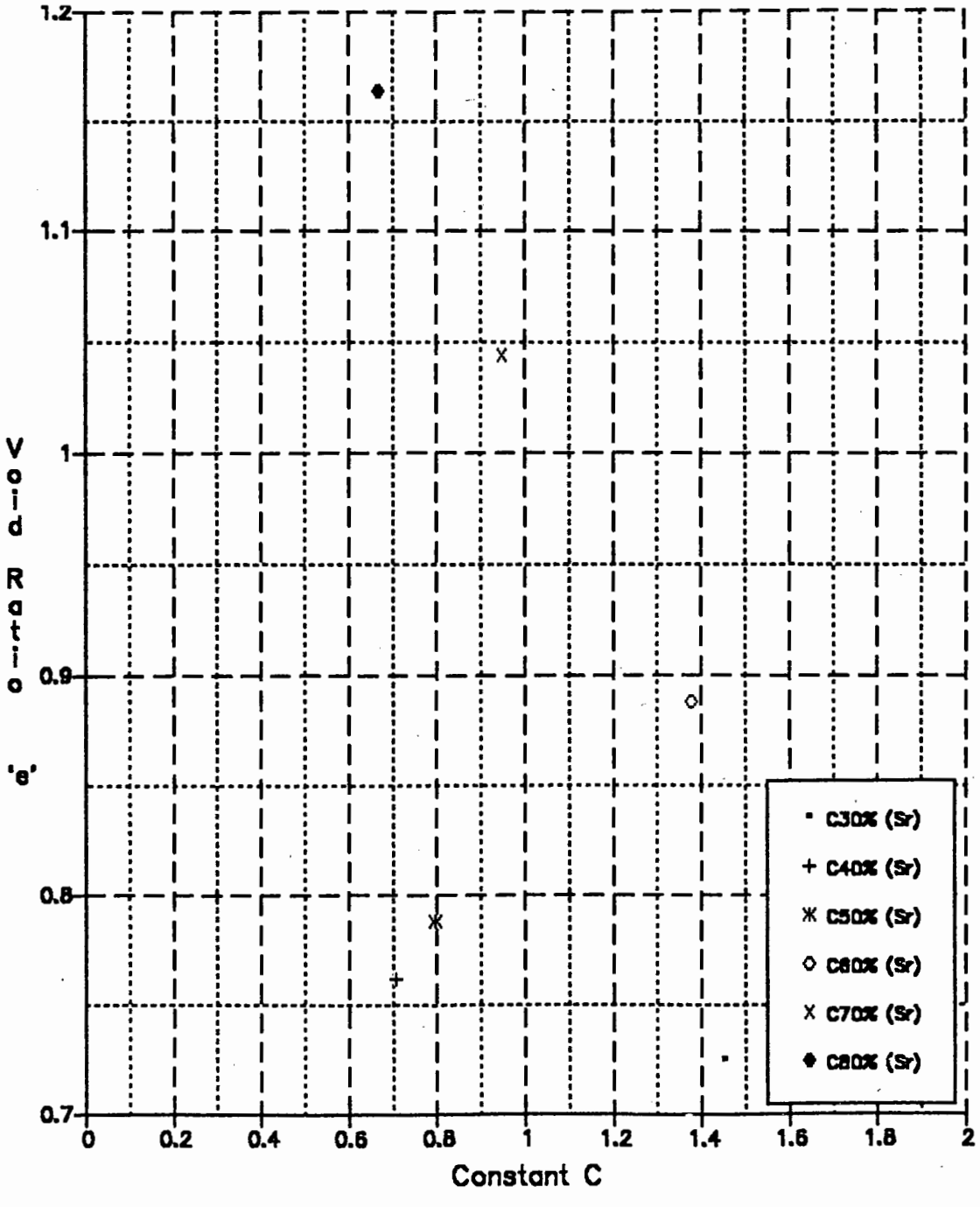

Figure 10.41: Bentonite B.2 (7% clay size) - 'C' as function of 'Sr' in the Free Swell Paths[1].

---

[1] - *see chapter four.*

Bentonite B.2 (7% clay size).

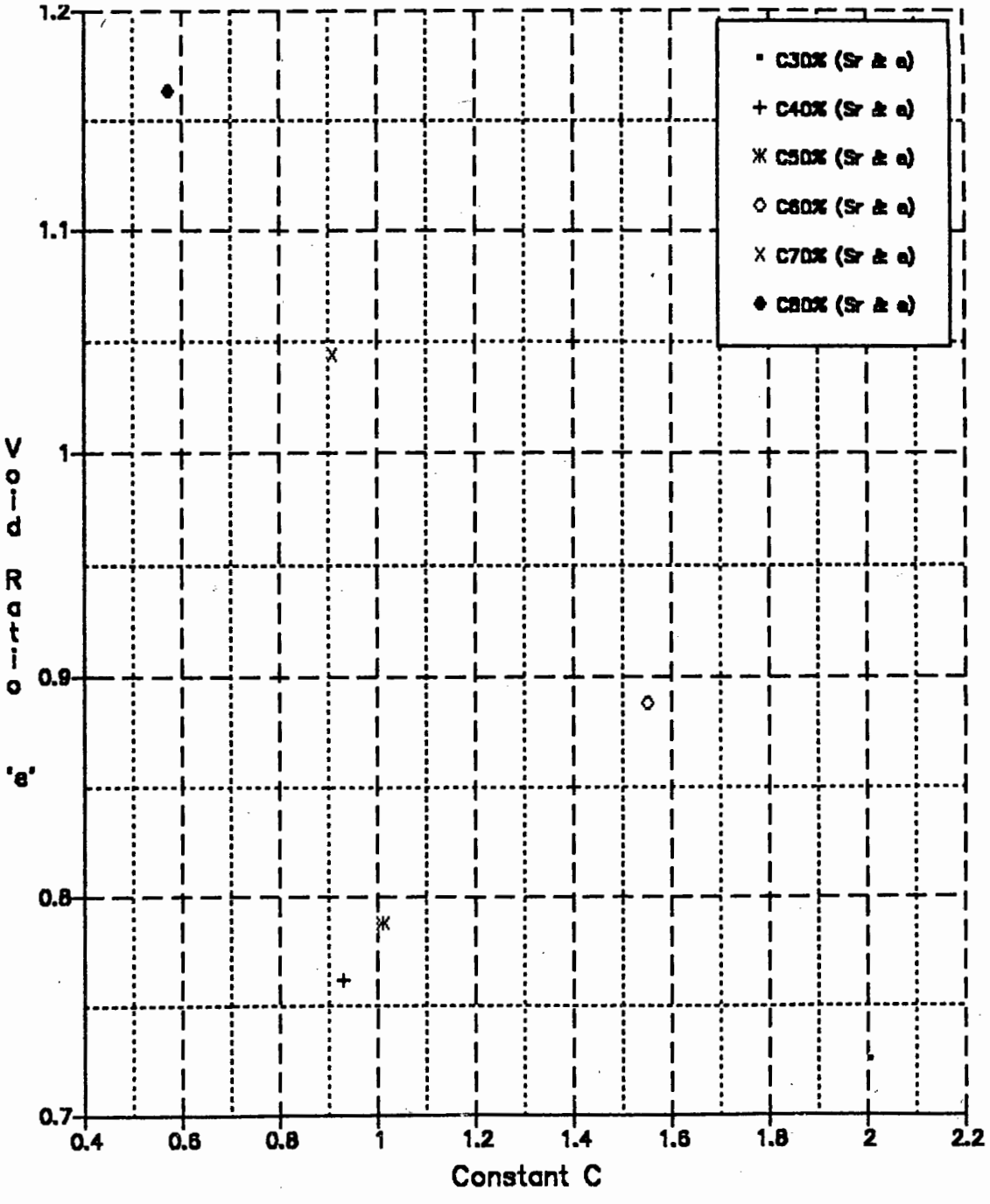

Figure 10.42: Bentonite B.2 (7% clay size) - 'C' as function of 'Sr' and 'e' in the Free Swell Path[1].

---

[1] - *see chapter four.*

Bentonite B.3 (11.5% clay).

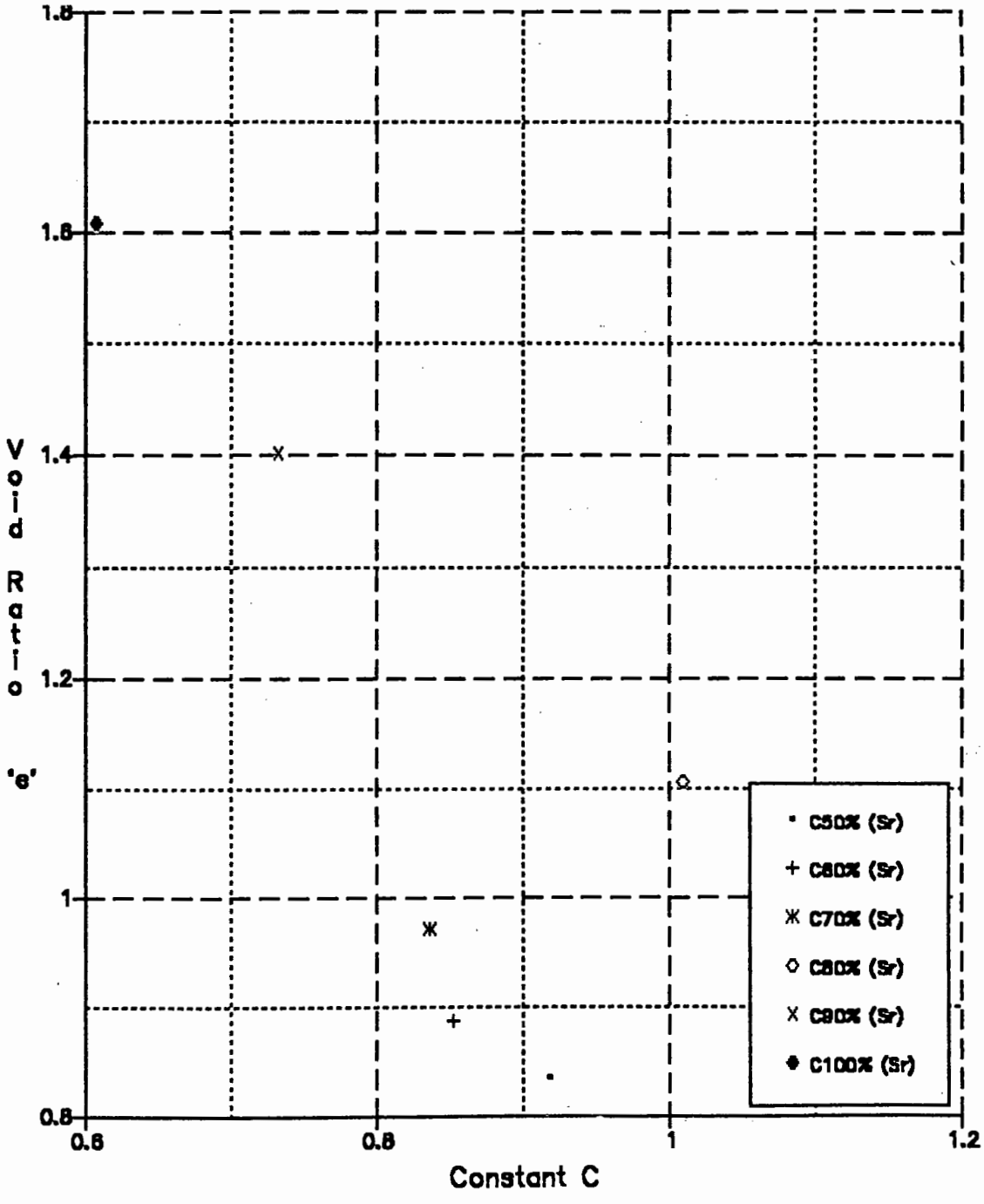

Figure 10.43: Bentonite B.3 (11.5% clay size) - 'C' as function of 'Sr' in the Free Swell Paths[1].

[1] - *see chapter four.*

Bentonite B.3 (11.5% clay size).

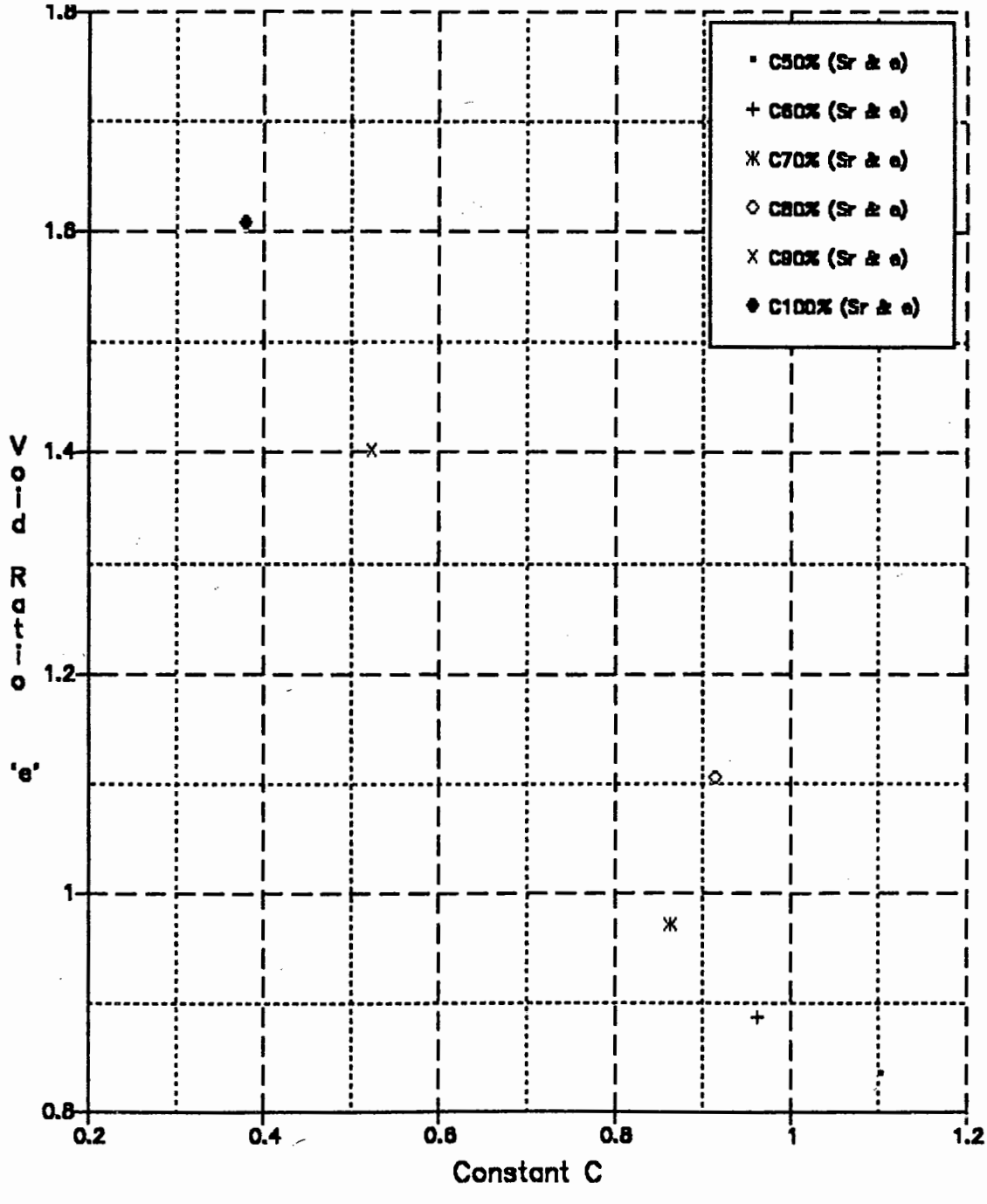

Figure 10.44: Bentonite B.3 (11.5% clay size) - 'C' as function of 'Sr' and 'e' in the Free Swell Path[1].

[1] - see chapter four.

Bentonite B.4 (15.5% clay).

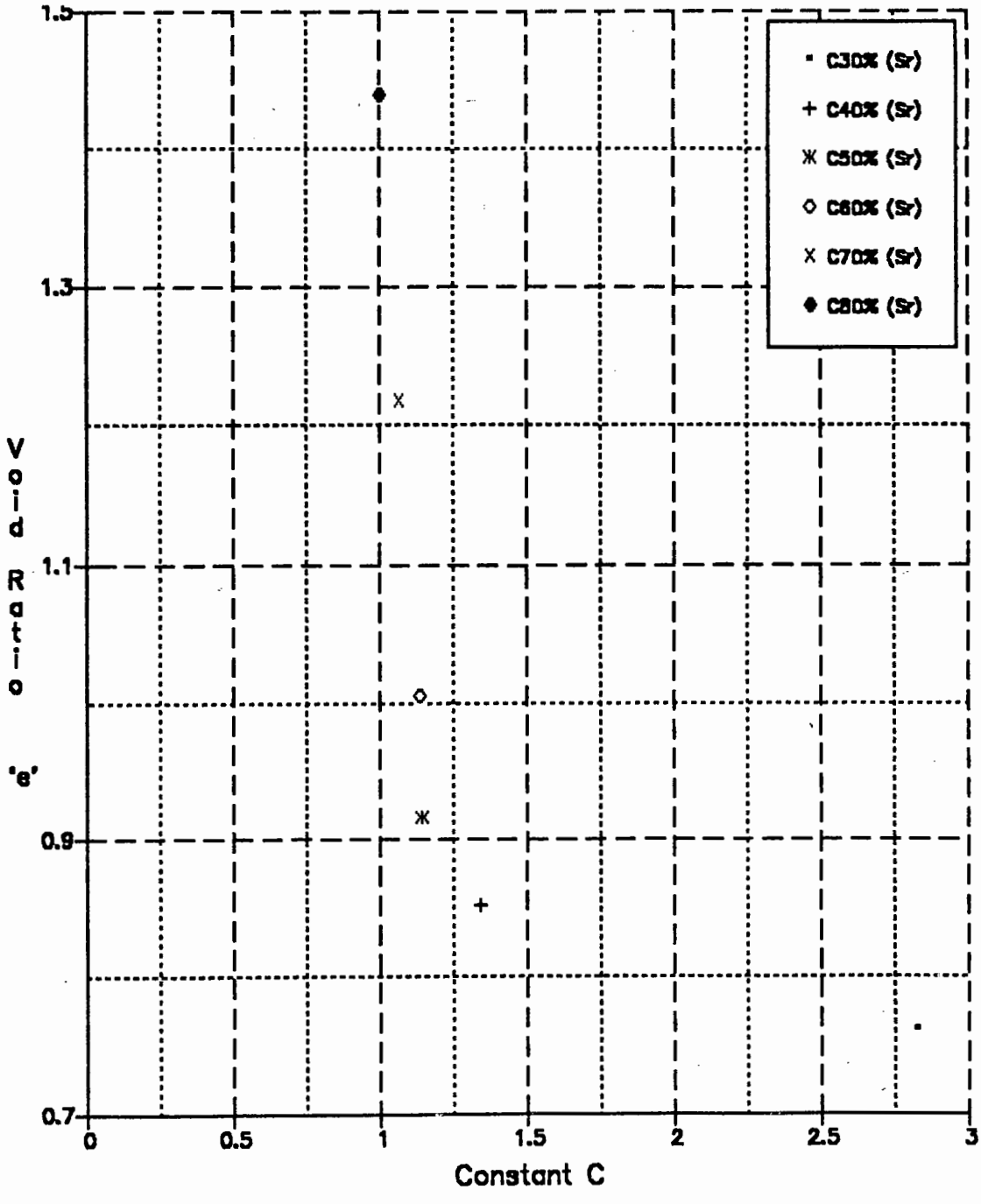

Figure 10.45: Bentonite B.4 (15.5% clay size) - 'C' as function of 'Sr' in the Free Swell Paths[1].

[1] - *see chapter four.*

Bentonite B.4 (15.5% clay size).

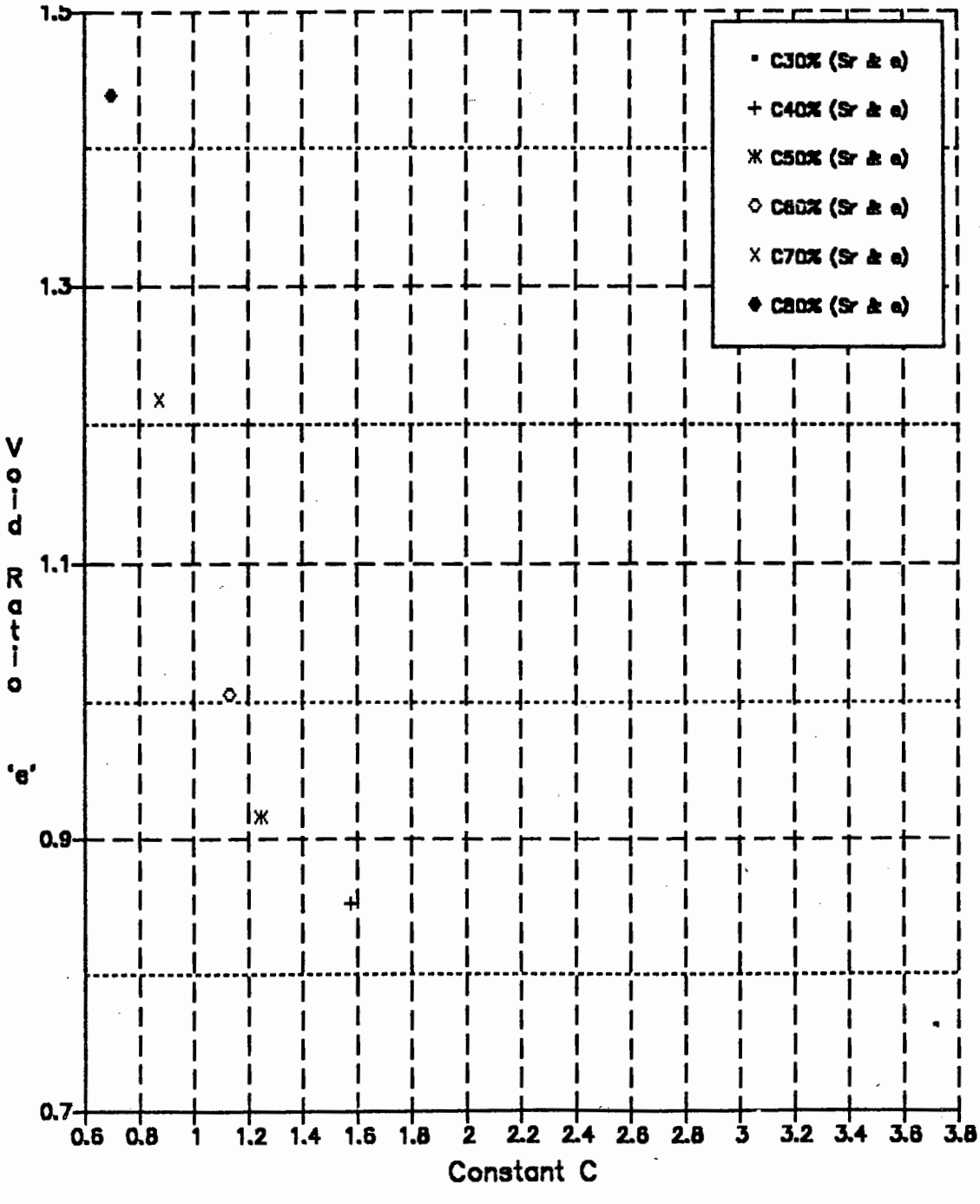

Figure 10.46: Bentonite B.4 (15.5% clay size) - 'C' as function of 'Sr' and 'e' in the Free Swell Path[1].

---

[1] - *see chapter four.*

Bentonite B.5 (35% clay).

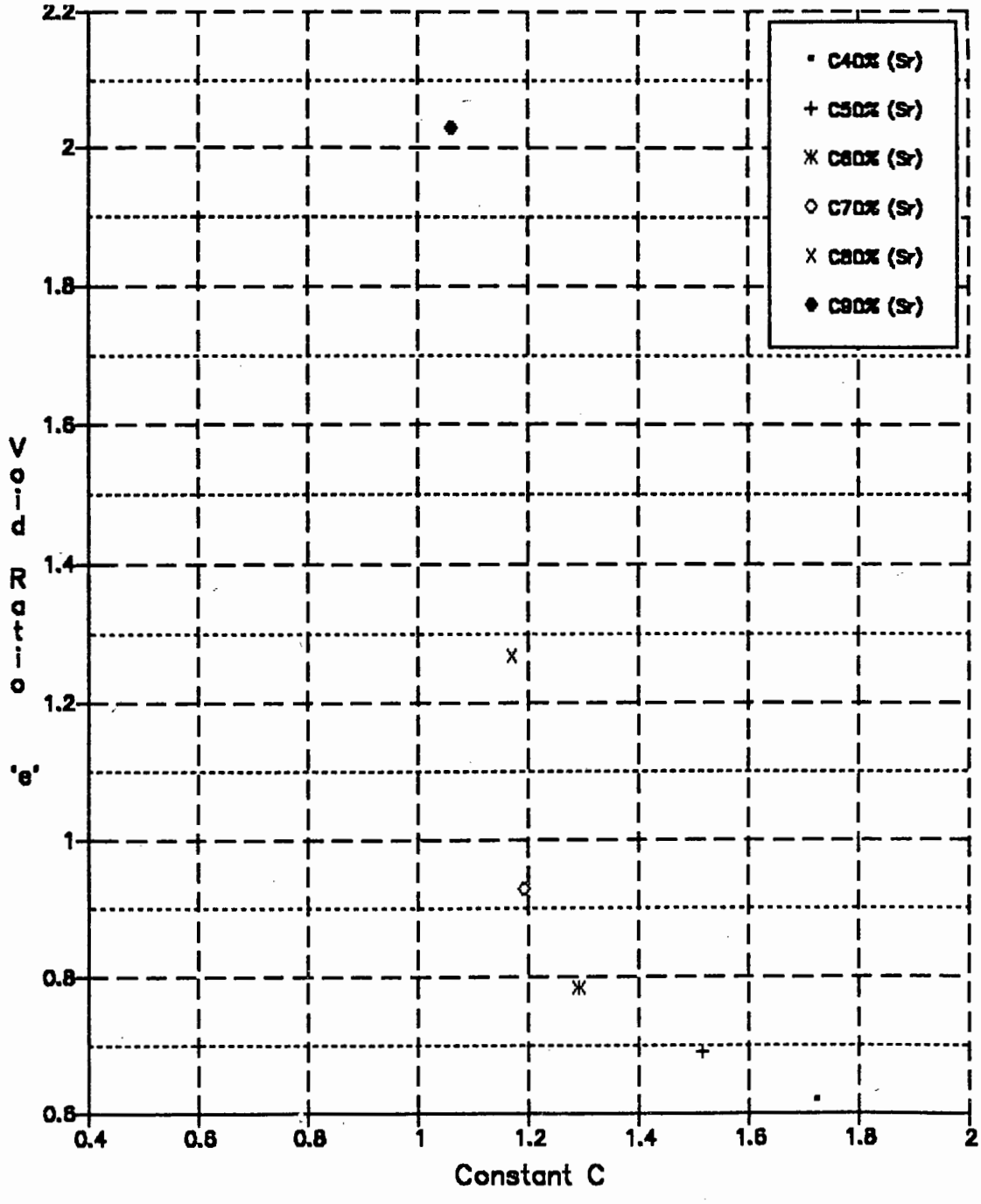

Figure 10.47: Bentonite B.5 (35% clay size) - 'C' as function of 'Sr' in the Free Swell Paths[1].

[1] - *see chapter four.*

Bentonite B.5 (35% clay size).

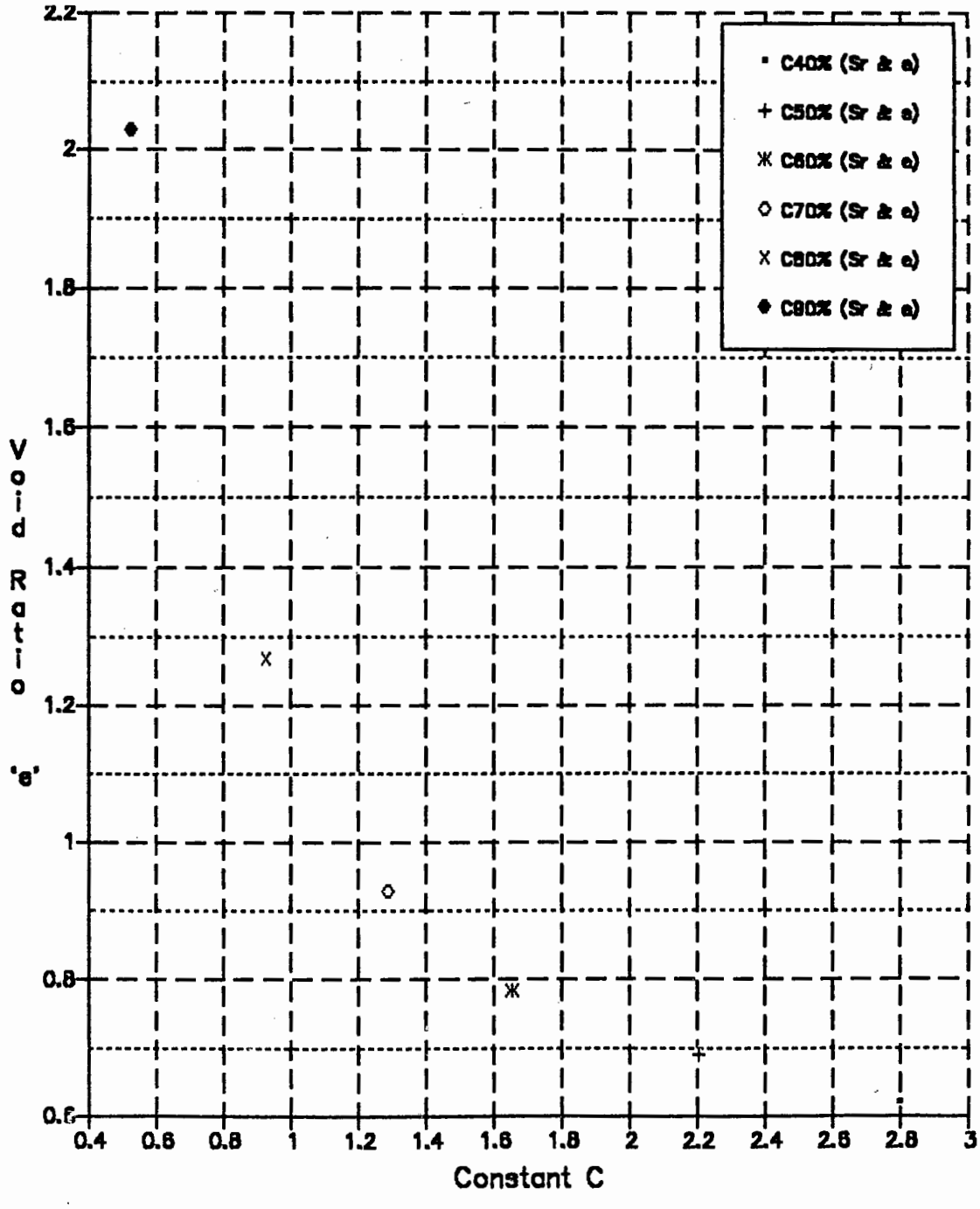

Figure 10.48: Bentonite B.5 (35% clay size) - 'C' as function of 'Sr' and 'e' in the Free Swell Path[1].

[1] - *see chapter four.*

10.3.4 Expansion or Collapse of samples due to wetting.

The relationships between void ratio and water ratio for the free swell paths of unrestrained samples were studied in Chapter Four.

Chapter Six dealt with the individual relationships between initial water content 'w_i', initial void ratio 'e_i', before wetting, and the percentage volume change 'dv', for the full range of applied external pressures.

Plots of these two types of volume change, namely Free Expansion and expansion while under load, have been combined for the remoulded and compacted test samples of the main soil types.

These combined plots, for each soil type, are shown in the figures below - refer to Figures 10.49 to 10.56. Both natural and artificial soil types have been included. Each plot also includes the full range of consistency limits, namely - the Shrinkage Limit 'SL', Plastic Limit 'PL', Liquid Limit 'LL' and the Free Expansion Limit 'FEL'.

In the case of expansive behaviour a number of preliminary conclusions can be made, as follows:-

1. Concerning the Natural Soil Types:[1]

(i) For the same initial void ratio and for the same value of the initial confining pressure, there appears to be a linear correlation between the initial water content (before wetting) and the percentage volume change resulting from wetting the sample.

(ii) The larger volume changes occur if the initial water content is low, and if the vertical confining pressure is also low.

(iii) As the effective vertical pressure restraining the sample increases, there is a gradual reduction in the amount of percentage volume change, until a certain pressure is reached where this volume change is zero. If the confining pressure is increased beyond this critical value the sample will decrease in volume when wetted.

---

[1] - *Figures 10.49 - 10.54.*

2. Artificial Soil Types:[1]

(iv) The volume change behaviour of the kaolin soil type is somewhat similar to that of soil types for sites 'A' Berea Road, 'B' Francois Road, 'C' Margaret Mayton Avenue, and 'D' Rose Hill.

(v) Concerning the volume change behaviour of the bentonite soil type, there is a noticeable change from a very high volume increase, due to wetting, under unrestrained conditions (that is, free swell), to a situation of no volume increase when the sample is restrained by the applied vertical pressure. This appears to indicate little or no development of shear strength in these soil types while under applied load conditions.

---

[1] - *Figures 10.55 and 10.56.*

Natural Soil Type: Site 11, Rosebank.

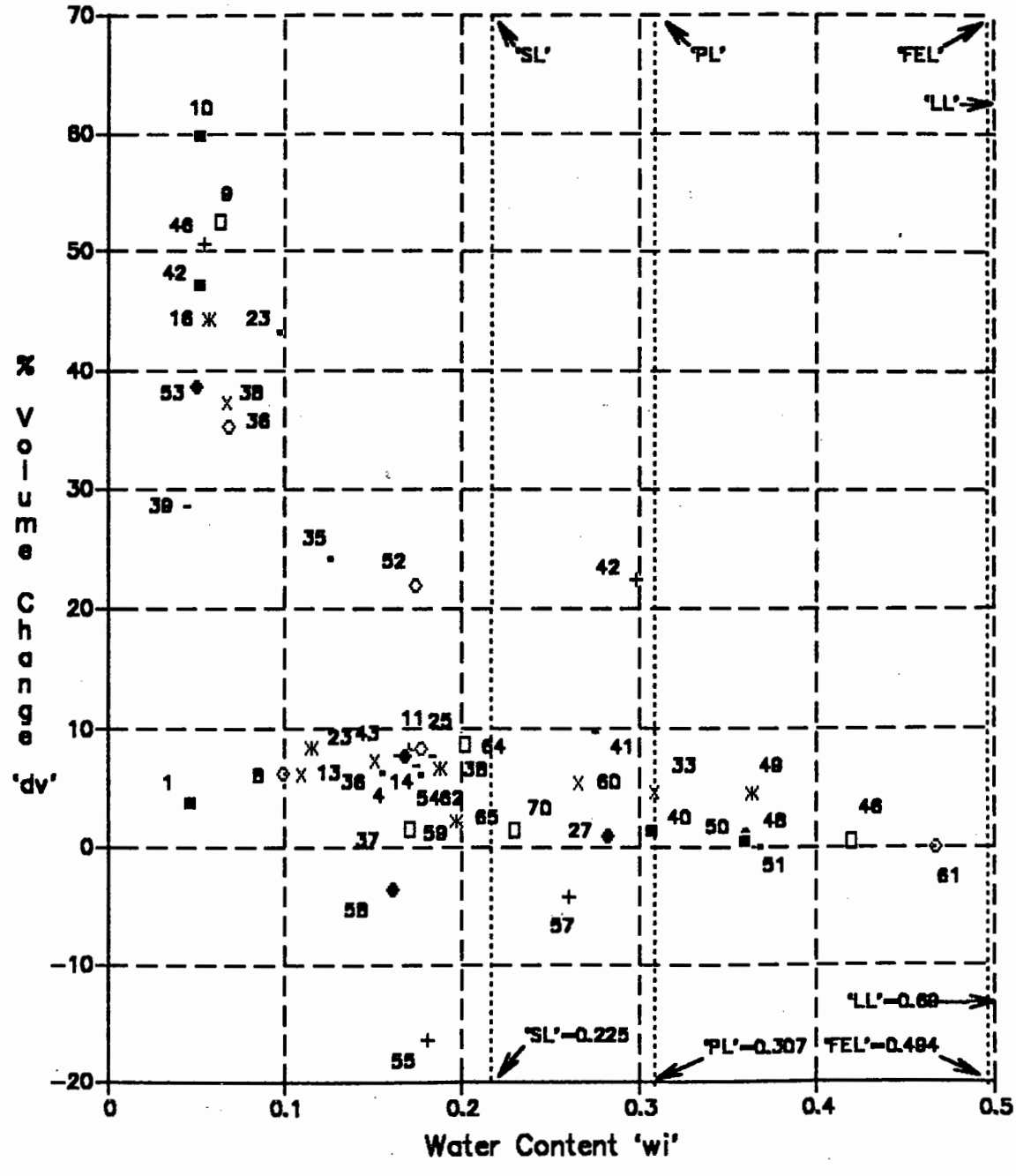

Figure 10.49: Site 11, Rosebank [Remoulded and Compacted samples][1] - Water Content[2] 'w_i' and Void Ratio 'e_i', before wetting, and the Percentage Volume Change, after wetting.

---

[1] - *See next page for Legend of soil types.*
[2] - *expressed as 'mass ratio'.*

Legend for Figure 10.49:

Key:

| * Soil Type, Initial Void Ratio, and Restraining Vertical Pressure |

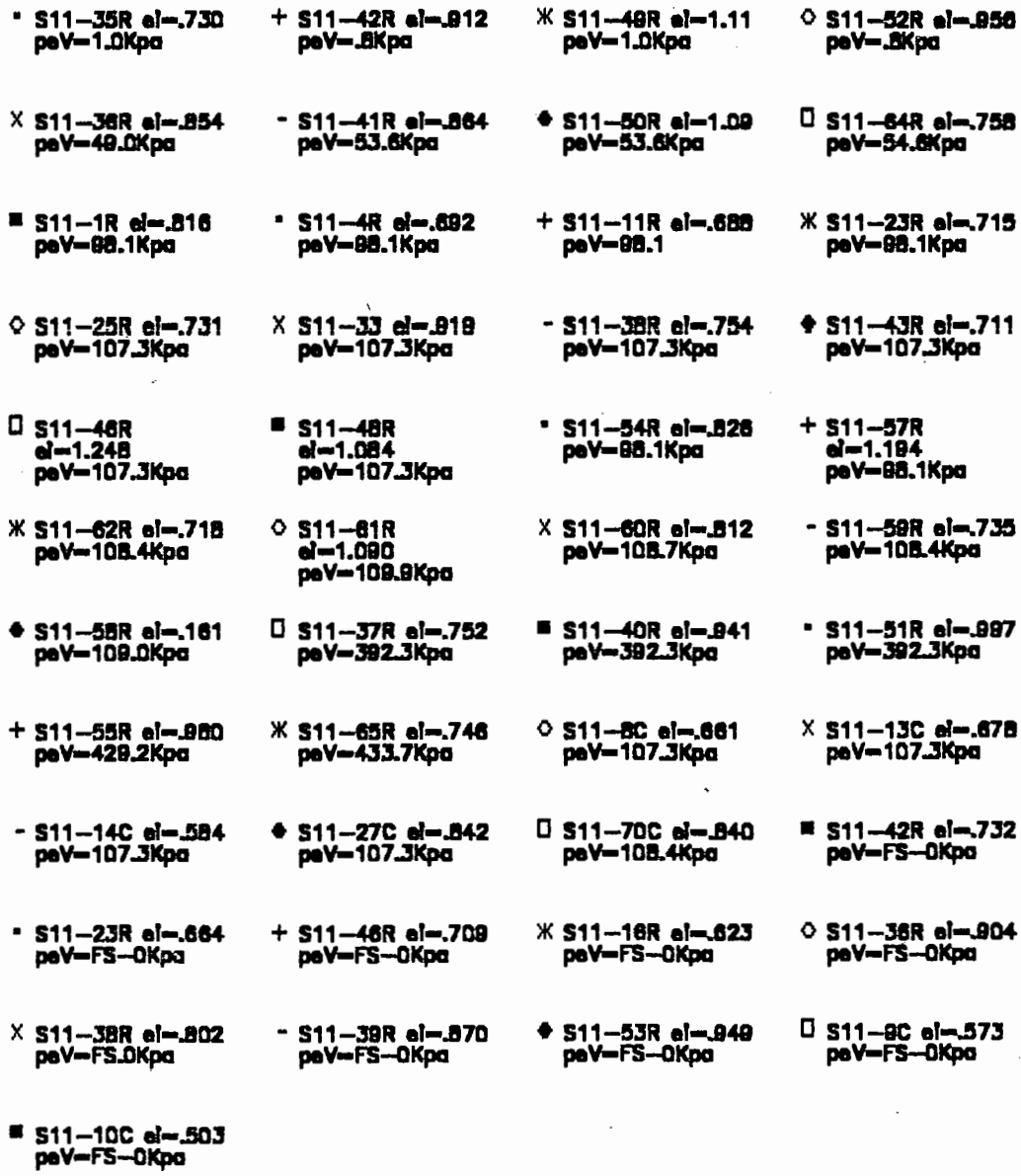

---

* - *symbol to identify each soil type.*

Natural Soil Type: Site 36, Rondebosch.

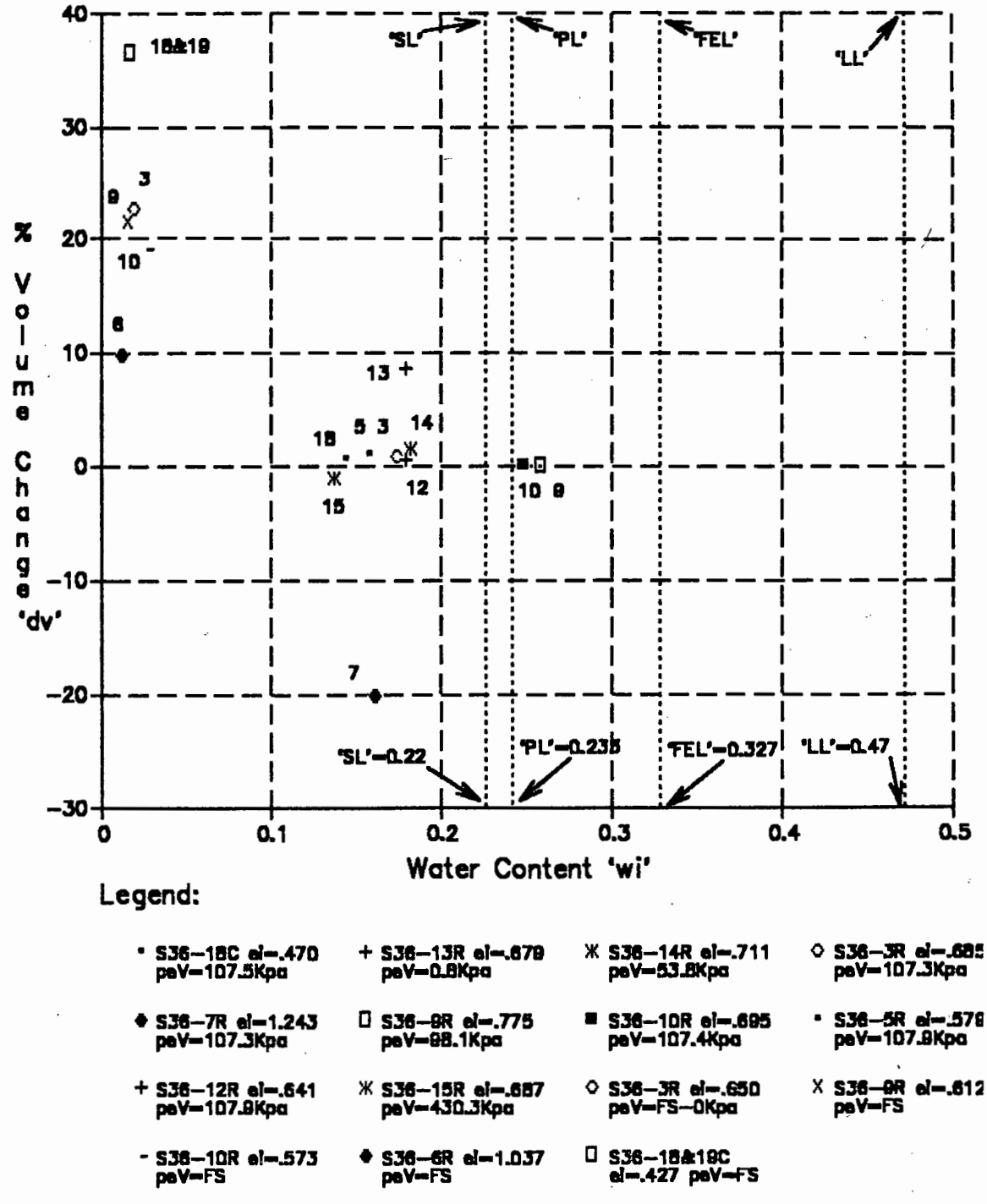

Figure 10.50: Site 36, Rondebosch [Remoulded and Compacted samples] - Water Content[1] 'w_i' and Void Ratio 'e_i', before wetting, and the Percentage Volume Change, after wetting.

---

[1] - *expressed as mass ratio.*

Natural Soil Type: Site 30, Hout Bay.

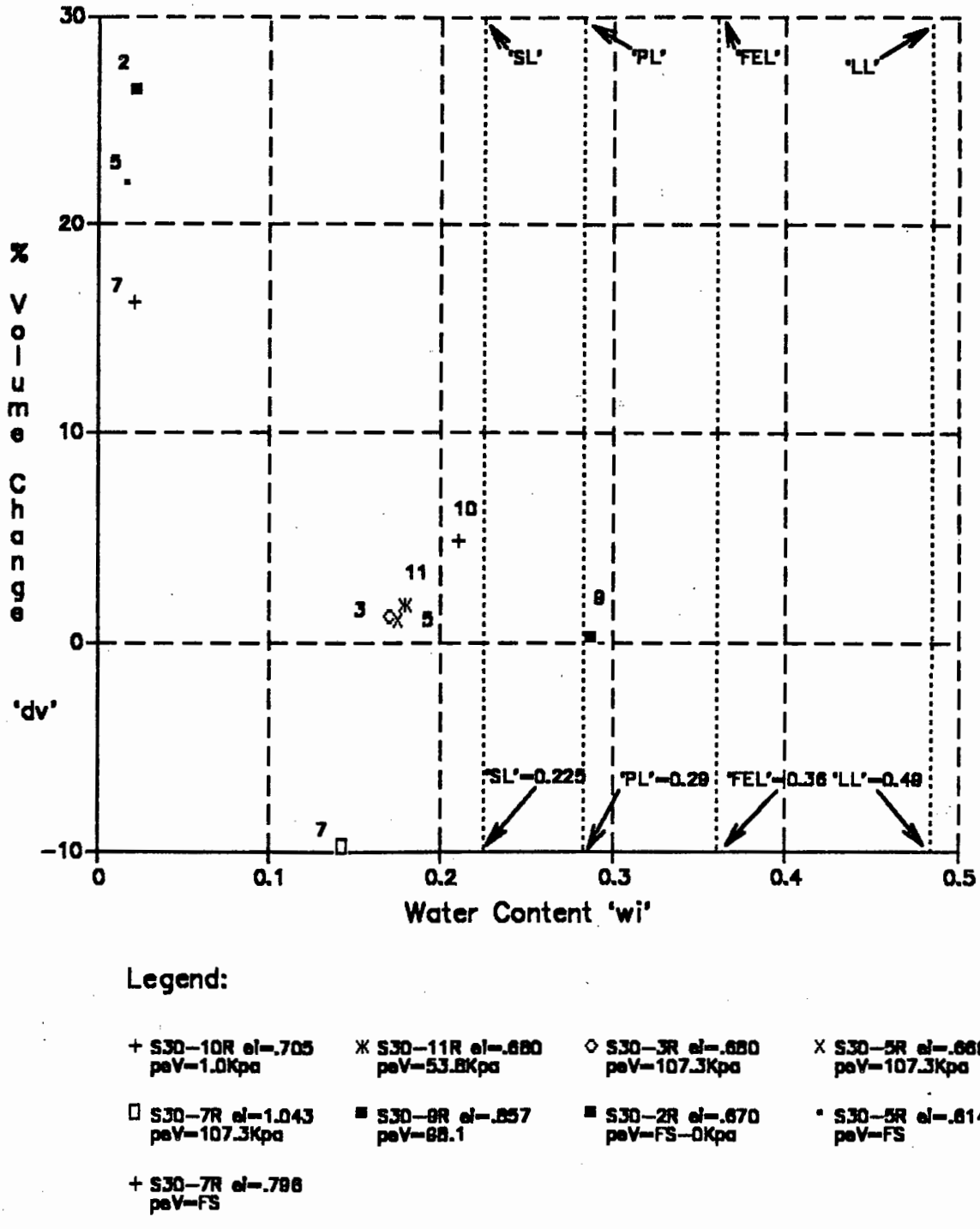

Figure 10.51: Site 30, Hout Bay [Remoulded samples] - Water Content[1] 'w_i' and Void Ratio 'e_i', before wetting, and the Percentage Volume Change, after wetting.

---

[1] - *expressed as mass ratio.*

Natural Soil Type: Site A, Berea Road.

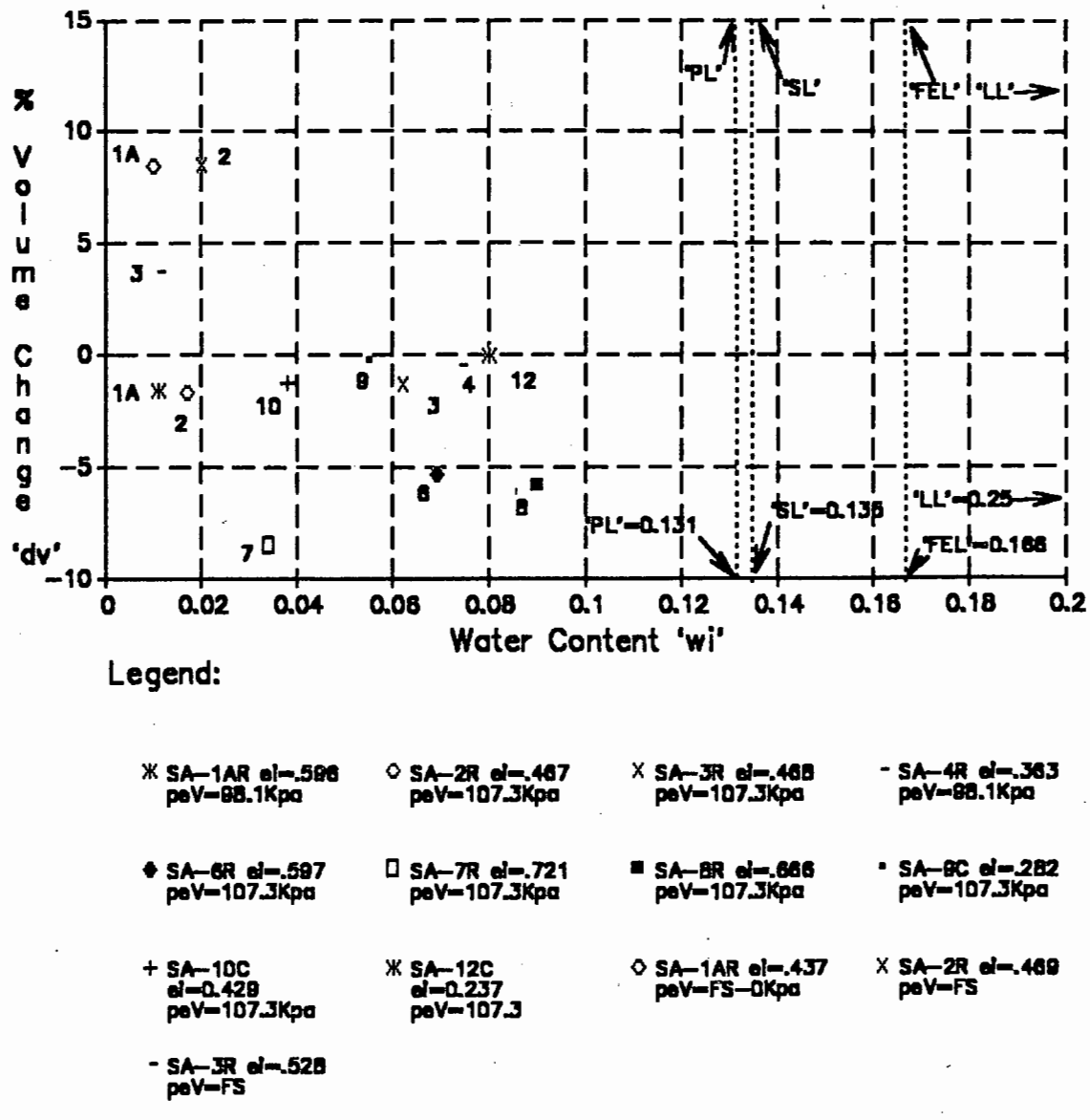

Figure 10.52: Site A, Berea Road [Remoulded and Compacted samples] - Water Content[1] 'w_i' and Void Ratio 'e_i', before wetting, and the Percentage Volume Change, after wetting.

---

[1] - *expressed as mass ratio.*

Natural Soil Type: Site 7, Mowbray.

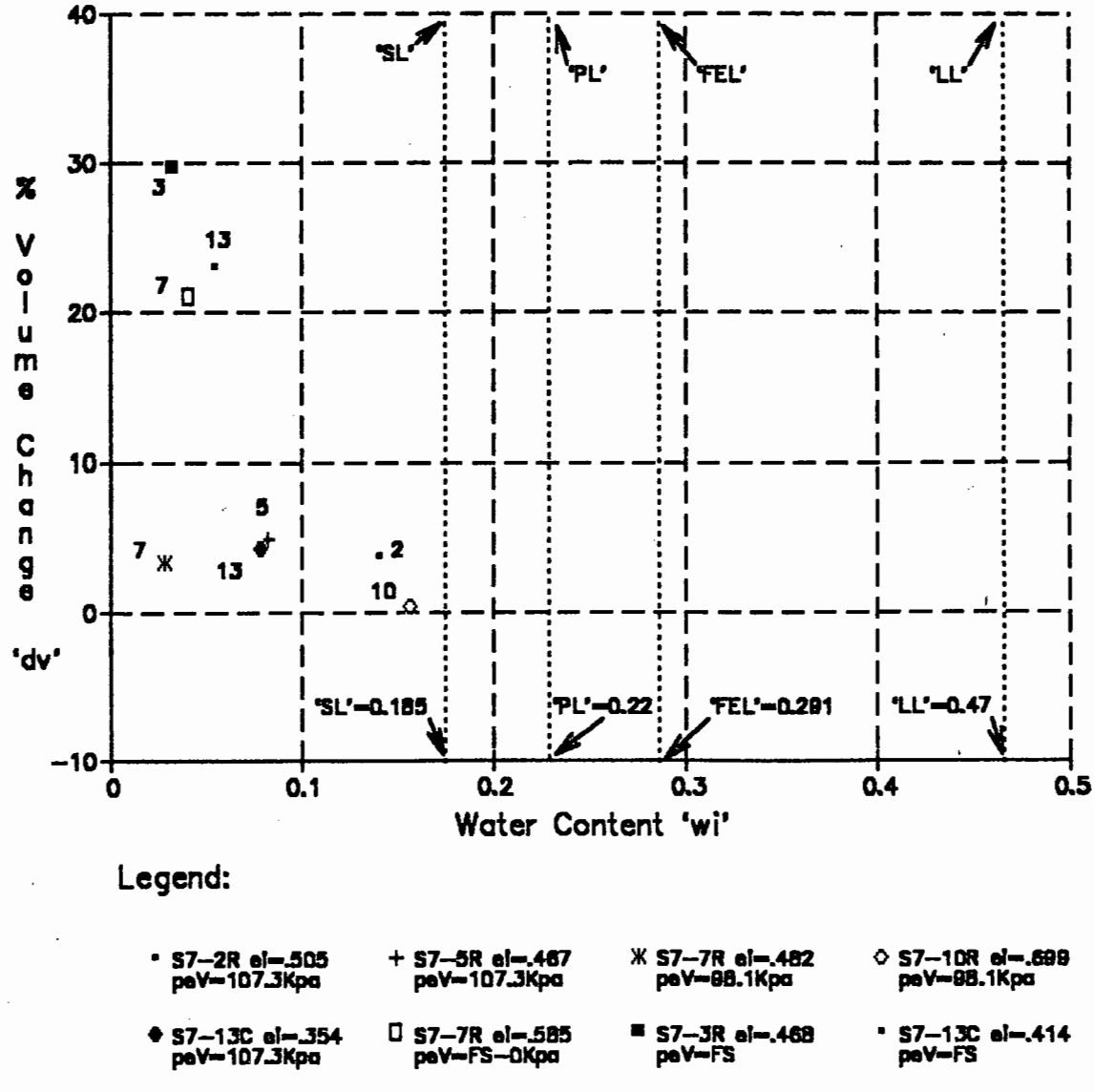

Figure 10.53: Site 7, Mowbray [Remoulded and Compacted samples] - Water Content[1] 'w_i' and Void Ratio 'e_i', before wetting, and the Percentage Volume Change, after wetting.

---

[1] - *expressed as mass ratio.*

Natural Soil Types: Site 'B' Francois Road, Site 'C' Margaret Mayton Avenue, and Site 'D' Rose Hill.

Site	'PL'	'SL'	'FEL'	'LL'
'B'	0.129	(0.135)	0.118	0.15
'C'	0.159	(0.135)	0.154	0.197
'D'	0.149	(0.135)	0.122	0.206

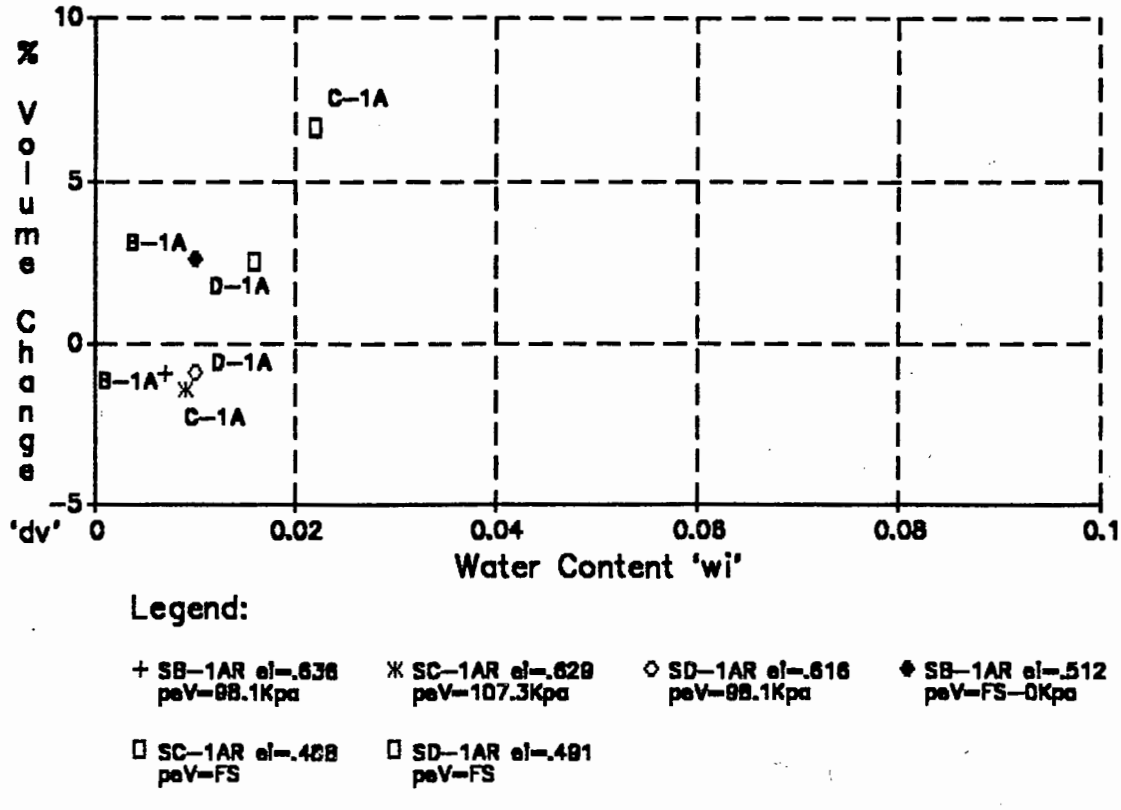

Figure 10.54: Site 'B' Francois Road, 'C' Margaret Mayton Avenue, and 'D' Rose Hill [Remoulded samples] - Water Content[1] 'w_i' and Void Ratio 'e_i', before wetting, and the Percentage Volume Change, after wetting.

---

[1] - *expressed as mass ratio.*

Artificial Soil Types: Kaolin K.1 (13% clay size), K.2 (20% clay), and Kaolin K.3 (8.5% clay size)

	'PL'	'SL'	'FEL'	'LL'
K.1	0.118	0.14	0.123	0.123
K.2	0.104	0.125	0.12	0.14
K.3	-	0.17	0.11	-

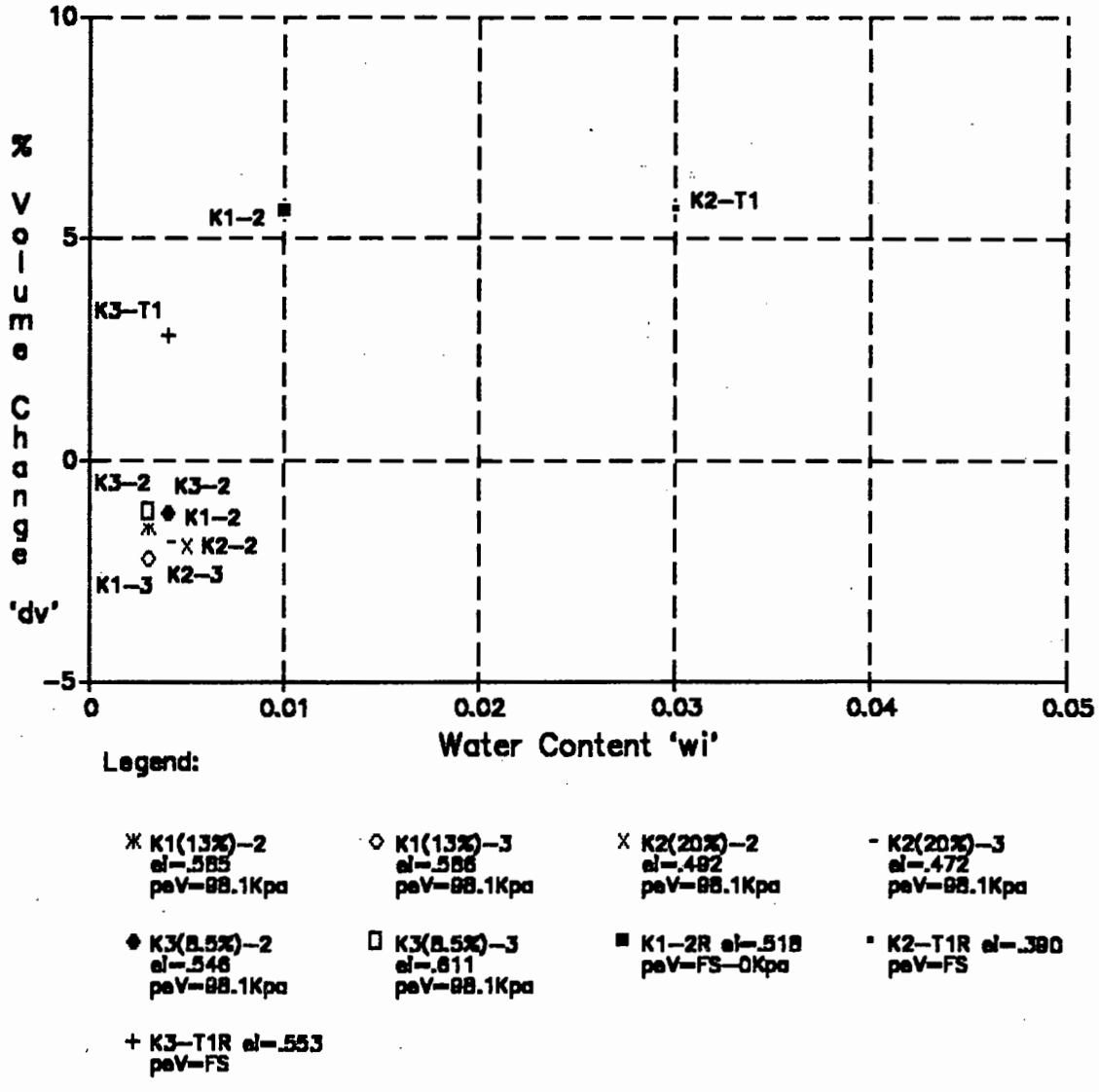

Figure 10.55: Kaolin K.1 (13% clay size), K.2 (20% clay), and Kaolin K.3 (8.5% clay size) [Remoulded samples] - Water Content[1] 'w_i' and Void Ratio 'e_i', before wetting, and the Percentage Volume Change, after wetting.

---

[1] - *expressed as mass ratio.*

Artificial Soil Types: Bentonite B.1 (3.5% clay size), B.2 (7% clay), B.3 (11.5% clay), B.4 (15.5% clay), and Bentonite B.5 (35% clay size).

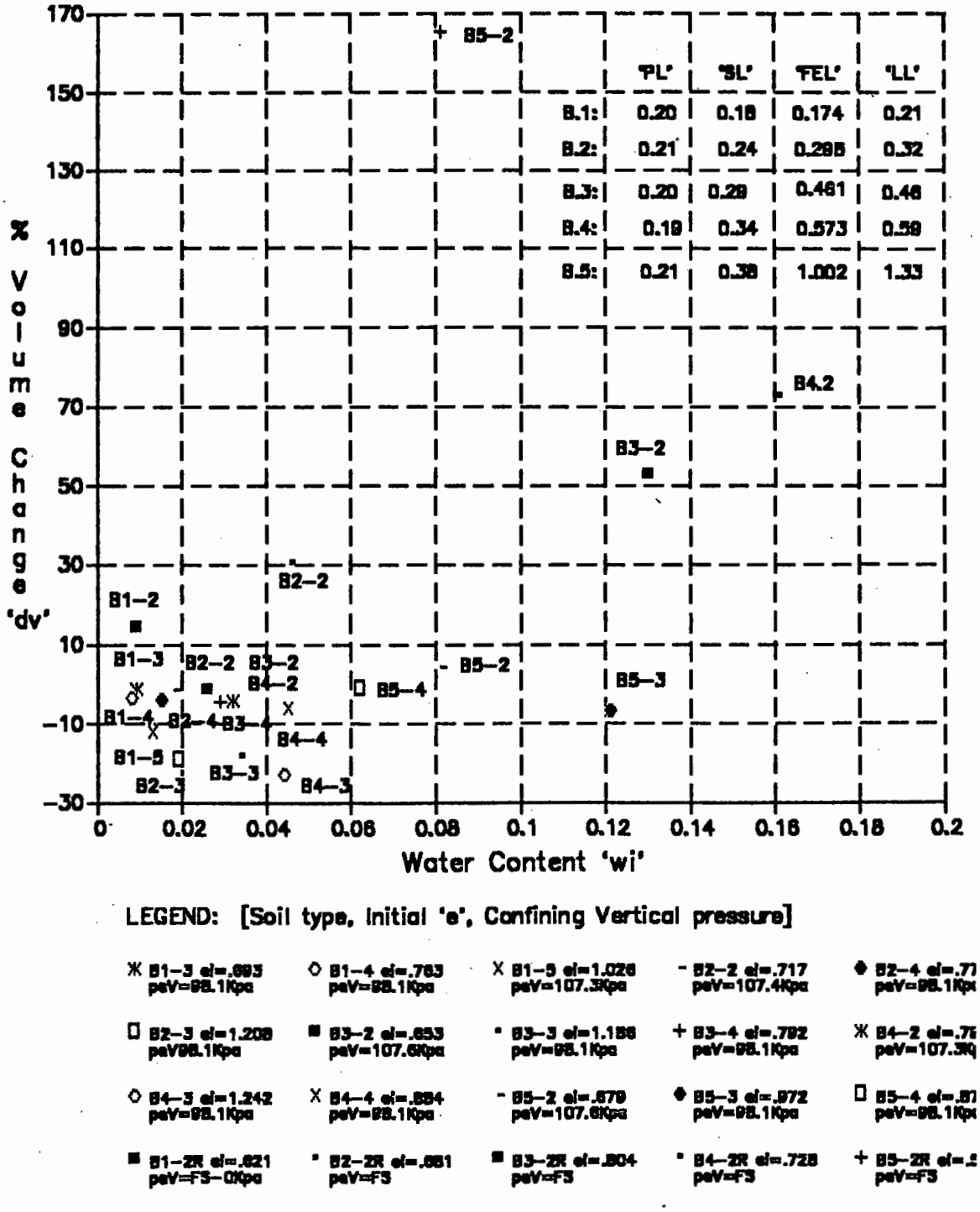

Figure 10.56: Bentonite B.1 (3.5% clay size), B.2 (7% clay), B.3 (11.5% clay), B.4 (15.5% clay), and Bentonite B.5 (35% clay size) [Remoulded samples] - Water Content[1] 'w_i' and Void Ratio 'e_i', before wetting, and the Percentage Volume Change, after wetting.

---

[1] - *expressed as mass ratio.*

10.3.5 Swell Pressures, Consistency Limits and Stress Scales.

It was noted from experiment, using the horizontal strain ring (refer to Chapter Eight - "Axisymmetric Stress Behaviour of Expansive and Collapsing Soils"), that in ordinary one-dimensional consolidation the ratio of horizontal to vertical stress seems to change during the test.
The plot of Vertical Pressure versus Horizontal Pressure, for the one-dimensional consolidation of Site 11 (Rosebank), is included in the next section[1] of this chapter.

The ratio, of horizontal to vertical stress, starts at zero and then increases to about one quarter in value.
This proves the anticipated trend expected by Prof. Sparks[2].

Figure 7.03 has been repeated as Figure 10.57. This new figure includes the 'void ratio versus water ratio' over the full range of degree of saturation, for swelling against constraint - it also includes the vertical swell pressures due to wetting, and the consistency limits for this soil type.

This diagram shows that in general the stress scales for confining stress increases down the Sr = 1 line, which is similar to the stress system anticipated in the modelling method used by Prof Sparks for his predictions (Durban Conference, 1975)[2].

However the results by the writer indicate that this general trend does display certain exceptions if a soil swells from an initial condition which is not very dry (higher water ratio).

---

1 - refer to Figure 10.58 in section 10.3.6.
2 - Reference 86.

Site 11, Rosebank.

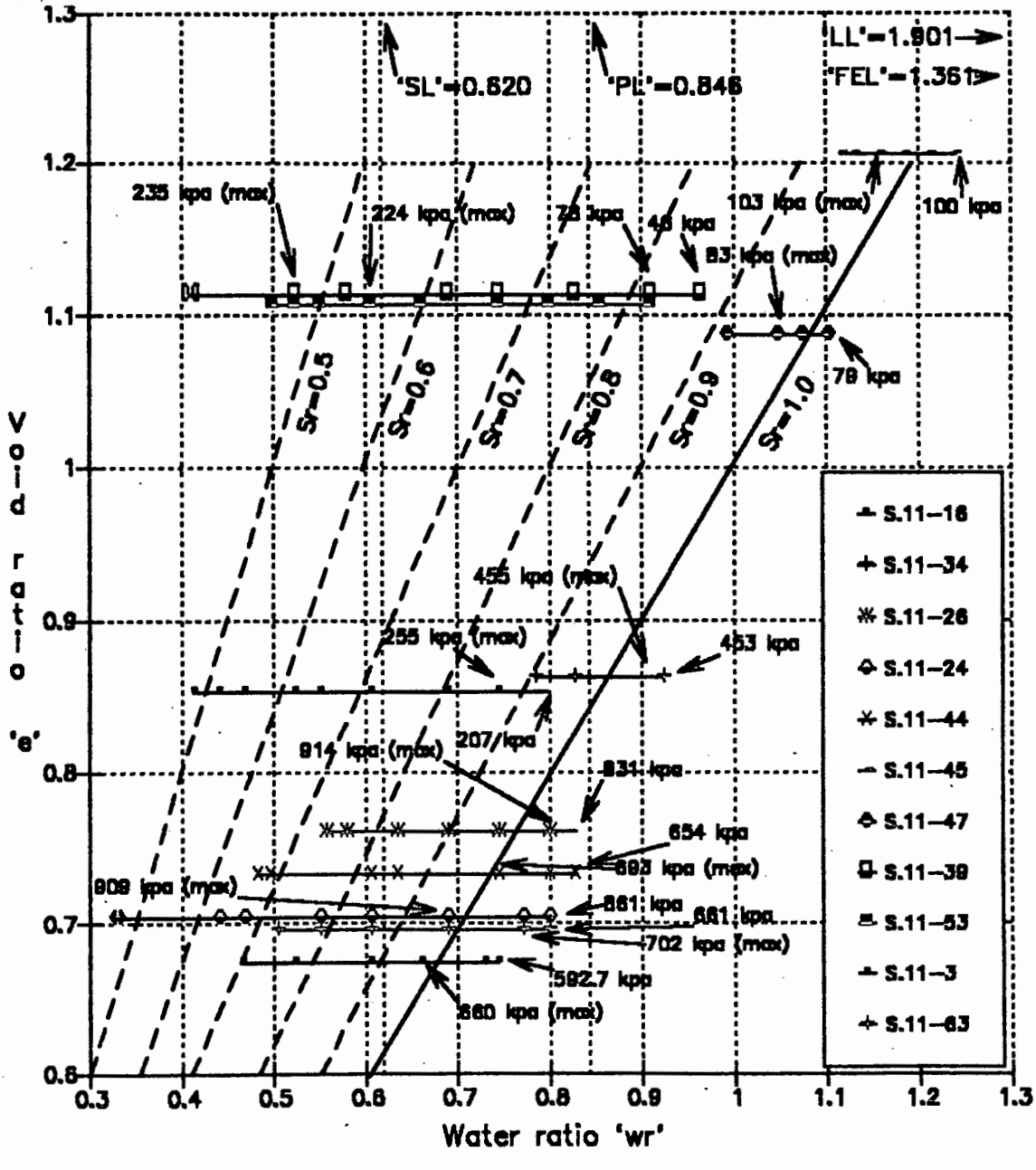

Figure 10.57: Site 11, Rosebank [Remoulded samples] - Observed stress scale system.
Comprises the void ratio 'e' vs water ratio 'wr' for swelling against constraint over the full range of degree of saturation 'Sr' and consistency limits.

10.3.6 Vertical Pressures versus Horizontal Pressures, or Stresses.

The ratio of horizontal to vertical stress, for one-dimensional consolidation, was discussed in the previous section.

It was observed from experiment that the ratio of horizontal to vertical stress can change during the test. In other words, the ratio of horizontal to vertical stress changes with changes in the applied stress.

Figures 10.58 to 10.63.

These figures show the observed ratios of horizontal to vertical stress in the samples.

The following soil/test types are illustrated:

(i) Site 11, Rosebank: Figure 10.58 - One-dimensional consolidation; Figure 10.59 - Expansion or collapse under load (50 Kpa, 100 Kpa, 400 Kpa, and swelling pressures).

(ii) Site 36, Rondebosch: Figure 10.60 - Expansion or collapse under 100 Kpa applied pressure.

Site A, Berea Road (Durban): Figure 10.61 - 100 Kpa.

Site 7, Mowbray: Figure 10.62 - 100 Kpa.

Site 48, Lady Grey: Figure 10.63 - 100 Kpa.

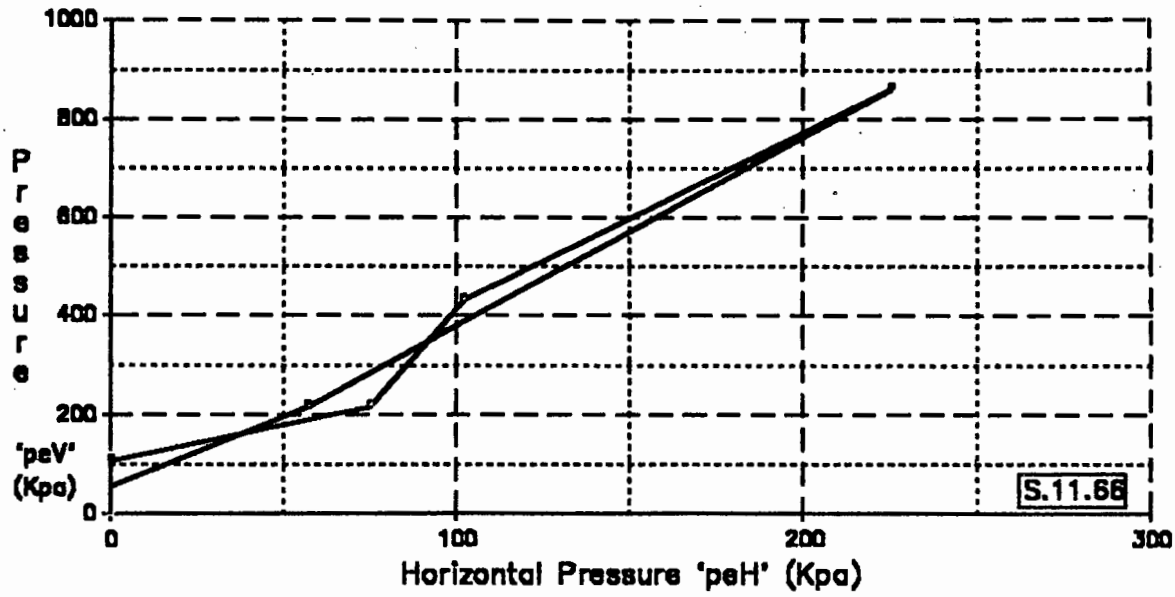

Figure 10.58: Site 11, Rosebank [One-dimensional consolidation] - Vertical pressure 'peV' versus Horizontal pressure 'peH'.

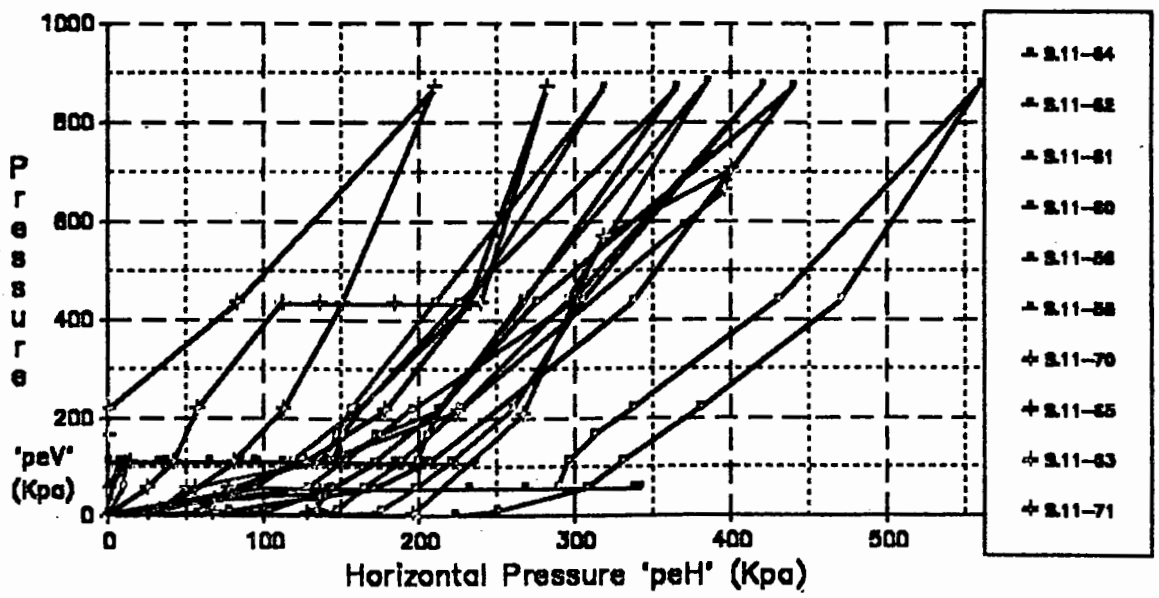

Figure 10.59: Site 11, Rosebank [50 Kpa, 100 Kpa, 400 Kpa and Swell Pressure] - Vertical pressure 'peV' versus Horizontal pressure 'peH'.

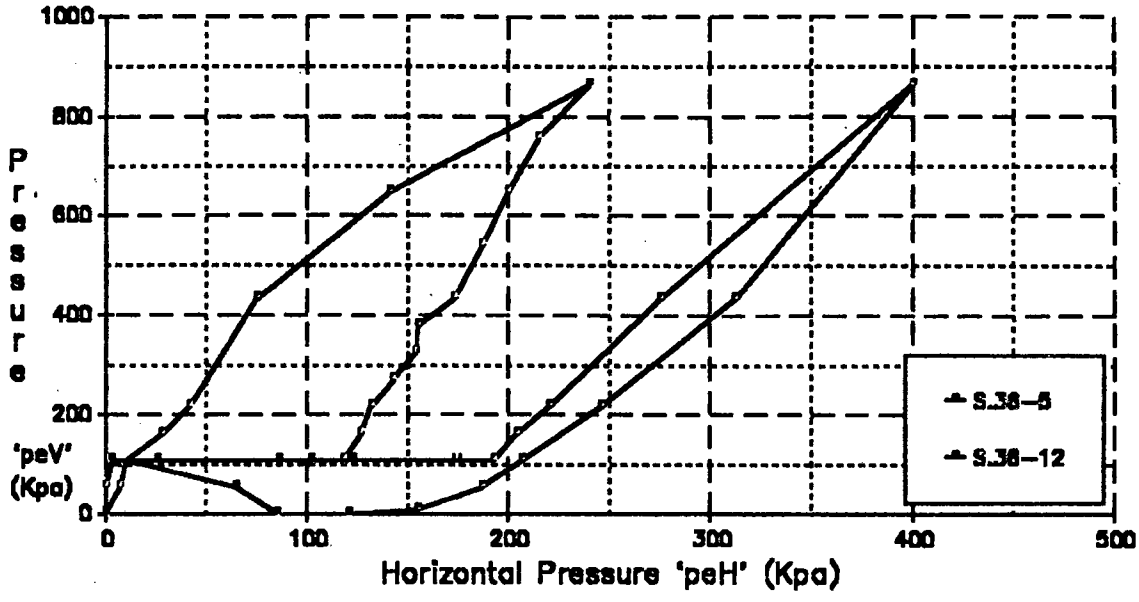

Figure 10.60: Site 36, Rondebosch [100 Kpa] - Vertical pressure 'peV' versus Horizontal pressure 'peH'.

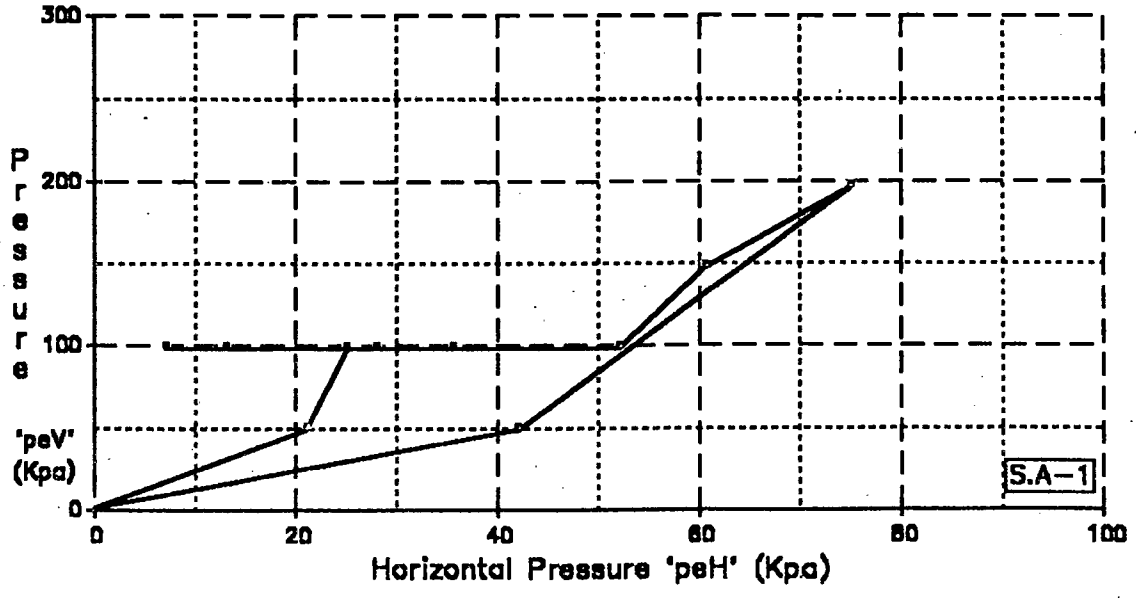

Figure 10.61: Site A, Berea Road [100 Kpa] - Vertical pressure 'peV' versus Horizontal pressure 'peH'.

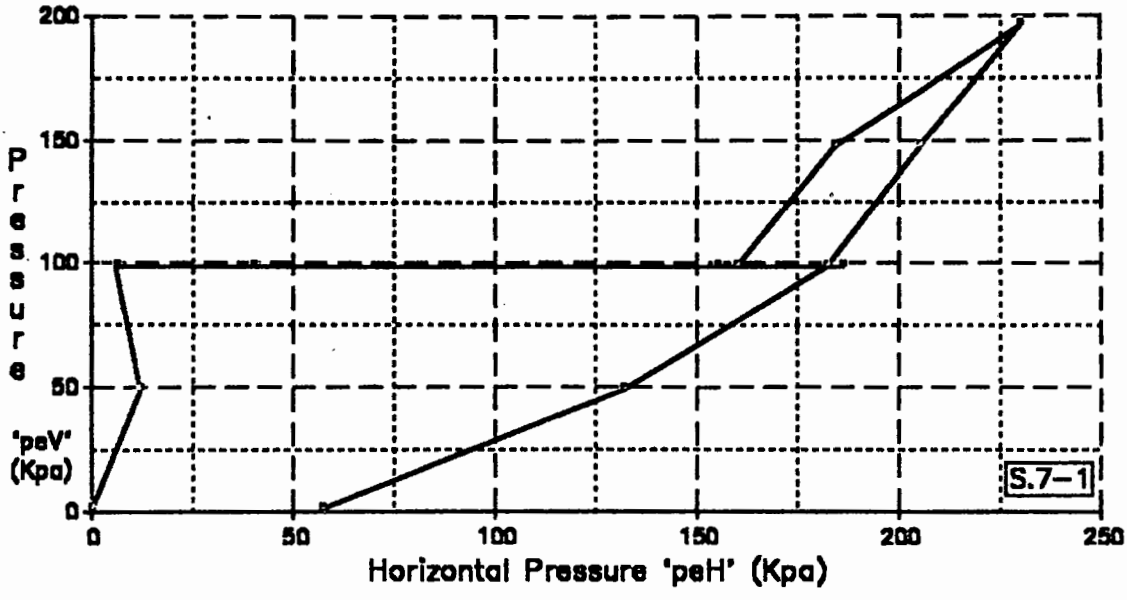

Figure 10.62: Site 7, Mowbray [100 Kpa] - Vertical pressure 'peV' versus Horizontal pressure 'peH'.

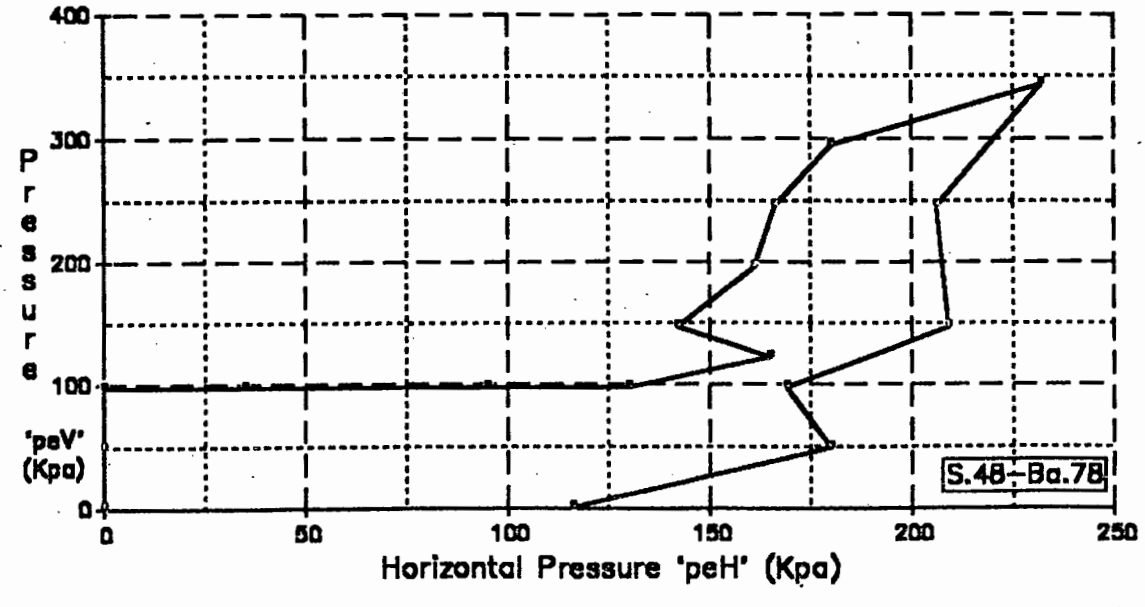

Figure 10.63: Site 48, Lady Grey [100 Kpa] - Vertical pressure 'peV' versus Horizontal pressure 'peH'.

10.3.7 Stress Paths of 'p' versus 'q'.

The stress path can be briefly described as a line joining stress points, each of which defines the Mohr's circle (ie, a graphical construction[1]) in position and size. Stress paths can be plotted on 'p' - 'q' diagrams either in terms of total stress or effective stress paths.

To be noted that: 'p' equals the vertical stress plus horizontal stress divided by 2, and 'q' the difference between the vertical and horizontal stresses divided by 2. The following are effective stress paths, or 'p' versus 'q' diagrams, for the soil types investigated[2].

Site 11, Rosebank.

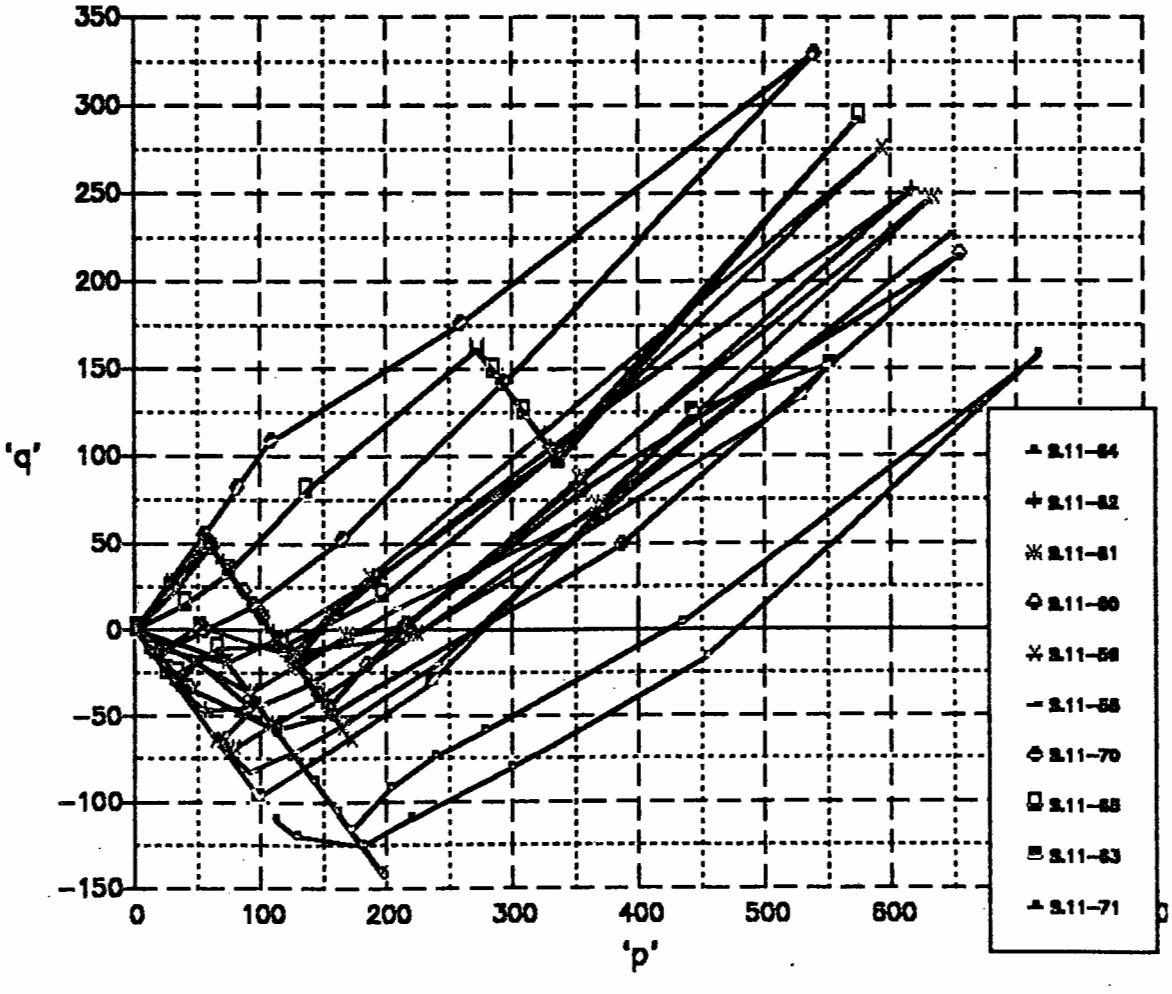

Figure 10.64: Site 11, Rosebank [One-dimensional; 50Kpa; 100Kpa; 400Kpa; Swell Pressure] Stress paths of 'p' vs 'q'.

---

[1] - *which defines the state of stress on a plane.*
[2] - *in chapter eight.*

Site 36, Rondebosch.

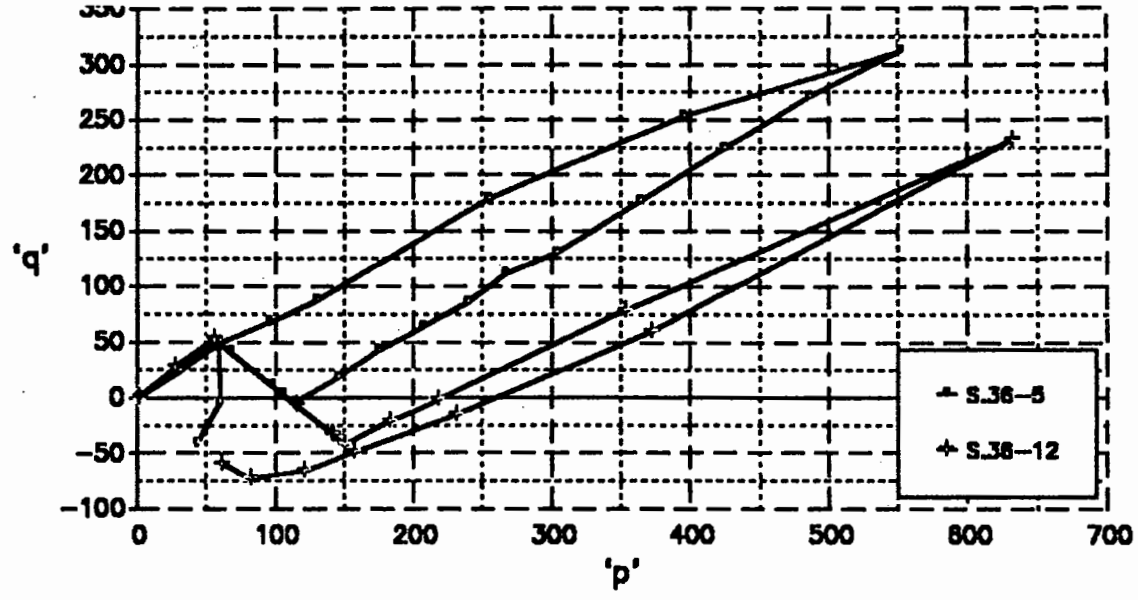

Figure 10.65: Site 36, Rondebosch [100 Kpa] - Stress paths of 'p' versus 'q'.

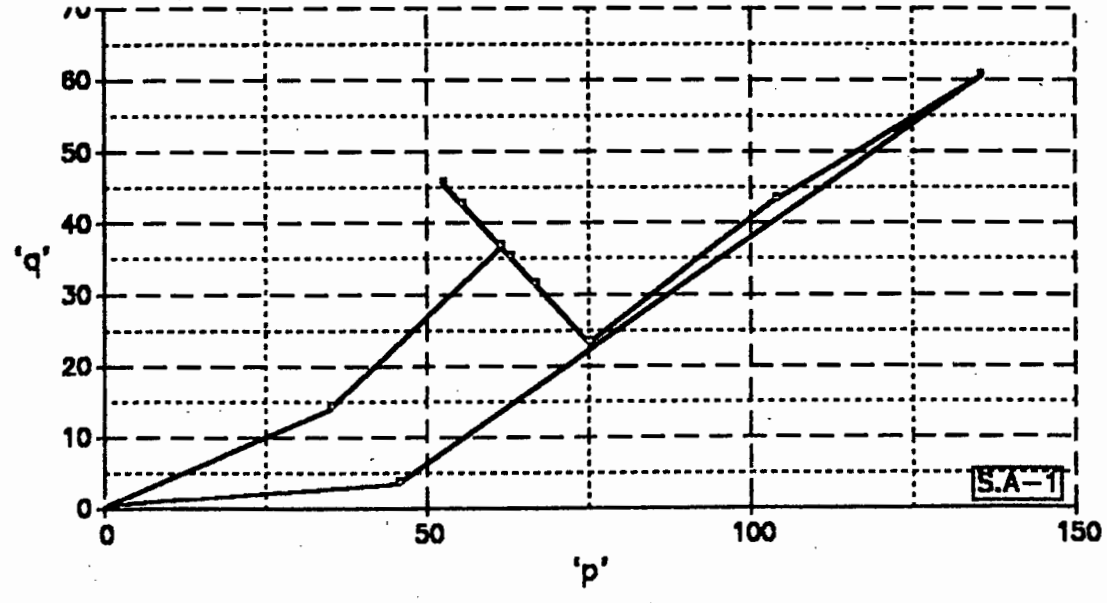

Figure 10.66: Site A, Berea Road [100 Kpa] - Stress paths of 'p' versus 'q'.

Site 7, Mowbray.

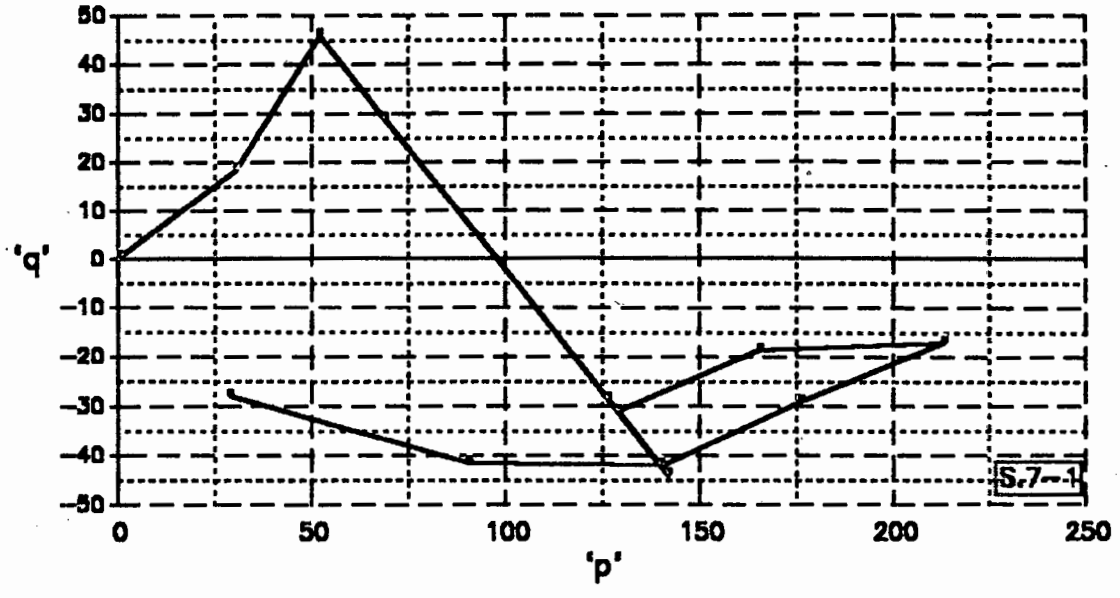

Figure 10.67: Site 7, Mowbray [100 Kpa] - Stress paths of 'p' versus 'q'.

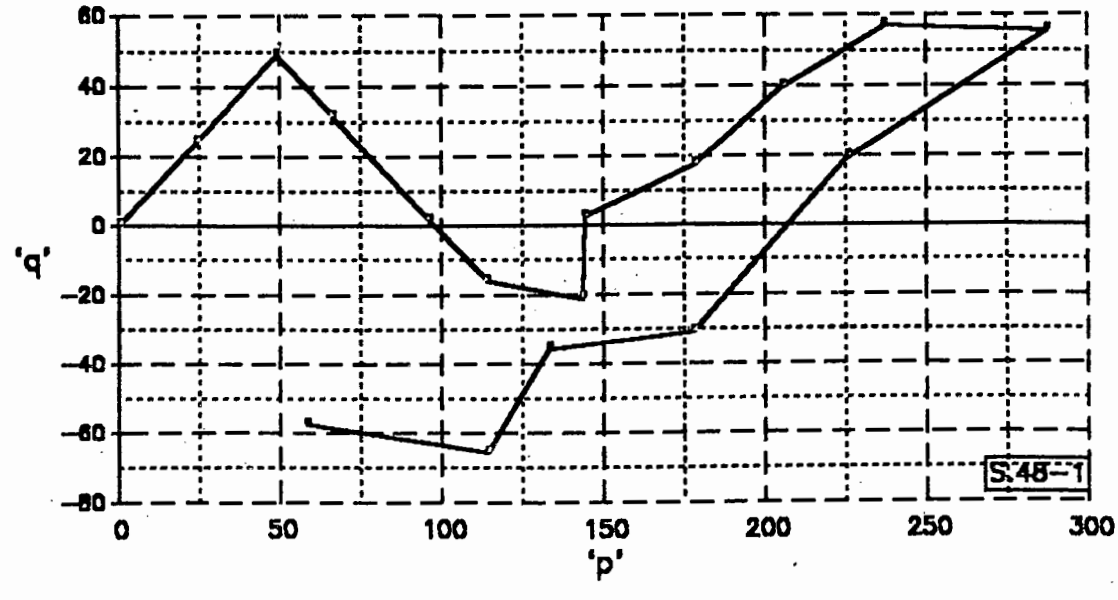

Figure 10.68: Site 48, Lady Grey [100 Kpa] - Stress paths of 'p' versus 'q'.

10.4 STRESS PATHS

The diagram in Figure 10.69 illustrates the main stages for a stress path.

Stages of stress path:

B : Loading of sample to the required effective vertical stress (in this case 100 Kpa).
B - C: The initial loading path - drained conditions -> k_O condition. (k_O = coefficient of lateral pressure at rest)
C - D: Water is gradually increasedin steps - if 'p' increases & 'q' decreases due to wetting -> Expansive soil (Note: If 'p' decreases & 'q' increases -> Collapsing soil).
D - E: Final loading - path reaches a 'k_O' line.
E - F: Unloading - tangent to line of path is a 'k_F' line.

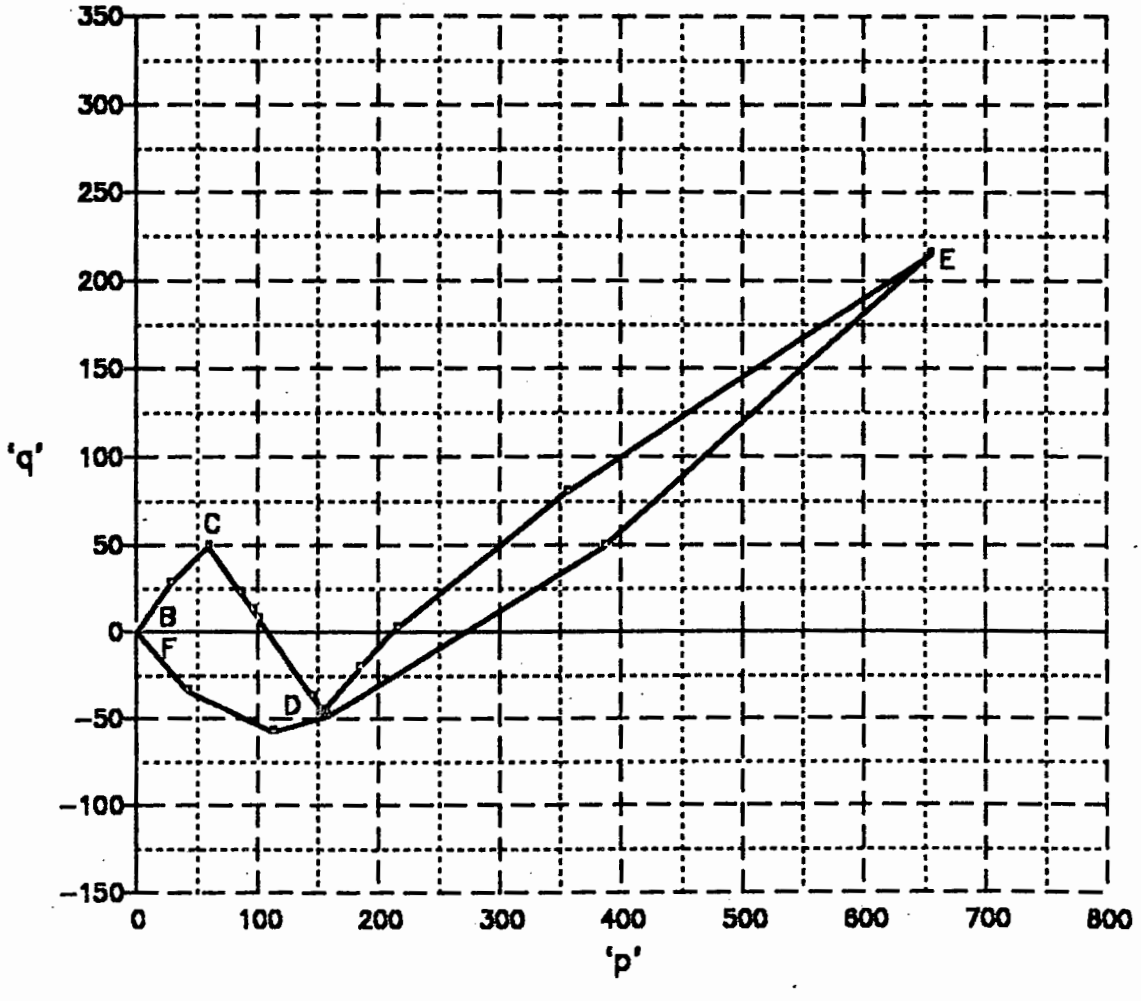

Figure 10.69: Site 11, Rosebank [100 Kpa] - The main stages for the 'p' versus 'q' diagram.

---

1 - *same sequence as used in Chapter Four, Figs. 8.01-03.*
2 - *in this case 100 Kpa.*

10.5 COMPACTED SOILS VS SOILS WHICH DRY FROM SLURRIES.

As described in Chapter Two of the thesis, to compact a soil is to place it into a denser state. The compaction effort imparts into the soil, amongst others, an increase in swell potential.

It was noted from experiment that compacted soil samples appear to exhibit greater potential for expansion and/or generate swell pressure.

Figure 7.44 has been repeated as Figure 10.70. The diagram in Figure 10.70 shows the void ratio versus effective vertical pressure versus water ratio, for Site A, Berea Road (Durban). This soil type is known for its collapse potential, however, this particular plot shows an effective vertical 'swell' pressure of approximately 13 Kpa.

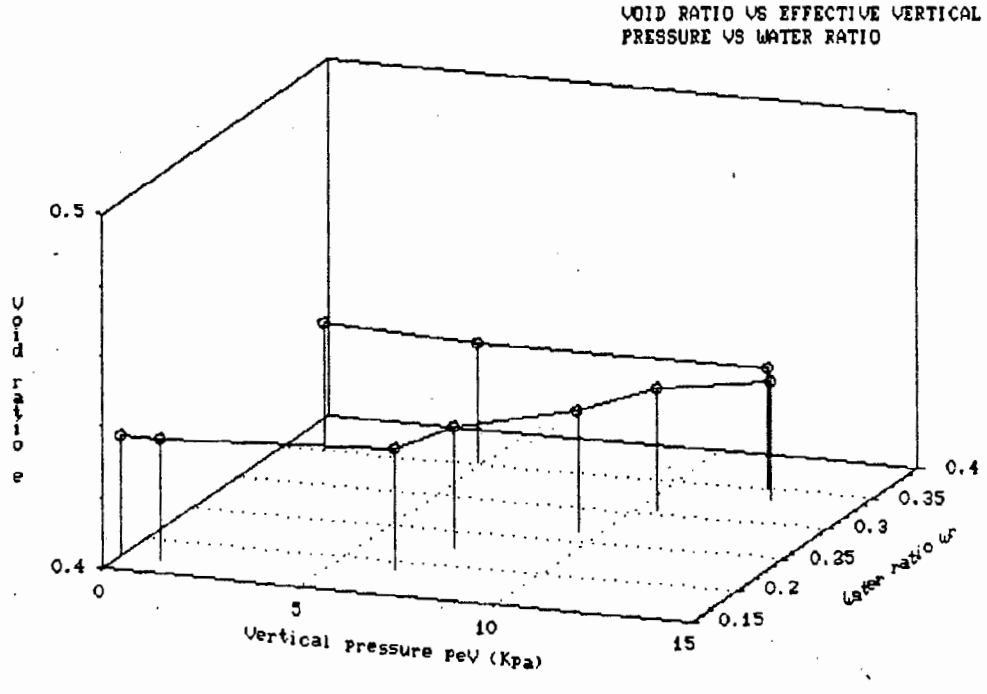

Figure 10.70: Site A, Berea Road [Compacted sample] - Void ratio 'e' vs effective vertical pressure 'peV' versus water ratio 'wr'.

10.6 FREE SWELL CURVES

These curves are useful because they illustrate the free swell paths for samples with different initial void ratios which are almost all at the same initial water ratio. Figure 4.81 has been repeated as Figure 10.71.

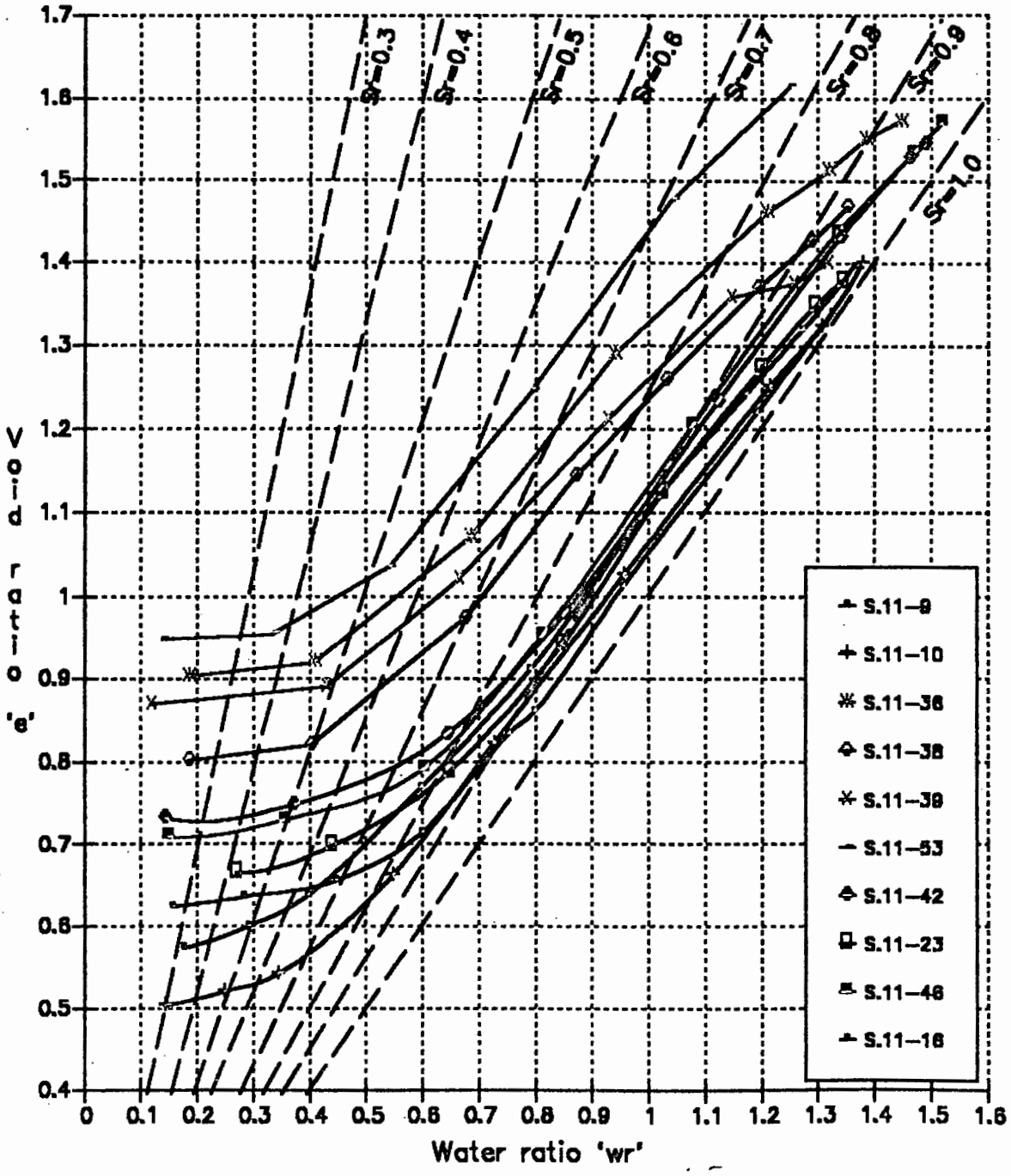

Figure 10.71: Site 11, Rosebank [Remoulded and Compacted samples] - Void Ratio 'e' vs Water Ratio 'wr' for Free Swell Paths over the full range of Degree of Saturation 'Sr'.

10.7 TIME VERSUS SWELL AND/OR SETTLEMENT BEHAVIOUR

It was noted from experiment that time to full heave (resulting from wetting the sample) is not the same as time to minimum strength (cohesion) due to this wetting. That is, time for swell pressure to reach a maximum, in an unconfined sample, is not the same as the time for it to decrease its shear strength to a minimum.

10.8 CONCLUDING REMARK

An extensive amount of data was obtained for this thesis. A major portion of this data was not analysed in this thesis. In particular, the 'Time versus Swell and/or Settlement' observations have not been included.

Future Research.

The writer proposes to extend this research work as follows: The inclusion of additional natural soil types; Time as a factor in the load-moisture behaviour of soils; The use of dynamic laboratory test methods (for example, dynamic triaxial testing) and the development of a Finite Element program to model the dynamic loading effect upon a volume change soil exhibiting expansive or collapsing behaviour.